NUCLEAR PHYSICS

JOURNAL DEVOTED TO THE EXPERIMENTAL AND THEORETICAL STUDY OF THE FUNDAMENTAL CONSTITUENTS OF MATTER AND THEIR INTERACTIONS

EDITOR: L. ROSENFELD - COPENHAGEN
ASSOCIATE EDITOR: O. NATHAN - COPENHAGEN

VOLUME VII

NORTH-HOLLAND PUBLISHING COMPANY - AMSTERDAM

NUCLEAR PHYSICS

EDITORIAL BOARD

AUSTRALIA & NEW ZEALAND:	H. Messel (Sydney), M. L. Oliphant (Canberra)
AUSTRIA:	B. Karlik (Vienna), H. Thirring (Vienna)
BELGIUM:	M. de Hemptinne (Louvain), J. Verhaeghe (Ghent)
CANADA:	G. Volkoff (Vancouver)
DENMARK:	C. Møller (Copenhagen), S. Rozental (Copenhagen)
FINLAND:	L. Simons (Helsinki)
FRANCE:	A. Berthelot (Saclay), S. Gorodetzky (Strasbourg), F. Joliot (Paris)
GERMANY (DEM. REP.):	G. Hertz (Leipzig)
GERMANY (FED. REP.):	W. Gentner (Freiburg i. B.), J. H. D. Jensen (Heidelberg)
GREAT BRITAIN:	S. Devons (Manchester), T. H. R. Skyrme (Harwell)
HUNGARY:	L. Janossy (Budapest)
INDIA:	H. Bhabha (Bombay), B. Peters (Bombay), R. Ramanna (Trombay)
IRISH REPUBLIC:	J. McConnell (Maynooth)
ISRAEL:	G. Racah (Jerusalem)
ITALY:	E. Amaldi (Rome)
JAPAN:	S. Kikuchi (Tokyo), S. Tomonaga (Tokyo)
MEXICO:	M. Moshinsky (Mexico)
NETHERLANDS:	H. Brinkman (Groningen), S. R. de Groot (Leiden)
NORWAY:	E. Hylleraas (Oslo), A. Lundby (Oslo), H. Wergeland (Trondheim)
POLAND:	L. Infeld (Warsaw)
PORTUGAL:	J. M. Araújo (Porto), J. R. de Almeida Santos (Coimbra)
SOUTH AMERICA:	G. Beck (Saõ Paulo), J. Leite Lopes (Rio de Janeiro)
SPAIN:	J. M. Otero (Madrid), C. Sanchez del Rio (Madrid)
SWEDEN:	O. Klein (Stockholm), K. Siegbahn (Uppsala), I. Waller (Uppsala)
SWITZERLAND:	P. Huber (Basel), P. Scherrer (Zürich)
U.A.R. & ARAB COUNTRIES:	F. El Bedewi (Alexandria), M. G. Nooh (Cairo)
U.S.A.	V. Weisskopf (Cambridge, Mass.)
U.S.S.R.:	M. A. Markov (Moscow), I. S. Shapiro (Moscow), D. V. Skobeltzyn (Moscow)
YUGOSLAVIA:	I. Supek (Zagreb)

NUCLEAR PHYSICS

MONTHLY JOURNAL DEVOTED TO THE EXPERIMENTAL AND THEORETICAL STUDY OF ATOMIC NUCLEI, NUCLEAR FIELDS AND THE FUNDAMENTAL ASPECTS OF COSMIC RADIATION

EDITOR: L. ROSENFELD - COPENHAGEN

VOLUME VII

JUNE 1958—AUGUST 1958

NORTH-HOLLAND PUBLISHING COMPANY - AMSTERDAM

PRINTED IN THE NETHERLANDS BY
DRUKKERIJ VOORHEEN GEBROEDERS HOITSEMA, GRONINGEN

1.E.1 : 2.L

Nuclear Physics 7 (1958) 1—9; © *North-Holland Publishing Co., Amsterdam*

Not to be reproduced by photoprint or microfilm without written permission from the publisher

QUASI-ELASTIC SCATTERING AND NUCLEAR STRUCTURE

TH. A. J. MARIS

The Gustaf Werner Institute for Nuclear Chemistry, University of Uppsala, and The Institute for Theoretical Physics, University of Copenhagen

and

PETER HILLMAN † and H. TYRÉN

The Gustaf Werner Institute for Nuclear Chemistry, University of Uppsala

Received 9 April 1958

Abstract: Energy and angular correlation measurements on the two protons emerging from high energy (p, 2p) processes may give direct information on the structure of the ground state of the bombarded nucleus and of certain excited states of the residual one. Expectations are derived on the basis of the assumptions of the approximative validity of the shell model and the Serber-Chew hypothesis of the reaction mechanism. The influence of multiple collisions in the nucleus is considered.

1. Introduction

In the bombardment of nuclei with protons †† of a hundred or more MeV, knock-out processes of the type

$$N_Z^A(\mathrm{p}, 2\mathrm{p})N_{Z-1}^{A-1}$$

in which both outcoming protons have high energies often occur. These processes have been discussed qualitatively by Serber [1]) and quantitatively by Chew [2]), Wolff [3]) and other authors. The leading idea in these treatments is that, assuming the absence of a strong clustering of the nucleons in the nucleus, the bombarding proton can, because of its small de Broglie wavelength and high energy, approximately be regarded as interacting with the individual nucleons in the nucleus, considering these as being free at the moment of the collision. Many experiments [4]) have verified the existence of such "quasi-elastic" scattering.

It is the purpose of this paper to show that quasi-elastic scattering may give direct information on the ground state of the bombarded nucleus, on certain states of the residual one, and on parameters of importance for the shell model.

Suppose the incoming protons have a well defined momentum and the

† CERN (European Organization for Nuclear Research, theoretical study division). Now at SC division, CERN, Geneva.

†† All conclusions are equally valid for bombarding or knocked-out neutrons.

momenta of two protons resulting from an interaction are simultaneously measured. In this case the energy momentum balance of the event is known and the energy of the residual nucleus in its centre of mass can be calculated. This energy will be located in the discrete or in the continuous part of the spectrum of the residual nucleus, depending on whether this nucleus remains intact or disintegrates.

Any model of the nucleus and the reaction will result in certain predictions concerning the observed energy spectra and angular correlations, and can be tested by comparison with experiments. At present only expectations on the basis of the approximate validity of the shell model for the nucleus and the Serber-Chew hypothesis for the reaction mechanism will be discussed.

2. Transparent Closed Shell Nuclei

The situation is most simple if the target consists of closed shell nuclei, say of O^{16}. Considerations quite analogous to the following can be applied to Ca^{40} and also to C^{12}, if the latter is assumed to be purely j–j-coupled.

We first assume that the process consists of a pure knock-out reaction, i.e. that the incoming and knocked-out proton after, and the incoming proton before, the p–p collision do not interact with the nucleus. In any coupling scheme of the shell model in which different shells do not mix with each other, only three types of protons can be knocked out of O^{16}. In j–j coupling, for example, these are two $p_{1/2}$, four $p_{3/2}$ and two $s_{1/2}$ protons. Only three states of N^{15} result, with the assignments $\frac{1}{2}-$, $3/2-$, and $\frac{1}{2}+$. The $\frac{1}{2}-$ state should be the ground state; the $3/2-$ state may be the known 6.33 MeV state with these assignments [5, 6]), and the $\frac{1}{2}+$ state is a dipole excitation [7]) and should lie in the lowest energy part of the giant γ-resonance, around 15 MeV.

3. Transparent Non-Closed Shell Nuclei

If the last shell of the target nucleus is not filled, the ground state can have many parents and the excitation caused by a knocking out of a proton from the unfilled shell may result in many states. There are of course restrictions; for example, a knocking out of a proton from the p-shell of a spin zero nucleus can only result in $3/2-$ and $1/2-$states.

Although in this case more definite conclusions can only be made on the basis of a knowledge of the wave functions of the ground states of the bombarded nucleus and of the excited states of the residual one, some general features may be predicted.

If both the original and residual nuclei are nearly spherical, the observed energy spectrum will consist of level groups roughly reflecting the shell structure of the bombarded nuclei. Differences of the pairing energies in the shells concerned might smear the spectrum out somewhat [8]).

The change of the spectra with atomic number may give information about the shell which is involved in a certain transition, and sudden changes in the nuclear structure like strong deformations of the initial or residual nucleus should show up.

At sufficiently high bombarding energies an analysis of the angular and energy correlations of the proton pairs which leave the residual nucleus in a definite excited state should indicate from which shell the protons are knocked out.

4. The Cross Section in Impulse Approximation

We still consider perfectly transparent non-refracting nuclei and calculate the cross section for the knock-out process in the impulse approximation, following Chew [2]). The differential cross section in the laboratory system for an event in which a proton of momentum $\mathbf{k}_0$ and spin function s_0 is scattered into the wave number interval $\mathrm{d}\mathbf{k}_1$ with spin function s_1 and another into $\mathrm{d}\mathbf{k}_2$ with spin function s_2 is

$$\frac{\mathrm{d}\sigma_{12,0}}{\mathrm{d}\mathbf{k}_1\,\mathrm{d}\mathbf{k}_2} = \frac{\pi}{\hbar} \cdot \frac{1}{v_0} \cdot \delta(E_1+E_2+E_\mathrm{n}+E_\mathrm{b}-E_0) \cdot |\sum_{m_3} R_{12,03}\, g_{m_3(\mathbf{k}_3)}|^2 \qquad (1)$$

Throughout this paper the indices 0, 3, 1, 2 and n, refer respectively to the incoming and the nuclear proton until they collide, to the two outcoming protons, and to the recoiling nucleus. The meaning of the other symbols is

v — a velocity;

$\mathbf{k}$ — a momentum;

E — a kinetic energy, except for E_b which means the binding energy of the knocked-out proton;

$R_{12,03}$ — the scattering amplitude which describes the free p–p scattering from an initial state in which the protons have the momenta $\mathbf{k}_0$, $\mathbf{k}_3 = \mathbf{k}_1+\mathbf{k}_2-\mathbf{k}_0$ and spin functions s_{m_0}, s_{m_3} into states with momenta $\mathbf{k}_1$, $\mathbf{k}_2$ with spin functions s_{m_1}, s_{m_2}; $|R_{12,03}|^2$ is, neglecting the binding energy, reducible to a measurable proton-proton cross section;

$$g_m(\mathbf{k}) = \ldots{}^{3/2}(2\pi)^{-3/2} \cdot \int \psi_f^*(2, \ldots, A) \cdot \exp(-i\mathbf{k}\cdot\mathbf{r}_1) \cdot s_m^*(1) \cdot t_\mathrm{p}^*(1)\psi_1(1, \ldots, A)\mathrm{d}1 \ldots \mathrm{d}A,$$

ψ_1 and ψ_f being the wave functions of the original and residual nuclei, s_m a spin function, and t_p the proton isobaric spin function; the integration is meant to be performed over the variables of all A particles of the initial nucleus.

The physical meaning of the function $|g_m(\mathbf{k})|^2$ is the probability density for the situation in which any one of the protons of the original nucleus has the

momentum $\mathbf{k}$ and the spin indicated by s_m, the rest of the nucleus being just in the relevant final state of the residual nucleus.

The antisymmetry of the wave function of the total system has been taken into account in (1).

The expression (1) may be simplified because in practice no observations are made of the orientations of the initial and residual nuclei. We will use a physical argument. The cross section (1), neglecting the binding energy, is equal to $\sum_m |g_m(\mathbf{k}_3)|^2$ times the corresponding one in which the target nucleus is replaced by a proton of momentum $\mathbf{k}_3 = \mathbf{k}_1+\mathbf{k}_2-\mathbf{k}_0$ and with a polarization corresponding to the normalized spin wave function $(\sum_m g_m(\mathbf{k}_3) \cdot s_m)/\sum_m |g_m(\mathbf{k}_3)|^2$. This is just a restatement of the physical meaning of the impulse approximation. The same replacement can be done for all orientations of the ground state of the initial nucleus and relevant excited state of the residual nucleus, and it is clear that the cross section for unpolarized nuclei equals $\sum_m \sum_f \overline{|g_{fm}|^2}$ times the cross section after the replacement of a target nucleus by an unpolarized † proton of momentum $\mathbf{k}_3$. The bar over $|g_{fm}|^2$ indicates the averaging over the different orientations of the initial state, and the index f refers to the orientations of the final state. We have explicitly

$$\frac{\mathrm{d}\sigma_{21,0}}{\mathrm{d}\mathbf{k}_1\,\mathrm{d}\mathbf{k}_2} = \Big(\sum_m \sum_f \overline{|g_{fm}(\mathbf{k}_3)|^2}\Big) \frac{\mathrm{d}\sigma_{\mathrm{pp}}}{\mathrm{d}\mathbf{k}_1} \tag{2}$$

with

$$\frac{\mathrm{d}\sigma_{\mathrm{pp}}}{\mathrm{d}\mathbf{k}_1} = \frac{\pi}{\hbar} \cdot \frac{1}{v_0} \cdot \sum_m |R_{21,03}|^2 \cdot \delta(E_1+E_2+E_{\mathrm{n}}+E_{\mathrm{b}}-E_0)$$

being, except for a slightly different energy conserving δ-function, the proton-proton cross section for this scattering on free unpolarized protons. There is some arbitrariness in the choice of this cross section because energy is not conserved for the momenta $\mathbf{k}_0, \mathbf{k}_3; \mathbf{k}_1, \mathbf{k}_2$, but assuming a smooth dependence of R on the momenta, this uncertainty is unimportant. If the bombarding beam is also unpolarized and the polarizations of the scattered particles are not measured, one has to take in (2) simply the corresponding unpolarized p–p cross section.

In the case of a closed shell target nucleus,

$$\sum_f \sum_m \overline{|g_{fm}(\mathbf{k}_3)|^2} = (2j+1)|g(\mathbf{k}_3)|^2, \tag{3}$$

j denoting the angular momentum of the final state of the residual nucleus and $|g(\mathbf{k}_3)|^2$ the normalized average momentum distribution of all the single particle states with definite angular momentum j in the shell from which the proton has been knocked out. From (2) and (3) it follows, for example, that,

† This is because, assuming parity conserving interactions, in a spherically symmetric situation there can be no direct correlation between a momentum and a polarization.

neglecting the effect of the spin-orbit coupling on $|g(\mathbf{k}_3)|^2$, quasi-elastic scattering on O^{16} should lead twice as often to the 3/2— as to the ground state of N^{15}. From an intuitive point of view this is expected, as there are twice as many $p_{3/2}$ as $p_{1/2}$ protons in similar conditions available in O^{16}. As will be shown, the same conclusion still holds if spin-independent absorption and refraction of the nucleus are taken into account.

5. The Influence of Refraction and Absorption

The approximation used should be good at energies of 150 MeV or more, except for the fact that multiple collisions have been neglected. Especially after the p–p interaction, as both particles have on the average less than half of the initial energy, this effect can be serious. It may be taken into account by replacing the nucleus by a complex potential well which distorts the plane incoming and outgoing waves. In a WKB approximation [9]), neglecting the change of the distortion over the radius of the nucleon-nucleon interaction and using for simplicity a spin independent square well potential, one has to replace the functions $g_m(\mathbf{k})$ by

$$g'_m(\mathbf{k}) = A^{-1/2}(2\pi)^{-3/2} \cdot \int \psi_f^*(2,\ldots,A) \exp(-i\mathbf{k}\cdot\mathbf{r}_1) s_m^*(1) t_p^*(1) \psi_i(1,\ldots,A) \exp\left[\sum_{n=0}^{2} \frac{d_n(\mathbf{r}_1)}{2}\left(i\frac{V_n}{E_n}k_n - \frac{1}{\lambda_n}\right)\right] \cdot \mathrm{d}1\ldots\mathrm{d}A. \quad (4)$$

In this expression V is the real part of the square well potential, λ the mean free path in nuclear matter, and $d(\mathbf{r})$ the distance travelled in the potential to or from the collision point r.

Even for simple final and initial wave functions the integration in (4) is not easy to do by hand. The general effect of the distorting exponential in (4) is to introduce additional real and purely imaginary momentum components. The former will mainly smear out the angular distributions and the latter decrease the intensity. It may be remarked that as long as the distorting factor is taken spin-independent it will enter in the same way in $|g(\mathbf{k}_3)|^2$ of eq. (3) for final states of different angular momenta resulting from a knocking out of a proton from states of the same orbital angular momentum in a closed shell. This shows that these processes will still occur with cross sections in the ratio of their statistical weights.

To get some idea of the reduction of the cross sections for quasi-elastic events in the different shells by multiple collisions, we replace the quantities $d_n(r)$ by a crude average value

$$\overline{d_n} = \sqrt{(\text{nuclear radius})^2 - \tfrac{2}{3}\langle r^2\rangle}.$$

For $\langle r^2\rangle$ we take the expectation value in the relevant shell for wave functions of a harmonic oscillator potential so chosen that the average value of

r^2 for all particles agrees with that of an isotropic sphere with radius $A^{1/3} \cdot 1.3 \times 10^{-13}$ cm, which is also used for the absorbing potential. The factor $\exp -\sum_n (d_n/\lambda_n)$ gives an impression of the intensity reduction by the absorption and is plotted in fig. 1 as a function of atomic number for bombarding energies of 200 and 400 MeV. The mean free paths for 100 MeV, 200 MeV and 400 MeV have been chosen to be 2, 4, and 4×10^{-13} cm respectively.

Especially at 200 MeV the absorption is large, and our estimate of it, which improves with decreasing absorption, has therefore not much more than a qualitative meaning. The "absorption" of a particle means that a multiple collision has taken place. This results in an extra energy loss and it

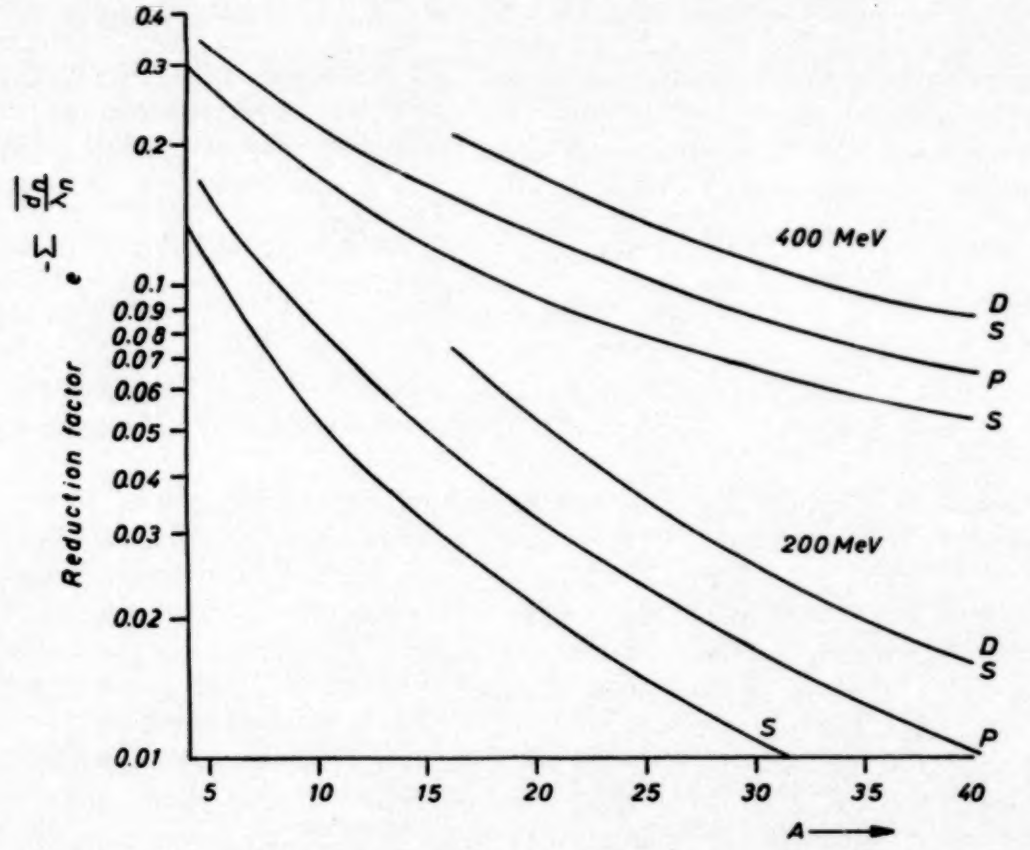

Fig. 1. Reduction factors for the cross sections of knockout processes occurring in various shells for 200 and 400 MeV bombarding energy.

might seem that the frequent occurrence of such events would spoil the spectrum caused by clean quasi-elastic collisions. However, the energy losses by multiple collisions will be smeared out over the whole available energy and angular range and result in a smooth background in the measured

energy spectrum of the residual nucleus. This background will start at the ground state of the residual nucleus and rise with excitation energy and atomic number. Superimposed on it one may expect to see the peaks caused by clean knock-out collisions, as long as a structure in the background does not become comparable with these peaks. This is also the general reason that the expected spectra are not very sensitively dependent on the applicability of the Serber-Chew hypothesis of quasi-elastic collisions.

Nevertheless, for the study of quasi-elastic collisions the absorption is an unfavourable effect, decreasing the peak heights and increasing the background. From this point of view fig. 1 shows that an initial energy of 400 MeV is much preferable to one of 200 MeV. Also, a measurement of angular and energy correlations will give more information on the momentum distributions at higher energies because of the smaller distortion of the ingoing and outgoing waves.

The figure shows that events in the shells of lower energy are more depressed than those in the higher ones. This is natural because the former are more concentrated towards the centre of the nucleus than the latter. The differences in absorption for different shells will have been underestimated in fig. 1, especially for the cases of very strong absorption, in which mainly the nuclear surface contributes.

6. Other Corrections

Besides the background created and the reduction of the peak heights by the absorption, there are some other corrections to our initial picture.

The knocking-out of a proton will often lead to a state of short lifetime, broadening the expected peaks. If, for example, an $s_{1/2}$ proton from a nucleus like carbon has been knocked out, the Pauli principle no longer excludes those collisions in the p-shell in which a proton falls into the hole of the s-shell ejecting another particle from the nucleus. The state in boron with a hole in the s-shell is a giant γ-resonance state and the typical width of the giant γ-resonance ($\approx$ 5 MeV) should be an upper limit for the width to be expected in this case. Holes in shells lying still deeper, for example in the s-shell in elements between oxygen and calcium, may have shorter lifetimes. This fact, together with the absorption, the relatively small number of occupying particles, and the location over a continuum, will make the detection of these shells only possible with large bombarding energies, say, at least 300 MeV.

If a particle is knocked out, the radius of the potential generating the shell model wave functions is suddenly decreased and this will cause additional excitations. However, it is easily shown that the probabilities for the new states excited are of the order of the square of the relative change in the

radius and even in the very light nuclei are negligible. On the other hand, a strong difference in the shape of the collective potentials of the initial and final nuclei may be noticeable by a broadening of the level structures, both because of a bad overlap of the initial and final states and because of the splitting up of the single particle levels by a deformation [10]).

7. Comparison with Deuteron Pick-Up

Quasi-elastic scattering has a strong similarity to the high energy deuteron pick-up process, in which, also a nucleon is taken out of the nucleus. It is interesting to compare these two reactions.

The experimental results and their analysis [11]) suggest that in deuteron pick-up the interaction is concentrated at the nuclear surface. The following reasons lead one to expect that, for the same incident energy, deuteron pick-up is more restricted to the nuclear surface than appropriately chosen quasi-elastic scattering:

a. In deuteron pick-up, especially at higher energies, high momentum nucleons are snatched out of the nucleus. Such nucleons are more present in shells of higher energy, which have a large density at the nuclear surface.

In symmetric quasi-elastic scattering at 45 degrees one is looking at very low momentum nucleons which belong more to the inner nuclear shells.

b. The absorption in the nucleus favours surface interactions. The choice of equal energies of the two outgoing particles, as obtainable in quasi-elastic scattering, results in the smallest total absorption. In deuteron pick-up the distorted deuteron wave function in the nucleus corresponds to a neutron and a proton of greatly differing absolute momenta, resulting in a strong increase of the absorption.

For these reasons we think that at a given bombarding energy quasi-elastic scattering offers a larger chance for studying inner shells than deuteron pick-up. The optimum energy for investigating these shells with quasi-elastic scattering will be about 400 MeV. At such energies the nucleons to be picked up in deuteron pick-up must have very high momenta, so the cross section for this reaction becomes very small, and secondary processes become important.

8. Concluding Remark

As shown above, quasi-elastic scattering may give direct information on some aspects of nuclear structure and enable one to measure important parameters of the shell model such as spin-orbit splitting and the energy differences of various shells. The essential reason that the spectra resulting from quasi-elastic scattering, as well as those from deuteron pick-up, should be so much simpler than, for example, those resulting from conventional high

energy inelastic scattering, is most easily seen in the shell model. In inelastic scattering the bombarding particle excites a neutron or proton from one of the filled single particle states into an unknown state, while in quasi-elastic scattering a proton is excited into a state which can be determined.

Preliminary measurements with 185 MeV protons of reactions of the type with which this paper is concerned have been reported [12]); the following paper contains improved and more complete results.

Professor The Svedberg has extended his kind support to this work. One of us (T. M.) is grateful to Professor Niels Bohr for the hospitality of the Institute for Theoretical Physics, Copenhagen. We thank Drs. G. E. Brown, D. Kurath and A. Turkevitch for useful contributions. The work was partly supported by the Swedish Atomic Energy Commission. One of us (T. M.) held a fellowship of the Ford Foundation.

References

1) R. Serber, Phys. Rev. **72** (1947) 1114
2) G. F. Chew, Phys. Rev. **80** (1950) 196
3) P. A. Wolff, Phys. Rev. **87** (1952) 434
4) O. Chamberlain and E. Segrè, Phys. Rev. **87** (1952) 81;
J. B. Cladis, W. N. Hess and B. J. Moyer, Phys. Rev. **87** (1952) 425
5) D. R. Inglis, Revs. Mod. Phys. **25** (1953) 390
6) F. Ajzenberg and T. Lauritsen, Revs. Mod. Phys. **27** (1955) 77
7) D. H. Wilkinson, Physica **22** (1956) 1039
8) A. M. Lane and D. H. Wilkinson, Phys. Rev. **97** (1955) 1199
9) L. I. Schiff, Phys. Rev. **103** (1956) 443
10) S. G. Nilsson, Mat. Fys. Medd. Dan. Vid. Selsk. **29** (1955) 16
11) J. Hadley and H. York, Phys. Rev. **80** (1950) 345;
W. Selove, Phys. Rev. **101** (1956) 231;
G. F. Chew and M. L. Goldberger, Phys. Rev. **77** (1950) 470
12) H. Tyrén, Th. A. J. Maris and P. Hillman, Nuovo Cimento **6** (1957) 1507

1.E.1 : 2.L | *Nuclear Physics* 7 (1958) 10—23; © *North-Holland Publishing Co., Amsterdam*

Not to be reproduced by photoprint or microfilm without written permission from the publisher

HIGH ENERGY (p, 2p) REACTIONS AND PROTON BINDING ENERGIES

H. TYRÉN, PETER HILLMAN † and TH. A. J. MARIS ††

The Gustaf Werner Institute for Nuclear Chemistry, University of Uppsala

Received 9 April 1958

Abstract: The energy carried away by each of the two coincident protons from (p, 2p) reactions in elements bombarded by 185 MeV protons has been measured by range analysis. To the extent that the collision is quasi-elastic, the difference between the sum of these energies and the incident energy, corrected for the recoil energy of the residual nucleus, gives the binding energy of the struck proton in the nucleus. Sharp groups which can be associated with the nuclear shell structure have been observed in the light elements. The results determine directly the spin-orbit splitting in the 1p-shell and the binding energy of the 1s-shell for the lightest nuclei. Only the spectrum of Be^9 might give some indication of an α-particle structure.

1. Introduction

As discussed in the preceding paper [1]), it is of interest for the theory of nuclear structure to study the (p, 2p) reaction initiated in nuclei by high energy protons. At proton energies (above 50 MeV or so) for which at least the light nuclei become appreciably transparent, such experiments have not been previously performed, and those at lower energies [2]) are complicated by the preponderance of multiple collisions. The experiments of Selove [3]) on the energy spectra of deuterons from high-energy (p, d) reactions give information somewhat similar to that obtained in the present work, but emphasizing surface interactions almost exclusively [1]). Earlier experiments have studied the energy distributions of protons scattered in the near-elastic [4]) and quasi-elastic [5]) regions, the energy distributions of one of two coincident protons [6]), and the angular correlations between proton pairs [7]). The significance of the results of most of these experiments, which established the existence of quasi-elastic scattering, is limited by the generally poor resolutions, and they yield mainly estimates of the average momentum distributions inside the nucleus. For discussions see refs. [6,7]).

The initial object of our experiment is the measurement of the energy required to remove a proton from a nucleus. For this purpose, it is necessary to measure simultaneously the energy carried away by the bombarding and

† CERN (European Organization for Nuclear Research, theoretical study division); now at SC Division, CERN, Geneva.

†† Now at the Institute for Theoretical Physics, Copenhagen.

recoil protons. A study of the correlations in angle and energy between the two protons, which we hope to pursue experimentally at a later stage, may yield information on the momentum distributions of the protons in each nuclear shell; for the moment we have measured only the spectra of the total energy carried away by two protons in coincidence and approximately 90° apart (45° on each side) in a plane with the incident momentum, when lithium, beryllium, boron, carbon, nitrogen, oxygen, and calcium are bombarded with 185 MeV protons. A preliminary report of this work has already appeared [8]).

2. Method and Apparatus

We use the range method to measure separately the energies of the two coincident protons, which we sum afterwards. Each proton is detected in a double- plus anti-coincidence channel. The geometry and electronic connections are shown schematically in fig. 1. There are on each side of the target four scintillators (L1, L2, L3, L4 and R1, R2, R3, R4 respectively), making up two channels; input channel I being $L1L2\overline{L3}$ (L1 in coincidence with L2, and L3 in anticoincidence), $II = R1R3\overline{R4}$, $III = L1L3\overline{L4}$, and $IV = R1R2\overline{R3}$. There are then four output channels, channel A consisting of coincidences between the outputs of channels I and IV, $B = I+II$, $C = III+IV$, and $D = II+III$. This arrangement minimizes the amount of electronic equipment required, as well as allowing a simultaneous measurement of input and output channel counting rates.

The channel positions are moved through the energy spectra by insertion of remotely variable aluminium absorbers between scintillators L1 and L2, and R1 and R2. A few millimeters of absorber are usually kept in front of L1 and R1 to prevent possible large numbers of evaporation protons from entering those scintillators.

The energy resolution is determined largely by the range straggling at the highest energies, but increasingly by the thicknesses of the crystals and associated aluminium covers, and to lesser extent of the target, at lower energies. The energy spread of the incident beam is negligible ($\approx$ 1 MeV). Although available beam intensity is not a limiting factor, the targets are shaped to give the maximum mass in the beam for optimum energy resolution, in order to minimize beam intensity (and therefore room background) required for a given counting rate. The targets have isosceles triangular cross sections, with bases towards the incident beam and vertex angles 30°. This shape ideally gives near-zero energy spread, where however the ideal vertex angle depends slowly on emergent proton angles and energies. The sizes are chosen to give a maximum of 2 MeV energy spread over the experimental range of energies. There are additional small contributions to the resolution from the fact that the absorbers are not shaped but flat, and from the fact

that a variation in the nuclear recoil energy is allowed by the large telescope geometries. (In the case of deuterium only, this latter effect is large, as may be seen from fig. 3 below.) The final total energy resolution is about 4.4 MeV

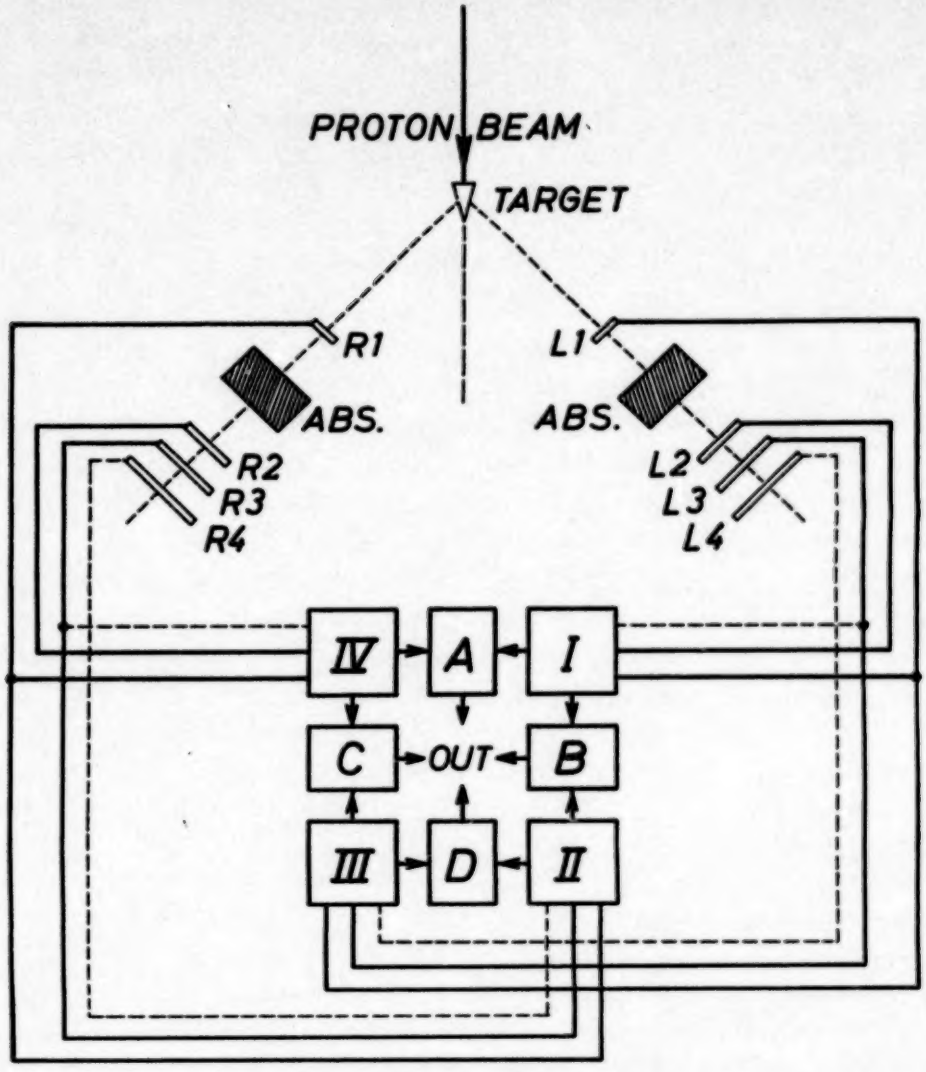

Fig. 1. Schematic diagram of counting geometry and electronic connections. Dashed lines indicate anticoincidence inputs. I, II, III, and IV are input mixers, and A. B. C, and D are final mixers.

full width at half height over the whole energy range, rising slightly at the highest binding energies.

The scintillators are all 3 mm thick NE102 plastic. L1 and R1 are 14 mm wide by 28 mm high, L2 and R2 26×52 mm, L3 and R3 34×68 mm, and L4 and R4 42.5×85 mm, spaced respectively 90, 165, 180, and 195 mm from the target centre. Each is wrapped in two layers of 0.02 mm aluminium foil.

The total angular width in each telescope is about 10° horizontally and 20° vertically.

The pulses from the RCA 6810A photomultipliers are clipped to 8mμsec length, shaped by series and parallel diodes, and fed through short 100 Ω cables into the coincidence circuits, those from the L scintillators via relay switches allowing remote insertion of delays. Each input mixer is a Garwin type double -plus anti-coincidence circuit modified to give, in addition to the normal slow output, a fast output of a size sufficient to feed directly two final mixers, which are of the same design but without the fast output and the anti-coincidence input. The eight mixers are mounted in a compact array to minimize the lengths of all internal leads. Resolving times are usually about 8 mμsec in the input mixers, and slightly longer in the final mixers. Conventional amplifiers and scalers complete each final channel. High voltage for the photomultipliers (about 2 mA at 2000 V for each) is provided by a 25 mA Oltronix Type LSH 12R unit, quoted stable to 0.4 V for 10 % line voltage variations.

The monitor is a two-scintillator telescope looking at the target, so that slight variations in the beam position (causing counting rate variations, since the target is not flat) are automatically taken into account. To normalize to the same incident beam intensity for the various targets, for purposes of absolute measurements, another two-scintillator telescope looks at a thin aluminium window at the exit of the proton beam tube in front of the target.

3. Checks and Procedure

Of the protons recorded in each channel (a few percent of those entering each telescope) only a fraction of a percent are in coincidence with protons recorded in the opposite channel. Most of the remainder are not in coincidence because of the poor angular and energy correlations between the two protons emerging from a quasi-elastic collision (spread out over more than a steradian and many MeV due to the nuclear momentum distribution), or because they are due to other nuclear processes. Accidental coincidences are therefore the main limiting factor on the counting rates and therefore on the statistical and total errors.

There are several pulse combinations possibly responsible for accidental coincidences, but by far the bulk come from non-accidental counts in the input channels, in accidental coincidence with each other. This is checked by observing the linear relationship between channel width and accidental rate, by putting absorbers in front of the appropriate anticoincidence counter. Accidentals can therefore be measured by remote insertion of equal delay cables into all L inputs. These delays must be longer than the coincidence resolution time ($\approx$ 8 mμsec) but, since the proton beam has a time-structure corresponding to the cyclotron radiofrequency, must be an integral number

(in our case one is sufficient) of r.f. cycles. We have determined the correct length ($\approx$ 40 mμsec) empirically by maximizing accidental rate versus cable length.

The accidental rate should not follow the spectrum, but should be a smooth function of absorber thickness. (For targets other than hydrogen the momentum distribution in the nucleus completely smoothes out all peaks in the *separate* telescopes.) This is illustrated in fig. 2 for carbon. Normally acci-

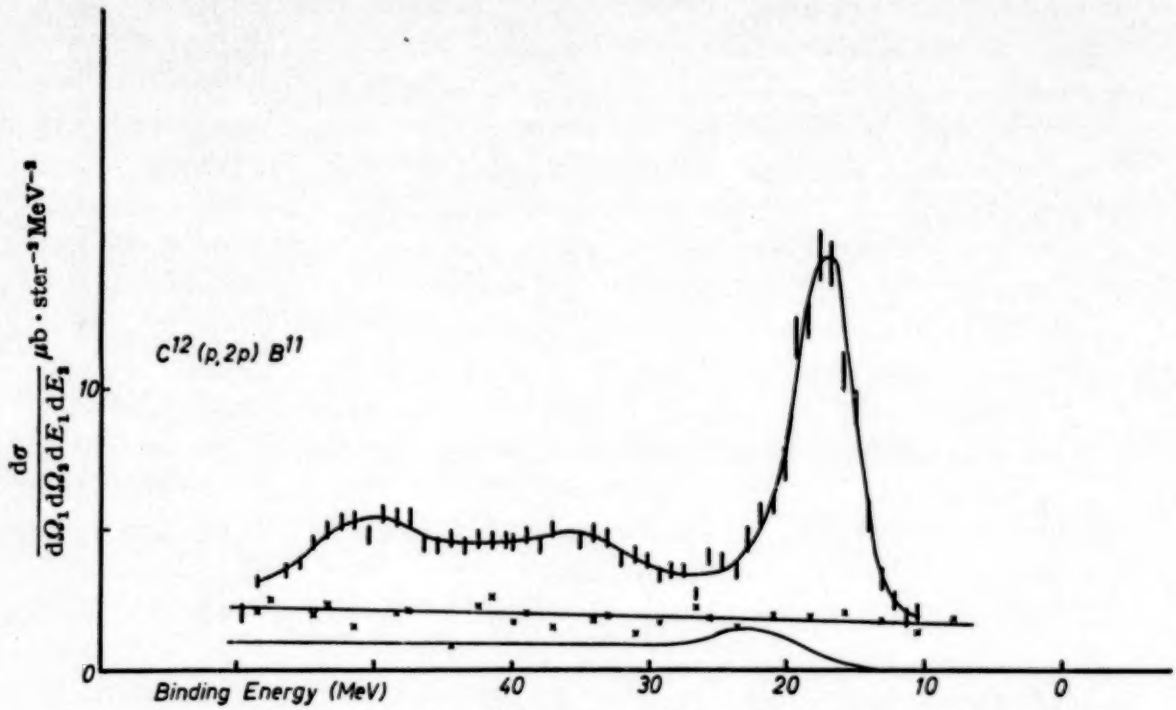

Fig. 2. The spectrum of summed proton energies for carbon, showing the accidental counting rates (crosses) and the correction for nuclear absorption in the scintillators (lowest curve).

dentals are only measured once every few absorber steps, except when unstable beam conditions are suspected.

While it is not possible to improve appreciably the radiofrequency duty-cycle (fractional on-time) of the external proton beam, it was found possible to increase the frequency modulation pulse length from a normal 12 μsec to about 40—60 μsec by lowering the cyclotron magnetic field, giving smaller energy gain per turn near the extraction radius, and thus a larger time spread. No other cyclotron controls had any noticeable effect. The effective total duty cycle was about 1/400.

We usually use only about 10^7 protons per second in the incident beam, much less than the full regenerated beam. The beam intensity is however reasonably steady only at full internal intensity. Therefore we use an aluminium diffusing screen in the regenerated beam before it enters the extraction channel, to reduce the external intensity while operating with full internal beam.

The most critical requirement of the experiment is on the efficiency of the anti-coincidence counters, because there are up to fifty times more protons passing through each channel-scintillator than stopping in it. An unavoidable source of inefficiency is the nuclear absorption of protons in that scintillator or the following aluminium foils, which will cause of the order of a percent of the transmitted protons to be lost to the respective anti-coincidence counter, and therefore to be recorded in each channel — amounting, in the lower energy regions, to a large fraction of the spectrum height. The number of transmitted protons in coincidence with normally recorded protons in the opposite channel is approximately given just by the integral of the observed real spectrum above that point. The fraction incorrectly counted due to the geometrical, optical, or electronic anti-coincidence inefficiencies is believed to be small, due to the good agreement among different channels at different times and under variable conditions, particularly at near-zero points on the spectra. These same points give upper limits to the nuclear absorption inefficiency, only a little higher than the values of this correction calculated from known carbon inelastic and hydrogen cross sections, corrected roughly for forward emission of secondary charged particles from carbon inelastic collisions, as estimated from the Monte-Carlo calculations of Rudstam [9]) and Metropolis *et al.* [10]). This calculated correction has been applied to all final spectra. Its magnitude is illustrated by the lowest curve in fig. 2.

The coincidence counter optical and electronic efficiencies are ensured by obtaining high-voltage and scaler-discriminator plateaus. This is done with anti-coincidences turned off, for greater speed and because a more critical test is obtained with protons not stopping in the scintillators, and therefore giving much smaller light pulses. The relative channel sizes, which depend on crystal thicknesses and sizes (no one crystal is defining) are calibrated by observing the relative heights of some prominent peak in the four channels. For reasons of counting rate this is conveniently that from deuterium in heavy water, the angular correlation between the two protons from deuterium being much better than that from other elements. (Ordinary hydrogen would give *exact* angular correlations, and if the two telescopes are not perfectly positioned, would give a distorted picture of the channel sizes.) The result is shown in fig. 3, indicating practically equal channel sizes. (The great width of the peak is due, as mentioned above, to the variation in "nuclear" recoil energies allowed by the finite telescope geometries.) The same test checks the calculated energy separations of the channels. The observed spectra from any three channels are thereafter simply normalized in energy to that of the fourth.

The energy variation of the channel efficiencies is due mainly to nuclear absorption in the absorbers, which reduces these a calculated maximum

of 22 % at the highest proton energies (lowest binding energies). This calculated correction has been applied to all spectra, assuming all protons inelastically scattered in the aluminium absorbers to be lost completely. The "anti-correction" due to those which are merely degraded in energy or create secondary charged particles, is calculated to be negligible.

For the present, we have always kept the left and right absorber thicknesses about equal. Channels B and C are then essentially similar. We change the sum of the absorber thicknesses in steps usually equal to one third of the

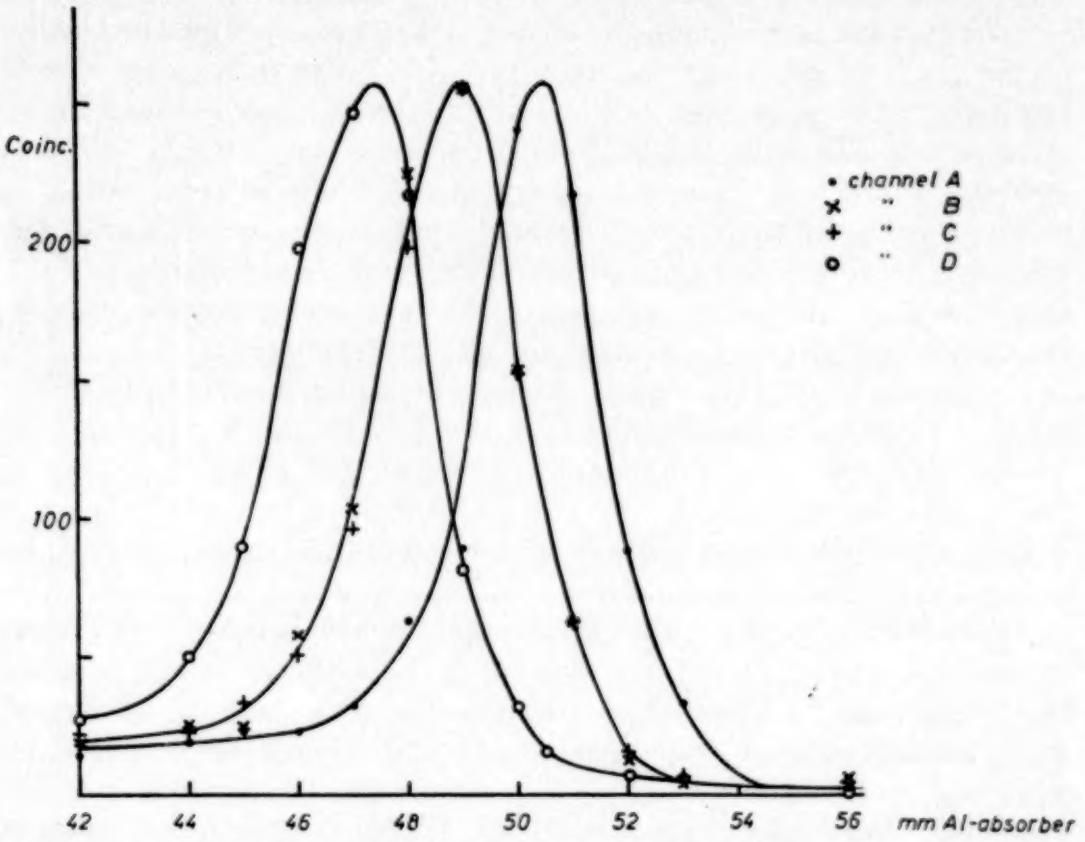

Fig. 3. The spectrum of summed proton energies as seen in the four separate channels for heavy water. The oxygen contribution is small. Numbers of coincidences are plotted versus total Al-absorber thickness.

A—D energy separation. Nearly every final point thus consists of at least two measurements, and alternating points belong respectively to channels A+D and B+C.

In converting the spectra to an energy scale, published range-energy tables are used [11]), and in addition a zero-point (free proton) check is obtained either from the natural water content of the targets, or from thin polythene foils attached to their front faces. The cross sections are corrected for the increase in energy width of each channel with decreasing proton energy, as calculated from the range energy tables. A correction is also made to the

energy scale for the recoil energy of the nucleus, which is kinematically determined except for the finite telescope resolutions. This correction is generally very small in the present cases, because of the angles chosen.

The beam is approximately 10 mm in diameter at the target position. The D_2O, Be, B, N_2, O_2, and Ca targets have base widths, facing the beam, of 10 mm, and the Li and C targets 15 and 7.5 mm respectively. The heavy water and powdered boron containers are of 0.1 mm aluminium. The cryostatic target container for oxygen and nitrogen is a 0.023 mm soldered nickel foil triangle, surrounded by a 40 mm diameter aluminium cylinder machined to 0.2 mm thickness. Helium gas is maintained at atmospheric pressure between the nickel and the aluminium to prevent distortion of the nickel by a pressure differential. The helium is supplied through a tube pleading up through the cryostat reservoir. The remainder of the cryostat is conventional. The background caused by the cryostatic, boron, and heavy water containers is separately measured and found to be small. For all other targets "target-out" counting rates are negligible. The liquid nitrogen is condensed under pressure by liquid air, from pure nitrogen gas, and should be sufficiently free of oxygen, though there was a trace of water present.

In order to obtain absolute values of the cross sections, activation of aluminium by Al^{27}(p, 3pn)Na^{24} is used to determine the incident proton intensity. (Na^{24} is practically the only activity present after a few hours of "cooling".) To make possible a direct transformation to the *effective* beam intensity over our non-flat (triangular) targets, a stack of thin aluminium foils arranged to have the same shape of mass distribution across the beam (though of course much thinner along the beam) is used. This is exposed for a known number of counts on the "target-independent" monitor mentioned above, which in turn is normalized to the target-dependent monitor counts for each target. Corrections then have to be made for the numbers of nuclei in the various targets, the telescope geometries and channel energy-widths, and for the absorption of protons in the aluminium absorbers and in the crystals as described above.

4. Results

The results are shown in figs. 4 and 5, plotted as $d\sigma/d\Omega_1 d\Omega_2 dE_1 dE_2$ in units of $\mu b \cdot ster^{-2}\ MeV^{-2}$. Smoothed values of the backgrounds of random coincidences have been subtracted from all experimental points. Only statistical errors are shown. Other errors should be small, except for those arising from the corrections for nuclear absorption in the crystals, which should however, as may be seen from fig. 2, be a smooth function of energy, and large only in the region of high binding energies. Because of some uncertainties in the determination of the zero point of the energy scale, the abso-

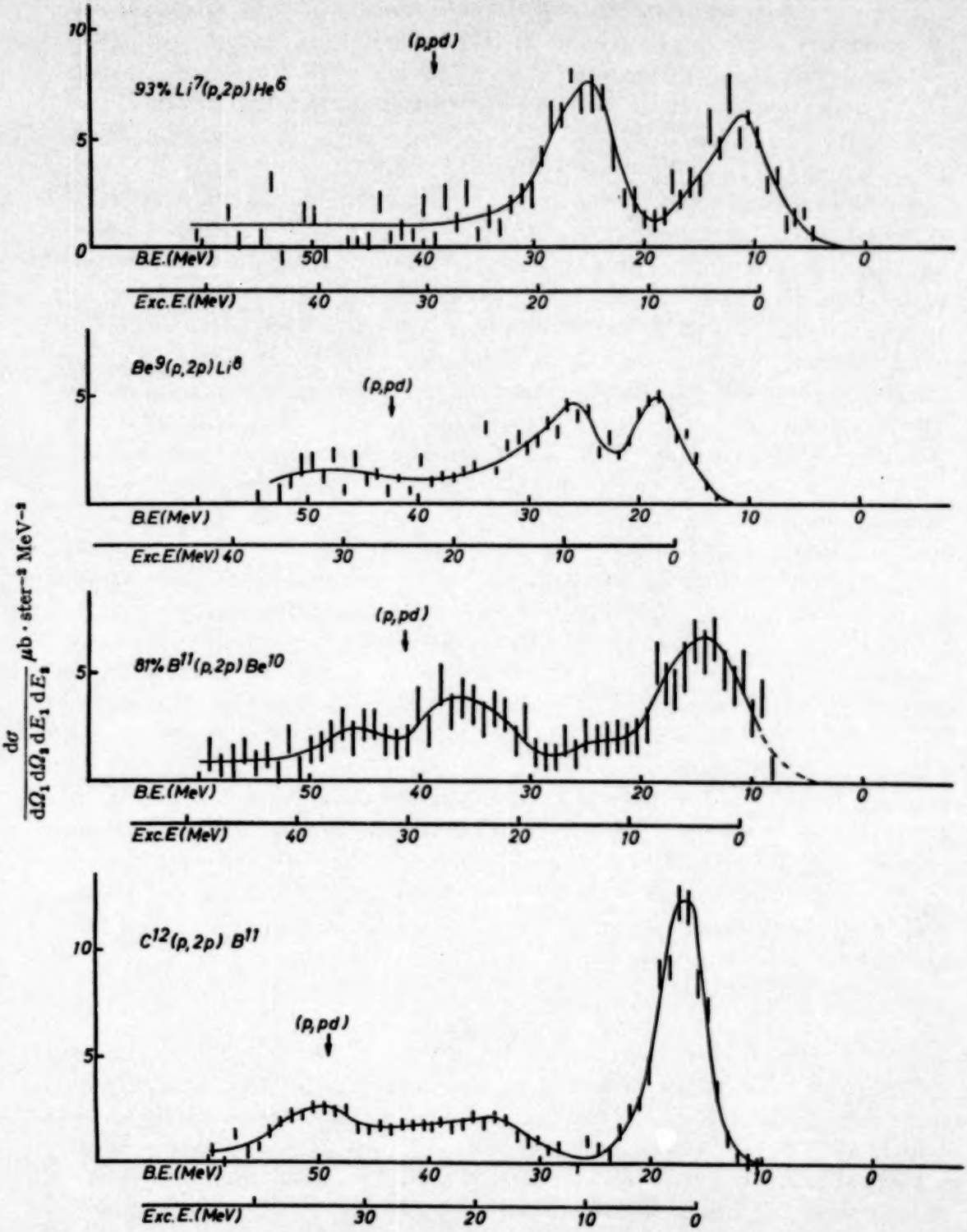

Fig. 4 and Fig. 5. Absolute cross sections for the (p, 2p) reaction at 185 MeV versus binding energy of the removed proton. Separate energy scales for each target also show the corresponding excitation energy of the residual nuclei. Relative errors should not be much larger than the statistical errors shown on each point; absolute errors should be less than 40 %, and the error in comparing two spectra somewhat less.

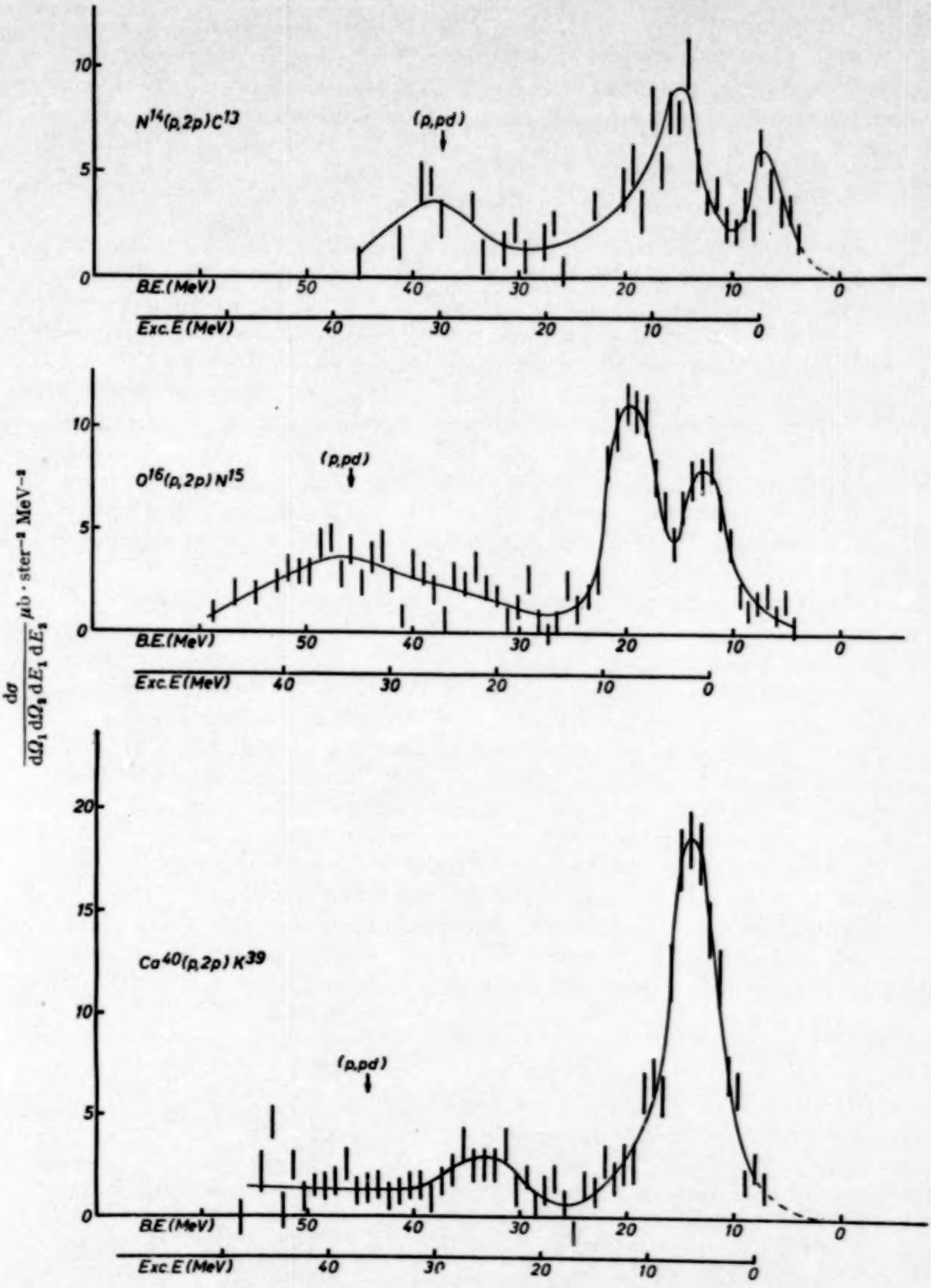
$N^{14}(p,2p)C^{13}$
(p,pd)
B.E.(MeV)
Exc.E(MeV)
$O^{16}(p,2p)N^{15}$
(p,pd)
B.E.(MeV)
Exc.E(MeV)
$Ca^{40}(p,2p)K^{39}$
(p,pd)
B.E.(MeV)
Exc.E(MeV)
$\frac{d\sigma}{d\Omega_1 d\Omega_2 dE_1 dE_2}$ μb · ster^{-2} MeV^{-2}

lute energies may have an error of ± 1.5 MeV. Contributions from (p, np) reactions should be negligible because of the low detection efficiency for neutrons. Arrows on the figures indicate the points in the spectra above which protons and deuterons from the (p, pd) reaction could not have sufficient range to be recorded in coincidence.

5. Discussion

The present measurements select proton pairs in which the protons are scattered 90° apart and symmetric in both angle and energy. This situation is similar to that for free proton scattering and it follows from momentum conservation that, neglecting the scattering in the nucleus and the large solid angles of the detectors, the measured events correspond to a knocking out of a proton which is almost at rest in the nucleus. From this point of view, we appear to favour the interactions in the lower shells which have a small mean kinetic energy, and especially those in the lowest s-shell. However, the strong scattering in the nuclear field and the large solid angles of the detectors will make this effect unimportant in comparison with the influence of the variation of the absorption in the nucleus for the various shells (fig. 1 of the preceding paper).

The lithium spectrum shows two peaks. The protons of the peak of lowest binding energy leave the residual nucleus with a small excitation energy and are evidently knocked out of the p-shell. The second maximum is made up of protons with binding energies of about 26 MeV. This is some MeV more than the binding energy of a proton in the α-particle, and therefore we suppose that the second maximum corresponds to a knocking out of an s-state proton. Its height might be expected to be at least twice that of the first one, because the s-shell contains two and the p-shell one proton, but the absorption in the nucleus evidently depresses the s-peak considerably more than the p-peak. This is in qualitative agreement with fig. 1 of the preceding paper.

Using the reduction coefficient of this figure and formula (2) of the preceding paper one may make the following estimate of the order of magnitude of the cross section for the s-peak in lithium. For our case $\mathbf{k}_3 \approx 0$ and therefore the conventional proton-proton cross section may be used. By integrating over the momentum one finds for this cross section

$$\frac{\mathrm{d}\sigma_{\mathrm{pp}}}{\mathrm{d}\Omega} = \int \frac{\mathrm{d}\sigma_{\mathrm{pp}}}{\mathrm{d}\mathbf{k}_1} \hbar^2 \, \mathrm{d}\mathbf{k}_1 = \frac{\pi}{\hbar} \frac{1}{v_0} \frac{m}{\hbar^2} k_0 \cos\Theta_1 \cdot \sum_m |R|^2.$$

Solving this equation for $\sum_m |R|^2$ and inserting the result in (2) gives

$$\frac{\mathrm{d}\sigma_{21,0}}{\mathrm{d}\mathbf{k}_1 \, \mathrm{d}\mathbf{k}_2} = \sum_m \sum_l \overline{|g_{lm}(\mathbf{k}_3)|^2} \left(\frac{m}{\hbar^2} k_0 \cos\Theta_1 \right)^{-1} \cdot \frac{\mathrm{d}\sigma_{\mathrm{pp}}}{\mathrm{d}\Omega_1} \delta(E_1 + E_2 + E_n + E_b - E_0).$$

The value of the function $\sum_m \sum_l \overline{|g_{lm}(\mathbf{k})|^2}$ for the 1s-state in a parabolic

potential with classical frequency ω at the point $\mathbf{k} = 0$ is $2(\hbar^2/m\hbar\omega\pi)^{3/2}$. With this value, taking $(\hbar^2/2m)k_1^2 = (\hbar^2/2m)k_2^2 = E$ and $\Theta = 45°$, we have

$$\frac{\delta\sigma_{21,0}}{\mathrm{d}\Omega_1\,\mathrm{d}E_1\,\mathrm{d}\Omega_2\,\mathrm{d}E_2} = \frac{\mathrm{d}\sigma_{21,0}}{\mathrm{d}\mathbf{k}_1\,\mathrm{d}\mathbf{k}_2}\left(\frac{m}{\hbar^2}\right)^2 |k_1||k_2|$$

$$= 4\pi^{-3/2}EE_0^{-1/2}(\hbar\omega)^{-3/2}\frac{\mathrm{d}\sigma}{\mathrm{d}\Omega}\delta(E_1+E_2+E_\mathrm{n}+E_\mathrm{b}-E_0).$$

For $\hbar\omega = 41\ A^{-1/3}$MeV [12]), $E = 75$ MeV, $E_0 = 180$ MeV and $\mathrm{d}\sigma/\mathrm{d}\Omega =$ 11 mb/sterad,

$$\frac{\mathrm{d}\sigma_{21,0}}{\mathrm{d}\Omega_1\,\mathrm{d}E_1\,\mathrm{d}\Omega_2\,\mathrm{d}E_2} = 0.44\delta(E_1+E_2+E_\mathrm{n}+E_\mathrm{b}-E_0).$$

Using the reduction factor 0.08 of fig. 1 of the preceding paper the cross section finally becomes

$$0.035\delta(E_1+E_2+E_\mathrm{n}+E_\mathrm{b}-E_0)\mathrm{mb}\cdot\mathrm{ster}^{-2}\,\mathrm{MeV}^{-2}.$$

Because of the level width and our finite energy resolution the δ-function is replaced by a Gaussian in the measurements. The area of this Gaussian in a plot of cross section versus (E_1+E_2) has to be compared with the value $0.035\mathrm{mb}\cdot\mathrm{ster}^{-2}\ \mathrm{MeV}^{-1}$. Experimentally it is $0.04\mathrm{mb}\cdot\mathrm{ster}^{-2}\,\mathrm{MeV}^{-1}$.

As has been remarked in the preceding paper, strong deformations of the initial or final nuclei cause deviations of the spectrum from the expectations on the basis of the simple shell model. This is probably the case for beryllium and to a lesser extend also for boron.

The spectrum of beryllium shows two maxima. The structure of Be^9 may be similar to that of Be^8, except for an additional neutron which we do not see. Therefore there could be some tendency to an α-particle structure. In case of a pure α-particle structure there would be one maximum of the same energy as the s-peak in lithium. If, on the other hand, the simple shell model were valid a spectrum like that of lithium but with a higher first peak would be expected. The measurements indicate an intermediate situation in which the first peak is moved considerably upwards, showing that the knocked out particles are strongly bound, though not so strongly as those in the α-core of lithium. This is the only indication of a possible α-particle structure in any of the light nuclei investigated.

A difficulty for the interpretation of the results for boron is caused by the fact that the target consisted of natural boron (81 % B^{11} and 19 % B^{10}). The proton group originating from the p-shell is clearly recognizable but the peak is deformed. The maximum at 36 MeV seems to originate from the s-shell collisions.

Carbon shows a high peak probably leading mainly to the ground state of B^{11}. Clearly the peak corresponds to p-shell particles being knocked out. In pure j–j coupling only the 3/2− ground state, would be excited. In L–S

coupling 1/2− and 3/2− states would be present in the ratios of their statistical weights, one to two. Mainly the ground state and the 2.14 MeV state would be expected to be involved. At higher binding energies there exists a clear residue of the s-peak, whose height is somewhat more depressed than one would calculate from the reduction factor, probably because of its large width.

Here and in all other spectra it is interesting to see how small and smooth the background from the multiple collisions indeed turns out to be. The small peak near 50 MeV is probably due to secondary deuteron pick-up.

The spectrum of N^{14} is like what one would expect for j–j coupling, which should be rather good for nuclei nearing a closed shell. Over the peak caused by $p_{3/2}$ particles the $p_{1/2}$ peak appears.

In oxygen the $p_{1/2}$ peak has increased in height to considerably more than half that of the $p_{3/2}$ maximum. This is probably caused by the difference in absorption originating from the fact that the $p_{1/2}$ wave function has a longer tail at the nuclear surface, because of its smaller binding energy. This explains also the relatively large size of the $p_{1/2}$ peak in the nitrogen spectrum. The separation of the two peaks in the oxygen spectrum agrees well with the interpretation of the 6.3 MeV state in N^{15} as a state with a hole in the $p_{3/2}$ shell.

In these last two nuclei the s-shell is no longer clearly visible.

The spectrum of calcium shows one peak about as sharp as our energy resolution allows, leading to about 6 MeV excitation in K^{39}. This result is not yet fully understood. Two maxima of the $d_{3/2}$ and $d_{5/2}$ particles, perhaps smeared out by multiple collisions, were expected. Also the height of the observed maximum is surprisingly large (see fig. 1 of preceding paper). A tentative explanation might be given by the assumption that the ground state of Ca^{40} contains a strong admixture of a state in which a nucleon pair is excited into the $f_{7/2}$ state of the next shell. This is in agreement with the existence of a 0^+ excited state in Ca^{40} as low as 3.3 MeV excitation energy. The mean radius of an f-state for harmonic oscillator wave functions is 13 % larger than that of a d-state. Because in a nucleus like Ca clean knock out processes strongly favour the surface the peak in the spectrum might be caused by f-state protons and the contribution of the d-state could be hidden under it. If a proton of an f-state pair is knocked out, the nucleus is left with an excited particle in the $f_{7/2}$ state and has $j = 7/2^-$.

Fig. 6 shows the binding energies of the different proton types we believe we have observed in the light nuclei, as a function of atomic number. The energy of 19 MeV required to eject a proton from He^4 leaving H^3 in its ground state falls well on the extrapolated s-curve.

Of course further measurements are required. Energy and angular correlations, especially for the lightest elements, might give information on the nuclear wavefunctions and, by comparison with a detailed calculation, on

the distortion of the incoming and outgoing waves. The building up of the s- and d-shells in the elements between oxygen and calcium should be studied.

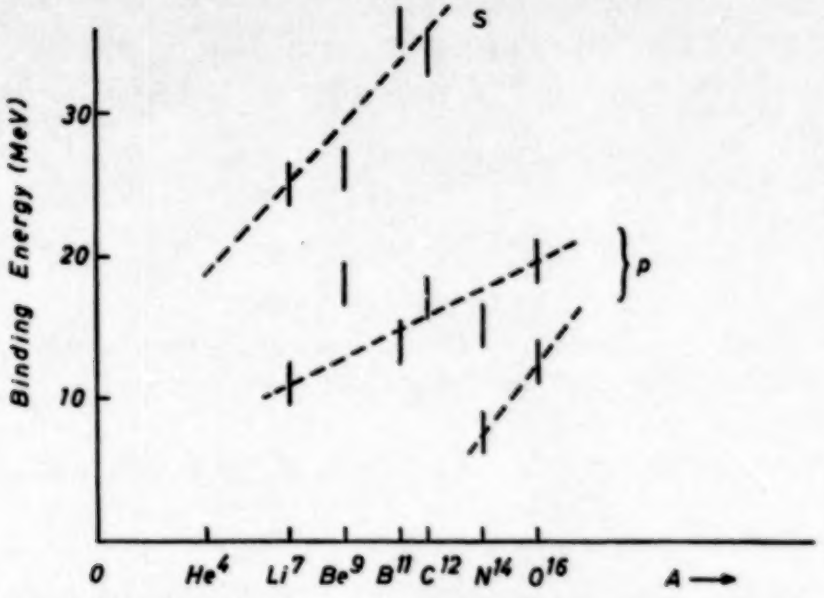

Fig. 6. The binding energies of the protons in various shells versus atomic number, as taken from the positions of the peaks in figs. 4 and 5.

By using higher bombarding energies one should be able to follow the inner shells further and to extend and improve fig. 6.

Prof. The Svedberg's support was as always very welcome. Per Isacsson was responsible for most of the electronic design, construction, and maintenance, and was at all times cheerfully helpful. We thank Å. Svanheden for making the aluminium foil activation measurements and together with the cyclotron crew for providing the proton beam. Two of us (P. H. and T. M.) express their gratefulness to Prof. Svedberg and all the members of the Institute for their great kindness and hospitality during their stay. The work was supported by the Swedish Atomic Energy Commission.

References

1) Th. A. J. Maris, P. Hillman and H. Tyrén, Nuclear Physics **7** (1958) 1
2) B. L. Cohen, Phys. Rev. **108** (1957) 768
3) W. Selove, Phys. Rev. **101** (1956) 231
4) H. Tyrén and Th. A. J. Maris, Nuclear Physics **4** (1957) 637
5) J. B. Cladis, W. N. Hess and B. J. Moyer, Phys. Rev. **87** (1952) 425
6) J. M. Wilcox and B. J. Moyer, Phys. Rev. **99** (1955) 875
7) O. Chamberlain and E. Segrè, Phys. Rev. **87** (1952) 81;
J. G. McEwen, W. M. Gibson and P. J. Duke, Phil. Mag. **2** (1957) 231
8) H. Tyrén, Th. A. J. Maris and P. Hillman, Nuovo Cimento **6** (1957) 1507
9) G. Rudstam, Doctoral Dissertation, University of Uppsala (1956)
10) N. Metropolis, R. Bivins, M. Storm, A. Turkevitch, J. M. Miller and G. Friedlander, Phys. Rev. to be published
11) M. Rich and R. Madey, UCRL **2301** (1954)
12) S. G. Nilsson, Mat. Fys. Medd. Dan. Vid. Selsk. **29** (1955) 16

2.L

Nuclear Physics 7 (1958) 24—26; © *North-Holland Publishing Co., Amsterdam*

Not to be reproduced by photoprint or microfilm without written permission from the publisher

INELASTIC SCATTERING OF 185 MeV PROTONS ON ELEMENTS BETWEEN Ca AND Zn

H. TYRÉN and TH. A. J. MARIS

The Gustaf Werner Institute for Nuclear Chemistry, University of Uppsala

Received 9 April 1958

Concluding the experiments [1]) on the inelastic scattering of 185 MeV protons on light nuclei we report the spectra of some elements between calcium and zinc. For the description of the experimental set-up and the errors see ref. [1]).

The spectra are shown in figs. 1 and 2. Where the natural isotopic composition of the targets contains more than one isotope with an abundance larger than 10 % this is indicated in the figures.

At 10 degrees around 16 MeV excitation energy the dipole peak is visible. Similar excitations have been observed in nearly all lighter nuclei. These peaks rise with decreasing scattering angles, but the tails of the high elastic peaks in these cases made measurements at angles smaller than 10 degrees uncertain.

TABLE 1

Element	Energy (MeV)
V	3.5±0.3
	6.4±0.3
Cr	≈ 5.5
Fe	4.4±0.3
	6.7±0.3
Co	3.8±0.3
Ni	3.9±0.3
	6.5±0.3
Cu	3.0±0.3
Zn	2.5±0.4

The spectra at larger angles show some excitations at lower energies, which are tabulated in table 1. Just as for all previously measured low excitations, the angular distributions are forward dipped.

References

1) H. Tyrén and Th. A. J. Maris, Nuclear Physics **3** (1957) 52;
H. Tyrén, G. Tibell and Th. A. J. Maris, Nuclear Physics **4** (1957) 277;
H. Tyrén and Th. A. J. Maris, Nuclear Physics **4** (1957) 637;
H. Tyrén and Th. A. J. Maris, Nuclear Physics **6** (1958) 82;
H. Tyrén and Th. A. J. Maris, Nuclear Physics **6** (1958) 446;
H. Tyrén, G. Tibell and Th. A. J. Maris, Nuclear Physics (to be published);
H. Tyrén and Th. A. J. Maris, Arkiv för Fysik (in press)

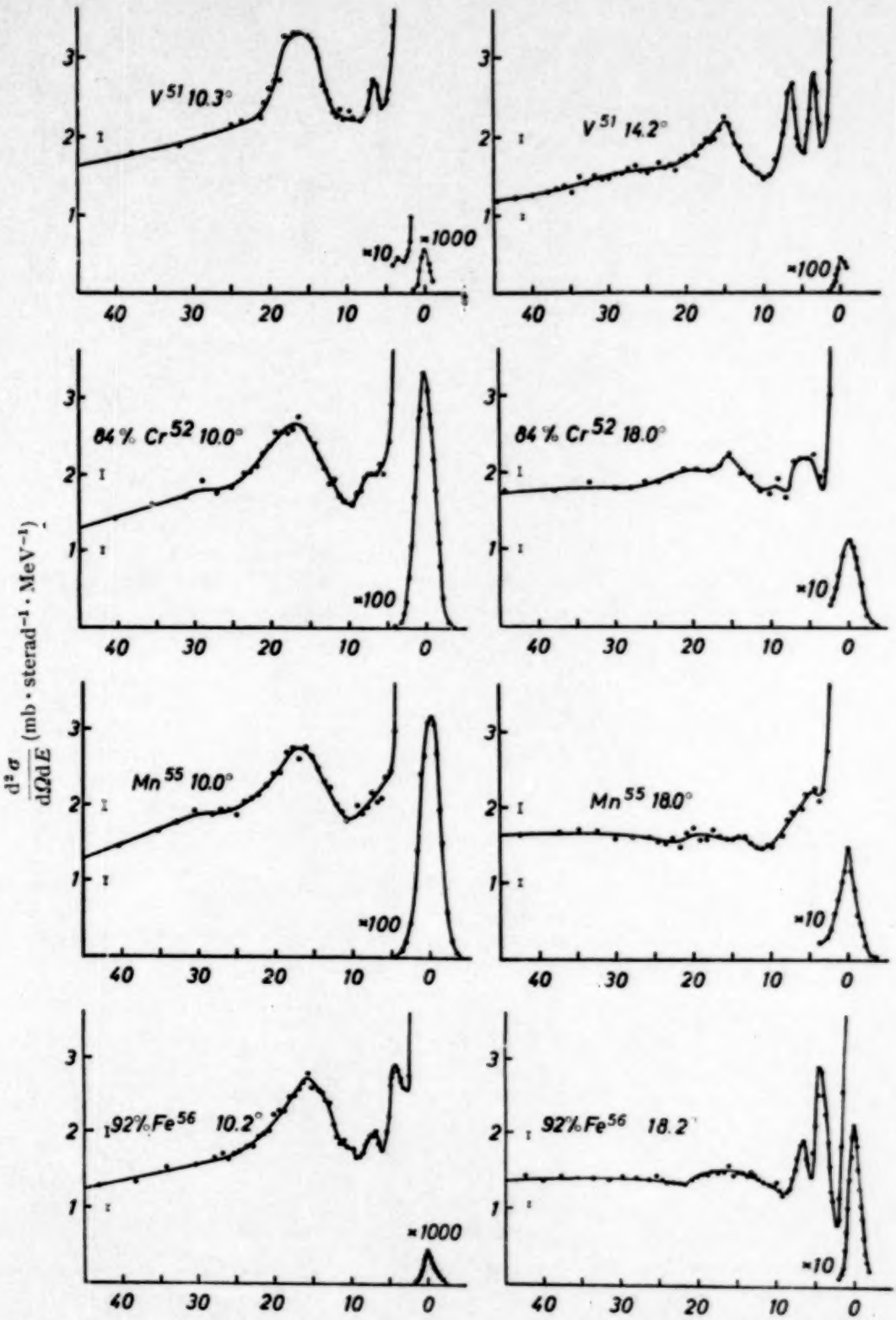

Fig. 1. Energy spectra for inelastic scattering of 185 MeV protons on natural V, Cr, Mn and Fe.

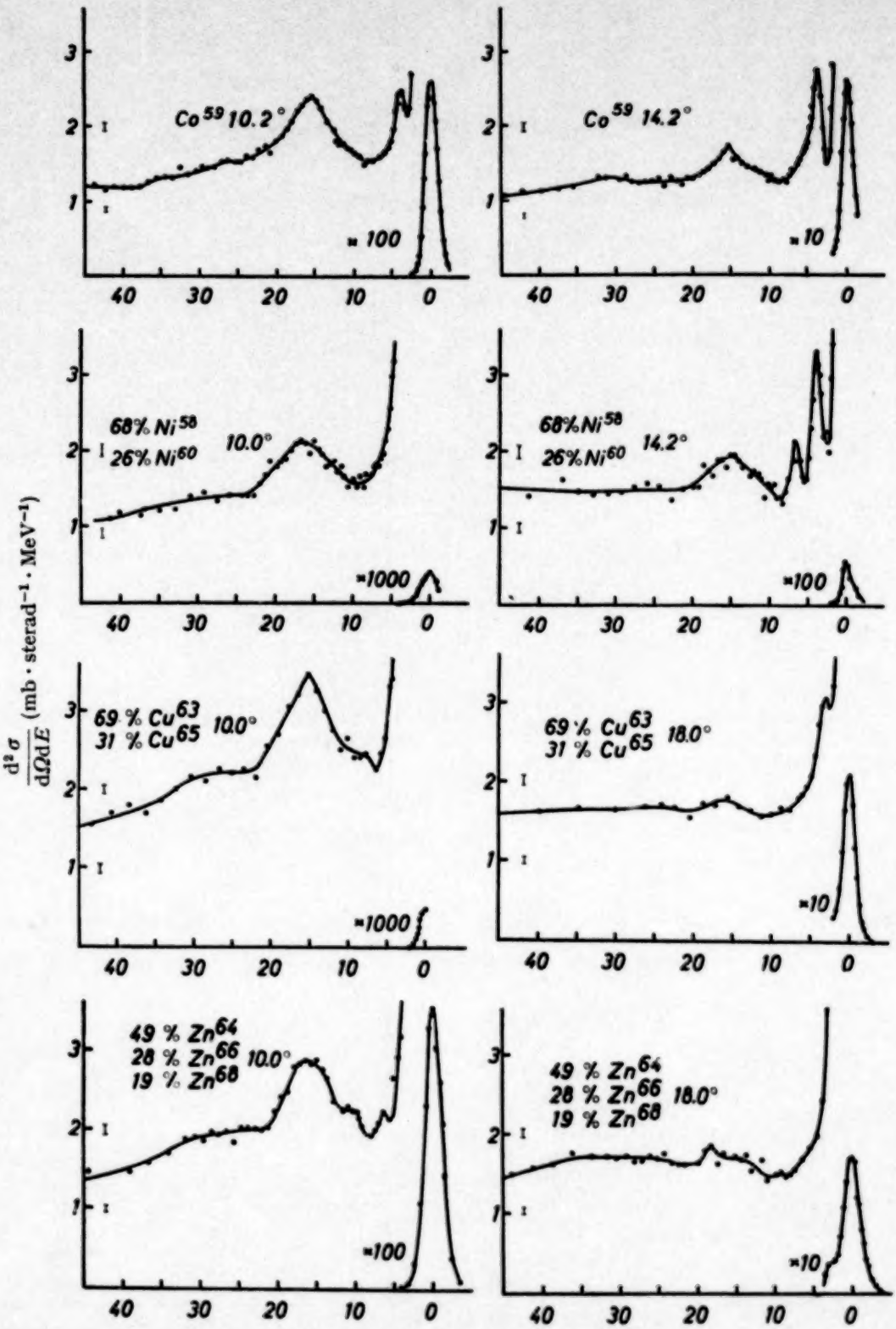

Fig. 2. Energy spectra for inelastic scattering of 185 MeV protons on natural Co, Ni, Cu and Zn.

1.D.1:
1.E.2

Nuclear Physics **7** (1958) 27—110; © *North-Holland Publishing Co., Amsterdam*
Not to be reproduced by photoprint or microfilm without written permission from the publisher

NUCLEAR ENERGIES AND THE SHELL MODEL †

NISSAN ZELDES ††

Department of Physics, The Hebrew University of Jerusalem, Israel

and

Department of Mathematical Physics, University of Birmingham, England

Received 12 December 1957

Abstract: Various nuclear energetics data are interpreted according to the shell model in its simplest form, characterized by the "single particle" approximation (states of seniority 0 for the even group and seniority 1 for the odd group). The information gained thereby is applied in discussing the problem of the competition between nuclear shells.

CONTENTS

INTRODUCTION 3

1. Subject Matter and Plan of the Work 3

2. The approximations Adopted 4

3. Energy Formulas 5

3.1 IDENTICAL NUCLEONS IN A GIVEN SHELL 5

3.2 IDENTICAL NUCLEONS IN TWO DIFFERENT SHELLS 6

3.3 NUCLEONS OF DIFFERENT KINDS 7

4. The nuclear binding energy 7

4.1 THE BINDING ENERGY OF A GIVEN NUCLEAR STATE 7

4.2 A CRITICAL REMARK 9

PART I. THE SYSTEMATICS OF NUCLEAR ENERGIES . 10

CHAPTER I. NUCLEON SEPARATION ENERGIES 10

A. Preliminary Discussion 10

5. Linear Relationships 10

6. Zig-Zag Relationships 11

6.1 NEUTRON SEPARATION ENERGIES OF THE ISOTOPES OF AN EVEN-Z ELEMENT 11

6.2 NEUTRON SEPARATION ENERGIES OF THE ISOTOPES OF AN ODD-Z ELEMENT 12

6.3 NEUTRON SEPARATION ENERGIES OF ISOTONES 12

6.4 PROTON SEPARATION ENERGIES 14

† Reprints of this article are available at the publishers.

†† Now on leave of absence at Birmingham University.

7. The Beginning of a New Shell 14

B. Analysis of the Experimental Data 15

8. The Signs and Qualitative Magnitude Relationships of the Parameters 15

8.1 SIGNS 15

8.2 MAGNITUDE RELATIONSHIPS 16

9. The Magic Numbers 17

10. Comparison with the Electrons in Atoms 19

11. Subshell Effects 25

12. Quantitative Treatment of Nucleon Separation Energy Systematics 29

13. The Interaction of the Odd Neutron and Odd Proton in Odd Nuclei 32

CHAPTER II. BETA AND ALPHA DECAY ENERGIES 34

A. Beta Decay Energies 34

14. Linear Relationships 34

15. Zig-Zag Relationships 39

15.1 Z OR N CONSTANT 39

15.2 MASS NUMBER A CONSTANT 42

15.3 NEUTRON EXCESS I CONSTANT 42

16. The Beginning of a New Shell 42

17. Subshell Effects 43

18. Quantitative Treatment of Beta Decay Energy Systematics 44

B. Alpha Decay Energies 46

19. Linear Systematics 46

20. Shell Effects 48

CHAPTER III. THE NUCLEAR MASS SURFACE 49

21. The Nuclear Mass Surface and its Splitting 49

22. Levy's Empirical Mass Equation 51

23. Section of the Mass Surface for Constant Z or N 53

23.1 PARABOLIC SECTION 53

23.2 SHELL EFFECTS 54

24. Section of the Mass Surface for Constant *A* 56
24.1 PARABOLIC SECTION 56
24.2 SHELL EFFECTS 57

25. The Line of Beta Stability 57
25.1 STRAIGHT LINE 57
25.2 SHELL EFFECTS 57

CHAPTER IV. EXCITED STATES OF NUCLEI. 61

26. Low-Lying Excited States of Odd-Mass Nuclei 61

27. Low-Lying Excited States of Odd Nuclei 62

28. Low-Lying Excited States of Even Nuclei. 64

PART II. THE COMPETITION BETWEEN NUCLEAR SHELLS 64

CHAPTER V. PRELIMINARY DISCUSSION 64

29. The Factors Governing the Order of Shell Filling . . . 65

CHAPTER VI. NUCLEAR GROUND-STATE CONFIGURATIONS IN ODD-MASS NUCLEI 67

30. The Competition Between the Neutron Shells $2p_{\frac{1}{2}}$ and $1g_{9/2}$ 68

31. The Competition Between the Proton Shells $2p_{\frac{1}{2}}$ and $1g_{9/2}$ 72

32. The Competition Between the Neutron Shells $3s_{\frac{1}{2}}$, $2d_{3/2}$ and $1h_{11/2}$ 73

33. The Competition Between the Proton Shells $3s_{\frac{1}{2}}$, $2d_{3/2}$ and $1h_{11/2}$, and the Competition Between the Neutron Shells $3p_{3/2}$, $3p_{\frac{1}{2}}$, $2f_{5/2}$ and $1i_{13/2}$ 78

INTRODUCTION

1. Subject Matter and Plan of the Work

The occurrence of linear relationships in the study of various nuclear systematics suggests their interpretation within the framework of the shell model. According to this model, the nuclear binding energy is a quadratic function of the numbers of nucleons in the various shells, and its differences, which determine the various nuclear disintegration energies, should, therefore, vary linearly with the nucleon numbers. It is the purpose of the present study to examine these problems rather closely.

After summarizing the pertinent energy formulas in the introduction, the work is divided into two parts: the first part deals with the various nuclear systematics and with the deductions obtained therefrom which pertain to the nuclear mass surface. The second part deals with the problem of nuclear shell filling, and is based on the knowledge gained from the study of the systematics.

2. The Approximations Adopted

We shall confine ourselves to the spin-orbit coupling model of Mayer and Jensen [1,2,3]). In the zeroth-order approximation, the nucleons are assumed to move independently in the various shells of the nuclear central field. The remainder of the interaction between the nucleons is treated as a perturbation.

The empirical facts concerning nuclear moments and isomerism on the one hand, and the odd-even alternations of nuclear binding energies on the other, lead to the assumption that in all but the lightest nuclei, the maximum possible number of identical nucleons in a given shell are paired off, each pair being in a $J = 0$ state. The mathematical formulation of this coupling is given by Racah's seniority concept [4]). We shall assume, therefore, that the seniority is a good quantum number of the nuclear ground states, an even nuclear shell always being in a $J = 0$ state with seniority zero, and an odd nuclear shell being in a $J = j$ state with seniority one †. This approximation is very useful in bringing into prominence the essential features of the interaction between the nucleons in the nucleus ††.

However, due to insufficient knowledge, we shall not make any special assumptions concerning internucleonic forces, except that they are derived from a two-body potential energy. The coupling of the nucleons according to the seniority then unequivocally determines the resulting very simple structure of the energy formulas. An obvious disadvantage of this approach is the absence of knowledge on the relationship between the parameters appearing in the energy formulas and those derived from other nuclear phenomena, losing thereby an important check on the plausibility of the results obtained from comparing the energy formulas with the experimental data.

The comparison between theory and experiment becomes possible when assuming that the parameters appearing in the energy formulas are more or less the same in neighbouring nuclei. Results obtained recently by workers of Rehovoth [5–12]), and also here [13]), seem to justify this assumption †††. On adopting it, the number of empirical data to be correlated by the

† A somewhat more detailed explanation of this 'single-particle' approximation, with references, is given in the introductory part of ref. [13]).

†† See also the discussion following formula (26) in § 11.

††† See, however, the remarks made in § 4.2.

formulas exceeds by far the number of parameters in the latter, and this allows to check the agreement between theory and experiment, by the usual methods of atomic spectroscopy.

3. Energy Formulas

Assume a nucleus having two incomplete neutron shells, j_1 and j_2, with n_1 and n_2 neutrons, respectively, and one incomplete proton shell, j_3, with p_3 protons; further, let there also be N_0 neutrons and Z_0 protons in closed shells. The nuclear binding energy is then given by

$$\begin{aligned} B(N_0 Z_0;\ j_1^{n_1} j_2^{n_2} j_3^{p_3}) = {} & B(N_0 Z_0)+n_1 c_1+n_2 c_2+p_3 C_3 \\ & +W(j_1^{n_1})+W(j_2^{n_2})+W(j_3^{p_3}) \\ & +I(j_1^{n_1} j_2^{n_2})+I(j_1^{n_1} j_3^{p_3})+I(j_2^{n_2} j_3^{p_3}). \end{aligned} \tag{1}$$

Here, B denotes binding energy, c_1 and c_2 the single-particle central-field energies of the j_1 and j_2 neutrons, respectively, C_3 the same for the j_3 protons; each W denotes the internal binding energy of the shell within its brackets, and each I denotes the interaction energy between the two shells within its brackets. All these binding energies are taken positive. One has to find formulas for the W's and the I's.

3.1. IDENTICAL NUCLEONS IN A GIVEN SHELL

The derivation of the pertinent formula is straightforward by using the results of Schwartz and de Shalit [14]). From their formula (A8), one obtains for an even group in a ${}_0 0$ state (where the 0 denotes the value of J and the subscript 0 denotes the seniority),

$$W(j^n{}_0 0) = \frac{n(2j+1-n)}{2(2j-1)} W(j^2 0) + \frac{n(n-2)}{(2j-1)(2j+1)} \sum_{J'} (2J'+1) W(j^2 J'), \tag{2}$$

where J' ranges over the allowed even J values of the j^2 configuration of identical nucleons. We shall rewrite (2) in the form

$$W(j^n{}_0 0) = \tfrac{1}{2} n\pi + \tfrac{1}{2} n(n-1) d \tag{3}$$

where

$$\pi = \frac{1}{2j-1}\left[2j W(j^2 0) - \frac{2}{2j+1} \sum_{J'} (2J'+1) W(j^2 J')\right], \tag{4a}$$

$$d = \frac{1}{2j-1}\left[-W(j^2 0) + \frac{2}{2j+1} \sum_{J'} (2J'+1) W(j^2 J')\right]. \tag{4b}$$

For an odd group in a ${}_1 j$ state, one obtains similarly to (2)

$$W(j^n{}_1 j) = \frac{(n-1)(2j-n)}{2(2j-3)} W(j^3{}_1 j) + \frac{(n-1)(n-3)}{(2j-3)(2j+1)} \sum_{J'} (2J'+1) W(j^2 J'). \tag{5}$$

To proceed further, one expands by fractional parentage

$$\psi(j^3\,_1j) = \sum_{J'} \psi(j^2J',\ jj)(j^2J',\ jj|\}j^3\,_1j), \tag{6}$$

and writes

$$W(j^3\,_1j) = 3\sum_{J'}(j^2J',\ jj|\}j^3\,_1j)^2 \cdot W(j^2J')$$
$$= \frac{2j-3}{2j-1}W(j^20) + \frac{4}{(2j-1)(2j+1)}\sum_{J'}(2J'+1)W(j^2J'). \tag{7}$$

The last step was made by using the explicit expression of the pertinent fractional parentage coefficients, given by formula (17) of Schwartz and de Shalit [14]). Inserting (7) in (5) one finally obtains, in analogy to (3),

$$W(j^n\,_1j) = \tfrac{1}{2}(n-1)\pi + \tfrac{1}{2}n(n-1)d. \tag{8}$$

(3) and (8) may be summarized as

$$W(j^n) = [\tfrac{1}{2}n]\pi + \tfrac{1}{2}n(n-1)d. \tag{9}$$

The energy is the same as if each pair of coupled nucleons has a 'pairing energy' π, and, furthermore, any two nucleons, irrespective of their relative orientation, interact with strength d. A formula equivalent to (9) was derived by Racan [15]) employing methods of group theory.

3.2. IDENTICAL NUCLEONS IN TWO DIFFERENT SHELLS

In this case, it is convenient to start from the interaction between two nucleons in the different shells. Their interaction energy depends on the relative orientation of their angular momenta, and may be written [16]) as

$$I(j_1j_2J) = \sum_k A^k(n_1l_1n_2l_2)(j_1j_2J|(\mathbf{t}_1^{(k)} \cdot \mathbf{t}_2^{(k)})|j_1j_2J)$$
$$= A^0(\mathbf{t}_1^{(0)} \cdot \mathbf{t}_2^{(0)}) + \sum_{k\neq 0} A^k(\mathbf{t}_1^{(k)} \cdot \mathbf{t}_2^{(k)}), \tag{10}$$

where the A^k are parameters depending on the radial parts of the nuclear states and the interaction, and $\mathbf{t}^{(k)}$ are tensor operators, irreducible with respect to **J**. The generalization of (10) to multi-nucleon configurations is

$$I(j_1^{n_1}j_2^{n_2}J) = n_1 \cdot n_2 \cdot A^0(\mathbf{t}_1^{(0)} \cdot \mathbf{t}_2^{(0)}) + \sum_{k\neq 0} A^{(k)}(\mathbf{T}_1^{(k)} \cdot \mathbf{T}_2^{(k)}), \tag{11}$$

where $\mathbf{T}_1^{(k)}$ is the sum $\sum_1 \mathbf{t}_1^{(k)}$ of the $\mathbf{t}^{(k)}$'s of the nucleons of shell j_1; $\mathbf{T}_2^{(k)}$ is the same for shell j_2.

In our approximation, at least one of the shells j_1 and j_2 is even, in a spherically symmetric state with $J = 0$. Therefore, the interaction of one shell with the nucleons of the other one does not depend on the former's orientation in relation to these nucleons, and the contribution of the tensors with $k \neq 0$, which depends on this orientation, vanishes. Then,

$$I(j_1^{n_1}j_2^{n_2}) = n_1 \cdot n_2 \cdot A^0(\mathbf{t}_1^{(0)} \cdot \mathbf{t}_2^{(0)}) = n_1 \cdot n_2 \cdot I_{12}^0, \tag{12}$$

where I_{12}^0 denotes the contribution of the scalars $\mathbf{t}^{(0)}$ to the interaction

between the two nucleons. It will be simply referred to as the scalar interaction between the two nucleons.

3.3. NUCLEONS OF DIFFERENT KINDS

In analogy to the reasoning leading to (11), one obtains, in an obvious notation,

$$I(j_1^{n_1} j_3^{p_3} J) = n_1 \cdot p_3 \cdot A^0(\mathbf{t}_1^{(0)} \cdot \mathbf{t}_3^{(0)}) + \sum_{k \neq 0} A^k(\mathbf{T}_1^{(k)} \cdot \mathbf{T}_3^{(k)}). \qquad (13)$$

For even nuclei or odd-mass nuclei, again at least one of the shells has $J = 0$; therefore, as in (12),

$$I(j_1^{n_1} j_3^{p_3}) = n_1 \cdot p_3 \cdot I^0_{13}. \quad \text{(even or odd-mass nuclei).} \qquad (14)$$

However, for odd nuclei one has also to consider the possibility that both shells are odd. In this case, it is convenient to decompose (13) further:

$$I(j_1^{n_1} j_3^{p_3} J) = n_1 \cdot p_3 \cdot A^0(\mathbf{t}_1^{(0)} \cdot \mathbf{t}_3^{(0)}) + \sum_{k\,\text{odd}} A^k(\mathbf{T}_1^{(k)} \cdot \mathbf{T}_3^{(k)}) + \sum_{k\,\text{even}} A^k(\mathbf{T}^{(k)} \cdot \mathbf{T}^{(k)}). \qquad (15)$$

Using formula (II38) [17]) and the jj-analogue of (III69a) [4]), the last two sums may be written in the form

$$I'_{13J} = I''_{13J} + \frac{2j_1+1-2n_1}{2j_1-1} \cdot \frac{2j_3+1-2p_3}{2j_3-1} \cdot I'''_{13J}, \qquad (16)$$

where I''_{13J} is the contribution of the odd tensors to the interaction between the two nucleons when they are coupled in a $(j_1 j_3 J)$-state, and I'''_{13J} is the contribution of the even tensors. (14) and (16) may be summarized as

$$I(j_1^{n_1} j_3^{p_3} J) = n_1 \cdot p_3 \cdot I^0_{13} + \tfrac{1}{4}[1-(-1)^{n_1}][1-(-1)^{p_3}] \cdot I'_{13J}. \qquad (17)$$

Whereas I^0 depends only on the shells, I' depends also on the value of the total angular momentum J of the nucleus, and on the numbers of nucleons in the odd shells.

4. The Nuclear Binding Energy

4.1. THE BINDING ENERGY OF A GIVEN NUCLEAR STATE

To approximate the conditions existing in heavy nuclei, in which several shells are being filled simultaneously, we shall use the above results in order to state the binding energy of a nucleus containing two incomplete neutron shells, $j_1^{n_1}$ and $j_2^{n_2}$, and two incomplete proton shells, $j_3^{p_3}$ and $j_4^{p_4}$, in addition to N_0 neutrons and Z_0 protons in closed shells. In this paper, the odd neutron shell, when it exists, will be called j_1, and the odd proton shell j_3. Neutron parameters are given in lower case, proton parameters in capitals. Then

$$
\begin{aligned}
B(N_0 Z_0;\ j_1^{n_1} j_2^{n_2} j_3^{p_3} j_4^{p_4}) = {} & B(N_0 Z_0)+n_1 c_1+n_2 c_2+p_3 C_3+p_4 C_4 \\
& +[\tfrac{1}{2}n_1]\pi_1+\tfrac{1}{2}n_2\pi_2+[\tfrac{1}{2}p_3]\Pi_3+\tfrac{1}{2}p_4\Pi_4 \\
& +\tfrac{1}{2}n_1(n_1-1)d_1+\tfrac{1}{2}n_2(n_2-1)d_2+\tfrac{1}{2}p_3(p_3-1)D_3+\tfrac{1}{2}p_4(p_4-1)D_4 \\
& +n_1 n_2 I^0_{12}+p_3 p_4 I^0_{34}+n_1 p_3 I^0_{13}+n_1 p_4 I^0_{14}+n_2 p_3 I^0_{23}+n_2 p_4 I^0_{24} \\
& +\tfrac{1}{4}[1-(-1)^{n_1}][1-(-1)^{p_3}]I'_{13}.
\end{aligned} \tag{18}
$$

The structure of (18) is seen better by rewriting it in the form:

$$
\begin{aligned}
B(N_0 Z_0;\ j_1^{n_1} j_2^{n_2} j_3^{p_3} j_4^{p_4}) = {} & B(N_0 Z_0)+n_1 c_1+n_2 c_2+p_3 C_3+p_4 C_4 \\
& +\tfrac{1}{2}n_1\pi_1+\tfrac{1}{2}n_2\pi_2+\tfrac{1}{2}p_3\Pi_3+\tfrac{1}{2}p_4\Pi_4 \\
& +\tfrac{1}{2}n_1(n_1-1)d_1+\tfrac{1}{2}n_2(n_2-1)d_2+\tfrac{1}{2}p_3(p_3-1)D_3+\tfrac{1}{2}p_4(p_4-1)D_4 \\
& +n_1 n_2 I^0_{12}+p_3 p_4 I^0_{34}+n_1 p_3 I^0_{13}+n_1 p_4 I^0_{14}+n_2 p_3 I^0_{23}+n_2 p_4 I^0_{24}-\delta,
\end{aligned} \tag{19}
$$

where the parity term δ is given by

$$
\begin{aligned}
\delta = {} & \tfrac{1}{4}[1-(-1)^{n_1}]\pi_1 \\
& +\tfrac{1}{4}[1-(-1)^{p_3}]\Pi_3-\tfrac{1}{4}[1-(-1)^{n_1}][1-(-1)^{p_3}]I'_{13},
\end{aligned} \tag{20a}
$$

or, more specifically,

$$
\delta = \begin{cases} 0 & \text{even nuclei} \\ \tfrac{1}{2}\pi_1 & \text{odd-}N\text{ nuclei} \\ \tfrac{1}{2}\Pi_3 & \text{odd-}Z\text{ nuclei} \\ \tfrac{1}{2}\pi_1+\tfrac{1}{2}\Pi_3-I'_{13} & \text{odd nuclei.} \end{cases} \tag{20b}
$$

We assume the parameters to be constant for given nuclear shells (see § 2), except for the δ term of odd nuclei, which still depends through the I'_{13} on the number of nucleons in the odd shells and on the coupling of their angular momenta.

It follows that for nuclei of the same parity type, in which the same shells are being filled, the energy is an essentially quadratic function of the numbers of nucleons in the various shells. There remains the J-dependence of the δ term for odd nuclei. However, for odd nuclei which are not too light, the δ values for different J's differ by a few tens keV at the most, as is seen from their low excitation energies, which are given by the differences of the δ's in the different states. This cannot, therefore, invalidate the quadratic dependence given by the orientation-independent interactions, d, D and the I^0's, which are of a different order of magnitude. As a matter of fact, nuclear binding energies, separation energies, and radioactive decay energies, are usually known with far less precision than the differences of the δ's for different J's, and therefore the neglect of the J-dependence of δ is unimportant for the study of these energies.

The quadratic dependence is essentially the same for the four types of nuclei, and the nuclear energy surface is merely split into four similar surfaces, vertically displaced with respect to one another, by amounts given

by the differences of the δ terms. Here, too, exists the n_1- and p_3-dependence of the δ term of odd nuclei, which might have changed the shape of the odd surface from that of the other three. However, this extra n_1- and p_3-dependence is given by a product of two fractions (eq. (16)), and might therefore be supposed to be negiglible as compared to the n_1- and p_3-dependence of the other terms, which is the same for all four types. In § 13 we shall investigate more closely, and further justify, the neglect of the I'_{13} dependence on n_1 and p_3. Here, it might be added, that for nuclei beyond the $1f_{7/2}$ shells, the exact form of the δ term for odd nuclei cannot even be applied, due to incomplete knowledge of the distribution of nucleons in the various incomplete shells of odd nuclei. In the following, δ will be treated as a constant, independent on both J and the numbers of nucleons.

From the quadratic dependence, it is clear that the binding energy differences in a sequence of nuclei of the same parity type, differing from each other by the same numbers of nucleons in the same shells, will vary linearly within the sequence. But when nuclei of different parity types alternate in the sequence, zig-zag lines will result. The various known nuclear systematics will be considered from this point of view in the following chapters.

4.2. A CRITICAL REMARK †

In this study we adopt the assumption that the nuclear parameters are approximately the same in neighbouring nuclei. This results in the quadratic dependence (19) of the binding energy on the nucleon numbers.

On the other hand, the nuclear radius varies slowly from lighter to heavier nuclei. The increase of the nuclear radius within a given shell region amounts usually to a few per cent of its value, which might result in a change of a similar order of magnitude of the nuclear field and the nuclear parameters. A change of such a relative order of magnitude is negligible as far as the two-body parameters π, Π, d, D and the I^0's are concerned. On the other hand, such a change of the single-nucleon binding energies c and C might be of the order of magnitude of the two-body parameters, and the change of the total binding energy of the closed shells, $B(N_0 Z_0)$, might be of the order of magnitude of c and C themselves.

Allowing for a linear variation of c and C and a quadratic variation of $B(N_0 Z_0)$ within a given shell region does not invalidate the quadratic dependence of the binding energy on the nucleon numbers. In fact, the binding energy might still be written in the form (19). However, the coefficients will then have a different meaning from those of (19) as defined in § 3.

While of no consequence for the correlation of experimental data and for

† I am indebted to Professor Peierls for directing my attention to this point.

most of the conclusions of the present paper, this possibility should still be borne in mind when attempting to derive the numerical values of the parameters, obtained from comparing formula (19) or its consequences with experimental nuclear energies, by theoretical considerations.

PART I. THE SYSTEMATICS OF NUCLEAR ENERGIES

CHAPTER I. NUCLEON SEPARATION ENERGIES

A. Preliminary Discussion

It is appropriate to begin with the binding energies of the last neutron and proton, or the neutron and proton separation energies, as they are called. In this way, the magnitudes of the various parameters are seen directly in the separation energy graphs, whose slopes and distances between the lines are given by these parameters. With the other nuclear energy differences, such as radioactive decay energies or excitation energies, one cannot achieve this, since their slopes are given by differences of parameters.

A consideration of the nuclear binding energy itself might give us the parameters as well. However, since it is a quadratic function of the numbers of nucleons, the parameters would appear only following some arithmetic manipulations, whereas the magnitudes of the slopes and distances between straight lines can be found visually from the graphs.

5. Linear Relationships

The neutron separation energy, S_n, of the sample nucleus of eq. (19), is given, in the simple case when a neutron is taken out of shell j_1, by

$$\begin{aligned} S_n(N_0 Z_0;\ & j_1^{n_1} j_2^{n_2} j_3^{p_3} j_4^{p_4}) \\ &= B(N_0 Z_0;\ j_1^{n_1} j_2^{n_2} j_3^{p_3} j_4^{p_4}) - B(N_0 Z_0;\ j_1^{n_1-1} j_2^{n_2} j_3^{p_3} j_4^{p_4}) \qquad (21) \\ &= c_1 + \tfrac{1}{2}\pi_1 + (n_1-1)d_1 + n_2 I^0_{12} + p_3 I^0_{13} + p_4 I^0_{14} - \Delta_n \delta, \end{aligned}$$

where

$$\Delta_n \delta = \tfrac{1}{2}(-1)^{n_1+1}\pi_1 + \tfrac{1}{2}(-1)^{n_1}[1-(-1)^{p_3}]I'_{13} \qquad (22)$$

is the difference of the parity terms of the two nuclei.

Thus, as long as we consider nuclei obtained from one another by adding pairs of neutrons and protons in the same shells, the separation energy will vary linearly with respect to the neutrons, with a slope given by d, or I^0_{12}, and also linearly with respect to the protons, with a slope given by I^0_{13} or I^0_{14}. The slopes directly give the orientation-independent parts of the interaction between the nucleons. Such linear graphs have been given on several occasions [18–20, 93–95].

Confining our attention to nuclei belonging to the same parity type, we thus obtain a network of parallelograms, arrived at by connecting the S_n value of each nucleus with those of its isotopes on the one hand, and with those of its isotones on the other. This might be considered the separation-energy analogue of the Way and Wood [21]) systematics for beta decay energies (§ 14). There are four independent parallel networks, corresponding to the four nuclear parity types.

Figs. 1a, b show parts of these four networks of parallelograms. The (nuclear) rare-earths region is not represented, as the experimental data here are comparatively too scanty. The region of the lighter nuclei, displaying considerable irregularities, is omitted too †. The data were taken directly, or calculated with the help of decay or reaction data, from refs.[18–20, 22–29, 73, 97]). Values whose calculation involved an estimated decay energy are starred (*)††, and values involving two or more estimates were altogether omitted.

In order to see the linear dependence of the separation energies on both N and Z, we have chosen as abscissa the mass number A in preference over N or Z. To avoid overcrowding of the lines we have segregated the S_n lines according to the parity of Z. This still shows the neutron pairing energies directly as the vertical distance between the line connecting the odd-N isotopes of a given element and the line connecting its even-N isotopes (see § 6.1).

Many other linear systems may be obtained by connecting selected points at regular intervals in the above networks. Thus, connecting S_n values of alternate isodiapheres ††† [39]), one obtains straight lines with a slope given by $d(\text{or } I^0_{12}) + I^0_{13}(\text{or } I^0_{14})$. We shall not consider these lines in this paper.

6. Zig-Zag Relationships

When one nucleon at a time is added, changing thereby the parity type of the nucleus, zig-zag lines are obtained. We shall consider three cases:

6.1. NEUTRON SEPARATION ENERGIES OF THE ISOTOPES OF AN EVEN-Z ELEMENT

Progressing from one isotope to its immediate neighbour, the neutron separation energy undergoes an alternating change $\pm\pi_1$, which is superposed

† In fact, light nuclei are not considered in the present paper. In these, neutrons and protons are coupled together, and the approximation (19) is certainly inapplicable. To obtain their binding energies quantitatively (19) has to be modified to take care of this common coupling [11, 15]). However, the qualitative trends discussed in the present chapter are displayed by lighter nuclei as well. Some separation energy graphs for light nuclei are given in ref. [96]).

†† Except for the heavier transmercury elements, where we took the values given in ref. [19]), without specifying estimated ones.

††† These are nuclei having a constant neutron excess.

on the regular increase of d or I^0_{12} discussed before. Thus, a zig-zag line is obtained, enveloped by two parallel straight lines, one connecting the odd-N isotopes of the given element, and the other vertically higher by π_1, connecting the even-N isotopes. This vertical distance is perhaps the most direct way to show the existence of pairing energy.

6.2. NEUTRON SEPARATION ENERGIES OF THE ISOTOPES OF AN ODD-Z ELEMENT

Here, too, a similar zig-zag line is obtained. The only difference being that the alternating part is no longer $\pm\pi_1$ but $\pm(\pi_1-2I'_{13})$, which is usually smaller (see § 8.1). Therefore, the vertical distance between the S_n lines of the even-N and odd-N isotopes is reduced relatively to the even-Z elements. The magnitude of this reduction [19,98]) gives us the value of $2I'_{13}$. This value will be obtained in a more direct way in § 6.3 below.

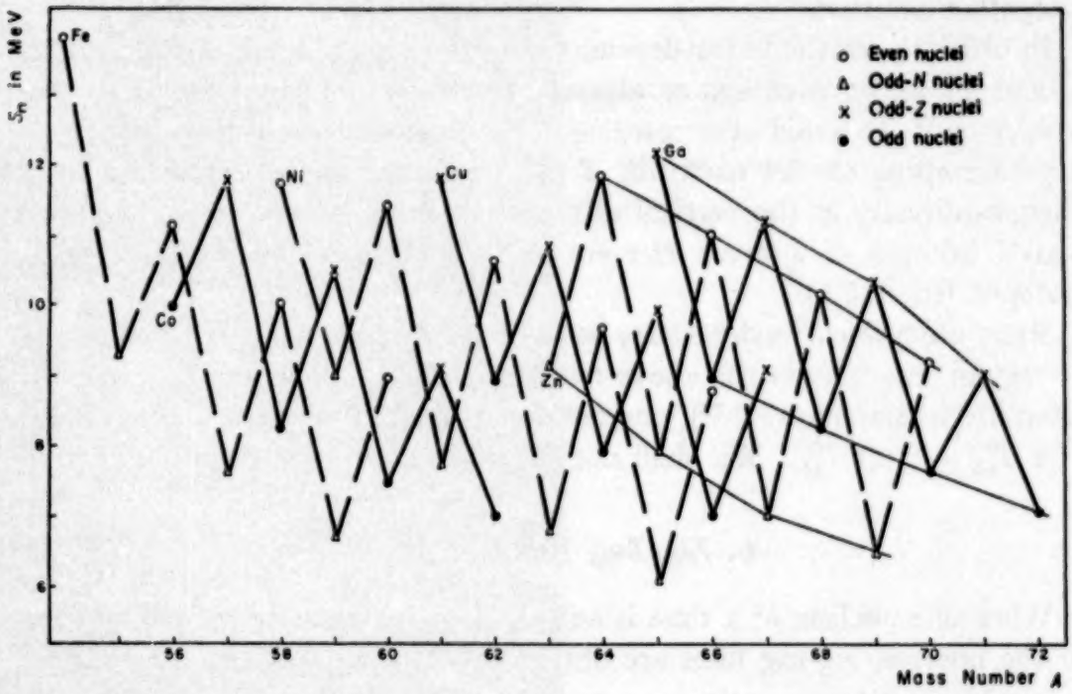

Fig. 2a. S_n values of consecutive isotopes (after Johnson and Bhanot [29])).

Zig-zag lines such as those mentioned hitherto have been drawn by Johnson and Bhanot [29]) and by Kravstov [93]). They are shown in fig. 2a. The enveloping straight lines for Zn and Ga are also shown (thin lines).

6.3. NEUTRON SEPARATION ENERGIES OF ISOTONES

Progressing from one isotone to its immediate neighbour, the neutron separation energy undergoes an alternating change of $\pm I'_{13}$, superposed on the regular increase of I^0_{13} or I^0_{14}, discussed in connection with the linear systematics. Thus, again a zig-zag line results, enveloped by two parallel

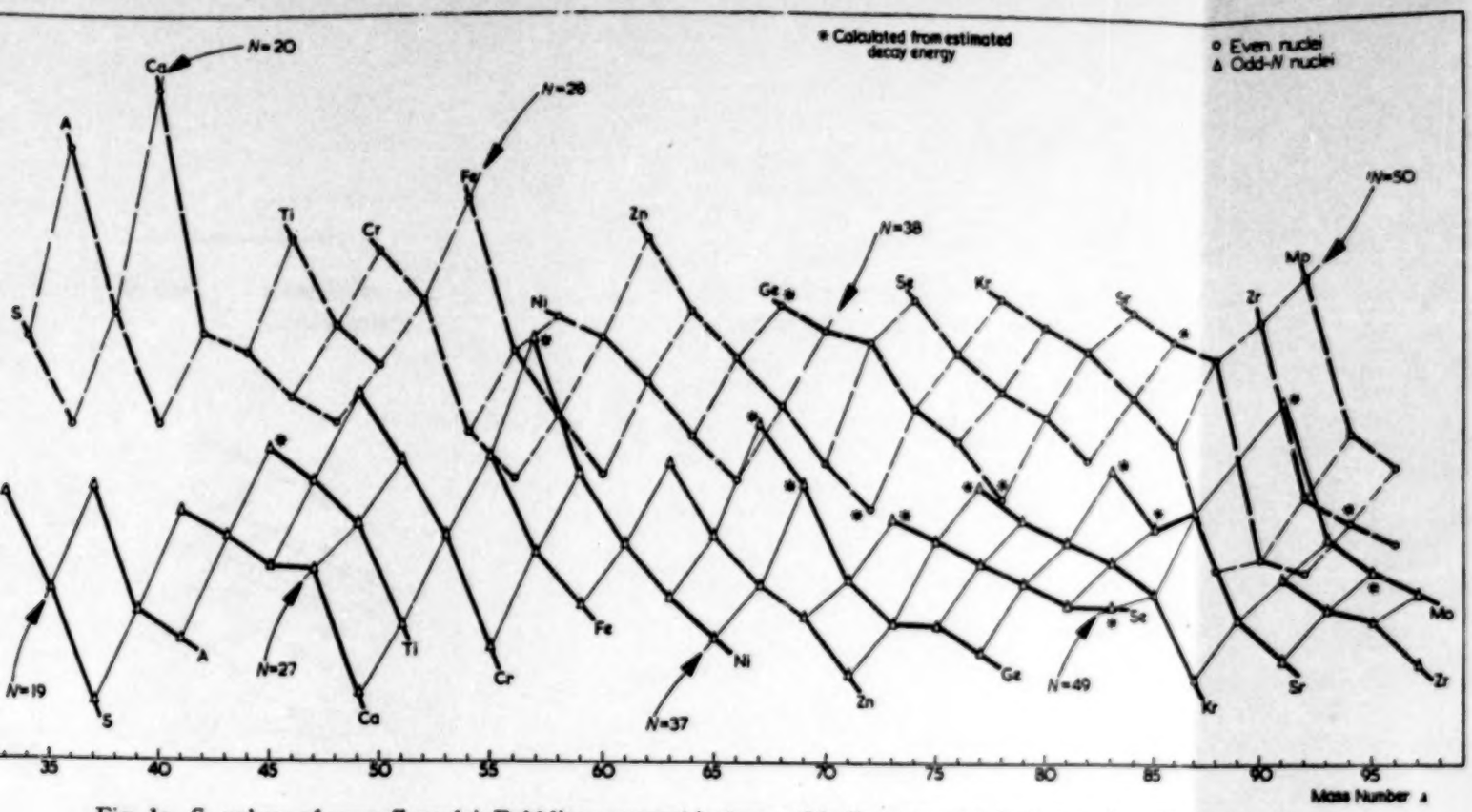

Fig. 1a. S_n values of even-Z nuclei. Bold lines connect isotopes, thin lines connect isotones $A = 33$ to $A = 97$.

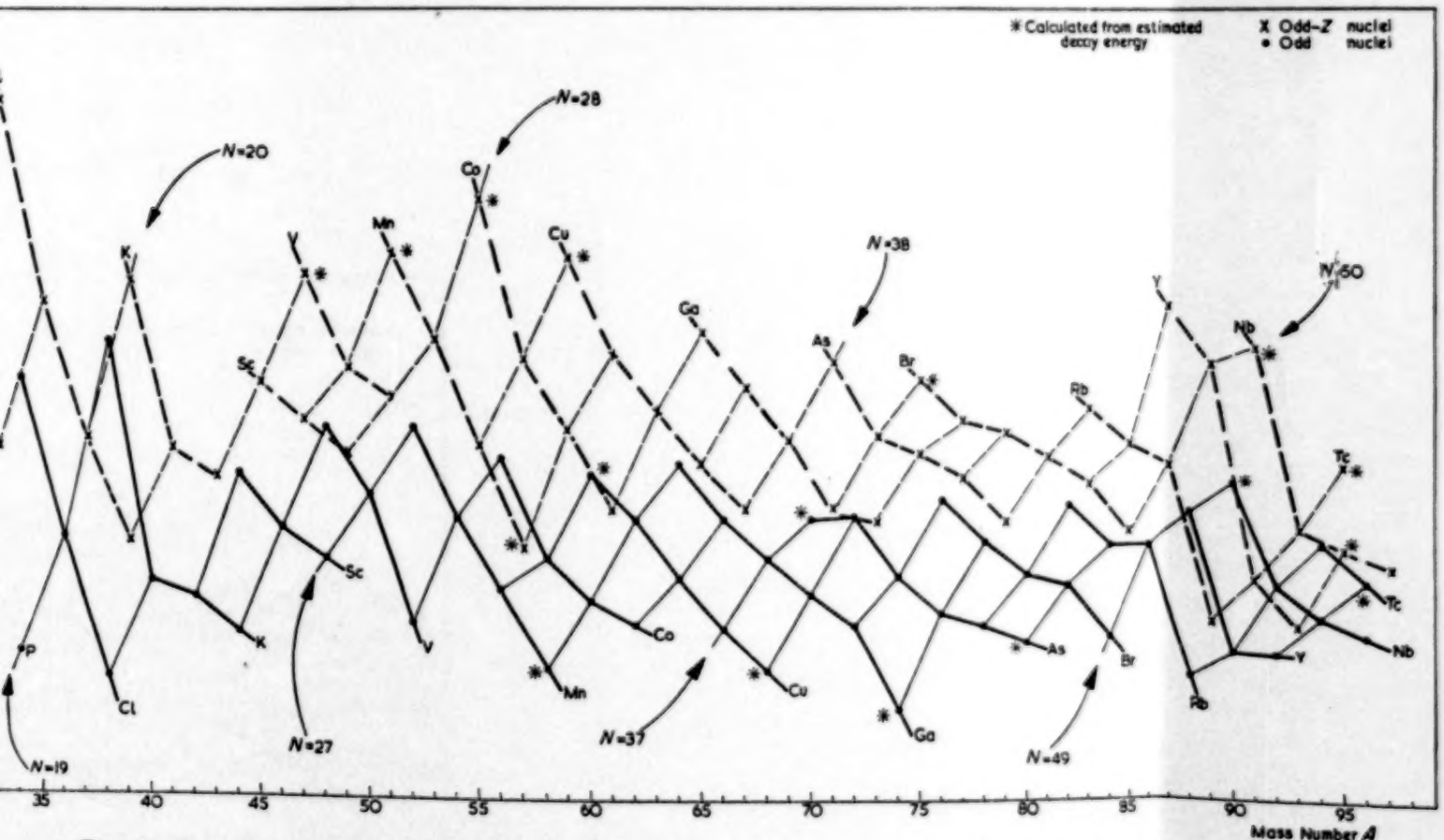

Fig. 1b. S_n values of odd-Z nuclei. Bold lines connect isotopes, thin lines connect isotones. $A = 33$ to $A = 97$.

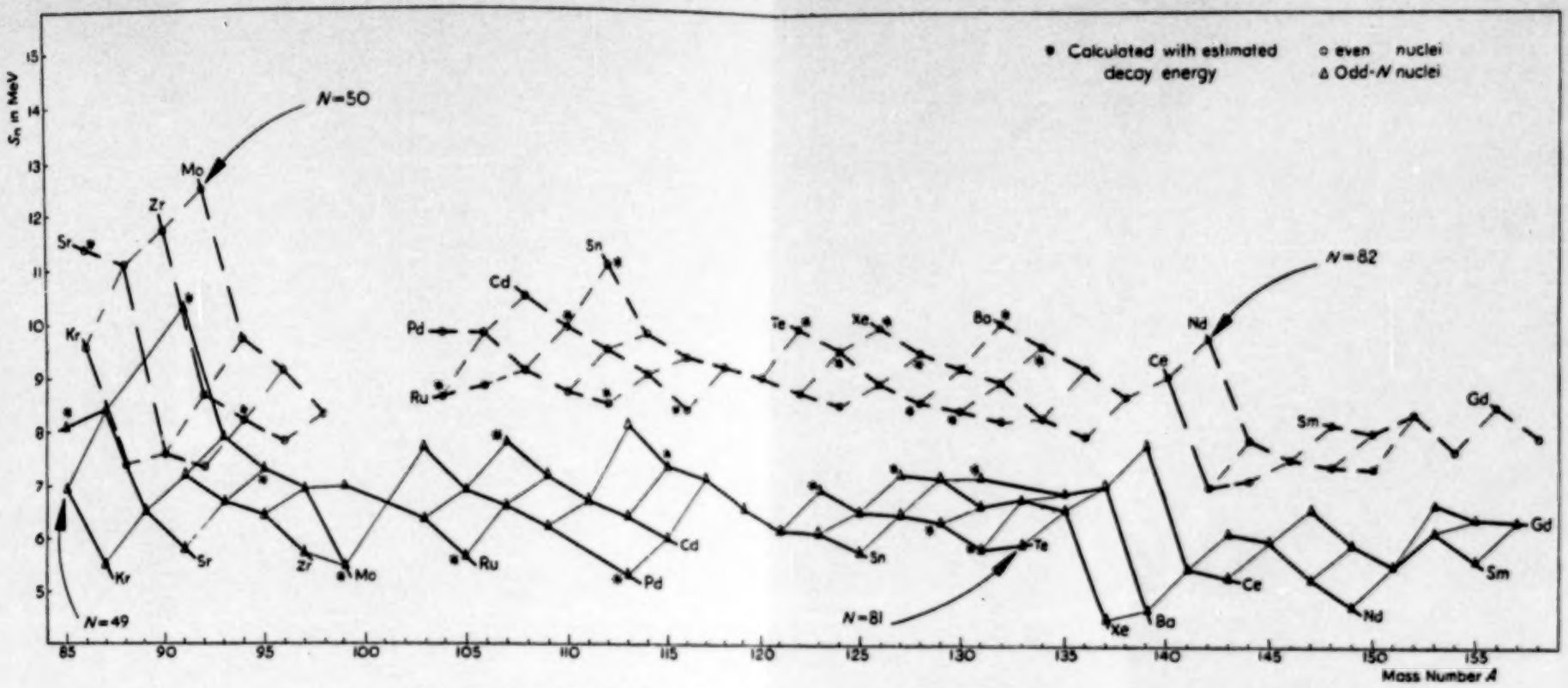

Fig. 1a. (continued). S_n values of even-Z nuclei. $A = 85$ to $A = 158$.

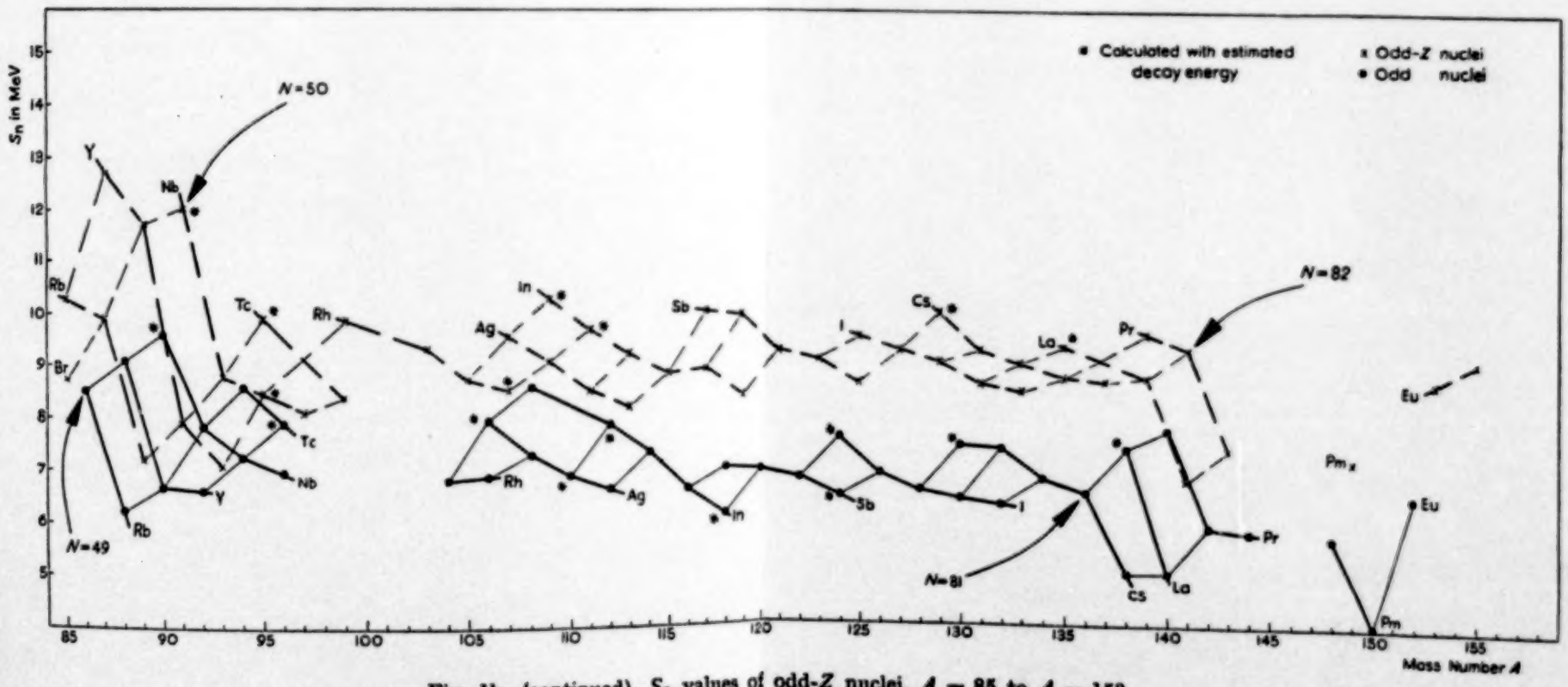

Fig. 1b. (continued). S_n values of odd-Z nuclei. $A = 85$ to $A = 158$.

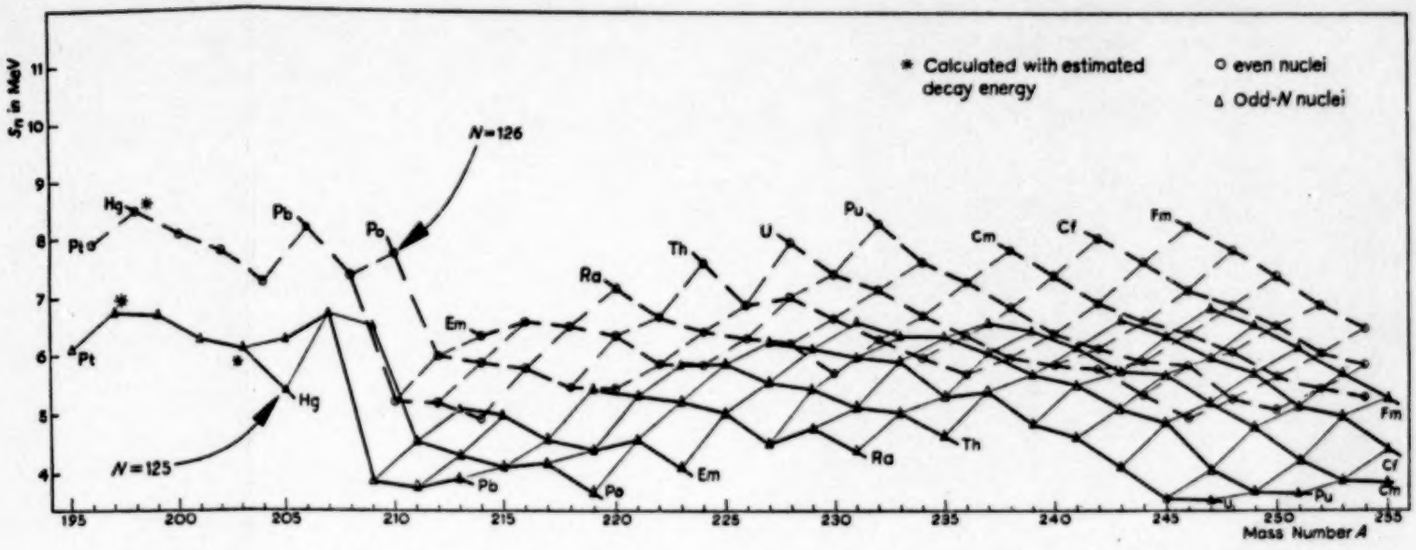

Fig. 1a. (continued). S_n values of even-Z nuclei. $A = 195$ to $A = 255$.

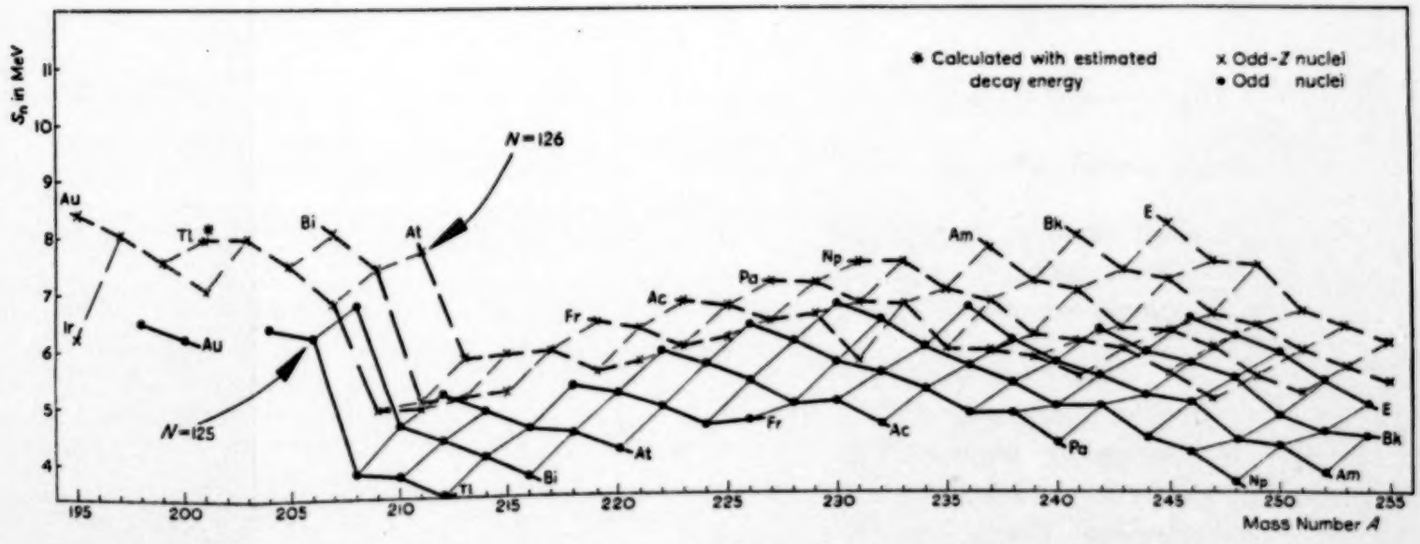

Fig. 1b. (continued). S_n values of odd-Z nuclei. $A = 195$ to $A = 255$.

straight lines, vertically apart by a distance I'_{13}. This vertical distance directly gives the orientation-dependent part of the interaction between

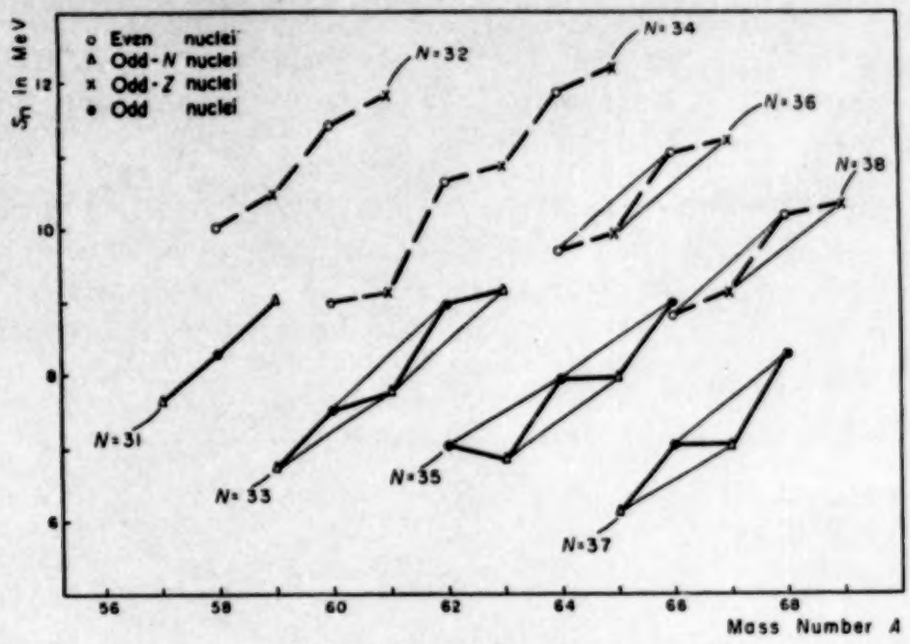

Fig. 2b. S_n values of consecutive isotones (after Ghoshal and Saxena [30]) and Way [31]).

the odd neutron and odd proton in the nucleus. If I'_{13} is positive, then for odd N, the line connecting odd-Z nucleides is above the line connecting

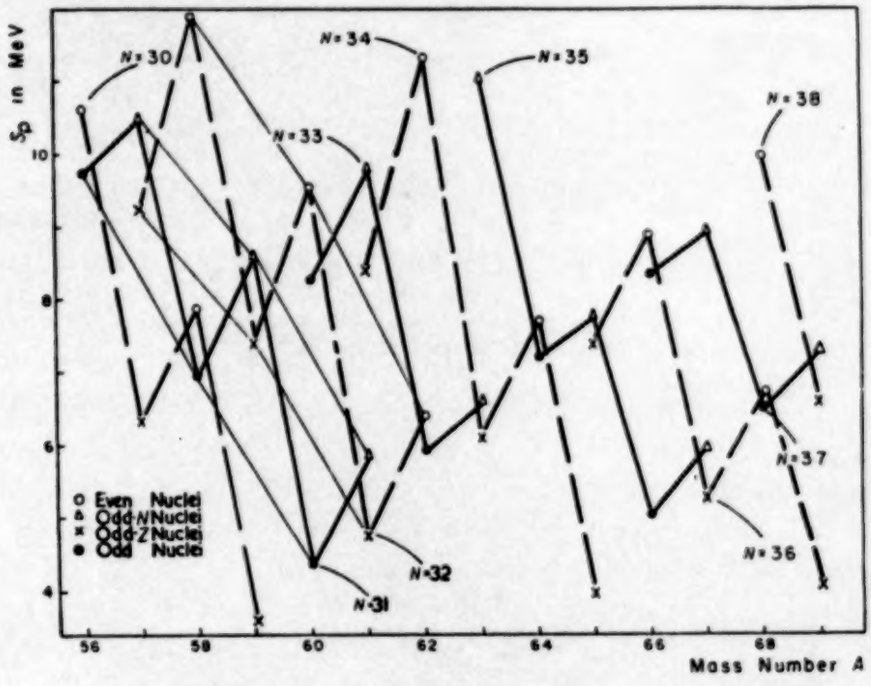

Fig. 4a. S_p values of consecutive isotones.

even-Z nucleides, and the situation is reversed for even N: the line connecting even-mass nuclei is always the higher. This is the regularity found by Ghoshal and Saxena [30]) in heavier nuclei and by Way [31]) † in lighter nuclei as well. It has already been indicated in the work of Edmonds [99]), and was interpreted according to the shell model by de Shalit [32]).

These zig-zag lines are shown in fig. 2b. Some of the enveloping straight lines are also shown (thin lines).

6.4. PROTON SEPARATION ENERGIES

The regularities observed above for neutrons are valid for protons as well, when changing the roles of neutrons and protons, isotopes and isotones. The corresponding graphs of the proton separation energies, S_p, are shown in figs. 3a, b and 4a, b.

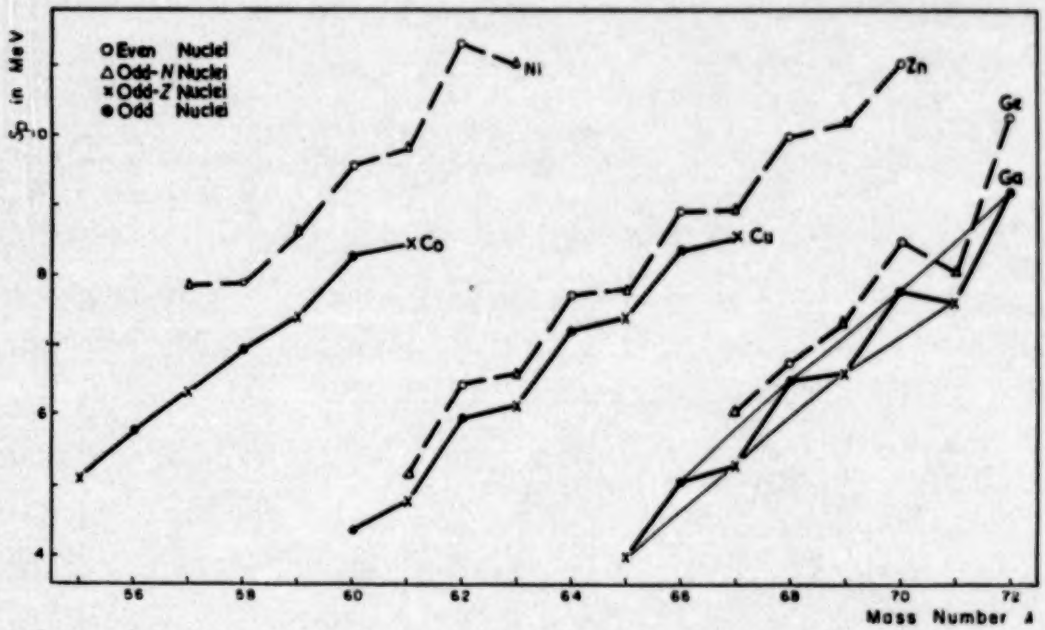

Fig. 4b. S_p values of consecutive isotopes (after Ghoshal and Saxena [30]) and Way [31])).

7. The Beginning of a New Shell

When a new shell begins to be filled, the parameters of formula (21) would generally change. This affects both the slopes of the straight lines considered above and the distances between them, and produces sharp breaks in the straight lines. In particular, since the single-particle binding energy is the smaller the later a shell is filled, the commencement of a new neutron shell should produce a downward discontinuity in the S_n lines connecting isotopes, and a similar discontinuity should occur in the S_p lines in the

† I thank Dr. Way for sending me copies of her graphs.

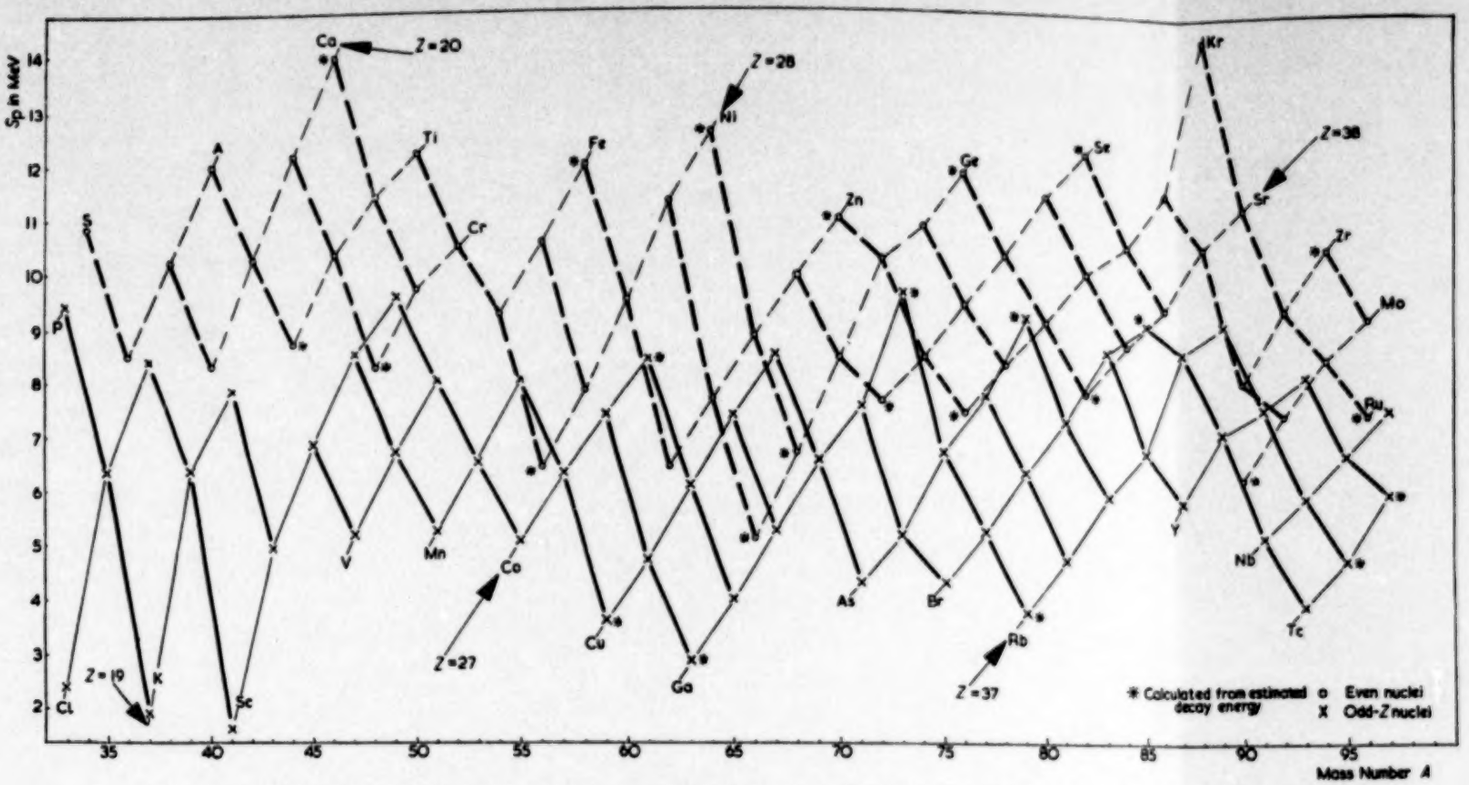

Fig. 3a. S_p values of even-N nuclei. Bold lines connect isotones, thin lines connect isotopes. $A = 33$ to $A = 97$.

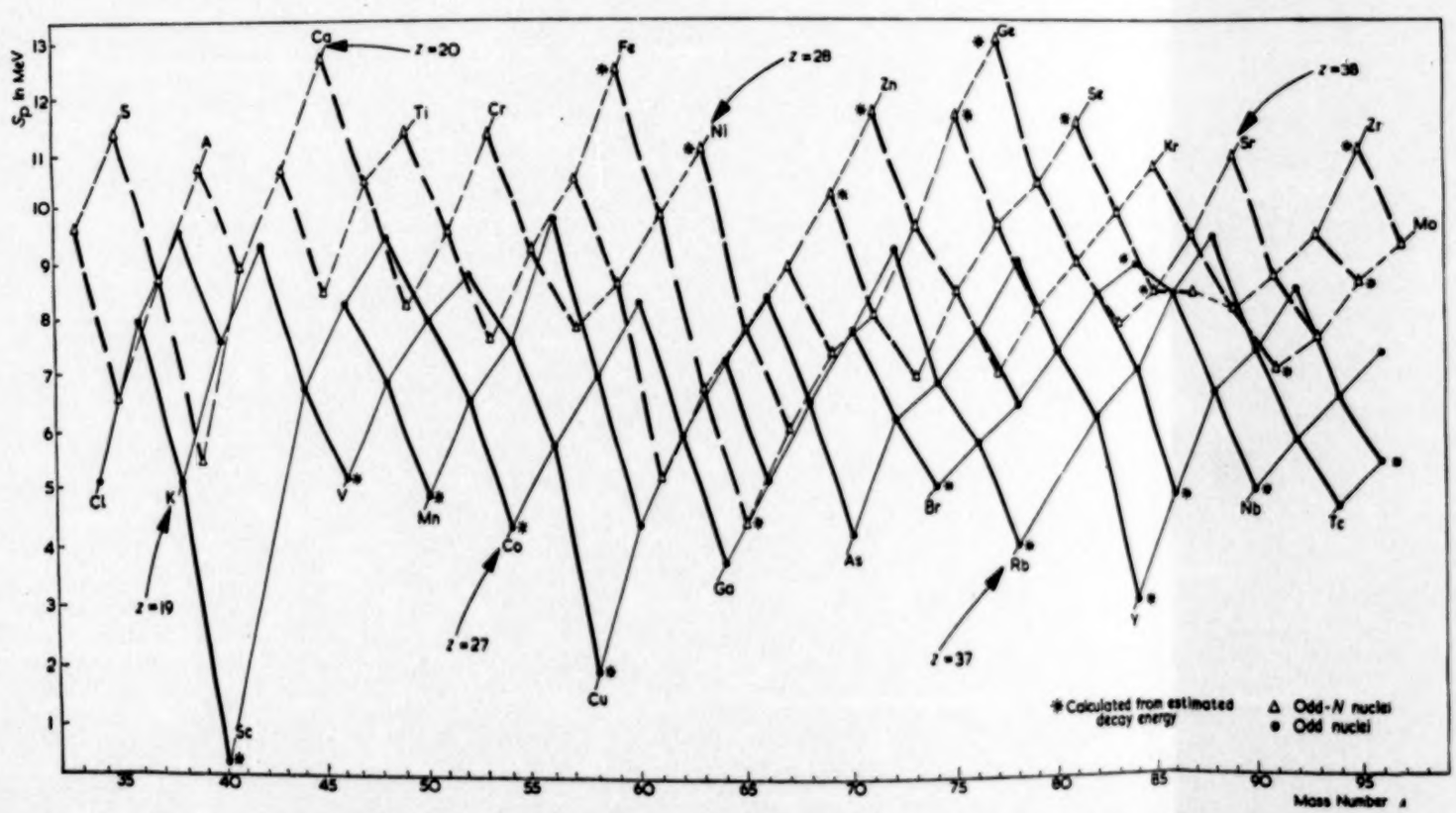

Fig. 3b. S_p values of odd-N nuclei. Bold lines connect isotones, thin lines connect isotopes. $A = 33$ to $A = 97$.

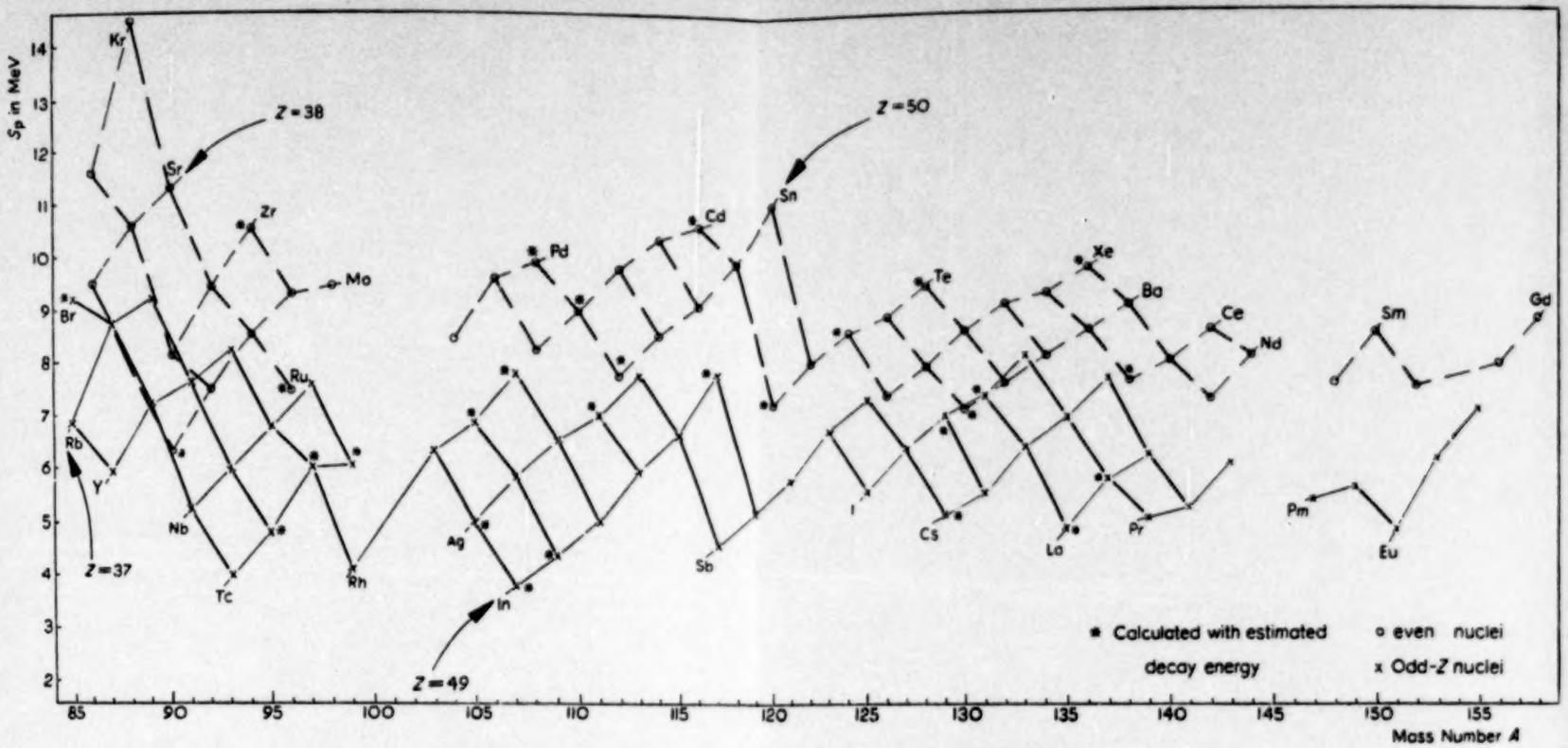

Fig. 3a. (continued). S_p values of even-N nuclei. $A = 85$ to $A = 158$.

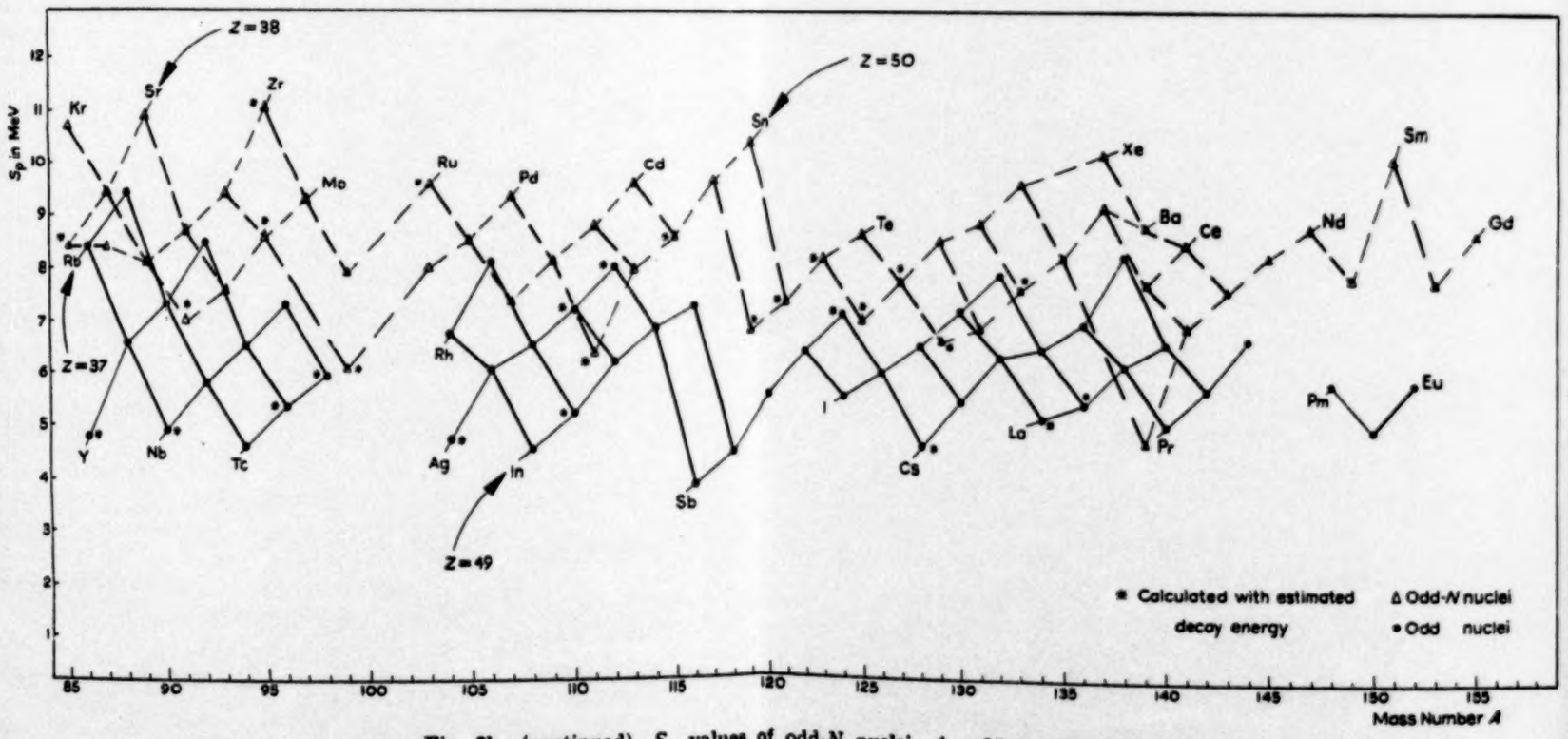

Fig. 3b. (continued). S_p values of odd-N nuclei. $A = 85$ to $A = 158$.

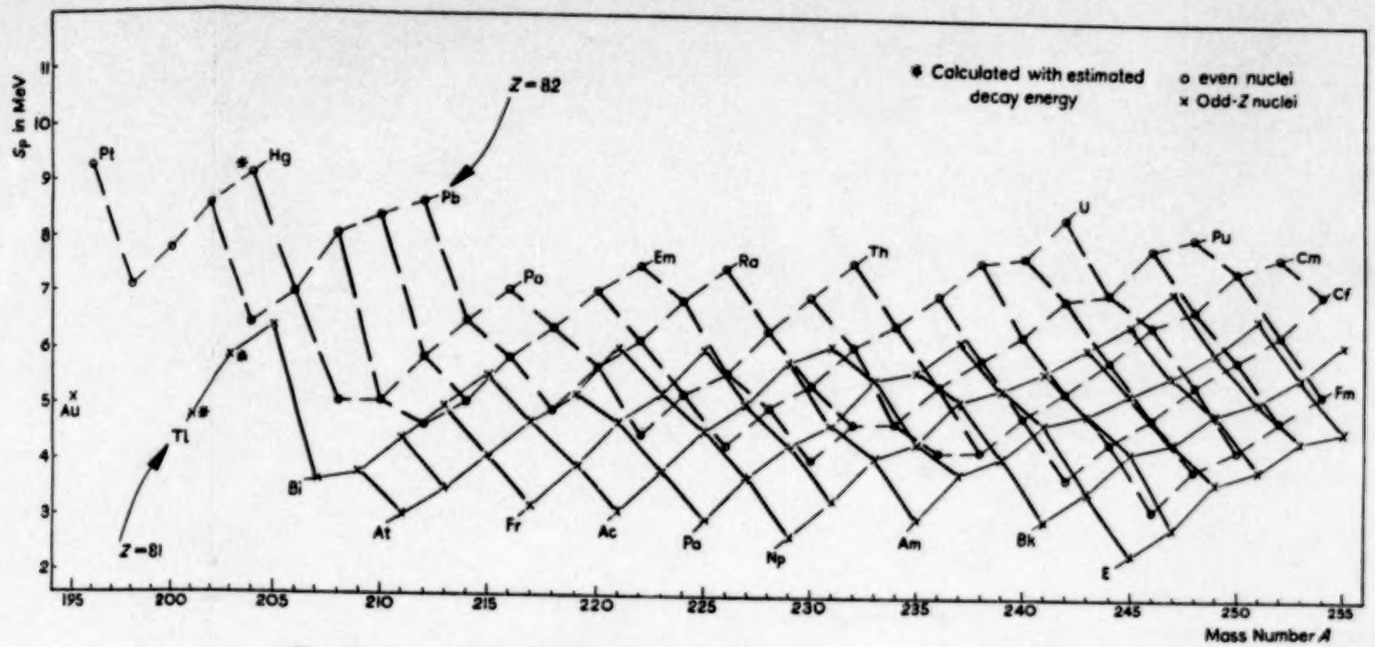

Fig. 3a. (continued). S_p values of even-N nuclei. $A = 195$ to $A = 255$.

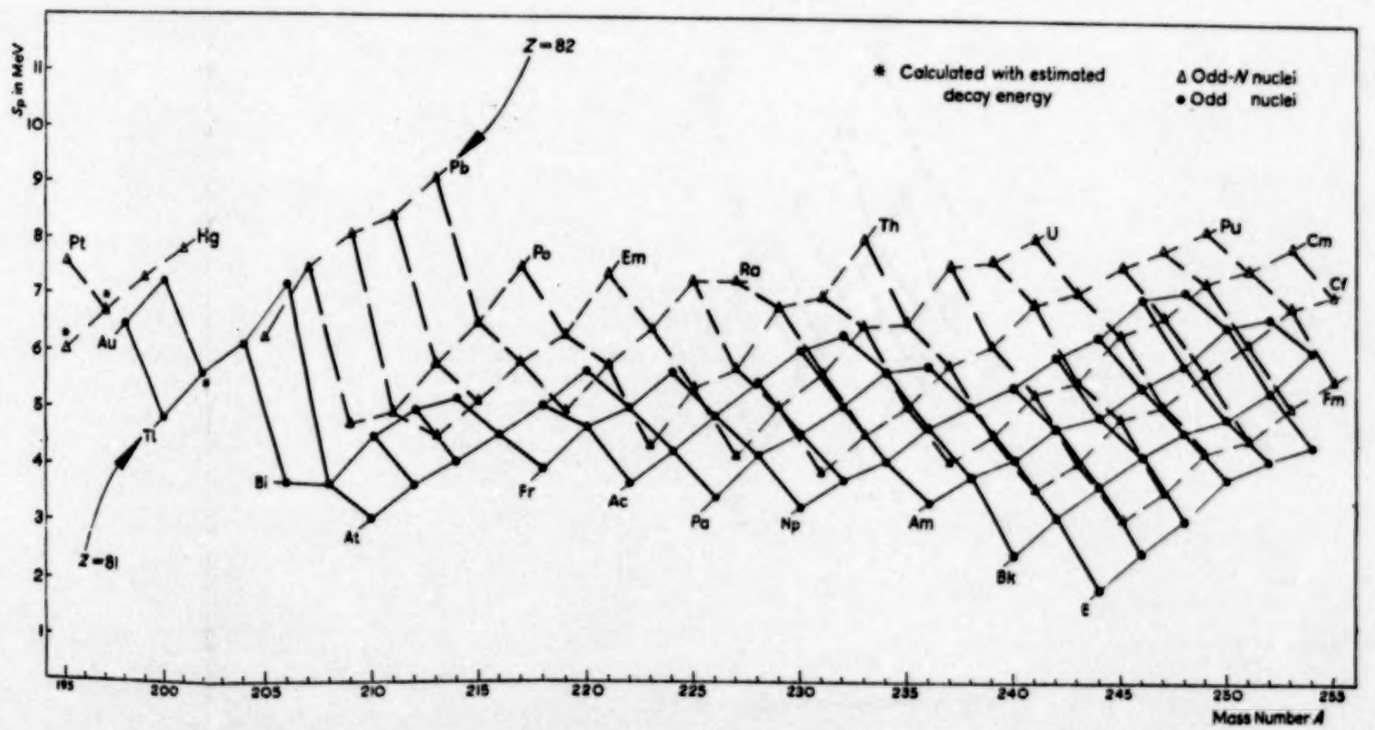

Fig. 3b. (continued). S_p values of odd-N nuclei. $A = 195$ to $A = 255$.

case of a new proton Shell. Such discontinuities are seen in figs. 1a, b and 3a, b, † and they are discussed in § 9.

B. Analysis of the Experimental Data

A glance at figs. 1a, b and 3a, b is sufficient to convince one that formula (21) would generally correlate the data fairly well. It is also worth mentioning that in the region below $A = 70$ and also in the trans-mercury elements, where the separation energies are known with greater accuracy [18, 19, 24, 25, 33]) than elsewhere, the parallelogram systems are most regular ††. We shall now proceed with a more systematic discussion.

Somewhat similar discussions have been carried out on several occasions [18–20, 29–32, 93–95, 98, 99, 101]).

8. The Signs and Qualitative Magnitude Relationships of the Parameters

8.1. SIGNS

The S_n lines connecting isotopes (bold lines †††) are almost invariably sloping downwards, and the lines connecting isotones (thin lines) are sloping upwards, and the opposite applies to the S_p lines *. From a study of nuclear moments [34]) and nuclear isomerism [13]), it is learned that there exists strong competition between nuclear shells, and that in passing from nucleus to nucleus along the lines of the diagrams, the pairs of nucleons sometimes fill one of the incomplete shells, sometimes the other. This means that the slopes of isotopic S_n lines are sometimes given by d and sometimes by I^0_{12}, and similarly the slopes for isotones are given by I^0_{13} and I^0_{14}. The signs of the slopes may therefore be summarized by saying that d, D, I^0_{nn} and I^0_{pp} are negative, and that I^0_{np} is positive **. *Thus the orientation-independent part of the interaction between any two identical nucleons, whether they are in the same or in different shells, is repulsive, and the analogous interaction between particles of different kinds is attractive.*

This very clearly explains both the neutron-proton balance in stable nuclei, and the saturation property of nuclear binding energy. The situation is essentially the same as that prevailing between the ions in a polar crystal,

† See also refs. [18, 20, 37–39, 93–95, 99]).

†† For the rare-earths region, very accurate S_n values were recently measured [39]) as the doublet separation between neighbouring isotopes. However, the data in this region are too scanty to display such regularities.

††† In the following discussion the reader is referred to figs. 1a, b and 3a, b.

* At least if we consider only values which are more or less precisely known. Thus one may observe that the very few violations of this rule in figs. 1a, b and 3a, b usually come from starred values, which were calculated with the help of estimated decay energies.

** $I_{nn}{}^0$, $I_{pp}{}^0$ and $I_{np}{}^0$ denote the scalar interaction between two neutrons, two protons, and one neutron and one proton, respectively, in different shells.

where ions of opposite charge attract one another, whilst ions of the same charge are mutually repulsive, thus preventing the binding energy from increasing quadratically with the number of particles †.

A second immediate consequence from the non-vanishing of d is that the nuclear forces do not possess the 'pairing property' as it was defined by Racah and Talmi [16]), viz. that the energy of a j^n configuration equals the sum of the pairing energies of its pairs, $[\frac{1}{2}n]\pi$. If this were the case, the S_n lines would quite often run horizontally, instead of sloping downwards. This entails, particularly, that an approximation based on a short-range delta-type interaction between the nucleons will be unable to explain the experimental facts about nuclear binding energies and separation energies. This conclusion could not have been arrived at from a consideration of beta decay energies or nuclear excitation energies, as there the slopes of the lines are always given by $(d-I^0)$'s (eqs. (31) and (57a, b) below), and one has no means of distinguishing the d from the I^0.

The S_n line for even N is invariably found above the line for odd N, and similarly the S_p line for even Z. This shows that the pairing energies π and Π are positive, which is in agreement with the known tendency of the nucleons to couple in pairs.

Finally, in the regions displaying a more or less regular systematics, the distance between the S_n lines of even and odd N, respectively, is usually †† smaller for odd Z than for even Z, as already mentioned in § 6.2, and an analogous situation holds for the proton separation energies [19, 98]). Thus I'_{13}, the analogue of the pairing energy for nucleons of different kinds, is usually also positive †††. The same conclusion might have been drawn from the Ghoshal-Saxena-Way zig-zag behaviour mentioned in § 6.3. As a matter of fact, the existence of each of these two regularities implies the existence of the other as well, since both depend on the non-vanishing of I'_{13}.

8.2. MAGNITUDE RELATIONSHIPS

A first conspicuous fact is the difference between the slopes of the S_n and S_p lines connecting isotopes and isotones, respectively. The slopes show that both D and I^0_{pp} are larger in absolute value than either d or I^0_{nn} (these parameters are negative!). This is qualitatively obvious, because of the additional Coulomb repulsion between the protons [93–95]).

From the slopes of the S_n and S_p lines connecting isotones and isotopes,

† In this simplified description, we have disregarded the orientation-dependent pairing energies, which are positive. However, since their contribution to the total binding energy (19) varies linearly with the nucleon numbers, they are outweighed by the quadratically-varying orientation-independent interactions, and the above description is essentially correct.

†† The only region systematically displaying the opposite behaviour is that of the heaviest alpha-emitting nuclei.

††† De Shalit [82]) has shown theoretically that it must be positive for the ground state of an odd nucleus.

respectively, one also finds that D and I^0_{pp} are larger in absolute value than I^0_{np}, which is larger than the absolute value of d or I^0_{nn}. We therefore find the results

$$\begin{Bmatrix} -D \\ -I^0_{pp} \end{Bmatrix} > I^0_{np} > \begin{Bmatrix} -d \\ -I^0_{nn} \end{Bmatrix} > 0. \tag{23}$$

This may also be replaced by an equivalent relation between the second derivatives of the nuclear binding energy with respect to the nucleon numbers:

$$-\frac{\partial^2 B(NZ)}{\partial Z^2} > \frac{\partial^2 B(NZ)}{\partial Z \partial N} > -\frac{\partial^2 B(NZ)}{\partial N^2} > 0. \tag{24}$$

These inequalities have been derived by Fuchs [35]) from very general considerations about the saturation character of nuclear forces, independently of any specific nuclear model.

A second significant fact is the decrease of both the absolute values of the slopes and the distances between the lines, when the mass number A becomes large [2,38,94,98]). Again, this is qualitatively very plausible, since in the larger heavy nuclei the average distance between any two outer nucleons is larger, and therefore their average interaction, as given by the magnitude of the parameters, is smaller.

9. The Magic Numbers

When looking for sharp changes in the linear graphs of the separation energies, which would reveal the beginning of new shells, the most significant of these are the downward discontinuities already mentioned in § 7, associated with the sudden decrease of the single-neutron or proton binding energy as a corresponding shell edge is crossed. Such downward discontinuities are observed in the S_n lines connecting isotopes at neutron numbers 28, 50, 82 and 126, and in the S_p lines connecting isotones at proton numbers 20, 28, 50 and 82. A typical such discontinuity is shown schematically in fig. 7a (§ 10).

A much smaller discontinuity in the S_p lines is also observed when passing from Sr to Zr. However, the corresponding discontinuity is not observed for the odd-Z lines between Rb and Y, and the observed effect is thus probably due to a reduction of the proton pairing energy rather than to a weakening of the single-proton binding energy. It will be further discussed in the later part of the present section, in connection with the reduction of pairing energies when shell edges are crossed.

The discontinuities of the S_n lines seem sharper than those of the S_p lines, due to the steeper downward slopes of the latter (eq. (23)). For the same reason, the discontinuities at the higher magic numbers, where the

slopes are milder (§ 8.2), are much more ovbious than at the lower ones.

Another type of discontinuity occurs at $N = 20$. Instead of a discontinuity of the above mentioned type, which would have taken place between $N = 19$ and $N = 21$ in the S_n lines connecting odd-N isotopes, and between $N = 20$ and $N = 22$ in the S_n lines connecting even-N isotopes, there is a very considerable decrease of the magnitude of the slope of the S_n lines connecting isotopes, taking place after $N = 20$ is already crossed, viz. at $N = 21$ for the odd-N line, and at $N = 22$ for the even-N line: the discontinuity does not appear, as the decrease of the single-neutron binding energy on crossing the shell edge is compensated here by the decrease of the repulsion d exerted on the neutron by its equivalents.

The discontinuities at the magic numbers are usually different for the lines connecting nuclei of different parity types. Thus at $N = 28$ the downward discontinuity in the S_n lines connecting the even-N isotopes exceeds that in the S_n lines connecting the odd-N isotopes, indicating a decrease of the pairing energy of the last neutron pair when this number is crossed. Similarly, the decrease of S_p from Ni to Zn exceeds the decrease from Co to Cu. This corresponds to the usual assumption [2, 3]) that the pairing energy is lower in $2p_{3/2}$ or $1f_{5/2}$ than in the $1f_{7/2}$ shell. A similar situation occurs at $N = 50$ and $Z = 50$, because the pairing energy is lower in $2d_{5/2}$ or $1g_{7/2}$ than in $1g_{9/2}$†. On the other hand, no such effect is observed in the S_n lines at $N = 82$ and in the S_p lines at $Z = 82$. However, we know here (see table 8 (§ 32) and table 10 (§ 33)) that the last neutron pairs before $N = 82$ are in $2d_{3/2}$ and the last proton pairs before $Z = 82$ are in $2d_{3/2}$ or $3s_{\frac{1}{2}}$, rather than in the $1h_{11/2}$ shells, whereas shells with higher j, having probably higher pairing energies, begin to fill beyond them. A similar behaviour is observed also for the S_n lines of the Pb isotopes at $N = 126$, and it might probably be similarly explained.

We have already seen at the beginning of the present section that the small discontinuity in the S_p lines connecting isotones from Sr to Zr should also probably be attributed to a reduction of the pairing energy of the last proton pair when passing from Sr to Zr. We know (tables 5 and 7) that the last proton pair of Zr is a $2p_{\frac{1}{2}}^2$ pair, and the above decrease is again in agreement with the usual assumption on the connection between pairing energy and angular momentum.

These even-odd differences are connected with a similar difference in the spacing between the odd and even S_n or S_p lines, when the neutron or proton magic numbers, respectively, are crossed. However, some distance beyond the magic numbers the pairing energies recover their "normal"

† For protons the effect is observed only in fig. 3a. In fig. 3b the decrease of Π is compensated by a decrease of a similar order of magnitude of $2I'$ (see fig. 8b below (§ 11)).

values, and the distances between the odd and even lines increase to their usual magnitude in the new shell region.

The decrease of the absolute values of the slopes of the S_n and S_p lines, given by the orientation-independent parameters, d, D and the I^0's, in heavier nuclei, was mentioned in § 8.2. There is a considerable increase of $|d|$ and also a smaller one of $|D|$ after the $1f_{7/2}$ shell is crossed. However, beyond 28 neutrons or protons, their decrease is more or less smooth, and does not seem to be particularly affected by crossing shell edges.

A detailed picture of the variation of the slopes and distances of the separation energy lines of figs. 1a, b and 3a, b is given in figs. 8a, b below (§ 11).

10. Comparison with the Electrons in Atoms

At this point, a somewhat detailed examination of the oft-mentioned analogy between nucleon separation energies and atomic ionization potentials would be profitable. In both cases we have a system composed of two kinds of particles, neutrons and protons in nuclei and electrons and protons in atoms. In both cases, particles of the same kind are mutually repulsive, while particles of different kinds attract one another. Finally, in both systems the numbers of particles of the two kinds may vary independently, resulting in various isotopes and isotones in the case of nuclei, and in atoms of various elements, in various degrees of ionization, in the case of atoms.

Fig. 5 shows the ionization potentials of various atoms and ions. The data were taken from Moore's "Atomic Energy Levels" [36]). To stress the similarity to nucleon separation energies, we have chosen as abscissa the sum of the nuclear charge Z and the number of electrons e, and have connected both the values of ions belonging to the same isoelectronic sequence (thin lines) and the values of the various ions of the same element (bold lines). We did not distinguish between even and odd lines, since there is no electrostatic pairing energy for the long-range Coulomb forces between the electrons.

The similarity to the graphs of the nuclear separation energies is very clear. When electrons are added, decreasing the degree of ionization of the same element, the ionization potential decreases, due to the mutual repulsion of the electrons. On the other hand, when the attractive nuclear charge increases along an isoelectronic sequence by the addition of protons, the ionization potential increases with it. Sometimes there are strong downward discontinuities in the lines connecting ions of the same element, corresponding to the completion of the electronic shells, which are also marked on the graph.

There are considerable quantitative differences, of course, over and above

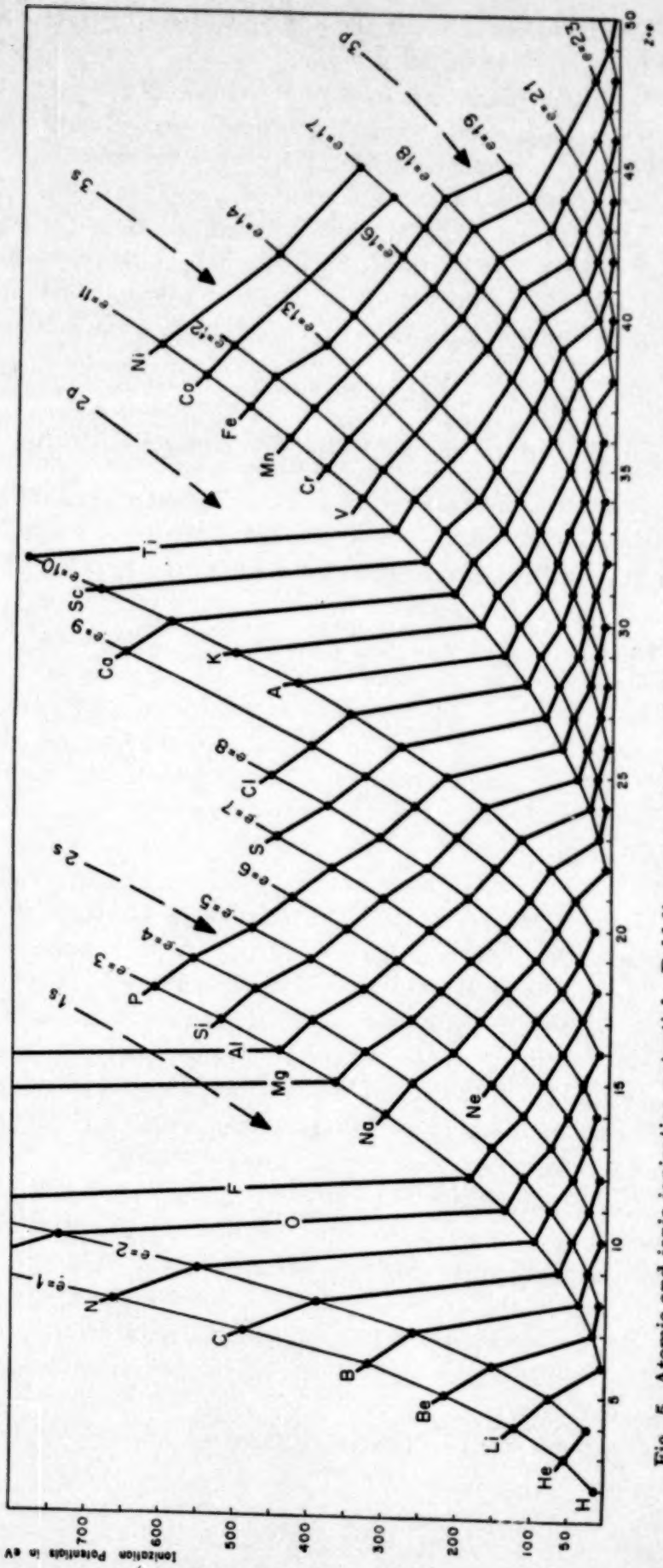

Fig. 5. Atomic and ionic ionization potentials. Bold lines connect ions of the same element, thin lines connect isoelectronic ions.

the very different order of magnitude of the involved energies. In the first place, there is the very clear parabolic dependence of the ionization potentials on the proton number, corresponding to the well known Z^2-dependence of the Rydberg constant in atomic spectroscopy. In the second place, there are the enormous relative magnitudes of the discontinuities associated with shell crossing. These discontinuities increase with the ionization in accordance with the above mentioned Z^2-dependence, so that subshell effects also become clearly distinguishable.

However, the usual comparison between nucleons and electrons is not the one carried out above. Usually [102, 119]), the first ionization potentials of

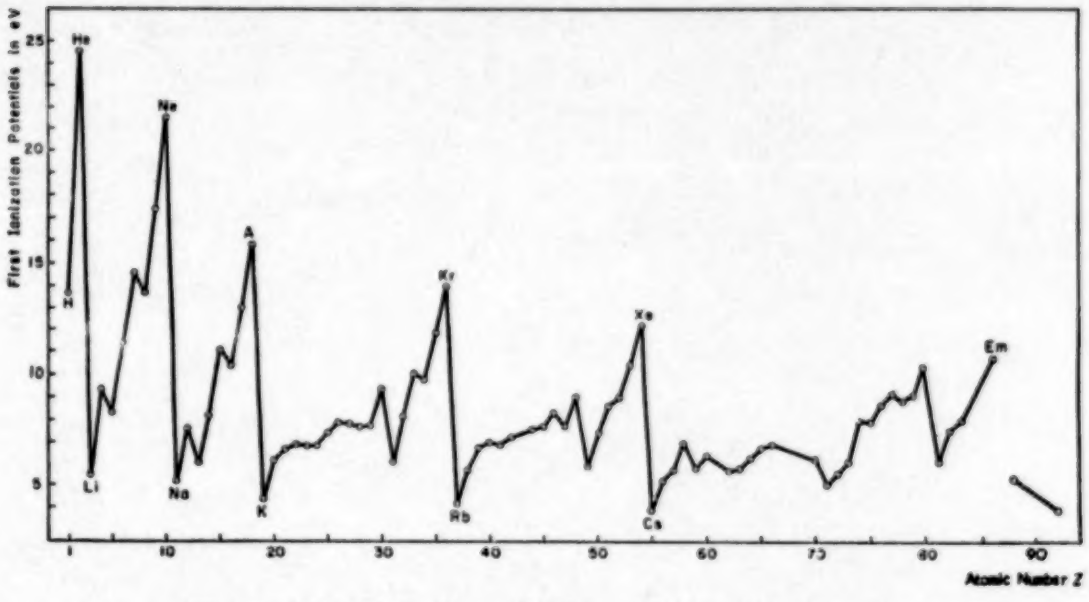

Fig. 6a. First ionization potentials of consecutive elements.

consecutive atoms are compared to the nucleon separation energies of the naturally-occurring beta-stable nucleides. This corresponds to the addition of a proton and an electron at a time in the case of the ionization potentials, and roughly to the addition of three neutrons for two protons in the case of the separation energies. A line so obtained for the ionization potentials consists of diagonals passing from left to right in the parallelograms of fig. 5. For nucleon separation energies it can similarly be roughly approximated to by diagonals of larger parallelograms obtained by adding four protons and six neutrons to a given nucleus in figs. 1a, b and 3a, b. A glance at figs. 5, 1a, b and 3a, b then suffices to make it clear, that electrons do indeed become more tightly bound as a shell is being filled, but the behaviour of the nucleons is different: their binding remains approximately constant within a given shell region, or even decreases slightly as the shell is being filled. This is shown more precisely in figs. 6a, b, c, showing the first ioniza-

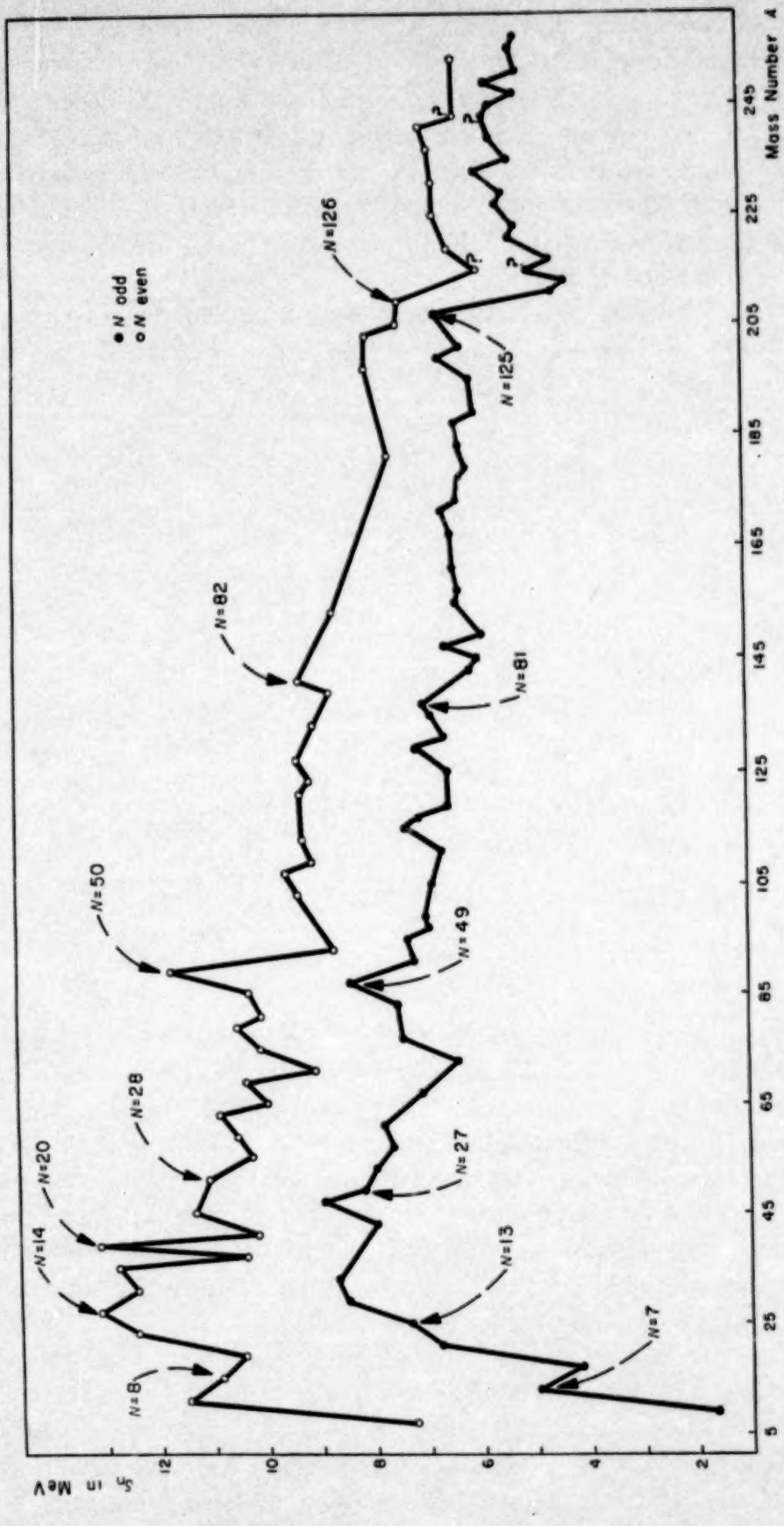

Fig. 6b. S_n values of odd-mass beta-stable nucleides.

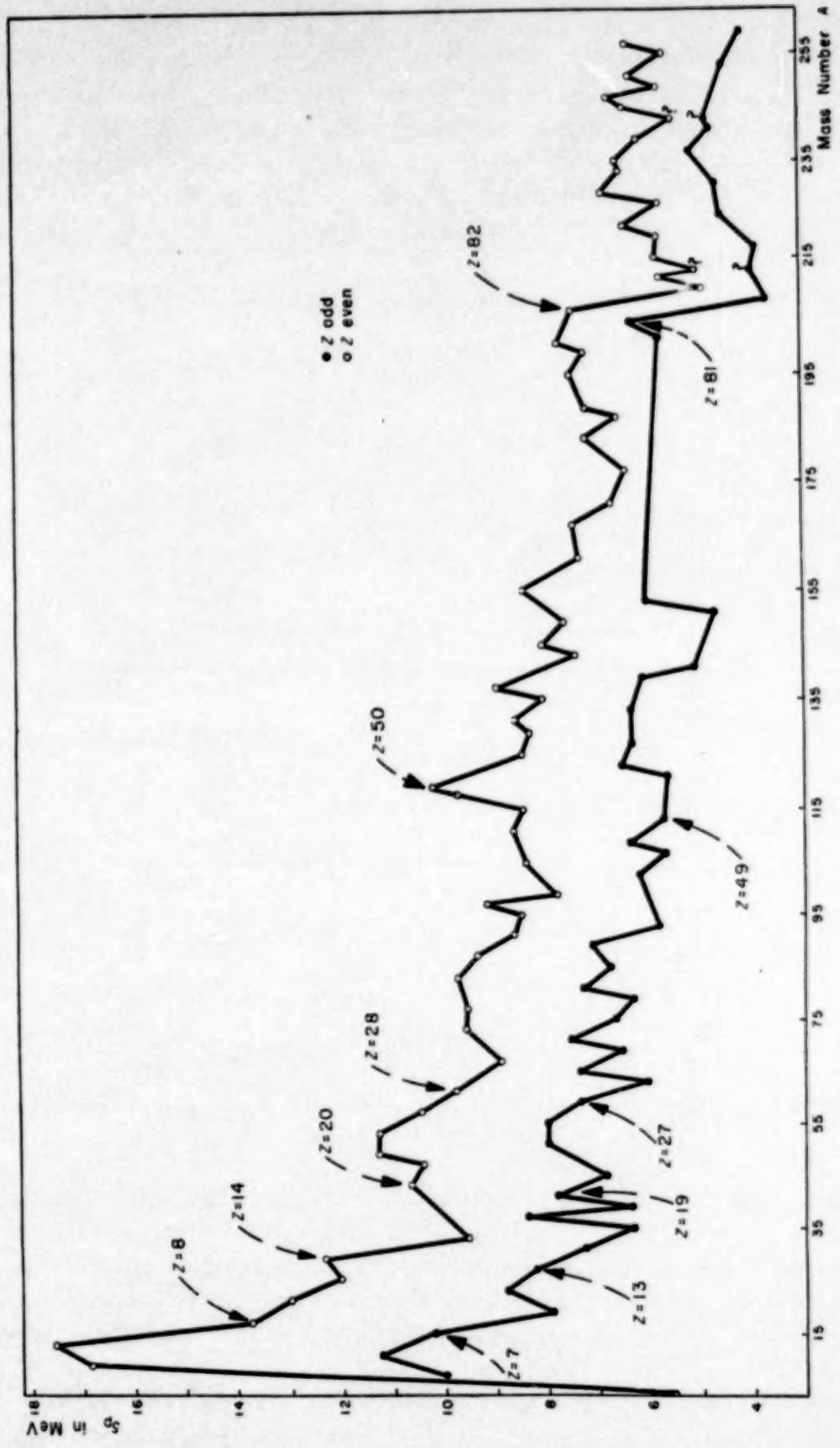

Fig. 6c. S_p values of odd-mass beta-stable nucleides.

tion potentials of atoms and the neutron and proton separation energies of odd-mass beta-stable nuclei, respectively. In order to best distinguish shell effects from pairing effects, we connected the S_n and S_p values of nuclei of the same parity type, thus obtaining two S_n and two S_p lines.

On the other hand, when considering not the separation energies themselves, but their deviations from a smooth semi-empirical or empirical mass

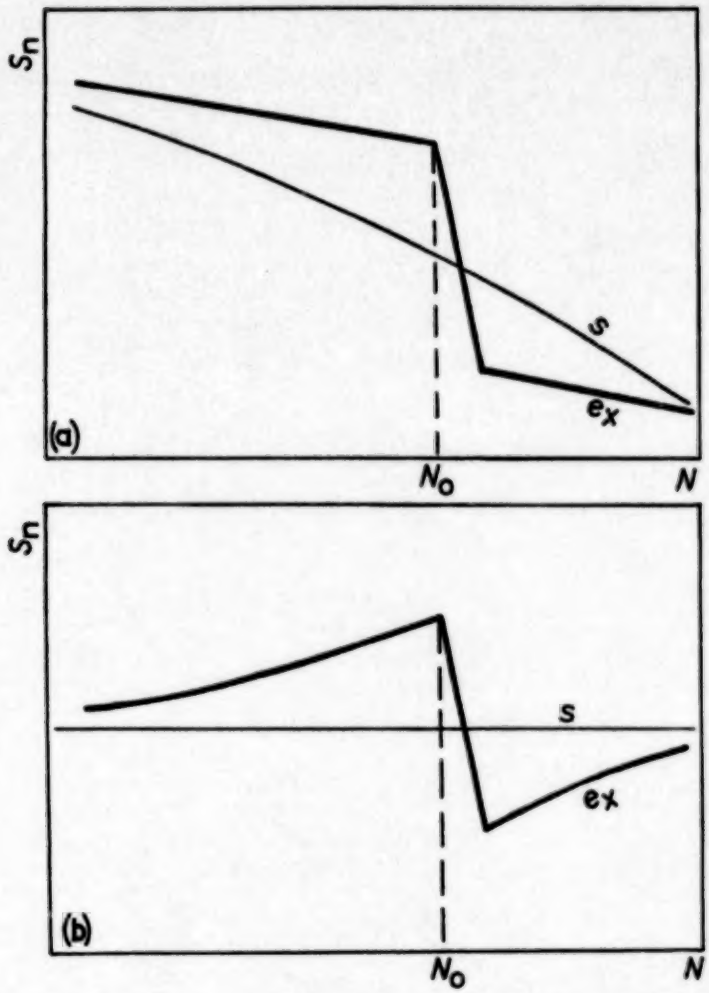

Fig. 7. Schematic illustration of the apparent increase of nucleon separation energies as a shell is gradually filled.

formula [37–39, 99, 102]), the impression is obtained that as the shell is filling, the nucleons gradually become more tightly bound, and very much so. This very current distortion of the actual situation is caused by the choice of the smooth base-line: relative to the smooth line s of fig. 7a the actually decreasing line ex of the separation energies seems to increase when approaching the magic number, and to recover slowly from its sudden decrease caused by crossing it, as the next shell is gradually filled (fig. 7b). Johnson and Nier [20]) have already remarked that the sudden decrease in neutron separation energies

when $N = 82$ is crossed is due to the relatively very low binding of the neutrons beyond $N = 82$, rather than a particularly high binding energy at $N = 82$.

Systematics of beta decay energies (§ 16), as well as of total binding energies (§ 23.2), also show that there is a sharp decrease in binding in "after magic" nuclei, rather than a particular increase at magic nuclei as compared to their predecessors.

11. Subshell Effects

The nuclear shell model predicts the completion of shells at additional nucleon numbers besides the magic ones. These so-called subshells, if regularly filled, should be revealed by discontinuities in the lines and their slopes, similar to those encountered in connection with the magic numbers.

Mayer [1]) had already postulated that there should be a strong competition between "pairs of spin levels arising from adjacent orbital levels in the square well in such a way that spin orbit coupling tends to bring their energy close together". A later study [34]) confirmed this competition within the groups of levels $2p_{3/2}$, $1f_{5/2}$; $2p_{\frac{1}{2}}$, $1g_{9/2}$; $2d_{5/2}$, $1g_{7/2}$; $3s_{\frac{1}{2}}$, $2d_{3/2}$, $1h_{11/2}$; $3p_{3/2}$, $3p_{\frac{1}{2}}$, $2f_{5/2}$, $1i_{13/2}$. One cannot then expect to find abrupt discontinuities in straight S_n or S_p lines at nucleon numbers corresponding to the completion of one of these subshells, whilst its competitors are still empty. On the contrary, since the competing subshells differ in energy by a few hundred keV at most, as evidenced by the low excitation energies of single-particle levels in the regions of competition, there should usually be a strong mixing of them [40]). The characterization of the nuclear states by the numbers of nucleons in the various subshells becomes meaningless, and discontinuities connected with subshells cannot be expected. This was the explanation suggested by Hogg and Duckworth [41]) for the negative results of their attempts to discover subshell effects in their mass data between $N = 82$ and $N = 126$. The observation of Quinsberry *et al.* [19]), that the variation of neutron pairing energy in nuclei from Fe to Zn cannot be accounted for by the angular momentum of the shell occupied by the pair, might be explained by the same argument.

Moreover, it is not at all obvious that under such circumstances the binding energies would still be adequately represented by a simple quadratic formula like (19), resulting in linear systematics of the separation energies. Nevertheless, figs. 1a, b and 3a, b show that the linear approximation is fairly good: as if there were no subshells at all.

A possible explanation is the following: the competing subshells have approximately equal single-particle binding energies. They also have similar radii, and therefore their two-body parameters are approximately

equal too. Then the binding energy (19) will depend only on the numbers of nucleons, and will be the same for any distribution among the subshells. As a matter of fact, if we assume

$$\begin{aligned} &c_1 = c_2 = c, \qquad d_1 = d_2 = I^0_{12} = d, \qquad \pi_1 = \pi_2 = \pi, \\ &C_3 = C_4 = C, \qquad D_3 = D_4 = I^0_{34} = D, \qquad \Pi_3 = \Pi_4 = \Pi, \\ &I^0_{13} = I^0_{14} = I^0_{23} = I^0_{24} = I^0, \qquad I'_{13} = I'_{14} = I'_{23} = I'_{24} = I', \end{aligned} \tag{25a}$$

and introduce

$$n_1+n_2 = n, \qquad p_3+p_4 = p, \tag{25b}$$

eq. (19) becomes

$$\begin{aligned} B(N_0+n,\ Z_0+p) = B(N_0 Z_0)+nc+pC+\tfrac{1}{2}n\pi+\tfrac{1}{2}p\Pi \\ +\tfrac{1}{2}n(n-1)d+\tfrac{1}{2}p(p-1)D+npI^0-\delta, \end{aligned} \tag{26}$$

which is the same as if there were but one incomplete neutron shell $j_n{}^n$ and one incomplete proton shell $j_p{}^p$.

In this reasoning, the non-diagonal elements of the energy matrix have not been considered. However, if they are small, the energies will remain essentially unaffected, though the mixing of the states produced by these non-diagonal elements will be very strong due to the degeneracy.

Similarly, possible mixing in of states of higher seniority, whose binding energy differs from that of the states of lowest seniority by the order of magnitude of the excitation energies of low-lying levels of even nuclei, should leave the binding energy (26) unaffected to the same order of magnitude. Thus, up to a fine structure of a few hundred keV, (26) may be expected to give a fairly general representation of nuclear binding energies. This expectation is indeed borne out by the facts (see § 22).

Returning to the problem of possible subshell effects, no strong competition has been observed between two subshells, each belonging to a different group of the adjacent competing subshells mentioned above. Thus, "submagic" numbers 38, 64 and 100 should still be possible.

It must be admitted that some competition exists here as well. A competition between the neutron shells $2p_{3/2}$ and $2p_{\frac{1}{2}}$ is revealed by the ground state $p_{\frac{1}{2}}$ of Fe^{57} [23, 28, 42]) and a competition between the same proton shells might be indicated by the low-lying, possibly-$p_{\frac{1}{2}}$, levels of As^{75} [43, 44, 45]), As^{77} [44]) and Br^{79} [46]). A competition between the neutron shells below $N = 64$ and the $3s_{\frac{1}{2}}$ neutron shell is revealed by the ground state $s_{\frac{1}{2}}$ of Cd^{111} [47]) and probably also of Mo^{99} [49, 50]) and Sn^{113} [48]), as well as by the $s_{\frac{1}{2}}$ level of 58 keV of Cd^{109} [28, 51]). A similar competition for the protons might be indicated by the ground state spins $\frac{1}{2}$ of Cs^{127} and Cs^{129} [52]). Finally, $Z = 64$ and $N = 100$ are reached in the rare-earths region, where there is a very high degree of configuration mixing, producing the big deformations revealed by the large nuclear quadrupole moments. Con-

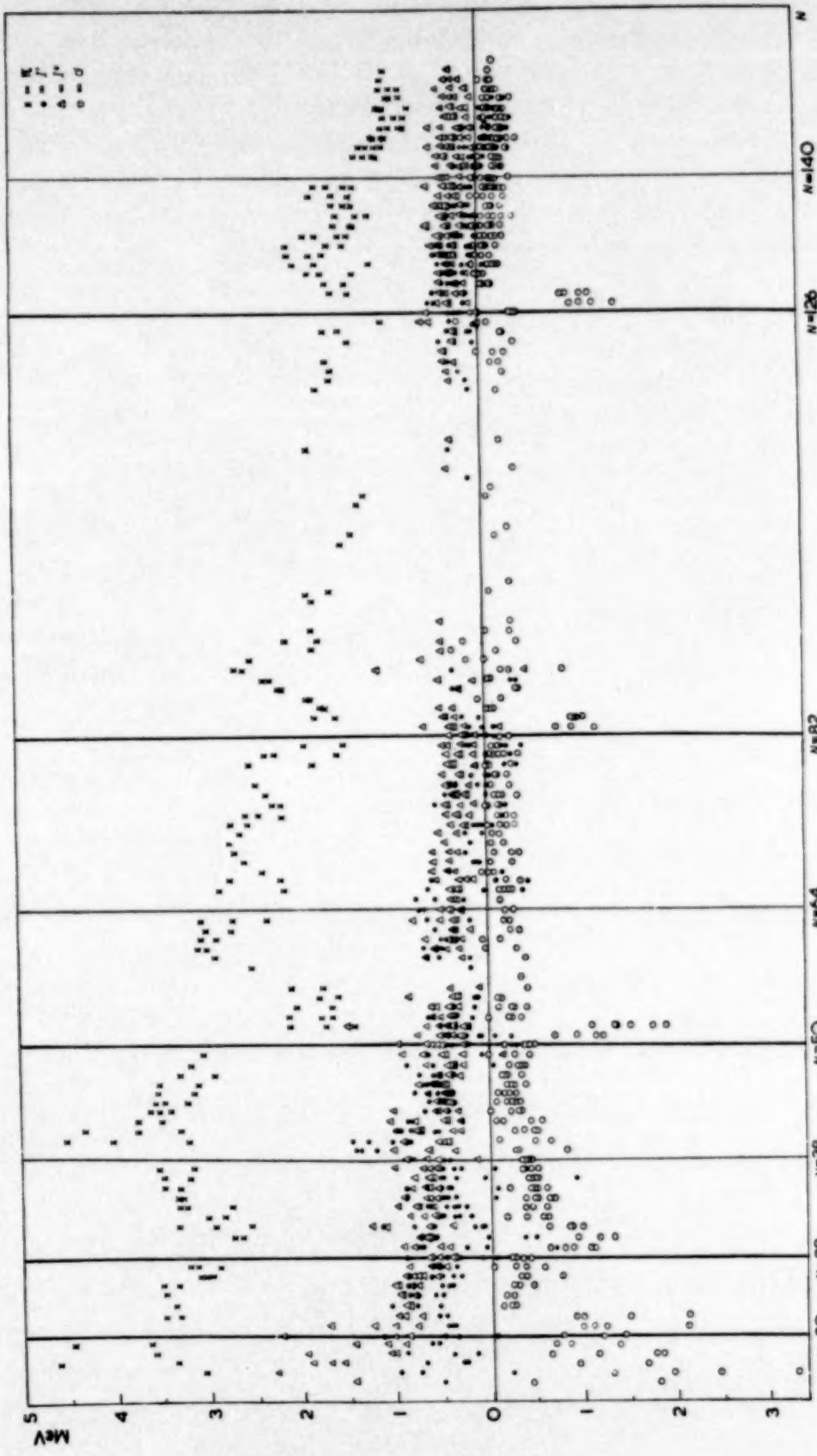

Fig. 8a. Variation of the parameters d, π, I^o and I' with neutron number.

sidering all this evidence, one can at most expect a gradual change in the slopes and distances of the separation energy lines, taking place around the above mentioned submagic numbers, rather than sharp changes at well defined nucleon numbers. As a matter of fact, the graphs of the separation energies do not show any particular changes associated with these numbers.

The situation can be seen somewhat more clearly by plotting the local values of the above mentioned slopes and distances, viz.†:

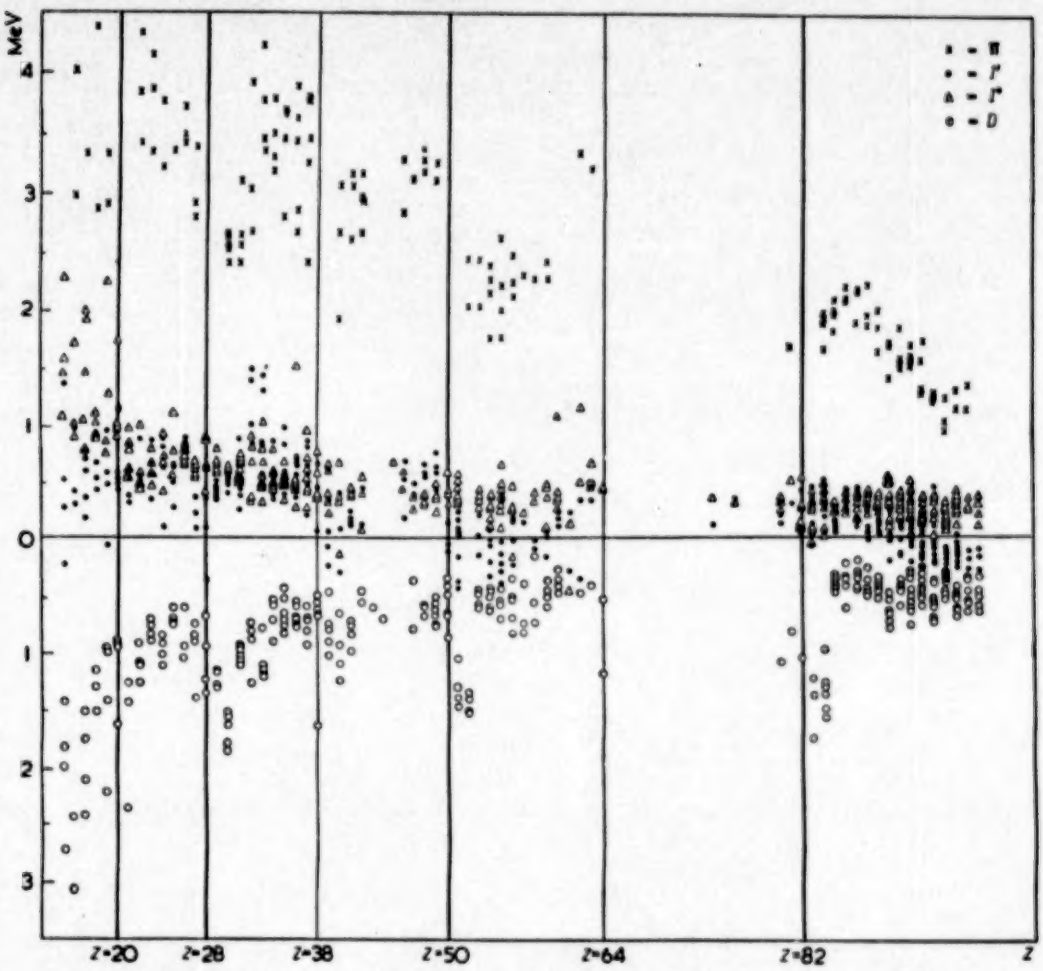

Fig. 8b. Variation of the parameters D, Π, I^0 and I' with proton number.

$$d(NZ) = \tfrac{1}{2}(S_n(NZ) - S_n(N-2,\ Z)),$$
$$D(NZ) = \tfrac{1}{2}(S_p(NZ) - S_p(N,\ Z-2)),$$
$$I^0(NZ) = \tfrac{1}{2}(S_n(NZ) - S_n(N,\ Z-2)) \text{ or } \tfrac{1}{2}(S_p(NZ) - S_p(N-2,\ Z)),$$
$$\pi(NZ) = \pm\tfrac{1}{2}(2S_n(NZ) - S_n(N-1,\ Z) - S_n(N+1,\ Z)) \quad (Z \text{ even}), \quad (27)$$

where the sign is + when N is even, and − when N is odd,

$$\Pi(NZ) = \pm\tfrac{1}{2}(2S_p(NZ) - S_p(N,\ Z-1) - S_p(N,\ Z+1)) \quad (N \text{ even}),$$

† We designate these slopes and distances by the symbols of the parameters to which they are equal. However, it should be noted that the value (27) of $\pi(NZ)$ for an odd-N nucleus, for example, is really due to the neutron pairing energies of its two even-N neighbours.

where the sign is + when Z is even, and − when Z is odd,

$$I'(NZ) = \pm\tfrac{1}{2}(2S_n(NZ) - S_n(N, Z-1) - S_n(N, Z+1)) \quad \text{or}$$
$$\pm\tfrac{1}{2}(2S_p(NZ) - S_p(N-1, Z) - S_p(N+1, Z)), \tag{27}$$

where the sign is + when $N+Z$ is even, and − when $N+Z$ is odd,

as functions of the neutron and proton numbers. These are shown in figs. 8a, b. One then finds all the effects connected with the magic numbers already discussed in § 9 †. However, the only definite submagic-number effect is the reduction of proton pairing energy after $Z = 38$ is crossed, mentioned in the same section. No particular effect is found at $N = 38$, 64 and 100 or at $Z = 64$. Though it must be admitted that precise experimental data in the region including $Z = 64$ and $N = 100$ are too scanty to allow a definite conclusion ††.

We shall later see (§ 17) that no definite subshell effects can be detected in beta decay systematics as well, and a similar situation has been recently found in the behaviour of total binding energies [12]).

12. Quantitative Treatment of Nucleon Separation Energy Systematics

The results of § 11 suggest ††† that in a local region not including a magic number, the separation energies may be fairly well represented by a linear formula with constant parameters, which is obtained from (26):

$$S_n(N_0+n, Z_0+p) = c + \tfrac{1}{2}\pi + (n-1)d + pI^0 - \Delta_n\delta \tag{28a}$$

$$S_p(N_0+n, Z_0+p) = C + \tfrac{1}{2}\Pi + (p-1)D + nI^0 - \Delta_p\delta, \tag{28b}$$

where

$$\Delta_n\delta = \tfrac{1}{2}(-1)^{n+1}\pi + \tfrac{1}{2}(-1)^n(1-(-1)^p)I' \tag{29a}$$

$$\Delta_p\delta = \tfrac{1}{2}(-1)^{p+1}\Pi + \tfrac{1}{2}(-1)^p(1-(-1)^n)I'. \tag{29b}$$

The numerical values of the parameters for each region should be obtained by comparing the formula with the experimental data.

There remains the problem of the appropriate nucleon numbers to be

† At a magic neutron number N_0, $d(N_0+1, Z)$ as defined above includes also the reduction of the single-neutron binding energy c when the shell edge is crossed, and is thus much lower than neighbouring $d(NZ)$. Similarly, $d(N_0+2, Z)$ includes both the above mentioned reduction of c, as well as the reduction of π, and is thus even lower than $d(N_0+1, Z)$ when the latter reduction exists. On the other hand, $\pi(N_0Z)$ and $\pi(N_0+1, Z)$, which are also influenced by the reduction of c, have not been drawn in the figures at all. Similar remarks apply to proton parameters at proton magic numbers.

†† Thus it has been recently [30, 29]) pointed out that the experimental data now available indicate discontinuities in the general trends of the separation energies around $N = 90$ and $N = 116$, where the transition into the region of rotational properties and out of it, respectively, take place.

††† This is entirely analogous to Levy's treatment [53, 54]) of beta decay energies (see § 18).

chosen for the region boundaries. The "official" magic numbers 20, 28, 50, 82 and 126 form natural such boundaries. In fact, the considerations of § 11 show that they are the only natural boundaries (with the possible exception of $Z = 38$, already mentioned (§§ 9 and 11)).

However, due to the variation of the nuclear parameters when the mass number increases, it is clear, that in order to achieve a satisfactory agreement of formulae (28a, b) with the experimental data, one has to introduce a finer division into subregions. The tradition in treatments of nuclear energies [53–56]) has been to introduce 40, 64, and sometimes also 106 and 140 as submagic numbers. From the practical point of view, at least as far as the smoothly varying direction-independent parameters d, D and the I^0's are concerned, the choice is quite appropriate, as the above mentioned numbers † lie more or less midway between magic numbers. However, choosing them in preference to any other of their neighbours, seems to be but a matter of tradition, based on the fact that these numbers correspond to complete subshells in the original Mayer [1, 57])-Haxel-Jensen-Suess [58]) scheme. Actually, the strong mixing of nuclear subshells causes nuclear shell filling to deviate considerably from this ideal scheme, and the above numbers are hardly more magic than any neighbouring number. We shall adopt Levy's [53, 54]) subdivision into shell and subshell regions.

Table 1 shows the results of a least-squares fit of the experimental separation energies to formulas (28a, b). In order to obtain useful values of the parameters, we fitted only separation energies known with a precision better than 250 keV. The table gives the "best" average values of the parameters

TABLE 1

Nuclear Parameters in the various shell regions, obtained by comparing formulae (28a, b) with experimental values of nucleon separation energies

Region Z	Region N	Parameters (MeV) c	C	π	Π	d	D	I^0	I'	Mean Deviation (MeV)	Number of data treated
21—28	21—28	8.686	3.738	3.269	3.816	—0.331	—0.795	0.732	0.672	0.455	58
21—28	29—40	5.077	9.907	2.844	3.296	—0.514	—0.836	0.624	0.375	0.325	61
29—40	29—40	6.421	1.968	3.564	2.920	—0.445	—0.934	0.642	0.611	0.273	62
29—40	41—50	4.839	8.871	3.344	3.260	—0.240	—0.736	0.511	0.566	0.304	95
29—40	51—82	2.069	17.115	1.514	2.623	—0.225	—1.028	0.427	0.199	0.202	26
41—50	51—82	6.817	5.240	2.452	2.975	—0.207	—0.501	0.351	0.309	0.266	86
51—64	51—82	7.400	4.160	2.238	2.295	—0.153	—0.521	0.299	—0.011	0.221	92
51—64	83—126	2.918	9.149	2.053	2.441	—0.086	—0.477	0.300	0.163	0.339	57
65—82	83—126	8.160	1.740	1.673	1.832	—0.205	—0.655	0.361	0.307	0.318	88
>82	127—140	3.975	3.781	1.569	1.884	—0.102	—0.433	0.317	0.203	0.173	178
>82	>140	3.409	8.933	1.071	1.438	—0.173	—0.496	0.245	—0.083	0.143	144

† This sentence, as well as the following one, apply only to the numbers 40, 64 and 106. There is no a priori expectation of a neutron subshell at $N = 140$ [53, 54]). However, the pairing parameters change appreciably around this neutron number. In particular, I' becomes negative on the higher-N side (fig. 8a).

in each region, as well as the mean deviation and the number of cases treated.

The table reproduces quantitatively the general features of the nuclear parameters along the periodic system of nuclei, already referred to in §§ 8 and 9. It is remarkable, that the specifically-proton parameters, such as D and Π, are affected by crossing a neutron shell edge to no lesser degree than the corresponding neutron parameters d and π, and vice versa. This is partly connected with the gradual variation of the absolute values of all these parameters when the mass number increases, irrespectively of shell edges.

The single-neutron energy c decreases when a neutron shell is crossed, and increases when a proton shell is crossed. This is comprehensible, since in the first case the repulsion of the neutrons in the newly closed shell becomes included in c, thus reducing its value, and in addition to this there is the weaker binding in the new outer shell †. In the second case, the attraction I^0 of the protons in the newly closed shell becomes included in c, increasing its value. This explanation is roughly quantitatively confirmed by the numerical values of the parameters of table 1. It might indicate a rough method of extrapolation of table 1 and of the use of eqs. (28a, b) to shell regions removed from the region of stable nuclei, for which no experimental separation energies are available (see also § 22).

Finally, the I' is on the average negative for the shell regions represented by the seventh and by the last line of table 1, whereas according to its shell model definition I' should be positive for the ground states of nuclei [32]) (§ 8.1). This might either indicate a complete breakdown of the shell model in these regions (which is comprehensible for the heaviest nuclei with $N > 140$, but not too plausible for nuclei with $N < 82$), or it might be due to our inadequate knowledge of the experimental data in these regions.

The mean deviations are of the order of 200—400 keV. This might then be considered the order of magnitude of the elements of the energy matrix which were neglected in the simplified treatment (28a, b), viz. the non-diagonal elements between the several competing subshells whose existence was altogether ignored in eqs. (26) and (28a, b), as well as the energy difference between these subshells, and also possible contributions of states of higher seniority (see the discussion following formula (26)).

The deviations are largest for the nuclei of the $1f_{7/2}$ shells. This might indicate that they are too light for the approximation (19), regarding neutrons and protons as coupled separately, to be valid for them ††.

It is worth mentioning that the agreement of the formulae with the data in the rare-earths region is hardly worse than in other regions showing shell

† This last cause applies only to main shells, beginning after one of the magic numbers.

†† Levy [53, 54]) altogether excluded the $1f_{7/2}$ nuclei from his treatment of beta decay energies and nuclear masses (see §§ 18 and 22, respectively), because of similar larger deviations.

model properties, and the best agreement is found in the region of the heavy alpha-decaying nuclei, though the shell model is known to be invalid for these two "rotational" regions. A parallel situation was found by Levy [53, 54] to hold for his empirical treatment of beta decay energies, which was likewise based on a formula equivalent to the energy formula (26). Again, total nuclear binding energies or nuclear masses of the transmercury elements were found by him to be represented by a formula equivalent to (26) even more adequately than nuclear masses in the conventional shell regions. A possible qualitative incorporation of such facts within the framework of the shell model was indicated in § 11.

Thus, although eq. (26) was derived by shell model considerations, it is largely independent of the assumption of an essentially spherically-symmetrical nucleus, characterizing this model. *Formula* (26) *holds for any system of nucleons, in which identical nucleons are paired off as far as possible, and there remain after this strong pairing interaction a weaker attraction towards nucleons of the opposite kind, and a similar repulsion from nucleons of the same kind, which are independent of the mutual orientation of the nucleons* †.

We conclude with some remarks concerning the practical applications of the treatment based on eqs. (28a, b). The parameters of table 1 may be used to predict unknown separation energies up to the order of two to four hundred keV, as shown by the mean deviations. This might also be useful in clarifying the assignment of (γ, n) and (p, d) reactions and their inverses. Similarly, the parameters may be used to predict Q-values of other nuclear reactions, as well as nuclear mass differences.

An even simpler use than that of table 1 in predicting unknown separation energies might be made of figures like 1a, b and 3a, b. As mentioned in § 5, these are the separation energy analogue of the Way and Wood beta-decay systematics, and might be used in the same manner. However, they may be used only in regions with well defined and not-too-short lines, whereas the parameters of table 1 may also be used to predict separation energies of nucleides having no isotopes or isotones with known separation energies.

13. The Interaction of the Odd Neutron and Odd Proton in Odd Nuclei

In this section we want to investigate somewhat more closely the dependence on n_1 and p_3 of the parity term I'_{13J} (eq. (16)).

In the first place we emphasize that I'''_{13J} does not, as a rule, vanish (which could make I'_{13J} n_1- and p_3-independent from the outset). Were it to vanish,

† See also appendix I of Part I of ref. [53]).

the order and the energies of the J-levels of different odd nuclei with the same odd shells would have to be the same, depending solely on the I''_{13J}. However, this is found not to be the rule in the few cases of odd nuclei where the configurations of the odd groups can be inferred from the values of the nuclear magnetic moments [47]). A conspicuous example is afforded by the three isotopes Co^{56}, Co^{58}, and Co^{60}, all having the odd configuration $p^n_{3/2}\, f^p_{7/2}$ according to an analysis of their magnetic moments [47, 59]), and having ground state spins $J = 4$, 2 and 5, respectively. As a matter of fact, an attempt [60]) to explain the variation as nucleons are added of the ground state spins of odd nuclei, depended essentially on the term

$$\frac{2j_n+1-2n}{2j_n-1}\cdot\frac{2j_p+1-2p}{2j_p-1}I'''_{npJ}$$

in eq. (16).

Nevertheless, in our cruder treatment of separation energies and binding energies, its neglect as in § 4.1 is justified. In order to see this we shall consider the neutron separation energies of the odd-Z $1f_{7/2}$ nuclei. For such nuclei one obtains from (21) and (16)

$$S_n(j_n{}^n j_p{}^p) = c+\tfrac{1}{2}\pi+(n-1)d+pI^0 + \begin{cases} -\left(\tfrac{1}{2}\pi-I''-\dfrac{2j_p+1-2p}{2j_p-1}\cdot\dfrac{2j_n+1-2n}{2j_n-1}I'''\right) & \text{odd } N \\ +\left(\tfrac{1}{2}\pi-I''-\dfrac{2j_p+1-2p}{2j_p-1}\cdot\dfrac{2j_n+3-2n}{2j_n-1}I'''\right) & \text{even } N \end{cases} \cdot \quad (30)$$

For isotopes of the same parity type this is again linear in n, however the slope depends on the parity of N, being

$$d-\frac{2(2j_p+1-2p)}{(2j_p-1)(2j_n-1)}I''' \text{ for odd } N, \text{ and } d+\frac{2(2j_p+1-2p)}{(2j_p-1)(2j_n-1)}I'''$$

for even N. In addition, the slope also depends on p, so that the S_n lines of different elements should no longer run parallel. Similar results hold for the S_n lines connecting isotones, and for the S_p lines. Thus the networks of parallelograms of the $1f_{7/2}$ nuclei in figs. 1b and 3b should be distorted as compared to those of figs. 1a and 3a. Actually they do not appear to be more distorted.

TABLE 2

Nuclear parameters in the $1f_{7/2}$ shell, obtained by comparing formula (30) with experimental values of nucleon separation energies

Parameters (MeV)									Mean Deviation (MeV)	Number of data treated
c	C	π	Π	d	D	I^0	I''	I'''		
8.831	3.739	3.309	3.825	−0.366	−0.795	0.732	0.710	0.170	0.451	58

In order to have a more quantitative check, we tried to fit formula (30), with its S_p-analogue, to the experimental separation energies of the $1f_{7/2}$ nuclei. The resulting parameters and deviations are given in table 2. The fit with (30) is hardly better than with (28a, b), as seen by comparing table 2 with the first line of table 1 †. The values of the parameters are likewise essentially the same, and I''' is much smaller than the mean deviation.

It seems, that the errors introduced by an approximation regarding the seniority as a good quantum number, far exceed the errors introduced by the neglect of the variation of I' with n and p ††.

CHAPTER II. BETA AND ALPHA DECAY ENERGIES

A. Beta Decay Energies

14. Linear Relationships

For the simple case of beta decay in which the nuclear configuration changes from $(j_1^{n_1} j_2^{n_2} j_3^{p_3} j_4^{p_4})$ to $(j_1^{n_1-1} j_2^{n_2} j_3^{p_3+1} j_4^{p_4})$, the decay energy is given by

$$\begin{aligned} Q_{\beta^-} &= (M_n - M_H) + B(j_1^{n_1-1} j_2^{n_2} j_3^{p_3+1} j_4^{p_4}) - B(j_1^{n_1} j_2^{n_2} j_3^{p_3} j_4^{p_4}) \\ &= (M_n - M_H) + (C_3 - c_1) + \tfrac{1}{2}(\Pi_3 - \pi_1) - (n_1 - 1)(d_1 - I^0_{13}) + n_2(I^0_{23} - I^0_{21}) \\ &\quad + p_3(D_3 - I^0_{13}) + p_4(I^0_{34} - I^0_{14}) - \Delta_{\beta^-}\delta \end{aligned} \tag{31}$$

where $\Delta_{\beta^-}\delta$, the change of the parity term (20) caused by the decay, is given by

$$\Delta_{\beta^-}\delta = \tfrac{1}{2}(-1)^{n_1}\pi_1 + \tfrac{1}{2}(-1)^{p_3}\Pi_3 - \tfrac{1}{2}(-1)^{n_1}\cdot(1+(-1)^{n_1+p_3})I'_{13}. \tag{32}$$

It follows that for nuclei of the same parity type, in which the nucleons enter the same shells, the Q_{β^-} will be a linear function of the numbers of neutrons and protons, and also of any linear combination of them, such as the total mass number $A(=N+Z)$ or the isotopic number $I(=N-Z)$.

Keeping Z constant and varying N, one obtains the Way and Wood [21] straight lines connecting alternate isotopes, which have an upward slope of $(I^0_{np} - I^0_{nn}$ (or $d))$. Keeping N constant and varying Z, one obtains straight lines connecting alternate isotones sloping downward with a gradient given by $(I^0_{pp}$ (or $D) - I^0_{np})$, which is even steeper (eq. (23)) than that of the lines connecting isotopes. Both the lines connecting isotopes and the lines connecting isotones will in the sequel be referred to as the Way and Wood

† It is worth mentioning, that when considering only the odd nuclei of the $1f_{7/2}$ shell, formula (30) gives a somewhat better fit than (28a, b), the mean deviation being 0.32 MeV with (28a, b) and 0.28 MeV with (30). However, this does not alter the following conclusion.

†† See also the treatment of K^{42} [7]) and of Cl^{40} [9]) by Talmi *et al.*

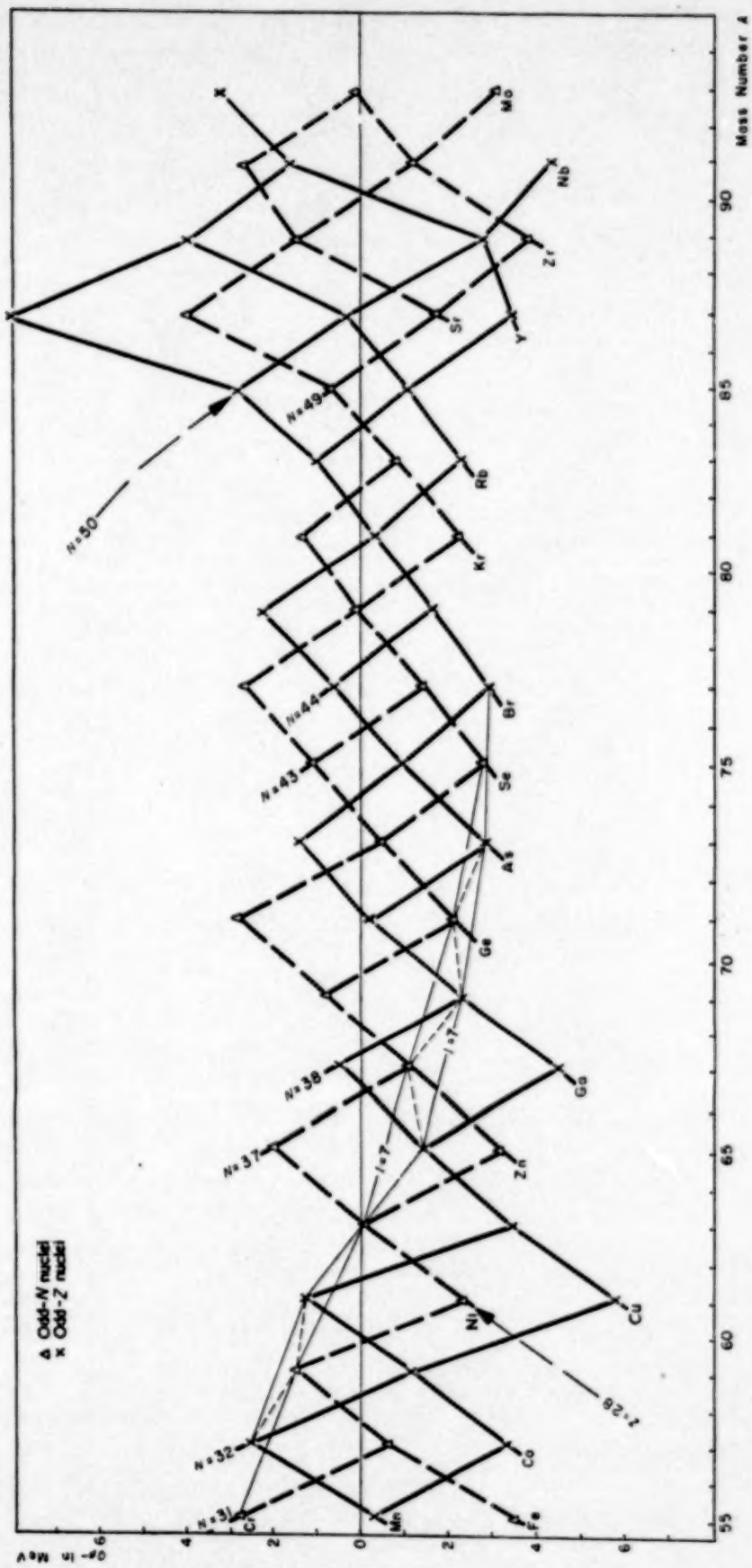

Fig. 9a. Way and Wood lines for odd-mass nuclei (bold lines). Two Suess and Jensen lines for $I = 7$ are also shown (thin lines).

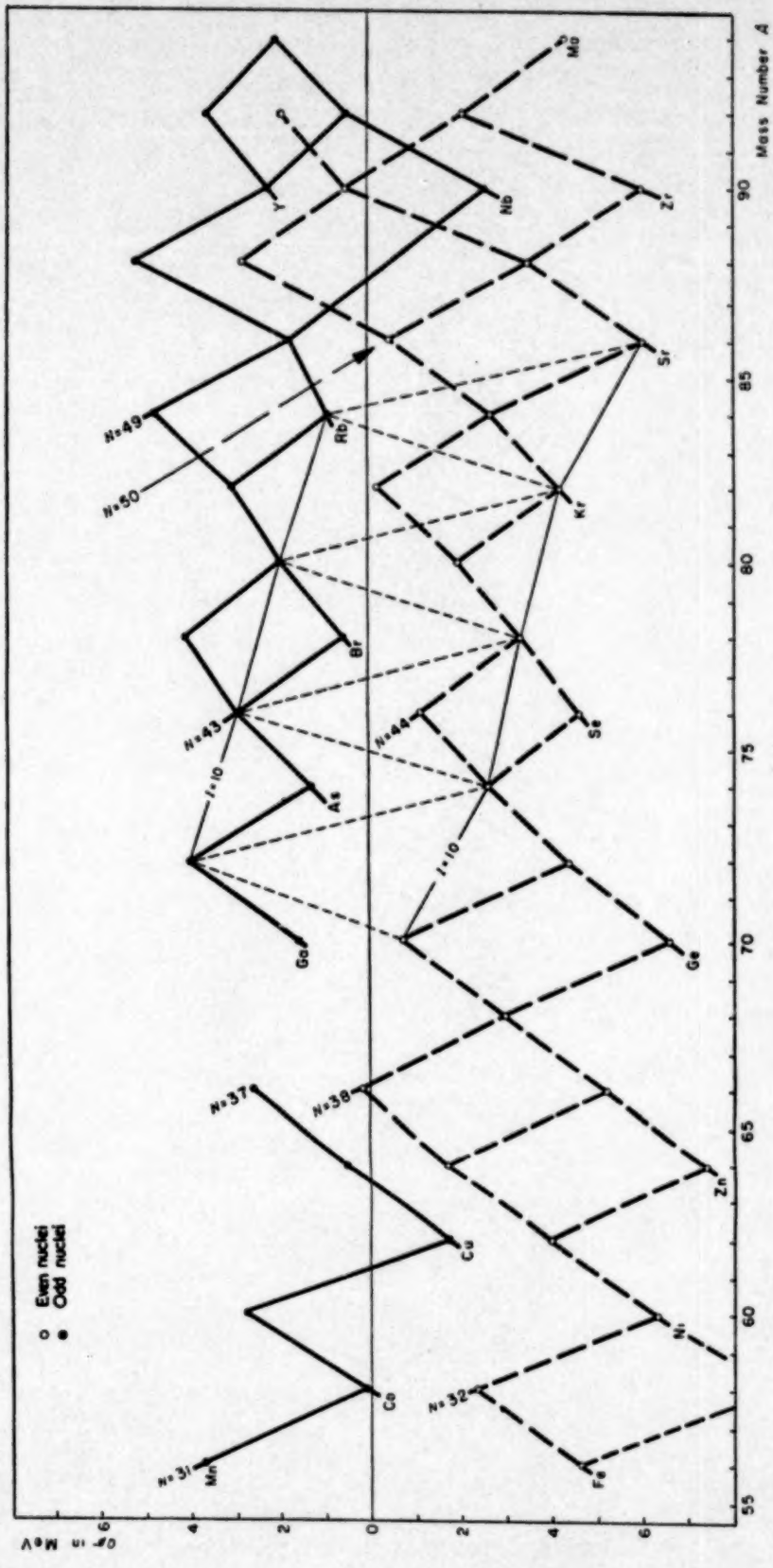

Fig. 9b. Way and Wood lines for even-mass nuclei (bold lines). Two Suess and Jensen lines for $I = 10$ are also shown (thin lines).

lines, even though only the former were originally given by Way and Wood. Their slopes are about twice that of the nucleon separation energy lines of figs. 1a, b and 3a, b, which is obvious when visualizing the beta decay process as a removal of a neutron from the nucleus, followed by the addition of a proton.

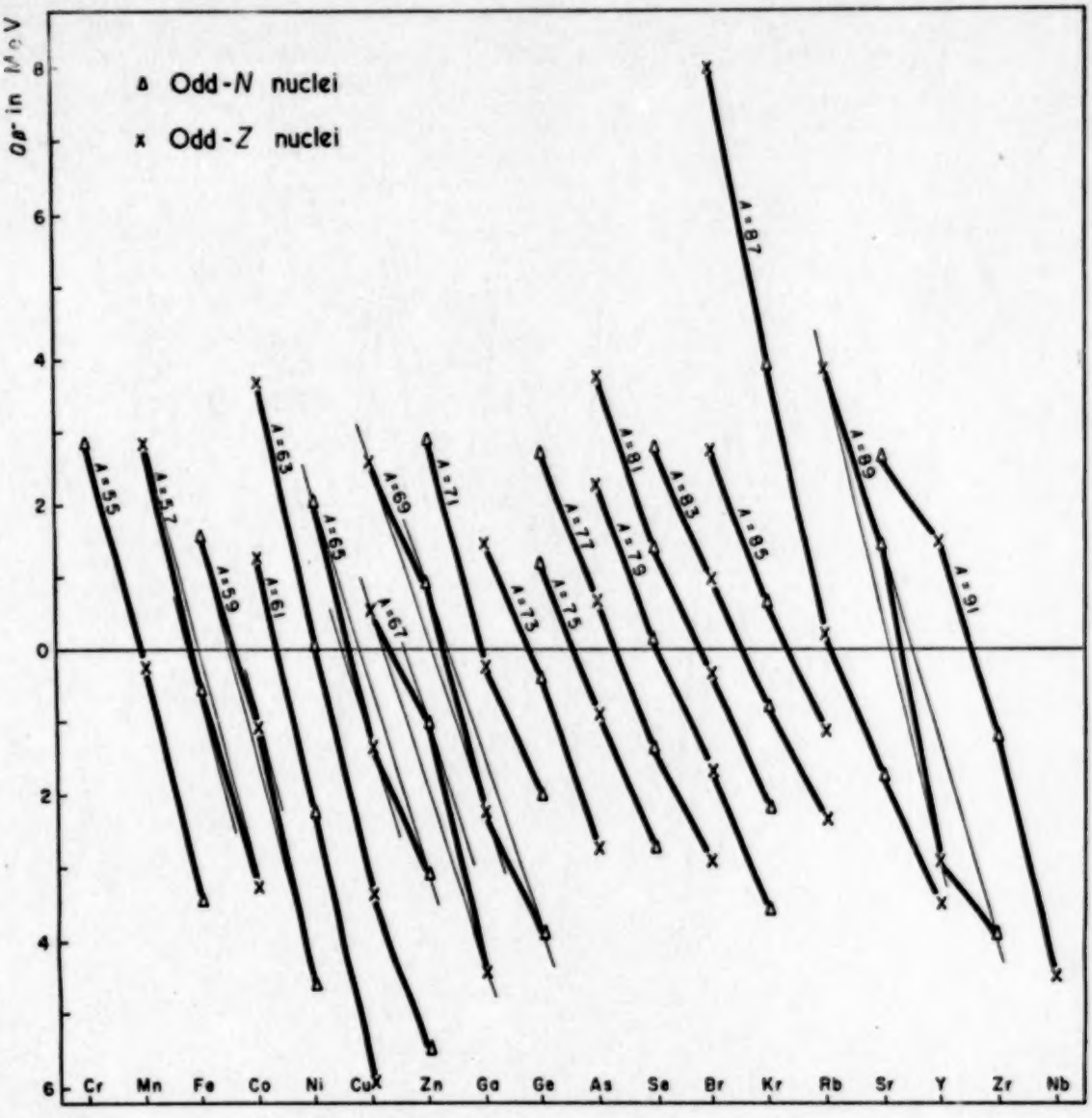

Fig. 10a. Beta decay Ghoshal and Saxena zig-zag lines for isobaric odd-mass nuclei (bold lines). Some enveloping Kumar and Preston lines are also shown (thin lines).

Figs. 9a, b show part of the Way and Wood systematics. The data were taken from refs. [26]) and [28]). Each line connecting isotopes is designated by the chemical symbol of the β^--decaying element. Some of the lines connecting isotones are designated by the neutron number of the β^--decaying nuclei. To avoid overcrowding of the lines, Way and Wood segregated them accord-

ing to the parity of the mass number A. Glass *et al.* [18]) continued the systematics into the region of the heavy alpha-decaying nuclei.

Connecting the beta decay energy values of alternate isobars, the Kumar

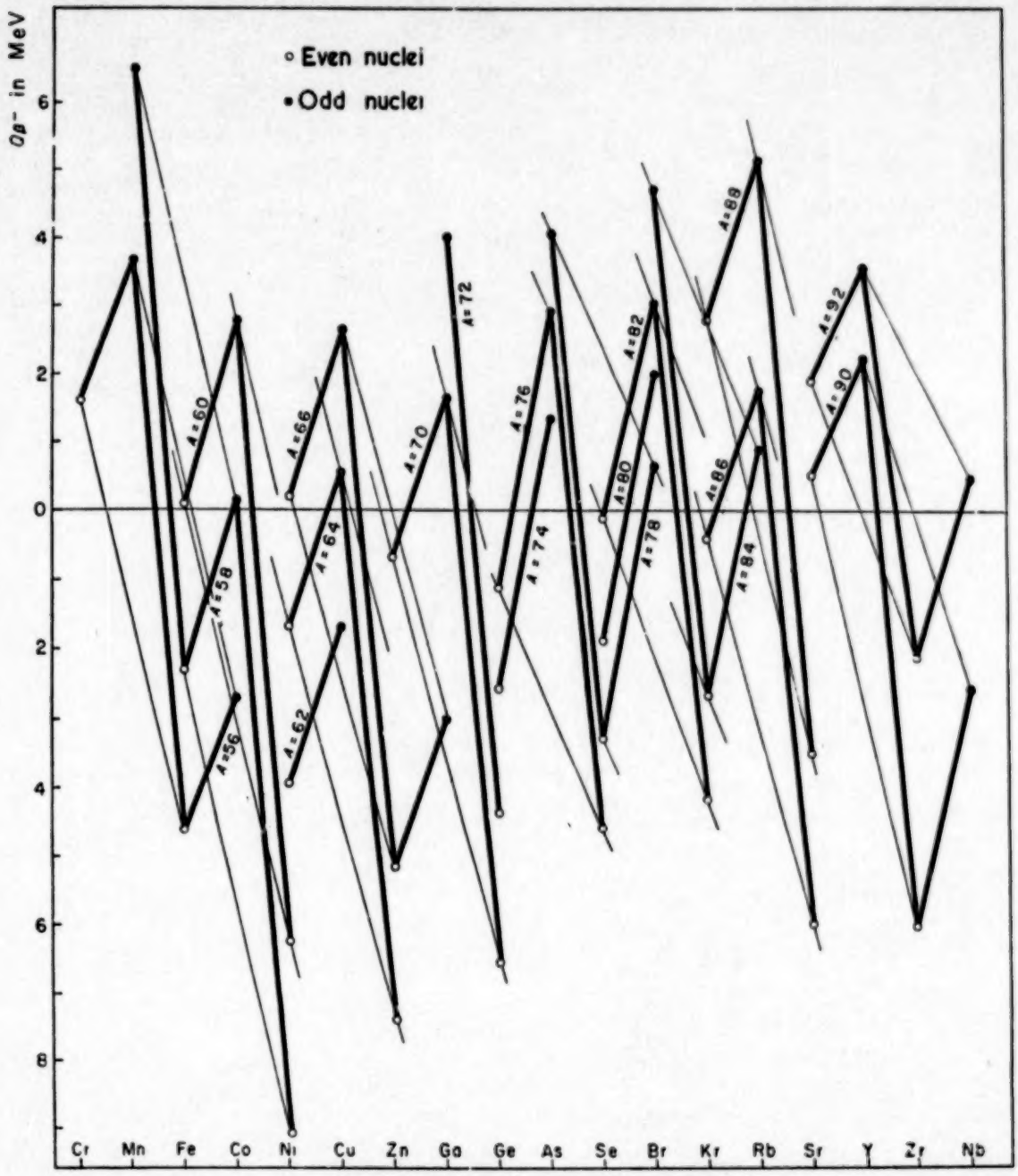

Fig. 10b. Beta decay zig-zag lines for isobaric even-mass nuclei (bold lines). Some enveloping Kumar and Preston lines are also shown (thin lines).

and Preston [61]) lines are obtained. Their slope, when Z increases, is given by $[d(\text{or } I^0_{nn})+D(\text{or } I^0_{pp})-2I^0_{np}]$, which is negative and about twice as steep as the Way and Wood lines. Its absolute value is usually called B_A †

† The subscript A is appended, since in most of these treatments B is considered a function of A.

in treatments of beta decay energetics [18, 55, 56, 61, 64, 103, 104]), and it gives the curvature of the parabolic section of the mass surface connecting isobars, at the vertex of the section.

Figs. 10a, b show (thin lines) some Kumar and Preston lines for odd-mass and even-mass nuclei, respectively.

Keeping I constant, the Suess and Jensen [62]) straight lines connecting alternate isodiapheres are obtained. Their slope is $(I^0_{pp}(\text{or } D)-I^0_{nn}(\text{or } d))$, which is slightly negative. Each of these lines possesses many more points than the Way and Wood lines. Figs. 9a, b show (thin lines) also four Suess and Jensen lines, for $I = 7$ and $I = 10$, respectively, each connecting nuclei of a different parity type.

Such lines have also been drawn on several other occasions [39,105–107]).

15. Zig-Zag Relationships

15.1 Z OR N CONSTANT

Let us, for the sake of definiteness, assume that from one isotope to its immediate successor, the neutrons are added in shell j_1. The increase of beta decay energy from one isotope to another will consist of an alternating part, $\pm(\pi_1-I'_{13})$, superposed on the steady increase of $(I^0_{np}-d)$. This results in a zig-zag line when connecting beta decay energy values of consecutive isotopes. The alternating part determines the vertical distance between the two Way and Wood lines of different parity types belonging to the same element †. The value of the brackets is always positive (see table 1), and the Way and Wood line connecting odd-N isotopes will therefore always be above the line connecting the even-N isotopes.

Similarly, assume that in a sequence of successive isotones, the protons are added in shell j_3. Then, if the beta decay energy values of consecutive isotones are connected, there is an alternating change $\pm(\Pi_3-I'_{13})$ superposed on the steady decrease $(D-I^0_{np})$. This again results in a zig-zag line when connecting beta-decay energy values of consecutive isotones. The alternating part equals in magnitude the vertical distance between the two Way and Wood lines of different parity type connecting isotones †. Here the line connecting the odd-Z isotones will always be above the line connecting the even-Z isotones.

Figs. 11a, b show such zig-zag lines connecting isotopes and isotones, respectively. The enveloping Way and Wood lines are also shown (thin lines).

† These two lines do not appear in the same diagram, since the lines are segregated according to the parity of A.

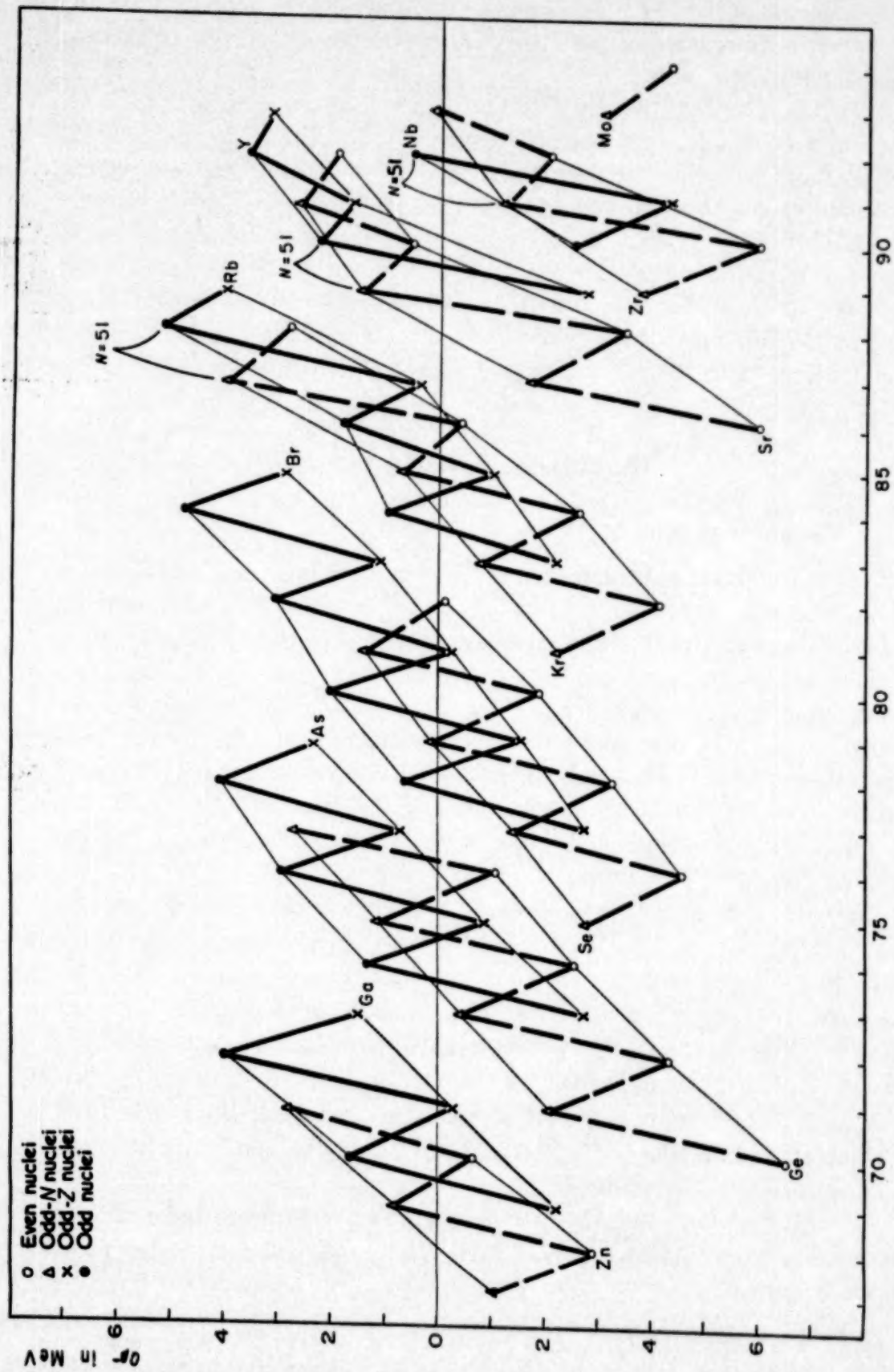

Fig. 11a. Zig-zag lines connecting beta decay energy values of consecutive isotopes (bold lines). The enveloping Way and Wood lines are also shown (thin lines).

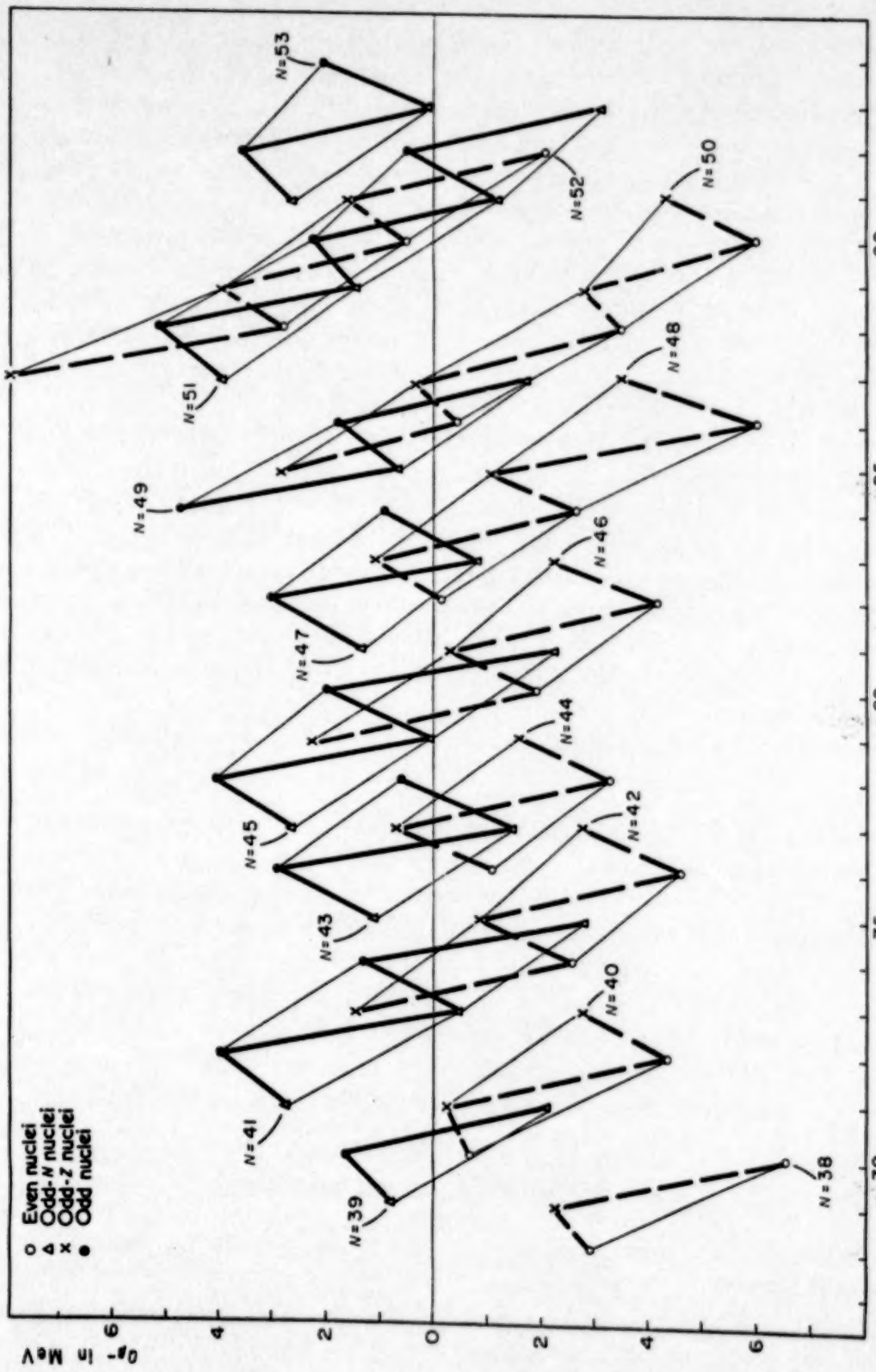

Fig. 11b. Zig-zag lines connecting beta decay energy values of consecutive isotones (bold lines). The enveloping Way and Wood lines are also shown (thin lines).

15.2 MASS NUMBER A CONSTANT

When progressing in a chain of isobars from one isobar to its higher-Z successor, the beta decay energy decrease will consist of an alternating part superposed on the steady decrease of $(d_1+D_3-2I^0_{13})$†. This results in a zig-zag line when connecting beta decay energy values of consecutive isobars. The alternating part determines the vertical distance between the Kumar-Preston lines. Its magnitude depends on the parity of the mass number A. For even A the odd-Z line lies above the even-Z line at a distance of $(\pi_1+\Pi_3-2I'_{13})$, which is of considerable magnitude. This distance is usually called $2\delta_A$ †† in treatments of beta decay energetics [18, 55, 61, 63, 103, 104]), and the existence of the related zig-zag line is perhaps the most direct way to show the splitting of the parabolic section of the mass surface at a given even A, according to the parity type.

For odd A the odd-Z line lies at a distance $(\Pi_3-\pi_1)$ above the even-Z line. This distance, which is much smaller than $2\delta_A$ and might change sign from one shell region to another, is usually [55, 56, 61, 63, 108]) denoted by $2\varepsilon_A$ ††. The related zig-zag lines were drawn by Ghoshal and Saxena [64]). The existence of the Ghoshal-Saxena zig-zag lines for odd A, connected with the non-vanishing of ε_A, is perhaps the most direct way to show the difference in pairing energy which might exist between neutrons and protons, and the splitting of the parabolic section of the mass surface for constant odd A caused thereby.

Isobaric beta-decay zig-zag lines are shown in figs. 10a, b (bold lines).

15.3. NEUTRON EXCESS I CONSTANT

Connecting the values of beta decay energies of successive isodiapheres, a zig-zag line is obtained, enveloped by two parallel straight Suess and Jensen lines. The vertical distance between the latter, which determines the magnitude of the zig-zag alternations, is the same as for the Kumar-Preston lines, viz.: $2\delta_A$ for even-A and $2\varepsilon_A$ for odd-A ones. In this way, Suess and Jensen [62]) demonstrated for the first time the generality of the occurrence of different pairing energies for neutrons and for protons, which was until then known only for the heaviest elements [65]).

Two isodiapheric zig-zag lines are shown in figs. 9a, b (broken thin lines).

16. The Beginning of a New Shell

When a new neutron shell begins to fill in the decaying nucleus, c_1 in eq. (31) decreases †††, resulting in an upward discontinuity in the straight

† For the sake of definiteness, we assume that here, too, the numbers of nucleons change from one isobar to another in shells j_1 and j_3.

†† Concerning the subscript A see footnote in § 14.

††† Naturally, the decaying neutron will be the less tightly bound neutron in the new shell.

lines connecting isotopes mentioned in § 14. Similarly, when a new proton shell begins to fill in the product nucleus, the C_3 decreases, and the straight lines connecting isotones break downwards. Such discontinuities are seen in figs. 9a, b, for the magic numbers $N = 50$ and $Z = 28$. Corresponding discontinuities for $N = 50$ are also seen in fig. 11a. The other magic numbers manifest themselves as well, as shown in the original graphs of Way and Wood, Suess [106]), Suess and Jensen, Feather [107]) and Glass *et al.* [18]).

It should be specially mentioned that no extraordinary increase in beta decay energy, due to extra binding of the product nucleus, is predicted by eq. (31) when the product nucleus is Z-magic, and likewise no extraordinary decrease when the decaying nucleus is N-magic. Conversely, the fact that such magic nuclei lie on the same line as their predecessors is a decisive demonstration of the fact that they are no more tightly bound relatively to their predecessors than the latter are bound relatively to their respective predecessors. This fact was already encountered in connection with the separation energies (§ 10) and will be further discussed in connection with the total binding energy of the nucleus (§ 23.2).

In addition to discontinuities, there might be changes in the slopes of, and distances between, the lines, corresponding to variations of the 'orientation-independent' and 'pairing' interactions, respectively, between the nucleons. In particular, since the pairing energy decreases abruptly after a corresponding shell edge is crossed, ε_A might abruptly reverse its sign [55, 56, 61, 62, 64, 108]) †. This is reflected in a reversal of the relative position of the isodiapheric lines in fig. 9a when the magic number $Z = 28$ is crossed, and of the odd-Z and odd-N Kumar-Preston lines in fig. 10a. Likewise, δ_A decreases considerably on crossing a shell edge [61, 64]).

17. Subshell Effects

It was pointed out by Way and Wood [21]) that their systematics is particularly suited for studying neutron and proton subshell effects, as it shows the beta decay energy variations when shells of one kind of nucleons are being filled, the number of nucleons of the other kind remaining constant. For this purpose it is certainly advantageous to choose as abscissa the mass number A, rather than N of the original graphs of Way and Wood, and draw the lines connecting both isotopes and isotones (see figs. 9a, b), in complete analogy to figs. 1a, b and 3a, b of the separation energy systematics. This allows proton shell effects to manifest themselves by changes of slopes of the lines connecting isotones ††, is complete analogy to neutron

† This is the Suess and Jensen [62]) rule: when one kind of nucleons crosses a magic number, its pairing energy is smaller than that of the other kind.

†† This idea is also due to Way and Wood [21]).

shell effects in the lines connecting isotopes, whereas with N as abscissa, proton shell effects are given by changes of the distances between the lines connecting isotopes.

Glass, Thompson and Seaborg [18]) also chose A as abscissa in their beta decay energy diagrams of the transmercury elements. However, they found it useful for their purpose to connect the values of isodiapheres instead of isotones.

A study of the analogous separation energy systematics exemplified in figs. 1a, b and 3a, b has shown that nuclear subshells are usually considerably mixed, and subshell effects can hardly be observed (figs. 8a, b). However, since beta decay energies are usually known with a much better precision than separation energies †, one might still expect that their study might reveal delicate subshell effects, which might have become unobservable in the separation energies due to small errors in the experimental data.

As far as the slopes of and distances between the lines are concerned, no definite subshell effects are observed in figs. 9a, b, corresponding to the proton subshells $1f_{5/2}$, $2p_{3/2}$ and $2p_{\frac{1}{2}}$ and the neutron subshells $1f_{5/2}$, $2p_{3/2}$ $2p_{\frac{1}{2}}$ and $1g_{9/2}$, which are being filled in this region. The only possibly-subshell effect is the decrease of the distance between the Suess and Jensen lines in fig. 9a after $N = 40$ is crossed. This corresponds to a decrease of $|\varepsilon_A|$. Similarly, no definite subshell effects in the Way and Wood graphs are observed in the other shell regions, as already remarked by Way and Wood. Likewise, no definite subshell effects are observed when plotting the local values of the slopes and distances between the Way and Wood lines as functions of N or Z, in the same manner as was done for the separation energy lines in figs. 8a, b.

Coryell [55]), Kumar and Preston [61]) and Fix [56]), studied the variation with nucleon numbers of beta decay parameters related to the parabolic section of the mass surface through isobaric nuclei (eq. (34), § 18). They also found no definite subshell effects associated with submagic numbers (Except at $Z = 64$? [55])).

Thus, as far as subshell effects are concerned, the situation with beta decay energies is the same as with separation energies, confirming the conclusion derived from the latter about the usually-considerable mixing of nuclear configurations.

18. Quantitative Treatment of Beta Decay Energy Systematics

The linearity of the Way and Wood systematics suggests in a natural way †† the treatment of beta decay energies as if in a given shell region there

† Which might be a reason for the better linearity of the Way and Wood lines as compared to that of figs. 1a, b and 3a, b.

†† This idea is due to Levy [53, 54]). A similar treatment of separation energies was carried out in § 12.

is but one incomplete neutron shell, j_n^n, and one incomplete proton shell, j_p^p. Beta decay energies are then given by

$$Q_{\beta-}=(M_n-M_H)+(C-c)+\tfrac{1}{2}(\Pi-\pi)-(n-1)(d-I^0)+p(D-I^0)-\Delta_{\beta-}\delta, \quad (33)$$

where $\Delta_{\beta-}\delta$ is obtained from (32) by dropping the indices 1 and 3.

Levy [53, 54]) fitted a formula equivalent to (33) to the experimental beta decay energies. When the parabolic section of the mass surface is expressed as [103])

$$M(Z, A) = M(Z_A, A)+\tfrac{1}{2}B_A(Z-Z_A)^2+\delta, \quad (34)$$

where Z_A is the Z value (usually not integer) of the minimum of the parabola, and B_A and δ have the usual meaning, then

$$Q_{\beta-}(Z, A) = B_A(Z_A-Z-\tfrac{1}{2})+(\delta_1-\delta_2), \quad (35)$$

where $(\delta_1-\delta_2)$ is the change of the parity term δ caused by the decay. According to Levy (see § 25.1)

$$Z_A = q_1 A+q_0. \quad (36)$$

He also writes α_4 for $\frac{1}{2}B_A$, thus obtaining

$$Q_{\beta-}(Z, A) = 2\alpha_4(q_1 A+q_0-Z-\tfrac{1}{2})+(\delta_1-\delta_2). \quad (37)$$

This is the same as (33), when the parameters are identified as follows:

$$\begin{aligned}
\alpha_4 &= I^0-\tfrac{1}{2}d-\tfrac{1}{2}D \\
q_1 &= \frac{I^0-d}{2I^0-d-D} \\
q_0 &= Z_0+\tfrac{1}{2}+\frac{(M_n-M_H)+(C-c)+\tfrac{1}{2}(\Pi-\pi)-(A_0+1)(I^0-d)}{2I^0-d-D} \\
(\delta_1-\delta_2) &= -\Delta_{\beta-}\delta,
\end{aligned} \quad (38a)$$

and reciprocally

$$\begin{aligned}
&(M_n-M_H)+(C-c)+\tfrac{1}{2}(\Pi-\pi) = 2\alpha_4(q_1(A_0+1)+q_0-Z_0-\tfrac{1}{2}) \\
&I^0-d = 2\alpha_4 q_1 \\
&I^0-D = 2\alpha_4(1-q_1) \\
&-\Delta_{\beta-}\delta = (\delta_1-\delta_2),
\end{aligned} \quad (38b)$$

where $A_0(=N_0+Z_0)$ is the mass number of the heaviest closed shells nucleus (Z_0, N_0) which is still contained in the nucleus (Z, A).

Levy adopted the numbers $Z = 28, 40, 50, 64, 82$ and $N = 28, 40, 50, 82, 126, 140$ as the boundaries of his shell regions. The appropriateness of this choice or of any other choice of a similar nature was discussed in § 12. The agreement of Levy's formula with the experimental data is remarkable, the deviation being less than 250 keV in 84 % of the 179 cases treated, and better than 0.5 MeV in 95 % of them. In fact, a better agreement

cannot be expected, considering the simplification introduced by disregarding the existence of competing subshells within each shell region, whose energy difference is of that order of magnitude. However, for the finer problems of beta stability such an accuracy is insufficient.

TABLE 3

Nuclear parameters related to beta decay systematics, obtained from Levy's coefficients by using eqs. (38b) †

Region Z	Region N	$(M_n-M_H)+(C-c)+\frac{1}{2}(\Pi-\pi)$	I^0-d	Parameters (MeV) I^0-D	$-\Delta_{\beta-}-\delta$ (A odd)	$-\Delta_{\beta-}-\delta$ (A even)
21–28	21–28	−4.476	1.170	1.401	0.314	2.980
21–28	29–40	6.053	1.246	1.549	0.105	2.644
29–40	29–40	−5.230	0.903	1.804	(−)0.708	2.468
29–40	41–50	4.245	0.653	1.110	0.019	2.868
29–40	51–82	12.292	0.497	1.019	0.484	1.881
41–50	51–82	0.182	0.518	0.865	0.093	2.868
51–64	51–82	−7.497	0.399	0.795	(−)0.009	2.346
51–64	83–126	7.361	0.415	0.793	0.214	1.946
65–82	83–126	−4.136	0.432	0.771	0.074	1.499
>82	127–140	0.780	0.406	0.735	0.121	1.546
>82	>140	6.192	0.369	0.692	0.196	1.238

† The values in the first two lines were obtained by fitting the corresponding beta decay energies to formula (33). Levy did not consider these lighter nuclei

It was mentioned by Levy that the success of the formula in the rare earths region is hardly worse than in other regions of the periodic table. The implications of this fact were discussed in § 12, in connection with the similar behaviour of the separation energies.

Table 3 gives the values of the beta decay parameters (38b), calculated from Levy's values of q_0, q_1, α_4 and $(\delta_1-\delta_2)$ [53, 54]). The parameters for the $1f_{7/2}$ shells, not considered by Levy, were calculated by comparing formula (33) with experimental beta decay energies [23, 26, 28]).

The practical application of the Way and Wood lines in predicting unknown beta decay energies by interpolation and extrapolation is too well known to be described here.

B. Alpha decay energies

19. Linear Systematics

For the simple alpha decay in which the nuclear configuration changes from $(j_1^{n_1}j_2^{n_2}j_3^{p_3}j_4^{p_4})$ to $(j_1^{n_1-2}j_2^{n_2}j_3^{p_3-2}j_4^{p_4})$, the decay energy is given by

$$\begin{aligned} Q_\alpha &= B\,(\mathrm{He}^4)+B(j_1^{n_1-2}j_2^{n_2}j_3^{p_3-2}j_4^{p_4})-B(j_1^{n_1}j_2^{n_2}j_3^{p_3}j_4^{p_4}) \\ &= B(\mathrm{He}^4)-2c_1-2C_3-\pi_1-\Pi_3+d_1+D_3 \qquad (39) \\ &\quad -(2n_1-2)(d_1+I^0_{13})-2n_2(I^0_{12}+I^0_{23})-(2p_3-2)(D_3+I^0_{13})-2p_4(I^0_{14}+I^0_{34}). \end{aligned}$$

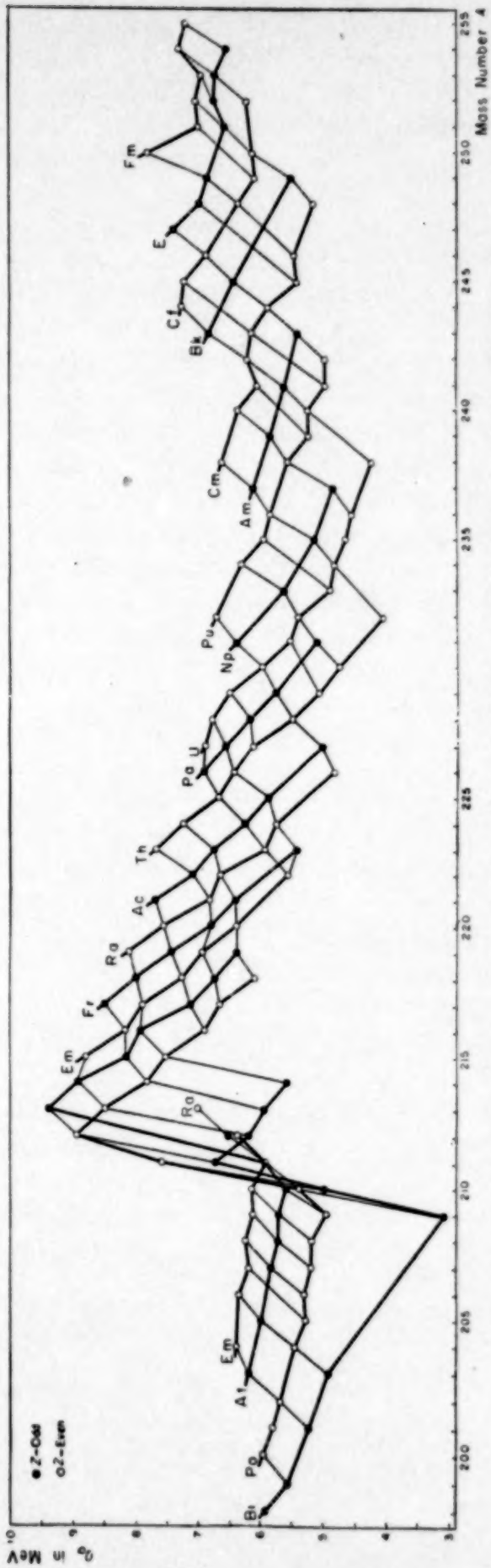

Fig. 12. Alpha decay energy systematics (after Perlman, Ghiorso and Seaborg [67]) and Sengupta [111, 113]).

Therefore, in a sequence of nuclei differing from one another by constant numbers of nucleons, the alpha decay energies will vary linearly within the sequence, as long as the neutrons and protons are entering the same shells. Contrary to the case of the separation energies or the beta decay energies, it is unnecessary to impose the condition that the sequence will consist of nuclei of the same parity type, since alpha decay does not involve a change of the parity type. Thus one obtains linear graphs by connecting the Q_α values of all isotopes of the same element or of all isotones. The density of points on these lines is double that on the straight lines of beta decay energies or of the separation energies, thus displaying general trends less ambiguously †.

The slopes of the lines connecting isotopes are $-(d_1+I^0_{13})$ or $-(I^0_{12}+I^0_{23})$, which means (eq. 23) that they are somewhat slanting downwards, and the slopes of the lines connecting isotones are $-(D_3+I^0_{13})$ or $-(I^0_{14}+I^0_{34})$, which means that they are somewhat slanting upwards.

The network of parallelograms obtained from these lines is shown in fig. 12. The data used in the drawing were

† The same situation holds for graphs showing double beta-decay energies [21]).

taken from the review article by Asaro and Perlman [66]), supplemented by newer data [28]). These lines were given by Perlman, Ghiorso and Seaborg [67]) in their *Systematics of Alpha Radioactivity* †, and also by others [100, 109–112]). They were also considered analytically [112, 113]).

Straight lines connecting alpha decay energy values of isodiapheres were also given [100, 110]).

Though the general trend is linear, yet there are here and there zig-zag variations. However, for a large number of the reported energies, it is not certain whether they really represent ground states transitions, and sometimes even the identification of the isotope is uncertain [66]). In particular, the reported value may be smaller than the true Q_α value for odd-mass and odd nuclei, where various selection rules are liable to operate. The observation that, when connecting only nuclei belonging to the same parity type, the parallelogram system of even nuclei is more regular than that of odd-N nuclei, ††, lends support to the expectation that when the Q values of alpha decay become better known, the linearity of the graph of fig. 12 will considerably improve. The zig-zag variations of the lines might serve as a guide where to look for wrong assignments, either of the Q value or of the mass number.

20. Shell Effects

When crossing a neutron magic number N_0, the straight lines connecting isotopes suffer an upwards discontinuity due to the decrease of the single-neutron binding energy. This increase, which is twice as large as the one encountered in the beta decay or the separation energy lines, is accomplished in two steps: from N_0 to N_0+1, thence from N_0+1 to N_0+2. A similar increase is observed for a proton magic number.

In fig. 12, these discontinuities are very clearly observed for $N = 126$ and for $Z = 82$†††. The increase for $Z = 82$ is only about half as large as that for $N = 126$, since the lightest alpha emitting element shown is Bi, having already 83 protons.

Strangely enough, the appreciable discontinuity from Bi to Po, due to the crossing of $Z = 82$, is observed only from Bi^{209} onwards, for isotopes above the magic number $N = 126$. With the values calculated by Glass *et al.* [18]) or by Huizenga [33]) for Bi^{207} and Bi^{208}, with $N = 124$ and $N = 125$, respectively, the $Z = 82$ discontinuity exists for them too. However, the

† In the original graphs of Perlman, Ghiorso and Seaborg, as well as in later versions [18, 68]), only the lines connecting isotopes are drawn. Lines connecting isotones have been drawn by Sengupta [111, 112]).

†† The data for odd-Z nuclei, and in particular for odd nuclei, are too scanty to enable a significant comparison of this kind.

††† See also refs. [18, 65–68, 100, 109–112, 114]).

lighter Bi^{199}, Bi^{201} and Bi^{203} show no such discontinuity. But it must be pointed out that the isotope identification is reported [66]) to be uncertain for $Bi^{198-203}$.

The above mentioned discontinuities in alpha decay energies at $Z = 82$, $N = 126$ were among the earliest [109]) indications of the existence of shells in nuclei.

CHAPTER III. THE NUCLEAR MASS SURFACE

21. The Nuclear Mass Surface and its Splitting

The results of the previous two chapters suggest that up to the order of magnitude of the perturbation caused by the non-diagonal elements of the energy matrix between subshells, which is about a few hundred keV (see § 12), the binding energy of a nucleus containing n neutrons and p protons in open shells beyond the magic or submagic numbers N_0 and Z_0, respectively, might fairly adequately be represented by formula (26), rewritten here for the sake of easier orientation:

$$B(N_0+n, Z_0+p) = B(N_0 Z_0)+nc+pC+\tfrac{1}{2}n\pi+\tfrac{1}{2}p\Pi + \tfrac{1}{2}n(n-1)d+\tfrac{1}{2}p(p-1)D+npI^0-\delta, \qquad (26)$$

where the parameters c, C, d, D, π, Π, I^0 and δ, of which the latter is to be considered different for the four parity types of nuclei†, are determined by a comparison of the formula with the experimental data, separately for each shell region.

From the well known relation between mass and energy, the nuclear mass surface would likewise be represented by the formula

$$M(N_0+n, Z_0+p)=M(N_0 Z_0)+n(M_n-c-\tfrac{1}{2}\pi+\tfrac{1}{2}d)+p(M_H-C-\tfrac{1}{2}\Pi+\tfrac{1}{2}D) -\tfrac{1}{2}n^2 d-\tfrac{1}{2}p^2 D-npI^0+\delta, \qquad (40)$$

and similarly mass defects by

$$\Delta M(N_0+n, Z_0+p) = M(N_0+n, Z_0+p)-A = \Delta M(N_0 Z_0)+n((M_n-1)-c-\tfrac{1}{2}\pi+\tfrac{1}{2}d)+p((M_H-1)-C-\tfrac{1}{2}\Pi+\tfrac{1}{2}D) \qquad (41)$$
$$-\tfrac{1}{2}n^2 d-\tfrac{1}{2}p^2 D-npI^0+\delta\,\dagger\dagger.$$

In the following, the surface represented by (41) is also referred to as the nuclear mass surface.

Thus, in each shell region, the mass surface consists of four similar quadratic surfaces, corresponding to the four parity types of nuclei, and

† It is equal to zero in even nuclei.

†† In this formula (M_n-1) and (M_H-1) are to be first written down in atomic mass units, and only then to be transformed to energy units if necessary.

displaced vertically one in relation to the other. The amount of the displacement from the even surface is given by the δ terms. From the values of the parameters obtained by the treatment of separation energies and beta decay energies we know, that the surface of even nuclei is invariably the lowest, and that the odd surface is invariably the highest, at a distance δ_A above the former. The surfaces for odd mass nuclei are situated between the two, the odd-Z surface lying above the odd-N surface when ε_A is positive, and vice versa. The distance between them is given by ε_A.

In studies of beta decay energetics, it is usually [55, 56, 61, 63, 64]) implicitly assumed, that the mean height of the mass surfaces of even-A nuclei coincides with that of odd-A. Expressed quantitatively, the assumption is

$$\tfrac{1}{2}(\delta(\text{even nuclei})+\delta(\text{odd nuclei}))=\tfrac{1}{2}(\delta(\text{odd-}Z\text{ nuclei})+\delta(\text{odd-}N\text{ nuclei})). \quad (42)$$

The conventional form [63]) of the pairing term leading to (42) is

$$\delta=\begin{cases}-\tfrac{1}{2}\delta_A & \text{even nuclei}\\ -\tfrac{1}{2}\varepsilon_A & \text{odd-}N\text{ nuclei}\\ +\tfrac{1}{2}\varepsilon_A & \text{odd-}Z\text{ nuclei}\\ +\tfrac{1}{2}\delta_A & \text{odd nuclei.}\end{cases} \quad (43)$$

Assumption (42) may usually be traced back to the assumptions [38, 69, 70, 102]) that pairing-and shell-correction terms to an otherwise-smooth mass-formula are independently contributed by the neutrons and the protons. In an obvious notation:

$$P(NZ)=P(N)+P(Z) \quad (44)$$

$$S(NZ)=S(N)+S(Z). \quad (45)$$

On the other hand, the shell model predicts (eq. (20b)) that eq. (44) will not hold, as long as the interaction I'_{13} between the odd neutron and odd proton does not vanish. Therefore, in those shell regions where this interaction occurs, as manifested by the Saxena-Ghoshal-Way systematics (§ 6.3), or by the reduction of neutron or proton pairing caused by the odd proton or neutron, respectively (§ 6.2), formulation (43), or any other formulation leading to (42), cannot be accepted †.

To be sure, for beta decay studies assumption (43) is quite sufficient, since the beta decay process always connects nuclei with the same parity of A, and thus can give no information concerning the relative displacement of the even-A and odd-A surfaces.

† It is worth pointing out explicitly, that the new revised semi-empirical mass equation of Cameron [69, 70]) is also based on assumption (44). Thus, separation energies calculated from it do not show the two last mentioned effects. Adopting an additional pairing term for odd nuclei would further improve its agreement with the experimental data in the mass regions displaying the above mentioned regularities.

22. Levy's Empirical Mass Equation

Formula (41) is essentially Levy's empirical mass equation. Levy [53, 54]) developed "a purely empirical equation for atomic masses. The form of the equation has been kept as simple as possible for ease of handling, while still remaining consistent with the experimental data". The experimental data referred to by Levy are the various straight-line relationships mentioned thus far, as well as other straight-line and parabolic relationships, to be mentioned below. For practical reasons, Levy chose to characterize nuclei by their nuclear charge Z and mass number A, and wrote his equation in the form

$$\Delta M(ZA) = \alpha_0+\alpha_1 A+\alpha_2 Z+\alpha_3 AZ+\alpha_4 Z^2+\alpha_5 A^2+\delta, \tag{46}$$

where the α_i and δ, which is regarded different for the four parity types of nuclei, are assumed constant in each shell region, to be determined by comparing the formula with the experimental data. It is evident that (45) is the same as (41), expressed in a different form. The relations of Levy's empirical coefficients to the "shell-model"-coefficients of (41) are given by

$$\begin{aligned}
\alpha_0 &= \Delta M(N_0 Z_0)-N_0((M_n-1)-c-\tfrac{1}{2}\pi+\tfrac{1}{2}d)\\
&\quad -Z_0((M_H-1)-C-\tfrac{1}{2}\Pi+\tfrac{1}{2}D)-\tfrac{1}{2}N_0^2 d-\tfrac{1}{2}Z_0^2 D-N_0 Z_0 I^0\\
\alpha_1 &= (M_n-1)-c-\tfrac{1}{2}\pi+\tfrac{1}{2}d+N_0 d+Z_0 I^0\\
\alpha_2 &= (M_H-M_n)-(C-c)-\tfrac{1}{2}(\Pi-\pi)+\tfrac{1}{2}(D-d)\\
&\qquad -N_0 d+Z_0 D+(N_0-Z_0)I^0 \qquad (47a)\\
\alpha_3 &= d-I^0\\
\alpha_4 &= -\tfrac{1}{2}d-\tfrac{1}{2}D+I^0\\
\alpha_5 &= -\tfrac{1}{2}d\\
\delta_{\text{Levy}} &= \delta_{\text{shell model}}\ \text{(eq. (20b))},
\end{aligned}$$

and reciprocally:

$$\begin{aligned}
\Delta M(N_0 Z_0) &= \alpha_0+\alpha_1 A_0+\alpha_2 Z_0+\alpha_3 A_0 Z_0+\alpha_4 Z_0^2+\alpha_5 A_0^2\\
c &= (M_n-1)-\alpha_1-\alpha_3 Z_0-\alpha_5(2A_0+1)-\delta_{\text{odd-}N\text{ nuclei}}\\
C &= (M_H-1)-\alpha_1-\alpha_2-\alpha_3(Z_0+A_0+1)-\alpha_4(2Z_0+1)-\alpha_5(2A_0+1)-\delta_{\text{odd-}Z\text{ nuclei}}\\
\pi &= 2\delta_{\text{odd-}N\text{ nuclei}}\\
\Pi &= 2\delta_{\text{odd-}Z\text{ nuclei}} \qquad (47b)\\
I' &= \delta_{\text{odd-}N\text{ nuclei}}+\delta_{\text{odd-}Z\text{ nuclei}}-\delta_{\text{odd nuclei}}\\
d &= -2\alpha_5\\
D &= -2(\alpha_3+\alpha_4+\alpha_5)\\
I^0 &= -\alpha_3-2\alpha_5.
\end{aligned}$$

The shell boundaries adopted by Levy were already given in § 12.

We have already seen that boundaries at the submagic numbers 40 and 64 are introduced mainly in order to account for the gradual variation of the nuclear parameters with mass number, rather than because of real shell-edge effects associated with these numbers.

The agreement of Levy's formula with the experimental data is better than 0.5 millimass units in 75 % of the 340 nucleides studied, and better than 1.5 millimass units in 95 % of them. The distribution of the deviations

TABLE 4

Nuclear parameters obtained from Levy's coefficients by using eqs. (47b)

Region Z	Region N	Parameters (MeV) $\Delta M(N_0 Z_0)$	c	C	π	Π	d	D	I^0	I'
29—40	29—40	(—)47.018	7.165	1.860	4.097	2.682	—0.215	—1.116	0.688	0.922
29—40	41—50	(—)45.304	4.940	8.380	3.389	3.427	—0.192	—0.648	0.461	0.540
29—40	51—82	(—)13.108	3.403	14.433	1.397	2.365	—0.187	—0.708	0.310	0.000
41—50	51—82	(—)64.055	6.352	5.661	2.682	2.868	—0.181	—0.528	0.336	(—)0.093
51—64	51—82	(—)44.601	8.995	0.726	2.104	2.086	—0.122	—0.519	0.276	(—)0.251
51—64	83—126	(—)38.757	3.046	9.406	1.359	1.788	—0.100	—0.478	0.315	(—)0.372
65—82	83—126	(—)32.642	7.914	2.922	1.415	1.564	—0.162	—0.501	0.269	(—)0.009
>82	127—140	38.625	3.959	3.835	1.639	1.881	—0.096	—0.425	0.309	0.214
>82	>140	101.277	3.843	9.048	0.931	1.322	—0.160	—0.483	0.209	(—)0.112

of the formula from the experimental data in the various shell regions is also shown by Levy. The deviations are largest in the rare earths region. However, the experimental mass values in this region are the least certain †. The deviations are smallest for the alpha decaying nuclei (see also §§ 12 and 18).

Table 4 gives the values of the nuclear parameters (47b) calculated from Levy's constants α_i and δ [53, 54]). The general features of the variation of these values from one shell region to the other are the same as those of the parameters of table 1. However, some individual values differ considerably. This might be due to the different procedures adopted in obtaining the two sets of values. However, the fact that in the transmercury elements, where the same experimental data [18]) were used in the calculations of both table 1 and table 4, the differences are smallest, suggests that the disagreement between the two tables might also be due in part to the fact that the experimental data used in calculating the two tables were different. It is worth mentioning, that with the newer data used in the calculation of table 1, the I' comes out positive, as it should be according to the shell model (§ 8.1) even in some regions where the data of table 4 give a negative value.

A rough method of extrapolation of Levy's formula to shell regions for which no experimental data are available has been indicated in § 12.

† Indeed, this situation does not occur with the more accurately known separation energies and beta-decay energies.

It is worth mentioning, that though Levy himself claimed no theoretical justification for his mass equation, yet he developed (see appendix I of part I of ref. [53]) a "model consistent with basic principles, that would give rise to an equation of the same type as the empirical equation". The model described by him is essentially an independent-particle model, with strong pairing between identical nucleons, and orientation-independent residual interaction, resulting in an equation equivalent to (26).

Independently of Levy, Thieberger and de-Shalit [12]) discovered that formula (26) reproduces quite well the experimental binding energies. They obtained values of the nuclear parameters by a least-squares fit of the formula to experimental binding energies. Their results show the same general trends as those of tables 1 and 4, but they cannot be directly compared with them, as they did not use the same division into shell regions. We have already mentioned (§ 11) that they found no definite subshell effect associated with any "submagic" number.

23. Section of the Mass Surface for Constant Z or N

23.1. PARABOLIC SECTION

Eq. (41) may be written as

$$\Delta M(N_0+n,\ Z_0+p) = \alpha_Z+\beta_Z n+\gamma_Z n^2+\delta, \tag{48}$$

where †

$$\begin{aligned}\alpha_Z &= \Delta M(N_0 Z_0)+p\left((M_{\mathrm{H}}-1)-C-\tfrac{1}{2}\Pi+\tfrac{1}{2}D\right)-\tfrac{1}{2}p^2 D\\ \beta_Z &= (M_{\mathrm{n}}-1)-c-\tfrac{1}{2}\pi+\tfrac{1}{2}d-pI^0\\ \gamma_Z &= -\tfrac{1}{2}d\end{aligned} \tag{49}$$

and δ is the usual parity term. Therefore, for a given parity type the section is parabolic in a given shell region. Such parabolas have been empirically found by Collins, Johnson and Nier [71]) when they studied combined mass spectroscopic and nuclear reaction data.

The slope of the parabola is given by

$$\left(\frac{\partial \Delta M}{\partial N}\right)_{Z=\mathrm{const}} = (M_{\mathrm{n}}-1)-c-\tfrac{1}{2}\pi-pI^0-(n-\tfrac{1}{2})d, \tag{50a}$$

which becomes positive for large n due to the repulsion d between the neutrons. On the other hand, when n decreases, it becomes negative if p is large enough, due to the attractive interaction I^0 between neutrons and protons. Thus the parabola has a minimum, for which n and p do not differ too much from one another.

Similarly, for constant N we have a parabolic section of the same qualita-

† The subscript Z designates the coefficients characterizing the section of the mass surface at constant Z.

tive features, obtained from (48), (49) and (50a) by interchanging the role of N and Z, n and p, and neutron and proton parameters. In particular, its slope is given by

$$\left(\frac{\partial \Delta M}{\partial Z}\right)_{N=\text{const}} = (M_H - 1) - C - \tfrac{1}{2}\Pi - nI^0 - (p - \tfrac{1}{2})D. \qquad (50b)$$

23.2. SHELL EFFECTS

Suppose that as N varies, shell j_1 becomes filled at $n = n_1$, and shell j_2 begins to fill. When it already contains n_2 neutrons, one has, similarly to (48),

$$\Delta M(N_0+n_1+n_2,\ Z_0+p) = \Delta M(N_0+n_1,\ Z_0+p) + \beta_Z' n_2 + \gamma_Z' n_2^2 + \delta', \quad (51)$$

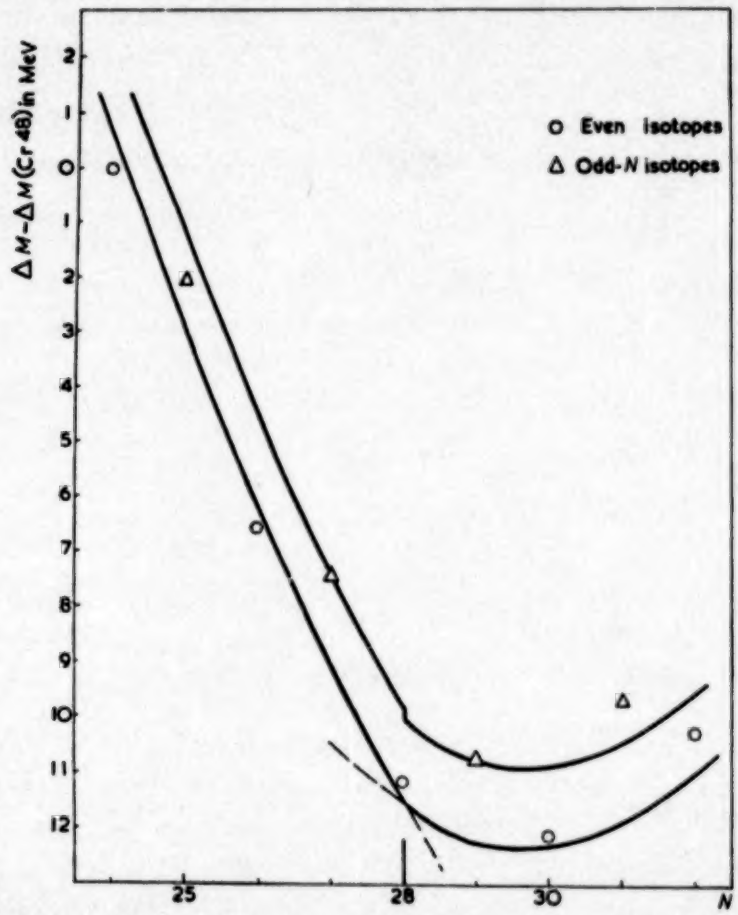

Fig. 13. Section of the mass surface through the Cr isotopes.

where the primes indicate that the parameters belong to the j_2 neutron shell. This is again a parabolic section, with a slope given by (50a) when the parameters are replaced by their primed equivalents. From the known variation of the nuclear parameters when shell edges are crossed, we see that

crossing a neutron shell edge will affect the slope of the mass surface mainly in the N direction, increasing it due to the decrease in binding c of the single neutrons. However, the increase of the slope when more neutrons are added, due to the repulsion d between the neutrons, will be slower than in shell j_1, owing to the smaller magnitude of this repulsion in the larger outer shell.

For even nuclei, *the two parts of the mass surface belonging to the two shell*

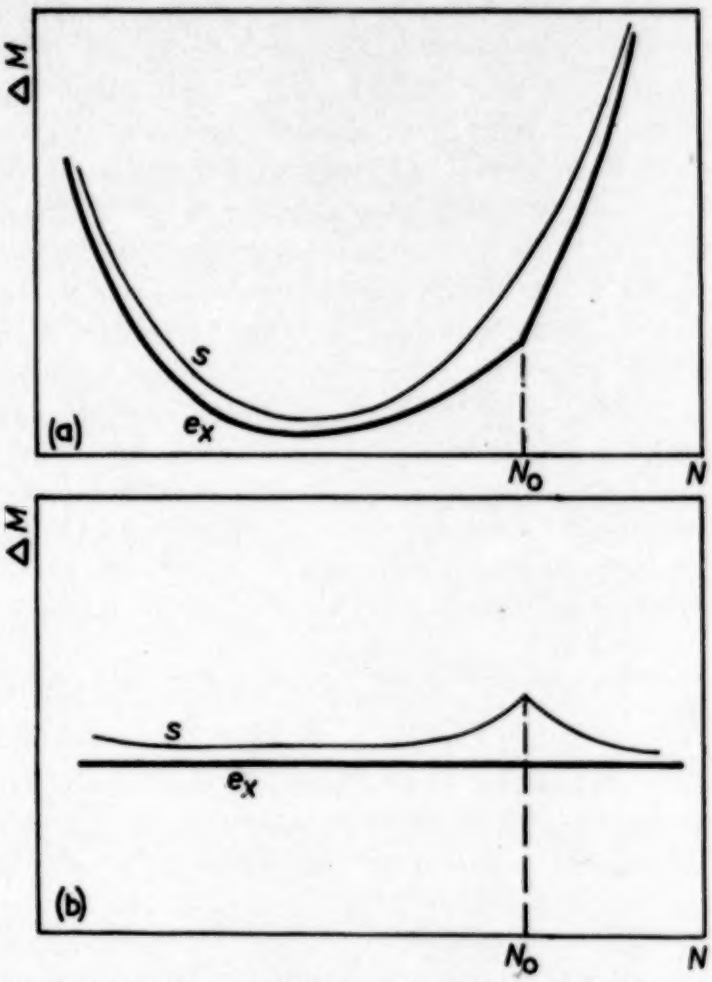

Fig. 14. Schematic illustration of the apparent exceptional stability of magic nuclei.

regions are continuously connected with one another along the magic or submagic line $N = N_0+n_1$, since the parity term δ vanishes for them. However, for the other three parity types of nuclei, there may also be a vertical discontinuity along the line $N = N_0+n_1$, due to a possible change of the δ term. Fig. 13 illustrates a section of the mass surface through the Cr isotopes. The mass data used in the drawing were taken directly or calculated from refs. [19, 23]) and [25]). The parabolas were drawn with the parameters of table 1 †.

† Since the $\Delta M(N_0Z_0)$ of (41) are not given by the table, we have chosen the vertical position of the parabolas so as to obtain the best possible agreement with the experimental points.

The essentially continuous crossing of the shell boundary, accompanied by a change of slope, was observed by Collins *et al.* [72]) and by Halsted [73]), when they tried to fit Wigner's mass formula to experimental mass values. Aten [74]) and Wapstra [115]) also came to the same conclusion.

Analogous results hold when proton magic numbers are crossed.

We want to stress here again, as already done in connection with the separation energies (§ 10) and beta decay energies (§ 16), that the shell model does not predict any extraordinary stability for magic nuclei, as compared to their neighbours in the shell region closed by them. The stability attributed to magic nuclei holds only in comparison to their neighbours in the next higher shell region, which are indeed much less tightly bound, as manifested by the increasing slope of the mass surface in the higher region. Levy has already emphasized this point.

On the other hand, when considering not the binding energies or the mass defects themselves, but their differences from the prediction of a smooth semi-empirical mass formula or any other similar difference [38, 41, 75, 94, 102, 115, 116]), the impression is easily obtained that magic nuclei are particularly stable with respect to all their neighbours. As in the case of the nucleon separation energies, this is due to the choice of the reference base line: relatively to the smooth line s of fig. 14a, the experimental mass defect line ex assumes the form shown in fig. 14b.

24. Section of the Mass Surface for Constant A

24.1. PARABOLIC SECTION

Here the famous parabolic section (34) of the mass surface is obtained †, with the appropriate amounts of splitting according to parity type. Choosing Z and A as independent variables we shall designate $n+p$ by a. Then (41) may be written as

$$\Delta M(Z_0+p,\ A_0+a) = \alpha_A+\beta_A p+\gamma_A p^2+\delta\ \text{††}, \tag{52}$$

where

$$\begin{aligned}\alpha_A &= \Delta M(Z_0A_0)+a\left((M_n-1)-c-\tfrac{1}{2}\pi+\tfrac{1}{2}d\right)-\tfrac{1}{2}a^2 d\\ \beta_A &= (M_H-M_n)-(C-c)-\tfrac{1}{2}(\Pi-\pi)+\tfrac{1}{2}(D-d)-a(I^0-d)\\ \gamma_A &= I^0-\tfrac{1}{2}d-\tfrac{1}{2}D\end{aligned} \tag{53}$$

and δ is the usual parity term.

The slope of this section may be obtained by the appropriate linear combination of the slopes (50a, b), or directly from (52) and (53):

† As a matter of fact, any plane section of the quadratic mass surface will be parabolic.

†† The subscript A designates the coefficients characterizing the section of the mass surface at constant A.

$$\left(\frac{\partial \Delta M}{\partial Z}\right)_{A=\text{const}} = (M_H - M_n) - (C-c) - \tfrac{1}{2}(\Pi - \pi) + \tfrac{1}{2}(D-d) - a(I^0-d) + p(2I^0-d-D). \quad (54)$$

It is seen again, that for large p it becomes positive, and for small p it is negative when a is not too small, resulting in a minimum mass defect for some p which is of the order of magnitude of a. This is also geometrically obvious from the behaviour of the sections of the mass surface at constant Z and N, considered in § 23.1.

24.2 SHELL EFFECTS

The beginning of a new proton shell increases the slope in the direction of increasing Z, whereas a beginning of a new neutron shell increases the slope in the opposite direction (increasing N). The further increase of the slope when receding from the shell edge is, however, slower for the new outer shell than for the inner one, due to the smaller value of the coefficient of p in eq. (54). For even nuclei the change in slope is the only manifestation of the beginning of new shell. For the other three parity types there might also exist the vertical discontinuity at the shell edge (§ 23.2), due to the change of the parity term. Magic isobars are found at the junction of two parabolas, but not below a single parabola representing the mass defects of all their other isobars.

25. The Line of Beta Stability

25.1. STRAIGHT LINE

The minimum of an isobaric section of the mass surface is found from (54) at

$$p_A = \frac{(M_n - M_H) + (C-c) + \tfrac{1}{2}(\Pi - \pi) - \tfrac{1}{2}(D-d)}{2I^0-d-D} + a\frac{I^0-d}{2I^0-d-D}. \quad (55)$$

This is a linear function of the mass number A for a given shell region. This fact has been first found empirically by Coryell and his co-workers [55]), and further investigated by Kumar and Preston [61]) and by Fix [56]), through careful analysis of beta decay data. Levy derived the linear dependence of p_A on A from his empirical mass equation, and expressed it in terms of Z_A and A in the form (36), which is easily seen to be identical with (55) by using eqs. (38a). The parameters determining the straight line (55) for each shell region are best obtained from beta decay data (table 3).

25.2. SHELL EFFECTS

Let us find how the straight line connecting the minima of isobaric sections of the mass surface in a given shell region is influenced by crossing

a shell edge. In the new region the line will again be represented by formula (55), this time with the parameters of the new shell region. Thus the

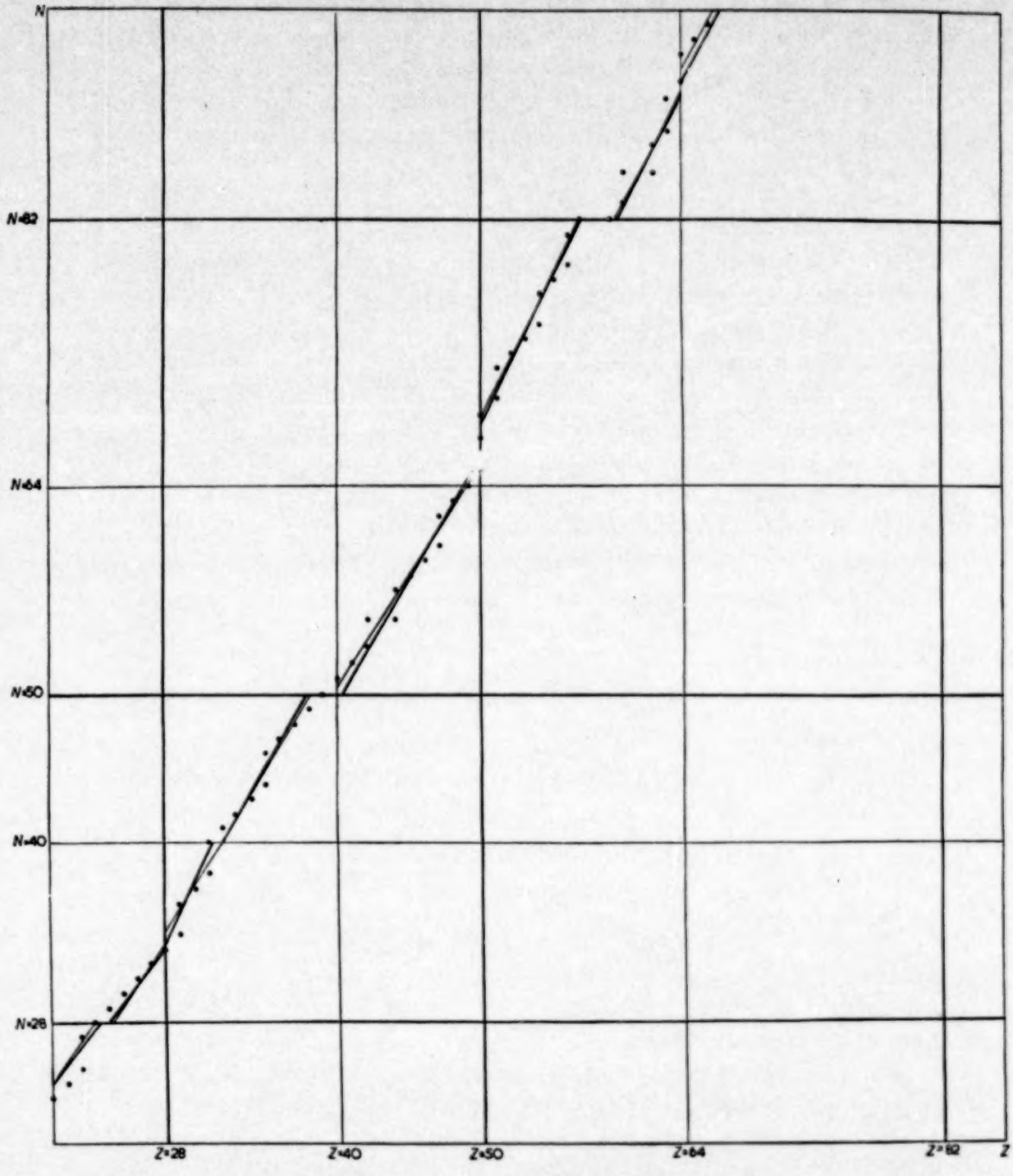

main change affecting the line in the transition from one region to another is a discontinuity due to the decrease in the single-nucleon binding energy. When a neutron magic number is crossed, c decreases, and p_A is shifted in the direction of increasing Z. Likewise, when a proton magic number is

crossed, p_A is shifted in the direction of increasing N. All this is also geometrically obvious from the considerations of §§ 23.2 and 24.2.

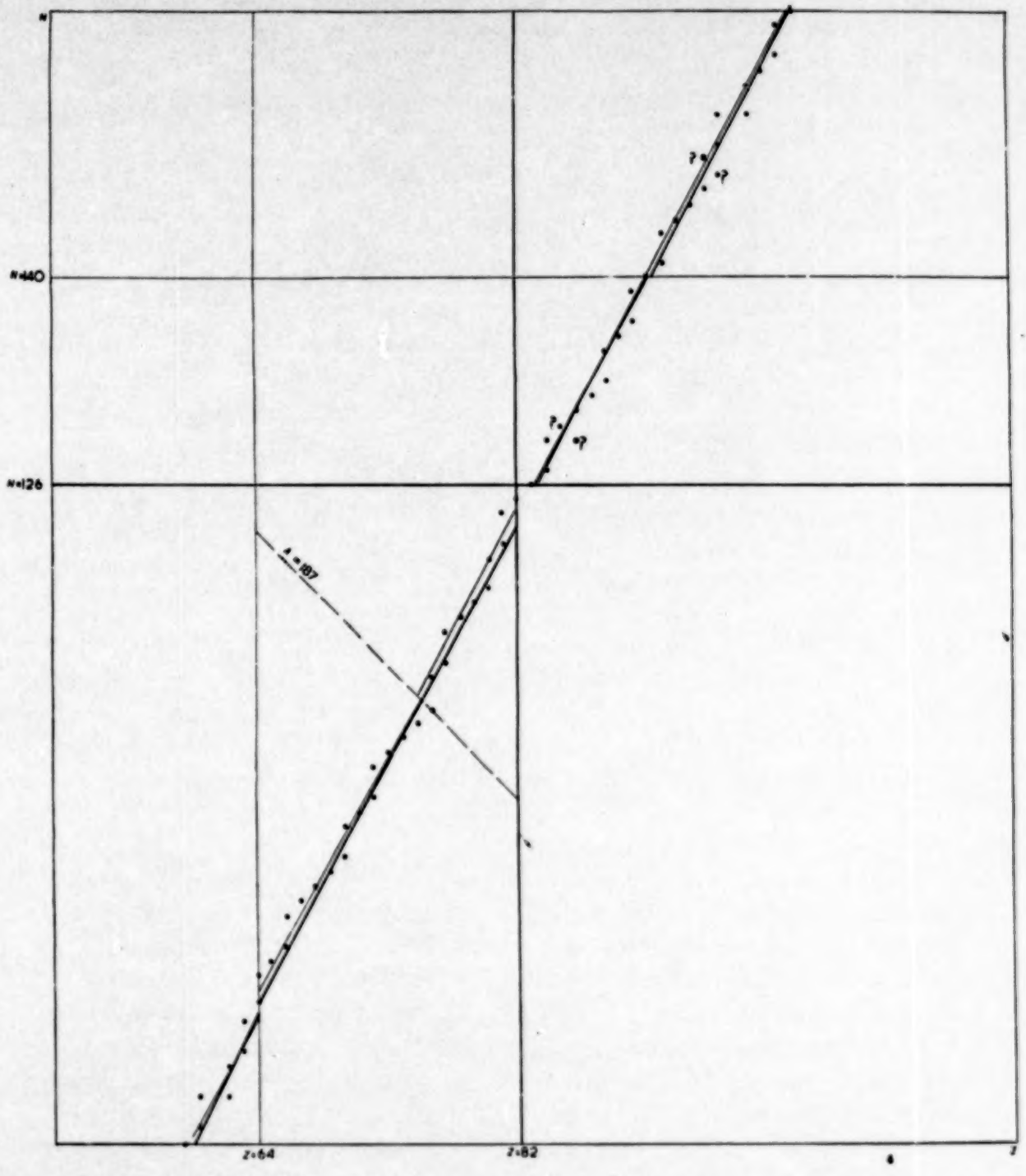

Fig. 15. The line of beta stability according to Levy [53])† (bold line), and according to Coryell and Fix [56]) (thin line), for $N > 20$, $Z > 20$. Beta-stable odd-mass nucleides are marked by solid circles.

† For the regions below 28 neutrons or protons the line was calculated from the corresponding parameters of table 3. Levy did not consider these lighter nuclei.

Besides, the slope of the line with respect to the N and Z axes in the (N, Z) plane may change, due to the change in absolute value of d, D and I^0. The change in the slope due to variation of the parameters may be roughly approximated to from eq. (55) as

$$\Delta\left(\frac{dp_A}{dA}\right) = \frac{1}{(2I^0-d-D)^2}\cdot[(D-I^0)\Delta d-(d-I^0)\Delta D+(d-D)\Delta I^0], \quad (56)$$

where a Δ written before a given quantity denotes the change which this quantity has undergone. When due regard is paid to the signs of the parameters and to their changes when a shell edge is crossed, it appears that the change of dp_A/dA due to the changes of I^0 and d is usually negative, while that due to the change of D is usually positive. Thus, the decrease of the repulsion between the neutrons, as well as the decrease of their attraction of the protons, tend to cause p_A to increase more slowly with the mass number. On the other hand, the decrease of the repulsion between the protons tends to cause p_A to increase more rapidly. Both these tendencies are intuitively evident.

Fig. 15 illustrates the line of beta stability computed by Levy [53, 54]) from eq. (36) with his values of the parameters (38a) (bold line). We have continued the line down to the magic numbers $N = 20$ and $Z = 20$ by using the corresponding values of the parameters of table 3. The stable odd-A nucleides are also marked in the figure (solid circles). The discontinuities of the line at the boundaries of the shell regions are very clear, being larger at the magic numbers and smaller at the "submagic" ones. In the lead region, the discontinuities connected with $Z = 82$ and $N = 126$ neutralize each other, resulting in an almost continuous transition of the line into the region of the heavy alpha decaying nuclei. Changes in slopes on crossing $Z = 50$ and $N = 82$ are clearly observed.

The line of beta stability of Coryell and Fix [56]) is also shown in fig. 15 (thin line), alongside Levy's line. Usually they are very close. The most conspicuous discrepancy is the discontinuity introduced by Fix at $A = 187$.

Finally, a word should be said about the variation of nuclear masses along the stability valley, the term $M(Z_A, A)$ of eq. (34). According to (52) and (55), this term increases quadratically with A. From § 23.2 it is geometrically obvious that when a shell edge is crossed, the bottom $M(Z_A, A)$ of the stability valley becomes steeper, but the increase of this steepness with A is slower than in the preceding shell region. This can also be seen from the rather cumbersome explicit expression of $M(Z_A, A)$ in terms of the various interaction parameters, which will not be given here†.

† See refs. [53, 54]) for an expression of $M(Z_A, A)$ in terms of Levy's empirical parameters.

CHAPTER IV. EXCITED STATES OF NUCLEI

On a much smaller scale, many regularities encountered in the study of the low lying nuclear energy level systematics are very similar to the larger scale linear regularities met with in connection with both nuclear separation energies and radioactive decay energies. This is so, because all these regularities are consequences of the same fundamental binding energy formula (19). In order to stress this uniformity in the behaviour of the various nuclear energies, we conclude Part I with some considerations concerning nuclear excitation energies.

The treatment of the above mentioned large scale nuclear energetics was based on eq. (26), which ignored the existence of separate subshells between two magic (or submagic) numbers. On the other hand, excitation energies of nuclear excited levels are intimately connected with the change in nuclear structure caused by the excitation, in particular with the distribution of the nucleons in the various subshells and with the interference between the different possible nuclear configurations thus obtained. Therefore, one can expect to understand the excitation energies only on the basis of more exact formulas distinguishing between various subshells, such as those based on the energy equation (19).

26. Low-Lying Excited States of Odd-Mass Nuclei

Let us consider an excited state of an odd-neutron nucleus having a ground state configuration $(j_1^{n_1} j_2^{n_2} j_3^{p_3} j_4^{p_4})$. The excitation energies of the states obtained from it by the transition of the odd neutron from shell j_1 to shell j_2, or by a neutron transition in the reverse direction, are given by formulas (57a) and (57b), respectively:

$$B(j_1^{n_1} j_2^{n_2} j_3^{p_3} j_4^{p_4}) - B(j_1^{n_1-1} j_2^{n_2+1} j_3^{p_3} j_4^{p_4})$$
$$= (c_1 - c_2) + (n_1 - 1)(d_1 - I_{12}^0) - n_2(d_2 - I_{12}^0) + p_3(I_{13}^0 - I_{23}^0) + p_4(I_{14}^0 - I_{24}^0) \quad (57a)$$

$$B(j_1^{n_1} j_2^{n_2} j_3^{p_3} j_4^{p_4}) - B(j_1^{n_1+1} j_2^{n_2-1} j_3^{p_3} j_4^{p_4})$$
$$= -(c_1 - c_2) - (\pi_1 - \pi_2) - n_1(d_1 - I_{12}^0) \quad (57b)$$
$$+ (n_2 - 1)(d_2 - I_{12}^0) - p_3(I_{13}^0 - I_{23}^0) - p_4(I_{14}^0 - I_{24}^0).$$

The analogous formulas for odd-proton nuclei are obtained from (57a, b) by interchanging the shells, the numbers and the parameters of neutrons and protons.

The formulas show, that when one considers a sequence of odd-N isotopes, in which the neutrons are filling the same shell, the excitation energy of a single-particle state, obtained by a neutron transition from one shell to another, will vary linearly within the sequence. The same applies to a

sequence of odd-N isotones, in which the protons are filling the same shell. Whether the excitation energy will increase or decrease depends on the signs of the $(d_1-I_{12}^0)$ and the $(I_{13}^0-I_{23}^0)$, of which nothing can be said a priori, as the two parameters within each bracket are of the same order of magnitude. This was shown in detail in the treatment of the separation energies (§ 11), and allowed us to treat nuclear binding energies and their differences by the crude approximation (26), altogether ignoring the existence of different subshells.

In particular, the linear energy differences (57a, b) may change sign when nucleons are added. Thus, the single-particle ground state of neighbouring nuclei may belong to different shells. Here we see that the systematics of single-particle excited levels is closely related to the competition between nuclear shells, and their simultaneous study should elucidate both. This problem will again be considered in the second part of this paper †.

Figs. 17, 18 and 20—22 in Chapter VI show the systematics of various single-particle levels. In some regions one observes parallelograms similar to those encountered in the graphs of the separation energies and disintegration energies (figs. 1a, b, 3a, b, 9a, b and 12). However, in most of the regions of the periodic system of nuclei no such parallelograms are observed, indicating that the mixing of the various states is large, and that the approximation (57a, b), which assumes pure nuclear configurations, will, therefore, be unable to explain the data ††. Actually, linear systematics occur only in the vicinity of the magic numbers, where the number of near configurations available for the mixing is rather small. The opposite extreme lies in the regions of the rare earths and the heavier alpha-emitting elements, where the opportunities for mixing are very numerous. Here the low lying levels are rotational collective levels [76]), indicating a complete breakdown of the independent-particle shell model.

27. Low-Lying Excited States of Odd Nuclei

In odd nuclei which are not too light, the low-lying excited levels are even much lower than the single-particle excited levels in neighbouring odd-mass nuclei. Therefore, one usually assumes that the configuration is the same in all these states, and their energy difference is due to the different couplings of the odd neutron and proton to form the total nuclear angular momentum J.

According to formula (16), the excitation energy of such an excited J'-state from the ground J-state is given by

† See ref. [13]) for a more detailed discussion.

†† This is in conformity with the results of §§ 11 and 17. As a matter of fact (see also § 32), the distortion of the parallelograms probably indicates that the amount of mixing is not negligible even in regions displaying "parallelogram" systematics, which is confirmed by more detailed calculations [80–82]).

$$B(j_1^{n_1} j_3^{p_3} J) - B(j_1^{n_1} j_3^{p_3} J') = (I''_J - I''_{J'}) + \frac{2j_1+1-2n_1}{2j_1-1} \cdot \frac{2j_3+1-2p_3}{2j_3-1} \cdot (I'''_J - I'''_{J'}). \quad (58)$$

The other incomplete even shells remain intact, and have, therefore, not been explicitly mentioned.

Here, too, the excitation energies vary linearly with the numbers of nucleons, as long as the added nucleons enter the same odd shells in neighbouring odd nuclei. However, this time the rate of their variation with respect

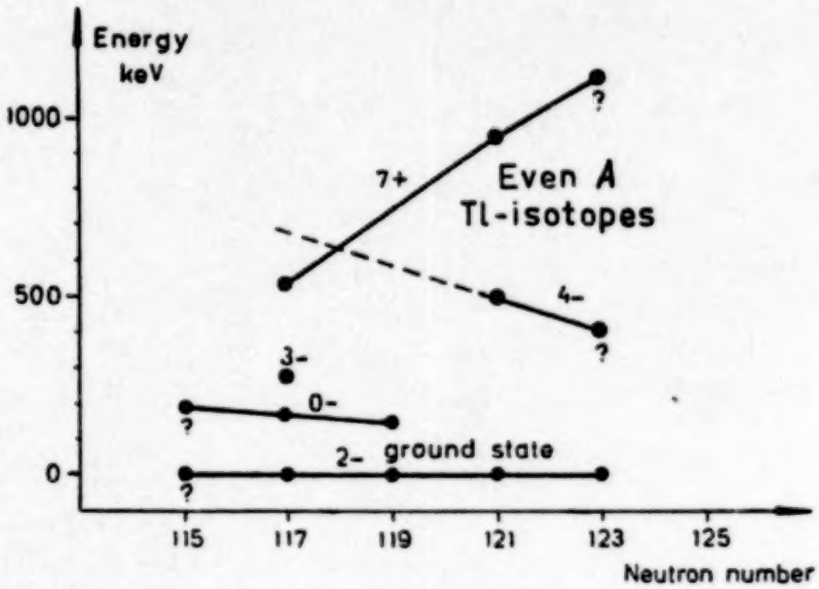

Fig. 16. Low lying excited levels of the even-mass Tl isotopes (a reproduction of fig. 12 of Bergström and Andersson [77]) †).

to the neutron number depends on the number of protons and vice versa, due to the bilinear form of (58), in contrast to the linear form of (57a, b). When the added nucleons enter the even shells, the excitation energy (58) should remain constant.

Again, the difference (58) may change sign when n_1 or p_3 vary. This means that the ground-state J might differ in odd nuclei with the same odd shells. The empirical occurrence of this fact has already been mentioned in § 13, as well as the attempt of Schwartz [60]) to explain it, which was based on the linear variation mentioned above.

Our empirical knowledge of excited states of odd nuclei is too scanty to allow the verification of the linear variations predicted by eq. (58). However, a possibility of such a linearity is indicated in fig. 16 ††.

† I am grateful to Dr. I. Bergström for permission to reproduce this figure.

†† Strictly speaking, this concerns only the 0^- levels. The linear variation of the 7^+ levels is probably [77]) a combination of the linear variation (58) and the linear variation (57a, b) of the $i_{13/2}$ excitation energies, shown in fig. 22 (§ 33).

28. Low-Lying Excited States of Even Nuclei

Since the pairing energy, as obtained from a study of separation energies or binding energies, is usually much larger than the energy difference between adjacent single-particle levels, it is plausible that the low-lying states of even nuclei will be 0^+ states, obtained by transferring coupled $j^2(0)$ pairs from shell to shell [40]). Some such states have indeed been observed experimentally †.

However, the known first excited states of even nuclei are almost invariably 2^+ states [79]). This does not decisively contradict the previous conclusion, since on the one hand the experimental identification of 0^+ states is rather difficult, and on the other hand, the interference between the 0^+ ground state and the other low-lying 0^+ states would depress the ground state, and repel the other states possibly even above other low-lying states with different J values, such as the observed 2^+ states mentioned above.

The low-lying 2^+ states in even nuclei are then explained by the shell model as 2^+ states of seniority 2, viz. states formed by breaking the tight coupling of one of the $j^2(0)$ pairs, transferring it into a $j^2(2)$ state, and leaving the other pairs unaffected. It is usually possible to break a pair in each of several incomplete shells, and the experimentally observed 2^+ states are probably produced by the interference of these various 2^+ states. In extreme cases, where the possibilities of interference are very numerous, it is altogether better to consider them as collective states [76]). Nevertheless, when the energy needed to break a pair in one of the shells considerably differs from that in others, one might with due reservation attribute a given 2^+ state to a given shell. Similar remarks apply to low-lying 4^+, 6^+ . . . states of even nuclei. Thus, the consideration of the systematics of excited levels of even nuclei might also give information about the filling of nuclear shells.

Fig. 19 in § 32 shows the systematics of some low-lying excited levels in even nuclei.

PART II. THE COMPETITION BETWEEN NUCLEAR SHELLS

CHAPTER V. PRELIMINARY DISCUSSION

When studying the competition between nuclear subshells, one should in the first place apply data which are known with greater precision than the energy difference of no more than a few hundred keV between two nuclear configurations differing from one another in the distribution of the nucleons

† See ref. [78]) for a review and discussion of these 0^+ states, and for further references.

in the various subshells. Thus, total binding energies and separation energies should usually be excluded †. Beta decay energies are quite often known much more precisely. However, their interpretation involves both neutron and proton configurations and might thus initially be less obvious. Besides, the magnitude of these energies is usually very much larger than the energy differences between neighbouring subshells, and therefore subshell effects are hardly distinguishable at a glance. The best way seems to begin with the study of the excitation energies of low-lying single-particle states, which are most precisely known, and are given directly by the energy difference between the competing configurations. The method suffers, however, from the incompleteness of our experimental knowledge of nuclear isomerism, as compared to the knowledge of decay energies ††.

In a previous study [13]) on the competition between nuclear shells, which was based on an investigation of the systematics of excited levels, we applied an approximation assuming a short-range delta-type interaction between the nucleons. The nuclear parameters were then unequivocally expressed in terms of the positive-by-definition Slater integrals, and the limitations thus imposed on their signs sufficed in some cases to deduce the configurations from the systematics. Since, however, the study of nuclear binding energies and separation energies shows that the forces between nucleons in the low-lying nuclear states are certainly not of a short-range delta type (§ 8.1), it seems worth while to examine the matter anew.

29. The Factors Governing the Order of Shell Filling

In order to see how the neutrons would arrange themselves for a given proton configuration, we shall write the binding energy (19) for an even nucleus in the form

$$
\begin{aligned}
&B(j_1^{n_1} j_2^{n_2} j_3^{p_3} j_4^{p_4}) \\
&= B_0 + p_3 C_3 + p_4 C_4 + \tfrac{1}{2} p_3 \Pi_3 + \tfrac{1}{2} p_4 \Pi_4 + \tfrac{1}{2} p_3 (p_3 - 1) C_3 + \tfrac{1}{2} p_4 (p_4 - 1) C_4 + p_3 p_4 I^0_{34} \\
&+ n_1 (c_1 + \tfrac{1}{2}\pi_1 + p_3 I^0_{13} + p_4 I^0_{14}) + n_2 (c_2 + \tfrac{1}{2}\pi_2 + p_3 I^0_{23} + p_4 I^0_{24}) \qquad (59a) \\
&+ \tfrac{1}{2} n_1 (n_1 - 1) d_1 + n_1 n_2 I^0_{12} + \tfrac{1}{2} n_2 (n_2 - 1) d_2 .
\end{aligned}
$$

For an odd-N nucleus we shall similarly write:

$$
\begin{aligned}
&B(j_1^{n_1} j_2^{n_2} j_3^{p_3} j_4^{p_4}) \\
&= B_0 + p_3 C_3 + p_4 C_4 + \tfrac{1}{2} p_3 \Pi_3 + \tfrac{1}{2} p_4 \Pi_4 + \tfrac{1}{2} p_3 (p_3 - 1) C_3 + \tfrac{1}{2} p_4 (p_4 - 1) C_4 + p_3 p_4 I^0_{34} \\
&+ (n_1 - 1)(c_1 + \tfrac{1}{2}\pi_1 + p_3 I^0_{13} + p_4 I^0_{14}) + n_2 (c_2 + \tfrac{1}{2}\pi_2 + p_3 I^0_{23} + p_4 I^0_{24}) \qquad (59b) \\
&+ \qquad (c_1 \qquad + p_3 I^0_{13} + p_4 I^0_{14}) \\
&+ \tfrac{1}{2} n_1 (n_1 - 1) d_1 + n_1 n_2 I^0_{12} + \tfrac{1}{2} n_2 (n_2 - 1) d_2 .
\end{aligned}
$$

† A conspicuous exception are the very precise mass measurements recently carried out at Minnesota [18, 28, 29]).

†† As a matter of fact, the desire to gain additional information concerning nuclear shell filling gave the impetus to the present study.

Let us investigate first the terms which are linear in n_1 and n_2. When the value of the sum multiplying n_2 in (59a) is bigger than that of the sum multiplying n_1, all the pairs of neutrons will tend to be concentrated in shell j_2. Thus, the competition between the subshells does not arise from the linear terms of (59a, b), except that the single odd neutron in an odd-N nucleus might be in shell j_1, even when all the other paired neutrons are in j_2, in case the bracketed value in the third line of (59b) is bigger for j_2, and yet the bracketed value in the fourth line is bigger for j_1. This might, of course, only happen when the pairing energy is higher in j_2 than in j_1.

When the interaction of the protons with the j_1 neutrons is stronger than with the j_2 neutrons, $I^0_{1p} > I^0_{2p}$ †, they will increase the tendency of the neutrons to be in shell j_1 rather than in j_2. This is the *stabilization effect* of de Shalit and Goldhaber [40]). The same stabilization effect will cause the excitation energy of the single-particle j_2-state, obtained by a neutron transition from shell j_1 to shell j_2 (eq. (57a)), to increase when protons favouring j_1 over j_2 are added in a sequence of odd-N isotones. The excitation energy of the single-particle j_2-state obtained by a neutron transition in the reverse direction (eq. (57b)) will likewise decrease. Similar results hold for odd-Z nuclei when neutrons are added.

As against the above, the orientation-independent interactions between identical nucleons are repulsive. Therefore, each of the quadratic terms contributed by the d's to eqs. (59a, b) resists the concentration of the neutrons within its shell, whereas the I^0_{12} tends to drive them all into the same shell. When the repulsion d_1 in one of the shells is weaker than the other two interactions, I^0_{12} and d_2, the contribution of the quadratic terms to the binding energy will be of maximum value when all the neutrons are concentrated within j_1. On the other hand, when the repulsion I^0_{12} between the two shells is weakest, the maximum binding due to the quadratic terms will usually be achieved when the nucleons are distributed between the shells, and the more equal the distribution, the higher are the differences $(I^0_{12}-d)$. This can also be seen from eqs. (57a, b).

When there is a third even neutron shell, $j_0^{n_0}$, its interaction with the two shells j_1 and j_2, given by an additional term $n_0 n_1 I^0_{01} + n_0 n_2 I^0_{02}$ which should be added to eqs. (59a, b), tends to concentrate all the n_1+n_2 neutrons in the shell for which the absolute value of the last sum is smallest (the parameters are negative). Thus, there exists, as a matter of fact, a stabilization effect for identical particles too, however it should more appropriately be called a *smaller destabilization effect* (see § 32 for an example).

When comparing the conclusions arrived at so far with the corresponding results for delta forces, it is seen that as far as the interaction between particles of different kinds with its various stabilization possibilities is

† In this case we say that the proton shells prefer or favour neutron shell j_1 over j_2.

concerned, the situation is qualitatively the same, due to the attractive character of the interaction in both cases. The possibility of a stabilization effect for particles of the same kind likewise exists, though the stabilization, due to attraction between like particles in different shells for the case of delta forces, is really a lesser destabilization for the actual repulsive interaction. On the other hand, the tendency of identical nucleons towards equal distribution between their shells, which is universal for delta forces, due to the attraction between the shells caused thereby, is no longer universally valid. The situation depends upon the sign of the (I^0-d)'s, which replace the positive $\frac{1}{2}F^0_{12}$ of delta forces in the energy differences formulas (57a, b). †

The foregoing discussion, based on eqs. (59a, b) and (57a, b), assumes pure nuclear configurations. Configurations assigned on its basis from an analysis of energy level systematics should thus not be regarded too reliable ††. Nevertheless, they might serve as a starting point for more detailed calculations taking configuration-interaction into account †††, and they offer a very simple explanation of the gross features of the systematics from which they were inferred.

CHAPTER VI. NUCLEAR GROUND-STATE CONFIGURATIONS IN ODD-MASS NUCLEI

In this final chapter we shall briefly reconsider the question of the ground state configurations of odd-mass nuclei. We shall not repeat the detailed arguments given elsewhere [13]).

Each section contains graphs, showing the systematics of the pertinent single-particle excited levels in odd-mass nuclei, and sometime also of low-lying excited levels of even nuclei. We likewise give tables showing nuclear configurations. The notation adopted previously [13]) is used in these tables, in particular the degree of reliability of the configurations is marked as follows:

a — an odd-group configuration determined by the nuclear moments or a configuration consisting of closed shells or subshells.

b — configurations determined by a quantitative consideration of energy-level systematics in odd-mass nuclei.

c — configurations determined by consistency considerations.

e — configurations determined by a qualitative discussion of the excited levels of even nuclei.

† The corresponding formulas for delta forces (eqs. (18a, b) of ref. [13])) are obtained from (57a, b) by putting $d = 0$, $I^0_{ss} = \frac{1}{2}F^0_{ss}$, $I^0_{sp} = F^0_{sp}$.

†† See the pertinent footnote in § 26.

††† Like those recently carried out by Kearsley [80]), True [81]) and Sheline [82]).

Configurations not designated by either of these letters are also sometimes given, but they are only tentative. Spins measured directly are designated by (d). Radioactive nuclei are marked (*).

Both the graphs and the tables are essentially a repetition [13]), with a few additional data [23, 28]). We do not give detailed references to the experimental data. These may be found in the three last-mentioned references.

30. The Competition Between the Neutron Shells $2p_{\frac{1}{2}}$ and $1g_{9/2}$

Fig. 17 shows the systematics of the binding energy difference $B(p_{\frac{1}{2}})-B(g_{9/2})$ for odd-N nuclei before $N = 50$. Table 5 gives the configurations assigned to these nuclei from an analysis of the systematics.

The last pair of protons was previously [13]) assumed to be in the $p_{\frac{1}{2}}$ shell. This still remains a plausible assumption, when considering both the

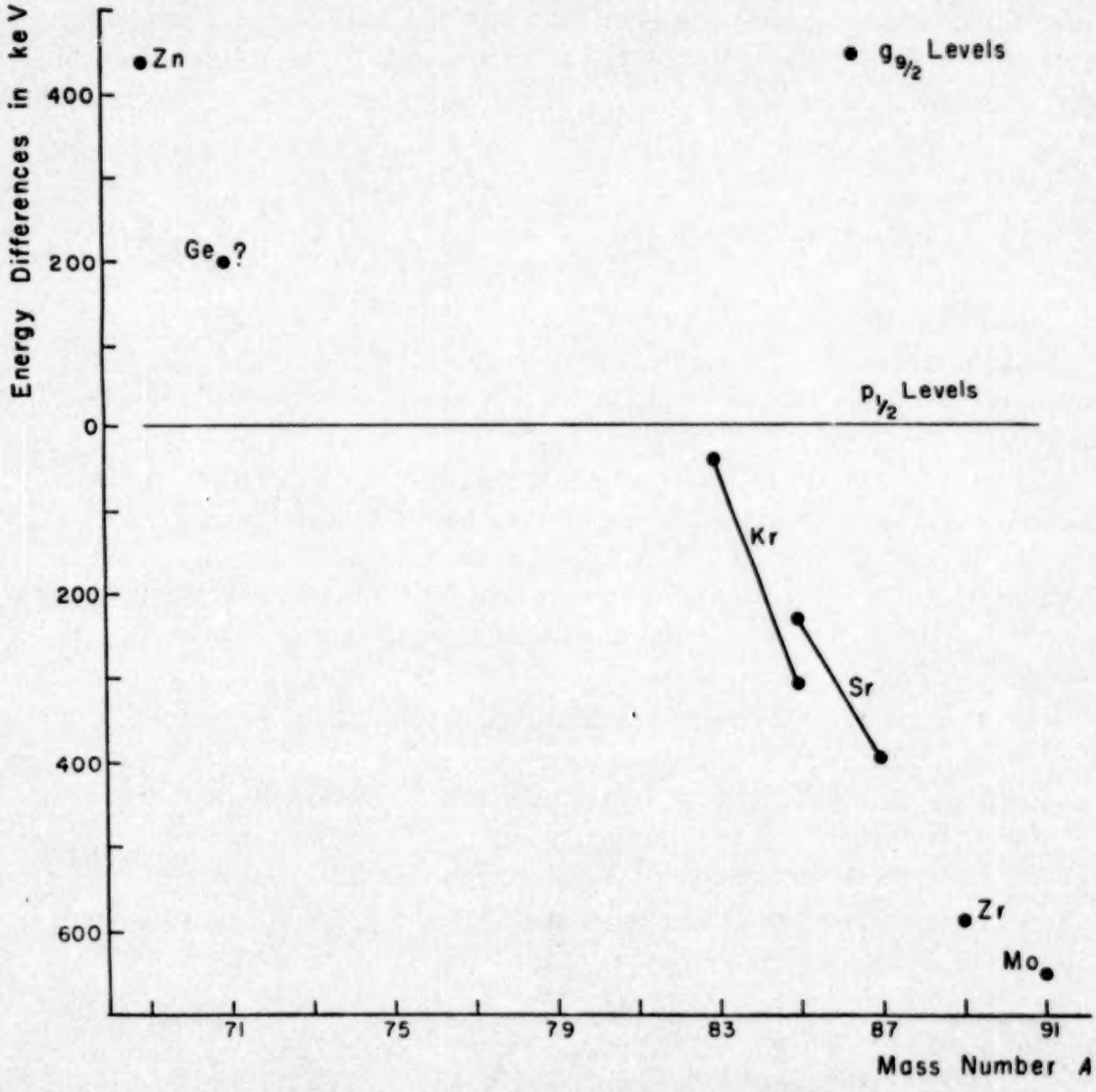

Fig. 17. $p_{\frac{1}{2}}$ and $g_{9/2}$ levels of odd-N nuclei before $N = 50$.

high difference of 913 keV of $B(p_{\frac{1}{2}})-B(g_{9/2})$ in Y^{89}, and the usual interpretation of the ground state and the first excited 0^+ state of Zr^{90} as arising from the proton configurations $p_{\frac{1}{2}}^2$ and $g_{9/2}^2$, respectively †. Thus the proton configurations of Sr, Zr and Mo are determined as in Table 5. The increase of the $p_{\frac{1}{2}}$ excitation energy from Sr^{87} to Zr^{89} and from this to Mo^{91} shows

TABLE 5

Ground-State Configurations of Odd-N Nuclei before $N = 50$

Nucleus	Z	N	$I^{\pm}$	μ	Q	Proton Shells $p_{3/2}$	$f_{5/2}$	$p_{\frac{1}{2}}$	$g_{9/2}$		Neutron Shells $p_{\frac{1}{2}}$	$g_{9/2}$	
Zn^{69*}	30	39	$1/2^-$			2					1		a
Ge^{71*}	32		$1/2^-$			?	?				1		a
Ge^{73}	32	41	$9/2^+$ (d)	−0.877	−0.22	?	?				?	?	
Se^{75*}	34		$5/2^{\dagger}$ (d)	−1.61	1.1	?	?				?	?	
Ge^{75*}	32	43	$1/2^-$			?	?				1	4	a
Se^{77}	34		$1/2^-$ (d)	0.533		?	?				1	4	a
Kr^{79*}	36		$1/2^-$			?	?				1	4	a
Sr^{81*}	38		$1/2^-$			4	6			a	1	4	a
Ge^{77*}	32	45	$7/2^{+\dagger}$			?	?				?	?	
Se^{79*}	34		$7/2^{+\dagger}$ (d)	−1.015	0.7	?	?				?	?	
Kr^{81*}	36		$7/2^{+\dagger}$			?	?				?	?	
Se^{81*}	34	47	$1/2^-$			?	?				1	8	a
Kr^{83}	36		$9/2^+$ (d)	−0.967	0.16	?	?				2	7	b
Sr^{85*}	38		$9/2^+$			4	6			a	2	7	b
Kr^{85*}	36	49	$9/2^+$ (d)	−1.001	0.27	?	?				2	9	a
Sr^{87}	38		$9/2^+$ (d)	−1.089		4	6			a	2	9	a
Zr^{89*}	40		$9/2^+$			4	6	2		b	2	9	a
Mo^{91*}	42		$9/2^+$			4	6	2	2	b	2	9	a

† Not a single-particle state.

that both proton shells $p_{\frac{1}{2}}$ and $g_{9/2}$ prefer the neutron shell $p_{\frac{1}{2}}$ over $g_{9/2}$, the $p_{\frac{1}{2}}$ proton shell much more so than the $9_{9/2}$.

A parallelogram is obtained by connecting the $g_{9/2}$ levels of Kr^{83}, Sr^{85}, Sr^{87} and Kr^{85} in fig. 17. The *parallelogram principle* deduced for the case of delta forces (eqs. (27) of ref. [13])) is valid for the more general formulas (57a, b) as well, as it depends only on the linearity of the formulas with respect to the nucleon numbers. Thus, the parallelogram suggests that the excited $p_{\frac{1}{2}}$ state is formed from the ground $g_{9/2}$ state by a neutron transition in the same direction in the above mentioned four nuclei, and that both isotopes of each element have identical proton configurations.

This is sufficient to determine the neutron configurations of Kr^{83} and Sr^{85}

† However, a recent work by Sheline [82]) shows, that though the main component of the ground state configuration is indeed $p_{\frac{1}{2}}^3$, the amount of $g^3_{9/2}$ is considerable.

as $p_{\frac{1}{2}}^2 g_{9/2}^7$. On the other hand, the available data do not allow the determination of the proton configuration of the Kr isotopes. The systematics show that from Kr to Sr the protons are added in a shell preferring the neutron shell $p_{\frac{1}{2}}$ over $g_{9/2}$. However, we do not even know whether only one or both proton shells prefer the $p_{\frac{1}{2}}$ neutrons. For a solution of this

TABLE 6

Ground-State Configurations of Odd-Z Nuclei before $N = 50$

Nucleus	Z	N	$I^{\pm}$	μ	Q	Proton Shells $p_{3/2}$ $f_{5/2}$	Neutron Shells $p_{3/2}$ $f_{5/2}$ $p_{\frac{1}{2}}$ $g_{9/2}$
Cu^{61*}	29	32	3/2 (d)			1 a	? ?
Cu^{63}		34	$3/2^-$ (d)	2.226	—0.16	1 a	? ?
Cu^{65}		36	$3/2^-$ (d)	2.386	—0.15	1 a	? ?
Cu^{67*}		38	$3/2^-$			1 a	4 6 a
Ga^{67*}	31	36	$3/2^-$ (d)	1.84	0.213	3	? ?
Ga^{69}		38	$3/2^-$ (d)	2.017	0.243	3 a	4 6 a
Ga^{71}		40	$3/2^-$ (d)	2.561	0.152	3 a	4 6 2
Ga^{73*}		42	$3/2^-$			3	4 6 2 2
As^{71*}	33	38	$5/2^-$			4 1	4 6 a
As^{73*}		40	$3/2^-$			3 2	4 6 2
As^{75}		42	$3/2^-$ (d)	1.439	0.3	3 2 a	4 6 2 2
As^{77*}		44	$3/2^-$			3 2	4 6 2 4
As^{79*}		46	$3/2^-$			3 2	4 6 2 6
Br^{77*}	35	42	$3/2^-$			3 4	4 6 2 2
Br^{79}		44	$3/2^-$ (d)	2.106	0.33	3 4 a	4 6 2 4
Br^{81}		46	$3/2^-$ (d)	2.269	0.28	3 4 a	4 6 2 6
Br^{83*}		48	$3/2^-$			3 4	4 6 2 8
Br^{85*}		50	$3/2^-$			3 4	4 6 2 10 a
Br^{87*}		52	$3/2^-$			3 4	4 6 2 10†
Rb^{81*}	37	44	$3/2^-$ (d)	2.00		3 6 a	4 6 2 4
Rb^{83*}		46	$5/2^-$			4 5 a	4 6 2 6
Rb^{85}		48	$5/2^-$ (d)	1.353	0.31	4 5 a	4 6 2 8
Rb^{87*}		50	$3/2^-$ (d)	2.749	0.15	3 6 a	4 6 2 10 a

† There is an additional neutron pair in $d_{5/2}$ or in $g_{7/2}$.

problem, it is very desirable to ascertain the $g_{9/2}$ state of Ge^{71} and also the relative position of the $p_{\frac{1}{2}}$ and $g_{9/2}$ levels of Se^{73}.

Moreover, the proton configurations of Kr are probably rather mixed, as may be inferred from the strong competition between the $p_{3/2}$ and $f_{5/2}$ states of the As, Br and Rb isotopes. The contributions of the various shells to the ground state configuration cannot be ascertained without higher-order calculations.

The increase of about 215 keV of the $p_{\frac{1}{2}}$ excitation energy from Kr^{83}

to Kr^{85} or from Sr^{85} to Sr^{87} is given (eq. (57b)) by $-2(d_{5/2}-I^0_{nn}(p_{\frac{1}{2}}\,g_{9/2}))$†. Thus, for these neutron shells the $(I^0_{nn}(p_{\frac{1}{2}}\,g_{9/2})-d_{5/2})$ is positive, resulting in the tendency of the neutrons to distribute themselves in the two subshells outweighing the mutual repulsion of the two subshells. The decisive factors determining the competition between these shells are therefore the same as in the case of delta forces.

Table 6 gives ground state configurations of odd-Z nuclei in this region, as deduced from the nuclear moments.

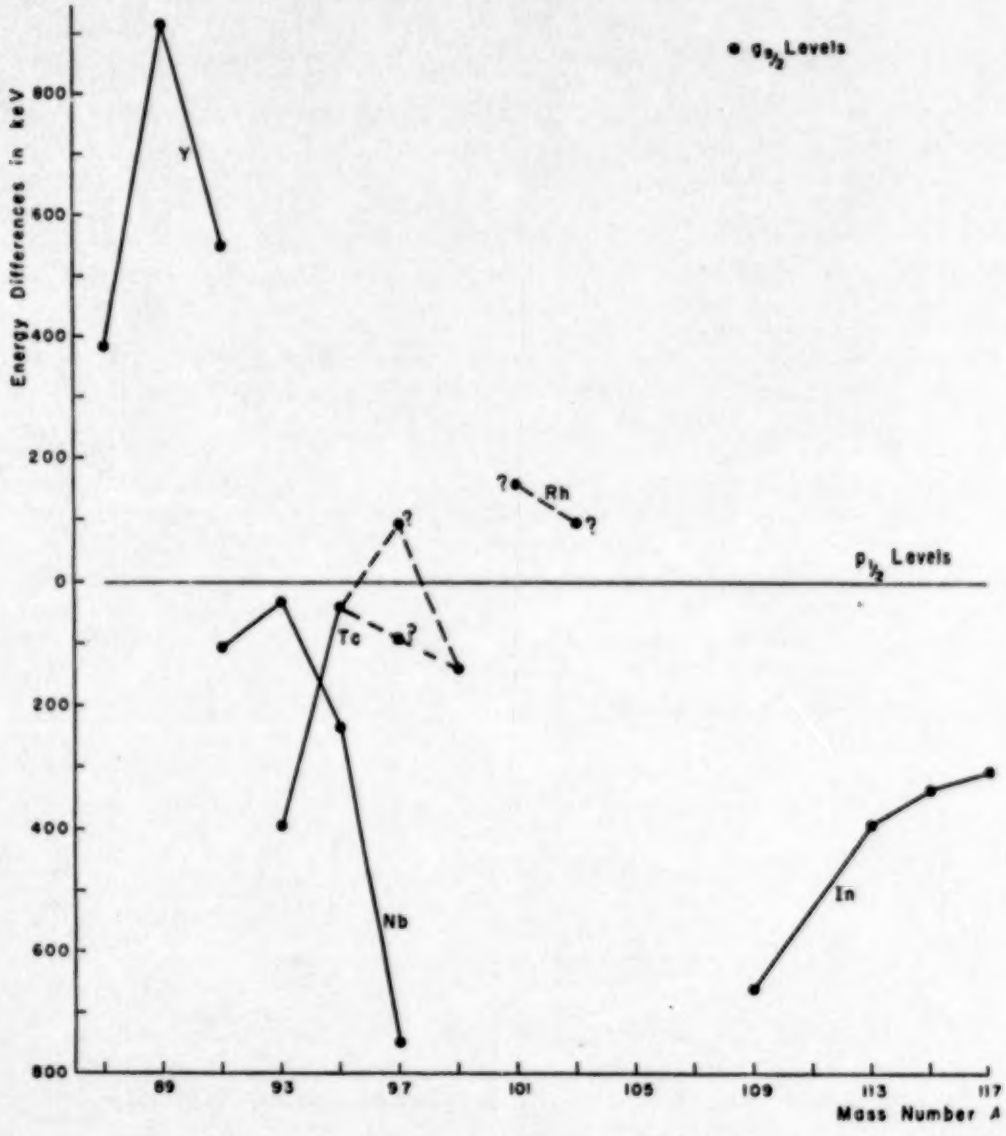

Fig. 18. $p_{\frac{1}{2}}$ and $g_{9/2}$ levels of odd-Z nuclei before $Z = 50$.

† Here $I^0{}_{nn}(p_{\frac{1}{2}}\,g_{9/2})$ denotes the I^0 between a $p_{\frac{1}{2}}$ and a $g_{9/2}$ neutron. Similarly, $I_{pp}{}^0(l_j\,l'_{j'})$ will denote an I^0 between an l_j and an $l'_{j'}$ proton, and $I_{np}{}^0(l_j\,l'_{j'})$ will denote an I^0 between an l_j neutron and an $l'_{j'}$ proton. This designation is more cumbersome than the one used with delta forces [13]), since there the I^0's depend only on the l-but not on the j-values of the shells.

31. The Competition Between the Proton Shells $2p_{\frac{1}{2}}$ and $1g_{9/2}$

Fig. 18 shows the systematics of $B(p_{\frac{1}{2}})-B(g_{9/2})$ for odd-Z nuclei before $Z = 50$. Table 7 gives the configurations deduced from the systematics.

Here too, the tendency of the protons to distribute themselves between the $p_{\frac{1}{2}}$ and $g_{9/2}$ shells dominates. This may be seen, for example, from

TABLE 7

Ground-State Configurations of Odd-Z Nuclei before $Z = 50$

Nucleus	Z	N	$I^{\pm}$	μ	Q	Proton Shells $p_{\frac{1}{2}}$	$g_{9/2}$		Neutron Shells $g_{9/2}$	$d_{5/2}$	$g_{7/2}$	$h_{11/2}$	
Y^{87*}	39	48	$1/2^-$			1		a	8				c
Y^{89}		50	$1/2^-$ (d)	—0.137		1		a	10				a
Y^{91*}		52	$1/2^-$			1		a	10	?	?		
Nb^{91*}	41	50	$9/2^+$			2	1	c	10				a
Nb^{93}		52	$9/2^+$ (d)	6.167	—0.2	?	?		10	?	?		
Nb^{95*}		54	$9/2^+$			?	?		10	?	?		
Nb^{97*}		56	$9/2^+$			?	?		10	?	?		
Tc^{93*}	43	50	$9/2^+$			2	3	c	10				a
Tc^{95*}		52	$9/2^+$			?	?		10	?	?		
Tc^{97*}		54	$1/2^-$?†			1	4	?	10	?	?		
Tc^{99*}		56	$9/2^+$ (d)	5.681		?	?		10	?	?		
Tc^{101*}		58	$9/2^+$			?	?		10	?	?		
Rh^{101*}	45	56	$1/2^-$? ††			1	6	?	10	?	?		
Rh^{103}		58	$1/2^-$ (d)	—0.088		1	6	a	10	?	?		
Rh^{105*}		60	$7/2^+$ †††			?	?		10	?	?		
Ag^{105*}	47	58	1/2 (d)			1	8	a	10	?	?		
Ag^{107}		60	$1/2^-$ (d)	—0.113		1	8	a	10	?	?		
Ag^{109}		62	$1/2^-$ (d)	—0.130		1	8	a	10	?	?		
Ag^{111*}		64	$1/2^-$ (d)	—0.145		1	8	a	10	6	8		a
Ag^{113*}		66	$1/2^-$			1	8	a	10	6	8	2	
Ag^{115*}		68	$1/2^-$			1	8	a	10	6	8	4	
In^{109*}	49	60	$9/2^+$			2	9	a	10	?	?		
In^{111*}		62	$9/2^+$			2	9	a	10	?	?		
In^{113}		64	$9/2^+$ (d)	5.522	1.181	2	9	a	10	6	8		a
In^{115*}		66	$9/2^+$ (d)	5.534	1.198	2	9	a	10	6	8	2	b?
In^{117*}		68	$9/2^+$			2	9	a	10	6	8	4	b?

† Way *et al.*[48]) also suggest a ground state $p_{\frac{1}{2}}$ for Tc^{97}.
†† We suggest a $p_{\frac{1}{2}}$ ground state from regularity considerations, as explained in the text.
††† Not a single-particle state.

the fact that the addition of two protons to Ag, resulting in In, changes the ground state proton configuration from $p_{\frac{1}{2}}g_{9/2}^8$ to $p_{\frac{1}{2}}^2g_{9/2}^9$. Thus $(I^0_{pp}(p_{\frac{1}{2}}g_{9/2})-D_{9/2})$ is positive, and the ground state proton configurations of Nb^{91} and Tc^{93} are $p_{\frac{1}{2}}^2g_{9/2}$ and $p_{\frac{1}{2}}^2g_{9/2}^3$, respectively, by reasoning along the same lines as in ref. [13]).

From the decrease of the excitation energy of the $p_{\frac{1}{2}}$ level from In^{109} to In^{113}, we infer that the neutron shell which is being filled prefers the proton shell $g_{9/2}$ over $p_{\frac{1}{2}}$, and much more so than the neutron shell $h_{11/2}$, which is probably filled in In^{115} and In^{117}.

We wish to add a remark concerning Tc^{97} and Rh^{101}. Regularity considerations [13]) led to the suggestion that the ground state of Tc^{97} is $p_{\frac{1}{2}}$, rather than $g_{9/2}$. This was likewise suggested by Way *et al.* [48]) from lifetime considerations. If the $g_{9/2}$ level of Rh^{103} suggested by Saraf[83] is correct †, and if the M4 transition of 158 keV found in Rh^{101} [84, 28]) also leads from an excited $g_{9/2}$ state to a ground state $p_{\frac{1}{2}}$, then the maximum of the $g_{9/2}$ curves in fig. 18 is regularly shifted from Y^{89} to Nb^{93}, thence to Tc^{97} and to Rh^{101}.

32. The Competition Between the Neutron Shells $3s_{\frac{1}{2}}$, $2d_{3/2}$ and $1h_{11/2}$

Fig. 19 shows the systematics of the low-lying 2^+ excited levels of the even isotopes of Cd, Sn, Te, Xe, Ba and Ce before $N = 82$. Fig. 20 shows

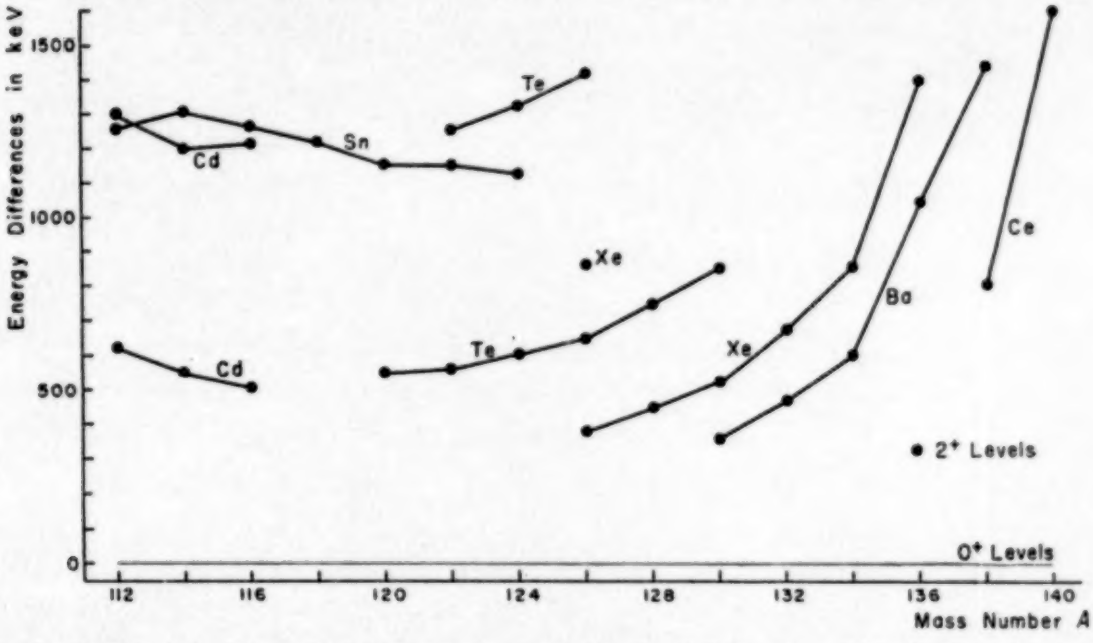

Fig. 19. Low-lying 2^+ levels of even isotopes of Cd, Sn, Te, Xe, Ba and Ce before $N = 82$.

the systematics of the single-particle $s_{\frac{1}{2}}$, $d_{3/2}$ and $h_{11/2}$ levels of the odd-N isotopes of the above elements with the exception of Cd. Table 8 gives ground state configurations of odd-N nuclei before $N = 82$.

The first 2^+ excited level in Sn is now [28, 118]) known from Sn^{112} up to and including Sn^{124} (fig. 19). It may be plausibly attributed to an $h^2_{11/2}(2)$ neutron pair, with the conclusion that up to Sn^{124}, with ten neutrons outside the closed shells $d_{5/2}$ and $g_{7/2}$, the $d_{3/2}$ neutron shell is empty. The same applies to the

† Recent investigation [117]) shows that this is probably the case.

Te isotopes, whose second excited level may be attributed to the $h_{11/2}$ shell as well. The recently [85]) Coulomb-excited second 2^+ levels of the Cd

TABLE 8

Ground-State Configurations of Odd-N Nuclei before $N = 82$

Nucleus	Z	N	$I^{\pm}$	μ	Q	Proton Shells $g_{9/2}$ $d_{5/2}$ $g_{7/2}$	Neutron Shells $s_{\frac{1}{2}}$ $d_{3/2}$ $h_{11/2}$
Cd^{111}	48	63	$1/2^+$ (d)	—0.592		8 e	1†
Sn^{113*}	50		$1/2^+$			10 a	1†
Cd^{113*}	48	65	$1/2^+$ (d)	—0.620		8 e	1 a
Sn^{115}	50		$1/2^+$ (d)	—0.913		10 a	1 a
Cd^{115*}	48	67	$1/2^+$			8 e	1 2
Sn^{117}	50		$1/2^+$ (d)	—0.995		10 a	1 2 b, e
Sn^{119}	50	69	$1/2^+$ (d)	—1.041		10 a	1 4 b, e
Te^{121*}	52		$1/2^+$			10 2 b	1 4 b
Sn^{121*}	50	71	$3/2^+$			10 a	? ? ?
Te^{123*}	52		$1/2^+$ (d)	—0.732		10 2 b	1 6 b, e
Sn^{123*}	50	73	$3/2^+$			10 a	? ? ?
Te^{125}	52		$1/2^+$ (d)	—0.882		10 2 b	1 8 b, e
Xe^{127*}	54		$3/2^+$			10 ? ?	? ? ?
Sn^{125*}	50	75	$11/2^-$?			10 a	? ? ?
Te^{127*}	52		$3/2^+$			10 ? ?	? ? ?
Xe^{129}	54		$1/2^+$ (d)	—0.773		10 4 b	1 10 b
Te^{129*}	52	77	$3/2^+$			10 ? ?	? ? ?
Xe^{131}	54		$3/2^+$ (d)	0.687	—0.12	10 4 b	1 12 b
Ba^{133*}	56		$1/2^+$			10 6 b	1 12 b
Te^{131*}	52	79	$3/2^+$			10 2 b	2 1 12 b, c
Xe^{133*}	54		$3/2^+$			10 4 b	2 1 12 b, c
Ba^{135}	56		$3/2^+$ (d)	0.835		10 6 b	2 1 12 b, c
Ce^{137*}	58		$3/2^+$			10 ? ?	2 1 12 b, c
Te^{133*}	52	81	$3/2^+$			10 2 b	2 3 12 a
Xe^{135*}	54		$3/2^+$			10 4 b	2 3 12 a
Ba^{137}	56		$3/2^+$ (d)	0.935		10 6 b	2 3 12 a
Ce^{139*}	58		$3/2^+$			10 8 b	2 3 12 a

† There are two holes either in the $d_{5/2}$ or in the $g_{7/2}$ neutron shell.

isotopes also fit the picture quite well †. It must, however, be pointed out, that the existence of this level as a first excited level in Sn^{114}, with 64 neutrons only, and even in the still lighter Sn^{112}, might indicate that the neutron configurations are really very mixed, and the attribution of a given level to a given shell is meaningless.

† Previously [13]), their absence was one of the objections to the above interpretation of the Sn 2^+ levels.

The first excited levels of the even isotopes of Cd, Te, Xe, Ba and Ce are naturally attributed to their incomplete proton shells. However, the steep rise of their lines on approaching the magic number $N = 82$ might point out that they, too, are quite mixed with the neutron 2^+ levels.

It would be very desirable to find whether the first excited level of Sn^{126} and the second excited level of Te^{128} smoothly continue the respective lines

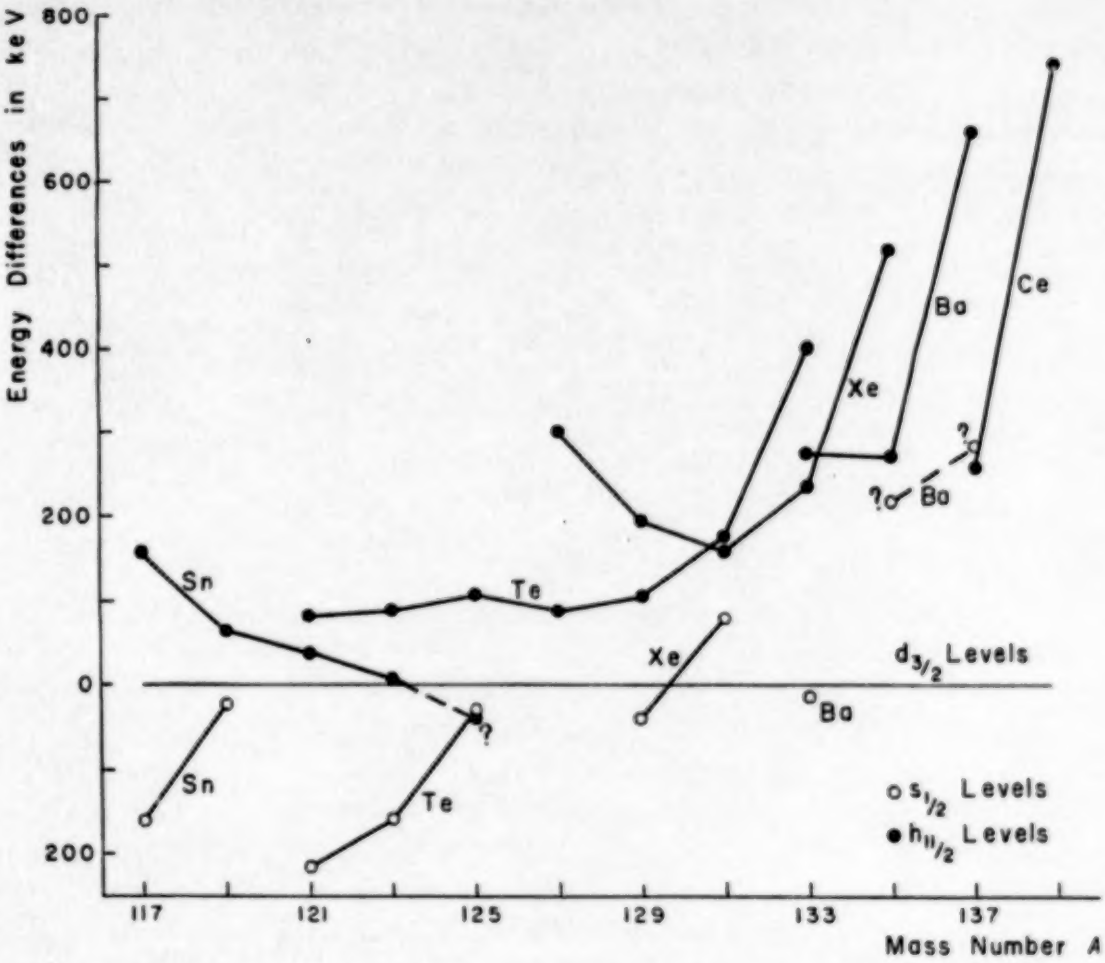

Fig. 20. $s_{\frac{1}{2}}$, $d_{3/2}$ and $h_{11/2}$ levels of odd-N nuclei before $N = 82$.

in fig. 19, in order to know whether the $s_{\frac{1}{2}}$ neutron shell is already filled in these nuclei or not.

In view of the strong tendency of neutron pairs to fill the $h_{11/2}$ shell, it is but natural to assume that they all also fill it in the odd-N lighter isotopes of Sn, Te, Xe and Ba. Then there is but one single neutron in $s_{\frac{1}{2}}$ or $d_{3/2}$, determining the j value of the nucleus. The change of the ground state from $s_{\frac{1}{2}}$ in the lighter isotopes of these elements to $d_{3/2}$ in the heavier ones, as well as the decrease of the $d_{3/2}$ excitation energy in the latter (fig. 20),

show then that the $h_{11/2}$ neutron shell repels the $d_{3/2}$ neutrons less strongly than those in $s_{\frac{1}{2}}$, thus pushing the odd neutron from $s_{\frac{1}{2}}$ to $d_{3/2}$ as $h_{11/2}$ gradually fills up. This assumes the form of a stabilization effect exerted on the $d_{3/2}$ neutron shell by the $h_{11/2}$ neutron shell, as already mentioned in § 29.

On the other hand, the last $g_{7/2}$ [13]) proton pairs of Te, Xe and Ba, prefer the neutron shell $s_{\frac{1}{2}}$ over $d_{3/2}$, which is reflected both in the ground state variations, and in the increase of the $d_{3/2}$ excitation energy, from the lighter to the heavier isotones.

There still remains unexplained the $d_{3/2}$-assigned [86]) ground state of Xe^{127}. Likewise, it is very desirable to find the $s_{\frac{1}{2}}$ states of the heavier Sn, Te and Xe odd-N isotopes, in connection with the question of when the $s_{\frac{1}{2}}$ neutron shell first becomes filled.

Turning now to the two heaviest isotopes before $N = 82$ of each of the odd-N isotopes of Te, Xe, Ba and Ce, we see three somewhat distorted parallelograms, whose vertices are formed by the $h_{11/2}$ levels of these nuclei, and whose sides connect the levels of isotopes and also the levels of isotones. This suggests the application of the parallelogram principle (§ 30). There are three possibilities for the neutron configuration of Te^{131}, Xe^{133}, Ba^{135} and Ce^{137}, viz.: $s_{\frac{1}{2}}^2 d_{3/2} h_{11/2}^{12}$, $d_{3/2}^3 h_{11/2}^{12}$ and $s_{\frac{1}{2}}^2 d_{3/2}^3 h_{11/2}^{10}$. In the case of delta forces [13]) the last one was excluded by the increase of the $h_{11/2}$ excitation energy from the lighter to the heavier isotopes. In the present approximation, when the last configuration is adopted, this increase is given by $-2(I^0_{nn}(d_{3/2}h_{11/2})-d_{11/2})$, and it cannot be said a priori whether (I^0-d) is positive, which would exclude the adopted neutron configuration, or whether it is negative.

However, Fagg [87]) suggests that the 218 keV and 281 keV levels in Ba^{135} and Ba^{137}, respectively, are $s_{\frac{1}{2}}$. If this is so, the configuration $s_{\frac{1}{2}}^2 d_{3/2}^3 h_{11/2}^{10}$ in Ba^{135} is excluded, as it implies a decrease of the $s_{\frac{1}{2}}$ excitation energy from Ba^{135} to Ba^{137} due to the addition of two $h_{11/2}$ neutrons 'preferring' $d_{3/2}$ to $s_{\frac{1}{2}}$, whereas experimentally the excitation energy increases.

The choice between the other two possibilities can be achieved most directly by measuring the quadrupole moment of Ba^{135}, or by discovering the $s_{\frac{1}{2}}$ level in either of Te^{131}, Xe^{133} and Ce^{137} and comparing it to that of Ba^{135}. Meanwhile, the configuration $d_{3/2}^3 h_{11/2}^{12}$ can be excluded by consistency considerations: the systematics of $B(s_{\frac{1}{2}})-B(d_{3/2})$ shows that the ground state neutron configuration of Ba^{133} is probably $s_{\frac{1}{2}} h_{11/2}^{12}$. Likewise, the ground state configuration of Ba^{137} is $s_{\frac{1}{2}}^2 d_{3/2}^3 h_{11/2}^{12}$ rather than $s_{\frac{1}{2}} d_{3/2}^4 h_{11/2}^{12}$. These two configurations imply that a configuration $s_{\frac{1}{2}}^2 d_{3/2} h_{11/2}^{12}$ in Ba^{135} would be more stable than $d_{3/2}^3 h_{11/2}^{12}$.

Thus the neutron configuration of Te^{131}, Xe^{133}, Ba^{135} and Ce^{137} is probably $s_{\frac{1}{2}}^2 d_{3/2} h_{11/2}^{12}$, and the increase of the excitation energy of the $h_{11/2}$ level, when

passing to the heavier isotopes, is given by $2(I^0_{nn}(d_{3/2}\,h_{11/2})-d_{11/2})$. Therefore this is positive, showing that the repulsion within the $h_{11/2}$ neutron shell still overcomes the repulsion between the $d_{3/2}$ and $h_{11/2}$ shells, resulting in a tendency of the neutrons to distribute themselves between the two shells, as was the case with delta forces.

The increase of the $h_{11/2}$ excitation energy from Te^{133} to Xe^{135}, from this to Ba^{137} and from the latter to Ce^{139}, shows that the $g_{7/2}$ protons prefer the $h_{11/2}$ neutron shell over $d_{3/2}$.

TABLE 9
Ground-State Configurations of Odd-Z Nuclei before $N = 82$

Nucleus	Z	N	$I^{\pm}$	μ	Q	Proton Shells $d_{5/2}$	$g_{7/2}$	$s_{\frac{1}{2}}$	Neutron Shells $s_{\frac{1}{2}}$	$d_{3/2}$	$h_{11/2}$	
Sb^{117*}	51	66	5/2+			1		a			2	
Sb^{121}		70	5/2+ (d)	3.360	—0.52	1		a			6	
Sb^{123}		72	7/2+ (d)	2.547	—0.67		1	a			8	
Sb^{125*}		74	7/2+				1	a			10	
I^{123*}	53	70	5/2 (d)			1	2				6	
I^{125*}		72	5/2+ (d)	3.0	—0.66	1	2	a			8	
I^{127}		74	5/2+ (d)	2.808	—0.75	1	2	a			10	
I^{129*}		76	7/2+ (d)	2.617	—0.47		3				12	
I^{131*}		78	7/2+ (d)	2.56	—0.29		3			2	12	
I^{133*}		80	7/2+				3			2 2	12	
Cs^{127*}	55	72	1/2 (d)	1.41†		?	?	1 ?			8	
Cs^{129*}		74	1/2 (d)	1.47†		?	?	1 ?			10	
Cs^{131*}		76	5/2+ (d)	3.48		1	4				12	
Cs^{133}		78	7/2+ (d)	2.579	—0.003		5††			2	12	
Cs^{135*}		80	7/2+ (d)	2.727			5			2 2	12	
Cs^{137*}		82	7/2+ (d)	2.840			5			2 4	12	a
La^{137*}	57	80	7/2+			?	?			2 2	12	
La^{139}		82	7/2+ (d)	2.778	0.268	?	?			2 4	12	a
Pr^{141}	59	82	5/2+ (d)	3.9	—0.054	3	6	a?		2 4	12	a

† The sign of the moment is somewhat uncertain [52]).
†† This state is really a mixture [13]).

It must be added, that $B(d_{3/2})-B(h_{11/2})$ decreases from Ba^{135} to Ce^{137}, whereas according to the parallelogram interpretation it should increase. This, as well as the overall distortion of the parallelograms, and the strong competition between the proton shells $2d_{5/2}$ and $1g_{7/2}$ in odd-Z nuclei, show that the interpretation of the data in terms of pure configurations cannot have more than a qualitative significance. The change of sign of the increase of the $h_{11/2}$ excitation energy from Ba^{135} to Ce^{137} might perhaps indicate that the main component of the proton configuration in Ce^{137} is $d^2_{5/2}\,g^6_{7/2}$ rather than $g^8_{7/2}$.

Table 9 gives ground state configurations of odd-Z nuclei before $N = 82$.

33. The Competition Between the Proton Shells $3s_{\frac{1}{2}}$, $2d_{3/2}$ and $1h_{11/2}$, and the Competition Between the Neutron Shells $3p_{3/2}$, $3p_{\frac{1}{2}}$, $2f_{5/2}$ and $1i_{13/2}$

Fig. 21 shows the systematics of the single-particle $s_{\frac{1}{2}}$, $d_{3/2}$, $d_{5/2}$ and $h_{11/2}$ levels of the odd-mass isotopes of Ir, Au and Tl. Table 10 gives ground

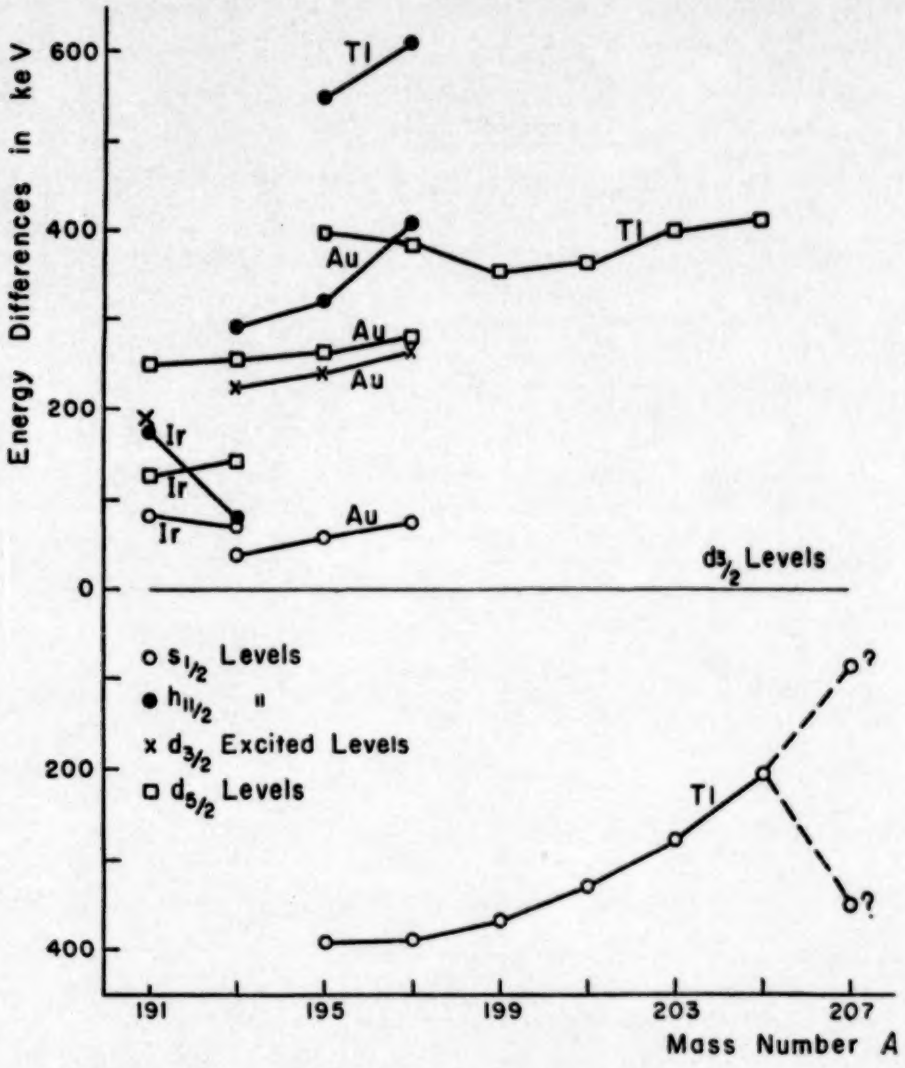

Fig. 21. $s_{\frac{1}{2}}$, $d_{3/2}$, $d_{5/2}$ and $h_{11/2}$ levels of odd-Z nuclei before $Z = 82$.

state proton configurations of odd-Z nuclei. An exhaustive summary of the experimental data in this region and of their theoretical interpretations has been recently published by Bergström and Andersson [77]).

The proton configurations of Au and Tl were deduced [13]) from the variation of excitation energies of isotopes when neutrons are added. They remain therefore unaffected. The change of the ground state from $d_{3/2}$ in Au to $s_{\frac{1}{2}}$ in Tl shows that the $h_{11/2}$ protons 'prefer' the $d_{3/2}$ proton shell

over $s_{\frac{1}{2}}$. The decrease of $B(s_{\frac{1}{2}})-B(d_{3/2})$ from the lighter to the heavier isotopes of Au and Tl shows that the neutrons added prefer the $s_{\frac{1}{2}}$ proton shell over $d_{3/2}$.

It is worth mentioning that the increase of the $h_{11/2}$ excitation energy in the heavier isotopes of both Au and Tl suggests that they are similarly produced in these nuclei, viz. by a proton transition from the $h_{11/2}$ shell.

TABLE 10

Ground-State Proton Configurations of Odd-Z Nuclei before $Z = 82$, $N = 126$

Nucleus	Z	N	$I^{\pm}$	μ	Q	Proton Shells $s_{\frac{1}{2}}$	$d_{3/2}$	$h_{11/2}$	
Ir^{191}	77	114	3/2+ (d)	0.17	1.5		3	10	b
Ir^{193}		116	3/2+ (d)	0.17	1.5		3	10	b
Au^{191*}	79	112	3/2+ (d)			2	3	10	
Au^{193*}		114	3/2+ (d)			2	3	10	b
Au^{195*}		116	3/2+			2	3	10	b
Au^{197}		118	3/2+ (d)	0.13	0.56	2	3	10	b
Au^{199*}		120	3/2+ (d)	|0.24|†		2	3	10	
Tl^{195*}	81	114	1/2+			1	4	12	a
Tl^{197*}		116	1/2+ (d)			1	4	12	a
Tl^{199*}		118	1/2+ (d)			1	4	12	a
Tl^{201*}		120	1/2+			1	4	12	a
Tl^{203}		122	1/2+ (d)	1.611		1	4	12	a
Tl^{205}		124	1/2+ (d)	1.627		1	4	12	a
Tl^{207*}		126	1/2+			1	4	12	a

† Only the absolute value of the moment is known.

If the neutron configuration is the same in the Au and Tl isotones, the increase of the $h_{11/2}$ excitation energy from Au to Tl shows that the mutual repulsion of protons in the $h_{11/2}$ shells is weaker than the repulsion between the proton shells $h_{11/2}$ and $d_{3/2}$, or $h_{11/2}$ and $s_{\frac{1}{2}}$ (the latter repulsion is even stronger, as evidenced by the preference of $d_{3/2}$ over $s_{\frac{1}{2}}$ by $h_{11/2}$). This is contrary to the situation in the lighter nuclei of the preceding sections, where the repulsion between the shells was always the weaker, and the tendency of the nucleons to distribute themselves among the shells was the prevailing one.

The suggested [88]) change of direction of the Tl $s_{\frac{1}{2}}$-line at Tl^{205} might immediately be interpreted in our approximation, since the last pair of neutrons in Tl^{207} begins a new shell, namely $p_{\frac{1}{2}}$. If the latter prefers the proton shell $d_{3/2}$ over $s_{\frac{1}{2}}$, it will become more difficult to excite the $d_{3/2}$ state. However, it is not certain [88]) whether the $s_{\frac{1}{2}}$ level lies 353 keV or only 85 keV below the $d_{3/2}$ level, in which case the $s_{\frac{1}{2}}$ line continues smoothly up to Tl^{207}.

The decrease of the $s_{\frac{1}{2}}$ excitation energy from Ir^{191} to Ir^{193}, as compared to its increase from the lighter to the heavier Au isotopes, suggests that the proton configuration of Ir is $d^3_{3/2}h^{10}_{11/2}$. The decrease of the $h_{11/2}$ excitation energy from Ir^{191} to Ir^{193} suggests that these $h_{11/2}$ states are formed by a proton transition from $d_{3/2}$ to $h_{11/2}$, contrary to the situation in Au and Tl.

Fig. 22 shows the systematics of the single-particle $p_{3/2}$, $p_{\frac{1}{2}}$, $f_{5/2}$ and $i_{13/2}$

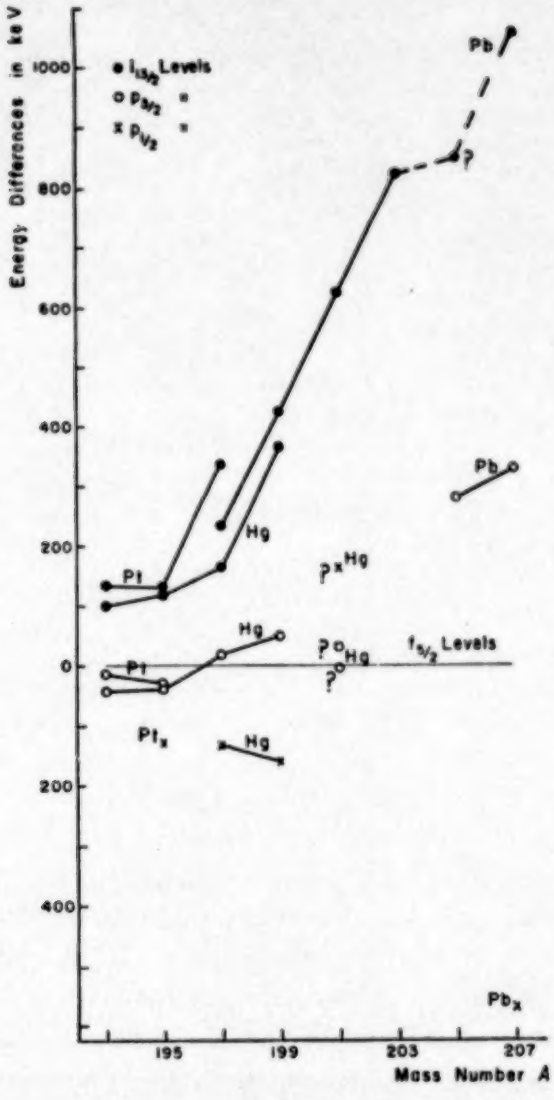

Fig. 22. $p_{3/2}$, $p_{\frac{1}{2}}$, $f_{5/2}$ and $i_{13/2}$ levels of odd-N nuclei before $N = 126$.

levels of the odd-mass isotopes of Pt, Hg and Pb †. We had no simple interpretation of this particularly linear systematics [13]).

Table 11 gives tentative ground state configurations of odd-N nuclei,

† From regularity considerations we assign the shells $p_{3/2}$, $f_{5/2}$ and $i_{13/2}$, to the ground and the two excited levels at 13 and 148 keV, respectively, of Pt^{193} measured by Ewan [89]), though he preferred the assignments $1/2^-$, $3/2^-$ and $11/2^+$, on the basis of Nilsson's model [90]).

as deduced previously [13]), and also neutron configurations of some Pb isotopes, as calculated by Pryce [91, 92]) assuming a delta interaction between the nucleons.

TABLE 11

Ground-State Configurations of Odd-N Nuclei before $Z = 82$, $N = 126$

Nucleus	Z	N	$I^{\pm}$	μ	Q	Proton Shells $s_{\frac{1}{2}}$ $d_{3/2}$ $h_{11/2}$	Neutron Shells $f_{5/2}$ $p_{3/2}$ $p_{\frac{1}{2}}$ $i_{13/2}$
Os^{187}	76	111	1/2 (d)	0.12		? ? ?	? ? ? ?
Os^{189}	76	113	3/2† (d)	0.65	0.6	? ? ?	? ? ? ?
Hg^{193*}	80		3/2⁻			2 2 12	? ? ? ?
Os^{191*}	76	115	9/2⁻†			? ? ?	? ? ? ?
Pt^{193*}	78		3/2⁻ ?††			2 2 10 e	? 3 ? †††
Hg^{195*}	80		3/2⁻			2 2 12	? 3 ? †††
Pb^{197*}	82		5/2-? ††††			2 4 12 a	? ? ? ?
Pt^{195}	78	117	1/2⁻ (d)	0.601		2 2 10 e	? 4 1 ? †††
Hg^{197*}	80		1/2⁻ (d)	0.52		2 2 12	? 4 1 ? †††
Pb^{199*}	82		5/2-? ††††			2 4 12 a	? ? ? ?
Pt^{197*}	78	119	1/2-?			2 2 10 e	? 4 1 ? ††† ?
Hg^{199}	80		1/2⁻ (d)	0.499		2 2 12 e	? 4 1 ? †††
Pb^{201*}	82		5/2⁻ ††††			2 4 12 a	1 4 14 †††††
Hg^{201}	80	121	3/2⁻ (d)	−0.554	0.45	2 2 12 e	? 3 ? †††
Pb^{203*}	82		5/2⁻††††			2 4 12 a	3 4 14 †††††
Hg^{203*}	80	123	5/2, 3/2⁻††††			2 2 12	? ? ? ?
Pb^{205*}	82		5/2⁻ ††††			2 4 12 a	5 4 14 †††††
Hg^{205*}	80	125	1/2⁻			2 2 12	6 4 1 14 a
Pb^{207}	82		1/2⁻ (d)	0.584		2 4 12 a	6 4 1 14 a

† Not a single-particle state.

†† We suggest a $p_{3/2}$ state from similarity considerations: there is a change of direction in the $i_{13/2}$ line of the Hg nuclei at Hg^{197} (fig. 22) accompanied by a change of the ground state spin from $p_{3/2}$ to $p_{\frac{1}{2}}$. There is a similar change at Pt^{195}, which brought us to the above suggestion. This assumption is also consistent with Ewan's [89]) results, as explained in the text.

††† These partial neutron configurations were derived [13]) by assuming a delta-type interaction between the nucleons. They should be accepted with reservation.

†††† J assignment taken from Bergström and Andersson [77]).

††††† Configuration according to Pryce [91, 92]).

I am grateful to Dr. W. H. Johnson and Dr. L. W. Fagg for communicating to me their results before publication. Likewise, I am grateful to Dr. H. B. Levy and to Dr. A. G. W. Cameron for sending me prepublication copies of their papers, and to Professor C. D. Coryell, for a copy of the thesis by Fix.

I also wish to express my gratitude to Mr. N. Spektor and Mr. J. Stuttard for help in the calculations.

The figures were drawn by Mr. S. Levy of the Weizman Scientific Press, Jerusalem, and also at Engineering Tracing Agency, Birmingham, and at the North Holland Publishing Company.

Thanks are also due to Mr. M. Spitz, Miss S. Paulin and Miss K. Sumner for typing the manuscript.

Finally, I am most grateful to Professor Racah for continuous encouragement and for several stimulating discussions. I likewise thank Professor R. E. Peierls for enabling me to complete this study at Birmingham University, and for several critical remarks.

A maintenance grant from the friends of the Hebrew University of Jerusalem is gratefully acknowledged.

References

1) M. G. Mayer, Phys. Rev. **78** (1950) 16
2) M. G. Mayer, Phys. Rev. **78** (1950) 22
3) M. G. Mayer and J. H. D. Jensen, Elementary Theory of Nuclear Shell Structure (John Wiley & Sons, New York, 1955)
4) G. Racah, Phys. Rev. **63** (1943) 367 (referred to as III in the present work)
5) B. C. Carlson and I. Talmi, Phys. Rev. **96** (1954) 436
6) S. Goldstein and I. Talmi, Phys. Rev. **102** (1956) 589
7) S. Goldstein and I. Talmi, Phys. Rev. **105** (1957) 995
8) I. Talmi, Phys. Rev. **107** (1957) 326
9) I. Talmi, Phys. Rev. **107** (1957) 1601
10) R. Thieberger and I. Talmi, Phys. Rev. **102** (1956) 923
11) I. Talmi and R. Thieberger, Phys. Rev. **103** (1956) 718
12) R. Thieberger and A. de Shalit, Phys. Rev. **108** (1957) 378
13) N. Zeldes, Nuclear Physics **2** (1956/57) 1
14) C. Schwartz and A. de Shalit, Phys. Rev. **94** (1954) 1257
15) G. Racah, Farkas Memorial Volume (Research Council of Israel, Jerusalem, 1952) p. 294
16) G. Racah and I. Talmi, Physica **18** (1952) 1097
17) G. Racah, Phys. Rev. **62** (1942) 438 (referred to as II in the present work)
18) R. A. Glass, S. G. Thompson and G. T. Seaborg, J. Inorganic and Nuclear Chemistry **1** (1955) 3
19) K. S. Quinsberry, T. T. Scolman and A. O. Nier, Phys. Rev. **104** (1956) 461
20) W. H. Johnson, Jr. and A. O. Nier, Phys. Rev. **105** (1957) 1014
21) K. Way and M. Wood, Phys. Rev. **94** (1954) 119
22) A. H. Wapstra, Physica **21** (1955) 367
23) K. Way, R. W. King, C. L. McGinnis and R. van Lieshout, Nuclear level schemes $A = 40$ to $A = 92$ (United States Government Printing Office, Washington 25, D.C., 1955)
24) P. M. Endt, W. W. Buechner, C. M. Braams, C. H. Paris and A. Sperduto, Phys. Rev. **105** (1957) 1002
25) C. F. Giese and J. L. Benson, BAPS II, **2** (1957) 223, and private communication from Dr. W. H. Johnson
26) R. W. King, Revs. Modern Phys. **26** (1954) 327
27) D. M. van Patter and W. W. Whaling, Revs. Modern Phys. **26** (1954) 402
28) New nuclear data, published in Nuclear Science Abstracts (6B quarterly cumulation, 12B semi-annual cumulation, 18B quarterly cumulation, 24B annual cumulation) (United States Atomic Energy Commission, Technical Information Service, Oak Ridge, Tennessee)
29) W. H. Johnson, Jr., and V. B. Bhanot, Phys. Rev. **107** (1957) 1669
30) S. N. Ghoshal and A. N. Saxena, Proc. Phys. Soc. A **69** (1955) 293

31) K. Way, Amsterdam Conference, July 1956 (Nederlandse Natuurkundige Vereniging, Amsterdam 1956); Nuclear masses and their determination, Proceedings of the conference held in Max Planck Institut für Chemie, Mainz, July 1956; edited by H. Hintenberger (Pergamon Press, London, 1957)
32) A. de Shalit, Phys. Rev. **105** (1957) 1528
33) J. R. Huizenga, Physica **21** (1955) 410
34) P. F. A. Klinkenberg, Revs. Modern. Phys. **24** (1952) 63
35) K. Fuchs, Proc. Camb. Phil. Soc. **35** (1939) 242
36) C. E. Moore, Atomic Energy Levels, N.B.S. Circular 467, Vol. I (1949); Vol. II (1952)
37) J. A. Harvey, Phys. Rev. **81** (1951) 353
38) A. E. S. Green and D. F. Edwards, Phys. Rev. **91** (1953) 46
39) N. Feather, Advances in Physics **2** (1953) 141
40) A. de Shalit and M. Goldhaber, Phys. Rev. **92** (1953) 1211
41) B. G. Hogg and H. E. Duckworth, Can. J. Phys. **32** (1954) 65
42) G. Trumpy, Nature **176** (1955) 507
43) A. W. Schardt and G. P. Welker, Phys. Rev. **99** (1955) 810
44) A. W. Schardt, Phys. Rev. **108** (1957) 398
45) W. H. Kelly and M. L. Wiedenbeck, Phys. Rev. **102** (1956) 1130
46) S. Thulin, Ark. f. Fysik **9** (1955) 137
47) R. J. Blin-Stoyle, Revs. Modern Phys. **28** (1956) 75
48) K. Way, D. N. Kundu, C. L. McGinnis and R. van Lieshout, Ann. Revs. Nuclear Sci. **6** (1956) 129
49) U. Capeller and R. Klingelhöfer, Z. Physik **139** (1954) 402
50) J. Varma and C. E. Mandeville, Phys. Rev. **94** (1954) 91
51) M. D. Petroff, BAPS II **1** (1956) 389; UCRL-3538 (1956)
52) H. B. Silsbee, W. A. Nierenberg, H. A. Shugart and R. A. Sunderland, BAPS II **2** (1957) 30
53) H. B. Levy, A new empirical mass equation:
I. Atomic masses in the fission product region, UCRL-4588 (November, 1955);
II. Atomic masses outside the fission product region UCRL-4713 (July, 1956)
54) H. B. Levy, Phys. Rev. **106** (1957) 1265
55) C. D. Coryell, Ann. Revs. Nuclear Sci. **2** (1953) 305
56) R. C. Fix, Beta-decay energies and nuclear systematics, Ph. D. thesis, M.I.T., Cambridge, Massachusetts (July 1956)
57) M. G. Mayer, Phys. Rev. **75** (1949) 1969
58) O. Haxel, J. H. D. Jensen and H. E. Suess, Phys. Rev. **75** (1949) 1766
59) W. Dobrolowski, R. V. Jones and C. D. Jeffries, Phys. Rev. **101** (1956) 1001
60) C. Schwartz, Phys. Rev. **94** (1954) 95
61) K. Kumar and M. A. Preston, Canad. J. Phys. **33** (1955) 298
62) H. E. Suess and J. H. D. Jensen, Ark. f. Fysik **3** (1951) 577
63) T. P. Kohman, Phys. Rev. **85** (1952) 530
64) S. N. Ghoshal and A. N. Saxena, Indian J. Phys. **29** (1955) 81
65) E. Glueckauf, Proc. Phys. Soc. A **61** (1948) 21
66) F. Asaro and I. Perlman, Revs. Modern Phys. **26** (1954) 456
67) I. Perlman, A. Ghiorso and G. T. Seaborg, Phys. Rev. **77** (1950) 26
68) I. Perlman and F. Asaro, Ann. Revs. Nuclear Sci. **4** (1954) 157
69) A. G. W. Cameron, A revised semi-empirical atomic mass formula A.E.C.L. No. 433 (March, 1957)
70) A. G. W. Cameron, Canad. J. Phys. **35** (1957) 1021
71) T. L. Collins, W. H. Johnson, Jr. and A. O. Nier, Phys. Rev. **94** (1954) 398
72) T. L. Collins, A. O. Nier and W. H. Johnson, Jr., Phys. Rev. **86** (1952) 408
73) R. E. Halsted, Phys. Rev. **88** (1952) 666
74) A. H. W. Aten, Jr., Science **110** (1949) 260
75) B. G. Hogg and H. E. Duckworth, Canad. J. Phys. **31** (1953) 942
76) A. Bohr and B. R. Mottelson, Mat. Fys. Medd. Dan. Vid. Selsk. **27** (1953) no. 16
77) I. Bergström and G. Andersson, Ark. f. Fysik **12** (1957) 415
78) A. S. Reiner, Physica **23** (1957) 338

79) G. Scharff-Goldhaber, Phys. Rev. **90** (1953) 587
80) M. J. Kearsley, Nuclear Physics **4** (1957) 157
81) W. W. True and K. W. Ford, Phys, Rev. **109** (1958) 1675
82) R. K. Sheline, Physica **23** (1957) 923
83) B. Saraf, Phys. Rev. **97** (1955) 715
84) D. J. Farmer, Phys. Rev. **99** (1955) 659
85) P. H. Stelson and F. K. McGowan, BAPS II **2** (1957) 267
86) H. B. Mathur and E. K. Hyde, Phys. Rev. **95** (1954) 708
87) L. W. Fagg, Phys. Rev. **109** (1958) 100
88) G. Andersson, E. Arbman and B. Jung, Ark. f. Fysik **11** (1956) 297
89) G. T. Ewan, Canad. J. Phys. **35** (1957) 672
90) S. G. Nilsson, Mat. Fys. Medd. Dan. Vid. Selsk. **29** (1955) no. 16
91) M. H. L. Pryce, Nuclear Physics **2** (1956/57) 226
92) M. H. L. Pryce, Private Communication to I. Bergström and G. Andersson, quoted as 5P56a in ref. [77])
93) V. A. Kravstov, Doklady Akad. Nauk SSSR **78** (1951) 43
94) V. A. Kravstov, Izv. Akad. Nauk SSSR, Ser. Fiz. **18** (1954) 5
95) K. Way and M. Wood, Phys. Rev. **86** (1952) 608
96) J. Mattauch and F. Everling, Progress in Nuclear Physics **6** (1957) 233
97) E. M. Pennington and H. E. Duckworth, Can. J. Phys. **32** (1954) 808
98) M. Nomoto, Progr. Theor. Phys. Japan **18** (1957) 483
99) A. R. Edmonds, Proc. Phys. Soc. A **66** (1953) 793
100) A. Berthelot, J. Phys. Rad. **3** (1942) 17.
101) K. Guggenheim, J. Phys. Rad. **5** (1934) 475
102) A. E. S. Green, Nuclear Physics (McGraw Hill, New-York, 1955)
103) N. Bohr and J. A. Wheeler, Phys. Rev. **56** (1939) 426
104) I. Joliot-Curie, J. Phys. Rad. **6** (1945) 209
105) M. N. Saha and A. K. Saha, Trans. Nat. Inst. Sci. India **2** (1946) 193
106) H. E. Suess, Phys. Rev. **81** (1951) 1071
107) N. Feather, Proc. Roy. Soc. Edinburgh A **63** (1952) 242
108) Y. F. Bow, Phys. Rev. **105** (1957) 1541
109) W. M. Elsasser, J. Phys. Rad. **5** (1934) 635
110) B. Karlik, Acta Phys. Austriaca **2** (1948) 182
111) S. Sengupta, Phys. Rev. **87** (1952) 1136
112) S. Sengupta, Z. Physik **134** (1953) 413
113) T. P. Kohman, Phys. Rev. **76** (1949) 448
114) M. H. L. Pryce, Proc. Phys. Soc. A **63** (1950) 692
115) A. H. Wapstra, Physica **17** (1951) 628
116) A. E. S. Green, Phys. Rev. **95** (1954) 1006
117) F. C. Flack and P. Mason, Proc. Phys. Soc. **71** (1958) 247
118) D. C. Alkhazov, I. K. Lemberg, D. S. Andreyev and K. I. Erokhina, Zhur. Eksptl. i Teoret. Fiz. **33** (1957) 1347
119) R. D. Evans, The Atomic Nucleus (McGraw Hill, New York, 1955)

Nuclear Physics 7 (1957) 111—112; © *North-Holland Publishing Co., Amsterdam*

BOOK REVIEW

S. V. FLÜGGE (Editor), *Handbuch der Physik — Encyclopedia of Physics* (Springer-Verlag, Berlin 1957—). Vol. 39. Bau der Atomkerne (vi-566 pages. DM 125). Vol. 40. Kernreaktionen I (vi-553 pages. DM 128). Vol. 42. Kernreaktionen III (vii-626 pages. DM 135).

The stately rows of volumes known as *Handbücher* represent the last stage, especially perfected by the Germans, of a tradition in the writing of encyclopedias, which goes back to the XVIIIth century, but has changed its character completely as the knowledge of which it was at first intended to give an all-embracing picture became more and more diversified. The aim of the modern *Handbuch* is essentially practical: its articles appear as so many treatises providing the specialists in any field with concise authoritative accounts of the state of knowledge both in their own and in other domains; they are intended both as stores of information to which the worker in the field can refer, and as introductory surveys for those who want a quick orientation in a domain less familiar to them.

Although the "blue" *Handbuch* — the previous edition of the work under review — was not the only one of its kind, it is chiefly through it that physicists were introduced to this type of literature: planned with typical German thoroughness and brought out by a publisher famous for his experience in this kind of undertaking, it served its purpose admirably. The volumes of the new edition, following each other in quick succession, show that this high standard of excellence has not only been kept up, but even improved in some respects: a larger appeal has been made to international collaboration, and the articles have been distributed over a larger number of smaller and handier volumes. There is no doubt that, viewed as a whole, the new encyclopedia will for years to come fulfil the same useful function as its predecessor.

When, however, we look more closely at the part of it which will eventually cover the vast and rapidly expanding field of nuclear physics, we cannot help noticing certain signs of strain, and we come to doubt whether the new situation created by the unprecedented rate of growth of this field is adequately met by a form of publication which was obviously conceived for a rather slower pace of development. It will perhaps not be out of place here to touch upon some of the general practical problems raised in this connexion, since these problems become more pressing every day and invite serious reflexion.

The first point to consider is that of the systematic arrangement of the subject matter. The larger subdivisions may be fairly straightforward, but very soon difficulties arise: groupings of subjects which might have appeared natural a few years ago (when the plan was drawn up) have ceased to be so at the time of publication, either because of a change of emphasis arising from deeper insight, or because the topics originally grouped together have in the meantime developed in diverging directions. This does not mean that the articles as originally planned have necessarily become useless, but their classification has become obsolete.

The following list of the articles contained in the three volumes hitherto published (out of the eight which will cover the field of nuclear physics) will illustrate this difficulty:

Volume 39 (nuclear structure): the two-nucleon system, the three-nucleon system, mass and charge distribution, the shell model, models of nuclear structure.

Volume 40 (nuclear reactions I): nuclear reaction levels and spectra of light nuclei, the same for heavy nuclei, resonance processes induced by neutrons, nuclear reactions at high energies.

Volume 42 (nuclear reactions III): nuclear isomerism, α-radioactivity, transuranic nucleides, nuclear photoeffect, angular correlation, oriented nuclei.

It is clear that the fitting of up-to-date accounts into this frame could not go without some straining and twisting, although it must be said that the authors of the articles have on the whole admirably succeeded in this none too easy task.

To take a specific example, the subject of "angular correlation" (treated in a masterly way

by S. Devons and L. Goldfarb in vol. 42) was originally confined to a limited type of nuclear reactions and was reasonably assigned a place under that general heading: nowadasy, however, the study of angular correlations has become a major technique, which has been successfully applied to problems of a quite different character, and has, moreover, become inseparably connected with the study of polarization effects. This powerful tool in the analysis of nuclear phenomena calls more than ever for a comprehensive treatment, which it has indeed received in the article just mentioned: however, the authors had to enlarge considerably the original set-up of their article, with the result that it no longer belongs to the place given to it, but ought to occupy a more prominent one among the articles dealing with the fundamental aspects of nuclear physics (including the physics of so-called "elementary particles").

In this example, the article is just misplaced, but as a treatise on the subject it may be expected to retain its value for a long time. More critical is the case of other articles, which, excellent as they are, risk to be rendered rapidly out-of-date by the very development of the subject they treat. I am not here alluding to the trivical circumstance that new information on almost any topic is continually accumulating: this is an unavoidable drawback, which can only be remedied by consultation of the current abstracting periodicals. What cannot be mended in this way, however, is the fact that the whole standpoint from which the article has been written may have to be abandoned for a better one: then the article loses most of its usefulness even though the information on which it is based remains largely valid. A case in point is the theory of nuclear models, which has been and is still undergoing such shifts of emphasis — a symptom, by the way, of the shakiness of its foundations. The article by S. Moszkowski devoted to this theory in vol. 39 is a remarkable and highly successful effort at well-ordered presentation, elucidating the mutual relationships of the various models and fixing their scope: yet its author would probably be the first to emphasize the provisional character of the scheme he has taken such pains to draw up. Quite soon the need will be felt for another stocktaking of our views on nuclear structure: another crop of survey articles will adorn the jungle of "progress reports", and a substantial part of an expensive volume of the encyclopedia will cease to fulfil the role for which it was conceived.

The difficulties just described rather compellingly lead one to the conclusion that the very idea of an encyclopedia as a systematic and unified exposition of some domain of knowledge has become illusory — at any rate for those domains in which research is especially active, and which are just those where prompt and up-to-date surveys are especially needed. Clearly, some more flexible type of publication is called for here. The collection of several articles in volumes has also some practical disadvantages: The rate of appearance of the volumes is fixed by the slowest contributors. The efficiency of use in libraries is reduced by the fact that consultation of a single article in a volume makes simultaneous consultation of the other articles impossible. Moreover, in ignorance of, or uncertainty about, the plan adopted for the classification and distribution of the articles, they can only be found by trying out volume after volume. Last, not least, these volumes are terribly costly. The only way for the average physicist to enter into possession of any article is to beg a reprint of the author: a method perfectly gratifying when it succeeds, but on the whole rather frustrating.

This review is threatening to grow to true *Handbuch* size, and it has given more prominence to criticism of formal aspects than to praise of substantial qualities. Yet, there is one further desideratum which must be formulated, because it is not too late to satisfy it. It is very regrettable that in a standard work of this importance no definite policy has been followed in respect of symbols, units and nomenclature: it would be so simple to adopt the recommendations of the IUPAP Commission and to streamline the articles in accordance with them. Insistence on criticism, however, ought not to obscure the essential fact that the production of this monumental encyclopedia is a magnificent achievement, for which the enterprising publisher and the eminent editor, who is carrying out his heavy task single-handed in such a masterly way, have earned the gratitude of the rising generation of physicists.

L.R.

1.B : 6.B *Nuclear Physics* **7** (1958) 113—115; © *North-Holland Publishing Co., Amsterdam*
Not to be reproduced by photoprint or microfilm without written permission from the publisher

ANALYTIC FORMS OF THE DEUTERON WAVE FUNCTION

MICHAEL J. MORAVCSIK
Brookhaven National Laboratory, Upton, L.I., N.Y.†

Received 15 February 1958

Recently Gartenhaus [1]) calculated a deuteron wave function from the cut-off meson theory. Since the theoretical background of his calculations is perhaps more reliable than the basis of the generally used Hulthén wave function, one would like to make use of this new wave function in various calculations. For this purpose, it is desirable to approximate the Gartenhaus wave function, which is given in a numerical form, by an analytic expression which is simple enough to be useful in the various integrals which arise when one calculates phenomena involving the deuteron. The purpose of this note is to give three such approximations of varying degrees of accuracy.

Following the notation of Gartenhaus we denote the deuteron wave function as follows:

$$\text{S wave} \qquad \psi_S(r) = \frac{u(r)}{r}, \qquad \text{D wave} \qquad \psi_D(r) = \frac{w(r)}{r}. \tag{1}$$

Also following Gartenhaus's convention, our functions will be normalized in such a way that

$$\int_0^\infty [u^2(r)+w^2(r)]\mathrm{d}r = 4.315 \tag{2}$$

where r is measured in units of 10^{-13} cm. In particular, Gartenhaus's functions are such that

$$\int_0^\infty u^2(r)\mathrm{d}r = 4.025, \tag{3}$$

$$\int_0^\infty w^2(r)\mathrm{d}r = 0.290 \tag{4}$$

and we will take over this normalization of the two functions.

Approximation I

First we will write down the "best" Hulthén type wave function defined by the form

$$u(r) = C(\mathrm{e}^{-\alpha r}-\mathrm{e}^{-\beta r}) \tag{5}$$

† Work carried out under the auspices of the U. S. Atomic Energy Commission.

June (2) 1958

and its parameters chosen in the following way: C and α are chosen to agree with the asymptotic behaviour of the Gartenhaus S function, and β is then chosen in such a way that the normalization of the two functions agree. This uniquely determines β. The result is

$$u(r) = 1.85\ (e^{-0.232r} - e^{-1.202r}). \tag{6}$$

This is normalized in accordance with eq. (3). If one wants to use this function for the whole deuteron wave function (that is, if one disregards the difference between the shape of the D and S functions), the best Hulthén function is

$$1.91\ (e^{-0.232r} - e^{-1.202r}) \tag{7}$$

which is now normalized so that

$$\int_0^\infty u^2(r)\mathrm{d}r = 4.315. \tag{8}$$

Fig. 1 shows that the Hulthén wave function is sufficiently in disagreement with the Gartenhaus function so that the difference between the S function and the D function (the latter contributing only 7 % to the total nor-

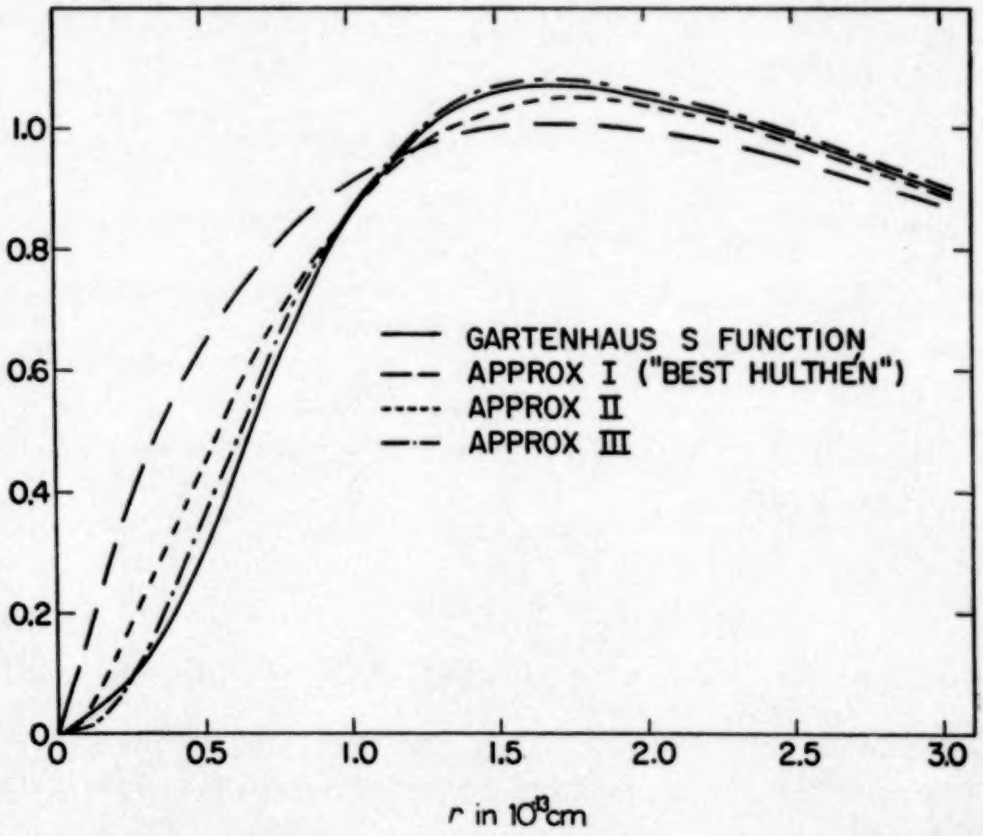

Fig. 1. Gartenhaus's deuteron S wave function and its approximations. The functions are normalized so that the integral of their square from zero to infinity is 4.025. Approximation III agrees with the Gartenhaus function within 2 % in the region of $0.9 < r < \infty$.

malization) can indeed be neglected. The Hulthén function is particularly bad at "small" distances, that is, below 2×10^{-13} cm. If the problem in question is dominated by the wave function at small distances the use of the Hulthén function can introduce a rather large error.

Approximation II

This function is a considerably better approximation to the Gartenhaus function but is essentially as simple as the Hulthén function. Its form is

$$u(r) = C(1-e^{-1.59r})(e^{-0.232r}-e^{-1.59r}) \tag{9}$$

where C is of course again 1.85 if the normalization is given by eq. (3) and 1.91 if the normalization is given by eq. (8).

Approximation III

An even better approximation, but still only a sum of exponential functions which are easy to treat under the integral sign, has the form

$$u(r) = C(1-e^{-2.5r})(1-e^{-1.59r})(e^{-0.232r}-e^{-1.90r}) \tag{10}$$

with C being again the same as it was in the previous approximations. As it can be seen from fig. 1, this function agrees with Gartenhaus's within 2 % for all $r > 0.9$, and is a considerable improvement over the other two functions for smaller r values as well.

All three approximating functions are shown in fig. 1, together with the Gartenhaus function itself.

Approximation to the D *Function*

It seems to be impossible to construct a good approximation to the D function using only exponential functions. A somewhat more cumbersome approximating function is the following:

$$w(r) = \begin{cases} 0.658\, r^3 & \text{for } 0 < r < 0.63 \\ 2.34\, r^3\, e^{-2r} & \text{for } 0.63 < r < 2.10 \\ 0.147\, e^{-0.256r} + 0.810\, e^{-0.577r} & \text{for } 2.10 < r < +\infty \end{cases}$$

which agrees with the Gartenhaus D function everywhere within 4 %. This function is normalized in accordance with eq. (4).

Since the Gartenhaus function is given to an accuracy of at best 1 % the parameters in the approximating functions are given to a corresponding degree of accuracy.

I am indebted to Dr. S. Gartenhaus for sending me the numerical tables of his wave function.

Reference

1) S. Gartenhaus, Physical Review **100** (1956) 900

2.B *Nuclear Physics* 7 (1958) 116—125; © *North-Holland Publishing Co., Amsterdam*
Not to be reproduced by photoprint or microfilm without written permission from the publisher

THE ANGULAR DISTRIBUTIONS OF THE LONG-RANGE ALPHA-PARTICLES FROM THE REACTION $F^{19}(p, \alpha_0)O^{16}$

AKIRA ISOYA†, HARUKO OHMURA

and

TERUO MOMOTA††

Department of Physics, Faculty of Science, University of Tokyo

Received 13 February 1958

Abstract: The angular distributions of the long-range alpha-particles from the reaction $F^{19}+p$, leading to the ground state of the residual nucleus O^{16}, have been measured. The energies of protons covered a range from 630 keV to 1460 keV, and measurements were made in steps of 5 to 10 keV with a proton energy spread of 0.2 per cent. Coefficients in the Legendre polynomial expansion of the angular distribution function were traced in this range.

1. Introduction

The excitation function of the ground state alpha-particles has been observed by Streib *et al.* [1]) from 0.3 to 1.5 MeV. Resonances were reported at 0.72, 0.84, 1.1 and 1.35 MeV. Angular distributions were studied by Asano [2]) and Rubin [3]) near resonances. The latter results have been analyzed by Chao[4]) and the assignment of $J = 2^+$ was made to the 1.35 MeV resonance. However, it was impossible to draw a definite conclusion about the other levels, because of overlap of the levels of the compound nucleus. It is naturally necessary to observe the angular distributions at many more energy points with an improved energy definition of the incident protons in order to disentangle such a complicated level structure as is encountered in this case.

Since the pair emitting state of O^{16} has the same spin and parity (0^+) as the ground state, the ground state alpha-particle α_0 and the short range alpha-particle α_π would be expected to show the same resonances; this is approximately so, although the 1236 keV pair resonance has not been found for long range alpha-particles. The angular distribution of α_π has been measured [5]) at many energy points in the same energy region as in the work by Streib *et al.*, and tentative assignments of J-value were made for the

† Now at the Institute for Nuclear Study, University of Tokyo, Tanashi-machi, Kitatama-gun, Tokyo.

†† Now at Japan Atomic Energy Research Institute, Shiba-Tamura-cho, Minato-ku, Tokyo.

resonances and broad background levels. For the 843 keV resonance the assignment (0^+) was made by Baranger [6]) from the analysis of elastic scattering of protons by fluorine [7]). This assignment, however, was different from that (2^+) obtained in the former work [5]). The purpose of the present work is to report the experimental data on the long range alpha-particles, which will be used to ascertain the J-value and the other nuclear properties of the resonance levels. These properties will be compared with the α_π data and the correspondence between the excitation functions of α_0 and α_π will be checked.

2. Apparatus

The reaction chamber which was described in the previous paper [5]) was used with a slight modification: a side-window type proportional counter of 2 cm diameter, which was to count the α-particles at various angles, was mounted on the movable upper lid of the chamber as before, but the thin-walled Geiger-Müller counter was replaced by an end-window type proportional counter which counted the long-range α-particles at a direction of 90° to the proton beam (see fig. 1). Both counters were filled with a mixture of argon and ethylformate at a pressure of 10 to 15 cm Hg. Their windows were covered with mica of 8 mg · cm^{-2} thickness, which was expected to be thick enough to stop protons scattered by the target and

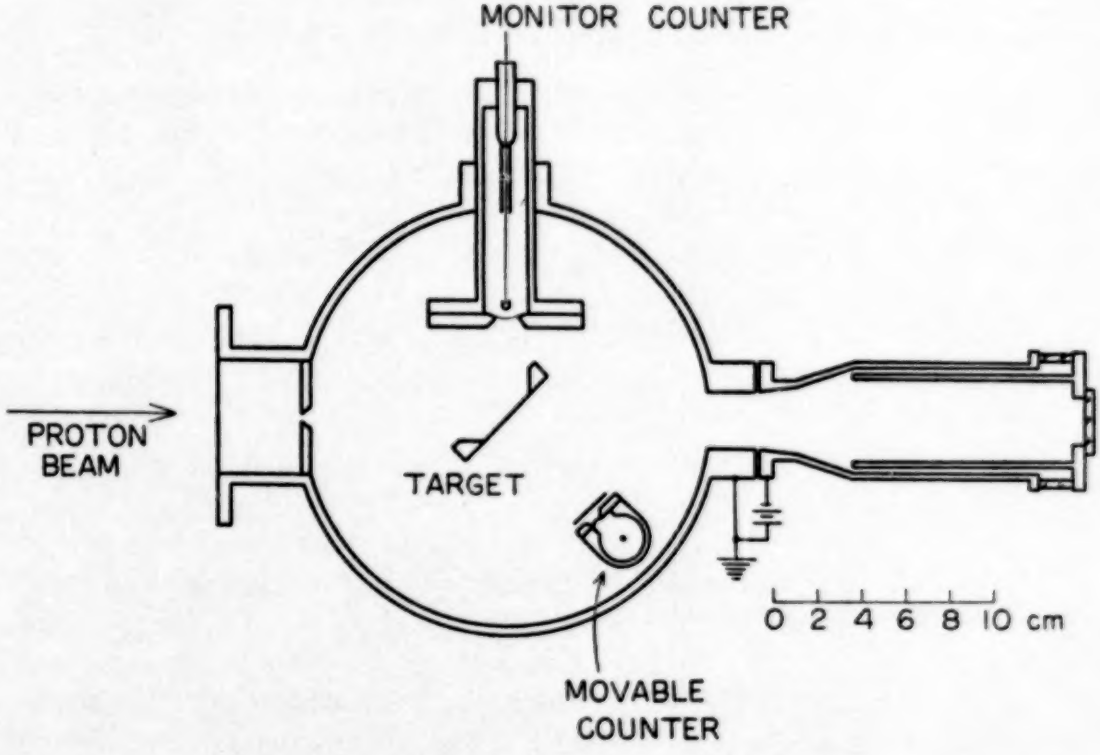

Fig. 1. Schematic diagram of the reaction chamber.

short range α-particles from the F+p reaction. But when the movable counter was set at forward positions relative to the proton beam, pulses of random height were observed. The largest of these were one half as high as those due to the long range α-particles, the latter, being, of course, uniform in height. These undesirable pulses were eliminated by proper pulse height discrimination. They might well be ascribed to a very small portion of scattered protons which had extraordinarily long ranges.

The angular resolution of the movable counter was 4° to 5°, which was considered to cause an error in the coefficients of the angular distribution not larger than 2 %, and the correction was neglected.

The target was made by evaporating CaF_2 onto an aluminium foil of about 50 μ g · cm^{-2}. The thickness of the CaF_2 film was about 8 keV at 840 keV. The target was placed at the centre of the chamber at an angle of 45° to the direction of incident beam, with the CaF_2 film facing the beam and with its normal pointing to a quadrant where the movable counter was set. At the forward directions, α-particles had to pass through the aluminium backing before they reached the movable counter, but the average angle of deflection they should suffer was estimated to be less than one degree. During this work the energy of the electrostatic generator was stabilized to within 0.2 %. Calibration of the voltage scale was done by observing the (p, $\alpha\gamma$) resonance in fluorine at 873.5 keV. Beam intensity was from 0.4 μA to 2μA.

3. Procedure of Measurement and Results

First we measured the angular distributions with quite good accuracy at the thirteen proton energies indicated on the yield curve of α_0 taken at 90° (fig. 2). Results are shown in fig. 3. Least squares fits were made using Legendre polynomial expansions to fourth order terms. Except for the distribution functions taken at 864 and 968 keV, good fits were obtained between the experimental points and the computed curves. At two energies mentioned above, slight systematic deviations of the fitted curves from the measurements were observed. These deviations did not contain terms of order higher than P_5 (cos θ). The coefficients of the angular distributions corrected for these deviations are listed in table 1 and the resulting curves are shown in fig. 3.

After these experiments it was felt that in order to analyse such a complicated excitation function as was encountered in the present case, it was necessary to trace the exact forms of the variation of the coefficients of the angular distribution with the proton energy. So we chose to use a method which has been described by P. C. Price [8]). In this method the experimental procedure to reduce the angular distributions by the least squares method is greatly simplified by using a particular set of a relatively small number

of experimental angles and of relative weights of the observations at each angle. Since in the present case the complexity of the angular distribution is limited to the terms of order less than $P_5(\cos\theta)$ at most energies investigated, it will be sufficient to measure the relative yields at five angles which

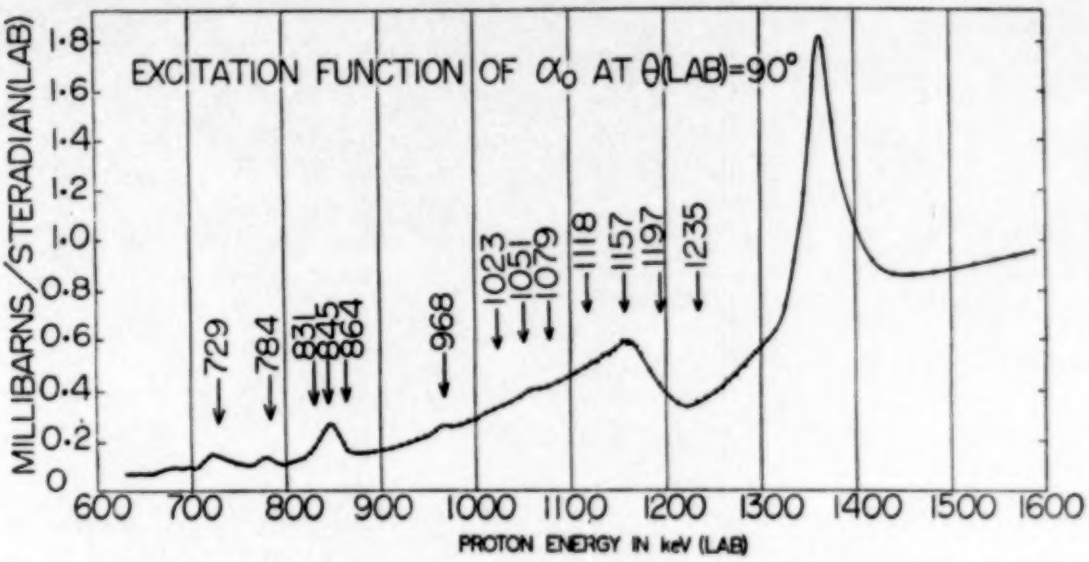

Fig. 2. Excitation function at 90° to the incident proton beam of the reaction $F^{19}(p, \alpha_0)O^{16}$. Arrows on the curve indicate the energies, where the angular distributions were measured. The energy scale is corrected for the energy loss in the target of incident protons.

TABLE 1

Coefficients of the Legendre polynomial fits to the $F^{19}(p, \alpha_0)O^{16}$ angular distributions by the method of least squares

$$d\sigma = \frac{\lambda^2}{8} \sum_{n=0} b_n P_n(\cos\theta) d\Omega.$$

E_p^{Lab} (keV)	b_1/b_0	b_2/b_0	b_3/b_0	b_4/b_0	b_5/b_0
729	0.65_5	0.93_4	0.42_6	1.45_2	—
784	-0.17_4	0.40_4	0.54_8	0.05_3	—
831	-0.01_3	0.82_6	0.16_8	0.20_8	—
845	0.03_6	0.29_7	0.09_4	0.12_7	—
864	−0.08	−0.66	0.05	0.40	0.04
968	−0.32	−0.54	0.09	0.08	0.05
1023	-0.47_9	-0.63_3	0.26_4	0.01_9	—
1051	-0.66_6	-0.33_4	0.30_7	0.12_7	—
1079	-0.99_5	0.25_9	0.31_6	0.11_7	—
1118	-0.59_9	0.28_7	-0.20_1	-0.15_2	—
1157	-0.49_3	0.31_2	-0.42_5	0.12_3	—
1195	-0.43_2	0.88_5	0.25_7	0.28_6	—
1235	-0.70_6	1.04_1	0.47_3	0.30_0	—

are the roots of $P_5(\cos\theta_{CM}) = 0$ ($\cos\theta_{CM} = 0, \pm 0.5385, \pm 0.9062$). The number of counts of the monitor counter in the measurement at $\vartheta_{CM} = 90°$ was fixed to 2000 for all energies. This meant that the standard errors of the counting at $\vartheta_{CM} = 90°$ were 4.0 %.

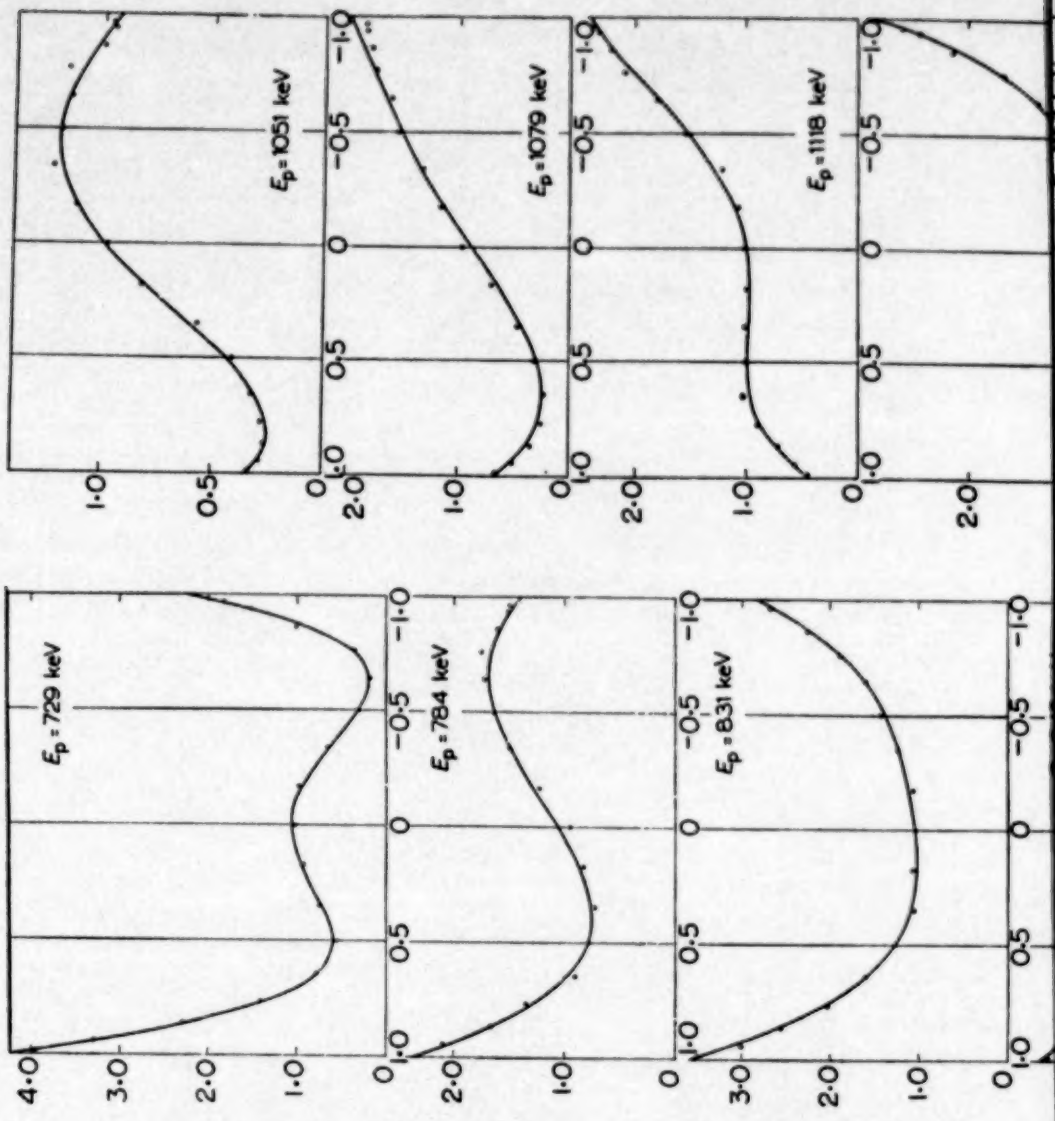
E_p = 729 keV
E_p = 784 keV
E_p = 831 keV
E_p = 1051 keV
E_p = 1079 keV
E_p = 1118 keV
E_p = 1157 keV

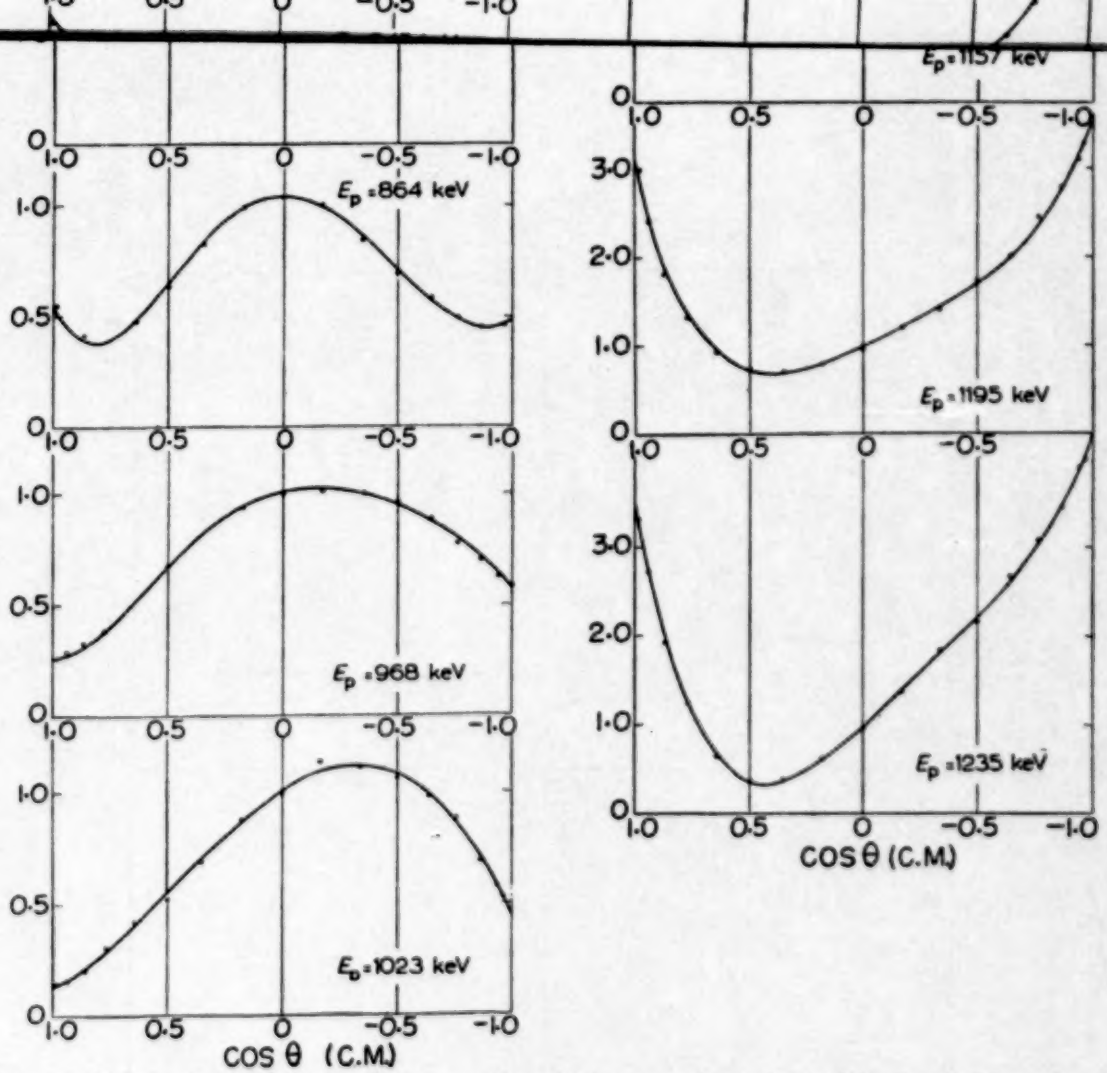

Fig. 3. Observed angular distributions taken at the energies indicated in fig. 2. The curves are the Legendre polynomial expansions which are shown in table 1.

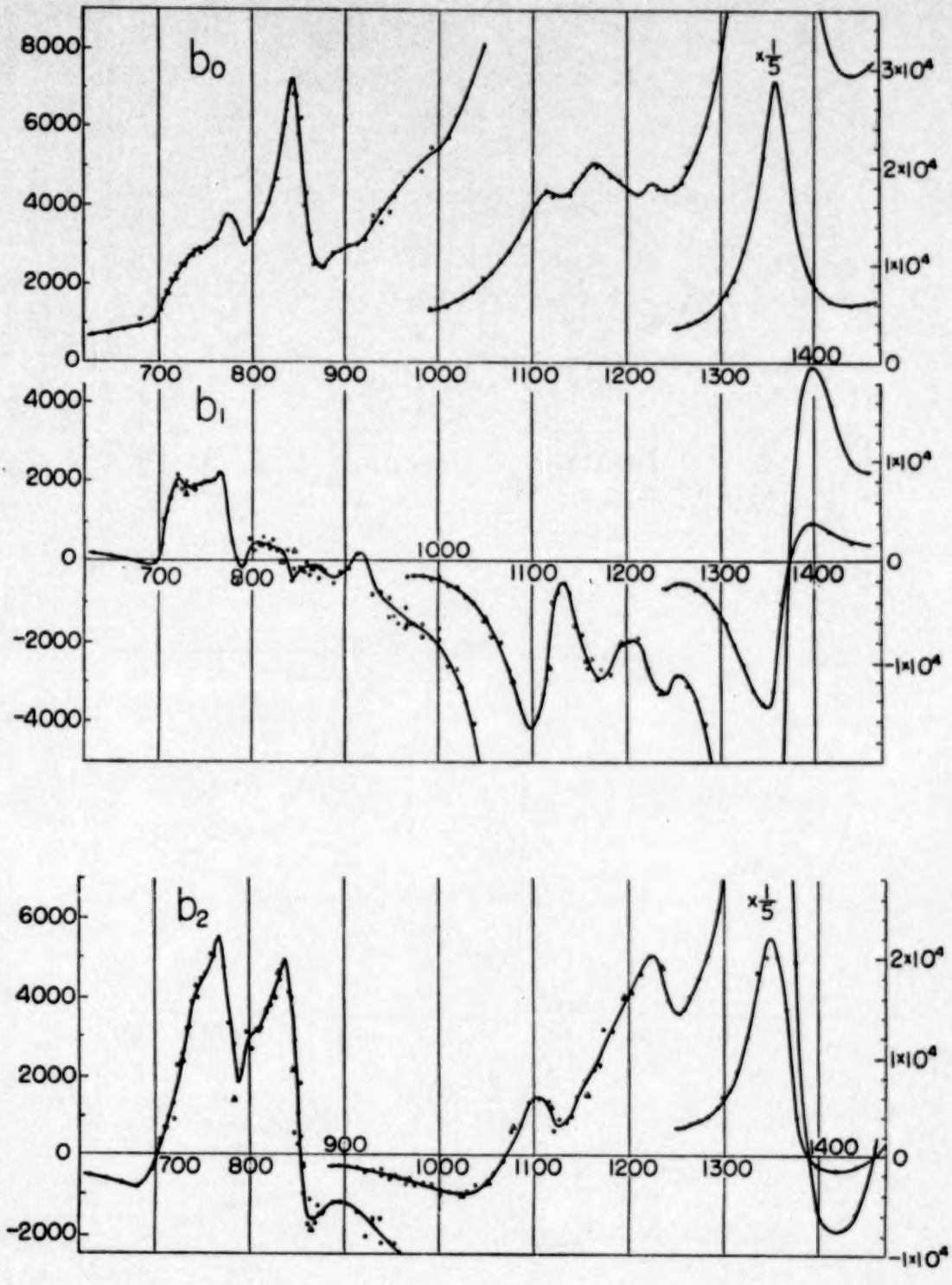
b0
b1
b2
×1/5
8000
6000
4000
2000
0
-2000
-4000
700
800
900
1000
1100
1200
1300
1400
3×10⁴
2×10⁴
1×10⁴
-1×10⁴

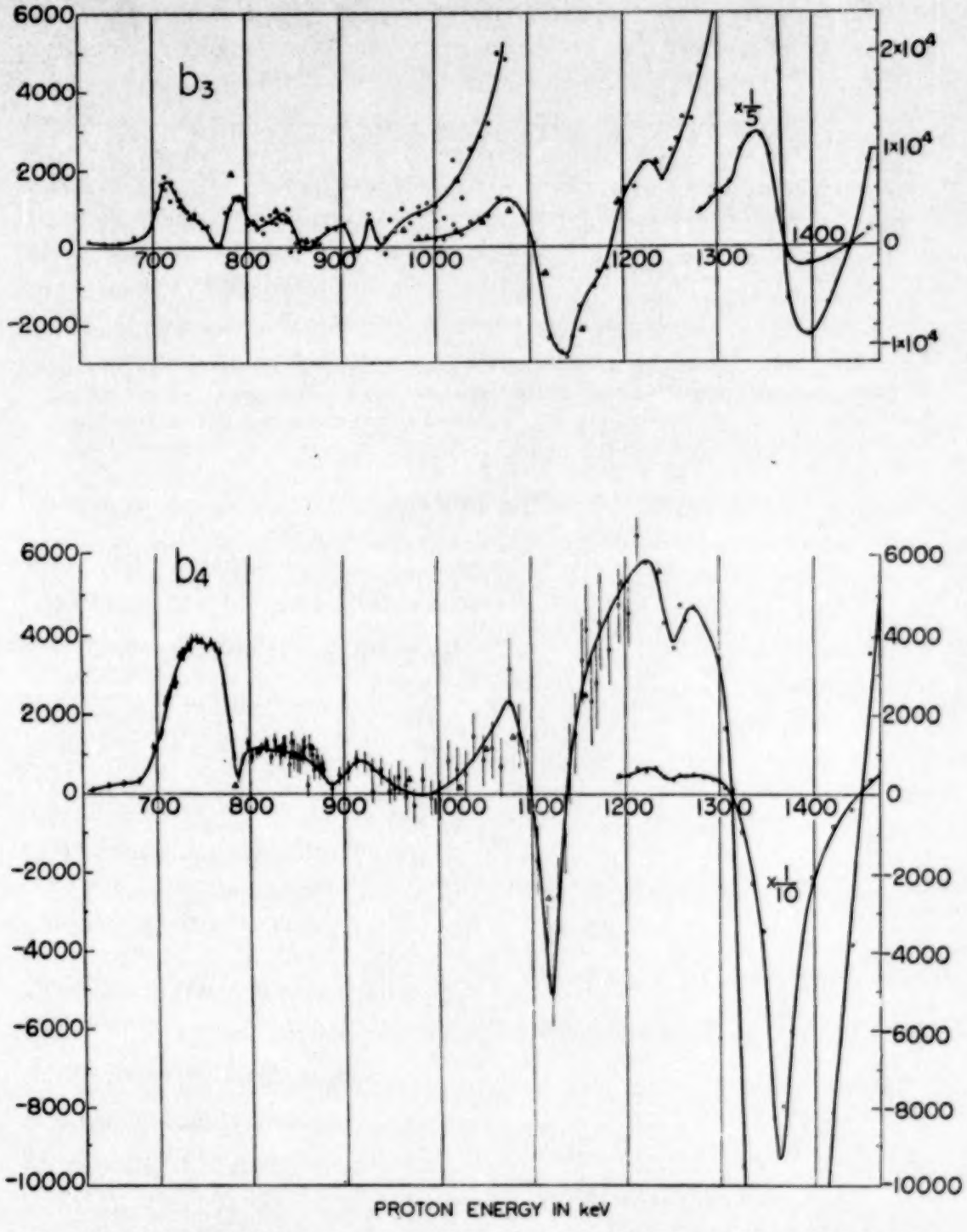

Fig. 4. Coefficients of the Legendre polynomial expansion of the $F^{19}(p, \alpha_0)O^{16}$ angular distribution as a function of the incident proton energy.

The ordinate is in arbitrary units. The ordinate of the graphs in the lower energy region refers to the scale on the left and that in the higher energy region refers to the scale on the right. The energy scale is corrected for the energy loss in the target of incident protons. No correction is made for the energy spread of proton energy. The points marked with triangles (△) are check points taken from table 1.

In this measurement the distance of the monitor counter from the target was shortened from 73.5 mm to 44.0 mm to reduce the statistical fluctuation in the monitor counter, and the width of the beam defining slit was enlarged from 2.0 mm to 3.3 mm to insure durability of the target under the ion bombardment by reducing the current density. These changes brought about the undesirable effect of increasing the systematic error, which was attributed to the deviation of the beam path from the centre of the chamber. Since the beam condition was fixed during one cycle of measurements involving five angles at a given energy, it should be possible to correct this error. When the ratio of the counts of both counters at 90° position deviated from the value which was expected from the geometry, the relative yield at different angles was corrected on the basis of magnitude of this deviation.

These measurements, which consisted of five different runs, were extended over the whole energy region in steps of 5 to 10 keV. The coefficients obtained at each energy were normalized to the yield curve at $\theta_{Lab} = 90°$ (fig. 2), which was carefully determined on the basis of several runs with the same target as was used in the angular distribution measurements. Results are shown in fig. 4.

For the determination of the cross section, target thickness was estimated from the amount of CaF_2 evaporated. As the most probable thickness we took a mathematical mean between the thickness determined on assuming uniform distribution of evaporated material over a half-sphere and that on assuming the distribution followed the cosine law. The value, thus determined was proved to be nearly the right one by the chemical method †. The cross section determined in the present work is larger by about one order than that obtained by Streib *et al.* [1, 9]) and the yields at resonances are comparable with those of the short range alpha particles α_π [5]). Recently the angular distribution and yield of α_0 in the higher energy region ($E_p > 1300$ keV) was published by Clarke and Paul [10]). Their results at the 1358 keV resonance agree quite well with the present work.

The authors wish to express their appreciation to Mr. Nogami and the other members of the Van de Graaf group who gave valuable assistance during the work. They are especially grateful to Mr. T. Kobayashi for his cooperation. They would like to thank Dr. K. Saito who made the chemical analysis of fluorine in the target.

† Quantitative analysis of fluorine was made by the zirconium alizalin colorimetric method.

References

1) J. F. Streib, W. A. Fowler and C. C. Lauritsen, Phys. Rev. **59** (1941) 253
2) Y. Asano, Proc. Phys. Math. Soc. Japan, **25** (1943) 432
3) S. Rubin, Phys. Rev. **72** (1947) 1176
4) C. Y. Chao, Phys. Rev. **80** (1950) 1053

5) A. Isoya, K. Goto and T. Momota, Jour. Phys. Soc. Japan **11** (1956) 899
6) E. U. Baranger, Phys. Rev. **99** (1955) 145
7) T. S. Webb, F. B. Hagedorn, W. A. Fowler and C. C. Lauritsen, Phys. Rev. **99** (1955) 138
8) P. C. Price, Phil. Mag. **45** (1954) 237
9) C. Y. Chao, A. V. Tollestrup, W. A. Fowler and C. C. Lauritsen, Phys. Rev. **79** (1950) 108
10) Clarke and Paul, Can. J. Phys. **35** (1957) 155

2.B *Nuclear Physics* 7 (1958) 126—145; © *North-Holland Publishing Co., Amsterdam*
Not to be reproduced by photoprint or microfilm without written permission from the publisher

ANALYSIS OF THE YIELD CURVES AND THE ANGULAR DISTRIBUTIONS OF THE REACTIONS F^{19} (p, α_0) O^{16} AND F^{19} (p, α_π) O^{16*}

AKIRA ISOYA
Institute for Nuclear Study, University of Tokyo

Received 13 February 1958

Abstract: By analysis of the angular distributions of α-particles from the reactions F^{19}(p, α)O^{16} leading to the ground state and first excited state of O^{16} (α_0 and α_π respectively), virtual levels of the nucleus Ne^{20} with spin and parity (even)$^+$ and (odd)$^-$ were investigated. Legendre polynomial expansions were adjusted to the data and the coefficients determined over the energy interval from 650 keV to 1500 keV. These results were then interpreted in terms of the resonance parameters of the compound levels presumed, and the following J-values were assigned: $J = 2$ levels at 731, 778, 843, 1115 and 1356 keV, a $J = 1$ level at 1250 keV and a $J = 0$ level at 1160 keV. Background yields are probably due to a few broad levels of $J = 0$ and 1. For the α_0-channel, vector diagrams of five elements of the collision matrix concerned, which correspond to two values of entrance channel spin and three values of relative orbital angular momentum, were drawn, which reproduce almost all details of observed excitation functions. This procedure gives information about the relative signs of the reduced width amplitudes of the virtual levels. This sign seems to be independent of the entrance channel spin in spite of large fluctuations of the relative yield in both channels from level to level. Yields of α_0, α_π and protons from each resonance are compared and the reduced widths of levels of Ne^{20} are estimated.

1. Introduction

The purpose of this paper is to carry out the analysis of two experiments on the angular distributions of α-particles from the reaction F^{19}(p, α)O^{16}; one is that of α-particles leaving the residual nucleus in the ground state [1]) and the other is that of α-particles leaving the residual nucleus in the pair-emitting state [2]). Analysis of these reactions gives information about the virtual levels of Ne^{20} having spin and parity (even)$^+$ or (odd)$^-$. The theoretical formula of the angular distribution for these reactions has been given by Chao [3]), and J-values have been assigned to some of the resonances on the basis of scanty data. In the present analysis the treatment is similar, but more extensive, and the complicated overlapping levels reveal themselves.

2. Collision Matrix Formulation of the Differential Cross Section

Since values of spin and parity of the ground and the first excited states of O^{16} are both 0^+, the reactions in question proceed via the same compound

states of Ne^{20}, and the angular distributions of two groups of α-particles are restricted by the same collision matrix formalism. Since the channel spin of the exit channel is 0, the orbital angular momentum l' of the exit channel is equal to the total angular momentum J, and the compound states concerned have spin and parity $(\text{even})^+$ or $(\text{odd})^-$. The entrance channel spin is either 0 or 1, because spin and parity of F^{19} are $\frac{1}{2}^+$. Hence the entrance channel partial wave is limited to the one with $l = J$, regardless of the channel spin value. The selection rule $l = J = l'$ reduces strikingly the complexity of the collision matrix formalism. Low incident energy may well limit the l-values of the incident partial waves to less than three. Then the differential cross section is described in terms of five elements of a collision matrix u_0^0, u_1^0, u_2^0, u_1^1 and u_2^1, where u_i^S denotes an element concerning the orbital angular momentum $l(=J)$ and the entrance channel spin S †:

$$\frac{d\sigma}{d\Omega} = \frac{\pi\lambda^2}{4}\{|\sum_{l=0}^{2}(2l+1)^{\frac{1}{2}}u_l^0 Y_{l0}(\theta\varphi)\, e^{i(\sigma_l+\sigma'_l)}|^2 + 2|\sum_{l=1}^{2}(2l+1)^{\frac{1}{2}}(1l;\ 10/1l;\ l1)u_l^1 Y_{l1}(\theta\varphi)\, e^{i(\sigma_l+\sigma'_l)}|^2\}, \quad (1)$$

where the first term in the bracket corresponds to the channel spin $S = 0$ and the second term to $S = 1$. The $Y_{lm}(\theta\varphi)$ are the usual spherical harmonics, σ_l is the Coulomb phase shift for scattering with orbital angular momentum l in the entrance channel and σ'_l is the similar quantity in the exit channel. Putting $u_i^S \exp\{i(\sigma_l+\sigma'_l)\} = A_i^S \exp(i\phi_i^S)$, $d\sigma/d\Omega$ is expressed as an expansion in $P_n(\cos\theta)$ $(n \leqq 4)$ as follows:

$$\frac{d\sigma}{d\Omega} = \frac{\lambda^2}{8}\{b_0+b_1 P_1(\cos\theta)+b_2 P_2(\cos\theta)+b_3 P_3(\cos\theta)+b_4 P_4(\cos\theta)\}, \quad (2)$$

where

$$b_0 = \tfrac{1}{2}(A_0^0)^2+\tfrac{3}{2}\{(A_1^0)^2+(A_1^1)^2\}+\tfrac{5}{2}\{(A_2^0)^2+(A_2^1)^2\}, \quad (3)$$

$$b_1 = 3A_0^0 A_1^0\cos(\phi_0^0-\phi_1^0)+6A_1^0 A_2^0\cos(\phi_1^0-\phi_2^0) + 3\sqrt{3}\,A_1^1 A_2^1\cos(\phi_1^1-\phi_2^1), \quad (4)$$

$$b_2 = 3(A_1^0)^2-\tfrac{3}{2}(A_1^1)^2+\tfrac{25}{7}(A_1^0)^2+\tfrac{25}{14}(A_2^1)^2+5A_2^0 A_0^0\cos(\phi_2^0-\phi_0^0), \quad (5)$$

$$b_3 = 9A_1^0 A_2^0\cos(\phi_1^0-\phi_2^0)-3\sqrt{3}A_1^1 A_2^1\cos(\phi_1^1-\phi_2^1), \quad (6)$$

and

$$b_4 = \tfrac{15}{7}\{3(A_2^0)^2-2(A_2^1)^2\}. \quad (7)$$

To determine the values of the A_i^S and ϕ_i^S from the values of b_n derived

† Eq. (1) was derived following the method of Breit and McIntosh [4]), which is the generalization of the theory of Wigner and Eisenbud [5]) to allow for Coulomb interactions between the particles within channels. It should be noted that we used $\exp\{\pm i(kr-\frac{1}{2}l\pi)\}$ instead of $\exp(\pm ikr)$ in the standard channel functions.

from the data, we employ the following linear combinations of b_n, equivalent to the original set of b_n:

$$b_0-\tfrac{7}{12}b_4=\tfrac{1}{2}(A_0^0)^2+\tfrac{3}{2}\{(A_1^0)^2+(A_1^1)^2\}+\tfrac{25}{4}(A_2^0)^2, \tag{8}$$

$$b_0-\tfrac{7}{18}b_4=\tfrac{1}{2}(A_0^0)^2+\tfrac{3}{2}\{(A_1^0)^2+(A_1^1)^2\}+\tfrac{25}{6}(A_2^0)^2, \tag{9}$$

$$b_0-b_2+\tfrac{1}{6}b_4=\tfrac{1}{2}(A_0^0)^2-\tfrac{3}{2}(A_1^0)^2+3(A_1^1)^2-5A_2^0A_0^0\cos(\phi_2^0-\phi_0^0), \tag{10}$$

$$b_1+b_3=3A_0^0A_1^0\cos(\phi_0^0-\phi_1^0)+15A_1^0A_2^0\cos(\phi_1^0-\phi_2^0), \tag{11}$$

$$b_1-\tfrac{2}{3}b_3=3A_0^0A_1^0\cos(\phi_0^0-\phi_1^0)+5\sqrt{3}\,A_1^1A_2^1\cos(\phi_1^1-\phi_2^1). \tag{12}$$

The differential cross section $d\sigma/d\Omega$ at $\theta_{CM}=90°$ is expressed by the following formula:

$$\left(\frac{d\sigma}{d\Omega}\right)_{\theta=90°}=\frac{\lambda\!\!\!^{-2}}{8}(b_0-\tfrac{1}{2}b_2+\tfrac{3}{8}b_4)$$

$$=\frac{\lambda\!\!\!^{-2}}{8}\{\tfrac{1}{2}(A_0^0)^2+\tfrac{9}{4}(A_1^1)^2+\tfrac{25}{8}(A_2^0)^2-\tfrac{5}{2}A_2^0A_0^0\cos(\phi_2^0-\phi_0^0)\}. \tag{13}$$

Since the number of parameters involved in these equations is ten, twice the number of the constants determined at each energy, it is impossible to determine values of the parameters uniquely. However, if we know the spins of all the resonance levels that appear in the energy range studied in this experiment, it is possible to evaluate approximately these parameters noting that they will have typical forms in the neighbourhood of the resonance energies.

In the case of isolated narrow resonances, u_l^S is described in the following manner [5]):

$$u_l^S=i\exp\left[-i\tan^{-1}\left(\frac{F_l}{G_l}\right)_p-i\tan^{-1}\left(\frac{F_l}{G_l}\right)_\alpha\right]\frac{g^S_{\lambda pl}g_{\lambda\alpha l}}{E_\lambda-E-\frac{1}{2}i\Gamma_\lambda}. \tag{14}$$

Here

$$g^S_{\lambda pl}=\left[\frac{2k_p}{(F_l^2+G_l^2)_p}\right]^{\frac{1}{2}}\gamma^S_{\lambda pl}=\pm(\Gamma^S_{\lambda pl})^{\frac{1}{2}}, \tag{15}$$

where $\gamma^S_{\lambda pl}$ is a reduced width amplitude of the level E_λ for the proton channel, and $\Gamma^S_{\lambda pl}$ is a corresponding partial width. $\gamma_{\lambda\alpha l}$ and $\Gamma_{\lambda\alpha l}$ are the similar quantities for the α-particle channel. Eq. (14) may be represented as follows:

$$A_l^S=\left[\frac{\Gamma^S_{pl}\Gamma_{\alpha l}}{(E_0-E)^2+\Gamma^2/4}\right]^{\frac{1}{2}}=(A_l^S)_0\left(\frac{1}{x^2+1}\right)^{\frac{1}{2}}=(A_l^S)_0|\sin\delta_l|$$

$$\phi_l^S=\sigma_l+\sigma'_l-\tan^{-1}\left(\frac{F_l}{G_l}\right)_p-\tan^{-1}\left(\frac{F_l}{G_l}\right)_\alpha+\delta_l+\frac{\pi}{2}, \tag{16}$$

where $(A_l^S)_0$ is the value of A_l^S at the observed resonance energy E_0

and $x = (E-E_0)/\frac{1}{2}\Gamma = -\cot\delta_l$. A resonant phase shift δ_l is defined such that

$$180° > \delta_l > \quad 0° \text{ when } g^S_{pl}g_{\alpha l} > 0$$
$$360° > \delta_l > 180° \text{ when } g^S_{pl}g_{\alpha l} < 0.$$

If a term $A_l{}^S \exp(i\phi_l{}^S)$ is plotted in the complex plane, it describes a circle of diameter $(A_l{}^S)_0$ counter-clockwise, starting from the origin as the incident energy is increased through a resonance (see fig. 1). It will be a fairly good approximation to assume that the total width Γ_λ is independent of the incident proton energy, because α-particle widths will be a main part of the total width and will be comparatively independent of the incident energy, owing to large Q-values (especially in the case of α_0). g_p or Γ_p depends on the incident energy through the barrier penetration factor $P_l = (F_l{}^2+G_l{}^2)^{-1}$ for protons. This situation allows the use of a resonant circle even for a broad resonance if $A_l{}^S/P_l{}^{\frac{1}{2}}$ is used in place of $A_l{}^S$.

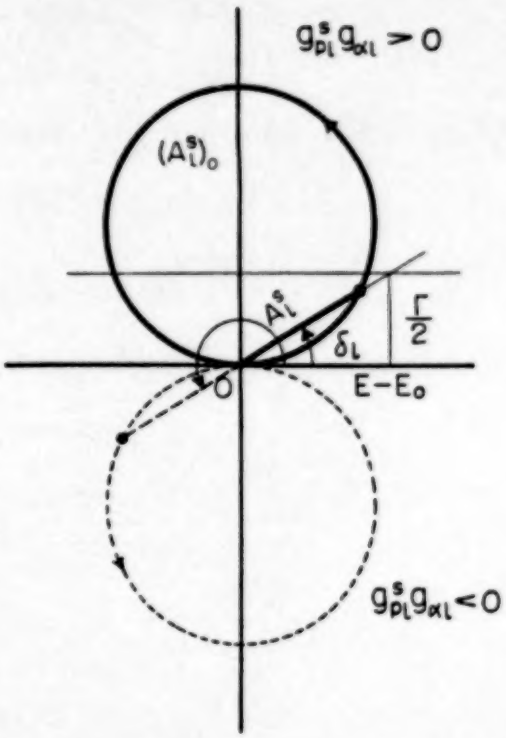

Fig. 1. Typical form of the vector diagram of collision matrix element $u_l{}^S$ due to a single resonance. Method of drawing a resonant circle in the complex plane is illustrated. Phase factors other than the resonant phase shift δ_l are omitted from this diagram. Two alternative cases, corresponding to different signs of $g_{pl}{}^S g_{\alpha l}$, are shown.

When the compound levels of the same spin and parity overlap, $u_l{}^S$ may be approximated by a superposition of one-level formulas (14). This approximation will be quite safe when the resonances are very widely separated, but rather large deviations are expected when the separation between levels is only several times larger than the width. Even in the

latter case the collision matrix can be formally expressed as a superposition of resonant terms of the form of (14) [6]. Then, however, g_p and g_α are in general complex and are complicated functions of the incident energy. Furthermore they are not simply related to the reduced widths. In the immediate vicinity of each resonance energy this feature can be represented by the rotation of the respective resonant circle by some angle around its origin along with change of the diameter.

In the present analysis four kinds of interference terms occur:

$$A_0^0 A_1^0 \cos(\phi_0^0-\phi_1^0),\quad A_1^0 A_2^0 \cos(\phi_1^0-\phi_2^0),$$
$$A_2^0 A_0^0 \cos(\phi_2^0-\phi_0^0),\quad A_1^1 A_2^1 \cos(\phi_1^1-\phi_2^1).$$

These terms take regular forms around the resonances. Especially at sharp $J=2$ resonances, around which matrix elements of s- and p-waves can be assumed constant, the interference terms are unambiguously discriminated from the b_n-plots. The following example illustrates the characteristic form of energy dependence of these terms when the d-wave matrix element is described in the form (16). Putting

$$\phi_1^S = \sigma_1+\sigma'_1-\tan^{-1}\left(\frac{F_1}{G_1}\right)_p-\tan^{-1}\left(\frac{F_1}{G_1}\right)_\alpha+\omega_1^S+\frac{\pi}{2},$$

one obtains

$$A_1^S A_2^S \cos(\phi_1^S-\phi_2^S) = A_1^S A_2^S \cos(\delta_2+\theta_{12}^S)$$
$$= -A_1^S (A_2^S)_0 \frac{\cos\theta_{12}^S\cdot x+\sin\theta_{12}^S}{x^2+1}\cdot\frac{g_{p2}^S g_{\alpha 2}}{|g_{p2}^S g_{\alpha 2}|}, \quad (17)$$

where

$$\theta_{12}^S = -(\sigma_1-\sigma_2)-(\sigma'_1-\sigma'_2)+\left(\tan^{-1}\frac{F_1}{G_1}-\tan^{-1}\frac{F_2}{G_2}\right)_p$$
$$+\left(\tan^{-1}\frac{F_1}{G_1}-\tan^{-1}\frac{F_2}{G_2}\right)_\alpha-\omega_1^S,$$

$$\sigma_1-\sigma_2 = -\tan^{-1}\frac{\eta}{2},$$

η denoting the Coulomb parameter $ZZ'e^2/\hbar v$. For the incident channel, $\tan^{-1}(F_l/G_l)$ can be taken to be zero because F_l is much less than G_l for all l. For the ground state α-particles ($E_\alpha \approx 8$ MeV) the magnitude of the term $\tan^{-1}(F_l/G_l)$ can be estimated from the numerical tables of Coulomb wave functions [7]. The above expression describes various profiles characteristic of the interference effect, corresponding to the value of θ_{12}^S, as a function of the incident energy. The difference between the maximum and the minimum of the curve is equal to $A_1^S(A_2^S)_0$, independent of the value of θ_{12}^S. This property is used to determine the magnitude of A_1^S at the $J=2$ resonance.

3. Analysis of Angular Distributions of α_π

Coefficients a_n of the angular distribution, which were obtained from experiment [2]), are plotted in fig. 3 as functions of the incident energy. Here we use an expansion in powers of $\cos\theta$, as was done in ref. [2]). The advantage of using this expansion rather that in Legendre polynomials

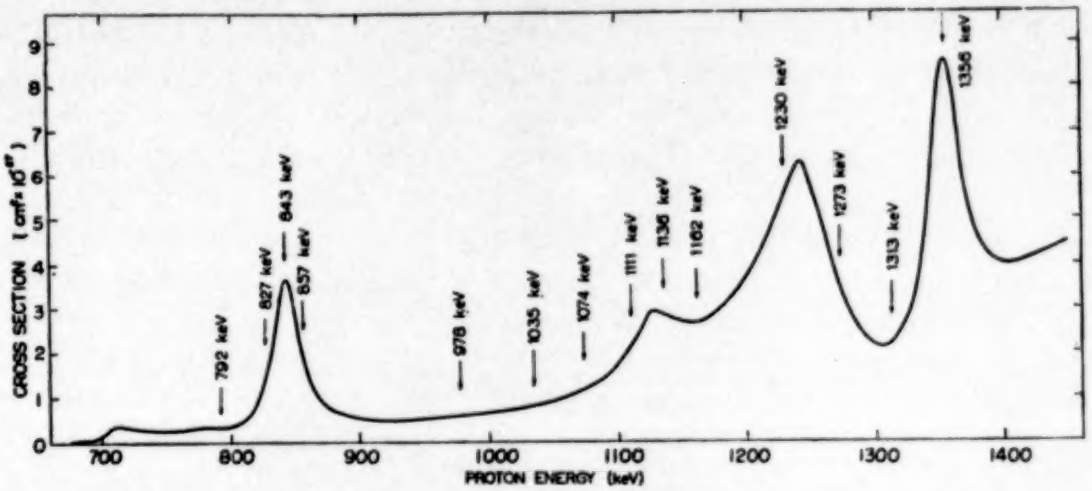

Fig. 2. Excitation function (total cross section) of α_π taken from ref. [2]). Arrows on the curve indicate the energy points where the angular distributions were measured.

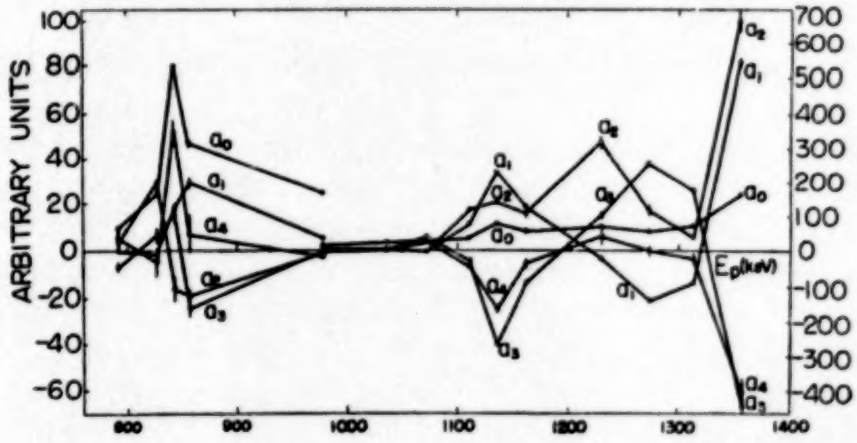

Fig. 3. Energy dependence of the coefficients in the expansion in powers of $\cos\theta_{CM}$ of the α_π angular distribution.

consists in the fact that coefficients of higher order terms are then relatively large compared to those of lower order terms †. Assignment of J-values to the resonance levels which appear in the excitation function is easily made by inspecting variation of a_n with the incident energy around the resonance peaks. J-values of resonances at 843, 1120 and 1355 keV are concluded to be 2 from the appearance of peaks in the a_4-plot. A peak of

† These two sets of coefficients are connected by the following relations:

$$a_0 = b_0 - \tfrac{1}{2}b_2 + \tfrac{3}{8}b_4, \quad a_1 = b_1 - \tfrac{3}{2}b_3, \quad a_2 = \tfrac{3}{2}b_2 - \tfrac{15}{4}b_4, \quad a_3 = \tfrac{5}{2}b_3, \quad a_4 = \tfrac{35}{8}b_4.$$

1243 keV is considered to be due to $J = 1$, because a_4 is small in this region and a_2 shows a large peak. The yield in the region of 1 MeV is predominantly due to the $l = 0$ wave with a small admixture of the $l = 1$ wave. We shall reveal more detailed structures by using the formulas (8) to (12).

The 843 keV ($J = 2$) *resonance*

This resonance peak extends so far above the background that the d-wave matrix element may be approximated by the single level formula (16), and the other matrix elements may be assumed constant in this region because of the sharpness of the resonance. The formula (17) is thus applicable to the interference terms $A_1^0 A_2^0 \cos(\phi_1^0 - \phi_2^0)$ and $A_1^1 A_2^1 \cos(\phi_1^1 - \phi_2^1)$. Results of fit are shown in fig. 4, where curves are drawn with the following values of relative amplitudes and phase differences between the elements of the collision matrix:

$$\frac{A_0^0}{(A_2^0)_0} = 0.99, \qquad \frac{A_1^0}{(A_2^0)_0} = 0.182, \qquad \frac{A_1^1}{(A_2^0)_0} = 0.313, \qquad \frac{(A_2^1)_0}{(A_2^0)_0} = 1.13,$$

$$\phi_2^0 - \phi_1^0 = \delta_2 + 270°, \qquad \phi_2^1 - \phi_1^1 = \delta_2 + 240°, \qquad \phi_2^0 - \phi_0^0 = \delta_2 + 60°,$$

where the resonant phase shift δ_2 is assumed to be $180° > \delta_2 > 0°$.

Higher energy region

A similar treatment was extended to the higher energy region. Plots of the experimental data are shown in fig. 5. In this region the interaction of overlapping levels is too complicated, and measurements of the angular distribution are too few to enable such an exact analysis as was made at the 843 keV resonance. A consistent interpretation is illustrated in the figure. In this energy range backgrounds seem to be composed of broad $J = 0$ and 1 levels. Roughly estimated magnitudes of these non-resonant parts are indicated with broken lines. A consistent set of values of adjustable parameters at the 1120 keV resonance ($J = 2$) are given as follows:

$$\frac{A_0^0}{(A_2^0)_0} = 2.4, \qquad \frac{A_1^0}{(A_2^0)_0} = 1.2, \qquad \frac{A_1^1}{(A_2^0)_0} = 1.0, \qquad \frac{(A_2^1)_0}{(A_2^0)_0} = 1.6,$$

$$\phi_2^0 - \phi_1^0 = \delta_2 + 210°, \qquad \phi_2^1 - \phi_1^1 = \delta_2 + 90°, \qquad \phi_2^0 - \phi_0^0 = \delta_2 + 30°.$$

Here δ_2 is assumed to be $180° > \delta_2 > 0°$. The $J = 1$ resonance at about 1240 keV interferes with the background. An abnormally steep gradient of the high energy wing of this resonance peak is probably due to a destructive interference which seems to occur there. Following this interpretation, the value of the resonance energy should be slightly higher than the peak position. This conclusion agrees with the fact that a corresponding resonance peak in an yield curve of protons scattered inelastically by F^{19}, measured

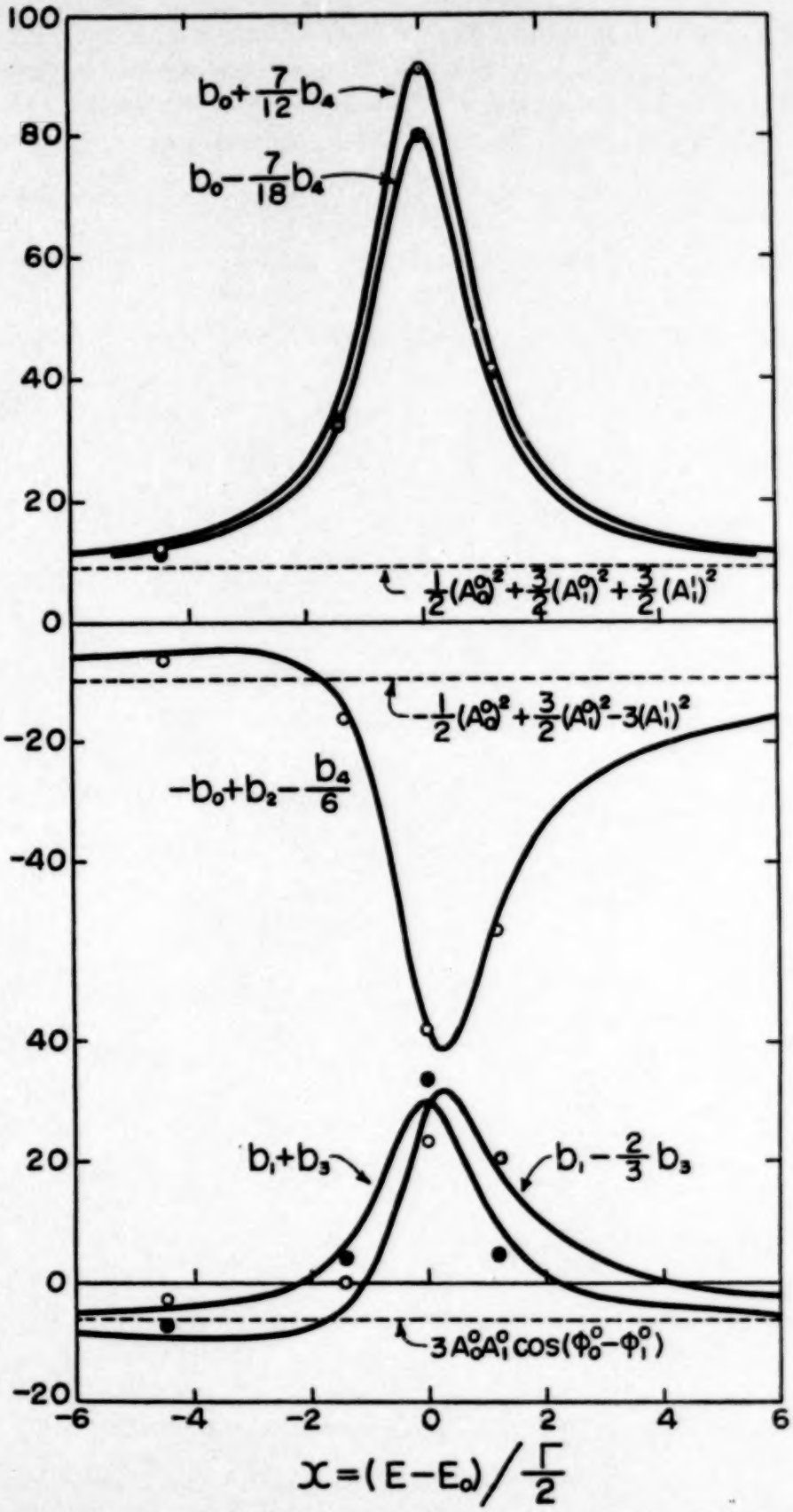

Fig. 4. Combinations (8) to (12) of the Legendre polynomial coefficients of the α_n angular distribution near the 843 keV ($J = 2$) resonance. (Γ=23 keV). Solid curves are calculated with the values of parameters listed in the text. Broken lines indicate the constant portions due to s- and p-wave elements.

by C. A. Barns [8]), appears near 1250 keV. From comparison between the two curves in fig. 5a, it is clear that this resonance state is excited predominantly through the channel of $S = 0$. On the other hand the main part of the $J = 1$ background seems to be the $S = 1$ component.

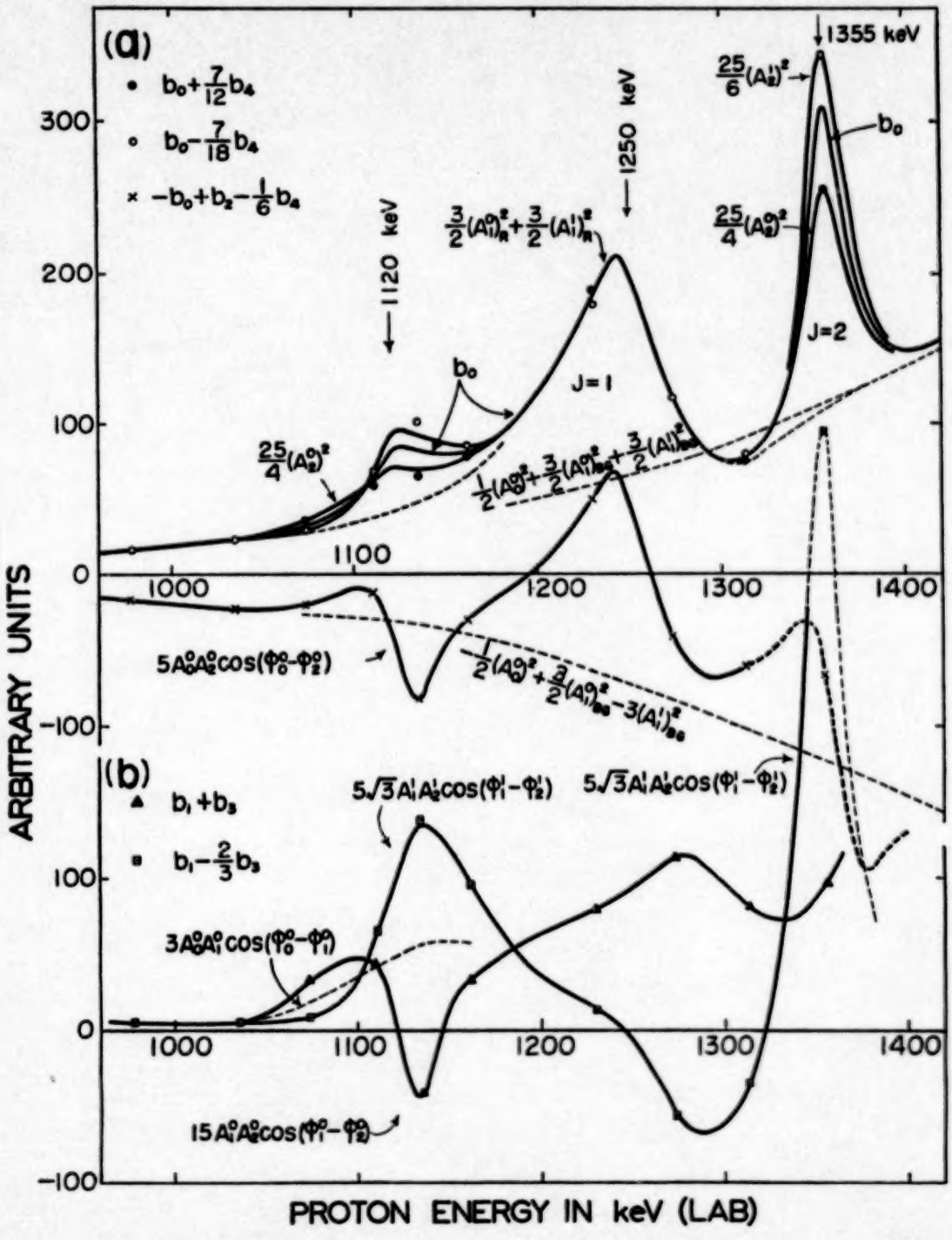

Fig. 5a and b. Plots of the combinations (8) to (12) of the Legendre polynomial coefficients of the α_π angular distribution in the higher energy region. Broken lines illustrate the contributions from the constituent terms in (8) to (12).

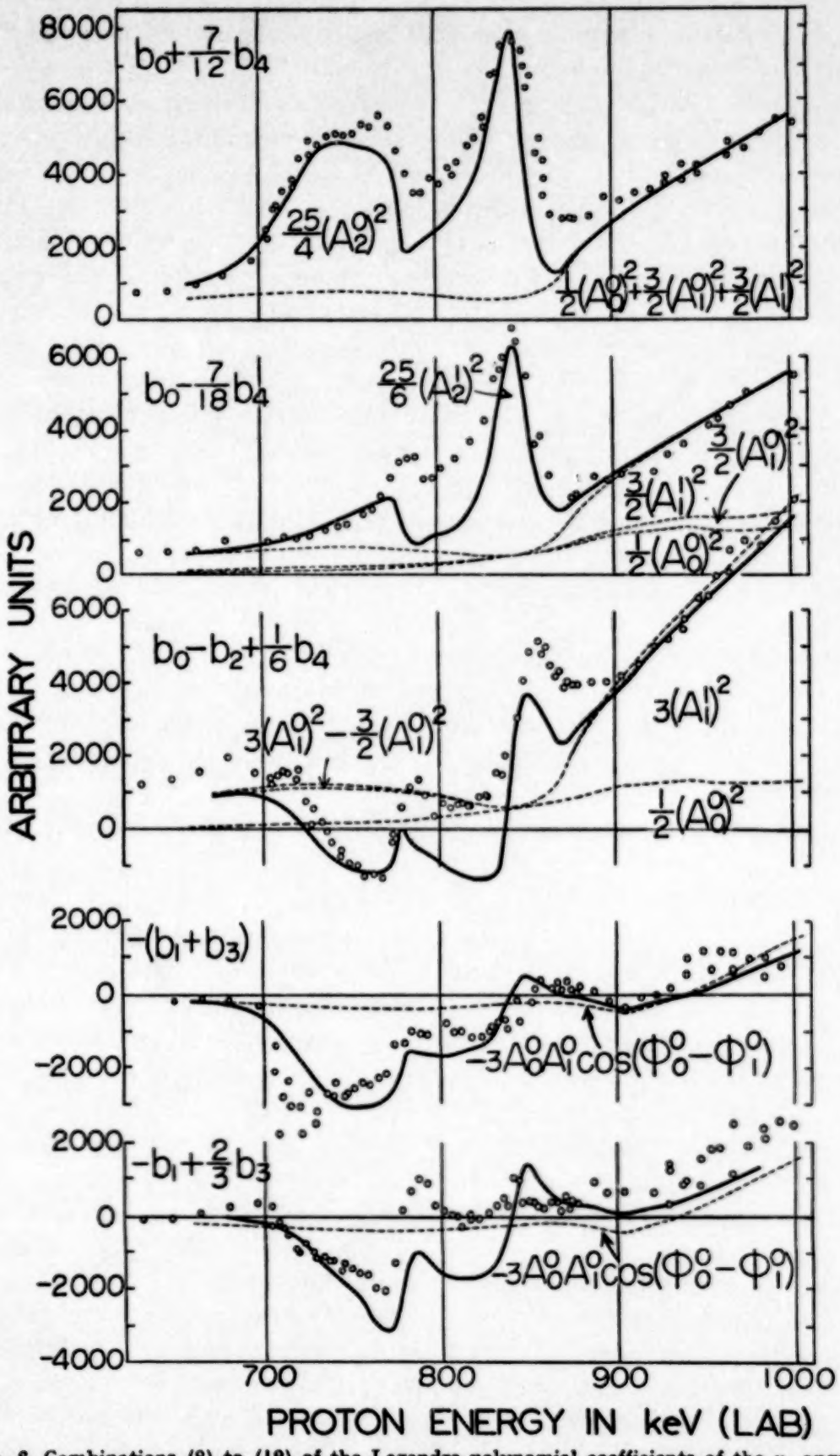

Fig. 6. Combinations (8) to (12) of the Legendre polynomial coefficients of the α_0 angular distribution in the lower energy region. Solid curves are reproduced from the vector diagrams in fig. 8. Broken lines illustrate the process of successive addition of the constituent terms to form the resultant curves.

4. Analysis of the Angular Distribution of α_0

Values of b_n are shown in fig. 4 of the preceding paper [1]) as functions of the incident proton energy. Values of the combinations (8) to (12), are shown in figs. 6 and 7 in the present paper. In these plots we find evidence of resonance levels at the following energies: 738, 778, 843, 1115, 1160, 1230 and 1360 keV. At 738, 778, 1115 and 1360 keV, a peak or undulation appears in the plot of b_4, and interference anomalies concerning the d-wave appear in the plots of the formulas (10), (11) and (12). Thus, the J-value 2 is assigned to these levels.

At 843 keV we find a sharp peak with nearly the same height in the plots of b_0, $b_0+\frac{7}{12}b_4$, and $b_0-\frac{7}{18}b_4$. The appearance of a small anomaly in the b_3-plot and an interference term $A_2^0 A_0^0 \cos(\phi_2^0-\phi_0^0)$ in the plot of $b_0-b_2+\frac{1}{6}b_4$ proved that these peaks are due to a $J=2$ resonance. A peak in the b_4-plot nearly vanishes on account of accidental cancellation between $\frac{45}{7}(A_2^0)^2$ and $\frac{30}{7}(A_2^1)^2$. A similar situation was also found in the α_π-group for which the magnitude of b_4 was very small compared to that of b_0.

At 1160 keV a peak appears in the plots of b_0, $b_0+\frac{7}{12}b_4$ $b_0-\frac{7}{18}b_4$ and $b_0-\frac{1}{2}b_2+\frac{3}{8}b_4$, but a corresponding peak of that height which is anticipated on an assumption of $J=1$ or 2, is not found in the b_2 and b_4 plots. Thus the J-value of tihs level is concluded to be 0. For the α_π-group no indication of this level was found.

At 1225 keV a peak is found in the plots of b_2 and $b_0-b_2+\frac{1}{6}b_4$. They have opposite signs and are attributed either to a term $A_2^0 A_0^0 \cos(\phi_2^0-\phi_0^0)$ or $(A_1^0)^2$. The appearance of a knob at just the same energy in the plots of b_0 and $b_0+\frac{7}{12}b_4$ makes one deduce that these peaks are due to a term $(A_1^0)^2$. This conclusion explains why the peak does not appear in the excitation function taken at $\theta=90°$: $b_0-\frac{1}{2}b_2+\frac{3}{8}b_4$ does not include the term $(A_1^0)^2$, and the peak height due to $(A_1^1)^2$ seems to be either negligible or negative. This level probably coincides with a level at about 1240 keV appearing in the excitation function of α_π and protons scattered inelastically. The large shift of the peak position of $15 \approx 20$ keV to the lower energy can be explained as caused by the interference with the background.

Besides the well established levels mentioned above, some indications of other levels appear. For the level at 710 keV, the existence of which is established by the excitation function of α_π evidence that $J=1$ is obtained from examination of the b_n plots. However, this assignment is not reliable because the experiment was not sufficiently accurate. In the region between two $J=2$ resonances at 843 and 1115 keV, the b_4 plot indicates complicated behaviour. We know that the $P_5(\cos\theta)$ term in the angular distribution does not vanish in this region and thus the present analysis which neglects

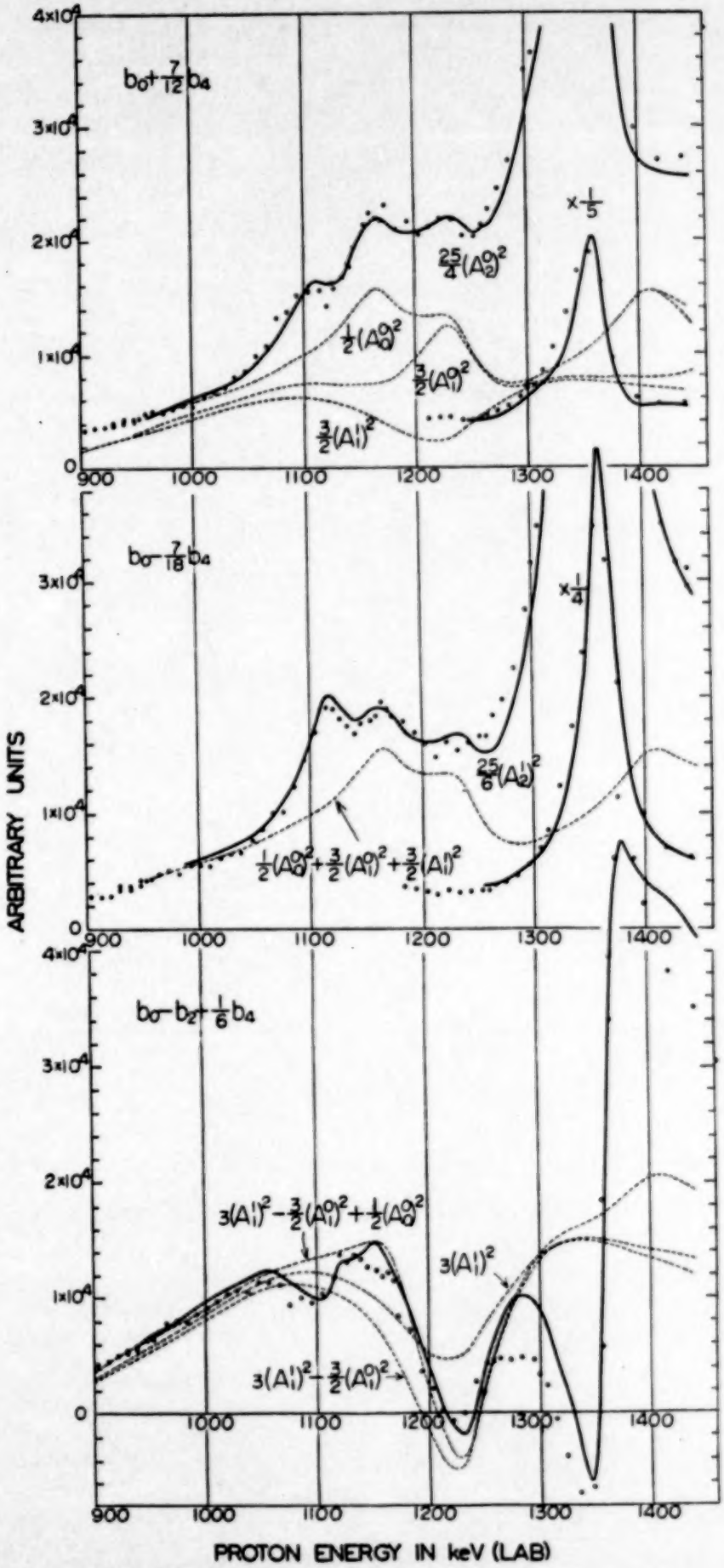
$b_0+\frac{7}{12}b_4$
$\frac{25}{4}(A_2^0)^2$
$\frac{1}{2}(A_0^0)^2$
$\frac{3}{2}(A_1^0)^2$
$\frac{3}{2}(A_1')^2$
$\times\frac{1}{5}$
$b_0-\frac{7}{18}b_4$
$\frac{25}{6}(A_2')^2$
$\frac{1}{2}(A_0^0)^2+\frac{3}{2}(A_1^0)^2+\frac{3}{2}(A_1')^2$
$\times\frac{1}{4}$
$b_0-b_2+\frac{1}{6}b_4$
$3(A_1')^2-\frac{3}{2}(A_1^0)^2+\frac{1}{2}(A_0^0)^2$
$3(A_1')^2$
$3(A_1')^2-\frac{3}{2}(A_1^0)^2$
ARBITRARY UNITS
PROTON ENERGY IN keV (LAB)

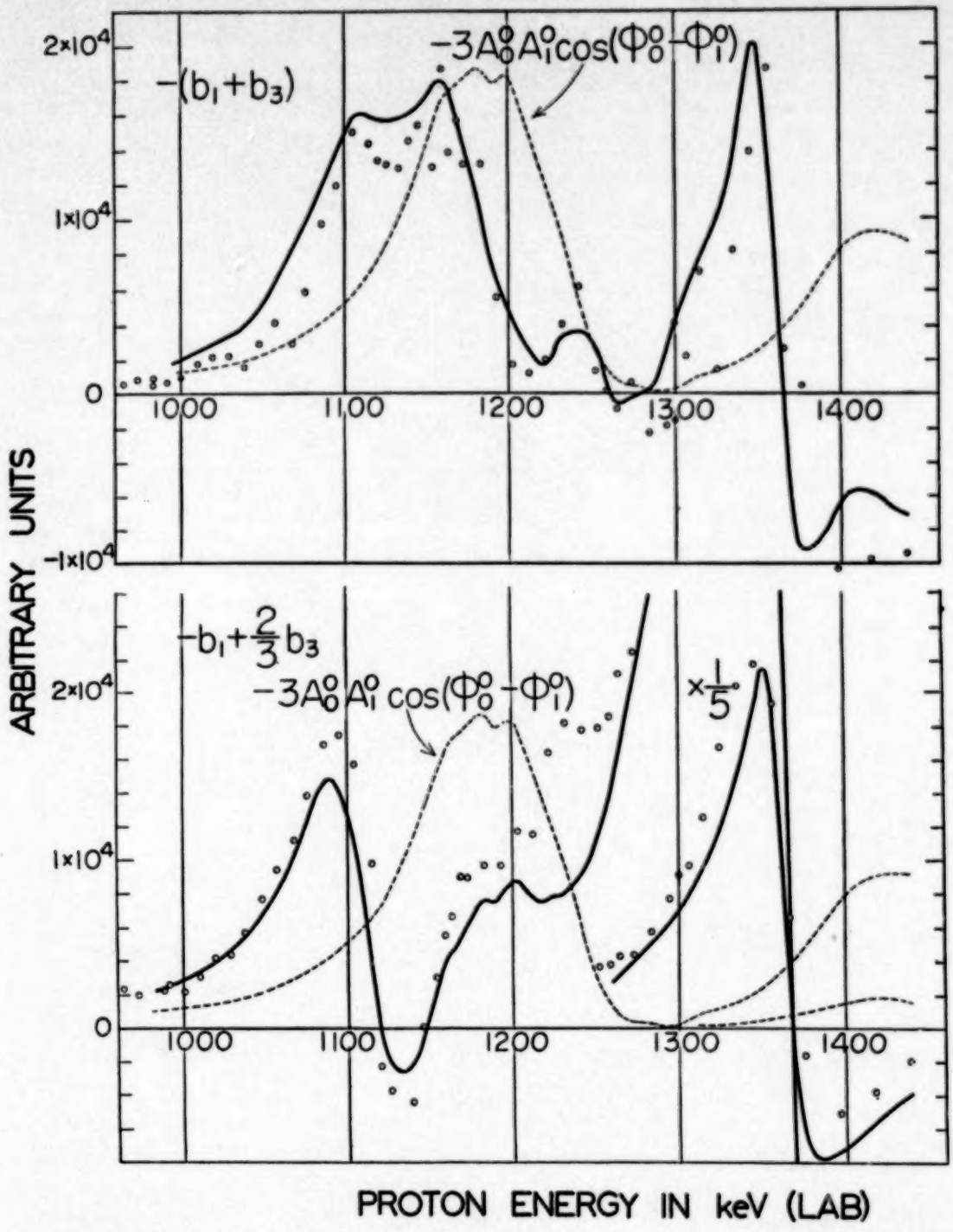

Fig. 7. Combinations (8) to (12) of the Legendre polynomial coefficients of the α_0 angular distribution in the higher energy region. Solid curves are reproduced from the vector diagrams in fig. 8. Broken lines illustrate the process of successive addition of the constituent terms to form the resultant curves.

the presence of this term is not accurate. It is not clear whether this structure is due to existence of resonances or merely due to experimental errors. In the region higher than 1000 keV, existence of a broad d-wave background is deduced from the b_4 plot. The $S=1$ component is probably small compared to the $S=0$ component. This background interferes with the $S=0$ component of the 1115 and 1360 keV resonances and shifts their peak positions in the plot of $b_0+\frac{7}{12}b_4$ (about 10 and 5 keV respectively to the lower energy relative to peaks of $S=1$ component in the plot of $b_0-\frac{7}{18}b_4$). The fact that the apparent level width of the 1360 keV resonance (≈ 40 keV) is quite large compared to that (26 keV) determined from the excitation function of α_n[9]) can be explained for the same reason. s- and p-wave components make up the broad background covering the whole energy range. To understand the nature of these background yields we must resort to a more detailed analysis.

The next step is to construct vector diagrams of the collision matrix elements. Tentatively assigned J-values of the resonance levels are confirmed by checking that consistent fits are obtained with the vector diagrams corresponding to these assignments. We shall sketch the procedure which was employed to construct a consistent set of vector diagrams. The most certain clues to this problem are obtained from analysis of the interference terms at the comparatively narrow $J=2$ resonances. As was done at the 843 keV resonance for the α_n-group, this analysis gives amplitudes and phases of the matrix elements of non-resonant waves at the resonance energies with reasonable accuracy, although it leaves a phase uncertainty of 180° due to the undetermined relative signs of $g^S_{p2}g_{\alpha 2}$ of the resonance levels. Also, the amplitude of each matrix element can be roughly estimated over the whole energy range from comparison between the plots of the coefficients or the combined coefficients of even order. On the basis of this information one can draw the locus of each matrix element, which is expressed, in a zero-approximation, as a superposition of rotated resonance circles as shown in section 2. Generally, the relative sign of $g^S_{pl}g_{\alpha l}$ of each level can be fixed, part by part, from the form of the interference terms between the overlapping levels of different J-values, and this linkage of the relative signs of $g^S_{pl}g_{\alpha l}$ can be extended to all resonances. The above rough loci must be refined by trial and error until the good over-all fit is attained. A set of vector diagrams of the collision matrix elements, obtained in this analysis, are shown in fig. 8 and the curves calculated from these diagrams are compared with the observed points in figs. 6 and 7.

In fig. 8 the quantities

$$\frac{A_l^S}{P_l^{\frac{1}{2}}}\exp\left(i\omega_l^S\right) \approx \sum_\lambda \frac{(g'^S_{\lambda pl}/P_l^{\frac{1}{2}})g'_{\lambda\alpha l}}{E'_\lambda - E - \frac{1}{2}i\Gamma''_\lambda} \tag{18}$$

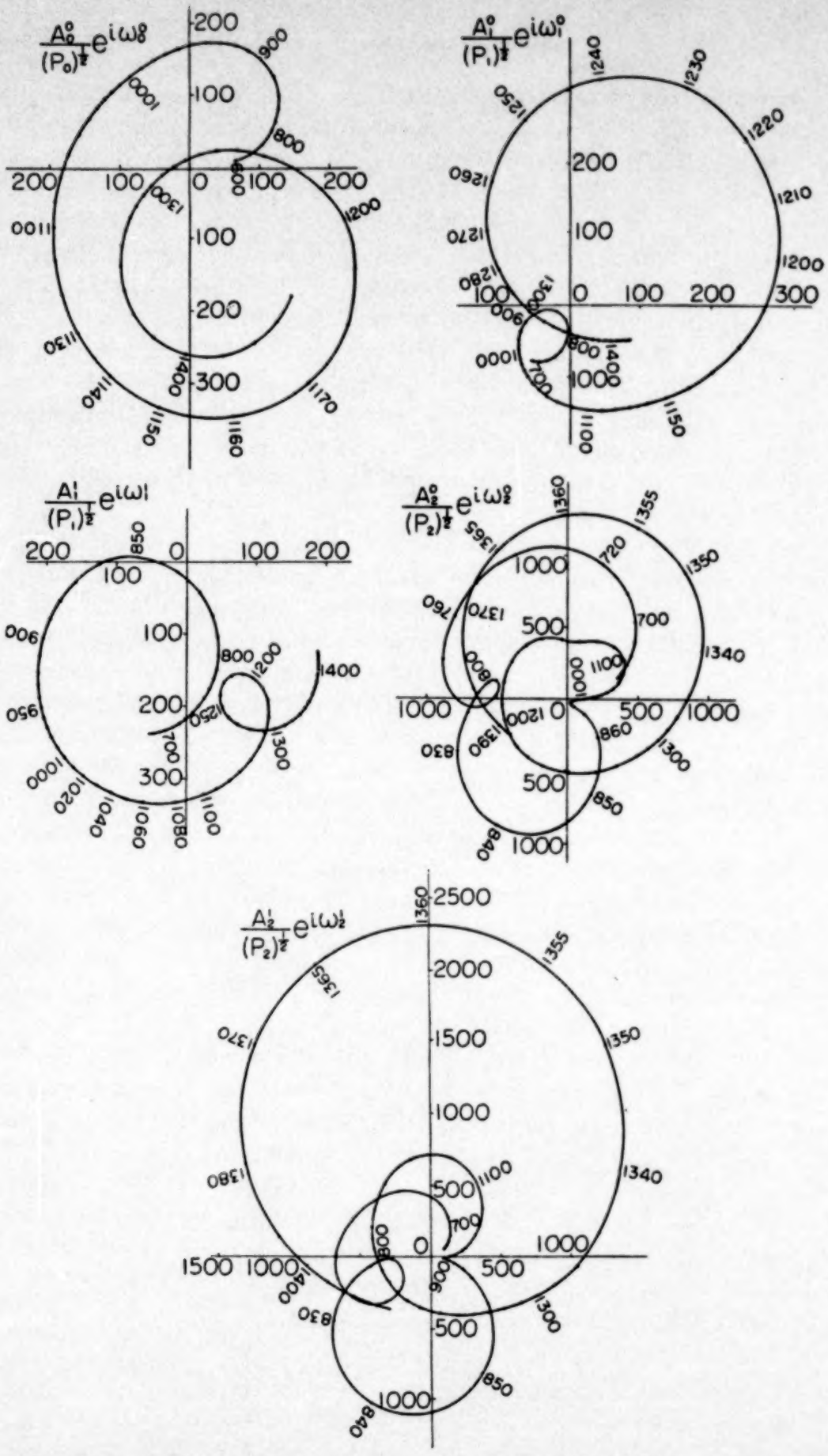

Fig. 8. Vector diagrams of the α_0 collision matrix elements. The scale is arbitrary but is consistent with that of figs. 6 and 7.

are shown, which must be multiplied by the factor

$$iP_l^{\frac{1}{2}} \exp\left[-i \tan^{-1}(F_l/G_l)_p - i \tan^{-1}(F_l/G_l)_\alpha\right] \quad \text{to get} \quad u_l^S.$$

The penetration factors for protons were estimated on assuming the interaction radius $R = 1.41 \times 10^{-13}\,(1+19^{1/3})$ cm. This set of vector diagrams is not the best one which might be attained; there is the possibility of refinement of over-all fit by further approximation.

In the low energy region ($E_p < 1000$ keV) the situation was comparatively simple, because the $J = 2$ resonance levels are close together and no sharp resonances of $J = 0$ and 1 appear. d-wave vector diagrams for $S = 0$ and 1 were constructed simply by superposing resonance circles. In the region between 900 and 1000 keV we have no information about the phases of the s- and p-wave matrix elements. However, the energy dependence of the s- and p-wave amplitudes and the locus interpolated between two neighbouring regions suggests broad $J = 0$ and 1 resonances here. The analysis at the 843 keV resonance required an abnormally small magnitude of A_1^0 and A_1^1 compared to the neighbouring regions and a fast variation of the phases ω_1^0 and ω_1^1 with proton energy. These properties were realized in the vector diagrams. This feature of the locus will occur if there is a $J = 1$ resonance in this neighbourhood which interferes with a broad non-resonant component to form a dip in the excitation function. On account of the formal treatment of the d-wave vector diagrams, which oversimplifies interference effects between the resonance levels with the same spin and parity, the obtained fit is not satisfactory †. However they are sufficient to allow assignment of the relative sign of $g_{pl}^S g_{\alpha l}$ to each resonance level.

In the high energy region ($E_p > 1000$ keV) for $S = 0$ components complicated level compositions of $J = 0$ and 1 and the further presence of the d-wave background make the analysis much more difficult. Interference terms do not always show regular patterns and may depend on trivial behaviours of the relevant vector diagrams. Thus we cannot draw any conclusions before attaining a satisfactory overall fit. After many trials a set of vector diagrams which reproduced almost all detailed features of the energy dependence of the coefficients b_n was obtained. For $S = 1$ components it was difficult to settle a vector diagram of $A_1^1 \exp(i\omega_1^1)$ definitely because of scanty information. We have no information about this locus in the intermediate region between the two resonances at 1115 and 1360 keV, other than the indication that the magnitude of $(A_1^1)^2$ is lowered in the vicinity of 1200 keV. We adopted the simplest interpretation that a dip occurs at the $\approx$ 1240 keV resonance on the broad $J = 1$ background, as shown in the vector diagram. The fact that the resonance amplitude of

† The fit of the curves $b_0 + (7/12)b_4$ and $b_0 - (7/18)b_4$ to the observed points could be considerably improved if the d-wave vector diagrams were modified by rotating the 778 keV resonant circles clockwise by 30° to 45°.

the $S = 1$ component for this resonance is small is consistent with the result of analysis of the α_π-group. The relative sign of $g^1_{p2}\, g_{\alpha 2}$ of the 1360 keV $J = 2$ resonance depends on the choice of phase $\omega_1{}^1$ at this energy. Present choice of this phase seems to be reasonable, because the locus of $(A_1{}^1/P_1^{\frac{1}{2}})$ exp $(i\omega_1{}^1)$, which passes through a point on the opposite side of the origin at this energy, does not allow a simple interpretation as a superposition of the resonance circles. The locus of $(A_0{}^0/P_0^{\frac{1}{2}})$ exp $(i\omega_0{}^0)$ in the region higher than 1360 keV is only a tentative one, and the fit obtained with this locus is not accurate. However, the general trend suggests the existence of a resonance with negative sign of $g^0_{p0}\, g_{\alpha 0}$ at a higher energy. It is plausible to assume that the locus of $(A_0{}^0/P_0^{\frac{1}{2}})$ exp $(i\omega_0{}^0)$ in this region is due to a strong resonance at 1709 keV, reported recently by Clarke and Paul [10]). According to their measurement, the amplitude $(A_0{}^0)_0/P_0^{\frac{1}{2}}$ of this resonance is 1080 on the scale of our vector diagram, and the amplitude at 1360 keV is just the magnitude required to explain the interference terms. If this assumption is made, a slight modification of the loci of $(A_1{}^0/P_1^{\frac{1}{2}})$ exp $(i\omega_1{}^0)$ and $(A_2{}^0/P_2^{\frac{1}{2}})$ exp $(i\omega_2{}^0)$ results in a better fit.

5. Summary

The information about the excited states of Ne^{20} obtained in this investigation and the results of ref. [8]) and [10]) are listed in table 1. For the

TABLE 1

Energy levels of Ne^{20} of spin and parity (even)$^+$ or (odd)$^-$

E^{Lab}_{res} (keV)	$J,\ \pi$	Γ^{Lab} (keV)	$\Gamma_p^{S=1}/\Gamma_p^{S=0}$ from $(p\alpha_0)$	$\Gamma_p^{S=1}/\Gamma_p^{S=0}$ from $(p\alpha_\pi)$	relative sign of $g^S_{pl}\, g_{\alpha l}$	$\sigma(p\alpha_0)$ (mb)	$\sigma(p\alpha_\pi)$ (mb)	$\sigma(pp_1)$[a] (mb)	$\sigma(pp_2)$[a] (mb)
≈ 930	0+	≈180			+	0.5			
1160	0+	≈ 70			—	5.1		<1	<1
1709[b]	0+[b]	148[b]			—	55±6[b]	≈18±5[b]		
710	1—[e]	35				≲0.5	≈0.2	<0.1	<0.1
≈ 860	1—	≈120	≈10.6		+	1.0			
≈1080	1—	≈200	≈ 5.1		—	3.4			
≈1240	1—	≈ 70	≈ 0.11	≲0.1	—	5.2	3±0.5	17±3	<1
733	2+	66	≈ 0.20		+	1.4	≲0.2	<0.1	<0.1
778	2+	≈ 10	≈ 1.6		—	≳0.5	≈0.2	<0.2	≈5
843	2+[c]	23	1.38	1.28	—	3.7	3.4	≈2	<0.3
1115	2+	50	≈ 2.2	2.5	+	2.4	1.5	<1	<0.5
≈1250	2+	≈150	≈ 0.64		—	0.26			
1360	2+[d]	≈ 30	2.52	≈2.4	+	81	6.0	<5	<5

a. From ref. [8]).
b. From ref. [10]).
c. This assignment is different from that of ref. [13]).
d. This assignment agrees with that of ref. [3]) and [10]).
e. This assignment is not certain.

(p, α_0) process, approximate values of the resonant amplitudes $(A_l{}^S)_0 = 2|g'^S_{pl}\, g'_{\alpha l}|/\Gamma'$ of each level were evaluated from the vector diagrams.

Using these amplitudes, the resonant cross sections $\sigma(p, \alpha_0) = \frac{1}{4}(2J+1)\pi\lambda^2\{(A_J{}^0)^2+(A_J{}^1)^2\}$ and the channel spin ratios $\Gamma_p^{S=1}/\Gamma_p^{S=0}$ were determined. It is to be noted that at some resonances the cross sections thus determined are considerably different from the observed peak cross sections. Level widths were also obtained from inspection of the vector diagrams. The values of $\Gamma_p^{S=1}/\Gamma_p^{S=0}$ (listed in the fifth column) derived from the analysis of the (p, α_π) process are to be compared with those mentioned above. Reasonable agreement is found between the values obtained from both processes. Assignments of the relative sign of $g_{pl}^S g_{\alpha l}$ were made consistent within the $S = 0$ and 1 components separately. For all observed $J = 1$ and 2 resonances we found the same sign of $g_{pl}^S g_{\alpha l}$ for the two values of entrance channel spin S. We may conclude that the sign of reduced width amplitude for proton channel $\gamma_{pl}^S (\propto g_{pl}^S)$ is very probably independent of the channel spin S.

The partial widths were calculated with the single level dispersion formula. The resonant cross sections for the competing modes of decay of each compound state, which are needed for this calculation, are listed in table 1. The (p, α_π) cross sections were obtained from the foregoing article by the author *et al.* [2]) (see fig. 2 of the present paper) and the inelastic proton scattering cross sections from the data of Barns [8]). The former cross sections were determined relative to the $(p, \alpha\gamma)$ cross sections due to Chao *et al.* [11]) and the results are in fair agreement with those of Devons *et al.* [12]). The (p, α_0) cross sections determined by the author *et al.* [1]) nearly agree with the result of Clarke and Paul [10]) which was also determined relative to the $(p, \alpha\gamma)$ cross section. Therefore, the values of the cross section for α-particle emission presented in table 1 may be considered to be quite reliable. For the 843 keV level a set of partial widths which gave a large value of Γ_p was abandoned because the resulting value of the reduced width $\gamma_p{}^2$ exceeded the Wigner limit $(\gamma_p{}^2/(3\hbar^2/2\mu_p R_p) = 4.1)$. For the other levels, sets of partial widths which gave the smaller value of Γ_p were adopted, because the elastic scattering cross sections for protons are likely to be small for these levels [13]). The reduced widths were calculated from the partial widths following the formula (15), assuming interaction radii $R = 1.41\times10^{-13}(A_1{}^{1/3}+A_2{}^{1/3})$cm as before. The orbital angular momenta of protons scattered inelastically were assumed to be the lowest possible ones. It is to be remembered that for most levels this procedure provides only order-of-magnitude estimates of the reduced widths, because the interference between the overlapping levels is generally too large. For most of the levels investigated the reduced α-particle widths $\gamma_{\alpha_0}^2$ and $\gamma_{\alpha_\pi}^2$ have magnitudes of a few per cent or somewhat less of the Wigner limit, $3\hbar^2/(2\mu_\alpha R_\alpha)$ (see table 2). One exception is a $J = 2$ level at 778 keV, where the α-particle widths are considerably less and on the other hand the reduced width of the channel corresponding

TABLE 2

Partial and reduced widths

E_{res}^{Lab} (keV)	$\Gamma_{\alpha_0}^{Lab}$ (keV)	$\gamma_{\alpha_0}^2 \times 10^{12}$ (keV · cm)	$\Gamma_{\alpha_\pi}^{Lab}$ (keV)	$\gamma_{\alpha_\pi}^2 \times 10^{12}$ (keV · cm)	$\Gamma_{p_0}^{Lab}$ (keV)	$\gamma_{p_0}^2 \times 10^{12}$ (keV · cm)	$\Gamma_{p_1}^{Lab}$ (keV)	$\gamma_{p_0}^2 \times 10^{12}$ (keV · cm)	$\Gamma_{p_2}^{Lab}$ (keV)	$\gamma_{p_2}^2 \times 10^{12}$ (keV · cm)
≈ 930	≈180	10 (0.029)			0.11	0.41(0.0003)				
1160		3.8 (0.011)			0.56	0.94(0.0007)				
1709										
710	≦ 25	≈ 2(0.006)	≈10	6 (0.02)	0.007	0.28(0.0002)				
≈ 860	≈120	7.2 (0.021)			0.048	0.77(0.0006)				
≈1080	≈200	11 (0.034)			0.34	2.1 (0.0016)				
≈1240	≈ 14	3.9 (0.012)	≈ 8	3.3(0.010)	1.05	3.8 (0.0030)	≈47	≈ 86(0.067)		
733	54	3.2 (0.010)	≦ 8	12 (0.034)	0.020	10 (0.008)				
778	≧ 0.9	0.05(0.0002)	≈ 0.4	0.5(0.0015)	0.12	44 (0.034)			≈9	≈340(0.3)
843	9.0	0.55(0.0016)	8.3	9.1(0.027)	0.051	11.5(0.0090)	≈ 5	≈180(0.094)		
1115	31	1.86(0.0055)	19	12 (0.036)	0.060	33 (0.0026)				
≈1250	≈150	9.0 (0.027)			0.015	0.5 (0.0004)				
1360	28	1.66(0.0049)	2.1	1.0(0.0029)	1.0	23 (0.018)				

The number in the bracket following the reduced width γ^2 indicates the ratio of γ^2 to the Wigner limit, $3\hbar^2/2\mu R$.

to the second excited state of F^{19} plus a proton is exceptionally large (≈ 0.3 of the Wigner limit). Differences between reduced widths of the α_0- and α_π- channels are generally small. These widths are also comparable to the usual reduced α-particle widths of the levels which are relevant to the process (p, $\alpha\gamma$) [13]). Levels at 843 keV and 1240 keV have considerably large reduced widths for the channel corresponding to the first excited state of F^{19} plus a proton (≈ 0.1 of the Wigner limit).

The author wishes to thank Professor T. Momota for his continued interest and encouragement. Thanks are also due to Dr. S. Yoshida and Mr. K. Kikuchi for their reading of the manuscript and helpful discussion.

References

1) A. Isoya, H. Ohmura and T. Momota, Nuclear Physics **7** (1958) 116
2) A. Isoya, K. Goto and T. Momota, Jour. Phys. Soc. Japan **11** (1956) 899
3) C. Y. Chao, Phys. Rev. **80** (1950) 1035
4) Breit and McIntosh, Phys. Rev. **106** (1957) 1246
5) E. P. Wigner and L. Eisenbud, Phys. Rev. **72** (1947) 29
6) R. G. Thomas, Phys. Rev. **97** (1955) 67
7) Bloch, Hull, Broyles, Bouricius, Freeman and Breit, Revs. Mod. Phys. **23** (1951) 147
8) C. A. Barns, Phys. Rev. **97** (1955) 1226
9) F. Ajenberg and T. Lauritsen, Revs. Mod. Phys. **27** (1955) 77
10) R. L. Clarke and E. B. Paul, Can. Jour. Phys. **35** (1957) 155
11) C. Y. Chao, A. V. Tollestrup, W. A. Fowler and C. C. Lauritsen, Phys. Rev. **79** (1950) 108
12) S. Devons, G. Goldring and G. R. Lindsey, Proc. Phys. Soc. A **67** (1954) 134
13) Webb, Hagedorn, Fowler and Lauritsen, Phys. Rev. **99** (1955) 138;
E. U. Baranger, Phys. Rev. **99** (1955) 145

8.B *Nuclear Physics* 7 (1958) 146—147; © *North-Holland Publishing Co., Amsterdam*
Not to be reproduced by photoprint or microfilm without written permission from the publisher

ON THE INTERACTION BETWEEN K-MESONS, PIONS, NUCLEONS AND HYPERONS

V. S. BARASHENKOV

Joint Institute of Nuclear Research, Laboratory of Theoretical Physics, Dubna, U.S.S.R.

Received 20 January 1958

A model for the description of plural creation of strange particles has been proposed in ref. [1, 2]). The structure of a "compound particle" resulting from the collision between two fast particles was found to depend markedly on the magnitude of the interaction assumed to exist between the various types of particles. Coupling constants do not explicitly enter the plural creation formulae of the statistical theory. "Strong" or "weak" are understood here with respect to the magnitude of the cross sections which determine statistical equilibrium between the created particles. In our opinion, conclusions regarding "strong" or "weak" interaction between various types of particles that can be drawn by comparing statistical theory computations with experiment in a broad energy range will probably yield information on the relative magnitude of the coupling constants for these particles †. Since at present diverse opinions are held regarding the magnitude of the interactions between π or K-mesons and hyperons, and between K-mesons and nucleons, even indirect information on these interactions would be of interest.

We shall proceed from the well known experimental fact that the interaction between pions and nucleons is a strong one ($g^2/4\pi\hbar c \gg 1$). If one assumes a strong interaction between pions and K-mesons (or between K-mesons and nucleons) the following choices of space volumes are possible for a "compound particle":

1) Statistical equilibrium between all secondary particles takes place in a single volume $V = V_1$ ††. In this case the ratio of created strange particles to pions and nucleons considerably exceeds the experimental value.

2) Statistical equilibrium between nucleons, pions and K-mesons occurs in the same space volumes $V = V_1$, whereas hyperon equilibrium takes place in a smaller volume. In this case the fraction of produced strange particles is close to the experimental value [6, 7]); however, for $E = 6.2$ GeV

† A detailed analysis of this problem will be presented at a later date.

†† The notations are those employed in ref. [1, 2]).

the ratio of K^- to K^+-mesons created in nucleon-nucleon collisions is $N^+/N^- \approx 3$. On the other hand a value $N^+/N^- \approx 100-150$ was observed in ref. [4]) for K-meson momenta $p \approx 250-350$ MeV/c. Even if the momentum distribution is taken into account it is difficult to remove a discrepancy of two orders of magnitude between these values †.

3) The K-meson equilibrium volume is larger than the respective volume for nucleons and pions. Neither the fraction of created strange particles nor the ratio N^+/N^- can be made to agree with the experimental data.

Agreement between the statistical theory of plural particle production and experiment can be attained only if weak interaction of K-mesons with pions and nucleons is assumed. Statistical equilibrium for K-mesons will then occur in a space volume that is smaller than that for pions and nucleons. The best agreement can be obtained by assuming, following ref. [5]), symmetrical interaction of pions with nucleons and hyperons ($V = V_2$[2]). Thus in this case the calculated effective cross section σ_s for strange particle production in 4.3 GeV π-meson-nucleon collisions is 3 mb. The mean experimental value for this cross section is approximately 2.2 mb. However, if one assumes that all strange particles interact weakly with pions and nucleons ($V = V_3$), one finds $\sigma_s = 0.3$ mb. The discrepancy between the theoretical and experimental values in this case considerably exceeds the experimental error ††. For $V = V_2$, $N^+/N^- \approx 160$ and for $V = V_3$, $N^+/N^- \approx 8$. Assuming again that all strange particles interact weakly with pions and nucleons, we find a large discrepancy between the computed values of N^+/N^- and the experimental ones.

The author wishes to thank D. I. Blokhintsev for numerous discussions and M. A. Markov, B. V. Medvedyev and V. I. Ogievetsky for discussion and valuable critical remarks. I am also thankful to K. D. Tolstov for discussion of the experiments [6]).

† Exact calculations with account of momentum distributions will be published in Acta Physica Polonica.

†† The experimental error is $\leqq 50$ %; $\sigma_{tot} = (25 \pm 2.5)$ mb.

References

1) V. S. Barashenkov, B. M. Barbashov, E. G. Bubelyev and V. M. Maksimenko, Nuclear Physics **5** (1957) 17
V. S. Barashenkov, B. M. Barbashov and E. G. Bubelyev, Nuovo Cimento (in print)
2) V. S. Barashenkov and V. M. Maltsev, Acta Physica Polonica (in print)
3) V. S. Barashenkov, Report at Conference on Pion and New Particle Physics, Padua-Venice 1957
4) W. W. Chapp *et al.*, Nuovo Cimento Suppl. **4** (1956) 359
5) M. Gell-Mann, Phys. Rev. **106** (1957) 1296
6) C. Besson *et al.*, Nuovo Cimento **6** (1957) 1168
7) Proceedings of the 7th Rochester Conference and of the Conference in Padua-Venice (1957)

8.B *Nuclear Physics* 7 (1958) 148—149; © *North-Holland Publishing Co., Amsterdam*
Not to be reproduced by photoprint or microfilm without written permission from the publisher

SPECULATIONS ON THE MASSES OF PARTICLES

H. FRÖHLICH
Department of Theoretical Physics, University of Liverpool

Received 5 February 1958

The discovery of mesons and baryons poses the obvious question whether the masses of these particles are related by a simple law. One would not expect this if these masses were to contain considerable contributions from field self-energies. In the following it will be shown, however, that a simple empirical relation between the masses does exist on the assumption that the electromagnetic self-energy E is the only self-energy involved. It has been pointed out [1, 2]) that E is of a corre . order to understand the mass difference of π^0 and $\pi^\pm$ mesons (about 9, using the electronic mass as unit) or of protons and neutrons (about 3 units). This invites the definition of basic masses M_0, which differ from the observed masses M by the electromagnetic self-energy E, i.e. by not more than about 10 units.

Table 1 now shows the striking fact that if M_0 is assumed to be eq ıal to the integer multiple of 137 nearest to M, the difference $E = M - M_0$ is of the order 10 or less for all particles except the μ-meson and the nucleons †.

TABLE 1

	π^+	π_0	K	Λ	Σ^0_+	Σ^-	Ξ
M	273	264	966	2180	2331	2341	2590
M_0	274		959	2192	2329		2603
$M_0/137$	2		7	16	17		19
E	−1	−10	7	−12	2	12	−13

The question arises whether the strange set of numbers 2, 7, 16, 17, 19 can be accounted for by a simple formula. This, no doubt, is possible in a number of ways. We note, for instance, that the series $(j+1)(j+2)+j^2$, $j = 0, 1, 2, 3$, starts with 2, 7, 16. We might then involve the baryonic number n ($n = 0$ for π's and K's; $n = 1$ for Λ, Σ, and Ξ's) to define $j \geqq 0$ by

$$n(n+1) = j(j-1)$$

and put

† However $\sqrt{2} \times 137 = 193.7$ differs from the μ-meson mass (207) by 13, and $(12+\sqrt{2}) \times 137 = 1837.7$ differs from proton (1836) and neutron (1839) mass by less than 2.

$$M_0 = (j+1)(j+2)+j^2+\tfrac{1}{2}nm(m+1)$$

where $m = 0, 1, \ldots, j$.

While the particular form of these relations may have no significance, I feel that it is very unlikely that the closeness of M, in five out of seven cases, to an integer multiple of the significant number 137 is a coincidence. If this were accepted then one might also conclude that nucleons and μ-mesons have certain other properties which distinguish them from the particles in the table †.

† After this note had been written, my attention was called to a note by Y. Nambu [3]), which has some similarity with this one.

References

1) R. O. Feynman and G. Speisman, Phys. Rev. **94** (1954) 500
2) A. Petermann, Helvet. Phys. Acta **27** (1954) 441
3) Y. Nambu, Progr. Theor. Phys. **7** (1952) 595

1.D.3 *Nuclear Physics* 7 (1958) 150—162; © *North-Holland Publishing Co., Amsterdam*
Not to be reproduced by photoprint or microfilm without written permission from the publisher

THE "CLUSTER MODEL" OF THE ATOMIC NUCLEI

K. WILDERMUTH and TH. KANELLOPOULOS
CERN, *Theoretical Study Division, Geneva*

Received 2 January 1958

Abstract: A method is discussed which makes it possible to see that in nuclei many different cluster structures are present. Which cluster structures are preferred depends on the form and strength of the interaction forces, the type of nucleus and the excitation levels of this nucleus. Some examples are discussed. The influence on the asymmetrical fission is mentioned briefly.

1. Introduction

The investigation of the ground states and of the excited levels, especially of light nuclei, has shown that it is necessary for the best description to apply different models according to the structure of these levels. Examples are the shell-model and the α-particle-model; in particular, it seems that the α-particle-model is especially good for the description of the low energy levels of nuclei which are composed of a whole number of α-particles as for instance Be^8, C^{12} and O^{16} [1, 2]). In this work we shall discuss in which way the different models can be understood in the frame of a generalized shell-model, the "cluster model" of nuclei. Especially we shall discuss in which way the "cluster model" can be used for the classification of the energy levels of nuclei. Here we restrict ourselves mainly to the light nuclei, because the mathematical formulation is especially simple for these nuclei. When going over to the medium and heavy nuclei nothing is changed physically, but the mathematical formulation becomes more complicated, because we have to pass from the oscillator potential to the square well potential as a representation of the average potential for the motion of the nucleons.

2. Description of the Method

As is well known, for the description of the motion of the nucleons in light nuclei in the frame of the independent particle model the oscillator potential is especially convenient. For a nucleus composed of A nucleons, we have the following Schrödinger equation for the motion of the nucleons:

$$\frac{1}{2M}\left\{\sum_{i=1}^{A}\mathbf{p}_i^2+a^2\hbar^2\sum_{i=1}^{A}\mathbf{r}_i^2\right\}\Psi(\mathbf{r}_1\ldots\mathbf{r}_A)=E\Psi(\mathbf{r}_1\ldots\mathbf{r}_A), \qquad (1)$$

where $\mathbf{p}_i$ is the operator of the momentum vector of the i^{th} nucleon and $\mathbf{r}_i$ is the position vector of the i^{th} nucleon.

The width parameter $a = M\omega/\hbar$ (ω = frequency of the oscillator potential) is defined, as is well known, in such a way (see e.g. ref. [3])), that the radius of the nucleus, composed of A nucleons, is in as good agreement with the experimental value as possible.

The eigenfunctions which belong to (1) are a complete set of orthogonal wave functions for the A variables $\mathbf{r}_i$. We can express the antisymmetrical wave functions of the states of a nucleus composed of A nucleons as a superposition of these eigenfunctions, if in addition we introduce the spin and the isobaric spin functions of the nucleons.

As is seen eq. (1) is completely separable in the variables $\mathbf{r}_i$. Therefore we can give a complete set of eigenfunctions (of 1) which are products of A one-particle wave functions. We shall call such a complete set of wave functions a one-particle wave-function system and the corresponding model a one-particle model.

If we now divide the A nucleons into clusters $n_1, n_2 \ldots n_k$ with $\sum_{i=1}^{k} n_k = A$ and introduce the centre of mass coordinates and the centre of mass momenta of these clusters, the Schrödinger equation (1) becomes

$$\left\{\sum_{i=1}^{k} H_i + \sum_{i=1}^{k} \frac{1}{2M} \cdot \frac{1}{n_i} P_i^2 + \sum_{i=1}^{k} \frac{a^2\hbar^2}{2M} n_i R_i^2\right\} \Psi = E\Psi; \qquad (2)$$

$$P_i = \sum_{s=1}^{n_i} p_s; \qquad R_i = \frac{1}{n_i} \sum_{s=1}^{n_i} r_i.$$

The Hamiltonian H_i depends only on the relative coordinates and the relative momenta of the nucleons in the i^{th} cluster. Therefore we can give a complete set of wave functions for (2), corresponding to that of (1). These eigenfunctions are products of functions †, in which every function either depends only on the relative coordinates of one cluster or depends on a single centre of mass coordinate $\mathbf{R}_i$ †. We characterize such a cluster function system by the indices $n_1, \ldots, n_i$.

After antisymmetrization all these cluster function systems are equivalent to the one-particle wave-function system, because we can expand all the states of a nucleus in terms of anyone of these cluster function systems.

It now depends on the nuclear forces, in which cluster function system the different states of nuclei are represented especially simply; i.e. what kind of correlation between the nucleons is particularly favoured in the different nuclear states. This favoured representation can change from nucleus to nucleus and from level to level. The practical criterion for an

† Special product functions of this kind have already been given by Elliott and Skyrme [4]) and Brink [5]). We thank Prof. Weisskopf very much for bringing the work of Brink to our attention.

especially simple description of a state in a certain cluster system is that in this system this state is described essentially by one or by only a small number of antisymmetrical cluster wave functions. This means that the corresponding expansion coefficients a_i must satisfy

$$|a_i|^2 \approx 1 \tag{3a}$$

or, respectively,

$$\sum_{i=1}^{m} |a_i|^2 \approx 1 \tag{3b}$$

where m is small number [(3b) is only true if the different wave functions are orthogonal to each other; see later].

3. States of Be^8

3.1. QUALITATIVE DESCRIPTION

The best way to understand the physical significance of such cluster states is to consider a special example. For this example we consider the ground state and the lowest excited states of Be^8.

Be^8 is composed of 4 protons and 4 neutrons. Further we know that the α-particle clusters are especially tightly bound. Therefore, it seems practical for energetical reasons to choose a representation, in which after the introduction of the spins and the isobaric spins we have two α-particle clusters i.e. for which $n_1 = 4$ and $n_2 = 4$. A wave function in this representation has then the general form

$$\Psi = \mathscr{A}\left\{\Psi_k(\alpha_1)\Psi_r(\alpha_2)X(\mathbf{R}_{\alpha_1}-\mathbf{R}_{\alpha_2})Y\left(\frac{\mathbf{R}_{\alpha_1}+\mathbf{R}_{\alpha_2}}{2}\right)\right\} \tag{4}$$

$\Psi_k(\alpha_1)$ depends on the relative coordinates of the first α-particle and $\Psi_r(\alpha_2)$ depends on the relative coordinates of the second α-particle. The indices k and r denote that the α-particles are in their k^{th} and r^{th} excited state respectively. Also we have introduced in (4) a splitting off of the centre of mass coordinates of the two α-particles in their relative coordinates on one hand, and the total centre of mass coordinates on the other. Thus the functions $X(\mathbf{R}_{\alpha_1}-\mathbf{R}_{\alpha_2})$ and $Y(\frac{1}{2}(\mathbf{R}_{\alpha_1}+\mathbf{R}_{\alpha_2}))$ depend on these relative coordinates and the total centre of mass coordinates respectively. The operator $\mathscr{A}$ denotes the complete antisymmetrization of the wave function with respect to its coordinates and also normalization of the wave function to 1. The set of functions (4) represents a complete set of antisymmetrical wave functions with respect to the coordinates $\mathbf{r}_1, \ldots, \mathbf{r}_A$ and the corresponding spin and isobaric spin coordinates. It must be mentioned that, in general, the wave functions are no longer orthogonal to each other as they are in the one-particle wave-function system. However, this is only a mathematical complication and presents no difficulty of principle.

It can be shown without difficulty that all functions (4) are oscillator wave functions or products of oscillator wave functions, if we make a linear transformation of the relative coordinates of the α-particles. The width is the same for all the oscillator wave functions. It seems therefore at first sight that the clustering of α-particles which we have considered here is very formal and has nothing to do with any real clustering of α-particles, since it seems that the single nucleons in an α-particle can move over the whole nucleus independently of each other. But this is not correct because especially for the region of very light nuclei (He^4 to O^{16}) the increase of the nuclear radius in going from light to heavier nuclei comes practically only from the filling up of the oscillator potential [6, 7]). For instance, if we use the two body forces given below, the calculated binding energy of He^4 with a width parameter a of the oscillator potential appropriate to Be^8 ($a = 4.7 \times 10^{25}$ cm^{-2}), is 28.5 MeV. As is seen, this value is very close to the experimental value. This means that the wave function (4) really describes a partial separation of the two α-particles †.

Since the nuclear forces in conjunction with the Pauli principle have the effect that the α-particles are especially tightly bound, we expect that the lowest levels of Be^8 are excitations of oscillation of the α-particles relative to each other without any internal excitation of the α-particles themselves. It can be seen very easily (for instance by consideration of the total kinetic energy of the nucleons in the oscillator potential) that $X(\mathbf{R}_{\alpha_1} - \mathbf{R}_{\alpha_2})$ must be an oscillator wave function of at least the 4th degree (highest power: $(\mathbf{R}_{\alpha_1} - \mathbf{R}_{\alpha_2})^4$), in order that at least four particles are lifted into the 1p-shell of the one-particle model as required by the Pauli principle. For lower excitations of the relative oscillation of the two α-particles, the wave functions vanish on antisymmetrization (see for this also ref. [2])). This means that already in the ground state the excitation of the relative oscillation of the two α-particles is relatively high ($E_{\text{kin}}^{\text{exc}} \approx 38$ MeV). It is well known that the oscillator wave functions of the 4^{th} degree are a 4s, a 4d and a 4g function. Every one of these three functions considered as a wave function for the relative oscillation of the two α-particles implies a certain correlation of the four 1p nucleons in the one-particle model. For a

† *Note added in proof:* For the calculated mean square radius of the α-particle in Be^8 we obtain the value 1.55×10^{-13} cm, in very good agreement with the experimental value [22]) 1.61×10^{-13} cm of the free α-particle radius. Nevertheless, this result should not be taken too seriously, because it is not valid for heavier α-particle nuclei. For these nuclei we have to take smaller a values to get their right binding energies and right experimental radii. This means that in these nuclei the α-particle clusters are less compact than the free α-particle. Therefore, the cluster model describes mainly the energetically favoured angular correlations of the nucleons in the nuclei. The radial part of the wave functions must essentially be guessed because of the failure of the assumed nuclear forces to produce saturation. A more detailed discussion of this topic will be presented in a forthcoming paper.

higher excitation of the relative oscillation, for instance the 6s oscillation †, it is necessary to lift a single 1p nucleon into the next but one shell in the one-particle model (see ref. [2, 4])). This is energetically very unfavoured and implies that these higher relative oscillations are energetically separated very clearly from the 4s, 4d and 4g oscillations.

In the same way all other excited states which originate from a superposition of one-particle states in the 1p shell (in the frame of the one-particle model) will be separated very clearly from the above 3 excitations of the relative oscillation of the two α-particles. Certainly in these other excited states no nucleon is lifted up into a higher shell, but an α-particle cluster is now broken up (this means internal excitation of an α-particle cluster). This is also energetically very unfavoured.

It can be seen directly that the 4s oscillation is energetically lower than the 4d oscillation and this oscillation in turn lower than the 4g oscillation. For the 4s oscillation the two α-particle clusters are on the average nearer to each other than for the 4d oscillation and for this in turn nearer to each other on the average than for the 4g oscillation. The potential interaction energy of the two α-particle clusters is more negative the nearer the two clusters are to each other on the average, since the nuclear forces are attractive if the mean distance between two nucleons is larger than the hard core of the nuclear forces (see also below). In all three states (for a given oscillator potential) the total kinetic energy of the nucleons is the same. Therefore, the ground state of Be^8 is that which corresponds to the 4s oscillation. It is identical with the α-particle model state given by Perring and Skyrme [2]).

The qualitative description of the position of the lowest energy levels of Be^8 is in complete agreement with experiment. The experimentally measured lowest energy levels are in fact successively s, d and g levels. The next higher levels are separated from the g level by a clear energy gap.

The d and g levels of Be^8 are very much smeared out because both levels are virtual. Also, as is well known, the ground state of Be^8 is unstable against decay into two α-particles.

3.2. QUANTITATIVE TREATMENT

We now come to the quantitative description. For this we have to specify the interaction between two nucleons. For the following calculations we assume two-body forces which describe the two-nucleon scattering data up to 50 MeV as well as possible and which are also such that the calculations do not become too complicated. We also neglect spin-orbit and

† It is easily seen that relative oscillations of odd orbital angular momentum vanish as a consequence of antisymmetrization if the α-particles are not internally excited. This is in accordance with the fact that the α-particles are bosons.

tensor forces. This is allowed to a good approximation, because in the excitations which we consider we have complete spin saturation of the clusters, which are completely spherically symmetrical, if we take into account only the α-particle states (no internal excitation of the α-particle clusters).

For the two-body forces we choose the following Serber potential, which satisfies the above conditions to a good approximation [8]):

$$V_{ik} = -V_0\, e^{-\left(\frac{r_{ik}}{\beta}\right)^2} \{w[1-\tfrac{1}{4}(1+\sigma_i \cdot \sigma_k)(1+\tau_i \cdot \tau_k)] + b[\tfrac{1}{2}(1+\sigma_i \cdot \sigma_k)-\tfrac{1}{2}(1+\tau_i \cdot \tau_k)]; \quad (5)$$

$$V_0 = 68.6 \text{ MeV}, \quad \beta = 1.55\times 10^{-13} \text{ cm}; \quad w = 0.41, \quad b = 0.09;$$

$$r_{ik} = |\mathbf{r}_i - \mathbf{r}_k|.$$

The potential (5) has no hard core and the proportion of exchange forces in it is too small to give saturation. However, it can be shown [9, 10, 7]) that with the potential (5) we can obtain the binding energies of nuclei within 10—20 % if we fix the radius of our model nucleus to agree with the experimentally measured nuclear radius (for instance the nuclear radii may be obtained from the Coulomb energy difference of mirror nuclei [6, 7])).

The agreement between the calculated and experimental values of the binding energies is to be considered as rather good, because the absolute value of the total kinetic and the total potential energies of the nucleons are respectively about a factor 2—3 and 3—4 larger than the corresponding binding energies.

This result leads to the supposition that the hard core of the nuclear forces is indeed required to prevent the collapse of nuclei, but that its direct contribution to the expectation value of the energy is rather small. Further we may conclude from these results and also from the proved validity of the shell-model, that the correlations of relatively long range, which are responsible for the nucleon clustering as already qualitatively discussed, can be separated rather unambiguously from the correlations of relatively short range. These last correlations arise from the hard core of the nuclear forces and are therefore connected with their saturating properties. Therefore, for the calculation of the wave functions and the excitation energies, we use the following procedure: We fix the width parameter a of the oscillator potential, as already mentioned, in such a way that the calculated nuclear radius is in agreement with the experimental radius †, or alternatively, what is more practical for our calculations, that the calculated binding energy of the nucleus in the ground state is in agreement with the experimental binding energy. We may then calculate the wave functions of the ground and excited states of a nucleus using the

† By fixing the radius we take into account the saturating properties of the nuclear forces in a rough way.

Ritz variational principle. For this the corresponding Hamiltonian is

$$H = \sum_{i=1}^{A} E_{\mathrm{kin}} + \tfrac{1}{2} \sum_{i,k} V_{ik}, \tag{6}$$

where the first term represents the kinetic energy of the nucleons and the second term the sum over the two-body interactions (5) between the nucleons.

For the variational procedure we superpose only those shell model wave functions which in the frame of the simple shell model are energetically relatively near to the ground state. If for this superposition we would use any highly excited shell model wave functions the variational principle would yield a state corresponding to a collapse of the nucleus. This is due, of course, to the non-saturating character of the interactions (5). This limitation of the shell model wave functions is a mathematical expression for the assumption that the correlations of relatively long range can be separated from the correlations of very short range.

We simplify the calculation of the energy levels of Be^8 by calculating at first only the expectation value of the energy for those wave functions which we assume to be essential for the description of the low lying states of Be^8. After this, we shall show that the expectation value of the energy for wave functions which correspond to a breaking up of an α-particle cluster or to excitations of higher oscillations (for instance the 6s oscillation) are energetically so much higher, that their contributions to the low energy levels are negligible in a first approximation.

If we calculate, for the 3 low lying α-particle states discussed qualitatively above, the expectation value of the energy

$$E = \int \Psi^* H \Psi \mathrm{d}\tau \tag{7}$$

where H is the Hamiltonian (6) and $\mathrm{d}\tau$ means integration and summation over all coordinates, we obtain

$$\frac{E_g - E_s}{E_d - E_s} = \frac{10}{3}. \tag{8}$$

This result is independent of the special form and exchange properties of the two-body forces. It is already contained in the calculations of Feenberg and Wigner [11, 12]), as can be seen very easily: this comes from the fact that we have pure LS-coupled states, all nucleons outside the closed shell being p-nucleons (Racah [21])†). We see that it is exactly what we should expect for three rotational states with the angular momenta $J = 0$, $J = 2$, $J = 4$, which is in rather good agreement with the experimental values.

† We are grateful to Dr. de Shalit for pointing this out to us.

It had already been tried long ago to explain these levels as rotational levels in the frame of the α-particle model. But in contrast to such an interpretation the ratio (8) results only from the change of the potential energy in the different states. The kinetic energy is, as already mentioned, the same in all three states.

Experimentally the g level lies a little higher than it ought to according to the ratio (8). This deviation partly comes from the fact that we have not taken into account spin-orbit coupling. If we carry out a variational calculation including spin-orbit coupling these three α-particle states will be slightly mixed with other states, corresponding to broken-up α-particle clusters. The ratio (8) then goes in the right direction [13]) †.

If we take $a = 4.7 \times 10^{25}$ cm^{-2}, we get very nearly the right binding energy for the ground state of Be^8. With this value of a we then obtain for the absolute values of the excitation energies of the α-particle states:

$$E_g - E_s = 12.5 \text{ MeV}, \qquad E_d - E_s = 3.75 \text{ MeV}. \tag{9}$$

Comparison with the experimental data shows that the theoretical values are larger by about 10—20 %.

The change of the energy differences (9) with a is relatively small. Thus, with $a = 3.6 \times 10^{25}$ cm^{-2} we obtain

$$E_g - E_s = 10.5 \text{ MeV}, \qquad E_d - E_s = 3.1 \text{ MeV}. \tag{10}$$

The calculated binding energy E_s of the ground state is then lowered from 56.3 MeV to 43.2 MeV. As examples for states in which the α-particle clusters are broken up, we have calculated the energies of the states ($J = 2$, $S = 1$, $T = 0$) and ($J = 2$, $S = 0$, $T = 1$). In doing this we have superposed only states for which (in the frame of the one-particle model) there is no excitation into higher levels. We get 20.7 MeV and 23 MeV. These energies, as already expected, are much higher than the excitation energies of the α-particle states previously considered ††. This is also true if for instance a 6s oscillation of the α-particles is excited, because this corresponds, as already mentioned, to a 1p nucleon being lifted up into the next but one level.

For explicit calculation it is most useful to represent the nuclear states in the one-particle model, because there the antisymmetrization and the normalization of the wave functions is particularly simple. We do not want to describe the calculations in more detail here because similar calculations

† We thank Prof. Inglis for pointing this out to us.

†† This is the reason, for instance, why the ($J = 2$, $S = 1$, $T = 0$) state, which can be mixed with the ($J = 2$, $S = 0$, $T = 0$) state, if a spin-orbit coupling is present, is practically absent from the energetically lowest state ($J = 2$, $T = 0$), unless the spin-orbit coupling is extremely large.

have already been given in the papers of Feenberg and Wigner [11]), Inglis [14, 15]) and Kurath [13]).

We would like to mention a point which is readily understandable in the frame of the "cluster model". The calculations of Inglis [14, 15]) and Kurath [13]) show that the energies of the higher excited levels of Be^8 and of the levels of Be^7, Li^7 and Be^9 change relatively rapidly with increase of the spin-orbit coupling, but in contrast the energies of α-particle levels do not. This comes from the fact that for the α-particle levels, the α-particle-clusters have to be broken up in order that the spin-orbit coupling can be effective. For the other levels, this is not the case and therefore the spin-orbit coupling is much more effective for these levels.

4. Other Light Nuclei

We now want to sketch out † for some nuclei the way in which it is possible to find the component states which are most important for the low lying levels. This method is related to the supermultiplet theory of Wigner [12]) and to the method of fractional parentage [18]).

For Be^9 and B^9 it is useful to choose a representation corresponding to two α-particle clusters and one extra nucleon. The ground states of Be^9 and B^9 are composed, then, mainly of the ground and the first excited state of Be^8, coupled together with a neutron or a proton, since for both states we can build up a resulting state with $J = 3/2$. With the help of the variational principle we can then calculate the relative proportion of the two states in the ground states of Be^9 and B^9. The interesting question can then be investigated of why the ground state of Be^9 is a bound state, whereas He^5 as well as Be^8 have ground states which are not bound.

Taking the low lying levels of C^{12} and O^{16} as another example we first consider a representation by 3 and 4 α-particles, respectively. It is very probable that also for these nuclei we can find ratios of different excitation energies which are independent of the particular characteristics of the two-body forces, as long as we neglect any mixing of states for which the α-particle structures are broken up.

For the low lying levels of Ne^{20}, we have two reasonable possibilities: we may consider either a representation by an O^{16} and an α-particle, or a five α-particle representation †. Since O^{16} is a cluster which is less tightly bound than an α-particle cluster, we expect that the first representation will not give such good results as the five α-particle representation, if we neglect internal cluster excitations. On the other hand the calculations are simpler in the former representation than in the five α-particle one.

† A more detailed discussion of these topics will be given in a forthcoming paper.

5. Giant Resonance in O^{16}

If we want to calculate the dipole excitations corresponding to the "giant" resonances it is not useful to start from an α-particle representation, because for the appropriate excitation energies some α-particle clusters will be broken up. Brink [5]) has shown that the Goldhaber-Teller model of the "giant" resonances is equivalent to a one-particle dipole excitation, as long as the oscillator potential is a good approximation for the average one-nucleon potential. For the proof of this equivalence in the case of O^{16} he has chosen a representation in which the 8 protons and the 8 neutrons are separately clustered together. With the help of the dipole wave function of Brink we have calculated, after the introduction of the spin and isobaric spin coordinates and after complete antisymmetrization, the expectation value of this dipole excitation. For the two-body forces we have again used the interaction (5). The width parameter has again been fixed in such a way as to obtain the right binding energy for the ground state of O^{16}. For the expectation value of the dipole excitation energy we then obtain †

$$E_{\mathrm{dip}} = 26.5 \text{ MeV}. \tag{11}$$

The excitation energy is in approximate agreement with the presumed experimental value [16]) of 22.5 MeV. It can further be seen that this excitation energy is of the order of magnitude which is required for the breaking up of an α-particle cluster in Be^8. Further we can see quite clearly from this example that the correlations between the nucleons can create a very large energy difference in the excitation energies. The "giant" resonance which we have considered here is a one-particle excitation created by lifting up a p nucleon into the next higher shell. It is defined by the following values of the total angular momentum, spin and isobaric spin: $J = 1$, $S = 0$, $T = 1$. We can get another one-particle excitation into the same shell, if we take $J = 1$, $S = 0$, $T = 0$. This corresponds to an excitation of the centre of mass oscillation having an energy of 6.1 MeV (no change in the potential energy, which is the same as for the ground state). We see that corresponding to these two different correlations in the same shells between the nucleons in O^{16} there is an energy gap of about 20 MeV.

6. Heavy Nuclei

If we go to heavier nuclei the mathematical description becomes more complicated, because the oscillator potential is then no longer a good approximation for the average one-nucleon potential. The physical facts,

† For the calculation of this excitation energy the integral tables of von Siemens [17]) were of great help to us.

however, are not changed. For instance, it is to be expected, in accordance with our previous considerations, that in very heavy nuclei the stable closed neutron shells $N = 50$ and $N = 82$ are present as clusters with a rather large probability. This makes asymmetric fission more readily understandable, at least qualitatively, since it will be easier to excite relative oscillations of these two clusters against each other than to break up one of these clusters.

We now want to discuss very briefly the question why, in the same nuclear state, different cluster structures may be present, depending upon the point of view from which we consider this state. For a heavy nucleus, it may be seen that every possible cluster structure which can be formed corresponds to a certain correlation between nucleons near the surface of the "Fermi sea". This is a consequence of the exclusion principle; for, if the nucleons were considered as distinguishable, the cluster structures would correspond to correlations which involve nucleons deep in the Fermi sea. The mathematical expression for this is that it is possible to form a large number of many-particle wave functions which are different from each other as long as they describe distinguishable particles, but which become identical to each other on antisymmetrization (see also ref. [2])). This is, for instance, the reason why a collective dipole oscillation can be exactly equivalent to a one-particle excitation [5]). Another simple example is a Fermi sea which is moving with a uniform velocity, as for instance the superconducting current in a superconductor. In the momentum space such a collective motion is described simply by a displacement of the Fermi sphere. It is clear that this collective motion may be obtained from the state of rest by changing the sign of the momentum vectors of the few particles on the surface of the hemisphere which is backwards with respect to the direction of the motion. In the interior of the Fermi sea all momentum changes of the indistinguishable particles cancel each other.

7. Concluding Remarks

Our considerations have shown that the nuclear interactions may give rise to energetically favoured correlation between the nucleons. We call such correlations cluster structures. For the investigation of these cluster structures, it is convenient to introduce eigenfunction systems specially adapted to them. It is then possible, with the aid of energetical considerations, to figure out which wave functions are especially important for a particular nuclear state and which wave functions may be neglected to a good approximation. The explicit calculations are usually best carried out in the eigenfunction system of the one-particle model, as in this system the normalization and the orthogonality relations are particularly simple.

For the existence of these cluster structures it is not important, to a first approximation, that the nuclear forces be exactly known; it is only important to know that the clusters are especially favoured energetically †. It is therefore possible to describe the kinematic behaviour of nuclei much better, in general, than the excitation energies of the levels. Even the usual shell model is an example of this. It is therefore of special interest to find properties of nuclei which depend only on this kinematic behaviour, such as, for instance, the ratios of certain excitation energies, which are independent, to a first approximation, of the refined characteristics of the two-body interactions. An example of this is given by the low lying levels of Be^8. Other examples are the energy ratios of the rotational levels of heavy nuclei pointed out by Bohr and Mottelson, and the γ-transition probabilities.

The method described here is, in a certain sense, a realization of Wheeler's conception of resonating group structure [19]).

Our considerations are similar to those of Skyrme and Perring [2]), but in contrast to the latter, they are kept within the framework of the usual shell model calculations with interactions.

We thank Dr. Bodmer, Prof. Inglis, Dr. de Shalit, Prof. Toyoda and Prof. Weisskopf for many helpful discussions. We also thank Dr. Bodmer for his very kind help in correcting our English. Finally, we wish to thank Prof. Rosenfeld for his active interest in our work.

† Another point of great importance is that the nuclear forces are of short range, because only then is it understandable that the structures of lighter nuclei may be contained in heavy nuclei.

References

1) D. M. Dennison, Phys. Rev. **96** (1954) 378;
S. L. Kameny, Phys. Rev. **103** (1956) 358;
A. Herzenberg and A. S. Roberts, Nuclear Physics **3** (1957) 314; and earlier papers
T. Toyoda, private communication
2) J. K. Perring and T. H. Skyrme, Proc. Phys. Soc. **69** (1956) 600
3) Heisenberg, Macke, Theorie des Atomkerns (Göttingen, 1951)
4) J. P. Elliot and T. H. R. Skyrme, Proc. Roy. Soc. A **232** (1955) 561
5) D. M. Brink, Nuclear Physics **4** (1957) 215
6) B. C. Carlson and I. Talmi, Phys. Rev. **96** (1954) 436
7) H. von Siemens, Dissertation (München, 1957)
8) Lederer, Diplomarbeit (München, 1956)
9) Florian, Urban und Wildermuth, Zeitschr. f. Naturf. **9A** (1954) 748
10) Wild und Wildermuth, Zeitschr. f. Naturf. **9A**, (1954) 799
11) Feenberg and Wigner, Phys. Rev. **51** (1937) 95
12) E. P. Wigner, Phys. Rev. **51** (1937) 106 and 947
13) D. Kurath, Phys. Rev. **101** (1956) 216
14) D. R. Inglis, Phys. Rev. **51** (1937) 531
15) D. R. Inglis, Revs. Mod. Phys. **25** (1953) 390
16) F. Ajzenberg and T. Lauritsen, Revs. Mod. Phys. **27** (1955) 77

17) Integral tables von Siemens, unpublished
18) S. Goudsmit and R. F. Bacher, Phys. Rev. **46** (1934) 948;
G. Racah, Phys. Rev. **63** (1943) 367;
G. Racah, Phys. Rev. **76** (1949) 1352
19) J. A. Wheeler, Phys. Rev. **52** (1937) 1083 and 1107;
D. L. Hill and J. A. Wheeler, Phys. Rev. **89** (1953) 1106;
J. J. Griffin and J. A. Wheeler, Phys. Rev. **108** (1957) 311;
J. J. Griffin, Phys. Rev. **108** (1957) 328
20) A. F. Tsander, Doklady Akademi Nauk SSSR. **90** (1953) 761
21) G. Racah, L. Farkas Memorial Volume (1952)
22) R. Hofstadter, Revs. Mod. Phys. **28** (1956) 214

7.A *Nuclear Physics* 7 (1958) 163—168; © *North-Holland Publishing Co., Amsterdam*
Not to be reproduced by photoprint or microfilm without written permission from the publisher

THE CAUSAL FUNCTION AND THE CAUSALITY CONDITION

S. T. MA

The F.B.S. Falkiner Nuclear Research and Adolph Basser Computing Laboratories, School of Physics, University of Sydney †

Received 14 February 1958

Abstract: This article is concerned with the connection between the Stueckelberg-Feynman causal function and the causality condition, i.e. the condition that no disturbance in a wave field can travel faster than light. It contains an analysis of the S-matrix for the scattering of electrons by electrons, and the scattering of nucleons by nucleons, which both involve the causal propagation function for the exchanged bosons. By means of certain mathematical relations for the causal function, the S-matrix is partitioned in such a way that each term by itself fulfils the causality condition for all distances, large or small. The mathematical treatment is applicable to the scattering of any number of fermions with the exchange of any number of bosons. A physical interpretation, according to which the partitioned S-matrix describes the various modes of the propagation of retarded action at a distance, is suggested.

1. Introduction

It was shown by Feynman, Dyson, Stueckelberg and Rivier [1, 2, 3, 4]) that the scattering matrix in local quantum field theory may be expressed in a simple way in terms of a propagation function of a special type. Discussions from the viewpoint of causality [3, 4, 5]) led to the name "causal function" and the notation Δ_c, which we adopt in the present article.

This article is concerned with the connection between the causal function and a condition which follows from causality in conjunction with relativistic invariance, namely the condition that no disturbance in a wave field can travel faster than light. This condition, to be referred to as the "causality condition", plays an important role in the discussion of the measurement of observable quantities in quantum field theory [6]) and in the derivation of the dispersion relations [7, 8]). The causality condition is fulfilled by the propagation function for the retarded potential, Δ_R, which vanishes (i) for negative values of the time variable and (ii) outside the light cone. The second property is shared by the propagation function for the advanced potential, Δ_A, and the function Δ which appears in the commutation and anticommutation relations. Neither property is shared by Δ_c, however, as was pointed out in ref. [4]). It therefore appears at first sight as if the causal function might describe events which violate the causality condition.

† Also supported by the Nuclear Research Foundation within the University of Sydney.

In order to clarify the situation, Fierz [9, 10]) analysed the S-matrix for the Møller scattering of electrons which involves the causal function D_c, the special case of Δ_c for the photons. Fierz reached the conclusion that the apparent discrepancy may be removed when the complementary of energy and time is taken into account and attention is confined to the wave zone. A similar analysis due to Stueckelberg was presented in Thirring's book [11]).

In this article we make use of some mathematical relations for the causal function which are suggested by mathematical analyses in ref. [9, 10, 11]). It will be shown that the S-matrix may be partitioned, by means of these relations, in such a way that each individual term contains only the boson propagator Δ_R but no longer Δ_c, and so fulfils the causality condition for all distances, large or small. Our mathematical treatment is applicable both to the scattering of electrons by electrons due to exchange of photons, and to the scattering of nucleons by nucleons due to exchange of pions according to the weak-coupling theory, irrespective of the number of scattered fermions or the number of exchanged bosons.

The possibility of expressing the S-matrix in terms of the boson propagation function Δ_R is not unexpected. In fact, Møller's scattering formula was originally derived from a semi-classical treatment of the retarded interaction of electrons [6]). Furthermore, the formalism which has been developed for the Heisenberg picture of quantum field theory [12, 13]) involves only the propagation functions Δ_R, Δ_A but not Δ_c.

It will also be shown that our mathematical manipulation admits of a plausible physical interpretation in terms of retarded action at a distance, which is a concept of long standing [14]). The relation between causal interaction and retarted action has previously been discussed in ref. [1]), but there is no discussion of the causality condition in that paper.

We shall derive in section 2 the needed mathematical relations for the causal function, and then proceed to a discussion of the S-matrix in section 3.

2. Mathematical Relations for the Causal Function

Let us first state a few known formulas for the sake of reference. Let the scalar product of the four-vectors $x = (\mathbf{x}, x_0)$, $p = (\mathbf{p}, p_0)$ be defined by

$$p \cdot x = \mathbf{p} \cdot \mathbf{x} - p_0 x_0. \tag{1}$$

Let

$$\mathrm{d}^4 p = \mathrm{d}^3 p \, \mathrm{d}p_0. \tag{2}$$

The Δ functions that concern us may be defined as follows [7]):

$$\Delta_R(x) = (2\pi)^{-4} \lim_{\lambda_0 \to +0} \int \exp(ip \cdot x)[(p+i\lambda)^2 + m^2]^{-1} \mathrm{d}^4 p \qquad (\lambda = 0), \tag{3}$$

$$\Delta_A(x) = \Delta_R(-x), \tag{4}$$

$$\Delta(x) = \Delta_R(x) - \Delta_A(x), \tag{5}$$

$$\Delta_c(x) = (2\pi)^{-4} \lim_{\varepsilon \to +0} \int \exp(ip \cdot x)(p^2+m^2-i\varepsilon)^{-1} d^4p. \tag{6}$$

The propagation functions $\Delta_R, \Delta_A, \Delta_c$ all satisfy the inhomogeneous equation

$$(\Box - m^2)\Delta_i(x) + \delta(x) = 0, \tag{7}$$

where $\delta(x)$ denotes the four-dimensional delta function

$$\delta(x) = \delta(\mathbf{x})\delta(x_0). \tag{8}$$

Any function $F(x)$ having a Fourier transform may be separated into two parts such that

$$F(x) = F_+(x) + F_-(x), \tag{9}$$

where $F_\pm(x)$ are functions whose Fourier transforms are the same as that of $F(x)$ for $p_0 \gtrless 0$ but vanish for $p_0 \lesseqgtr 0$. They will be referred to as the positive and negative frequency parts of $F(x)$. According to this definition, the four-dimensional delta function $\delta(x)$ has the positive and negative frequency parts

$$\delta_\pm(x) = \delta(\mathbf{x})\delta_\pm(x_0), \tag{10}$$

with

$$\delta_\pm(x_0) = (\tfrac{1}{2})[\delta(x_0) \pm \mathrm{P}/\pi i x_0]. \tag{11}$$

It follows from eqs. (3)–(6) that

$$\Delta_{c+}(x) = \Delta_{R+}(x), \qquad \Delta_{c-}(x) = \Delta_{A-}(x), \tag{12}$$

$$\Delta_c(x) = \begin{cases} \Delta_+(x) \\ -\Delta_-(x) \end{cases} \qquad (x_0 \gtrless 0). \tag{13}$$

Eq. (12) expresses the decomposition of Δ_c according to the sign of the frequency, and eq. (13) the decomposition according to the sign of the time. The former plays a major part in the following considerations. In the case of $m = 0$, explicit expressions may be easily written down. In particular,

$$\begin{aligned} \mathrm{D}_{R\pm}(x) &= (4\pi r)^{-1}\delta_\pm(x_0 - r) \\ \mathrm{D}_{A\pm}(x) &= (4\pi r)^{-1}\delta_\pm(x_0 + r) \end{aligned} \qquad (r = |\mathbf{x}|). \tag{14}$$

Consider, for a given $s(x)$, the function $\phi_i(x)$ defined by

$$\phi_i(x) = \int \Delta_i(x - x')s(x')d^4x', \tag{15}$$

which is, on account of eq. (7), a solution of the equation

$$(\Box - m^2)\phi_i(x) + s(x) = 0. \tag{16}$$

In the case of Δ_R and Δ_A, the value of $\phi_i(x)$ depends only on the values of $s(x')$ at points x' inside the light cone of x. As mentioned in the introduction, this condition is not satisfied in the case of Δ_c. The situation is different, however, if the positive and negative frequency parts are considered separately. An application of the convolution theorem in the theory

of Fourier transforms [15]) leads to the following orthogonality relations:

$$\int \Delta_{i\pm}(x-x')s_{\mp}(x')\mathrm{d}^4x' = 0, \tag{17}$$

$$\int s_{\pm}(x)\Delta_{i\pm}(x-x')\mathrm{d}^4x = 0. \tag{18}$$

Using eq. (12) and then eq. (17) twice, we obtain

$$\int \Delta_c(x-x')s(x')\mathrm{d}^4x' = \int \Delta_R(x-x')s_+(x')\mathrm{d}^4x' + \int \Delta_A(x-x')s_-(x')\mathrm{d}^4x'. \tag{19}$$

The two integrals on the right-hand side, which are the positive and negative frequency parts of the integral on the left-hand side, involve only Δ_R and Δ_A but no longer Δ_c. The same is true of the relation

$$\int s(x)\Delta_c(x-x')\mathrm{d}^4x = \int s_-(x)\Delta_R(x-x')\mathrm{d}^4x + \int s_+(x)\Delta_A(x-x')\mathrm{d}^4x. \tag{20}$$

It was shown by the writer [16]) that the integral $\int \Delta_c(x-x')s(x')\mathrm{d}^4x'$ represents asymptotically at large distances outward moving waves of positive frequencies together with inward moving waves of negative frequencies. This statement may be derived from eq. (19), which holds exactly for all distances.

The orthogonality relations expressed by eqs. (17), (18) may be directly verified when $m = 0$ and $s(x) = \delta(x)$. In that special case, by eqs. (10), (14), they reduce to

$$\int_{-\infty}^{\infty} \delta_{\pm}(\rho-\tau)\delta_{\mp}(\tau-\sigma)\mathrm{d}\tau = 0. \tag{21}$$

By eq. (11), the validity of eq. (21) depends on the validity of the equation

$$\mathrm{P}\int_{-\infty}^{\infty} \frac{\mathrm{d}\tau}{(\rho-\tau)(\tau-\sigma)} + \pi^2\delta(\rho-\sigma) = 0, \tag{22}$$

which is the fundamental relation for the Hilbert transforms.

3. Partition of the Scattering Matrix

From now on we shall use the following abbreviated notation:

$$\mathrm{dV} = \mathrm{d}^4x, \tag{23}$$

$$\Delta_c(1, 2) = \Delta_c(x_2-x_1). \tag{24}$$

Consider first the Møller scattering, i.e. the scattering of two fermions with the exchange of one boson. Let ψ and $\bar{\psi}$ denote the quantized Dirac wave functions for the fermions, and γ a Dirac matrix whose form depends on the coupling of the fermions with the bosons. Let

$$s(1, 2) = \bar{\psi}(2)\gamma\psi(2)\bar{\psi}(1)\gamma\psi(1). \tag{25}$$

The dependence of the S-matrix on the space and time variables is contained in the factor

$$I_1 = \int \Delta_c(1, 2)s(1, 2)\mathrm{dV}_1\,\mathrm{dV}_2, \tag{26}$$

where the subscript 1 indicates that one boson is exchanged.

The scattering of two fermions involving the exchange of two bosons is represented by two Feynman diagrams which consist of two disconnected fermion lines and two internal boson lines, namely the ladder diagram and the diagram with crossing boson lines. In each case the S-matrix contains an integral of the form

$$I_2 = \int \Delta_c(1, 2)\Delta_c(3, 4)s(1, 2, 3, 4)\mathrm{dV}_1 \ldots \mathrm{dV}_4. \tag{27}$$

The fermion distribution function $s(1, 2, 3, 4)$ involves not only the Dirac wave functions ψ, $\bar{\psi}$ but also the causal propagators for the fermions in the intermediate states.

A general expression which is applicable to the scattering of any number of fermions with the exchange of any number of bosons is

$$I_n = \int \Delta_c(1, 2) \ldots \Delta_c(2n-1,\ 2n)s(1, \ldots, 2n)\mathrm{dV}_1 \ldots \mathrm{dV}_{2n}. \tag{28}$$

It is well known that the distinction between Δ_c and Δ_R is immaterial for the integral I_1 in the case of free fermions. We shall now show generally that the mathematical relations of section 2 enable us to express the integrals $I_1, I_2, \ldots$ in terms of Δ_R instead of Δ_c, without using any special property of the distribution functions s. Note that, just as the function $s(x)$ in section 2 is separable into two parts s_+ and s_-, so the function $s(1, 2)$ is separable into four parts s_{++}, s_{+-}, s_{-+}, s_{--}, and the function $s(1, \ldots, 2n)$ is separable into 2^{2n} parts. Similarly to eqs. (19) and (20), we obtain

$$I_1 = \int [\Delta_R(1, 2)s_{+-}(1, 2)+\Delta_A(1, 2)s_{-+}(1, 2)]\mathrm{dV}_1\,\mathrm{dV}_2. \tag{29}$$

This becomes, on using eq. (4),

$$I_1 = \int [\Delta_R(1, 2)s_{+-}(1, 2)+\Delta_R(2, 1)s_{-+}(1, 2)]\mathrm{dV}_1\,\mathrm{dV}_2. \tag{30}$$

Similarly,

$$\begin{aligned} I_2 = \int [&\Delta_R(1, 2)\Delta_R(3, 4)s_{+-+-}(1, 2, 3, 4) \\ &+\Delta_R(1, 2)\Delta_R(4, 3)s_{+--+}(1, 2, 3, 4) \\ &+\Delta_R(2, 1)\Delta_R(3, 4)s_{-++-}(1, 2, 3, 4) \\ &+\Delta_R(2, 1)\Delta_R(4, 3)s_{-+-+}(1, 2, 3, 4)]\ \mathrm{dV}_1 \ldots \mathrm{dV}_4, \end{aligned} \tag{31}$$

$$I_n = \int [\Delta_R(1, 2) \ldots \Delta_R(2n-1, 2n)s_{+-\ldots+-}(1, \ldots, 2n)+\ldots]\mathrm{dV}_1 \ldots \mathrm{dV}_{2n}. \tag{32}$$

It seems plausible to the writer that eqs. (30)—(32) may be interpreted as a description of the propagation of retarded action at a distance. For example, the first term on the right-hand side of eq. (30) describes the

propagation of retarded action from 1 to 2, and the first term on the right-hand side of eq. (31) describes the propagation of retarded action from 1 to 2 and from 3 to 4. A general feature of the various terms in these equations is that each retarded action originates from a point which is associated with a plus sign, and is received at a point which is associated with a minus sign. Borrowing a terminology of hydrodynamics, we shall refer to the points associated with the plus and minus signs as the sources and sinks respectively. The situation may then be summarized by saying that the S-matrix in its partitioned form describes the various modes of the propagation of retarded action from the sources to the sinks.

The significance of the sources and sinks is particularly clear in the case of the distribution function expressed by eq. (25). Consider a particular transition in which the fermion at point 1 is scattered from a state a to a state a′ and the fermion at point 2 from a state b to a state b′. Conservation of energy requires

$$E_a - E_{a'} = -(E_b - E_{b'}). \tag{33}$$

The two source-sink distributions s_{+-} and s_{-+} are responsible for the transitions in which $E_a - E_{a'} \gtrless 0$ respectively. Hence a retarded action carries with it a positive amount of energy from a source to a sink.

Note added in proof: Our treatment of the scattering processes whose diagrams contain two or more internal boson lines may be simplified by focusing attention on one of the lines at a time. Using 1 and 2 to denote the two points joined by the particular boson line under consideration, we can express all the integrals $I_2, I_3, \ldots$ in the form of I_1 by taking $s(1, 2)$ to be an integral over the other points. Thus eq. (30) alone is sufficient for dealing with all the internal boson lines, each of which is associated with its own pair of source-sink distributions.

References

1) R. P. Feynman, Phys. Rev. **76** (1949) 769
2) F. J. Dyson, Phys. Rev. **75** (1949) 486
3) D. Rivier, Helv. Phys. Acta **22** (1949) 265
4) E. C. G. Stueckelberg and D. Rivier, Helv. Phys. Acta **23** (1950) 215
5) H. Umezawa, Quantum Field Theory (North-Holland, 1956)
6) W. Heitler, Quantum Theory of Radiation (Oxford, 1954)
7) J. M. Jauch and F. Rohrlich, Theory of Photons and Electrons (Addison-Wesley, 1955)
8) M. Gell-Mann, M. L. Goldberger and W. Thirring, Phys. Rev. **95** (1954) 1612
9) M. Fierz, Helv. Phys. Acta **23** (1950) 731
10) W. Pauli, Lectures on "Feldquantisierung" (Zürich, 1950/1)
11) W. Thirring, Einführung in die Quantenelektrodynamik (Franz Deuticke, 1955)
12) C. N. Yang and D. Feldman, Phys. Rev. **79** (1950) 972
13) G. Källén, Arkiv for fysik **2** (1950) no. 19, no. 37
14) J A. Wheeler and R. P. Feynman, Revs. Mod. Phys. **17** (1945) 157
15) I. N. Sneddon, Fourier Transforms (McGraw-Hill, 1951)
16) S. T. Ma, Phys. Rev. **68** (1945) 166

8.B *Nuclear Physics* 7 (1958) 169—183; © *North-Holland Publishing Co., Amsterdam*
Not to be reproduced by photoprint or microfilm without written permission from the publisher

THE HYPERON DECAYS AND THE STRUCTURE OF INTERACTIONS

HIROOMI UMEZAWA, MICHIJI KONUMA and KIMIKO NAKAGAWA
Department of Physics, University of Tokyo

Received 13 February 1958

Abstract: Experiments have shown that, in cases of the weak fermion interactions and π-decay interaction, the coupling constant for the parity conserving term and that for the parity non-conserving term are almost equal to each other. Assuming that this is the situation in every case of the weak interactions, we show that the Λ-decay interaction is of the derivative (vector and axial vector) coupling type. This belongs to the 2nd kind interactions, as do the weak fermion interactions.

We discuss various features which stem from the basic assumption that all the weak interactions violating the parity conservation belong to the 2nd kind. A result coming from this basic assumption is the universality of the coupling constants for the weak interactions. The two-neutrino decay of K is forbidden as it should be. The situation for the processes π, $K \to e+\nu$ and $e+\nu+\gamma$ is much better than in the case of the weak interactions of the 1st kind.

A dimensional analysis is used to obtain information on the strength of interactions in each energy region. It suggests that the weak interactions belonging to the 2nd kind predominate over all the other interactions in the high energy region corresponding to a scale smaller than 10^{-20} cm. The violation of the parity conservation may be due to some feature of space for such small distances. It is suggested that multiple production of leptons may occur at extremely high energies. The high energy behaviour of the strong interactions like the π-nucleon coupling is briefly discussed; the nucleon Compton wavelength may characterize a region where the strong interactions behave in a way different from ordinary notions. In this sense, we may meet various strata of nature in high energy regions.

1. Interactions for the Hyperon Decay

1.1. GENERAL CONSIDERATIONS

It is now common to classify known interactions into three classes according to their strength. They are called the strong, electromagnetic and weak interactions. The first consists of interactions having coupling constants of about the same magnitude as the π-nucleon coupling constant. This class also includes the hyperon-nucleon interactions whose coupling constants seem to be slightly smaller than the π-nucleon coupling constant. The third class is sometimes divided into two groups: weak interactions between bosons and fermions and those between fermions, like the beta interactions. It has long been noticed that the stronger the interactions, the more laws of invariance are established for them.

It is now well established [1]) that the parity is not conserved in the processes due to the weak fermion interactions. This is also true for some of the weak boson-fermion interactions, viz. the interactions for the $\pi-\mu$ decay [1]) and Λ-decay processes [2]). The latter decay process is especially important, because it seems to have nothing to do with the neutrino. The non-conservation of the parity is not a peculiarity of the neutrino interactions, but rather one of the weak interactions.

As for the weak interactions concerning neutrinos, experiments have shown that *the coupling constant for the parity conserving term is of a magnitude almost equal to that belonging to the parity non-conserving term. Assuming that this is the situation in every case of the weak interactions violating the parity conservation* (*one-to-one law*), we shall show that experiments exclude the non-derivative (scalar and pseudoscalar) type for the Λ-decay interaction. A reason for assuming the "one-to-one law" will be discussed in section 3.

Let us consider the following types for a weak boson-fermion interaction:

$$H_1 = g_1 \bar{\psi}(a_1+b_1\gamma_5)\psi' \varphi + \text{h.c.} \tag{1}$$

or

$$H_2 = ig_2 \bar{\psi}(a_2+b_2\gamma_5)\gamma_\mu \psi' \partial_\mu \varphi + \text{h.c.} \tag{2}$$

Here, the spins of the fermions ψ, ψ' and that of the boson φ are assumed to be $\frac{1}{2}$ and 0 respectively. The constants a_1, a_2, b_1 and b_2 are, in general, complex numbers. The "one-to-one law" implies that

$$|a_i|^2 = |b_i|^2 = 1, \qquad i = 1, 2.$$

The coupling constants $g_i a_i$ and $g_i b_i$ stand in the following relations:

$$g_1 a_1 = (m'-m) g_2 a_2, \tag{3}$$

$$g_1 b_1 = (m'+m) g_2 b_2, \tag{4}$$

as far as the lowest order term of the perturbation series is concerned. The relations (3) and (4) result from the equivalence theorem. The quantities m and m' are the masses of the fermions ψ and ψ'.

To decide the type of the interaction, we take advantage of the interference effect between the parity conserving and non-conserving terms. It is well known [3]) that this interference effect must appear in the angular distribution of the pion produced in the polarized hyperon decay. The angular distribution has the form

$$1+P\alpha \cos\theta.$$

Here, θ is the angle between the pion momentum and the polarization axis. The quantity P is the magnitude of the polarization, i.e. the expectation value of the spin matrix of the hyperon in the direction of the polarization

axis. The interference effect leads to a finite anisotropy coefficient †

$$\alpha = \frac{\mathrm{Re}\,(a_1^* b_1)\{m_Y^2-(m_N-m_\pi)^2\}^{\frac{1}{2}}\{m_Y^2-(m_N+m_\pi)^2\}^{\frac{1}{2}}}{m_Y^2+m_N^2-m_\pi^2} \tag{5}$$

$$\alpha = \frac{\mathrm{Re}\,(a_2^* b_2)(m_Y^2-m_N^2)\{m_Y^2-(m_N-m_\pi)^2\}^{\frac{1}{2}}\{m_Y^2-(m_N+m_\pi)^2\}^{\frac{1}{2}}}{(m_Y^2-m_N^2)^2-m_\pi^2(m_Y^2+m_N^2)} \tag{6}$$

for the types (1) and (2) respectively. Here m_Y, m_N and m_π are the masses of the hyperon, nucleon and pion, respectively. The anisotropy coefficient α becomes maximum when $a_i = b_i$. This is the case when the interaction is invariant under time reversal. The coefficient α is zero when $a_i^* b_i$ is imaginary. For example, α is zero when the interaction is invariant under charge conjugation. The numerical results for the maximum values of α are listed in the table 1.

TABLE 1

Up-down asymmetry for hyperon decays

Processes	Maximum Anisotropy Coefficients	
	α_{max} for type (1)	α_{max} for type (2)
$\Lambda \to p+\pi^-$	0.10	0.91
$\Sigma^- \to n+\pi^-$	0.20	0.99
$\Sigma^+ \to p+\pi^0$	0.20	1.00
$\Sigma^+ \to n+\pi^+$	0.20	1.00
$\Xi^- \to \Lambda+\pi^-$	0.13	0.97

1.2. THE Λ AND Σ DECAYS

Experiments have been done on the following two processes:

$$\pi^-+p \to \Lambda+\theta^0, \quad \Lambda \to p+\pi^-, \tag{7}$$

$$\pi^-+p \to \Sigma^-+K^+, \quad \Sigma^- \to n+\pi^-. \tag{8}$$

The polarization in the direction normal to the production plane is a function of the production angle. It has been shown by recent experiments [2]) that $|\alpha| \geqq 0.67 \pm 0.13$ for the process $\Lambda \to p+\pi^-$. This, according to table 1, excludes the interaction (1) for the Λ-decay process; *this decay process is caused by a derivative-type interaction.*

Taking account of the final state interaction between the pion and the nucleon does not change our conclusion. Briefly, the final state interaction affects the anisotropy coefficient α by way of changing a_i into $a_i \exp(i\delta_1)$ or $a_i \exp(i\delta_3)$ and b_i into $b_i \exp(i\delta_{11})$ or $b_i \exp(i\delta_{31})$, if δ_1, δ_3, δ_{11} and δ_{31} denote the well-known phase shifts for the π-nucleon scattering. Thus, the

† The asymmetry coefficient α for the Λ-decay due to the Hamiltonians (1) and (2) without the assumption $|a_i|^2 = |b_i|^2$ is shown in the appendix for purposes of reference.

coefficient α cannot exceed the values listed in table 1, even if the final state interaction is taken into account.

It should be noted that in the case of interactions invariant under charge conjugation the coefficient α may be different from zero because of the effect of the final state interaction. However, experiments on the Λ-decay have shown that α is large enough to exclude interactions invariant under charge conjugation [4]).

Not much asymmetry has been observed in the angular distribution of the Σ-decay † ($\Sigma^- \to \pi^- + \mathrm{n}$). The reason for this may be that the polarization of Σ produced in the process $\pi + \mathrm{p} \to \Sigma + \mathrm{K}$ is not large enough to give us an observable asymmetry. Another possibility is that the relative phase between a_i and b_i is not small.

1.3. THE Ξ-DECAY PROCESSES

Let us now turn our attention to the Ξ-decay process [5]) ††:

$$\left.\begin{aligned} &\mathrm{K}^- + \mathrm{p} \to \Xi^- + \mathrm{K}^+, \\ \text{or} \qquad &\\ &\pi^- + \mathrm{p} \to \Xi^- + \mathrm{K}^+ + \mathrm{K}^0, \end{aligned}\right\} \Xi^- \to \Lambda + \pi^- \qquad (9)$$

$$\Xi^- \to \Lambda + \pi^-, \quad \Lambda \to \mathrm{p} + \pi^-. \qquad (10)$$

The asymmetry coefficient α for the process (9) is also listed in table 1. For this case, it is not easy to estimate the magnitude of the polarization of Ξ, because Ξ is produced by a strong interaction. The situation is different in the case of the cascade decay process (10). Indeed, if conservation of parity were violated for Ξ-decay, the decay product Λ should be polarized in the direction of the momentum of Λ. The degree P of the polarization of Λ is just equal to the asymmetry coefficient α, i.e. (5) or (6) for the Ξ-decay. Accordingly, the distribution of the pions due to the subsequent Λ-decay should show a forward-backward asymmetry. Theoretical results for the two coupling types are given in table 2. One could get support for the derivative coupling type of the weak boson-fermion interactions $\Xi^- \to \Lambda + \pi^-$ and $\Lambda \to \mathrm{p} + \pi^-$, if the Λ-decay following the Ξ decay would show a large forward-backward asymmetry such as $P\alpha > 0.12$.

More information on the weak Λ-nucleon interaction might be obtained from the ratio of the cross sections for the non-mesonic and mesonic decays of the hyperfragments. This ratio is closely related to the quantity $|a_i|/|b_i|$. Experiments combined with recent calculations [6]) for the ratio in question

† The branching ratios of various channels of the Σ-decay are of use for determining the type of the Σ-decay interactions. Assuming the one-to-one law and a change of the isobaric spin $|\Delta I| = \frac{1}{2}$ for Σ-decay, we can show that experiments on the above ratios support the derivative type for the Σ-decay interaction.

†† The threshold energy for the Ξ production is 660 MeV for the $\mathrm{K}^- + \mathrm{p}$ collision and 2.22 GeV for the $\pi^- + \mathrm{p}$ collision.

suggest that the parity is not conserved in the Λ-decay process. The results are also not contradictory with the weak interaction for the Λ-decay being a derivative coupling which satisfies the one-to-one law.

TABLE 2

Forward-backward asymmetry for the cascade decay

Interaction types		P_{max} of Λ	α_{max} for Λ-decay	$(P\alpha)_{max}$
Ξ-decay	Λ-decay			
(1)	(1)	0.13	0.10	0.013
(1)	(2)	0.13	0.91	0.12
(2)	(1)	0.97	0.10	0.097
(2)	(2)	0.97	0.91	0.88

2. Structure of the Weak Interactions

2.1. INTERACTIONS OF THE FIRST AND THE SECOND KIND

We discussed in the last section a phenomenological classification of known interactions. There is another classification of interactions which has been many times discussed in the history of quantum field theory: in this theory, all the interactions are classified into two groups, called the 1st kind and 2nd kind interactions, according to the dimension of their coupling constants [7, 8]):

$$\begin{aligned} &\eta \leqq 0 \text{ for the 1st kind interactions} \\ &\eta > 0 \text{ for the 2nd kind interactions.} \end{aligned} \tag{11}$$

Here η is the dimension † of the coupling constant †† g:

$$[g] = [\mathrm{L}]^{\eta}.$$

It has been firstly pointed out by Heisenberg [7, 10]) that the interactions of the 1st and 2nd kind behave differently at high energies. The latter depends essentially on the energy, whereas the former does not. The important significance of this classification became clear when it was proved [8]) that the renormalization theory can successfully eliminate the divergence difficulties in any approximation of the perturbation series when and only when we have to do with interactions of the 1st kind. We have, however, weak fermion interactions like beta interaction and μ-decay interaction which belong to the 2nd kind (with $\eta = 2$).

† [L] means the dimension of a length. Here, use is made of units for which $\hbar = c = 1$.

†† The constant η can be evaluated from the number of the field operators, the sum of the true degrees [8]) of the derivative operators acting on the field operators and the spins of the fields. There are two exceptions, viz. the vector couplings of the real vector field with a spinor field and the couplings with a scalar field: these belong to the 1st kind [9]).

2.2. A BASIC ASSUMPTION

In section 1 it was shown that the one-to-one law leads to an interaction of the 2nd kind for the Λ-decay process. Thus, it is quite interesting to examine the basic conjecture that *all the weak interactions violating parity conservation belong to the 2nd kind* †. We shall show in the next section that this assumption finds a reasonable position in the recent development of the quantum field theory.

In this section we briefly discuss some of the results coming from this basic assumption. A way of examining its validity is to study detailed structure of weak boson-fermion interactions. In section 1 use was made of the Λ-decay process in order to clarify the weak Λ-nucleon interaction.

It has been once noted [11]) that all the coupling constants of the weak boson-fermion interactions come very close to each other when we assume interactions of the vector or axial vector types: this is called the universal coupling of the weak boson-fermion interactions. In table 3 are shown the coupling constants for the weak boson-fermion interactions whose forms are assumed to be

$$g\bar{\psi}(1\pm\gamma_5)\gamma_\mu\psi\partial_\mu\varphi. \tag{12}$$

In computing them, use is made of the life times of the decay processes, shown in the table, and the branching ratios of the various decay channels

TABLE 3

Coupling constants for the weak interactions

Processes	Coupling constants g or $\sqrt{g_V}$ (cm)	Life time (sec)
$\Lambda \to p+\pi^-$	3.6×10^{-20}	3.7×10^{-10}
$\Sigma^+ \to p+\pi^0$	4.9×10^{-20}	3.4×10^{-11}
$\Xi^- \to \Lambda+\pi^-$	$\approx 7 \times 10^{-20}$	$\approx 10^{-10}$
$K^+ \to \mu^+ + \nu$	5.3×10^{-21} †	1.27×10^{-8}
$\pi^\pm \to \mu^\pm + \nu$	3.5×10^{-20}	2.5×10^{-8}
beta decay††	6.7×10^{-17}	

† The branching ratio 57 % for $K^+ \to \mu^+ + \nu$ is taken into account to determine g.
†† The coupling constant $\sqrt{g_V}$ for the beta decay is obtained from the ft value of O^{14}.

of the K-meson are also taken into account. The dimension of the coupling constant g_F of the beta interaction is known to be $[L]^2$. In table 3 we give $\sqrt{g_F}$ obtained from the ft value [12]) of the beta decay of O^{14}. It is well known that all the weak fermion interactions have about the same coupling constant. These apparent coincidences between the coupling constants seem to give some substance to the basic assumption. This will be further discussed in the next section.

† It should be noted that the V and A types are the simplest ones for the boson-fermion interactions of the 2nd kind. Thus, we may further conjecture that all the boson-fermion interactions are of the V and A types. This viewpoint will be discussed elsewhere.

It is worthwhile to point out that, among the unobserved decay modes, the process

$$K \to \text{two neutrinos}$$

is forbidden by the basic assumption. This is due to the fact that the mass of the neutrino is zero.

2.3. THE π-DECAY PROCESSES

Let us now turn to the problem of the π-decay. It is known that the branching ratios for the decay modes $\pi \to e+\nu$ and $\pi \to e+\nu+\gamma$ to the mode $\pi \to \mu+\nu$ are very small ($< 10^{-5}$) [13]). Taking into account only the weak boson-fermion interactions of the types (12) with the universal coupling, we obtain for the ratio of decay rates

$$\frac{w(\pi \to e+\nu)}{w(\pi \to \mu+\nu)} = \left(\frac{m_e}{m_\mu}\right)^2 \left\{1-\left(\frac{m_e}{m_\pi}\right)^2\right\}^2 \Big/ \left\{1-\left(\frac{m_\mu}{m_\pi}\right)^2\right\}^2 = 1.3 \times 10^{-4}. \quad (13)$$

The situation here is much better than in the case of the weak interactions of the 1st kind, i.e., of the scalar and pseudoscalar interactions. The problem of the π-electron decay is, however, still left open; as is well known, this decay can also occur through the π-nucleon and beta interactions.

The transition probability of the $\pi-e$ decay due to the latter interactions depends on the types of the beta interaction. It also depends very much on the cut-off momentum for the contribution of the virtual nucleon pairs. The cut-off momentum could be assumed to be small enough to make the effect of the virtual nucleon pairs negligibly small. Further, the contribution due to the virtual hyperon pairs might diminish the transition probability. It is worthwhile to note that such a cut-off procedure has no relation to the life time of the neutral pion. Indeed, the latter life time is free from divergences as far as the π-nucleon interaction is of the pseudoscalar coupling type. This is due to the gauge invariance of the theory.

Let us now consider the radiative electron decay of the pion. Taking into account the weak boson-fermion interaction (12) with the electromagnetic interaction, the ratio of the decay rates is given by [14]) †

$$R_\gamma \equiv \frac{w(\pi \to e+\nu+\gamma)}{w(\pi \to \mu+\nu)} \approx 10^{-6}. \quad (14)$$

The radiative electron decay occurs also through the beta interactions (except that of scalar type) via virtual nucleon loops. A way of getting rid of this difficulty is to assume global symmetry for the baryon interactions. This symmetry law leads to an extremely long life time [15]) in the case of beta interactions of the V, T-types: contributions due to the nucleon and

† This is consistent with experiments. A comprehensive discussion for the pion decay will be published elsewhere.

Ξ-particle almost cancel each other, $R_\gamma \approx 10^{-5}$ for T, $\approx 10^{-8}$ for V. Furthermore, it is well known [14]) that the beta interaction of the A type gives us a reasonable value ($\approx 10^{-8}$) for the ratio R_γ. Thus, any combination of V, A and T types contributes to the ratio R_γ by a negligible amount ($< 10^{-5}$) in a theory exhibiting global symmetry. To obtain a reasonable value for the ratio without assuming the global symmetry, we need to choose the cut-off momentum smaller than the nucleon mass; a cut-off momentum equal to the nucleon mass leads [14]) to a ratio of the order 10^{-3}.

The absence of the decay mode $K \to e + \nu$ can be explained in a similar way.

3. High Energy Behaviour of the Elementary Particles

3.1. VARIATION IN STRENGTH OF INTERACTIONS OF THE SECOND KIND

A current classification of the natural laws and various forms of matter is expressed in terms of the scale of the phenomena: the quantum mechanics of atoms is characterized by the scale 10^{-8} cm, nuclear physics by 10^{-13} cm, etc. It has often been said [7, 10, 16]) that the present theory of elementary particles may exceed the limit of its applicability in the region of extremely high energies. The non-local theory [16]) has been motivated by this standpoint. It has also been said that the present theory may not be applicable to the case of extremely strong interactions. Heisenberg's classification of the interactions is typical of the latter viewpoint. He suggested that the present theory may be applicable only to the case of interactions of the 1st kind and not to those of the 2nd kind, whose strength increases with the energy concerned. We now know that Heisenberg's classification is closely related to the limit of applicability of the renormalization theory; Dyson's formulation of the latter theory is applicable only to the case of interactions of the 1st kind. We may also expect phenomena quite different from our present notions for the elementary particles when any interaction of the 1st kind appears to be extremely strong [17]). Thus, there arises the question how strong the interactions realized in nature are. This is not a simple problem; some interactions could be very strong in the high energy region, even though they would appear to be weak in the ordinary energy phenomena. The phenomenological classification of the interactions discussed in section 1 has been established only in the ordinary energy region ($\lesssim 10^{10}$ eV). It may not correspond to the real situation in the extremely high energy region, e.g., in the region $> 10^{15}$ eV. Anyway, it is important to get as much information as possible on the strength of the interactions in each energy region.

The problem of the limit of applicability of the present theory has hitherto been of academic character. This is because it arose from the fact that the theory can make no exact prediction because of the well known divergence

difficulties. The problem has been concerned mainly with the question of the internal consistency of quantum field theory. To make the problem realistic, we must take into account various features of known phenomena.

Let us first call attention to the universal couplings of the weak interactions (cf. table 3); they suggest that, in exploring higher and higher energy phenomena, we shall meet with a hitherto unknown stratum, which is characterized by the scale of about 10^{-20} cm. To have a general idea about this stratum, we shall study the potentials due to the weak interactions. The beta interaction induces a part of the nuclear potential, because two nucleons can exchange electrons and neutrinos. The nuclear potential due to the beta interaction has been estimated by Tamm [18]) and Iwanenko [19]) in the lowest order approximation of the perturbation calculation. Briefly, it is of the form

$$V \approx \frac{g_F^2}{r^5} \tag{15}$$

for small r, where g_F is the coupling constant of the beta interaction. Such a potential contributes to the binding energy of the deuteron by an extremely small amount, because the radius of the deuteron is much larger than $\sqrt{g_F} \approx 10^{-17}$ cm. However, the potential is not at all weak for small r. Taking the Yukawa potential (with the unit coupling constant) $e^{-\mu r}/r$ as a standard of comparison, the nuclear potential (15) due to the beta interaction exceeds the Yukawa potential within the small region defined by

$$r \lesssim g_F^{\frac{1}{2}} \approx 10^{-17} \text{ cm}. \tag{16}$$

3.2. MULTIPLE LEPTON PRODUCTION

It is worthwhile to note that multiple production of leptons may occur in an extremely high energy region where the 2nd kind interactions are of importance. The high energy regions $E > 10^{12}$ eV and $E > 10^{15}$ eV (in the centre of mass system) correspond to the short distances $r < 10^{-17}$ cm and $r < 10^{-20}$ cm, respectively. In such an extremely high energy region, we can expect that contributions due to the 2nd kind interactions compete with those due to the 1st kind interactions. The higher the energy becomes, the larger the cross sections due to interactions of the 2nd kind will be. To see the situation in detail, we give two examples. The first is the production of 2 pions together with N electron-neutrino or μ meson-neutrino pairs in the nucleon-antinucleon annihilation:

$$\mathrm{n}+\tilde{\mathrm{n}} \to 2\pi+\mathrm{N}(\mathrm{e}+\nu)$$

or

$$\mathrm{n}+\tilde{\mathrm{n}} \to 2\pi+\mathrm{N}(\mu+\nu).$$

We apply the LOW method for the Fermi interactions [20]) to this phenomena in the following way. Lepton pairs are produced in the first step by succes-

sive changes of the states of the n ñ system, and in the second step the annihilation of n ñ leads to the 2-pion production. The latter step is treated by a perturbation calculation. Then, the cross section appears to be

$$\sigma(E_{\mathrm{L}}, N) \approx \sigma_0 \frac{(32\sqrt{2}\,\pi g_{\mathrm{F}} M E_{\mathrm{L}})^{2N}}{4(N!)^2(4N)!} \equiv \sigma_0 R(E_{\mathrm{L}}, N). \tag{17}$$

Here E_{L} is the antinucleon energy in the laboratory system, M is the mass of the nucleon and σ_0 is the cross section for the process n ñ $\rightarrow 2\pi$. The $R(E_{\mathrm{L}}, N)$ is the correction factor due to the interactions of the 2nd kind. For large multiplicity, the most probable number of the lepton pairs $\bar{N}$ is given by

$$\bar{N} \approx (2\sqrt{2}\,\pi g_{\mathrm{F}} M E_{\mathrm{L}})^{1/3}.$$

The second example is the process of production of $(N+1)$ electron-neutrino or μ meson-neutrino pairs in the nucleon-antinucleon annihilation. We treat the N-pair production in this process by the LOW method and evaluate the last one-pair production by a perturbation calculation. The cross section is found to be

$$\sigma_{\mathrm{II}}(E_{\mathrm{L}}, N+1) \approx \frac{9 g_{\mathrm{F}}^2 M E_{\mathrm{L}} (N+1)(32\sqrt{2}\,\pi g_{\mathrm{F}} M E_{\mathrm{L}})^{2N}}{32\pi (N!)^2 (4N)!}. \tag{19}$$

The most probable multiplicity $\bar{N}+1$ is again given by eq. (18).

The order of magnitude of these results are shown in table 4. They may be compared with the value for the one pair production at 10^{12} eV:

$$R(10^{12}\ \mathrm{eV},\ 1) = 2 \times 10^{-13}.$$

TABLE 4

Cross sections for multiple lepton pair production

$\bar{N}$	E_{L} (eV)	$R(E_{\mathrm{L}}, \bar{N})$	$\sigma_{\mathrm{II}}(E_{\mathrm{L}}, \bar{N}+1)$ (cm^2)
1	3×10^{13}	1.5	10^{-34}
5	5×10^{15}	5×10^{7}	10^{-24}
10	3×10^{16}	10^{13}	3×10^{-18}

It may be that the results in these two examples are overestimated. For the damping factor is not taken into consideration in the LOW method. The damping effect may be quite effective when the interaction becomes strong.

At the moment, we do not have any reliable method for treating the interactions of the 2nd kind. Thus, we should not take the values in table 4 too seriously; we are only interested in the rising tendency of the cross section due to the 2nd kind interactions. Moreover, even if the cross section becomes large, we should be confronted by many difficulties in identifying such processes experimentally: a similar increasing tendency of the cross

section is expected for various collision processes. Nevertheless, it is of importance to look for multiple production of μ-mesons and electrons in extremely high energy phenomena. The multiple production of μ-mesons may lead to multiple penetrating showers [21]) in high energy cosmic ray events. Measurements on cosmic ray events deeper underground † may give us important knowledge about the 2nd kind interactions.

3.3 UNIVERSAL FEATURES OF INTERACTIONS OF THE SECOND KIND

We should not take any result of the LOW method and perturbation theory too seriously, because the latter theory may not be applicable to our subject. The result (16), however, is based on a dimensional consideration. The interaction for the π-meson decay gives rise to a potential between π and μ-mesons, and the interaction for the Λ-decay to part of the Λ-nucleon potential. Let us consider a potential due to an interaction of the 2nd kind. In studying the behaviour of the potential at short distances, we may neglect the masses of particles. Here, the static approximation is assumed. Then, dimensional consideration leads us to a potential of a form

$$\frac{1}{r} f\left(\frac{g}{r^7}\right), \tag{20}$$

where g is a coupling constant of the dimension $[\mathrm{L}]^7$. Assuming an ordinary value (≈ 1) for the function $f(x)$ at $x \approx 1$, we see that the potential (20) exceeds the Yukawa potential at a point around

$$r \approx g^{1/7}.$$

Thus, the weak boson-fermion and fermion-fermion interactions turn out to become strong at $r \approx 10^{-20}$ cm and $r \approx 10^{-17}$ cm, respectively. It is remarkable that all the weak boson-fermion interactions become strong at about the same point. The same is true for the weak fermion interactions. This reflects the universality of the coupling constants of the weak interactions and is based on our fundamental assumption. Let us call attention to the fact that the weak interactions do not seem to be invariant under ordinary space inversion. This suggests that the violation of the invariance under the latter transformation manifests a feature of space in the region $r \lesssim 10^{-20}$ cm and, in this sense, has its origin in the structure of the particles. From such a viewpoint the one-to-one law (cf. section 1) appears to be quite plausible. Indeed, the ratio of the absolute magnitudes of the coupling constants for the parity-conserving and non-conserving terms should be the same for all the weak interactions and depend only on the laws that govern the small region.

† The effect of the neutrino underground has been once estimated by Hayakawa *et al.* [22]). The authors express their sincere thanks to Prof. Hayakawa for discussions with him at a Meeting on High Energy Physics held in January 1958.

3.4. RELATIONS WITH RENORMALIZATION THEORY

Our viewpoint on the weak interactions finds a reasonable position in the recent development of quantum field theory. We know that Dyson's formulation of the renormalization theory can remove all the divergences appearing in the case of the interactions of the 1st kind. This does not mean, however, that the renormalization theory for the latter interactions is internally consistent. The theory may be consistent as far as we describe its results in terms of the renormalized charge e_r (not the obsereved charge e_{ob}). However, it is not at all clear that the renormalized charge can be consistently replaced by the observed charge. Since 1951, great progress[23]) has been made in formulating the renormalization theory in the Heisenberg representation, and it has been shown that the renormalization constant Z_3, as a function of the renormalized charge, should satisfy the condition

$$0 \leqq Z_3(e_r) \leqq 1. \tag{21}$$

We call the zone of e_r satisfying (21) the normal zone of the renormalized charge [24]). Nobody has proved th: the observed charge $e_{ob} = 1/\sqrt{137}$ lies in the normal zone. The relation (21) can be intuitively understood from the hole theory. In the hole theory we must consider an electron in polarizable matter, i.e. in an ocean of vacuum electrons and, therefore, the effect of the electric charge of the electron must be weakened on account of the Lenz Law. Thus Z_3 cannot be larger than 1. Since the charge distribution of the point electron has a strong singularity, it is quite possible that the whole charge of the electron is cancelled by the polarized charge, and therefore, that the renormalized charge is zero for the point electron. This is not a fact proved rigorously. Landau applied an approximation method to calculate the renormalized charge and found that it is zero [25]). He showed that to obtain the renormalized charge equal to the observed one, we are forced to introduce a cut-off momentum Λ such that $1/\Lambda$ is much smaller than 10^{-20} cm. Since the effects of the proper fields due to interactions of the 1st kind are quite small in extremely high energy regions ($E > \mu$; μ stands for the masses of particles), no interaction of the 1st kind can change Landau's result [25]). At present we are not in a position to decide whether or not Landau's result is correct. We may only say that his result is possible. Taking Landau's viewpoint, we see that quantum electrodynamics is open, inasmuch as only the interactions of the 1st kind are taken into account. It would be not at all surprising if the interactions of the 2nd kind turn out to be strong in the region $r \lesssim 10^{-20}$ cm. We shall further note that the gravitational interaction is effective in a region $r \lesssim 10^{-34}$ cm. The problems concerning the gravitation field, weak interactions, non-conservation of parity and Landau's cut-off seem to be closely related to each other and depend essentially on the behaviour of space for $r \lesssim 10^{-20}$ cm.

3.5. THE STRONG INTERACTIONS

We have not discussed strong interactions, like the π-nucleon interaction. Our basic assumption does not say anything about these interactions. However, taking the viewpoint that the violation of the invariance under ordinary space inversion is a feature of space at short distances, we are led to the conclusion that the interactions being invariant under the latter transformation cannot be strong in small regions. This supports the view that the strong interactions are of the 1st kind.

It is, however, premature to conclude that our present notions of quantum field theory are applicable to these strong interactions. It was pointed out by Blokhintsev [17]) that there seems to appear a region 10^{-13} cm $\lesssim r \lesssim 10^{-15}$ cm where the π-nucleon interaction of the pseudoscalar type becomes extremely strong. Such a situation appears because the nucleon mass cannot be neglected in the above domain of variation of r. Blokhintsev suggested that we may meet with such a situation in the problem of the multiple production of pions. Another example might be given by the nucleon core. These problems are concerned with the region $r \approx 10^{-14}$ cm.

It is quite interesting to see whether or not any drastic change in the behaviour of the pions and nucleons (e.g., the ratio of produced pions and nucleons in the multiple production phenomena) appears at energies larger than 10^9 eV in the centre of mass system. It should be noted that the π-nucleon interaction could be proved to be of the 1st kind if the effects of the lepton interactions exceed those of the π-nucleon interaction.

3.6. THE MASS SPECTRUM

It is a consequence of our viewpoint, that most of the fundamental quantities of the elementary particles come out of the effects of the weak interactions. For example, we have to ask the question how the weak interactions are effective in explaining the main features of the mass spectrum. At present, it is hard to find a clear answer to this question, because we have not yet formulated any theory applicable to the case of the interactions of the 2nd kind. It is clear, however, that no interaction of the 1st kind can explain the mass spectrum, because it is impossible to form any constant of the dimension of a mass by using only $\hbar$ and c; some constant of the dimension of a length is necessary for explaining the mass spectrum. Such a constant may be given by the coupling constants of the weak interactions.

A promising speculation on the mass spectrum is the following one. The weak interactions may lead us to four levels of fermion masses, viz. baryons, μ-meson, electron and neutrino. The mass level of the baryons may be split into the masses of the Ξ, Σ, Λ and nucleon by effects of strong interactions. Further fine structures of the mass levels, e.g. the mass difference of the

proton and neutron, may be explained by effects of the electromagnetic interaction. In the same way, the two levels of boson masses, viz. mesons and photon, may be given by the weak interactions. The strong interactions may split the mass level of the mesons into two levels, the K and π-mesons. In this way, the idea of the global symmetry [26]) of the heavy particles may be extended to all the elementary particles.

3.7 CONCLUSION

Summarizing the results, there are two strata in the structure of the elementary particles; they are characterized by the two constants $r \approx 10^{-14}$ cm and $r \approx 10^{-20}$ cm. The latter constant is about the range of the region where the weak interactions become strong. Two steps are essential in examining the validity of our viewpoint. One is to show that all the weak interactions violating the parity conservation belong to the 2nd kind. The other is to look for high energy phenomena in which the weak interactions are effective.

If the weak interactions would not by any means be effective at sufficiently high energies, we should be forced to conclude that the present theory of quantized fields is applicable only to the phenomena in the outer region $r_0 \gg 10^{-20}$ cm.

We are grateful to Professor S. Sakata and Professor S. Nakamura for their inspiring discussions. We are also indebted to Professor S. Machida, Dr. S. Sato and Dr. J. Otokozawa for their excellent cooperation.

Appendix

We give here the angular distribution of the pion in the polarized hyperon decay, resulting from the general Hamiltonian (1) or (2) (in section 1). Here the condition $|a_i|^2 = |b_i|^2 = 1$ is not assumed.

$$\begin{aligned} w_1(\theta) = {} & \frac{{g_1}^2}{4\pi}\frac{1}{4m_Y}\left\{\frac{(m_Y-m_N)^2-m_\pi^2}{{m_Y}^2}\right\}^{\frac{1}{2}}\left\{\frac{(m_Y+m_N)^2-m_\pi^2}{{m_Y}^2}\right\}^{\frac{1}{2}} \\ & \times [|a_1|^2\{(m_Y+m_N)^2-m_\pi^2\}+|b_1|^2\{(m_Y-m_N)^2-m_\pi^2\}] \\ & \times \{1+P\alpha_1\cos\theta\} \end{aligned} \tag{A.1}$$

and

$$\begin{aligned} w_2(\theta) = {} & \frac{{g_2}^2}{4\pi}\frac{1}{4m_Y}\left\{\frac{(m_Y-m_N)^2-m_\pi^2}{{m_Y}^2}\right\}^{\frac{1}{2}}\left\{\frac{(m_Y+m_N)^2-m_\pi^2}{{m_Y}^2}\right\}^{\frac{1}{2}} \\ & \times [|a_2|^2(m_Y-m_N)^2\{(m_Y+m_N)^2-m_\pi^2\} \\ & + |b_2|^2(m_Y+m_N)^2\{(m_Y-m_N)^2-m_\pi^2\}] \\ & \times \{1+P\alpha_2\cos\theta\} \end{aligned} \tag{A.2}$$

for (1) and (2) respectively.

Here, α_1 and α_2 are written as

$$\alpha_1 = \frac{2\,\mathrm{Re}\,(a_1^* b_1)\{m_Y^2-(m_N-m_\pi)^2\}^{\frac{1}{2}}\{m_Y^2-(m_N+m_\pi)^2\}^{\frac{1}{2}}}{|a_1|^2\{(m_Y+m_N)^2-m_\pi^2\}+|b_1|^2\{(m_Y-m_N)^2-m_\pi^2\}},$$

$$\alpha_2 = \frac{2\,\mathrm{Re}\,(a_2^* b_2)(m_Y^2-m_N^2)\{m_Y^2-(m_N-m_\pi)^2\}^{\frac{1}{2}}\{m_Y^2-(m_N+m_\pi)^2\}^{\frac{1}{2}}}{|a_2|^2(m_Y-m_N)^2\{(m_Y+m_N)^2-m_\pi^2\}+|b_2|^2(m_Y+m_N)^2\{(m_Y-m_N)^2-m_\pi^2\}}.$$

References

1) C. S. Wu, E. Ambler, R. W. Hayward, D. D. Hoppes and R. P. Hudson, Phys. Rev. **105** (1957) 1413; R. L. Garwin, L. M. Lederman and M. Weinrich, Phys. Rev. **105** (1957) 1415
2) F. S. Crawford *et al.*, Phys. Rev. **108** (1957) 1102; F. Eisler *et al.*, Phys. Rev. **108** (1957) 1353
3) T. D. Lee, J. Steinberger, G. Feinberg, P. K. Kabir and C. N. Yang, Phys. Rev. **106** (1957) 1367
4) R. Gatto, Phys. Rev. **108** (1957) 1103
5) S. Minami and Y. Yamaguchi, Prog. Theor. Phys. **18** (1957) 39
6) F. Cerulus, Nuovo Cimento **5** (1957) 1685
7) W. Heisenberg, Solvay Bericht (1939) Kap. III, IV
8) S. Sakata, H. Umezawa and S. Kamefuchi, Prog. Theor. Phys. **7** (1952) 377
9) H. Umezawa, Prog. Theor. Phys. **7** (1952) 551
10) W. Heisenberg, Zs. für Phys. **101** (1936) 533; **113** (1939) 61
11) K. Iwata, S. Ogawa, H. Okonogi, B. Sakita and S. Oneda, Prog. Theor. Phys. **13** (1955) 19
12) D. A. Bromley, E. Almqvist, H. E. Gove, A. E. Litherland, E. B. Paul and A. J. Ferguson, Phys. Rev. **105** (1957) 957
13) S. Lokanathan and J. Steinberger, Nuovo Cimento Suppl. **2** (1957) 151; J. M. Cassels, M. Rigby, A. M. Wetherell and J. R. Wormald, Proc. Phys. Soc. A **70** (1957) 729
14) S. B. Treiman and H. W. Wyld, Jr., Phys. Rev. **101** (1957) 1552
15) M. Kawaguchi and K. Nishijima, Phys. Rev. **108** (1957) 905
16) G. Wataghin, Zs. für Phys. **88** (1934) 92
17) D. Blokhintsev, Usp. Fis. Nauk USSR, **61** (1956) 137; **62** (1957) 381
18) I. Tamm, Nature **133** (1934) 981
19) D. Iwanenko, Nature **133** (1934) 981
20) H. W. Lewis, T. R. Oppenheimer and S. A. Wouthuysen, Phys. Rev. **73** (1947) 127; H. Umezawa, Y. Takahashi and S. Kamefuchi, Phys. Rev. **85** (1952) 505
21) S. Higashi, T. Oshio, H. Shibata, K. Watanabe and Y. Watase, Nuovo Cimento **5** (1957) 597
22) S. Hayakawa, S. Machida and M. Umezawa, Soryushiron Kenkyu **1** (1949) 74
23) H. Umezawa and S. Kamefuchi, Prog. Theor. Phys. **6** (1951) 543; G. Källén, Helv. Phys. Acta **25** (1952) 417; H. Lehmann, Nuovo Cimento **11** (1954) 342
24) H. Umezawa, S. Kamefuchi, Y. Tomozawa and M. Konuma, Nuovo Cimento **3** (1956) 772
25) L. D. Landau, A. A. Abrikosov and I. M. Halatnikov, Dok. Akad. Nauk USSR **95** (1954) 497, 733, 1177; **96** (1954) 261; G. Källén and W. Pauli, Mat. Fys. Medd. Dan. Vid. Selsk. **30** (1955) no. 7
26) J. Schwinger, Phys. Rev. **104** (1956) 1164; M. Gell-Mann, Phys. Rev. **106** (1957) 1296

1.D.2 *Nuclear Physics* 7 (1958) 184—194; © *North-Holland Publishing Co., Amsterdam*
Not to be reproduced by photoprint or microfilm without written permission from the publisher

ROTATIONAL PROPERTIES OF THE TWO-DIMENSIONAL ANISOTROPIC HARMONIC OSCILLATOR

II. The Collective-Intrinsic Description

H. J. LIPKIN and S. GOLDSTEIN

Department of Physics, The Weizmann Institute of Science, Rehovoth

Received 13 February 1958

Abstract: Harmonic oscillator wave functions are examined from the point of view of the collective rotational motion characteristic of the unified nuclear model. An oscillatory collective rotation is defined. Conditions are formulated for the separability of this motion from the other degrees of freedom of the system. Separability is demonstrated to good approximation in systems of large numbers of particles with large deformations.

1. Introduction

In the unified nuclear model [1]), the anisotropic harmonic oscillator potential is frequently used to calculate the motion of nucleons in a deformed central field [2]). The wave functions describing the motion of a system of particles in an anisotropic potential are not eigenstates of the total angular momentum; they therefore cannot be considered as approximations of the wave functions of a real nucleus. The relation connecting the oscillator and nuclear wave functions is not uniquely defined and is not yet well understood. Some insight into this problem can be gained by an examination of the oscillator system using a slightly different point of view from the usual one; namely by introducing the concepts of collective and intrinsic motion as used in the unified model.

1.1. DEFINITION AND NOTATION

The system treated in this paper is that of A particles moving in a two-dimensional anisotropic harmonic oscillator potential. The Hamiltonian for the system is

$$H = \sum_{i=1}^{A} (p_{x_i}^2+p_{y_i}^2)/2M+M \sum_{i=1}^{A} \tfrac{1}{2}(\omega_x^2 x_i^2+\omega_y^2 y_i^2), \qquad (1)$$

where x_i, y_i, p_{x_i}, and p_{y_i} are the co-ordinates and the momenta of the i-th particle, M is the particle mass, and ω_x and ω_y are the constants characterizing the oscillator potential. The expectation values for a number of operators describing collective properties of the ground state wave function of this

system are given in the first paper of this series [3]), referred to as I. As in I, we take

$$\omega_y > \omega_x. \tag{2}$$

The states of the system are specified by the x and y oscillator quantum numbers for each particle, n_{x_i} and n_{y_i}, and the following quantities are defined as in I:

$$N_x = \sum_{i=1}^{A} (n_{x_i}+\tfrac{1}{2}), \quad N_y = \sum_{i=1}^{A} (n_{y_i}+\tfrac{1}{2}); \tag{3}$$

$$I_{\text{rig}} = \hbar \left[\frac{N_x}{\omega_x} + \frac{N_y}{\omega_y}\right] = \sum_{i=1}^{A} M\langle x_i^2+y_i^2\rangle; \tag{4}$$

$$\delta = \frac{(N_x/\omega_x)-(N_y/\omega_y)}{(N_x/\omega_x)+(N_y/\omega_y)} = \frac{\sum_i \langle x_i^2-y_i^2\rangle}{\sum_i \langle x_i^2+y_i^2\rangle}. \tag{5}$$

$$L = \sum_i (x_i p_{y_i} - y_i p_{x_i}). \tag{6}$$

The Bohr-Mottelson condition for equilibrium deformation is

$$N_x\omega_x = N_y\omega_y. \tag{7}$$

As discussed in I, the numbers N_x and N_y are large if the number of particles is large, being of the order 200—350 for nuclei in the rare earth and transuranium regions of the periodic table where rotational states are observed. This makes possible expansions in powers of $1/N_x$ or $1/N_y$ which are called in these papers expansions in powers of $1/N$. Expansions in powers of $1/N\delta$ and $1/N\delta^2$ are also used.

2. The Collective-Intrinsic Description

Rotational states in nuclei are most conveniently described with reference to a body-fixed co-ordinate system rotating with the nucleus. In two dimensions this body-fixed system is defined by a single angle co-ordinate characterizing the orientation of the nucleus. The collective motion of the nucleus is described by this angle and is a free rotation with constant angular momentum. The intrinsic motion of the particles is described by the particle co-ordinates with respect to the rotating system.

The anisotropic harmonic oscillator system does not have rotational states and it is very easily described in terms of the particle co-ordinates with respect to axes fixed in the laboratory. Since the individual particles move independently, there does not seem to be any good reason for introducing a collective description. However, oscillator wave functions do possess certain collective properties which are of interest when these functions are used in unified model calculations. These properties become

evident when a collective-intrinsic type of description is used for the oscillator system. In this paper the feasibility of such a description is demonstrated, along with some of its principal properties. The explicit canonical transformation from the Hamiltonian (1) to the collective-intrinsic Hamiltonian will be treated in a subsequent paper.

2.1. THE COLLECTIVE CO-ORDINATE

The collective description is characterized by an angle co-ordinate θ describing the orientation of the nucleus. θ is a function of the particle co-ordinates and momenta which is not uniquely determined. It can be any function which satisfies the following two conditions:

1) it must be symmetric in all the particles;

2) it must be an angle; i.e. it must be canonically conjugate to the total angular momentum L (eq. (6)), satisfying the commutation rule $[L, \theta] = -i\hbar$.

Two examples of such angle variables are the angles θ_1 and θ_2 treated in I:

$$\theta_1 = \tfrac{1}{2}\tan^{-1} 2\{\sum_i x_i y_i / \sum (x_i^2 - y_i^2)\} \tag{8}$$

$$\theta_2 = \tfrac{1}{2}\tan^{-1} 2\{[\sum_i x_i y_i + \sum_i p_{x_i} p_{y_i}/M^2\omega_y^2] \\ [\sum_i (x_i^2 - y_i^2) + \sum_i (p_{x_i}^2 - p_{y_i}^2)/M^2\omega_y^2]^{-1}\} \tag{9}$$

θ_1 is just the angle defining the orientation of the principal axes of the tensor of inertia of the system. θ_2 can be considered as defining the principal axes of a tensor depending upon both the co-ordinates and momenta of the particles.

It is possible to choose a particular angle variable θ and to define a set of intrinsic co-ordinates q^α and their canonically conjugate momenta p^α such that all the p^α and q^α commute with both L and θ. The Hamiltonian (1) can then be transformed canonically to a representation in terms of these collective and intrinsic variables. The ground state wave function of the system has then the form

$$\psi_0 = \psi_0(\theta, q^\alpha). \tag{10}$$

2.2. SEPARABILITY

The wave function ψ_0 will be called *separable* if there exists a representation in which it can be written as a product of two factors, one depending only upon θ and one depending only upon the intrinsic co-ordinates q^α:

$$\psi_0 = f_0(\theta)\varphi(q^\alpha). \tag{11}$$

In this paper certain general conditions for separability will be developed and it will be shown that the ground state oscillator wave function is separable to a good approximation if $N\delta$ is large.

The collective part $f_0(\theta)$ of a separable wave function cannot describe a free rotation, since the original Hamiltonian (1) does not possess rotational symmetry and does not commute with L. It must rather describe some sort of oscillation about an equilibrium orientation in which the energy of the system is a minimum with respect to changes in θ.

In order to get a general idea of the properties of the separated system, let us assume that a collective co-ordinate θ has been found which separates the ground state wave function. Let us examine the form which the Hamiltonian (1) must have after a canonical transformation to the co-ordinates θ, q^α and their canonically conjugate momenta L, p^α. The transformed Hamiltonian can be written conveniently as the sum of three terms

$$H^{\mathrm{T}} = H_{\mathrm{coll}}(L, \theta)+H_{\mathrm{int}}(p^\alpha, q^\alpha)+H_{\mathrm{coupl}}(L, \theta, p^\alpha, q^\alpha). \tag{12}$$

The separation (11) requires of course that H_{coupl} satisfy the relation

$$H_{\mathrm{coupl}}\,\psi_0 = 0. \tag{13}$$

Let us now consider the possible form of the collective term H_{coll}. If we expand it in a power series in L and θ ,the first non-vanishing terms will be quadratic, giving a harmonic-oscillator-type Hamiltonian. It seems reasonable to neglect the higher terms on the basis of the expectation value results obtained in I. The expectation values of the squares of typical angle variables θ_1^2 and θ_2^2 indicate that the wave function is appreciable only at small angles and that therefore the contribution of higher order terms in θ is small. The relation between the expectation values of L^4 and L^2 is just that of a gaussian distribution, i.e. of a harmonic oscillator wave function. It is therefore reasonable to expect that a good approximation for the function f_0 in (11) should be the ground state wave function of the harmonic oscillator Hamiltonian

$$H_{\mathrm{coll}}(L, \theta) = \frac{L^2}{2\mathscr{I}} + \frac{\mathscr{I}\Omega^2\theta^2}{2}. \tag{14}$$

This Hamiltonian describes a harmonic oscillation of the orientation of the system of particles with angular frequency Ω and moment of inertia $\mathscr{I}$.

3. Separability Theorems

3.1. STATEMENTS AND PROOFS

Using the above reasoning as a guide, the following useful separability theorems can be proved:

Theorem 1. Given a particular function $\psi_0(x_i, y_i)$ and a particular angle function $\theta(x_i, y_i, p_{x_i}, p_{y_i})$. Let ψ_0 be transformed canonically to be expressed in terms of θ and a set of intrinsic co-ordinates q^α commuting with L and θ. Then a sufficient condition that the transform of ψ_0 have the separated

form (11) is that there exist two numbers $\mathcal{I}$ and Ω such that the expectation value of (14) in the state of ψ_0 is equal to $\hbar\Omega/2$.

Proof: Let us expand ψ_0 in eigenfunctions of (14):

$$\psi_0 = \sum_{n=0}^{\infty} a_n f_n(\theta)\varphi_n(q^a), \tag{15}$$

where f_n is the n-th normalized eigenfunction of (14) corresponding to the eigenvalue $(n+\frac{1}{2})\hbar\Omega$, and the functions φ_n are normalized but not necessarily orthogonal. Then the expectation value of (14) in the state (15) is just

$$\langle H_{\text{coll}}\rangle = \sum_{n=0}^{\infty} (n+\tfrac{1}{2})\hbar\Omega|a_n|^2. \tag{16}$$

If this expression (16) is equal to exactly $\hbar\Omega/2$, then all the coefficients a_n must vanish except a_0 which must be equal to unity. Thus ψ_0 has the form (11) and is separable.

Theorem 2. Given ψ_0 and θ as in theorem 1. Then ψ_0 can be expressed as the sum of a separable wave function and a remainder, such that the square of the amplitude of the remainder is less than or equal to $\langle H_{\text{coll}}/\hbar\Omega\rangle - \frac{1}{2}$.

Proof: Divide eq. (16) by $\hbar\Omega$ and substitute $|a_0|^2 = 1 - \sum_{n=1}^{\infty}|a_n|^2$ to obtain

$$\langle H_{\text{coll}}/\hbar\Omega\rangle - \tfrac{1}{2} = \sum_{n=1}^{\infty} n|a_n|^2 \geqq \sum_{n=1}^{\infty} |a_n|^2. \tag{17}$$

Theorem 3. Given ψ_0 and θ as in theorem 1. A sufficient condition for separability is that

$$\langle L^2\rangle\langle\theta^2\rangle = \hbar^2/4. \tag{18}$$

Proof: Let $\mathcal{I}$ and Ω be any two numbers such that

$$\mathcal{I}\Omega = \sqrt{\langle L^2\rangle/\langle\theta^2\rangle}. \tag{19}$$

Then by direct substitution of (18) and (19) into (14) it is evident that the conditions of theorem 1 are satisfied.

Theorem 4. Given ψ_0 and θ as in theorem 1. Then ψ_0 can be expressed as the sum of a separable wave function and a remainder, such that the square of the amplitude of the remainder is less than or equal to $\hbar^{-1}\sqrt{(\langle L^2\rangle\langle\theta^2\rangle)} - \frac{1}{2}$.

Proof: Choose $\mathcal{I}$ and Ω in accordance with eq. (19), substitute into eq. (14) and use the result in theorem 2.

Theorem 5. Given ψ_0 and θ as in theorem 1. Then a sufficient condition for separability is the existence of a positive real number a such that

$$(L - ia\theta)\psi_0 = 0. \tag{20}$$

Proof: Multiply eq. (20) by $L + ia\theta$ and set $a = \mathcal{I}\Omega$ to obtain

$$(L^2 + \mathcal{I}^2\Omega^2\theta^2 - \hbar\mathcal{I}\Omega)\psi_0 = 0.$$

The conditions of theorem 1 are therefore satisfied.

3.2. APPLICATIONS TO THE ANISOTROPIC HARMONIC OSCILLATOR

Let us now attempt to find a collective angle co-ordinate which separates the ground state wave function for a system of particles moving in a deformed harmonic oscillator potential. The simplest choice for θ is the angle θ_1 defined by eq. (8) which defines the orientation of the principal axes of inertia of the system. Whether or not θ_1 gives a good separation of the oscillator ground state wave function can be determined by the use of theorems 3 and 4 and the calculated expectation values given in I. The result obtained is

$$\langle L^2\rangle\langle\theta_1^2\rangle = \frac{\hbar^2}{4}\frac{(1+\delta)}{2\delta}\left\{1-\hbar\frac{(1+\delta)/\omega_x+(7+\delta)/3\omega_y}{2\delta^2 I_{\text{rig}}}\right\}. \tag{21}$$

This is considerably greater than $\hbar^2/4$; thus θ_1 is not the proper co-ordinate to separate the deformed oscillator.

A clue to the proper form for θ is given by theorem 5. It is necessary to find an operator $a\theta$ such that $(L-ia\theta)\,\psi_0$ vanishes. From the form of the operator L, eq. (6), and the characteristics of the harmonic oscillator, it is evident that if the ground state wave function is specified by the total quantum numbers (N_x, N_y), then the operator L has non-vanishing matrix elements between this state and only two other states; namely those specified by the total quantum numbers (N_x+1, N_y+1) and (N_x-1, N_y+1). The operators $\sum_i x_i y_i$ and $\sum_i p_{x_i} p_{y_i}$ have exactly the same property as do also all linear combinations

$$L+\alpha\sum_i x_i y_i+\beta\sum_i p_{x_i} p_{y_i} \tag{22}$$

of the three operators. Since there are only two non-vanishing matrix elements and there are two free parameters at our disposal, α and β, it is possible to determine values of α and β for which all matrix elements of (22) connecting the ground state vanish. If with these values of α and β, the operator $\alpha\sum_i x_i y_i+\beta\sum_i p_{x_i} p_{y_i}$ is set equal to $-ia\theta$, the resulting θ satisfies the condition (20) for theorem 5 but does not satisfy the proper commutation rule with L to be an angle variable. One can modify this operator slightly to construct an angle variable, thereby obtaining the angle θ_2 defined by eq. (9). The numerator in the argument of the inverse tangent is just that operator appearing in (22) with the proper values α and β. The addition of the denominator and the inverse tangent results in an angle variable satisfying $[L, \theta] = -i\hbar$ exactly and satisfying (20) except for terms of higher order in $1/N$. The denominator can be considered as diagonal except for terms of higher order in N, and the inverse tangent differs from its argument also only in higher order. The extent to which these changes disturb the validity of theorem 5 can be estimated by testing θ_2 with

theorems 3 and 4. The result, using expectation values given in I, is

$$\langle L^2\rangle\langle\theta_2^2\rangle \approx \frac{\hbar^2}{4}\left\{1+(4\hbar^2/3\langle L^2\rangle)-\frac{\hbar^4}{4}N_x\left(\frac{\omega_x}{\omega_y}-\frac{\omega_y}{\omega_x}\right)^2/\langle L^2\rangle^2\right\}. \quad (23)$$

Since L^2 is a large number eq. (23) is very close to eq. (18) if the number of particles is large and the deformation is not too small. Thus θ_2 gives a separation of the ground state oscillator wave function to a good approximation. This can be expressed quantitatively by the use of theorem 4; the ground state oscillator wave function can be expressed as the sum of a separable wave function and a remainder whose amplitude squared is of the order $1/\langle L^2\rangle$ or one per cent in cases of interest.

4. Implications of Separability

Now that the ground state oscillator wave function has been shown to be separable to good approximation, this property can be used to clarify a number of points in the calculation of nuclear moments of inertia using oscillator wave functions.

4.1. GENERATOR WAVE FUNCTIONS

In the method of generator co-ordinates [4, 5, 6]) the deformed shell model wave functions are used to generate eigenfunctions of the total angular momentum. Let $\psi(x_i, \beta)$ be a deformed shell model wave function for a system whose axes have been rotated by an angle β with respect to the laboratory axes. Then

$$\varphi_M(x_i) = \int_0^{2\pi} e^{iM\beta}\psi(x_i, \beta)d\beta \quad (24)$$

is an eigenfunction of the total angular momentum with eigenvalue M.

If $\psi(x_i, \beta)$ is the ground state oscillator wave function, the expression (24) assumes a particularly simple form after the transformation to the collective-intrinsic representation. We have seen that the function $\psi(x_i, 0)$ which corresponds to a non-rotated system transforms to the form

$$\psi_0(x_i, 0) \to f(\theta_2)\varphi(q^\alpha), \quad (25)$$

where the transformation used is of course that defined by the angle θ_2. A rotation of the system to the co-ordinate axes by an angle β does not change the intrinsic co-ordinates q^α and changes θ to $\theta-\beta$. Thus

$$\psi_0(x_i, \beta) \to f(\theta_2-\beta)\varphi(q^\alpha). \quad (26)$$

The transform of eq. (24) is therefore

$$\varphi_M(x_i) \to \int_0^{2\pi} e^{iM\beta}f(\theta_2-\beta)\varphi(q^\alpha)d\beta = C\, e^{iM\theta_2}\varphi(q^\alpha), \quad (27)$$

where

$$C = \int_0^{2\pi} e^{iM(\beta-\theta_2)}f(\theta_2-\beta)d\beta \quad (28)$$

is clearly a constant, independent of θ_2, since $f(\theta)$ must be a periodic function. The value of C depends upon M, but is irrelevant, since generator wave functions are not normalized.

The set of wave functions generated from the ground state oscillator wave function by using different values of M in eq. (24) thus correspond to what is usually called a "rotational band". They all have the same intrinsic wave function $\varphi(q^\alpha)$ and different values of the total angular momentum M. This is true only because of the separability of the deformed shell model wave function used. It is easily shown that if the wave function used is not separable, a rotational band is not obtained.

Consider a case of a function $\psi(x_i)$ which is not separable in any collective-intrinsic representation. The transform of $\psi(x_i)$ can be written

$$\psi(x_i) \rightarrow \sum_k f_k(\theta)\varphi_k(q^\alpha) \tag{29}$$

where the functions $\varphi_k(q^\alpha)$ represent a complete set of intrinsic wave functions and the functions $f_k(\theta)$ are not necessarily normal or orthogonal. In all representations there will be at least two non-vanishing terms in the sum on k.

The transform of the wave function generated by introducing (29) into the generator formula (24) is just

$$\varphi_M(x_i) \rightarrow e^{iM\theta}\sum_k C_{Mk}\varphi_k(q^\alpha), \tag{30}$$

where

$$C_{Mk} = \int_0^{2\pi} e^{iM(\beta-\theta)} f_k(\theta-\beta)\mathrm{d}\beta. \tag{31}$$

The dependence of C_{Mk} upon M and k is now significant, since there are at least two terms in the sum on k in eq. (30). The intrinsic part of the wave function, $\sum C_{Mk}\varphi_k(q^\alpha)$ now depends upon M, and the set of wave functions generated for different values of M no longer correspond to a "rotational band".

Note that the trivial "separability" of the generated wave function into the product of $e^{iM\theta}$ and an intrinsic wave function follows directly from the fact that $\varphi_M(x_i)$ is an eigenfunction of the total angular momentum regardless of the separability properties of the deformed shell model wave function $\psi(x_i)$.

4.2. OVERLAP INTEGRALS

It is sometimes of interest to estimate the value of the overlap integrals [4]) between the ground state wave function of the Hamiltonian (1) and that of the same system rotated in space by a small angle β. Although this is difficult to calculate in the x_i, p_i representation, it is very simple in terms

of the co-ordinates θ_2, q^α. The wave function has the separated form

$$\psi_0 = N e^{-\mathscr{I}\Omega\theta_2^2/2\hbar}\varphi(q^\alpha) \tag{32}$$

where N is a normalization constant. The wave functions for systems rotated with respect to (1) by an angle $\pm\beta$ are given by

$$\psi_0(\pm\beta) = N e^{-\mathscr{I}\Omega(\theta_2\pm\beta)^2/2\hbar}\varphi(q^\alpha). \tag{33}$$

The overlap integral of two wave functions rotated with respect to one another by an angle β is therefore given by

$$\begin{aligned}\int \psi_0^*(-\beta/2)\psi_0(\beta/2)\mathrm{d}\theta\mathrm{d}q^\alpha &= e^{-\mathscr{I}\Omega\beta^2/4\hbar}\int N^2 e^{-\mathscr{I}\Omega\theta_2^2/\hbar}\varphi^*(q^\alpha)\varphi(q^\alpha)\mathrm{d}\theta\mathrm{d}q^\alpha \\ &= e^{-\mathscr{I}\Omega\beta^2/4\hbar}\int \psi_0^*(0)\psi_0(0)\mathrm{d}\theta\mathrm{d}q^\alpha = e^{-\mathscr{I}\Omega\beta^2/4\hbar}.\end{aligned} \tag{34}$$

From eq. (19) using the expectation values given in I,

$$\mathscr{I}\Omega = \sqrt{\langle L^2\rangle/\langle\theta_2^2\rangle} = 2\langle L^2\rangle/\hbar. \tag{35}$$

Since $\langle L^2\rangle$ is of the order of $100\hbar^2$ in most cases of interest, the exponent in (34) is of the order $100\beta^2$ and i small except when β is of the order 0.1 or smaller.

4.3. THE MOMENT OF INERTIA

Since the ground state oscillator wave function has been shown to describe approximately a collective rotational oscillation corresponding to the collective Hamiltonian (14), it is of interest to calculate the moment of inertia of this rotational motion. In the collective-intrinsic representation the ground state wave function is

$$|0\rangle = f_0(\theta_2)\varphi(q^\alpha), \tag{36}$$

where $f_0(\theta_2)$ is the ground state wave function of the harmonic oscillator Hamiltonian (14) having moment of inertia $\mathscr{I}$ and angular frequency Ω. The operator L operates only on θ_2 and not on q^α. Thus

$$L\,|0\rangle = cf_1(\theta_2)\varphi(q^\alpha) = c|1\rangle, \tag{37}$$

where c is a normalization constant and $f_1(\theta_2)$ is the wave function of the first excited state of the oscillator (14). The energy of the state $|1\rangle$ is greater than that of the state $|0\rangle$ by just $\hbar\Omega$. Thus

$$\langle 1|H|1\rangle = \frac{\langle 0|LHL|0\rangle}{\langle 0|L^2|0\rangle} = \langle 0|H|0\rangle + \hbar\Omega. \tag{38}$$

Because of the properties of the harmonic oscillator ground state,

$$\hbar\Omega = 2\langle 0|L^2|0\rangle/\mathscr{I}. \tag{39}$$

Inserting eq. (39) into eq. (38) and solving for $\mathscr{I}$, we obtain a formula for the moment of inertia

$$\mathscr{I} = 2\langle 0|L^2|0\rangle^2/\langle 0|L(H-\langle 0|H|0\rangle)L|0\rangle. \tag{40}$$

This formula is the same as that given by Skyrme [5]) and by Peierls and Yoccoz [4]) for the nuclear moment of inertia under certain assumptions. Our derivation has shown it to give the moment of inertia of the collective motion in the oscillator wave function, which is a property only of the oscillator wave function. The treatments leading to the formula (40) for a real nucleus must therefore contain implicitly an assumption of the equivalence of the oscillator collective motion and that of the real nucleus.

5. An Angle Variable of Interest for the Cranking Model

In treatments attempting to derive the cranking model [7, 8]) on a completely quantal basis, [9, 10]) a collective angle θ_3 is defined which satisfies the relation

$$[H,\ \theta_3] = i\hbar\, L/\mathscr{I}, \tag{41}$$

where $\mathscr{I}$ is the moment of inertia of the cranking model.

An angle variable satisfying this relation to good approximation can be defined for the deformed oscillator system (1):

$$\theta_3 = \tfrac{1}{2}\tan^{-1} 2\{[\sum_i x_i y_i + \sum_i 2p_{x_i} p_{y_i}/M^2(\omega_x^2+\omega_y^2)]$$
$$[\sum_i (x_i^2-y_i^2)+2\sum(p_{x_i}^2-p_{y_i}^2)/M^2(\omega_x^2+\omega_y^2)]^{-1}\}. \tag{42}$$

The commutator $[H, \frac{1}{2}\tan 2\theta_3]$ can be calculated directly. Letting F and G be the two expressions in the square brackets in (42), we have

$$[H, \tfrac{1}{2}\tan 2\theta_3] = [H, (FG^{-1})] = \{[H,\ F]-\tfrac{1}{2}\tan 2\theta_3\,[H, G]\}G^{-1}$$
$$= -i\hbar\{L-\tfrac{1}{2}\tan 2\theta_3 \sum_i (x_i p_{x_i}+p_{x_i}x_i+y_i p_{y_i}+p_{y_i}y_i)\}G^{-1}(\omega_y^2-\omega_x^2)/4. \tag{43}$$

The right hand side of eq. (43) can be expanded in powers of $1/\sqrt{N}$ by the method described in I. The term proportional to LG^{-1} is seen to be of order $1/\sqrt{N}$, whereas the term proportional to $\frac{1}{2}\tan 2\theta_3$ is of order $1/N$ and can therefore be neglected. Furthermore the operator G^{-1} can be replaced by $\langle G\rangle^{-1}$ with the loss only of terms of higher order in $1/N$. The difference between $\frac{1}{2}\tan 2\theta_3$ and θ_3 is also of higher order in $1/N$. Thus to the lowest order in $1/\sqrt{N}$, eq. (43) reduces to eq. (41), with the moment of inertia given by

$$\mathscr{I} = 4\langle G\rangle/(\omega_y^2-\omega_x^2)$$
$$= \frac{\hbar}{2}\frac{1}{\omega_y\omega_x}\left[\frac{(\omega_y-\omega_x)^2}{\omega_y+\omega_x}(N_y+N_x)+\frac{(\omega_y+\omega_x)^2}{\omega_y-\omega_x}(N_x-N_y)\right] \tag{44}$$

using the expectation values tabulated in I. This result (44) is just the value of the moment of inertia given by the cranking model [6]).

It is now of interest to check the separability of the ground state oscil-

lator wave function in the collective-intrinsic representation defined by the co-ordinate θ_3.

The expectation value of θ_3^2 is given by

$$\langle\theta_3^2\rangle \approx \frac{\hbar^2}{8\langle L^2\rangle}(1+\delta)(2-\delta) \tag{45}$$

o the order $1/N$. Then

$$\langle L^2\rangle\langle\theta_3^2\rangle = \frac{\hbar^2}{8}(1+\delta)(2-\delta) = \frac{\hbar^2}{8}[\tfrac{9}{4}-(\delta-\tfrac{1}{2})^2]. \tag{46}$$

Unlike the case of the co-ordinate θ_2 which gives separation except for terms of order $1/N$, eq. (46) differs from $\hbar^2/4$ by an expression of zero order in $1/N$. This expression however is still reasonably small, having a maximum value of $\frac{9}{8}\hbar^2/4$ for $\delta = \frac{1}{2}$. According to theorem 4 of section 3.1 the ground state oscillator wave function can be expressed as the sum of a wave function separable in θ_3 and a remainder whose amplitude squared

$$a_r^2 \leqq \sqrt{\tfrac{1}{8}[\tfrac{9}{4}-(\delta-\tfrac{1}{2})^2]}-\tfrac{1}{2} \leqq \sqrt{\tfrac{9}{32}}-\tfrac{1}{2} \approx 0.03. \tag{47}$$

References

1) K. Alder, A. Bohr, T. Huus, B. Mottelson and A. Winther, Revs. Mod. Phys. **28** (1956) 432
2) S. G. Nilsson, Mat. Fys. Medd. Dan. Vid. Selsk. **29** (1955) no. 16
3) H. J. Lipkin and S. Goldstein, Nuclear Physics **5** (1958) 202
4) R. E. Peierls and J. Yoccoz, Proc. Phys. Soc. A **70** (1957) 381; J. Yoccoz, Proc. Phys. Soc. A **70** (1957) 388
5) T. H. R. Skyrme, Proc. Phys. Soc. A **70** (1957) 433
6) J. J. Griffin and J. A. Wheeler, Phys. Rev. **108** (1957) 311
7) D. R. Inglis, Phys. Rev. **96** (1954) 1059
8) A. Bohr and B. Mottelson, Mat. Fys. Medd. Dan. Vid. Selsk. **30** (1955) no. 1
9) H. J. Lipkin, A. de-Shalit, and I. Talmi, Phys. Rev. **103** (1956) 1773
10) B. Mottelson, Proc. Rehovoth Conference on Nuclear Structure (North Holland Publishing Company, Amsterdam, 1958)

1.B *Nuclear Physics* 7 (1958) 195—201; © *North-Holland Publishing Co., Amsterdam*
Not to be reproduced by photoprint or microfilm without written permission from the publisher

NOTE ON EFFECTIVE RANGE THEORY

N. AUSTERN †

The F.B.S. Falkiner Nuclear Research and Adolph Basser Computing Laboratories, School of Physics, University of Sydney††

Received 28th January 1958

Abstract: It is shown that the basic formula of effective range theory may be derived from the orthogonality of wave functions. The results of this theory therefore are not limited in their application to systems which can be described by a phenomenological Schrödinger equation. Some discussion is given of n—p scattering with tensor forces, of the Bethe-Longmire theory of deuteron photodisintegration, and of partial waves of angular momentum greater than zero. It is remarked that the Bethe-Longmire result for the electric dipole photodisintegration may be derived without any consideration of the nature of the neutron-proton interaction.

1. General Method

The ordinary "effective range theory" is made up of two distinct parts: (1) a certain formula [eq. (10) of ref. [1])], which is a mathematical identity, (2) certain qualitative ideas about nuclear forces †††. The formula is useful if the qualitative properties of the forces are such that one part of it must vary slowly with energy, it then being convenient for interpolating between differing energies and for correlating different sorts of experiments.

Derivations of the basic formula generally start from an explicit form of the Schrödinger equation for the system, and would seem to be only as valid as the particular sort of phenomenological interaction in terms of which that equation was written. A simplified derivation will be given here. It will be shown that orthogonality * of the solution functions in fact is the only property of the Schrödinger equation which must be employed; that the formula therefore may be applied without consideration of the detailed nature of the two-body interaction. It is not even necessary that a phenomenological description of the system be possible.

† Fulbright Research Scholar, on leave from University of Pittsburgh.

†† Also supported by the Nuclear Research Foundation within the University of Sydney.

††† The qualitative ideas must be built into the theory separately, and are in no way automatically embodied in the basic formula, which is only a context for them. Attempts to use the basic formula with unrealistic nuclear interactions have been shown to lead to paradoxical results. See ref. [2]).

* Other authors have noted the appearance of the orthogonality property in the basic formula, but apparently did not attempt to use it as a basis for the derivation. See ref. [3]).

The approach to be followed here is based upon a new interpretation of the usual calculations. Its nature is rather fully exhibited by a discussion of the familiar s wave neutron-proton system. For this case the effective range formula is

$$\frac{k_1 \cot \delta_1 - k_2 \cot \delta_2}{k_1^2 - k_2^2} = \tfrac{1}{2}\rho(E_1, E_2), \tag{1}$$

with

$$\tfrac{1}{2}\rho(E_1, E_2) = \int_0^\infty (U_1 U_2 - N_1 N_2 u_1 u_2)\mathrm{d}r. \tag{2}$$

The subscripts 1 and 2 refer throughout to the energies E_1 and E_2, δ and k are the phase shift and wave number at the energy E, and u_E is the radial S wave function at the energy E, with the usual plane wave normalization. Also U_E is the asymptotic function

$$U_E = \frac{\sin(kr+\delta)}{\sin\delta}, \tag{3}$$

and N_E is a normalization constant, so chosen that

$$\lim_{r\to\infty} N_E u_E = U_E. \tag{4}$$

In the present circumstance N_E is seen to be $(\sin\delta)^{-1}$.

Eq. (1) becomes interesting when it is pointed out, in the usual way, that $\rho(E_1, E_2)$ is a slowly varying function of its arguments. This follows because in (2) the two terms of the integrand are identically equal outside the region of the nuclear force. The integrand then is large only where the potential energy is much larger than the total energy, where the latter therefore is of minor importance in determining the shape of the wave function. The normalization of the wave function, in addition, is defined to be $U_E(r = 0) = 1$, a constant; accordingly, both the shape and amplitude of the integrand are nearly energy independent.

Now, the new point of view to be discussed in this paper is that the integral $\frac{1}{2}\rho(E_1, E_2)$ defined in (2) may be understood as an integral representation of the algebraic expression which is the left hand side of (1). With this understanding of the meaning of the integral it then becomes natural to ask which other integral forms might be equally valid representations of the algebraic expression, and whether these alternative forms also might be convenient for physical discussion.

It is important that the two terms in the integrand in (2) do not play equal roles. Except where $E_1 = E_2$, the second term contributes exactly zero to the integral, u_1 and u_2 being orthogonal. It is the $U_1 U_2$ term, composed entirely of elementary functions, which actually gives the integral representation. If this term is evaluated separately, a convergence factor

being employed, the result is

$$\lim_{\omega \to 0} \int_0^\infty U_1 U_2 e^{-\omega r} dr$$
$$= \lim_{\omega \to 0} \left[\frac{\omega}{\omega^2 + (k_1 - k_2)^2} \right] \frac{\cos(\delta_1 - \delta_2)}{2 \sin \delta_1 \sin \delta_2} + \frac{k_1 \cot \delta_1 - k_2 \cot \delta_2}{k_1^2 - k_2^2}$$
$$= \frac{\pi}{2} \frac{\delta(k_1 - k_2)}{\sin \delta_1 \sin \delta_2} + \tfrac{1}{2} \rho(E_1, E_2). \tag{5}$$

From a purely formal point of view, then, the only role of the $u_1 u_2$ term in (2) is to serve as a counter-term to the $\delta(k_1 - k_2)$ term of (5), making the integral representation continuous at $E_1 = E_2$.

Eq. (5) is useful in emphasizing the mathematical structure of (2), showing that for (2) to be a mathematical identity it is only required of the system that its wave functions be orthogonal, so as to yield the function $\delta(k_1 - k_2)$. The various other physical statements which are built into the usual developments of the theory are used at a latter stage, for the qualitative discussion of the energy variation of $\rho(E_1, E_2)$.

The generalization of (2), which is the result of this paper, is obtained by representing $\delta(k_1 - k_2)$ in terms of the relevant wave functions, according to the expression

$$\frac{\pi}{2} \delta(k_1 - k_2) = (\psi_{k_1}^{(\alpha)}, \psi_{k_2}^{(\alpha)}),$$

rather than in the more elementary fashion employed in (2). Here $\psi_k^{(\alpha)}$ is the eigenstate (α) of the S matrix, with energy $E = \hbar^2 k^2 / 2m$. The generalization of (2) then is

$$\tfrac{1}{2} \rho_{(\alpha)}(E_1, E_2) = \int_0^\infty U_1 U_2 \, dr - N_1 N_2 (\psi_{k_1}^{(\alpha)}, \psi_{k_2}^{(\alpha)}). \tag{6}$$

Eq. (6) gives the effective range for the eigenwave (α), and may be used as it stands even if the hamiltonian for the system contains velocity-dependent potentials, or non-local potentials, or tensor potentials, or even if a phenomenological description of the system is not possible. In this last case, where a field theory must be used, $\psi_k^{(\alpha)}$ describes the collision of two "dressed" nucleons; N must be so chosen that $N \psi_k^{(\alpha)}$ gives U_k for the relative motion of the mass centres of the two nucleons, at distances sufficiently large for the polarization of their meson clouds to be negligible.

Similar discussions may be carried out also for those physical systems for which different asymptotic functions must be used. In the case of proton-proton scattering, for example, the standard function $v_E(r)$ appears [1, 4]) in place of the function $U_E(r)$ of eq. (3), and the phase shift occurs not in the form $k \cot \delta$, but in the form of the Smorodinsky f function, the logarithmic derivative of $v_E(r)$ at $r = 0$. In any event, all discussions of this sort always have in common the use of a scalar product of two state

functions to cancel out a $\delta(k_1-k_2)$ infinity from an integral representation of some simple expression.

Section 2, below, shows how the method may be used for low-energy n—p scattering with tensor forces. Section 3 shows that the Bethe-Longmire treatment of deuteron photodisintegration is always valid, whatever the nature of the n—p interaction. Section 4 comments about the procedure to be used for partial waves having angular momentum greater than zero.

2. The Case of Tensor Forces

As a simple illustration of the utility of eq. (6) the low energy neutron-proton triplet state scattering will be discussed in this section †.

Each relevant eigenstate of the S matrix is a mixture of S and D waves, such that the S and D parts of the mixture each have the same scattering phase shift. Two such eigenstates exist ††. At low energy one is mostly S wave, and dominates the scattering, while the other is mostly D wave. For either state the form of the wave function is

$$\psi_k^{(\alpha)} = \frac{1}{r\sqrt{4\pi}}\left\{u_k^{(\alpha)}(r) + \frac{1}{\sqrt{8}} S_{12} w_k^{(\alpha)}(r)\right\} \chi_1^m, \tag{7}$$

where for large r

$$u_k^{(\alpha)} \sim \sin(kr+\delta^{(\alpha)}), \tag{8}$$

$$w_k^{(\alpha)} \sim -\eta^{(\alpha)} \sin(kr+\delta^{(\alpha)}). \tag{9}$$

For the important state, $\eta^{(\alpha)}$ is very small at low energy, and proportional to the energy. (For the other state, γ, it may be shown that $\eta^{(\gamma)} = -1/\eta^{(\alpha)}$.) The various symbols in (7) are standard, S_{12} denoting the tensor operator, and χ_1^m the triplet spin function.

Substitution of (7) into (6) gives

$$\tfrac{1}{2}\rho(E_1, E_2) = \int_0^\infty \{U_1 U_2 - N_1 N_2 (u_1 u_2 + w_1 w_2)\} \mathrm{d}r, \tag{10}$$

for convenience the label (α) now being omitted. To evaluate $N_1 N_2$, completing the formal derivation, we recall that the integrand must be made to vanish at large r. Then from (3), (8), (9) it follows that

$$N_1 N_2 = [\sin\delta_1 \sin\delta_2 (1+\eta_1\eta_2)]^{-1}. \tag{11}$$

It is interesting that in the special case where $\rho(0, E)$ is desired, often the case of interest, the product $\eta_1\eta_2$ reduces to zero. This happens because η_E vanishes linearly with E. Indeed, it is customary to approximate $\eta_1\eta_2$

† A very extensive analysis of this problem has been given in ref. [5]). The present approach first was applied during a recent discussion with Dr. Elizabeth Baranger, for whose interest I am grateful.

†† For a complete analysis of the S matrix of the neutron-proton system with spin-orbit coupling see ref. [6]).

as zero even when neither of the energies actually vanishes. This is reasonable, because for energies of a few MeV the order of magnitude of η is about 10^{-2}.

3. Extension of the Bethe-Longmire Theory

Bethe and Longmire [7]) demonstrate a connection between the scattering effective range and the normalization of the asymptotic part of the ground state wave function for the deuteron. Since low-energy electric dipole photodisintegration can be computed very accurately in terms of just this asymptotic wave function, it follows that the scattering experiments give enough information for a complete calculation of the low energy E1 photoeffect. It will now be shown that the Bethe-Longmire connection between the effective range and the ground state normalization is true in a far wider context than the one in which it was first demonstrated. In particular, it is true even if the wave function of field theory is used, involving all the internal variables describing virtual mesons †.

As discussed so far $\rho(E_1, E_2)$ has been defined only for both E_1 and E_2 positive. Fortunately the integral representation is sufficiently general to be easily extended to negative energies. For $U_{-\varepsilon}$, where ε is the deuteron binding energy, we merely use the deuteron asymptotic wave function. This is given the normalization

$$U_{-\varepsilon}\,(r = 0) = 1,$$

in accord with the energy-independent normalization used for $U_E\ (r = 0)$ in section 1 ††. Then the same examination of the integral representation formula which suggested that $\rho(E_1, E_2)$ is a slowly varying function of E_1 and E_2 when in the continuum now suggests that $\rho(E_1, E_2)$ again has much the same value when either one or both of E_1 and E_2 equals $-\varepsilon$. In detail, the expressions become

$$U_{-\varepsilon} = \mathrm{e}^{-\gamma r}, \tag{12}$$

$$\tfrac{1}{2}\rho(-\varepsilon,\ -\varepsilon) = \int_0^\infty (\mathrm{e}^{-\gamma r})^2\,\mathrm{d}r - N_{-\varepsilon}^2(\psi_{-\varepsilon},\ \psi_{-\varepsilon}) = \frac{1}{2\gamma} - N_{-\varepsilon}^2. \tag{13}$$

Here in (13) advantage has been taken of the fact that $\psi_{-\varepsilon}$ by definition is normalized to unity; and that for the bound state the two terms of the integral expression are separately convergent. These two terms have been evaluated explicitly.

† This result of the present paper first was obtained in 1954, at Cornell University, as an initial part of an investigation, with A. M. Sessler, of the corrections to the Bethe-Longmire paper arising from quantum field theory.

†† No account should be taken in $U_{-\varepsilon}$ of the higher Fock space terms of $\psi_{-\varepsilon}$, just as none was taken of them for the continuum case. That the two cases be discussed in terms of effective ranges which are as nearly alike as possible is the property we most desire.

We may follow Bethe-Longmire, and solve (13) for $N^2_{-\varepsilon}$:

$$N^2_{-\varepsilon} = \frac{1}{2\gamma} - \tfrac{1}{2}\rho(-\varepsilon, -\varepsilon). \tag{14}$$

It is seen that $N_{-\varepsilon}$ can be evaluated in terms of the scattering effective range, since, on account of the slow energy variation of $\rho(E_1, E_2)$, the value $\rho(-\varepsilon, -\varepsilon)$ is nearly equal to the directly measured $\rho(0, 0)$ or $\rho(0, -\varepsilon)$. Finally, the definition of $N_{-\varepsilon}$ (see section 1) requires that $N_{-\varepsilon}\psi_{-\varepsilon}$ go asymptotically to $e^{-\gamma r}$, so the asymptotic $\psi_{-\varepsilon}$ is

$$\lim_{r\to\infty} \psi_{-\varepsilon} = e^{-\gamma r}/N_{-\varepsilon}; \tag{15}$$

all the constants in this expression are known. The E1 photodisintegration may now be computed.

4. Higher Angular Momenta

The effective range theory is somewhat awkward for partial waves having angular momentum greater than zero. Nevertheless, insofar as useful expressions have been obtained the method of the present paper simplifies and generalizes their derivations.

The difficulty lies entirely in the nature of the asymptotic wave function of the two-body system. For each partial wave it is a linear combination of spherical Bessel and Neumann functions:

$$u_l^{(\infty)}(r) = kr\{\cos\delta \cdot j_l(kr) - \sin\delta \cdot n_l(kr)\}. \tag{16}$$

The j_l and n_l reduce to the well-behaved sine and cosine only for $l = 0$. For $l > 0$ they are made up from sines and cosines multiplied by polynomials in $(kr)^{-1}$. The function n_l diverges at $kr = 0$, its variation there being as $(kr)^{-l}$. The correct scattering wave function for the system has, of course, no such divergence, but an effective range formula must be built principally from the asymptotic function, and the divergence of n_l accordingly leads to trouble.

The trouble is two-fold. (1) It is difficult to employ divergent functions to build an integral which is a well-behaved function (of E_1, E_2, δ_1, δ_2) everywhere except at $E_1 = E_2$, and which has a $\delta(k_1 - k_2)$ singularity at that point. (2) It is impossible to adjust the normalization of the divergent $u_l^{(\infty)}(r)$ to give a function having the nature of $U_E(r)$ of eq. (2), whose amplitude at $r = 0$ will be independent of energy.

These difficulties have been circumvented by various authors in one or the other of two ways: either by building an integral formula which involves a cut-off [8]), or by building an integral formula from other functions than the $u_l^{(\infty)}(r)$, and which are not divergent †.

† See ref. [8]). Similar methods also have been developed by M. Baranger (unpublished).

If a cut-off is used the effective range formula simply becomes

$$\tfrac{1}{2}\rho_l(E_1,\ E_2) = \int_b^\infty U_1^{(l)} U_2^{(l)}\,\mathrm{d}r - N_1 N_2(\psi_1^{(l)},\ \psi_2^{(l)}), \tag{17}$$

with

$$\tfrac{1}{2}\rho_l(E_1,\ E_2) = \frac{1}{k_1^2 - k_2^2}\left\{\frac{\mathrm{d}}{\mathrm{d}r}U_1^{(l)}(r) - \frac{\mathrm{d}}{\mathrm{d}r}U_2^{(l)}(r)\right\}_{r=b}, \tag{18}$$

$$U_E^{(l)}(r) = u_l^{(\infty)}(r)/u_l^{(\infty)}(b). \tag{19}$$

This procedure was used by Brueckner [8]) when he set up an effective range treatment of meson-nucleon scattering. Most of the calculation done in his paper led only to the demonstration that the $\psi_E^{(l)}$ form an orthogonal set, which here is presumed to be true without demonstration. It is interesting that in the limit $kb \to 0$ the energy dependence of δ_l may be expressed [8]) in terms of only one effective range parameter, a composite of b and ρ_l.

If the other procedure is followed, in which the $u_l^{(\infty)}$ functions are modified to give $\tilde{u}_l^{(\infty)}$ functions which are finite at $r = 0$, the introduction of a more or less arbitrary cut-off is avoided. The modification of $u_l^{(\infty)}$ to give $\tilde{u}_l^{(\infty)}$ is achieved by subtracting from $u_l^{(\infty)}$ the singular terms. The resulting integral representation formula † then tends to be somewhat more complicated than (17), but still involves the exact wave functions of the system in just the same way. They form a $\delta(k_1 - k_2)$ counterterm which makes the integral representation continuous at $E_1 = E_2$.

I am grateful to Drs. M. Baranger, J. M. Blatt, E. E. Salpeter and A. M. Sessler for helpful discussions concerning this paper.

† The mathematical analysis is given in full by Biedenharn and Blatt [5]) for the case of D waves, in their discussion of the "β state".

References

1) H. A. Bethe, Phys. Rev. **76** (1949) 38
2) R. G. Newton, Phys. Rev. **105** (1957) 763
3) J. M. Blatt and V. F. Weisskopf, Theoretical Nuclear Physics (John Wiley and Sons, New York, 1952)
4) R. G. Sachs, Nuclear Theory (Addison-Wesley Publishing Co., 1953) pp. 125–127
5) L. C. Biedenharn and J. M. Blatt, Phys. Rev. **93** (1954) 1387; R. S. Christian, Phys. Rev. **75** (1949) 1675; Y. Yamaguchi, Prog. Theor. Phys. **6** (1951) 439
6) J. M. Blatt and L. C. Biedenharn, Phys. Rev. **86** (1952) 399
7) H. A. Bethe and C. Longmire, Phys. Rev. **77** (1950) 647
8) K. A. Brueckner, Phys. Rev. **87** (1952) 1026

2.I *Nuclear Physics* **7** (1958) 202—208; © *North-Holland Publishing Co., Amsterdam*
Not to be reproduced by photoprint or microfilm without written permission from the publisher

MEASUREMENTS OF (γ, d) AND (γ, np) REACTIONS IN THE THRESHOLD REGION

J. GOLDEMBERG
Departamento de Fisica, Universidade de São Paulo, São Paulo
and
L. MARQUEZ
Centro Brasileiro de Pesquisas Fisicas, Rio de Janeiro, Brazil †

Received 10 January 1958

Abstract: The yield of the combined nuclear reactions (γ, d) and (γ, np) has been measured for Zn^{64}, Zn^{66}, Fe^{54} and S^{32} by isolating and measuring the activity of the residual nucleus. In the first two cases we found a curve for the cross section with two peaks. In the third case, no residual activity was found and an upper limit is given for the yield. In the fourth case the results found coincide with the results of other workers who had measured this reaction.

1. Introduction

The investigation of (γ, d) reactions at low energies has attracted some interest recently [1, 2]. Sawicki [1]) calculated the cross section for the photoemission of deuterons assuming a mechanism in which the outgoing proton "picks up" a neutron in the outside shells of the nucleus; using the independent particle model he obtains cross sections of a few millibarns, which are of the correct order of magnitude, although bigger than expected on the evaporation model.

It has been noticed in all the investigated cases that the reactions (γ, d) and (γ, np) occur about 10—100 times more frequently than expected. This is the case in sulphur [3]) and copper [4, 5]). These measurements, however, give no more information than the cross section at a few energies.

At higher energies (50—150 MeV) a number of measurements have been made [6, 7]), including the energy distribution of the emitted protons and the angular correlation of protons and neutrons. The "quasi-deuteron" model of Levinger [8]) seems to be quite successful in explaining the results.

In the low energy experiments, Katz and Penfold used the residual activity in P^{30} formed in the reactions (γ, d) and (γ, np) in S^{32} to measure the cross section for the reaction. Preliminary work of the same type has been made by S. S. Villaça and J. Goldemberg in several other elements [9]). In

† This work was done under the auspices of the Conselho Nacional de Pesquisas of Brazil.

this type of experiment the only hope of distinguishing between the emission of deuterons and uncorrelated neutrons and protons is the threshold for the reaction which is 2.23 MeV smaller for (γ, d) than (γ, np). No peculiarity was found in this region by Katz and Penfold, who report, however, the existence of a "bump" in the cross section at higher energies, attributed to the fall of (γ, d) and rise of (γ, np) reaction. This interpretation can, however, be seriously criticized.

In this paper a report is made on measurements of reactions (γ, d) and (γ, np) in S^{32}, Zn^{64}, Zn^{66} and Fe^{54}; radiochemical methods were used to separate the parent from the daughter nucleus, respectively P^{30}, Cu^{62}, Cu^{64} and Mn^{54}.

Great care was taken in measurements in the 2 MeV region above the (γ, d) and below the (γ, np) threshold. The results show that in this region the (γ, d) cross section goes through a resonance with a maximum of about 1 mb; at energies above the (γ, np) threshold the cross section rises again to ≈ 3 mb and goes probably through a second maximum.

2. Experimental Procedure

Sample of materials containing sulphur, zinc and iron were irradiated in the X-ray beam of the 22 MeV Betatron of the University of São Paulo in energies ranging from 16 to 22 MeV variable in steps of 500 keV. In table 1 pertinent data on the irradiation are given. Table 2 gives the thresholds for

TABLE 1
Data on irradiation

Parent nucleus	Material used	Quantity of sample (g)	Daughter nucleus	Half-life	Time of irradiation (min)
S^{32}	$(NH_4)_2SO_4$	150	P^{30}	2.55 min	5
Zn^{64}	ZnO	20	Cu^{62}	10 min	10
Zn^{66}	ZnO	20	Cu^{64}	12.9 h	20
Fe^{54}	$Fe(NO_3)_3$	5	Mn^{52}	21 min + 6.5 d	20

TABLE 2
Reaction thresholds

Parent nucleus	Daughter nucleus	Threshold for (γ, d) (MeV)	Threshold for (γ, np) (MeV)
S^{32}	P^{30}	19.15	21.38
Zn^{64}	Cu^{62}	16.01	18.24
Zn^{66}	Cu^{64}	16.42	18.65
Fe^{54}	Mn^{52}	16.54	18.77

the pertinent reactions, calculated from the work of Wapstra [10]). The chemical separations are described in the appendix. In each case a test of purity of the substance used was made, following carefully the decay of one sample and checking the half-life; chemical tests of purity were also made. In the case of Zn^{64} the absolute activity was found by comparison with the activity induced in Cu^{63} by a (γ, n) reaction, which gives exactly the same end product Cu^{62}.

3. Results

The excitation function and cross section for the reaction $Zn^{64}(\gamma, d)Cu^{62} + Zn^{64}(\gamma, np)Cu^{62}$ are shown in fig. 1.

In the measurements of Zn^{66} a difficulty arises due to the fact that the reaction $Zn^{68}(\gamma, p)Cu^{67}$ contributes appreciably to the counting rate; it was decided not to eliminate this reaction in order to have something to compare with the (γ, d) reaction. The excitation function for the $Zn^{66}(\gamma, d)Cu^{64} + Zn^{66}(\gamma, np)Cu^{64}$ is shown in fig. 2 together with the results of the reaction $Zn^{68}(\gamma, p)Cu^{67}$. The cross section for the (γ, d) and (γ, np) is also shown.

The excitation function of fig. 2 clearly shows the slope change in the (γ, d) and (γ, np) curve responsible for the first maximum in the cross section curve. This change of slope is absent in the (γ, d) reaction although this is a reaction in which charged particles are emitted too.

It was thought that a good check of the experimental procedure was to remeasure the (γ, d) reaction in S^{32} and the results obtained are shown in fig. 3, normalized to those of Katz and Penfold at 22 MeV. The good agreement in shape of the two curves indicates that no peculiarity of the kind found in Zn is present between 19.15 and 21.38 MeV; our measurements do not extend to 25 MeV.

Finally a careful search was made of any activity provenient from the 21 min isomeric state of Mn^{52} and the same was done with the 6.5 day activity; none of these were found and this enables us to put an upper limit in the reaction $Fe^{54}(\gamma, d)Mn^{52} + Fe^{54}(\gamma, np)Mn^{52}$ of 1/30 the value found for the reaction $Zn^{64}(\gamma, d)Cu^{62} + Zn^{64}(\gamma, np)Cu^{62}$. The upper limit of the yield per mole per 100 R/min in Fe^{54} is 2.5×10^4 at our maximum energy. No reason for this anomalous low yield was found.

4. Discussion

The curves of the reactions in Zn show a peculiar shape which does not appear in Sawicki's paper; this behaviour could apparently not arise from competition due to the onset of the (γ, np) reaction. The results are more of the kind of the photodisintegration of the deuteron, with a sudden rise and falling down in the cross section; we feel tempted to say that some outgoing

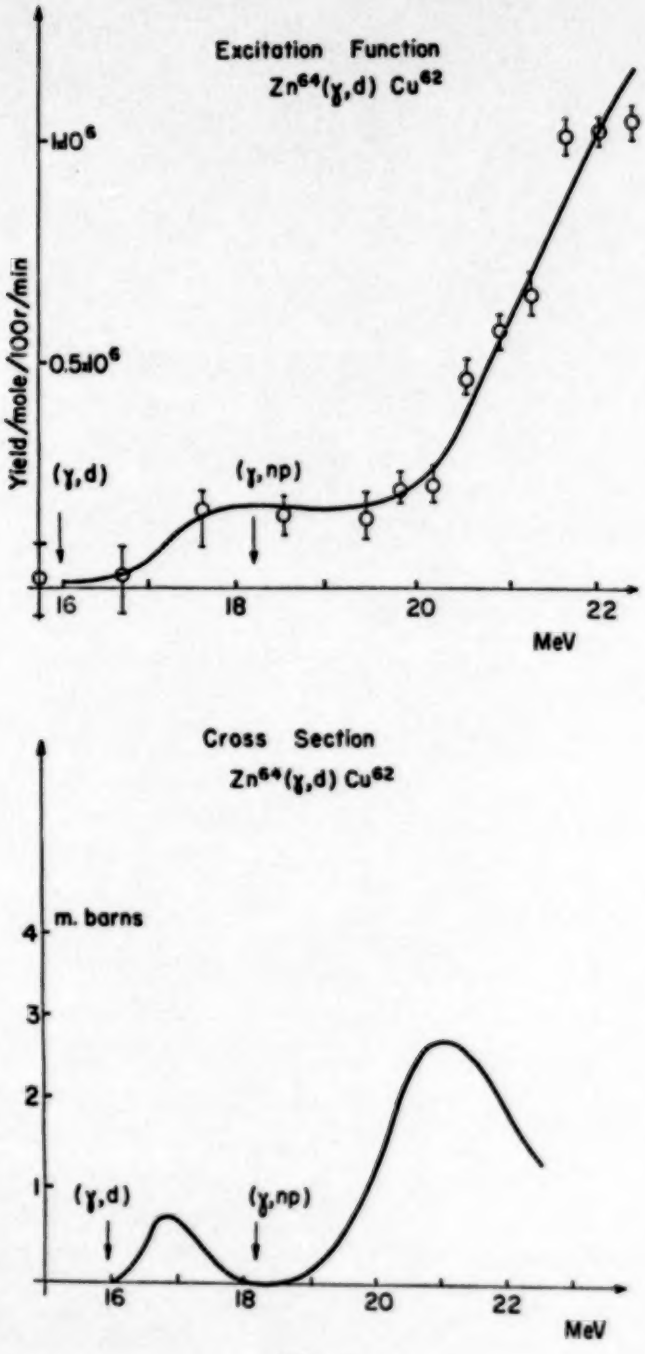
Excitation Function
Zn64(γ,d) Cu62
1.0^6
0.5.10^6
Yield/mole/100r/min
(γ,d)
(γ,np)
16
18
20
22
MeV
Cross Section
Zn64(γ,d) Cu62
m. barns
4
3
2
1
(γ,d)
(γ,np)
16
18
20
22
MeV

Fig. 1

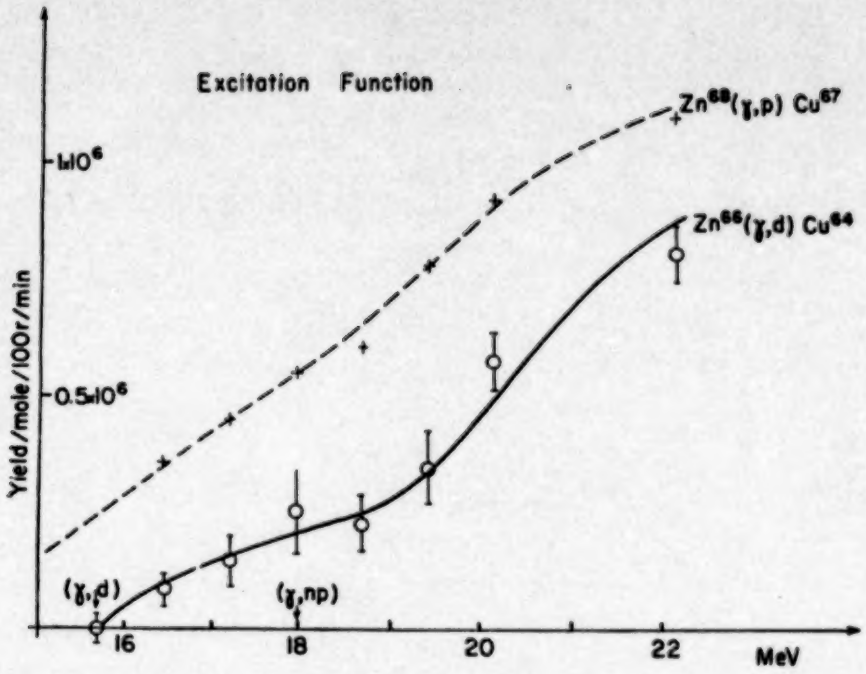
Excitation Function
$Zn^{68}(\gamma,p)\ Cu^{67}$
$Zn^{66}(\gamma,d)\ Cu^{64}$
1.10^6
0.5.10^6
Yield/mole/100r/min
(γ,d)
(γ,np)
16
18
20
22
MeV

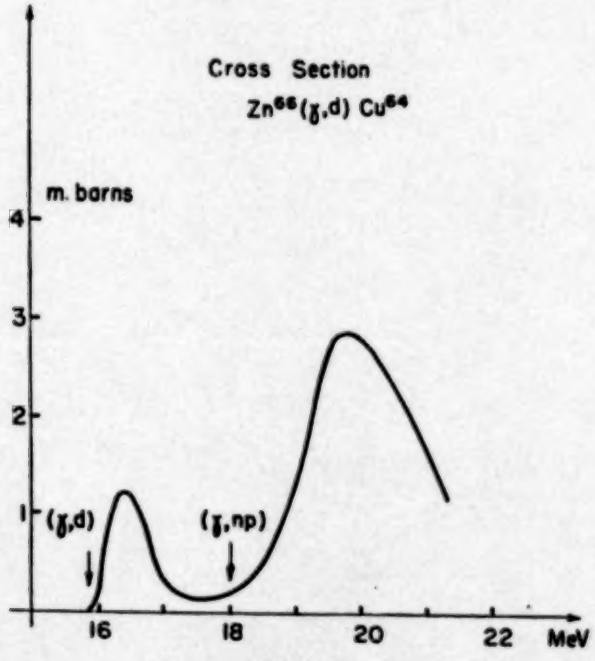
Cross Section
$Zn^{66}(\gamma,d)\ Cu^{64}$
m. barns
4
3
2
1
(γ,d)
(γ,np)
16
18
20
22
MeV

Fig. 2

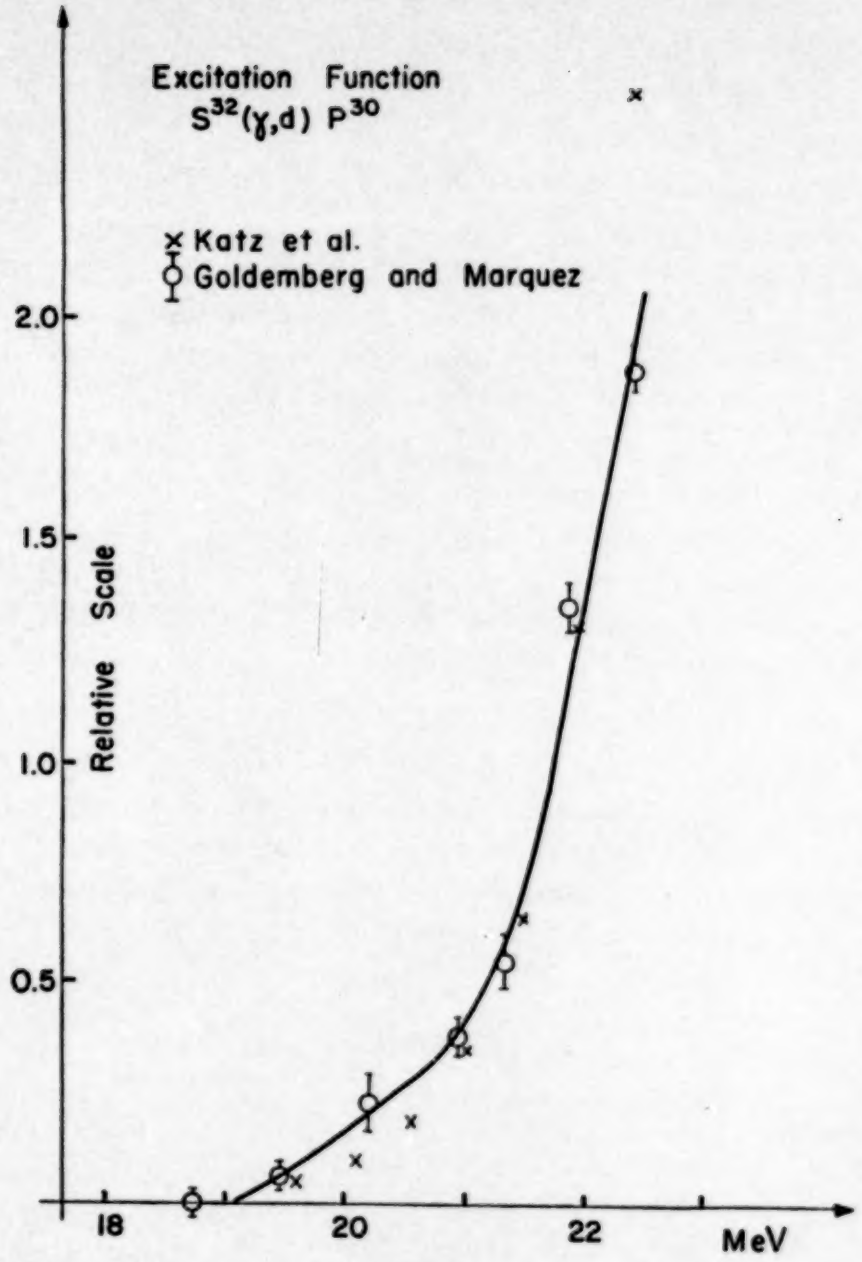
Excitation Function
$S^{32}(\gamma,d)\ P^{30}$
Katz et al.
Goldemberg and Marquez
Relative Scale
2.0
1.5
1.0
0.5
18
20
22
MeV

Fig. 3

neutrons of the nucleus (there are about 100 times as many neutrons as deuterons in this energy region) can "pick-up" protons with the right momentum to form bound deuterons and come out. As the energy of the neutrons increases, less of these processes occur until there is enough energy for the emission of uncorrelated neutrons and protons.

More experimental work is in progress in other elements.

Appendix

SEPARATION OF Cu FROM Zn

The irradiated ZnO was dissolved in 12NHCl, 20 mg of Cu^{++} added, diluted with H_2O and the Cu^{++} reduced to Cu^{+} with sodium bisulphite. The Cu was precipitated with NH_4SCN, the precipitate of CuSCN was coagulated in an ice bath, filtered, dried, weighed and counted with a NaI scintillation counter.

SEPARATION OF P FROM S

The irradiated $(NH_4)_2SO_4$ was dissolved in hot water, 1 mg of P as PO_4^{-3} added, then were added NO_2^-, HNO_3 and 20 mg of Fe^{+++}. The Fe was precipitated with an excess of NH_4OH and it carried the P. The precipitate was quickly filtered and counted with a thin wall Geiger counter.

SEPARATION OF Mn FROM Fe

The irradiated hydrated ferric nitrate was dissolved in hot HNO_3 and 20 mg of Mn^{++} added. The Mn was precipitated as MnO_2 with $KClO_3$, the solution was diluted with water, cooled, filtered, weighed and placed in a test tube thick enough to absorb all the positons. The samples were counted with a well crystal scintillation spectrometer, set to count annihilation radiation.

References

1) J. Sawicki, Nuclear Physics **4** (1957) 248
2) B. Forkman, Ark. Fys. **11** (1956) 265
3) L. Katz and A. S. Penfold, Phys. Rev. **81** (1951) 815
4) P. R. Byerly and W. E. Stephens, Phys, Rev. **83** (1951) 54
5) W. H. Smith and L. J. Laslett, Phys. Rev. **86** (1952) 523
6) M. M. Hoffman and A. G. W. Cameron, Phys. Rev. **92** (1953) 1184
7) J. H. Smith and M. Q. Barton, Phys. Rev. **100** (1955) 126
8) J. S. Levinger, Phys. Rev. **84** (1951) 43
9) S. S. Villaça and J. Goldemberg, An. Acad. Bras. Ciencias **27** (1955) 427
10) A. H. Wapstra, Physica **21** (1955) 367 and 385

1.D.2 *Nuclear Physics* 7 (1958) 209—216; © *North-Holland Publishing Co., Amsterdam*
Not to be reproduced by photoprint or microfilm without written permission from the publisher

SOME PROPERTIES OF THE IRREGULAR ROTATIONAL SPECTRA IN ODD-MASS NUCLEI

LENNART SIMONS
University of Helsinki

Received 4 November 1957

Abstract: An investigation is made of the spin sequence in the rotational spectra of odd-mass nuclei for the case $K = \frac{1}{2}$. One feature of this investigation is that it leads to a method for rapidly obtaining a survey of the spin sequence in various cases. An alternative interpretation is given, as an example, of the spectrum of Tm^{171} which differs essentially from an earlier interpretation.

1. Investigation of the Spin Sequence

It is well known that heavy odd-mass atomic nuclei with the lowest spin $K = \frac{1}{2}$ have irregular rotational spectra. This is considered to be due to the partial decoupling of the last odd-particle from the rotational motion. The energy of a rotational level with spin I, which has a half-integer value $\geqq \frac{1}{2}$, is, according to Bohr and Mottelson's theory [1]), given by

$$E = \frac{\hbar^2}{2J}[I(I+1)+a(-1)^{I+\frac{1}{2}}(I+\tfrac{1}{2})], \tag{1}$$

where J is an "irrotational" moment of inertia, and

$$a = \sum_j (-1)^{j-\frac{1}{2}}(j+\tfrac{1}{2})|c_j|^2, \tag{2}$$

$|c_j|^2$ representing the probability that the last odd particle has angular momentum j.

If we imagine such an extreme case that $j = 9/2$ and $|c_{9/2}|^2 = 1$, then $a = +5$, and in an extreme case with $j = 7/2$ and $|c_{7/2}|^2 = 1$ then $a = -4$. In general, however, $|a| < 2$.

For the case $K = \frac{1}{2}$, in contrast with other cases with $K \neq \frac{1}{2}$, the energy E does not always increase when I increases. By "spin sequence" we understand here the sequence of spins obtained in order of increasing energy, which is not the same as the sequence of spins in order of increasing I values. It frequently happens, for example, that the I value I_0 for the ground state, which has the lowest energy, is larger than K, i.e. $I_0 > \frac{1}{2}$.

A study is now made of the spin sequence in odd-mass nuclei. We consider the spins I to be in two groups:

June (3) 1958

$$I_- = \tfrac{1}{2}, 5/2, 9/2, \ldots$$
$$I_+ = 3/2, 7/2, 11/2, \ldots.$$

We may then rewrite eq. (1) in the form

$$E = \frac{\hbar^2}{2J}[I_-(I_-+1)-(I_-+\tfrac{1}{2})a]$$

or (3)

$$E = \frac{\hbar^2}{2J}[I_+(I_++1)+(I_++\tfrac{1}{2})a]$$

according to the particular group to which the spin value belongs. Introducing the parameters

$$u_- = \tfrac{1}{2}(a-2I_--1) \text{ and } u_+ = \tfrac{1}{2}(a+2I_++1) \quad (4)$$

eqs. (3) become

$$E = \frac{\hbar^2}{2J}\left[u_-{}^2 - \frac{a^2+1}{4}\right], \qquad E = \frac{\hbar^2}{2J}\left[u_+{}^2 - \frac{a^2+1}{4}\right]. \quad (5)$$

The term $\frac{1}{4}(a^2+1)$, which is independent of I, has no influence upon the derived spectrum (the difference between the level energies and the ground-state energy). We see from eqs. (4) that the expressions (5) coincide for $I_+ = 0$ and $I_- = -1$, i.e. when $u_\pm$ has the value $\frac{1}{2}(a+1)$.

We consider now the parabola $z = u^2$ drawn in rectangular coordinates with arbitrary scale. On a movable strip of paper we mark the spins I_+ and I_-, with the same numerical scale, on each side of the centre point P, where P corresponds with the position $I_+ = 0$ and $I_- = -1$ (see fig. 1). The strip

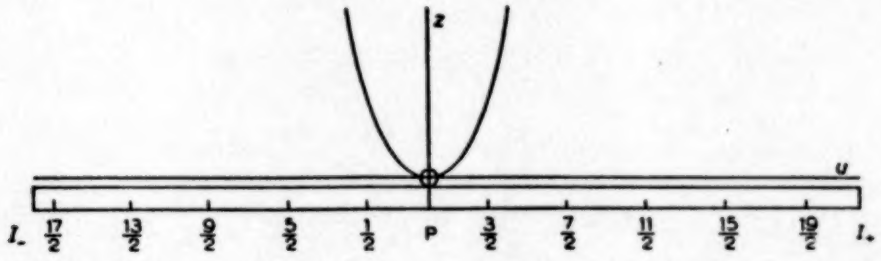

Fig. 1. The ordinates of the parabola give the energies of the levels. The paper strip is in a position corresponding to $a = -1$.

should be placed below the u-axis in such a way that the point P coincides with the point $u = \frac{1}{2}(a+1)$. The spectrum is then obtained by the subtraction of the smallest ordinate from the other ordinates and subsequent multiplication by the factor $\hbar^2/2J$ in accordance with eq. (5). The ordinates can thus be considered to constitute spectral terms from which the spectrum is obtained. The magnitude of the energy levels (z and therefore E) is obviously increased as the interval between the respective I-points and the origin O

(for which $u = 0$) is increased. Folding the strip at O one immediately obtains the spin sequence.

Since z is given by the square of the distance from the fold we see that the parabola itself is quite superfluous once the position of the folding place O has been determined. This position may be determined in the following manner:

$$\text{for } u = 0, \begin{cases} \text{if } a \geqq -1,\ I_- = \dfrac{a-1}{2}\ (\text{i.e. } I_- \geqq -1); \\ \text{if } a \leqq -1,\ I_+ = \dfrac{-a-1}{2}\ (\text{i.e. } I_+ \geqq 0); \end{cases}$$

the value of a, therefore, determines the position O.

In fig. 1 the paper strip is in the position where P and O coincide. This occurs at $a = -1$ and is a special case. In this case only, all levels coincide in pairs.

Instead of folding the strip the same results are obtained more conveniently with the aid of a second strip which is graduated in the opposite direction. The values to the right (or to the left) of the dividing line O are of actual interest. This dividing line can be marked by the edge of a sheet covering the values not required.

As an example let us consider the rotational spectrum[2]) of Pu^{239} for which $\hbar^2/2J = 4.62$ keV and $a = +3.146$. In order to obtain the spin sequence we first calculate I_- (since $a > -1$) and obtain $I_- = \frac{1}{2}(a-1) = 1.07$. In fig. 2 the strips have been displaced in such a way that the points $I_- = 1.07$

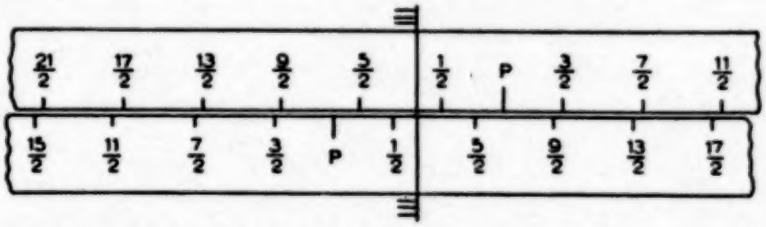

Fig. 2. The two paper strips indicate the spin sequences in the case $a = 3.146$.

of both strips coincide. To the right of the dividing line at 1.07 (or equally well to the left) we may now read the spin sequence: 1/2, 5/2, 9/2, 3/2, 13/2, 7/2, etc. The corresponding energy differences ΔE, in keV, are 0.0, 7.9, 52.8, 57.5, 134.7, 142.1, etc.

2. Coincidences

We may now deduce a number of interesting properties of the system, particularly with regard to the possible coincidence of levels. Levels may coincide only in pairs and this can occur only for integer a values. The properties which are of interest are shown in table 1. We may summarize these results in the following manner:

TABLE 1

Coincidences of levels

a	I_-	I_+	Coincidences			Comments
			I_- with I_+	I_- with I_-	I_+ with I_+	
10	9/2			√		$I_- = (\frac{1}{2}, \frac{17}{2})$, $(\frac{5}{2}, \frac{13}{2})$ only. Lowest level $I_- = \frac{9}{2}$ has no pair
9	4		√			$I_- < \frac{21}{2}$ have no pair. Lowest level $I_- = \frac{9}{2}$ has no pair
8	7/2			√		$I_- = (\frac{1}{2}, \frac{13}{2})$, $(\frac{5}{2}, \frac{9}{2})$ only. $(\frac{5}{2}, \frac{9}{2})$ are the lowest levels
7	3		√			$I_- < \frac{17}{2}$ have no pair. Lowest level $I_- = \frac{5}{2}$ has no pair
6	5/2			√		$I_- = (\frac{1}{2}, \frac{9}{2})$ only. Lowest level $I_- = \frac{5}{2}$ has no pair
5	2		√			$I_- < \frac{13}{2}$ have no pair. Lowest level $I_- = \frac{5}{2}$ has no pair
4	3/2			√		$I_- = (\frac{1}{2}, \frac{5}{2})$ only. $(\frac{1}{2}, \frac{5}{2})$ are the lowest levels
3	1		√	///// /////	///// /////	$I_- < \frac{9}{2}$ have no pair. Lowest level $I_- = \frac{1}{2}$ has no pair
2	1/2			//////	//////	No coincidences
1	0		√	//////	//////	Lowest level $I_- = \frac{1}{2}$ has no pair
0	−1/2			//////	//////	No coincidences
− 1	−1	0	√	///// /////	///// /////	No level is without pair. $(\frac{1}{2}, \frac{3}{2})$ are the lowest levels
− 2		1/2		//////	//////	No coincidences
− 3		1	√	//////	//////	Lowest level $I_+ = \frac{3}{2}$ has no pair
− 4		3/2		//////	//////	No coincidences
− 5		2	√	///// /////	///// /////	$I_+ < \frac{11}{2}$ have no pair. Lowest level $I_+ = \frac{3}{2}$ has no pair
− 6		5/2			√	$I_+ = (\frac{3}{2}, \frac{7}{2})$ only. $(\frac{3}{2}, \frac{7}{2})$ are the lowest levels
− 7		3	√			$I_+ < \frac{15}{2}$ have no pair. Lowest level $I_+ = \frac{7}{2}$ has no pair
− 8		7/2			√	$I_+ = (\frac{3}{2}, \frac{11}{2})$ only. Lowest level $I_+ = \frac{7}{2}$ has no pair
− 9		4	√			$I_+ < \frac{19}{2}$ have no pair. Lowest level $I_+ = \frac{7}{2}$ has no pair
−10		9/2			√	$I_+ = (\frac{7}{2}, \frac{11}{2})$ $(\frac{3}{2}, \frac{15}{2})$ only. $(\frac{3}{2}, \frac{15}{2})$ are the lowest levels

For odd a (i) Only levels belonging to different spin groups can coincide (i.e. only I_- with I_+).

(ii) All levels belonging to *one* spin group (i.e. I_+ *or* I_-) will form coincidences, while levels (with low spin values) belonging to the other group will not.

(iii) The lowest energy level is always without pair.

The singlest exception to results (ii) and (iii) occurs for $a = -1$: for this case only, no level is without pair.

For even a (iv) Only levels belonging to one and the same spin group can coincide (i.e. I_- with I_- or I_+ with I_+, not both).

(v) For $4 > a > -6$ there are no coincidences.

(vi) For $a \geqq 4$ and $a \leqq -6$ coincidences occur: for $a \geqq 4$, I_- with I_-; for $a \leqq -6$, I_+ with I_+.

(vii) For every second even spin value

$$a = \begin{cases} 4, 8, 12, 16, \ldots & \text{the lowest energy level is always paired;} \\ -6, -10, -14, -18, \ldots & \end{cases}$$

$$a = \begin{cases} 6, 10, 14, 18, \ldots & \text{the lowest energy level is never paired †.} \\ -8, -12, -16, -20, \ldots & \end{cases}$$

It is important to note that the ground state has the lowest spin ($\frac{1}{2}$) *only for* $-1 < a < 4$. When a increases, or decreases, a change in the spin sequence will occur at each coincidence.

The spin sequences for $-5 < a < 3$ are given in table 2. We see that only in the range $-1 < a < +1$ is the "normal" spin sequence obtained.

TABLE 2

Spin sequences

$-5 < a < -3$	$\frac{3}{2}\ \frac{7}{2}\ \frac{1}{2}\ \frac{11}{2}\ \frac{5}{2}\ \frac{15}{2}\ \frac{9}{2} \ldots .$
$a = -3$	$\frac{3}{2}\ \frac{1}{2}\ \frac{5}{2}\ \frac{9}{2} \ldots .$ $\frac{7}{2}\ \frac{11}{2}\ \frac{15}{2} \ldots .$
$-3 < a < -1$	$\frac{3}{2}\ \frac{1}{2}\ \frac{7}{2}\ \frac{5}{2}\ \frac{11}{2}\ \frac{9}{2}\ \frac{15}{2} \ldots .$
$a = -1$	$\frac{1}{2}\ \frac{5}{2}\ \frac{9}{2} \ldots .$ $\frac{3}{2}\ \frac{7}{2}\ \frac{11}{2} \ldots .$
$-1 < a < +1$	$\frac{1}{2}\ \frac{3}{2}\ \frac{5}{2}\ \frac{7}{2}\ \frac{9}{2}\ \frac{11}{2}\ \frac{13}{2} \ldots .$
$a = +1$	$\frac{3}{2}\ \frac{7}{2}\ \frac{11}{2} \ldots .$ $\frac{1}{2}\ \frac{5}{2}\ \frac{9}{2}\ \frac{13}{2} \ldots .$
$+1 < a < +3$	$\frac{1}{2}\ \frac{5}{2}\ \frac{3}{2}\ \frac{9}{2}\ \frac{7}{2}\ \frac{13}{2}\ \frac{11}{2} \ldots .$

For levels with equal energies the corresponding spins are placed one above the other.

† Only for these cases, and for the lowest energy levels when $a = 2$ and $a = -4$, does $z = 0$.

It should be noted that if a more accurate expression for E is used (eq. (1') in the following section) the spin sequence obtained may differ from that derived from eq. (1) in certain cases, viz. when I has large values and when a has near-integral values.

Among peculiar examples the following may be mentioned. For $a = +5$ a spectrum is obtained with the relative energy values, shown in fig. 3. The same spectrum, although with different spin sequence, is obtained for $a = -7$. We have initially three single levels (the ground state having spin 5/2) and thereafter double levels. Qualitatively this spectrum resembles quite strikingly that of W^{183} (see ref. [3]), p. 18, fig. 1). Quantitatively, however, the calculations reveal great differences. The spectrum of W^{183} is explained [3]) as the superposition of three different rotational spectra with $K = 1/2$, 3/2 and 7/2.

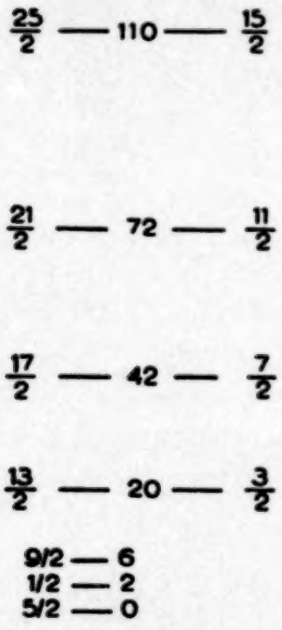

Fig. 3. Spin and relative energy values in the example $a = 5$. The three lowest levels are simple, the other are double levels.

3. Discussion of Tm^{171}

When levels occur close to each other and a therefore has a near-integral value, the determination of the spin sequence (and consequently the determination of a) can be difficult in certain cases, particularly as numerous possibilities exist with regard to the multipolarity of the γ-radiations. Such a case is the spectrum of Tm^{171}.

Assuming a rotational spectrum with $I_0 = K = \frac{1}{2}$ and normal spin sequence, Johansson [4]) has calculated from the 5 keV and 118 keV levels the values $\hbar^2/2J = 1215$ keV and $a = -0.86$. For the next level the experimen-

tal value of 130 keV is obtained with very great accuracy. For the subsequent level, however, the theoretical value 334 keV is found, which is less than the experimental value of 337 keV.

According to Bohr and Mottelson's theory [1]), eq. (1) is only approximate and for more accurate calculations a correction term, due to the spin dependence of the irrotational moment of inertia, is required. The exact formula is

$$E = E_{\text{rot}} - k\frac{\hbar^2}{2J}E_{\text{rot}}^2 \tag{1'}$$

where E_{rot} is identical with the E of eq. (1), and

$$k = \frac{12}{(\hbar\omega_\beta)^2} + \frac{4}{(\hbar\omega_\gamma)^2}.$$

The phonon energies $\hbar\omega_\beta$ and $\hbar\omega_\gamma$ will, for $A = 171$, have the order of magnitude of 1 MeV.

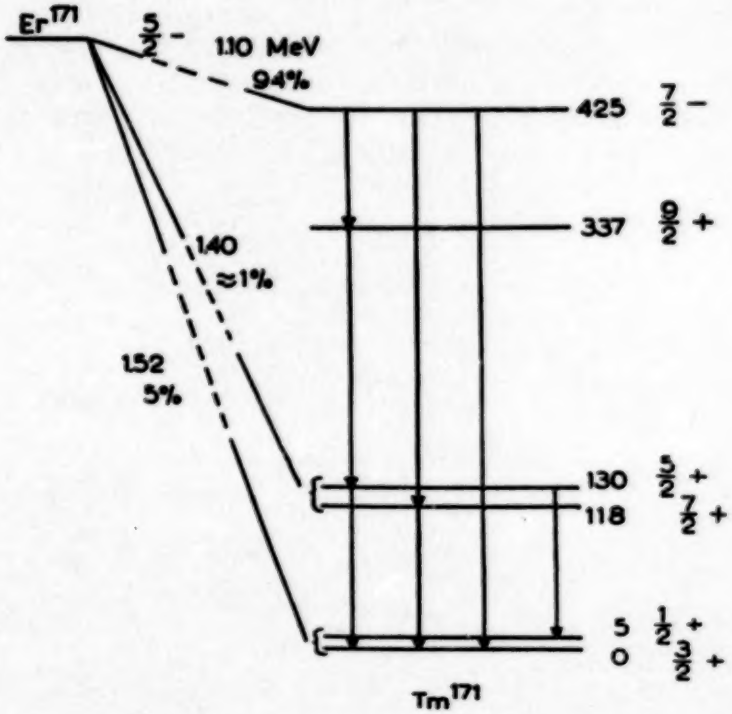

Fig. 4. Proposed level scheme for Tm^{171}.

The correction term is always negative, and therefore if eq. (1') rather than eq. (1) were used in the calculation of the above energy levels, a value lower than 334 keV would result. The level energies are in better agreement with the experimental values for $a = -1.14$, $\hbar^2/2J = 12.5$ keV and $k = 1.41 \times 10^{-5}$ keV^{-2}, which corresponds with phonon energies of the order

of magnitude of 1 MeV. The spin sequence is now 3/2, 1/2, 7/2, 5/2, 11/2, 9/2, etc., and the corresponding energies, in keV, are 0, 5, 118, 130, 320, 337, etc. This includes the energies of the rotational levels of Tm^{171} obtained [4]) from the beta decay of Er^{171}. The ground state is now assumed to have spin $I_0 = 3/2$.

Fig. 4 shows the scheme of energy levels with the new spin sequence, together with the β and γ transitions which can be considered to have measurable intensities. Also the ground state of Er^{171} is considered to have spin 5/2 and odd parity, the metastable 425 keV level of Tm^{171} to have spin 7/2 and odd parity, and the usual even parity is ascribed to the rotational levels. The originating γ-radiation is mainly of E2 or M1 character, but E1 and M2 radiation can be considered to occur.

It is not possible by means of the beta decay of Er^{171} to establish experimentally the energy of the Tm^{171} level with spin $I = 11/2$. On the basis of the above discussion the energy of this level would be 320 keV, whereas if the system is considered to possess a normal spin sequence the energy would be $\approx$ 352 keV. It would be interesting therefore if, by means of Coulomb excitation or other experiments, the existence of a level having one or other of the above energy values could be established. Similarly it would be of interest if, experimentally, it could be decided with certainty whether the ground state of Tm^{171} has spin 3/2 or 1/2.

References

1) A. Bohr and B. R. Mottelson, Mat. Fys. Medd. Dan. Vid. Selsk. **27** (1955) no. 16
2) J. O. Newton, Nuclear Physics **3** (1957) 345
3) A. Kerman, Mat. Fys. Medd. Dan. Vid. Selsk. **30** (1956) no. 15
4) S. A. E. Johansson, Phys. Rev. **105** (1957) 189

7.C *Nuclear Physics* 7 (1958) 217—222; © *North-Holland Publishing Co., Amsterdam*
Not to be reproduced by photoprint or microfilm without written permission from the publisher

CHARGE DEPENDENT EFFECTS ON SCATTERING LENGTHS OF np AND pp SYSTEMS

RIAZUDDIN

Department of Mathematics, Imperial College of Science and Technology, London†

Received 28 February 1958

Abstract: The effects of the electromagnetic structure of a nucleon on the singlet scattering lengths a_{np}, a_{pp} of np and pp systems are calculated. They are found to be much too small to remove the discrepancy between a_{np} and a_{pp}. It is shown to be plausible that the discrepancy between a_{np} and a_{pp} may be due to $\pi^{\pm}-\pi^{0}$ mass difference when its kinematic and dynamical effects, as defined in the text, are taken into account.

1. Introduction

The discrepancy between the singlet scattering lengths a_{np}, a_{pp} of np and pp systems is a problem of long standing, even after elimination of the effects of the Coulomb force. The hypothesis of charge independence of nuclear forces will be greatly strengthened if this discrepancy could be explained as due to non-nuclear interactions. In this paper we discuss the charge dependent effects on a_{np} and a_{pp} and see whether the discrepancy between a_{np} and a_{pp} is due to such effects, which are of the following two types:

(ia) The magnetic interaction energy between two nucleons: this gives different contributions to np and pp systems. Schwinger [1]) made calculations of this effect and he assumed no spread of the magnetic moment of the nucleon. He obtained a very satisfactory agreement between a'_{np} and a'_{pp} for a Yukawa potential, where a'_{np}, a'_{pp} are the effective scattering lengths for nuclear interaction alone. Salpeter [2]) showed that this agreement is destroyed if a repulsive core is added to the Yukawa potential.

(ib) The effects due to electromagnetic structure of a nucleon, i.e. due to its spread-out moment and charge. Electron-nucleon scattering data now enable us to make a calculation of these effects on the scattering lengths. Such a calculation is made in section 3 by using the electromagnetic vertex operator of a nucleon as determined from electron-nucleon scattering data. It is shown there that the agreement between a'_{np} and a'_{pp} is destroyed even for the Yukawa potential if spread-out moment and charge are assumed. The electromagnetic vertex operator of a nucleon is discussed in section 2.

(ii) The effect of the $\pi^{\pm}-\pi^{0}$ mass difference which is also presumably of electromagnetic origin. The kinematic effect of the mass difference on scat-

† Grant provided by the Department of Scientific and Industrial Research.

tering lengths was estimated by A. Sugie [3]), H. P. Noyes [4]) and the present author [5]). It was found in ref. [5]) (quoted here as I) that the effect was in the right direction to remove the discrepancy between a_{np} and a_{pp} but was much larger in magnitude than required. It is shown in section 4 that the dynamical effects of mass difference may reduce the contribution of the kinematic effect to the right magnitude. The sense in which the terms "kinematic" and "dynamical" effects of mass difference are used is also defined in section 4.

2. Electromagnetic Vertex Operator of a Nucleon

The matrix element for the scattering of an electron with a nucleon, when exchange of only one photon is considered between the two particles, is given by [6])

$$-4\pi i J_\mu(p, p') \frac{1}{q^2} j_\mu^{\,e}(k', k) \tag{1}$$

where $q = p'-p = -(k'-k)$ is the 4-momentum transfer. The operator $j_\mu^{\,e}(k', k) = -ieU_e(k')\gamma_\mu U_e(k)$ refers to the electron and the electromagnetic vertex operator $J_\mu(p', p)$ for the nucleon is of the form

$$J_\mu(p', p) = e\bar{u}(p') \left[\gamma_\mu(f_1(q^2)+\tau_3 g_1(q^2)) + \frac{\sigma_{\mu\gamma}}{2M} q_\gamma(f_2(q^2)+\tau_3 g_2(q^2))\right] u(p). \tag{2}$$

In terms of f_i, g_i, the form factors $F_i^{n,p}$ for neutron and proton are given by

$$\begin{aligned} F_1^{(p)} &= f_1+g_1, & F_1^{(n)} &= f_1-g_1 \\ \mu_p F_2^{(p)} &= f_2+g_2, & \mu_n F_2^{(n)} &= f_2-g_2 \end{aligned} \tag{3}$$

where μ_p, μ_n are the anomalous magnetic moments of proton and neutron respectively.

The vertex operator for neutron or proton is thus

$$J_\mu^{n,p}(p', p) = e\bar{u}(p') \left[\gamma_\mu F_1^{n,p}(q^2) + \frac{\sigma_{\mu\gamma}}{2M} q_\gamma \mu_{n,p} F_2^{n,p}(q^2)\right] u(p). \tag{4}$$

We now discuss the information which we can get about the form factors F_i from electron-nucleon scattering data. From electron-proton scattering [7]) we know that the best fit to the experimental data at all energies is given by the following choice of F_i:

$$F_1^{(p)}(q^2) = F_2^{(p)}(q^2) = F = \left(1-\frac{q^2a^2}{60}\right)\left(1+\frac{q^2a^2}{20}\right)^{-3} \tag{5}$$

where a, the root mean square radius, in the notation of ref. [6]), is given by

$$a = (\langle r^2\rangle_{1,p})^{\frac{1}{2}} = (\langle r^2\rangle_{2,p})^{\frac{1}{2}} = 0.77\times 10^{-13} \text{ cm}. \tag{6}$$

With the above choice of F's, J_μ is known for the proton.

For the neutron we know that $F_1^{(n)}(0) = 0$ and that the mean square

radius [6]) corresponding to the form factor $F_1^{(n)}$ is $\langle r^2\rangle_{1,n} = (0.000 \pm 0.006) \times 10^{-26}$ cm^{-2}. Therefore we shall take $F_1^{(n)}(q^2) \approx 0$. For $F_2^{(n)}(q^2)$ it has been shown experimentally [8]) that at large angles, where the scattering is mainly magnetic, the cross-section in the electron-neutron case is about $\frac{1}{2}$ of that in the electron-proton case; this gives $F_2^{(n)}(q^2) \approx F_2^{(p)}(q^2)$. Thus for the neutron we shall take

$$\begin{aligned} F_1^{(n)}(q^2) &= 0 \\ F_2^{(n)}(q^2) &= F_2^{(p)}(q^2) = F, \end{aligned} \tag{7}$$

where F is given by (5).

The vertex operator $J_\mu(\mathrm{p}', \mathrm{p})$ being thus determined for proton as well as neutron we can now easily calculate the effect of the electromagnetic structure of the nucleon on scattering lengths. This is done in the next section.

3. Effect of Electromagnetic Structure of Nucleon on Scattering Lengths

Let us consider the scattering of two nucleons due to their electromagnetic interaction alone. The process is shown in fig. 1. The matrix element for this process is given by

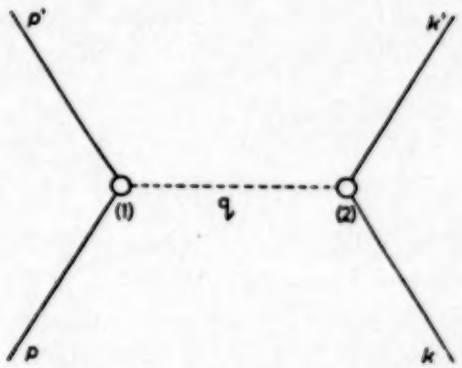

Fig. 1

$$T = \frac{M}{p_0} J_\mu^{(1)}(p', p) \frac{1}{q^2} J_\mu^{(2)}(k', k) \tag{8}$$

where the J_μ's are given by (4). For our purposes it will be sufficient to consider the non-relativistic approximation. Then in the cm. frame J_μ is given by

$$\begin{aligned} J_0 &\approx e\left[F_1 - \frac{q^2}{8M^2}(F_1 + 2\mu F_2)\right] \\ \mathbf{J} &\approx e\left[\frac{\mathbf{p}+\mathbf{p}'}{2M} F_1 + \frac{1}{2M} i\boldsymbol{\sigma} \wedge \mathbf{q}(F_1 + \mu F_2)\right]. \end{aligned} \tag{9}$$

From eqs. (8) and (9), on substituting the values of F_i given by eqs. (5)

and (7), we get the matrix elements for the singlet states of np and pp systems

$$M_{ss}^{np} = Q_n \mu_0^2 F^2$$
$$M_{ss}^{pp} = Q_p \mu_0^2 F^2 + \frac{F^2-1}{q^2} e^2 + \frac{e^2}{q^2} + \frac{F^2}{q^2} \mu_0^2 4k^2 \tag{10}$$

where $Q_n = 8\pi\mu_n(\mu_p+\frac{1}{2})$, $Q_p = 8\pi(\mu_p^2+\mu_p+\frac{1}{2})$, k is the c.m. momentum and $\mu_0 = e/2Mc$. We take the Fourier transforms of these and get what may be called the electromagnetic potentials for the np and pp systems in singlet states

$$V_{np}^{e.m.} = S_n f(r/a)$$
$$V_{pp}^{e.m.} = S_p f(r/a) - e^2 g(r/a) - 4\mu_0^2 \mathbf{p} \cdot g(r/a)\mathbf{p} + 4\mu_0^2 \mathbf{p} \cdot \frac{1}{r}\mathbf{p}. \tag{11}$$

The expressions for $S_{n,p}$, f, g are

$$S_{n,p} = \frac{Q_{n,p}\mu_0^2}{4\pi a^3} \frac{(20)^{\frac{1}{2}}}{3^3 \times 4};$$

$$f(r/a = \left[45+45(20)^{\frac{1}{2}} r/a + (20)^2 \left(\frac{r}{a}\right)^2 + 5(20)^{3/2} \left(\frac{r}{a}\right)^3 + (20)^2 \left(\frac{r}{a}\right)^4\right] e^{-\gamma r},$$

$$g(r/a) = \frac{1}{4\pi} \frac{e^{-\gamma r}}{r} + \frac{(20)^{\frac{1}{2}}}{16\pi \cdot 3^3 a} \left[\frac{333}{4} + \frac{117}{4} (20)^{\frac{1}{2}} \frac{r}{a} + 120 \left(\frac{r}{a}\right)^2 + 15(20)^{\frac{1}{2}} \left(\frac{r}{a}\right)^3 + 20 \left(\frac{r}{a}\right)^4\right] e^{-\gamma r},$$

$$\gamma = (20)^{\frac{1}{2}}/a.$$

In deriving $V_{pp}^{e.m.}$ we have omitted the term e^2/q^2 in the second eq. (10) because its effect has already been taken care of, in the value of the pp scattering length a_{pp} which we shall use, by the conventional treatment of Coulomb effect. These formulae reduce to those of Schwinger's [1]) if F is taken to be unity.

We now calculate the effect of $V_{np}^{e.m.}$ and $V_{pp}^{e.m.}$ on the scattering lengths a_{np} and a_{pp}. Following Schwinger's [1]) method and notation we find for the Yukawa potential

$$\delta\left(-\frac{b_0}{a_{np}}\right) = -0.0564, \qquad \delta\left(-\frac{b_0}{a_{pp}}\right) = 0.0653, \tag{12}$$

with $-b_0/a_{np} = 1.216$ and $-b_0/a_{pp} = 1.573$,
so that,

$$\frac{-b_0}{a'_{np}} = \frac{-b_0}{a_{np}} - \delta\left(\frac{-b_0}{a_{np}}\right) = 1.272,$$
$$\frac{-b_0}{a'_{pp}} = \frac{-b_0}{a_{pp}} - \delta\left(\frac{-b_0}{a_{pp}}\right) = 1.508. \tag{13}$$

Schwinger's results were

$$\delta\left(\frac{-b_0}{a_{np}}\right) = -0.145, \qquad \delta\left(\frac{-b_0}{a_{pp}}\right) = 0.195.$$

We thus find considerably smaller values than Schwinger's when charge and current distributions in the form suggested by electron-nucleon scattering experiments are taken into account. This was noted qualitatively by Salpeter [2]). Eq. (13) shows that a sizeable discrepancy remains between a'_{np} and a'_{pp} even for the Yukawa potential when charge and current distributions are assumed. For a Yukawa potential with a repulsive core the values of $\delta(-b_0/a_{np})$ and $\delta(-b_0/a_{pp})$ will be smaller than those given by (11); for a repulsive core of radius 0.5×10^{-13} cm, we find $\delta(-b_0/a_{np}) \approx -0.02$.

We may remark in passing that eqs. (4), (5), (7) and (8) may be used to calculate the relativistic electromagnetic effects on the scattering of two nucleons when their structure is also taken into consideration. Calculation of such effects may give additional information for the determination of nuclear phase shifts at high energies.

4. Effect of the π^0—$\pi^\pm$ Mass Difference on Scattering Lengths

For symmetric pseudo-scalar meson theory with pseudo-scalar coupling, the result of I for the 2nd order potential may be written as

$$V'_2 = \boldsymbol{\tau}^{(1)} \cdot \boldsymbol{\tau}^{(2)} V_2(\mu^\pm) - \tau_3^{(1)} \tau_3^{(2)} (V_2(\mu^\pm) - V_2(\mu^0)) \tag{14}$$

where $V_2(\mu^\pm)$ is the potential due to exchange of a charged meson and $V_2(\mu^0)$ is that due to a neutral meson. Here we have not made the approximation of expanding the last term of (14) in powers of $\delta\mu/\mu \equiv (\mu^+ - \mu^0)/\mu^+$ and retaining terms of order $\delta\mu/\mu$ only, as we did in I. It is more correct to use (14) than the corresponding expression in I because the scattering lengths are very sensitive to small changes of potential. H. P. Noyes [4]) has shown that the expression (14) for the 2nd order potential holds for any theory in which the basic interaction, as far as the meson variables are concerned, is of the form $\tau^{(1)}\phi^{(1)} + \tau^{(2)}\phi^{(2)} + \tau^{(3)}\phi^{(3)}$ where the mesons of type 1 and 2 have mass $\mu^\pm$ while the meson of type 3 has mass μ^0.

For singlet states we get from (14)

$$\begin{aligned} V^{pp} &= V_2(\mu^0) \\ V^{np} &= 2V_2(\mu^\pm) - V_2(\mu^0) \end{aligned} \tag{15}$$

where $V_2(\mu)$ is of the form $-(g^2/4\pi)(\mu/2M)^2(e^{-\mu r}/r)$ and $\delta\mu/\mu = 0.032$. As suggested by eq. (15) we write the effective np and pp potentials in ^1S states

$$V^{pp} = -\frac{V_0}{\beta}\frac{e^{-\beta r}}{r}, \qquad V^{np} = -\frac{V_0}{\beta}\left[2a^2\frac{e^{-a\beta r}}{r} - \frac{e^{-\beta r}}{r}\right], \tag{16}$$

with $a = 1.032$, and fix V_0 and β so as to obtain the experimental values of scattering length and effective range for the pp system. With the values of V_0 and β thus found we get

$$\frac{1}{a_{np}} - \frac{1}{a_{pp}} = 0.322 \times 10^{12} \text{ cm}^{-1}$$

while the experimental value is 0.130×10^{12} cm^{-1}.

Let us now examine our calculation a little more closely. The value 0.322×10^{12} cm^{-1} which we got for $a_{np}^{-1} - a_{pp}^{-1}$ is due to the term $(\mu_0^2 - \mu^2)\phi_3^2$ which appears in the renormalized Hamiltonian $\mu^2 \phi_i \phi_i + (\mu_0^2 - \mu^2)\phi_3^2$ for the free meson field to take account of the kinematic effect of the $\pi^{\pm} - \pi^0$ mass difference. As also noted by A. Sugie [3]) and H. P. Noyes [4]) the above value for $a_{np}^{-1} - a_{pp}^{-1}$ is bound to be affected by the dynamical effects of the mass difference which may make the renormalized coupling constants for π^0 and $\pi^{\pm}$ slightly different. Such a difference of coupling constants can exist, since the pion-nucleon vertex operator, when the nucleon and meson lines are real, is a function of the meson mass. In fact, our result for $a_{np}^{-1} - a_{pp}^{-1}$ is reduced to its experimental value if we take the coupling constant $g^2_{\pi^{\pm}pn}$ to be smaller by about 1.5 % than $g^2_{\pi^0 pp}$. As will be shown in the following paper, second order perturbation theory gives $g_{\pi^0 pp} - g_{\pi^{\pm} pn} = g(7\alpha/8\pi) \log (\Lambda^2/M^2)$, where $\alpha = e^2/4\pi\hbar c$ and Λ is the cut-off energy. A cut-off at $\Lambda = 4M$ will make $g^2_{\pi^0 pp}$ greater than $g^2_{\pi^{\pm} pn}$ by about 1.14 %. It seems, thus, quite plausible that the discrepancy between a_{np} and a_{pp} may be due to the $\pi^{\pm} - \pi^0$ mass difference when its kinematic and dynamical effects are taken into account.

The author is deeply indebted to Prof. A. Salam for encouragement and advice. He is also indebted to Dr. H. P. Noyes for communicating his results and to Prof. R. E. Peierls who suggested to him to look into the effect of the $\pi^{\pm} - \pi^0$ mass difference on the scattering lengths.

References

1) J. Schwinger, Phys. Rev. **78** (1950) 135
2) E. Salpeter, Phys. Rev. **91** (1953) 994
3) A. Sugie, Prog. Theor. Phys. **11** (1954) 333
4) H. P. Noyes, unpublished
5) Riazuddin, Nuclear Physics **2** (1956) 188
6) D. R. Yennie, M. M. Levy and D. G. Ravenhall, Revs. Mod. Phys. **29** (1957) 144
7) R. Hofstadter, Revs. Mod. Phys. **28** (1956) 214
8) R. Hofstadter, Proc. of 7th Ann. Rochester Conference on high energy Physics (Interscience Publishers, New York, 1957)

7.C *Nuclear Physics* **7** (1958) 223—224; © *North-Holland Publishing Co., Amsterdam*
Not to be reproduced by photoprint or microfilm without written permission from the publisher

ON THE DIFFERENCE OF π^0-NUCLEON AND $\pi^\pm$-NUCLEON COUPLING CONSTANTS

RIAZUDDIN

Department of Mathematics, Imperial College of Science and Technology, London†

Received 28 February 1958

In the preceding paper [1]) (hereafter called II) the effect of the $\pi^\pm - \pi^0$ mass difference on the scattering lengths a_{np}, a_{pp} was estimated. The kinematic effect of the mass difference as defined in II gave a larger contribution than was required to remove the discrepancy between a_{np} and a_{pp}. In order to reduce this contribution so as to get agreement with the experimental value for $a_{np}^{-1} - a_{pp}^{-1}$, the π^0-coupling constant was required in II to be larger by about 1.5 % than the $\pi^\pm$-coupling constant. The purpose of this note is to show that second order perturbation theory indicates that the π^0-coupling constant is indeed greater than the $\pi^\pm$-coupling constant.

Let us consider the renormalization of the π^0 and $\pi^\pm$-coupling constants due to the electromagnetic interaction to 2nd order. Let us denote by $g_{\pi^0 pp}$, $g_{\pi^0 nn}$ and $g_{\pi^\pm pn}$ the three renormalized coupling constants. We get

$$\begin{aligned} g_{\pi^0 pp} &= g(1-\tfrac{1}{2}B-\tfrac{1}{2}B+L_1) \\ g_{\pi^0 nn} &= -g \\ g_{\pi^+ pn} &= g(1-\tfrac{1}{2}B+\tfrac{1}{2}C+L_2); \end{aligned} \tag{1}$$

$\frac{1}{2}B$, $\frac{1}{2}C$ are the contributions due to the insertions of the proton and meson self-energy parts, respectively; L_1, L_2 are the contributions from the "true" vertex parts corresponding to the $p\pi^0 p$ and $p\pi^+ n$ vertices respectively. The values of these divergent constants, as defined by Feynman's [2]) method, are as far as the cut-off dependent parts are concerned,

$$\begin{gathered} B = \tfrac{1}{4}a, \qquad L_1 = a, \qquad C = \tfrac{1}{2}a, \qquad L_2 = -\tfrac{1}{4}a; \\ a = \frac{\alpha}{\pi}\log\frac{\Lambda^2}{M^2}, \qquad \alpha = \frac{e^2}{4\pi\hbar c}, \end{gathered} \tag{2}$$

Λ = cut-off energy, M = nucleon mass.

From eqs. (1) and (2), we get

$$\frac{g_{\pi^0 pp} - g_{\pi^+ pn}}{g} = \frac{7\alpha}{8\pi}\log\frac{\Lambda^2}{M^2} \tag{3}$$

† Grant provided by the Department of Scientific and Industrial Research.

showing that $g_{\pi^0 pp} > g_{\pi^+ pn}$. A cut-off at $\Lambda = 4M$ makes $g^2_{\pi^0 pp}$ greater than $g^2_{\pi^+ pn}$ by about 1.14 %.

It may be noted that the interaction Lagrangian for the pion-nucleon system can now be written in the form

$$L_{int} = G\bar{N}\boldsymbol{\tau}\Gamma_5 N \cdot \boldsymbol{\pi} + G\bar{N}(b + c\tau_3)\Gamma_5 N\pi^0.$$

The hope that b, c are zero is not borne out by the above calculation.

D. M. Greenberger [3]) has considered the possible difference between the three coupling constants $g_{\pi^0 pp}$, $g_{\pi^0 nn}$ $g_{\pi^\pm pn}$ from another point of view.

This investigation was suggested by Prof. A. Salam, to whom the author is deeply indebted for encouragement and advice.

References

1) Riazuddin, Nuclear Physics **7** (1958) 217
2) R. P. Feynman, Phys. Rev. **76** (1949) 769
3) D. M. Greenberger, Bull. Am. Phys. Soc. **3** (1958) 11

1.D.1:
1.E.1

Nuclear Physics **7** (1958) 225—232; © *North-Holland Publishing Co., Amsterdam*

Not to be reproduced by photoprint or microfilm without written permission from the publisher

ENERGY LEVELS IN ODD-MASS AND EVEN NUCLEI

A. DE-SHALIT
CERN, *Geneva* †

Received 17 March 1958

Abstract: Methods developed by Racah and first used by Talmi for the study of nuclear spectra are used to derive relations between energy level spacings in even and odd-mass nuclei in the scheme of the jj-coupling shell model. It is found that the occurrence of close lying states near the ground states of odd-mass nuclei and the absence of such states in even nuclei can be accounted for.

1. Introduction

The nuclear shell model can predict, in addition to the spin and parity of ground states, also that of excited states. As a matter of fact the identification of a definite state of the configuration j^n with the "ground state" implies at least qualitative information on the other states of the same configuration. A number of attempts have been made in the past to estimate the relative positions of the different states of a given configuration assuming various kinds of interactions between the particles [1]). The main purpose of these studies was to see whether one could explain the occurrence of states with total angular momentum $J = j-1$ as ground states in configurations containing an odd number of nucleons in the state j. Usually, as is well known, the ground states of such configurations have $J = j$, but a number of cases show the exceptional behaviour of having $J = j-1$ or even $J = j-2$ [1]). Ordinarily one may expect that roughly the same energy would to be required to excite the first few states of an odd-n configuration or of an even-n configuration. This expectation is actually fulfilled in the regions of high deformations where the lowest excitations have rotational character. However, in the regions of non-deformed nuclei where rotational spectra are not observed, it looks as if considerably less energy is required to excite the first few states of odd-n configurations than to excite the first states of a neighbouring even-n configuration. Thus in the analysis made by Lawson and Uretsky [2]) it was shown that about 1 MeV was needed to excite the first two states in the configurations $f^3_{7/2}$ or $f^5_{7/2}$, whereas more than 2.5 MeV were required for the excitation of the first two states in the configurations $f^2_{7/2}$, $f^4_{7/2}$ and $f^6_{7/2}$. The

† On leave of absence from the Weizmann Institute of Science, Rehovoth, Israel, on a Ford Foundation Fellowship.

energy required for the excitation of the first state shows even a bigger difference: about 0.4 MeV for odd n and more than 1.4 MeV for even n. Then again, in the region of $g_{9/2}$ nucleons where in several cases one knows both the states $(g^n_{9/2})_{9/2}$ and $(g^n_{9/2})_{7/2}$ (for odd n's) it is found that the difference between these two states can be as low as 0.014 MeV (Ge^{73}) or even 0.009 MeV (Kr^{83}) with a typical excitation of 0.600 MeV required for the lowest excitation of a neighbouring even-n nucleus.

These big differences in the behaviour of even nuclei and odd-mass nuclei poses the question as to whether or not it is due to some basic differences in their mode of excitation. In the next section we treat this question using the simple, though powerful, methods of Bacher and Goudsmit [3]), first introduced into nuclear spectroscopy by Talmi and his collaborators [4]). We derive the explicit relations for the energy spectra of configurations j^n in terms of the energy spectrum of the configuration j^2. These relations then enable us to see to what an extent the general behaviour of odd-n configurations is consistent with that of even-n ones.

2. Details of the Method

A state of n particles in the jj coupling shell (lj) is characterized by its total angular momentum J, its projection J_z and if necessary other quantum numbers α; its eigenfunction, assumed to be normalized and anti-symmetric in all n particles, is denoted by $\psi(j^n, \alpha JM)$. A state of n particles in the shell (lj) can also be created by combining any state of $n-2$ particles in that shell with any other state of 2 particles in the same shell. Such a state will be denoted by $\psi(j^{n-2}(\alpha' J')j^2(J''); JM)$. It is implied in this notation that an anti-symmetric state of the $n-2$ particles 3, 4, ... n characterized by the total angular momentum J' and the additional quantum numbers (if necessary) α', is coupled to an anti-symmetric state of the two particles 1 and 2 characterized by the total angular momentum J''; the coupling is carried out in such a way as to yield a normalized state of total angular momentum J and z-component M. It is clear that whereas the functions $\psi(j^{n-2}(\alpha' J')$ $j^2(J''); JM)$ are anti-symmetric separately in the particles 1 and 2, and in particles 3, 4, ..., n, they are not necessarily anti-symmetric under the exchange of either 1 or 2 with any of the particles 3, 4, ... or n. The space spanned by the totality of all wave functions of the type $(j^{n-2}(\alpha' J')j^2(J''); JM)$ with different values of α', J' and J'' (fixed J and M) is thus generally bigger than the space spanned by the totality of all wave functions of the type $\psi(j^n \alpha JM)$ with different values of α (again: JM fixed). One can therefore express any state $\psi(j^n \alpha JM)$ as a linear combination of the states $\psi(j^{n-2}(\alpha' J')j^2(J''); JM)$, and the coefficients of this expansion are at least partially determined by the requirement on the complete anti-symmetry of

$\psi(j^n\alpha JM)$ [5, 6]). Thus,

$$\psi(j^n\alpha JM) = \sum_{\alpha' J' J''} a^{(\alpha J)}_{\alpha' J' J''}\psi(j^{n-2}(\alpha' J')j^2(J''); JM) \tag{1}$$

where we have denoted the coefficients by $a^{(\alpha J)}_{\alpha' J' J''}$ instead of using the more explicit conventional notation of these fractional parentage coefficients: $a^{(\alpha J)}_{\alpha' J' J''} \equiv (j^{n-2}(\alpha' J')j^2(J'')J|\}j^n\alpha J)$. Since both $\psi(j^n\alpha JM)$ and $\psi(j^{n-2}(\alpha' J')j^2(J''); JM)$ are orthonormal, we find that

$$\sum_{\alpha' J' J''} |a^{(\alpha J)}_{\alpha' J' J''}|^2 = 1. \tag{2}$$

In the shell model all the states of the configuration j^n are degenerate in zeroth order, and are split in first order by the introduction of a two-body residual interaction V_{ij} as a perturbation. We have, therefore, the following relation for the first order energies:

$$-[E(j^n\alpha J)-E(j^n\alpha_0 J_0)] = (j^n\alpha JM|\sum_{i<k} V_{ik}|j^n\alpha JM) - (j^n\alpha_0 J_0 M_0|\sum_{i<k} V_{ik}|j^n\alpha_0 J_0 M_0) \tag{3}$$

where $E(j^n\alpha J)$ is the excitation energy of the state $\psi(j^n\alpha JM)$ (it is independent of M) measured from the ground state of the configuration j^n.

Since the wave function $\psi(j^n\alpha JM)$ is antisymmetric in all n-particles, we have

$$(j^n\alpha JM|\sum_{i<k} V_{ik}|j^n\alpha JM) = \frac{n(n-1)}{2}(j^n\alpha JM|V_{12}|j^n\alpha JM). \tag{4}$$

Substituting in (4) the expression (1) for $\psi(j^n\alpha JM)$ and recalling that V_{12}, like any permissible two-body interaction, connects only states with the same angular momentum J'', we find that

$$(j^n\alpha JM|\sum_{i<k} V_{ik}|j^n\alpha JM) = \frac{n(n-1)}{2}\sum_{\alpha' J' J''} |a^{(\alpha J)}_{\alpha' J' J''}|^2(j^2 J'' M''|V_{12}|j^2 J'' M'') \tag{5}$$

where M'' has any arbitrary value. Using eq. (3), also for the case $n = 2$, and making use of eq. (2), we find that

$$E(j^n\alpha J)-E(j^n\alpha_0 J_0) = \frac{n(n-1)}{2}\sum_{J''}[b^{(\alpha J)}_{J''}-b^{(\alpha_0 J_0)}_{J''}][E(j^2 J'')-E(j^2 0)] \tag{6}$$

where we have introduced the coefficients b defined by

$$b^{(\alpha J)}_{J''} = \sum_{\alpha' J'} |a^{(\alpha J)}_{\alpha' J' J''}|^2. \tag{7}$$

Eq. (6) is the relation we need. Similar relations have been derived previously [4, 7]). It gives the structure of the configuration j^n in terms of the structure of the configuration j^2. The coefficients b, being entirely determined by the structure of the zeroth order wave function, do not depend, of course, on the interaction and can be readily calculated from available tables of

fractional parentage coefficients [8])†. The explicit form of the interaction V_{ij} is thus eliminated from eq. (6) at the cost of being able to check only the consistency between different configurations and not the actual excitation energy derived from "first principles". Thus it is a matter of simple algebra to show that if the two-particle spectrum shows a rotational structure $E(j^2 J'')-E(j^2 0) = \alpha J''(J''+1)$ the same will be true of the n-particle configuration, but still the rotational spectra in the highly deformed nuclei cannot be explained on the basis of the shell model because of the magnitude of the excitation energy (and for many other reasons as well).

To simplify the analysis of eq. (6) we introduce as our scale for energy measurement the separation between the ground state ($J'' = 0$) and first excited state ($J'' = 2$) in the configuration j^2. We further choose as the reference state $\alpha_0 J_0$ of the configuration j^n the state of seniority zero ($J_0 = 0$) whenever n is even and seniority one ($J_0 = j$) whenever n is odd. Denoting then

$$\delta_{\alpha J}^{(n)} = \frac{E(j^n \alpha J)-E(j^n \alpha_0 J_0)}{E(j^2 2)-E(j^2 0)},$$

we can rewrite eq. (6) in the form

$$\delta_{\alpha J}^{(n)} = \frac{n(n-1)}{2} \sum c_{J''}^{(\alpha J)} \delta_{J''}^{(2)} \tag{8}$$

where now

$$c_{J''}^{(\alpha J)} = b_{J''}^{(\alpha J)} - b_{J''}^{(\alpha_0 J_0)}$$

and, of course,

$$\delta_0^{(2)} = 0, \qquad \delta_2^{(2)} = 1.$$

The following is a summary of the results obtained in this way for various j's and n's. It should be emphasized that the δ's depend on j as well as on n, α and J; and $\delta_{J''}^{(2)}$, say, appearing in the equations for $j = 5/2$ should not be confused with $\delta_{J''}^{(2)}$ appearing in the equations for $j = 7/2$ or $9/2$.

a) $j = 5/2$. There are only three states in the configuration $(5/2)^3$ with $J = 3/2,\ 5/2$ and $9/2$. We find

$$\delta_{3/2}^{(3)} = \tfrac{1}{42}(55-27\delta_4^{(2)}),$$
$$\delta_{9/2}^{(3)} = \tfrac{1}{21}(-4+18\delta_4^{(2)}).$$

me err: were found in these tables; for maximum T the following are the corrected s:

$$((5/2)^2\ 2\ 5/2\ 5/2|)(5/2)^3 v = 1, 5/2)) = \tfrac{1}{3}\sqrt{\frac{5}{2}},$$

$$((5/2)^2\ 4\ 5/2\ 5/2|)(5/2)^3 v = 1, 5/2)) = \frac{1}{\sqrt{2}},$$

$$((9/2)^2\ 4\ 9/2\ 9/2|)(9/2)^3 v = 1, 9/2)) = \tfrac{1}{2}\sqrt{\frac{3}{5}},$$

$$((9/2)^2\ 2\ 9/2\ 5/2|)(9/2)^3 v = 3, 5/2)) = -\tfrac{1}{3}\sqrt{\frac{5}{2}}.$$

b) $j = 7/2$. For the configuration $(7/2)^n$ the seniority v is always a good quantum number [6]), and the states can therefore be classified according to it without any further assumption. For $(7/2)^3$ there are the states with $J = 7/2$ ($v = 1$) and $J = 3/2$, $5/2$, $9/2$, $11/2$ and $15/2$ (all with $v = 3$). For $(7/2)^4$ there are the states $J = 0$ ($v = 0$), $J = 2$, 4 and 6 ($v = 2$), and $J = 2$, 4, 5 and 8 ($v = 4$). For $(7/2)^3$ we find

$$\delta^{(3)}_{3/2} = \tfrac{1}{84}(19+135\delta_4{}^{(2)}-91\delta_6{}^{(2)}),$$
$$\delta^{(3)}_{5/2} = \tfrac{1}{132}(187-75\delta_4{}^{(2)}-13\delta_6{}^{(2)}),$$
$$\delta^{(3)}_{9/2} = \tfrac{3}{308}(-11+123\delta_4{}^{(2)}-35\delta_6{}^{(2)}),$$
$$\delta^{(3)}_{11/2} = \tfrac{1}{132}(55-21\delta_4{}^{(2)}+65\delta_6{}^{(2)}),$$
$$\delta^{(3)}_{15/2} = \tfrac{1}{132}(-55-9\delta_4{}^{(2)}+163\delta_6{}^{(2)}).$$

For $(7/2)^4$ we find ($\delta^{(n)}_{v,J}$ corresponds to a state of seniority v and total angular momentum J)

$v = 2$:

$$\delta^{(4)}_{2,2} = \delta^{(2)}_{2,2} = 1,$$
$$\delta^{(4)}_{2,4} = \delta^{(2)}_{2,4},$$
$$\delta^{(4)}_{2,6} = \delta^{(2)}_{2,6};$$

$v = 4$:

$$\delta^{(4)}_{4,2} = \tfrac{1}{66}(11+153\delta^{(2)}_{2,4}-65\delta^{(2)}_{2,6}),$$
$$\delta^{(4)}_{4,4} = \tfrac{1}{2}(3-\delta^{(2)}_{2,4}+\delta^{(2)}_{2,6}),$$
$$\delta^{(4)}_{4,5} = \tfrac{1}{462}(143+459\delta^{(2)}_{2,4}+91\delta^{(2)}_{2,6}),$$
$$\delta^{(4)}_{4,8} = \tfrac{1}{462}(-165+81\delta^{(2)}_{2,4}+777\delta^{(2)}_{2,6}).$$

c) $j = 9/2$. Only the levels of $(9/2)^3$ were calculated. Some fractional parentage coefficients which were not calculated in ref. [3]) were evaluated here using a modification of a relation given in ref. [6]). A complete table of these coefficients with the method used for their derivation is given in the appendix.

For the energy levels of $(9/2)^3$ with seniority 3 we then find

$$\delta^{(3)}_{3/2} = \tfrac{1}{220}[-55+381\delta_4{}^{(2)}+37\delta_6{}^{(2)}-187\delta_8{}^{(2)}],$$
$$\delta^{(3)}_{5/2} = \tfrac{1}{660}[385+93\delta_4{}^{(2)}+611\delta_6{}^{(2)}-561\delta_8{}^{(2)}],$$
$$\delta^{(3)}_{7/2} = \tfrac{1}{8580}[11375-261\delta_4{}^{(2)}-5525\delta_6{}^{(2)}+1275\delta_8{}^{(2)}],$$
$$\delta^{(3)}_{9/2} = \tfrac{1}{4290}[-650+3582\delta_4{}^{(2)}+3458\delta_6{}^{(2)}-2958\delta_8{}^{(2)}],$$
$$\delta^{(3)}_{11/2} = \tfrac{1}{8580}[2275+6339\delta_4{}^{(2)}-2665\delta_6{}^{(2)}+915\delta_8{}^{(2)}],$$
$$\delta^{(3)}_{13/2} = \tfrac{1}{2860}[1885-747\delta_4{}^{(2)}+351\delta_6{}^{(2)}+799\delta_8{}^{(2)}],$$
$$\delta^{(3)}_{15/2} = \tfrac{1}{2860}[-715-147\delta_4{}^{(2)}+3601\delta_6{}^{(2)}-451\delta_8{}^{(2)}],$$
$$\delta^{(3)}_{17/2} = \tfrac{1}{2860}[-715+1213\delta_4{}^{(2)}-377\delta_6{}^{(2)}+2167\delta_8{}^{(2)}],$$
$$\delta^{(3)}_{21/2} = \tfrac{1}{20}[-5-9\delta_4{}^{(2)}+\delta_6{}^{(2)}+29\delta_8{}^{(2)}].$$

3. Discussion

The relations obtained above for $(5/2)^n$ are plotted in fig. 1. An inspection of this figure as well as of the more explicit relations obtained above, reveals that whereas generally the first few levels of an odd-n configuration are as widely spread as those of an even-n configuration, this is not true for some specific values of $\delta_4^{(2)}$, $\delta_6^{(2)}$ and $\delta_8^{(2)}$. Thus for the configuration $(5/2)^n$ we find that for $\delta_4^{(2)} \approx 2$, the configuration $(5/2)^3$ has two very close states of spins 3/2 and 5/2 whose separation in energy is only 10 % of the separation between the ground state and the first excited state in $(5/2)^2$. For $(7/2)^{2,3,4}$ we find a similar situation for $\delta_4^{(2)} = 1.70$ and $\delta_6^{(2)} = 2.5$ or $\delta_4^{(2)} = 2.2$ and $\delta_6^{(2)} = 3.5$, or other similar combinations. It is now interesting to note that in fact pure configuration j^2 (like Ca^{42} or Fe^{54}) do indicate values of $\delta_4^{(2)}$ and $\delta_6^{(2)}$ that are in the neighbourhood of the above specific values. The analysis

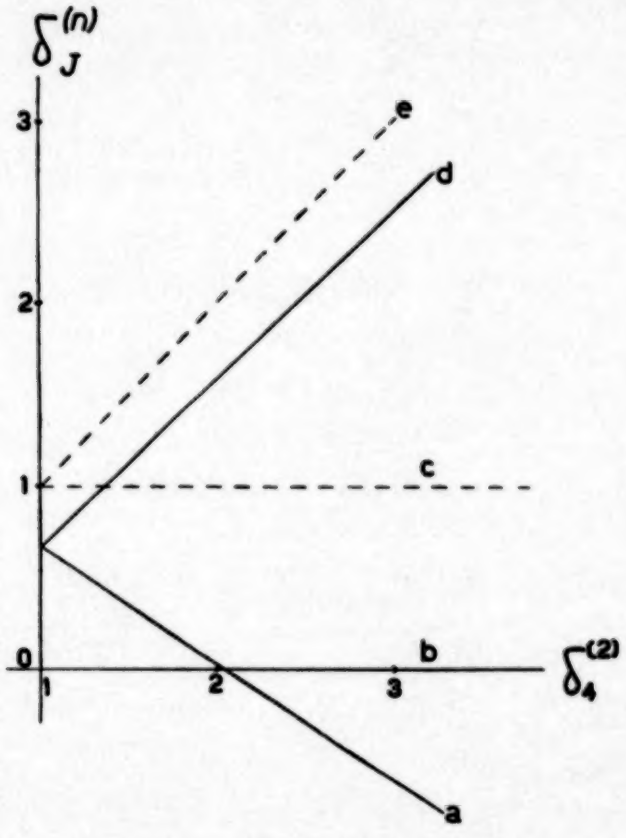

Fig. 1. Energy levels of the configurations $(5/2)^2$ (broken lines) and $(5/2)^3$ (full lines) as a function of $\delta_4^{(2)}$. The line b $\delta_J^{(n)} = 0$ corresponds to the state $J = 0$ in the configuration $(5/2)^2$ and $J = 5/2$ in $(5/2)^3$. The other lines refer to the following states: a $-(5/2)^3_{3/2}$, c $-(5/2)^2_2$, d $-(5/2)^3_{9/2}$, e $-(5/2)^2_4$.

of Scharff-Goldhaber and Weneser [9]) also shows that for non-deformed nuclei one can expect a value of 2.2 for $\delta_4^{(2)}$ and perhaps 3.5 for $\delta_6^{(2)}$.

We thus see that whereas generally we could have been surprised to find that non-deformed odd-mass nuclei require systematically less energy for the excitation of their first few states than their neighbouring even nuclei, this behaviour may very well result from the very special pattern of excitations in even nuclei which have shown such outstanding regularities. Our analysis also suggests that some of the excited states in odd-mass nuclei believed to result from the excitation of a single nucleon, may actually be excited states of the ground state configuration. This point, however, needs further study.

Appendix

It was shown in ref. [6]) that the fractional parentage coefficients for seniority $v = 3$ in configurations j^3 are given by

$$(j^2(J')jJ|\}j^3, v = 3, J) = C(J_0)\left[[\delta(J'J_0) + (2J_0+1)^{\frac{1}{2}}(2J'+1)^{\frac{1}{2}}[1+(-1)^{J'}]\begin{Bmatrix} jjJ' \\ jJJ_0 \end{Bmatrix}\right] \tag{A1}$$

where J_0 is an even number satisfying the triangular condition with j and J:

$$|j-J| \leqq J_0 \leqq |j+J|$$

and $\{^{jjJ'}_{jJJ_0}\}$ is a Racah coefficient. The normalization factor $C(J_0)$ was given in ref. [6]) as

$$C(J_0) = \pm\left[3[1+2(2J_0+1)]\begin{Bmatrix} jjJ_0 \\ jJJ_0 \end{Bmatrix}\right]^{-\frac{1}{2}}. \tag{A2}$$

Since (A1) is true for any J_0 satisfying the above conditions, and since J' always satisfies these conditions, we can take (provided v and J determine the state of j^3 uniquely) $J_0 = J'$ and obtain

$$(j^2(J')jJ|\}j^3 v = 3J) = \frac{\pm 1}{\sqrt{3}}\left[1+2(2J'+1)\begin{Bmatrix} jjJ' \\ jJJ' \end{Bmatrix}\right]^{\frac{1}{2}}. \tag{A3}$$

Eq. (A3) does not give the phase of the fractional parentage coefficient; however in many applications one is interested only in the square of the f.p.c. and this relation is then very practical for both general relations as well as for actual computation of f.p.c.'s, since the Racah coefficient involved is relatively simple to calculate.

The following is a complete table of fractional parentage coefficients for the configuration $(9/2)^3$. Part of it ($J = 3/2, 5/2, 7/2, 9/2$ and $21/2$) is taken from Flowers [8]). The rest was calculated with the help of an unpublished table of some Racah coefficients by A. Szöke.

TABLE 1

Fractional parentage coefficients $(j^3(vJ_2)jJ \,|\}\, j^3 v' J)$

$(9/2)^3$ \ $(9/2)^3$		$v = 0$	$v = 2$			
		$J_2 = 0$	$J_2 = 2$	$J_2 = 4$	$J_2 = 6$	$J_2 = 8$
$v' = 1$	$J = 9/2$	$-\frac{2}{\sqrt{15}}$	$\frac{1}{2\sqrt{15}} \times \sqrt{5}$	$\times \sqrt{9}$	$\times \sqrt{13}$	$\times \sqrt{17}$
$v' = 3$	$J = 3/2$			$-\frac{2\sqrt{2}}{11}$	$\sqrt{\frac{3}{11}}$	
	5/2		$-\frac{1}{3}\sqrt{\frac{5}{2}}$	$\sqrt{\frac{13}{66}}$	$\frac{2}{3}\sqrt{\frac{13}{11}}$	
	7/2		$\frac{2}{3}\sqrt{\frac{13}{11}}$	$2\sqrt{\frac{5}{143}}$	$\frac{1}{3}\sqrt{\frac{1}{55}}$	$-\sqrt{\frac{238}{715}}$
	9/2		$-\frac{1}{6}\sqrt{\frac{13}{11}}$	$\frac{7}{2}\sqrt{\frac{5}{143}}$	$-\frac{31}{6}\sqrt{\frac{1}{55}}$	$\frac{3}{2}\sqrt{\frac{17}{715}}$
	11/2		$\frac{1}{3}\sqrt{\frac{17}{11}}$	$-\sqrt{\frac{170}{429}}$	$-\frac{2}{3}\sqrt{\frac{14}{55}}$	$6\sqrt{\frac{19}{2145}}$
	13/2		$\sqrt{\frac{10}{33}}$	$-3\sqrt{\frac{1}{143}}$	$-\sqrt{\frac{17}{66}}$	$-\sqrt{\frac{323}{858}}$
	15/2			$\sqrt{\frac{19}{143}}$	$-\sqrt{\frac{7}{11}}$	$\sqrt{\frac{3}{13}}$
	17/2			$5\sqrt{\frac{5}{429}}$	$-\sqrt{\frac{19}{110}}$	$-\sqrt{\frac{209}{390}}$
	21/2				$-\sqrt{\frac{7}{30}}$	$\sqrt{\frac{23}{30}}$

References

1) For references see, for instance, K. Way, D. N. Kundu, C. L. McGinnis and R. van Lieshout, Ann. Rev. Nuc. Sci. **6** (1956) 129
2) R. D. Lawson and J. L. Uretsky, Phys. Rev. **106** (1957) 1369;
I. Talmi, unpublished
3) R. F. Bacher and S. Goudsmit, Phys. Rev. **46** (1934) 948
4) S. Goldstein and I. Talmi, Phys. Rev. **102** (1956) 589; **105** (1957) 995;
I. Talmi and R. Thieberger, Phys. Rev. **103** (1956) 718
5) G. Racah, Phys. Rev. **62** (1942) 438
6) C. Schwartz and A. de-Shalit, Phys. Rev. **94** (1954) 1257
7) S. P. Pandya, Phys. Rev. **103** (1956) 956;
G. Racah, Farkas Memorial Volume (Research Council of Israel, Jerusalem 1952)
8) A. R. Edmonds and B. H. Flowers, Proc. Roy. Soc. A **214** (1952) 515;
B. H. Flowers, Proc. Roy. Soc. A **215** (1952) 398
9) G. Scharff-Goldhaber and J. Weneser, Phys. Rev. **98** (1955) 212

1.B:2.B:
2.L

Nuclear Physics **7** (1958) 233—236; © *North-Holland Publishing Co., Amsterdam*
Not to be reproduced by photoprint or microfilm without written permission from the publisher

POLARIZATION IN THE ELASTIC SCATTERING OF 2—3 MeV NEUTRONS BY DEUTERONS

R. E. WHITE †, A. CHISHOLM and D. BROWN
University of Auckland, Auckland, New Zealand

Received 9 January 1958

Abstract: Large polarization effects have been observed in the elastic scattering of polarized neutrons from the D—D reaction by deuterons. The polarization for 90° centre of mass scattering is 0.58±0.05 at 2.26 MeV and 0.86±0.19 at 3.1 MeV and was measured by studying the asymmetry in the distribution of recoil deuterons in deuterium filled proportional counters.

1. Introduction

A recent theoretical study of n—d elastic scattering in the 0—5 MeV neutron energy range, to be described in a forthcoming publication by L. M. Delves and D. Brown, predicts that small polarization effects should be observed. Theoretically, the polarization is maximum for scattering near 90° centre of mass and has a maximum value of −28 % at 0.4 MeV; it then becomes positive, attaining a value of 6 % at 2.4 MeV, after which it again decreases, becoming zero at 3.0 MeV. The experiment to be described was aimed at checking these predictions by studying the angular distribution of polarized neutrons scattered by deuterons. If these neutrons receive a polarization $\mathbf{P}_2(\theta_2)$ in the scattering, and if their initial polarization is $\mathbf{P}_1(\theta_1)$, the angular distribution will exhibit an asymmetry given by

$$R = \frac{I(+\theta_2)}{I(-\theta_2)} = \frac{1+\mathbf{P}_1 \cdot \mathbf{P}_2}{1-\mathbf{P}_1 \cdot \mathbf{P}_2} \tag{1}$$

with the geometry shown in fig. 1; i.e.

$$\mathbf{P}_1 \cdot \mathbf{P}_2 = \frac{R-1}{R+1}. \tag{2}$$

In this experiment partially polarized neutrons from the D—D reaction were used, and R was obtained from the number of deuteron recoils at $\mp\beta_2$ (lab.), corresponding to neutrons scattered through $+\theta_2$ and $-\theta_2$, observed in deuterium filled proportional counters with directional properties. The principle of this method, developed for the study of helium polarization, has been described in detail elsewhere [1, 2]). Briefly, a counter with

† Now at the Massachussetts Institute of Technology, Boston, Mass.

directional properties is achieved by arranging that the track length for the recoils to be studied is larger than the counter diameter. Then by orienting the counter with its axis at $+\beta_2$ say to the neutron beam, these recoils expend all their energy in the counter, giving a pulse height corresponding to this energy. Recoils at $-\beta_2$, however, can expend only a fraction of their energy in the counter, since they travel only a distance of about one dia-

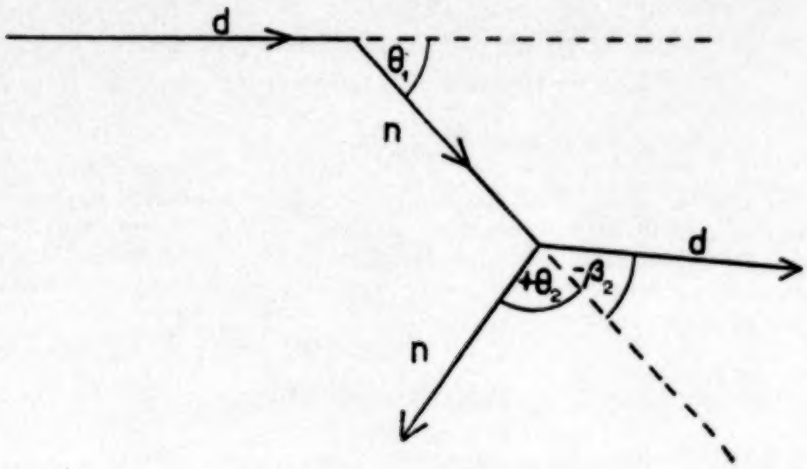

Fig. 1

meter in the counter, and give a smaller pulse. Recoils at $+\beta_2$ may therefore be counted selectively by using pulse-height analysis. The range of angles about β_2 in which recoils are accepted is then fixed in the main by the width of the pulse-height channel used.

2. Experimental

The only neutrons of known polarization available in this laboratory are those produced in the D—D reaction for deuteron energies between 100 keV and 450 keV. The polarization is known accurately only for neutrons emerging at 53° centre of mass (45° lab.), and therefore at 127° centre of mass (117° lab.), to the deuteron beam, and is −0.10 at 45° lab. and +0.10 at 117° lab. [3]). The neutron energies at these angles become more divergent as the deuteron bombarding energy is increased, and using 400 keV deuterons on a thick heavy ice target have mean values of 3.1 MeV and 2.26 MeV at 45° and 117° respectively. These energies were convenient since 2.26 MeV is near the theoretical polarization maximum; while at 3.1 MeV the theoretical polarization is almost zero. For these energies the theory predicts that the polarization is maximum for 90° c.m. scattering which corresponds to observing recoils at ±45° lab.

Two counters were constructed using a range-energy relation for deuterons in deuterium deduced from data for protons in hydrogen [4]). The recoil

deuteron energy at 45° is 0.44× neutron energy, i.e. 0.99 MeV and 1.36 MeV for 2.26 and 3.1 MeV neutrons. The counters were filled by introducing deuterium through a palladium leak, after inserting appropriate amounts of argon and carbon dioxide to produce satisfactory operation from a normal filling bench. This limited the pressure to about 0.5 atmospheres giving recoil ranges of the order 10 cm. To allow a reasonable range to diameter ratio and counting rate the counters were made 30 cm long and 3.8 cm in diameter with 0.003 inch diameter wires. The counters were filled to a pressure of 39 cm deuterium, 2.8 cm of argon, and 1.5 cm of carbon dioxide so that the ranges of 0.99 MeV and 1.36 MeV recoils were 7.3 cm and 12.4 cm respectively, giving range to diameter ratios of 1.9 and 3.3 .The counters were mounted with an included angle of 90° between their axes which crossed at the midpoints of their active lengths, this being less than the total lengths by approximately the recoil range. Mica windows on the counter bodies permitted the entry of natural alpha particles for checking the behaviour and stability of the counters.

To calibrate the pulse height scales the counters were exposed to an axial beam of neutrons emerging at 100° to the deuteron beam. These neutrons are almost monoergic with an energy of 2.44 MeV and give an integral recoil pulse spectrum whose cut-off corresponds to 0° recoils of 2.17 MeV energy. By studying the end region of this spectrum a calibration figure accurate to ± 2 % was obtained [1]).

Asymmetry measurements were made using single channel pulse-height analyses with a channel width corresponding to a spread of $\pm 6°$ lab. about the 45° recoil direction. The counters were interchanged regularly throughout the measurements and the asymmetry as given by each counter calculated to check for any geometrical differences. However the individual results agreed within statistics. Background effects were looked for in two ways, firstly by repeating the asymmetry measurements for $\theta_1 = 0°$ when $\mathbf{P}_1 = 0$ and R should become 1, and secondly by repeating the measurements at 117°, where the range to diameter ratio is least and background effects might be expected to be worst, using an identical counter filled with hydrogen. In this case $\mathbf{P}_2 = 0$ [5]) and R should again be 1. The hydrogen pressure was adjusted to give the same range to diameter ratio as for the deuterium case.

Typically, with an 80—100 μA deuteron beam, the channel counting rate was between 0.5 and 1 count per second for a mean target to counter distance of 60 cm. The counters then subtended $\pm 5°$ at the target.

Tests with natural 8.78 MeV alpha particles showed that the corresponding group peak varied in pulse height by less than ± 2 %, the group variance being 0.05. The background rate in the counters when not exposed to neutrons was only about one count in five minutes.

3. Results

A number of measurements of the asymmetry R were made at each θ_1 position. Weighted means were then calculated by weighting the individual R values with the squares of the reciprocals of their standard deviations. The results obtained are as follows:

Neutron Energy (MeV)	R	P_1	P_2
2.26	1.100±0.012	0.10	0.48±0.05
3.1	0.922±0.036	−0.10	0.40±0.2
0° position	1.009±0.025	0.00	
2.26 (hydrogen counter)	0.990±0.025	0.10	−0.05±0.12

The asymmetry vanishes for $P_1 = 0$ as it should. The hydrogen counter measurements show that while there may be a small spurious asymmetry from background effects, this by no means accounts for the asymmetry observed in the n—d scattering. It seems reasonable, therefore, to conclude that genuine large polarization effects are present at these energies.

The polarization observed is much greater in magnitude than that predicted by the theoretical treatment of Delves and Brown, but has the same sign. It is hoped that a more detailed theoretical study will give better agreement.

We would like to acknowledge the assistance received from Mr. H. Naylor and Mr. A. L. McCarthy in taking the measurements.

References

1) I. I. Levintov, A. V. Miller and V. N. Shamshev, Nuclear Physics **3** (1957) 221
2) R. E. White and F. J. M. Farley, Nuclear Physics **3** (1957) 476
3) I. I. Levintov, A. V. Miller, E. Z. Tarumov and V. N. Shamshev, Nuclear Physics **3** (1957) 237
4) E. Segrè, Experimental Nuclear Physics, vol. I (Wiley, 1953)
5) J. C. Allred, A. H. Armstrong, and L. Rosen, Phys. Rev. **91** (1953) 90

8.B *Nuclear Physics* 7 (1958) 237—250; © *North-Holland Publishing Co., Amsterdam*
Not to be reproduced by photoprint or microfilm without written permission from the publisher

RIGHT-LEFT ASYMMETRY AND TWO-COMPONENT NEUTRINO

T. TAKABAYASI
Institut Henri Poincaré, Paris

Received 31 March 1958

Abstract: The two-component neutrino theory is formulated irrespectively of the handedness of the coordinate frame. This is made possible by introducing a constant pseudoscalar η_l and by ascribing the two-component spinor slightly new transformation properties under Lorentz transformations. The method automatically exhibits the reflection properties of the various physical quantities of the system and eliminates some confusing inconveniences of the current theory, which restricts one to either right-handed or left-handed coordinate frame. It is emphasized that η_l is an effective instrument in specifying the description of any objectively right-left asymmetrical process.

1. Introduction

Since the recognition of the violation of reflection symmetry in weak interaction phenomena [1]) it has been usual to describe those processes in arbitrarily restricting one-self to a right-handed coordinate system. Such descriptions have the drawback that they obscure the reflection properties of various physical quantities and apt to lead to confusion. Especially, the two-component neutrino field [2, 3]) seems to have been treated from the viewpoint that it is describable by restricting oneself to one kind of handedness of coordinate frames on account of its intrinsic violation of reflection invariance.

It should, however, be remarked that any objectively real physical relation must always be describable in a right-handed and a left-handed frame at the same time, as we can observe the same phenomenon in both frames without mutual interference. Both descriptions must be equivalent and are connected in a definite manner. The connection is formally expressed as a certain transformation.

This general principle applies irrespectively of whether or not the physical process in question be symmetrical to right and left. Right-left asymmetry of the process, as is the case with the polarized neutrino, just means that a description in a right-handed frame and one in a left-handed frame do not take perfectly the same form; namely, the description is not reflection invariant.

This non-invariance, however, can be eliminated by introducing a con-

stant pseudoscalar η_t, and in so doing we can treat any right-left asymmetrical process in an arbitrary coordinate frame regardless of the handedness of the frame. We may call such representation "inversion covariant" in a broad sense.

It is to be emphasized that when the process is a right-left asymmetrical one, the more is it significant to describe it in such an "inversion covariant" manner so as to manifest the reflection properties of the physical quantities of the system. In fact we shall see that this method clears up some obscurities in the current representations. The inconvenience that the handedness of the neutrino is liable to be confused with the handedness of the reference frame is also eliminated.

In this paper we are mainly concerned with the treatment of the two-component neutrino. It is to be noted, however, that the pseudoscalar parameter η_t, specifying the handedness of the frame, always occurs for any right-left asymmetrical process in the "inversion covariant" representation. Thus, η_t is also essential in the representation of the polarized neutrino by means of a four-component spinor (see sec. 7).

2. Right or Left Handed Relation in the Classical Case

As a preliminary it is useful to consider how a right (or left) handed relation is represented in classical case in an arbitrary reference frame. Suppose for example a 3-dimensional polar vector $\mathbf{V}$ and a right-screwed rotation around it. If we use an axial vector $\mathbf{A}$ to represent the rotation, the relation is expressed, in a right-handed coordinate frame, as

$$\mathbf{A} = k\mathbf{V}, \tag{2.1}$$

where k is a positive scalar. The same relation is written in a left-handed frame as $\mathbf{A} = -k\mathbf{V}$.

Let us now introduce a constant unit pseudoscalar η_t by

$$\eta_t = \begin{cases} +1 \text{ for a right-handed frame,} \\ -1 \text{ for a left-handed frame.} \end{cases} \tag{2.2}$$

Then the above right-screwed relation is expressed by

$$\mathbf{A} = \eta_t k\mathbf{V}, \qquad k > 0, \tag{2.3}$$

in any frame. This is regarded as reflection covariant since both sides of (2.3) are axial vectors. If $k < 0$, (2.3) means a left-screwed relation, the helicity is properly defined by the scalar,

$$\eta_t \mathbf{A} \cdot \mathbf{V}/(|\mathbf{A}||\mathbf{V}|) = k/|k|. \tag{2.4}$$

The second example is the right-handed relation of three polar vectors $\mathbf{U}$, $\mathbf{V}$ and $\mathbf{W}$. This is expressed as

$$\mathbf{W} = \eta_t k'[\mathbf{U} \times \mathbf{V}], \tag{2.5}$$

i.e.

$$W_i = \eta_l k' \varepsilon_{ijk} U_j V_k, \tag{2.5'}$$

where ε_{ijk} is the alternating symbol and k' is a positive scalar. This is again covariant under rotation and reflection, since both sides of (2.5') are vectors. (Note that ε_{ijk} is a pseudotensor.)

In this way any objectively right (or left) handed relation can be written in a covariant form with the use of η_l. Indeed the occurrence of η_l signifies that the relation is right-left asymmetric. The case of the two-component neutrino will be somewhat more subtle as we are dealing with a spinor and Lorentz transformations, but the problem is essentially similar to the above classical case †.

3. Inversion Covariant Formulation of Two-Component Neutrino Field

We consider the two-component neutrino field in its simplest form, i.e., the c-number free neutrino field, as it is sufficient in order to illustrate the essential points of the problem. Two kinds of polarized neutrino field are conceivable, which we shall call d- and g-fields (signifying "droite" and "gauche"): the d-field, e.g., corresponds to right-screw neutrinos and left-screw antineutrinos. To fix our ideas we consider the d-field for the present. The usual method to describe this with a two-component spinor $\varphi^{(d)}$ is to restrict oneself to right-handed coordinate systems and assume the wave equation

$$\partial_0 \varphi^{(d)} + \sigma_k \partial_k \varphi^{(d)} = 0 \quad (\partial_0 = \partial/\partial x_0, \quad x_0 = ct, \quad \partial_k = \partial/\partial x_k), \tag{3.1}$$

where the σ_k's are Pauli matrices satisfying the relations

$$\sigma_i \sigma_j = i\varepsilon_{ijk}\sigma_k + \delta_{ij}. \tag{3.2}$$

The above description is not covariant under space inversion in any sense, simply because it lacks any statement whatsoever about how the theory should be expressed in left-handed coordinate frames. To supplement this defect we replace (3.1) by

$$\partial_0 \varphi^{(d)} + \eta_l \sigma_k \partial_k \varphi^{(d)} = 0, \tag{3.3}$$

which applies equally in right and left handed frames and is covariant under the inversion

$$x_k \to -x_k, \tag{3.4}$$

since $\eta_l \sigma_k \partial_k$ is invariant under this transformation.

† Furthermore it is possible to represent the two-component neutrino theory in terms of vector variables alone [4]). If we adopt such a representation the problem becomes more similar to classical cases.

Of course we need at the same time to postulate the inversion property of $\varphi^{(d)}$, and indeed we assume simply that †

$$\varphi^{(d)} \text{ is invariant under space inversion.} \tag{3.5}$$

It is well-known that in non-relativistic theory, where a two-component spinor φ is employed to describe a Pauli particle, φ is assumed to be inversion invariant [6]). Thus the prescription (3.5) is just the natural extension of this assumption to the relativistic case. In non-relativistic theory the inversion invariance of φ was legitimate because we then need to consider only spatial rotation and inversion, and the former operation commutes with the latter. On the other hand, in the relativistic case a two-component spinor is known to be capable of representing proper Lorentz transformations alone, excluding the inversion. However, we shall show that it is possible to include the inversion according to the simple rule (3.5), if we adopt a slightly new prescription for the proper Lorentz transformation properties of $\varphi^{(d)}$.

Now, it is convenient to introduce the notation

$$\sum_{\mu}^{(d)} = \{\eta_l \sigma_k, \sigma_4\}, \tag{3.6}$$

with

$$\sigma_4 = i\sigma_0, \qquad \sigma_0 = \begin{pmatrix} 1 & 0 \\ 0 & 1 \end{pmatrix}.$$

Eq. (3.3) is then written as ††

$$\sum_{\mu}^{(d)} \partial_{\mu} \varphi^{(d)} = 0, \tag{3.7}$$

while its complex conjugate is

$$\partial_{\mu} \varphi^{(d)\dagger} \sum_{\mu}^{(d)} = 0. \tag{3.8}$$

We assume that for a proper Lorentz transformation L:

$$x'_{\mu} = a_{\mu\nu} x_{\nu}, \tag{3.9}$$

$\varphi^{(d)}$ transforms as

$$\varphi^{(d)} \to \varphi^{(d)\prime} = \Lambda^{(d)} \varphi^{(d)} \qquad (\varphi^{(d)\dagger} \to \varphi^{(d)\dagger} \Lambda^{(d)\dagger}) \tag{3.10}$$

through a 2×2 matrix $\Lambda^{(d)}$. In order that (3.7) and (3.8) be covariant, $\Lambda^{(d)}$ must satisfy

$$\Lambda^{(d)} \sum_{\mu}^{(d)} \Lambda^{(d)} = a_{\mu\nu} \sum_{\nu}^{(d)}. \tag{3.11}$$

Such a $\Lambda^{(d)}$ is explicitly written, for the infinitesimal Lorentz transformation $a_{\mu\nu} = \delta_{\mu\nu} + \omega_{\mu\nu}$, $(\omega_{\mu\nu} = -\omega_{\nu\mu})$, as

† It is also possible to assume that under inversion $\varphi \to -\varphi$, or $\varphi \to \pm i\varphi$, instead of (3.5), but the difference is inmaterial for the case of no interaction.

†† In this paper Greek suffixes run from 1 to 4, $\partial_4 = \partial/\partial x_4$, $x_4 = ix_0$. Latin suffixes run from 1 to 3. Summation convention is applied. * denotes complex conjugate, † Hermitian conjugate, and T transposed.

$$\Lambda^{(d)} = 1+\tfrac{1}{2}i(\tfrac{1}{2}\varepsilon_{ijk}\omega_{ij}+\eta_l\omega_{k4})\sigma_k. \tag{3.12}$$

The characteristic fact is that $\Lambda^{(d)}$ depends on η_l as shown in (3.12). This means that the same proper Lorentz transformation L is represented in $\varphi^{(d)}$-space in a two-fold manner (besides the usual two-valued character of the spinor representation) depending on whether L operates on a right-handed frame or on a left-handed frame. More explicitly, L corresponds to $\Lambda_1(L)$ satisfying

$$\Lambda_1^\dagger \sigma_\mu \Lambda_1 = a_{\mu\nu}\sigma_\nu, \qquad \sigma_\mu = \{\sigma_k, \sigma_4\} \tag{3.13}$$

when it acts to transfer a right-handed frame into another right-handed frame, while the same L corresponds to $\Lambda_2(L)$ satisfying

$$\Lambda_2^\dagger \sigma'_\mu \Lambda_2 = a_{\mu\nu}\sigma'_\nu, \qquad \sigma'_\mu = \{-\sigma_k, \sigma_4\} = -\sigma_\mu^\dagger \tag{3.14}$$

when it operates to alter a left-handed frame into another left-handed frame. In general $\Lambda_1(L)$ and $\Lambda_2(L)$ are different †, but we have

$$\Lambda_1(L) = \Lambda_2(L^*), \tag{3.15}$$

where L^* denotes the proper Lorentz transformation defined by the coefficients $(a^*_{\mu\nu})$.

The meaning of L^* is expressed by the relation

$$L^* = PLP, \tag{3.16}$$

P denoting the space inversion: Suppose we transfer a right-handed frame I_r into another right-handed one II_r by means of L, and on the other hand we transfer the left-handed frame I_l which is the inversion of I_r into another left-handed one II_l by means of L^*, then II_l is the inversion of II_r. If we take account of this fact, the relation (3.15) ensures that our transformation rule for $\varphi^{(d)}$ under proper Lorentz transformations is consistent with the other rule, the reflection invariance of $\varphi^{(d)}$.

4. Densities

From the transformation rule for $\varphi^{(d)}$ given in sec. 3 it follows immediately that

$$S_\mu^{(d)} = \varphi^{(d)\dagger} \sum_\mu^{(d)} \varphi^{(d)} = \{\eta_l \varphi^\dagger \sigma_k \varphi, i\varphi^\dagger \varphi\} \tag{4.1}$$

is a 4-vector. This is evident for inversion owing to the vector character of $\sum_\mu^{(d)}$; it is also clear for proper Lorentz transformations on account of (3.11):

$$\varphi^{(d)\dagger} \sum_\mu^{(d)} \varphi^{(d)} \to \varphi^{(d)\dagger} \Lambda^{(d)\dagger} \sum_\mu^{(d)} \Lambda^{(d)} \varphi^{(d)} = a_{\mu\nu}(\varphi^{(d)\dagger} \sum_\nu^{(d)} \varphi^{(d)}).$$

We see how the η_l-dependence of the proper Lorentz transformation property of $\varphi^{(d)}$ drops out in the transformation of these tensor quantities.

† If, in particular L is a spatial rotation, this is commutable with P, and so $L = L^*$. Hence we have $\Lambda_1(L) = \Lambda_2(L)$.

The 4-vector $S_\mu^{(d)}$ is the current 4-vector, satisfying

$$S_0^{(d)} = S_4^{(d)}/i \geqq 0, \qquad S_\mu^{(d)2} = 0, \tag{4.2}$$

and

$$\partial_\mu S_\mu^{(d)} = 0. \tag{4.3}$$

Next, the Lagrangian density which gives rise to our field equation (3.3) is given by

$$\mathscr{L}^{(d)} = -\frac{\hbar c}{2i}(\varphi^{(d)\dagger} \sum_\mu^{(d)} \partial_\mu \varphi^{(d)} - \partial_\mu \varphi^{(d)\dagger} \sum_\mu^{(d)} \varphi^{(d)}), \tag{4.4}$$

which is invariant under either proper Lorentz transformation or inversion.

The canonical energy-momentum tensor of the field is given by

$$\mathscr{T}_{\mu\nu} = \frac{\hbar c}{2i}(\varphi^{(d)\dagger} \sum_\nu^{(d)} \partial_\mu \varphi^{(d)} - \partial_\mu \varphi^{(d)\dagger} \sum_\nu^{(d)} \varphi^{(d)}), \tag{4.5}$$

and satisfies the relations [4])

$$\partial_\nu \mathscr{T}_{\mu\nu}^{(d)} = 0, \qquad \partial_\mu \mathscr{T}_{\mu\nu}^{(d)} = 0, \tag{4.6}$$

$$\mathscr{T}_{\mu\mu}^{(d)} = 0, \qquad \mathscr{T}_{\mu\nu}^{(d)} S_\nu^{(d)} = 0, \tag{4.7}$$

and

$$\mathscr{T}_{\mu\nu}^{(d)} - \mathscr{T}_{\nu\mu}^{(d)} = \partial_\rho \mathscr{M}_{\mu\nu\rho}^{(d)}, \tag{4.8}$$

with

$$\mathscr{M}_{\mu\nu\rho}^{(d)} = -\frac{i\hbar c}{2} \eta_t \varepsilon_{\mu\nu\rho\lambda} S_\lambda^{(d)}. \tag{4.9}$$

The relation (4.8) is the conservation law of angular momentum, indicating at the same time that $\mathscr{M}_{\mu\nu\rho}^{(d)}$ is the intrinsic angular momentum density tensor of the field. The pseudovector dual to $\mathscr{M}_{\mu\nu\rho}^{(d)}$ is

$$\hat{S}_\mu^{(d)} = \eta_t S_\mu^{(d)} = \{\varphi^{(d)\dagger} \sigma_k \varphi^{(d)}, i\eta_t \varphi^{(d)\dagger} \varphi^{(d)}\}, \tag{4.10}$$

whose space part gives the spin density, since

$$(\text{intrinsic angular momentum density})_k = \frac{1}{ic} \mathscr{M}_{ij4}^{(d)} = \tfrac{1}{2}\hbar \hat{S}_k^{(d)}, \tag{4.11}$$

$$(ijk) = \text{even permutation of } (123).$$

The relation (4.10) indicates that the spin pseudovector $\hat{S}_\mu^{(d)}$ and current vector $S_\mu^{(d)}$ coincide apart from the difference in their reflection properties. According to the explanations given in sec. 2 the relation tells us that the spin and current densities are in objectively right-screwed relation everywhere. Such fixed correlation is the characteristic simplification of the polarized neutrino field.

5. Particle Aspect

We now write the equation (3.3) in the form

$$\frac{\hbar}{i}\frac{\partial \varphi^{(d)}}{\partial t} + \mathsf{H}^{(d)}\varphi^{(d)} = 0, \tag{5.1}$$

with

$$\mathsf{H}^{(d)} = c\eta_t \boldsymbol{\sigma}\cdot\boldsymbol{p} \quad (\mathsf{p}_k = \frac{\hbar}{i}\partial_k). \tag{5.2}$$

Eq. (5.2) then means the particle Hamiltonian of the system, exhibiting that $\mathsf{H}^{(d)}$ is reflection invariant. (Note that η_t is a pseudoscalar and $\boldsymbol{\sigma}$ an axial vector.)

It is easy to derive the conservation laws in operator form:

$$\begin{gathered}\mathsf{p}_i = \text{const}, \qquad \mathsf{H}^{(d)} = \text{const}, \\ \varepsilon_{ijk}\mathsf{x}_j^{(d)}\mathsf{p}_k + \tfrac{1}{2}\hbar\sigma_i = \text{const},\end{gathered} \tag{5.3}$$

where $\boldsymbol{x}^{(d)}$ is the particle position operator conjugate to $\boldsymbol{p}$.

On the other hand we get the relation

$$\dot{\mathsf{x}}_i^{(d)} = \frac{i}{\hbar}[\mathsf{H}^{(d)}, \mathsf{x}_i^{(d)}] = \eta_t c\sigma_i, \tag{5.4}$$

which again indicates that the velocity $\dot{\mathsf{x}}_i^{(d)}$ is always connected to the spin σ_i as a right-handed screw, taking eigenvalues $\pm c$. Eq. (5.4) also yields the relation $\mathsf{H}^{(d)} = \dot{\mathsf{x}}_k^{(d)}\mathsf{p}_k$.

Furthermore by integrating the equation of motion for σ_i (i.e., for $\dot{\mathsf{x}}_i^{(d)}$ owing to (5.4)), we get

$$\dot{\mathsf{x}}_i^{(d)} = \tfrac{1}{2}i\hbar c\eta_t \dot{\sigma}_i^0 \exp\left(-\frac{2i}{\hbar}\mathsf{H}^{(d)}t\right)\cdot(\mathsf{H}^{(d)})^{-1} + c^2\mathsf{p}_i(\mathsf{H}^{(d)})^{-1}, \tag{5.5}$$

where the $\dot{\sigma}_i^0$'s are constant matrices denoting the initial values of the $\dot{\sigma}_i$'s. Eq. (5.5) shows that the velocity consists of two parts, the constant classical part $c^2\mathsf{p}_i\cdot(\mathsf{H}^{(d)})^{-1}$, and the Zitterbewegung part, just as in the case of a Dirac particle [7]).

6. g-Field, Helicity Conjugation, Plane Wave Solutions

6.1. THE g-FIELD

Hitherto we have considered the d-field. The oppositely polarized g-field can be treated in a similar manner: This is described by another two-component spinor $\varphi^{(g)}$, obeying

$$\partial_0\varphi^{(g)} - \eta_t\sigma_k\partial_k\varphi^{(g)} = 0, \tag{6.1}$$

i.e.,

$$\sum_\mu{}^{(g)}\partial_\mu\varphi^{(g)} = 0, \tag{6.2}$$

with

$$\sum_{\mu}^{(g)} = \{-\eta_1 \sigma_k, \sigma_4\} = -\sum_{\mu}^{(d)\dagger}. \tag{6.3}$$

$\varphi^{(g)}$ is assumed again to be reflection invariant, while it transforms, under the proper Lorentz transformation (3.9), by

$$\varphi^{(g)} \to \varphi^{(g)\prime} = A^{(g)} \varphi^{(g)}, \tag{6.4}$$

with

$$A^{(g)\dagger} \sum_{\mu}^{(g)} A^{(g)} = a_{\mu\nu} \sum_{\nu}^{(g)}. \tag{6.5}$$

This $A^{(g)}$ is connected to $A^{(d)}$ of (3.11) by

$$A^{(g)} = (A^{(d)\dagger})^{-1}, \qquad A^{(g)}(\mathrm{L}^*) = A^{(d)}(\mathrm{L}). \tag{6.6}$$

The current 4-vector and spin pseudovector are respectively

$$S_{\mu}^{(g)} = \varphi^{(g)\dagger} \sum_{\mu}^{(g)} \varphi^{(g)} = \{-\eta_1 \varphi^{(g)\dagger} \sigma_k \varphi^{(g)}, i\varphi^{(g)\dagger} \varphi^{(g)}\}, \tag{6.7}$$

$$\hat{S}_{\mu}^{(g)} = -\eta_1 S_{\mu}^{(g)} = \{\varphi^{(g)\dagger} \sigma_k \varphi^{(g)}, -i\eta_1 \varphi^{(g)\dagger} \varphi^{(g)}\}, \tag{6.8}$$

while the particle Hamiltonian and velocity are given by

$$\mathbf{H}^{(g)} = -c\eta_1 \boldsymbol{\sigma} \cdot \boldsymbol{p} \quad \text{and} \quad \mathbf{x}_i^{(g)} = -\eta_1 c \sigma_i.$$

Evidently, every expression or relation for the g-field is immediately obtained by the substitution

$$\eta_1 \to -\eta_1 \tag{6.9}$$

from the corresponding relation for the d-field.

6.2. HELICITY CONJUGATION

As is well-known, the two-component field has no "charge conjugation" invariance. As the analogue of the charge transformation in the 4-component spinor case, however, we may consider the transformation (e.g. for the d-field),

$$\varphi^{(d)} \to \varphi^{\Gamma} = \Gamma \varphi^{(d)*}, \tag{6.10}$$

where the matrix † Γ is defined by

$$\Gamma^{\mathrm{T}} = -\Gamma, \qquad \Gamma^{\dagger}\Gamma = 1, \qquad \sigma_k^{\mathrm{T}} = -\Gamma^{\dagger} \sigma_k \Gamma. \tag{6.11}$$

The new field φ^{Γ} then is no longer a d-field but a g-field, as it satisfies (6.1) and (6.4). Thus it is adequate to call (6.10) "helicity conjugation".

The current and spin densities of the helicity conjugated field are connected to those of the original field by

$$S_{\mu}^{\Gamma} = S_{\mu}^{(d)}, \qquad \hat{S}_{\mu}^{\Gamma} = -\hat{S}_{\mu}^{(d)}. \tag{6.12}$$

† In the usual representation of Pauli matrices,

$$\Gamma = -i\sigma_2 = \begin{pmatrix} 0 & 1 \\ -1 & 0 \end{pmatrix}.$$

6.3. SIMULTANEOUS EQUATIONS FOR d- AND g- FIELDS

In order to treat both d- and g-fields together, we use a suffix h representing d or g, and introduce a new dichotomic parameter

$$\eta_{\mathrm{h}} = \begin{cases} +1 & \text{for h} = \mathrm{d}, \\ -1 & \text{for h} = \mathrm{g}. \end{cases} \tag{6.13}$$

Then the field equations (3.3) and (6.1) are written together as

$$\partial_0 \varphi^{(\mathrm{h})} + \eta_{\mathrm{h}} \eta_{\mathrm{f}} \sigma_k \partial_k \varphi^{(\mathrm{h})} = 0, \tag{6.14}$$

or

$$\sum_{\mu}{}^{(\mathrm{h})} \partial_\mu \varphi^{(\mathrm{h})} = 0 \qquad (\mathrm{h} = \mathrm{d} \text{ or } \mathrm{g}), \tag{6.15}$$

with

$$\sum_{\mu}{}^{(\mathrm{h})} = \{\eta_{\mathrm{h}} \eta_{\mathrm{f}} \sigma_k, \sigma_4\}. \tag{6.16}$$

Similarly, any other pair of corresponding relations for d- and g-fields is also brought together; one has simply to replace η_{f} occurring in any relation for the d-field by $\eta_{\mathrm{h}} \eta_{\mathrm{f}}$:

$$\eta_{\mathrm{f}} \to \eta_{\mathrm{h}} \eta_{\mathrm{f}}. \tag{6.17}$$

Thus in the resulting representation the η-symbols occur only through the product $\eta_{\mathrm{h}} \eta_{\mathrm{f}}$. This expresses the evident fact that a $\varphi^{(\mathrm{d})}$-field viewed in a right-handed frame (or left-handed frame) and a $\varphi^{(\mathrm{g})}$-field viewed in a left-handed frame (or right-handed frame) behave exactly in the same manner. As the $\varphi^{(\mathrm{g})}$-field here we can specifically take the helicity conjugate of the $\varphi^{(\mathrm{d})}$-field (6.10); then the above statement expresses the well-known CP-invariance of the two-component theory [8]).

6.4. PLANE WAVE SOLUTIONS

Finally we shall write down the plane wave solutions of our wave equation. To each eigenstate of momentum with an eigenvalue $\hbar \boldsymbol{k}$ belong two independent eigenstates with energy values $\hbar c k \eta_\xi$ ($k \equiv |\boldsymbol{k}|$), where the suffix ξ is the specification of positive and negative energy states with

$$\eta_\xi = \begin{cases} +1 & \text{for } \xi = 1, \\ -1 & \text{for } \xi = 2. \end{cases} \tag{6.18}$$

Such solutions are explicitly written as follows †:

$$\varphi_\rho{}^{(\mathrm{h})(\xi)} = \tfrac{1}{2} \eta_\xi \frac{K_{\rho\xi}}{K_{\xi\xi}} \exp i(\boldsymbol{k} \cdot \boldsymbol{x} - \eta_\xi k x_0), \tag{6.19}$$

with

$$K = \eta_{\mathrm{h}} \eta_{\mathrm{f}} \boldsymbol{k} \cdot \boldsymbol{\sigma} + \eta_\xi k \sigma_0. \tag{6.20}$$

In (6.19) the common factor $K_{\xi\xi}^{-1}$ was introduced to normalize the solution in such a way that

† In $K_{\rho\xi}$ or $K_{\xi\xi}$ the subscripts apply to the σ-matrices, and summation must not be taken over ξ in $K_{\xi\xi}$.

$$S_0^{(h)(\xi)} = \varphi^{(h)(\xi)\dagger}\varphi^{(h)(\xi)} = k. \tag{6.21}$$

We have then

$$S_i^{(h)(\xi)} = \eta_h\eta_t\varphi^{(h)(\xi)\dagger}\sigma_i\varphi^{(h)(\xi)} = \eta_\xi k_i, \tag{6.22}$$

so the current is parallel or antiparallel to the momentum depending on the energy sign.

7. Four-Component Representation

Lee and Yang [3]) have shown that the polarized neutrino can equally be described by a 4-component spinor ψ, obeying the Dirac equation

$$\gamma_\mu\partial_\mu\psi = 0, \tag{7.1}$$

and a subsidiary condition,

$$\gamma_5\psi = -\psi, \tag{7.2}$$

which is consistent with (7.1).

It must, however, again be noted that such a definition has only a definite meaning if one restricts oneself to either right-handed or left-handed coordinate frames, since under the inversion $\psi \to \psi' = \gamma_4\psi$, the condition (7.2) goes over into

$$\gamma_5\psi' = +\psi',$$

and hence is not invariant.

In order to define a polarized neutrino, e.g. the d-field, by means of a Dirac spinor irrespectively of the handedness of the frame employed, we need to replace (7.2) by

$$\gamma_5\psi^{(d)} = -\eta_t\psi^{(d)}, \qquad \text{i.e.,} \qquad (1+\eta_t\gamma_5)\psi^{(d)} = 0, \tag{7.3}$$

and combine this with the field equation

$$\gamma_\mu\partial_\mu\psi^{(d)} = 0. \tag{7.4}$$

The verification of the equivalence of this formalism with our two-component formulation given in sec. 3 is effected by taking the representation of γ-matrices in which

$$\gamma_5 = \begin{pmatrix} -\sigma_0 & \cdot \\ \cdot & \sigma_0 \end{pmatrix}, \quad \gamma_k = \begin{pmatrix} \cdot & i\sigma_k \\ -i\sigma_k & \cdot \end{pmatrix}, \quad \gamma_4 = \begin{pmatrix} \cdot & \sigma_0 \\ \sigma_0 & \cdot \end{pmatrix}, \tag{7.5}$$

and making the identification

$$\psi^{(d)} = \begin{cases} \begin{pmatrix} \varphi^{(d)} \\ 0 \end{pmatrix} & \text{in a right-handed frame,} \\ \begin{pmatrix} 0 \\ \varphi^{(d)} \end{pmatrix} & \text{in a left-handed frame.} \end{cases} \tag{7.6}$$

Also the various densities such as the current vector† $S_\mu^{(d)} = i\bar{\psi}^{(d)}\gamma_\mu\psi^{(d)}$,

† $\bar{\psi} = \psi^\dagger\gamma_4$.

the spin density pseudovector $\hat{S}_\mu{}^{(d)}=i\bar{\psi}^{(d)}\gamma_5\gamma_\mu\psi^{(d)}$, etc., are proved to coincide exactly with those given for the two-component field $\varphi^{(d)}$; in particular, we find again the relation $\hat{S}_\mu{}^{(d)} = \eta_t S_\mu{}^{(d)}$.

8. Majorana Field

It has been noticed [9]) that the Majorana field is essentially equivalent to the two-component neutrino field. The meaning of such an equivalence is made clearer by means of our η_t-method. Again we consider the free field case. The Majorana field ϕ is defined by the Dirac equation

$$\gamma_\mu\partial_\mu\phi = 0 \tag{8.1}$$

and the subsidiary condition

$$\phi = \phi^C, \tag{8.2}$$

where ϕ^C is the charge conjugate defined by

$$\phi^C = C\bar{\phi}^T \tag{8.3}$$

with

$$C^\dagger C = 1, \qquad C^T = -C, \qquad \gamma_\mu{}^T = -C^{-1}\gamma_\mu C.$$

Now we define

$$\psi^{(d)} = (1-\eta_t\gamma_5)\phi; \tag{8.4}$$

this is a d-field in the 4-component representation (sec. 7), because this field clearly satisfies the condition (7.3). Conversely, ϕ can be expressed in terms of $\psi^{(d)}$ as follows: Taking the charge conjugate of (8.4) and using (8.2) we get

$$\psi^{(d)C} = (1+\eta_t\gamma_5)\phi. \tag{8.5}$$

Thus we have

$$\phi = \tfrac{1}{2}(\psi^{(d)}+\psi^{(d)C}). \tag{8.6}$$

Relations (8.4) and (8.6) yield a one-to-one correspondence † between ϕ and $\psi^{(d)}$. In spite of the equivalent correspondence between the Majorana field ϕ and a polarized field $\psi^{(d)}$ (or $\psi^{(g)}$), the former is intrinsically right-left symmetric while the latter is not. This is just the effect of the occurrence of η_t in the connection formula (8.4). This situation results in differences in free field properties of both fields; in particular the spin pseudovector vanishes for the Majorana field, $\hat{S}_\mu{}^M = i\bar{\phi}\gamma_5\gamma_\mu\phi = 0$, whereas for the polarized field we had $\hat{S}_\mu{}^{(h)} = \eta_h\eta_t S_\mu{}^{(h)}$.

9. Supplementary Remarks

9.1. TIME REVERSAL

As is well-known the polarized neutrino field is invariant under time reversal

† As $\psi^{(d)C}$ is a g-field we may write it as $\psi^{(g)}$: then the relations (8.4) and (8.6) are replaced by $\psi^{(g)} = (1+\eta_t\gamma_5)\phi$ and $\phi = \frac{1}{2}(\psi^{(g)}+\psi^{(g)C})$.

$$x_0 \to x'_0 = -x_0, \quad (x'_k = x_k). \tag{9.1}$$

This is ensured, in our two-component representation, by assuming that $\varphi^{(d)}$ transforms, along with (9.1), as

$$\varphi^{(d)} \to \varphi^{(d)\prime} = \varepsilon \Gamma \varphi^{(d)*} \quad (\varepsilon = \pm 1 \text{ or } \pm i) \tag{9.2}\dagger$$

In fact it is readily observed that we have

$$\partial'_0 \varphi^{(d)\prime} + \eta_l \sigma_k \partial'_k \varphi^{(d)\prime} = 0, \tag{9.3}$$

as the consequence of the original field eq. (3.3).

We can verify also that the above rule (9.2) is consistent with the rule for proper Lorentz transformations, (3.11), in a similar way as stated for the case of space inversion (sec. 3); namely we consider the following successive Lorentz transformations: First we transform the original frame I into another frame II through a proper Lorentz transformation L, and then we go to $\overline{\text{II}}$ by time reversal T, next we go, through a suitable proper Lorentz transformation $\overline{\text{L}}$, to the frame $\overline{\text{I}}$ that is the time reflection of the original frame I, and finally we come back to I by T. By these successive transformations the spinor $\varphi^{(d)}$ transforms as

$$\varphi^{(d)} \to \varphi^{(d)\prime} = \varepsilon \Gamma [\Lambda^{(d)}(\overline{\text{L}}) \varepsilon \Gamma \{\Lambda^{(d)}(\text{L}) \varphi^{(d)}\}^*]^*. \tag{9.3}$$

Noting that††

$$\overline{\text{L}} = \text{T}\text{L}^{-1}\text{T} = (\text{L}^{-1})^* \tag{9.4}$$

and using the relation (6.6), we get

$$\varphi^{(d)\prime} = \Gamma \Lambda^{(g)}(\text{L}^{-1})^* \Gamma^* \Lambda^{(d)}(\text{L}) \varphi^{(d)}. \tag{9.5}$$

Here we take account of the relation

$$\Lambda^{(d)} \Gamma = \Gamma \Lambda^{(g)*} \tag{9.6}$$

satisfied by the Λ-matrix, then we reach

$$\varphi^{(d)\prime} = \Lambda^{(d)}(\text{L}^{-1}) \Gamma \Gamma^* \Lambda^{(d)}(\text{L}) \varphi^{(d)} = -\varphi^{(d)}. \tag{9.7}$$

Originally the spinor $\varphi^{(d)}$ is double-valued, alternating its sign by a spatial rotation of 2π. We have seen that $\varphi^{(d)}$ changes its sign also by a loop of transformations containing time reversals. The above result (9.7) ascertains the consistency of our prescription for time reversal with that for proper Lorentz transformations.

The time reversal transformation properties of various bilinear covariants are derivable from (9.2); in particular we observe that both the current $S_\mu^{(d)}$ and spin density $\hat{S}_\mu^{(d)}$ transform as pseudovectors for (9.1):

† This transformation must not be confused with the helicity conjugation stated in sec. 6, in which $\varphi^{(d)}$ transforms by (6.10), keeping the coordinates (x_k, x_0) unchanged, so that the transformed field φ^Γ satisfied the equations for a g-field.

†† The meaning of the notation $(\text{L}^{-1})^*$ was given in the sentence following eq. (3.15).

$$\begin{aligned} S_k^{(d)} &\to -S_k^{(d)}, \quad S_4^{(d)} \to S_4^{(d)}, \\ \hat{S}_k^{(d)} &\to -\hat{S}_k^{(d)}, \quad \hat{S}_4^{(d)} \to \hat{S}_4^{(d)}, \end{aligned} \tag{9.8}$$

in accord with the physical meanings of these quantities.

9.2. PERFECTLY REFLECTION-INVARIANT TWO-COMPONENT THEORY

There exists a relativistic two-component spinor theory which is perfectly invariant to space inversion. This is formulated as follows: The field equation is

$$\sigma_\mu \partial_\mu \varphi = 0, \qquad \sigma_\mu = \{\sigma_k, \, i\sigma_0\} \tag{9.9}$$

which is assumed to hold equally in right-handed and left-handed coordinate frames. This is made possible by assigning to φ the following transformation rule under space inversion:

$$\begin{aligned} &\varphi \to \varphi' = \varepsilon_1 \Gamma \varphi^* \\ &(\varepsilon_1 = \pm 1, \text{ or } \pm i). \end{aligned} \tag{9.10}$$

For proper Lorentz transformation (3.9), φ transforms like

$$\varphi \to \Lambda \varphi, \qquad \Lambda^\dagger \sigma_\mu \Lambda = a_{\mu\nu} \sigma_\nu; \tag{9.11}$$

and for time reversal,

$$\begin{aligned} &\varphi \to \varepsilon_2 \Gamma \varphi^*, \\ &(\varepsilon_2 = \pm 1, \quad \text{or} \quad \pm i). \end{aligned} \tag{9.12}$$

We can verify that the above prescriptions are mutually consistent.

This theory contains nothing to distinguish between right and left as is evident from the fact that it is formulated in inversion-covariant form with no use of η_t.

In fact the theory is identical with the Majorana field and is just the one considered by Case [5]). Apparently this theory is rather similar to the theory of polarized neutrino treated in the present paper, but the physical features of both theories are quite different, in so far as we consider the free field properties; for instance the former does not imply any handed relation such as $\hat{S}_\mu^{(d)} = \eta_t S_\mu^{(d)}$ which was characteristic to the latter. More detailed considerations about the two-component representation of the Majorana field will be given in a separate note.

In conclusion the author would like to express his sincere gratitude to Professor L. de Broglie and also to the other members of the Institut Henri Poincaré for kind discussions in this work.

References

1) T. D. Lee and C. N. Yang, Phys. Rev. **104** (1956) 254
2) H. Weyl, Z.f. Phys. **56** (1929) 330;
W. Pauli, Handb. d. Phys. **24/1** (Berlin 1933) p. 225
3) T. D. Lee and C. N. Yang, Phys. Rev. **105** (1957) 1671

4) T. Takabayasi, Compte-rendus Acad. Sci. **246** (1958) 1010
5) K. M. Case, Phys. Rev. **107** (1957) 307
6) B. L. van der Waerden, Die gruppentheoretische Methode in der Quantenmechanik (Springer, Berlin 1932) p. 92
7) P. A. M. Dirac, The Principles of Quantum Mechanics (Oxford, 1935) p. 260
8) e. g. L. Landau, Nuclear Physics **3** (1957) 127
9) J. Serpe, Physica **18** (1952) 295;
Mac Lennan, Phys. Rev. **106** (1957) 821;
L. A. Radicati and B. Touschek, Nuovo Cimento **5** (1957) 1693;
W. Pauli, Nuovo Cimento **6** (1957) 204

2.L *Nuclear Physics* 7 (1958) 251–262; © *North-Holland Publishing Co., Amsterdam*
Not to be reproduced by photoprint or microfilm without written permission from the publisher

INELASTIC SCATTERING OF PROTONS AT INTERMEDIATE ENERGIES

N. ODA

Department of Physics, Rikkyo (St. Paul's) University, Tokyo

and

K. HARADA

Japan Atomic Energy Research Institute, Tokai-mura, Ibaragi-ken

Received 24 February 1958

Abstract: The differential cross sections for the inelastic scattering of protons at intermediate energies are calculated in an analytical way on the basis of the statistical independent particle model with a diffuse nuclear surface, assuming that main contribution to the cross section comes from the direct interactions of incident protons with the target nucleons penetrating out beyond some critical radius in the diffuse rim of the nucleus, and taking the Pauli principle exactly into consideration. The contribution of the compound nucleus formation process to the cross section was also estimated. The application to the inelastic scattering of 31 MeV protons by Sn leads to values of the cross sections in good agreement with the experiment.

1. Introduction

Experiments by Eisberg and Igo [1]) on the inelastic scattering of 31 MeV protons by medium and heavy elements have given results completely incompatible with the predictions derived from the statistical theory of the compound nucleus [2]): (a) the angular distributions were strongly peaked forward, (b) the energy distribution was relatively flat, and (c) the observed total cross sections were at least an order of magnitude larger than the compound nucleus cross section for boiling off protons through the Coulomb barrier.

Hayakawa *et al.* [3]) tried with fair success to explain these results by direct knock-on processes taking place throughout the whole nuclear volume assumed as a Fermi gas (having constant density and a sharp boundary). This case was first treated analytically by Goldberger [4]) in order to interpret the nuclear reactions induced by 90 MeV neutrons.

Along this line, recently, a more detailed calculation, omitting the simplifying assumptions made by Hayakawa *et al.*, has been performed by Elton and Gomes [5]). The results of their reexamination show that the direct volume processes are no more effective than the compound nucleus processes and the calculated total cross section is more than ten times

smaller than the experimental one. The large reduction of the direct volume interaction cross section obtained by them is essentially due to the realistic inclusion of the effect of total internal reflection at the nuclear boundary: the reflection effect due to the Coulomb barrier hinders more strongly the escape of protons from the nucleus than in the case of Hayakawa *et al.*, and almost all protons, once they have penetrated into the nucleus, are trapped to form a compound nucleus. Then, Elton and Gomes discussed a different explanation, by the direct surface processes occurring in the diffuse rim of the nucleus, which was first proposed in a qualitative form by Eisberg and Igo [1]), and found a result in fair agreement with experiment.

Their analytical calculation is based on the assumptions that (i) the momentum distribution of the target nucleons in the diffuse rim is given by $\rho(k) = |\psi(k)|^2 = \exp(-k^2/K^2)$ (i.e., a Gaussian function), and (ii) the Pauli principle is not operative in the diffuse rim. However, the above assumptions do not seem to have any physically unique and consistent grounds, so that the calculations based on other models are desirable for comparison†.

Among the various models thus far proposed, the Fermi gas model, as is well known, is unexpectedly valid in a wide range of nuclear phenomena. Particularly, the absolute magnitude of the imaginary part of complex potential used in the optical model of nuclear reactions, and its dependence upon the energy of the incident particle, could be successfully calculated by many authors [6–8]), assuming that (a) the nucleus can be represented by a Fermi gas, and (b) the incident particle interacts individually with the bound nucleons of the target, with a cross section which differs from that for free particles only through the restrictions due to the Pauli principle. Various calculations of direct volume interaction processes were also essentially based on the above assumptions (a) and (b).

In this paper we shall extend this approach, without losing its essential characteristics and internal consistency, and make it applicable to the direct surface processes produced in the diffuse rim of the nucleus, so as to provide a useful basis for the future development of theoretical investigations of the phenomena concerned. The actual application of our method is made to the results of Eisberg and Igo [1]).

Calculations are carried out according to the following prescriptions:

1) For the (p, p′) reaction in the intermediate energy region, since the direct volume and compound processes may be largely suppressed due to the reflection effect of nuclear Coulomb barrier, the main contributions will come from the scattering of the incident protons by the outside part of the nucleus, which diffuses out beyond the top of the Coulomb barrier.

† Further, eqs. (2.6) and (3.3) given in their paper are incorrect.

2) The semi-classical statistical model (the independent particle model) is assumed as a model of the nucleus having a diffuse rim; the Fermi gas of constant density and sharp boundary of assumption (a) above is replaced by a Thomas-Fermi gas of variable density.

3) On the other hand, assumption (b) is completely retained. Since the nucleus is treated as a gas consisting of independent nucleons, the Pauli exclusion principle should operate not only inside the nucleus but also in the diffuse rim.

4) The Coulomb barrier, acting so as to define the effective scattering region of the diffuse rim and reduce the energy of the incident protons, is modified from the conventional form, taking into account the effect of the diffuseness of nuclear surface.

5) An estimate based upon the evaporation model is given to see to what extent the compound processes increase the differential cross sections in backward directions.

2. The Independent Particle Model of a Nucleus with a Diffuse Rim

According to the prescriptions 1)—3) just mentioned it is first necessary to find the nucleon density and the momentum distribution of nucleons in the diffuse rim, on the basis of the independent particle model. To do this it is assumed that the simple Thomas-Fermi formula, stating the proportionality of the density ρ and the 3/2-power of the maximum kinetic energy $T_F(r)$, will be valid in the diffuse rim:

$$\rho(\mathbf{r}) = \sum|\psi_i|^2 \approx \frac{2}{\hbar^3}\frac{4\pi}{3}[2M(E-V(\mathbf{r}))]^{3/2} = \frac{2}{\hbar^3}\frac{4\pi}{3}p_F^3(\mathbf{r}), \qquad (1)$$
$$-(\hbar^2/2M)\nabla^2\psi_i + V(\mathbf{r})\psi_i = E_i\psi_i,$$

where the sum is over all filled states, E being the total energy of the most energetic particle, and $p_F(\mathbf{r})$ being the maximum momentum of any particle at the point $\mathbf{r}$. Instead of proceeding to derive the self-consistent "Thomas-Fermi equation" from the formula (1) as in the usual Thomas-Fermi theory, we shall simply make use of the relation (1) in order to fix the values of $p_F(\mathbf{r})$ from the knowledge of $\rho(\mathbf{r})$. On the other hand, given E and $V(\mathbf{r})$, the values of $\rho(\mathbf{r})$ and $p_F(\mathbf{r})$ can be uniquely derived from eq. (1): the actual calculation on this line was performed by Swiatecki [9]) for a nuclear potential well with rather gently sloping sides. His results show that on the basis of the independent particle model the surface energy can be simply connected with the slope of the potential in the surface reigon; the density of protons for the diffuse potential, adjusted to obtain the empirical magnitude of the surface energy, is not inconsistent with high-energy electron scattering experiments [10]) and for a nucleus with $N > Z$ it

is possible to have a neutron radius greater than the proton radius [11]). These results seem to be supporting the use of eq. (1) in our case.

The density of protons ρ_p can be fairly well determined from the high-energy electron scattering [10]). As for the density of neutrons ρ_n, there is no definite experimental evidence; ρ_n was assumed to have the same type of distribution as ρ_p, only with a difference of the parameter values, expressing the enrichment of neutrons at the surface. Referring to electron scattering [10]) we have assumed a Fermi type function for the actual shape of ρ_p and ρ_n:

$$\rho(r) = a\{\exp[(r-c)/b]+1\}^{-1}, \tag{2}$$

where a is a normalization factor to make the integral of $\rho_p(r)$ or $\rho_n(r)$ over the whole space equal to Z or N respectively; c is the radius at which $\rho(r)$ has half its central value, b a diffuseness parameter.

Near the rim of the surface eq. (2) may be approximated by

$$\rho(r) \approx a \exp[-(r-c)/b], \tag{3}$$

from which $p_F(r)$ in the rim is evaluated. The parameters b and c for $\rho_p(r)$ could be exactly determined from the analysis of electron scattering †; $b = 0.57\ f$ and $c = 1.1 \times A^{1/3} f$. The similar parameters for $\rho_n(r)$ were varied within a reasonable range in view of our present ignorance of the law of nuclear force ††.

Next, according to the prescription 4), we shall derive the critical radius R_0 determining the effective rim region in question. From the analysis of the proton elastic scattering experiments in the 20 MeV range, it was proved that the nuclear potential should have a rounded edge. Following Woods and Saxon [13]) we have assumed the following shape of potential:

$$V(r) = V_n(r)+V_c(r), \tag{4}$$

where

$$V_n(r) = -V_0\{\exp[(r-R_1)/d]+1\}^{-1}, \tag{5}$$

and V_c is the Coulomb potential for a point charge Ze, $V_c = Ze^2/r$. We assumed the following values for the parameters: $V_0 = 40$ MeV, $d = 0.5f$ and $R_1 = 1.35 \times A^{1/3} f$. We have tentatively assumed that R_0 is taken equal to the radius at which the potential (4) has a maximum value, according to the prescription 1). This choice of R_0 means that the nucleon-nucleon interaction is approximately taken to be a contact interaction, similar to the one adopted by Austern *et al.* [14]) in their calculation of direct surface interaction.

As an illustration, ρ_p, ρ_n and the Coulomb barrier (4) for Sn^{120} ($N = 70$,

† We express all lengths in terms of $f = 10^{-13}$ cm.

†† For example, see ref. [13]) for the relation between the nuclear density and the nuclear potential.

$Z = 50$), are shown in fig. 1 and $p_F^2(r)$ derived from eq. (1) for the adopted values for the parameters is given in fig. 2.

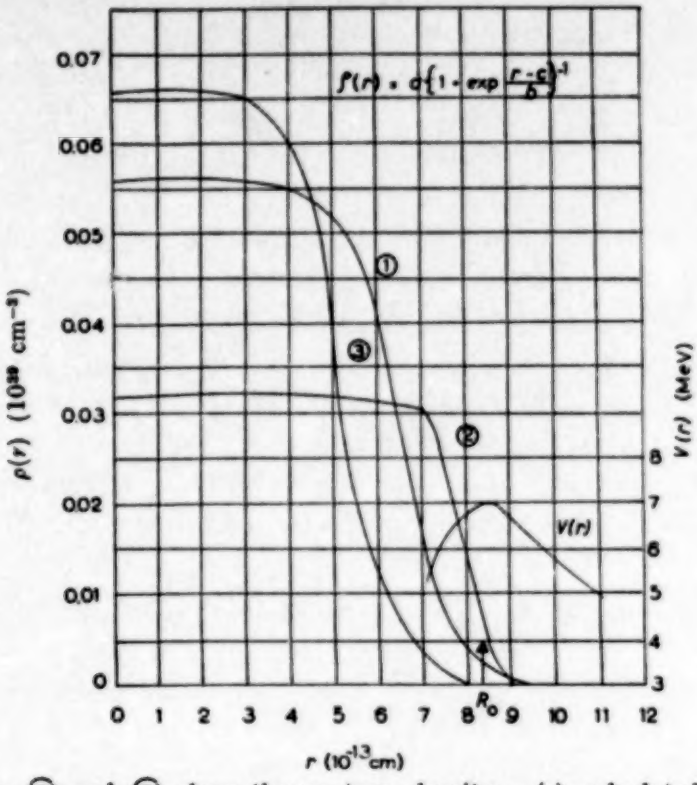

Fig. 1. Curves (1) and (2) show the neutron density $\rho_n(r)$ calculated with parameters $b = 0.57 \times 10^{-13}$ cm, $c = 6.66 \times 10^{-13}$ cm, and $b = 0.3 \times 10^{-13}$ cm, $c = 8 \times 10^{-13}$ cm, respectively. Curve (3) shows the proton density $\rho_p(r)$ calculated with parameters $b = 0.57 \times 10^{-13}$ cm, $c = 5.42 \times 10^{-13}$ cm determined from experiment.

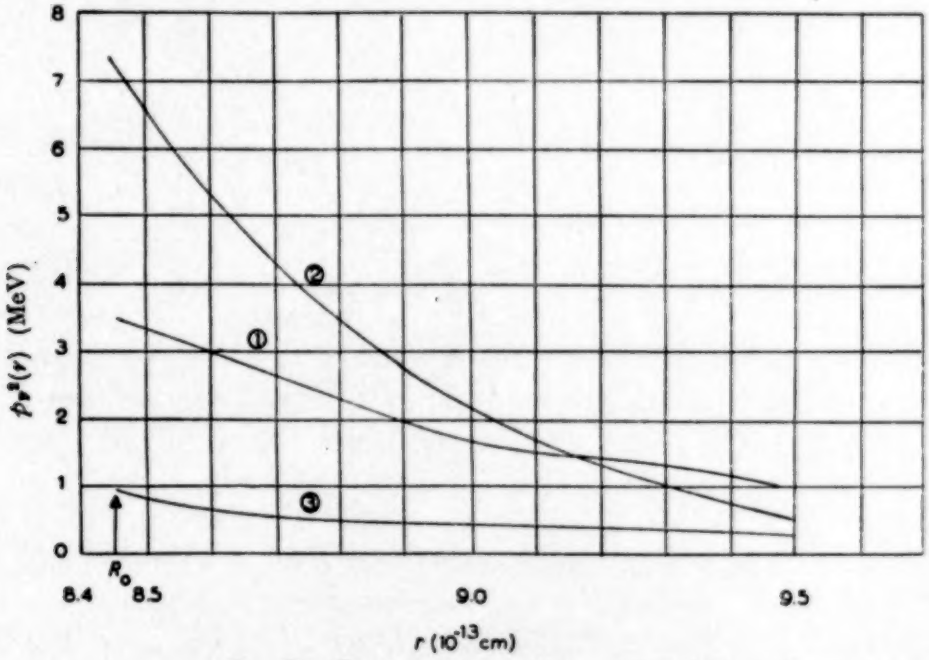

Fig. 2. The curves (1), (2), (3) show the Fermi-momentum $p_F^2(r)$ calculated from curves (1), (2), (3) of $\rho(r)$ in fig. 1, using eq. (1).

3. The Differential Cross Section for the Diffuse Rim Scattering

According to the prescriptions 1) and 3), the differential cross section $\sigma(\mathbf{p}_f)d\mathbf{p}_f$ for the scattered protons having a final momentum between $\mathbf{p}_f$ and $\mathbf{p}_f+d\mathbf{p}_f$ in the laboratory system is derived as the result of the interaction which occurs through a single collision of the incident proton with either a neutron or proton in the effective diffuse rim of the target nucleus defined in the preceding section.

Let the momenta of incident and target nucleons be $\mathbf{p}_1$ and $\mathbf{p}_2$ and those of outgoing and residual nucleons be $\mathbf{p}_f$ and $\mathbf{p}'_2$, respectively. The distribution of the momenta $|\mathbf{p}_2|$ of the target nucleons, from the centre of the nucleus, extends uniformly from zero to the value $p_{2F}(r)$, given in the preceding section. The Pauli principle requires $|\mathbf{p}_f| > p_{1F}(r)$ and $|\mathbf{p}'_2| > p_{2F}(r)$ for the collision occurring at distance r. The two-body scattering cross section for these nucleons is a function of half the relative momenta of the initial and final states, $\mathbf{p}$ and $\mathbf{p}'$, respectively, and is assumed to be the same as for free particles of the same relative momenta, according to the prescription 3). The above cross section $\sigma(\mathbf{p}, \mathbf{p}')$ in the centre of mass system is very nearly inversely proportional to $|\mathbf{p}|^2(=|\mathbf{p}'|^2)$ over a considerably wide range of energies [15]), and is assumed to be isotropic. Although this assumption is not correct for n–p scattering, the error introduced is negligible in this calculation.

The differential cross section $\sigma(\mathbf{p}_f)d\mathbf{p}_f$ may be expressed as

$$\sigma(\mathbf{p}_f)d\mathbf{p}_f = \frac{1}{v_1}\frac{2}{\hbar^3}\frac{N_{eff}}{N_{rim}}\int d\mathbf{r}\int d\mathbf{p}_2 v_{rel}\sigma(\mathbf{p}, \mathbf{p}')\frac{\delta(p-p')}{p^2}d\mathbf{p}_f, \tag{7}$$

where

$$v_{rel} = 2p, \tag{8}$$

$$N_{rim} = \frac{2}{\hbar^3}\int_{R_0}^{\infty} d\mathbf{r}\int_0^{p_F(r)} d\mathbf{p}_2 = \int_{R_0}^{\infty}\rho(\mathbf{r})\,d\mathbf{r}, \tag{9}$$

$$N_{eff} = \alpha N_{rim}; \tag{10}$$

N_{rim} defined in eq. (9), in terms of the density $\rho(\mathbf{r})$ given by eq. (1), is an average number of nucleons in the effective rim region and is introduced in eq. (7) to play the role of a normalization. N_{eff} expresses the part of N_{rim} truly effective to the cross section in question: not all members of N_{rim} may be effective for our case, since nucleons at the back of the nucleus do not contribute to the scattering, and scattering from the front of the nucleus is likely to lead to a compound nucleus process. Accordingly, the value of the reduction factor α has been tentatively assumed to be 1/3.

The integration $\int d\mathbf{r}\int d\mathbf{p}_2$ should be first performed with respect to $\mathbf{p}_2$ for a fixed $\mathbf{r}$, under the restriction of the Pauli exclusion principle operating locally. This method of integration originates from the fact that

in our case of variable density the Fermi momentum $p_F(r)$ is a function of the space coordinates of the target nucleons.

Assuming $\sigma(\mathbf{p}, \mathbf{p}') = \sigma_t(p)/4\pi$, we get

$$\sigma(\mathbf{p}_f)\mathrm{d}\mathbf{p}_f = \frac{2\sigma_t\alpha}{h^3 q p_1}\int_{R_0}^{\bar{R}} \mathrm{d}\mathbf{r} \times \begin{cases} (p_f^2 - p_1^2) & \text{for } p_F^2(r)+p_f^2-p_1^2-z_0^2 \geqq 0 \\ (p_F^2(r) - z_0^2) & \text{for } p_F^2(r)+p_f^2-p_1^2-z_0^2 \leqq 0, \end{cases} \tag{11}$$

where †

$$q = |\mathbf{q}| = |\mathbf{p}_f - \mathbf{p}_1|, \tag{12}$$

$$z_0 = \frac{1}{2q}(p_f^2 + q^2 - p_1^2), \tag{13}$$

and $\bar{R}$ is a root of the equation $p_F^2(r) = z_0^2$. If the Pauli principle is disregarded, we uniquely get $p_F^2(r) - z_0^2$ for the integrand of eq. (11). The Coulomb effect on the scattered protons has been taken into account through the reduction of the kinetic energy in the collision region.

The actual calculation has been performed for the inelastic scattering of 31 MeV protons by Sn. The values of N_{rim} for several choices of b and c are listed in table 1.

TABLE 1

Values of N_{rim} for $_{50}\mathrm{Sn}^{70}$, $R_0 = 8.5 \times 10^{-13}$ cm

Target Nucleons	b	c	r_0 †	N_{rim}
Protons	0.57	5.42	1.1	0.19
Neutrons	0.57	6.66	1.35	1.32
	1.00	6.66	1.35	8.46
	0.30	7.15	1.45	0.16
	0.30	8.00	1.6	2.02

† $c = r_0 A^{1/3}$ f.

The calculated cross sections due to the target protons only are shown in fig. 3: they are much smaller than the experimental ones. Those due to the target neutrons only, for two choices of $\rho_n(r)$, of which the one has a smaller radius c and a larger diffuseness b than the other, are shown in figs. 4 and 5, respectively. The latter gives larger cross sections in backward directions than the former, reflecting the fact that the relative increase of the higher momentum components of target nucleons in the diffuse rim gives rise to a relative increase of the backward cross sections. The agreement of these cross sections with the experimental ones is fairly satisfactory, except for the backward direction. It is to be noted that $p_F^2(r)+p_f^2-p_1^2-z_0^2$ with the values of parameter adopted here has always been negative due to

† For the convenience of comparison we used the same notations as those of ref. [3]).

the smallness of the values of $p_F^2(r)$. Thus, the the differential cross sections computed from eq. (11) actually give the same values as those calculated without regard to the Pauli principle. The effect of the Pauli principle appears if the value of $p_F^2(r)+p_f^2-p_1^2-z_0^2$ becomes positive. This is the case for the scattering taking place in a region of the nucleus more central than that considered here.

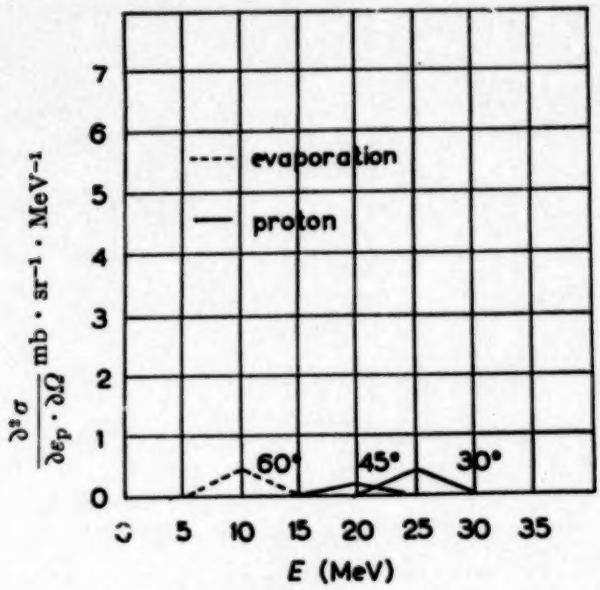

Fig. 3. The solid curves are differential cross sections for diffuse rim scattering of 31 MeV protons due to the target protons only. The dotted curve is the differential cross section calculated from the evaporation theory.

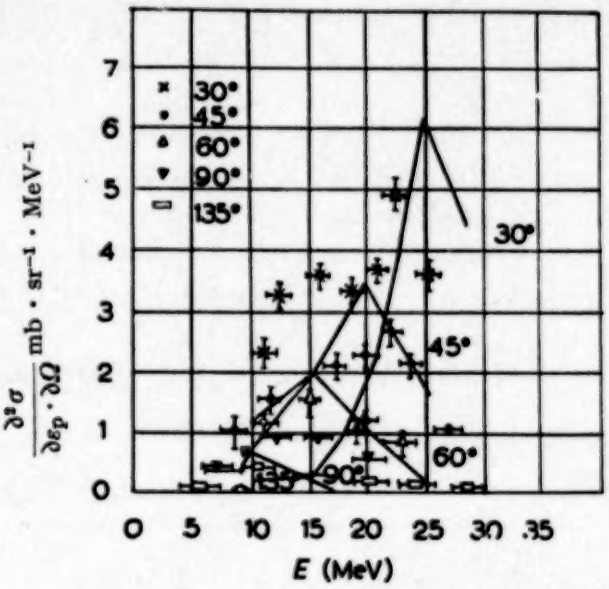

Fig. 4. Differential cross sections for diffuse rim scattering of 31 MeV protons due to the target neutrons only. The parameters adopted are the same as those for $\rho_n(r)$ (1) in fig. 1.

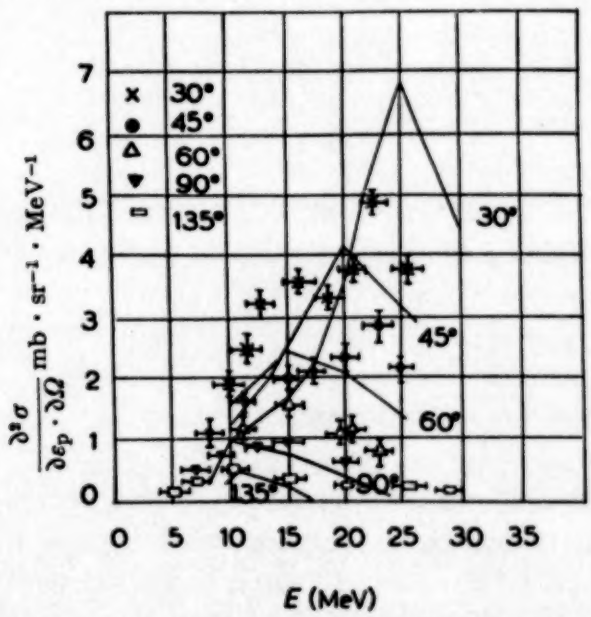

Fig. 5. Differential cross sections for diffuse rim scattering of 31 MeV protons due to the target neutrons only. The parameters adopted are the same as those for $\rho_n(r)$ (2) in fig. 1.

4. The Effect of the Compound Nucleus Processes

There is a possibility that the observed cross sections in backward directions might have been largely contributed by the protons evaporating from a compound nucleus, formed as a final result of the multiple collisions of the incident protons with the target nucleus occurring in the region within the radius R_0 defined previously. We shall here give a estimate of this process.

While the excitation of a compound nucleus accompanying the nucleon emission due to direct volume collisions may have a wide range of energies, these states of excitation cannot contribute significantly to the processes considered here. Therefore, the excitation energy of the compound nucleus E_{exc} may be assumed to be

$$E_{\text{exc}} = E_{\text{p}}+S_{\text{p}},$$

where E_{p} and S_{p} are the channel energy and the binding energy of the incident proton in the compound nucleus.

The cross section σ_{c} for the formation of a compound nucleus with excitation energy E_{exc} may be defined by

$$\sigma_{\text{c}} = \sigma_{\text{a}}-\sigma_{\text{direct volume}}-\sigma_{\text{direct surface}}; \tag{14}$$

σ_{a} is the absorption (reaction) cross section on the optical model, defined as the total cross section minus the shape-elastic scattering cross section, and can be calculated by the use of a complex potential [16]). For σ_{a}, we take the value 1.5 *b*, interpolated from the cross sections computed by Melkanoff *et al.* [17]), who used a diffuse optical potential for 31.5 MeV protons. The cross section $\sigma_{\text{direct volume}}$ was computed for the Fe nucleus and 18 MeV protons by Hayakawa *et al.* [3]). From their results, taking into account the difference of target nuclei and incident energies, we can estimate this direct cross-section for neutron emission to be 10 to 20 mb (that for proton emission being negligible). The cross section $\sigma_{\text{direct surface}}$ is theoretically given by integration of the differential cross section of eq. (7) over the whole range of angles and energies; actually, it was estimated from the experimental data [1]) to be 200 to 250 mb, depending upon the amount subtracted as the contribution from the compound processes. After all, σ_{c} has a value from 1.2 to 1.3 b.

The differential cross section for the emission of protons with energy ε_{p}, through the evaporation process is given, in the usual way [2, 18]), by

$$\frac{\partial^2\sigma}{\partial\varepsilon_{\text{p}'}\partial\Omega} = \frac{\sigma_{\text{c}}}{4\pi}\frac{2M_{\text{p}}}{\hbar^2}\frac{\varepsilon_{\text{p}'}\sigma_{\text{c}}(\varepsilon_{\text{p}'})w_{\text{R}}^{(\text{p}')}(E_{\text{exc}}-S_{\text{p}}-\varepsilon_{\text{p}'})}{\sum_{\text{k}}F_{\text{k}}(E_{\text{exc}}-S_{\text{k}})}, \tag{15}$$

where M_{p} is the mass of proton, $w_{\text{R}}^{(\text{p}')}$ the level density of the residual nucleus left after the evaporation of protons with energy $\varepsilon_{\text{p}'}$, and $\sigma_{\text{c}}(\varepsilon_{\text{p}'})$

the cross section for the formation of a compound nucleus with energy E_{exc} by a proton with energy $\varepsilon_{p'}$ in the inverse process; F_k is defined by

$$F_k(E_{exc}-S_k) = \frac{2M_k}{\hbar^2}\int_0^{E_{exc}-S_k} \varepsilon_k \sigma_c^{(k)}(\varepsilon_k) w_R^{(k)}(E_{exc}-S_k-\varepsilon_k)\mathrm{d}\varepsilon_k, \quad (16)$$

where the suffix k stands for the emitted particle k and all notations with suffix k have the same meaning as for the proton. F_γ for the emission of gammas was found to be negligible. For the level density $w(E)$ we used the semi-empirical formula

$$w(E) = C \exp 2\sqrt{aE}, \quad (17)$$

$$C_{even} = \tfrac{1}{2}C_{odd\text{-}mass} = \tfrac{1}{4}C_{odd},$$

where a was assumed to be 8 MeV^{-1} for every residual nucleus and C to be 0.02 MeV^{-1} for odd-mass nuclei, according to Blatt and Weisskopf [18]). Actual evaluations of F_k have been done for protons, neutrons, deuterons, alphas and tritons. The required separation energies S_k were estimated with the aid of experimental dat [9]):

$$S_p = 6.2\ \text{MeV},\ S_n = 9.7\ \text{MeV},\ S_d = 13.2\ \text{MeV},$$
$$S_\alpha = 4\ \text{MeV},\ S_t = 13.7\ \text{MeV}.$$

For the evaluation of $\sigma_c^{(k)}(\varepsilon_k)$ we have employed the formula given in ref. [18]).

With 31 MeV protons, the emission of protons through (p, np) and (p, 2p) processes should be also considered, but we have not included them because the exact values S_{nn} and S_{pp} which significantly affect the results were not known from the experimental data, and these processes would not contribute much to the energy spectrum of protons except for the lower energy part. We have therefore chosen for σ_c the lower limit 1.2 b to see to what extent even the evaporation processes without (p, np) and (p, 2p) contribute to the cross sections in backward directions. The result is given in fig. 3, which corresponds to the lower limit of the contribution from the compound processes. While the lower energy part of the experimental proton spectrum can be fully explained by the compound processes, on the other hand in the higher energy region the contributions of the compound processes are not sufficient to fit the experimental curve, and other effects will be required.

5. Conclusion

We have developed for the interpretation of the inelastic scattering of intermediate energy protons a formulation of the direct surface interaction in the diffuse rim of the target nucleus, on the basis of the statistical theory of the independent particle model of the nucleus with diffuse nuclear boundary, with exact inclusion of the Pauli principle. Actual application

has been made to the differential cross section for inelastic scattering of 31 MeV protons by the Sn nucleus, and the results show that with the appropriate values for the parameters the agreement with the experimental cross sections is quite good, except for backward directions, and that the Pauli principle is not effective in this case. It seems, however, to be very interesting to derive the radial dependence of the absorption potential in the optical model from our theory, in which the Pauli principle is exactly taken into account.

Next, a lower limit of the contribution from the compound nucleus processes has been given, using a reasonable value of the cross section for compound nucleus formation σ_c and neglecting (p, np) and (p, 2p) processes. One finds that, in the backward direction, (i) the lower energy part of the experimental proton spectrum is mostly covered by the contribution from the compound nucleus processes and leaves little room for any contribution from direct surface processes, and (ii) on the other hand the higher energy part should mostly come from processes other than compound processes.

These results indicate in what way to refine the theory in future. The refinement of the theory will require a more detailed examination of the following points: (i) the detailed shape of the neutron density in the diffuse rim, (ii) the replacement of the assumption of contact interaction used in our calculation by a more realistic interaction of finite range, and (iii) a more realistic estimate of the effective numbers of nucleons in the diffuse rim, N_{eff}.

In this connection other experiments, with 14 MeV neutrons [20]), 18 MeV protons [21]) and 40 MeV alphas [22]), should be reexamined in the light of the direct surface processes which might give large contributions in these cases as well.

We should like to thank Professor Y. Sugiura for his interest and stimulating discussions on the subject of this work, Professor S. Yoshida for his valuable advice for the manuscript. One of the authors (K. Harada) would like to express his sincere thanks to Professor S. Kikuchi and members of theoretical division of the Institute for Nuclear Study, University of Tokyo, for the hospitality they have extended to him, especially to Dr. K. Kikuchi for his kind criticism and encouragement.

References

1) R. M. Eisberg and G. Igo, Phys. Rev. **93** (1954) 1039
2) V. F. Weisskopf and D. H. Ewing, Phys. Rev. **57** (1940) 472
3) S. Hayakawa, M. Kawai and K. Kikuchi, Prog. Theor. Phys., **13** (1955) 415
4) M. L. Goldberger, Phys. Rev. **74** (1948) 1269

5) L. R. B. Elton and L. C. Gomes, Phys. Rev. **105** (1957) 1027
6) A. M. Lane and C. F. Wandel, Phys. Rev. **98** (1955) 1524
7) E. Clementel and C. Villi, Nuovo Cimento **11** (1955) 176
8) G. C. Morrison, H. Muirhead and P. A. B. Murdoch, Phil. Mag. **44** (1955) 795
9) W. J. Swiatecki, Phys. Rev. **98** (1955) 203, 204
10) R. Hofstadter, Revs. Mod. Phys. **28** (1956) 214
11) M. H. Johnson and E. Teller, Phys. Rev. **93** (1954) 357
12) K. A. Brueckner, Phys. Rev. **103** (1956) 1121
13) R. D. Woods and D. S. Saxon, Phys. Rev. **95** (1954) 577
14) N. Austern, S. T. Butler and H. McManus, Phys. Rev. **92** (1953) 350
15) Millburn, Birnbaum, Crandall and Schecter, Phys. Rev. **95** (1954) 1268
16) V. F. Weisskopf, Revs. Mod. Phys. **29** (1957) 174
17) Melkanoff, Nodvik, Saxon and Woods, Phys. Rev. **106** (1957) 793
18) J. M. Blatt and V. F. Weisskopf, Theoretical Nuclear Physics (John Wiley and Sons, 1952)
19) A. H. Wapstra, Physica **21** (1955) 385
20) L. Rosen and L. Stewart, Phys. Rev. **107** (1957) 824
21) P. C. Gugelot, Phys. Rev. **93** (1954) 425
22) G. Igo, Phys. Rev. **106** (1957) 256

1.E.4:
3.A

Nuclear Physics 7 (1958) 263—275; © *North-Holland Publishing Co., Amsterdam*
Not to be reproduced by photoprint or microfilm without written permission from the publisher

TRANSITIONS IN Hg^{199} FOLLOWING THE DECAY OF Au^{199}

G. BÄCKSTRÖM, O. BERGMAN and J. BURDE †

The Institute of Physics, Uppsala, Sweden

Received 24 February 1958

Abstract: The energies of the three γ-lines in Hg^{199} were measured absolutely, using an iron-free double focusing spectrometer. The atomic binding energy was also absolutely determined. Relative L-subshell conversion intensities were found to yield accurate information on the multipolarity. Relative M-shell conversion coefficients were compared with theory. Partial transition probabilities were computed, and the effect of l-forbiddenness was studied.

1. Introduction

The absolute measurement of γ energies in Hg^{199} is connected with our present work on neutron deficient gold isotopes. These isotopes, being produced by cyclotron bombardment of Pt, are generally obtained as mixed with Au^{199}, which thus produces a set of accurate reference lines. When constructing a complicated decay scheme, it is particularly important to measure the conversion line energies on an absolute scale, since otherwise sum relations and atomic shell differences are not accurately conserved.

Au^{199} is indeed a rather suitable standard source. Its γ-energies are convenient for absolute determination; it can easily be produced pure and carrier-free, and the half-life is reasonably long. Advantage can further be taken of the fact that one of the gamma energies is the sum of two others.

2. Experimental Method

The momentum of electrons measured in an iron-free double focusing spectrometer, as used in this work, is proportional to the current through the coils, or to the potentiometer reading R. If the momenta of a K and an L_i internal conversion line, of the same transition, are recorded as R_K and R_{Li} respectively, the calibration constant c, defined as $c = B\rho/R$, is given by the equation

$$f(cR_{Li}) - f(cR_K) = E(K, L_i) \qquad (1)$$

where f is the electron energy as a function of $B\rho$ and $E(KL_i)$ is the X-ray transition energy between the shells involved. Although the equation may be solved explicitly for c, it is simpler to apply successive approximations,

† On leave from the Hebrew University, Jerusalem, Israel.

using tabulated values [1]) of $f(B\rho)$. Obviously the accuracy of the calibration procedure is higher the larger the ratio of R_{L_i}/R_K. It is advantageous to compute the calibration constant from L_{II} or L_{III} subshells, as $E(KL_i)$ then corresponds simply to a K_α emission line, which is generally carefully measured. In our case, Hg appeared to be an exception, obviously due to the experimental difficulty of obtaining emission lines from this element. Probably the best measurement of the Hg K_α lines has been made by Beckman [2]), who reports $K_{\alpha 1} = 70.824 \pm 0.020$ keV and $K_{\alpha 2} = 68.902 \pm 0.020$ keV. This accuracy is not satisfactory for our purposes. The neighbouring elements however, Ir, Pt, Au as well as Tl, Pb, Bi have been carefully investigated in the X-ray emission work of Ingelstam [3]), who reports relative errors of a few parts in 10^5. From a compilation of these data [21]) we have tried to obtain the Hg emission lines by interpolation. Plotting the ratio K_α/Z^2 as a function of Z results in a rather straight but sloping curve. Subtraction

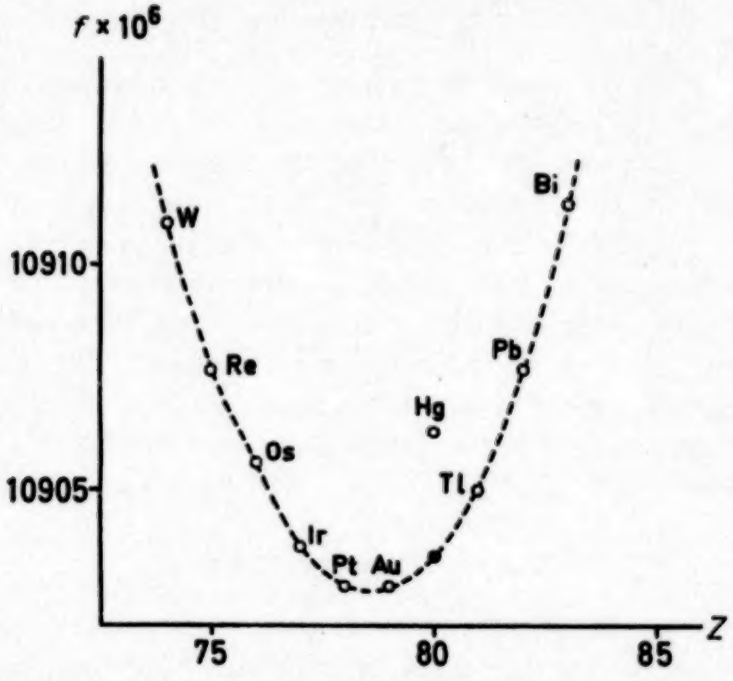

Fig. 1. Plot of $f = K_\alpha/Z^2 + c(Z-80)$, using published values for K_α. The full dot at $Z = 80$ corresponds to the interpolated value of the K_α energy; the open one to the experimental data.

of a suitable linear function of Z, shows that the experimental points lie on a parabola with its apex at about $Z = 80$ (fig. 1). Physically, there is no reason to expect a marked deviation from the smooth curve at $Z = 80$, and the $K_{\alpha 1}$ value for Hg was interpolated on this assumption. As an alternative, the three first terms in the Taylor expansion of $K_\alpha(Z)$ were subtracted from the function $K_\alpha(Z)$. The derivatives were taken as the mean values of the 1st and 2nd differences. Both treatments were found to yield

the same results: 70.807 keV and 68.881 keV for $K_{\alpha 1}$ and $K_{\alpha 2}$, respectively. The errors in these energies are believed to be only slightly larger than in the primary data used for the interpolation. However, should future X-ray work on mercury yield different values from those adopted here, it will be easy to correct accordingly the present final results. Precise evaluation of gamma energies from the conversion electron energies can be done if $K_{\alpha 1}$, $K_{\alpha 2}$, the $(L_I L_{II})$ difference and the L_I binding energy are known accurately. $E(L_I L_{II})$ is found to be 0.634 keV by means of simple interpolation.

Atomic binding energies have, with few exceptions, been determined by measuring the energy of the absorption edge. As has been pointed out by Sokolowski *et al.* [4]), this is not the best way of obtaining absolute data. Furthermore Parrat *et al.* [5]) pointed out that in a practical case the absorption edge shifts as the absorbing layer becomes thicker, an effect which has recently been experimentally demonstrated by Beckman [6]) for a heavy element. This necessitates an extrapolation to zero thickness, a precaution which has perhaps not been taken by all workers. However, the present method opens a new possibility of simultaneous absolute measurement of electron energies and binding energies. There is no doubt that the three transitions involved in the decay of Au^{199}, are two cascades E_1 and E_2 and a cross-over line (E_3), related by

$$E_1(S_i)+S_i+E_2(S_m)+S_m = E_3(S_n)+S_n \qquad (2)$$

where $E_i(S_j)$ are electron energies from the i-th transition and the shell given in parenthesis, and S_j signifies the corresponding binding energies. If S_n is chosen to be equal to S_i or S_m, eq. (2) gives immediately the value of the binding energy of shell S_m or S_i respectively. By choosing, in the present work, $S_i = L_I$ and $S_m = S_n = K$, L_I was evaluated from eq. (2). It can be shown that in this case, with the electron energies 36 keV, 75 keV and 125 keV for $E_1(L_I)$, $E_2(K)$ and $E_3(K)$ respectively, L_I is very insensitive to the value of the calibration constant c. For this reason, it was chosen to compute L_I, the other binding energies being obtained by adding the pertinent emission energies.

3. Experimental Arrangement

About 1 g of very pure platinum was irradiated during one week in a slow neutron flux of $10^{12}/cm^2$ sec. The (n, γ) reaction produces Pt^{199} decaying with short half-life (33 min) to Au^{199} ($T_{\frac{1}{2}} = 3.1$ d). The latter can thus be separated carrier-free, and isotopically pure. After dissolving the platinum target in boiling aqua regia, the gold fraction is extracted with ethyl-acetate and then transferred to an aqueous solution†. The source preparation was made by electroplating the gold on a 1×10 mm² mylar strip with a thin layer of evaporated silver. The efficiency of this source

† We are much endebted to Miss I. B. Svensson for carrying out this separation.

preparation was about 30 %. The strip was cemented diametrically across a ring-shaped source holder and special care was taken to ensure good electrical contact to the vacuum tank. The cut-off energy of the Geiger tube was 6 keV. The details of the instrument used for this investigation have been described elsewhere[7]). The double focusing magnetic field is achieved by means of two concentric solenoids, wound on watercooled cores. In order to have a momentum accuracy of one part in 10^5 it is necessary to know the temperatures of the coils to within 1° C. In our experiments the temperatures of the coil frames were measured by thermocouples and the water stream regulated so that the temperature was constant within $\pm 5°$ C. For each line recorded, the current was switched off and the earth's magnetic field compensation checked. A systematic investigation was made on the instrument and its surroundings in order to discover factors which could possibly disturb the momentum linearity.

The spectrometer was set to a relative line halfwidth $\Delta B\rho/B\rho = 0.16$ % and the crucial conversion lines were recorded twice. One of the runs was more extensive, including M-groups and weaker components of the L-groups. A typical part of the spectrum is shown in fig. 2.

Apart from electrical charging, there are two source effects which could impair the energy measurements, namely straggling due to some thickness of the gold deposit, and back-scattering. Most electrons scattered back from the 1 mg/cm² mylar foil will have lost too much energy to reappear under the conversion peak, but from the silver film, which also has a much higher atomic number, an almost elastic scattering would be conceivable. This would then show up as an energy dependent tail. As we indeed observe closely the same halfwidth and the same line shape for as different energies as 36 keV and 146 keV, these sources of error must be unimportant in our case.

4. Experimental Results and Discussion

4.1. ENERGIES

The energies of the electron lines are given in table 1. The mean value for the binding energy found from these data is $L_I = 14.846 \pm 0.010$ keV, to be compared with the measured absorption edge value[21]) 14.841 keV. L_I has been used as the basis for calculating other binding energies, as mentioned above. The resulting absolute energies, with their limits of error are

$$E_{\gamma 1} = 49.817 \pm 0.015$$
$$E_{\gamma 2} = 158.359 \pm 0.025$$
$$E_{\gamma 3} = 208.176 \pm 0.030.$$

TABLE 1

Results of the absolute energy measurements

Conversion line	Energy (keV)		γ-energy (keV) mean value
	Run 1	Run 2	
50 L_I	34.976	34.972	49.820
50 L_{II}	35.602		49.814
158 K	75.265	75.266	158.359
158 L_{II}	144.145		158.357
158 L_{III}	146.073	146.073	158.359
208 K	125.080	125.092	208.179
208 L_I	193.314	193.342	208.174

4.2. MULTIPOLARITIES

The following relative intensities given in brackets have been obtained by comparing the line areas per unit momentum, after correction for the decay and the small counting losses:

$50L_I(160)$, $50L_{II}(19.6)$, $50L_{III}(3.52)$, $50\sum M_i(46)$ $158K(875)$, $158L_I(146)$, $158L_{II}(850)$, $158L_{III}(620)$ $158\sum M_i(420)$, $158\sum N_i(120)$. $208K(600)$, $208L_I(93)$, $208L_{II}(16.9)$, $208L_{III}(4.8)$.

The experimental L subshell conversion ratios are summarized in table 2

TABLE 2

Multipole assignments

γ-line	L_I/L_{III}			L_{II}/L_{III}			Multipolarity
	Exp.	Theor. M1	Theor. M2	Exp.	Theor. M1	Theor. E2	
50	46 $\pm$7	105	0.022	5.6 $\pm$0.9	8.7	1	M1+E2(0.19$\pm$0.06%)
158	0.23$\pm$0.03	140	0.24	1.37$\pm$0.14	9.8	1.46	E2(< 1.5 % M1)
208	19.3 $\pm$3	147	0.44	3.5 $\pm$0.7	10.0	1.65	M1+E2(11$\pm$3%)

together with the theoretical ratios for the only possible competing multipolarities, M1 and E2. The mixing fractions inferred from these are also given. The computations have been based on the finite-nucleus conversion coefficients for the K and L shells, according to Rose [8]).

It is evident that the relative conversion coefficients for the L subshells are much more sensitive to mixing than $K/\sum L$ ratios. It has been preferred therefore to calculate these mixing values exclusively from the L subshell-intensities and use the resulting admixture in order to check the experimental $K/\sum L$ ratios. The experimental $K/\sum L$ for the 158 keV and the 208 keV transitions are 0.54 ± 0.06 and 5.2 ± 0.5 against the theoretical values 0.62 and 5.7. The agreement might be considered as fair, bearing in mind that the K and L lines were not recorded in immediate succession, and some slow drift of the Geiger tube cannot be quite eliminated.

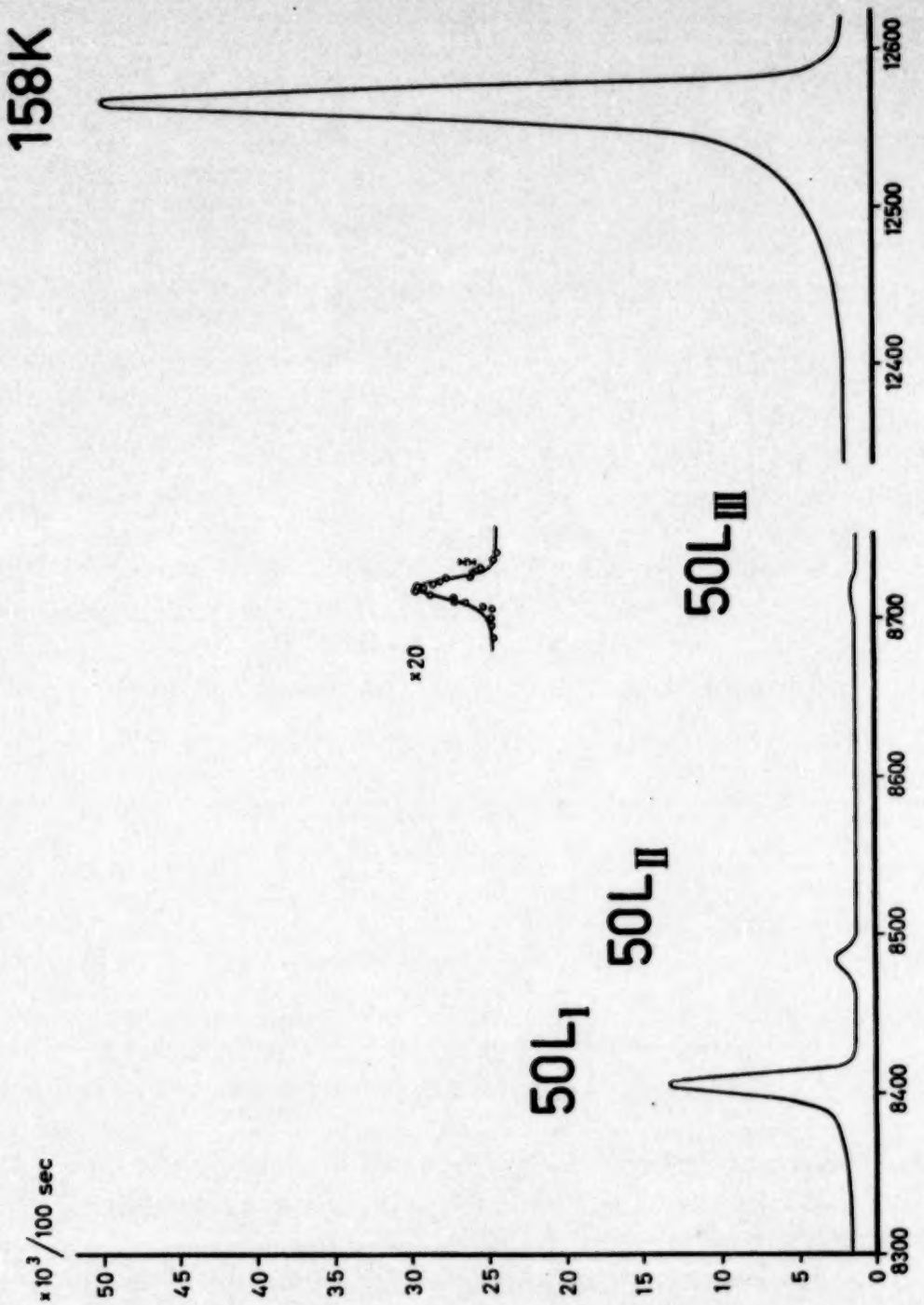
158K
×10³/100 sec
50
45
40
35
30
25
20
15
10
5
0
8300
8400
8500
8600
8700
12400
12500
12600
50L_I
50L_II
50L_III
×20

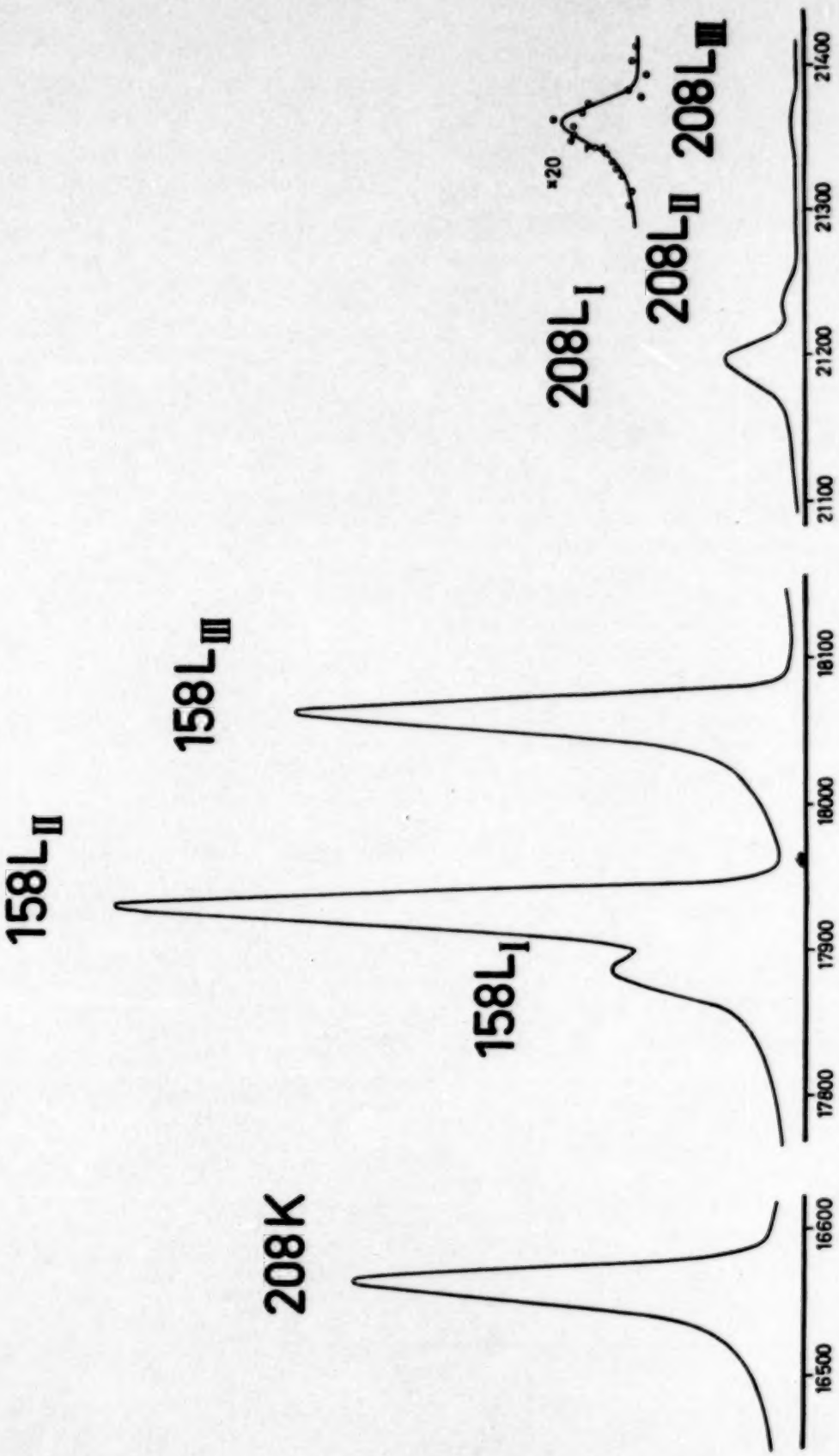

Fig. 2. The internal conversion spectrum of Au^{199}, taken with the iron-free double focusing spectrometer at a resolution of 0.16 %. The statistical error is negligible except in the two cases where the standard deviation has been indicated.

4.3. M SUBSHELL CONVERSION

Rose [8]) has calculated conversion coefficients for the M sub-shells neglecting finite nuclear size and screening. He emphasizes that absolutely the values may thus be wrong by as much as a factor of two but that taken relatively they should be far more accurate. Since the present spectrum contains an almost pure M1 and a pure E2 transition, it has been found wortwhile to make a comparison with theory for these two different cases. Table 3 contains the relevant data derived from an analysis of the line

TABLE 3

Relative M subshell conversion coefficients

$E_\gamma = 50$ keV (M1) †

	M_I	M_{II}	M_{III}	M_{IV}	M_V	$\Sigma L_i/\Sigma M_i$
Theory	1	1.07(—1)	9.7(—3)	1.15(—3)	6.8(—4)	2.11
Experiment	1	1.24(—1)	<2.5(—2)	<2.5(—2)	<2.5(—2)	3.97

† The numbers in brackets indicate powers of 10.

$E_{\gamma 2} = 158$ keV (E2)

	M_I	M_{II}	M_{III}	M_{IV}	M_V	$\Sigma L_i/\Sigma M_i$
Theory	1.27(—1)	1	7.5(—1)	1.3(—2)	1.0(—2)	2.06
Experiment	1.26(—1)	1	7.6(—1)	<3.0(—2)	<3.0(—2)	3.85

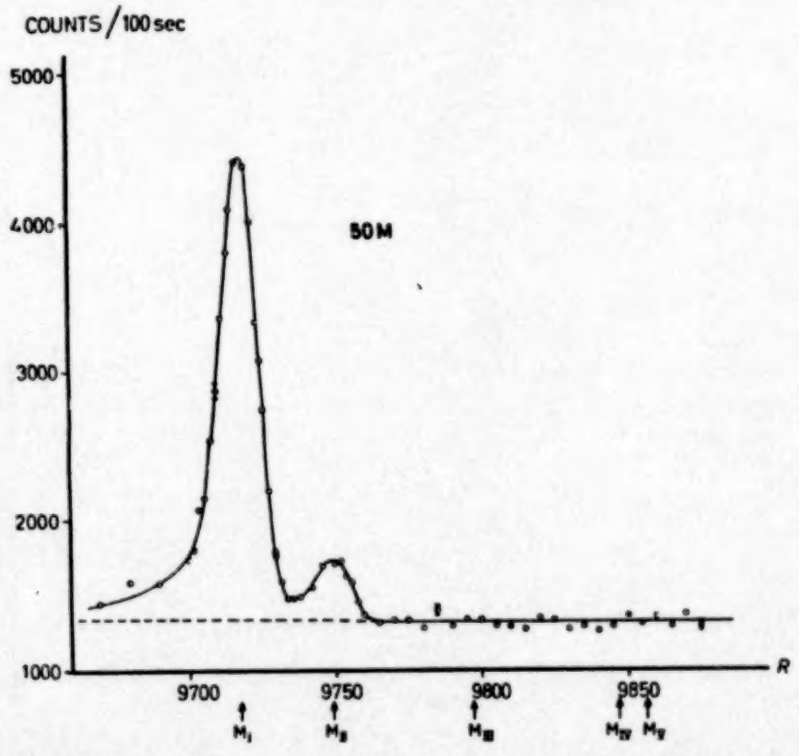

Fig. 3. The M shell conversion group of the 50 keV transition, of multipolarity M1. The arrows under the base line show the computed positions of the individual sub-lines.

shapes as shown in figs. 3 and 4. The measured M_i subshells have been divided in each case by the most intense line and compared with Rose's tables, after normalizing these data in the same manner. No discrepancy has been observed within the experimental error. However Rose's values are in disagreement in their absolute value with the experimental M shell intensity as is shown through the $(\sum L_i)/(\sum M_i)$ ratio in the last column of table 3.

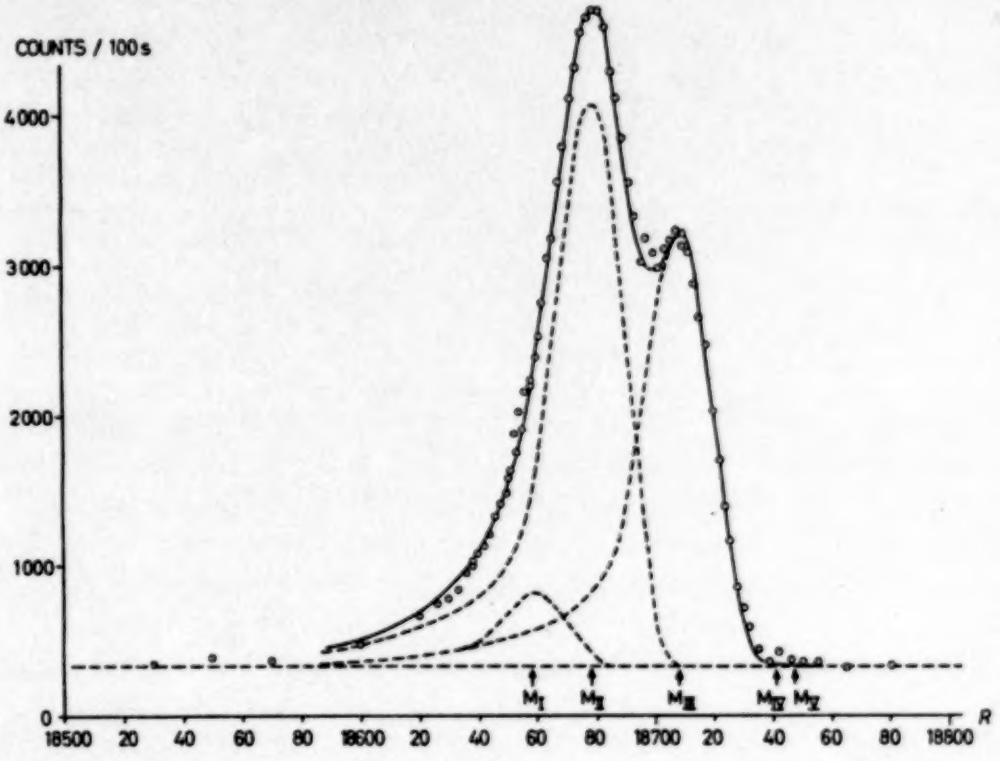

Fig. 4. The M conversion group of the 158 keV E2 transition. The structure has been resolved using the calculated positions of the sub-lines. The points represent experimental data; the full curve is the sum of the three window curves shown. The lines corresponding to M_{IV} and M_V are not observed.

4.4. β-DECAY BRANCHING RATIOS

The β-decay of Au^{199} (fig. 5) proceeds through three branches to the Hg^{199} levels. By analyzing the Kurie plot, Haynes and Achor [9]) have separated the components and determined the intensities: 24.3 % (251 keV), 69.3 % (302 keV) and 6.4 % (460 keV). The present results provide even more reliable values for the first two branches. The total transition probability is the sum of the total conversion intensity and the γ-decay rate, which can be accurately calculated. The total conversion line set has been recorded only for γ158. However, compiling L/(M+N) ratios from previous works one finds the ratio to be about 3.2 and there is no systematic trend with energy or multipolarity. Using this fact we obtain 21 ± 2 % and 73 ± 2 % for the β branching of the second and third components.

4.5. γ-TRANSITION PROBABILITIES

The knowledge of multipole mixing, together with level life-times given in the literature, enables one to compute a number of transition life-times. Table 4 is a compilation of available life-time data, obtained by means of

TABLE 4

Compilation of published mean life-times in Hg^{199}

Level energy	$\tau_{\gamma E2}$ (ns)	τ_{total} (ns)	method	authors
158	7700		Coul. exc.	Barloutaud *et al.*[10])
	15000		Coul. exc.	Davis *et al.*[11])
	6200	3400 ± 300	Delayed coinc.	Graham and Bell [12])
208	1550	78 ± 12	Res. scatt	Knapp [13])
	1320		Res. scatt	Metzger [14])
	1400	70 ± 40	Delayed coinc.	Graham *et al.*[15])
	2000	100 ± 60	Delayed coinc.	Graham *et al.*[16])
	6400		Coul. exc.	Davis *et al.*[11])
	3500		Coul. exc.	Barloutaud *et al.*[10])

resonant scattering, Coulomb excitation and delayed coincidences. In the cases where the results are based on assumptions concerning the conversion probability, these have been made reasonably enough not to change the life-times seriously. In order to facilitate comparison, τ_{E2}, the mean life-time, has been computed in all cases. The agreement between different authors is unfortunately only slight owing to the fact that the time range is unfavourable to most methods, except in one case. The mean values adopted are $\tau_{E2}(208) = 2.0\times10^{-9}$ sec and $\tau_{E2}(158) = 7.0\times10^{-9}$ sec. The computed transition probabilities using the branching data of the present work, have been summed up in table 5. The table also presents the ratios to

TABLE 5

Computed γ transition probabilities, compared to the single particle estimate

Energy (keV)	P(M1) (sec^{-1})	P (E2) (sec^{-1})	P (M1)/P(M1)$_{sp}$	P (E2)/P(E2)$_{sp}$
50	1.35×10^{5}	2.5×10^{5}	2.1×10^{-2}	8 ± 3
158	$<1.4\times10^{6}$	1.4×10^{9}	$<10^{-3}$	7.6
208	4.5×10^{9}	5.0×10^{8}	1.8×10^{-2}	7.0

the theoretical estimate, obtained by using Moszkowsky's formulae[17]: $P_{M1} = 2.8\times10^{13}E^{3}S$ and $P_{E2} = 1.6\times10^{8}A^{4/3}E^{5}S$, where E stands for transition energy in MeV and S for the statistical factor[24]). The values of S have been chosen in accord with the spin assignments of fig. 5.

The estimate for M1 is approximately valid for a single neutron as well as a single proton, whereas with E2 the ratios of table 5 would become larger

by a factor of 500 using the single neutron estimate. It is noticed that while the M1 transitions are retarded, the E2 probabilities are enhanced by collective motion. Within each group the comparative transition rates are found to be remarkably constant.

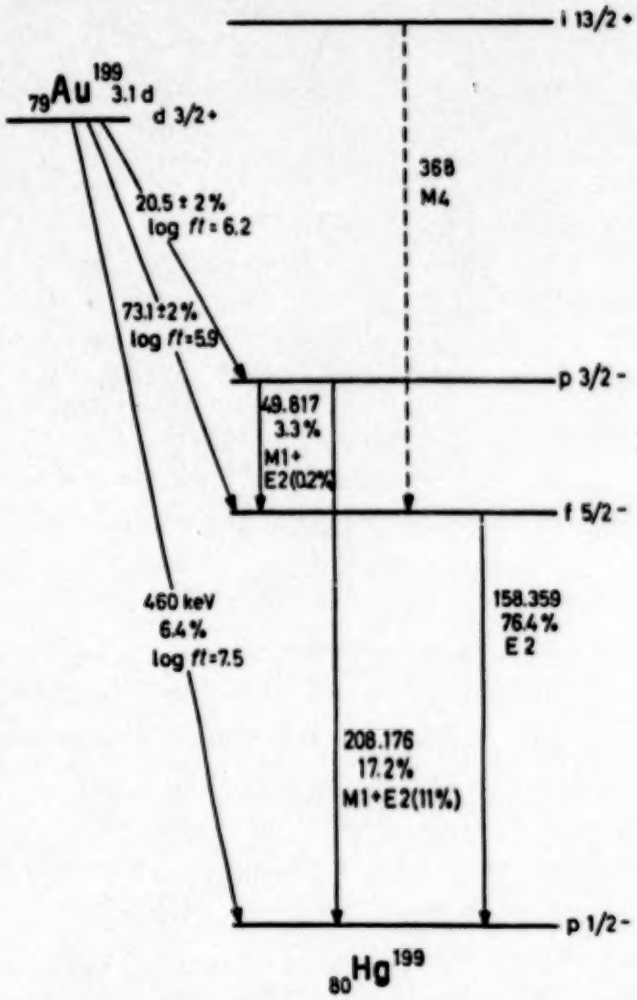

Fig. 5. The decay scheme as known from previous investigations. Energies, total intensities and multipole characters are given as found in the present work.

4.6. SPINS AND PARITIES

The decay scheme of Au^{199} is shown in fig. 5. The ground state spins 3/2 and $\frac{1}{2}$ for Au^{199} and Hg^{199} respectively, have been determined by magnetic resonance methods[22, 23]). Parity change is necessary to explain the doubtless forbiddenness of the connecting β-transition, the minus parity being assigned to Hg^{199} in consistency with the systematics of magnetic moments. In the theoretical level scheme according to Klinkenberg [18]) the 79th proton in Au may fill into a $d_{3/2}^{+}$ state, while for the 119th neutron in Hg there is a choice between $p_{\frac{1}{2}}^{-}$, $p_{3/2}^{-}$, $f_{5/2}^{-}$ and $i_{13/2}^{+}$. There exists indeed an isomeric state [19]) in Hg^{199}, decaying by emission of a 368 keV M4 transition in cascade with the 158 keV γ-line. The only possible shell model interpretation is the sequence $i_{13/2}$ (M4) $f_{5/2}$ (γ158)$p_{\frac{1}{2}}$. The pure E2 multipolarity for

$\gamma 158$ that we have found, is an experimental confirmation of the spin 5/2− for the first excited state. The spin of the 208 keV state must be $J \leqq 3/2$ and negative parity, since we observe an M1 branch to the ground state. The alternative $\frac{1}{2}-$ is excluded by the doubtless E2 admixure in the same transition and the result is 3/2−. Finally it is seen that the shell model supports the parity assignments in several ways. It could thus be believed that the orbital angular momentum would have a definite meaning and would be predicted by the same shell model. This means that the 50 keV gamma ray should be an l-forbidden M1 transition, i.e. $\Delta l = 2$. Now its M1 probability has been found to be closely equal to that of the l-allowed 208 keV transition. Attention has earlier been drawn to this fact by Graham and Bell [12]), although an accurate comparison of transition rates had not been done at the time. In a corresponding comparison [20]) for the odd proton nucleus Tl^{203} the reported ratio is approximately 10^{-3}. We evidently come to the conclusion that although there are too many neutron holes in Hg^{199} for it to be treated as an independent particle system, the same model does, curiously enough, predict correct spins and parities for the states involved.

The authors wish to thank professor K. Siegbahn for his interest in this work and for the use of the iron-free spectrometer. C. Nordling's and E. Sokolowski's hints concerning the use of the instrument are greatly appreciated. We further wish to thank A. Bäcklin for his assistance in taking readings.

One of us, J. Burde, likes to express his sincere thanks to professor Kai Siegbahn for the hospitality which has been shown to him during his stay at the institute and gratefully acknowledges a UNESCO fellowship and an adv. I. Philipson family's scholarship.

Note added in proof: The energy of the first excited state in Pt^{194} has since been measured by means of the iron-free instrument, the source containing both Au^{199} and Au^{194}. Using the conversion line momenta reported in this article, a relative measurement of the ground state transition in Pt^{194} yielded $E_\gamma = 328.45 \pm 0.06$ keV. O. Beckman *et al.* (Ark. Fys., to be published) have recently measured the same gamma ray from the decay of Ir^{194} with a curved crystal spectrometer, calibrated against a number of well known X-ray emission lines. Their value, 328.42 ± 0.05 keV, thus supports independently the present results on Hg^{199}.

References

1) T. R. Gerholm in Beta- and Gamma Ray Spectroscopy, edited by K. Siegbahn, p. 926
2) O. Beckman, Phys. Rev., to be published
3) E. Ingelstam, Dissertation (Uppsala 1937)
4) E. Sokolowski, C. Nordling and K. Siegbahn, Arkiv för fysik **12** (1957) 301
5) L. G. Parrat, C. F. Hempstead and E. L. Jossem, Phys. Rev. **105** (1957) 1228
6) O. Beckman, The Institute of Physics, Uppsala, private communication
7) K. Siegbahn and K. Edvarson, Nuclear Physics **1** (1956) 137
8) M. E. Rose, Oak Ridge National Laboratories, privately circulated papers

9) S. K. Haynes and W. T. Achor, J. Phys. radium **16** (1955) 635
10) R. Barloutaud, T. Grejebine and M. Riou, Comptes rendus **242** (1956) 1284
11) R. H. Davis, A. S. Divatia, D. A. Lind and R.D. Moffat, Phys. Rev. **103** (1956) 1801
12) R. L. Graham and R. E. Bell, Can. J. Phys. **31** (1953) 377
13) V. Knapp, Proc. Phys. Soc. A **70** (1957) 142
14) F. A. Metzger, J. Franklin Inst. (1956) 261, 219
15) R. L. Graham, R. E. Bell, L. Yaffe and J. S. Geiger, Phys. Rev. **99** (1955) 1646
16) R. L. Graham *et al.*, Bull. Am. Phys. Soc. **30** (1955) 20
17) S. A. Moszkowski in Beta- and Gamma Spectroscopy, edited by K. Siegbahn, p. **373**
18) P. F. A. Klinkenberg, Revs. Mod. Phys. **24** (1952) 63
19) N. Hole, Arkiv Mat. Astron. Fys. **36** A (1949) no. 9
20) T. Lindqvist and I. Marklund, Nuclear Physics **3** (1957) 367
21) S. Fine, C. F. Hendee, Nucleonics **13**, no. 3 (1955) 36
22) D. R. Hamilton *et al.*, Phys. Rev. **101** (1956) 1389
23) W. G. Proctor, F. C. Yu, Phys. Rev. **81** (1951) 20
24) S. A. Moszkowski, Phys. Rev. **89** (1953) 474

8.B *Nuclear Physics* **7** (1958) 276—280; © *North-Holland Publishing Co., Amsterdam*
Not to be reproduced by photoprint or microfilm without written permission from the publisher

NOTES ON MESON DECAYS

R. F. STREATER and J. C. TAYLOR
Imperial College of Science and Technology, London

Received 18 March 1958

Abstract: Some meson decay rates are examined as closely as possible, particularly to see if they are consistent with a universal Fermi interaction of V and A type. A possible connection is noted between the pion lifetime and the bare pion mass.

1. Introduction

If the He^6 beta decay recoil experiments prove to be wrong, the idea of a universal Fermi interaction will be a very attractive one [1]). This note analyses some meson decay rates with such a possibility in mind. The best that can be done in general is to write down the simplest direct interaction, corresponding to the decay in question, which is compatible with the V and A form of the Fermi interaction. The effect of the strong interactions is accounted for approximately by means of multiplicative constants, and the values found for these from the different decays are compared. In some cases, particularly $K_{\mu 3}$ and K_{e3}, more rigorous comparisons can be made.

The conclusions are discussed in the final section. We find some support for the belief that the K-meson interactions are significantly less strong than the pion interactions [2]). We note also the possibility that the π^+ life-time may afford a direct measure of the bare pion mass.

2. $K_{\mu 3}$ and K_{e3}

The strong interactions are identical in these decays, and, if the Fermi interactions of muons and electrons are sufficiently similar, an exact comparison is possible.

Let P, k, p, q be the momenta of the K, π, μ (or e), ν, and ψ, ϕ be the μ (e) and ν spinors, the latter being two-component. The amplitudes for the decays then have the form

$$g_S f_S \bar{\psi}\phi + g_T f_T P_\mu k_\nu \bar{\psi}\sigma_{\mu\nu}\phi + g_V f_{V1} P_\mu \bar{\psi}\gamma_\mu\phi + g_V f_{V2} k_\mu \bar{\psi}\gamma_\mu\phi.$$

Here the g's are the Fermi coupling constants. The factors $f = f(P, k, p, q) = f(P, k)$ represent the effect of the strong interactions. We have assumed the K-meson to be pseudo-scalar, but this is unimportant. The corresponding decay rate is then

$$(\hbar/\tau) = \int |g'_S f'_S(E)|^2 \rho_S(E)\mathrm{d}E + \int |g_T f_T(E)|^2 \rho_T(E)\mathrm{d}E + \int |g_V f'_V(E)|^2 \rho_V(E)\mathrm{d}E$$
$$+2\mathrm{Re}\int [g_S^* g_V f_S^* f'_V \rho_{SV} + g_V^* g_T f'^*_V f_T \rho_{VT}]\mathrm{d}E,$$

where

$$g'_S f'_S = g_S f_S - m_{\mu,e} g_V f_{V2}, \qquad f'_V = f_{V1} - f_{V2}.$$

Here E is the pion energy, and the kinematical factors $\rho(E)$ which are different for the two decays, have been computed by, for instance, MacDowell [3]).

Let us assume that present experimental indications are correct and that $(1/\tau)_\mu > (1/\tau)_e$ [4]). Then one definite conclusion can be drawn: that the universal Fermi interaction, if it exists, is not of the types S, T and P *alone*. This statement follows from the inequalities [3])

$$\rho_S^{(e)}(E) > \rho_S^{(\mu)}(E), \qquad \rho_T^{(e)}(E) > \rho_T^{(\mu)}(E), \quad \text{for all } E.$$

If the Fermi interaction contains S, V and T terms, it is difficult to make any definite statement. Therefore we assume henceforth the popular V and A form. Even then no rigorous conclusion can be drawn. However, it is probable that the factors $f(E)$ do not vary appreciably over the available range of values of E. So, replacing these functions by constants f, we obtain

$$(\hbar/\tau)_\mu \approx |g_V|^2 [11|f_{V1}|^2 + |f_{V2}|^2 - 5\mathrm{Re}\, f_{V1}^* f_{V2}] \times 10^7 \text{ MeV},$$
$$(\hbar/\tau)_e \approx |g_V|^2 [12|f_{V1}|^2] \times 10^7 \text{ MeV}.$$

It follows that

$$(1/\tau)_\mu \gtrsim \tfrac{1}{2}(1/\tau)_e.$$

This is certainly consistent with experiment. It also shows that it *cannot* be true of these decays that the effective value of g_V for muons is significantly greater than for electrons (as appears to be true of pion decay). Finally, assuming an experimental value $(1/\tau)_e \approx 1.6 \times 10^6\ \mathrm{sec}^{-1}$ and $g_V \approx 10^{-11}$ MeV^{-2}, we conclude that

$$|f_{V1}| \approx 0.3.$$

This is not considered an unreasonable value for a dimensionless number. Note that these decays are particularly suitable for making this kind of estimation, just because the contributions from the strong interactions are dimensionless. When the ratio of the two decay rates is known more accurately, it will be possible to determine the ratio f_{V1}/f_{V2}. Present results indicate $|f_{V2}| \lesssim 1$.

3. Other Meson Decay Modes

Firstly we compare the two (possible) decay modes $\pi^+ \to e^+ + \nu + \gamma$, $\pi^0 \to 2\gamma$. These are probably suitable for comparison, since in each case the strong interactions are represented by a "triangle" of similar structure. The simplest direct interactions consistent with the V and A Fermi interaction

are

$$(n_1/M)e^2\pi\varepsilon_{\lambda\mu\nu\rho}F_{\lambda\mu}F_{\nu\rho}$$

and

$$(n_2/M)eg_\Lambda(\bar{\psi}\gamma_\mu\phi)F_{\mu\nu}\partial_\nu\pi.$$

Here π is the pion field. The nucleon mass, M, has been inserted arbitrarily as a dimensional factor, and the numbers n_1 and n_2 are to be determined to represent the contribution from the strong interactions. Experimentally it is known that [5])

$$(1/\tau)_{e3} < 400 \text{ sec}^{-1}, \qquad (1/\tau)_{\pi^0} > 2\times 10^{15} \text{ sec}^{-1},$$

and comparison with the above interactions yield

$$n_1 \lesssim 0.1, \qquad n_2 \gtrsim 1.$$

Thus these two results are certainly consistent with one another, and with both factors n being of the order unity. Each experimental limit would have to be tightened up by a factor of order 10 at least before there could be any conflict.

Secondly we compare the three decay modes

$$\mathrm{K}^+ \to \mu^+ + \nu, \qquad \pi^+ \to \mu^+ + \nu, \qquad \Lambda \to \mathrm{P} + \pi^-.$$

As before, we represent the strong interactions by the constants n in the following direct couplings

$$n_3 g_\Lambda M(\bar{\psi}\gamma_\mu\phi)\partial_\mu \mathrm{K}, \qquad n_4 g_\Lambda M(\bar{\psi}\gamma_\mu\phi)\partial_\mu\pi, \qquad n_5 g_\Lambda M(\bar{\mathrm{P}}\gamma_\mu\Lambda)\partial_\mu\pi,$$

in an obvious notation. The nucleon mass is again inserted as a dimensional factor. The formal similarity between the three interactions is the justification for comparing them. The Λ decay is less suitable than the other two, because more than one strongly interacting particle is involved; but as the energies concerned are small this may not be too important. Comparison with known decay rates yields

$$n_3 \approx 0.04, \qquad n_4 \approx 0.16, \qquad n_5 \approx 0.2.$$

We consider the interpretation of these numbers in the next section.

4. Conclusion

Gell-Mann [2]) has suggested that baryons may be coupled less strongly with K-mesons than with pions. Preliminary results from dispersion relations support this notion [6]). Our result above, that $(n_3/n_4)^2 \approx 10$, may be an indication that this difference between pions and K-mesons has its consequences in the decays. The similarity between n_4 and n_5 lends support to the reliability of this sort of comparison.

Gell-Mann's idea may help in understanding other decay rates. For instance, the slowness of $\mathrm{K}^+_{\pi 2}$ would be explained if, by some collaboration

between selection rules, this decay must take place through *three*, at least, K-meson interactions. The other feature of Gell-Mann's scheme is that, when the K-mesons are neglected, the baryons and the pion interaction take on a higher symmetry. The principle controlling the form of a universal Fermi interaction might be expected to be connected with this "global" symmetry. Then it is possible that cancellation between the various intermediate baryon states might account for the anomalous slowness of π_{e2} decay. One detailed scheme incorporating these two possibilities has been described by d'Espagnat and Prentki [7]). Whether or not their proposals prove correct in detail, they at least demonstrate the possibility of developing these ideas.

Continuing this line of argument, we should expect that for $\pi_{\mu 2}$ decay, in contrast with π_{e2} decay, the different intermediate states should conspire to reinforce one another. The simplest way this can happen is when the baryon (and possibly meson) current, j_μ, interacting with $\bar{\psi}\gamma_\mu\phi$ in the Fermi interactions is similar to the source of the π^+ field. If, as is quite possible on our present knowledge, the pion coupling is pseudo-*vector*, then the interactions might be *identical*. That is, if the pion coupling is $f j_\mu \partial_\mu \pi$, the axial vector part of the Fermi interaction might be $g_A j_\mu(\bar{\psi}\gamma_\mu\phi)$.

If all this is indeed the case, one can draw a remarkable conclusion. The irreducible closed-loop graphs appearing in the pion decay would be almost identical with the pion self-energy graphs. Specifically, if

$$\delta\mu^2 = [k_\mu k_\nu C_{\mu\nu}(k)]_{k^2=\mu^2},$$

then the contribution from the strong interactions to $\pi_{\mu 2}$ decay is

$$[(1/f)k_\mu C_{\mu\nu}(k)]_{k^2=\mu^2} = k_\nu \delta\mu^2/(\mu^2 f).$$

The factor n_4, defined in section 3, is then given by

$$M n_4 = |\delta\mu^2/(\mu^2 f)|.$$

We can then determine $\delta\mu^2$. The value for g_A to be used is almost, but not quite, the experimental value from muon capture. It turns out that the correct value to use is that found from nuclear beta decay (the reason being that virtual processes in which a single pion is first emitted and then decays presumably give neglible contribution, and such virtual processes are not included in the renormalization of g_A above). Taking, then, $g_A = 1.15\times 10^{-11}$ MeV^{-2} and $1/f = 120$ MeV, we find

$$|\delta\mu^2/\mu^2| = 0.8.$$

The above ratio is considered to be a reasonable result. Whether or not the assumptions we have made to get it are all exactly correct, this would probably remain the best available method of estimating the absolute values of n_4 and n_5.

This result might be taken as evidence that the bare pion mass is exactly zero. According to Lehmann [8], $\delta\mu^2$ can be positive only if j_μ itself contains the pion field. But this is quite possible. It might, for instance, imply the existence of a direct interaction corresponding to $\pi^+ \to \pi^0 + e^+ + \nu$; an interaction which has been proposed for different reasons elsewhere [1].

References

1) R. P. Feynman and M. Gell-Mann, Phys. Rev. **109** (1958) 193
2) M. Gell-Mann, Phys. Rev. **106** (1957) 1296
3) S. W. MacDowell, Nuovo Cimento **6** (1957) 1445
4) R. H. Dalitz, Reports on Progress in Physics **20** (1957) 163
5) J. M. Cassels *et al.*, Proc. Phys. Soc. **70** (1957) 729;
J. Orear, Proceedings of the Rochester Conference (1957)
6) P. T. Matthews and A. Salam, Phys. Rev. (to be published)
7) B. d'Espagnat and J. Prentki, Nuclear Physics **6** (1958) 596
8) H. Lehmann, Nuovo Cimento **11** (1954) 342

2.L *Nuclear Physics* 7 (1958) 281—283; © *North-Holland Publishing Co., Amsterdam*
Not to be reproduced by photoprint or microfilm without written permission from the publisher

THE SCATTERING OF 185 MeV PROTONS FROM DEUTERIUM AND NEON

H. TYRÉN, G. TIBELL and TH. A. J. MARIS†
The Gustaf Werner Institute for Nuclear Chemistry, University of Uppsala

Received 27 March 1958

Abstract: The energy spectra of 185 MeV protons scattered off deuterium and neon have been recorded with a magnetic analyser. Gaseous targets were used, and five angles in the region 10° to 28° were studied.

1. Experimental Arrangements

Some further measurements on the inelastic scattering of 185 MeV protons on gaseous targets have been performed.

After scattering from the target contained in a high pressure gas chamber the protons passed a 90° magnetic analyser and were detected in a double coincidence telescope with plastic scintillators. The details of the experimental set-up have been described earlier [1]).

Deuterium and neon at pressures around 85 and 150 atm respectively were studied at five angles ranging from 10.2° to 28.2° in the laboratory system. The average scattering energy was 183 MeV in the deuterium case and 177 MeV in the neon case. The counting rates in the detecting telescope were transformed into differential cross sections after a calibration with gaseous hydrogen and plotted against the excitation energy of the residual nucleus.

2. Results

The results are given in figs. 1 and 2 with representative statistical errors shown. The cross section scale is thought to be good to 20 %. The energy resolution decreased with increasing angle as may be seen from the variation from 2 to 3.5 MeV of the full width at half height of the elastic peaks. In neon this effect is primarily caused by the changing geometry. In the deuterium case another contribution comes from the variation of recoil losses as the scattering angle varies across the entrance slit of the magnet, the slit being about 1° wide as seen from the target.

In each deuterium spectrum the continuum has the shape expected for quasi-elastically scattered protons. The points in the spectra where protons

† Present address: Institute for Theoretical Physics, Copenhagen.

from free nucleon-nucleon collisions with a bombarding energy 185 MeV minus the binding energy of the deuteron would appear are indicated by arrows in the figures.

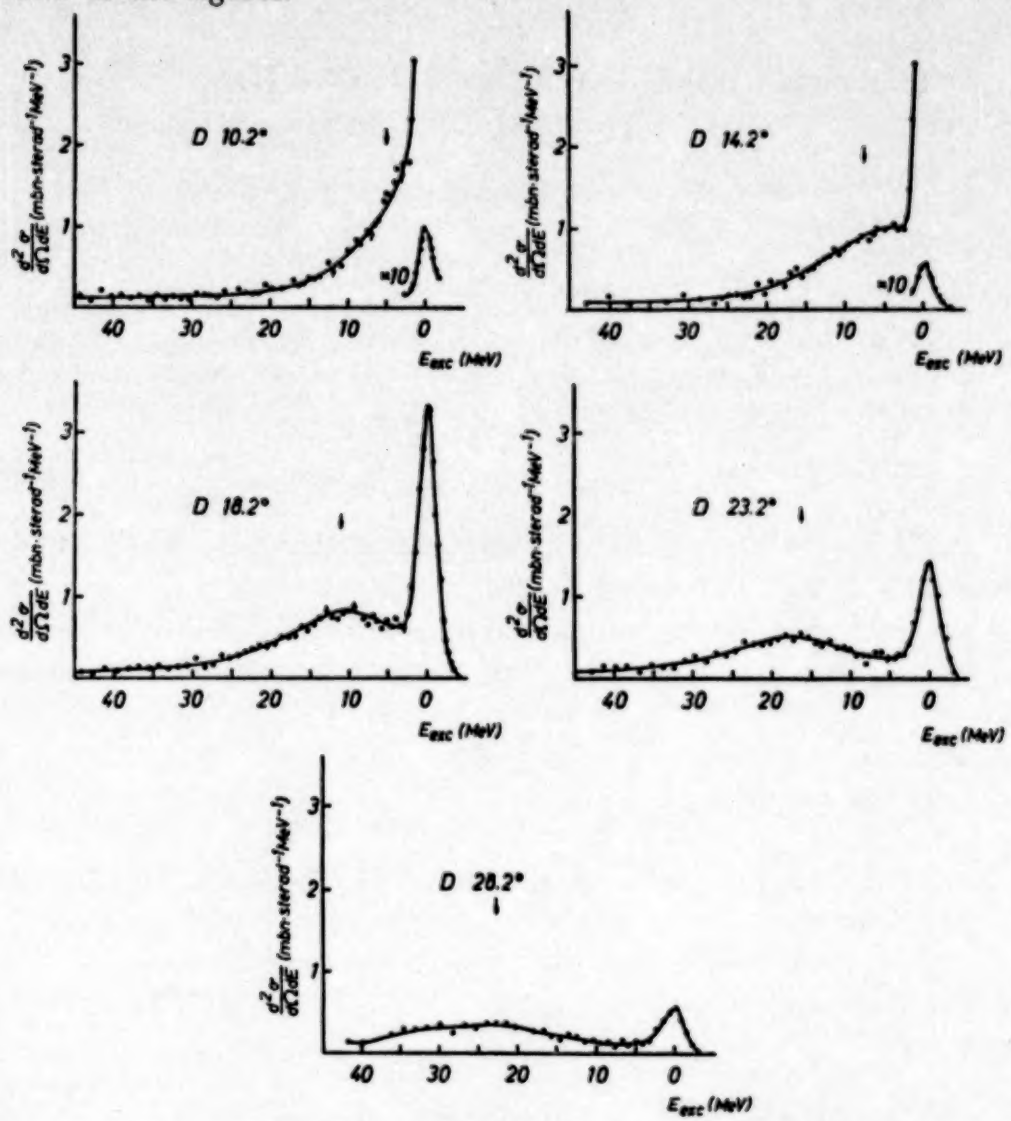

Fig. 1. The differential cross section of 183 MeV protons scattered off D_2 versus energy loss in the centre of mass system. The cross section and scattering angle are given in the laboratory system. Representative statistical errors are shown. The arrows are explained in the text.

The neon spectra at the larger angles show a maximum at 5.5 ± 0.5 MeV. At smaller angles this maximum broadens towards higher excitation energies and seems to decrease. The level structure at around 20 MeV for the 10° measurement probably corresponds to the giant γ-resonance excitations [2]).

The authors wish to thank Prof. The Svedberg for his interest in this work. We are indebted to Prof. J. O. Linde and Mr. C. Svensson for help with the compression of the gases, and to Prof. P. Ohlin and Prof. K. Siegbahn for permission to use their electrolyzer unit for the deuterium production. The work was supported by the Swedish Atomic Energy Commission.

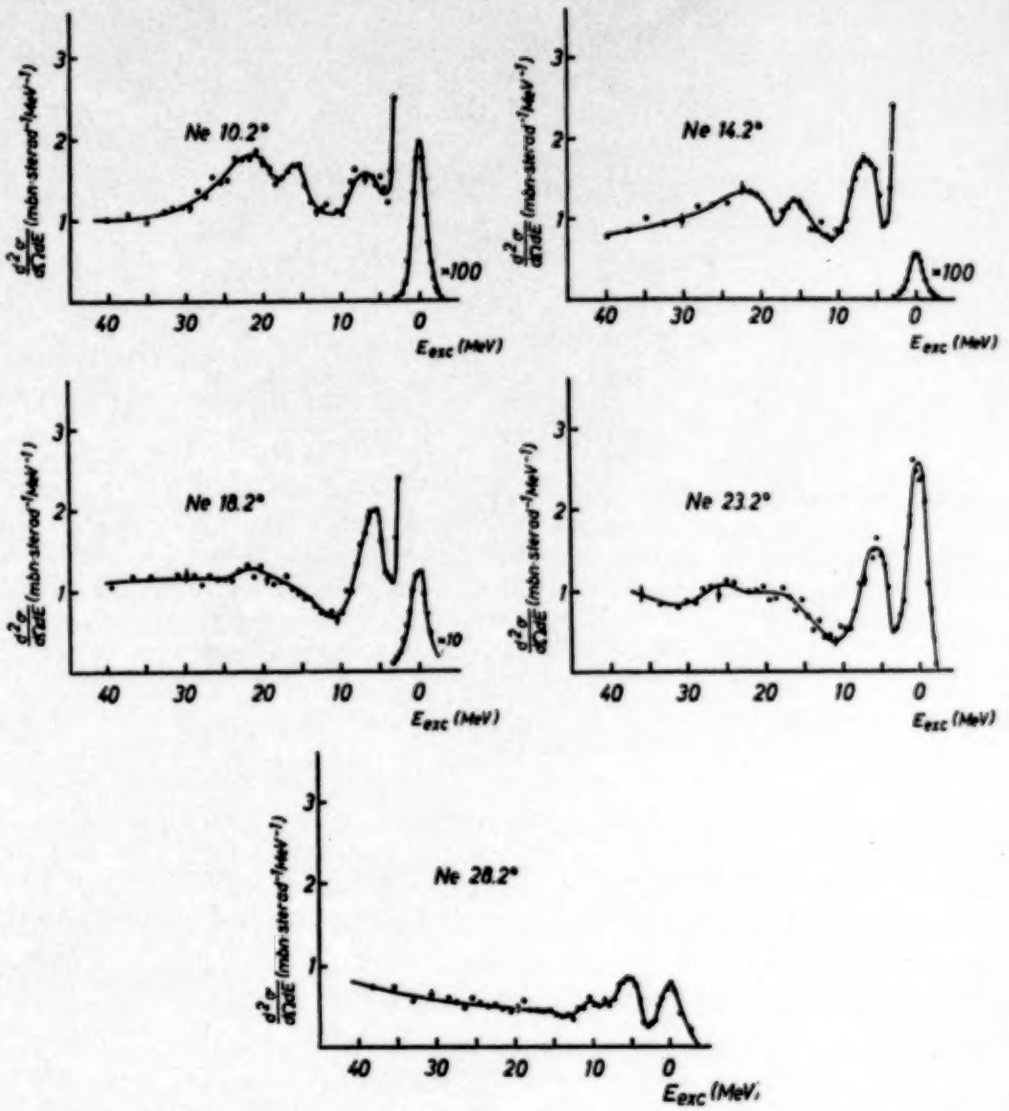

Fig. 2. The differential cross section of 177 MeV protons scattered off Ne versus energy loss in the centre of mass system. The cross section and scattering angle are given in the laboratory system. Representative statistical errors are shown.

References

1) H. Tyrén, G. Tibell and Th. A. J. Maris, Nuclear Physics **4** (1957) 277
2) Th. A. J. Maris and H. Tyrén, Nuclear Physics **4** (1957) 662

2.L *Nuclear Physics* 7 (1958) 284—288; © *North-Holland Publishing Co., Amsterdam*
Not to be reproduced by photoprint or microfilm without written permission from the publisher

AZIMUTHAL SYMMETRY IN PROTON SCATTERING AT 980 MeV

N. E. BOOTH, F. L. HEREFORD, M. HUQ, G. W. HUTCHINSON, MARGARET E. LAW, A. M. SEGAR and D. H. WHITE

Department of Physics, University of Birmingham

Received 24 March 1958

Abstract: The relative intensities of protons scattered near the vertical and near the horizontal planes at the second event of a double scattering process have been studied, the first scattering having taken place in the horizontal plane. Protons of kinetic energy 980 MeV were scattered first from carbon at 4° and then from either carbon or polyethylene at 14°. They were detected by an array of scintillation counters which could be rotated about an axis along the flight path of the protons between the two scatterers, and which was arranged so as to detect preferentially the elastic proton-proton scattering in the polyethylene. The ratio of horizontal to vertical scattering was found to be 0.940 ± 0.056, in proton-proton collisions.

1. Introduction

During experiments using photographic plates, in conjunction with the Birmingham proton synchrotron, to investigate proton-proton scattering, Duke *et al.* [1]) found a significantly larger number of events in which the scattering plane lay within 45° of the horizontal plane than within 45° of the vertical plane. This apparent asymmetry in azimuth was attributed to scanning losses, the plane of the emulsions having been horizontal.

Proton-proton scattering has also been investigated in this laboratory using a diffusion cloud chamber [2]). A first scan of the photographs taken in this experiment resulted once again in an apparent azimuthal asymmetry for cases in which the scattering angle was less than 20°.

Both these experiments were done in a beam scattered out from the synchrotron by an internal carbon target. They were thus experiments on the second event of a double scattering process in which the first event took place in a horizontal plane.

It would not appear possible for particles of spin $\frac{1}{2}\hbar$ to produce an azimuthal asymmetry of this complexity. It is known from the experiments of Chamberlain *et al.* [3]) that for proton scattering from carbon at 380 MeV the azimuthal asymmetry is less than 1 %. However, since no effect of this kind appears to have been looked for at energies approaching 1 GeV or above, it was not inconceivable that protons of this energy might be excited to some state in which they could carry more intrinsic angular momentum

during the time of flight between the two scattering events. It therefore seemed worthwhile to investigate the double scattering by an independent method not involving any photographic or scanning procedures which might themselves produce an asymmetric result.

Such an experiment has been carried out using scintillation counters in coincidence to detect elastic events at the second scattering. The other conditions were as closely analogous as possible to those of the previous experiments in this laboratory. The flight path between the two scatterings was longer than in the photographic plate experiment but shorter than in the cloud chamber experiment.

2. Apparatus

The counting apparatus, shown in fig. 1, consisted of two identical sets of three scintillation counters in triple coincidence, $C_1 C_2 C_3$ and $C'_1 C'_2 C'_3$.

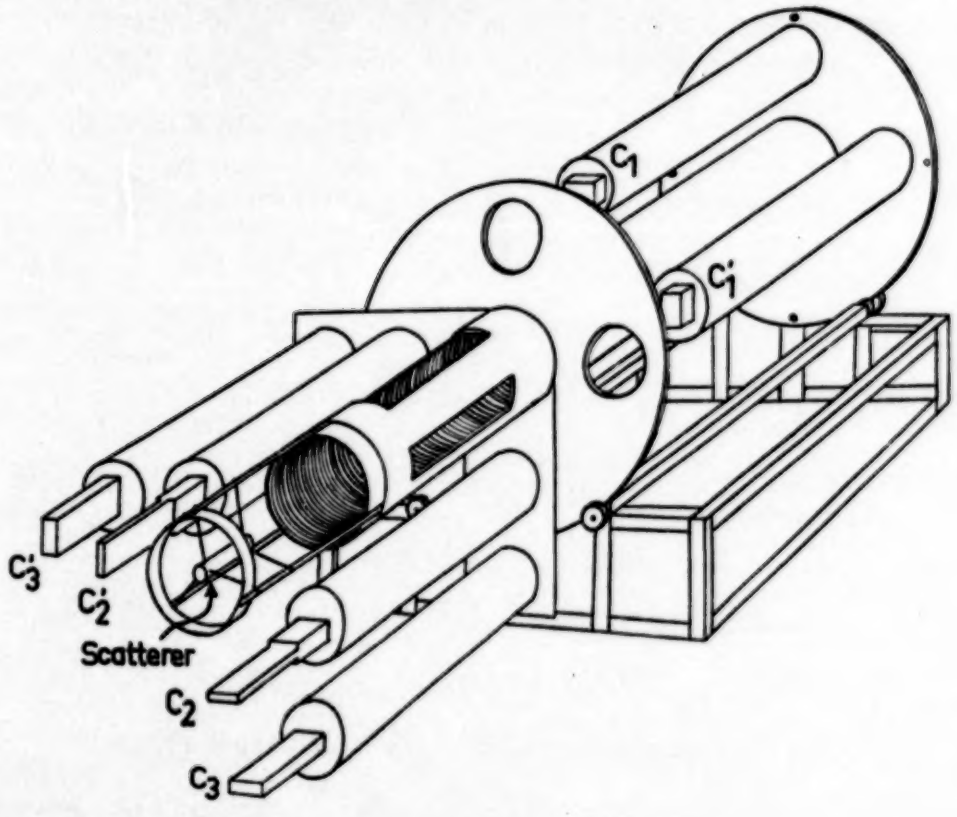

Fig. 1. Experimental arrangement.

Conventional fast electronic techniques were used to form and count the coincidences. The planes of the two sets of counters were at right angles and intersected along the beam axis. Fig. 2 shows the geometrical arrangement of the scintillators of one set. The dimension of C_1 perpendicular to the plane of the figure was 5.0 cm and of C_2 and C_3 3.7 cm. The beam was monitored by placing a seventh counter in the beam, behind the apparatus. Twenty centi-

metres of lead was placed in front of this counter to diffuse the beam and minimize the effect of target changes.

The asymmetries previously observed have been at forward angles. The scatterer and counter geometry was therefore chosen to achieve the smallest forward scattering angle compatible with detection of the lower energy recoil protons.

There were three target units, each quickly interchangeable on the apparatus so that its alignment was accurately reproduced. One unit held a cylindrical carbon scatterer, another a polyethylene scatterer of the same dimensions, each suspended on nylon threads, and the third was a dummy having only the threads. The latter was used in measuring backgrounds, and in checking the alignment. The axis of rotation, the axis of the target and either set of scintillators were coplanar to within 0.05 cm.

Protons were scattered at an angle of 4° by a carbon target inside the vacuum box of the synchrotron and were focussed to a nearly parallel beam of cross section 2.5 cm × 5.0 cm. The flight path between the first and second scatterers was 950 cm corresponding to a time of flight of 3.7×10^{-8} sec.

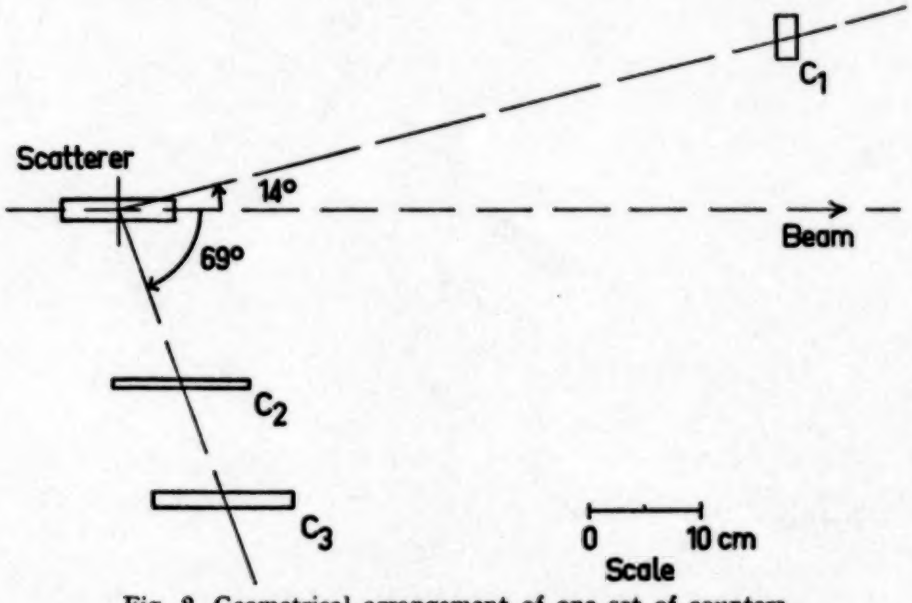

Fig. 2. Geometrical arrangement of one set of counters.

The beam passed down the axis of the apparatus so that only the scatterers and the nylon threads were exposed to it. The axis of rotation of the apparatus was aligned to the beam centre to 0.1 cm, and to the beam direction to 0.1°, by exposing X-ray films at the front and at the back.

3. Experimental Procedure

Triple coincidences from each set of counters were recorded simultaneously but independently. Cycles of measurements were made in both orientations

in the horizontal and in the vertical planes (i.e. with C_1 in the positions right, left, up and down). In each position counts were recorded for the carbon target, the polyethylene target and the dummy assembly. These counts were normalized to one another using the monitor counter. The rates from the carbon scatterer and the background were about 50 % and 15 % respectively of that from the polyethylene scatterer.

The results of 10 such cycles were separately analysed and found to be internally consistent.

To obtain the asymmetries for hydrogen, the effect of the carbon in the polyethylene scatterer must be subtracted. The relative number of interactions in the carbon of the two scatterers was calculated from the known absorption cross section for carbon [4]). Since the density of the carbon scatterer was about twice that of the polyethylene scatterer, account had to be taken of absorption and multiple scattering of the quasi-elastic recoils. The effect of this correction upon the results is small. An uncertainty of 5 % has been ascribed to the correction and this has been taken into account in assessing the final uncertainty of the results.

The ratio of the number of proton-proton elastic events at 14° to quasi-elastic proton-proton events per carbon nucleus at 14° was 1.56 ± 0.10. This ratio will be somewhat greater than the ratio of the differential cross sections at 14° because of the unknown fraction of quasi-elastic events not detected.

The possible mis-alignment of the axis of rotation to the beam direction (by $\pm 0.1°$) could result in an error of up to 1 % in the asymmetry in any plane (i.e. right v. left or up v. down). The error in a result comparing any two normal planes (i.e. right + left v. up + down) is very much smaller.

4. Results

The final mean results are shown in table 1. The total errors quoted are statistical errors combined with an estimate of the uncertainties discussed above.

TABLE 1

	$\frac{R}{L}$	$\frac{U}{D}$	$\frac{R+L}{U+D}$
Carbon (Quasi-elastic)	0.805	1.11	1.065
Statistical Error	0.098	0.15	0.096
Total Error	0.104	0.16	0.096
Hydrogen (Elastic)	1.123	1.098	0.940
Statistical Error	0.095	0.088	0.054
Total Error	0.109	0.099	0.056

In the table of results R and L are right and left second scattering intensities in the horizontal plane. U and D are upward and downward scattering intensities in the vertical plane. On this convention the first scatter is in the direction of R.

5. Conclusion

The right-left asymmetry, in so far as it is significant, is considered to be due to the polarization of protons by the first scattering. The other ratios are not significantly different from one. The ratio (R+L)/(U+D) observed with nuclear emulsion and cloud chamber techniques at 14° was about 1.4.

Our thanks are due to Professor P. B. Moon and the Cloud Chamber group for drawing our attention to this problem, and to the latter for making available their data prior to publication. N.E.B. is indebted to I.C.I. Ltd. for a research fellowship, F. L. H. to the U.S. Education Commission for a Fulbright Award, M. H. to the Government of East Pakistan for a research scholarship, M. E. L. to D. S. I. R. for a research scholarship, and A. M. S. to the Royal Society for a Rutherford scholarship.

References

1) P. J. Duke, W. O. Lock, P. V. March, W. M. Gibson, J. G. McEwen, I. S. Hughes and H. Muirhead, Phil. Mag. **2** (1957) 204
2) A. P. Batson, B. B. Culwick and L. Riddiford, private communication
3) O. Chamberlain, E. Segrè, R. D. Tripp, C. Wiegand and T. Ypsilantis, Phys. Rev. **102** (1956) 1689
4) N. E. Booth, B. Ledley, D. Walker and D. H. White, Proc. Phys. Soc. A **70** (1957) 209

1.D.2 : 2.G

Nuclear Physics **7** (1958) 296; © *North-Holland Publishing Co., Amsterdam*

Not to be reproduced by photoprint or microfilm without written permission from the publisher

SHAPE EFFECTS IN DEUTERON STRIPPING ON SPHEROIDAL NUCLEI

J. SAWICKI

Palmer Physical Laboratory, Princeton University, Princeton †

and

G. R. SATCHLER

Clarendon Laboratory, Oxford

Received 4 April 1958

Abstract: The geometrical effect of the spheroidal shape of strongly deformed nuclei on the angular distributions from deuteron stripping reactions is discussed. The usual boundary conditions are assumed, not on a Butler sphere of radius r_0, but rather on a corresponding spheroidal boundary. This gives rise to contributions to the reaction amplitude, additional to the "spherical" parts, which correspond to angular momenta L different in general from the orbital angular momentum l of the captured nucleon. They do not, however, violate the strong coupling model selection rule $L \geqq |K_f - K_i| - \frac{1}{2}$; in particular $L = 0$ can only occur if $|K_f - K_i| = \frac{1}{2}$. These shape contributions are in general rather small, but must be considered when attempts are made to correlate experimental widths with the nuclear collective model and to detect small configuration mixing effects.

1. Introduction

It has been shown in recent papers [1,2,3,4]) that deuteron stripping on strongly deformed nuclei is characterized by very specific selection rules, branching ratios, and mixing of values of l, the orbital angular momentum of the captured nucleon, predicted by the strong coupling collective model [5]). The theory is consistent with the experimental data for nuclei around $A = 25$ [4]). In particular it has been suggested that suitable Nilsson-type wave functions [5]) for nucleons moving in a spheroidal potential could explain quantitatively, and in a natural way, the experimental ratio of mixing of two l-values in a number of reactions. Other cases seem to require configuration mixing to explain the simultaneous appearance of two such l-values. By "quantitative" one means on the basis of some particular approximate treatment of the kinematic factors, namely the overlap integral of the captured nucleon wave function and the Fourier transform of the internal deuteron wave function. The uncertainties introduced there seem to be unimportant when plane waves are used to describe the incident deuterons and outgoing nucleons since the Butler, Bhatia and other prescriptions [6]) are known to produce similar results. This will not be true in general for distorted wave calculations [7]).

† On leave of absence from Warsaw, Poland. Work supported in part by the U. S. Atomic Energy Commission and the Higgins Scientific Trust Fund.

Let us call "dynamical" the strong coupling collective model effects, being of nuclear dynamical origin, which are described elsewhere [2,3]). There are additional "geometrical" effects due to the non-spherical nuclear shape. In fact the incoming deuterons and outgoing nucleons see a spheroid rather than a sphere. It is the aim of the present note to make some estimate of these geometrical contributions and to see how they may affect our interpretation of experimental data.

2. Theory

We shall treat the reaction adiabatically, that is, assume that the nuclear shape does not change its orientation appreciably while the reaction is proceeding. This is justified for strongly deformed nuclei. The most realistic approach would be then to use deuteron and nucleon waves distorted by scattering from the corresponding spheroidal optical potentials [7]). However, even the phase shifts for elastic scattering from a spheroid are difficult to compute [8]). We confine ourselves therefore to using plane waves. The shape effects will still be present because we argue on physical grounds that the reaction is mostly localized near the nuclear surface, which is now non-spherical. Deeper penetration of the deuterons is likely to lead to their absorption into a compound nucleus. The Butler prescription gives for the overlap integral for the captured nucleon [2])

$$S(lm) = \int_{r_0}^{\infty} \mathrm{d}\mathbf{r} \exp(i\mathbf{Q}\cdot\mathbf{r}) R_{Nl}(r) Y_l^m(\omega)^*, \tag{1}$$

where $\mathbf{Q} = \mathbf{K}_d - (M_1/M_t)\mathbf{K}_p$ and R_{Nl} is the radial part of that component of the captured nucleon wave function with principal quantum number N and orbital momentum l [2,3]). The shape effects are taken into account by modifying $S(lm)$ so that the cut-off follows the nuclear surface. We replace r_0 by $r_0(1+\zeta)$ where $\zeta = \beta \sum_\nu D^2_{\nu 0}(\theta_i)^* Y_2^\nu(\omega)$ (or $\beta Y_2^0(\omega')$ in body-fixed coordinates). β is the value of the equilibrium deformation [5]) and $D^2_{\nu 0}(\theta_i)$ is the usual rotation matrix for angular momentum 2, the Euler angles θ_i referring to the orientation of the nuclear symmetry axis [9]). The evaluation of such a modified $\tilde{S}(lm)$ is difficult. To first order in β we may write

$$\begin{aligned} \tilde{S}(lm) &= S(lm) + \delta S(lm) \\ \delta S(lm) &= -r_0^3 \beta \sum_\nu D^2_{\nu 0}(\theta_i)^* R_{Nl}(r_0) \int \mathrm{d}\omega \exp(i\mathbf{Q}\cdot\mathbf{r}_0) Y_l^m(\omega)^* Y_2^\nu(\omega). \end{aligned} \tag{2}$$

It is not certain that such an expansion of $\tilde{S}(lm)$ in powers of β always converges rapidly for values of β that are of interest. However, it gives a qualitative description of the shape effect and is a guide to its magnitude.

The geometrical coefficients we obtain below are independent of any particular treatment [6]) of the plane wave theory, and are indeed still valid if waves distorted by spherical potential [7]) are used. They arise simply

from the angular and rotational (Eulerian angle) integrations. The integrands of the reaction amplitude are the same as for a spherical boundary times 1, ζ, $\zeta^2, \ldots, \zeta^n \ldots$ for successive terms of an expansion in powers of β. It is then obvious that the general strong coupling selection rule [2,3]) for the projections of the nuclear spins on the symmetry axis remains unmodified, $K_f = K_1 + \Omega$, where Ω is the projection for the orbit entered by the captured nucleon [5]).

A straightforward calculation with strong coupling wave functions [2,3,5]) gives the differential cross-section

$$\frac{\mathrm{d}\sigma}{\mathrm{d}\omega} \propto \sum_{JLM} (I_f K_f | I_1 J K_1 \Omega)^2 |A(JLM)|^2. \tag{3}$$

With plane waves and quantization axis along the recoil $\mathbf{Q} = \mathbf{K_d} - (M_1/M_f)\mathbf{K_p}$ only $M = 0$ appears, and the reaction amplitude becomes, to order β †,

$$\begin{aligned} A(JL) = \sum_{jl} c_{jl}(\Omega)[I_{il}\delta_{iL}\delta_{jJ} \\ + \beta\left(\frac{5}{4\pi}\right)^{\frac{1}{2}} (j\tfrac{1}{2}\,|J2\tfrac{1}{2}0)(J\Omega|j2\Omega 0) r_0 I'_{iL}] \end{aligned} \tag{4a}$$

$$\begin{aligned} = \sum_{i\Lambda} a_{i\Lambda}(\Omega)(J\Omega|L\tfrac{1}{2}\Lambda,\ \Omega-\Lambda)[I_{il}\delta_{iL} \\ + \beta\left(\frac{5}{4\pi}\right)^{\frac{1}{2}} (l0|L200)(L\Lambda|l2\Lambda 0) r_0 I'_{iL}]. \end{aligned} \tag{4b}$$

The primes denote differentiation with respect to r_0. The two forms (4a) and (4b) correspond to the two ways of expanding the wave function for the captured nucleon moving in a deformed potential well [2,3]). The coefficients $a_{i\Lambda}(\Omega)$ have been given by Nilsson [5]) for a particular choice of well, and the $c_{jl}(\Omega)$ for many orbits appropriate to nuclei around $A = 25$ have been displayed graphically [4]). The $(c\gamma|ab\alpha\beta)$ are the usual Clebsch-Gordan coefficients. The first term in eqs. (4) with $l = L$ is the normal term; in addition, the nuclear shape allows captures with $l = L \pm 2$ (providing $l \geqq |\Omega| - \frac{1}{2}$) to contribute coherently to the normal $l = L$ term. Because of the phase convention $c_{jl}(-\Omega) = (-)^{j-\frac{1}{2}} c_{jl}(\Omega)$ or $a_{i-\Lambda}(-\Omega) = a_{i\Lambda}(\Omega)$, the corrections have the same sign for $\pm\Omega$ captures.

† In deriving (4a) we have used the relation

$$[(2l+1)(2L+1)]^{\frac{1}{2}} (k0\,|lL00) W(jlJL;\ \tfrac{1}{2}k) = (k0|\,jJ\tfrac{1}{2},\ -\tfrac{1}{2}).$$

The form (4b) is probably most easily obtained from (4a) before this contraction has been applied, by using

$$c_{jl}(\Omega) = \sum_{\Lambda} a_{i\Lambda}(\Omega)(j\Omega\,|l\tfrac{1}{2}\Lambda,\ \Omega-\Lambda)$$

and the standard Racah algebra [9]).

The Butler cut-off for the radial overlap integral as in (1) gives

$$\begin{aligned} I_{lL} &= \int_{r_0}^{\infty} r^2 \mathrm{d}r R_{Nl}(r) j_L(Qr_0) \\ I'_{lL} &\equiv \frac{\mathrm{d}}{\mathrm{d}r_0} I_{lL} = -r_0^2 R_{Nl}(r_0) j_L(Qr_0). \end{aligned} \tag{5a}$$

If we replace the integral by its value close to the nuclear surface we get, to within a constant,

$$\begin{aligned} I_{lL} &= r_0^2 R_{Nl}(r_0) j_L(Qr_0) \\ I'_{lL} &= r_0[2R_{Nl}(r_0) j_L(Qr_0) + r_0 R_{Nl}(r_0) j'_L(Qr_0) + r_0 R'_{Nl}(r_0) j_L(Qr_0)]. \end{aligned} \tag{5b}$$

The j_L are the usual spherical Bessel functions [10]).

3. Applications

The normal stripping selection rules are maintained, $|I_f - I_i| - \frac{1}{2} \leqq L \leqq I_i + I_f + \frac{1}{2}$, and parity change $(-)^L$. What is changed is the relation between the L term in the angular distribution and the width for nucleon capture with orbital momentum l. To illustrate this we consider the amplitude A for $L = 0$; then $J = |\Omega| = \frac{1}{2}$, but we may have contributions from captures with $l = 0$ or 2, to order β.

$$\begin{aligned} A(\tfrac{1}{2}0) &= a_{00}(\tfrac{1}{2}) I_{00} + \beta \left(\frac{1}{4\pi}\right)^{\frac{1}{2}} a_{20}(\tfrac{1}{2}) r_0 I'_{20} \\ &= c_{\frac{1}{2}0}(\tfrac{1}{2}) I_{00} + \beta \left(\frac{1}{4\pi}\right)^{\frac{1}{2}} [(\tfrac{3}{5})^{\frac{1}{2}} c_{5/2\,2}(\tfrac{1}{2}) - (\tfrac{2}{5})^{\frac{1}{2}} c_{3/2\,2}(\tfrac{1}{2})] r_0 I'_{20}. \end{aligned} \tag{6}$$

Without the shape effects it would be possible for such an $L = 0$ transition to be inhibited if the $l = 0$ part of the $\Omega = \frac{1}{2}$ orbit were small (that is, if a_{00} or $c_{\frac{1}{2}0}$ were small). The shape effects, allowing $l \neq L$, relax this inhibition to some extent. For a reaction with a Q-value of about 5 MeV, nuclear radius $r_0 = 5f$ ($f = 10^{-13}$ cm), and with $Qr_0 = 0$ (that is, on the $L = 0$ peak), (5a) in (6) gives

$$A(\tfrac{1}{2}0) = (a_{00} + 0.63\,\beta\, a_{20}) I_{00} \tag{7a}$$

while (5b) gives

$$A(\tfrac{1}{2}0) = (a_{00} + 0.76\,\beta\, a_{20}) I_{00}. \tag{7b}$$

In obtaining these figures we have assumed that the s and d wave functions have the same value at $r = r_0$ and may be described by Hankel functions $h_l^{(1)}(i\alpha r)$ for $r > r_0$ [10]). We may use Nilsson's values for the a_{lA} [5]) for the $\Omega = \frac{1}{2}$ orbits 6, 9 and 11 at a deformation $\beta = 0.3$ (appropriate to nuclei around $A = 25$). We find from (7a) that the amplitudes $A(\frac{1}{2}0)$ are enhanced by 28 % and 3 % for orbits 6 and 9, and decreased by 15 % for orbit 11, from their values ignoring the shape effects. Thus the

ratio of cross sections on the $L = 0$ peak for capture into orbits 11 and 9 may be some 31 % less than predicted from the ratio of the $c_{\frac{1}{2}0}$'s; there seems to be some evidence for this effect [4]). Eq. (7b) predicts slightly larger corrections.

Two particular $L = 0$ captures in the reaction Al^{27}(d, p)Al^{28} were considered in ref. [2]), those with Q values 5.49 MeV ($I_f = K_f = 3$, +) and 4.48 MeV ($I_f = 3$, $K_f = 2$, +). Since $I_1 = K_1 = 5/2$, we have $|\Omega| = \frac{1}{2}$ in both cases. We have computed the shape corrections for the $L = 0$ parts of these captures, using the values of c_{jl} given by Litherland *et al.* [4]) for $\beta = 0.20$, and taking a radius $r_0 = 5.27\,f$. With the prescription (5b) and the oscillator radial functions given by Nilsson [5]) we get the angular distributions (to order β),

$$\frac{d\sigma}{d\omega}(K_f = 3) \propto [34.5\, j_0^2 + 7.5\, j_2^2] + [1.07\, j_0^2 + 0.18\, Qr_0 j_1 j_0],$$

$$\frac{d\sigma}{d\omega}(K_f = 2) \propto [5.7\, j_0^2 + 5.9\, j_2] + [0.18\, j_0^2 + 0.03\, Qr_0 j_1 j_0].$$

The first bracket gives the 'normal' angular distribution, the second contains the shape correction to $L = 0$. In both cases the correction is quite small. The argument of the Bessel functions j_L is Qr_0 as usual.

As a further example consider an $\Omega = 5/2$, even parity, capture. For light nuclei ($A \approx 25$) this means $l = 2$ only, since the $l = 4$ components of the wave function will be very small. Also, $c_{5/2\,2}(\frac{5}{2}) = a_{22}(\frac{5}{2})$. Then $J = \frac{5}{2}$, $L = 2$, and the amplitude is

$$A(\tfrac{5}{2}2) = F\, c_{5/2\,2}(\tfrac{5}{2})\, I_{22}$$

where

$$F = 1 - 0.18\, \beta r_0 (dI_{22}/dr_0)/I_{22}. \tag{8}$$

$F-1$ is a measure of the shape correction to the amplitude. In the reaction Mg^{25}(d, p) Mg^{26} leading to the 1.83 MeV level [11]) we have the Q-value 7.06 MeV. Again assuming the radial function for the neutron for $r > r_0$ can be approximated by a Hankel function, and taking $r_0 = 5.2f$, (5a) and (5b) give

$$F - 1 = 0.18\beta \frac{12.25 + (Qr_0)^2}{5.14 + (r_0 j'_2(Qr_0)/j_2(Qr_0))} \tag{8a}$$

or

$$F - 1 = 0.18\beta [3.14 - (r_0 j'_2(Qr_0)/j_2(Qr_0))]. \tag{8b}$$

For a deuteron energy of about 8 MeV, and deformation $\beta = 0.3$, the value of F on the $L = 2$ peak is 1.17 from (8a), 1.24 from (8b). Thus the shape contributions enhance the peak intensity by 37 % and 54 % respectively. If oscillator radial functions [5]) are used for R_{Nl} the results depend upon the

definition of nuclear radius used, but they seem to give results similar to the Hankel functions used in (8). The general shape of the angular distribution is little changed by the shape dependent terms except for an increase at large proton angles which tends to shift the peak towards larger angles. The experimentally observed [11]) $L = 0$ contribution is not given by the shape effect; as already remarked [2,3]) this is presumably due to configuration mixing in the nuclear wave function which relaxes the $L \geqq 2$ selection rule.

4. Second Order Corrections

In view of the approximate nature of our model we do not intend to attach much physical significance to higher order terms. However, we will consider the β^2 corrections in order to get a feeling for the convergence of the expansion in powers of β. The addition to the amplitudes (4a) and (4b) is

$$\delta A(JL) = \tfrac{1}{2} \sum_{jlp} c_{jl}(\Omega) \left(\frac{5}{4\pi}\right) \beta^2 r_0^2 I''_{lL}(p0|2200)^2 \times (J\Omega|jp\Omega 0)(j\tfrac{1}{2}|Jp\tfrac{1}{2}0) \tag{9a}$$

$$= \tfrac{1}{2} \sum_{l\Lambda p} a_{l\Lambda}(\Omega) \left(\frac{5}{4\pi}\right) \beta^2 r_0^2 I''_{lL}(p0|2200)^2 \times (J\Omega|L\tfrac{1}{2}\Lambda,\ \Omega-\Lambda)(l0|Lp00)(L\Lambda|lp\Lambda 0). \tag{9b}$$

The sum over p includes only $p = 0$, 2 and 4. The new radial overlap may be obtained from (5a), (5b), since

$$I''_{lL} = \mathrm{d}^2 I_{lL}/\mathrm{d}r_0^2. \tag{10}$$

Using the figures appropriate to the Mg^{25}(d, p) Mg^{26} reaction discussed above, we find an addition to the correction factor F of (8a) and (8b) due to these β^2 terms. Near the $L = 2$ peak, the addition to (8a) is $-0.40\beta^2$, and to (8b) is $-0.15\beta^2$. Thus the convergence in this case is not too bad. However, the shape corrections are very sensitive to the binding energy of the captured nucleon (through the variation of R_{Nl} in(5)) and to the nuclear radius r_0. On the main stripping L-peak the variation of $j_L(Qr_0)$ is small, but away from the peak its contributions to the shape effects vary quite rapidly with deuteron energy and the angle of emission of the nucleons.

5. Discussion

The nuclear shape contributions we have described are in general rather small. They do not violate the general selection rule for the orbit of the captured nucleon, $\Omega = K_f - K_i$. In particular they admix $L = 0$ terms into the angular distribution only when $|\Omega| = \frac{1}{2}$, that is when they are already present naturally from $l = 0$ captures. Terms of the type $Qr_0 \cdot j_{L-1}(Qr_0)$ appear in addition to the normal "spherical" amplitudes $j_L(Qr_0)$,

but change the angular distribution very little. However, the shape contributions may be important when quantitative deductions about the wave function of the captured nucleon are to be made, since captures with $l \neq L$ can contribute to the L-peak of the angular distribution.

The model we have used, with plane waves and a sharp cut-off at the nuclear surface, will overestimate the shape effect in general. The true deuteron wave function will fall off less rapidly inside the nuclear surface, thus reducing the effect of a change in shape. Similarly the radial wave function for the captured nucleon in a more realistic (diffuse edge) potential well [12]) will fall off less rapidly for $r > r_0$ than either the eigenfunctions for a square well or an oscillator well. Since the diffuseness may well depend on the deformation, being greater at the poles than on the equator for a prolate nucleus, the effect may be further reduced. It is difficult to predict the results of using waves distorted by the appropriate non-spherical optical potentials, except to argue that the shape effect would be less than that calculated using spherically distorted waves, since the waves would tend to "follow" the deformation.

Finally we should note that there are additional dynamic effects which may be present when the nuclei are deformed. Owing to the dynamical (non-adiabatic) coupling between the incident and outgoing particles and the nuclear rotational motion, it would be possible for nuclear rotational levels to be excited before and after the nucleon capture. An estimate of these could be made by including such excitations in the distorted waves [13]) used in a distorted wave calculation.

One of us (J. S.) is indebted to Dr. J. Blair for several stimulating discussions.

References

1) S. Yoshida, Progr. Theoret. Phys. **12** (1954) 141;
G. R. Satchler, Phys. Rev. **97** (1955) 1416
2) J. Sawicki, Nuclear Physics **6** (1958) 575
3) G. R. Satchler, Annals of Physics, in print
4) D. A. Bromley, H. E. Gore and A. E. Litherland, Can. J. Phys. **35** (1957) 1057;
A. E. Litherland, H. McManus, E. B. Paul, D. A. Bromley and H. E. Gore, Chalk River Report PD – 289 (1957)
5) A. Bohr and B. Mottelson, Mat. Fys. Medd. Dan. Vid. Selsk. **27** (1953) no. 16;
S. G. Nilsson, Mat. Fys. Medd. Dan. Vid. Selsk. **29** (1955) no. 16
6) S. T. Butler, Phys. Rev. **106** (1957) 272;
A. B. Bhatia, K. Huang, R. Huby and H. C. Newns, Phil. Mag. **43** (1952) 485
7) W. Tobocman and M. M. Kalos, Phys. Rev. **97** (1955) 132
8) B. Margolis and E. S. Troubetskoy, Phys. Rev. **106** (1957) 105
9) A. R. Edmonds, Angular Momentum in Quantum Mechanics (Princeton Univ. Press)
10) L. I. Schiff, Quantum Mechanics (McGraw-Hill, New York) Ch. 4
11) J. R. Holt and T. N. Marsham, Proc. Phys. Soc. A **66** (1953) 527
12) A. A. Ross, H. Mark and R. D. Lawson, Phys. Rev. **102** (1956) 1613
13) D. M. Brink, Proc. Phys. Soc. A **68** (1955) 994

2.I

Nuclear Physics **7** (1958) 296; © *North-Holland Publishing Co., Amsterdam*

Not to be reproduced by photoprint or microfilm without written permission from the publisher

THE HALF-LIVES OF SOME SHORT-LIVED ISOTOPES

M. V. MIHAILOVIĆ and B. POVH

Institute "J. Stefan", Ljubljana, Yugoslavia

Received 10 April 1958

The half-lives of the isotopes Mg^{23}, Al^{26}, Si^{27}, S^{31}, Cl^{34}, K^{38} and Ca^{39} have been measured with better precision than before [1]). The activities were produced by (γ, n) reactions induced by X-rays from a 31-MeV betatron. In each case the maximum energy was chosen below the threshold for (γ, 2n) reactions.

The irradiated samples were transferred from the X-ray beam by a pneumatic tube to an anthracene scintillation counter. The output pulses from a scaler were registered by a chronograph upon teledeltos paper tape [2]). By plotting the remaining number of counts [3]) instead of the activity, it has been possible to reduce the error below 1 % with rather poor activities. The activities of the target impurities were counted as background.

The results are illustrated in table 1.

TABLE 1

Isotope	Substance irradiated	Half-lives (seconds)	Number of measurements	Total number of counts
Mg^{23}	Mg	12.1 (1 ± 0.008)	6	62 000
Al^{26}	Al	$6.74(1\pm0.004)$	6	80 000
Si^{27}	Si	$4.14(1\pm0.007)$	10	46 000
S^{31}	S	$2.72(1\pm0.006)$	8	120 000
Cl^{34*}	C_6Cl_6	$1.61(1\pm0.007)$	12	46 000
K^{38*}	KJ	$0.97(1\pm0.007)$	12	37 000
Ca^{39}	Ca	$0.86(1\pm0.006)$	15	40 000

References

1) W. A. Hunt, R. M. Kline and D. J. Zaffarano, Phys. Rev. **95** (1954) 611A;
F. I. Boley and D. J. Zaffarano, Phys. Rev. **84** (1951) 1059;
R. M. Kline and D. J. Zaffarano, Phys. Rev. **96** (1954) 1620;
D. W. Green, J. C. Harris and J. N. Cooper, Phys. Rev. **96** (1954) 817A

2) I. Kuščer and M. V. Mihailović, Reports J. Stefan Inst. **2** (1955) 51

3) I. Kuščer, M. V. Mihailović and E. C. Park, Phil. Mag. **20** (1957) 998

Nuclear Physics **7** (1958) 297—298; © *North-Holland Publishing Co., Amsterdam*

BOOK REVIEWS

N. N. Bogoliubov i D. V. Shirkov, *Vvedenie v teoriiu kvantovannych polei* [Introduction into the theory of quantized fields] (Gos. Izd. Tech.-teor. Lit. Moskva 1957. 442 str. 18.50 rubl.)

With the present review Nuclear Physics inaugurates a service to those of its readers who know or are learning Russian. These form an increasing number of people who will be interested in being informed of the appearance of new books on the Russian market; these books are now easily available through the ordinary trade channels, and are usually much cheaper than comparable products of our specialized publishing firms.

The first book to be reviewed in these columns is a major production in the domain of quantum electrodynamics, and it would certainly deserve a wide circulation also in translation. It is the most comprehensive text-book in existence concentrating on the mathematical methods extensively used in this field: it may be compared, in set-up and also in excellence, with Weyl's *Gruppentheorie und Quantenmechanik*. Here and there the same happy blending of physics and mathematics, with distinct emphasis on the latter, both limited to fundamentals, but treated very fully and with exemplary lucidity and precision. In both cases also we have a book written from first-hand knowledge and embodying important original contributions to the subject.

The treatment is very complete and self-contained: naturally, a thorough knowledge of quantum mechanics, as well as a sound mathematical training, are presupposed; but the fundamental ideas of field theory are developed from the beginning and gradually carried to their last development in a harmonious sequence of well-constructed chapters: classical theory of free fields, quantal theory of free fields, the scattering matrix, the elimination of divergencies from the S-matrix, the Schrödinger equation and the dynamical variables, the method of functional averaging, the renormalization group, the dispersion relations. This last chapter contains a full account of the fundamental results obtained by Prof. Bogoliubov and his school. Everywhere the presentation of the argument is carefully thought-out and gives the rather austere subject such a freshness that the whole book makes fluent and highly enjoyable reading. I would even have praised the authors for the elegance of their style, if I had not encountered the phrase 'this situation takes place' which is awful in any language.

The unified treatment so brilliantly achieved entails a critical selection of the abundant literature: this is all to the good and contrasts most pleasantly with the dismal patchwork and endless lists of papers which are too often found even in widely used text-books. In one respect, however, I must raise a protest: to suggest that the history of the subject begins in 1947 is grossly unfair to the 'old guard'. The ideas known nowadays under the new-fangled names of 'renormalization', 'manifestly covariant formulation', 'interaction representation' had been introduced and discussed at a very early stage: they were perfectly familiar by 1938 to all workers in the field, for whom the problems raised by the Lamb-Retherford experiment appeared as the natural continuation of an unbroken line of development. The powerful conception of the S-matrix was introduced by Heisenberg as early as 1943: in that year Heisenberg paid a private visit to the Dutch physicists and in two long discussion meetings (the first in my house in Utrecht, the second in Kramers' house near Leyden) the physical implications of the new idea could be fully recognized, even though we lacked the wonderful techniques which have since made their exact formulation possible. It is pardonable that mathematicians should not know all this, but then they should refrain from reckless statements.

As a matter of fact, the weakest point in the book is the discussion of the physical basis of the laws and concepts whose mathematical formulation is developed in such a masterly fashion. The name of Niels Bohr occurs only as an adjective to the word magneton, and although there are three invocations to the 'principle of correspondence', one at least is highly irrelevant: there is certainly no 'correspondence' between the Poisson bracket and the *anti-*

commutator! However, such slight imperfections are of no consequence: after all, physicists able to read this book will also be able to correct them.

The production is of a very high standard. The typography closely imitates the best German models (including such refinements as the use of smaller type for fractions); it even improves upon these models by using bold-face type for vectors: here, however, the Russians ought to go all the way and adopt the Gibbs or Milne-Chapman system of vector notation in its entirety.

L.R.

S. V. FLÜGGE (Editor), *Handbuch der Physik — Encyclopedia of physics*, Vol. 5/1: Principles of quantum theory I (Springer, Berlin 1958. 376 pages. DM 90).

This volume of the Encyclopedia was planned to consist of three articles, by Pauli, Källén and Schwinger: the only trace of the last article, however, is an allusion to its conceptual existence in a footnote to the first. We are thus deprived of what would presumably have been a masterly exposition of the way to pack a complete description of the universe into a Lagrangian. What we do find in the book is in the first place Pauli's imperfectible presentation of the principles of quantum mechanics, which is accordingly reprinted *verbatim* from the previous edition, with addition of some footnotes and imperfect correction of the misprints. The last 30 pages of the old article, however, have been left out, and are now replaced by a fully-fledged treatment of quantum electrodynamics by Källén: a task which might well have daunted anyone else, but which he has brilliantly accomplished.

The student has by now at his disposal a fair number of treatises in which the thorny problems of quantum field theory are approached in very different moods, ranging from the sternly mathematical to the drearily pragmatical. Quite in keeping with the character of this volume of the Encyclopedia, Källén's standpoint is decidedly olympian: his article is no beginner's reading, but to those who are to some degree initiated, it offers a survey of the subject of unequalled clarity, precision and elegance. Although the emphasis is upon the most general and fundamental features, a good sample of important special problems is given, the discussion of which is presented in such a way as to throw light upon the essential aspects. In this domain, in which a careful formulation of the presuppositions, and a severe assessment of the rigour, of every argument is more needed than anything else, the author's well-known critical acumen confers to his analysis a special value: the general discussion of the renormalization problem, in particular, is a most original and authoritative contribution. The author's friends will be delighted to recognize, and others to make acquaintance with, his pungent and picturesque mode of expression and his fine sense of humour. Against the background of uniform dullness of scientific literature in our days, he must be highly commended for daring to write in a style which reveals something of his personality.

L.R.

Recommendations of the International Union of Pure and Applied Physics

Commission for symbols, units and nomenclature †

The Commission for Symbols, Units and Nomenclature, meeting in Rome 17–19 September 1957, has considered the remarks and criticism received from several National Committees of the I.U.P.A.P. on the draft proposals contained in the 'Short Report of the Meeting of the S.U.N. Commission in Paris 20–23 March 1956' (Doc. S.U.N. 56–7). The improved version of these draft proposals has been accepted by the General Assembly of the International Union of Pure and Applied Physics on 19 September 1957 in Rome. These recommendations have to be added to the previous recommendations included in 'Symbols and Units' (Doc. U.I.P. 6 (1955)).

Additions to Ch. I: General principles and recommendations.

(1) *Use of the decimal sign and of the multiplication sign between figures and numbers*:

It is recommended to use the decimal sign and the multiplication sign between figures or numbers according to the following principles:

decimal sign: , or(but only in *English* texts) .

multiplication sign between figures: × or(but only in *non English* texts) .

(2) *Nomenclature and symbols for particles and quanta*:

(2a) It is recommended that symbols indicating particles or quanta should be printed in upright latin or Greek type. *Examples*:

neutron	n	pion	π
proton	p	muon	μ
deuteron	d	electron	e
triton	t	neutrino	ν
α-particle	α	photon	γ

† Communicated by Prof. Dr. J. de Boer, Secretary of the S.U.N., Instituut voor Theoretische Physica, Roetersstraat 1A, Amsterdam.

(2b) It is recommended that the following notation should be used:

Hyperons: Y-particles; Upright capital Greek letters to indicate particular particles, *e.g.* Λ, Ξ, Σ.

Nucleons: N-particles; Upright lower case n and p to indicate neutron and proton respectively.

Mesons: Upright lower case Greek letters to indicate particular particles, *e.g.* π, μ, τ.

Leptons: L-particles; *e.g.* e, ν.

(2c) It is recommended that the charge of particles may be indicated by adding the superscript $+$, $-$ or 0. *Examples*:

$$\pi^+ \ \pi^- \ \pi^0 \ , \ p^+ \ , \ p^- \ , \ e^+ \ , \ e^-.$$

If in connection with the symbols p and e no charge is indicated, these symbols should refer to the positive proton and the negative electron respectively.

(2d) The symbol $\sim$ above the symbol of a particle has been used to indicate the anti-particle of that particle (e.g. $\tilde{\nu}$ for anti-neutrino) and it is recommended to use the same indication when needed in other cases.

(3) *Symbols for quantum state*:

It is recommended that symbols indicating the quantum state of a system or a particle should be printed in upright (roman) type. *Examples*:

$^2P_{\frac{1}{2}}$ state s electron.

(4) *Printing of indices*:

It is recommended to consider as a guiding principle for the printing of indices the criterion: only indices which are symbols for physical quantities should be printed in sloping (italic) type. *Examples*:

Upright indices:	*Sloping indices*:
C_{g} (g = gas)	p in C_p
g_{n} (n = normal)	n in $\sum_n a_n \varphi_n$
m_{p} (p = proton)	x in $\sum_x a_x b_x$
μ_{r} (r = relative)	i, k in g_{ik}
E_{k} (k = kinetic)	x in p_x
χ_{e} (e = electric)	

Additions to Ch. II: Symbols for physical quantities.

physical quantity:	*symbol*:
magnetization: ($M = B/\mu_0 - H$)	M
electromagnetic moment: (dimension: M/n)	μ, m
magnetic polarization: ($J = B - \mu_0 H$)	J
magnetic dipole moment: (dimension: J/n)	j
electric potential:	V, Φ

Additions to Ch. III: Mathematical operations and symbols.

(1) *Use of the solidus in mathematical equations and in fractions*: The solidus may be used in a fraction to separate the numerator from the denominator. When there is any doubt where the numerator starts or where the denominator ends, brackets should be used. *Examples*:

Expressions with a horizontal bar:	Same expressions with a solidus:
$\dfrac{a}{bcd}$	a/bcd
$\dfrac{2}{9}\sin kx, \quad \dfrac{1}{2}RT$	$(2/9)\sin kx$, $(1/2)RT$ or $RT/2$
$\dfrac{a}{b} - c$	$a/b - c$
$\dfrac{a}{b - c}$	$a/(b - c)$
$\dfrac{a - b}{c - d}$	$(a - b)/(c - d)$
$\dfrac{a}{c} - \dfrac{b}{d}$	$a/c - b/d$

It is recommended that in expressions like:

$\sin(2\pi(x - x_0)/\lambda)$, $\exp((r - r_0)/\sigma)$

$\exp(-V(r)/kT)$, $\sqrt{(\varepsilon/c^2)}$

the argument should always be placed between brackets, except when the argument is a simple product of two quantities: *e.g.* $\sin kx$.
When the horizontal bar above the square root is used, no brackets are needed.

Additions to Ch. IV: Units.

(1) *Definition of the unit 'mole';*

(1a) It is recommended that the unit 'mole' should be considered in physics as a unit for *quantity of substance* (indicated by the symbol Q).
Its definition should be: 1 mole (symbol: mole) is the quantity of substance which contains the same number of molecules (or ions, or atoms, or electrons, as the case may be) as there are atoms in exactly 16 gram of pure oxygen isotope ^{16}O.
This quantity and the corresponding unit should be considered in the field where they are used as a fundamental (or basic) quantity and unit respectively.

(1b) *Related quantities*, defined in terms of this quantity are: The molar mass (Definition: $M = m/Q$, m = mass of quantity of substance Q) with CGS unit: g/mole. The molar volume (Definition: v/Q, v = volume of quantity of substance Q) with the CGS unit: cm^3/mole. The 'molecular weight' with the definition: physical molecular weight =

$$\frac{16 \times \text{molar mass of substance}}{\text{molar mass of (atomic) } ^{16}O}$$

which quantity thus should be considered as a pure number.
Avogadro's constant (Definition: N/Q, N is number of molecules in a quantity of substance Q) with the unit: mole^{-1}. Its present value should thus be expressed as:

$$N_0 = N/Q = 6{,}025 \times 10^{23} \text{ mole}^{-1}.$$

(1c) *Remark*: The unit 'grammole' (symbol: g-mole) should be considered as a non-coherent unit of mass characteristic for any particular substance.

(2) *Units and unit symbols*:

The following corrections resp. additions are made in the tables of units and unit symbols:

unit:	*symbol*:
microbar; *barye* (= dyn/cm^2)	μbar
bar; *bar* (= 10^6 dyn/cm^2)	bar
electronvolt: *electronvolt*	eV

(3) *Use of solidus in unit expressions*:

In expressions for units not more than one solidus should be used. *Examples:*

Not: cm/s/s,	*but*: cm/s^2 = cm s^{-2}
Not: neutrons/cm/sr,	*but*: neutrons/cm sr = neutrons cm^{-1} sr^{-1}
Not: 1 poise = 1 g/s/cm,	*but*: 1 poise = 1 g/s cm = 1 g s^{-1} cm^{-1}
Not: J/°K/mole,	*but*: J/°K mole = J °K^{-1} mole^{-1}

(4) *Double prefixes*:

The use of double prefixes should be avoided whenever single prefixes are available. *Examples*:

Not: mμs,	*but*: ns	(nanosecond)
Not: kMW	*but*: GW	(gigawatt)
Not: μμF,	*but*: pF	(picofarad)

(5) *Unit with prefix*:

(5a) When a prefix is placed before the symbol of a unit, the combination of prefix and symbol should be considered as *one new symbol* which can be squared or cubed without using brackets. *Examples*:

cm^2 , mA^2 , μs^2 .

(5b) *Remark*: A prefix should never be used before a unit which is squared. *Example*:

cm^2 *means always* (0,01 m)^2 *and never* 0,01 m^2.

Misprint to be corrected in U.I.P. 6 (1955)

[Nuclear Physics 1 (1956) 555]

The symbol for the quantity indicated in connection with the unit kilowatt-hour should be: *E*.

Editor's Note:

All the above recommendations have already been adopted in Nuclear Physics, with one minor exception: for the sake of uniformity the *English* convention for the decimal sign is always used, irrespective of the language in which the article is written.

Nuclear physicists are not likely to use the unit 'mole'. They might be puzzled by the new definition proposed by the Commission: what in the name of Burleus, Duns Scot, Oresme and all the scholastic doctors is a *quantity of substance?*

8.B *Nuclear Physics* 7 (1958) 305—372; © *North-Holland Publishing Co., Amsterdam*
Not to be reproduced by photoprint or microfilm without written permission from the publisher

PARTICLES AND SYMMETRIES

E. CORINALDESI
University College of North Staffordshire, Keele, England

Received 5 December 1957

CONTENTS

Chapter I: Introduction

1. VACUUM, PARTICLE STATES AND TRANSITION AMPLITUDES 306
2. SPINLESS PARTICLES 307
3. PARTICLES OF SPIN $\frac{1}{2}$ 310
4. PHOTONS 317
5. PARTICLES OF SPIN 1 321
6. THE ELECTRON-PHOTON-NUCLEON-π-MESON SYSTEM 321

Chapter II: Space Inversion

1. SPINLESS PARTICLES 323
2. PARTICLES OF SPIN $\frac{1}{2}$ 325
3. PHOTONS 328
4. PARITY CONSERVING INTERACTIONS 329
5. SELECTION RULES 330
6. PARITY NON-CONSERVING INTERACTIONS 333

Chapter III: Particle-Antiparticle Conjugation

1. SPINLESS AND SPIN 1 PARTICLES 334
2. PARTICLES OF SPIN $\frac{1}{2}$ 337
3. DO THE OPERATIONS OF SPACE-INVERSION AND PARTICLE-ANTI-PARTICLE CONJUGATION COMMUTE? 339
4. C-PARITY OF A PARTICLE-ANTIPARTICLE SYSTEM (SPIN $\frac{1}{2}$, POSITONIUM; NUCLEON-ANTINUCLEON PAIR) 340
5. SELECTION RULES FROM CONSERVATION OF C-PARITY 340

Chapter IV: Charge Symmetry

1. PRELIMINARIES 341
2. INTERACTIONS OF BOSONS AND NUCLEONS 342
3. SELECTION RULES FROM CONSERVATION OF CD 344
4. BREAKING OF SELECTION RULES BY THE ELECTROMAGNETIC FIELD 345

July (1) 1958

Chapter V: **Time Reversal**

1. OUTLINE. SPINLESS PARTICLES 347
2. TIME REVERSAL FOR PARTICLES OF SPIN $\frac{1}{2}$ 349

Chapter VI: **Weak Interactions**

1. GENERAL FEATURES 352
2. SALAM'S GAUGE TRANSFORMATION AND THE TWO-COMPONENT THEORY OF NEUTRINOS 356
3. MORE GENERAL GAUGE TRANSFORMATIONS 362

Chapter VII: **New Particles**

1. RÉSUMÉ OF EXPERIMENTAL RESULTS 364
2. CONSERVATION OF BARYONS 366
3. ISOBARIC SPIN 367
4. CLASSIFICATION OF NEW PARTICLES 370

CHAPTER I

PARTICLES AND FIELDS

1. Vacuum, particle states and transition amplitudes

Any portion of the world, defined, for instance, as the enclosure of a box, can be described in many different ways. For our purpose it is convenient to give the number and nature of the particles present, together with the momentum of each. Further degrees of freedom may have to be specified if the particles possess an internal structure, and occasionally the angular momentum will be given instead of the momentum.

The formalism embodying this mode of description defines first the vacuum state, denoted by the ket $|0)$. Particle states are constructed by applying to the vacuum certain creation operators $\mathbf{c}^*(\mathbf{k}, \lambda)$, where $\mathbf{k}$ stands for the momentum of a particle and λ for any additional information, e.g. charge, spin, needed to make the representation complete. Thus

$$\mathbf{c}^*(\mathbf{k}_1, \lambda_1)\mathbf{c}^*(\mathbf{k}_2, \lambda_2) \ldots \mathbf{c}^*(\mathbf{k}_m, \lambda_m) |0) \tag{1}$$

is a state with m particles, each having a given momentum and additional degrees of freedom.

Multiplication of (1) by a function $\varphi(\mathbf{k}_1, \mathbf{k}_2 \ldots \mathbf{k}_m)$, followed by integration over the momenta $\mathbf{k}_1, \mathbf{k}_2 \ldots \mathbf{k}_m$, produces a state in which the particles are localized in space. Whereas the function φ can then be regarded as a momentum wave function, in the non-relativistic limit its Fourier transform can be identified with the ordinary Schroedinger wave function $\psi(\mathbf{r}_1, \mathbf{r}_2 \ldots \mathbf{r}_m)$ ($\mathbf{r}_i$ denoting the position of the i-th particle).

Interactions are the agents which induce transitions from one state to another. The probability of a certain transition taking place is proportional to the square of the modulus of the transition amplitude

$$(0|\, \mathsf{c}(\mathbf{k}'_n, \lambda'_n) \ldots \mathsf{c}(\mathbf{k}'_1, \lambda'_1) \mathsf{U} \mathsf{c}^*(\mathbf{k}_1, \lambda_1) \ldots \mathsf{c}^*(\mathbf{k}_m, \lambda_m)\, |0). \tag{2}$$

The state vector to the left of the transition operator U is a bra, the conjugate of the ket $\mathsf{c}^*(\mathbf{k}'_1, \lambda'_1) \ldots \mathsf{c}^*(\mathbf{k}'_n, \lambda'_n)\, |0)$. It results from the latter by the operation of Hermitian conjugation, which replaces the ket vacuum $|0)$ by the bra vacuum $(0|$, each creation operator by its Hermitian conjugate, which is a destruction operator, and reverses the order of all the factors †.

U is a Lorentz invariant functional of the interaction Lagrangian $\mathscr{L}(x)$, which is always Lorentz invariant of its own accord and a product of field operators $\psi(x)(x \equiv \mathbf{r}, t)$. These are related to the creation and destruction operators before mentioned in much the same way as a function is to the coefficients of its Fourier expansion. The relationship will be explicitly written in the following sections, and lists of Lorentz invariant interactions given in appropriate places.

Expanded in powers of the interaction, the transition operator it given by

$$\mathsf{U} = \sum_{n=1}^{\infty} \frac{i^n}{n!} \int \mathrm{d}^4 x_1 \ldots \mathrm{d}^4 x_n \left(\mathscr{L}(x_1) \ldots \mathscr{L}(x_n)\right)_+, \tag{3}$$

where $\mathrm{d}^4 x \equiv \mathrm{d}\mathbf{r}\, \mathrm{d}t$, and the integrations cover the whole space-time. The chronological ordering $(\ \ )_+$ signifies that for any two factors $\mathscr{L}(x_j)$ and $\mathscr{L}(x_k)$, $\mathscr{L}(x_j)$ must take the left of $\mathscr{L}(x_k)$ if $t_j > t_k$, and the right if $t_j < t_k$.

2. Spinless particles

2.1. CREATION AND DESTRUCTION OPERATORS

For neutral †† spinless particles the creation and destruction operators $\mathsf{c}^*(\mathbf{k})$ and $\mathsf{c}(\mathbf{k})$ are functions of the momentum only. The field operator $\phi(x)$ is Hermitian and is given by

$$\phi(x) = \sum [\mathsf{c}(\mathbf{k}) \mathrm{e}^{i(k,x)} + \mathsf{c}^*(\mathbf{k}) \mathrm{e}^{-i(k,x)}], \tag{4}$$

where $(k, x) \equiv \mathbf{k} \cdot \mathbf{r} - \omega t$, and $\omega = \sqrt{\mathbf{k}^2 + \mu^2}$, μ being the mass of the particles.

We have introduced the abbreviation $\sum \equiv \sum_{\mathbf{k}} (2V\omega)^{-\frac{1}{2}}$, V being the volume of the box in which the particles are contained.

† The Hermitian conjugate of a c-number $\gamma = \alpha + i\beta$ (α, β real) is the complex conjugate $\gamma^* = \alpha - i\beta$. If c_1 and c_2 are destruction operators, the Hermitian conjugate of the operator $\mathsf{c} = \mathsf{c}_1 + i\mathsf{c}_2$ is $\mathsf{c}^* = \mathsf{c}_1^* - i\mathsf{c}_2^*$. An operator is said to be Hermitian when it is equal to its Hermitian conjugate.

†† Or rather, particles which are in all respects indistinguishable from their antiparticles. In Ch. VII we shall mention an uncharged spinless particle, the θ_0 meson, which is not identical with its antiparticle $\overline{\theta}_0$. Therefore the field operator of $(\theta_0, \overline{\theta}_0)$ will be non-Hermitian, and must be expanded according to eq. (5).

For charged spinless particles, two kinds of creation and destruction operators must be introduced, $\mathsf{a}^*(\mathbf{k})$ and $\mathsf{a}(\mathbf{k})$ for positive particles (particles) $\mathsf{b}^*(\mathbf{k})$ and $\mathsf{b}(\mathbf{k})$ for negative particles (antiparticles). The expansion of the field operator $\boldsymbol{\phi}(x)$ contains both,

$$\boldsymbol{\phi}(x) = \sum [\mathsf{a}(\mathbf{k})e^{i(k,x)} + \mathsf{b}^*(\mathbf{k})e^{-i(k,x)}]. \tag{5}$$

In contrast with the case of neutral particles, (5) is not Hermitian. This is true of any field of charged particles, the reason being that only with a non-Hermitian field is it possible to construct a non-vanishing interaction † with the electromagnetic field.

2.2. ANGULAR MOMENTUM REPRESENTATION

If the energy and the angular momentum are chosen as degrees of freedom for the individual particles, appropriate creation and destruction operators $\mathsf{c}^*(k, l, m)$, $\mathsf{c}(k, l, m), \ldots$ must be introduced [3, 10]). Then, for instance,

$$\mathsf{c}^*(k, l, m)|0), \qquad \mathsf{a}^*(k, l, m)|0), \qquad \mathsf{b}^*(k, l, m)\,|0)$$

are states with one (neutral, positive, negative) spinless particle of energy $\omega = \sqrt{k^2+\mu^2}$ and angular momentum quantum numbers $\mathbf{l}^2 = l(l+1)$, $l_z = m$. An expansion for the field operator equivalent to (5) is [3, 10])

$$\boldsymbol{\phi}(x) = \sum_{klm} [\mathsf{a}(k, l, m)\, Y_l^{(m)}(\theta, \phi)e^{-i\omega t} + \mathsf{b}^*(k, l, m)Y_l^{(m)*}(\theta, \phi)e^{i\omega t}] \tag{6}$$

(for neutral particles $\mathsf{a} \to \mathsf{c}$, $\mathsf{b} \to \mathsf{c}$). Here θ and ϕ are the polar angles of $\mathbf{r}$, $Y_l^{(m)}(\theta, \phi)$ is a spherical harmonic defined so that $Y_l^{(m)*} = (-1)^m Y_l^{(-m)}$, and $\sum_{klm}$ stands for $\sum_{klm} (2\omega)^{-\frac{1}{2}} g_{lk}(r)$, where the radial functions $g_{lk}(r)$ are given by

$$g_{lk}(r) = \sqrt{\frac{\pi k}{rR}} \cdot J_{l+\frac{1}{2}}(kr), \tag{7}$$

and are solutions of the radial Laplace equation.

R is the (large) radius of a spherical box, and $J_{l+\frac{1}{2}}$ is a Bessel function.

The application of the differential operator $(\Box^2-\mu^2)$ to each term of (4), (5) and (6) gives zero, so that

$$(\Box^2-\mu^2)\boldsymbol{\phi}(x) = 0. \tag{8}$$

Comparison of eqs. (5) and (6) yields the relation

$$\mathsf{a}^*(\mathbf{k}) = \frac{\pi}{k}\sqrt{\frac{8R}{V}} \sum_{l=0}^{\infty} \sum_{m=-l}^{+l} i^l\, Y_l^{(m)*}(\mathbf{k})\mathsf{a}^*(k, l, m) \tag{9}$$

between creation operators in the momentum representation and those in

† Which interaction may be a multipole of any order, so long as it discriminates between particles and antiparticles. It is not, however, known whether the distinction between the mesons θ_0 and $\overline{\theta}_0$ is of electromagnetic origin (see footnote p. 3).

the angular momentum representation. Applying the two members of (9) to the vacuum $|0)$, a relation ensues between corresponding one particle states.

The angular momentum representation may also be used for the description of particles acted upon by a central static field. The creation and destruction operators then refer to non-free particles of given angular momentum and energy. The expansion (6) is still valid with g_{lk} replaced by the solutions of a radial equation including the static potential.

2.3. TWO-PARTICLE STATES

Two-particle states are generated by operating on the vacuum with two creation operators. Thus

$$\mathsf{a}^*(\mathbf{k})\mathsf{b}^*(\mathbf{k}')\,|0) \tag{10}$$

is a state with one particle of momentum $\mathbf{k}$ and one antiparticle of momentum $\mathbf{k}'$, and

$$\mathsf{a}^*(k, l, m)\mathsf{b}^*(k', l', m')\,|0) \tag{10'}$$

is a state with one particle with the quantum numbers (k, l, m) and one antiparticle with (k', l', m') in the angular momentum representation.

More interesting is the construction of a particle-antiparticle state of relative angular momentum (L, M) in the centre-of-momentum frame. This can be done by superposing states (10) with $\mathbf{k}' = -\mathbf{k}$. The expression for the state in question is [3])

$$|k, L, M) = \int \mathrm{d}\Omega_{\mathbf{k}}\, Y_L^{(M)}(\mathbf{k})\mathsf{a}^*(\mathbf{k})\mathsf{b}^*(-\mathbf{k})\,|0), \tag{11}$$

where $Y_L^{(M)}(\mathbf{k})$ is a spherical harmonic whose arguments are the polar angles of $\mathbf{k}$, and $\mathrm{d}\Omega_{\mathbf{k}}$ is an element of solid angle around $\mathbf{k}$. Using the Clebsch-Gordan coefficients [1]), states with any number of particles and antiparticles and given total angular momentum can be formed.

2.4. BOSE-EINSTEIN STATISTICS

Particles of spin zero obey the Bose-Einstein statistics, a property which is formally expressed by the commutation relations † among creation and destruction operators,

$$[\mathsf{c}(\mathbf{k}), \mathsf{c}^*(\mathbf{k}')] = [\mathsf{a}(\mathbf{k}), \mathsf{a}^*(\mathbf{k}')] = [\mathsf{b}(\mathbf{k}), \mathsf{b}^*(\mathbf{k}')] = \delta_{\mathbf{k}\mathbf{k}'}$$

all the other commutators being zero.

Let us consider, for instance, neutral particles. There is no restriction on the number of particles of momentum $\mathbf{k}$ in the state $\mathsf{c}^*(\mathbf{k})\mathsf{c}^*(\mathbf{k})\ldots\mathsf{c}^*(\mathbf{k})\,|0)$, since $[\mathsf{c}^*(\mathbf{k}), \mathsf{c}^*(\mathbf{k})] = 0$ is only a trivial identity. On the other hand, this state is an eigenstate of the operator $\mathsf{N}(\mathbf{k}) = \mathsf{c}^*(\mathbf{k})\mathsf{c}(\mathbf{k})$ (number of particles of momentum $\mathbf{k}$) whose eigenvalue is the number of factors $\mathsf{c}^*(\mathbf{k})$ which operate on the vacuum. For example, omitting $\mathbf{k}$ for brevity, $\mathsf{N}\mathsf{c}^*\mathsf{c}^*\,|0) =$

† Here $[a, b] = ab - ba$, $\delta_{\mathbf{k}\mathbf{k}'}$ $(= 1$ for $\mathbf{k} = \mathbf{k}'$, $= 0$ for $\mathbf{k} \neq \mathbf{k}')$.

$c^* cc^* c^* |0) = c^*(1+c^* c)c^* |0) = c^* c^* cc^* |0)+c^* c^* |0) = c^* c^* (1+c^* c) |0)+ c^* c^* |0) = 2c^* c^* |0)$ since $c |0) = 0$ (destruction operators give zero when applied to the ket vacuum; note, however, that $(0|c \neq 0$, since it results from $c^* |0)$ by Hermitian conjugation).

3. Particles of spin $\frac{1}{2}$

3.1. SPIN STATES AND SPIN MATRICES

We denote by $a^*(\mathbf{k}, \lambda)$, $a(\mathbf{k}, \lambda)$ the creation and destruction operators for a particle of momentum $\mathbf{k}$ and with spin either parallel, $\lambda = \uparrow$, or antiparallel, $\lambda = \downarrow$, to the momentum. The analogous operators for an antiparticle will be $b^*(\mathbf{k}, \lambda)$ and $b(\mathbf{k}, \lambda)$.

Particles of spin $\frac{1}{2}$ obey the Fermi-Dirac statistics. The creation and destruction operators satisfy anticommutation † relations

$$\{a(\mathbf{k}, \lambda), a^*(\mathbf{k}', \lambda')\} = \{b(\mathbf{k}, \lambda), b^*(\mathbf{k}', \lambda')\} = \delta_{\lambda\lambda'}\delta_{\mathbf{k}\mathbf{k}'}.$$

All the other anticommutatores are zero. E.g.,

$$\{a^*(\mathbf{k}, \lambda), a^*(\mathbf{k}', \lambda')\} = 0,$$

which, for $\mathbf{k} = \mathbf{k}'$ and $\lambda = \lambda'$ reduces to $a^*(\mathbf{k}, \lambda)a^*(\mathbf{k}, \lambda) = 0$, so that states with more than one particle of given $(\mathbf{k}, \lambda)$ do not exist.

The operator $N(\mathbf{k}, \lambda) = a^*(\mathbf{k}, \lambda)a(\mathbf{k}, \lambda)$ represents the number of particles of momentum $\mathbf{k}$ and spin orientation λ and has the eigenvalues 1 and 0, for the eigenstates $a^*(\mathbf{k}, \lambda) |0)$ and $|0)$, respectively. Similarly $\bar{N}(\mathbf{k}, \lambda) = b^*(\mathbf{k}, \lambda)b(\mathbf{k}, \lambda)$ represents the number of antiparticles of momentum $\mathbf{k}$ and spin orientation λ.

The expansion of the field operator $\psi(x)$ must be done with care. In analogy with eq. (5)

$$\psi(x) = \sum [a(\mathbf{k}, \lambda)u(\mathbf{k}, \lambda)e^{i(k,x)} + b^*(\mathbf{k}, \lambda)v(\mathbf{k}, \lambda)e^{-i(k,x)}], \tag{12}$$

where now $\sum \equiv \sum_{\mathbf{k}} \sum_{\lambda} (2V\omega)^{-\frac{1}{2}}$ includes a sum over the direction of the spin.

If $u(\mathbf{k}, \lambda)e^{i(k,x)}$ and $v(\mathbf{k}, \lambda)e^{-i(k,x)}$ are solutions of the Dirac equation, one has also

$$\left(\gamma_\mu \frac{\partial}{\partial x_\mu} + m\right)\psi(x) = 0. \tag{13}$$

We here anticipate that, whereas $u(\mathbf{k}, \uparrow)$ and $u(\mathbf{k}, \downarrow)$ are positive energy solutions for momentum $\mathbf{k}$ and spin parallel and antiparallel to $\mathbf{k}$, respectively, $v(\mathbf{k}, \uparrow)$ and $v(\mathbf{k}, \downarrow)$ are negative energy solutions for momentum $-\mathbf{k}$ and spin parallel and antiparallel to $-\mathbf{k}$, respectively. The reason for this is that when we insert eq. (12) into, e.g., the expression for the total momen-

† Here $\{a, b\} = ab+ba$. Cf. footnote on page 5 for the definition of $\delta_{\mathbf{k}\mathbf{k}'}$. That of $\delta_{\lambda\lambda'}$ is $\delta_{\uparrow\uparrow} = \delta_{\downarrow\downarrow} = 1, \delta_{\uparrow\downarrow} = \delta_{\downarrow\uparrow} = 0$.

tum $\mathbf{P}$ of the field, of the form $\int \psi^* \ldots \psi \, d\mathbf{r}$, by virtue of the anticommutativity of the creation and destruction operators we find

$$\mathbf{P} = \sum_{\mathbf{k}\lambda} [\mathsf{N}(\mathbf{k}, \lambda) \times \text{momentum of } u(\mathbf{k}, \lambda) \\ -\overline{\mathsf{N}}(\mathbf{k}, \lambda) \times \text{momentum of } v(\mathbf{k}, \lambda)]$$

where N and $\overline{\mathsf{N}}$ denote the numbers of particles and antiparticles. Clearly the momentum of $v(\mathbf{k}, \lambda)$ must be $-\mathbf{k}$, if $\mathbf{P}$ is to be the sum of the momenta of particles and antiparticles present. A similar consideration would hold for the energy and the spin.

Since the γ_μ are 4×4 matrices, $u(\mathbf{k}, \lambda)$ and $v(\mathbf{k}, \lambda)$ are four-component c-numbers, and $\psi(x)$ four-component operators.

It is to be borne in mind that the form of the γ-matrices is not unique [8]). If γ_μ and γ'_μ ($\mu = 1, 2, 3, 4$) are two sets of Hermitian matrices satisfying the anticommutation relations

$$\gamma_\mu\gamma_\nu + \gamma_\nu\gamma_\mu = 2\delta_{\mu\nu} \tag{14}$$

a unitary matrix exists connecting them, $\gamma'_\mu = S\gamma_\mu S^{-1}$, and for our purpose are entirely equivalent.

The following are the most usual choices for the γ's (with $\boldsymbol{\gamma} \equiv (\gamma_1, \gamma_2, \gamma_3)$, and we give also $\gamma_5 = \gamma_1\gamma_2\gamma_3\gamma_4$):

$$\begin{array}{lllll}
\text{(Pauli) [2,7])} & \boldsymbol{\gamma} = \rho_y \times \boldsymbol{\sigma}, & \gamma_4 = \rho_z \times I, & \gamma_5 = -\rho_x \times I; \\
\text{(Kramers) [4,5])} & \boldsymbol{\gamma}' = -\rho_y \times \boldsymbol{\sigma}, & \gamma'_4 = \rho_x \times I, & \gamma'_5 = -\rho_z \times I; \\
\text{(Majorana) [6])} & \gamma''_1 = -I \times \sigma_x, & \gamma''_2 = -\rho_y \times \sigma_y, & \gamma''_3 = I \times \sigma_z, \\
 & & \gamma''_4 = \rho_z \times \sigma_y, & \gamma''_5 = \rho_x \times \sigma_y.
\end{array} \tag{15}$$

We have introduced the matrices

$$\sigma_x = \begin{pmatrix} 0 & 1 \\ 1 & 0 \end{pmatrix}, \quad \sigma_y = \begin{pmatrix} 0 & -i \\ i & 0 \end{pmatrix}, \quad \sigma_z = \begin{pmatrix} 1 & 0 \\ 0 & -1 \end{pmatrix}, \quad I = \begin{pmatrix} 1 & 0 \\ 0 & 1 \end{pmatrix} \tag{16}$$

and $\rho_x, \rho_y, \rho_z, I$, which are defined in the same way. If the four components of u, say, are written $u_1 \equiv u_{1,1}$, $u_2 \equiv u_{-1,1}$, $u_3 \equiv u_{1,-1}$, $u_4 \equiv u_{-1,-1}$ the σ's operate on the first indices as they would on the two-components of a non-relativistic spin function, whereas the ρ's operate on the second indices in the same manner. For instance

$$\rho_x \times \sigma_x \begin{pmatrix} u_1 \\ u_2 \\ u_3 \\ u_4 \end{pmatrix} = \rho_x \begin{pmatrix} u_2 \\ u_1 \\ u_4 \\ u_3 \end{pmatrix} = \begin{pmatrix} u_4 \\ u_3 \\ u_2 \\ u_1 \end{pmatrix}. \tag{17}$$

The main advantage of the Pauli set is that γ_4 is diagonal, which, at low energy, causes the components u_1 and u_2 to be large (proportional to $\omega+m \approx 2m$) and u_3 and u_4 to be small (proportional to $\omega-m$).

In the Kramers set, the matrix γ_5, which occurs in the coupling of spin $\frac{1}{2}$ particles (e.g., mucleons) with pseudoscalar particles (e.g., π-mesons), is diagonal. The use of this set is convenient in studying space inversions.

Finally, the Majorana matrices $\gamma''_1, \gamma''_2, \gamma''_3$ are real like the space coordinates x, y, z and γ''_4 is imaginary like $x_4 = it$ †. All four matrices are, of course, Hermitian. Thus $\gamma''_1, \gamma''_2, \gamma''_3$ are equal to their transposes, since the Hermiticity condition $a_{ik} = a^*_{ki}$ reduces for them to $a_{ik} = a_{ki}$, whereas γ''_4 is equal to minus its transpose. The formula $\gamma''^{\mathrm{T}}_\mu = -\gamma''_4 \gamma''_\mu \gamma''_4$, where T denotes transposition, concisely expresses this property. The Majorana set turns out to be the most convenient when defining the operation of particle-antiparticle conjugation.

For completeness we add the expressions for the components of the spin matrices in the different sets:

$$\begin{aligned}
&\text{(Pauli)} && \mathbf{s} \equiv \tfrac{1}{2}(I\times\sigma_x, && I\times\sigma_y, && I\times\sigma_z);\\
&\text{(Kramers)} && \mathbf{s}' \equiv \tfrac{1}{2}(I\times\sigma_x, && I\times\sigma_y, && I\times\sigma_z); \qquad (15')\\
&\text{(Majorana)} && \mathbf{s}'' \equiv \tfrac{1}{2}(\rho_y\times\sigma_z, && I\times\sigma_y, && -\rho_y\times\sigma_x).
\end{aligned}$$

The reader may find it useful to have in full the relations between the three sets of matrices (15). These are

$$\gamma'_\mu = S_{\mathrm{K,P}}\gamma_\mu S^{-1}_{\mathrm{K,P}}, \qquad \gamma''_\mu = S_{\mathrm{M,K}}\gamma'_\mu S^{-1}_{\mathrm{M,K}}, \qquad \gamma''_\mu = S_{\mathrm{M,P}}\gamma_\mu S^{-1}_{\mathrm{M,P}}, \quad (18)$$

with ††

$$\begin{aligned}
S_{\mathrm{K,P}} &= \frac{1}{\sqrt{2}}(1+i\rho_y)\rho_x,\\
S_{\mathrm{M,K}} &= \frac{e^{i\pi/4}}{\sqrt{2}}(1+i\rho_y\sigma_y), \qquad (19)\\
S_{\mathrm{M,P}} &= \frac{e^{i\pi/4}}{\sqrt{2}}(1+i\rho_y\sigma_y)(1+i\rho_y)\rho_x,
\end{aligned}$$

(the inverse matrices being the Hermitian conjugates of these, e.g., $S^{-1}_{\mathrm{K,P}} = (1/\sqrt{2})\,\rho_x(1-i\rho_y)$). The corresponding transformations for the field operator ψ are

$$\psi' = S_{\mathrm{K,P}}\psi, \qquad \psi'' = S_{\mathrm{M,K}}\psi', \qquad \psi'' = S_{\mathrm{M,P}}\psi. \quad (20)$$

3.2. EXPLICIT SOLUTIONS

Tables 1 and 2 show the components of the solutions of given momentum for the three sets of γ-matrices. The symbols used are

† i.e., all the elements of $\gamma''_1, \gamma''_2, \gamma''_3$ are real numbers, while those of γ''_4 are purely imaginary.

†† For simplicity we write $\rho_i\sigma_k$ instead of $\rho_i\times\sigma_k$ in these formulae, and replace unit matrices by 1.

TABLE 1
Particle solutions

	$\sqrt{2}\,u(\mathbf{k},\uparrow)$	$\sqrt{2}\,u(\mathbf{k},\downarrow)$	$u'(\mathbf{k},\uparrow)$	$u'(\mathbf{k},\downarrow)$	$\sqrt{2}\,e^{-\pi i/4}\cdot u''(\mathbf{k},\uparrow)$	$\sqrt{2}\,e^{-\pi i/4}\cdot u''(\mathbf{k},\downarrow)$
(1)	$\alpha(c+s)$	$-\beta^*(c+s)$	$c\alpha$	$-s\beta^*$	$c\alpha-is\beta$	$-s\beta^*-ic\alpha^*$
(2)	$\beta(c+s)$	$\alpha^*(c+s)$	$c\beta$	$s\alpha^*$	$c\beta+is\alpha$	$s\alpha^*-ic\beta^*$
(3)	$\alpha(c-s)$	$\beta^*(c-s)$	$s\alpha$	$-c\beta^*$	$ic\beta+s\alpha$	$is\alpha^*-c\beta^*$
(4)	$\beta(c-s)$	$-\alpha^*(c-s)$	$s\beta$	$c\alpha^*$	$-ic\alpha+s\beta$	$is\beta^*+c\alpha^*$

TABLE 2
Antiparticle solutions

	$\sqrt{2}v(\mathbf{k},\uparrow)$	$\sqrt{2}v(\mathbf{k},\downarrow)$	$v'(\mathbf{k},\uparrow)$	$v'(\mathbf{k},\downarrow)$	$\sqrt{2}\,e^{-\pi i/4}\cdot v''(\mathbf{k},\uparrow)$	$\sqrt{2}\,e^{-\pi i/4}\cdot v''(\mathbf{k},\downarrow)$
(1)	$-\beta^*(c-s)$	$\alpha(c-s)$	$s\beta^*$	$c\alpha$	$s\beta^*-ic\alpha^*$	$c\alpha+is\beta$
(2)	$\alpha^*(c-s)$	$\beta(c-s)$	$-s\alpha^*$	$c\beta$	$-s\alpha^*-ic\beta^*$	$c\beta-is\alpha$
(3)	$\beta^*(c+s)$	$\alpha(c+s)$	$-c\beta^*$	$-s\alpha$	$-is\alpha^*-c\beta^*$	$ic\beta-s\alpha$
(4)	$-\alpha^*(c+s)$	$\beta(c+s)$	$c\alpha^*$	$-s\beta$	$-is\beta^*+c\alpha^*$	$-ic\alpha-s\beta$

$$c=\cos\frac{\chi}{2},\qquad s=\sin\frac{\chi}{2},\qquad \operatorname{ctg}\chi=\frac{|\mathbf{k}|}{m},\qquad k_z=k\cos\theta,$$
$$k_x+ik_y=k\sin\theta\cdot e^{i\phi},\qquad \alpha=\cos\frac{\theta}{2}\cdot e^{-i\phi/2},\qquad \beta=\sin\frac{\theta}{2}\cdot e^{i\phi/2}. \tag{21}$$

It is easy to verify that $\uparrow$ and $\downarrow$ correspond to a spin orientation parallel and antiparallel to $\mathbf{k}$ for the particle solutions, and to a spin orientation parallel and antiparallel to $-\mathbf{k}$ for the antiparticle solutions. For example, for the Kramers set

$$\frac{1}{k}(\mathbf{s}'\cdot\mathbf{k})u'(\mathbf{k},\uparrow)=\tfrac{1}{2}u'(\mathbf{k},\uparrow),$$
$$\frac{1}{k}(\mathbf{s}'\cdot\mathbf{k})u'(\mathbf{k},\downarrow)=-\tfrac{1}{2}u'(\mathbf{k},\downarrow), \tag{22}$$

and

$$\frac{1}{k}(\mathbf{s}'\cdot-\mathbf{k})v'(\mathbf{k},\uparrow)=\tfrac{1}{2}v'(\mathbf{k},\uparrow),$$
$$\frac{1}{k}(\mathbf{s}'\cdot-\mathbf{k})v'(\mathbf{k},\downarrow)=-\tfrac{1}{2}v'(\mathbf{k},\downarrow). \tag{22'}$$

Another important point is that, for the Majorana set, the particle and antiparticle solutions are the complex conjugate of one another,

$$(u''_\alpha(\mathbf{k}, \uparrow))^* = v''_\alpha(\mathbf{k}, \uparrow),$$
$$(u''_\alpha(\mathbf{k}, \downarrow))^* = v''_\alpha(\mathbf{k}, \downarrow) \qquad (\alpha = 1, 2, 3, 4). \tag{23}$$

That this must be so can be seen by writing the Dirac equation for the two kinds of solutions,

$$(i\boldsymbol{\gamma}'' \cdot \mathbf{k} - \omega\gamma''_4 + m)u''(\mathbf{k}, \lambda) = 0,$$
$$(-i\boldsymbol{\gamma}'' \cdot \mathbf{k} + \omega\gamma''_4 + m)v''(\mathbf{k}, \lambda) = 0, \tag{24}$$

and by noticing that, $\boldsymbol{\gamma}''$ being real and γ''_4 purely imaginary, the second equation results from the first by complex conjugation (not to be confused with Hermitian conjugation).

The relationship between particle and antiparticle solutions is more complicated for the other two sets. Taking

$$\psi^* \gamma, \tag{25}$$

where γ is a matrix and ψ is a four-component quantity, to mean a quantity with components $\alpha = 1, 2, 3, 4$ given by

$$\psi_\beta^* \gamma_{\beta\alpha} \tag{26}$$

we see that

$$v(\mathbf{k}, \lambda) = u^*(\mathbf{k}, \lambda)\gamma_2, \qquad v'(\mathbf{k}, \lambda) = u'^*(\mathbf{k}, \lambda)\gamma'_2 \tag{27}$$

and conversely

$$u(\mathbf{k}, \lambda) = v^*(\mathbf{k}, \lambda)\gamma_2, \qquad u'(\mathbf{k}, \lambda) = v'^*(\mathbf{k}, \lambda)\gamma'_2. \tag{27'}$$

3.3. MAJORANA'S NEUTRINO THEORY

Some neutral particles of spin $\frac{1}{2}$ (e.g. neutrons) are distinguishable from their antiparticles by virtue of their electromagnetic properties, such as their magnetic moment.

The Majorana theory of neutrino [6, 9]) concerns itself with particles which are identical with their antiparticles. The transition from the ordinary theory to the Majorana theory is effected by writing

$$\mathsf{a} \to \mathsf{c}, \qquad \mathsf{a}^* \to \mathsf{c}^*, \qquad \mathsf{b} \to \mathsf{c}, \qquad \mathsf{b}^* \to \mathsf{c}^* \tag{28}$$

in eq. (12) i.e. by identifying the creation and destruction operators for particles and antiparticles. The consequences of doing so are particularly evident if Majorana's own set of γ-matrices is employed. In fact, from (12), (28) and tables 1 and 2, we find

$$\begin{pmatrix} \psi''_1 \\ \psi''_2 \\ \psi''_3 \\ \psi''_4 \end{pmatrix} = \begin{pmatrix} \psi''^*_1 \\ \psi''^*_2 \\ \psi''^*_3 \\ \psi''^*_4 \end{pmatrix} \tag{29}$$

so that the components of the field operator for Majorana particles are

Hermitian for the Majorana set. For the Pauli and Kramers sets we have

$$\psi_\alpha = \psi_\beta^* \gamma_{2,\beta\alpha}, \qquad \psi'_\alpha = \psi'^*_\beta \gamma'_{2,\beta\alpha} \tag{30}$$

so that

$$\begin{pmatrix} \psi_1 \\ \psi_2 \\ \psi_3 \\ \psi_4 \end{pmatrix} = \begin{pmatrix} -\psi_4^* \\ \psi_3^* \\ \psi_2^* \\ -\psi_1^* \end{pmatrix} = \begin{pmatrix} \psi_1 \\ \psi_2 \\ \psi_2^* \\ -\psi_1^* \end{pmatrix} \tag{31}$$

in the former, and

$$\begin{pmatrix} \psi'_1 \\ \psi'_2 \\ \psi'_3 \\ \psi'_4 \end{pmatrix} = \begin{pmatrix} \psi'_1 \\ \psi'_2 \\ -\psi'^*_2 \\ \psi'^*_1 \end{pmatrix} \tag{31'}$$

in the latter. This shows that the Majorana theory uses only two independent non-Hermitian components, or four independent Hermitian components in the Majorana set.

3.4. ANGULAR MOMENTUM REPRESENTATION

In the angular momentum representation, particles of spin $\frac{1}{2}$ are described by the eigenvalues $j(j+1)$ of the square of the total angular momentum $\mathbf{j} = \mathbf{l}+\mathbf{s}$ $(j = \frac{1}{2}, \frac{3}{2}, \ldots)$ and by the component $j_z = m (m = \pm\frac{1}{2}, \pm\frac{3}{2}, \ldots)$. For each pair of values j and m and a given sign of the energy, the Dirac equation is known to have two independent solutions (according as to whether $j = l \mp \frac{1}{2}$, l being the orbital angular momentum, they will be denoted by $j^{(\pm)}$). For positive energy and for the Pauli set of γ-matrices these are of the form [3])

$$u(k, j^{(\pm)}, m; \mathbf{r}, t) = \begin{pmatrix} a^{(\pm)} Y^{(m-\frac{1}{2})}_{j\pm\frac{1}{2}} \\ b^{(\pm)} Y^{(m+\frac{1}{2})}_{j\pm\frac{1}{2}} \\ ic^{(\pm)} Y^{(m-\frac{1}{2})}_{j\mp\frac{1}{2}} \\ id^{(\pm)} Y^{(m+\frac{1}{2})}_{j\mp\frac{1}{2}} \end{pmatrix} \cdot e^{-i\omega t}. \tag{32}$$

Where two signs occur, only the upper signs or the lower signs must be taken.

The (real) coefficients $a^{(\pm)}, \ldots, d^{(\pm)}$ need not be specified. For what follows it is, however, necessary to notice that

$$a^{(\pm)}(-m) = \mp b^{(\pm)}(m), \qquad c^{(\pm)}(-m) = \pm d^{(\pm)}(m). \tag{33}$$

It follows immediately from $Y_l^{(m)}(-\mathbf{r}) = (-1)^l Y_l^{(m)}(\mathbf{r})$ that

$$u(k, j^{(\pm)}, m; -\mathbf{r}, t) = (-1)^{j\pm\frac{1}{2}} \gamma_4 \, u(k, j^{(\pm)}, m; \mathbf{r}, t), \tag{34}$$

from which it is apparent that, j being a half integer, the solutions with $j^{(+)}$ and $j^{(-)}$ are of different parity.

Antiparticle solutions for $j_z = m$ (which are negative energy solutions

for $j_z = -m$) are given by

$$v(k, j^{(\pm)}, m; \mathbf{r}, t) = (-1)^{m+\frac{1}{2}} \begin{pmatrix} id^{(\pm)} Y_{j\mp\frac{1}{2}}^{(-m-\frac{1}{2})} \\ ic^{(\pm)} Y_{j\mp\frac{1}{2}}^{(-m+\frac{1}{2})} \\ b^{(\pm)} Y_{j\pm\frac{1}{2}}^{(-m-\frac{1}{2})} \\ a^{(\pm)} Y_{j\pm\frac{1}{2}}^{(-m+\frac{1}{2})} \end{pmatrix} \cdot e^{-i\omega t} \tag{35}$$

and are related to the particle solutions by the equation

$$v(k, j^{(\pm)}, m; \mathbf{r}, t) = u^*(k, j^{(\pm)}, m; \mathbf{r}, t)\gamma_2, \tag{36}$$

as is easy to show by using the properties of the spherical harmonics. Eq. (36) is analogous to (27) for the momentum representation.

The analogue of (34) is

$$v(k, j^{(\pm)}, m; -\mathbf{r}, t) = (-1)^{j\mp\frac{1}{2}} \gamma_4 v(k, j^{(\pm)}, m; \mathbf{r}, t). \tag{37}$$

The expansion of the field operators is

$$\psi = \sum [\mathfrak{a}(k, j^{(\pm)}, m)u(k, j^{(\pm)}, m; \mathbf{r}, t) + \mathfrak{b}^*(k, j^{(\pm)}, m)v(k, j^{(\pm)}, m; \mathbf{r}, t)], \tag{38}$$

which defines creation and destruction operators for particles and antiparticles characterized by the quantum numbers $k, j^{(\pm)}, m$.

3.5. TWO-PARTICLE STATES

To construct state vectors for two particles of spin $\frac{1}{2}$, we proceed as in the case of spinless particles. For a particle and an antiparticle in the centre-of-momentum frame, the most general state of definite energy is

$$\int d\Omega_{\mathbf{k}} \phi(\mathbf{k}; s_a s_b)\mathfrak{a}^*(\mathbf{k}, s_a)\mathfrak{b}^*(-\mathbf{k}, s_b) \quad |0), \tag{39}$$

where now it is convenient to use as one-particle states those of given momentum and spin parallel and antiparallel to the z-axis ($s = \pm 1$). The corresponding creation operators are related to the creation operators for spin parallel and antiparallel to the momentum by the formulae

$$\mathfrak{a}^*(\mathbf{k}, 1) = \alpha^* \mathfrak{a}^*(\mathbf{k}, \uparrow) - \beta \mathfrak{a}^*(\mathbf{k}, \downarrow), \tag{40}$$

$$\mathfrak{a}^*(\mathbf{k}, 2) = \beta^* \mathfrak{a}^*(\mathbf{k}, \uparrow) + \alpha \mathfrak{a}^*(\mathbf{k}, \downarrow) \tag{41}$$

(non-relativistic).

The magnitude of the total spin $\mathbf{S} = \mathbf{s}_a + \mathbf{s}_b$ of the particle-antiparticle system is a good quantum number, so that we have triplet and singlet states.

For the singlet states, the orbital angular momentum L is also a good quantum number. For the triplet, orbital angular momenta are mixed to form ${}^3P_0$, ${}^3S_1 + {}^3D_1$, ${}^3P_1$, ${}^3P_2 + {}^3F_2$, ${}^3D_2$ etc. states. (The subscript denotes the total angular momentum J.) In both cases, the momentum wave function has the property

$$\phi(-\mathbf{k}, s_a s_b) = (-1)^L \phi(\mathbf{k}, s_a a_b), \tag{42}$$

which holds also for mixtures such as ${}^3S_1 + {}^3D_1$, since the orbital angular

momenta of the two components differ by 2. On the other hand, for interchange of s_a and s_b, $\phi(\mathbf{k}, s_a s_b)$ is symmetrical for the triplet, antisymmetrical for the singlet. The non-relativistic expressions

$$Y_L^{(M)}\left[\delta_{s_a,1}\,\delta_{s_b,1},\ \frac{\delta_{s_a,1}\,\delta_{s_b,-1}+\delta_{s_a,-1}\,\delta_{s_b,1}}{\sqrt{2}},\ \delta_{s_a,-1}\,\delta_{s_b,-1}\right] \tag{43}$$

$$Y_L^{(M)}\,\frac{\delta_{s_a,1}\,\delta_{s_b,-1}-\delta_{s_a,-1}\,\delta_{s_b,1}}{\sqrt{2}} \tag{44}$$

for the triplet (no mixture) and the singlet satisfy these general conditions.

4. Photons [11])

4.1. POLARIZATION STATES

For a photon of momentum $\mathbf{k}$ two independent polarization states are possible, from which states with any other polarization can be constructed by linear combination. They are represented by the unit vectors $\mathbf{e}(\mathbf{k}, \lambda)$ ($\lambda = 1, 2$) perpendicular to $\mathbf{k}$ and to each other. Creation and destruction operators $\mathfrak{a}^*(\mathbf{k}, \lambda)$ and $\mathfrak{a}(\mathbf{k}, \lambda)$ can be defined, so that

$$\mathfrak{a}^*(\mathbf{k}, \lambda)\,|0) \tag{45}$$

is a state with a photon of momentum $\mathbf{k}$ and polarization λ.

The field operator is the vector potential, which can be represented as

$$\mathbf{A}(x) = \sum \mathbf{e}(\mathbf{k}, \lambda)\,[\mathfrak{a}(\mathbf{k}, \lambda)e^{i(k,x)}+\mathfrak{a}^*(\mathbf{k}, \lambda)e^{-i(k,x)}], \tag{46}$$

where

$$\sum \equiv \sum_{\mathbf{k}} \sum_{\lambda} \frac{1}{\sqrt{2Vk_0}} \text{ and } k_0 = |\mathbf{k}|.$$

Consider now the simple case of two classical waves both circularly polarized. The first,

$$\begin{aligned} A_x^{(R)} &= A_0 \cos\,(kz-k_0t+\delta^R), \\ A_y^{(R)} &= A_0 \sin\,(kz-k_0t+\delta^R) \end{aligned} \tag{47}$$

propagates with wave length $2\pi k$ in the z-direction and has right-circular polarization, and

$$\begin{aligned} A_x^{(L)} &= A_0\,\cos\,(kz-k_0t+\delta^L), \\ A_y^{(L)} &= -A_0 \sin\,(kz-k_0t+\delta^L) \end{aligned} \tag{48}$$

has left-circular polarization and propagates in the same direction as the first.

We compare (47) and (48) with the vector potentials for two waves both propagating in the z-direction, one

$$\mathbf{A}^{(1)} = A_0\,\mathbf{e}(1)e^{i(kz-k_0t)}+\text{c.c.} \tag{49}$$

with $\mathbf{e}(1) \equiv (1, 0, 0)$, polarized in the x-direction, the other,

$$\mathbf{A}^{(2)} = A_0 \mathbf{e}(2) e^{i(kz - k_0 t)} + \text{c.c.} \tag{50}$$

with $\mathbf{e}(2) \equiv (0, 1, 0)$, polarized in the y-direction. We can now write

$$\mathbf{A}^{(R)} = \frac{A_0}{\sqrt{2}} \mathbf{e}(R) e^{i(kz - k_0 t + \delta^R)} + \text{c.c.} \tag{51}$$

and

$$\mathbf{A}^{(L)} = \frac{A_0}{\sqrt{2}} \mathbf{e}(L) e^{i(kz - k_0 t + \delta^L)} + \text{c.c.} \tag{52}$$

Here

$$\mathbf{e}(R) = \frac{\mathbf{e}(1) - i\mathbf{e}(2)}{\sqrt{2}}, \qquad \mathbf{e}(L) = \frac{\mathbf{e}(1) + i\mathbf{e}(2)}{\sqrt{2}} \tag{53}$$

and

$$\mathbf{e}^*(R) \cdot \mathbf{e}(R) = \mathbf{e}^*(L) \cdot \mathbf{e}(L) = 1.$$

We can now proceed to define circularly polarized photons. We introduce

$$a(\mathbf{k}, R) = \frac{1}{\sqrt{2}} [a(\mathbf{k}, 1) + i a(\mathbf{k}, 2)] \tag{54}$$

as the destruction operator for a right-circular photon of momentum $\mathbf{k}$ and polarization vector

$$\mathbf{e}(\mathbf{k}, R) = \frac{1}{\sqrt{2}} [\mathbf{e}(\mathbf{k}, 1) - i\mathbf{e}(\mathbf{k}, 2)], \tag{55}$$

and

$$a(\mathbf{k}, L) = \frac{1}{\sqrt{2}} [a(\mathbf{k}, 1) - i a(\mathbf{k}, 2)] \tag{56}$$

and

$$\mathbf{e}(\mathbf{k}, L) = \frac{1}{\sqrt{2}} [\mathbf{e}(\mathbf{k}, 1) + i\mathbf{e}(\mathbf{k}, 2)] \tag{57}$$

for left-circular photons. Then the right member in the expression (46) for the vector potential can be rearranged to read

$$\mathbf{A}(x) = \sum \{ [\mathbf{e}(\mathbf{k}, R) a(\mathbf{k}, R) + \mathbf{e}(\mathbf{k}, L) a(\mathbf{k}, L)] e^{i(k,x)} + [\mathbf{e}^*(\mathbf{k}, R) a^*(\mathbf{k}, R) + \mathbf{e}^*(\mathbf{k}, L) a^*(\mathbf{k}, L)] e^{-i(k,x)} \}. \tag{58}$$

States with one circularly polarized photon of momentum $\mathbf{k}$ will be given by

$$a^*(\mathbf{k}, R) |0) \quad \text{and} \quad a^*(\mathbf{k}, L) |0)$$

according to whether the polarization is right or left. By eqs. (54) and (56) they can be expressed as superpositions of states with linear polarization.

4.2. TWO-PHOTON STATES

Later on, in connection with the selection rules for positronium decay, we shall have to consider states with two photons of equal

and opposite momenta. For simplicity we shall assume that the momenta are along the z-axis, and denote by $a^*(+, R)$, $a^*(-, R)$, $a^*(+, L)$, $a^*(-, L)$ the creation operators for photons with right- and left-circular polarization, travelling in the positive $(+)$ and negative $(-)$ z-direction.

By applying to the vacuum state the product of two of the above operators we can construct the four states $|+R, -R)$, $|+L, -L)$, $|+R, -L)$, $|+L, -R)$. It is convenient, however, to consider mixtures of the first two:

$$\begin{aligned} |+R, -R)+|+L, -L) &= [a^*(+, R)a^*(-, R)+a^*(+, L)a^*(-, L)]\,|0) \\ &= [a^*(+, 1)a^*(-, 1)-a^*(+, 2)a^*(-, 2)]\,|0), \qquad (59) \\ |+R, -R)-|+L, -L) &= -i[a^*(+, 1)a^*(-, 2)+a^*(+, 2)a^*(-, 1)]\,|0). \end{aligned}$$

The first represents two photons travelling in opposite directions with planes of polarization always parallel. There is an equal chance that the planes of polarization are either both in the x-direction or both in the y-direction. The second represents the state of two photons having planes of polarization always perpendicular to one another. On the other hand

$$\begin{aligned} |+R, -L) &= \tfrac{1}{2}[a^*(+, 1)a^*(-, 1)+a^*(+, 2)a^*(-, 2) \\ &\qquad +ia^*(+, 1)a^*(-, 2)-ia^*(+, 2)a^*(-, 1)]\,|0), \\ |+L, -R) &= \tfrac{1}{2}[a^*(+, 1)a^*(-, 1)+a^*(+, 2)a^*(-, 2) \\ &\qquad -ia^*(+, 1)a^*(-, 2)+ia^*(+, 2)a^*(-, 1)]\,|0) \end{aligned} \qquad (60)$$

are states where there is an equal chance that the planes of polarization are parallel or perpendicular to one another.

4.21. TRANSFORMATION PROPERTIES OF PHOTON STATES

We cannot dispense with a few remarks about transformation properties of photons under space rotations, later to be used for deriving selection rules for the decay of particles into two photons.

A rotation by the angle ϕ around the z-axis

$$\begin{aligned} x' &= x\cos\phi + y\sin\phi, \\ y' &= -x\sin\phi + y\cos\phi, \qquad (61) \\ z' &= z \end{aligned}$$

transforms the classical vector potential as

$$\begin{aligned} A'_x &= A_x\cos\phi + A_y\sin\phi, \\ A'_y &= -A_x\sin\phi + A_y\cos\phi, \qquad (62) \\ A'_z &= A_z. \end{aligned}$$

In the quantized theory the rotation is associated with a unitary operator R_ϕ such that

$$R_\phi A R_\phi^{-1} = A' \qquad (63)$$

is the transformation law for the vector potential operator, $\mathbf{A}'$ being expressed in terms of $\mathbf{A}$ through (62). In order to determine R_ϕ we consider one typical term in the expansion (58). According to (61) and (62) the polarization vectors $\mathbf{e}(\mathbf{k}, R)$ and $\mathbf{e}(\mathbf{k}, L)$ transform as †

$$\begin{aligned} \mathbf{e}'(\mathbf{k}, R) &= e^{-i\phi} \cdot \mathbf{e}(\mathbf{k}, R), \\ \mathbf{e}'(\mathbf{k}, L) &= e^{i\phi} \cdot \mathbf{e}(\mathbf{k}, L), \end{aligned} \tag{64}$$

if $\mathbf{k}$ is in the z-direction. For (63) to be realized we must have

$$R_\phi[\mathbf{e}(\mathbf{k}, R)\mathbf{a}(\mathbf{k}, R)]R_\phi^{-1} = \mathbf{e}'(\mathbf{k}, R)\mathbf{a}(\mathbf{k}, R) \tag{65}$$

and similarly for left polarization, and therefore

$$\begin{aligned} R_\phi\, \mathbf{a}(\mathbf{k}, R)R_\phi^{-1} &= e^{-i\phi} \cdot \mathbf{a}(\mathbf{k}, R), \\ R_\phi\, \mathbf{a}(\mathbf{k}, L)R_\phi^{-1} &= e^{i\phi} \cdot \mathbf{a}(\mathbf{k}, L). \end{aligned} \tag{66}$$

For the creation operators we have

$$\begin{aligned} R_\phi\, \mathbf{a}^*(\mathbf{k}, R)R_\phi^{-1} &= e^{i\phi} \cdot \mathbf{a}^*(\mathbf{k}, R) \\ R_\phi\, \mathbf{a}^*(\mathbf{k}, L)R_\phi^{-1} &= e^{-i\phi} \cdot \mathbf{a}^*(\mathbf{k}, L). \end{aligned} \tag{67}$$

We now apply R_ϕ to states with one and two photons. For instance

$$R_\phi\, \mathbf{a}^*(\mathbf{k}, R)\,|0) = R_\phi\, \mathbf{a}^*(\mathbf{k}, R)R_\phi^{-1} \cdot R_\phi\,|0). \tag{68}$$

If we assume that the vacuum is invariant under rotations,

$$R_\phi\,|0) = |0), \tag{69}$$

comparing (68) with (67) we find

$$R_\phi\, \mathbf{a}^*(\mathbf{k}, R)\,|0) = e^{i\phi} \cdot \mathbf{a}^*(\mathbf{k}, R)\,|0) \tag{70}$$

and similarly

$$R_\phi\, \mathbf{a}^*(\mathbf{k}, L)\,|0) = e^{-i\phi} \cdot \mathbf{a}^*(\mathbf{k}, L)\,|0). \tag{71}$$

Thus states with one right or left circularly polarized photon moving along the z-axis are eigenstates of R_ϕ with eigenvalues $e^{-i\phi}$ and $e^{+i\phi}$ respectively. It is useful to remind the reader of the connection between the angular momentum component in a certain direction, say z, and the operator R_ϕ for rotations around that direction,

$$J_z = \frac{1}{i}\left(\frac{dR_\phi}{d\phi}\right)_{\phi=0}. \tag{72}$$

It is apparent from this formula and from (70), (71) that $\mathbf{a}^*(\mathbf{k}, R)\,|0)$ and $\mathbf{a}^*(\mathbf{k}, L)\,|0)$ are photons with $J_z = \pm 1$ respectively.

The discussion of two photon states follows similar lines. We have

$$R_\phi\{|+R, -R) \pm |+L, -L)\} = |+R, -R) \pm |+L, -L) \tag{73}$$

$$R_\phi|+R, -L) = e^{2i\phi}|+R, -L), \tag{73'}$$

$$R_\phi|+L, -R) = e^{-2i\phi}|+L, -R). \tag{73''}$$

† The exponentials $e^{\pm i(k, x)}$ are invariant under rotations.

Thus the states $|+R, -R)\pm|+L, -L)$, which are eigenstates of R_ϕ with eigenvalue 1, are also eigenstates of J_z with eigenvalue $J_z = 0$. On the other hand, $|+R, -L)$ and $|+L, -R)$ correspond to $J_z = \pm 2$.

The operator R_ξ for rotations around the x-axis through 180°, $x' = x$, $y' = -y$, $z' = -z$ will also be employed in Ch. II. We leave it to the reader to show that the states $|+R, -R)\pm|+L, -L)$ are both eigenstates of R_ξ with the eigenvalue $+1$.

5. Particles of spin 1 [9])

The formalism for the description of neutral particles of spin 1 is an extension of that for photons. In the expansion (46), $\sum$ must be taken to mean $\sum_{\mathbf{k}} \sum_{\lambda=1,2,3} (2Vk_0)^{-\frac{1}{2}}$, with $k_0 = (\mathbf{k}^2+\mu^2)^{\frac{1}{2}}$, μ being the particle mass; the additional polarization $\lambda = 3$, with a polarization vector $\mathbf{e}(\mathbf{k}, 3)$ which is parallel to the momentum $\mathbf{k}$, goes by the name of longitudinal polarization, and the particles described by the corresponding creation and destruction operators $\mathfrak{a}^*(\mathbf{k}, 3)$ and $\mathfrak{a}(\mathbf{k}, 3)$ are sometimes called longitudinal particles. Their spin component in the direction of $\mathbf{k}$ is zero. On the other hand, the transversal particles with $\lambda = 1, 2$ can exist in states of circular polarization, with complex polarization vectors (55) and (57) and corresponding destruction operators (54) and (56). The two modes of circular polarization correspond to spin parallel and antiparallel to $\mathbf{k}$, as in the case of photons.

Charged particles of spin 1 are described by the modified version of the formalism of section 4 just outlined, with $\mathfrak{a}^*(\mathbf{k}, \lambda)$ replaced by $\mathfrak{b}^*(\mathbf{k}, \lambda)$ in eq. (46) and in the remaining ones. The field operator $\mathbf{A}(x)$ is no longer Hermitian.

We finally remark that the fourth component of the field operator, $A_0(x)$, does not need to be specified in either the photon or the spin 1 particle case. We must only require that whatever transformation properties we may assign to it in the following, these must be consistent with the condition

$$\frac{\partial A_\mu}{\partial x_\mu} = \operatorname{div} \mathbf{A} + \frac{\partial A_0}{\partial t} = 0, \tag{74}$$

which is an operator identity for spin 1 particles, and a subsidiary condition for photons.

6. The Electron-Photon-Nucleon-π-Meson System

Let the electron field be described by the four-component operator ψ, the photon field by A_μ, the nucleon field by the eight-component operator $\Psi = \begin{pmatrix}\psi_n \\ \psi_p\end{pmatrix}$, ψ_p and ψ_n being each four-component operators for the proton and the neutron field respectively, and let $\phi = (1/\sqrt{2})(\phi_1+i\phi_2)$, $\phi^* = (1/\sqrt{2})(\phi_1-i\phi_2)$ describe the charged π-mesons and ϕ_3 the neutral π^0-mesons.

The complete set of interactions within the system is known to be

$$\begin{aligned}\mathscr{L} = &-ie\bar{\psi}\gamma_\mu\psi\cdot\mathsf{A}_\mu+ie\bar{\Psi}\frac{1-\tau_3}{2}\gamma_\mu\Psi\cdot\mathsf{A}_\mu \\ &-ie\left(\phi^*\frac{\partial\phi}{\partial x_\mu}-\phi\frac{\partial\phi^*}{\partial x_\mu}\right)\mathsf{A}_\mu-e^2\mathsf{A}_\mu{}^2\phi^*\phi \\ &-ig\bar{\Psi}\gamma_5\tau_i\Psi\cdot\phi_i-if\bar{\Psi}\gamma_5\gamma_\mu\tau_i\Psi\cdot\frac{\partial\phi_i}{\partial x_\mu} \\ &(\bar{\Psi}=\Psi^*\gamma_4)\end{aligned} \tag{75}$$

with the usual summation convention for the indices $\mu = 1, 2, 3, 4$ and $i = 1, 2, 3$. The matrices τ_1, τ_2, τ_3 are the isobaric spin matrices, identical in form with the spin matrices (16).

The nucleon-meson interaction is dictated by the experimental evidence on nuclear forces and meson scattering and is consistent with the assumption that π-mesons are pseudoscalar particles and that charge independence obtains if the electromagnetic interactions are neglected. This latter is exhibited by the occurrence of the scalar product $\tau_i\phi_i = \boldsymbol{\tau}\cdot\boldsymbol{\phi}$, which is invariant under rotations in the isobaric spin space in which the π-meson components ϕ_1, ϕ_2, ϕ_3 are regarded as the components of a vector †. Charge independence (not to be confused with charge symmetry) causes the total isobaric spin of a nucleus to be a good quantum number if electromagnetic interactions are neglected.

The interactions (75) will be referred to as strong interactions ††.

† This will be shown in detail in Ch. VII.

†† Some authors put the electromagnetic interactions in a class apart.

References to Chapter I

1) J. M. Blatt and V. F. Weisskopf, Theoretical Nuclear Physics (New York, 1952) p. 790
2) P. A. M. Dirac, Proc. Roy. Soc. A **117** (1928) 610
3) J. Hamilton, Proc. Camb. Phil. Soc. **52** (I) (1956) 97
4) H. A. Kramers, Proc. of Amsterdam Academy **40** (1937) 814
5) H. A. Kramers, Hand. u. Jahrb. d. Chem. Physik I (1934) 63, 64
6) E. Majorana, Nuovo Cimento **14** (1937) 171
7) W. Pauli, Handbuch der Physik, Vol. 24/1, pp. 220–227
8) W. Pauli, Ann. Inst. H. Poincaré **6** (1936) 109
9) W. Pauli, Revs. Mod. Phys. **13** (1941) 203
10) R. G. Sachs, Phys. Rev. **87** (1952) 1100
11) C. N. Yang, Phys. Rev. **77** (1950) 242

CHAPTER II

SPACE INVERSION

In this chapter we shall study the effect of the coordinate transformation

$$x' = -x, \qquad y' = -y, \qquad z' = -z \tag{1}$$

on particle states and field operators. This transformation, which is called a space inversion or a space reflection leads from a right-handed system of axes to a left-handed one, and vice versa. It is known to change the sign of all components of polar vectors, such as the momentum, the electric field etc., and to leave unaltered those of axial vectors, such as the angular momentum, the magnetic field, etc..

1. Spinless Particles

The transformation (1) causes the components (k_x, k_y, k_z) of the momentum of a particle to change their sign. Therefore we must expect (1) to correspond to a unitary operator P which transforms the state $\mathsf{c}^*(\mathbf{k})\,|0)$ into the state with one particle of opposite momentum $\mathsf{c}^*(-\mathbf{k})\,|0)$.

In Quantum Mechanics, however, state vectors which differ by a numerical factor of modulus one are to be regarded as equivalent. Thus the definition of P is

$$\mathsf{P}\mathsf{c}^*(\mathbf{k})|0) = \eta_P\,\mathsf{c}^*(-\mathbf{k})\,|0), \tag{2}$$

where η_P is a complex number of modulus one.

One further restriction on η_P results from applying P to the two members of (2). We then obtain

$$\mathsf{P}^2\,\mathsf{c}^*(\mathbf{k})\,|0) = \eta_P\,\mathsf{P}\mathsf{c}^*(-\mathbf{k})\,|0) = \eta_P{}^2\,\mathsf{c}^*(\mathbf{k})\,|0), \tag{3}$$

and, since two successive applications of (1) merely re-establish the initial coordinate system, $\mathsf{P}^2 = 1$ †, and therefore $\eta_P{}^2 = 1$, $\eta_P = \pm 1$.

Particles which obey (2) with $\eta_P = +1$ are called scalar, those with $\eta_P = -1$ pseudoscalar.

We assume that the vacuum is scalar, i.e.

$$\mathsf{P}|0) = |0). \tag{4}$$

Then (2) can be written

$$\mathsf{P}\mathsf{c}^*(\mathbf{k})\mathsf{P}^{-1}\mathsf{P}\,|0) = \mathsf{P}\mathsf{c}^*(\mathbf{k})\mathsf{P}^{-1}\,|0) = \eta_P\,\mathsf{c}^*(-\mathbf{k})\,|0). \tag{5}$$

From this and similar relations for states with any number of particles, the transformation properties of the creation and destruction operators can be derived. For spinless neutral particles

† Thus $\mathsf{P} = \mathsf{P}^{-1} = \mathsf{P}^*$, and P is Hermitian.

$$\mathsf{P}c^*(\mathbf{k})\mathsf{P}^{-1} = \eta_P\, c^*(-\mathbf{k}), \qquad \mathsf{P}c(\mathbf{k})\mathsf{P}^{-1} = \eta_P\, c(-\mathbf{k}), \tag{6}$$

and for spinless charged particles

$$\mathsf{P}a^*(\mathbf{k})\mathsf{P}^{-1} = \eta_P\, a^*(-\mathbf{k}), \qquad \mathsf{P}a(\mathbf{k})\mathsf{P}^{-1} = \eta_P a(-\mathbf{k}), \tag{6a}$$

$$\mathsf{P}b^*(\mathbf{k})\mathsf{P}^{-1} = \eta_P\, b^*(-\mathbf{k}), \qquad \mathsf{P}b(\mathbf{k})\mathsf{P}^{-1} = \eta_P\, b(-\mathbf{k}). \tag{6b}$$

Each type of particle is characterized by a certain η_P. Thus the η_P in (6) may, of course, be different from that appearing in (6a) and in (6b). Nevertheless, η_P in (6a) must be equal to that in (6b) if a^*, b^*, a, b are creation and destruction operators for positive and negative particles of the same field. Another thing to note is that, as seen from (6a) and (6b), the operator P does not mix particles and antiparticles. As concerns space inversions, there is no essential difference between neutral and charged particles.

Let us now consider the transformation induced by P in the field operator $\phi(\mathbf{r}, t)$. We have

$$\begin{aligned}\mathsf{P}\phi(\mathbf{r}, t)\mathsf{P}^{-1} &= \sum[\mathsf{P}a(\mathbf{k})\mathsf{P}^{-1}\, e^{i(k,x)} + \mathsf{P}b^*(\mathbf{k})\mathsf{P}^{-1}\, e^{-i(k,x)}] \\ &= \eta_P \sum [a(-\mathbf{k})e^{i(k,x)} + b^*(-\mathbf{k})e^{-i(k,x)}], \end{aligned} \tag{7}$$

and, changing the summation variable from $\mathbf{k}$ to $\mathbf{k}' = -\mathbf{k}$, and writing $\mathbf{r}$ in terms of the new coordinates as $\mathbf{r} = -\mathbf{r}'$, we find, since $(k, x) = \mathbf{k}\cdot\mathbf{r} - \omega t = \mathbf{k}'\cdot\mathbf{r}' - \omega t$,

$$\mathsf{P}\phi(\mathbf{r}, t)\mathsf{P}^{-1} = \eta_P\, \phi(\mathbf{r}', t), \tag{8}$$

which is the transformation law for fields of spinless particles. The transformed field operator is obtained by writing $\mathbf{r}'$ instead of $\mathbf{r}$ and by multiplying by $\eta_P = +1$ if the field is scalar, by $\eta_P = -1$ if the field is pseudoscalar.

A word must be said about the eigenstates of P. Clearly, a state with one particle of non-zero momentum $\mathbf{k}$ is not an eigenstate of P, since P changes it into an altogether different state. If, however, $\mathbf{k} = 0$ we have

$$\mathsf{P}a^*(0)\,|0) = \eta_P\, a^*(0)\,|0), \tag{9}$$

so that a state with one spinless particle at rest is an eigenstate of P with eigenvalue η_P. This justifies calling η_P the intrinsic P-parity of the particle in question [10]). In general, a state with any number of spinless particles at rest, e.g. $a^*(0)b^*(0)\ldots|0)$, is an eigenstate of P with an eigenvalue which is the product of the individual intrinsic parities η_P, e.g. $(-1)^n$ if there are n pseudoscalar particles.

Let us now consider states with particles of definite orbital angular momentum. Inserting in (8) the expression (I, 6) of the field operator in the angular momentum representation, and recalling that, if (θ, ϕ) are the polar angles of $\mathbf{r}$ those of $\mathbf{r}' = -\mathbf{r}$ will be $(\pi-\theta, \pi+\phi)$ and therefore $Y_l^{(m)}(\mathbf{r}) = (-1)^l Y_l^{(m)}(\mathbf{r}')$ we find, writing $t = 0$ for brevity,

$$\sum_{klm} [\mathsf{P}a(k, l, m)\mathsf{P}^{-1} Y_l^{(m)}(\theta, \phi) + \mathsf{P}b^*(k, l, m)\mathsf{P}^{-1} Y_l^{(m)*}(\theta, \phi)]$$
$$= \eta_P \sum_{klm} (-1)^l [a(k, l, m) Y_l^{(m)}(\theta, \phi) + b^*(k, l, m) Y_l^{(m)*}(\theta, \phi)]. \quad (10)$$

We infer that

$$\mathsf{P}a(k, l, m)\mathsf{P}^{-1} = \eta_P(-1)^l a(k, l, m),$$
$$\mathsf{P}a^*(k, l, m)\mathsf{P}^{-1} = \eta_P(-1)^l a^*(k, l, m), \text{ etc.}, \quad (11)$$

so that for a particle (or antiparticle) state we have

$$\mathsf{P}a^*(k, l, m)\,|0) = \eta_P(-1)^l a^*(k, l, m)\,|0). \quad (12)$$

Thus states with one particle (or antiparticle) of definite angular momentum are eigenstates of the space inversion operator P with eigenvalues $\eta_P(-1)^l$. That this should be so is evident from the fact that the angular momentum is an axial vector whose components are left unchanged by the transformation (1).

We finally mention the case of two spinless particles of intrinsic parities η_{P_1} and η_{P_2}, forming a system of relative angular momentum (L, M) in the centre-of-momentum frame. The corresponding state vector is

$$|k, L, M) = \int d\Omega_{\mathbf{k}}\, Y_L^{(M)}(\mathbf{k}) c_1^*(\mathbf{k}) c_2^*(-\mathbf{k})\,|0) \quad (13)$$

according to eq. (I, 11). Now

$$\mathsf{P}|k, L, M) = \int d\Omega_{\mathbf{k}}\, Y_L^{(M)}(\mathbf{k}) \eta_{P_1}\eta_{P_2} c_1^*(-\mathbf{k}) c_2^*(\mathbf{k})\,|0)$$
$$= \eta_{P_1}\eta_{P_2}(-1)^L |k, L, M), \quad (14)$$

as follows by changing $\mathbf{k}$ into $-\mathbf{k}$ in the integral and remembering once more the properties of the spherical harmonics. The result (14) holds for any two spinless particles, irrespective of their charge.

2. Particles of spin $\frac{1}{2}$

A space inversion transforms a particle of momentum $\mathbf{k}$ into one of momentum $-\mathbf{k}$, while leaving the spin direction unchanged. If $a^*(\mathbf{k}, \lambda)$ and $b^*(\mathbf{k}, \lambda)$ are creation operators for particles and antiparticles of the same field, the correct transformation is

$$\mathsf{P}a^*(\mathbf{k}, \lambda)\,|0) = \eta_P^*\, a^*(-\mathbf{k}, \lambda')\,|0),$$
$$\mathsf{P}b^*(\mathbf{k}, \lambda)\,|0) = \eta_P\, b^*(-\mathbf{k}, \lambda')\,|0), \quad (15)$$

with $\lambda' \neq \lambda$. It is worth remembering that $a^*(\mathbf{k}, \uparrow)$ is the creation operator for a particle of momentum $\mathbf{k}$ and spin parallel to $\mathbf{k}$, and $a^*(\mathbf{k}, \downarrow)$ that for a particle of momentum $\mathbf{k}$ and spin antiparallel to $\mathbf{k}$. Similarly $a^*(-\mathbf{k}, \uparrow)$ refers to a particle of momentum $-\mathbf{k}$ and spin parallel to $-\mathbf{k}$ (i.e. antiparallel to $\mathbf{k}$) and $a^*(-\mathbf{k}, \downarrow)$ to a particle of momentum $-\mathbf{k}$ and spin antiparallel to $-\mathbf{k}$ (i.e. parallel to $\mathbf{k}$). The notation being thus clarified, we proceed to

notice that we have anticipated the possibility that the intrinsic parity factor η_P may be complex. This is necessary, because two successive applications of P reproduce the original state up to a factor ± 1. In fact the states of particles of spin $\frac{1}{2}$ are two-valued, since a rotation of 360° around any axis reproduces the original state multiplied by -1. Therefore $\mathsf{P}^4 = 1$, $\eta_P{}^4 = 1$, $\eta_P = (\pm 1, \pm i)$ [6, 12]).

The right members of eqs. (15) must one contain $\eta_P{}^*$ and the other η_P, if the field operator $\psi(x)$ is to have definite transformation properties for space inversions. Thus we must have

$$\begin{aligned} \mathsf{P}a^*(\mathbf{k},\lambda)\mathsf{P}^{-1} &= \eta_P{}^*\, a^*(-\mathbf{k},\lambda'), \\ \mathsf{P}a(\mathbf{k},\lambda)\mathsf{P}^{-1} &= \eta_P\, a(-\mathbf{k},\lambda'), \\ \mathsf{P}b^*(\mathbf{k},\lambda)\mathsf{P}^{-1} &= \eta_P\, b^*(-\mathbf{k},\lambda'), \\ \mathsf{P}b(\mathbf{k},\lambda)\mathsf{P}^{-1} &= \eta_P{}^*\, b(-\mathbf{k},\lambda'). \end{aligned} \qquad (\lambda' \neq \lambda) \quad (16)$$

The transformation properties of the creation operators $a^*(\mathbf{k}, s)$ ($s = \pm 1$ meaning $s_z = \pm\frac{1}{2}$) can be found by comparing (16) with (I, 40). We find for instance

$$\begin{aligned} \mathsf{P}a^*(\mathbf{k},s)\mathsf{P}^{-1} &= i\eta_P{}^*\, a^*(-\mathbf{k},s), \\ \mathsf{P}b^*(\mathbf{k},s)\mathsf{P}^{-1} &= i\eta_P\, b^*(-\mathbf{k},s), \end{aligned}$$

where the spin index is now the same in the two members. In fact, the spin orientation is referred to the z-axis, whereas in (16) is referred to the direction of the momentum.

Applying the P transformation to the field operator $\psi(x)$ (I, 12) for the Pauli set of γ-matrices, we obtain

$$\begin{aligned} \mathsf{P}\psi(\mathbf{r},t)\mathsf{P}^{-1} = \eta_P \sum \{ &[u(\mathbf{k},\uparrow)a(-\mathbf{k},\downarrow) + u(\mathbf{k},\downarrow)a(-\mathbf{k},\uparrow)]\, e^{i(k,x)} \\ &+ [v(\mathbf{k},\uparrow)b^*(-\mathbf{k},\downarrow) + v(\mathbf{k},\downarrow)b^*(-\mathbf{k},\uparrow)]\, e^{-i(k,x)}\}. \end{aligned} \quad (17)$$

However,

$$u(-\mathbf{k},\lambda) = i\gamma_4\, u(\mathbf{k},\lambda') \text{ and } v(-\mathbf{k},\lambda) = i\gamma_4\, v(\mathbf{k},\lambda'), \qquad (\lambda' \neq \lambda) \quad (18)$$

which can easily be derived by noticing that, when the direction of $\mathbf{k}$ is reversed, the polar angles (θ, ϕ) become $(\pi-\theta, \pi+\phi)$ so that α and β defined in (I, 21) become equal to $-i\beta^*$ and $i\alpha^*$ respectively. It is then easy to show that the two first columns of tables 1 and 2 satisfy eq. (18) with $\gamma_4 = \rho_z \times I$. By inserting (18) in (17) and changing $\mathbf{k}$ into $-\mathbf{k}$ in the summation we finally find

$$\mathsf{P}\psi(\mathbf{r},t)\mathsf{P}^{-1} = i\eta_P\, \gamma_4\, \psi(\mathbf{r}',t) \qquad (19)$$

with $\mathbf{r}' = -\mathbf{r}$.

Similarly

$$\mathsf{P}\bar{\psi}(\mathbf{r},t)\mathsf{P}^{-1} = -i\eta_P{}^*\, \bar{\psi}(\mathbf{r}',t)\gamma_4 \qquad (19')$$

with $\bar{\psi} = \psi^*\gamma_4$. These transformations (with γ_4 replaced by γ'_4 and γ''_4) hold also for the Kramers and for the Majorana sets of γ's.

Only the $\eta_P = \pm 1$ intrinsic parities are allowed for the Majorana particles described in Ch. I, subsection 3.3. In fact. working with Majorana matrices γ''_μ for which the elements of $i\gamma''_4$ are all real, we see that only for $\eta_P = \pm 1$ are the components of the transformed field operator $\mathsf{P}\psi''(\mathbf{r}, t)\mathsf{P}^{-1}$ Hermitian if those of ψ'' are so, which is necessary for the consistency of the theory.

In the angular momentum representation, comparing eq. (19) with (I, 38) and (I, 34), (I, 37) we find

$$\begin{aligned} \mathsf{P}a(k, j^{(\pm)}, m)\mathsf{P}^{-1} &= i\eta_P(-1)^{j\pm\frac{1}{2}}\, a(k, j^{(\pm)}, m), \\ \mathsf{P}b^*(k, j^{(\pm)}, m)\mathsf{P}^{-1} &= i\eta_P(-1)^{j\mp\frac{1}{2}}\, b^*(k, j^{(\pm)}, m), \text{ etc.} \end{aligned} \tag{20}$$

so that one particle and one antiparticle states are eigenstates of P with eigenvalues $i\eta_P^*(-1)^{j\mp\frac{1}{2}}$ and $i\eta_P(-1)^{j\mp\frac{1}{2}}$, respectively,

$$\mathsf{P}a^*(k, j^{(\pm)}, m)\,|0) = i\eta_P^*(-1)^{j\mp\frac{1}{2}}\, a^*(k, j^{(\pm)}, m)\,|0), \tag{21}$$

$$\mathsf{P}b^*(k, j^{(\pm)}, m)\,|0) = i\eta_P(-1)^{j\mp\frac{1}{2}}\, b^*(k, j^{(\pm)}, m)\,|0). \tag{21'}$$

For Majorana particles ($\eta_P = \eta_P^*$) the two eigenvalues are equal, as should be.

For electrons η_P is imaginary. Writing $\eta_{P_e} = \varepsilon i$ with $\varepsilon = \pm 1$, and recalling that $j^{(\pm)} = l \mp \frac{1}{2}$, we find from (21) that for orbital angular momentum l the parity of a negaton is $-\varepsilon(-1)^l$ and that of a positon $+\varepsilon(-1)^l$.

2.1. TRANSFORMATION PROPERTIES OF BILINEAR FORMS OF SPIN $\frac{1}{2}$ FIELDS

Let ψ_1 and ψ_2 be two fields of particles of spin $\frac{1}{2}$. The following bilinear forms

$$\bar{\psi}_1 O_1 \psi_2 \qquad (\mathrm{i} = \mathrm{S, V, T, A, P}) \tag{22}$$

with the Hermitian matrices O_1 given by

$$\begin{aligned} &O_\mathrm{S} = 1, \qquad O_\mathrm{V} = \gamma_\mu, \qquad O_\mathrm{T} = -\frac{i}{2\sqrt{2}}(\gamma_\lambda\gamma_\mu - \gamma_\mu\gamma_\lambda) \\ &O_\mathrm{A} = -i\gamma_\mu\gamma_5, \qquad O_\mathrm{P} = \gamma_5 \end{aligned} \tag{23}$$

occur in many important interactions. They transform under space inversions as

$$\mathsf{P}\bar{\psi}_1 O_1 \psi_2 \mathsf{P}^{-1} = \eta_{P_1}^*\eta_{P_2}\varepsilon_{P,1}\bar{\psi}_1 O_1 \psi_2 \tag{24}$$

with

i =	S	V	T	A	P
$\varepsilon_{P,1} =$	1	$-1(\mu = 1, 2, 3)$ $+1(\mu = 4)$	$+1(\lambda, \mu = 1, 2, 3)$ $-1(\lambda = 4 \text{ or } \mu = 4)$	$+1(\mu = 1, 2, 3)$ $-1(\mu = 4)$	-1

(25)

as can be shown by using eqs. (19) and (19') and the anticommutation relations of the γ's (I, 14).

Since the O_1 are Hermitian

$$
\begin{aligned}
(\bar{\psi}_1 O_1 \psi_2)^* &= (\psi^*_{1\alpha}\gamma_{4,\alpha\beta} O_{1,\beta\gamma}\psi_{2\gamma})^* \\
&= \psi^*_{2\gamma}\gamma^*_{4,\alpha\beta} O^*_{1,\beta\gamma}\psi_{1\alpha} = \psi^*_{2\gamma} O_{1,\gamma\beta}\gamma_{4,\beta\alpha}\psi_{1\alpha} \\
&= \psi_2{}^* O_1 \gamma_4 \psi_1 = \zeta_1 \bar{\psi}_2 O_1 \psi_1,
\end{aligned} \tag{26}
$$

with $\zeta_1 = \varepsilon_{P,1}$.

On the other hand

$$
\mathsf{P}\bar{\psi}_1 O_1 \gamma_5 \psi_2 \mathsf{P}^{-1} = -\eta^*_{P_1}\eta_{P_2}\varepsilon_{P,1}\bar{\psi}_1 O_1 \gamma_5 \psi_2, \tag{27}
$$

but

$$
(\bar{\psi}_1 O_1 \gamma_5 \psi_2)^* = \psi_2{}^* \gamma_5 O_1 \gamma_4 \psi_1 = \xi_1 \bar{\psi}_2 O_1 \gamma_5 \psi_1 \tag{28}
$$

with

i =	S	V	T	A	P
$\xi_1 =$	-1	$-1(\mu = 1, 2, 3)$ $+1(\mu = 4)$	$-1(\lambda, \mu = 1, 2, 3)$ $+1(\lambda = 4$ or $\mu = 4)$	$+1(\mu = 1, 2, 3)$ $-1(\mu = 4)$	$+1$

(29)

2.2. PARITY OF A SYSTEM OF A PARTICLE AND AN ANTIPARTICLE OF SPIN $\frac{1}{2}$ (POSITONIUM; NUCLEON-ANTINUCLEON PAIR)

The state (I, 39) with $\phi(\mathbf{k}, s_a s_b)$ restricted by (I, 42) is an eigenstate of P. In fact

$$
\begin{aligned}
&\mathsf{P}\int d\Omega_{\mathbf{k}}\phi(\mathbf{k}, s_a s_b)\mathfrak{a}^*(\mathbf{k}, s_a)\mathfrak{b}^*(-\mathbf{k}, s_b)\,|0) \\
&\qquad = -\int d\Omega_{\mathbf{k}}\phi(\mathbf{k}, s_a s_b)\mathfrak{a}^*(-\mathbf{k}, s_a)\mathfrak{b}^*(+\mathbf{k}, s_b)\,|0) \\
&\qquad = -\int d\Omega_{\mathbf{k}}\phi(-\mathbf{k}, s_a s_b)\mathfrak{a}^*(\mathbf{k}, s_a)\mathfrak{b}^*(-\mathbf{k}, s_b)\,|0),
\end{aligned} \tag{30}
$$

so that both the triplet and the singlet are eigenstates of P with the eigenvalue

$$
P' = (-1)^{L+1} \qquad \text{(triplet and singlet)}.
$$

3. Photons

We start from the remark that, under the coordinate transformation (1), a right-circular polarized wave propagating in the z-direction,

$$
\begin{aligned}
A_x^{(\mathrm{R})} &= A_0 \cos\,(kz - k_0 t + \delta), \\
A_y^{(\mathrm{R})} &= A_0 \sin\,(kz - k_0 t + \delta),
\end{aligned} \tag{31}
$$

becomes

$$
\begin{aligned}
A_{x'} &= -A_0 \cos\,(-kz' - k_0 t + \delta) \\
A_{y'} &= -A_0 \sin\,(-kz' - k_0 t + \delta)
\end{aligned} \tag{32}
$$

i.e., a left-circular polarized wave propagating in the $-z'$-direction. The four possible states of circular polarization and propagation in the positive or negative z-direction are transformed by P as

$$
\begin{aligned}
&\mathsf{P}|+, \mathrm{R}) = \eta|-, \mathrm{L}), \qquad \mathsf{P}|+, \mathrm{L}) = \eta|-, \mathrm{R}), \\
&\mathsf{P}|-, \mathrm{R}) = \eta|+, \mathrm{L}), \qquad \mathsf{P}|-, \mathrm{L}) = \eta|+, \mathrm{R}).
\end{aligned} \tag{33}
$$

To ensure definite transformation properties for the vector potential, the factor η must be the same in all these formulae, and can be equal to either $+1$

or -1 since $\mathsf{P}^2 = 1$. Using eqs. (33) and $\mathsf{P}|0) = |0)$, we find, by the usual reasoning,

$$\begin{aligned} \mathsf{P}a(+,\mathrm{R})\mathsf{P}^{-1} &= \eta a(-,\mathrm{L}), \qquad \mathsf{P}a(+,\mathrm{L})\mathsf{P}^{-1} = \eta a(-,\mathrm{R}), \\ \mathsf{P}a(-,\mathrm{R})\mathsf{P}^{-1} &= \eta a(+,\mathrm{L}), \qquad \mathsf{P}a(-,\mathrm{L})\mathsf{P}^{-1} = \eta a(+,\mathrm{R}) \end{aligned} \tag{34}$$

for the destruction operators, and identical formulae for the creation operators of circularly polarized photons.

The next step is to use these equations to derive from (I, 58) the transformation law for the vector potential

$$\mathsf{P}\mathbf{A}(\mathbf{r})\mathsf{P}^{-1} = \eta\mathbf{A}(\mathbf{r}'). \tag{35}$$

The value of η cannot be assigned a priori, but only upon examining the interaction of the electromagnetic field with charged matter. We see from the equation $[\Delta - (\partial^2/\partial t^2)]\mathbf{A} = -\mathbf{j}$ that $\mathbf{A}$ must behave like $\mathbf{j}$ under space inversions. On the other hand, $\mathbf{j}$ will be proportional to the velocities $\mathbf{v}$ of the charged particles, whose components under space inversions change their signs. The proper choice in (35) is therefore $\eta = -1$: the vector potential is an ordinary vector. Vector meson fields which transform according to (35) with $\eta = +1$ are pseudovectors; their existence in nature is in no way excluded.

Systems of two photons of equal and opposite momentum are particularly interesting for the discussion of the 2γ-decay of positonium and of the neutral π-meson. Using eqs. (33) and (34), and the notation of Ch. I, we find

$$\begin{aligned} \mathsf{P}|+\mathrm{R}, -\mathrm{R}) &= |+\mathrm{L}, -\mathrm{L}), \qquad \mathsf{P}|+\mathrm{L}, -\mathrm{L}) = |+\mathrm{R}, -\mathrm{R}), \\ \mathsf{P}|+\mathrm{R}, -\mathrm{L}) &= |+\mathrm{R}, -\mathrm{L}), \qquad \mathsf{P}+\mathrm{L}, -\mathrm{R}) = |+\mathrm{L}, -\mathrm{R}). \end{aligned} \tag{36}$$

Thus $|+\mathrm{R}, -\mathrm{L})$ and $|+\mathrm{L}, -\mathrm{R})$, for which the z-component of the angular momentum is $+2$ and -2, respectively, are eigenstates of P with eigenvalue $+1$. On the other hand, the mixtures $|+\mathrm{R}, -\mathrm{R})+|+\mathrm{L}, -\mathrm{L})$ and $|+\mathrm{R}, -\mathrm{R})-|+\mathrm{L}, -\mathrm{L})$, for which the z-component of the angular momentum is zero, are eigenstates of P with eigenvalue $+1$ and -1, respectively, as can be seen by summing and subtracting the first two of eqs. (36).

4. Parity Conserving Interactions

The interaction Lagrangian (I, 75) for the electron-photon-nucleon-π meson system, which we write once more for convenience,

$$\begin{aligned} \mathscr{L} = &-ie\bar{\psi}\gamma_\mu\psi\cdot\mathsf{A}_\mu + ie\bar{\psi}_\mathrm{p}\gamma_\mu\psi_\mathrm{p}\cdot\mathsf{A}_\mu + ie\mathsf{A}_\mu\left(\phi^*\frac{\partial\phi}{\partial x_\mu} - \phi\frac{\partial\phi^*}{\partial x_\mu}\right) - e^2\mathsf{A}_\mu{}^2\phi^*\phi \\ &-i\left(\bar{\psi}_\mathrm{n}\gamma_5\left[g\phi^* + f\gamma_\mu\frac{\partial\phi^*}{\partial x_\mu}\right]\psi_\mathrm{p} + \bar{\psi}_\mathrm{p}\gamma_5\left[g\phi + f\gamma_\mu\frac{\partial\phi}{\partial x_\mu}\right]\psi_\mathrm{n}\right) \\ &-i\left(\bar{\psi}_\mathrm{p}\gamma_5\left[g\phi_3 + f\gamma_\mu\frac{\partial\phi_3}{\partial x_\mu}\right]\psi_\mathrm{p} - \bar{\psi}_\mathrm{n}\gamma_5\left[g\phi_3 + f\gamma_\mu\frac{\partial\phi_3}{\partial x_\mu}\right]\psi_\mathrm{n}\right) \end{aligned} \tag{37}$$

is known to be parity conserving. In fact, transitions between any two states A and B of the system, which are eigenstates of the operator P with eigenvalues P'_{A} and P'_{B}, are forbidden for $P'_{\mathrm{A}} \neq P'_{\mathrm{B}}$.

This selection rule is connected with the invariance of $\mathscr{L}$, $\mathsf{P}\mathscr{L}\mathsf{P}^{-1} = \mathscr{L}$, from which $\mathsf{PUP}^{-1} = \mathsf{U}$. In fact, since

$$(\mathrm{A}|\mathsf{U}|\mathrm{B}) = (\mathrm{A}|\mathsf{P}^{-1} \cdot \mathsf{PUP}^{-1} \cdot \mathsf{P}|\mathrm{B}) = P'_{\mathrm{B}} P'^{-1}_{\mathrm{A}} (\mathrm{A}|\mathsf{PUP}^{-1}|\mathrm{B}) \tag{38}$$

we find employing the invariance of U

$$(\mathrm{A}|\mathsf{U}|\mathrm{B})(P'_{\mathrm{B}} P'^{-1}_{\mathrm{A}} - 1) = 0 \tag{39}$$

so that

$$(\mathrm{A}|\mathsf{U}|\mathrm{B}) = 0 \qquad \text{for } P'_{\mathrm{B}} \neq P'_{\mathrm{A}}. \tag{40}$$

The specific set of transformations under which $\mathscr{L}$ is invariant is

$$\begin{aligned} &\psi' = i\eta_{\mathrm{e}}\gamma_4\psi(-\mathbf{r}), \qquad \psi'_{\mathrm{p}} = i\eta_{\mathrm{p}}\gamma_4\psi_{\mathrm{p}}(-\mathbf{r}), \qquad \psi'_{\mathrm{n}} = i\eta_{\mathrm{n}}\gamma_4\psi_{\mathrm{n}}(-\mathbf{r}), \\ &\phi' = \eta_{\pi^\pm}\phi(-\mathbf{r}), \qquad \phi'_3 = \eta_{\pi^0}\phi_3(-\mathbf{r}), \\ &\mathbf{A}' = -\mathbf{A}(-\mathbf{r}), \qquad A'_0 = A_0(-\mathbf{r}), \end{aligned} \tag{41}$$

where for simplicity we write $\psi' = \mathsf{P}\psi\mathsf{P}^{-1}$ etc..

The intrinsic parities $\eta_{\mathrm{e}}, \eta_{\mathrm{p}}, \eta_{\mathrm{n}}$ of electrons, protons and neutrons may take the values ± 1, $\pm i$, while $\eta_{\pi^\pm}$ and η_{π^0} for charged and neutral mesons are ± 1. $\mathscr{L}$ is invariant if

$$\eta_{\pi^\pm}\eta_{\mathrm{n}}\eta_{\mathrm{p}}^* = \eta_{\pi^\pm}\eta_{\mathrm{n}}^*\eta_{\mathrm{p}} = -1 \quad \text{and} \quad \eta_{\pi^0} = -1, \tag{42}$$

as can be seen by employing the transformation properties of bilinear forms given in subsection 2.1.

It is usually assumed that the proton and the neutron have equal intrinsic parity, so that these conditions are fulfilled if

$$\eta_{\mathrm{p}} = \eta_{\mathrm{n}} \quad \text{and} \quad \eta_{\pi^\pm} = \eta_{\pi^0} = -1. \tag{43}$$

Charged and neutral π-mesons are pseudoscalar according to this assignment.

The alternative assignment

$$\eta_{\mathrm{p}} = -\eta_{\mathrm{n}}, \qquad \eta_{\pi^\pm} = +1, \qquad \eta_{\pi^0} = -1, \tag{43'}$$

in which charged and neutral mesons have different parity would also be consistent with the experimental evidence, since it satisfies (42).

5. Selection Rules

Conservation of parity, in connection with conservation of angular momentum, is responsible for a number of selection rules for decay processes. We list a few examples.

5.1. DECAY OF A PARTICLE OF INTEGER SPIN INTO TWO PHOTONS [8, 11]

Two-photon states in the centre-of-momentum frame were discussed in Ch. I. The following table summarizes their properties:

	$\|+R,-R)$ $+\|+L,-L)$	$\|+R,-R)$ $-\|+L,-L)$	$\|+R,-L)$	$\|+L,-R)$
R_ϕ rotation of an angle ϕ around z-axis	1	1	$e^{2i\phi}$	$e^{-2i\phi}$
R_ξ rotation of 180° around x-axis, $x'=x$, $y'=-y$, $z'=-z$	1	1		
P space inversion	1	−1	1	1
J_z z-component of angular momentum	0	0	2	−2

Therefore:

a) For an odd initial state ($P=-1$) the only possible mode of disintegration is to go into the two-photon state $|+R,-R)-|+L,-L)$. For an even initial state ($P=+1$) the three final states $|+R,-R)+|+L,-L)$, $|+R,-L)$ and $|+L,-R)$ are possible. (By parity conservation.)

b) For an initial state with total angular momentum $J=1,3,5,\ldots$ the only possible final states are $|+R,-L)$ and $|+L,-R)$. This is so because $|+R,-R)\pm|+L,-L)$ are both eigenstates of R_ϕ and R_ξ with eigenvalue 1, while the initial state which is an eigenstate of R_ϕ with eigenvalue 1 has the rotation properties of the spherical harmonics $Y_J^{(0)}$, and therefore changes sign † under R_ξ for $J=1,3,5,\ldots$

c) For an initial state with $J=0,1$ the only possible final states are $|+R,-R)\pm|+L,-L)$, because the states $|+R,-L)$ and $|+L,-R)$ have $J_z=\pm 2$, which is too large for $J=0$ and 1. (By conservation of angular momentum.)

The following table illustrates these selection rules:

parity \ J	0	1	2, 4, 6 . . .	3, 5, 7 . . .
even	$\|\|$	forbidden	$\|\| \geqq 50\,\%$ $\perp \leqq 50\,\%$	$\|\|$ 50 % $\perp$ 50 %
odd	$\perp$	forbidden	$\perp$	forbidden

where $\|\|$ and $\perp$ mean that the planes of polarization of the two photons are parallel and perpendicular, respectively.

† E.g., $Y_1^{(0)}=z/r$, $Y_3^{(0)}=(5z^3-3z^2r)/r^3$ etc. change sign under R_ξ.

More specific examples of forbidden 2γ-decay processes are:

1) A vector or pseudovector meson (spin 1) cannot decay into two photons [2,7,8]).

2) Positonium in the ^3S state cannot decay into two photons [5,9]).

On the other hand:

1) Positonium in the ^1S state (odd parity) may decay into two photons, whose planes of polarization are always perpendicular to one another.

2) Scalar and pseudoscalar neutral mesons may decay into two photons. These have parallel planes of polarization for scalar mesons, perpendicular planes of polarization for pseudoscalar mesons. A full investigation of the polarization of the photons emitted in the decay $\pi^0 \to 2\gamma$ would decide whether the π^0-meson is scalar or pseudoscalar, a question which is still to some extent doubtful.

5.2. DECAY OF A PARTICLE OF INTEGER SPIN INTO TWO OR THREE PARTICLES OF SPIN ZERO [5])

The parity of a system of two spinless particles in the centre-of-momentum frame was discussed in section 1, and the results are embodied in the formula $\mathsf{P}|k, L, M) = \eta_{P_1}\eta_{P_2}(-1)^L|k, L, M)$, where L is the orbital angular momentum and η_{P_1} and η_{P_2} are the intrinsic parities of the two particles. This formula holds for any two spinless particles or antiparticles.

We find:

a) Decay into two identical spin zero particles is forbidden for odd J. This is so since for two identical particles (I, 11) must be symmetrized and we have

$$|k, L, M) = \frac{1}{\sqrt{2}}\int d\Omega_{\mathbf{k}}\,[Y_L^{(M)}(\mathbf{k}) + Y_L^{(M)}(-\mathbf{k})]\,c^*(\mathbf{k})c^*(-\mathbf{k})\,|0),$$

so that the sum of spherical harmonics is zero for L odd, in which case the state does not exist. On the other hand, conservation of angular momentum requires that L be equal to J, from which the selection rule ensues.

b) Decay into two spin zero particles of parities η_{P_1} and η_{P_2} is permitted only if the parity η_P of the decaying particle of spin J satisfies $\eta_P = (-1)^J\eta_{P_1}\eta_{P_2}$. This is a consequence of the conservation of parity and angular momentum.

c) If the decaying particle has spin zero and parity η_P, it may decay into three spinless particles of parities η_{P_1}, η_{P_2}, η_{P_3} only if $\eta_P = \eta_{P_1}\eta_{P_2}\eta_{P_3}$. In fact, the parity of a state of zero orbital angular momentum of three spin zero particles is equal to the product of the intrinsic parities, as can be seen by constructing the three particle analogue of (I, 11). This is clearly the case if the three particles are all at rest. For this question, which is relevant to the study of the decay of τ-mesons into three π-mesons, we refer the reader to the original paper of Dalitz [1]).

6. Parity Non-Conserving Interactions

Interactions such that the transition amplitude, unlike that of the strong interactions dealt with in section 4, is *not* invariant under space inversions, will be considered in Ch. VI.

These are the weak β-decay interactions and those, equally weak, which are responsible for the decay of π and μ-mesons and possibly of some other particles recently discovered.

The weak interaction Lagrangians can be expressed as sums of two terms $\mathscr{L}_1$ and $\mathscr{L}_2$, one of which is parity conserving, $\mathsf{P}\mathscr{L}_1\mathsf{P}^{-1} = \mathscr{L}_1$, while $\mathsf{P}\mathscr{L}_2\mathsf{P}^{-1} = -\mathscr{L}_2$ for the other.

Thus $\mathsf{P}\mathscr{L}\mathsf{P}^{-1} = \mathsf{P}(\mathscr{L}_1+\mathscr{L}_2)\mathsf{P}^{-1}$ differs from $\mathscr{L}$ not merely by a numerical factor, but in such a way that experiments which distinguish between a right-handed and a left-handed system of axes may lead to the determination of the ratio of the coupling constants of the parity conserving and the parity non-conserving parts.

References to Chapter II

1) R. H. Dalitz, Phil. Mag. **44** (1954) 1068
2) R. J. Finkelstein, Phys. Rev. **72** (1947) 415
3) L. D. Landau, Dokl. Akad. Nauk. USSR **60** (1948) 207
4) D. C. Peaslee, Helv. Phys. Acta **23** (1950) 845
5) M. H. L. Pryce and J. C. Ward, Nature **160** (1947) 435
6) G. Racah, Nuovo Cimento **14** (1937) 322
7) S. Sakata and Y. Tanikawa, Phys. Rev. **57** (1948) 548
8) J. Steinberger, Phys. Rev. **76** (1949) 1180
9) J. A. Wheeler, Ann. N. Y. Acad. Sci. **48** (1946) 219
10) G. C. Wick, A. S. Wightman and E. P. Wigner, Phys. Rev. **88** (1952) 101
11) C. N. Yang, Phys. Rev. **77** (1950) 242
12) C. N. Yang and J. Tiomno, Phys. Rev. **79** (1950) 495

CHAPTER III

PARTICLE-ANTIPARTICLE CONJUGATION

This operation, first introduced by Kramers [1]), transforms particles into antiparticles and vice versa. If the particles are charged, this amounts to transforming a positive (negative) into a negative (positive) particle, which has given rise to the occasional use of the term charge conjugation. This usage is inexact, since neutral particles may exist, such as the neutron, which are distinguishable from their antiparticles by virtue of their dipole interaction with the electromagnetic field † or even of a higher multipole

† The magnetic moments of neutron and antineutron are expected to be equal in magnitude and respectively antiparallel and parallel to the spin.

interaction, or perhaps on account of their interaction with a field other than the electromagnetic.

Strictly neutral particles are such that there is no distinction between particles and antiparticles. These might be more correctly called self-conjugate particles, the π^0-meson and the photon being of this type, and they are described by Hermitian field operators. To speak of particle-antiparticle conjugation is meaningless when these particles are free. If, however, they are considered together with their sources, it is no longer senseless to enquire whether, if particles are replaced by antiparticles in the sources, the field operator of the self-conjugate particles will not have to change accordingly. This is indeed the case for the electromagnetic field, since the sign of the vector potential must be changed if negatons are everywhere replaced by positons, though not for the π^0-mesons, since as far as we know these interact in exactly the same way with nucleons and antinucleons.

1. Spinless and Spin 1 Particles

We shall first discuss the case of charged † spinless particles. The operator C of particle-antiparticle conjugation is defined by

$$\begin{aligned} \mathsf{C}\mathsf{a}^*(\mathbf{k})\,|0) &= \eta_C\,\mathsf{b}^*(\mathbf{k})\,|0), \\ \mathsf{C}\mathsf{b}^*(\mathbf{k})\,|0) &= \eta_C^*\,\mathsf{a}^*(\mathbf{k})\,|0) \end{aligned} \tag{1}$$

for one-particle states i.e. it transforms particles into antiparticles of the same momentum and vice versa.

Assuming that C twice applied reproduces the initial state, we must have $\mathsf{C}^2 = 1$, so that $\eta_C\,\eta_C^* = 1$, and η_C is a complex number of modulus one, the intrinsic C-parity characteristic of the field. We also assume that C is unitary, and that the vacuum state has C-parity one, i.e. is an eigenstate of C with eigenvalue 1. We have then

$$\begin{aligned} \mathsf{C}\mathsf{a}^*(\mathbf{k})\mathsf{C}^{-1} &= \eta_C\,\mathsf{b}^*(\mathbf{k}), \qquad \mathsf{C}\mathsf{a}(\mathbf{k})\mathsf{C}^{-1} = \eta_C^*\,\mathsf{b}(\mathbf{k}), \\ \mathsf{C}\mathsf{b}^*(\mathbf{k})\mathsf{C}^{-1} &= \eta_C^*\,\mathsf{a}^*(\mathbf{k}), \qquad \mathsf{C}\mathsf{b}(\mathbf{k})\mathsf{C}^{-1} = \eta_C\,\mathsf{a}(\mathbf{k}), \end{aligned} \tag{2}$$

and from the expansion (I, 5) we infer that

$$\mathsf{C}\boldsymbol{\phi}(x)\mathsf{C}^{-1} = \eta_C^* \sum [\mathsf{b}(\mathbf{k})e^{i(k,x)} + \mathsf{a}^*(\mathbf{k})e^{-i(k,x)}] = \eta_C^*\,\boldsymbol{\phi}^*(x) \tag{3}$$

and

$$\mathsf{C}\boldsymbol{\phi}^*(x)\mathsf{C}^{-1} = \eta_C\,\boldsymbol{\phi}(x). \tag{4}$$

Therefore the operator C transforms the field operator into its Hermitian conjugate.

Only states with an equal number of particles and antiparticles can be eigenstates of C. Two trivial examples of such states are

$$\mathsf{a}^*(\mathbf{k})\mathsf{b}^*(\mathbf{k})\,|0)$$

† Or, in general, particles which are not self-conjugate.

with one particle and one antiparticle of the same momentum, and

$$[\mathsf{a}^*(\mathbf{k})\mathsf{b}^*(\mathbf{k}')+\mathsf{a}^*(\mathbf{k}')\mathsf{b}^*(\mathbf{k})]\,|0)$$

consisting in equal proportions of a particle of momentum $\mathbf{k}$ and an antiparticle of momentum $\mathbf{k}'$, and a particle of momentum $\mathbf{k}'$ and an antiparticle of momentum $\mathbf{k}$. They both correspond to the eigenvalue $C' = 1$. Of greater interest is the C-parity of the two-particle state (I, 11), representing e.g. a state of a π^+- and a π^--meson with relative angular momentum L in the centre-of-momentum frame. We have

$$\mathsf{C}|k, L, M) = \int \mathrm{d}\Omega_{\mathbf{k}}\, Y_L^{(M)}(\mathbf{k})\mathsf{b}^*(\mathbf{k})\mathsf{a}^*(-\mathbf{k})\,|0),$$

and changing the variable of integration from $\mathbf{k}$ to $-\mathbf{k}$ and remembering that the creation operators a^* and b^* commute we find †

$$\mathsf{C}|k, L, M) = (-1)^L|k, L, M). \tag{5}$$

Instead of the field operator ϕ, it is sometimes convenient to introduce two Hermitian fields ϕ_1 and ϕ_2 defined by ††

$$\phi_1 = \frac{1}{\sqrt{2}}(\sqrt{\eta_C}\phi+\sqrt{\eta_C^*}\phi^*), \qquad \phi_2 = \frac{1}{\sqrt{2}i}(\sqrt{\eta_C}\phi-\sqrt{\eta_C^*}\phi^*) \tag{6}$$

with the transformations ($\eta_C\eta_C^* = 1$)

$$\mathsf{C}\phi_1\mathsf{C}^{-1} = \phi_1, \qquad \mathsf{C}\phi_2\mathsf{C}^{-1} = -\phi_2 \tag{7}$$

i.e. two fields of even and odd C-parity. The particles associated with these fields ††† might be described by creation and destruction operators c_1^*, c_1 and c_2^*, c_2. A state with n_1 particles of the type 1 and n_2 of the type 2 is an eigenstate of C with eigenvalue $(-1)^{n_2}$.

1.1. PARTICLE-ANTIPARTICLE CONJUGATION AND THE ELECTROMAGNETIC FIELD

The transformations (3) and (4) for the field operator followed from those for the creation and destruction operators by virtue of the fact that, in the expansion (I, 5) of the field operator, the destruction operator of a particle

† The state in question is an eigenstate of the space inversion operator P having also the eigenvalue $(-1)^L$, if, of course, the particle and the antiparticle belong to the same field as tacitly assumed in deriving (5).

†† For $\eta_C = 1$, ϕ_1 and ϕ_2 are the Hermitian fields by which a field of charged particles is usually represented [3])

$$\phi_1 = \frac{1}{\sqrt{2}}(\phi+\phi^*), \qquad \phi_2 = \frac{1}{\sqrt{2}i}(\phi-\phi^*) \text{ so that } \phi = \frac{1}{\sqrt{2}}(\phi_1+i\phi_2).$$

††† A particle of the type 1, e.g., is represented by a state vector which is obtained by applying to the vacuum the coefficient of the exponential $\exp[-i(k, x)]$ in the expansion of ϕ_1 in plane waves. This coefficient is the creation operator c_1^*, and the state in question is a mixture of particle and antiparticle states of equal momentum.

and the creation operator of an antiparticle of equal momentum are multiplied by functions of $\mathbf{r}$ and t which are complex conjugate.

What happens if the particles are not free, but are acted upon by, say, an electrostatic field? This case would be of actual physical interest in the theory of $\pi^{\pm}$-mesons in the Coulomb field of a nucleus. The expansion of $\phi(x)$ would then be

$$\phi(\mathbf{r}, t) = \sum_{E,\alpha} [\mathsf{a}(E, \alpha)u(V; E, \alpha; \mathbf{r})e^{-iEt} + \mathsf{b}^*(E, \alpha)u^*(V; -E, \alpha; \mathbf{r})e^{iEt}]. \quad (8)$$

Here $\mathsf{a}(E, \alpha)$ is the destruction operator for a particle of charge $+e$ with wave function $u(V; E, \alpha; \mathbf{r})$ characterized by the energy E and by certain other quantum numbers α, which is a solution of the equation

$$[\Delta + (E - eV)^2 - \mu^2]u(V; E, \alpha; \mathbf{r}) = 0. \quad (9)$$

V is the potential of the electrostatic field.

Similarly $\mathsf{b}^*(E, \alpha)$ is the creation operator for an antiparticle with wave function $u(V; -E, \alpha; \mathbf{r})$ which is a solution of the equation

$$[\Delta + (E + eV)^2 - \mu^2]u(V; -E, \alpha; \mathbf{r}) = 0. \quad (9')$$

Instead of changing the sign of E we might have replaced e by $-e$ in going from (9) to (9').

Particle-antiparticle conjugation transforms a state $\mathsf{a}^*(E, \alpha)\,|0)$ of one particle of energy E in the electrostatic field of potential V into a state with one antiparticle of the same energy in the electrostatic field of potential $-V$. Therefore, with an improvement of notation, we might write

$$\mathsf{C}\mathsf{a}^*(V; E, \alpha)\,|0) = \eta_{\mathsf{C}}\,\mathsf{b}^*(-V; E, \alpha)\,|0) \quad (10)$$

and analogous formulae for the transformation of the other operators.

Then, denoting by $\phi(V; x)$ the operator for a field of spinless charged particles in an electrostatic field V, we have

$$\mathsf{C}\phi(V; x)\mathsf{C}^{-1} = \eta_{\mathsf{C}}^* \sum_{E,\alpha} [\mathsf{b}(-V; E, \alpha)u(V; E, \alpha; \mathbf{r})e^{-iEt} + \mathsf{a}^*(-V; E, \alpha)u^*(V; -E, \alpha; \mathbf{r})e^{iEt}]. \quad (11)$$

Noticing now that $u(V; E, \alpha; \mathbf{r}) = u(-V; -E, \alpha; \mathbf{r})$ we see that

$$\mathsf{C}\phi(V; x)\mathsf{C}^{-1} = \eta_{\mathsf{C}}^*\,\phi^*(-V; x). \quad (12)$$

Therefore, particle-antiparticle conjugation must be accompanied by a change of sign of the potential V, or, what is equivalent, by the replacement of the charge e by $-e$ (change of the sign of the coupling constant).

This is a special case of a general result which can be obtained by requiring that the interaction Lagrangian

$$\mathscr{L} = -ie\mathsf{A}_\nu \left(\phi^* \frac{\partial \phi}{\partial x_\nu} - \phi \frac{\partial \phi^*}{\partial x_\nu}\right) - e^2 \mathsf{A}_\nu^2 \phi^* \phi \quad (13)$$

of the field ϕ with a (classical or quantized) electromagnetic field be invariant under the transformations (3) and (4). As the coefficient of A_μ (the current) changes its sign under C the invariance of $\mathscr{L}$ can only be achieved by requiring either that the coupling constant change its sign or that A_μ do so. We shall always keep to the second alternative, and assume from now on that †

$$CA_\mu C^{-1} = -A_\mu. \tag{14}$$

If the electromagnetic field is quantized, (14) implies that one-photon states are eigenstates of C with eigenvalue -1, since $Ca^*(\mathbf{k}, \lambda)C^{-1} = -a^*(\mathbf{k}, \lambda)$ is the transformation of creation operators of photons following from (14). States with n photons are eigenstates of C with eigenvalue $(-1)^n$, irrespective of momentum and polarization ††.

Finally we mention the particle-antiparticle conjugation for charged spin 1 fields, defined by

$$C\phi_\mu C^{-1} = \eta_C^* \phi_\mu^* \qquad (\mu = 0, 1, 2, 3) \tag{15}$$

(η_C being any complex number of modulus one), whereas for neutral vector mesons

$$C\phi_\mu C^{-1} = \pm\phi_\mu, \tag{15'}$$

of which (14) for the electromagnetic field is an example. In analogy with eqs. (6) and (7), charged vector meson fields can be expressed in terms of Hermitian fields of C-parity ± 1.

2. Particles of Spin $\frac{1}{2}$

For particles of spin $\frac{1}{2}$ the operator C transforms a state with a particle of given momentum and spin into an antiparticle of the same momentum and spin. Thus

$$\begin{aligned} Ca(\mathbf{k}, \lambda)C^{-1} &= \eta_C^* b(\mathbf{k}, \lambda), \\ Cb(\mathbf{k}, \lambda)C^{-1} &= \eta_C a(\mathbf{k}, \lambda). \end{aligned} \tag{16}$$

As usual we require that $C^2 = 1$, so that the eigenvalues of C will be ± 1, and the intrinsic C-parity must have modulus one.

The transformation properties of the field operator will depend on the particular set of γ-matrices used. In the Majorana set, in which particle and antiparticle solutions are complex conjugate (cf. eq. (I, 23)), we have

$$C\psi''(x)C^{-1} = \eta_C^* \psi''^*, \qquad C\psi''^* C^{-1} = \eta_C \psi''. \tag{17}$$

C merely transforms the field operator into its Hermitian conjugate as for spinless particles. The Majorana theory of neutrinos, in which particles

† Thus A_μ is a field with the same transformation law as ϕ_3 defined in eq. (7)

†† Incidentally, a π^0-meson state is an eigenstate of C with eigenvalue $+1$, since $C\phi_3 C^{-1} = \phi_3$ as remarked before. Thus, if C-parity is conserved in the γ-decay of π^0, no decay into an odd number of photons is allowed.

and antiparticles are indistinguishable and the field operator is Hermitian, clearly corresponds to C = identity and $\eta_{\mathsf{C}} = 1$.

In the Majorana set, the transformation (17) in conjunction with (14) for the electromagnetic field, is immediately seen to leave invariant the electromagnetic interaction of spin $\frac{1}{2}$ particles. In fact, if

$$\mathscr{L} = -ie\mathsf{A}_\mu \bar{\psi}'' \gamma''_\mu \psi'' \tag{18}$$

with $\bar{\psi}'' = \psi''^* \gamma''_4$, we have

$$\mathsf{C}\mathscr{L}\mathsf{C}^{-1} = \mathsf{C}[-ie\mathsf{A}_\mu \psi''^*_\alpha \gamma''_{4,\alpha\beta} \gamma''_{\mu,\beta\gamma} \psi''_\gamma]\mathsf{C}^{-1}$$
$$= +ie\mathsf{A}_\mu \psi''_\alpha \gamma''_{4,\alpha\beta} \gamma''_{\mu,\beta\gamma} \psi''^*_\gamma. \tag{19}$$

We now notice two independent facts: 1) that in the Majorana set the matrices γ''_k ($k = 1, 2, 3$) are equal to their transposes, whereas γ''_4 is equal to minus its transpose; 2) that field operators of spin $\frac{1}{2}$ particles anticommute †, so that $\psi''_\alpha \psi''^*_\gamma = -\psi''^*_\gamma \psi''_\alpha$. As a consequence of 1) and of the anticommutativity of the γ's by renaming indices we obtain

$$\mathsf{C}\mathscr{L}\mathsf{C}^{-1} = ie\mathsf{A}_\mu \psi''_\gamma \gamma''_{4,\alpha\beta} \gamma''_{\mu,\beta\gamma} \psi''^*_\alpha$$

which, by 2), yields

$$\mathsf{C}\mathscr{L}\mathsf{C}^{-1} = \mathscr{L} \tag{20}$$

showing that the interaction (18) is invariant under (17) accompanied by (14) or by the replacement of e by $-e$, as was the case for particles without spin.

With the Pauli set of γ's, using eqs. (I, 27) and (I, 27′) we obtain

$$\mathsf{C}\psi\mathsf{C}^{-1} = \eta_{\mathsf{C}}^* \bar{\psi}\gamma_4\gamma_2, \qquad \mathsf{C}\bar{\psi}\mathsf{C}^{-1} = \eta_{\mathsf{C}}\gamma_4\gamma_2\psi, \tag{21}$$

so that

$$\mathsf{C}\mathscr{L}\mathsf{C}^{-1} = ie\mathsf{A}_\mu(\gamma_4\gamma_2\psi)_\alpha \gamma_{\mu,\alpha\beta}(\bar{\psi}\gamma_4\gamma_2)_\beta, \tag{22}$$

or, using the anticommutativity of the field operators,

$$\mathsf{C}\mathscr{L}\mathsf{C}^{-1} = -ie\mathsf{A}_\mu(\bar{\psi}\gamma_4\gamma_2)_\beta \gamma_{\mu,\alpha\beta}(\gamma_4\gamma_2\psi)_\alpha. \tag{23}$$

Now the transposed matrices γ_μ^{T} with elements $\gamma^{\mathrm{T}}_{\alpha\beta} = \gamma_{\beta\alpha}$ are related to the original matrices by the formula

$$\gamma_\mu^{\mathrm{T}} = -\gamma_2\gamma_4 \cdot \gamma_\mu \cdot \gamma_4\gamma_2 \text{ and } \gamma_\mu = -\gamma_2\gamma_4 \cdot \gamma_\mu^{\mathrm{T}} \cdot \gamma_4\gamma_2 \tag{24}$$

i.e. the unitary transformation $S_{\mathsf{C}}\gamma_\mu S_{\mathsf{C}}^{-1}$ with $S_{\mathsf{C}} = \gamma_2\gamma_4$ and $S_{\mathsf{C}}^{-1} = \gamma_4\gamma_2$ transforms a γ-matrix into $-\gamma^{\mathrm{T}}$. Therefore we can write $\gamma_{\mu,\alpha\beta} = \gamma^{\mathrm{T}}_{\mu,\beta\alpha} = -(\gamma_2\gamma_4 \cdot \gamma_\mu \cdot \gamma_4\gamma_2)_{\beta\alpha}$, which inserted into (23) yields $\mathsf{C}\mathscr{L}\mathsf{C}^{-1} = \mathscr{L}$. A similar discussion, with $\gamma_2\gamma_4$ replaced by $\gamma'_2\gamma'_4$, can be made in the Kramers set.

† This is not strictly true, since $\psi_\alpha(x)\psi^*_\beta(x') + \psi^*_\beta(x')\psi_\alpha(x)$ is equal to a function which is divergent for $x = x'$, which is precisely the case we are considering. To avoid this difficulty, it is customary in field theory to take $\frac{1}{2}(\bar{\psi}\gamma_\mu\psi - \mathsf{C}^{-1}\bar{\psi}\gamma_\mu\psi\mathsf{C})$ instead of $\bar{\psi}\gamma_\mu\psi$ in the interaction, which then clearly changes sign under C. We shall not do this here, since it amounts to introducing inessential complications.

The crucial point is certainly the replacement of the γ's by their transposes, so that a general formulation of the C-conjugation of field operators following from (16) is

$$\mathsf{C}\psi\mathsf{C}^{-1} = \eta_{\mathsf{C}}^{*}\bar{\psi}S_{\mathsf{C}}, \qquad \mathsf{C}\bar{\psi}\mathsf{C}^{-1} = \eta_{\mathsf{C}}S_{\mathsf{C}}\psi, \tag{25}$$

where S_{C} is a matrix such that

$$\gamma_{\mu}^{\mathsf{T}} = -S_{\mathsf{C}}\gamma_{\mu}S_{\mathsf{C}}^{-1} \tag{26}$$

($S_{\mathsf{C}} = \gamma_2\gamma_4$ (Pauli), $S'_{\mathsf{C}} = \gamma'_2\gamma'_4$ (Kramers), $S''_{\mathsf{C}} = \gamma''_4$ (Majorana)).

A final word about the angular momentum representation. By comparing (21) with (I, 38) and (I, 36) we find

$$\begin{aligned}\mathsf{C}a^{*}(k, j^{(\pm)}, m)\mathsf{C}^{-1} &= \eta_{\mathsf{C}}\,b^{*}(k, j^{(\pm)}, m),\\ \mathsf{C}a(k, j^{(\pm)}, m)\mathsf{C}^{-1} &= \eta_{\mathsf{C}}^{*}b(k, j^{(\pm)}, m)\end{aligned} \tag{27}$$

etc., so that C transforms a particle with quantum numbers $(k, j^{(\pm)}, m)$ into an antiparticle with the same quantum numbers, and vice versa.

2.1. TRANSFORMATION PROPERTIES OF BILINEAR FORMS

The bilinear forms

$$\bar{\psi}_1 O_i \psi_2 \qquad (i = S, V, T, A, P) \tag{28}$$

defined in Ch. II sect. 2.1 have the following transformation properties under particle-antiparticle conjugation:

$$\mathsf{C}\bar{\psi}_1 O_i \psi_2 \mathsf{C}^{-1} = \eta_{\mathsf{C}_1}\eta_{\mathsf{C}_2}^{*}\varepsilon_{\mathsf{C},i}\bar{\psi}_2 O_i \psi_1 \tag{29}$$

with

$$\varepsilon_{\mathsf{C},\mathrm{S}} = \varepsilon_{\mathsf{C},\mathrm{A}} = \varepsilon_{\mathsf{C},\mathrm{P}} = 1, \qquad \varepsilon_{\mathsf{C},\mathrm{V}} = \varepsilon_{\mathsf{C},\mathrm{T}} = -1. \tag{30}$$

This can easily be proved in the same way as (II, 24) by noticing that

$$O_i^{\mathsf{T}} = \varepsilon_{\mathsf{C},i}S_{\mathsf{C}}O_i S_{\mathsf{C}}^{-1}. \tag{31}$$

3. Do the Operations of Space Inversion and Particle-Antiparticle Conjugation Commute?

Beginning with the case of spinless particles, we apply the operators P and C in a different order to a one-particle state. From (I, 6) and (1) we obtain

$$\begin{aligned}\mathsf{PC}a^{*}(\mathbf{k})\,|0) &= \mathsf{P}\eta_{\mathsf{C}}\,b^{*}(\mathbf{k})\,|0) = \eta_{\mathsf{C}}\eta_{\mathsf{P}}\,b^{*}(-\mathbf{k})\,|0),\\ \mathsf{CP}a^{*}(\mathbf{k})\,|0) &= \mathsf{C}\eta_{\mathsf{P}}a^{*}(-\mathbf{k})\,|0) = \eta_{\mathsf{P}}\eta_{\mathsf{C}}\,b^{*}(-\mathbf{k})\,|0),\end{aligned} \tag{32}$$

so that the outcome does not depend on the order in which the two operations are performed. This result, which is valid also for the electromagnetic field and spin 1 meson fields is quite general: P and C commute for particles of integer spin.

This is not the case for particles of spin $\frac{1}{2}$. Consider, as a special instance,

$$\begin{aligned} \mathsf{PC}a^*(\mathbf{k},\lambda)\,|0) &= \mathsf{P}\eta_C\, b^*(\mathbf{k},\lambda)\,|0) = \eta_C\eta_P\, b^*(-\mathbf{k},\lambda')\,|0), \\ \mathsf{CP}a^*(\mathbf{k},\lambda)\,|0) &= \mathsf{C}\eta_P^*\, a(-\mathbf{k},\lambda')\,|0) = \eta_P^*\eta_C\, b^*(-\mathbf{k},\lambda')\,|0), \end{aligned} \tag{33}$$

so that P and C will in general commute only for spin $\frac{1}{2}$ particles of a real parity type, $\eta_P = \eta_P^*$. We have assumed that negatons and positons are not particles of this kind. In any case, it is apparent from (33) and the analogous equations for antiparticles, that PC and CP give the same result when applied to states containing, for each type of spin $\frac{1}{2}$ field, an equal number of particles and antiparticles.

When P and C commute, P-parity and C-parity can be simultaneous quantum numbers of a system.

4. C-Parity of a Particle-Antiparticle System (Spin $\frac{1}{2}$; Positonium; Nucleon-Antinucleon Pair)

It is easy to show that the state (I, 39) of a particle and an antiparticle in the centre-of-momentum frame is an eigenstate of C. In fact,

$$\begin{aligned} &\mathsf{C}\int \mathrm{d}\Omega_{\mathbf{k}}\phi(\mathbf{k};s_a s_b)a^*(\mathbf{k};s_a)b^*(-\mathbf{k};s_b)\,|0) \\ &= \int \mathrm{d}\Omega_{\mathbf{k}}\phi(\mathbf{k};s_a s_b)b^*(\mathbf{k};s_a)a^*(-\mathbf{k};s_b)\,|0) \\ &= -\int \mathrm{d}\Omega_{\mathbf{k}}\phi(-\mathbf{k};s_b s_a)a^*(\mathbf{k};s_a)b^*(-\mathbf{k};s_b)\,|0) \end{aligned} \tag{34}$$

since the creation operators anticommute.

Remembering that $\phi(-\mathbf{k};s_b s_a) = \pm(-1)^L\phi(\mathbf{k};s_a s_b)$ (+ for the triplet, − for the singlet) we find that the triplet state of positonium is an eigenstate of C with eigenvalue $C' = (-1)^{L+1}$, and the singlet state is one with eigenvalue $C' = (-1)^L$.

5. Selection Rules from Conservation of C-Parity

We assume that the interaction for the electron-photon-nucleon-meson system is invariant under particle-antiparticle conjugation. This restricts the possible choices of intrinsic C-parities. In fact, the condition for invariance is that the intrinsic C-parities η_{Cp}, η_{Cn}, $\eta_{C\pi^\pm}$ and $\eta_{C\pi^0}$ of protons, neutrons, charged and neutral π-mesons satisfy

$$\eta_{C\pi^\pm}\eta_{Cn}\eta_{Cp}^* = \eta_{C\pi^\pm}^*\eta_{Cn}^*\eta_{Cp} = -1 \quad \text{and} \quad \eta_{C\pi^0} = 1. \tag{35}$$

For the proof, which is similar to that given on page 330 for the invariance under space inversions, the transformations of bilinear forms of spin $\frac{1}{2}$ fields given in sect. 2.1 must be employed. We assume that the conditions (35) are satisfied and that the strong interactions conserve C-parity. The following selection rules are then found [2, 4]):

a) Positonium decay. The singlet state has $C' = (-1)^L$, the triplet

$C' = (-1)^{L+1}$. A state with n photons has $C' = (-1)^n$. Thus singlet states with $\binom{\text{even}}{\text{odd}}$ L and triplet states with $\binom{\text{odd}}{\text{even}}$ L can decay only into an $\binom{\text{even}}{\text{odd}}$ number of photons;

b) π^0 decay. Since $\mathsf{C}\phi_3\mathsf{C}^{-1} = \phi_3$, a π^0-state is an eigenstate of C with eigenvalue 1. If the decay of π^0 into photons is due entirely to C-conserving interactions, π^0 cannot decay into an odd number of photons.

References to Chapter III

1) H. A. Kramers, Proc. of Amsterdam Academy **40** (1937) 814
2) L. Michel, Nuovo Cimento **10** (1953) 319
3) G. Wentzel, Quantum Theory of Fields (New York, 1949)
4) L. Wolfenstein and D. G. Ravenhall, Phys. Rev. **88** (1952) 279

CHAPTER IV

CHARGE SYMMETRY

SELECTION RULES FROM CHARGE SYMMETRY AND PARTICLE-ANTIPARTICLE CONJUGATION

1. Preliminaries

If electromagnetic interactions are neglected, the strong interaction (I, 75) of the nucleon-π meson system is invariant under the operation of charge symmetry. This, denoted by D, transforms protons into neutrons † and vice versa, π^+-mesons into π^--mesons and vice versa, and may also affect neutral mesons in a way which is discussed below. The most striking consequence of the approximate invariance of nuclear physics under D, is the equality of the binding energy of a nucleus with Z protons and N neutrons with that of one with N protons and Z neutrons (mirror nuclei) if the electric repulsion between protons is neglected.

Explicitly

$$\mathsf{D}\psi\mathsf{D}^{-1} = \tau_1\psi, \qquad \mathsf{D}\bar{\psi}\mathsf{D}^{-1} = \bar{\psi}\tau_1, \tag{1}$$

where $\tau_1 = \left(\begin{smallmatrix}0 & 1\\ 1 & 0\end{smallmatrix}\right)$ interchanges the first and second row of $\psi = \binom{\psi_n}{\psi_p}$. Therefore $\mathsf{D}\psi_n\mathsf{D}^{-1} = \psi_p$ and $\mathsf{D}\psi_p\mathsf{D}^{-1} = \psi_n$.

On the π-meson components the effect of D is

$$\mathsf{D}\phi_1\mathsf{D}^{-1} = \phi_1, \qquad \mathsf{D}\phi_2\mathsf{D}^{-1} = -\phi_2, \tag{2}$$

† A more appropriate name for the operation might be „doublet inversion", since it interchanges the two components of the proton-neutron isobaric spin doublet.

so that

$$\mathsf{D}\phi\mathsf{D}^{-1} = \phi^*, \qquad \mathsf{D}\phi^*\mathsf{D}^{-1} = \phi, \tag{2'}$$

and

$$\mathsf{D}\phi_3\mathsf{D}^{-1} = -\phi_3. \tag{3}$$

It is easy to see that the g and f coupling terms in (I, 75), (II, 37) are invariant under this transformation, since $\tau_1 \cdot \tau_i \mathsf{D}\phi_i \mathsf{D}^{-1} \cdot \tau_1 = \tau_i \phi_i$. Indeed, D is equivalent to a rotation of 180° around the 1st axis in the isobaric spin space, so that invariance under D is merely a special case of "charge independence". On the other hand, it is interesting to speculate that a neutral spinless meson π^0, may exist whose interaction with the nucleons is of the type

$$-i\bar{\Psi}\gamma_5\left[g_0\phi_0 + f_0\gamma_\mu \frac{\partial\phi_0}{\partial x_\mu}\right]\Psi, \tag{4}$$

in which case

$$\mathsf{D}\phi_0\mathsf{D}^{-1} = \phi_0. \tag{5}$$

This type of neutral meson is unaffected by the operation of charge symmetry.

The creation and destruction operators of π^+-mesons (a^*, a), π^--mesons (b^*, b), π^0-mesons of the type $\phi_3(\mathsf{c}^*, \mathsf{c})$ and neutral spinless mesons $\pi^{0\prime}$ of the type $\phi_0(\mathsf{c}_0{}^*, \mathsf{c}_0)$ transform under D as

$$\begin{aligned} &\mathsf{D}\mathsf{a}\mathsf{D}^{-1} = \mathsf{b}, && \mathsf{D}\mathsf{a}^*\mathsf{D}^{-1} = \mathsf{b}^*, \\ &\mathsf{D}\mathsf{b}^*\mathsf{D}^{-1} = \mathsf{a}^*, && \mathsf{D}\mathsf{b}\mathsf{D}^{-1} = \mathsf{a}, \end{aligned} \tag{6}$$

and

$$\begin{aligned} &\mathsf{D}\mathsf{c}\mathsf{D}^{-1} = -\mathsf{c}, && \mathsf{D}\mathsf{c}^*\mathsf{D}^{-1} = -\mathsf{c}^*, \\ &\mathsf{D}\mathsf{c}_0\mathsf{D}^{-1} = \mathsf{c}_0, && \mathsf{D}\mathsf{c}_0{}^*\mathsf{D}^{-1} = \mathsf{c}_0{}^*. \end{aligned} \tag{7}$$

Together with the invariance of the interactions under particle-antiparticle conjugation, invariance under charge symmetry produces selection rules for reactions among nucleons and mesons. It is convenient to formulate them in a general way, so that they may embrace, together with the π-mesons, also other, yet undiscovered, or not well known bosons of any parity and spin zero or one. For this purpose the most general interaction will be given in the next section.

2. Interactions of Bosons and Nucleons

As usual we denote by Ψ the two-component nucleon operator. We introduce the spin matrices $\tau^{(\alpha)}$, such that $\tau^{(k)} \equiv \tau_k$ $(k = 1, 2, 3)$ and $\tau^{(0)} \equiv I = \left(\begin{smallmatrix} 1 & 0 \\ 0 & 1 \end{smallmatrix}\right)$. The most general list of couplings is then †:

† We do not specify the transformation properties of the mesons under space inversion.

Spinless bosons and nucleons †

$$\begin{aligned}
&\text{Scalar coupling} && g^{\alpha}\,\overline{\Psi}O_{\mathrm{S}}\tau^{(\alpha)}\Psi\cdot\phi_{\alpha}\\
&\text{Vector coupling} && f^{\alpha}\,\overline{\Psi}O_{\mathrm{V}\mu}\tau^{(\alpha)}\Psi\cdot\frac{\partial\phi_{\alpha}}{\partial x_{\mu}}\\
&\text{Pseudoscalar coupling} && g^{\alpha}\,\overline{\Psi}O_{\mathrm{P}}\tau^{(\alpha)}\Psi\cdot\phi_{\alpha}\\
&\text{Pseudovector coupling} && f^{\alpha}\,\overline{\Psi}O_{\mathrm{A}\mu}\tau^{(\alpha)}\Psi\cdot\frac{\partial\phi_{\alpha}}{\partial x_{\mu}}
\end{aligned}\qquad (8)$$

Spin one bosons and nucleons

$$\begin{aligned}
&\text{Vector coupling} && g^{\alpha}\,\overline{\Psi}O_{\mathrm{V}\mu}\tau^{(\alpha)}\Psi\cdot\phi_{\alpha,\mu}\\
&\text{Tensor coupling} && f^{\alpha}\,\overline{\Psi}O_{\mathrm{T}\mu\nu}\tau^{(\alpha)}\Psi\cdot\left(\frac{\partial\phi_{\alpha,\nu}}{\partial x_{\mu}}-\frac{\partial\phi_{\alpha,\mu}}{\partial x_{\nu}}\right)\\
&\text{Pseudovector coupling} && g^{\alpha}\,\overline{\Psi}O_{\mathrm{A}\mu}\tau^{(\alpha)}\Psi\cdot\phi_{\alpha,\mu}\\
&\text{Pseudotensor coupling} && f^{\alpha}\,\overline{\Psi}\gamma_{5}O_{\mathrm{T}\mu\nu}\tau^{(\alpha)}\Psi\cdot\left(\frac{\partial\phi_{\alpha,\nu}}{\partial x_{\mu}}-\frac{\partial\phi_{\alpha,\mu}}{\partial x_{\nu}}\right)
\end{aligned}\qquad (8')$$

where

$$O_{\mathrm{S}}=1,\qquad O_{\mathrm{V}}=\gamma_{\mu},\qquad O_{\mathrm{T}}=-\frac{i}{2\sqrt{2}}(\gamma_{\lambda}\gamma_{\mu}-\gamma_{\mu}\gamma_{\lambda}),\qquad O_{\mathrm{A}}=-i\gamma_{\mu}\gamma_{5},\qquad O_{\mathrm{P}}=\gamma_{5}\qquad (9)$$

and ϕ_{α} are the components of spinless boson fields as in the previous section, whereas $\phi_{\alpha,\mu}$, μ being a relativistic index, are their analogue for a spin one field. Thus the transformation properties for charge symmetry are determined by the index α and given by eqs. (2), (3) and (5). The interactions (8), (8′) are invariant under **D** for any choice of the coupling constants.

If the additional property of invariance under rotations in isobaric spin space is required we must have $g_1 = g_2 = g_3$ and $f^1 = f^2 = f^3$ ††.

The purely neutral theory is obtained by setting all the coupling constants g, f equal to zero, except g^0 and f^0.

On the assumption that the interactions (8) (8′) are invariant under particle-antiparticle conjugation, we must determine the transformation properties of the various boson fields under this operation. We take it for simplicity that the neutron and proton C-parities η_{Cp} and η_{Cn} are equal.

† Here $g^{\alpha}\ldots\tau^{(\alpha)}\ldots\phi_{\alpha}$ stands for $\sum_{\alpha=0}^{3} g^{\alpha}\ldots\tau^{(\alpha)}\ldots\phi_{\alpha}$.

†† We then have a "charge independent" theory, which is called "symmetrical theory" [3]) by some authors, in spite of the fact that a theory invariant under charge symmetry would not be necessarily "symmetrical" in their terminology. This makes the name of "doublet inversion" for **D** preferable to that of "charge symmetry".

Thus we have †

$$C\bar{\Psi}O_1\tau^{(\alpha)}\Psi C^{-1} = \varepsilon_{C,i}\zeta_\alpha\bar{\Psi}O_1\tau^{(\alpha)}\Psi \tag{10}$$

with

$$\varepsilon_{C,S} = 1, \quad \varepsilon_{C,V} = -1, \quad \varepsilon_{C,T} = -1, \quad \varepsilon_{C,A} = 1, \quad \varepsilon_{C,P} = 1 \tag{11}$$

and

$$\zeta_1 = \zeta_3 = \zeta_0 = 1, \quad \zeta_2 = -1\ \dagger\dagger. \tag{11'}$$

Thus, if (8) is to be invariant under particle-antiparticle conjugation, we must have

$$C\phi_\alpha C^{-1} = \zeta_\alpha\varepsilon_{C,i}\phi_\alpha$$

and (12)

$$C\phi_{\alpha,\mu}C^{-1} = \zeta_\alpha\varepsilon_{C,i}\phi_{\alpha,\mu},$$

so that $\varepsilon_{C,i} = +1$ for spinless bosons with scalar, pseudoscalar and pseudovector coupling and for spin one bosons with pseudovector coupling, and $\varepsilon_{C,i} = -1$ for spinless bosons with vector coupling and for spin one bosons with vector, tensor and pseudotensor coupling.

For the creation and destruction operators we have

$$\begin{aligned} CaC^{-1} &= \varepsilon_{C,i}b, & Ca^*C^{-1} &= \varepsilon_{C,i}b^*, \\ CbC^{-1} &= \varepsilon_{C,i}a, & Cb^*C^{-1} &= \varepsilon_{C,i}a^* \end{aligned} \tag{13}$$

for charged bosons (spinless or spin one) and

$$\begin{aligned} CcC^{-1} &= \varepsilon_{C,i}c, & Cc^*C^{-1} &= \varepsilon_{C,i}c^*, \\ Cc_0C^{-1} &= \varepsilon_{C,i}c_0, & Cc_0^*C^{-1} &= \varepsilon_{C,i}c_0^* \end{aligned} \tag{14}$$

for neutral bosons.

3. Selection Rules from Conservation of CD [7, 4])

The effect of the successive application of the operations of particle-antiparticle conjugation and charge symmetry on creation and destruction operators of bosons is merely to multiply them by a constant:

$$CD(a, b, a^*, b^*, c, c^*, c_0, c_0^*)D^{-1}C^{-1} = \varepsilon_{C,i}(a, b, a^*, b^*, -c, -c^*, c_0, c_0^*). \tag{15}$$

Thus in a transition amplitude initial and final states consisting only of bosons are eigenstates of CD. If (8), and therefore the transition amplitude U, is invariant under CD, which is true if electromagnetic interactions are excluded, the eigenvalue of CD for the initial state must be equal to that for the final state. We have the selection rules:

a) A reaction is forbidden [1, 5, 6]) if

† To see this remember that for any two fields ψ_1 and ψ_2

$$C\bar{\psi}_1O_i\psi_2C^{-1} = \eta_{c_1}\eta_{c_2}^*\varepsilon_{c,i}\bar{\psi}_2O_i\psi_1 \text{ with } \varepsilon_{c,i} \text{ given by (III, 30)}$$

In proving (10) the bilinear forms must be reexpressed in terms of proton and neutron components.

†† The transformation of the bilinear form with γ_5O_T is the same as that of the form with O_T.

$$n_3+n(\mathrm{v})+n(\mathrm{t}) = \text{odd}, \tag{16}$$

where n_3 denotes the number of bosons of the type ϕ_3, $n(\mathrm{v})$ the number of bosons with vector coupling, $n(\mathrm{t})$ the number of bosons with tensor or pseudotensor coupling, irrespective of spin, occurring in the initial and final state, on the assumption that no nucleons are present in either.

Example: The process

$$B_v^+ \to \pi^+ + \pi^{0\prime}, \tag{17}$$

where B_v^+ is a positively charged vector boson with vector and/or tensor coupling, π^+ is a positive π-meson, and $\pi^{0\prime}$ the hypothetical neutral π-meson of the ϕ_0 type, is forbidden. Likewise

$$B_v^0 \to \pi^+ + \pi^- \tag{17'}$$

is forbidden if B^0 is of the ϕ_0 type.

b) If no charged bosons are involved in the initial and final state, these are eigenstates of D, and we have the selection rule:

A reaction is forbidden if

$$n_3 = \text{odd}. \tag{18}$$

Combined with a), also

$$n_3 = \text{even}, \qquad n(\mathrm{v})+n(\mathrm{t}) = \text{odd} \tag{19}$$

is forbidden.

Examples: The process

$$B_3^0 \to (2\pi^0, 2\pi^{0\prime}) \tag{20}$$

is forbidden, if B_3^0 is a neutral boson of the type ϕ_3, and the final state consists of $2\pi^0$ both of the type ϕ_3 or of two hypothetical $\pi^{0\prime}$ both of the type ϕ_0.

4. Breaking of Selection Rules by the Electromagnetic Field

If electromagnetic interactions are taken into account, the invariance of the theory under charge symmetry no longer obtains. We still have selection rules for particle-antiparticle conjugation, according to which a reaction is forbidden if

$$n(\text{photons})+n(\mathrm{v})+n(\mathrm{t}) = \text{odd}, \tag{21}$$

where $n(\mathrm{v})$ and $n(\mathrm{t})$ are defined as before, and $n(\text{photons})$ is the number of photons in the initial and final state †.

The processes

$$B_v^+ \to \pi^+ + \pi^0 + \gamma \tag{17a}$$

$$B_v^0 \to \pi^+ + \pi^- + \gamma \tag{17'a}$$

† The coupling of photons and nucleons is "vector", $(-j_\mu A_\mu)$, or "tensor", if a Pauli term [9]) is introduced to account for the anomalous magnetic moments of the nucleons.

are now possible, which differ from (17) and (17′) by the presence of a photon in the final state. However, if the transition operator U is no longer invariant under CD, the reactions (17) and (17′) themselves become possible.

The reader familiar with the language of Feynman graphs [2]), which has deliberately never been used in these notes can convince himself that the probabilities of (17a) and (17′a) are proportional to e^2, and those of (17) and (17′) are proportional to e^4, so that the process involving the production of the photon is always more probable than the radiationless one. In fact, the simplest forbidden graph for (17′), say, is

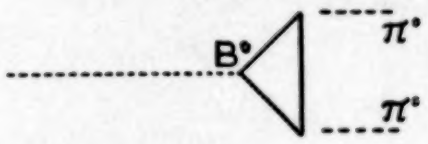

(the continuous lines represent nucleons), which can be turned into a non-forbidden graph for (17′a)

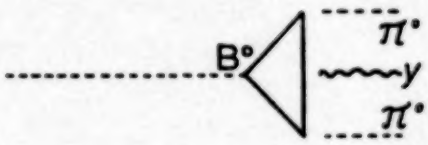

by adding an external photon line (which involves only one electromagnetic interaction, $\approx e$), or into the non-forbidden graph

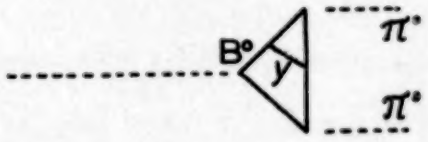

by adding an internal photon line (which involves two electromagnetic interactions, $\approx e^2$). Hence, taking the square of the matrix elements, our statement about the probabilities of the two processes taking place is proved.

The selection rule (21) forbids for example:

(1) The 2γ decay of a neutral spin one meson [9])

(2) The 3γ decay of a neutral spin one meson with pseudovector coupling.

References to Chapter IV

1) H. Fukuda and Y. Miyamoto, Progr. Theor. Phys. **4** (1950) 389

2) J. M. Jauch and F. Rohrlich, The Theory of Photons and Electrons (Cambridge, Mass., 1955)

3) N. Kemmer, Proc. Camb. Phil. Soc. **34** (1938) 354
4) L. Michel, Progress in Cosmic Ray Physics, Vol. I (Amsterdam, 1952) Ch. III
5) K. Nishijama, Progr. Theor. Phys. **6** (1951) 614
6) A. Pais, Phys. Rev. **86** (1952) 663
7) A. Pais and R. Jost, Phys. Rev. **87** (1952) 871
8) W. Pauli, Handbuch der Physik, 24/1, p. 233
9) S. Sakata and Y. Tanikawa, Phys. Rev. **57** (1949) 548

CHAPTER V

TIME REVERSAL †

1. Outline. Spinless particles

Consider a reaction leading from a state with m particles of momenta $\mathbf{k}_1 \ldots \mathbf{k}_m$ at the time $t = -\infty$ to a state with n particles of momenta $\mathbf{k}'_1, \ldots \mathbf{k}'_n$ at the time $t = +\infty$. The transition amplitude is

$$(0|\mathsf{b}(\mathbf{k}'_n) \ldots \mathsf{a}(\mathbf{k}'_1)\mathsf{U}\mathsf{a}^*(\mathbf{k}_1) \ldots \mathsf{b}^*(\mathbf{k}_m)\,|0), \tag{1}$$

where U is the transition operator. The particles, assumed all to be spinless for simplicity's sake, are part positive (a^*, a) and part negative (b^*, b). The order of the creation and destruction operators in (1) is arbitrary, although a definite choice must be made. Ours is that the operators for positive particles are as near as possible to U, those for negative particles are as far as possible.

The time reversed reaction is the one in which the n final particles of the original reaction are found at the time $t = -\infty$ with momenta $-\mathbf{k}'_1$, $-\mathbf{k}'_2$ $\ldots -\mathbf{k}'_n \ldots$, and the m initial particles are at the time $t = +\infty$ with momenta $-\mathbf{k}_1$, $-\mathbf{k}_2 \ldots -\mathbf{k}_m$. The corresponding transition amplitude is

$$(0|\mathsf{b}(-\mathbf{k}_m) \ldots \mathsf{a}(-\mathbf{k}_1)\mathsf{U}\mathsf{a}^*(-\mathbf{k}'_1) \ldots \mathsf{b}^*(-\mathbf{k}'_n)\,|0), \tag{2}$$

where the creation and destruction operators are chosen in a definite order. The transition operator U is the same as in (1).

The relationship between the amplitudes (1) and (2) depends on the transformation properties of the transition operator U, and therefore of the interaction Lagrangian, under the operation T of time reversal. This is defined as follows:

(1) The transformed of a ket is a bra, e.g.

$$\mathsf{T}|0) = (0| \tag{3}$$

† Our time reversal T coincides with that of Wigner [7]), with the weak time reversal of Pauli [4]) and with the time reversal of the second kind of Lüders [2, 3]). Pauli's strong time reversal [4, 5]) and Lüders' time reversal of the first kind [2, 3]) are the product of T with the particle-antiparticle conjugation C.

for the vacuum, and that of a bra is a ket,

$$(0|\mathsf{T}^{-1} = |0) \tag{3'}$$

also for the vacuum.

If $\mathsf{T}|A) = (A'|$ and $(B|\mathsf{T}^{-1} = |B')$, we have

$$(B|A) = (B|\mathbf{1}|A) = (B|\mathsf{T}^{-1} \cdot \mathsf{T}|A) = (A'|B'). \tag{4}$$

Thus T is not a unitary operator, since $(B|A)$ is in general different from $(A|B)$, so that (4) implies that the product of two state vectors is not invariant. The word antiunitary [7]) is sometimes used to describe a transformation with the property (4).

(2) If O is any operator, the time reversed operator $\mathsf{O}' = \mathsf{T}\mathsf{O}\mathsf{T}^{-1}$ has the property

$$(B|\mathsf{O}|A) = (B|\mathsf{T}^{-1}\mathsf{O}'\mathsf{T}|A) = (A'|\mathsf{O}'|B'). \tag{5}$$

(3) A more precise definition of T depends on the particles considered. For spinless particles we require that

$$\begin{aligned} &\mathsf{T}\mathsf{a}^*(\mathbf{k}_1) \ldots \mathsf{b}^*(\mathbf{k}_m)\,|0) = \varepsilon_m (0|\mathsf{b}(-\mathbf{k}_m) \ldots \mathsf{a}(-\mathbf{k}_1), \\ &(0|\mathsf{b}(\mathbf{k}'_n) \ldots \mathsf{a}(\mathbf{k}'_1)\mathsf{T}^{-1} = \varepsilon_n\, \mathsf{a}^*(-\mathbf{k}'_1) \ldots \mathsf{b}^*(-\mathbf{k}'_n)\,|0), \end{aligned} \tag{6}$$

where ε_m and ε_n are numbers of modulus one depending on the number of operators involved. (3) and (3') are special cases of (6).

Thus T changes kets into bras and vice versa, and reverses the order of all factors, while its effect on creation and destruction operators is

$$\begin{aligned} &\mathsf{T}\mathsf{a}(\mathbf{k})\mathsf{T}^{-1} = \eta_{\mathrm{T}}^*\, \mathsf{a}^*(-\mathbf{k}), \qquad &&\mathsf{T}\mathsf{b}(\mathbf{k})\mathsf{T}^{-1} = \eta_{\mathrm{T}}\, \mathsf{b}^*(-\mathbf{k}), \\ &\mathsf{T}\mathsf{a}^*(\mathbf{k})\mathsf{T}^{-1} = \eta_{\mathrm{T}}\, \mathsf{a}(-\mathbf{k}), \qquad &&\mathsf{T}\mathsf{b}^*(\mathbf{k})\mathsf{T}^{-1} = \eta_{\mathrm{T}}^*\, \mathsf{b}(-\mathbf{k}). \end{aligned} \tag{7}$$

Since $\mathsf{T}^2 = 1$, η_{T} must be a number of modulus one.

For the field operator $\boldsymbol{\phi}(\mathbf{r}, t)$ we have

$$\mathsf{T}\boldsymbol{\phi}(\mathbf{r}, t)\mathsf{T}^{-1} = \eta_{\mathrm{T}}^* \sum [\mathsf{a}^*(-\mathbf{k})e^{i(k,x)} + \mathsf{b}(-\mathbf{k})e^{-i(k,x)}] = \eta_{\mathrm{T}}^*\, \boldsymbol{\phi}^*(\mathbf{r}, t') \tag{8}$$

with $t' = -t$.

1.1.

From the above definition of time reversal, we are led to expect that the expression for the charge density should be left unchanged, whereas the sign of the current components should change †. This is in fact the case, as can be seen by applying T to

$$\mathsf{j}_\mu = ie\left(\frac{\partial \boldsymbol{\phi}^*}{\partial x_\mu}\,\boldsymbol{\phi} - \boldsymbol{\phi}^*\,\frac{\partial \boldsymbol{\phi}}{\partial x_\mu}\right) \tag{9}$$

† In classical mechanics, for instance, the time reversed motion is defined in such a way that the particles move backwards along their original trajectories, the direction of the velocities (and, therefore, of the current density) having been reversed. Note that together with the momentum $m\mathrm{d}\mathbf{r}/\mathrm{d}t$, also the angular momentum $\mathbf{r} \times m\mathrm{d}\mathbf{r}/\mathrm{d}t$ changes sign under time reversal since t is replaced by $-t$.

and remembering that, by definition, the order of the factors must be reversed. We have, with $t' = -t$,

$$\begin{aligned} \mathsf{T}\mathbf{j}(\mathbf{r}, t)\mathsf{T}^{-1} &= -\mathbf{j}(\mathbf{r}, t'), \\ \mathsf{T}\rho(\mathbf{r}, t)\mathsf{T}^{-1} &= \rho(\mathbf{r}, t'). \end{aligned} \tag{10}$$

If we require the invariance of the interaction with the electromagnetic field, the vector and scalar potential of this latter must transform as

$$\begin{aligned} \mathsf{T}\mathbf{A}(\mathbf{r}, t)\mathsf{T}^{-1} &= -\eta_T \mathbf{A}(\mathbf{r}, t'), \\ \mathsf{T}A_0(\mathbf{r}, t)\mathsf{T}^{-1} &= \eta_T A_0(\mathbf{r}, t') \end{aligned} \tag{11}$$

with $\eta_T = 1$. Eqs. (11) with η_T equal to a complex number of modulus one, is also the time reversal transformation of any vector field.

By comparing (11) with (I, 58) and taking into account that $\mathbf{e}^*(-\mathbf{k}, \mathrm{L}) = \mathbf{e}(\mathbf{k}, \mathrm{L})$ and $\mathbf{e}^*(-\mathbf{k}, \mathrm{R}) = \mathbf{e}(\mathbf{k}, \mathrm{R})$, we find that T reverses the momentum and the spin † of the photons, since e.g.

$$\mathsf{T}a(\mathbf{k}, \mathrm{R})\mathsf{T}^{-1} = -a^*(-\mathbf{k}, \mathrm{R}). \tag{12}$$

1.2.

We can now write (1) in the form

$$\begin{aligned} &(0|b(\mathbf{k}'_n) \ldots a(\mathbf{k}'_1)\mathsf{T}^{-1}\mathsf{T}\mathsf{U}\mathsf{T}^{-1}\mathsf{T}a^*(\mathbf{k}_1) \ldots b^*(\mathbf{k}_m)|0) \\ &\qquad = \varepsilon_m \varepsilon_n (0|b(-\mathbf{k}_m) \ldots a(-\mathbf{k}_1)\mathsf{T}\mathsf{U}\mathsf{T}^{-1}a^*(-\mathbf{k}'_1) \ldots b^*(-\mathbf{k}'_n)|0), \end{aligned}$$

so that for interactions which are invariant under $\mathsf{T}(\mathsf{T}\mathsf{U}\mathsf{T}^{-1} = \mathsf{U})$ the transition amplitude (1) differs from (2) for the time reversed reaction only by the factor $\varepsilon_m \varepsilon_n$ of modulus one.

This being the case the probability of the reaction (1) is equal to that of the time reversed reaction (2), an occurrence which is not to be confused with the condition for detailed balance.

2. Time Reversal for Particles of Spin $\frac{1}{2}$

As was the case with vector particles, the operation of time reversal must invert momentum and spin alike. The transformation law for creation and destruction operators is ††

$$\begin{aligned} \mathsf{T}a(\mathbf{k}, \lambda)\mathsf{T}^{-1} &= \eta_T^*(\delta_{\lambda\downarrow} - \delta_{\lambda\uparrow})a^*(-\mathbf{k}, \lambda), \\ \mathsf{T}b(\mathbf{k}, \lambda)\mathsf{T}^{-1} &= \eta_T(\delta_{\lambda\uparrow} - \delta_{\lambda\downarrow})b^*(-\mathbf{k}, \lambda), \end{aligned} \tag{13}$$

† Under time reversal the spin behaves like an orbital angular momentum.

†† It is apparent from (13) and (II, 16) that e.g.

$$\begin{aligned} \mathsf{P}\mathsf{T}a(\mathbf{k}, \uparrow)\mathsf{T}^{-1}\mathsf{P}^{-1} &= -\eta_T^*\eta_P^* a(\mathbf{k}, \downarrow) \\ \mathsf{T}\mathsf{P}a(\mathbf{k}, \uparrow)\mathsf{P}^{-1}\mathsf{T}^{-1} &= \eta_T^*\eta_P a(\mathbf{k}, \downarrow). \end{aligned}$$

Thus the operations P, T commute for spin $\frac{1}{2}$ particles with η_P imaginary, as electrons have been assumed to be. The possibility of the existence of spin $\frac{1}{2}$ particles for which P and T anticommute has been studied by J. C. Taylor in an attempt to classify the new heavy particles of spin $\frac{1}{2}$ (baryons, cf. Ch. VII).

so that neutral Majorana particles must have $\eta_T = \pm i$.

For the field operator in the Pauli set we obtain

$$\begin{aligned}\mathsf{T}\psi(\mathbf{r},t)\mathsf{T}^{-1} = \eta_T^* \sum \{&[-\mathsf{a}^*(\mathbf{k},\uparrow)u(-\mathbf{k},\uparrow)+\mathsf{a}^*(\mathbf{k},\downarrow)u(-\mathbf{k},\downarrow)] \\ &\cdot \exp[-i(\mathbf{k}\cdot\mathbf{r}+\omega t)] \\ +&[\mathsf{b}(\mathbf{k},\uparrow)v(-\mathbf{k},\uparrow)-\mathsf{b}(\mathbf{k},\downarrow)v(-\mathbf{k},\downarrow)] \\ &\cdot \exp[i(\mathbf{k}\cdot\mathbf{r}+\omega t)]\}\end{aligned} \tag{14}$$

having changed the summation variable from $\mathbf{k}$ to $-\mathbf{k}$.

We now notice that

$$\begin{aligned}&\gamma_1\gamma_3 u(\mathbf{k},\uparrow) = [-iu(-\mathbf{k},\uparrow)]^*, \qquad \gamma_1\gamma_3 u(\mathbf{k},\downarrow) = [iu(-\mathbf{k},\downarrow)]^*, \\ &\gamma_1\gamma_3 v(\mathbf{k},\uparrow) = [iv(-\mathbf{k},\uparrow)]^*, \qquad \gamma_1\gamma_3 v(\mathbf{k},\downarrow) = [-iv(-\mathbf{k},\downarrow)]^*,\end{aligned} \tag{15}$$

where $\gamma_1\gamma_3$ is essentially the y-component of the spin, in fact $\gamma_1\gamma_3 = -iI\times\sigma_y = -2s_y$. Employing (15), eq. (14) gives

$$\mathsf{T}\psi(\mathbf{r},t)\mathsf{T}^{-1} = (\eta_T i\gamma_1\gamma_3\psi(\mathbf{r},t'))^*. \tag{16}$$

Similarly

$$\mathsf{T}\psi^*(\mathbf{r},t)\mathsf{T}^{-1} = \eta_T i\gamma_1\gamma_3\psi(\mathbf{r},t'). \tag{16'}$$

Eqs. (16) and (16') are also valid in the Kramers set with ψ, γ_1, γ_3 replaced by ψ', γ'_1, γ'_3. Note, however, that $\gamma'_1\gamma'_3 = -iI\times\sigma_y = \gamma_1\gamma_3$. This is due to the fact that the transformation matrix $S_{K,P}$ given in (I, 19) is a real matrix, so that, when applied to the right member of (16), it can be brought inside the Hermitian conjugation sign without any change. This is not the case for the Majorana set. The appropriate steps in going over from (16) to the analogous expression in the Majorana set are

$$S_{M,P}(\eta_T i\gamma_1\gamma_3\psi(\mathbf{r},t'))^* = (\eta_T i S^*_{M,P}\gamma_1\gamma_3 S^{-1}_{M,P} S_{M,P}\psi)^* = \left(\eta_T \frac{2}{i}\rho_y\times I\psi''(\mathbf{r},t')\right)^*.$$

Thus when going from the Pauli and the Kramers sets to the Majorana, $-iI\times\sigma_y$ must be replaced by $-2i\rho_y\times I$, which is not the y-component of the spin.

2.1.

The transformations (16) and (16'), together with the convention of reversing the order of the ψ operators † give for

$$\mathscr{L} = -ie\mathsf{A}_\mu\bar{\psi}\gamma_\mu\psi$$

the transformed

$$\begin{aligned}\mathsf{T}\mathscr{L}\mathsf{T}^{-1} = -ie[&-\bar{\psi}(\mathbf{r},t')\gamma\psi(\mathbf{r},t')\cdot\mathsf{T}\mathbf{A}(\mathbf{r},t)\mathsf{T}^{-1} \\ &+\bar{\psi}(\mathbf{r},t')\gamma_4\psi(\mathbf{r},t')\cdot\mathsf{T}A_4(\mathbf{r},t)\mathsf{T}^{-1}].\end{aligned} \tag{17}$$

This, in conjunction with (11), yields

† But not using in any way the anticommutativity of these, which was employed in the corresponding discussion of particle-antiparticle conjugation.

$$\mathsf{T}\mathscr{L}\mathsf{T}^{-1} = -ieA_\mu(\mathbf{r}, t')\bar{\psi}(\mathbf{r}, t')\gamma_\mu\psi(\mathbf{r}, t'). \tag{18}$$

Thus the interaction Lagrangian is invariant under the transformation T, which, as for spinless particles, changes the sign of the current but not that of the charge density.

2.2. TRANSFORMATION OF BILINEAR FORMS

The familiar bilinear forms,

$$\bar{\psi}_1 O_i \psi_2 \qquad (i = S, V, T, A, P)$$

have the following transformation properties under time reversal:

$$\mathsf{T}\bar{\psi}_1 O_i \psi_2 \mathsf{T}^{-1} = \eta_{T_1}\eta^*_{T_2}\varepsilon_{T,i}\bar{\psi}_2 O_i \psi_1$$

with

	S	V	T	A	P
$\varepsilon_{T,i} =$	1	-1 $\mu = 1, 2, 3$	$+1$ λ or $\mu = 4$	-1 $\mu = 1, 2, 3$	-1
		$+1$ $\mu = 4$	-1 $\lambda, \mu = 1, 2, 3$	$+1$ $\mu = 4$.	

It is interesting to consider the results of applying simultaneously the operations P of space inversion and T of time reversal †. We have

$$\mathsf{PT}\bar{\psi}_1 O_i \psi_2 \mathsf{T}^{-1}\mathsf{P}^{-1} = \eta_{T_1}\eta_{P_1}\eta^*_{T_2}\eta^*_{P_2}\varepsilon_{PT,i}\bar{\psi}_2 O_i \psi_1$$

with

	S	V	T	A	P
$\varepsilon_{PT,i} =$	$+1$	$+1$	-1	-1.	$+1$

For the operation CPT †† we have

$$\mathsf{CPT}\bar{\psi}_1 O_i \psi_2 \mathsf{T}^{-1}\mathsf{P}^{-1}\mathsf{C}^{-1} = \eta_{T_1}\eta_{P_1}\eta_{C_2}\eta^*_{T_2}\eta^*_{P_2}\eta^*_{C_1}\varepsilon_{CPT,i}\bar{\psi}_1 O_i \psi_2$$

with

	S	V	T	A	P
$\varepsilon_{CPT,i} =$	$+1$	-1	$+1$	-1	$+1$.

Notice that CPT transforms the scalar S like the pseudoscalar P, and the vector V like the axial vector A. Thus the transformation properties for proper ††† Lorentz transformations determine also the transformation character of the bilinear forms under CPT, a fact of the greatest importance [1, 3, 4]) which will be used in Ch. VI.

† Pauli calls PT "weak reflection" [4]).

†† Pauli's "strong reflection" [4]).

††† I.e., excluding space inversions, so that S and P are transformed in the same way, and so are also V and A.

References to Chapter V

1) J. S. Bell, Proc. Roy. Soc. A **231** (1955) 479
2) G. Lüders, Zeits. f. Physik **133** (1952) 325
3) G. Lüders, Mat. Fys. Medd. Dan. Vid. Selsk. **28** (1954) no. 5

4) W. Pauli, Niels Bohr and the Development of Physics (London, 1955) p. 30
5) J. Schwinger, Phys. Rev. **82** (1951) 914
6) J. C. Taylor, Nuclear Physics **3** (1957) 606
7) E. P. Wigner, Gött. Nachr. (Math. Naturw. Klasse) (1932) 546

CHAPTER VI

WEAK INTERACTIONS

1. General Features

The p-n-e-ν interaction †, which is responsible for β-decay, and the π-μ-ν and μ-e-ν interactions, which produce the decay of the π-meson and of the μ-meson, respectively, all come under this heading. As briefly mentioned at the end of Ch. II, they differ in several respects from the strong interactions:

(i) Because of the small value of the coupling constants only the first term of the power expansion of the transition operator needs to be considered in the calculation of transition probabilities. This first term is by itself capable of producing real processes, in which the total energy and momentum are conserved ††;

(ii) It has recently been discovered that the weak interactions do not conserve parity [5, 6, 20]) so that, if P as usual denotes the operation of space inversion defined in Ch. II, $\mathsf{PUP}^{-1} \neq \mathsf{U}$. Non-conservation of parity will be revealed by experiments which differentiate a right-handed system of axes from a left-handed one. The crucial experiment of this type is the measurement of the angular distribution of the β-rays coming from the decay of oriented nuclei, which is found to be of the form [20])

$$I(\theta)\mathrm{d}\theta \propto \left(1+\alpha \frac{\mathbf{J}\cdot\mathbf{k}}{|\mathbf{J}|\,|\mathbf{k}|}\right) \sin\theta\, \mathrm{d}\theta$$

with $\theta \triangleq \mathbf{Jk}$. The term $\mathbf{J}\cdot\mathbf{k}/|\mathbf{J}|\,|\mathbf{k}|$ expresses a correlation between the nuclear spin $\mathbf{J}$, which is an axial vector, and the β-ray momentum $\mathbf{k}$, which is a polar vector, and is a pseudoscalar. Its occurrence together with the scalar 1 must be due to a violation of the law of space inversion invariance in β-decay. This invariance appears equally to be infringed in the decay of the π-meson into a μ-meson and a neutrino, and of the μ-meson into an a negaton and two neutrinos;

(iii) The question of the invariance of the weak interactions under

† The abbreviations p, n, e, ν, π, μ stand for proton, neutron, electron, neutrino, π-meson and μ-meson, respectively.

†† This is a very fortunate occurrence. The successive terms of the expansion of U are marred by non-renormalizable divergences, so that U cannot be given a well defined mathematical meaning.

particle-antiparticle conjugation and time reversal has also been raised [8]).

The most general expression for a parity non-conserving (but Lorentz invariant) β-decay interaction is

$$\mathscr{L} = \sum_{i} (\bar{\psi}_p O_{1\mu} \ldots \psi_n)(\bar{\psi}_e O_{1\mu} \ldots (C_1 + C'_1\gamma_5)\psi_\nu) + \text{H.C.}, \tag{1}$$

where $i = S, V, T, A, P$ denotes the various combinations of γ-matrices listed in Ch. II, sect. 2.1; $\mu \ldots$ stands for the respective tensor indices, and C_1 and C'_1 are the coupling constants of the parity conserving (even) and parity non-conserving (odd) part of the interaction.

For the following it is convenient to have $\mathscr{L}$ in an explicit form:

$$\begin{aligned}
\mathscr{L} = {} & C_S(\bar{\psi}_p O_S \psi_n)(\bar{\psi}_e O_S \psi_\nu) + C_S^*(\bar{\psi}_n O_S \psi_p)(\bar{\psi}_\nu O_S \psi_e) \\
& + C_V(\bar{\psi}_p O_{V\mu} \psi_n)(\bar{\psi}_e O_{V\mu} \psi_\nu) + C_V^*(\bar{\psi}_n O_{V\mu} \psi_p)(\bar{\psi}_\nu O_{V\mu} \psi_e) \\
& + C_T(\bar{\psi}_p O_{T\mu\nu} \psi_n)(\bar{\psi}_e O_{T\mu\nu} \psi_\nu) + C_T^*(\bar{\psi}_n O_{T\mu\nu} \psi_p)(\bar{\psi}_\nu O_{T\mu\nu} \psi_e) \\
& + C_A(\bar{\psi}_p O_{A\mu} \psi_n)(\bar{\psi}_e O_{A\mu} \psi_\nu) + C_A^*(\bar{\psi}_n O_{A\mu} \psi_p)(\bar{\psi}_\nu O_{A\mu} \psi_e) \\
& + C_P(\bar{\psi}_p O_P \psi_n)(\bar{\psi}_e O_P \psi_\nu) + C_P^*(\bar{\psi}_n O_P \psi_p)(\bar{\psi}_\nu O_P \psi_e) \\
& + C'_S(\bar{\psi}_p O_S \psi_n)(\bar{\psi}_e O_S \gamma_5 \psi_\nu) - C'^*_S(\bar{\psi}_n O_S \psi_p)(\bar{\psi}_\nu O_S \gamma_5 \psi_e) \\
& + C'_V(\bar{\psi}_p O_{V\mu} \psi_n)(\bar{\psi}_e O_{V\mu} \gamma_5 \psi_\nu) + C'^*_V(\bar{\psi}_n O_{V\mu} \psi_p)(\bar{\psi}_\nu O_{V\mu} \gamma_5 \psi_e) \\
& + C'_T(\bar{\psi}_p O_{T\mu\nu} \psi_n)(\bar{\psi}_e O_{T\mu\nu} \gamma_5 \psi_\nu) - C'^*_T(\bar{\psi}_n O_{T\mu\nu} \psi_p)(\bar{\psi}_\nu O_{T\mu\nu} \gamma_5 \psi_e) \\
& + C'_A(\bar{\psi}_p O_{A\mu} \psi_n)(\bar{\psi}_e O_{A\mu} \gamma_5 \psi_\nu) + C'^*_A(\bar{\psi}_n O_{A\mu} \psi_p)(\bar{\psi}_\nu O_{A\mu} \gamma_5 \psi_e) \\
& + C'_p(\bar{\psi}_p O_P \psi_n)(\bar{\psi}_e O_P \gamma_5 \psi_\nu) - C'^*_p(\bar{\psi}_n O_P \psi_p)(\bar{\psi}_\nu O_P \gamma_5 \psi_e).
\end{aligned} \tag{2}$$

The interaction Lagrangian (1) and (2) is that for the process

$$n \to p + e + \bar{\nu},$$

where $\bar{\nu}$ denotes an antineutrino. The process

$$n \to p + e + \nu$$

is described by the Lagrangian obtained by replacing ψ_ν by the conjugate $\psi_\nu^c = C\psi_\nu C^{-1}$ in (1) and (2), since the antineutrino creation operator b_ν^* must appear instead of the neutrino a_ν^*. The Lagrangian remains Lorentz invariant, since ψ_ν and ψ_ν^c transform in the same way †.

1.1. TRANSFORMATION PROPERTIES OF LAGRANGIAN

As mentioned in the previous section, experiments have been devised to study the transformation properties of the Lagrangian of the weak interactions under space inversion, particle-antiparticle conjugation and time reversal. The observed effects are all described by formulae in which the coupling constants occur bilinearly as $C_1 C_k^*$, $C'_1 C_k^*$, $C_1 C'^*_k$, $C'_1 C'^*_k$. Thus the

† If Majorana matrices are used $\psi_\nu^{c\prime\prime} = \psi_\nu^{\prime\prime *}$. With the other sets, however, merely to replace ψ_ν by ψ_ν^* would destroy Lorentz invariance.

physical content of the theory remains unaltered if all the coupling constants C_1, C'_1 in $\mathscr{L}$ are multiplied by the *same* phase factor $e^{i\alpha}$, and C_1^*, $C_1'^*$ by $e^{-i\alpha}$.

In the following we shall use the expression "physically invariant" to mean that the transformed Lagrangian differs from the original one in that the coupling constants C_1, C'_1 are multiplied by the same factor of modulus one. Moreover, the discussion of the transformation properties of $\mathscr{L}$ can be simplified by omitting the intrinsic parities η_P, η_C and η_T of the various fields. These can contribute only factors of modulus one, which can be absorbed in the coupling constants.

Using the results given in Ch. II, sect. 2.1, Ch. III, sect. 2.1 and Ch. V, sect. 2.2, we find the following sufficient conditions for the invariance of $\mathscr{L}$ under P, C and T:

(i) P invariance: all $C'_1 = 0$;

(ii) T invariance: all C_1, C'_1 real;

(iii) C invariance: all C_1 real, all C'_1 purely imaginary. (3)

These conditions, however, are not necessary.

We have already mentioned that (i) does not seem to be satisfied. Studies of Lüders [9]), Bell [1]) and Pauli [11]) have led to the important result that the Lagrangian (1) is always physically invariant under the product of the operators P, C and T taken in any order. For the order CPT this can be verified by employing the transformation properties of bilinear forms listed in Ch. V, sect. 2.2. As we there stressed, such properties are determined only by the Lorentz type, so that a scalar transforms like a pseudoscalar and a vector like a pseudovector. In this chapter we shall assume that all weak interactions are invariant under CPT, as the Bell-Lüders-Pauli theorem applies also to the π-μ-ν and the μ-e-ν interactions. If $\mathscr{L}$ is *not* invariant under one of the operators C, P, T, then it must also be not invariant under at least one of the others. Instead of giving a general proof, we content ourselves with remarking that the truth of the statement would be self-evident if the conditions (i), (ii) and (iii) for P, T and C invariance were necessary rather than sufficient. Assume for instance that P conservation is violated and that $C'_1 \neq 0$. Then either C'_1 is imaginary, and the Lagrangian is not invariant under T, or C'_1 is real, in which case the Lagrangian is not invariant under C. On the other hand, both C and T invariance are lost if C'_1 has both a real and an imaginary part.

1.2. β-DECAY OF ORIENTED NUCLEI

The angular distribution of the β-ray in the decay of oriented nuclei can be expressed in terms of the coupling constants C_1 and C'_1 by a straightforward calculation. Thus in an allowed transition $J \to J-1$ (no), the quantity α occurring in the formula for the angular correlation of the momentum of the β-ray and the spin of the polarized nuclei is given by

$$\alpha = \beta \langle J_z \rangle / J$$

with

$$\beta = \mathrm{Re}\left[(C_\mathrm{T} C'^{*}_\mathrm{T} - C_\mathrm{A} C'^{*}_\mathrm{A}) + i \frac{Ze^2}{k_e} (C_\mathrm{A} C'^{*}_\mathrm{T} + C'_\mathrm{A} C_\mathrm{T}^{*}) \right] \times |M_{\mathrm{G.T.}}|^2 \cdot v_e \cdot \frac{2}{\xi + \xi b / W}, \quad (4)$$

where

$$\begin{aligned} \xi &= (|C_\mathrm{S}|^2 + |C_\mathrm{V}|^2 + |C'_\mathrm{S}|^2 + |C'_\mathrm{V}|^2)|M_{\mathrm{F.}}|^2 \\ &\quad + (|C_\mathrm{T}|^2 + |C_\mathrm{A}|^2 + |C'_\mathrm{T}|^2 + |C'_\mathrm{A}|^2)|M_{\mathrm{G.T.}}|^2 \\ b\xi &= \gamma[(C_\mathrm{S}^{*} C_\mathrm{V} + C_\mathrm{S} C_\mathrm{V}^{*}) + (C'^{*}_\mathrm{S} C'_\mathrm{V} + C'_\mathrm{S} C'^{*}_\mathrm{V})]|M_{\mathrm{F.}}|^2 \\ &\quad + \gamma[(C_\mathrm{T}^{*} C_\mathrm{A} + C_\mathrm{A}^{*} C_\mathrm{T}) + (C'^{*}_\mathrm{T} C'_\mathrm{A} + C'^{*}_\mathrm{A} C'_\mathrm{T})]|M_{\mathrm{G.T.}}|^2. \end{aligned}$$

W, k_e and v_e are the energy, momentum and velocity of the electron and $\langle J_z \rangle$ is the average spin component of the initial nucleus. For an allowed transition $J \to J+1$ (no), α is given by

$$\alpha = -\beta \frac{\langle J_z \rangle}{J+1}.$$

The energy dependence of the square bracket in β has its origin in the distortion of the electron wave function due to the Coulomb field. It vanishes in the free electron approximation.

If the condition (i) for P invariance is satisfied, β is equal to zero. On the other hand, the energy dependent term Ze^2/k_e is missing if the condition (ii) for T invariance obtains, since $C_\mathrm{A} C'^{*}_\mathrm{T} + C'_\mathrm{A} C_\mathrm{T}^{*} = 0$. The first term $C_\mathrm{T} C'^{*}_\mathrm{T} - C_\mathrm{A} C'^{*}_\mathrm{A}$ vanishes if C is conserved. In general $\beta \neq 0$ rules out the possibility that both C and T are conserved.

If C is conserved, there is no asymmetry in the angular distribution of the β-rays if the Coulomb distortion of the electron wave function is neglected. This is the consequence of a general theorem:

"If the interaction is strictly invariant under particle-antiparticle conjugation ($\mathsf{C}\mathscr{L}\mathsf{C}^{-1} = \mathscr{L}$), and if the products of the decay of a particle A are free particles a, b, c, . . ., then to the lowest order in the coupling constants there is no interference between the parity conserving and the parity non-conserving parts of $\mathscr{L}$ in the decay of A".

Assume for simplicity that A is a particle of spin zero † at rest. The transition amplitude to the lowest order in the coupling constants is $(\mathrm{B}|\mathsf{U}|\mathrm{A})$ with $\mathsf{U} = i\int \mathscr{L}(x)\mathrm{d}^4x$. Since A is spinless and at rest $\mathsf{T}|\mathrm{A}) = (\mathrm{A}|$, whereas $(\mathrm{B}|\mathsf{T}^{-1} = |-\mathrm{B})$, in which $-\mathrm{B}$ signifies that T has reversed the momenta of all the particles of B. Moreover, $(\mathrm{A}|\mathsf{P}^{-1} = \varepsilon_\mathrm{A}(\mathrm{A}|$ and $\mathsf{P}|-\mathrm{B}) = \varepsilon_\mathrm{B}|\mathrm{B})$, where ε_A is the intrinsic parity of A and ε_B is the product of the intrinsic parities of the decay products. By reversing the momenta P replaces $-\mathrm{B}$ by B.

† This is the actual case for π-meson decay.

We can now write

$$\mathscr{L} = \mathscr{L}_1 + \mathscr{L}_2$$

with

$$\mathscr{L}_1 = \tfrac{1}{2}[\mathscr{L} + \mathsf{P}\mathscr{L}\mathsf{P}^{-1}],$$
$$\mathscr{L}_2 = \tfrac{1}{2}[\mathscr{L} - \mathsf{P}\mathscr{L}\mathsf{P}^{-1}].$$

$\mathscr{L}_1$ and $\mathscr{L}_2$ respectively commute and anticommute with P ($\mathsf{P}\mathscr{L}_1\mathsf{P}^{-1} = \mathscr{L}_1$ and $\mathsf{P}\mathscr{L}_2\mathsf{P}^{-1} = -\mathscr{L}_2$). Similarly $\mathsf{U} = \mathsf{U}_1 + \mathsf{U}_2$, where U_1 and U_2 have the same properties as $\mathscr{L}_1$ and $\mathscr{L}_2$.

Consider now the transition amplitudes $(B_1|\mathsf{U}_1|A)$ and $(B_2|\mathsf{U}_2|A)$ from A to B_1 through U_1 and to B_2 through U_2. B_1 and B_2 are states of different parities. Moreover

$$(B_1|\mathsf{U}_1|A) = (A|\mathsf{T}\mathsf{U}_1\mathsf{T}^{-1}|-B_1) = \varepsilon_A\varepsilon_{B_1}(A|\mathsf{P}\mathsf{T}\mathsf{U}_1\mathsf{T}^{-1}\mathsf{P}^{-1}|B_1),$$

and, since U, U_1 and U_2 commute with C by assumption, we find $(B_1|\mathsf{U}_1|A) = \varepsilon_A\varepsilon_{B_1}\alpha(A|\mathsf{U}_1|B_1)$, where α is a factor by which all the coupling constants of $\mathscr{L}$ are multiplied as a result of the transformation CPT ("physical invariance"). From this, since U_1 is parity conserving ($\varepsilon_A = \varepsilon_{B_1}$) and $\mathsf{U}_1^* = -\mathsf{U}_1$, we find $(B_1|\mathsf{U}_1|A) = -(B_1|\mathsf{U}_1|A)^*\alpha$. In a similar fashion we find $(B_2|\mathsf{U}_2|A) = (B_2|\mathsf{U}_2|A)^*\alpha$, with the same factor α as before. For the square of the modulus of the whole transition amplitude $(B|\mathsf{U}|A) = (B_1|\mathsf{U}_1|A) + (B_2|\mathsf{U}_2|A)$ we then have $|(B|\mathsf{U}|A)|^2 = [(B_2|\mathsf{U}_2|A)^2 - (B_1|\mathsf{U}_1|A)^2]\alpha$, so that as already stated there are no interference terms between the parity conserving and non-conserving transition amplitudes.

2. Salam's Gauge Transformation and the Two-Component Theory of Neutrinos

Following the discovery that the β-decay interaction is not invariant under space inversion, the hope has arisen that it may be so under some more general transformation.

One such is the neutrino gauge transformation proposed by Salam [15]), which is defined by

$$\psi_\nu \to \pm\gamma_5\psi_\nu, \qquad \bar{\psi}_\nu \to \pm\psi_\nu^*\gamma_5\gamma_4 = \mp\bar{\psi}_\nu\gamma_5. \tag{5}$$

We shall now investigate the implications of postulating that the theory is invariant under (5), an assumption which may eventually be contradicted by the experimental evidence.

It must be stressed that the free neutrino Lagrangian

$$\mathscr{L}_\nu = \bar{\psi}_\nu\left(\gamma_\mu\frac{\partial}{\partial x_\mu} + m_\nu\right)\psi_\nu \tag{6}$$

is transformed into

$$\mathscr{L}'_\nu = \bar{\psi}_\nu \left(\gamma_\mu \frac{\partial}{\partial x_\mu} - m_\nu \right) \psi_\nu \tag{6'}$$

by (5), as can be seen by using the anticommutativity of γ_5 and γ_μ. Thus only a field of massless neutrinos ($m_\nu = 0$) can be invariant under (5). Moreover, neutrinos cannot have a magnetic moment μ_ν. In fact, the Pauli interaction †

$$i\mu_\nu F_{\rho\sigma} \bar{\psi}_\nu \gamma_{[\rho\sigma]} \psi_\nu \tag{7}$$

changes sign under (5), since $\gamma_5 \gamma_{[\rho\sigma]} \gamma_5 = \gamma_{[\rho\sigma]}$, so that μ_ν must be zero.

The interaction Lagrangian (1) is transformed by (5) into

$$\mathscr{L}' = \sum_i (\bar{\psi}_p O_{1\mu} \ldots \psi_n)(\bar{\psi}_e O_{1\mu} \ldots (\pm\gamma_5 C_1 \pm C'_1)\psi_\nu), \tag{8}$$

so that invariance requires that

$$C_1 + C'_1\gamma_5 = \pm C'_1 \pm C_1\gamma_5, \tag{9}$$

and therefore

$$C_1 = \pm C'_1. \tag{10}$$

It is apparent from this result that in a theory invariant under (5) only one of the two dynamically independent components ψ_1 and ψ_2 †† of the neutrino field, defined by

$$\psi_\nu = \psi_1 + \psi_2 \tag{11}$$

and

$$\psi_1 = \tfrac{1}{2}(1-\gamma_5)\psi_\nu, \qquad \psi_2 = \tfrac{1}{2}(1+\gamma_5)\psi_\nu \tag{12}$$

interacts with the other particles. This fact, together with the vanishing of the neutrino rest mass, makes it possible to use a two-state theory of neutrinos [8,10,14,16]). This can be shown as follows.

We employ the Kramers set of γ-matrices. For $m = 0$, the four independent plane wave solutions of the Dirac equation reduce to

$$\begin{aligned} u'(\mathbf{k}, \uparrow) &= \begin{pmatrix} \alpha \\ \beta \\ 0 \\ 0 \end{pmatrix}, \qquad u'(\mathbf{k}, \downarrow) = \begin{pmatrix} 0 \\ 0 \\ -\beta^* \\ \alpha^* \end{pmatrix}, \\ v'(\mathbf{k}, \uparrow) &= \begin{pmatrix} 0 \\ 0 \\ -\beta^* \\ \alpha^* \end{pmatrix}, \qquad v'(\mathbf{k}, \downarrow) = \begin{pmatrix} \alpha \\ \beta \\ 0 \\ 0 \end{pmatrix}, \end{aligned} \tag{13}$$

since $\operatorname{ctg} \kappa = \infty$ and $c = 1$, $s = 0$. In the same set

† Here $\gamma_{[\rho\sigma]} = \frac{1}{2}(\gamma_\rho \gamma_\sigma - \gamma_\sigma \gamma_\rho)$.

†† For $m_\nu = 0$, ψ_1 and ψ_2 separately obey the Dirac equation if ψ does so.

$$\gamma'_5 = -\rho_2 \times I = \left(\begin{array}{cc|cc} -1 & 0 & & \\ 0 & -1 & 0 & \\ \hline & & 1 & 0 \\ 0 & & 0 & 1 \end{array}\right), \tag{14}$$

so that

$$\psi'_1 = \tfrac{1}{2}(1-\gamma'_5)\psi'_\nu = \sum_{\mathbf{k}} \begin{pmatrix} \alpha \\ \beta \\ 0 \\ 0 \end{pmatrix} [a_\nu(\mathbf{k}, \uparrow)e^{i(k,x)} + b_\nu^*(\mathbf{k}, \downarrow)e^{-i(k,x)}]. \tag{15}$$

This goes to show that an interaction with $C_1 = -C'_1$, in which only the component ψ_1 occurs, involves only neutrinos with spin parallel to the momentum and antineutrinos with spin antiparallel.

We can now write

$$\psi'_1 = \tfrac{1}{2}(1-\gamma'_5)\psi'_\nu = \begin{pmatrix} \phi' \\ 0 \end{pmatrix}, \tag{16}$$

where ϕ' is a two-component field operator. Since

$$\gamma'_\mu \frac{\partial}{\partial x_\mu} \psi'_1 = 0$$

we have

$$\sigma \cdot \operatorname{grad} \phi' + \frac{\partial \phi'}{\partial t} = 0, \tag{17}$$

which is the basis of the two state or two component theory for particles of spin $\frac{1}{2}$ and zero rest mass. That a two component relativistic theory of spin $\frac{1}{2}$ particles is possible has long been known [19]). Such a theory has always been rejected because of its intrinsic violation of space and time inversion invariance, a reason which is no longer valid †.

† In sect. 3.3 of Ch. I we stated that the Majorana theory of neutrinos makes use of only two independent components. Thus, in the Kramers set,

$$\psi' = \begin{pmatrix} \psi'_1 \\ \psi'_2 \\ -\psi'^*_2 \\ \psi'^*_1 \end{pmatrix}$$

is the field operator of Majorana particles, and the Dirac equation for zero rest mass reduces to

$$\sigma \cdot \operatorname{grad} \begin{pmatrix} \psi'_1 \\ \psi'_2 \end{pmatrix} + \frac{\partial}{\partial t} \begin{pmatrix} \psi'_1 \\ \psi'_2 \end{pmatrix} = 0$$

and its Hermitian conjugate.

Nevertheless, the expansion of the field operator, also for zero rest mass, is different from (15).

From (12) it is apparent that particles have spin parallel to the momentum and antiparticles have it antiparallel. In fact, for a solution of momentum $\mathbf{k}$ we have

$$\boldsymbol{\sigma} \cdot \mathbf{k} - k_0 = 0,$$

with $k_0 = |\mathbf{k}|$, which can be interpreted as meaning either that for energy $|\mathbf{k}|$ and momentum $\mathbf{k}$ the component of $\boldsymbol{\sigma}$ in the direction of $\mathbf{k}$ is equal to 1, or that for energy $-k_0$ the component of $\boldsymbol{\sigma}$ along $-\mathbf{k}$ is -1. In the hole theory, the positive energy state of momentum $\mathbf{k}$ corresponds to a particle of momentum $\mathbf{k}$ and spin parallel to $\mathbf{k}$. On the other hand, the state with energy $-k_0$, momentum $-\mathbf{k}$ and spin antiparallel to $-\mathbf{k}$, will correspond to an antiparticle of energy k_0, momentum $\mathbf{k}$ and spin antiparallel to $\mathbf{k}$.

This outlines the equivalence of the two state theory of spin $\frac{1}{2}$ particles with the ψ_1-component theory of the neutrino.

Similarly, the ψ_2-component theory is equivalent to a two-state theory in which the particles have spin antiparallel to the momentum and the antiparticles have it parallel. The essential point of these theories is that a neutrino of given momentum has only one spin state. The spin and the momentum together define automatically the sense of a screw, so that the name "screwon" has been suggested for the particles. The theory does not conserve parity, since the space inversion P inverts the momentum of a neutrino but not its spin. As in the theory the two are always either parallel (ψ_1) or antiparallel (ψ_2), P applied to a neutrino state of the type ψ_1 leads to a state of the type ψ_2 and vice versa, so that the ψ_1- and ψ_2-component theories cannot separately be P-invariant. They are, however, separately invariant under CP, as can easily be seen by applying our previous reasoning for example to eq. (15), since CP changes a neutrino into an antineutrino and simultaneously reverses its momentum while keeping the spin direction fixed.

If in the Lagrangian (1) ψ_ν is replaced by ψ_ν^c, so that the reaction $n \to p+e+\nu$ takes place, the preceding considerations are still valid with the words neutrino and antineutrino interchanged and a_ν and b_ν also interchanged.

Summarizing we have:

$$\psi' = \Sigma \left\{ \begin{pmatrix} \alpha \\ \beta \\ 0 \\ 0 \end{pmatrix} [c(\mathbf{k}, \uparrow) e^{i(k,x)} + c^*(\mathbf{k}, \downarrow) e^{-i(k,x)}] + \begin{pmatrix} 0 \\ 0 \\ -\beta^* \\ \alpha^* \end{pmatrix} [c(\mathbf{k}, \downarrow) e^{i(k,x)} + c^*(\mathbf{k}, \uparrow) e^{-i(k,x)}] \right\},$$

and ψ' can emit *and* absorb both right handed and left handed neutrinos. This makes possible the process of double beta decay, in which a (Majorana) neutrino (say, right-handed) is emitted by a neutron,

$$n \to p + \beta^- + \nu(\uparrow)$$

and absorbed by another neutron

$$n + \nu(\uparrow) \to p + \beta^-,$$

so that two β-rays, unaccompanied by neutrinos, are emitted.

$$\begin{aligned} \mathscr{L}(\psi_\nu): \quad & C_1 = -C'_1, \qquad n \to p+e+\bar{\nu}(\downarrow), \\ & C_1 = +C'_1, \qquad n \to p+e+\bar{\nu}(\uparrow), \end{aligned} \tag{19}$$

$$\begin{aligned} \mathscr{L}(\psi_\nu^c): \quad & C_1 = -C'_1, \qquad n \to p+e+\nu(\downarrow), \\ & C_1 = +C'_1, \qquad n \to p+e+\nu(\uparrow), \end{aligned} \tag{19'}$$

where $\bar{\nu}$ and ν denote an antineutrino and a neutrino, respectively, and $(\downarrow)$ and $(\uparrow)$ signify that the spin is antiparallel or parallel to the momentum. If neutrinos are Majorana particles, $\nu \equiv \bar{\nu}$, so that one neutral massless particle of spin $\frac{1}{2}$ is emitted in the neutron decay, with spin antiparallel to the momentum if $C_1 = -C'_1$ and parallel if $C_1 = C'_1$. We shall say that a right-handed screwon is emitted if $C_1 = C'_1$, and a left-handed one if $C_1 = -C'_1$.

In the two-state theory of neutrinos the coefficient β for the correlation between the momentum of the β-ray and the spin of the oriented nucleus is[8])†

$$\beta = \mp v_e \frac{|C_T|^2 - |C_A|^2 - \dfrac{2Ze^2}{k_e} \operatorname{Im}(C_A C_T^*)}{|C_T|^2 + |C_A|^2}, \tag{20}$$

where the $(-)$ sign refers to the emission of a left-handed screwon and the $(+)$ sign to the emission of a right-handed one.

2.1. ANGULAR CORRELATIONS IN SUCCESSIVE MESON DECAYS[2, 3, 4, 9])

We here consider the decay of a π-meson into a μ-meson (spin $\frac{1}{2}$) and a neutrino. With an interaction Lagrangian of the form

$$\mathscr{L} = i \frac{\partial \phi}{\partial x_\alpha} g \bar{\psi}_\mu \gamma_\alpha (1 \pm \gamma_5) \psi_\nu + \text{H.C.}, \tag{21}$$

which is invariant under (5), we then have the following possibilities:

$$\begin{aligned} &\text{(A)} \quad \begin{cases} \pi^+ \to \mu^+ + \bar{\nu}(\uparrow), \\ \pi^- \to \mu^- + \nu(\downarrow), \end{cases} \\ &\text{(B)} \quad \begin{cases} \pi^+ \to \mu^+ + \bar{\nu}(\downarrow), \\ \pi^- \to \mu^- + \nu(\uparrow). \end{cases} \end{aligned} \tag{22}$$

In the rest frame of the π-meson, the neutrino and μ-meson momenta are equal and opposite. We consider the conservation of the component of the angular momentum along the direction of $\mathbf{p}_\mu$, the momentum of the μ-meson. The orbital angular momentum contributes nothing to this component, so that the component of the spin of the μ-meson is determined by that of the neutrino or antineutrino. We therefore have that for (A) the components of the spins of $\mu^\pm$ along the momenta $\mathbf{p}_{\mu^\pm}$ are $\pm\frac{1}{2}$, respectively, whereas for (B)

† In conformity with the experimental evidence Re $[C_A C_T^*]$ has been set equal to zero (vanishing of the Fierz interference terms).

they are $\mp\frac{1}{2}$. The μ-mesons produced in the decay are completely polarized, and if they remain so while they slow down, their decay into an electron and two neutrinos should be characterized by an asymmetry in the angular distribution of the electron emitted. Thus the study of the correlation between the momentum of the μ-meson emitted in the decay of a π-meson and that of the electron emitted in the decay of the μ-meson will establish whether parity is conserved in π-meson decay.

Using the previously proved theorem, according to which, if any left-right asymmetry exists, the part of the asymmetry which is independent of the distortion of the final state wave functions can arise only if particle-antiparticle conjugation symmetry breaks down, we must conclude that, since the particles in the final states of the decays $\pi \to \mu+\nu$ and $\mu \to e+\nu+\nu$ are free, the detection of parity non-conservation becomes impossible if C is strictly conserved.

It is important to stress that the invariance of the π-meson decay interaction under C does *not* follow from the equality of the π^+ and π^- lifetimes.

The reasoning leading to the belief that it would was the following:

If a particle A decays by virtue of an interaction which is invariant under C into certain decay products a, b, c . . ., and the antiparticle $\overline{A}$ decays into the decay products $\bar{a}, \bar{b}, \bar{c}, \ldots$ ($\bar{a}, \bar{b}, \bar{c} \ldots$ being the antiparticles of a, b, c . . .), the lifetimes of A and $\overline{A}$ will be equal. In fact, the transition amplitudes for the two processes can differ only by a factor of modulus one, since schematically

$$(abc \ldots |U|A) = (abc \ldots |C^{-1} \cdot CUC^{-1} \cdot C|A) = \varepsilon(\bar{a}\bar{b}\bar{c} \ldots |U|\overline{A}), \quad (23)$$

where ε is a number of modulus one.

This would seem to prove the C-invariance of the weak interactions responsible for the decays

$$\pi^+ \to \mu^+ + \tilde{\nu}, \qquad \pi^- \to \mu^- + \nu,$$

since the differences between the lifetimes of the particle π^+ and of the antiparticle π^- are within the experimental error.

However, Lee, Oehme and Yang [7]) have shown that the equality of the lifetimes is already insured by the physical invariance under CPT, which, as has been previously stressed, is a consequence of the invariance under proper Lorentz transformations.

Thus we have the theorem: "If a particle A decays through a weak interaction, and if the particle and its antiparticle $\overline{A}$ do not decay into the same final products (as e.g. when A is charged), then to the lowest order in the interaction the lifetimes of A and $\overline{A}$ are the same, even if the weak interaction is *not* invariant under particle-antiparticle conjugation".

Proof: Considering for simplicity a spinless system and A and $\overline{A}$ at rest, we have

$$(B|U|A) = \alpha(B|T^{-1}P^{-1}C^{-1}UCPT|A) = \alpha\varepsilon_A\varepsilon_B(A|C^{-1}UC|B) = \alpha\varepsilon'_A\varepsilon'_B(\overline{A}|U|\overline{B}), \tag{24}$$

α, ε_A, ε_B, ε'_A, ε'_B being all numbers of modulus one, from which the theorem readily follows.

We conclude by remarking [15]) that the Lagrangians

$$\mathscr{L}_A = \sum_i f_i(\bar{\psi}_\mu O_i \psi_e)(\bar{\psi}_\nu O_i \psi_\nu) + \text{H.C.} \tag{25}$$

and

$$\mathscr{L}_B = \sum_i f_i(\bar{\psi}_\mu O_i \psi_e^c)(\bar{\psi}_\nu^c O_i \psi_\nu) + \text{H.C.} \tag{25'}$$

for μ-meson decay correspond the former to the emission of a neutrino and an antineutrino, the latter to the emission of two neutrinos or two antineutrinos.

If invariance under the transformation $\psi_\nu \to \pm\gamma_5\psi_\nu$ is postulated, $\mathscr{L}_A$ may consist only of V and A, $\mathscr{L}_B$ of S, T, P interactions.

3. More General Gauge Transformations

Parity non-conservation is still at the time of writing these notes an open question. Attempts are being made to find out wheter the weak interactions are not by any chance invariant under transformations even more general than (5). Pursey [13, 12]) has studied the transformations

$$\psi_\nu \to e^{i\alpha\gamma_5 + i\beta}\psi_\nu \tag{26}$$

($\exp(i\alpha\gamma_5) = \cos\alpha + i\gamma_5\sin\alpha$), of which (5) are special cases for $\beta = \pm\pi/2$, $\alpha = \pi/2$, and which are compatible only with neutrinos of zero rest mass and zero magnetic moment in analogy with what was shown in eqs. (6), (7).

If the Lagrangian is invariant, the coupling constants (C_1, C'_1) and (B_1, B'_1) in

$$(\bar{\psi}_p O_1 \psi_n)(\bar{\psi}_e O_1(C_1 + C'_1\gamma_5)\psi_\nu) = (\bar{\psi}_p O_1 \psi_n)(\bar{\psi}_e O_1(B_1 + B'_1\gamma_5)e^{i\alpha\gamma_5 + i\beta}\psi_\nu) \tag{27}$$

are physically equivalent. From

$$C_1 + C'_1\gamma_5 = (B_1 + B'_1\gamma_5)e^{i\alpha\gamma_5 + i\beta} \tag{28}$$

we find

$$\begin{cases} C_1 = e^{i\beta}(B_1\cos\alpha + iB'_1\sin\alpha), \\ C'_1 = e^{i\beta}(B'_1\cos\alpha + iB_1\sin\alpha). \end{cases} \tag{29}$$

It is easy to show that certain bilinear forms of the coupling constants are invariant. E.g. for $\beta = 0$

$$\begin{cases} C_1C_1 - C'_1C'_1 = B_1B_1 - B'_1B'_1, \\ C_1C'_1 - C'_1C_1 = B_1B'_1 - B'_1B_1, \end{cases} \tag{30}$$

and, for any α and β,

$$C_1 C'_j{}^* + C'_1 C_j{}^* = B_1 B'_j{}^* + B'_1 B_j{}^*,$$
$$C_1 C_j{}^* + C'_1 C'_j{}^* = B_1 B_j{}^* + B'_1 B'_j{}^*. \tag{31}$$

It is important to stress that necessary and sufficient conditions for P, T and C invariance of the β-decay interaction are:

(i) P-invariance: $C_j C'_k{}^* + C'_j C_k{}^* = 0$ (all j and k);

(ii) T-invariance: $\mathrm{Im}\,(C_j C_k{}^* + C'_j C'_k{}^*) = 0$

and $\mathrm{Im}\,(C_j C'_k{}^* + C'_j C_k{}^*) = 0$ (all j and k);

(iii) C-invariance: $\mathrm{Im}\,(C_j C_k{}^* + C'_j C'_k{}^*) = 0$

and $\mathrm{Re}\,(C_j C'_k{}^* + C'_j C_k{}^*) = 0$ (all j and k), (32)

so that they are expressed in a form which is invariant under the transformation (26). The sufficient conditions (3) are special ways of satisfying (32). The coefficients of the energy dependent and of the energy independent parts in (4) are also clearly invariant under (26).

Along the same lines, Touschek [17,18,12,13]) has attempted to postulate the invariance of the weak interactions under the simultaneous transformation

$$\psi_\nu \to e^{i\alpha\gamma_5}\psi_\nu \tag{33}$$

for the neutrino field, and

$$\psi_l \to e^{i\alpha l_l}\psi_l \tag{34}$$

for the other particles, which are designated by the index i, so that l_l plays the part of a "lepton charge" characteristic of the i-th type of particle.

In this way selection rules can be found for the various decay processes, which are consistent only with certain assignments of lepton charges. To give an example, if the Lagrangian for π-meson decay is to be invariant, from

$$\phi(\bar\psi_\mu(C+C'\gamma_5)\psi_\nu) \to e^{i\alpha l_{\pi^+}}(\bar\psi_\mu e^{-i\alpha l_{\mu^+}+i\alpha\gamma_5}(C+C'\gamma_5)\psi_\nu) \tag{35}$$

we find that $C = \pm C'$ and $l_{\pi^+} - l_{\mu^+} = \pm l$. Such attempts are, however, still in a very speculative stage.

References to Chapter VI

1) J. S. Bell, Proc. Roy. Soc. A **231** (1955) 479
2) C. Castagnoli, C. Franzinetti and A. Manfredini, Nuovo Cimento **5** (1957) 684
3) J. I. Friedman and V. L. Telegdi, Phys. Rev. **105** (1957) 1681
4) R. L. Garwin, L. M. Lederman and M. Weinrich, Phys. Rev. **105** (1957) 1415
5) T. D. Lee and C. N. Yang, Phys. Rev. **104** (1956) 254
6) T. D. Lee and C. N. Yang, Phys. Rev. **104** (1956) 822
7) T. D. Lee, R. Oehme and C. N. Yang, Phys. Rev. **106** (1957) 340
8) T. D. Lee and C. N. Yang, Phys. Rev. **105** (1957) 1671
9) G. Lüders, Mat. Fys. Medd. Dan. Vid. Selsk. **28** (1954) no. 5
10) J. A. McLennan, Phys. Rev. **106** (1957) 821
11) W. Pauli, Niels Bohr and the Development of Physics (London, 1955) p. 30
12) W. Pauli, Nuovo Cimento **6** (1957) 204

13) D. L. Pursey, Nuovo Cimento **6** (1957) 266
14) L. A. Radicati and B. Touschek, Nuovo Cimento **5** (1957) 1693
15) A. Salam, Nuovo Cimento **5** (1957) 299
16) J. Serpe, Physica **18** (1952) 295
17) B. Touschek, Nuovo Cimento **5** (1957) 754
18) B. Touschek, Nuovo Cimento **5** (1957) 1281
19) H. Weyl, Z. für Phys. **56** (1929) 330
20) C. S. Wu, R. Hudson, R. Hayward, D. D. Hopper and R. P. Hudson, Phys. Rev. **105** (1957) 1413

CHAPTER VII

NEW PARTICLES

1. Résumé of Experimental Results

With the particles so far considered physicists have been acquainted for at least ten years, so that their properties are fairly well known. Their number has been increased by the discovery of a host of new particles. Some of these have mass greater than the nucleon mass M †. They have been given the name of "hyperons", and are denoted by the following symbols:

Λ^0 (neutral, mass 1.2 M),

Σ^+, Σ^0, Σ^- (positive, neutral, negative, having masses approximately equal to 1.3 M),

Ξ^- (negative, mass 1.4 M).

They all have spin $\frac{1}{2}$. The existence of the hyperon Σ^0 is not well ascertained, and that of Ξ^0, the neutral partner of Ξ^- has been suggested. Together with the nucleons, the hyperons form the "baryon" family.

The meson family has also been enriched by the discovery of the K-particles. These are the parent particles in a varying series of decay processes, such as

$$\begin{aligned}
K^+_{\pi 2} &\to \pi^+ + \pi^0,\\
\theta^0 &\to \pi^+ + \pi^-,\\
\tau^+ &\to 2\pi^+ + \pi^-,\\
\tau'^+ &\to \pi^+ + 2\pi^0,\\
\tau^- &\to 2\pi^- + \pi^+,\\
K^+_{\mu 2} &\to \mu^+ + \nu,\\
K^+_{\mu 3} &\to \mu^+ + 2?,\\
K^+_{e3} &\to e^+ + 2?.
\end{aligned}$$

The different symbols used for the particles in the left members of these

† We neglect the difference between the neutron and the proton mass.

reaction formulae signify that, in spite of their having approximately equal masses ($\approx 966\ m_e$) and being all of integer spin, they are not necessarily identical. The two modes of decay θ^0 and τ^+, for instance, imply that θ^0 and τ^+ should have opposite intrinsic parity, unless their spin is greater than one, an assumption we should make with some reluctance [1]). The recent discovery that parity is not conserved in β-decay has made this type of argument less stringent. In fact, the long lifetimes of the K-mesons ($\tau_{K^\pm} \approx 1.7 \times 10^{-8}$ sec, $\tau_{K^0} \approx 10^{-10}$ sec) would seem to point to the weakness and, by analogy with β-decay, to the likely parity violation of the K-meson decay interactions.

The hyperon decay processes:

$$\begin{aligned} \Lambda^0 &\to p+\pi^-, \\ \Sigma^+ &\to p+\pi^0 \\ &\to n+\pi^+, \\ \Sigma^- &\to n+\pi^-, \end{aligned} \qquad \Xi^- \to \Lambda^0+\pi^-,$$

with lifetimes of the order of 10^{-10} sec are also due to fairly weak interactions.

We are confronted with two problems, which, for the time being, must be regarded as distinct.

The first is to classify the new particles in terms of quantum numbers derived from the conservation laws with which we are already familiar, or from new ones. It appears that, for this purpose, the idea of an isobaric spin space (isospace) should be taken more seriously than in the past [6, 7]).

The second problem is of a more specific nature. It arises from the necessity of reconciling the weakness of the hyperon decay interactions, as evidenced by the comparatively long lifetimes, with the frequency with which production reactions such as

$$\pi^-+p \to \Lambda^0+\theta^0, \qquad \pi^-+p \to \Sigma^-+K^+$$

are found to occur.

A striking difference between production and decay reactions is that in the former at least two "new" particles are involved ("associated production") [5]) whereas only one occurs in the latter. In order to be "strong" a reaction must conserve some quantity which is an attribute of the "new" particles alone. This quantity seems to have been found in the "strangeness" [3, 4]) of Gell-Mann and the "attribute" of Sachs [10]). The two are to some extent equivalent, so we shall mention only the former. The strangeness quantum number S takes the values: 0 (nucleons), -1 (Λ^0), -1 ($\Sigma^+, \Sigma^0, \Sigma^-$), -2 (Ξ^-), 0 (π-mesons), $+1$ (K^+, K^0), -1 ($K^-, \overline{K}^0$) †. A strong reaction is one which

† $\overline{K}^0$ is the antiparticle of K^0. We now conform to the idea of a unique K-meson type.

conserves strangeness, i.e. one for which the sum of the S's of the initial particles is equal to that of the final particles. For example

$$\begin{array}{cccccc} \pi^- & + & \mathrm{p} & \rightarrow & \Lambda^0 & + & \theta^0 \\ (0) & & (0) & & (-1) & & (+1). \end{array}$$

On the other hand

$$\begin{array}{cccccc} \mathrm{n} & + & \mathrm{n} & \rightarrow & \Lambda^0 & + & \Lambda^0 \\ (0) & & (0) & & (-1) & & (-1) \end{array}$$

cannot be a strong reaction, neither can any of the decay reactions previously mentioned.

It is certainly worth noticing that K^0 has been given a strangeness opposite to that of the antiparticle $\overline{\mathrm{K}}^0$. Though neutral and spinless, K^0 and $\overline{\mathrm{K}}^0$ must be regarded as distinct, a circumstance which justifies the remark made in the footnote on page 307.

The necessity for this distinction is indeed compelling, lest the very law of conservation of strangeness in the strong reactions be circumvented. Take for instance the strangeness conserving reaction $\pi^- + \mathrm{p} \rightarrow \Lambda^0 + \theta^0$. The two reactions $\theta^0 \rightarrow \mathrm{n} + \bar{\Lambda}^0$, $\bar{\theta}^0 \rightarrow \bar{\mathrm{n}} + \Lambda^0$ differ from the above in that a π-meson has been absorbed (which is a strong process, due to the large value of the π-meson-nucleon coupling constant), and that particles have been shifted from one member to another and replaced by antiparticles. This, of course, violates energy conservation. If, however, the two reactions were to be regarded as two steps in a perturbation calculation of the process $\mathrm{n} + \bar{\Lambda}^0 \rightarrow \theta^0 \overset{?}{\equiv} \bar{\theta}^0 \rightarrow \bar{\mathrm{n}} + \Lambda^0$, which would be based on the identity of θ^0 and $\bar{\theta}^0$, this would be strong, and the process $\mathrm{n} + \mathrm{n} \rightarrow \Lambda^0 + \Lambda^0$ derived from it would also occur strongly at sufficiently high energy. But this last reaction does not conserve strangeness and indeed has not been encountered in the experiments. We must therefore insist on θ^0 and $\bar{\theta}^0$ being distinct particles.

2. Conservation of Baryons

No reaction has ever been observed in which a baryon has disappeared without the formation of another baryon. All the processes listed in these notes and consequently the interactions which cause them, conform to this rule. The law of conservation of baryons is therefore generally accepted. It states that in a reaction $\mathrm{A} \rightarrow \mathrm{B}$,

$$n_{\mathrm{A}} - \bar{n}_{\mathrm{A}} = n_{\mathrm{B}} - \bar{n}_{\mathrm{B}}, \tag{1}$$

where n_{A} is the number of baryons and $\bar{n}_{\mathrm{A}}$ the number of antibaryons in the initial state, and n_{B}, $\bar{n}_{\mathrm{B}}$ are the analogous numbers for the final state.

This law stems from the invariance of all interactions under the baryon gauge transformation B, which multiplies all one-baryon states by $e^{i\alpha}$ and

all one-antibaryon states by $e^{-i\alpha}$, without affecting any of the degress of freedom:

$$\mathsf{B}a^*|0) = e^{i\alpha}a^*|0), \qquad \mathsf{B}b^*|0) = e^{-i\alpha}b^*|0), \tag{2}$$

α being the same for all types of baryons, but otherwise arbitrary. The corresponding transformation law for all baryon operators $\psi_n, \psi_p, \psi_{\Lambda^0}, \psi_\Sigma, \psi_\Xi$ is

$$\mathsf{B}\psi\mathsf{B}^{-1} = e^{-i\alpha}\psi, \qquad \mathsf{B}\psi^*\mathsf{B}^{-1} = e^{i\alpha}\psi^*.$$

The strong (I, 75) and weak (VI, 1) interactions for the „old" particles are invariant under B, since the proton and neutron operators occur only in the bilinear forms $\psi^*\psi$ †. The interactions among "new" particles must also be built from such bilinear forms of the baryon field operators ††.

The conservation law is immediately derived from $\mathsf{BUB}^{-1} = \mathsf{U}$ and

$$(\mathrm{B}|\mathsf{U}|\mathrm{A}) = (\mathrm{B}|\mathsf{B}^{-1}\cdot\mathsf{BUB}^{-1}\cdot\mathsf{B}|\mathrm{A}) = e^{i\alpha(n_A-\bar{n}_A-n_B+\bar{n}_B)}(\mathrm{B}|\mathsf{U}|\mathrm{A}), \tag{4}$$

since the transition amplitude will vanish unless the exponent $(n_A-\bar{n}_A-n_B+\bar{n}_B)$ is zero.

3. Isobaric spin

Already in the study of low energy nuclear physics it becomes clear that there is more to the idea of isobaric spin than a mere way of labelling the proton and neutron components in the 8-component operator $\Psi \equiv \binom{\psi_n}{\psi_p}$ of the nucleon field. As before mentioned the components $\binom{\psi_n}{0}$ and $\binom{0}{\psi_p}$ are eigenvectors of the matrix $\frac{1}{2}\tau_3 = \frac{1}{2}\left(\begin{smallmatrix}1 & 0\\ 0 & -1\end{smallmatrix}\right)$ with eigenvalues ± 1. Once the idea of an *isospace* is accepted, protons and neutrons can be regarded as particles of spin $\frac{1}{2}$ *at rest* in that space, or rather as particles of spin $\frac{1}{2}$ with zero "orbital" angular momentum. Some years ago Pais made an attempt to identify the hyperons with states of non-zero orbital angular momentum in isospace [6, 7]), and later he went as far as adding a new dimension, extending to the "iso-space-time" the familiar particle representations of ordinary space-time [8, 11]). Such speculations, however, did not bear fruit, and in the following we shall consider exclusively particles which have isospin I_3, but no isobaric orbital angular momentum.

† Conservation of charge is a consequence of the invariance under the gauge transformation of the second kind $\psi_j \to e^{iq_j\alpha}\psi_j$ for all fields of charged particles, q_j denoting the charge of the particles of the field j.

†† Here we make no distinction between phase transformations (α an arbitrary constant) and gauge transformations ($\alpha(x)$ an arbitrary function of $(\mathbf{r}, t)$), thus tacitly assuming that no derivatives of the baryon field operators occur in the interaction Lagrangian. Note, however, that the free baryon Lagrangian does involve such derivatives, and is not invariant under the baryon gauge transformation ($\psi \to e^{-i\alpha(x)}\psi$). Invariance can be achieved by introducing a neutral vector meson field $\mathfrak{A}_\mu$, interacting in the same way with all the baryons, which undergoes a gauge transformation of the first kind, $\mathfrak{A}_\mu \to \mathfrak{A}_\mu + \partial\alpha(x)/\partial x_\mu$ matching that of the baryons [12]). Similarly Lagrangians of fields of charged particles are invariant under gauge transformations of the second kind † accompanied by gauge transformations of the first kind $A_\mu \to A_\mu + \partial\alpha/\partial x_\mu$ for the electromagnetic field.

A rotation ϕ around the third axis in isospace will be represented, as in ordinary space, by a transformation $\mathfrak{R}_\phi$ of the field operators which is equivalent to applying the operator $\exp(iI_3\phi)$ from the left. For the nucleons $I_3 = \frac{1}{2}\tau_3$ and therefore

$$\mathfrak{R}_\phi \Psi \mathfrak{R}_\phi^{-1} = e^{+\frac{1}{2}i\tau_3\phi}\Psi, \tag{5}$$

from which

$$\mathfrak{R}_\phi \psi_p \mathfrak{R}_\phi^{-1} = e^{-i\phi/2}\psi_p, \qquad \mathfrak{R}_\phi \psi_n \mathfrak{R}_\phi^{-1} = e^{+i\phi/2}\psi_n, \tag{6}$$

since τ_3 takes the values ± 1 for the neutron and proton components respectively.

If we write

$$\psi_p = \sum(a_p + b_p^*)$$

from which the free particle solutions of the Dirac equation are omitted for brevity's sake and where a_p and b_p^* are respectively destruction operators for protons and creation operators for antiprotons, we find

$$\mathfrak{R}_\phi a_p \mathfrak{R}_\phi^{-1} = e^{-i\phi/2}a_p, \qquad \text{but } \mathfrak{R}_\phi b_p \mathfrak{R}_\phi^{-1} = e^{+i\phi/2}b_p. \tag{7}$$

Thus one-proton and one-antiproton states are eigenstates of $\mathfrak{R}_\phi$ with the eigenvalues $e^{\pm i\phi/2}$ respectively,

$$\mathfrak{R}_\phi |p) = e^{i\phi/2}|p), \qquad \mathfrak{R}_\phi |\bar{p}) = e^{-i\phi/2}|\bar{p}). \tag{8}$$

The connection between the operator of rotations around an axis and the component of the angular momentum along the same axis may be taken over in isospace, so that $I_3 = (1/i)(d\mathfrak{R}_\phi/d\phi)_{\phi=0}$ from which

$$I_3 |p) = \tfrac{1}{2}|p), \qquad I_3 |\bar{p}) = -\tfrac{1}{2}|\bar{p}). \tag{9}$$

Similarly for neutrons and antineutrons

$$I_3 |n) = -\tfrac{1}{2}|n), \qquad I_3 |\bar{n}) = \tfrac{1}{2}|\bar{n}). \tag{10}$$

In isospace the π-meson components (ϕ_1, ϕ_2, ϕ_3) play the same role as the components (A_x, A_y, A_z) of a spin 1 field in ordinary space. Since (ϕ_1, ϕ_2, ϕ_3) are Hermitian operators, "particles" of the type i $(i = 1, 2, 3)$ are identical with the antiparticles of the same type. However, mesons of the (1, 2) types or, pursuing our analogy, "polarized" in the 1 and 2 directions, have no direct physical meaning and are not eigenstates of the iso-angular-momentum. On the other hand, "circularly polarized" mesons

$$(a_1^* - ia_2^*)|0) = a^*|0), \qquad (a_1^* + ia_2^*)|0) = b^*|0) \tag{11}$$

correspond to the values ± 1 of the third component of the isospin. They describe $\pi^\pm$-mesons †. Similarly

$$a_3^*|0) \tag{11'}$$

† Note that the particle π^+ and the antiparticle π^- have opposite values of I_3, as was the case for nucleons and antinucleons.

is a "longitudinal" meson with $I_3 = 0$.

To see this we summarize the formulae for rotations around the third axis:

$$\mathfrak{R}_\phi \boldsymbol{\phi} \mathfrak{R}_\phi^{-1} = \boldsymbol{\phi}', \tag{12}$$

with †

$$\phi'_1 = \phi_1 \cos\phi + \phi_2 \sin\phi, \qquad \phi'_2 = -\phi_1 \sin\phi + \phi_2 \cos\phi \qquad \phi'_3 = \phi_3 \tag{13}$$

and

$$\mathfrak{R}_\phi \phi \mathfrak{R}_\phi^{-1} = e^{-i\phi}\phi, \qquad \mathfrak{R}_\phi \phi^* \mathfrak{R}_\phi^{-1} = e^{+i\phi}\phi^*, \qquad \mathfrak{R}_\phi \phi_3 \mathfrak{R}_\phi^{-1} = \phi_3 \tag{14}$$

with

$$\phi = \frac{\phi_1 + i\phi_2}{\sqrt{2}}, \qquad \phi^* = \frac{\phi_1 - i\phi_2}{\sqrt{2}}.$$

Therefore

$$\mathfrak{R}_\phi a^* |0) = e^{i\phi} a^* |0), \qquad \mathfrak{R}_\phi b^* |0) = e^{-i\phi} b^* |0), \tag{15}$$

$$\mathfrak{R}_\phi a_3^* |0) = a_3^* |0), \tag{15'}$$

and, using once more the expression for the angular momentum in terms of $\mathfrak{R}_\phi$ our assertion is easily proved.

3.1.

When dealing with the strong interactions among old particles, we stated that, if electromagnetic interactions are neglected, there obtains complete invariance under rotations in isospace ††.

There is no preferred direction in this latter. An arbitrary one can be chosen as an "axis of quantization" to distinguish between protons and neutrons and between charged mesons by the isospin components along it. The electromagnetic field, on the other hand, fixes a direction, which is conventionally chosen as that of the third axis. This is apparent from the form of the electromagnetic interaction of nucleons, i.e. $\overline{\Psi}\frac{1}{2}(1-\tau_3)\gamma_\mu \Psi \cdot A_\mu$ and of mesons

$$-ie\left(\phi^* \frac{\partial\phi}{\partial x_\mu} - \phi \frac{\partial\phi^*}{\partial x_\mu}\right) A_\mu - e^2 A_\mu^2 \phi^* \phi$$

$$= e\left(\phi_1 \frac{\partial\phi_2}{\partial x_\mu} - \phi_2 \frac{\partial\phi_1}{\partial x_\mu}\right) A_\mu - e^2 A_\mu^2 \frac{\phi_1^2 + \phi_2^2}{2}.$$

Invariance for rotations around the third axis still obtains. This is clear

† In general (ϕ_1, ϕ_2, ϕ_3) transform like the components of a vector under rotations around an arbitrary axis.

†† Using the results of the previous section, we can easily prove that the π-meson-nucleon interaction $\overline{\Psi}\boldsymbol{\tau} \cdot \boldsymbol{\phi}\Psi$ is invariant under rotations around the third axis. In fact,

$$\mathfrak{R}_\phi \overline{\Psi}\boldsymbol{\tau}\boldsymbol{\phi}\Psi\mathfrak{R}_\phi^{-1} = \overline{\Psi} e^{-i\tau_3\phi/2}(\tau_1\phi'_1 + \tau_2\phi'_2 + \tau_3\phi'_3) e^{+i\tau_3\phi/2}\Psi = \overline{\Psi}\boldsymbol{\tau} \cdot \boldsymbol{\phi}\Psi,$$

since τ_3 anticommutes with τ_1 and τ_2 so that e.g.

$$e^{-i\tau_3\phi/2}\tau_1 e^{+i\tau_3\phi/2} = \tau_1 e^{-i\tau_3\phi} = \tau_1(\cos\phi + i\tau_3 \sin\phi) = \tau_1 \cos\phi + \tau_2 \sin\phi.$$

from eq. (5) for the nucleon interaction, and for the π-meson interaction from the manifest invariance of the vector product component $[\boldsymbol{\phi} \times (\partial \boldsymbol{\phi}/\partial x_\mu)]_3$ and of $\boldsymbol{\phi}^2 - \phi_3^2$.

In conclusion, within the electron-photon-nucleon-π-meson system there is invariance under rotations in isospace around the third axis. For any reaction $A \to B$ the selection rule

$$I_3(A) = I_3(B) \tag{16}$$

can be established by proceeding as in sect. 2. $I_3(A)$ and $I_3(B)$ are the sums of the third components of the isospin ($+\frac{1}{2}$: proton and antineutron, $-\frac{1}{2}$: neutron and antiproton, $+1 : \pi^+$-meson, $-1 : \pi^-$-meson, $0 : \pi^0$-meson) of the particles in the initial and final state.

If electromagnetic effects are neglected, the selection rule

$$|\mathbf{I}(A)| = |\mathbf{I}(B)| \tag{17}$$

for the magnitudes of the total isospin vectors also holds.

We finally remark that the weak β-decay interactions are in no way invariant under rotations in isospace. There has so far been no definite answer to the question whether leptons (μ-mesons, electrons, neutrinos) possess an isobaric spin.

4. Classifications of new Particles

The most successful classification of new particles employs the isobaric spin together with either the strangeness S of Gell-Mann [3, 4]) and the "baryon number" n defined in sect. 2 (+1 for baryons, −1 for antibaryons) or the "isoparity" U of Prentki and d'Espagnat. This is shown by the following table:

	I_3	n	S	U
p, n	$\frac{1}{2}, -\frac{1}{2}$	1	0	1
Λ^0	0	1	−1	0
$\Sigma^+, \Sigma^0, \Sigma^-$	1, 0, −1	1	−1	0
Ξ^0, Ξ^-	$\frac{1}{2}, -\frac{1}{2}$	1	−2	−1
K^+, K^0	$\frac{1}{2}, -\frac{1}{2}$	0	+1	+1
$K^-, \overline{K}^0$	$-\frac{1}{2}, \frac{1}{2}$	0	−1	−1

The isospin is $\frac{1}{2}$ for all the new particles except Λ^0 and the Σ's. In isospace the former is spinless, while the latter have the same properties as the π-mesons. It is important to notice that some of the new particles have ordinary spin $\frac{1}{2}$ and isospin zero or one (Λ^0 and the Σ's), or the converse (K-mesons). This causes a certain amount of complication in writing down the field operators. For example, the Σ's should be described by field operators (ψ_1, ψ_2, ψ_3) each having four components. The four component fields

$(\psi_1+i\psi_2)/\sqrt{2}$ and $(\psi_1-i\psi_2)/\sqrt{2}$ would represent respectively $(\Sigma^+, \bar{\Sigma}^+)$ and $(\Sigma^-, \bar{\Sigma}^-)$. Only if the fictitious "particles" of the fields 1 and 2 were Majorana particles and the components of ψ_1 and ψ_2 were Hermitian in the Majorana set, would $\bar{\Sigma}^+$ be identical with Σ^-. But this is not expected to be the case, as can be seen by inspecting the values of the baryon number n. Since $n = 1$ for both Σ^+ and Σ^-, it is clear that $\Sigma^- \neq \bar{\Sigma}^+$, since n should be -1 for this last. Note, however, that $I_3 = -1$ for both Σ^- and $\bar{\Sigma}^+$. Similarly it is doubtful whether $K^- \equiv \overline{K}^+$. The field operators of K-particles will be (Φ_1, Φ_2, Φ_3), Φ_i being a two-component (isospin $\frac{1}{2}$) operator not necessarily Hermitian. Thus $(\Phi_1+i\Phi_2)/\sqrt{2}$ describing K^+ and $\overline{K}^+$, and $(\Phi_1-i\Phi_2)/\sqrt{2}$ describing K^- and $\overline{K}^-$, would be transformed into one another by particle-antiparticle conjugation only if Φ_1 and Φ_2 were Hermitian. We have already mentioned that Φ_3 is certainly not Hermitian, since $K^0 \neq \overline{K}^0$.

The strangeness S was introduced by Gell-Mann as a purely empirical quantity. The basic postulate is that the charge of a particle is expressed by

$$Q = I_3 + \frac{n}{2} + \frac{S}{2}. \tag{18}$$

For instance, $Q(\Xi^-) = -\frac{1}{2}+\frac{1}{2}-\frac{2}{2} = -1$ and $Q(\bar{p}) = -\frac{1}{2}-\frac{1}{2}+0 = -1$.

Then the assumption is made that:

1) All interactions conserve Q and n;
2) Strong interactions conserve Q, n, $|\mathbf{I}|$, I_3 and therefore also S;
3) Strong and electromagnetic interactions conserve Q, n, I_3 and S;
4) Weak interactions do not conserve I_3, but $\Delta S = \pm 1$ for all reactions due to them;
5) There are no interactions yielding transitions with $|\Delta S| > 1$.

These rules account for the associated production, and are in agreement with the various weak decay processes listed so far, and with a number of experimental facts, such as the positive excess (K^+ occurs more frequently than K^-) which is due to the absorption of K^- by protons ($K^- + p \to \Lambda^0$, though weak, has $\Delta S = 1$, whereas $K^+ + n \to \Sigma^+$ cannot occur since $\Delta S = 2$).

Of greater interest from our viewpoint is the suggestion made by Prentki and d'Espagnat [2, 9] that, rather than S, the quantum number $U = n+S$ should be used and be interpreted as an intrinsic parity for inversions in isospace, so that

$$\mathfrak{P}\psi\mathfrak{P}^{-1} = e^{-i\frac{1}{2}\pi U}\psi, \tag{19}$$

U having a definite value for each field. This implies that the one-particle states of a certain field ψ are multiplied by $e^{i\frac{1}{2}\pi U}$, when acted upon by $\mathfrak{P}$, and one-antiparticle states by $e^{-i\frac{1}{2}\pi U}$, no other change taking place, since the particles are "at rest" in isospace and I_3 is not altered by an inversion.

The charge is now expressed by

$$Q = I_3 + \frac{U}{2}. \tag{20}$$

It is attractive to think of it in terms of a rotation of 90° around the third axis and an inversion in isospace, since

$$\mathfrak{R}_{\frac{1}{2}\pi}\mathfrak{P}\psi\mathfrak{P}^{-1}\mathfrak{R}_{\frac{1}{2}\pi}^{-1} = \mathrm{e}^{-i\frac{1}{2}\pi U - \frac{1}{2}i\pi I_3}\psi = i^{-Q}\psi, \tag{21}$$

though the meaning of this is rather obscure.

Gell-Mann's selection rules can now be straightforwardly expressed in terms of U. Strong interactions conserve isoparity. Weak interactions are parity non-conserving in isospace, as they are in ordinary space.

This review was inspired by a memorable lecture by Prof. W. Pauli on Parity Non-Conservation (March 1957, Tait Institute of Mathematical Physics, Edinburgh). The Author was then an I. C. I. Research Fellow at the University of Glasgow. He is indebted in several ways to Profs. J. C. Gunn and D. S. Jones, and to Prof. L. Rosenfeld and Dr. P. Roman for a critical and helpful perusal of the manuscript.

References to Chapter VII

1) R. H. Dalitz, Phil. Mag. **44** (1954) 1068; and subsequent papers
2) B. d'Espagnat and J. Prentki, Nuclear Physics **1** (1956) 33
3) M. Gell-Mann, Phys. Rev. **92** (1953) 833
4) M. Gell-Mann and A. Pais, Proc. of the 1954 Glasgow Conference on Nuclear and Meson Physics (London, 1955)
5) A. Pais, Phys. Rev. **86** (1952) 663
6) A. Pais, Prog. Theor. Phys. **10** (1953) 457
7) A. Pais, Physica **19** (1953) 869
8) A. Pais, Proc. Nat. Acad. Sci. U.S. **40** (1954) 484, 835
9) G. Racah, Nuclear Physics **1** (1956) 302
10) R. G. Sachs, Phys. Rev. **99** (1955) 1573
11) A. Salam and J. C. Polkinghorne, Nuovo Cimento **2** (1955) 685
12) C. N. Yang and R. L. Mills, Phys. Rev. **96** (1954) 191

8.B *Nuclear Physics* 7 (1958) 373—383; © *North-Holland Publishing Co., Amsterdam*
Not to be reproduced by photoprint or microfilm without written permission from the publisher

DIRAC MATRICES, TELEPARALLELISM AND PARITY CONSERVATION

H. S. GREEN
University of Adelaide

Received 13 February 1958

Abstract: This paper puts on a more fundamental basis a proposal of Green and Hurst for reconciling failures of parity conservation. It is shown that teleparallelism is a necessary consequence of the introduction of Dirac matrices in general relativity, and that these matrices require a reducible 8-dimensional representation. A suggestion is made for the representation of all fermion fields by a single spinor. The problem of particle-antiparticle conjugation is solved for general relativity. Finally it is shown how the formalism introduced by Green and Hurst, and Watanabe, is contained in the theory.

1. Introduction

One of the most promising attempts by Einstein [1]) to construct a synthesis of general relativity and electrodynamics was his 'unitary' theory of 1928—30, with its concept of teleparallelism (*Fernparallelismus*). This is distinguished from the general theory of relativity in its best known form by the existence, at every point of space-time, of a uniquely determined vector which is 'parallel' to a vector at any given point. It was soon observed, by Schouten [2]) and by Pauli and Solomon [3]) among others, that Einstein's theory had a special importance for the relativistic generalization of Dirac's equation, because it furnished a simple representation of a set of four matrices γ_λ, satisfying

$$\{\gamma_\lambda, \gamma_\mu\} \equiv \gamma_\lambda\gamma_\mu+\gamma_\mu\gamma_\lambda = 2g_{\lambda\mu}, \tag{1}$$

where $g_{\lambda\mu}$ is the metric tensor.

The representation of the Dirac matrices obtained in this way is not, however, the most general one. After the similarity transformation

$$\gamma_\lambda \rightarrow \gamma'_\lambda = V\gamma_\lambda V^{-1} \tag{2}$$

is applied, the transformed matrices γ'_λ still satisfy (1), whether the matrix V depends on the co-ordinates or not. For this reason, many authors have preferred to develop the theory of Dirac's equation in general relativity in a different way, following the method of Infeld and van der Waerden [4]). One feature of this method is that the ordinary derivative $\gamma_{\lambda,\mu}$ of γ_λ with respect to x_μ can be expressed in the form

$$\gamma_{\lambda,\mu} = \Gamma^{\nu}_{\lambda\mu}\gamma_\nu + [\Gamma_\mu, \gamma_\lambda],$$
$$[\Gamma_\mu, \gamma_\lambda] \equiv \Gamma_\mu\gamma_\lambda - \gamma_\lambda\Gamma_\mu, \tag{3}$$

where $\Gamma^{\nu}_{\lambda\mu}$ is the Christoffel affinity:

$$\Gamma^{\nu}_{\lambda\mu} = \tfrac{1}{2}g^{\nu\rho}(g_{\lambda\rho,\mu} + g_{\mu\rho,\lambda} - g_{\lambda\mu,\rho}) \tag{4}$$

and Γ_μ is a matrix which might be called the spinor affinity. There are several questions which might be asked about this approach. Does it still carry the implication of teleparallelism? Also, suppose one is given Γ_μ in an explicit form, how would one proceed to construct a representation for the γ_λ? These are purely mathematical questions, for which answers will be provided in this paper.

But there as also some very interesting physical questions which deserve attention. Dirac's equation, assumed to be invariant with respect to general co-ordinate transformations and similarity transformations, has the form

$$\gamma^\lambda(\psi_{,\lambda} - \Gamma_\lambda\psi) = 0, \tag{5}$$

where ψ is a general spinor. Is there any evidence that this equation describes the behaviour of the elementary particles better than its counterpart in special relativity, i.e., that general relativity has anything useful to say about atomic or nuclear physics? If so, what is the interpretation of the apparently unique spinor field ψ; how could it describe particles as dissimilar as the electron and the proton; and how can the invariance properties postulated by general relativity be reconciled with the observed failures of parity conservation? These are questions to which at present no complete answer can be expected. The present paper will have fulfilled its purpose if it encourages the hope that satisfactory answers to the outstanding questions may still be found.

2. Dirac Matrices in General

The main purpose of this section is to symmarize for the reader's convenience some relevant properties of the generalized Dirac matrices and spinors; a more extended account will be found in a review article by Bade and Jehle [5]). An attractive point of view is that the set of four Dirac matrices γ_λ is the fundamental geometrical invariant, and the metric tensor $g_{\lambda\mu}$ is defined by (1). Then the geometry of space-time is properly described by a linear matrix form $ds = \gamma_\lambda dx_\lambda$. But as $g_{\lambda\mu}$ is a multiple of the unit matrix, it is necessary to introduce as a postulate

$$[g_{\lambda\mu}, \gamma_\nu] = 0. \tag{6}$$

Defining

$$\gamma_{\lambda\mu} = \tfrac{1}{2}[\gamma_\lambda, \gamma_\mu]; \quad \gamma_{\lambda\mu\nu} = \tfrac{1}{2}\{\gamma_\lambda, \gamma_{\mu\nu}\};$$
$$\gamma_{\lambda\mu\nu\rho} = \tfrac{1}{2}[\gamma_\lambda, \gamma_{\mu\nu\rho}], \tag{7}$$

one finds that these are anti-symmetrical in all pairs of suffixes, so that

$$\gamma_{\lambda\mu\nu\rho} = \varepsilon_{\lambda\mu\nu\rho}\gamma_5, \tag{8}$$

where $|\varepsilon_{\lambda\mu\nu\rho}| = 1$, defining γ_5. Further,

$$\begin{aligned}
&\tfrac{1}{2}[\gamma_\lambda, \gamma_{\mu\nu}] = g_{\lambda\mu}\gamma_\nu - g_{\lambda\nu}\gamma_\mu;\\
&\tfrac{1}{2}\{\gamma_\lambda, \gamma_{\mu\nu\rho}\} = g_{\lambda\mu}\gamma_{\nu\rho} + g_{\lambda\nu}\gamma_{\rho\mu} + g_{\lambda\rho}\gamma_{\mu\nu};\\
&\gamma_{\lambda 5} \equiv \gamma_\lambda\gamma_5 = -\gamma_5\gamma_\lambda = 1/6\, g_{\lambda\mu}\varepsilon^{\mu\nu\rho\sigma}\gamma_{\nu\rho\sigma};\\
&\gamma_5{}^2 = g,
\end{aligned} \tag{9}$$

in which g means the determinant of the $g_{\lambda\mu}$, which is empirically negative. One defines $g^{\lambda\mu}$, γ^λ and γ^5 by

$$g^{\lambda\mu}g_{\mu\nu} = \delta_\nu{}^\lambda; \quad \gamma^\lambda = g^{\lambda\mu}\gamma_\mu; \quad \gamma^5\gamma_5 = 1. \tag{10}$$

The ring generated by the γ_λ has only 16 independent elements, e.g. the unit matrix δ, the γ_λ, γ_5, $\gamma_{\lambda\mu}$ and $\gamma_{\lambda 5}$. It will be postulated that the derivative $\gamma_{\lambda,\mu}$ is an element of this ring and can therefore be expressed in the form

$$\gamma_{\lambda,\mu} = E_{\lambda\mu}\delta + E^\nu_{\lambda\mu}\gamma + E^5_{\lambda\mu}\gamma_5 + E^{\rho\sigma}_{\lambda\mu}\gamma_{\rho\sigma} + E^{\rho 5}_{\lambda\mu}\gamma_{\rho 5}. \tag{11}$$

But from (10) it follows on differentiation that

$$\tfrac{1}{2}\{\gamma_{\lambda,\nu}, \gamma_\mu\} + \tfrac{1}{2}\{\gamma_\lambda, \gamma_{\mu,\nu}\} = g_{\lambda\mu,\nu} \tag{12}$$

and by substituting (11) into (12) one finds

$$\begin{aligned}
&E_{\lambda\mu} = 0; \quad E^\rho_{\lambda\nu}g_{\rho\mu} + E^\rho_{\mu\nu}g_{\rho\lambda} = g_{\lambda\mu,\nu};\\
&E^{\rho\sigma}_{\lambda\nu}\gamma_{\mu\rho\sigma} + E^{\rho\sigma}_{\mu\nu}\gamma_{\lambda\rho\sigma} = 0;\\
&E^{\rho 5}_{\lambda\nu}\gamma_{\mu\rho} + E^{\rho 5}_{\mu\nu}\gamma_{\lambda\rho} = 0.
\end{aligned} \tag{13}$$

From the third and fourth of these equations it follows that $E^{\rho\sigma}_{\lambda\nu}$ and $E^{\rho 5}_{\lambda\nu}$ have the form

$$\begin{aligned}
E^{\rho\sigma}_{\lambda\nu} &= \tfrac{1}{2}(E_\nu{}^\sigma\delta_\lambda{}^\rho - E_\nu{}^\rho\delta_\lambda{}^\sigma);\\
E^{\rho 5}_{\lambda\nu} &= E_\nu{}^5\delta_\lambda{}^\rho,
\end{aligned} \tag{14}$$

defining $E_\nu{}^\mu$ and $E_\nu{}^5$, so that (11) reduces to

$$\gamma_{\lambda,\mu} = E^\nu_{\lambda\mu}\gamma_\nu + E^5_{\lambda\mu}\gamma_5 + E_\mu{}^\nu\gamma_{\lambda\nu} + E_\mu{}^5\gamma_{\lambda 5}. \tag{15}$$

This result can also be written in the form of (3), where

$$\Gamma_\mu = -\tfrac{1}{2}(\tfrac{1}{2}C^\nu_{\lambda\mu}\gamma^\lambda\gamma_\nu + E^5_{\lambda\mu}\gamma^\lambda\gamma_5 + E_\mu{}^\nu\gamma_\nu + E_\mu{}^5\gamma_5) \tag{16}$$

and

$$C^\nu_{\lambda\mu} \equiv E^\nu_{\lambda\mu} - \Gamma^\nu_{\lambda\mu}. \tag{17}$$

To establish the equivalence of (15) and (3), it is necessary to use the fact that the tensor $C^\rho_{\lambda\nu}g_{\rho\mu}$ is anti-symmetric in λ and μ, which follows from (4) and the second of equations (13).

When (16) is substituted into the generalized form (5) of Dirac's equation,

this reduces to

$$\gamma^\lambda \psi_{,\lambda} - \tfrac{1}{2}\{g^{\lambda\mu} C^\nu_{\lambda\mu} \gamma_\nu + g^{\lambda\mu} E^5_{\lambda\mu} \gamma_5 + E_\mu{}^\mu + (E_\mu{}^\nu g^{\mu\rho} - \tfrac{1}{2} E^5_{\lambda\mu} \varepsilon^{\lambda\mu\nu\rho})\gamma_{\rho\nu} + (E_\mu{}^5 g^{\mu\rho} - \tfrac{1}{2} g^{-1} g_{\nu\sigma} C^\sigma_{\lambda\mu} \varepsilon^{\lambda\mu\nu\rho})\gamma_{\rho 5}\}\psi = 0. \quad (18)$$

The physical interpretation of this result will be considered in more detail later (§ 6). But it may be noticed immediately that the imaginary part of $g^{\lambda\mu} C^\nu_{\lambda\mu}$ has the character of an electromagnetic field, that $g^{\lambda\mu} E^5_{\lambda\mu}$ has the character of a pseudo-scalar meson field, and that the imaginary part of $E_\mu{}^\mu$ acts as a mass field. The coefficients of $\gamma_{\rho\nu}$ and $\gamma_{\rho 5}$ in (18) have not yet any firm physical interpretation, but could represent fields involved in such phenomena as β-decay.

3. The Field Identities

The coefficients $E^\nu_{\lambda\mu}$, $E^5_{\lambda\mu}$, $E_\mu{}^\nu$ and $E_\mu{}^5$ which appear in (15) cannot be assigned arbitrarily, but must satisfy a set of identities in order that (15) be integrable. These identities are obtained from $(\gamma_{\lambda,\mu})_{,\nu} = (\gamma_{\lambda,\nu})_{,\mu}$ by working out each side of this equation with the help of (15). But first one requires the following results:

$$\begin{aligned}
\gamma_{\lambda\mu,\nu} &= (E^\rho_{\mu\nu}\gamma_{\lambda\rho} - E^\rho_{\lambda\nu}\gamma_{\mu\rho}) + (E^5_{\mu\nu}\gamma_{\lambda 5} - E^5_{\lambda\nu}\gamma_{\mu 5}) + (E^6_{\mu\nu}\gamma_\lambda - E^6_{\lambda\nu}\gamma_\mu);\\
\gamma_{\lambda 5,\nu} &= (E^\rho_{5\nu}\gamma_{\lambda\rho} - E^\rho_{\lambda\nu}\gamma_{5\rho}) + E^5_{5\nu}\gamma_{\lambda 5} + (E^6_{5\nu}\gamma_\lambda - E^6_{\lambda\nu}\gamma_5); \qquad (19)\\
\gamma_{5,\nu} &= E^\rho_{5\nu}\gamma_\rho + E^5_{5\nu}\gamma_5 + E_\nu{}^\rho \gamma_{5\rho},
\end{aligned}$$

where, to point the symmetry, the notation

$$E^6_{\mu\nu} = g_{\mu\rho} E_\nu{}^\rho, \quad E^\rho_{5\nu} = -g g^{\rho\mu} E^5_{\mu\nu}, \quad E^5_{5\nu} = E^\mu_{\mu\nu}, \quad E^6_{5\nu} = g E_\nu{}^5, \quad (20)$$

has been introduced. These results follow easily from (7), (8) and (15).

On working out $(\gamma_{\lambda,\mu})_{,\nu}$ with the help of (15) and (19), one finds that the conditions that the result should be symmetric in μ and ν are

$$\begin{aligned}
&E^\sigma_{\lambda\mu,\nu} + E^\rho_{\lambda\mu} E^\sigma_{\rho\nu} + E^5_{\lambda\mu} E^\sigma_{5\nu} + E^6_{\lambda\mu} E^\sigma_{6\nu}\\
&= E^\sigma_{\lambda\nu,\mu} + E^\rho_{\lambda\nu} E^\sigma_{\rho\mu} + E^5_{\lambda\nu} E^\sigma_{5\mu} + E^6_{\lambda\nu} E^\sigma_{6\mu};\\
&E^5_{\lambda\mu,\nu} + E^\rho_{\lambda\mu} E^5_{\rho\nu} + E^5_{\lambda\mu} E^5_{5\nu} + E^6_{\lambda\mu} E^5_{6\nu}\\
&= E^5_{\lambda\nu,\mu} + E^\rho_{\lambda\nu} E^5_{\rho\mu} + E^5_{\lambda\nu} E^5_{5\mu} + E^6_{\lambda\nu} E^5_{6\mu}; \qquad (21)\\
&E^\sigma_{\mu,\nu} + E_\mu{}^\rho E^\sigma_{\rho\nu} + E_\mu{}^5 E^\sigma_{5\nu} = E^\sigma_{\nu,\mu} + E_\nu{}^\rho E^\sigma_{\rho\mu} + E_\nu{}^5 E^\sigma_{5\mu};\\
&E^5_{\mu,\nu} + E_\mu{}^\rho E^5_{\rho\nu} + E_\mu{}^5 E^5_{5\nu} = E^5_{\nu,\mu} + E_\nu{}^\rho E^5_{\rho\mu} + E_\nu{}^5 E^5_{5\mu},
\end{aligned}$$

where

$$E^\sigma_{6\mu} = E_\mu{}^\sigma; \quad E^5_{6\mu} = E_\mu{}^5. \quad (22)$$

These relations may also be obtained by a similar process from (3). If $R_{\mu\nu}$ is the spinor curvature, defined by

$$R_{\mu\nu} = \Gamma_{\mu,\nu} + \Gamma_\mu \Gamma_\nu - \Gamma_{\nu,\mu} - \Gamma_\nu \Gamma_\mu, \quad (23)$$

and $R^\rho_{\lambda\mu\nu}$ is the Riemann Christoffel tensor, constructed entirely from the

Christoffel affinity, one has

$$[\gamma_\lambda, R_{\mu\nu}] = R^\rho_{\lambda\mu\nu}\gamma_\rho. \tag{24}$$

On decomposing this identity, one obtains

$$\begin{aligned}
&C^\sigma_{\lambda\mu/\nu} - C^\sigma_{\lambda\nu/\mu} + (C^\rho_{\lambda\mu} C^\sigma_{\rho\nu} + E^5_{\lambda\mu} E^\sigma_{5\nu} + E^6_{\lambda\mu} E^\sigma_{6\nu}) \\
&\quad - (C^\rho_{\lambda\nu} C^\sigma_{\rho\mu} + E^5_{\lambda\nu} E^\sigma_{5\mu} + E^6_{\lambda\nu} E^\sigma_{6\mu}) = R^\sigma_{\lambda\mu\nu}; \\
&E^5_{\lambda\mu/\nu} + C^\rho_{\lambda\mu} E^5_{\rho\nu} + E^6_{\lambda\mu} E^5_{6\nu} = E^5_{\lambda\nu/\mu} + C^\rho_{\lambda\nu} E^5_{\rho\mu} + E^6_{\lambda\nu} E^5_{6\mu}; \\
&E^6_{\lambda\mu/\nu} + C^\rho_{\lambda\mu} E^6_{\rho\nu} + E^5_{\lambda\mu} E^6_{5\nu} = E^6_{\lambda\nu/\mu} + C^\rho_{\lambda\nu} E^6_{\rho\mu} + E^5_{\lambda\nu} E^6_{5\mu}; \\
&E^5_{\mu/\nu} - E^5_{\nu/\mu} = E_\nu{}^\rho E^5_{\rho\mu} - E_\mu{}^\rho E^5_{\rho\nu},
\end{aligned} \tag{25}$$

where $/\nu$ means the covariant derivative with respect to x_ν, in the usual sense of general relativity. It is readily verified that (25) and (24) are equivalent.

4. Teleparallelism

Consider the simultaneous differential equations

$$\begin{aligned}
h_{\lambda,\mu} &= E^\rho_{\lambda\mu} h_\rho + E^5_{\lambda\mu} h_5 + E^6_{\lambda\mu} h_6; \\
h_{5,\mu} &= E^\rho_{5\mu} h_\rho + E^6_{5\mu} h_6; \\
h_{6,\mu} &= E^\rho_{6\mu} h_\rho + E^5_{6\mu} h_5.
\end{aligned} \tag{26}$$

The conditions that they are integrable are obtained by working out $(h_{\lambda,\mu})_{,\nu}$, $(h_{5,\mu})_{,\nu}$, and $(h_{6,\mu})_{,\nu}$ and expressing the fact that these must be symmetric in μ and ν. But these conditions are found to be satisfied identically by virtue of (21). Thus equations (26) are integrable, by virtue of (15).

There is one integral of (26) which does not depend on the E's, so long as they satisfy the integrability conditions; this is

$$h^\lambda h_\lambda + g^{-1} h_5{}^2 - h_6{}^2 = \text{constant}. \tag{27}$$

This enables one to prove the theorem: *corresponding to any vector $h_\lambda(0)$ at the point* 0 *of space-time, there exists a uniquely defined 'parallel'* vector *at any other point* P *of space-time.*

The proof is as follows. Let h be any fixed constant, and at 0 let $h_\lambda = h_\lambda(0)$, $h_6 = h$, and $h_5 = \{(-g)(h^\lambda h_\lambda - h^2)\}^{\frac{1}{2}}$; then the constant on the right-hand side of (27) is zero. Furthermore, the solution of (27) is uniquely determined throughout space-time. Hence the vector hh_λ/h_6 is uniquely determined everywhere, in particular at the point P.

It will be noticed that the "uniqueness" of the parallel vector at a distance depends on a special choice for the value (h) of h_6 at 0, which thereafter plays a fundamental role in the metrical properties of the space-time manifold. In this respect the present concept of teleparallelism is more general than Einstein's where no such parameter was involved. Einstein's theory is obtained by imposing the restrictions $g^{-\frac{1}{2}}h_5 = \text{constant}$ and $h_6 = \text{constant}$,

which have the effect of reducing $E_{\lambda\mu}$, $E_{\mu}{}^{\nu}$ and $E_{\mu}{}^{5}$ to zero. The author [6]) has recently discussed the application of this theory to electrodynamics, concluding that it is still tenable. Generalizations of Einstein's theory in which only $E_{\mu}{}^{\nu}$ and $E_{\mu}{}^{5}$ vanish, and not $E^{5}_{\lambda\mu}$, were discussed by Einstein himself [7]), by Pauli and Solomon [3]), and by Schouten and van Dantzig [8]).

5. Representation

In this section, it will be shown how one can construct an explicit representation of the γ_λ, given the components $E^{\nu}_{\lambda\mu}$, $E^{5}_{\lambda\mu}$, $E_{\mu}{}^{\nu}$ and $E_{\mu}{}^{5}$ of the spinor affinity. As a by-product of this work, a general solution will be obtained of the set of simultaneous equations (21).

The first step is to determine a set of six independent solutions $h_{r\lambda}$, h_{r5}, h_{r6} ($r = 1, 2, 3, 4, 5, 6$) of the simultaneous equations (26). This is done by taking any solution of the equations

$$\begin{aligned} &\textstyle\sum_r h_{r\lambda} h_{r\mu} = g_{\lambda\mu}; && \textstyle\sum_r h_{r\lambda} h_{r5} = 0; \\ &\textstyle\sum_r h_{r5} h_{r5} = g; && \textstyle\sum_r h_{r\lambda} h_{r6} = 0; \\ &\textstyle\sum_r h_{r5} h_{r6} = 0; && \textstyle\sum_r h_{r6} h_{r6} = h^2 \end{aligned} \tag{27}$$

at the point 0; the solution, which relates only to this point, is a set of numbers, not field variables. But, by means of the integrable equations (26), the values so obtained can be continued to any point of space-time. Moreover, since $g_{\lambda\mu}$, 0, g, 0, 0, h^2, satisfy the same simultaneous differential equations [by virtue of the second of eqs. (13)] as $\sum_r h_{r\lambda} h_{r\mu}$, etc., the relations (27) hold not merely at 0 but throughout space-time.

Let

$$h_r{}^{\lambda} = g^{\lambda\mu} h_{r\mu}, \quad h_r{}^{5} = g^{-1} h_{r5}, \quad h_r{}^{6} = h^{-2} h_{r6}; \tag{28}$$

then from (27) it follows that

$$h_r{}^{\lambda} h_{s\lambda} + h_r{}^{5} h_{s5} + h_r{}^{6} h_{s6} = \delta_{rs}. \tag{29}$$

Also, by multiplying (29) by $h_{5\lambda,\,\mu}$, $h_{s5,\,\mu}$ and $h_{s6,\,\mu}$, one finds that the simultaneous equations (26) are satisfied identically, provided

$$\begin{aligned} E^{\nu}_{\lambda\mu} &= \textstyle\sum_r h_r{}^{\nu} h_{r\lambda,\,\mu}, \quad E^{5}_{\lambda\mu} = \sum_r h_r{}^{5} h_{r\lambda,\,\mu}, \\ E_{\mu}{}^{\nu} &= \textstyle\sum_r h_r{}^{\nu} h_{r6,\,\mu}, \quad E_{\mu}{}^{5} = \sum_r h_r{}^{5} h_{r6,\,\mu}. \end{aligned} \tag{30}$$

It can also be verified that, by virtue of (26), the relations (30) furnish a solution of the simultaneous differential equations (21). The most general solution of (21) is therefore provided by (30), with $h_{r\lambda}$, h_{r5} and h_{r6} unrestricted except by (27).

To achieve a representation of the γ_λ, let α_r ($r = 1, 2, 3, 4, 5, 6$) be a set of 6 constant mutually anti-commuting matrices:

$$\{\alpha_r, \alpha_s\} = 2\delta_{rs}; \tag{31}$$

these generate a Clifford algebra and as there are 2×3 of them, they have well-known representations in $2^3 = 8$ dimensions. Let

$$\beta_\lambda = \sum_r h_{r\lambda}\alpha_r, \qquad \beta_5 = \sum_r h_{r5}\alpha_r, \qquad \beta_6 = \sum_r h_{r6}\alpha_r \tag{32}$$

so that, by (27) one has

$$\begin{gathered}\tfrac{1}{2}\{\beta_\lambda, \beta_\mu\} = g_{\lambda\mu}; \qquad \{\beta_\lambda, \beta_5\} = 0; \qquad \beta_5{}^2 = g; \\ \{\beta_\lambda, \beta_6\} = \{\beta_5, \beta_6\} = 0; \qquad \beta_6{}^2 = h^2,\end{gathered} \tag{33}$$

and by (26) one has

$$\begin{aligned}\beta_{\lambda,\mu} &= E^\nu_{\lambda\mu}\beta_\nu + E^5_{\lambda\mu}\beta_5 + E^6_{\lambda\mu}\beta_6; \\ \beta_{5,\mu} &= E^\nu_{5\mu}\beta_\nu + E^6_{5\mu}\beta_6; \\ \beta_{6,\mu} &= E^\nu_{6\mu}\beta_\nu + E^5_{6\mu}\beta_5.\end{aligned} \tag{34}$$

Let

$$24\beta_7 = \varepsilon^{\lambda\mu\nu\rho}\beta_\lambda\beta_\mu\beta_\nu\beta_\rho\beta_5\beta_6/(gh); \tag{37}$$

it satisfies

$$\begin{gathered}\{\beta_\lambda, \beta_7\} = \{\beta_5, \beta_7\} = \{\beta_6, \beta_7\} = 0; \\ \beta_7{}^2 = -1; \qquad \beta_{7,\mu} = 0.\end{gathered} \tag{38}$$

Then, according to (33), (34) and (38), $\frac{1}{2}\beta_\lambda\beta_6(1\pm i\beta_7)$ satisfy the same equations as γ_λ; and one can make the identification

$$\gamma_\lambda = \tfrac{1}{2}\beta_\lambda\beta_6(1\pm i\beta_7). \tag{39}$$

The representation thus obtained is 8-dimensional, but reducible to two four-dimensional representations of which $\frac{1}{2}(1+i\beta_7)$ and $\frac{1}{2}(1-i\beta_7)$ are the unit elements. There appears to be no way of obtaining the 4-dimensional representations without introducing the dichotomic variable β_7, which appears in a perfectly natural way in the theory. One is therefore impelled to regard ψ in (5) as an eight-component spinor, and to consider the generalization

$$\beta^\lambda\beta^6(\psi_{,\lambda} - B_\lambda)\psi \tag{40}$$

of (5), in which

$$B_\mu = -\tfrac{1}{2}(\tfrac{1}{2}C^\nu_{\lambda\mu}\beta^\lambda\beta_\nu + E^5_{\lambda\mu}\beta^\lambda\beta_5 + E^6_{\lambda\mu}\beta^\lambda\beta_6 + E^5_{6\mu}\beta_5\beta^6) \tag{41}$$

is the spinor affinity. One concludes that the natural generalization of the 4-component spinor equation of special relativity is an 8-component spinor equation. The significance of the extra components will be discussed in § 8.

It should be mentioned that the above results could be expected on arguments derived from group theory. The group of similarity transformations under which the theory is invariant is isomorphic with the group of rotations in an abstract 6-dimensional space. This group is well-known to require a $2^3 = 8$-dimensional representation.

6. Physical Identifications

The physical interpretation of this theory is naturally somewhat tentative because no field equations — apart from the identities (21) — have yet been postulated, and no attempt to do so will be made in the present paper. However, certain identifications can be made with confidence even in the absence of a set of field equations, assuming of course that there is some physical sense in the theory at all.

If e is the 'bare' electonic charge and φ_λ the electro-magnetic four-vector potential, one sees from (18) that †

$$ie\varphi^\nu = \mathscr{I}(\tfrac{1}{2}g^{\lambda\mu}C^\nu_{\lambda\mu}). \tag{42}$$

A similar identification was made by Einstein, though, as he was unaware of the connection of his theory with Dirac's equation, he did not introduce imaginaries. The pseudo-scalar meson potential φ_5 can be identified in a similar way:

$$ie'\varphi^5 = \mathscr{I}(g^{\lambda\mu}E^5_{\lambda\mu}), \tag{43}$$

where e' is the appropriate coupling constant, which, in an 'unrenormalized' theory, might well be the same as e. From (18) one sees also that

$$i\mu = \mathscr{I}(E_\mu{}^\mu)$$

defines an unrenormalized mass field μ, which ought to be constant over regions comparable with the de Broglie wave-length, even at low energies.

The real parts of $C_{\lambda\mu}$, $E^5_{\lambda\mu}$ and $E_\mu{}^\mu$ do not play any part in the account given of the elementary particles by special relativity, and are therefore connected with gravitational phenomena. This is confirmed in part by (25), where the Riemann-Christoffel tensor $R^\sigma_{\lambda\mu\nu}$ appears linearly with the real part of $C^\sigma_{\lambda\mu/\nu}-C^\sigma_{\lambda\nu/\mu}$.

So far there is no direct discrepancy with observation. However, one question demands immediate consideration. How is it that, with a single spinor equation (40), the several different kinds of fermions found in nature can be represented?

To answer this question, it must be stated how ψ is related, for example, to the wave-spinor of the electron, which has no interaction with the meson field φ^5, though it interacts with the electromagnetic field. It will be shown that there are unique, relativistically invariant, similarity transformations V_0, V_5, V_6 which 'switch off' the interaction of the electromagnetic field, the meson field, and the mass field, respectively, with the spinor field ψ. Then, if ψ represented the proton field, $V_0\psi$ might represent the neutron field, $V_5V_6\psi$ might represent the positon field, and $V_0V_5V_6\psi$ might represent the neutrino field. There are, of course, other possibilities such

† The symbol $\mathscr{I}$ denotes i times the imaginary part.

as $V_5\psi$, $V_6\psi$, $V_0V_5\psi$ and $V_0V_6\psi$ which might be needed to represent the μ-meson and the hyperons.

To construct V_0 explicitly, let $k_u{}^\lambda$, for $u = 1, 2, 3, 4$, be eigenvectors of $g_{\lambda\mu}$, regarded as a four-dimensional matrix, so that

$$g_{\lambda\mu}k_u{}^\mu = g'_{\lambda\mu}k_u{}^\mu,$$

where $g'_{\lambda\mu}$ is diagonal. Let the $k_u{}^\lambda$ be normalized so that

$$\sum_u k_u{}^\lambda k_u{}^\mu = g^{\lambda\mu}.$$

Then if α^λ is defined by

$$\alpha^\lambda = \sum_u k_u{}^\lambda \alpha_u, \tag{44}$$

where the u-summation is from 1 to 4, one has

$$\begin{aligned} V_0 &= 1+\alpha^\lambda\beta_\lambda+\tfrac{1}{2}\alpha^{\lambda\mu}\beta_{\mu\lambda}+\tfrac{1}{6}\alpha^{\lambda\mu\nu}\beta_{\nu\mu\lambda}+\tfrac{1}{24}\alpha^{\lambda\mu\nu\rho}\beta_{\rho\nu\mu\lambda}, \\ V_5 &= 1+\alpha^5\beta_5; \qquad V_6 = 1+\alpha^6\beta_6, \end{aligned} \tag{45}$$

where $\alpha^{\lambda\mu}$ and $\beta_{\mu\lambda}$ are formed from α^λ and β_λ in the same way as $\gamma^{\lambda\mu}$ and $\gamma_{\lambda\mu}$ are formed from γ^λ and γ_λ (sec eq. (7)), $\alpha^5 = \alpha_5$, and $\alpha^6 = \alpha_6$. The reciprocals of V_0, V_5 and V_6 are given by

$$\begin{aligned} V_0{}^{-1} &= \lambda_0(1+\beta_\lambda\alpha^\lambda+\tfrac{1}{2}\beta_{\lambda\mu}\alpha^{\mu\lambda}+\tfrac{1}{6}\beta_{\lambda\mu\nu}\alpha^{\nu\mu\lambda}+\tfrac{1}{24}\beta_{\lambda\mu\nu\rho}\alpha^{\rho\nu\mu\lambda}); \\ V_5{}^{-1} &= \lambda_5(1+\beta_5\alpha^5); \qquad V_6{}^{-1} = \lambda_6(1+\beta_6\alpha^6), \end{aligned} \tag{46}$$

where λ_0, λ_5 and λ_6 are constants which can be determined in a straightforward way.

If the above suggestion is correct, an interaction which involves, for example, the emission of a positively charged meson, has an amplitude proportional to $V_0\gamma_5\psi$, when a similar interaction involving the emission of a neutral meson has an amplitude proportional to $\gamma_5\psi$.

It is worth noticing that V_0, V_5 and V_6 commute, so that it is unnecessary to distinguish between V_0V_5, for example, and V_5V_0. But $V_0\beta_\lambda V_5$ is distinct from $V_5\beta_\mu V_0$, because

$$V_0\beta_\lambda = \alpha_\lambda V_0; \qquad V_5\beta_5 = \alpha_5 V_5; \qquad V_6\beta_6 = \alpha_6 V_6. \tag{47}$$

These formulae enable one to bring V_0, V_5 and V_6 to the left- or right-hand side of any amplitude in which they occur.

7. Particle-Antiparticle Conjugation

In spinor field theory, the view is generally held that a Dirac spinor represents simultaneously two rather different things: particles and 'holes', or, in the quantized theory, the annihilation of particles and the creation of anti-particles. Another spinor, obtained from the first by particle-antiparticle conjugation, represents the creation of particles and the annihilation of antiparticles. This operation of particle-antiparticle conjugation, is per-

formed by taking the complex conjugate and multiplying by the transpose of a matrix η. In the general theory of relativity this matrix cannot be identified with γ_4 as in the special theory, and the object of this section is to show how it may be constructed.

If $\gamma_\lambda{}^*$ represents the hermitean conjugate of γ_λ, η must have the property

$$\eta\,\gamma_\lambda = \gamma_\lambda{}^*\,\eta. \tag{48}$$

By differentiation with respect to x_μ and multiplication from the left by η^{-1}, one finds

$$[\eta^{-1}\eta_{,\mu},\ \gamma_\lambda] = \eta^{-1}\gamma^*_{\lambda,\mu}\eta - \gamma_{\lambda,\mu} = -2(I^\nu_{\lambda\mu}\gamma_\nu + I^5_{\lambda\mu}\gamma_5 + R_\mu{}^\nu\gamma_{\lambda\nu} + R_\mu{}^5\gamma_{\lambda 5}) \tag{49}$$

from (15), if $I^\nu_{\lambda\mu}$ and $I^5_{\lambda\mu}$ represent i times the imaginary parts of $C^\nu_{\lambda\mu}$ and $E^5_{\lambda\mu}$, and $R_\mu{}^\nu$ and $R_\mu{}^5$ represent the real parts of $E_\mu{}^\nu$ and $E_\mu{}^5$. Since $g_{\nu\rho}C^\nu_{\lambda\mu}$, and hence $g_{\nu\rho}I^\nu_{\lambda\mu}$ are anti-symmetrical in λ and ρ, (49) is satisfied by

$$\eta^{-1}\eta_{,\mu} = \tfrac{1}{2}I^\nu_{\lambda\mu}\gamma^\lambda\gamma_\nu + I^5_{\lambda\mu}\gamma^\lambda\gamma_5 + R_\mu{}^\nu\gamma_\nu + R_\mu{}^5\gamma_5. \tag{50}$$

One can verify by a straightforward though tedious calculation that $(\eta_{,\mu})_{,\nu}$ computed with the help of this formula is symmetric in μ and ν, by virtue of the identities (21). So (50) is integrable, and requires only a boundary condition to make η uniquely determinate. This boundary condition is supplied by assuming the Galilean value γ_4 for η in regions remote from matter.

Under similarity transformation, η transforms somewhat differently from the Dirac matrices. Corresponding to (2), one must have

$$\eta \to \eta' = (V^{-1})^*\,\eta V^{-1}, \tag{51}$$

in order that the property (48) should be invariant with respect to such transformations.

8. Conservation of Parity

As general relativity usually presupposes the invariance of physical laws with respect to all co-ordinate transformations, including reflections of the spatial co-ordinate system, it is in apparent contradiction with recent experimental evidence [9]) that parity is not conserved in the weak interactions affecting the decay of certain elementary particles. A crucial test of the theory is therefore to examine whether it is consistent with the failure of parity conservation.

In a recent paper, Green and Hurst [10]) have suggested that the condition of invariance with respect to spacial reflections might be relaxed, by requiring only invariance with respect to parity conjugation in the sense of Lee and Yang [11]). In Watanabe's terminology [12]), this implies that chirality, rather than parity, is conserved. Green and Hurst [10]) and Watanabe [12]) independently introduced 8-component spinors to allow the

representation of the chirality operator, and Green and Hurst defined a set of operators ρ_1, ρ_2 and ρ_3 operating on the 8-component spinors. The matrix ρ_3 always commuted with the Dirac matrices; ρ_1 and ρ_2 commuted with the Dirac matrices in representations for particles of 'pure' parity and anti-commuted with the Dirac matrices in representations for particles of 'mixed' parity. Failures of parity conservation could be attributed to the interaction of particles of pure and mixed parity.

All these considerations are automatically validated by the theory of the previous sections. One can make the following identifications:

$$\rho_1 = (-g)^{-\frac{1}{2}}\beta_5, \qquad \rho_2 = (g)^{-\frac{1}{2}}\beta_5\beta_7, \qquad \rho_3 = -i\beta_7 \tag{52}$$

and the conservation of chirality is ensured by the requirement

$$\rho_3\psi = \psi \tag{53}$$

which is equivalent to the choice of $\frac{1}{2}(1+i\beta_7)$ as the unit element. There are two possible and equivalent representations of the Dirac matrices, furnished by the $\gamma_\lambda = \beta_\lambda\beta_6$ and the $\beta_\lambda\beta_5$ of this paper. The γ_λ commute with ρ_1 and ρ_2, as well as ρ_3 and are therefore appropriate to particles of pure parity. The $\beta_\lambda\beta_5$ on the other hand, commute with ρ_3 but anticommute with ρ_1 and ρ_2, and are appropriate to particles of mixed parity.

The following may therefore be asserted: the failure of parity conservation is not merely consistent with general relativity, but is an almost necessary consequence of the theory.

References

1) A. Einstein, Sitz. Preuss. Akad. Wiss., P.-M. Klasse (1928) 217, 224; (1928) 2, 156; (1930) 18, 401
2) J. A. Schouten, J. of Math. and Phys. (Mass.) **10** (1932) 239
3) W. Pauli and J. Solomon, J. Physique **3** (1932) 452, 582
4) L. Infeld and B. L. van der Waerden, Sitz. Preuss. Akad. Wiss., P.-M. Klasse (1933) 380
5) W. L. Bade and H. Jehle, Revs. Mod. Phys. **25** (1953) 714
6) H. S. Green, Proc. Roy. Soc. A
7) A. Einstein and W. Mayer, Sitz. Preuss. Akad. Wiss., P.-M. Klasse (1931) 541
8) J. A. Schouten and D. van Dantzig, K. Akad. Amst., **35** (1932) 642, 843
9) C. S. Wu, E. Ambler, R. W. Hayward, D. D. Hoppes and R. P. Hudson, Phys. Rev. **105** (1957) 1413 and subsequent publications by these and others
10) H. S. Green and C. A. Hurst, Nuclear Physics **4** (1957) 589
11) T. D. Lee and C. N. Yang, Phys. Rev. **102** (1956) 290
12) S. Watanabe, Nuovo Cimento **6** (1957) 187

2.C:6.A *Nuclear Physics* 7 (1958) 384—388; © *North-Holland Publishing Co., Amsterdam*
Not to be reproduced by photoprint or microfilm without written permission from the publisher

BEAMS OF DIFFERENT MASSES IN ELECTROSTATIC ACCELERATORS

S. L. ANDERSEN, K. GJÖTTERUD, T. HOLTEBEKK and O. LÖNSJÖ
Institute of Physics, University of Oslo, Blindern

Received 26 March 1958

Abstract: The use of the H_2^+ beam to obtain yield curves for (p, γ) reactions is shown to introduce an additional energy spread of about 0.5 keV at 500 keV proton energy. A simple explanation for this effect is suggested. We also find that the use of the H_2^+ beam leads to lower values for the resonance energies. Resonance energies and upper limits for the half-widths are given for three resonances in the Al^{27} (p, γ) Si^{28} reaction.

1. Introduction

In experiments with protons accelerated in electrostatic generators, the proton energy range may be extended towards lower values by the use of H_2^+ and H_3^+ ions. It is also an accepted practise to check the voltage scale of the generator by comparing the voltage values for which the same reaction is found to take place when beams of different masses are used. We have compared the use of the H^+ and H_2^+ beams in a series of experiments, and find some discrepancy in the results obtained.

2. Experimental Methods

The experimental procedure is about the same as that described in an earlier paper [1]). The protons from our Van de Graaff generator are analyzed in the electrostatic analyzer. The slit widths have been varied between 0.5 mm and 0.2 mm with the same width being used on the entrance and exit slits.

The energy calibration has been checked by repeated measurements of certain resonances, and is shown to be reproducible within 0.05 %. The larger part of this variation occurs over a period of several hours. Relative energy calibration of a higher accuracy may therefore be obtained by successive runs on two resonances within a short period of time. Also width measurements will be reliable to a much higher degree when observations are taken during short time-intervals. The energy variation in this case will arise from voltage instability on the analyzer deflecting plates only and is usually less than 0.02 %.

The effect of using different beams has been most carefully studied in

aluminium, where the resonances are generally found to be narrow and the γ-ray yield is rather high.

To avoid the oxide layer which forms when aluminium is exposed to air, a new target chamber has been built. The essential features of the chamber, which will be described in more detail later, are as follows:

1) The target material is evaporated in the target chamber, and is not exposed to air after evaporation.

2) The target is shaped as a cylinder which may be turned in small steps, so that several hundred observation spots may be obtained on each target.

In work of highest precision, a fresh target spot is used for each new voltage setting. The exposure time of each target spot is of the order of one minute, and the changes taking place in the target surface in such a time interval are negligible. In addition, two liquid air traps are placed close to the target to prevent carbon contamination.

The targets used have been between 5 and 10 keV thick, thus giving a thick target yield curve without influence from lower lying resonances.

3. Experimental Results

In fig. 1 are shown the resonances at 504, 506 and 630 keV, measured with the H^+ and the H_2^+ beam and slit widths 0.3 mm. The results obtained are summarized in table 1 which includes one more set of runs in addition to

TABLE 1

Observed resonance energy E_{res} and width Γ_{obs} for three resonances in aluminium

H^+ beam		H_2^+ beam	
E_{res}(keV)	Γ_{obs}(eV)	E_{res}(keV)	Γ_{obs}(eV)
504.6	130	504.2	530
506.6	120	506.2	490
632.1	120	631.4	650

those shown in fig. 1. Because of the long-time variation in the energy scale, we do not draw the yield curves for the two sets of runs, but estimate the width from each run and then give the average of the estimates.

The widths are defined to be the inter-quartile range on the curves. In cases when the yield curves are describable by a Breit-Wigner formula, this would correspond to the halfwidth of the resonance. In most other cases the inter-quartile range would be considerably less than the half width.

The energies tabulated are determined relative to the 990.8 keV resonance in aluminium and each represents the average of several measurements.

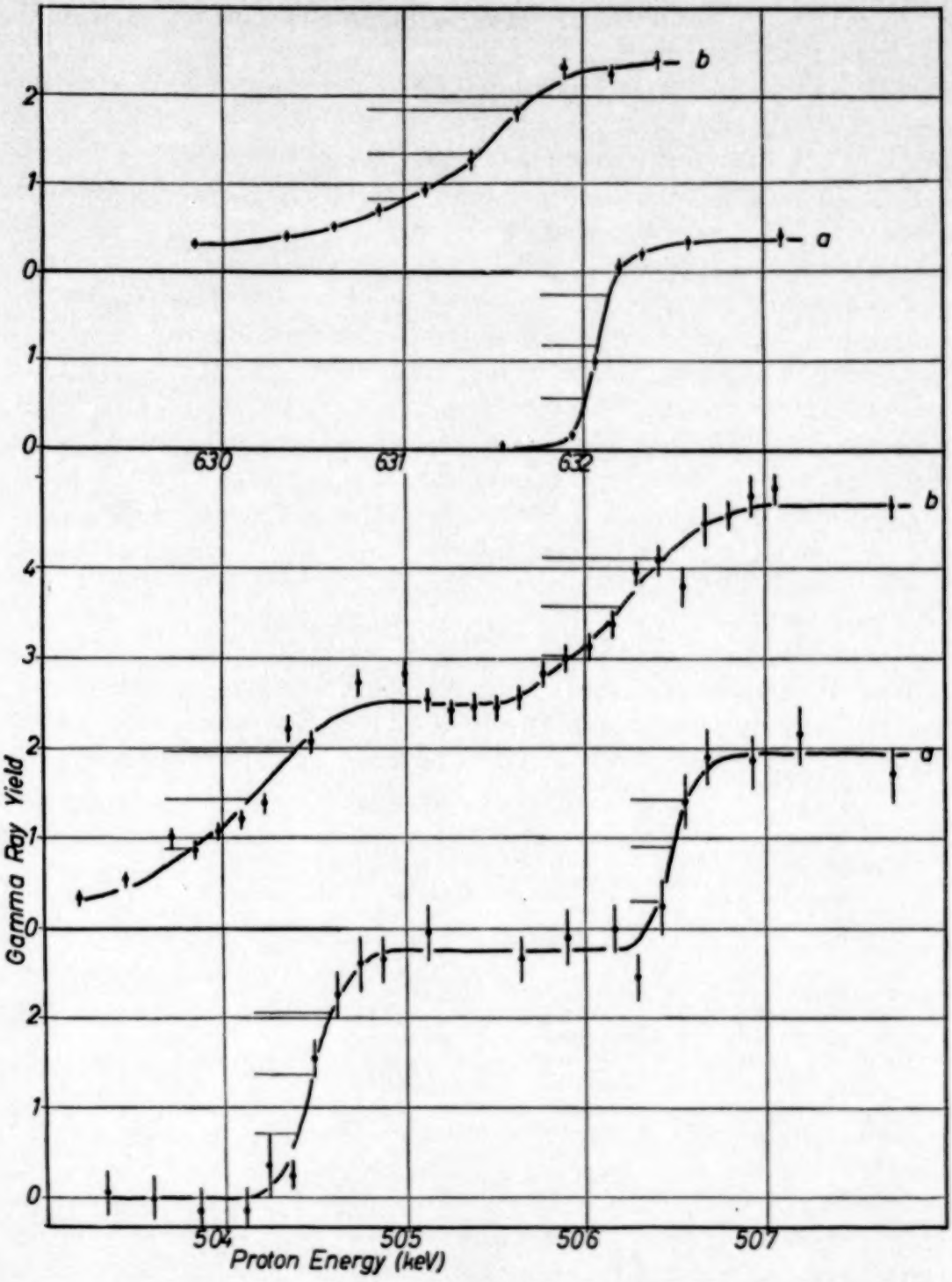

Fig. 1. Three resonances in aluminium.
curves a: measured with the H^+ beam
curves b: measured with the H_2^+ beam.

Values obtained with the H_2^+ beam are corrected for the mass of the electron. It is to be noted that all the values are lower when determined with the H_2^+ beam than with the H^+ beam.

4. Discussion

4.1. ENERGY SPREAD

It has been suggested to us by A. Storruste that the widths measured with the H_2^+ beam are due to the internal motion of the protons in the molecules. This effect is analogous to the Doppler broadening of the resonance widths because of the motion of the target atoms.

A classical treatment taking account of this effect would give an energy spread of $\pm\sqrt{(2E_n E_m)}$ centered about the value E_m of the protons observed in the laboratory system. Here E_n is the total vibrational energy of the molecule and E_m is the mean energy of the proton in the laboratory system.

The H_2^+ molecule has a number of bound vibrational states between 0.14 and 2.6 eV with the electron in the $^2\Sigma_g^+$ state. For a mean proton energy of 500 keV one would expect to find a total energy spread of ± 370 eV if the molecule is in its lowest state and of 1600 eV if the molecule is in the highest vibrational state.

A detailed quantal calculation has been carried out [2]) for the situation in which the molecule is in its vibrational and rotational ground state. It follows mainly the procedure used by Serber [3]) for the deuteron stripping process. We give here a brief summary of the calculations.

Using the ground state function of the linear harmonic oscillator, we get the probability function for the momentum p of each proton

$$P(p) = (\pi m E_0)^{-\frac{1}{2}} \exp(-p^2/mE_0)$$

where E_0 is the zero point energy of the molecule, and m the proton mass. Taking into account the random orientation of the molecule and using the approximation

$$p_z = (E - E_m)(m/2E_m)^{\frac{1}{2}}$$

where p_z is the momentum component in the beam direction and E the total proton energy, we get the energy distribution

$$P(E) = (8\pi E_0 E_m)^{-\frac{1}{2}} \int_\tau^\infty \frac{e^{-t}}{t}\,dt$$

where $\tau = (E - E_m)^2/2E_0 E_m$. This function is valid for $E_0 \ll E_m$. For $E_0 = 0.14$ eV and $E_m = 500$ keV, numerical calculation gives the inter-quartile range $\Delta E = 140$ eV. Although this is much smaller than the observed width, such a result makes it reasonable to believe that the effect would be fully explained if the distribution of molecules on different vibrational levels were taken into account.

Since there is no dipole transition between the vibrational levels in the H_2^+ molecule, the lifetimes of the excited levels are large compared to the time used by a molecule in passing from the ion source to the target. Thus the ions might still be in an excited state while hitting the target. Further calculation

can be carried out only if it is possible to get an estimate of the distribution of states of the H_2^+ molecules in the ion source.

4.2. ENERGY DISPLACEMENT

If the method of checking the energy scale by the use of beams of different masses is accepted, our measurements show that our energy scale is not exactly proportional to the voltage of the analyzer. It is not clear to us if this is so, or if it is only an apparent non-linearity that is due to effects arising with the use of H_2^+ masses as suggested by Bondelid *et al.* [4]). We find it, however, more reasonable to believe that it is a non-linearity in the energy scale. It is well known that electrostatic charges may arise on the deflecting plates of the analyzer, an effect which might easily account for the differences between absolute energy calibration made with an electrostatic analyzer as is done by Herb et *al.* [5]) and by Hunt *et al.* [6]), and with a magnetic analyzer as done by Bumiller *et al.* [7]). If the voltage drop across the insulating films is not strictly proportional to the applied voltage, relative energy measurements will also be affected.

If the displacement arises in this way, the most precise values for the resonance energies would be those obtained with the generator voltage nearest to the calibration voltage. For example the energy of the resonances at 505 keV is most precisely determined with the H_2^+ beam at a voltage near 1010 keV, i.e. close to the 990.8 keV calibration voltage.

5. Conclusion

We have observed a broadening of several resonances when using the H_2^+ beam, as compared to measurements using the H^+ beam. In the region around 500 keV this broadening is about 500 eV. It is apparently due to the internal motion of the protons in the molecule.

We have also observed a displacement towards lower values of the energies when determined with the H_2^+ beam as compared with the H^+ beam.

Precise measurements are carried out for 3 resonances in Al^{27}. The observed widths of these resonances obtained with the H^+ beam agree well with those expected from the resolution of the analyzer, and we conclude that each of these three resonances has a width of less than 100 eV.

References

1) Andersen, Holtebekk, Lönsjö and Tangen, Nuclear Physics **4** (1957) 39
2) K. Gjötterud, Hovedoppgave i fysikk, University of Oslo (1958)
3) R. Serber, Phys. Rev. **72** (1947) 1008
4) Bondelid, Butler and Kennedy, Bull. Am. Phys. Soc. **2** (1957) 381
5) Herb, Snowdon and Sala, Phys. Rev. **75** (1949) 246
6) Hunt and Firth, Phys. Rev. **99** (1955) 786
7) Bumiller, Staub and Weaver, Helv. Phys. Acta **29** (1956) 83

2.L *Nuclear Physics* 7 (1958) 389—396; © *North-Holland Publishing Co., Amsterdam*

Not to be reproduced by photoprint or microfilm without written permission from the publisher

RELATION OF SCATTERING PHASES TO INTERACTION PARAMETERS

E. VAN DER SPUY and H. J. PIENAAR

Department of Physics, University, Stellenbosch

Received 27 March 1958

Abstract: An analysis is introduced which relates the parameters of suitable functions of experimental scattering phases, in the presence of Coulomb forces, to parameters which define the nuclear interaction. A feature of the analysis is to circumvent the need for the troublesome continuous bivariate interpolation of Coulomb-functions, and requires instead the knowledge of a number of coefficients which are functions of one nuclear parameter which assumes only certain discrete values, corresponding to nuclear quantities (such as charge, reduced mass, and outer nuclear radius) which need in practice be tried only at discrete values. A further advantage of the analysis is the direct relation which it establishes between experimental phase parameters and the nuclear interaction parameters.

1. Introduction

A previous analysis [1]) established a direct connection between scattering phase parameters and the parameters defining interaction of the two-body velocity-independent type, without Coulomb-forces, for any angular momentum quantum number l. It is now proposed to extend this analysis to the case where Coulomb-forces have to be included, and to show how this can be done in a way avoiding the troublesome use of a number of Coulomb-functions. Instead the analysis introduces certain coefficients which are functions of r_N, the outer radius of the nuclear interaction concerned, and the charges and reduced masses of the particles concerned. The latter nuclear quantities have discrete values: even in a phenomenological analysis r_N need only be tried at certain discrete values which may be generally selected for all cases over quite a limited range. With the use of Coulomb-functions one requires them to be known for the whole range of the discrete set of nuclear quantities and continuously over the energy range. One is then generally involved in bivariate continuous interpolation.

2. The General Analysis

We consider a two-body scattering problem, assuming velocity-independent forces. After the usual elimination of the angular dependence from the

Schrödinger equation, the radial part of the wave-function, $R_l(r)/r$, is governed by the equation

$$\frac{d^2}{dr^2}R_l(r)+\left\{k^2-\frac{l(l+1)}{r^2}-U_c(r)-U_N(r)\right\}R_l(r)=0, \tag{1}$$

where $k^2=2\mu E/\hbar^2$; here μ is the reduced mass of the two particles having centre-of-mass energy E, and

$$\begin{aligned} U_c(r) &= 2\mu Z_1 Z_2 e^2/\hbar^2 r \qquad \text{for } r > r_N, \\ &= 0 \qquad\qquad\qquad\quad \text{for } r < r_N, \end{aligned}$$

$Z_1 e$, $Z_2 e$ being the charges of the two interacting particles; for $r < r_N$ the Coulomb-potential is included in the nuclear potential;

$$U_N(r)=2\mu V_N(r)/\hbar^2, \qquad \text{with } V_N(r)=0 \qquad \text{for } r > r_N.$$

Although velocity-dependence will not be discussed, simple types of the latter, as for example spin-orbit coupling, could be treated by a simple extension of the present analysis.

The boundary conditions of $R_l(r)$ are defined by $R_l(0)=0$ and $R_l(r_N)=1$. Then, the logarithmic derivative at the interaction boundary, at $r=r_N$, namely

$$f_l=\left\{\frac{r\dfrac{d}{dr}R_l(r)}{R_l(r)}\right\}_{r=r_N}=\left\{r\frac{d}{dr}R_l(r)\right\}_{r=r_N}. \tag{2}$$

Now select a comparison function $R'_l(r)$ with the same defining equation and boundary conditions as $R_l(r)$, except that now $V_N(r)\equiv 0$ for all r. Let f'_l be the logarithmic derivative of $R'_l(r)$. Clearly $R'_l(r)=j_l(kr)/j_l(kr_N)$ for $r<r_N$, $j_l(kr)$ being the spherical Bessel-function. Also

$$f'_l=\left\{\frac{r\dfrac{d}{dr}j_l(kr)}{j_l(kr)}\right\}_{r=r_N}. \tag{3}$$

As usual the Wronskian

$$R'_l(r)\frac{d}{dr}R_l(r)-R_l(r)\frac{d}{dr}R'_l(r)=\text{constant for } r>r_N,$$

and

$$\left\{R'_l(r)\frac{d}{dr}R_l(r)-R_l(r)\frac{d}{dr}R'_l(r)\right\}_0^\infty=\int_0^\infty U_N(r)R'_l(r)R_l(r)dr.$$

Therefore,

$$(f_l-f'_l)\cdot\frac{1}{r_N}=\frac{1}{j_l(kr_N)}\cdot\int_0^{r_N}U_N(r)R_l(r)j_l(kr)dr. \tag{4}$$

One can proceed with the right-hand side of (4) as in the previous analysis [1]) without Coulomb-forces: the function $C(r) = U_N(r)R_l(r)$ is fairly generally $= 0$ for $r = 0, r_N$. This means one can expand $G(r)$ in terms of the orthogonal functions $j_l(k_n r)$ where k_n is given by $j_l(k_n r_N) = 0$; n indicates the number of loops in $j_l(k_n r)$ for $0 \leqq r \leqq r_N$. Thus

$$G(r) = \sum_{n=1}^{\infty} A_n j_l(k_n r). \tag{5}$$

Therefore (4) now changes to

$$(-f_l + f'_l)\frac{1}{r_N} = -\sum_{n=1}^{\infty} \frac{A_n}{j_l(kr_N)} \int_0^{r_N} j_l(k_n r) j_l(kr)\mathrm{d}r$$
$$= \sum_{n=1}^{\infty} \frac{A_n k_n}{(k_n^2 - k^2)} \cdot j_{l-1}(k_n r_N). \tag{6}$$

Eqs. (5) and (1) with the $R_l(r)$ boundary conditions lead to

$$R_l(r) = \frac{j_l(kr)}{j_l(kr_N)} + \sum_{n=1}^{\infty} \frac{A_n}{(k^2 - k_n^2)} \cdot j_l(k_n r), \tag{7}$$

and

$$U_N(r)\left\{\frac{j_l(kr)}{j_l(kr_N)} + \sum_{n=1}^{\infty} \frac{A_n}{(k^2 - k_n^2)} \cdot j_l(k_n r)\right\} = \sum_{n=1}^{\infty} A_n j_l(k_n r), \tag{8}$$

for $r \leqq r_N$.

Eq. (8) clearly shows how the A_n can be regarded as nuclear interaction parameters: the A_n determine $U_N(r)$ and vice versa. As in the analysis without Coulomb-forces [1]), the right-hand side of eq. (6) can be expanded in powers of k^2 (or of the energy E). To do this, and put the result in its simplest form, one expands

$$\frac{A_n}{k_1^2} = C_{n0} + C_{n1}(k/k_1)^2 + C_{n2}(k/k_1)^4 + \ldots, \tag{9}$$

and uses the relations between the C_{nm} which can be deduced from the equations one obtains by expanding (8) in powers of k^2 and equating coefficients of the same powers. In the process the coefficient of each power of k^2 in the expansion of (8) gives rise to a separate energy-independent equation. The latter equations relate the C_{nm} to $U_N(r)$. Though these steps can be effected generally, they will be exemplified here in the case of $l = 0$ alone. Here $j_0(k_n r) = \sin k_n r$, $k_1 r_N = \pi$, and $k_n = nk_1$. For $l = 0$,

$$(f'_0 - f_0) \cdot \frac{1}{\pi} = \sum_{n=1}^{\infty} (-1)^n \frac{C_{n0}}{n} + \sum_{n=1}^{\infty} \left\{(-1)^n \frac{2C_{n0}}{n^3} + \frac{\pi}{2}\frac{C_{n0}^2}{n^4}\right\} \left(\frac{k}{k_1}\right)^2$$
$$+ \sum_{n=1}^{\infty} \left\{(-1)^n \frac{2C_{n0}}{n^5} + (-1)^n \frac{C_{n1}}{n^3} + \frac{\pi}{2}\left(\frac{C_{n0}}{n^6} + \frac{C_{n0}C_{n1}}{n^4}\right)\right\} (k/k_1)^4 + \ldots, \tag{10}$$

and the expansion of (8) leads to

$$\frac{U_N(r)}{k_1^2}\cdot\left\{\frac{r}{r_N}-\sum_{n=1}^{\infty}\frac{C_{n0}}{n^2}\sin(k_n r)\right\}=\sum_{n=1}^{\infty}C_{n0}\sin(k_n r),$$

or

$$\frac{U_N(r)}{k_1^2}\cdot\left\{-\frac{\pi^2}{6}\cdot\left(\frac{r}{r_N}\right)^3-\sum_{n=1}^{\infty}\frac{\sin(k_n r)}{n^2}\left(C_{n1}+\frac{C_{n0}}{n^2}-\frac{\pi^2}{6}C_{n0}\right)\right\}$$
$$=\sum_{n=1}^{\infty}\left(C_{n1}-\frac{\pi^2}{6}C_{n0}\right)\sin(k_n r), \quad (11)$$

etc..

Eq. (11) shows the C_{nm} as interaction parameters; the lowest order equation suffices to determine $U_N(r)$ in terms of C_{n0}, and vice versa, and the higher order equations fix successively C_{n1}, etc.. Eq. (10) hence establishes that (f'_0-f_0) may be given explicitly as a k^2 (or E) power series whose coefficients are functions of the interaction parameters. For the first two terms in the expansion of (10) one needs only the C_{n0}; but for higher order expansions, a knowledge of C_{n1}, etc. is successively needed. Note the zero-energy solution

$$R_0(r)_{k=0}=\frac{r}{r_N}-\sum_{n=1}^{\infty}\frac{C_{n0}}{n^2}\sin(nk_1 r).$$

Now (11) gives an infinite number of energy-independent equations. Another set may be obtained from eq. (10), by expanding the left-hand side into a k^2 (or E) power series, and equating coefficients of like powers of k^2.

Consider now f_0: it may be obtained from the outside solution of eq. (1):

$$R_0(r)=\{\cos\delta_0^N F_0(r)+\sin\delta_0^N G_0(r)\}/N_0,$$

where $F_0(r)$ and $G_0(r)$ are the regular and irregular Coulomb-wavefunctions as normalized by Breit *et al.* [2]); δ_0^N is the nuclear phase-shift with Coulomb forces present, and N_0 is selected to make $R_0(r_N)=1$.
With these $F_0(r)$, $G_0(r)$,

$$G_0(r)\frac{\mathrm{d}}{\mathrm{d}r}F_0(r)-F_0(r)\frac{\mathrm{d}}{\mathrm{d}r}G_0(r)=k.$$

Therefore,

$$f_0/r_N=\left(\frac{\cos\delta_0^N\frac{\mathrm{d}}{\mathrm{d}r}F_0(r)+\sin\delta_0^N\frac{\mathrm{d}}{\mathrm{d}r}G_0(r)}{\cos\delta_0^N F_0(r)+\sin\delta_0^N G_0(r)}\right)_{r=r_N}$$
$$=\left\{\frac{\frac{\mathrm{d}}{\mathrm{d}r}F_0(r)}{F_0(r)}-\frac{k}{F_0(r)G_0(r)+\cot\delta_0^N F_0^2(r)}\right\}_{r=r_N}$$

Therefore,

$$f_0=f''_0-kr_N\{F_0(r_N)G_0(r_N)+F_0^2(r_N)\cot\delta_0^N\}^{-1}=f''_0-f'''_0, \quad (12)$$

where

$$f''_0 = \left(r \frac{\mathrm{d}}{\mathrm{d}r} F_0(r) \over F_0(r) \right)_{r=r_N}$$

is the logarithmic derivative of the regular Coulomb-wavefunction at the nuclear boundary.

Introduce the symbols

$$\rho_N = kr_N, \qquad \eta = \mu Z_1 Z_2 e^2/\hbar^2 k,$$
$$a_N = \rho_N \eta = \mu Z_1 Z_2 e^2 r_N/\hbar^2.$$

The dimensionless quantity a_N is generally quite small; for example, $a_N = 1.38$ for the $\alpha-\alpha$ interaction at $r_N = 5\times 10^{-13}$ cm. Using the auxiliary functions of Breit *et al.* [2]) one immediately gets from (12)

$$\frac{1}{f'''_0} = \{F_0(r_N)G_0(r_N)+F_0^2(r_N)\cot\delta_0^N\}/\rho_N$$
$$= \Phi_0(r_N)\Psi_0(r_N)+2a_N\Phi_0^2(r_N)\left\{\frac{\pi}{(\mathrm{e}^{2\pi\eta}-1)}\cot\delta_0^N+Q+2\gamma'-1+\log 2a_N\right\}, \quad (13)$$

where

$$Q = \mathrm{Re}\frac{\Gamma'(i\eta)}{\Gamma(i\eta)} - \log\eta$$

and γ' is Euler's constant. The quantity

$$\mathscr{E} = \frac{\pi}{(\mathrm{e}^{2\pi\eta}-1)}\cot\delta_0^N+Q$$

is an experimental phase function of k^2 (or E) which may be written as a k^2-power series [3]). This will also appear explicitly from the following analysis. One assumes that the experimental phase δ_0^N has already been analyzed in this form:

$$\mathscr{E} = \alpha+\beta k^2+\gamma k^4+\ldots = \alpha+(\beta/r_N^2)\rho_N^2+(\gamma/r_N^4)\rho_N^4+\ldots, \quad (14)$$

or

$$\mathscr{E}+2\gamma'-1+\log 2a_N = \alpha_1+\beta_1\rho_N^2+\gamma_1\rho_N^4+\ldots,$$

where

$$\alpha_1 = \alpha+2\gamma'-1+\log 2a_N, \qquad \beta_1 = \beta/r_N^2, \qquad \gamma_1 = \gamma/r_N^4.$$

Now one introduces the convergent series for $\Phi_0(r_N)$, $\Psi_0(r_N)$, and $\Phi_0^*(r_N)$, given by Breit *et al.* [2]), noting that

$$f''_0 = \left(r \frac{\mathrm{d}}{\mathrm{d}r} F_0(r) \over F_0(r) \right)_{r=r_N} = \frac{\Phi_0^*(r_N)}{\Phi_0(r_N)};$$

these are

$$\begin{aligned}
\Phi_0(r_N) &= \alpha_2+\beta_2\rho_N{}^2+\gamma_2\rho^4{}_N+\ldots,\\
\alpha_2 &= 1+a_N+\tfrac{1}{3}a_N{}^2+\tfrac{1}{18}a_N{}^3+\tfrac{1}{180}a_N{}^4+\tfrac{1}{2700}a_N{}^5+\tfrac{1}{56700}a_N{}^6+\ldots,\\
-\beta_2 &= \tfrac{1}{6}+\tfrac{1}{9}a_N+\tfrac{1}{36}a_N{}^2+\tfrac{1}{270}a_N{}^3+\tfrac{1}{3240}a_N{}^4+\tfrac{1}{56700}a_N{}^5+\ldots,\\
\gamma_2 &= \tfrac{1}{120}+\tfrac{23}{5400}a_N+\tfrac{7}{8100}a_N{}^2+\tfrac{11}{113400}a_N{}^3+\ldots;
\end{aligned} \tag{15}$$

$$\begin{aligned}
\Phi_0{}^*(r_N) &= \alpha_3+\beta_3\rho_N{}^2+\gamma_3\rho_N{}^4+\ldots,\\
\alpha_3 &= 1+2a_N+a_N{}^2+\tfrac{2}{9}a_N{}^3+\tfrac{1}{36}a_N{}^4+\tfrac{1}{450}a_N{}^5+\tfrac{1}{8100}a_N{}^6+\ldots,\\
-\beta_3 &= \tfrac{1}{2}+\tfrac{4}{9}a_N+\tfrac{5}{36}a_N{}^2+\tfrac{1}{45}a_N{}^3+\tfrac{7}{3240}a_N{}^4+\tfrac{8}{56700}a_N{}^5+\ldots,\\
\gamma_3 &= \tfrac{1}{24}+\tfrac{23}{900}a_N+\tfrac{49}{8100}a_N{}^2+\tfrac{11}{14175}a_N{}^3+\ldots;
\end{aligned} \tag{16}$$

$$\begin{aligned}
\Psi_0(r_N) &= \alpha_4+\beta_4\rho_N{}^2+\gamma_4\rho_N{}^4+\ldots,\\
\alpha_4 &= 1-3a_N{}^2-\tfrac{14}{9}a_N{}^3-\tfrac{35}{108}a_N{}^4-\tfrac{101}{2700}a_N{}^5-\tfrac{28}{10125}a_N{}^6+\ldots,\\
-\beta_4 &= \tfrac{1}{2}-\tfrac{1}{9}a_N-\tfrac{43}{108}a_N{}^2-\tfrac{77}{540}a_N{}^3-\tfrac{373}{16200}a_N{}^4-\tfrac{247}{113400}a_N{}^5+\ldots,\\
\gamma_4 &= \tfrac{1}{24}-\tfrac{2}{225}a_N-\tfrac{172}{10125}a_N{}^2-\tfrac{2687}{567000}a_N{}^3-\ldots.
\end{aligned} \tag{17}$$

Note that

$$f'_0 = \rho_N \cot \rho_N = 1-2B_1\rho_N{}^2-\tfrac{2}{3}B_2\rho^4{}_N-\ldots,$$

where B_r is the rth Bernoulli number. The formulae have been given explicitly in powers of $\rho_N{}^2$ up to the third order (this is sufficient for most practical purposes); they show the α_n, β_n, γ_n to the lower orders in a_N, but they could be calculated to any order of accuracy by using the appropriate recursion formulae [2]). The fact is that α_n, β_n, γ_n, ... for $n = 2, 3, 4$, may be calculated and tabulated for any discrete set of values which the dimensionless quantity a_N would normally take. In practice it is useful to take for r_N a few of a discrete set of values extending over quite a small range which will cover all problems. One will finally interpolate from the final results for such trial values of r_N (4 values for a given problem, say) to the precise r_N demanded by the experiments. Since one is inevitably limited to the class of 2-body problems that may effectively be analysed, $\mu Z_1 Z_2$ and $a_N = \mu Z_1 Z_2 e^2 r_N/\hbar^2$ need have only a limited number of values. For the required values of a_N, the formulae (15), (16), (17) give the α_n β_n, γ_n for $n = 2, 3, 4$, which is normally all that is required, since the experiments usually only permit to derive from $\mathscr{E}$ 2 or 3 of the parameters α, β, γ. Thus for any particular r_N, or a_N, one has energy-independent values of α_n, β_n, γ_n for $n = 1, 2, 3, 4$. Using these expansions of $\Phi_0(r_N)$, $\Phi_0{}^*(r_N)$, $\Psi_0(r_N)$, $\mathscr{E}$, $\rho_N \cot \rho_N$ one may expand the left-hand side of (10) in a power series in $\rho_N{}^2$, or $(k/k_1)^2 \cdot (k_1 r_N)^2 = \pi^2(k/k_1)^2$, and hence by equating coefficients of like powers of $(k/k_1)^2$ obtain a number of equations relating interaction parameters to the phase parameters α_1, β_1, γ_1 through the intermediary of certain energy-independent coefficients α_n, β_n, γ_n (for $n = 2, 3, 4$) which have to be known only for a discrete set of values of a_N. Since the latter equations relating interaction and phase para-

meters may be more simply arrived at with numerical values for the α_n, β_n, γ_n the general relations will only be quoted for the first two coefficients of the $(k/k_1)^2$-power expansion of (10):

$$1-\frac{\alpha_3}{\alpha_2}+(\alpha_2\alpha_4+2a_N\alpha_1\alpha_2^2)^{-1}=\pi\sum_{n=1}^{\infty}(-1)^n\frac{C_{n0}}{n},$$

$$\frac{\beta_2\alpha_3}{\alpha_2^2}-\frac{\beta_3}{\alpha_2}-\frac{1}{3}-\frac{\alpha_2\beta_4+\beta_2\alpha_4+2a_N(2\alpha_1\alpha_2\beta_2+\alpha_2^2\beta_1)}{(\alpha_2\alpha_4+2a_N\alpha_1\alpha_2^2)^2} \tag{18}$$

$$=\frac{1}{\pi}\sum_{n=1}^{\infty}\left\{(-1)^n\frac{2C_{n0}}{n^3}+\frac{\pi}{2}\cdot\frac{C_{n0}^2}{n^4}\right\}.$$

Being energy-independent, the equations of the type (18) presumably have a wider validity than indicated by the radius of convergence of the expansions involved. Using these relations has the advantage of establishing the connection between the phase parameters and interaction parameters only with the help of energy-independent coefficients α_n, β_n, γ_n $(n = 2, 3, 4)$, which have to be known in terms of the discrete variable a_N. In any case, a_N also determines the values of the normal Coulomb-functions, but in using the above parameters α_n, β_n, γ_n, ... one avoids the general need for continuous interpolation of Coulomb-wave functions over a practically continuous energy range. This is even more important if one realizes that in the normal use of Coulomb-wavefunctions one has bivariate continuous interpolation in terms of ρ and η. Furthermore the advantage of the direct connection of phase and interaction parameters in the above form is that it gives a direct method of selecting in a general way useful phenomenological parameters corresponding to the amount of information contained in the experimental data. In such a general phenomenological analysis, equations such as (11) relate $U_N(r)$ and C_{nm} while eq. (18) relates C_{nm} and the experimental α_1, β_1, γ_1, etc. The selection of useful interaction parameters proceeds on the same lines as in the previous analysis without Coulomb-forces [1]), and one may refer to this paper for a further discussion of this aspect; in fact, for phenomenological potentials which are smooth, reasonably slowly varying and non-oscillating with distance, one can limit the analysis to the lower harmonics, i.e. the lower n in C_{nm}; by (11) higher harmonics correspond to rapidly changing or oscillatory potentials, and (18) shows the reduced effect of higher harmonics). In the opposite sense, any velocity-independent potential $V_N(r)$ of finite range can be analysed by relations such as (11) to as many harmonics as are required, and relations (18), (14) will immediately give the phases.

The analysis for higher l can follow in the same way, the relations becoming, however, progressively more complicated.

One of the authors (H. J. P.) wishes to acknowledge the benefit of a bursary of the South African Council for Scientific and Industrial Research during the present investigations.

References

1) E. van der Spuy, Nuclear Physics **1** (1956) 381
2) Breit, Wheeler and Yost, Phys. Rev. **49** (1936) 174
3) G. F. Chew and M. L. Goldberger, Phys. Rev. **75** (1949) 1637

2.L *Nuclear Physics* 7 (1958) 397—410; © *North-Holland Publishing Co., Amsterdam*
Not to be reproduced by photoprint or microfilm without written permission from the publisher

THE INTERACTION OF TWO ALPHA-PARTICLES

E. VAN DER SPUY and H. J. PIENAAR
Department of Physics, University, Stellenbosch

Received 27 March 1958

Abstract: It is investigated whether the phase shift data for alpha-alpha scattering up to bombardment energies ≈ 6 MeV can be represented by a velocity-independent alpha-alpha interaction potential, or a two-body interaction. It is found on the basis of square well potentials and of a general purely phenomenological analysis, which is here developed for interactions with an infinite repulsive core, that this is not possible even for this low energy domain. The results indicate, however, that an outer interaction radius ≈ 4×10^{-13} cm with a strong repulsive core of radius ≈ 1.8×10^{-13} cm is required. These dimensions are in line with fundamental group resonance calculations of the alpha-alpha interaction starting from nucleon-nucleon forces, which also indicated that the repulsive core of the interaction is velocity-dependent. This velocity-dependence may, for example, be phenomenologically indicated by a lower effective repulsive core radius for higher l.

1. Introduction

The scattering of α-particles on He^4 has recently been experimentally investigated with improved accuracy over an extended bombardment energy range, $E' = 0$ to 22.9 MeV [1,2,3]), and the results could be fitted with a unique set of phases for the S, D, F, G waves. It is therefore appropriate to investigate the phenomenological $\alpha-\alpha$ interaction potential that will represent these results.

The α-particle is a saturated and tightly bound system. One might hence expect, in the collision of two such particles at sufficiently low energies, that the two interacting groups will act as two invariable, "rigid" units. For such a situation one would expect that polarization of the α-particles, and exchange of its constituents would play no major role. At higher energies of collision the particles would interpenetrate more, and hence polarize each other, and call into play repulsive forces which will counteract the overlap of these two saturated groups, as is probably demanded by the exclusion principle. One should, however, note that the exclusion principle does not necessarily demand repulsive forces in all cases of overlap of identical spin-$\frac{1}{2}$ particles, but rather that the overall wave-function for groups of such particles should be appropriately antisymmetrized. This antisymmetrization suffices in some cases [4]) to secure the vanishing of the total wavefunction without the explicit intermediary of a repulsive force.

At sufficiently low energies one would therefore expect that two such α-particles would interact according to a velocity-independent two-body interaction potential. The velocity-independence would include independence of l, the orbital angular momentum quantum number. It is the purpose of the investigation reported in this paper to examine whether the experimental results permit of the latter interpretation at all, and what features of the interaction are phenomenologically indicated. A sufficiently low energy of collision in the above sense is probably one which is, say, an order smaller than the high excitation energy of an α-particle ($\approx$ 20—30 MeV). Since a bombardment energy of $E' = 6$ MeV (centre of mass energy $E = 3$ MeV) would seem to be amply allowed on this score, it seems natural to limit this investigation to the results of Heydenburg and Temmer [1]) and Russell *et al.* [2]). These results go up to $E' = 5.63$ MeV and only involve S and D phases. The next results [3]) start at 12.3 MeV, and are only used here to check the range of application of some of the potentials. Nevertheless, it should be mentioned that the phase results from the different sources [1,2,5]) all fall on one smooth continuous graph for any value of l.

The analysis [2]) of the S wave phases up to $E' = 5.63$ MeV indicates that these phases may be described by 3 parameters. The S wave phases may therefore determine 3 parameters of the S wave interaction unambiguously. The D wave phases will determine at least two further parameters of a velocity-independent interaction. If the latter is permitted, one may get not only the outer interaction radius, core radius, depth of the attractive well, but also two shape-defining parameters.

The discussion of the experimental results [2]), as well as the theoretical discussion of Herzenberg [6]), indicate an outer radius of the $\alpha-\alpha$ nuclear interaction $r_N \approx 5f$ (we express distance r in terms of $f = 10^{-13}$ cm). Therefore, in the phenomenological analysis, the logarithmic derivative of the wavefunction was calculated from the phases using Coulomb-functions [7]), at assumed values of $r_N = 4, 4.5, 5f$. Reaction data, but not clearly the scattering data, show an S wave resonance at 94.5 keV, at which energy it is permissible to take the phase shift $\delta_0^N = 90°$ [1]). Unless otherwise stated all potentials were selected to give $\delta_0^N = 90°$ at $E = 94.5$ keV. It does not make much difference to the interaction whether this point is counted in or not, but that actual interaction potential may have a relatively large effect on the resonance energy.

In section 2 it is investigated which square well parameters give the best fit to the S and D wave results. This indicates the features of the interaction schematically.

In section 3 we develop a general analysis for finding interaction parameters from parameters describing the calculated logarithmic derivatives at r_N, for the case of a nuclear interaction with an infinite repulsive core.

This analysis is a logical extension of a previously published [4]) analysis relating phase parameters to interaction parameters. With a repulsive core, the analysis can be put in a simple form, only needing sinusoidal radial wavefunctions, even for $l > 0$.

The general analysis is applied in section 4 to the S wave data to find a 3 or 4 parameter interaction giving a fit. These interactions are then tested for the D wave case. The general technique is finally applied to the $\alpha-\alpha$ interaction deduced by Herzenberg [6]) from fundamental considerations.

In all cases for $r < r_N$, the Coulomb-potential is understood as being added to the nuclear potentials.

2. Square Well Analysis

If one starts from the Schrödinger equation for two identical, spin-less, charged α-particles with velocity-independent interaction, one obtains in the usual way, after elimination of the angular dependence, the following equation for the radial part of the wave-function $R_l(r)/r$:

$$\frac{d^2 R_l(r)}{dr^2} + \left\{ k^2 - U(r) - \frac{l(l+1)}{r^2} \right\} R_l(r) = 0, \tag{1}$$

where only even values of l need be considered; $k^2 = 2\mu E/\hbar^2$, where $\mu = \frac{1}{2}m_\alpha$ denotes the reduced mass of the two α-particles; and

$$U(r) = U_c(r) + U_N(r),$$

$$U_c(r) = \begin{cases} 8\mu e^2/\hbar^2 r & \text{for } r > r_N \\ 0 & \text{for } r < r_N; \end{cases}$$

$$U_N(r) = \begin{cases} 0 & \text{for } r > r_N \\ 2\mu V_N(r)/\hbar^2 & \text{for } r < r_N, \end{cases}$$

where $V_N(r)$ is the nuclear interaction potential.

Now for the square well nuclear interaction of a sufficiently general type for the present purposes one restricts $V_N(r)$ as follows:

$$V_N(r) = +\infty \text{ for } r \leqq r_1, = -V \quad \text{for } r_1 < r < r_N, \; = 0 \quad \text{for } r > r_N, \tag{2}$$

which allows for an infinite repulsive core and has three parameters (r_1, r_N V); $r_1 = 0$ was always included as one possibility. The attractive outside well is demanded by the presence of a very low energy S wave resonance, the absence of bound states, and the δ_0^N phase, which goes up to 180°, at low energies, and then decreases from 180° and becomes negative at $E' \approx 19$ MeV; as well as by the positive D phases. Recognizing the possibility of velocity-dependence of V_N at high energies, the fact that δ_0^N becomes negative indicates a strong repulsive core at least at high energies. Such qualitative features have been noted by Russell *et al.* [2]).

The derivation of $R_l(r)$ for the inside domain, $r < r_N$, follows in the well-known way from (1), (2), and one immediately deduces for the inside solution the logarithmic derivative

$$f_l = \left\{ r \frac{dR_l(r)}{dr} \Big/ R_l(r) \right\}_{r=r_N}:$$

$$f_0 = Kr_N \cot K(r_N - r_1), \tag{3}$$

$$f_2 = -2 + \frac{x_N^2}{3} + \frac{x_N^2}{3\left\{\left(\frac{3}{x_N^2} - 1\right) - \frac{3}{x_N}\cot(x_N + \phi)\right\}},$$

with

$$\cot(Kr_1 + \phi) = \frac{1}{Kr_1} - Kr_1/3, \qquad x_N = Kr_N, \qquad K^2 = k^2 + (2\mu V/\hbar^2).$$

Now for both S and D one can select a set (r_N, r_1, V) to give the best fit to the values for the outside logarithmic derivative as calculated in the usual way from the observed phases at the selected values of $r_N = 4, 4.5, 5f$.

The results were as follows:

(a) For the S wave, the best compromise fit for $r_N = 4f$ is near $r_1 = 1.7f$, $V = 7.2$ MeV, if one includes the 94.5 keV resonance point; and near $r_1 = 1.8f$, $V = 7.9$ MeV, if one ignores the 94.5 keV resonance point. The corresponding parameters for $r_N = 5f$, are $r_1 = 0.7f$, $V = 2.4$ MeV (including resonance point); $r_1 = 0.8f$, $V \approx 2.4$ MeV (not including resonance point). There is, if anything, a somewhat better fit when the curve is not made to pass through the exact resonance point, and for $r_N = 4f$.

(b) For the D wave, the best compromise fit for $r_N = 4f$, is probably reached for $r_1 = 1.8f$, $V = 10.5$ MeV. Lower radii r_1 for lower V values are possible if one improves the fit at low energies at the expense of that in middle energy range. For $r_N = 5f$ the fit is generally much worse; $r_1 = 0$ to f and $V = 3.9$ MeV give a good fit in the middle energy range (here $E' = 4$ to 5 MeV); but the well is too shallow at the higher energy end (here $E' = 5.63$ MeV) by ≈ 0.1 MeV, and much too deep at low energies (here $E' \approx 3$ MeV, where δ_2^N first deviates from zero).

(c) Since we found a better fit for $r_N = 4f$ for both S and D waves, the value $r_N = 6f$ was not tried. The conclusion was checked by taking $r_N = 4.5f$. Actually, the fit at $r_N = 4f$ also extrapolates more satisfactorily to energies as high as $E' = 12.3$ MeV.

Hence one deduces, for both the S and D wave, that the best fit requires r_N as low as $4f$, and demands a repulsive core of considerable radius: $r_1 = 1.8f$, but indicates $V_S = 7.9$ MeV, $V_D = 10.5$ MeV. The disparity between the latter two will increase for lower r_N on account of the centrifugal potential. The investigation thus indicates for this square well type that even for

$E' < 6$ MeV one has a velocity-dependent interaction with a large radius core ($r_1 = 1.8f$). From the fundamental discussion of Herzenberg [6]) it appears that the two aspects: repulsive core and velocity-dependence, can be made one, because his calculations show that the velocity-dependence resides in the repulsive core, while the outside attraction is mainly velocity-independent. If one may schematize the velocity-dependence of the core as a pure l-dependence of r_1, the outside attraction V being common to all l, then, for example, interpolation indicates that at $r_N = 4f$, for $r_{1S} = 2.0f$, $r_{1D} = 0.8f$; $V = 9.5$ MeV a reasonable fit is obtained. It is outside the scope of the present investigation to examine velocity-dependence, which anyway can only be done most arbitrarily without more precise fundamental indications, but if the correct type of velocity-dependence is that with V common to all l, and r_1 velocity-dependent, then the above potential will probably give very nearly the best compromise fit.

Continuing the search for a velocity-independent potential, one notices that the best solution given above has the D attractive well deeper than the S well. On account of the centrifugal potential the D wave wants considerable attractive potentials at large radii. One would therefore think that a compromise could be reached by means of a stepwise variation of the potential:

$$\begin{aligned} V_N(r) &= \infty \quad \text{for } r \leqq r_1, \\ &= -V_1 \quad \text{for } r_1 < r < r_2 \\ &= -V_2 \quad \text{for } r_2 < r < r_N \\ &= \quad 0 \quad \text{for } r > r_N, \end{aligned}$$

with $(-V_1) > (-V_2)$. The domain $r < r_2$ would then have relatively less effect on the D wave than on the S wave; V_2 can perhaps be selected large enough to give a sufficiently large δ_2^N, while $(-V_1)$ would still be shallow enough to give the right δ_0^N. This potential is much more arbitrary (for one thing it has 4 free parameters) and was hence only investigated in one example. Take $r_N = 4f$, $r_1 = 1.8f$ and $V_2 = 10.5$ MeV, to agree with the best D well above; further, $V_1 = 5$ MeV (note $V_S = 7.9 \approx \frac{1}{2}(10.5+5)$), and select r_2 to give an S wave fit: one finds $r_2 = 3.3f$. However, this well does not fit the D wave data at all. It is too shallow, or the filling up for $r_1 < r < r_2$ still has a considerable D wave effect. One notes, however, that this device brings the best fitting S well somewhat nearer fitting the D wave data than for the square well without step, but not so much as to make this a promising type of compromise.

With reference to the types of interaction potentials discussed by Haefner [8]) and by Herzenberg [6]), and which we shall consider in section 4, one should note here that the type of change from the pure square well to the above step well works in the same sense as the change to the Haefner well, but in the opposite direction to the change to Herzenberg's interaction.

3. General Analysis

A former analysis [4]) relating phase parameters to potential parameters is extended here to the case of an interaction with an infinitely repulsive core. For convenience one writes (1) in a different form:

$$\frac{\mathrm{d}^2}{\mathrm{d}r^2} R_l(r)+\{k^2-U_l(r)-U_{cc}(r)\}R_l(r) = 0, \tag{4}$$

where

$$U_{cc}(r) = \begin{cases} \dfrac{l(l+1)}{r^2}+\dfrac{8\mu e^2}{\hbar^2 r} & \text{for } r > r_N, \\ 0 & \text{for } r < r_N; \end{cases}$$

$$U_l(r) = \begin{cases} 0 & \text{for } r > r_N, \\ \dfrac{2\mu V_N(r)}{\hbar^2}+\dfrac{l(l+1)}{r^2} = \dfrac{2\mu V_{Nl}(r)}{\hbar^2} \equiv U_{Nl}(r) & \text{for } r_1 < r < r_N, \\ V_c = +\infty & \text{for } r < r_1; \end{cases}$$

here r_1 is the radius of the repulsive core, and $U_{Nl}(r) = 0$ outside the domain $r_1 < r < r_N$.

In the usual way the boundary conditions for $R_l(r)$ are

$$R_l(r) \sim \frac{1}{N_l} \sin\,(kr-\tfrac{1}{2}l\pi+\delta_l^{\,c}+\delta_l^{\,N}), \quad R_l(r \leqq r_1) = 0,$$

where δ_l is expressed as the sum of $\delta_l^{\,N}$, and the usual Coulomb phase shift

$$\delta_l^{\,c} = -\eta \log 2kr + \arg \Gamma(l+1+i\eta),$$

with

$$\eta = 4\mu e^2/\hbar^2 k.$$

In the above case the outside solution ($r > r_N$) is

$$R_l(r) = \frac{1}{N_l}\{\cos \delta_l^{\,N} F_l(r)+ \sin \delta_l^{\,N} G_l(r)\},$$

where $F_l(r)$, $G_l(r)$ are the regular and irregular Coulomb-functions as defined by Breit *et al.* [10]); the normalization constant N_l is now chosen so that $R_l(r_N) = 1$:

$$N_l = \cos \delta_l^{\,N} F_l(r_N) + \sin \delta_l^{\,N} G_l(r_N).$$

Introduce now the auxiliary function $R'_l(r)$ defined as follows:

$$\frac{\mathrm{d}^2}{\mathrm{d}r^2} R'_l(r)+\{k^2-U'_{cc}(r)\}R'_l(r) = 0, \tag{5}$$

where

$$U'_{cc}(r) = \begin{cases} V_c = +\infty & \text{for } r < r_1 \\ 0 & \text{for } r_1 < r < r_N, \\ \dfrac{l(l+1)}{r^2}+\dfrac{8\mu e^2}{\hbar^2 r} & \text{for } r > r_N. \end{cases}$$

The normalization of $R'_l(r)$ is effected in the same way to that for $R_l(r)$, except for the substitution of δ_l^0 for δ_l^N above.

It follows in the usual way that the Wronskian

$$R'_l(r)\frac{dR_l(r)}{dr} - R_l(r)\frac{dR'_l(r)}{dr} = \text{const.} \quad \text{for } r > r_N. \tag{6}$$

In general from (4) and (5),

$$\left\{R'_l(r)\frac{dR_l(r)}{dr} - R_l(r)\frac{dR'_l(r)}{dr}\right\}_0^\infty = \int_0^\infty U_{Nl}(r)R_l(r)R'_l(r)dr.$$

Therefore

$$(f_l - f^0)\cdot\frac{1}{r_N} = \int_{r_1}^{r_N} U_{Nl}(r)R_l(r)R'_l(r)\,dr, \tag{7}$$

using the definition of $U_{Nl}(r)$ and the boundary conditions for $R_l(r)$ and $R'_l(r)$, and eq. (6); f_l, f^0 are the logarithmic derivatives of $R_l(r)$, $R'_l(r)$ at $r = r_N$.

Now $R'_l(r)$ clearly is only required for the domain $r_1 < r < r_N$, when, with the boundary conditions,

$$R'_l(r) = \sin k(r - r_1)\ \text{cosec}\ k(r_N - r_1). \tag{8}$$

Similarly f^0 may be found by continuity at $r = r_N$ from (8):

$$f^0 = kr_N \cot k(r_N - r_1). \tag{9}$$

Eq. (7) is clearly an integral equation for

$$G'_l(r) = U_{Nl}(r)R_l(r), \tag{10}$$

in terms of the experimental function f_l (for assumed values of the parameters r_1, r_N) and the analysis can now proceed substantially as detailed in a previous paper [4]); it will therefore only be briefly sketched. The only differences are that now f_l, rather than the phase function $k^{2l+1}\cot\delta_l^N$ of the previous analysis, is the experimental function; that one now has a repulsive core; and that the analysis need now only use the simple $l = 0$ type radial functions for all l: this effects a great simplification in practice. The analysis, starting from f_l but without core, follow analogous lines and will not be given. The final form of the analysis below apply also if one has no Coulomb forces for $r > r_N$.

Since $G'_l(r) = 0$ for $r = r_1$ and $r = r_N$, the solution of the integral equation in (7) may be obtained by expanding in terms of orthogonal functions:

$$G'_l(r) = \sum_{n=1}^{\infty} A_n \sin k_n(r - r_1), \tag{11}$$

where $k_n = nk_1$ is defined by $k_1(r_N - r_1) = \pi$. The integer n denotes in fact the nth harmonic of the representation. A_n depends of course on l, but the

dependence has no formal significance. Hence eq. (7) reduces to

$$\{f_l - kr_N \cot k(r_N - r_1)\} \cdot \frac{1}{r_N} = \sum_{n=1}^{\infty} (-1)^{n+1} \frac{k_n A_n}{(k_n^2 - k^2)}. \tag{12}$$

Now in the domain $r_1 < r < r_N$ eq. (4) reads

$$\frac{d^2}{dr^2} R_l(r) + k^2 R_l(r) = U_{Nl}(r) R_l(r) = G'_l(r) = \sum_{n=1}^{\infty} A_n \sin k_n(r - r_1).$$

Thus, on account of the boundary conditions,

$$R_l(r) = \frac{\sin k(r - r_1)}{\sin k(r_N - r_1)} + \sum_{n=1}^{\infty} \frac{A_n}{(k^2 - k_n^2)} \sin k_n(r - r_1),$$

$$\text{for} \quad r_1 < r < r_N.$$

With (10) and (11) this leads to

$$U_{Nl}(r) \left\{ \frac{\sin k(r - r_1)}{\sin k(r_N - r_1)} + \sum_{n=1}^{\infty} \frac{A_n}{(k^2 - k_n^2)} \sin k_n(r - r_1) \right\}$$

$$= \sum_{n=1}^{\infty} A_n \sin k_n(r - r_1). \tag{13}$$

Eq. (13) clearly shows that the A_n, functions of k^2 or the energy, are "interaction parameters" defining $U_{Nl}(r)$. If one knows f_l as a function of energy, the parameters defining the latter are related to the interaction parameters by (12), and hence to the interaction by (13). Again, (12) and (13) may be used to calculate f_l if $U_{Nl}(r)$ is known. The practical way of effecting these connections is to expand both sides of equations (12) and (13), as one may [4]), in power series in $k^2 \propto E$, and to equate coefficients of the same powers. The equations thus obtained do not contain k^2 and hence probably apply over a larger energy range than that determined by the radius of convergence of the relevant expansions. To illustrate the procedure:

$$\frac{A_n}{k_1^2} = C_{n0} + C_{n1}\rho^2 + C_{n2}\rho^4 + \ldots, \text{ with } \rho = k/k_1. \tag{14}$$

Experimentally one has cot δ_l^N and using Coulomb functions here one may calculate f_l for any chosen r_N. This may be fitted with a polynomial in powers of E'

$$f_l = \alpha + \beta E' + \gamma E'^2 + \ldots. \tag{15}$$

Since $k^2 = 2\mu E/\hbar^2 = \mu E'/\hbar^2$,

$$\rho^2 = \mu E'/\hbar^2 k_1^2 = \mu(r_N - r_1)^2 E'/\hbar^2 \pi^2;$$

and

$$f_l = a + \pi^2 b\rho^2 + \pi^4 c\rho^4 + \ldots, \tag{16}$$

where

$$a = \alpha, \qquad b = \hbar^2\beta/\mu(r_N - r_1)^2, \qquad c = \hbar^4\gamma/\mu^2(r_N - r_1)^4, \ldots.$$

The a, b, c are thus experimental parameters determining the logarithmic derivatives for a given set (r_1, r_N), from the parameters $\alpha, \beta, \gamma, \ldots$ which are generally applicable for a given r_N.

Eq. (13) now yields a number of equations, of which the following comes from the lowest order term in the expansion in powers of k^2 (it may be directly deduced from (13) by letting $k \to 0$):

$$\frac{U_{Nl}(r)}{k_1^2}\left\{\left(\frac{r-r_1}{r_N-r_1}\right) - \sum_{n=1}^{\infty}\frac{C_{n0}}{n^2}\sin k_n(r-r_1)\right\} = \sum_{n=1}^{\infty} C_{n0}\sin k_n(r-r_1). \quad (17)$$

Note that the function in the curly brackets is the zero-energy form of $R_l(r)$. This equation read at a sufficient number of r values in the domain $r_1 < r < r_N$, yields the C_{n0} in terms of $U_{Nl}(r)/k_1^2$ or vice versa. Having C_{n0}, the next order in the expansion of (13) yields an equation for the C_{n1} and so on. All such equations shall be collectively indicated by (17).

Expanding (12) and using certain identities between C_{n0}, C_{n1}, etc. derived from eqs. (17), one readily arrives at

$$\begin{aligned}
\frac{1}{\pi}\{1-a(r_N-r_1)/r_N\} &= \sum_{n=1}^{\infty}(-1)^n\frac{C_{n0}}{n},\\
\pi\{-1/3-b(r_N-r_1)/r_N\} &= \sum_{n=1}^{\infty}\left\{(-1)^n\frac{2C_{n0}}{n^3}+\frac{\pi}{2}\cdot\frac{C_{n0}^2}{n^4}\right\}, \qquad (18)\\
\pi^3\{-1/45-c(r_N-r_1)/r_N\} &= \sum_{n=1}^{\infty}\left\{(-1)^n\frac{2C_{n0}}{n^5}+(-1)^n\frac{C_{n1}}{n^3}+\frac{\pi}{2}\left[\frac{C_{n0}^2}{n^6}+\frac{C_{n0}C_{n1}}{n^4}\right]\right\}.
\end{aligned}$$

One notices that (18) relates the experimental parameters a, b, c to the interaction parameters C_{nm}. If the experiments can be described by only 2 parameters, the first two equations may suffice, in which case we only need calculate the C_{n0}. If the next order coefficient is important, or has to be checked, the C_{n1} must be calculated from the next order equation of (17) above. Note that (17) only uses sinusoidal and power functions of $(r-r_1)$. It is clear from (17) that on the left hand side the effect of the higher harmonics is reduced in the term in the curly brackets which means that this term is usually a smooth function of $(r-r_1)$. Hence C_{n0} will only be appreciable for higher n, if $U_{Nl}(r)$ has sharp or rapid changes with $(r-r_1)$. Since in all the equations (18), the higher harmonics are relatively weighed down, one need, except for very rapidly changing potentials, only determine the lower harmonics to any accuracy. One further has a natural way of selecting a number of potential parameters: namely to use just the lower harmonics or C_{n0}. The only arbitrariness involved herein is the perhaps natural one of the consequent limitation of the investigation to smooth potentials which do not show rapid fluctuations. The advantage of introducing r_1 explicitly is that all l may be dealt with by one set of simple functions and that the

infinite repulsive core need not be represented by the C_{n0}—which would have called for many higher harmonics.

4. Application of the General Analysis

The quantity f_l is determined from the phases for $r_N = 4$ and $5f$ (found useful in the square well analysis) for both S and D waves. These functions are then fitted by least squares with polynomials as in (15), using the least number of parameters demanded to fit the results within the experimental errors, and letting the S curve pass through the 94.5 keV resonance. This yields 3 parameters for the S wave, and at least 2 more for the D wave. The former number agrees with that calculated by Russell *et al.* [2]), using another phase function. One therefore has 4 to 5 parameters altogether if a velocity-independent potential is possible; because one must recognize that one of the parameters for the S wave, γ, has relatively little effect and may perhaps not be insisted on.

The general analysis is first of all applied to the S wave to find, for a given (r_N, r_1) combination, the C_{10}, C_{20} from (18) which will give the correct α, β of (15), (16). This gives 4 parameters $(r_N, r_1, C_{10}, C_{20})$, or 3 when one takes the case $r_1 = 0$, which fixes a potential by the first of eqs. (17). The C_{n1} follow for the latter potential from the second of the eqs. (17). The γ corresponding to this potential may then be calculated by (16), (18), and hence the corresponding f_0 compared with the experimental f_0. One may then try other sets of r_N, r_1 (and C_{10} and C_{20}) till the γ is equal to that required by the experimental fit, or if this is not accurately possible, till the f_0 calculated from the potential, found in this way, agrees as nearly as can be with the experimental data, over the chosen energy range. The above procedure always ensures a fit at low energies for a start. Potentials which are found in this way to fit the S wave data well, are then tested for their fit of the D wave data. In this way, the 4 to 5 parameters from the S and D phases may suffice to determine the 4 parameters of the potential uniquely, if the latter can be velocity-independent at all. There is little reason to start with 5 interaction parameters (adding C_{30}, say), since one of the experimental parameters (γ from f_0) gives a small contribution in the chosen energy range, and it is doubtful whether it may be insisted on. In any case, C_{30} for the class of smooth, non-rapidly varying potentials will contribute little to f_0, but would tend to make the analysis prohibitively cumbersome for a desk calculating machine. Since the infinite repulsive core is explicitly introduced (and need hence not be represented by the harmonics), and since one knows from the phases that $R_0(r)$, $R_2(r)$ have only part of a loop over the chosen low energy range, two harmonics can permit of a $U_{Nl}(r)$ with one sign reversal in the domain $r_1 < r < r_N$ (see eq. (17)), which should suffice to cover as general a class

of potentials as one can perhaps expect from the nature of the problem in hand.

One finds then:

(a) Neither $r_N = 4f$, nor $r_N = 5f$, with $r_1 = 0$, allows of any real solutions for C_{10}, C_{20}. This does not mean that there are no solutions possible if one were to take sufficiently strong higher harmonics to describe the sharply changing potentials, with large values for low r, which seem to be demanded by the results given below for $r_1 > 0$. In this sense this finding is in line with the requirement of a strong repulsive core.

(b) With $r_N = 5f$ no value for $r_1 > 0$ permits of a real solution for C_{10}, C_{20}, or a smooth non-steep potential.

(c) With $r_N = 4f$, the values $r_1 = 1.2$, 1.4, $1.8f$ all permit of solutions; 2 each, in fact. The one solution could be selected as being of the same order of general depth as for the square well potentials; the other solution corresponds to much deeper wells and hence to a bound state. The two solutions come from the quadratic nature of (18) for 2 harmonics C_{n0}. With this selection the complete interaction potential curve can be drawn and the corresponding f_0 calculated. As higher values of r_1 are taken in the above set the fit becomes slightly better. Together with the D wave findings below, $r_1 \approx 1.8f$ is perhaps the best compromise for the S well. Comparing the corresponding wells in the order $r_1 = 1.2$, 1.4, $1.8f$, the first two show, for r just greater than r_1, a repulsive part which is strongest for $r_1 = 1.2f$. The effect of this is to indicate clearly the need for a bigger repulsive core radius, which supports the finding that $r_1 \approx 1.8f$ is probably the best compromise. Furthermore for $r_1 = 1.8f$ the potential (for $r_1 < r < r_N$) is purely negative, and up to radii $r \approx 3f$, resembles the square well of best fit in being nearly of constant depth, and of its order of depth. For larger r the potential rises gradually to 0 at $r_N = 4f$.

(d) Testing these three potentials for the D wave one finds that none nearly represents the results, the larger r_1 being further from a fit. Even potentials of this kind with lower r_1 do not come close to a D wave fit. It is for this reason that in (c) above, the compromise S wave fit is taken as corresponding to $r_1 \approx 1.8f$. The lack of D wave fit is not unexpected from the square well results (especially in view of the potential for $r = 1.8f$ being so similar to the square well); and as an estimate from the latter, one would say that the wells required by the S wave results are too shallow for the D wave phases by $\approx$ 2.7 MeV.

These results indicate, more generally, that a velocity-independent potential fitting both S and D results is not possible, even for the low energy domain. For the S waves, the results confirm the demand, for an infinite repulsive core of the considerable radius $r_1 \approx 1.8f$. They also indicate $r_N \approx 4f$. It is outside the scope of the present analysis to determine the na-

ture of the velocity dependence, but it is nevertheless clear that if the outside attractive well is to have the same shape up to the core, the velocity dependence could consist in r_1 depending on l, being in fact smaller for the D wave than for the S wave (for which, say, $r_1 = 1.8f$). The order of the compromise core dimension is near the suggestion of Herzenberg [6]), $r_1 = 2$ to $3f$. The latter analysis in any case shows from fundamental arguments that the core interaction is repulsive and velocity-dependent.

Since it is possible to test any interaction with a core and an effectively finite range r_N, the analysis was used to test the potential given in the paper by Herzenberg [6]), with $r_1 = 2.5f$. Using this potential for the S wave, the f_0 was nowhere near a fit, the attractive well being, effectively speaking, too shallow, or alternatively the core radius being too large, to a considerable degree. Although no calculations were made, this may also be said with great probability of f_2. Since the Herzenberg potential [6]) is uncertain in actual detail and velocity dependence below $r = 2.5f$, this analysis cannot usefully be pursued further at this stage. The fact is that if one permits of velocity-dependent effects a purely phenomenological analysis becomes impossible or at least quite arbitrary, unless a fairly precise indication of the type of velocity-dependence is furnished from other considerations (for example, fundamental considerations).

Even so the question may well arise of the possible use of such a phenomenological potential, apart from being a mere shorthand for scattering results (which may be done more simply with square wells). Indeed, the mere fact that, in spite of the considerations in the introduction, the interaction is velocity-dependent indicates that the problem is not precisely enough a two-body problem. It is hence natural to expect that a velocity-dependent phenomenological potential deduced for the α—α interaction would only apply strictly to it, and not to α—α cluster interaction in the Be^9 and C^{12} problems, for example. The need for such care is further indicated by the consideration that whereas the α—n interaction [4]) involves no sensible velocity-dependence (apart from the spin-orbit coupling, of course), the α—α interaction does. There is another difficulty in the way of an application of velocity-dependent forces such as is likely here: namely, that the strong repulsive forces would require due allowance for cluster correlation effects in problems involving α-clusters, in line with the work of Brueckner [11]). Since one would then have to deal with repulsive velocity-dependent forces within a region of large radius, involving in general a few clusters which are themselves compound particles, the use of a phenomenological potential looks very unpromising.

However, if it is possible to formulate the velocity-dependence in a reasonably simple form (l-dependence of core radius, say), connecting it with nucleon-nucleon forces by means of a group-resonance calculation, then the

phenomenological potential could provide an avenue for testing these forces and the $\alpha-\alpha$ interaction derived from such a calculation. It may then furnish information on the properly velocity-independent part of the $\alpha-\alpha$ interaction, and indicate features of the velocity-dependence which may qualitatively elucidate the application of the α-cluster model. With electronic computers a direct calculation of $\alpha-\alpha$ scattering from nucleon-nucleon forces may be possible, using the group-resonance formalism. The equivalent velocity-dependent potential may then be calculated from this solution. This would be another way of arriving at the $\alpha-\alpha$ potential, and would presumably have the restricted use indicated above.

The trend of the above phenomenological conclusions, arrived at by using square wells and more general smooth potentials, is confirmed by Nilson *etal.*'s [5]) † fitting of the experimental data to the Haefner potential [8])

$$V_N(r) = 0 \quad \text{for} \quad r > r_N, \quad = -D + \frac{q^2\hbar^2}{2\mu r^2} \quad \text{for} \quad r < r_N,$$

where $q^2 = 30$ for convenience. To fit the 94.5 keV resonance, D may be calculated as a function of r_N. The rest of the data then provide r_N, and hence D. Since these fits cover a wider energy range, the experimental points naturally have a somewhat wider scatter round the theoretical curves than was found in the present investigation over a more limited energy range. Nilson *et al.* [5]) found with the Haefner potential (the subscripts S, D, G refer to the partial wave):

(a) $r_{NS} = 3.49f$ for E' up to 20 MeV.

(b) $r_{ND} = 4.44f$ for E' up to 6 MeV. No fit here could represent D wave phases at $E' > 6$ MeV as well, the well with $r_{ND} = 4.44f$ being too shallow for higher energy data.

(c) r_{NG} just smaller than $4.44f$ would represent the G wave data up to $E' = 20$ MeV, but rapidly becomes too shallow at larger energies up to $E' = 22.9$ MeV.

These results thus also indicate velocity-dependence, inasmuch as r_N is not common to all the l values, and as a fit at lower energies deteriorates at higher energies. Similar results have been presented in a different form by Humphrey [9]): he used a modified Haefner potential and found a general fit up to $E' = 22$ MeV with $r_N = 3.75f$ and

$$D = 21 \text{ MeV for the S wave,}$$
$$D = 25 \text{ MeV for the D wave,}$$
$$D = 32 \text{ MeV for the G wave.}$$

† The result of this work became available when the calculations of the present paper were nearly completed; the authors are indebted to Prof. Jentschke for communicating these results to them before publication.

The value of r_N and the trend of D agrees with the general findings of the present paper. These modified Haefner potentials go through zero at a radius between 1 and $2f$, and rise rapidly for smaller r. This indicates a repulsive core with an effective radius comparable to that, $r_1 \approx 1.8f$, found in this paper, and this effective radius also becomes smaller for higher l. It should be noted that the Haefner potential, like the square well potential, is merely a convenient form for expressing repulsion between overlapping systems, which to some extent can fit the results, but has no theoretical foundation as yet.

One of the authors (H. J. P.) wishes to acknowledge the benefit of a bursary of the South African Council for Scientific and Industrial Research during the present investigations.

References

1) N. P. Heydenburg and G. M. Temmer, Phys. Rev. **104** (1956) 123
2) J. L. Russell, G. C. Phillips and C. W. Reich, Phys. Rev. **104** (1956) 135
3) Nilson, Kerman, Briggs and Jentschke, Phys. Rev. **104** (1956) 1673
4) E. van der Spuy, Nuclear Physics **1** (1956) 381
5) Nilson, Jentschke, Briggs, Kerman and Snyder, to be published
6) A. Herzenberg, Nuclear Physics **3** (1957) 1
7) Bloch, Hull, Broyles, Bouricius, Freeman and Breit, Revs. Mod. Phys. **23** (1951) 147
8) R. R. Haefner, Revs. Mod. Phys. **23** (1951) 228
9) C. H. Humphrey, quoted by Nilson *et al.* [5])
10) Breit, Wheeler and Yost, Phys. Rev. **49** (1936) 174
11) H. A. Bethe, Phys. Rev. **103** (1956) 1353

8.B *Nuclear Physics* 7 (1958) 411—420; © *North-Holland Publishing Co., Amsterdam*
Not to be reproduced by photoprint or microfilm without written permission from the publisher

REFORMULATION OF THE THEORY OF THE NEUTRINO

S. KAMEFUCHI
Universitetets Institut for teoretisk Fysik, Copenhagen

Received 14 March 1958

Abstract: A reformulation of the theory of the neutrino is attempted by generalizing the free Lagrangian so as to include from the outset terms violating parity and particle number conservations. It is shown that, so far as the free field is concerned, our generalized field is equivalent to the usual field and that a difference appears only when interactions are included. An application is also given to the discussion of coupling constant invariants of β-decay.

1. Introduction

Since the parity conservation is violated in some weak interactions comprising neutrinos, it would be a tempting idea to attribute the origin of this violation to the intrinsic nature of the neutrino. When we take such a viewpoint, it becomes possible to formulate a field theory of the neutrino in a way more general than the usual theories. This is because, in this case, we need not take into account the restriction of parity conservation and can thus start with a free Lagrangian which is not invariant under space reflection. The two-component theory developed by Lee and Yang, and others, is an example of this kind of approach [1]).

The question of the conservation of the lepton number is not yet fully settled by experiments and thus there exists, at present, further latitude to extend the theory in this direction, i.e., so as to introduce into the free Lagrangian terms violating this conservation law.

In this note, an attempt is made to reformulate the theory of the neutrino by generalizing the Lagrangian in the above sense. An application of our formalism is also given to the problem of coupling constant invariants, discussed recently by Pauli and Pursey [2]).

Our main conclusion is the following: so far as the free field is concerned, our generalized field is equivalent to the usual Dirac, Majorana or two-component neutrino field, which may have, in general, indefinite parities under the transformations of space reflection and of charge conjugation. Characteristic features of our field become explicit, however, when the interaction comes in. It is also found that our formalism is convenient for discussing coupling constant invariants of the β-decay interaction; it can easily be extended to the case of non-vanishing mass of the neutrino and,

moreover, with the use of a perturbation expansion, it enables us to reach somewhat more explicit conclusions than the above mentioned authors.

An appendix is devoted to the discussion of some identities which exist between Pauli's covariants of coupling constants.

2 Neutrino Field of Vanishing Mass

In this section, the case of a neutrino field with vanishing mass will be considered. The most general form of the free Lagrangian, which takes into account both the violation of parity and that of the lepton number, is given by†

$$L = -\tfrac{1}{2}[\xi\bar{\psi}(1+a\gamma_5)\Gamma\psi+\xi\psi\Gamma^{\mathrm{T}}(1+a\gamma_5{}^{\mathrm{T}})\bar{\psi}+\eta\bar{\psi}\Gamma C\bar{\psi}-\eta^*\psi C^{-1}\Gamma\psi], \quad (1)$$

where Γ is defined by $\gamma_\mu\partial/\partial x_\mu$, ξ and a are real constants, η in general a complex constant and C the usual charge conjugation matrix.

Now, the Lagrangian (1) shows different features according to the values of the parameters, and therefore we shall consider several cases separately.

2.1. $\xi^2(1-a^2)-|\eta|^2 \neq 0, \quad a \neq \pm 1$

The quantization in this case is carried out by using the standard method and most easily by using Umezawa-Takahashi's formula [3] ††. The anti-commutators for field quantities are as follows:

$$\begin{aligned}\{\psi(x),\ \psi(x')\} &= \frac{1}{i}\,\frac{\eta}{\xi^2(1-a^2)-|\eta|^2}\,S_0(x-x')C,\\ \{\psi(x),\ \bar{\psi}(x')\} &= \frac{1}{i}\,\frac{\xi}{\xi^2(1-a^2)-|\eta|^2}\,(1+a\gamma_5)S_0(x-x');\end{aligned} \quad (2)$$

$S_0(x)$ is defined by $\Gamma D(x)$, where $D(x)$ is the usual invariant function for massless fields.

In this case, we see from the consistency of the theory that there exist further restrictions on the parameters, which can be found in the following way. First, as seen from the second of eqs. (2), the constant a has to satisfy the condition $|a| < 1$, which is required in order that each component of ψ has the anti-commutators with the right sign. And, if this is the case, we can eliminate the γ_5-terms from (1) by making a linear transformation $\psi = k_1\psi'+k_2\gamma_5\psi'$, where $k_1{}^2+k_2{}^2 = 1$, $2k_1k_2 = a$.

† Terms like $\bar{\psi}\gamma_5\Gamma C\bar{\psi}$, which do not contribute to the variation of the action function, have been omitted. We can easily see that $\delta\int\bar{\psi}\gamma_5\Gamma C\bar{\psi}\mathrm{d}^4x = 0$, for any variation such that $\{\delta\psi(x), \psi(x')\} = 0$.

†† In order to apply this formula to our case, we have only to rewrite the Lagrangian (1) in the form $L = \tfrac{1}{2}\Psi^{\mathrm{T}}\Lambda\Psi$, where $\Psi = \begin{pmatrix}\psi\\ \bar{\psi}\end{pmatrix}$ and $\Lambda \equiv -\begin{pmatrix}\eta^*\Gamma^{\mathrm{T}}C^{-1}, & \xi\Gamma^{\mathrm{T}}(1+a\gamma_5{}^{\mathrm{T}})\\ \xi\Gamma(1-a\gamma_5), & \eta\Gamma C\end{pmatrix}$. Then, the anti-commutator is immediately given by the formula $\{\Psi^{\mathrm{T}}(x),\ \Psi(x')\} = iRD(x-x')$, where R is the solution to $\Lambda R = (\Gamma)^2$.

After this transformation the Lagrangian becomes $L = -\frac{1}{2}\sqrt{1-a^2} \times [2\xi\sqrt{1-a^2}\bar{\psi}'\Gamma\psi' + \eta\bar{\psi}'\Gamma C\bar{\psi}' - \eta^*\psi' C^{-1}\Gamma\psi']$, which can further be rewritten in terms of two real fields ϕ_1 and ϕ_2, defined by $\psi' = (1/\sqrt{2})(\phi_1 + i\phi_2)$, as follows:

$$L = -\frac{\sqrt{1-a^2}}{2}[(\xi\sqrt{1-a^2}+\eta)\phi_1\gamma_4\Gamma\phi_1 + (\xi\sqrt{1-a^2}-\eta)\phi_2\gamma_4\Gamma\phi_2],$$

where we have used the Majorana representation for the γ-matrices and changed the phase of ψ' in such a way that η becomes real. Thus, from the requirement that the commutators for ϕ_1 and ϕ_2 have the right signs, follow the conditions $\xi\sqrt{1-a^2} \pm \eta > 0$, which, in general, lead to $\xi > 0$ and $\xi^2(1-a^2) - |\eta|^2 > 0$. When these conditions are satisfied, we can further eliminate η-terms from the Lagrangian by making a transformation $\psi' = k_3\psi'' + k_4 C\bar{\psi}''$, where $k_3^2 + k_4^2 = 1$, $2k_3k_4 = -\eta/\xi\sqrt{1-a^2}$.

Thus, it is shown that the Lagrangian (1) in this case can ultimately be brought into a "canonical" form by making a linear transformation of the type

$$\psi = \alpha_1\varphi + \alpha_2\gamma_5\varphi + \beta_1 C\bar{\varphi} + \beta_2\gamma_5 C\bar{\varphi}. \tag{3}$$

Here, by the canonical form of the Lagrangian we mean the familiar form

$$L_c = -\bar{\varphi}\Gamma\varphi. \tag{4}$$

It is also to be noted that the transformation (3) reduces to Pauli's canonical transformation [2]) only when some conditions are imposed on the coefficients α's and β's †.

For convenience in later discussions we here define the following quantities:

$$\begin{aligned} K &\equiv |\alpha_1|^2 + |\alpha_2|^2 + |\beta_1|^2 + |\beta_2|^2, \\ L &\equiv \alpha_1\alpha_2^* + \alpha_1^*\alpha_2 + \beta_1\beta_2^* + \beta_1^*\beta_2, \\ I &\equiv 2(-\alpha_1^*\beta_1^* + \alpha_2^*\beta_2^*), \\ M &\equiv |\alpha_1|^2 - |\alpha_2|^2 - |\beta_1|^2 + |\beta_2|^2 + \alpha_1\alpha_2^* - \alpha_1^*\alpha_2 - \beta_1\beta_2^* + \beta_1^*\beta_2. \end{aligned} \tag{5}$$

In order to bring (1) into the form (4), the coefficients α's and β's have only to satisfy the conditions

$$\xi = \frac{K}{|M|^2}, \qquad a = \frac{L}{K}, \qquad \eta = \frac{I^*}{|M|^2}. \tag{6}$$

In terms of quantities defined by (5) the anti-commutators (2) can be rewritten in the form

† It can be proved that our transformation (3), which contains 8 real parameters, reduces to a canonical transformation, provided that the following four conditions are satisfied, viz., $K = L = I = I^* = 0$. (This is also seen from (2') below.) This result means that the most general type of canonical transformations for the neutrino fields consists of a 4-parameter group, just as given by Pauli.

$$\{\psi(x),\ \psi(x')\} = \frac{1}{i} I^* S_0(x-x')C,$$
$$\{\psi(x),\ \bar{\psi}(x')\} = \frac{1}{i} (K+L\gamma_5)S_0(x-x'), \tag{2'}$$

where we have used the identity $K^2-L^2-|I|^2 = |M|^2$.

Our results (2) or (2′) can be regarded as a further generalization of the anti-commutators discussed by Jauch and others [4]); if we put $a = 0$, the expressions (2) or (2′) go into Jauch's anti-commutators. Thus, the fields ψ corresponding to $a = 0$, $\eta = 0$ and $a = 0$, $0 < |\eta| < \xi$ describe the usual Dirac neutrino and what may be called the Jauch neutrino, respectively. As $|\eta| \to \xi$, the anti-commutators of the Jauch neutrino tend to those of the Majorana neutrino.

2.2. $\xi^2(1-a^2)-|\eta|^2 = 0, \qquad a \neq \pm 1$

As mentioned above, we can regard η as real and positive without loss of generality; $|a| < 1$ in this case.

First, we shall consider the case $\xi > 0$. Then $\eta = \xi\sqrt{(1-a^2)}$, and, by a transformation $\psi' = c_1\psi + c_2\gamma_5\psi$ with real c_1, c_2 such that $c_1 > c_2$, $c_1^2+c_2^2 = 1$, $a = -2c_1c_2$, we can bring the Lagrangian into the following form:

$$L = \frac{-\xi}{2}[2\bar{\psi}'\Gamma\psi' + \bar{\psi}'\Gamma C\bar{\psi}' - \psi' C^{-1}\Gamma\psi'] = \xi\left(\frac{\psi'+C\bar{\psi}'}{\sqrt{2}}\right) C^{-1}\Gamma\left(\frac{\psi'+C\bar{\psi}'}{\sqrt{2}}\right).$$

This means that in this case the Lagrangian describes just the usual Majorana field. As is evident from the above argument, the case $\xi < 0$ is unphysical. We also remark that in general any Majorana field can be written in the same form as (3) in terms of the Dirac field, but with the additional conditions that $\alpha_1^* = \beta_1$ and $\alpha_2^* = -\beta_2$.

2.3. $a = \pm 1$

First, let us consider the case $\xi \neq 0$. In this case, the ξ-terms in (1) just correspond to the free Lagrangian of a neutrino with a definite helicity, whereas the η-terms describe couplings between this neutrino and another kind with opposite helicity, the free Lagrangian of which is missing in (1), however. To exclude such an unphysical case, we must put $\eta = 0$. Needless to say we must have $\xi > 0$. Therefore, this case just corresponds to the well-known two-component neutrino field, which can again be written in a form like (3) with the conditions $\alpha_1 = \pm\alpha_2$ and $\beta_1 = \pm\beta_2$. Now the case $\xi = 0$ has to be excluded: for the Lagrangian in this case contains only the coupling term between neutrinos with different helicities and no term corresponding to free Lagrangians. Or, what is the same thing, the Lagrangian, being written in terms of Majorana fields, in the form

$$L = -\tfrac{1}{2}\eta[\phi_1\gamma_4\Gamma\phi_1 - \phi_2\gamma_4\Gamma\phi_2],$$

evidently leads to some inconsistency after quantization, i.e. to commutators with wrong signs irrespective of η.

It is also to be remembered here that the cases 2.2 and 2.3 differ from each other only by their representations. As shown by many authors [5]), they are completely equivalent so far as the free field is concerned. In fact, we can easily show that by changing the variable ψ into $(1/\sqrt{2})\{(c_1+c_2\gamma_5)\psi + (c_1-c_2\gamma_5)C\bar{\psi}\}$, with c_1 and c_2 defined above, the Lagrangian of the two-component neutrino $L = -\xi\bar{\psi}(1 \pm \gamma_5)\Gamma\psi$ can be transformed into the form $-\frac{1}{2}\xi\{2\bar{\psi}(1+a\gamma_5)\Gamma\psi+\sqrt{(1-a^2)}\,(\bar{\psi}\Gamma C\bar{\psi}-\psi C^{-1}\Gamma\psi)\}$, which is nothing else than the Lagrangian of the Majorana neutrino discussed above.

From the above arguments we conclude that, so far as the free field is concerned, our generalized Lagrangian can always be brought into the canonical form, and so our field is equivalent to the usual field of Dirac, Majorana and the two-component theory, respectively. It is to be noted, however, that in general the latter fields would have indefinite transformation properties under both space reflection and charge conjugation, as is easily seen from (3). The difference between our field and the usual fields appears only when the interaction is introduced. For, if the interaction is present, the transformation (3) induces corresponding changes in the interaction terms, too†.

3. Neutrino Field with Non-Vanishing Mass

Our method can be extended to the case of non-vanishing mass. Along similar lines as above we shall consider the general field defined by

$$\psi_i = \alpha_{1i}\varphi+\alpha_{2i}\gamma_5\varphi+\beta_{1i}C\bar{\varphi}+\beta_{2i}\gamma_5 C\bar{\varphi}, \tag{7}$$

where φ is a Dirac field with non-vanishing mass κ, which therefore satisfies the usual anti-commutators, and α_i's and β_i's are arbitrary constants.

Now, it is of special interest to note the commutation relations between two fields ψ_i and ψ_j, defined by (7), with different coefficients α_i, β_i and α_j, β_j:

$$\begin{aligned}
\{\psi_i(x),\ \psi_j(x')\} &= -\frac{1}{i}S(x-x')\{-I^*_{ij}+J^*_{ij}\gamma_5\}C-\frac{\varkappa}{i}\Delta(x-x')\{I'^*_{ij}-J'^*_{ij}\gamma_5\}C.\\
\{\psi_i(x),\ \bar{\psi}_j(x')\} &= \frac{1}{i}S(x-x')\{K_{ij}-L_{ij}\gamma_5\}+\frac{\varkappa}{i}\Delta(x-x')\{-K'_{ij}+L'_{ij}\gamma_5\},
\end{aligned} \tag{8}$$

where $\Delta(x)$ is the usual delta-function for a field with mass κ and $S(x) = \Gamma\Delta(x)$. The constants I_{ij} etc. are defined in the following way:

† However, we can also say that the Dirac neutrino with the most general kind of interaction, whose Lagrangian is, for instance, $L_e(\varphi)+L_{\text{int}}(\alpha_1\varphi+\alpha_2\gamma_5\varphi+\beta_1 C\bar{\varphi}+\beta_2\gamma_5 C\bar{\varphi})$, is entirely equivalent to our neutrino with a simple form of interaction, whose Lagrangian is $L(\psi)+L_{\text{int}}(\psi)$. In this connection, see ref. [4]).

$$
\begin{aligned}
I_{ij} &= \quad I_{ji} \equiv -\alpha^*_{1i}\beta^*_{1j}+\alpha^*_{2i}\beta^*_{2j}-\beta^*_{1i}\alpha^*_{1j}+\beta^*_{2i}\alpha^*_{2j},\\
J_{ij} &= -J_{ji} \equiv \quad \alpha^*_{1i}\beta^*_{2j}-\alpha^*_{2i}\beta^*_{1j}+\beta^*_{1i}\alpha^*_{2j}-\beta^*_{2i}\alpha^*_{1j},\\
K_{ij} &= \quad K^*_{ji} \equiv \quad \alpha_{1i}\alpha^*_{1j}+\alpha_{2i}\alpha^*_{2j}+\beta_{1i}\beta^*_{1j}+\beta_{2i}\beta^*_{2j},\\
L_{ij} &= \quad L^*_{ji} \equiv \quad \alpha_{1i}\alpha^*_{2j}+\alpha_{2i}\alpha^*_{1j}+\beta_{1i}\beta^*_{2j}+\beta_{2i}\beta^*_{1j},\\
I'_{ij} &= \quad I'_{ji} \equiv -\alpha^*_{1i}\beta^*_{1j}-\alpha^*_{2i}\beta^*_{2j}-\beta^*_{1i}\alpha^*_{1j}-\beta^*_{2i}\alpha^*_{2j},\\
J'_{ij} &= \quad J'_{ji} \equiv \quad \alpha^*_{1i}\beta^*_{2j}+\alpha^*_{2i}\beta^*_{1j}+\beta^*_{1i}\alpha^*_{2j}+\beta^*_{2i}\alpha^*_{1j},\\
K'_{ij} &= \quad K'^*_{ji} \equiv \quad \alpha_{1i}\alpha^*_{1j}-\alpha_{2i}\alpha^*_{2j}+\beta_{1i}\beta^*_{1j}-\beta_{2i}\beta^*_{2j},\\
L'_{ij} &= -L'^*_{ji} \equiv \quad \alpha_{1i}\alpha^*_{2j}-\alpha_{2i}\alpha^*_{1j}+\beta_{1i}\beta^*_{2j}-\beta_{2i}\beta^*_{1j}.
\end{aligned}
\tag{9}
$$

These definitions are just the same as those given by Pauli and others [2]†. The anti-commutators (8) include those of (2) or (2′) as a special case. In the case of $\kappa = 0$, they are invariant under Pauli's canonical transformation.

4. Interacting Fields

In this section, the case of interacting fields will be considered; as an example, let us take the β-decay problem. In terms of our field quantities ψ_i, the most general interaction of β-decay is written in the form

$$H_\beta = \sum_i (\bar{\psi}_\mathrm{p} O_i \psi_\mathrm{n})(\bar{\psi}_\mathrm{e} O_i \psi_i) + \mathrm{h.c.}, \tag{10}$$

where the O_i's ($i = 1, 2, \ldots, 5$) denote the usual covariant γ-matrices describing S, V, T, A, and P couplings, and the ψ_i's are defined by (7).

Now it is to be recalled that any physical quantity which does not depend upon the neutrino variables explicitly, such as the S-matrix element for a neutrino-less double β-process or the cross-section of a simple β-decay summed over neutrino variables, can always be written in terms of vacuum expectation values of chronological products of neutrino field quantities $\langle \mathrm{P}(\psi_i(x),\ \psi_j(x'))\rangle_0$ or $\langle \mathrm{P}(\psi_i(x),\ \bar{\psi}_j(x'))\rangle_0$. It can also easily be shown that these vacuum expectation values are given by the same expressions as the right-hand sides of (8), but with a simple replacement $\Delta(x) \to -\frac{1}{2}i\Delta_\mathrm{F}(x)$, where $\Delta_\mathrm{F}(x)$ is the usual Feynman function††.

From this argument we can derive the conclusion that the coupling constants α_i and β_i enter into the physical quantities mentioned above only through the combinations given by (9). Thus, we have generalized Pauli's result to the case of non-vanishing mass. It might be somewhat unexpected that in the case of $\kappa = 0$ some of Pauli's covariants (viz. M_{ij}, $N_{\mathrm{I}ij}$ and $N_{\mathrm{II}ij}$) do not appear in our result, and so the quantities

† The relation between our notation and Pauli's is as follows:

$$\alpha_{1i} = g^*_{1i},\ \alpha_{2i} = f^*_{1i},\ -\beta_{1i} = g^*_{\mathrm{II}i},\ \beta_{2i} = f^*_{\mathrm{II}i}.$$

†† This results from the fact that for our fields ψ_i we still have the property $\psi_i^{(+)}|0\rangle = 0$, where $(+)$ means the positive frequency part and $|0\rangle$ is the vacuum state.

under consideration, being written in terms of the invariant combinations only, remain invariant under Pauli's canonical transformation. However, we show in the appendix that there exist many identities between $(M_{ij}, N_{\mathrm{I}ij}, N_{\mathrm{II}ij})$ and $(K_{ij}, L_{ij}, I_{ij}, J_{ij})$: thus we can say that the former can appear in the physical quantities only through the intermediary of these identities.

We also remark that as far as the spin states of neutrinos are not measured, the quantities to be compared directly with experiments are limited to those which can be written in terms of the vacuum values of neutrino field operators. Thus, the properties of coupling constants can be discussed only through the combinations given by (9).

Now, we shall consider the P, C and T transformations. Under these transformations all the field operators in (10) obey the well-known transformation laws, except the neutrino operator, which can, in general, be a mixture of different "parities". Therefore, if we require the physical quantity under consideration to be invariant under these transformations, the vacuum expectation values like $\langle \mathrm{P}(\psi_i(x), \psi_j(x'))\rangle_0$ or $\langle \mathrm{P}(\psi_i(x), \bar{\psi}_j(x'))\rangle_0$ as a whole must in effect have just the same transformation properties as the corresponding expressions of usual fields like ψ_p, ψ_n and ψ_e. This can be seen in the following way.

As an example let us consider the P-transformation of the S-matrix element of the neutrino-less double β-process

$$S = \text{const.} \sum_{ij} \int \mathrm{d}\mathbf{x}_1 \mathrm{d}t_1 \int \mathrm{d}\mathbf{x}_2 \mathrm{d}t_2 (\bar{\psi}_\mathrm{p}(\mathbf{x}_1, t_1) O_i \psi_\mathrm{n}(\mathbf{x}_1, t_1))(\bar{\psi}_\mathrm{p}(\mathbf{x}_2, t_2) O_j \psi_\mathrm{n}(\mathbf{x}_2, t_2)) \times (\bar{\psi}_\mathrm{e}(\mathbf{x}_1, t_1) O_i F_{ij}(\mathbf{x}_1 - \mathbf{x}_2, t_1 - t_2) O_j^{\mathrm{T}} \bar{\psi}_\mathrm{e}(\mathbf{x}_2, t_2)),$$

where we have put $\langle \mathrm{P}(\psi_i(x_1), \psi_j(x_2))\rangle_0 = F_{ij}(\mathbf{x}_1 - \mathbf{x}_2, t_1 - t_2)$. In the variables of the reflected coordinates, $\psi'_\mathrm{p}(-\mathbf{x}, t) = \rho_\mathrm{p} \gamma_4 \psi_\mathrm{p}(\mathbf{x}, t)$, etc., the matrix element can be rewritten in the following form:

$$S = \text{const.} \sum_{ij} \int \mathrm{d}(-\mathbf{x}_1) \mathrm{d}t_1 \int \mathrm{d}(-\mathbf{x}_2) \mathrm{d}t_2 (\rho_\mathrm{p}^* \rho_\mathrm{n} \rho_\mathrm{e}^*)^{-2} \times (\bar{\psi}'_\mathrm{p}(-\mathbf{x}_1, t_1) O_i \psi'_\mathrm{n}(-\mathbf{x}_1, t_1))(\bar{\psi}'_\mathrm{p}(-\mathbf{x}_2, t_2) O_j \psi'_\mathrm{n}(-\mathbf{x}_2, t_2)) \times (\bar{\psi}'_\mathrm{e}(-\mathbf{x}_1, t_1) O_i \gamma_4 F_{ij}(\mathbf{x}_1 - \mathbf{x}_2, t_1 - t_2) \gamma_4^{\mathrm{T}} O_j^{\mathrm{T}} \bar{\psi}'_\mathrm{e}(-\mathbf{x}_2, t_2)).$$

Therefore, in order that this matrix element be invariant under P-transformation, we have to require that $F_{ij}(-\overline{\mathbf{x}_1 - \mathbf{x}_2}, t_1 - t_2) = (\rho_\mathrm{p}^* \rho_\mathrm{n} \rho_\mathrm{e}^*)^{-2} \gamma_4 F(\mathbf{x}_1 - \mathbf{x}_2, t_1 - t_2) \gamma_4^{\mathrm{T}}$. This relation is nothing but the usual transformation property for the quantity $\langle \mathrm{P}(\psi(x_1), \psi(x_2))\rangle_0$ of the field ψ, which transforms like $\psi(\mathbf{x}, t) \to \psi'(-\mathbf{x}, t) = (\rho_\mathrm{p}^* \rho_\mathrm{n} \rho_\mathrm{e}^*)^{-1} \gamma_4 \psi(\mathbf{x}, t)$. The other cases can be discussed in the same manner.

Now, from the above requirement we can obtain the necessary and sufficient conditions for invariance under P, C, and T transformations. These are as follows:

for P:

$$L_{ij} = L'_{ij} = 0,$$

and

$$\text{either } I_{ij} = I'_{ij} = 0, \quad \text{or} \quad J_{ij} = J'_{ij} = 0; \qquad \text{(all } i, j\text{)} \qquad (11)$$

for C:

$$\begin{aligned} &K_{ij} \text{ real}, && K'_{ij} \text{ real},\\ &L_{ij} \text{ pure imaginary}, && L'_{ij} \text{ pure imaginary},\\ &I^{(0)}_{ij}\, I^{(0)*}_{kl} \text{ real}, && \text{(all } i, j, k, l\text{)} \qquad (12)\\ &J^{(0)}_{ij}\, J^{(0)*}_{kl} \text{ real},\\ &I^{(0)}_{ij}\, J^{(0)*}_{kl} \text{ pure imaginary}; \end{aligned}$$

for T:

$$\begin{aligned} &K_{ij},\ L_{ij},\ K'_{ij},\ L'_{ij} \text{ real},\\ &I^{(0)}_{ij}\, I^{(0)*}_{kl} \text{ real}, && \text{(all } i, j, k, l\text{)} \qquad (13)\\ &J^{(0)}_{ij}\, J^{(0)*}_{kl} \text{ real},\\ &I^{(0)}_{ij}\, J^{(0)*}_{kl} \text{ real}; \end{aligned}$$

here $I^{(0)}_{ij}$, for example, means the same quantity with or without prime. The above result is a generalization of that of Kahana and Pursey [2]),who have given the conditions for the unprimed quantities only. It is to be noted that, if the neutrino has a non-vanishing mass, however small it may be, the number of conditions is almost doubled.

In this connection, it should also be noted that the conditions for P, C and T invariance as given by (11), (12) and (13) are weaker than those usually imposed on the interaction Hamiltonian itself (or the coupling constants). (For example, in the case of only one type of coupling present and of $\kappa = 0$, (13) gives no restrictions at all for T invariance). This results from the fact that, in our case, the invariance is required only for the expressions which are quadratic in coupling constants. In the case of $\kappa = 0$, it can also be explained by the fact that the existence of Pauli transformation allows us to generalize the operation of P, C and T transformations, and so for the invariance of the theory one has only to require the invariance under these generalized operations which are defined by $P' = U_1 T U_2$, $C' = U_1 C U_2$, and $T' = U_1 T U_2$, respectively, where P, C and T are the usual operations and U_1 and U_2 appropriate Pauli transformations.

The necessary and sufficient condition for lepton number conservation in our formalism is given by vanishing of the expression $\langle \mathrm{P}(\psi_i(x), \psi_j(x')) \rangle_0$:

$$I_{ij} = J_{ij} = I'_{ij} = J'_{ij} = 0 \qquad \text{(all } i, j\text{)}. \qquad (14)$$

Our method can also be applied to the similar problem in μ-meson decay interaction, which was recently discussed by Ferretti and others [6]).

The author likes to thank Professors G. Källén and L. Rosenfeld for their critical comments and valuable discussions. He wishes to express his gratitude to Professor Niels Bohr for the hospitality at the Institute for Theoretical Physics. It is also a pleasure to acknowledge the financial aid received from the Ford Foundation.

Appendix

Here we shall discuss the identities which hold between the unprimed quantities listed in (9) and M_{ij}, $N_{\mathrm{I}ij}$ and $N_{\mathrm{II}ij}$ defined by Pauli [2]).

To this purpose, it is convenient to use the quantities F_i and G_i defined by

$$\begin{aligned} F_i &= \begin{pmatrix} F_{1i} \\ F_{2i} \end{pmatrix} = \begin{pmatrix} \alpha_{1i}^* - \alpha_{2i}^* \\ \beta_{2i}^* - \beta_{1i}^* \end{pmatrix}, \\ G_i &= \begin{pmatrix} G_{1i} \\ G_{2i} \end{pmatrix} = \begin{pmatrix} \alpha_{1i}^* + \alpha_{2i}^* \\ \beta_{2i}^* + \beta_{1i}^* \end{pmatrix}. \end{aligned} \tag{A1}$$

Under Pauli's canonical transformation with respect to the neutrino variables, F_i and G_i, apart from phase factors, transform according to the spinor representation of the three-dimensional rotation group.

In terms of F_i and G_i the quantities under consideration can be written in the following way:

$$\begin{aligned} K_{ij} + L_{ij} &= G_{1i}^* G_{1j} + G_{2i}^* G_{2j}, \\ K_{ij} - L_{ij} &= F_{1i}^* F_{1j} + F_{2i}^* F_{2j}, \\ I_{ij} + J_{ij} &= G_{1i} F_{2j} - G_{2i} F_{1j}, \\ I_{ij} - J_{ij} &= F_{2i} G_{1j} - F_{1i} G_{2j}, \\ M_{ij} &= F_{1i}^* G_{1j} + F_{2i}^* G_{2j}, \\ N_{\mathrm{I}ij} &= F_{1i} F_{2j} - F_{2i} F_{1j}, \\ N_{\mathrm{II}ij} &= G_{1i} G_{2j} - G_{2i} G_{1j}. \end{aligned} \tag{A2}$$

Now, M_{ij}, $N_{\mathrm{I}ij}$ and $N_{\mathrm{II}ij}$ are not invariant quantities under Pauli's transformation, but change by phase factors $\exp(2i\alpha)$, $\exp(-2i\alpha)$ and $\exp(2i\alpha)$, respectively; therefore, all possible invariant quantities built up from M_{ij}, $N_{\mathrm{I}ij}$ and $N_{\mathrm{II}ij}$ only are given by the following expressions: $M_{ij} M_{kl}^*$, $N_{\mathrm{I}ij} N_{\mathrm{I}kl}^*$, $N_{\mathrm{II}ij} N_{\mathrm{II}kl}^*$, $N_{\mathrm{I}ij} N_{\mathrm{II}kl}$, $N_{\mathrm{I}ij} M_{kl}$ and $N_{\mathrm{II}ij} M_{kl}^*$. Therefore, it is to be expected that all these quantities can be expressed in terms of the invariants K_{ij}, L_{ij}, I_{ij} and J_{ij}, and, in fact, the following identities hold:

$$
\begin{aligned}
M_{ij}\ M^*_{kl} &= (K_{ij}+L_{ij})(K_{ik}-L_{ik})-(I_{jk}+J_{jk})(I^*_{il}-J^*_{il}),\\
N_{\mathrm{I}ij}\ N^*_{\mathrm{I}kl} &= (K_{ki}-L_{ki})(K_{lj}-L_{lj})-(K_{kj}-L_{kj})(K_{li}-L_{li}),\\
N_{\mathrm{II}ij} N^*_{\mathrm{II}kl} &= (K_{ki}+L_{ki})(K_{lj}+L_{lj})-(K_{kj}+L_{kj})(K_{li}+L_{li}),\\
N_{\mathrm{I}ij}\ N_{\mathrm{II}kl} &= (I_{ij}+J_{ij})(I_{ik}-J_{ik})-(I_{kj}+J_{kj})(I_{il}-J_{il}),\\
N_{\mathrm{I}ij}\ M_{kl} &= (I_{ij}+J_{ij})(K_{ki}-L_{ki})-(I_{ii}+J_{ii})(K_{kj}-L_{kj}),\\
N_{\mathrm{II}ij} M^*_{kl} &= (I_{ki}-J_{ki})(K_{lj}+L_{lj})-(I_{kj}-J_{kj})(K_{li}+L_{li}),\\
&\qquad\qquad \text{(all } i,\ j,\ k,\ l\text{).}
\end{aligned}
\tag{A3}
$$

These are easily checked by substituting the expressions given in (A2).

References

1) T. D. Lee and C. N. Yang, Phys. Rev. **105** (1957) 1671;
L. D. Landau, Nuclear Physics **3** (1957) 127;
A. Salam, Nuovo Cimento **5** (1957) 299
2) W. Pauli, Nuovo Cimento **6** (1957) 204;
C. P. Enz, *ibid.* **6** (1957) 250;
D. L. Pursey, *ibid.* **6** (1957) 266;
S. Kahana and D. L. Pursey, *ibid.* **6** (1957) 1469;
G. Lüders, *ibid.* **7** (1958) 171
3) Y. Takahashi and H. Umezawa, Prog. Theor. Phys. **9** (1953) 14, 501
4) J. M. Jauch, Helv. Phys. Acta **27** (1954) 89;
Y. Takahashi, Nuovo Cimento **1** (1955) 414;
S. Kamefuchi and S. Tanaka, Prog. Theor. Phys. **14** (1955) 225
5) J. Serpe, Physica **18** (1952) 295; Nuclear Physics **4** (1957) 183;
J. A. McLennan, Phys. Rev. **106** (1957) 821;
K. M. Case, *ibid.* **107** (1957) 307;
L. A. Radicati and B. Touschek, Nuovo Cimento **5** (1957) 1693
6) B. Ferretti, Nuovo Cimento **6** (1957) 997;
R. Gatto and G. Lüders, *ibid.* **7** (1958) 806

1.C *Nuclear Physics* 7 (1958) 421—424; © *North-Holland Publishing Co., Amsterdam*
Not to be reproduced by photoprint or microfilm without written permission from the publisher

BOUND STATES OF A MANY-PARTICLE SYSTEM

F. COESTER

Department of Physics, State University of Iowa, Iowa City, Iowa

Received 10 April 1958

Abstract: Rigorous formal solutions of the bound state Schrödinger equation are constructed in terms of an arbitrary complete set of single particle wave functions. From these solutions one sees without effort that the Rayleigh Schrödinger perturbation expansion of the energy does not contain matrix elements represented by products of unlinked diagrams. The components of the state vector are related in a simple manner to functions represented by linked diagrams only.

The validity of the Brueckner approximation to the bound state energy of a many particle system depends on the absence of "unlinked clusters" in the perturbation expansion of this energy. Brueckner [1]) has shown that such terms are absent from a few orders of the perturbation series. General proofs for all orders of the perturbation series have been given by several authors [2–4]). All these proofs are based on a detailed inspection of perturbation terms of arbitrary order. The purpose of this note is to cast the basic equations into such a form that the absence of unlinked terms from the energy becomes evident without detailed inspection of all n'th order perturbation matrix elements.

We are concerned with the formal perturbation expansion of the bound state Ω of a many particle system in terms of the eigenstates of a suitable independent particle Hamiltonian H_0. The expansion in powers of the perturbation $W \equiv H - H_0$ need not converge. However, if the interaction potential is bounded, the perturbation expansion of the state Ω_η,

$$(H_0 + \eta W)\Omega_\eta = E_\eta \Omega_\eta \tag{1}$$

converges for sufficiently small η, $0 < \eta \leqq 1$. There is an unambiguous correspondence between Ω_η and the zero order eigenstate ϕ defined by † $\phi = \lim_{\eta \to 0} \Omega_\eta$,

$$H_0 \phi = E_0 \phi.$$

The formal properties of the terms in the perturbation series are the same for all values of η. After a suitable selective summation of the leading terms in the series [2]) the limit $\eta \to 1$ may exist even if it did not exist for the original series. The correspondence $\phi \longleftrightarrow \Omega$ persists. ϕ is the "model state" of Eden and Francis [6]) and the "chosen configuration" of Bethe [7]). For an

† For proof of these statements see for instance F. Riesz and B. Sz. Nagy, ref. [5]).

infinite repulsive core W is not bounded and the above considerations are not directly applicable. However, we may replace the infinite repulsive core by a finite one and go to the limit after the potential has been eliminated in favor of the reaction matrix [2,8]). The discussion of useful approximation procedures and the convergence for $\eta = 1$ and infinite repulsive cores is beyond the scope of this note. We merely intend to establish formal properties of the bound state solution of the Schrödinger equation. We shall therefore put $\eta = 1$ in the following for the sake of simplicity and without regard for questions of convergence. We assume that the eigenvalues E and E_0 are non-degenerate. However, our formalism can be easily adapted to the important case of a $(2I+1)$ fold degeneracy of a state with spin I.

Ω is represented by the amplitudes for the excitation of k particles from the configuration ϕ. It is normalized by the condition

$$(\phi, \Omega) = 1. \tag{2}$$

Let the indices ρ and ν label respectively the single particle states which are occupied or empty in the configuration ϕ. Ω can be represented in the form

$$\Omega = \mathbf{F}\phi \tag{3}$$

with

$$\mathbf{F} = 1 + \sum_{k=1}^{N} \mathbf{F}_k \tag{4}$$

$$\mathbf{F}_k = \sum_{\rho_1 \cdots \rho_k} \sum_{\nu_1 \cdots \nu_k} a^+_{\rho_1} \cdots a^+_{\rho_k} b^+_{\nu_1} \cdots b^+_{\nu_k} \frac{1}{(k!)^2} F_k(\rho_1 \cdots \rho_k, \nu_1 \cdots \nu_k) \tag{5}$$

where $a_\rho{}^+$ and $b_\nu{}^+$ are anticommuting Jordan-Wigner operators which create respectively a particle in the state ρ and a hole in the state ν of the configuration ϕ. The function ϕ satisfies by definition the equations $a_\rho \phi = 0$ and $b_\nu \phi = 0$ for all ρ and ν if a_ρ and b_ν are respectively particle and hole annihilation operators. N is the total number of particles. One might proceed from here to derive the formal perturbation solution for the functions F_k and examine the structure of these functions to all order. However, the discussions of Hubbard [4]) and Hugenholtz [3]) indicate that simpler results can be expected if one defines an operator $\mathbf{S}$ by

$$\mathbf{F} = e^{\mathbf{S}} \tag{6}$$

with

$$\mathbf{S} = \sum_{k=1}^{N} \mathbf{S}_k, \tag{7}$$

$$\mathbf{S}_k = \sum_{\rho_1 \cdots \rho_k} \sum_{\nu_1 \cdots \nu_k} a^+_{\rho_1} \cdots a^+_{\rho_k} b^+_{\nu_1} \cdots b^+_{\nu_k} \frac{1}{(k!)^2} S_k(\rho_1 \cdots \rho_k, \nu_1 \cdots \nu_k).$$

Eq. (6) generates a finite set of equations for the $\mathbf{F}_k$ in terms of the $\mathbf{S}_k$:

$$\begin{aligned}\mathbf{F}_1 &= \mathbf{S}_1\\ \mathbf{F}_2 &= \mathbf{S}_2+\tfrac{1}{2}\mathbf{S}_1^2\\ \mathbf{F}_3 &= \mathbf{S}_3+\mathbf{S}_1\mathbf{S}_2+\frac{1}{3!}\mathbf{S}_1^3\\ &\cdots\cdots\end{aligned} \tag{8}$$

These equations can always be solved for the $\mathbf{S}_k$. The definition (6) of $\mathbf{S}$ is therefore always possible. Multiplying eq. (1) ($\eta = 1$) by $e^{-\mathbf{S}}$ we have

$$\{[H_0, \mathbf{S}]+e^{-\mathbf{S}}We^{\mathbf{S}}-E-E_0\}\,\phi = 0 \tag{9}$$

since

$$e^{-\mathbf{S}}H_0e^{\mathbf{S}} = H_0+[H_0, \mathbf{S}].$$

The expansion

$$e^{-\mathbf{S}}We^{\mathbf{S}} = W+[W, \mathbf{S}]+\frac{1}{2!}[[W, \mathbf{S}], \mathbf{S}]+\ldots \tag{10}$$

breaks off with the forth order term if H contains only two-body forces. From (9) follows

$$E-E_0 = (\phi, e^{-\mathbf{S}}We^{\mathbf{S}}\phi) = (\phi, \{W+[W, (\mathbf{S}_1+\mathbf{S}_2)]+\tfrac{1}{2}[[W, \mathbf{S}_1]\,\mathbf{S}_1]\}\,\phi). \tag{11}$$

Let Λ be the projection into ϕ. Multiplying (9) by $1-\Lambda$ we have

$$([H_0, \mathbf{S}]+(1-\Lambda)e^{-\mathbf{S}}We^{\mathbf{S}})\phi = 0. \tag{12}$$

In order to solve (12) for $\mathbf{S}$ it is convenient to define an operator $\mathbf{G}$

$$\mathbf{G} = \sum_{k=1}^{N}\mathbf{G}_k$$

with

$$\mathbf{G}_k = \sum_{\rho_1\cdots\rho_k}\sum_{\nu_1\cdots\nu_k} a^+_{\rho_1}\ldots a^+_{\rho_k}b^+_{\nu_1}\ldots b^+_{\nu_k}\frac{1}{(k!)^2}G_k(\rho_1\ldots\rho_k, \nu_1\ldots\nu_k) \tag{13}$$

by

$$G_k(\rho_1\ldots\rho_k, \nu_1\ldots\nu_k) = (\phi, b_{\nu_k}\ldots b_{\nu_1}a_{\rho_k}\ldots a_{\rho_1}e^{-\mathbf{S}}We^{\mathbf{S}}\phi). \tag{14}$$

In other words $\mathbf{G}$ is obtained from $e^{-\mathbf{S}}We^{\mathbf{S}}$ by shifting all annihilation operators to the right and retaining only those terms which contain after ordering no annihilation operators and at least one pair of creation operators. With these definitions there follows from (12)

$$[H_0, \mathbf{S}]+\mathbf{G} = 0 \tag{15}$$

since $[H_0, \mathbf{S}]$ and $\mathbf{G}$ contain only creation operators. Eq. (15) can be solved for $\mathbf{S}$ by [9])

$$\mathbf{S} = -i\lim_{\varepsilon\to 0}\int_{-\infty}^{0}d\tau\, e^{\varepsilon\tau}\,e^{iH_0\tau}\,\mathbf{G}e^{-iH_0\tau}. \tag{16}$$

On account of the definition of $\mathbf{G}$ the energy denominator in (16) is guaranteed not to vanish. Eqs. (16) and (14) together with the definition (6)

take the place of the original Schrödinger equation. No approximations and no infinite expansions have been used so far. (14) and (16) can be solved by systematic expansion in powers of W. The result is equivalent to the Rayleigh-Schrödinger perturbation series. The matrix elements in this expansion may be represented by diagrams quite similar to Feynmann diagrams†.

It is now easy to prove the following theorem [3,4]):

The diagrams representing the matrix elements of **S** *contain no unlinked parts.*

It is clear from (14), (10) and (16) that **G** contains no unlinked diagrams if **S** does not contain any. In an iteration solution the n'th order term $\mathbf{G}^{(n)}$ is according to (14) equal to an expression containing only $\mathbf{S}^{(n-1)}$ and lower order terms. Since the theorem is true for $n = 1$ it is thereby proven by mathematical induction for all orders. The matrix elements of **F** do have unlinked parts but there are no diagrams or unlinked parts of diagrams without external lines. Since **S** contains no unlinked parts the energy shift (11) also contains no unlinked parts. The choice of the single particle wave functions and energies has been quite arbitrary. Our results are independent of a "self-consistent" choice for these wave functions.

† These diagrams are the same as those used by J. Hubbard (ref. [4])).

References

1) K. A. Brueckner, Phys. Rev. **100** (1955) 36
2) J. Goldstone, Proc. Roy. Soc. A **239** (1957) 267
3) A. Hugenholtz, Physica **23** (1957) 481, 533
4) J. Hubbard, Proc. Roy. Soc. A **240** (1957) 539
5) F. Riesz and B. Sz. Nagy, Functional Analysis (New York, 1955) p. 373 ff
6) R. J. Eden and N. C. Francis, Phys. Rev. **97** (1955) 1366
7) H. A. Bethe, Phys. Rev. **103** (1956) 1353
8) H. A. Bethe and J. Goldstone, Proc. Roy. Soc. A **238** (1957) 551
9) J. M. Jauch and F. Rohrlich, Theory of Photons and Electrons (Addison Wesley, Cambridge, Mass., 1955) p. 129

1.D.4 : 2.L

Nuclear Physics 7 (1958) 425—428; © *North-Holland Publishing Co., Amsterdam*

Not to be reproduced by photoprint or microfilm without written permission from the publisher

INELASTIC SCATTERING OF 96 MeV PROTONS

KEIICHI NISHIMURA

Rutgers University, New Brunswick, New Jersey

Received 20 March 1958

Abstract: An analysis is made of the angular distribution of 96 MeV protons inelastically scattered by carbon. It was found that by using the collective model of the nucleus the agreement to the experimental results is as good as the previous calculations based upon the individual particle model of the nucleus.

In the recent double scattering experiments measurements have been made of polarization and differential cross sections of high-energy nucleons exciting low lying energy levels of target nuclei [1,2,3,4]). Analyses of these data are instrumental to determining the nature of the nuclear states involved as well as that of the scattering process itself. No quantitative analysis, however, has yet been made of the polarization by any method more accurate than the Born approximation [5]) and the angular distribution of the scattered beam has been analysed only with the independent particle model of the nucleus [6,7]).

In this paper the 96 MeV proton data of Strauch and Titus [8]) will be analysed with the collective model of the nucleus. Since the aim of this paper lies in determining the general adequacy of the method and the model, and not in obtaining the best fit of the experimental data, we shall use, instead of a more realistic potential with a rounded edge, a square well potential with a complex well parameter

$$V = -(V_R + iV_I)\rho(\mathbf{r}) \tag{1}$$

where $\rho = 1$ inside the spheroidal nuclear boundary given by

$$r = R[1+\beta Y_2^0(\Omega')] \tag{2}$$

and $\rho = 0$ outside. Here β is the familiar deformation parameter and the solid angle Ω' is measured from a symmetry axis of the spheroid, corresponding to an angle Ω_0 in our coordinate system. The target nucleus is in its ground state before the scattering takes place; for C^{12} this is a 0+ state, and the 4.3 MeV level is known to be a 2+ state. Using the nuclear collective model, these nuclear states may be represented by spherical harmonics, $Y_0^0(\Omega_0)$ and $Y_2^m(\Omega_0)$, respectively. If we write the initial and final nucleon wave function as ψ_0 and ψ_F, the transition amplitude is proportional to

$$I_m = \int Y_2^m(\Omega_0)\psi_F^*(\mathbf{r})V(\mathbf{r})Y_0^0(\Omega_0)\psi_0(\mathbf{r})\mathrm{d}\Omega_0\,\mathrm{d}\mathbf{r}. \tag{3}$$

July (2) 1958

In this paper the nucleon wave functions will be treated as functions of space coordinates only. The differential cross section is then proportional to

$$\frac{d\sigma}{d\Omega} \propto \sum_{m=-2}^{2} |I_m|^2. \tag{4}$$

In the Born approximation the nucleon wave functions in eq. (3) are plane waves. The differential cross section, then, varies as $[j_2(KR)]^2$ where $\hbar K$ is the momentum transfer. This means that the forward scattering cross section vanishes in this approximation. This fact was not observed in the experiment of Strauch and Titus [8]) but the more recent experiments at Uppsala [4]) as well as calculations based upon the independent particle model [6, 7]) show that the differential cross section indeed decreases in the forward direction. On the other hand, $j_2(KR)$ has a node at $KR \approx 5.8$. For the 96 MeV protons scattered by C^{12}, this corresponds to a centre-of-mass scattering angle of about 50°. The expected diffraction minimum in this neighborhood is not observed [8]). Instead the differential cross section decreases smoothly from 20° to 90°.

An improved approximation method was introduced by Schiff [9]) for high energy potential scattering. In this approximation, the distortions of the incident and outgoing plane waves, $e^{i\mathbf{k}_0 \cdot \mathbf{r}}$ and $e^{i\mathbf{k}_F \cdot \mathbf{r}}$, due to the scattering potential are taken into consideration. Then ψ_0 and ψ_F will be replaced by

$$\exp\left[i\mathbf{k}_0 \cdot \mathbf{r} - \frac{i}{\hbar v}\int_0^\infty V(\mathbf{r} - \hat{\mathbf{p}}_0 s)ds\right] \tag{5}$$

and

$$\exp\left[i\mathbf{k}_F \cdot \mathbf{r} + \frac{i}{\hbar v}\int_0^\infty V(\mathbf{r} + \hat{\mathbf{p}}_0 s)ds\right] \tag{6}$$

where Schiff's notations are used. Now in calculating I_m the simplifying assumption $\beta \ll 1$ will be made, although it may not actually hold: As a matter of fact, the C^{12} nucleus on the alpha particle model is a triangle and the nuclear boundary may be appreciably oblate. In addition to this assumption we shall also assume that the second terms in the exponentials (5) and (6) are small. The nuclear well depth at 96 MeV is expected to be less than 20 MeV [10, 11, 12]) and the order of magnitude of these terms is approximately $RV/\hbar v < 0.5$, and this is satisfactorily small.

The differential cross section thus calculated is shown in fig. 1. The well parameters chosen for this curve are $V_R = 2$ MeV, $V_I = 10$ MeV, $R = 1.4 \times 10^{-13} \times (12)^{1/3}$ cm, and $\beta = 0.03$.

The agreement with the experimental results [8]) is not worse than that obtained in a previous attempt [6]) using the independent particle model (shown in fig. 1 by a dotted line). The differential cross section drops for small scattering angles and this fact is not in disagreement with the experiment. This

decrease is not as sharp as that indicated by the dotted line. This is in a better qualitative agreement with ref. [4]). The diffraction minimum is much shallower than what the Born approximation would give and this dip may almost completely disappear if some more realistic potential is employed.

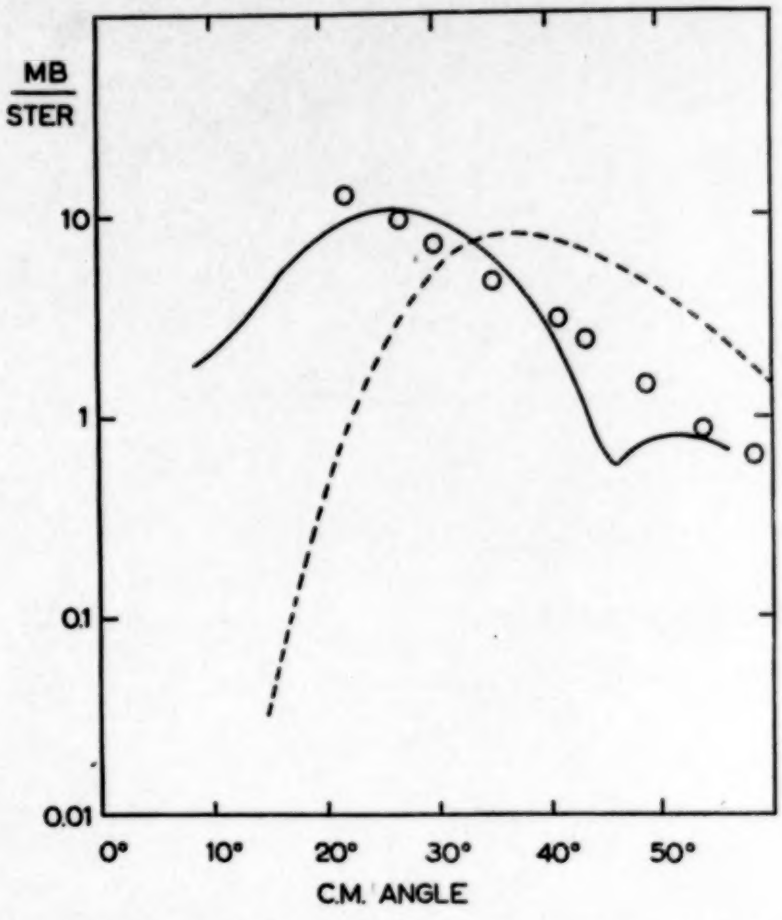

Fig. 1. The calculated differential cross section of 96 MeV protons exciting a 2 + collective level of C^{12}. The dotted line is the calculation based upon the individual particle model [6]). The circles are experimental results of Strauch and Titus [5]).

Thus the 4.3 MeV level of C^{12} can be regarded either as a collective state or as an individual particle excitation. In order to push the present investigation still further it is desirable to analyse the polarization experiments, adding a spin-orbit coupling term to the potential (1). This calculation is now in progress.

References

1) W. G. Chesnut, E. M. Hafner and A. Roberts, Phys. Rev. **104** (1956) 449
2) P. Hillman, A. Johansson and H. Tyrén, Nuclear Physics **4** (1957) 648
3) R. Alphonce, A. Johansson and G. Tibell, Nuclear Physics **4** (1957) 672
4) H. Tyrén and Th. A. J. Maris, Nuclear Physics **4** (1957) 637
5) Th. A. J. Maris, Nuclear Physics **3** (1957) 213
6) P. Benoist, C. Marty and Ph. Meyer, Physica **22** (1956) 1173

7) Th. A. J. Maris and H. Tyrén, Nuclear Physics **4** (1957) 662
8) K. Strauch and F. Titus, Phys. Rev. **103** (1956) 200
9) L. I. Schiff, Phys. Rev. **103** (1956) 443
10) T. B. Taylor, Phys. Rev. **92** (1953) 831
11) E. Clementi and C. Villi, Nuovo Cimento **2** (1955) 176
12) A. M. Lane and C. F. Wandel, Phys. Rev. **98** (1955) 1524

1.D.1 :
1.E.1

Nuclear Physics 7 (1958) 429—442; © *North-Holland Publishing Co., Amsterdam*
Not to be reproduced by photoprint or microfilm without written permission from the publisher

STUDIES IN LITHIUM-7 AND NITROGEN-13 †

FRANK R. HAIG

The Catholic University of America, Washington, D.C. ††

Received 10 March 1958

Abstract: The Pinkston-Brennan treatment of Li^6 and the Elliott treatment of N^{14} are tested by extending their assumptions to the respective three-body isotopes, Li^7 and N^{13}. The Li^7 analysis assigns a spin of 5/2 to the level at 4.61 MeV. The N^{13} analysis uses the Meshkov and Ufford tables for the expression of p^3 matrix elements in terms of p^2 elements. The phase conventions needed for the application to the $p^{-3} \rightarrow p^{-2}$ reduction are discussed. The results are favourable to Elliott's approach.

1. Introduction

Several investigators have shown that a potential consisting of a central force with exchange and a spin-orbit interaction term is capable of predicting the low-lying energy level structure in the case of the p^2 and p^{-2} configurations in P shell nuclei [1]). Wave functions determined by such a potential, however, are not accurate enough to account for other nuclear data, such as [2]) the vanishing of the beta-decay matrix element of the C^{14}—N^{14} decay or the static moments of Li^6.

The discovery of the quadrupole moment of the deuteron had earlier given rise to a similar problem. In that case, to correct the wave functions Schwinger and Rarita introduced a tensor force term into the nuclear Hamiltonian[3]). Elliott, and, independently, Visscher and Ferrell have followed the same approach in the nitrogen problem [4]). They have devised a tensor force which leaves the energy level structure basically unaltered but strongly affects the wave function. The resulting wave function is sufficiently accurate to predict the vanishing of the beta-decay element. In a similar study Pinkston and Brennan [5]) have, with apparent success, sought to account for the small size of the Li^6 quadrupole moment by introducing a small tensor term.

In the present study a test is made of the Pinkston-Brennan and Elliott approach by extending their assumptions for the two-body nuclear systems to the respective three-body cases, Li^7 and N^{13}. The choice of the three-body systems makes it possible not only to observe the reasonableness of the tensor

† This article was composed for the fulfilment of the publication requirement for the degree of Doctor of Philosophy in the Graduate School of Arts and Sciences of the Catholic University of America, Washington, D.C.

†† Now at Woodstock College, Woodstock, Maryland.

parameters chosen but also to investigate the exchange character of the central force. This possibility is due to the much greater sensitivity of the three-body systems as contrasted with the two-body ones to the exchange assumed.

In any such study where the dependence of the three-body matrix elements on the two-body matrix elements is considered, a powerful tool is the Bacher-Goudsmit method [6]) as applied to nuclear spectroscopy by Meshkov and Ufford [7]). In fact, their actual application was to the lithium isotopes here studied where, however, they did not feel justified in including a tensor term. By extending the Pinkston-Brennan results it is felt that such a term can now be reasonably included. Section 2 reviews the theoretical method of Meshkov and Ufford to extend their table to cover the $p^{-3} \rightarrow p^{-2}$ reduction and to simplify and correct their original equations. Section 3 then treats Li^7 and section 4 handles N^{13}.

2. The Bacher and Goudsmit Method

In the Meshkov and Ufford presentation of the Bacher and Goudsmit method, the matrix elements of the l^n configuration are expressed as linear combinations of the matrix elements of the l^{n-1} configuration. As a result the n-particle energy levels are determined once the $(n-1)$-particle system is known. Most importantly, the method directly exhibits the consequences for the n-particle system of any given $(n-1)$-particle assumption.

In order to give the l^n matrix elements in terms of the l^{n-1} matrix elements, Meshkov and Ufford express the wave function of the n-particle system in the $SLJTM_J M_T$ representation, transform it by means of the Clebsch-Gordan expansion to the $SLTM_S M_L M_T$ representation, and expand the resulting functions in terms of one-nucleon states vector-coupled to the $(n-1)$-particle parent states. In this expansion the terms are weighted by the coefficients of fractional parentage as worked out for L-S coupling by Jahn and Van Wieringen [8]). On coupling the parent and the one-particle states back into the $S'L'J'M_{J'}M_{T'}$ representation one obtains

$$\Psi(l^n \gamma TSLJM_T M_J) = \sum_{\substack{M_S M_L \gamma' T' S' L' \\ M_{S'} m_s M_{L'} m M_{T'} m_t J' M_{J'} j m_j}} \langle l^n \gamma TSL | l^{n-1} \gamma' T' S' L' \rangle (SLM_S M_L | JM) \tag{1}$$
$$\times (S' s M_{S'} m_s | SM_S)(L' l M_{L'} m_l | LM_L)(T' t M_{T'} m_t | TM_T)(S' L' M_{S'} M_{L'} | J' M_{J'})$$
$$\times (slm_s m_l | jm_j)\psi(l^{n-1} \gamma' T' S' L' J' M_{T'} M_{J'})\phi(tslm_t m_s m_l)$$

where the $\langle l^n \gamma TSL | l^{n-1} \gamma' T' S' L' \rangle$ are the coefficients of fractional parentage, $(SLM_S M_L | JM)$ is a Clebsch-Gordan coefficient, and $\phi(tslm_t m_s m_l)$ is a one-nucleon wave function. The equation is simplified by the introduction of an X function:

$$\Psi(l^n\gamma TSLJM_TM_J) = \sum_{\substack{\gamma' T' S' L' \\ M_{T'} m_t J' M_{J'} j m_j}} \langle l^n\gamma TSL|l^{n-1}\gamma' T' S' L'\rangle (J' j M_{J'} m_j|JM_J)$$
$$\times (T' tM_{T'} m_t|TM_T)\,[(2J'+1)(2j+1)(2S+1)(2L+1)]^{\frac{1}{2}} X\begin{Bmatrix} S' & L' & J' \\ s & l & j \\ S & L & J \end{Bmatrix} \qquad (2)$$
$$\times \psi(l^{n-1}\gamma' T' S' L' J' M_{T'} M_{J'})\phi(tsljm_t m_j).$$

Tables of X functions in a form suitable to calculate with, i.e., expressed as radicals rather than as decimals, are not easy to obtain. Many have been calculated by the Chalk River group, particularly in their tables for the transformation from L-S to j-j coupling [9, 10, 11]). For values of the parameters not contained in these tables, recourse must be had to the definition of the X function in terms of Racah coefficients.

The above equation may now be substituted into any given n-particle matrix element. In the expansion that results, the coefficient of the contribution of the l^{n-1} matrix element specified by the quantum numbers $(\gamma'_1 T' S'_1 L'_1 J')$ and $(\gamma'_2 T' S'_2 L'_2 J')$ to the l^n matrix element specified by the quantum numbers $(\gamma_1 TS_1 L_1 J)$ and $(\gamma_2 TS_2 L_2 J)$ becomes

$$d(1'2';12) = \frac{n}{n-2}\sum_j (2J'+1)(2j+1)\,[(2S_1+1)(2S_2+1)(2L_1+1)(2L_2+1)]^{\frac{1}{2}}$$
$$X\begin{Bmatrix} S'_1 & L'_1 & J'_1 \\ s & l & j \\ S_1 & L_1 & J \end{Bmatrix} X\begin{Bmatrix} S'_2 & L'_2 & J'_2 \\ s & l & j \\ S_2 & L_2 & J \end{Bmatrix} \langle l^n\gamma_1 TS_1 L_1|l^{n-1}\gamma'_1 T' S'_1 L'_1\rangle \qquad (3)$$
$$\langle l^n\gamma_2 TS_2 L_2|l^{n-1}\gamma'_2 T' S'_2 L'_2\rangle.$$

The summation must be carried out again with $(\gamma'_1 T' S'_1 L'_1 J')$ and $(\gamma'_2 T' S'_2 L'_2 J')$ interchanged if these two sets of quantum numbers are not the same †.

Eqs. (1) and (2) follow the same numbered equations of Meshkov and Ufford but with the isobaric spin dependence explicit. Eq. (3) simplifies their eq. (3) by using the orthonormality of the Clebsch-Gordan coefficients. Meshkov and Ufford have tabulated the equation for $n = 3$, thereby covering the reduction of the p^3 matrix elements to their p^2 parents ††. These tables are also applicable to the reduction of the p^{-3} matrix elements to the p^{-2}. Here, however, a wrong choice of phase conventions can render the table useless so that a discussion of these conventions is necessary.

Two different sets of phase conventions are in common use, the one due to Jahn and Van Wieringen[8]), and the other to Racah and Condon and Shortley [12]). Basically the difference between them begins with the considerable arbitrariness that exists with respect to the phases of wave functions. From

† This procedure is not, of course, equivalent to multiplying the first summation by 2.

†† One misprint occurred in the table. The $\langle {}^{13}D_1|{}^{11}P_1\rangle$ contribution to $\langle [21]^{24}P_{\frac{1}{2}}|[111]^{23}S_{\frac{1}{2}}\rangle$ should not be $-(30)^{\frac{1}{2}}/12$ but $-(30)^{\frac{1}{2}}/18$.

any complete set of wave functions, an equally valid complete set may be generated by changing the phases of one or more of the original set †. Then a matrix element involving one of these new wave functions will also change sign. So too will the coefficients of fractional parentage connecting this state with the states of $(n-1)$-particles.

Since Jahn and Van Wieringen desired to maintain the greatest possible generality, they determined the phases of their wave functions and correspondingly of their coefficients of fractional parentage from the standard Young-Yamanouchi orthogonal representations of the permutation group[14]). Such a phase choice gives a perfectly acceptable set of wave functions and fractional parentage coefficients but has the disadvantage of determining no clear relationship between wave functions and matrix elements for holes and particles. In particular, the spin-orbit matrix does not simply change sign on passing from a nucleus to its conjugate. Mandl's tables for the nuclear P shell follow this convention so that the elements starred in the tables do not change sign while all the rest do [15]). Such a phase convention makes the Meshkov and Ufford tables unusable for the p^{-3} to p^{-2} reduction.

Racah, on the other hand, may be said to define his coefficients of fractional parentage so that on the transition from particles to holes the entire spin-orbit matrix will change sign. He consequently derived the relationship[16])

$$\langle m-n;\gamma SLT|m-(n+1);\gamma' S' L' T'\rangle = (-1)^{L+L'+S+S'+T+T'-1}$$

$$\times \left[\frac{(n+1)}{(m-n)}\,\frac{(2L'+1)(2S'+1)(2T'+1)}{(2L+1)(2S+1)(2T+1)}\right]^{\frac{1}{2}} \langle (n+1);\gamma' S' L' T'|n;\gamma LST\rangle. \qquad (4)$$

Here m is the number of particles in a closed shell. This equation is also given by Jahn and Van Wieringen [17]) †† in their article in terms of group theory but is not used by them to determine their table for $n > 6$. To illustrate the difference in conventions table 1 contains for the reduction $\langle p^{10}|p^9 p\rangle$ both the corrected results of Jahn and Van Wieringen in slightly simpler form and the values as determined by eq. (4). The upper sign follows Jahn and Van Wieringen and the lower sign follows eq. (4).

For most purposes it is indifferent which convention is used for the spin-orbit matrix, provided consistency is maintained. The eigenvalues, for example, are the same in either case. Here, however, we must use the Racah convention. Then the Meshkov and Ufford table describes both the $p^3 \to p^2$ and the $p^{-3} \to p^{-2}$ reduction. So too, their eq. (3) describes the reduction of $p^n \to p^{n-1}$ and $p^{-n} \to p^{-(n-1)}$.

† Only real phases are considered. Cf. ref. [13]).

†† The author is indebted to Dr. J. B. French (private communication) for much of the preceding development.

3. Lithium-7

3.1. CALCULATIONS

The potential found by Pinkston and Brennan for Li^6 employs a central force stronger than that indicated by the two and three body problems and a much stronger spin exchange than that needed for the deuteron. A small tensor force is introduced. Its effect is to leave the energy level spectrum almost unchanged but to correct the wave function so as to reduce the quadrupole moment within the bounds set by experiment.

As is usual with two body problems, the exchange character of the central force is not completely determined by the Li^6 analysis. The value of the P state elements in Li^6 is a good measure of whatever exchange character is assumed. Pinkston and Brennan found good agreement for values of the matrix element $^{11}P_1$ varying from about -1.00 to 2.00 MeV.

In the present section, the effect on Li^7 of the Pinkston-Brennan assumptions for Li^6 is examined both to test whether the same parameters can fit both nuclei and to estimate the exchange character of the central force. Four calculations were made corresponding to assuming $^{11}P_1$ equal to -1.00, 0.00, 1.00, and 2.00 MeV. For this a straight shell model calculation was used. The central potential was expressed in the form

$$H(12) = J(r_{12})(a_0 + a_\sigma\, \sigma_1 \cdot \sigma_2 + a_\tau \tau_1 \cdot \tau_2 + a_{\sigma\tau}(\sigma_1 \cdot \sigma_2)(\tau_1 \cdot \tau_2)) \quad (5)$$

where σ_1 and τ_1 are the Pauli operators

TABLE 1

The coefficients of fractional parentage for the reduction $p^{10} \rightarrow p^9 p$. The table illustrates the two common phase conventions, the upper sign following the convention of Jahn and Van Wieringen and the lower sign that of Racah

	$[333]^{45}S$	$[333]^{44}S$	$[432]^{43}P$	$[432]^{34}P$	$[432]^{45}P$	$[441]^{43}P$	$[432]^{43}D$	$[432]^{34}D$	$[432]^{45}D$	$[441]^{43}F$
$[442]^{15}S$	0	0	$\mp(2/15)^{\frac{1}{2}}$	$\pm(8/15)^{\frac{1}{2}}$	0	$\mp(1/3)^{\frac{1}{2}}$	0	0	0	0
$[442]^{31}S$	0	0	$+(2/15)^{\frac{1}{2}}$	0	$\mp(8/15)^{\frac{1}{2}}$	$\mp(1/3)^{\frac{1}{2}}$	0	0	0	0
$[433]^{11}P$	$\pm(1/5)^{\frac{1}{2}}$	0	$\mp(3/10)^{\frac{1}{2}}$	0	0	0	$\mp(1/2)^{\frac{1}{2}}$	0	0	0
$[433]^{33}P$	$\pm(1/45)^{\frac{1}{2}}$	$\pm(8/45)^{\frac{1}{2}}$	$+(1/30)^{\frac{1}{2}}$	$+(2/15)^{\frac{1}{2}}$	$+(2/15)^{\frac{1}{2}}$	0	$+(1/18)^{\frac{1}{2}}$	$\mp(2/9)^{\frac{1}{2}}$	$\pm(2/9)^{\frac{1}{2}}$	0
$[442]^{13}D$	0	0	$+(1/30)^{\frac{1}{2}}$	$\mp(2/15)^{\frac{1}{2}}$	0	$\mp(4/75)^{\frac{1}{2}}$	$\mp(1/10)^{\frac{1}{2}}$	0	$\pm(2/5)^{\frac{1}{2}}$	$\mp(7/25)^{\frac{1}{2}}$
$[442]^{31}D$	0	0	$\mp(1/30)^{\frac{1}{2}}$	0	$+(2/15)^{\frac{1}{2}}$	$\mp(4/75)^{\frac{1}{2}}$	$+(1/10)^{\frac{1}{2}}$	0	$\mp(2/5)^{\frac{1}{2}}$	$\mp(7/25)^{\frac{1}{2}}$

TABLE 2

Exchange parameters of Li^6

$^{11}P_1$	−1.00	0.00	1.00	2.00
a_0	0.31	0.28	0.25	0.22
a_σ	−0.06	−0.03	0.00	0.04
a_τ	−0.18	−0.15	−0.12	−0.10
$a_{\sigma\tau}$	−0.06	−0.09	−0.12	−0.16
W	0.49	0.37	0.25	0.12
M	0.24	0.37	0.50	0.62
H	0.25	0.13	0.00	−0.12
B	0.01	0.13	0.25	0.38

The W, M, H and B symbols give the percentage of Wigner, Majorana, Heisenberg and Bartlett exchange. The a's are an equivalent set of parameters used by Elliott [18]). The four sets of values sample the region of acceptable central force elements in the Pinkston-Brennan treatment of Li^6 and are used to determine the central force elements in the four Li^7 calculations.

TABLE 3

Calculated energies of Li^7

No.	Term	$^{11}P_1$			
		−1.00	0.00	1.00	2.00
21	$[111]^{4}S_{3/2}$	15.83	15.82	15.81	14.31
20	$[111]^{2}S_{1/2}$	14.43	15.70	17.01	19.18
19	$[21]^{4}D_{3/2}$	12.08	12.07	12.45	13.40
18	$[21]^{2}D_{1/2}$	11.71	11.88	12.08	12.70
17	$[21]^{2}D_{3/2}$	11.68	12.02	12.06	12.71
16	$[21]^{4}D_{5/2}$	11.58	11.56	11.55	12.27
15	$[21]^{4}P_{1/2}$	10.40	10.39	10.38	11.06
14	$[21]^{2}D_{5/2}$	10.27	10.73	11.25	12.21
13	$[21]^{2}D_{3/2}$	9.67	10.18	10.65	11.45
12	$[21]^{2}D_{5/2}$	8.90	8.98	9.03	9.20
11	$[21]^{4}P_{3/2}$	8.84	8.83	8.82	9.49
10	$[21]^{2}P_{1/2}$	7.88	8.10	8.50	9.19
9	$[21]^{2}P_{1/2}$	7.38	7.77	7.91	7.97
8	$[21]^{2}P_{3/2}$	6.87	7.20	7.61	8.27
7	$[21]^{2}D_{7/2}$	6.58	7.05	7.04	7.14
6	$[21]^{2}P_{3/2}$	5.82	6.02	6.11	6.14
5	$[3]^{2}F_{5/2}$	5.67	5.71	5.74	5.95
4	$[21]^{2}P_{5/2}$	4.60	4.61	4.71	4.86
3	$[3]^{2}F_{7/2}$	4.35	3.86	3.85	4.01
2	$[3]^{2}P_{1/2}$	0.18	0.24	0.28	0.27
1	$[3]^{2}P_{3/2}$	0.00	0.00	0.00	0.00

All energies are in units of MeV. The four calculations correspond to the four sets of exchange parameters determined from the Pinkston-Brennan article on Li^6 when the $^{11}P_1$ element is taken as equal to −1.00, 0.00, 1.00 and 2.00 MeV.

in spin and isobaric spin spaces [18]). The a's are the exchange parameters. They are related to the M, W, B and H symbols expressing percentage of Majorana, Wigner, Bartlett and Heisenberg exchange by eq. (5.32) of Blatt and Weiss-

TABLE 4

Observed levels of Li^7

Energy (MeV)	0.00	0.477	4.454	4.61	5.5	6.53	6.6	7.46	9.6	10.8	12.4	14.0	17.5
J	3/2	1/2					1/2, 3/2 5/2						
Parity	−	−					+	−					

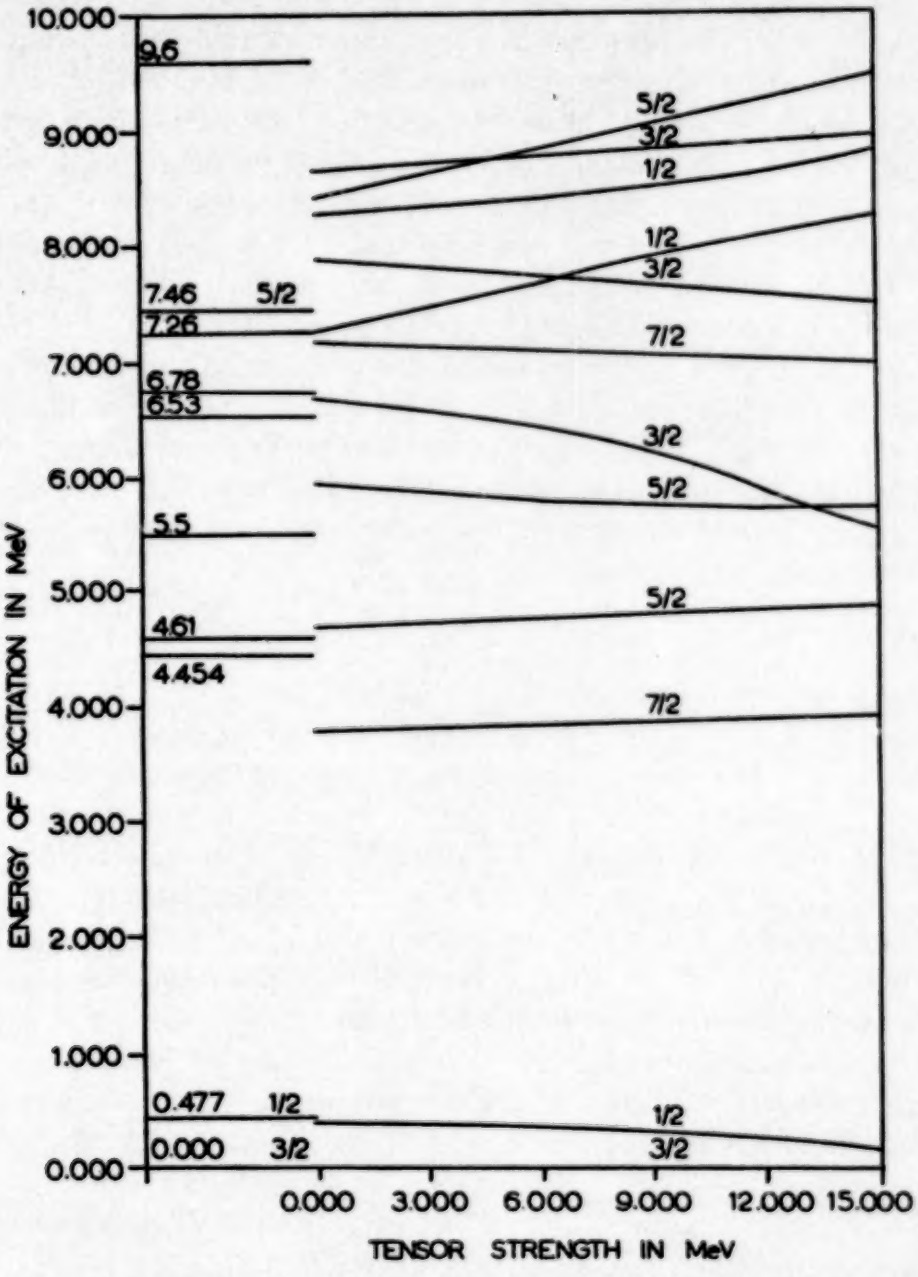

Fig. 1. Effect of the tensor force on Li^7 spectrum. The curves show the change in energy of levels of less than 10 MeV excitation as the tensor force increases from zero to 15 MeV strength. Gaussian shape and simple harmonic wave functions are assumed with $\beta/\alpha = 1$. Here β is the parameter determining the rate of fall-off of the radial wave function and α is the tensor force range.

kopf [19]). Table 2 gives the values of the a's and the related M, W, B and H derived from the Pinkston-Brennan article. The Li^7 central force and spin-orbit matrices are determined by putting the Pinkston-Brennan values for the central force exchange from table 2 in Elliott's matrices. Pinkston and Brennan assume for the direct central force radial integral L the value -5.6, for the exchange central force integral K the value -1.2, and for the spin-orbit parameter ζ the value -1.7. These values correspond to $\zeta/K = 1.42$ and $L/K = 4.66$. The Pinkston-Brennan tensor assumptions amount in Elliott's notation to writing the tensor force integrals as $A = 0.027$, $B = -0.115$, and $C = 0.154$, implying a tensor strength of 9 MeV, all integrals here being in units of MeV. The matrices were diagonalized on the Georgetown Astronomical Observatory's Burroughs' E102 digital computer with the results shown in table 3. The experimental data as taken from Ajzenberg and Lauritsen [20]) with the additional levels of Chromchenko and Blinov mentioned by Meshkov and Ufford [7]) are given in table 4.

Since the effect of the tensor force on three-body states is not well known, a series of calculations was carried out for $^{11}P_1 = 1.00$ MeV with the tensor strength varying in steps of 3 MeV from 0 to 15. The results for levels of less than 10 MeV excitation are shown in fig. 1. The numerical value chosen for the P state element was unfortunate but the qualitative picture is undoubtedly accurate.

3.2. DISCUSSION

As can be seen by a comparison of tables 3 and 4, the best fit occurs for the value $^{11}P_1 = -1.00$. Fair agreement is achieved with the $J = \frac{1}{2}$ level at 0.477. A more interesting result is the suggested assignment of $J = 5/2$ for the level at 4.61. Such an assignment would be in good agreement with the experimental conclusions of Conzett [21]). He found that although the usual theoretical assignment of 7/2 is not impossible, it is not indicated by the experiments. With this assignment the level of Chromchenko and Blinov [22]) at 4.454 could then be the 7/2 level. The rather close spacing of levels predicted with this potential leaves no $J = 5/2$ state free to associate with the observed 5/2 state at 7.46 MeV and it probably belongs to a different odd parity configuration. It is noteworthy that assigning $J = 7/2$ to the 4.454 level and considering the 5.5 level reported by Stoll [23]) as the corresponding $[3]\,^{22}F_{5/2}$ level would give as the ratio of ^2F to ^2P separation $1.046/0.477 = 2.2$. Such a result fits in well with the small spin-orbit parameter and the near L-S coupling of this nucleus.

With respect to the tensor force calculation the first point to be noted is the relatively small effect on the position of the energy levels caused by changing the tensor depth from 0 to 15 MeV. Only four of the levels plotted change by as much as 1 MeV. This feature is characteristic of the way in

which Pinkston and Brennan introduce the tensor force. The changes that do occur are not in general such as to produce a better fit. The ^{2}P splitting, for example, already too small, is decreased further. The tensor force would seem to have a tendency to distort the energy level structure which, indeed, is adequately described by central and spin-orbit forces alone. It is therefore the need for more accurate wave functions and not for improved eigenvalues that necessitates the inclusion of the tensor force.

3.3. COMPARISON WITH PREVIOUS RESULTS

The above assignments are considerably different from those given in previous treatments of Li^7. Inglis [1]) identified the 4.61 level as $J = 7/2$ and considered it together with the 7.46, $J = 5/2$ level as the two components of the F doublet. This assumption gave the ratio of ^{2}F/^{2}P separations as $2.9/0.48 = 6$. This result conflicts sharply with the largely L-S character of the nucleus. Inglis had shown in the same article that this ratio should be 7/3 in the limit of pure L-S coupling. The same difficulty has plagued most subsequent authors also.

Auerbach as mentioned by French and Fujii [24]) showed that by considering the off-diagonal P state contributions to the central force matrix and their exchange dependence, this conflict could be minimized but not easily eliminated. They then pointed out that good experimental reasons exist for not taking the 7.46 and the 4.61 levels as members of the same doublet system. This opinion agreed with the work of Meshkov and Ufford [7]) which had identified the 7.46 level as $[21]^{24}P_{5/2}$ and had put the $[3]^{22}F_{5/2}$ state between 5 and 6 MeV. Thereby a value for the disputed ratio of about 2 had been obtained. Lane [25]) in his extensive treatment of Li^7 followed the older assignments and consequently was unable to explain the high ratio these assignments give †. Finally, none of these authors used a tensor force in their investigations.

The results of the present study differ from those of previous investigators in that a considerable compression of the total energy level spectrum is observed. Kurath [26]) has pointed out that such a compression would result from a low L/K ratio which pulls down the higher states preferentially and a low ζ/K which pulls down the low-lying states. Since the Pinkston and Brennan assumptions give low values for both ratios, the compression is explained.

4. Nitrogen-13

The N^{14} nucleus has proved the greatest conundrum in the P shell. The

† A treatment of Li^7 that appeared too recently to be considered in this study is ref. [29]). The major difference from our analysis stems from our radical assumption that the level at 4.454 MeV reported in ref. [22]) is in fact a new level.

difficulty stems from the long half-life of the C^{14}-N^{14} beta decay, viz. 5580 years. Inglis [1]) had mentioned the possibility of explaining this phenomenon by invoking configuration interaction but Standing's experiments [27]) seem to preclude any sizeable admixture of higher configurations. The problem here again has been what might be called a second order effect on the wave function in the sense that the basic energy level structure is adequately described by a central force with exchange and a spin-orbit interaction but the wave functions are not accurately enough determined to explain other nuclear data such as the vanishing of the beta-decay matrix element. Consequently, the tensor force has been introduced to improve the wave functions. The first introduction of the tensor force, that by Talmi and Jancovici [28]), did prove that the tensor force can give a cancellation of terms in the beta-decay matrix element but it also resulted in a severe distortion of the energy level spectrum. The problem is to devise a tensor force that contributes heavily to the off-diagonal elements $\langle {}^{13}S_1|S_{12}|{}^{13}D_1\rangle$ and thereby alters the ground state wave function, but does not contribute strongly to the diagonal elements or it will produce distortion.

A Gaussian or mesonic shape tensor force has this property. Exploiting this fact, both Elliott and Visscher and Ferrell [4]) have published solutions to the N^{14} problem. However, the restrictions placed on the N^{14} wave function by the requirement of the vanishing of the C^{14}-N^{14} beta-decay matrix element are so severe as to suggest that the effectiveness of their procedure may be fortuitous. The large values both authors are forced to use for the ${}^{11}P_1$ matrix element, about 10 MeV for Elliott and -4.91 MeV for Visscher and Ferrell, emphasizes this doubt. These values in N^{14} contrast sharply with the almost zero value in Li^6 above.

To meet this difficulty, Visscher and Ferrell used initially and with some success what they call a "first principles" approach. By this term they mean that only experimental data from sources other than the mass-14 system are used in their calculation. Elliott for his part showed that his results agree fairly well with the static moments of N^{14} and some reaction data.

The Bacher and Goudsmit method is an ideal instrument in such problems for it makes possible a quick testing of the reasonableness of any set of assumptions for one nucleus by allowing them easily to be applied to a neighbouring nucleus. For example, any unreasonable assumption for a p^{-2} matrix element would immediately make its presence felt by throwing off the p^{-3} energy level spectrum and in a way that could be explicitly checked by reference to the Meshkov and Ufford tables. Accordingly, the Elliott results were submitted to a preliminary Bacher and Goudsmit analysis. The analysis is termed preliminary because the energy level structure of N^{13} is so incompletely known.

The procedure for adapting Elliott's results to this method is as follows.

First of all, care must be taken to change the sign of the proper matrix elements of the spin-orbit force since Elliott follows the Jahn and Van Wieringen convention. One then notices that Elliott uses a parameter y to define the region of acceptable values for his matrix elements. Elliott's y relates his tensor force radial integral A to the central force exchange radial integral K. He finds acceptable values for the N^{14} matrix elements for y equal to 1 and 2.

TABLE 5

Radial integrals of N^{14} assumed by Elliott

	$y = 1$	$y = 2$
L	−9.000	−10.800
K	−1.500	−1.800
ζ	−6.000	−7.200
L/K	6.000	6.000
ζ/K	4.000	4.000
A	−0.029	−0.068
B	0.133	0.237
C	0.200	0.237

The two columns give the values corresponding to two acceptable values of the parameter y connecting the exchange radial integral K and the tensor radial integral A. Integrals are in units of MeV.

The values for the N^{14} radial integrals as deduced from Elliott's article are given in table 5. The exchange is not determined by the data on N^{14} as was also the case with Li^6. Elliott assumes as probable a set of values that amount to setting $W = -0.18$, $M = 1.03$, $H = -0.37$ and $B = 0.52$. This set of exchange parameters does not resemble the set which was used in Li^7. Unfortunately, as will be seen, the present N^{13} data are themselves insensitive to exchange and so do not provide a critique of Elliott's choice.

Table 5 lists the values of the radial integrals of N^{14}, although they are not actually needed. The Meshkov and Ufford table requires knowledge only of the matrix elements and so is excellent for phenomenological procedures. In the present calculation the values of the matrix elements of N^{14} were extracted from Elliott's article and used in Meshkov and Ufford's table to determine the N^{13} matrices.

The matrices so obtained were then diagonalized and the resultant energy level structure is given in table 6 with the observed level structure for comparison shown in table 7, data again from Ajzenberg and Lauritsen [20]). Both for $y = 1$ and $y = 2$ the first excited state lies 1 MeV too low. The Meshkov and Ufford table gives some insight into the factors responsible for this. The two most important elements in the splitting of the P doublet are $\langle [441]^{22}P_{1/2} | [441]^{22}P_{1/2} \rangle$ and $\langle [441]^{22}P_{3/2} | [441]^{22}P_{3/2} \rangle$. Unfortunately they are not heavily determined by the character of the exchange assumed and so no conclusion on the exchange character of the central force can be obtained.

However, the tensor force does enter into the off-diagonal elements connecting $\langle[441]^{22}P_{1/2}|[441]^{22}P_{1/2}\rangle$ with the remaining elements of the $J=\frac{1}{2}$, $T=\frac{1}{2}$ matrix and always so as to raise the energy of the $^{22}P_{1/2}$ state and decrease the P doublet splitting. The calculation of the ground and first excited state of negative parity was therefore repeated with the tensor force set equal to zero. This time the splitting was 1 MeV too great for both values of y. Thus the tensor force would seem too strong.

TABLE 6

Calculated energies of N^{13}

No.	Term	$y=1$	$y=2$
21	$[333]^{22}S_{1/2}$	49.90	59.41
20	$[333]^{44}S_{3/2}$	38.67	46.08
19	$[432]^{22}D_{5/2}$	35.11	41.75
18	$[432]^{22}P_{3/2}$	31.87	38.22
17	$[432]^{24}D_{7/2}$	29.39	35.07
16	$[432]^{42}D_{3/2}$	28.34	33.06
15	$[432]^{22}D_{3/2}$	27.25	31.93
14	$[432]^{22}P_{1/2}$	26.82	31.15
13	$[432]^{42}D_{5/2}$	25.12	29.57
12	$[432]^{42}P_{1/2}$	23.02	27.05
11	$[432]^{24}P_{5/2}$	19.86	23.04
10	$[432]^{24}D_{5/2}$	19.64	22.24
9	$[432]^{24}P_{3/2}$	17.29	19.86
8	$[432]^{42}P_{3/2}$	16.36	19.20
7	$[432]^{24}P_{1/2}$	15.56	18.37
6	$[432]^{24}D_{3/2}$	13.52	15.74
5	$[441]^{22}F_{7/2}$	13.29	15.28
4	$[432]^{24}D_{1/2}$	11.34	13.51
3	$[441]^{22}F_{5/2}$	6.20	7.01
2	$[441]^{22}P_{3/2}$	2.43	2.24
1	$[441]^{22}P_{1/2}$	0.00	0.00

All energies are in units of MeV. Results are listed for two values of the parameter y which connects the exchange integral K and the tensor integral A.

TABLE 7

Observed levels of N^{13}

Energy (MeV)	0.00	2.37	3.51	3.56	6.4	6.90	7.40
J	1/2	1/2	3/2	5/2			
Parity	−	+	−	+			

The predicted energy level spectrum of N^{13} is of the expanded type in contrast to the results obtained for Li^7. This situation is reasonable if one makes the usual assumption that the ground and 3.51 states are the components of the P doublet. Then the P doublet splitting in N^{13} is seven times

that in Li^7. One would conclude therefore that results of Elliott's N^{14} assumptions on N^{13} are reasonable though a fuller knowledge of the N^{13} spectrum is needed before a final evaluation can be reached.

5. Conclusion

The Pinkston-Brennan results for Li^6 when applied to Li^7 yield a rather new picture of that nucleus. In particular, the 4.61 level is identified as 5/2, in better agreement with experiment than the received assignment of 7/2. This assignment considers the 4.454 level of Chromchenko and Blinov as a separate level with spin 7/2. The results of extending Elliott's assumptions for N^{14} to N^{13} are not decisive but seem favourable though Elliott's tensor force may still be large. Both isotope pairs seem to support the hypothesis that the specific function of the nuclear tensor force is to provide more accurate wave functions while the basic energy level structure is determined by the central and spin-orbit forces alone.

Special acknowledgment is due to Doctors Meshkov and Ufford for introducing the author to their method and for constant patience with his questions. The author also wishes to thank Doctors J. B. French and J. P. Elliott for clarifying his difficulties on various questions in hole-particle theory. Special thanks are due to Rev. Mr. James C. Carter, S.J., Ph. D., for help with the hand calculations, to Rev. Francis J. Heyden, S.J., Ph. D., of the Georgetown Astronomical Observatory for permission to use the computational facilities of the Observatory, and to Owen Mattingly of the Observatory staff for devising the program. Finally, the author recalls with pleasure the constant encouragement and advice of Dr. James G. Brennan.

References

1) D. R. Inglis, Revs. Mod. Phys. **25** (1953) 390; Phys. Rev. **85** (1952) 915; G. E. Tauber and T. Y. Wu, Phys. Rev. **93** (1954) 295; T. Auerbach and J. B. French **98** (1955) 1276
2) R. Schulten, Z. Naturforsch. **8** (1953) 759; D. R. Inglis, ref. [1])
3) W. Rarita and J. Schwinger, Phys. Rev. **59** (1941) 436
4) J. P. Elliott, Phil. Mag. **1** (1956) 503; W. M. Visscher and R. A. Ferrell, Phys. Rev. **107** (1957) 781
5) W. T. Pinkston and J. G. Brennan, Phys. Rev. **109** (1958) 499
6) R. F. Bacher and S. Goudsmit, Phys. Rev. **46** (1934) 948; S. Meshkov and C. W. Ufford, Phys. Rev. **94** (1954) 75; R. E. Trees, J. Research Nat. Bur. Standards **53** (1954) 35
7) S. Meshkov and C. W. Ufford, Phys. Rev. **101** (1956) 734
8) H. A. Jahn and H. van Wieringen, Proc. Roy. Soc. A **209** (1951) 502; J. P. Elliott, J. Hope and H. A. Jahn, Phil. Trans. **246** (1953) 241 contains some phase corrections to the preceding
9) W. T. Sharp, J. M. Kennedy, B. J. Sears and M. G. Hoyle, Chalk River Report CRT-556 (AECL 97)
10) J. M. Kennedy, B. J. Sears and W. T. Sharp, Chalk River Report CRT-569 (AECL 106)

11) J. M. Kennedy and M. J. Cliff, Chalk River Report CRT-609 (AECL 224)
12) G. Racah, Phys. Rev. **63** (1943) 367; E. U. Condon and G. H. Shortley, Theory of Atomic Spectra (Cambridge, 1953) esp. p. 299 ff.
13) Robert Sachs, Nuclear Theory (Addison-Wesley Publishing Company, Cambridge, Mass., 1953) app. 3
14) T. Yamanouchi, Proc. Phys.-Math. Soc. Japan **19** (1937) 436; D. E. Rutherford, Substitutional Analysis (Edinburgh University Press, 1948) contains a complete presentation of Young's work
15) M. E. Mandl, U.S. AEC Report NYO-7135 (1955) (unpublished)
16) G. Racah, ref. [12]), eq. (19), slightly altered to fit the nuclear case
17) H. A. Jahn and H. van Wieringen, ref. [8]) p. 518
18) J. P. Elliott, Proc. Roy. Soc. A **218** (1953) 345; Ref. [7]) contains some corrections to this
19) J. M. Blatt and V. F. Weisskopf, Theoretical Nuclear Physics (John Wiley and Sons, New York, 1952)
20) F. Ajzenberg and T. Lauritsen, Revs. Mod. Phys. **27** (1955) 77
21) H. E. Conzett, Phys. Rev. **105** (1957) 1324
22) L. M. Chromchenko and V. A. Blinov, JETP **28** (1955) 741
23) P. Stoll, Helv. Phys. Acta. **27** (1954) 395
24) J. B. French and A. Fujii, Phys. Rev. **105** (1957) 652
25) A. M. Lane, Proc. Phys. Soc. A **66** (1955) 189
26) D. Kurath, Phys. Rev. **101** (1956) 216
27) K. G. Standing, Phys. Rev. **101** (1956) 152
28) B. Jancovici and I. Talmi, Phys. Rev. **95** (1954) 289
29) J. M. Soper, Phil. Mag. **2** (1957) 1219

8.B *Nuclear Physics* 7 (1958) 443—450; © *North-Holland Publishing Co., Amsterdam*
Not to be reproduced by photoprint or microfilm without written permission from the publisher

REPRÉSENTATION DU SPIN ISOBARIQUE DES PARTICULES À INTERACTIONS FORTES

D. RUELLE
Service de Physique Mathématique, Université Libre de Bruxelles

Reçu le 22 mars 1958

Abstract: The behaviour of all known particles in isobaric spin space is represented by 2 × 2 matrices or "quaternions". In particular an isospin-zero particle introduced by d'Espagnat et Prentki and others disappears from the Lagrangian of the strong interactions as a consequence of invariance under charge conjugation.

This representation gives a simple form to the isospin, charge and isofermion number as infinitesimal operators. Although not irreducible when only rotations in isospin space and charge-conserving gauge transformations are considered, it may prove useful in the study of very strong or weak interactions.

1. Introduction

L'examen du spin isobarique des particules élémentaires à interactions fortes suggère le groupement de divers champs en grandeurs ne formant pas des représentations irréductibles du groupe des rotations dans l'espace du spin isobarique, mais peut-être d'un groupe plus général pour lequel les interactions très fortes seraient invariantes [1]). L'avantage d'un tel groupement ($\Lambda-\Sigma$ et nucléons $-\Xi$) apparaît aussi dans l'étude des interactions faibles où le changement des variances isobariques des groupements ($\Lambda-\Sigma$) et ($\mathcal{N}-\Xi$) etc. permettrait d'interpréter les règles de sélection sur le spin isobarique agissant dans ces interactions. De telles possibilités ont été discutées par d'Espagnat, Prentki et Salam [2]). Enfin nous montrerons † qu'il y a moyen d'établir une transformation de jauge et que celle-ci ne traite pas irréductiblement $\mathcal{N}$ et Ξ, ce qui est une raison supplémentaire de les associer.

En raison de ces résultats, nous représenterons les particules à interactions fortes par des grandeurs qui ne sont pas irréductibles si l'on ne considère que les rotations dans l'espace du spin isobarique. On obtiendra ainsi une représentation simple du spin isobarique, de la charge et du nombre d'isofermions [4]) sous forme d'opérateurs infinitésimaux. De plus, on n'introduira pas dans les interactions fortes d'autres particules que celles qui sont physiquement observées. Un boson d'isospin zéro introduit

† L'existence de cette transformation de jauge a été établie par Hanawa [3]) dans un article qui présente beaucoup d'analogies avec ce qui est fait ici.

par d'Espagnat et Prentki [4]) sera en particulier éliminé par conjugaison de charge.

2. Quaternions

Posons

$$\varphi = \begin{pmatrix} \varphi_0 - \mathscr{I}\varphi_3 & -\varphi_2 - \mathscr{I}\varphi_1 \\ \varphi_2 - \mathscr{I}\varphi_1 & \varphi_0 + \mathscr{I}\varphi_3 \end{pmatrix} = -\mathscr{I}\begin{pmatrix} \varphi_3 + \mathscr{I}\varphi_0 & \varphi_1 - \mathscr{I}\varphi_2 \\ \varphi_1 + \mathscr{I}\varphi_2 & -(\varphi_3 - \mathscr{I}\varphi_0) \end{pmatrix} = \varphi_0 I + \sum_l \varphi_l \rho_l$$

$$\varphi^+ = \begin{pmatrix} \varphi_0 + \mathscr{I}\varphi_3 & \varphi_2 + \mathscr{I}\varphi_1 \\ -\varphi_2 + \mathscr{I}\varphi_1 & \varphi_0 - \mathscr{I}\varphi_3 \end{pmatrix} = \mathscr{I}\begin{pmatrix} \varphi_3 - \mathscr{I}\varphi_0 & \varphi_1 - \mathscr{I}\varphi_2 \\ \varphi_1 + \mathscr{I}\varphi_2 & -(\varphi_3 + \mathscr{I}\varphi_0) \end{pmatrix} = \varphi_0 I - \sum_l \varphi_l \rho_l$$

(où $\mathscr{I}^2 = -1$, $\rho_l = -\mathscr{I}\tau_l$ et les τ_l sont les matrices de Pauli. Si les φ_λ $\lambda = 0, 1, 2, 3$) sont réels, les matrices φ forment une représentation isomorphe du corps des quaternions

$$\boldsymbol{\varphi} = \varphi_0 + \mathbf{i}\varphi_1 + \mathbf{j}\varphi_2 + \mathbf{k}\varphi_3 = \varphi_0 + \boldsymbol{\varphi}, \tag{2.1}$$

c'est-à-dire qu'en particulier si $\varphi \to \boldsymbol{\varphi}$, $\varphi' \to \boldsymbol{\varphi}'$ et $\varphi'' \to \boldsymbol{\varphi}''$ par (2.1)

$$\varphi\varphi' = \varphi'' \text{ implique } \boldsymbol{\varphi}\boldsymbol{\varphi}' = \boldsymbol{\varphi}''. \tag{2.2}$$

Le produit des quaternions est défini par

$$\boldsymbol{\varphi}\boldsymbol{\varphi}' = (\varphi_0 + \boldsymbol{\varphi})(\varphi'_0 + \boldsymbol{\varphi}') = \varphi_0\varphi'_0 - \boldsymbol{\varphi}\cdot\boldsymbol{\varphi}' + \varphi_0\boldsymbol{\varphi}' + \boldsymbol{\varphi}\varphi'_0 + \boldsymbol{\varphi}\wedge\boldsymbol{\varphi}'. \tag{2.3}$$

La définition (2.3) reste formellement exacte au sens de (2.2) si l'on applique la définition (2.1) au cas où les φ_λ ne sont plus réels mais définis avec une unité imaginaire i, considérée comme différente de $\mathscr{I}$ (c'est un simple artifice de calcul).

Posant

$$\boldsymbol{\varphi}^+ = \varphi_0 - \mathbf{i}\varphi_1 - \mathbf{j}\varphi_2 - \mathbf{k}\varphi_3 = \varphi_0 - \boldsymbol{\varphi}$$

on voit que si $\varphi \to \boldsymbol{\varphi}$ par (2.1) de même $\varphi^+ \to \boldsymbol{\varphi}^+$. On a

$$\varphi^+\varphi = \boldsymbol{\varphi}^+\boldsymbol{\varphi} I \text{ et } ||\varphi|| = ||\varphi^+|| = \boldsymbol{\varphi}^+\boldsymbol{\varphi}.$$

Si les φ_λ sont réels, φ^+ est l'hermitienne conjuguée de φ et les deux formules ci-dessus montrent que si $\boldsymbol{\varphi}^+\boldsymbol{\varphi} = 1$ (si φ correspond à un quaternion "normé"), φ est unitaire et de déterminant égal à 1.

L'algèbre des matrices φ possède un groupe d'automorphismes intérieurs définis par la variance

$$\varphi \to \tau\varphi\tau^+, \tag{2.4}$$

où τ représente une matrice unitaire et unimodulaire. A cela correspondent pour les quaternions les automorphismes

$$\boldsymbol{\varphi} \to \boldsymbol{\tau}\boldsymbol{\varphi}\boldsymbol{\tau}^+ \tag{2.5}$$

où $\boldsymbol{\tau}$ représente un quaternion normé. De la matrice φ ou du quaternion $\boldsymbol{\varphi}$ on peut tirer un scalaire (invariant) pour (2.4) ou (2.5); c'est $\boldsymbol{\varphi} + \boldsymbol{\varphi}^+ = \mathrm{Tr}\,\varphi$. D'autre part, le scalaire associé au produit $\boldsymbol{\varphi} = \boldsymbol{\varphi}_B \ldots \boldsymbol{\varphi}_A$ n'est pas modifié si l'on remplace la variance (2.5) par

$$\varphi_A \to \tau\varphi_A \tag{2.6}$$

et

$$\varphi_B \to \varphi_B\tau^+ \tag{2.6'}$$

respectivement pour φ_A et φ_B.

Nous appellerons désormais quaternions vrais les grandeurs φ se transformant suivant (2.5), quaternions spineurs et spineurs conjugués, celles qui se transforment selon (2.6) et (2.6'). La conjugaison $\varphi \to \varphi^+$ conserve la variance des quaternions vrais, elle échange celles des spineurs et des spineurs conjugués. Il sera avantageux pour la suite de considérer toujours un quaternion spineur conjugué comme le conjugué d'un quaternion spineur et de poser en conséquence

$$\varphi_B = \varphi^+_{A'}$$

Les quaternions vrais φ ne sont pas irréductibles pour la variance (2.5). Par (2.5), $\varphi = \varphi_0 + \boldsymbol{\varphi}$ devient en effet $\tau\varphi\tau^+ = \varphi_0 + \tau\boldsymbol{\varphi}\tau^+$. On voit que φ_0 est invariant et que $\boldsymbol{\varphi}$ devient $\tau\boldsymbol{\varphi}\tau^+$. Si l'on écrit τ sous la forme $\tau = \cos\frac{1}{2}\theta + \mathbf{u}\sin\frac{1}{2}\theta$ avec $\mathbf{u}\cdot\mathbf{u} = 1$, on voit que la transformation

$$\boldsymbol{\varphi} \to \tau\boldsymbol{\varphi}\tau^+ = (\mathbf{u}\cdot\boldsymbol{\varphi})\mathbf{u} + \cos\theta(\boldsymbol{\varphi} - (\mathbf{u}\cdot\boldsymbol{\varphi})\mathbf{u}) + \sin\theta\,\mathbf{u}\wedge\boldsymbol{\varphi} \tag{2.7}$$

correspond à une rotation d'angle θ du vecteur $\boldsymbol{\varphi}$ autour du vecteur unitaire $\mathbf{u}$ dans l'espace euclidien de base orthonormée $\mathbf{i}$, $\mathbf{j}$, $\mathbf{k}$.

Les quaternions spineurs φ_A ne sont pas non plus irréductibles pour la variance (2.6). On s'en rend compte d'après la représentation matricielle introduite au début: les deux colonnes se transforment indépendamment. Cette décomposition n'est d'ailleurs pas unique, elle dépend de la représentation matricielle employée.

Si l'on appelle φ_{A1} et φ_{A2} les colonnes de φ_A : $\varphi_A = (\varphi_{A2}\varphi_{A2})$, on voit par (2.6) que φ_{A1} et φ_{A2} se transforment comme des spineurs pour le groupe des rotations (2.7) d'un espace euclidien tridimensionnel. On voit d'ailleurs que φ_{A1} et φ_{A1} sont conjugués de charge si les φ_λ sont réels.

Remarquons finalement que pour obtenir le scalaire associé à $\varphi = \varphi^+_{A'}\ldots\varphi\ldots\varphi_A$ où φ_A et $\varphi_{A'}$ sont des quaternions spineurs, il suffira de prendre

$$\varphi^+_{A'1}\ldots\varphi\ldots\varphi_{A1} + \varphi^+_{A1}\ldots\varphi^+\ldots\varphi_{A'1}.$$

3. Lagrangien des Interactions Fortes

Nous allons maintenant considérer des champs qui, en plus de leurs propriétés de transformation caractéristiques dans les changements de coordonnées sont des quaternions au sens indiqué plus haut. Pour des raisons de renormalisabilité, nous n'envisagerons que des champs scalaires et spinoriels dans l'espace ordinaire. Nous excluons aussi un champ vectoriel réel [5]) renormalisable, mais qui entraînerait ici l'existence de champs

vectoriels chargés non renormalisables. Pour les champs scalaires, nous prenons les φ_λ réels; quant aux champs spinoriels, dans la théorie de Dirac ils sont nécessairement complexes (mais avec une unité imaginaire i et non $\mathscr{I}$). Les champs ainsi introduits devront représenter le spin isobarique et la charge des particules à interaction forte. Ce sont

$$\begin{aligned} \text{spin } 0 &\begin{cases} \boldsymbol{\varphi}_V : \text{quaternion vrai} \\ \boldsymbol{\varphi}_S : \text{quaternion spineur} \end{cases} \\ \text{spin } \tfrac{1}{2} &\begin{cases} \boldsymbol{\psi}_V : \text{quaternion vrai} \\ \boldsymbol{\psi}_S : \text{quaternion spineur.} \end{cases} \end{aligned} \tag{3.1}$$

Nous utiliserons la représentation vectorielle et la représentation matricielle (ou spinorielle) de ces quaternions.

Donnons les attributions physiques des champs introduits:

$$\boldsymbol{\varphi}_V = \varphi_{V0} + \boldsymbol{\varphi}_V,$$

φ_{V0} représentera une particule neutre de spin isobarique 0, non observée,

$$\boldsymbol{\varphi}_V = \boldsymbol{\varphi}_\pi;$$

$$\varphi_S = -\mathscr{I}\sqrt{2}\begin{pmatrix} -\overline{K}^0 & K^+ \\ K^- & K^0 \end{pmatrix} = -\mathscr{I}\sqrt{2}\,(\varphi_{\overline{K}}\varphi_K);$$

$$\boldsymbol{\psi}_V = \psi_{V0} + \boldsymbol{\psi}_V,$$

$$\psi_{V0} = \psi_\Lambda, \qquad \boldsymbol{\psi}_V = \boldsymbol{\psi}_\Sigma;$$

$$\psi_S = -\mathscr{I}\sqrt{2}\begin{pmatrix} \Xi^0 & P \\ \Xi^- & N \end{pmatrix} = -\mathscr{I}\sqrt{2}\,(\psi_\Xi \psi_\mathscr{N}).$$

Nous allons maintenant former au moyen des champs introduits une "densité de lagrangien des interactions fortes", basée sur les hypothèses suivantes:

1. $\mathscr{L}_S$ doit être un scalaire dans l'espace ordinaire.
2. $\mathscr{L}_S$ doit être un scalaire pour les variances (2.5) et (2.6) des quaternions vrais et spineurs suivant les attributions (3.1) (conservation du spin isobarique).
3. Nous admettons les lois de conservation du nombre de baryons, de la parité et de la charge.
4. $\mathscr{L}_S$ doit être invariant pour la conjugaison de charge.
5. Pour la simplicité, nous ne considérons que les couplages de Yukawa directs.

Nous représentons ici l'antiparticule d'un baryon par $\bar{\psi} = \psi^{+*}\gamma_4$, où $^+$ désigne la conjugaison du quaternion (donc relativement à l'unité imaginaire $\mathscr{I}$ et * le passage à l'hermitien conjugué relativement à l'imaginaire i. Nous omettrons dans les termes de couplage les matrices γ qui peuvent intervenir, laissant ouvert le choix d'un couplage soit scalaire, soit pseudo-

scalaire. En ce qui concerne la conservation de la charge, notons que pour le quaternion $\phi = \varphi^{+}_{A'}\varphi\varphi_{A}$, où φ_{A} et $\varphi_{A'}$ sont des quaternions spineurs, les 4 composantes ϕ_λ sont des scalaires en vertu de (2.6). La conservation de la charge sera réalisée, comme on le verra plus loin, en n'introduisant dans $\mathscr{L}_{S}$ que ϕ_0 et ϕ_3.

On obtient ainsi †

$$\begin{aligned}
\mathscr{L}_{S} &= \mathscr{L}_{S\pi}+\mathscr{L}_{SK},\\
\mathscr{L}_{S\pi} &= \tfrac{1}{4}\tilde{g}_{\pi 1}[i\bar{\psi}_{S}\varphi_{V}\psi_{S}+\text{c.}]+\tfrac{1}{4}\tilde{g}_{\pi 2}[\rho_3\bar{\psi}_{S}\varphi_{V}\psi_{S}+\text{c.}]\\
&\quad +\tfrac{1}{4}\tilde{g}_{\pi 3}[i\bar{\psi}_{V}\varphi_{V}\psi_{V}+\text{c.}]+\tfrac{1}{4}g_{\pi 4}[i\bar{\psi}_{V}\psi_{V}\varphi_{V}+\text{c.}] \qquad (3.2)\\
\mathscr{L}_{SK} &= \tfrac{1}{2}\tilde{g}_{K1}[i\bar{\psi}_{S}\psi_{V}\varphi_{S}+\text{c.}]+\tfrac{1}{2}\tilde{g}_{K2}[\rho_3\bar{\psi}_{S}\psi_{V}\varphi_{S}+\text{c.}]\\
&\quad +\tfrac{1}{2}\tilde{g}_{K3}[i\bar{\psi}_{S}\psi_{V}{}^{+}\varphi_{S}+\text{c.}]+\tfrac{1}{2}\tilde{g}_{K4}[\rho_3\bar{\psi}_{S}\psi_{V}{}^{+}\varphi_{S}+\text{c.}]
\end{aligned}$$

où

$$A+\text{c.}=A+A^{+}+A^{*}+A^{+*}=(A+A^{+*})+(A+A^{+*})^{+}=(A+A^{+})+\text{h.c.}. \qquad (3.3)$$

En ce qui concerne $\mathscr{L}_{S\pi}$, il faut remarquer que φ_{V} contient une partie hermitienne et une partie antihermitienne. Si l'on n'introduit pas un facteur de phase complexe $e^{i\theta}$ devant le terme d'interaction, une de ces parties disparaît dans $\mathscr{L}_{S}$. Comme la partie vectorielle (antihermitienne) φ_{π} représente les pions connus (π^0, $\pi^{\pm}$) et la partie scalaire (hermitienne) une particule inobservée (π'_0), c'est cette dernière que nous rendons inobservable dans les interactions fortes. On peut rendre le raisonnement plus rigoureux en utilisant l'invariance de $\mathscr{L}_{S}$ pour la conjugaison de charge $\phi \to \phi^{c}$. On sait en effet que cette invariance implique la réalité des constantes de couplage [6]). Pour les pions, on a

$$\varphi^{c}_{\pi^+} = \varphi_{\pi^-},\ \varphi^{c}_{\pi^-} = \varphi_{\pi^+} \text{ et } \varphi^{c}_{\pi^0} = \varphi_{\pi^0},$$

soit

$$\varphi^{c}_{V1} = \varphi_{V1},\quad \varphi^{c}_{V2} = -\varphi_{V2},\quad \varphi^{c}_{V3} = \varphi_{V3}.$$

Comme $\varphi_{\pi'_0} = \varphi_{V0}$ n'apparaît dans la matrice φ_{V} que par les combinaisons linéaires $\varphi_{V3}+\mathscr{I}\varphi_{V0}$ et $\varphi_{V3}-\mathscr{I}\varphi_{V0}$, il est tentant, par analogie avec les mésons K [7]), d'admettre que $\varphi^{c}_{V0} = -\varphi_{V0}$. Cela revient à admettre que φ_{V} et φ_{S} se transforment exactement de la même façon dans la conjugaison de charge. On sait d'ailleurs que ψ_{V} et ψ_{S} se transforment de la même façon ††. Si l'on fait cette hypothèse, on peut voir que le π'_0 est exclu des interactions fortes, que le couplage soit scalaire ou pseudoscalaire. On obtient par exemple pour le premier terme de $\mathscr{L}_{S\pi}$

$$\begin{aligned}
\tfrac{1}{2}[i\bar{\psi}_{S}\varphi_{V}\psi_{S}+\text{h.c.}] &= i\bar{\psi}_{S}\varphi_{V}\psi_{S} \to i\bar{\psi}_{S}{}^{c}\varphi_{V}{}^{c}\psi_{S}{}^{c} = i\bar{\psi}_{S}\varphi_{V}\psi_{S},\\
\tfrac{1}{2}[\bar{\psi}_{S}\varphi_{V}\psi_{S}+\text{h.c.}] &= \bar{\psi}_{S}\varphi_{V0}\psi_{S} \to \bar{\psi}_{S}{}^{c}\varphi^{c}_{V0}\psi_{S}{}^{c} = -\bar{\psi}_{S}\varphi_{V0}\psi_{S}.
\end{aligned}$$

La démonstration est analogue pour les autres termes; elle utilise la pro-

† *Note sur épreuves:* Le ρ_3 des formules (3.2) correspond au "spurion" de Polkinghorne [9]) (d'Espagnat: communication privée).

†† Il faut noter à cet égard le changement de signe dans la définition de $\psi_{A}{}^{c}$ provenant de ce que notre définition diffère par un facteur $\mathscr{I}$ de la définition habituelle pour ψ_{A}.

priété Tr (AB) = Tr (BA). Notons cependant que l'élimination de π'_0 est basée sur la linéarité en φ_V de l'interaction. Si un couplage fort non linéaire tel que

$$\varphi_S{}^+\varphi_V{}^+\varphi_V\varphi_S = 2(\varphi_K{}^+\varphi_K)(\varphi_\pi\cdot\varphi_\pi+\varphi_{\pi'_0}\varphi_{\pi'_0})$$

existe, il peut y avoir émission simultanée de deux π'_0.

Revenons à la forme (3.2) de la densité de lagrangien des interactions fortes. On peut la ramener à la forme habituelle † en posant

$$g_1 = \tilde{g}_{\pi 1}+\tilde{g}_{\pi 2},\quad g_4 = \tilde{g}_{\pi 1}-\tilde{g}_{\pi 2},\quad g_2 = \tilde{g}_{\pi 4}+\tilde{g}_{\pi 3},\quad g_3 = \tilde{g}_{\pi 4}-\tilde{g}_{\pi 3},$$
$$g_5 = \tilde{g}_{K1}+\tilde{g}_{K3}+\tilde{g}_{K2}+\tilde{g}_{K4},\qquad g_7 = \tilde{g}_{K1}+\tilde{g}_{K3}-(\tilde{g}_{K2}+\tilde{g}_{K4}),$$
$$g_6 = \tilde{g}_{K1}-\tilde{g}_{K3}+\tilde{g}_{K2}-\tilde{g}_{K4},\qquad g_8 = \tilde{g}_{K1}-\tilde{g}_{K3}-(\tilde{g}_{K2}-\tilde{g}_{K4}).$$

Le calcul est direct et fournit après identification de $\mathscr{I}$ et i

$$\mathscr{L}_{S\pi} = [g_1\bar{\psi}_N\tau\psi_N+g_4\bar{\psi}_\Xi\tau\psi_\Xi+g_2 i(\overline{\psi}_\Sigma\psi_\Lambda-\bar{\psi}_\Lambda\psi_\Sigma)+g_3 i\overline{\psi}_\Sigma\wedge\psi_\Sigma]\cdot\varphi_\pi, \quad (3.4)$$
$$\mathscr{L}_{SK} = \bar{\psi}_N[g_5 i\psi_\Lambda+g_6(\tau\cdot\psi_\Sigma)]\varphi_K+\text{h.c.}+\bar{\psi}_\Xi[g_7 i\psi_\Lambda+g_8(\tau\cdot\psi_\Sigma)]\varphi_{\bar{K}}+\text{h.c.}. \quad (3.5)$$

L'intérêt de la forme (3.2) de $\mathscr{L}_S$ se manifeste par exemple si l'on exige le même couplage des π avec tous les baryons [1]). Il faut alors évidemment faire $\tilde{g}_{\pi 1} = \tilde{g}_{\pi 3} = g$ et $\tilde{g}_{\pi 2} = \tilde{g}_{\pi 4} = 0$ soit $g_1 = g_2 = -g_3 = g_4 = g$. Il vient ainsi en adoptant le couplage pseudoscalaire

$$\mathscr{L}_{S\pi} = \tfrac{1}{4}g\{[\psi_S^{+*}\gamma_4\gamma_5\varphi_V\psi_S+\text{c.}]+[\psi_V^{+*}\gamma_4\gamma_5\varphi_V\psi_V+\text{c.}]\}$$
$$= g\{-i[\bar{\psi}_N\gamma_5\tau\psi_N+\bar{\psi}_\Xi\gamma_5\tau\psi_\Xi]+[\overline{\psi}_\Sigma\gamma_5\psi_\Lambda-\bar{\psi}_\Lambda\gamma_5\psi_\Sigma-\overline{\psi}_\Sigma\gamma_5\wedge\psi_\Sigma]\}\cdot\varphi_\pi.$$

Cette expression est compatible indifféremment avec les variances (2.5) et (2.6) de ψ_V et ψ_S.

4. Lois de Conservation

La façon dont nous avons interprété les quaternions en termes de scalaires, vecteurs et spineurs ainsi que la façon dont on a construit la lagrangien d'interaction (3.2) assurent la conservation du spin isobarique. Nous allons redéfinir le spin isobarique en utilisant la représentation matricielle des quaternions. On a pour les quaternions vrais et les quaternions spineurs respectivement les variances

$$\varphi'_V = \tau\varphi_V\tau^+, \quad (4.1)$$
$$\varphi'_S = \tau\varphi_S, \quad (4.2)$$

où τ est une matrice unitaire de déterminant égal à 1 de la forme

$$\tau = \cos\tfrac{1}{2}\theta\, I+\sin\tfrac{1}{2}\theta\sum_l u_l\rho_l,$$

† A part la différence de définition de ψ_Λ, cf. note précédente.

où les u_i sont les composantes d'un vecteur unitaire **u**. Les opérateurs infinitésimaux correspondant à τ pour les 3 composantes de **u** sont

$$I + \tfrac{1}{2}\rho_i \, \mathrm{d}\theta = I - \tfrac{1}{2}\mathscr{I} \, \mathrm{d}\theta \, \tau_i .$$

Le lagrangian (3.2) étant invariant pour les transformations (4.1) et (4.2), on a conservation du spin isobarique **I**, défini par

$$\begin{aligned} \mathbf{I}\varphi_{\mathrm{V}} &= \tfrac{1}{2}(\boldsymbol{\tau}\varphi_{\mathrm{V}} - \varphi_{\mathrm{V}}\boldsymbol{\tau}) \quad \text{pour un quaternion vrai,} \\ \mathbf{I}\varphi_{\mathrm{S}} &= \tfrac{1}{2}\boldsymbol{\tau}\varphi_{\mathrm{S}} \qquad\quad \text{pour un quaternion spineur.} \end{aligned} \tag{4.3}$$

Introduisons les représentations $\varphi_{\mathrm{V}} = \varphi_0 I - \mathscr{I}\boldsymbol{\varphi}\cdot\boldsymbol{\tau}$ et $\varphi_{\mathrm{S}} = -\mathscr{I}\sqrt{2}\,(\psi_2\psi_1)$ en termes de scalaire, vecteur et spineurs. On a

$$\tfrac{1}{2}[\boldsymbol{\tau}, \varphi_0] = 0,$$

$$\tfrac{1}{2}[\boldsymbol{\tau}, \boldsymbol{\varphi}\cdot\boldsymbol{\tau}] = \tfrac{1}{2}\sum_k [\boldsymbol{\tau}, \tau_k]\varphi_k = \sum_i \tau_i \Big(\sum_k A_{ik}\varphi_k\Big) \text{ avec } A^{(i)}_{ik} = -i\varepsilon_{iik}.$$

Ainsi

$$\mathbf{I}\varphi_0 = 0, \quad \mathbf{I}\varphi_i = \sum_k \mathbf{A}_{ik}\varphi_k, \quad \mathbf{I}\psi_1 = \tfrac{1}{2}\boldsymbol{\tau}\psi_1, \quad \mathbf{I}\psi_2 = \tfrac{1}{2}\boldsymbol{\tau}\psi_2.$$

Pour former les scalaires dans (3.2), nous n'avons utilisé, dans le cas où le terme d'interaction contenait deux quaternions spineurs, que les composantes 0 et du 3 quaternion formé. Le lagrangien (3.2) est donc encore invariant pour la transformation

$$\varphi''_{\mathrm{V}} = \omega\varphi_{\mathrm{V}}\omega^+, \quad \varphi''_{\mathrm{S}} = \omega\varphi_{\mathrm{S}}\omega^+$$

avec

$$\omega = \cos\tfrac{1}{2}\theta \, I + \sin\tfrac{1}{2}\theta \, \rho_3. \tag{4.4}$$

Cette transformation est une transformation de jauge. Passant à la transformation infinitésimale, on peut définir l'opérateur charge Q par la relation, valable pour φ_{V} comme φ_{S},

$$Q\varphi = \tfrac{1}{2}[\tau_3, \varphi]. \tag{4.5}$$

Il existe encore une transformation qui laisse invariant le lagrangien (3.2), mais elle n'est pas indépendante des deux premières; c'est

$$\varphi'''_{\mathrm{V}} = \varphi_{\mathrm{V}}, \quad \varphi'''_{\mathrm{S}} = \varphi_{\mathrm{S}}\chi^+$$

avec

$$\chi = \cos\tfrac{1}{2}\theta \, I + \sin\tfrac{1}{2}\theta \, \rho_3. \tag{4.6}$$

Elle permet de définir l'opérateur nombre d'isofermions U de d'Espagnat et Prentki:

$$U\varphi_{\mathrm{V}} = 0, \quad U\varphi_{\mathrm{S}} = -\varphi_{\mathrm{S}}\tau_3,$$

soit, puisque l'on a $(\psi_2 \ \psi_1)\tau_3 = (\psi_2 \ -\psi_1)$,

$$U\varphi_0 = 0, \quad U\boldsymbol{\varphi} = 0, \quad U\psi_1 = \psi_1, \quad U\psi_2 = -\psi_2.$$

On a ainsi l'identité entre opérateurs

$$Q = I_3 + \tfrac{1}{2}U. \tag{4.7}$$

Faisant $\theta = -\pi$ dans (4.6), on trouve que le lagrangien est invariant pour la transformation $\varphi \to p\varphi$ avec

$$p\varphi_V = \varphi_V, \quad p\varphi_S = -\mathcal{I}\varphi_S\tau_3; \tag{4.8}$$

$p = e^{\frac{1}{2}\mathcal{I}\pi U}$ est l'isoparité de Racah [8]). Si l'on considère la transformation $\varphi \to p\varphi$ comme une inversion par rapport à l'origine dans l'espace du spin isobarique, le lagrangien est donc invariant pour les rotations et les retournements de cet espace, avec les attributions:

φ_0 isoscalaire, φ isopseudovecteur,

$\psi_1(\psi_2)$ isospineur de première (deuxième) espèce.

Je suis heureux de pouvoir remercier ici Monsieur le Professeur J. Géhéniau pour plusieurs discussions intéressantes au sujet de cette note.

Bibliographie

1) M. Gell-Mann, Phys. Rev. **106** (1957) 1296
2) B. d'Espagnat, J. Prentki and A. Salam, Nuclear Physics **5** (1958) 447
3) S. Hanawa, Progr. Theor. Phys. **17** (1957) 592
4) B. d'Espagnat et J. Prentki, Nuclear Physics **1** (1956) 33
5) Y. Nambu, Phys. Rev. **106** (1957) 1366, Proceedings of the Seventh Annual Rochester Conference (1957) I–26
6) A. Salam, Nuclear Physics **2** (1956) 173
7) M. Gell-Mann and A. Pais, Phys. Rev. **97** (1955) 1387
8) G. Racah, Nuclear Physics **1** (1956) 302
9) J. C. Polkinghorne, Nuovo Cimento **6** (1957) 864

1.C *Nuclear Physics* **7** (1958) 451—458; © *North-Holland Publishing Co., Amsterdam*
Not to be reproduced by photoprint or microfilm without written permission from the publisher

SUR LA DÉTERMINATION DE L'ÉTAT FONDAMENTAL D'UN SYSTÈME DE PARTICULES

CLAUDE BLOCH

Centre d'Études Nucléaires de Saclay, Gif-sur-Yvette (S. & O.)

Reçu le 18 mars 1958

Abstract: The linked diagram expansions of the ground state energy and wave function of a system of particles are derived by a method involving the use of the time-dependent as well as the time-independent formulations of perturbation theory. The essential step is the derivation, in the time-dependent formulation, of a simple exponential formula obtained by summation of the disconnected vacuum-vacuum diagrams.

1. Introduction

Les formules donnant l'énergie de liaison et la fonction d'onde de l'état fondamental sous la forme d'une somme de termes relatifs à des diagrammes liés (linked diagrams) ou connexes jouent un rôle fondamental dans l'étude des systèmes composés d'un grand nombre de particules. Ces formules, établies per Brueckner [1]) jusqu'au quatrième ordre, ont été démontrées dans toute leur généralité par Goldstone [2]) puis par Hugenholtz [3]).

Nous nous proposons d'en donner ici une démonstration basée sur l'utilisation simultanée de la méthode des perturbations dépendantes du temps et de la méthode des perturbations indépendantes du temps. L'intérêt de ce procédé réside dans le fait que certaines propriétés s'expriment simplement dans la formulation indépendante du temps, alors que d'autres et en particulier la formule exponentielle qui sera établie au paragraphe 3 ne s'expriment simplement que dans la formulation dépendante du temps.

La méthode décrite ici conduit par une généralisation très naturelle [4]) à un développement du potentiel de Gibbs qui présente sur les développements habituels de la mécanique statistique l'avantage de tenir compte beaucoup mieux du caractère de symétrie des fonctions d'onde des bosons ou des fermions.

2. Les Fonctions $G(\varepsilon)$ et $U(t)$

Les méthodes des perturbations indépendantes du temps et dépendantes du temps reposent essentiellement sur les fonctions respectives

$$G(\varepsilon) = \frac{1}{\varepsilon - H}, \qquad (1)$$

$$U(t) = \mathrm{e}^{iH_0 t}\,\mathrm{e}^{-iHt},$$

où H est l'Hamiltonien du système

$$H = H_0 + V, \tag{2}$$

et H_0 l'Hamiltonien décrivant le système correspondant de particules indépendantes. La fonction $G(\varepsilon)$, où ε est une variable complexe ayant la dimension d'une énergie, est la fonction de Green du système † alors que $U(t)$ est l'opérateur d'évolution en fonction du temps dans la représentation d'interaction.

Ces deux fonctions sont reliées par une transformation du type de Fourier:

$$\begin{aligned} U(t) &= \frac{1}{2\pi i}\int_C e^{i(H_0-\varepsilon)t} G(\varepsilon)\, d\varepsilon, \\ G(\varepsilon) &= \frac{1}{i}\int_0^{\pm\infty} e^{i(\varepsilon-H_0)t} U(t)\, dt, \end{aligned} \tag{3}$$

où C est un contour composé d'une parallèle à l'axe réel en dessous de celui-ci parcourue dans le sens positif et d'une parallèle au-dessus parcourue dans le sens négatif (fig. 1). Dans la seconde formule, il faut étendre l'intégrale jusqu'à $+\infty$ lorsque la partie imaginaire de ε est positive et jusqu'à $-\infty$ dans le cas contraire.

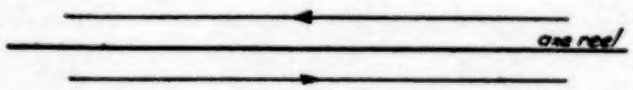

Fig. 1. Le contour d'intégration C de la formule (3) dans le plan complexe des ε.

Pour démontrer ces relations, il suffit d'écrire $G(\varepsilon)$ et $U(t)$ sous la forme

$$\begin{aligned} G(\varepsilon) &= \sum_n |n\rangle \frac{1}{\varepsilon - E_n} \langle n|, \\ U(t) &= e^{iH_0 t} \sum_n |n\rangle\, e^{-iE_n t} \langle n|, \end{aligned} \tag{4}$$

en appelant $|n\rangle$ et E_n les fonctions propres et les valeurs propres de H. En substituant ces expressions dans (3), la vérification des formules de transformation se ramène à des calculs d'intégrales élémentaires.

Les fonctions $G(\varepsilon)$ et $U(t)$ peuvent être développées en puissances de V sous la forme bien connue

$$\begin{aligned} G(\varepsilon) &= \frac{1}{\varepsilon - H_0} \sum_{p=0}^{\infty} \left(V \frac{1}{\varepsilon - H_0} \right)^p, \\ U(t) &= \sum_{p=0}^{\infty} (-i)^p \int_{t > t_1 > \ldots > t_p > 0} dt_1\, dt_2 \ldots dt_p\, V(t_1) V(t_2) \ldots V(t_p). \end{aligned} \tag{5}$$

Dans le second développement nous avons supposé $t > 0$, et nous avons posé

$$V(t) = e^{iH_0 t} V\, e^{-iH_0 t}. \tag{6}$$

† Hugenholtz [3]) appelle résolvante la fonction $-G(z)$.

Il est extrêmement commode pour analyser les développements (5) d'utiliser le formalisme de la seconde quantification. Nous suivrons de très près dans cet article les notations de Goldstone, et nous utiliserons le formalisme de la seconde quantification en prenant par définition pour état du vide l'état fondamental (supposé non dégénéré) du système de particules indépendantes.

Ceci conduit à mettre les développements (5) sous la forme de sommes de termes associés à tous les diagrammes qu'on peut dessiner. Les termes des deux développements correspondant au même diagramme se transforment l'un dans l'autre sous l'effet des transformations (3).

Rappelons qu'on appelle *partie liée* (linked) d'un diagramme toute la partie du diagramme qui peut être atteinte en suivant les lignes du diagramme lorsqu'on entre dans celui-ci par les lignes extérieures. On appelle *partie connexe* d'un diagramme une partie qui peut être parcourue entièrement en suivant les lignes intérieures. Un diagramme est dit lié lorsqu'il n'a qu'une partie liée, et connexe lorsqu'il n'a qu'une partie connexe.

3. La Formule Exponentielle

Supposons que nous voulions calculer la quantité

$$\langle 0|U(t)|0\rangle. \tag{7}$$

Les diagrammes qui interviennent ici sont tous les diagrammes sans lignes extérieures ou diagrammes vide-vide. Un diagramme de ce type est en général composé de plusieurs parties connexes. Désignons par $\Gamma_1, \Gamma_2, \Gamma_3, \ldots$ l'ensemble des diagrammes vide-vide connexes. Le diagramme vide-vide le plus général sera de la forme

$$\Gamma = n_1\Gamma_1 + n_2\Gamma_2 + \ldots, \quad (n_1, n_2, \ldots = 0, 1, 2, \ldots).$$

Pour un diagramme déterminé, les temps auxquels se produisent les interactions sont ordonnés d'une manière bien déterminée. Lorsqu'un diagramme est composé de plusieurs parties connexes on peut former une *famille de*

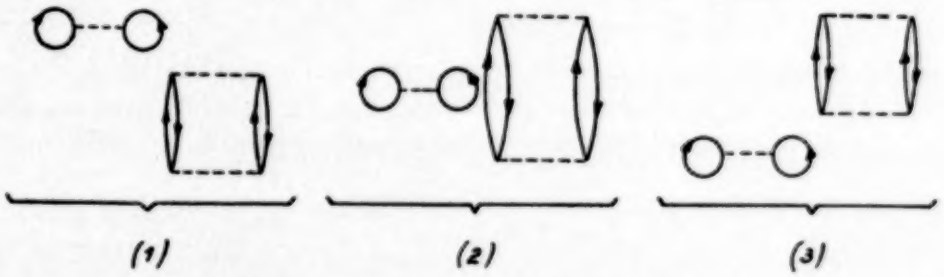

Fig. 2. Une famille de diagrammes vide-vide composés de deux parties connexes distinctes.

diagrammes semblables qui ne diffèrent les uns des autres que par la façon dont sont ordonnés les temps relatifs à des parties connexes différentes. Ainsi, les fig. 2 et 3 représentent des familles de diagrammes semblables

comprenant deux parties connexes. Lorsqu'on considère la somme des contributions provenant de tous les diagrammes d'une famille, seuls les temps relatifs aux interactions d'une même partie connexe sont ordonnés les uns

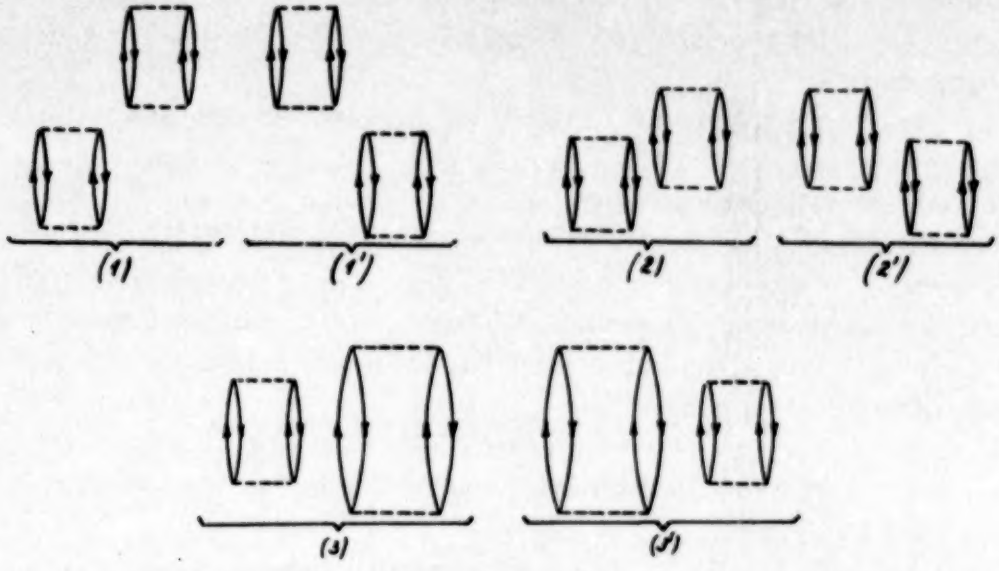

Fig. 3. Une famille de diagrammes vide-vide composés de deux parties connexes identiques.

par rapport aux autres. Il en résulte que la somme de ces contributions s'écrit

$$\langle 0|U_\Gamma(t)\,|0\rangle = \langle 0|\,U_{\Gamma_1}(t)|0\rangle^{n_1}\langle 0|\,U_{\Gamma_2}(t)|0\rangle^{n_2}\ldots \tag{8}$$

où $\langle 0|U_{\Gamma_i}(t)|0\rangle$ désigne la contribution à (7) provenant du diagramme Γ_i.

Lorsqu'un diagramme comprend plusieurs parties connexes identiques, les membres de la famille ne sont pas tous distincts. Ainsi, la fig. 3 représente les membres d'une famille composée de diagrammes formés de deux parties connexes identiques. Ces diagrammes sont classés par groupes de deux qui se déduisent l'un de l'autre par permutation des deux parties connexes. Cette opération ne donnant pas naissance à des diagrammes nouveaux, on voit que chaque diagramme est compté deux fois dans la famille. Plus généralement, si une partie connexe figure n fois, la famille obtenue en modifiant de toutes les façons possibles l'ordre des temps relatifs à des parties distinctes se composera de groupes $n!$ diagrammes se déduisant les uns des autres par permutation des parties connexes identiques. Il en résulte que (7) peut s'écrire

$$\begin{aligned}\langle 0|U(t)|0\rangle &= \sum_{n_1,n_2,\ldots}\frac{1}{n_1!\,n_2!\ldots}\langle 0|U_{\Gamma_1}(t)|0\rangle^{n_1}\langle 0|U_{\Gamma_2}(t)|0\rangle^{n_2}\ldots \\ &= \exp\left[\langle 0|U_{\Gamma_1}(t)|0\rangle+\langle 0|U_{\Gamma_2}(t)|0\rangle+\ldots\right],\end{aligned}$$

ou encore

$$\boxed{\langle 0|U(t)|0\rangle = \exp\langle 0|U(t)|0\rangle_c,} \tag{9}$$

où $\langle 0|U(t)|0\rangle_c$ désigne *la somme des contributions provenant des diagrammes connexes*. Il faut ici faire la convention que le diagramme ne comprenant aucune ligne (auquel correspond le terme 1 dans le développement (5) de $U(t)$) n'est pas un diagramme connexe, et ne doit, par conséquent, pas être pris en considération dans le calcul de $\langle 0|U(t)|0\rangle_c$.

On remarquera que, dans le développement de $G(\varepsilon)$, l'équivalent de la factorisation (8) est beaucoup moins facile à mettre en évidence parce que les dénominateurs $(\varepsilon - H_0)^{-1}$ dépendent des états des particules dans l'ensemble du diagramme, et non pas seulement à l'intérieur d'une partie connexe. On peut cependant établir la propriété correspondante, soit directement comme l'a fait Hugenholtz [3]), soit en transformant par les formules (3) la propriété établie ici.

La formule (9) s'étend immédiatement aux autres éléments de matrice de $U(t)$ sous la forme

$$\boxed{U(t) = U_L(t) \exp \langle 0|U(t)|0\rangle_c,} \tag{10}$$

où $U_L(t)$ désigne *la somme des contributions dues aux diagrammes liés*, avec la convention que le diagramme ne comprenant aucune ligne est un diagramme lié. En effet, le diagramme le plus général est la somme d'une partie liée (pouvant comprendre plusieurs parties connexes) et d'une partie vide-vide (fig. 4). En faisant, comme plus haut, la sommation des diagrammes

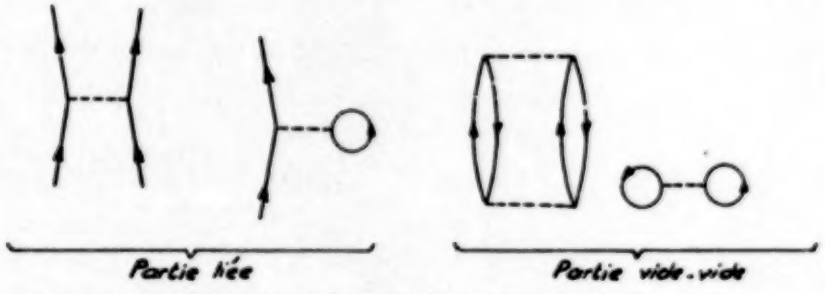

Fig. 4. Le diagramme le plus général.

vide-vide comprenant plusieurs parties connexes, on obtient immédiatement la formule (10).

4. L'Énergie de l'État Fondamental

Nous allons maintenant, dans les développements précédents, poser $it = \beta$, où β est réel. Dans le calcul du potentiel de Gibbs du système (4), on verra que β sera l'inverse de la température. Ici nous n'utiliserons que le passage à la limite $\beta \to \infty$. Avec ce changement de notation, la première relation (3) devient

$$U(\beta) = \frac{1}{2\pi i} \int_C e^{\beta(H_0 - \varepsilon)} G(\varepsilon)\, d\varepsilon. \tag{11}$$

De la seconde relation (4) nous déduisons que

$$\langle 0|U(\beta)|0\rangle = \sum_n |\langle 0|n\rangle|^2 \, e^{\beta(E_0-E_n)}.$$

Lorsque $\beta \to +\infty$, le terme dominant dans le second membre de cette expression est celui pour lequel E_n est le plus petit, c'est-à-dire l'état fondamental:

$$\lim_{\beta\to+\infty} \langle 0|U(\beta)|0\rangle = |\langle 0|f\rangle|^2 \, e^{-\beta\Delta E_0}, \tag{12}$$

où $|f\rangle$ désigne la fonction d'onde de cet état, et où

$$\Delta E_0 = E_f - E_0.$$

D'après la relation (9), il nous suffit, pour évaluer le premier membre de (12), de calculer la quantité

$$\lim_{\beta\to+\infty} \langle 0|U(\beta)|0\rangle_c = \lim_{\beta\to+\infty} \frac{1}{2\pi i}\int_C e^{\beta(E_0-\varepsilon)} \langle 0|G(\varepsilon)|0\rangle_c \, d\varepsilon, \tag{13}$$

où $\langle 0|G(\varepsilon)|0\rangle_c$ désigne la somme des diagrammes vide-vide connexes de $G(\varepsilon)$ qui peut s'écrire

$$\langle 0|G(\varepsilon)|0\rangle_c = \frac{1}{(\varepsilon-E_0)^2} F(\varepsilon)$$

en posant

$$F(\varepsilon) = \langle 0|V + V\frac{1}{\varepsilon-H_0}V + V\frac{1}{\varepsilon-H_0}V\frac{1}{\varepsilon-H_0}V + \ldots|0\rangle_c.$$

Les différents termes du développement de la fonction $F(\varepsilon)$ présentent des singularités pour toutes les valeurs propres de H_0 *sauf* E_0. En effet, un diagramme connexe ne peut pas comprendre le vide comme état intermédiaire, et le vide est le seul état intermédiaire pour lequel $(\varepsilon-H_0)^{-1}$ a un pôle en E_0.

Compte tenu de ces propriétés analytiques, le contour C de la fig. 1 pour l'intégrale (13) peut être décomposé en C_0+C_1 suivant la fig. 5. Lorsque

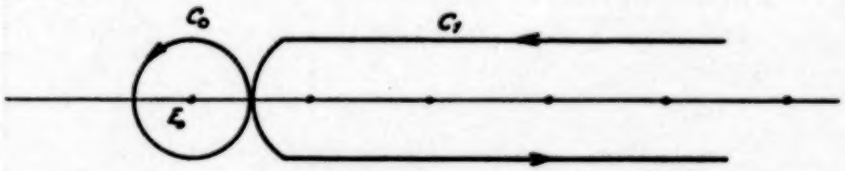

Fig. 5. Le contour d'intégration de la formule (13) dans le plan complexe des ε.

$\beta \to +\infty$, le rapport de la contribution de C_1 à la contribution de C_0 qui est entièrement à gauche de C_1 tend vers zéro, et on peut écrire

$$\lim_{\beta\to+\infty} \langle 0|U(\beta)|0\rangle_c = \frac{1}{2\pi i}\int_{C_0} e^{\beta(E_0-\varepsilon)} F(\varepsilon) \frac{d\varepsilon}{(\varepsilon-E_0)^2}$$
$$= F'(E_0) - \beta F(E_0),$$

comme le montre le calcul du résidu en E_0. D'après (10) on a

$$\lim_{\beta \to +\infty} \langle 0|U(\beta)|0\rangle = e^{F'(E_0)-\beta F(E_0)},$$

et en identifiant avec (12) on obtient enfin les résultats que nous voulions établir:

$$\Delta E_0 = F(E_0) = \langle 0|V+V\frac{1}{E_0-H_0}V+\ldots|0\rangle_c, \qquad |\langle 0|f\rangle|^2 = e^{F'(E_0)}.$$

La première relation est la formule de Goldstone [2]); la seconde, donnant le facteur de normalisation de la fonction d'onde de l'état fondamental a été établie pour la première fois par Hugenholtz [3]).

On remarquera que ces raisonnements supposent qu'on peut effectuer les intégrales de contour séparément sur chaque terme du développement en puissances de l'interaction, et sommer ensuite le développement obtenu. Cette hypothèse qui est bien dans l'esprit de la méthode des perturbations n'est pas forcément toujours justifiée.

La Fonction d'Onde de l'État Fondamental

La méthode du paragraphe précédent s'étend facilement au calcul de la fonction d'onde $|f\rangle$ de l'état fondamental. D'après (4) on a

$$U(\beta)|0\rangle = e^{\beta H_0}\sum_n |n\rangle\, e^{-\beta E_n}\langle n|0\rangle,$$

et

$$|f\rangle = \lim_{\beta \to +\infty} e^{\beta(E_f-H_0)}\, U(\beta)|0\rangle / \langle f|0\rangle.$$

La relation (10) et les résultats du paragraphe précédent sur la limite de $\langle 0|U(\beta)|0\rangle_c$ permettent alors d'écrire $|f\rangle$ sous la forme

$$\begin{aligned}|f\rangle &= \lim_{\beta \to +\infty} e^{\beta(E_0-H_0)}\, U_L(\beta)|0\rangle\langle 0|f\rangle \\ &= \lim_{\beta \to +\infty} \frac{1}{2\pi i}\int_C e^{(E_0-\varepsilon)\beta} G_L(\varepsilon)|0\rangle d\varepsilon\, \langle 0|f\rangle.\end{aligned}$$

Les différents termes du développement de la fonction

$$G_L(\varepsilon)|0\rangle = \frac{1}{\varepsilon-E_0}\left[1+\frac{1}{\varepsilon-H_0}V+\frac{1}{\varepsilon-H_0}V\frac{1}{\varepsilon-H_0}V+\ldots\right]_L|0\rangle$$

ont des singularités pour toutes les valeurs propres de H_0, mais en E_0 ils n'ont qu'un pôle simple.

Le contour d'intégration peut à nouveau être décomposé en C_0 et C_1 suivant la fig. 4 et la partie dominante pour $\beta \to +\infty$ provient de C_0. Le calcul du résidu en ce point donne enfin l'expression de Goldstone:

$$|f\rangle = \sum_{p=0}^{\infty}\left(\frac{1}{E_0-H_0}V\right)^p_L|0\rangle\langle 0|f\rangle.$$

Bibliographie

1) K. A. Brueckner, Phys. Rev. **100** (1955) 36
2) J. Goldstone, Proc. Roy. Soc. A **239** (1957) 267
3) N. M. Hugenholtz, Physica **23** (1957) 481
4) C. Bloch et C. De Dominicis, Nuclear Physics **7** (1958) 459

1.C *Nuclear Physics* **7** (1958) 459—479; © *North-Holland Publishing Co., Amsterdam*
Not to be reproduced by photoprint or microfilm without written permission from the publisher

UN DÉVELOPPEMENT DU POTENTIEL DE GIBBS D'UN SYSTÈME QUANTIQUE COMPOSÉ D'UN GRAND NOMBRE DE PARTICULES

CLAUDE BLOCH et CYRANO DE DOMINICIS
Centre d'Études Nucléaires de Saclay, Gif-sur-Yvette (S & O)

Reçu le 18 mars 1958

Abstract: The Gibbs potential is expressed as an expansion in terms of linked diagrams. In the limit of zero temperature, it reduces to the Goldstone expansion for the ground state energy. At a finite temperature, the only difference with the latter comes from temperature dependent weight factors associated with every line of the diagrams. For a fermion particle (hole) line, the weight factor is given by the probability of the corresponding state being empty (occupied) in the independent particle gas at the given temperature. The general case of a system of interacting bosons and fermions is treated. Wick's theorem has been extended to the expectation value of a product of operators for a system of independent particles at a given temperature.

1. Introduction

La fonction de partition de la mécanique statistique présente avec l'opérateur d'évolution de la mécanique quantique une analogie très étroite qui a conduit de nombreux auteurs [1]) à utiliser les techniques développées pour la mécanique quantique dans les problèmes de mécanique statistique. Récemment, des progrès considérables ont été accomplis dans l'étude de l'état fondamental d'un système composé d'un grand nombre de particules [2]). Ils ont abouti à la création d'un formalisme très élaboré permettant de classer les différents termes à l'aide de diagrammes de Feynman, comme dans la théorie des champs. Nous nous proposons ici de reprendre l'analogie entre la mécanique statistique et la mécanique quantique et de montrer que le développement du potentiel de Gibbs peut être mis sous une forme généralisant d'une manière très naturelle le développement de Goldstone [2]) pour l'énergie de l'état fondamental.

L'approximation d'ordre zéro dans la théorie de Goldstone est constituée par le système de particules sans interactions, dont l'état fondamental peut être décrit dans le cas des fermions en spécifiant que tous les états des particules indépendantes sont occupés jusqu'à l'énergie de Fermi et vides au-delà. L'énergie de l'état fondamental du système de particules en inter-

action est alors donnée par un développement dont chaque terme est associé à un diagramme connexe sans lignes extérieures. Les lignes constituant un diagramme sont affectées de flèches. Les lignes dont la flèche est dirigée dans le sens des temps croissants correspondent aux états vides dans l'état fondamental du système non perturbé ("particules") alors que les lignes dirigées en sens inverse correspondent aux états occupés ("trous").

Dans le développement que nous allons établir l'approximation d'ordre zéro est constituée par le gaz de particules sans interactions à la température choisie. Chacun des états des particules indépendantes a alors une probabilité d'être occupé ou vide donnée par la distribution statistique de Fermi. Nous montrerons que le développement du potentiel de Gibbs du système de particules en interaction est donné par un développement tout à fait analogue à celui de Goldstone. La seule différence réside dans le fait que quel que soit le sens de leurs flèches les lignes peuvent correspondre à tous les états. Il faut cependant affecter leur contribution d'un poids qui est égal pour les lignes dirigées dans le sens du temps à la probabilité pour que l'état correspondant soit vide dans le gaz sans interactions, et pour les lignes dirigées en sens inverse à la probabilité pour que l'état soit occupé.

Ce développement est différent de celui qu'on obtient [3]) en généralisant aux systèmes quantiques le développement classique de Ursell et Yvon [4]). Contrairement à ce dernier, il repose essentiellement sur un développement en puissances de l'interaction. Par contre, il tient mieux compte du caractère de symétrie des fonctions d'onde, et on doit donc s'attendre à ce que sa validité soit meilleure aux basses températures. La méthode de sommation des diagrammes en échelle sur laquelle repose la théorie de Brueckner [5]) s'étend sans difficulté de principe et conduit au remplacement du potentiel d'interaction par une matrice t dépendant de la température. Ainsi complétée, la théorie évite les inconvénients du développement en puissances de l'interaction et, en particulier, elle peut s'appliquer à des potentiels singuliers.

La théorie exposée ici constitue essentiellement une généralisation de la démonstration du développement de Goldstone décrite dans l'article précédant celui-ci [6]). Elle repose sur un emploi simultané des formulations dépendante et indépendante du temps de la théorie des perturbations qui conduit naturellement à la formule exponentielle. Celle-ci résulte de la sommation des diagrammes vide-vide non connexes. Nous avons également été conduits à démontrer une généralisation du théorème de Wick [7]) relative au calcul de la valeur moyenne d'un produit d'opérateurs pour un système de particules indépendantes à une température donnée. Le résultat final peut être mis sous plusieurs formes entre lesquelles le choix dépendra du problème traité. Le cas des bosons et le cas des fermions ont toujours été considérés parallèlement.

2. La Grande Fonction de Partition

Les propriétés thermodynamiques d'ensemble d'un système de particules peuvent être déterminées à l'aide des théorèmes généraux de la mécanique statistique lorsqu'on a réussi à calculer la *grande fonction de partition*

$$Z(\alpha, \beta) = \sum_{N,i} \exp\{-\beta E_i^N + \alpha N\}, \tag{1}$$

où β est l'inverse de la température et les E_i^N sont les niveaux d'énergie du système de N particules. La quantité qui intervient effectivement dans le calcul des propriétés thermodynamiques étant en réalité le logarithme de $Z(\alpha, \beta)$, il est commode de définir le potentiel de Gibbs $A(\alpha, \beta)$ par la relation

$$Z(\alpha, \beta) = \exp\{-\beta A(\alpha, \beta)\}. \tag{2}$$

Le système peut comprendre des particules de nature différente: bosons ou fermions. Il faut distinguer les particules dont le nombre est conservé au cours des interactions de celles qui peuvent être créées ou annihilées. S'il existe plusieurs groupes de particules dont le nombre est conservé par les interactions, on introduit plusieurs paramètres $\alpha_1, \alpha_2, \ldots$, et on définit la grande fonction de partition de la manière suivante:

$$Z(\alpha_1, \alpha_2, \ldots \beta) = \sum_{N_1, N_2, \ldots i} \exp\{-\beta E_i^{N_1 N_2 \cdots} + \alpha_1 N_1 + \alpha_2 N_2 + \ldots\};$$

où $N_1, N_2 \ldots$ sont les nombres de particules des différents groupes conservés.

Par exemple, dans le système électrons-phonons, seul le nombre des électrons est conservé, alors que dans un mélange d'atomes d'hélium 3 et 4, les nombres des particules des deux types sont conservés.

Les raisonnements qui suivent peuvent être appliqués à des systèmes très divers, mais pour fixer les idées nous nous appuierons sur le système électrons-phonons.

Nous utiliserons le formalisme de la seconde quantification. Les indices $r, s, \ldots$ d'une part, $k, l, \ldots$ d'autre part seront utilisés pour énumérer un ensemble complet quelconque d'états des électrons et des phonons libres, respectivement. Nous désignerons par η_r^+, η_r et q_k^+, q_k les opérateurs de création et d'annihilation des électrons et des phonons dans les états de base choisis. Ces opérateurs satisfont aux relations de commutation

$$[\eta_r, \eta_s^+]_+ = \delta_{rs}, \quad [q_k, q_l^+] = \delta_{kl}, \quad [\eta_r, \eta_s]_+ = [q_k, q_l] = [\eta_r, q_k] = 0. \tag{3}$$

Nous écrirons l'hamiltonien du système sous la forme

$$H = H_0 + V,$$

où

$$H_0 = \sum_r \varepsilon_r n_r + \sum_k \omega_k n_k \tag{4}$$

décrit le système des particules indépendantes, et

$$V = \sum_{r,s,k} \langle s,\ k|v|r\rangle q_k^+ \eta_s^+ \eta_r + \text{complexe conj.} \tag{5}$$

leurs interactions. Dans (4) les ε_r et ω_k sont les énergies des états des électrons et des phonons et les n_r et n_k désignent les opérateurs nombres d'occupation

$$n_r = \eta_r^+ \eta_r, \quad n_k = q_k^+ q_k. \tag{6}$$

La grande fonction de partition (1) peut s'écrire sous la forme d'une trace

$$Z(\alpha,\ \beta) = \mathrm{Tr}\, e^{-\beta H + \alpha N} \tag{7}$$

calculée sur l'ensemble des états du système doublement quantifié. Dans cette expression N est l'opérateur nombre total d'électrons

$$N = \sum_r n_r. \tag{8}$$

Nous partirons du développement de la fonction exponentielle bien connu en mécanique quantique

$$e^{\beta H_0} e^{-\beta H} = \sum_{p=0}^{\infty} (-)^p \int_{\beta > u_1 > u_2 \ldots > u_p > 0} du_1 du_2 \ldots du_p V(u_1) V(u_2) \ldots V(u_p); \tag{9}$$

où on a posé

$$V(u) = e^{uH_0} V e^{-uH_0}. \tag{10}$$

Par cette transformation, l'interaction (5) devient

$$V(u) = \sum_{r,s,k} \langle s,\ k|v|r\rangle q_k^+ \eta_s^+ \eta_r\, e^{u\Delta E(r;\,s,\,k)} + \langle r|v|s,\ k\rangle \eta_r^+ \eta_s q_k\, e^{u\Delta E(s,\,k;\,r)}, \tag{11}$$

où les ΔE sont les *énergies d'excitation corrrespondant à l'interaction*, c'est-à-dire les différences entre les énergies après et avant l'interaction. Par exemple,

$$\Delta E(r;\ s,\ k) = \omega_k + \varepsilon_s - \varepsilon_r = -\Delta E(s,\ k;\ r) \tag{12}$$

est le changement d'énergie correspondant à l'annihilation d'un électron dans l'état r et à la création d'un électron dans l'état s et d'un phonon dans l'état k.

Il sera commode pour la suite d'introduire la grande fonction de partition du système de particules indépendantes

$$Z_0(\alpha,\ \beta) = \mathrm{Tr}\, e^{-\beta H_0 + \alpha N}; \tag{13}$$

et *l'opérateur statistique du système de particules indépendantes*

$$\rho = \frac{1}{Z_0(\alpha,\ \beta)} e^{-\beta H_0 + \alpha N}. \tag{14}$$

D'après (4) et (8) on a

$$\alpha N - \beta H_0 = \sum_r (\alpha - \beta\varepsilon_r) n_r + \sum_k -\beta\omega_k n_k.$$

Les différents termes de cette somme commutant entre eux, on peut écrire l'opérateur statistique (14) sous la forme d'un produit d'opérateurs statistiques relatifs à chacun des états d'électron ou de phonon

$$\rho = \prod_r \rho_r \prod_k \rho_k, \tag{15}$$

où

$$\rho_r = \frac{e^{(\alpha-\beta\varepsilon_r)n_r}}{1+e^{\alpha-\beta\varepsilon_r}}, \qquad \rho_k = (1-e^{-\beta\omega_k})e^{-\beta\omega_k n_k}; \tag{16}$$

car

$$\mathrm{Tr}\, e^{(\alpha-\beta\varepsilon_r)n_r} = \sum_{n_r=0}^{1} e^{(\alpha-\beta\varepsilon_r)n_r} = 1+e^{\alpha-\beta\varepsilon_r},$$

$$\mathrm{Tr}\, e^{-\beta\omega_k n_k} = \sum_{n_k=0}^{\infty} e^{-\beta\omega_k n_k} = \frac{1}{1-e^{-\beta\omega_k}}.$$

De ces expressions, on tire aussi la valeur bien connue de $Z_0(\alpha, \beta)$:

$$\log Z_0(\alpha, \beta) = \sum_r \log(1+e^{\alpha-\beta\varepsilon_r}) - \sum_k \log(1-e^{-\beta\omega_k}). \tag{17}$$

Pour tout opérateur A agissant sur les variables dynamiques du système, nous définirons une moyenne prise sur le *système de particules indépendantes* par la relation

$$\langle A \rangle = \mathrm{Tr}\,(\rho A); \tag{18}$$

où ρ est l'opérateur statistique (14), (15) du système de particules indépendantes.

Cette définition permet en reportant (9) dans (7) d'écrire le développement suivant de la grande fonction de partition:

$$\frac{Z(\alpha, \beta)}{Z_0(\alpha, \beta)} = \sum_{p=0}^{\infty} (-)^p \int_{\beta > u_1 > u_2 \ldots > u_p > 0} du_1 du_2 \ldots du_p \langle V(u_1)V(u_2)\ldots V(u_p)\rangle. \tag{19}$$

3. La Valeur Moyenne d'un Produit d'Opérateurs de Création et d'Annihilation †

Lorsqu'on substitue dans le développement (19) l'expression (10) de $V(u)$ on obtient une somme de valeurs moyennes au sens défini par (18) de produits d'opérateurs de création et d'annihilation. Nous allons établir pour ces moyennes un théorème semblable au théorème de Wick pour le calcul de l'amplitude vide-vide d'un produit d'opérateurs.

Rappelons que Wick [7]) introduit pour deux opérateurs a et b la notion de *contraction* $a^\bullet b^\bullet$. C'est un nombre pur que nous définirons ici comme la valeur moyenne du produit des opérateurs:

$$a^\bullet b^\bullet = \langle ab \rangle. \tag{20}$$

† *Note ajoutée sur épreuves:* Nous sommes reconnaissants à M. J. Lascoux de nous avoir signalé l'article de J. Thouless [9]) où des considérations semblables sont développées.

Les seules contractions non nulles sont celles qui font intervenir un opérateur de création et un opérateur d'annihilation relatifs au même état. Toute autre combinaison d'opérateurs, en effet, n'a pas d'éléments diagonaux et sa moyenne définie par (18) est nulle puisque ρ est purement diagonal.

Les relations de commutation (3) entraînent pour les contractions les relations suivantes:

$$\begin{cases} \eta_r^{\bullet}\eta_r^{+\bullet}+\eta_r^{+\bullet}\eta_r^{\bullet}=1, \\ q_k^{\bullet}q_k^{+\bullet}-q_k^{+\bullet}q_k^{\bullet}=1, \end{cases} \tag{21}$$

car la moyenne de 1 au sens (18) est égale à 1.

Le calcul effectif des contractions est immédiat car

$$\eta_r^{+\bullet}\eta_r^{\bullet}=\langle n_r\rangle=\mathrm{Tr}\,(n_r\rho_r),$$
$$q_k^{+\bullet}q_k^{\bullet}=\langle n_k\rangle=\mathrm{Tr}\,(n_k\rho_k).$$

En utilisant les expressions (16) des opérateurs statistiques ρ_r et ρ_k ainsi que les relations (21), on trouve pour l'ensemble des contractions non nulles les expressions suivantes que nous désignerons dans la suite par $f_r^{\pm}$ et $g_k^{\pm}$:

$$\begin{aligned} \eta_r^{\bullet}\eta_r^{+\bullet} &= f_r^{+}=\frac{1}{1+e^{\alpha-\beta\epsilon_r}}, \\ q_k^{\bullet}q_k^{+\bullet} &= g_k^{+}=\frac{1}{1-e^{-\beta\omega_k}}, \\ \eta_r^{+\bullet}\eta_r^{\bullet} &= f_r^{-}=\frac{1}{e^{\beta\epsilon_r-\alpha}+1}=1-f_r^{+}, \\ q_k^{+\bullet}q_k^{\bullet} &= g_k^{-}=\frac{1}{e^{\beta\omega_k}-1}=g_k^{+}-1. \end{aligned} \tag{22}$$

Les $f_r^{\pm}$ se rapportent aux électrons, les $g_k^{\pm}$ aux phonons, les f_r^{+} et g_k^{+} se rapportent aux produits où l'opérateur de création est à droite de l'opérateur d'annihilation; les g_r^{-} et f_k^{-} au cas inverse.

Suivant Wick, nous définirons ensuite un *système de contractions* dans un produit de plusieurs facteurs. Pour cela, on associe les facteurs par groupes de deux entre lesquels on effectue des contractions. Nous nous occuperons ici exclusivement des *systèmes complets de contractions* qui ne laissent aucun opérateur non contracté. Un produit complètement contracté est un nombre pur. Par exemple,

$$a^{\bullet}b^{\bullet\bullet}c^{\bullet}d^{\bullet\bullet\bullet}e^{\bullet\bullet}f^{\bullet\bullet\bullet}=(-)^{\nu}\,(a^{\bullet}c^{\bullet})(b^{\bullet\bullet}e^{\bullet\bullet})(d^{\bullet\bullet\bullet}f^{\bullet\bullet\bullet}),$$

où ν est le nombre de permutations d'opérateurs agissant sur les fermions nécessaires pour amener l'un à côté de l'autre les groupes de facteurs contractés.

On a alors le théorème suivant: *la valeur moyenne* $\langle abc\ldots\rangle$ *d'un produit*

d'opérateurs de création et d'annihilation est égale à la somme de tous les systèmes complets de contractions de ce produit.

L'opérateur ρ servant à définir la valeur moyenne étant diagonal, les seuls produits d'opérateurs dont la moyenne n'est pas nulle se composent de paires d'opérateurs de création et d'annihilation relatifs aux mêmes états. D'autre part, d'après (15), ρ est le produit de facteurs relatifs aux différents états. Il en résulte que dans la démonstration du théorème, on peut raisonner *séparément* sur les opérateurs relatifs à chacun des états. Ainsi, lorsque le produit se compose de paires d'opérateurs relatives à des états tous différents, le théorème devient évident. Il n'y a alors qu'un seul système de contractions non nulles et d'après la définition (20), le produit de ces contractions est égal à la moyenne du produit.

Le cas où le produit comprend $p > 1$ opérateurs de création et p opérateurs d'annihilation *relatifs tous au même état* † doit être examiné avec plus de soin. On notera que l'ordre de ces $2p$ facteurs joue un rôle important. Nous ferons la démonstration en deux étapes:

1) Nous montrerons que si le théorème est vrai pour *tous* les produits de $2(p-1)$ opérateurs, et s'il est vrai pour *un* produit de $2p$ facteurs, il est aussi vrai pour tout produit qui s'en déduit par une permutation de deux facteurs voisins.

*†† Supposons que nous ayons un produit de $2p$ opérateurs agissant sur les bosons pour lequel le théorème soit vrai. Nous l'écrirons sous la forme Aq^+qB, où A et B désignent les $2(p-1)$ facteurs non explicités. Nous allons démontrer que le théorème est vrai aussi pour le produit Aqq^+B.

D'après les relations de commutation (3) on a

$$Aqq^+B = Aq^+qB + AB.$$

Le produit AB comprend $2(p-1)$ opérateurs, et nous supposons que le théorème peut lui être appliqué. Nous voyons alors que $\langle Aqq^+B\rangle$ est égal à la somme de tous les systèmes de contractions de Aq^+qB et de AB.

Les systèmes de contractions de Aqq^+B et de Aq^+qB dans lesquels les facteurs q et q^+ soumis à la permutation ne sont pas contractés ensemble sont visiblement identiques. Les systèmes de contractions de Aqq^+B et de Aq^+qB dans lesquels les facteurs permutés sont contractés ensemble sont les produits de $q^\bullet q^{+\bullet}$ et de $q^{+\bullet}q^\bullet$, respectivement, par les systèmes de contractions des autres facteurs, c'est-à-dire du produit AB. Mais d'après (21) on a

$$q^\bullet q^{+\bullet} = q^{+\bullet}q^\bullet + 1.$$

† Jusqu'à la fin de ce paragraphe, nous omettrons les indices r ou k spécifiant les états auxquels se rapportent les opérateurs.

†† Les passages encadrés par des astérisques • sont des démonstrations purement mathématiques qui peuvent être sautées en première lecture afin de mieux suivre l'enchaînement des idées.

Il en résulte que la somme des contractions de Aq^+qB et de AB est égale à la somme des contractions de Aqq^+B, ce qui établit la proposition à démontrer.

Le cas des fermions se traite de la même façon.*

2) Nous allons maintenant démontrer que le théorème est vrai pour un produit particulier de 2 ,4, 6, ... $2p$, ... facteurs.

* Commençons par le cas des bosons et prenons comme produit particulier

$$q^{+p}q^p, \quad (p = 1, 2, \ldots).$$

Les relations de commutation (3) entraînent pour l'opérateur nombre d'occupation (6) les relations

$$\begin{aligned} \boldsymbol{n}q &= q(\boldsymbol{n}-1), \\ \boldsymbol{n}q^2 &= q^2(\boldsymbol{n}-2), \\ &\text{- - - - - - - - -} \\ \boldsymbol{n}q^m &= q^m(\boldsymbol{n}-m). \end{aligned}$$

D'où

$$\begin{aligned} q^{+p}q^p &= q^{+p-1}\boldsymbol{n}q^{p-1} = q^{+p-1}q^{p-1}(\boldsymbol{n}-p+1) \\ &= q^{+p-2}q^{p-2}(\boldsymbol{n}-p+2)(\boldsymbol{n}-p+1) = \boldsymbol{n}(\boldsymbol{n}-1)\ldots(\boldsymbol{n}-p+1). \end{aligned}$$

D'autre part, les contractions sont toutes égales à

$$(q^{+\bullet}q^\bullet)^p = \langle \boldsymbol{n} \rangle^p,$$

et leur nombre est égal à $p!$ car le premier facteur q^+ peut être contracté avec chacun des p facteurs q, le second facteur q^+ peut être contracté avec chacun des $p-1$ facteurs q restant, et ainsi de suite.

La propriété à établir s'exprime donc par l'égalité

$$\langle \boldsymbol{n}(\boldsymbol{n}-1)\ldots(\boldsymbol{n}-p+1) \rangle = p!\langle \boldsymbol{n} \rangle^p, \tag{23}$$

que nous allons vérifier pour l'opérateur statistique (16). En posant pour simplifier l'écriture

$$z = \mathrm{e}^{-\beta\omega}, \tag{24}$$

on a

$$\begin{aligned} \langle \boldsymbol{n}(\boldsymbol{n}-1)\ldots(\boldsymbol{n}-p+1) \rangle &= (1-z)\sum_{n=0}^{\infty} n(n-1)\ldots(n-p+1)z^n \\ &= (1-z)z^p\left(\frac{\mathrm{d}}{\mathrm{d}z}\right)^p \sum_{n=0}^{\infty} z^n = (1-z)z^p\left(\frac{\mathrm{d}}{\mathrm{d}z}\right)^p \frac{1}{1-z} = p!\left(\frac{z}{1-z}\right)^p. \end{aligned}$$

En appliquant cette relation pour $p = 1$ on obtient

$$\langle \boldsymbol{n} \rangle = \frac{z}{1-z}. \tag{25}$$

Les deux dernières relations entraînent la relation (23) qui est démontrée.

Il reste à examiner le cas des fermions, qui est plus simple. Pour $p = 1$ la proposition à démontrer n'est rien de plus que la définition des contractions. Pour $p > 1$ on a

$$\eta^{+p}\eta^{p} = 0,$$

car le carré des opérateurs η et η^{+} est nul. Il faut donc vérifier que la somme des systèmes de contractions est nulle pour un tel produit.

Plus généralement, nous allons montrer que la somme des contractions est nulle pour un produit tel que $A\eta^{2}B$ comprenant deux facteurs η (ou η^{+}) l'un à côté de l'autre. Pour cela nous allons montrer que les systèmes de contractions peuvent être associés par paires dont les contributions ont une somme nulle. Soit en effet un système de contractions ou le premier facteur η dans le produit considéré est contracté avec un premier facteur η^{+} et le second facteur η avec un second facteur η^{+}. Il existe alors aussi un second système de contractions qui ne diffère du premier que par le fait que le premier facteur η est contracté avec le second facteur η^{+} et le second facteur η avec le premier facteur η^{+}. Les contributions de ces deux systèmes ne diffèrent que par le signe car elles sont formées du produit des mêmes contractions de paires, tandis que les nombres de permutations nécessaires pour amener l'un à côté de l'autre les groupes de facteurs contractés diffèrent d'une unité.*

Les propositions 1 et 2 contiennent la démonstration complète du théorème. Il suffit de considérer de proche en proche les produits de 2, 4, 6, 8 ... facteurs et de s'appuyer sur le fait que tout produit de $2p$ facteurs peut être obtenu à partir d'un produit particulier par une succession de permutations de facteurs voisins.

Mentionnons pour terminer ce paragraphe que les distributions des probabilités d'occupation données par les opérateurs statistiques (16) sont les seules pour lesquelles le théorème soit vrai d'une manière générale.

Dans le cas des fermions, cette affirmation est triviale car les nombres d'occupation ne prenant que deux valeurs, toute distribution de probabilité de ceux-ci peut être mise sous la forme (16) moyennant un choix approprié de la quantité $\alpha - \beta\varepsilon$.

Dans le cas des bosons, on peut montrer que les relations (23) impliquent que l'opérateur statistique est de la forme (16) avec une certaine valeur de $\beta\omega$.

* Soit en effet $\rho(n)$ la probabilité pour qu'il y ait n bosons dans l'état considéré. On peut écrire (23) sous la forme

$$\sum_{n=p}^{\infty} \frac{n!}{p!(n-p)!}\,\rho(n) = \langle n\rangle^{p}.$$

En multipliant ces équations par x^{p} où x est une variable telle que

$$\langle n\rangle |x| < 1,$$

et en sommant sur toutes les valeurs de p, on obtient dans les deux membres des séries absolument convergentes qui s'écrivent

$$\sum_{p=0}^{\infty} x^p \langle n \rangle^p = \frac{1}{1-x\langle n \rangle} = \sum_{p=0}^{\infty} x^p \sum_{n=p}^{\infty} \frac{n!}{p!(n-p)!} \rho(n)$$

$$= \sum_{n=0}^{\infty} \rho(n) \sum_{p=0}^{n} \frac{n!}{p!\,(n-p)!} x^p = \sum_{n=0}^{\infty} \rho(n)(1+x)^n.$$

En posant $y = 1+x$ on obtient ainsi la relation

$$\sum_{n=0}^{\infty} \rho(n) y^n = \frac{1}{1+\langle n \rangle - y\langle n \rangle}.$$

En développant le second membre en puissances de y et en identifiant avec le premier on obtient

$$\rho(n) = \frac{1}{1+\langle n \rangle} \left(\frac{\langle n \rangle}{1+\langle n \rangle} \right)^n.$$

Cette expression prend la forme (16) quand on introduit le paramètre $\beta\omega$ par les relations (24) et (25).*

4. Le Potentiel de Gibbs

Comme le théorème de Wick dans la théorie des champs, le théorème établi au paragraphe précédent conduit à représenter les différents termes du développement (19) par des *diagrammes de Feynman.*

Nous représenterons les interactions avec les "temps" croissant vers le haut, les lignes d'électrons par des traits pleins et les lignes de phonons par des traits pointillés.

Les contractions $\eta^{+\bullet}\eta^{\bullet}$ et $q^{+\bullet}q^{\bullet}$ seront représentés par des lignes avec des flèches dirigées vers le bas, et les contractions $\eta^{\bullet}\eta^{+\bullet}$ et $q^{\bullet}q^{+\bullet}$ par des lignes à flèches dirigées vers le haut (dans tous les cas, la flèche va de la création vers l'annihilation). On notera que, contrairement aux calculs d'énergie de l'état fondamental, nous sommes obligés de mettre des flèches sur les lignes de bosons aussi bien que sur celles de fermions.

Les seuls diagrammes à considérer sont les *diagrammes vide-vide*, c'est-à-dire sans lignes extérieures, puisque seuls les systèmes complets de contractions interviennent.

La contribution au développement (19) associée à chaque diagramme s'obtient en formant le produit de plusieurs facteurs:

1) *à chaque interaction est associé un terme de* (11), *c'est-à-dire un élément de matrice de v et un facteur exponentiel dépendant de l'instant auquel se produit l'interaction*;

2) *à chaque ligne est associée la valeur de la contraction correspondante donnée par* (22), *c'est-à-dire des facteurs* f^+ *et* g^+ *pour les lignes montantes*

d'électrons et de phonons et des facteurs f^- et g^- pour les lignes descendantes;

3) *Chaque terme est affecté du signe $(-)^{h+l}$, où h est le nombre de lignes descendantes de fermions et l le nombre de boucles fermées de lignes de fermions.*

Ce signe provient, comme d'habitude, des permutations des opérateurs agissant sur les fermions nécessaires pour amener les uns à côté des autres les groupes d'opérateurs contractés. On n'oubliera pas non plus le signe $(-)^p$ qui figure devant chaque terme du développement (19).

Il faut enfin effecteur *l'intégration ordonnée des temps d'interaction dans l'intervalle $0-\beta$ et la sommation sur l'ensemble des valeurs des états associés à chacune des lignes du diagramme.*

Par exemple, le diagramme de la figure 1 donne la contribution

Fig. 1. Un diagramme du second ordre.

$$\sum_{r,s,k} f_r^+ f_s^- g_k^- \int_{\beta > u_1 > u_2 > 0} du_1\, du_2 \langle sk|v|r\rangle\, e^{u_1 \Delta E_1} \langle r|v|sk\rangle e^{u_2 \Delta E_2}, \qquad (26)$$

où ΔE_1 et ΔE_2 sont les énergies d'excitation aux temps u_1 et u_2 données par

$$\Delta E_2 = -\Delta E_1 = \varepsilon_r - \varepsilon_s - \omega_k.$$

Le diagramme vide-vide le plus général est formé d'un certain nombre de parties connexes. La contribution au développement (19) associée à un diagramme formé de plusieurs parties connexes est le produit de facteurs associés à chacune des composantes connexes du diagramme. On peut alors répéter exactement le raisonnement qui a été fait à propos du calcul de l'état fondamental d'un système [6]), introduire les mêmes *familles de diagrammes semblables*, et montrer que le développement (19) est égal à l'exponentielle de la somme des contributions des diagrammes connexes. En introduisant la notion de *potentiel de Gibbs*, nous obtenons alors pour cette fonction le développement suivant:

$$A = A_0 - \frac{1}{\beta} \sum_{p=1}^{\infty} (-)^p \int_{\beta > u_1 \ldots > u_p > 0} du_1 \ldots du_p \langle V(u_1) \ldots V(u_p)\rangle_c; \qquad (27)$$

où l'indice c rappelle qu'*il ne faut prendre que les diagrammes connexes*, et où A_0 est le potentiel de Gibbs du système sans interaction, obtenu en remplaçant Z par Z_0 dans la relation (2).

5. L'Invariance Cyclique de la Trace

Il est bien connu que la trace d'un produit d'opérateurs n'est pas modifiée par une permutation circulaire des facteurs. Pour traduire cette invariance dans le problème qui nous intéresse, il est commode de porter les temps d'interaction $u_1, u_2, \ldots u_p$ à partir d'une origine O sur un *cercle de circonférence égale à* β (fig. 2).

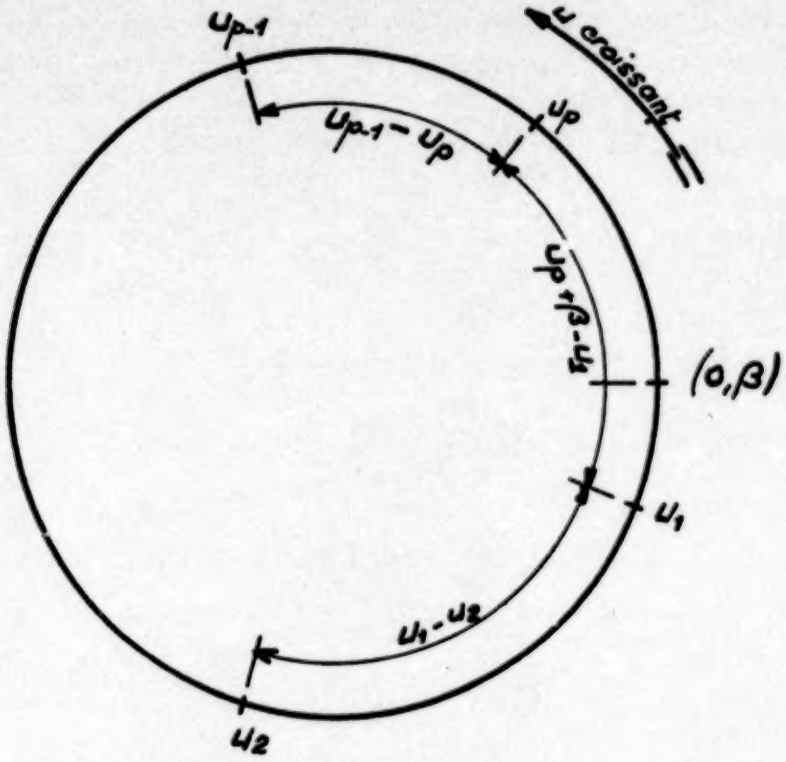

Fig. 2. Le cercle β des "temps".

On a alors la propriété suivante: *la quantité*

$$\langle V(u_1)V(u_2)\ldots V(u_p)\rangle \tag{28}$$

est invariante sous l'effet d'une rotation d'ensemble des points $u_1, u_2, \ldots u_p$ *sur le cercle* β.

Cette quantité peut, en effet, s'écrire sous la forme

$$\frac{1}{Z_0}\,\mathrm{Tr}\,\{e^{\alpha N}\,e^{(u_1-u_p-\beta)H_0}\,V\,e^{(u_2-u_1)H_0}\,V\ldots V\,e^{(u_p-u_{p-1})H_0}\,V\},$$

où le temps ne figure que par les combinaisons

$$u_p+\beta-u_1,\ u_1-u_2,\ u_2-u_3,\ldots u_{p-1}-u_p,$$

qui sont les longueurs des p arcs séparés sur le cercle β par les points $u_1, u_2 \ldots u_p$. Une rotation d'ensemble de ces points ne change pas les longueurs des arcs. Son seul effet pourra être une permutation circulaire des

facteurs, ce qui ne change pas la trace de leur produit. Il est important dans ce raisonnement que N commute avec H_0 et V, de sorte que la position du facteur contenant cet opérateur soit indifférente.

Nous allons maintenant analyser l'invariance de (28) plus en détail et montrer qu'on peut *classer les diagrammes d'ordre p en familles de p diagrammes équivalents qui se déduisent les uns des autres par rotation des temps sur le cercle β et donnent des contributions égales* †.

Raisonnons, pour fixer les idées, sur le diagramme du 4ème ordre de la figure 3(a) dont le cercle des temps est représenté sur la fig. (4a). Si on fait tourner les temps de façon à arriver à la configuration 4(b), l'interaction

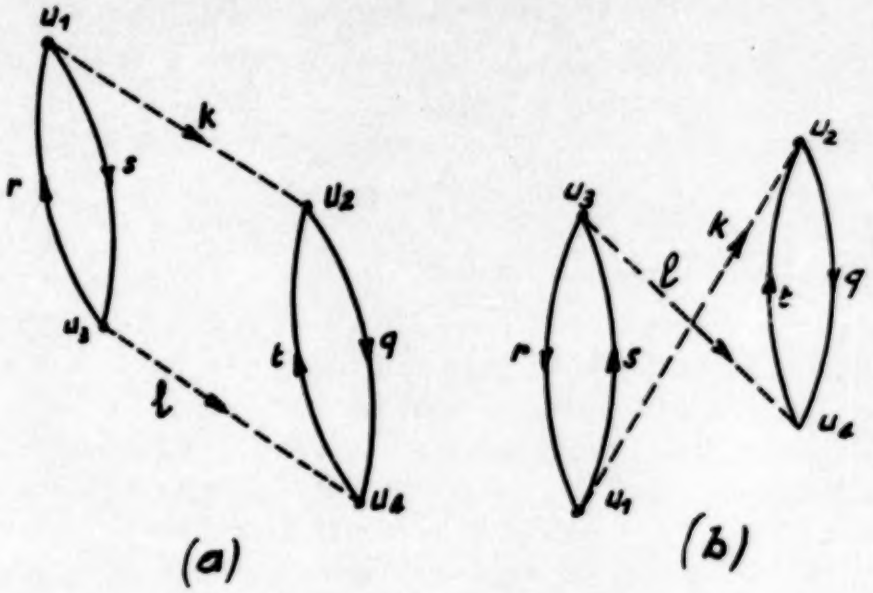

Fig. 3. Deux diagrammes équivalents.

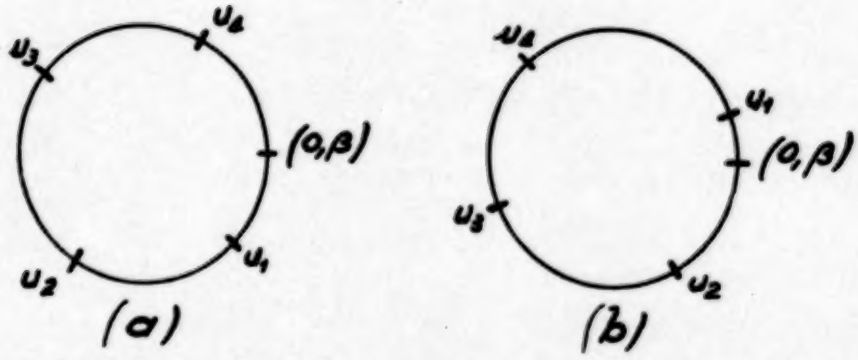

Fig. 4. La rotation sur le cercle β correspondant aux diagrammes de la fig. 3.

u_1 qui se trouvait au sommet du diagramme passe à la base et le diagramme prend l'aspect 3(b). En continuant la rotation on obtiendra en tout 4 diagrammes équivalents.

† On notera que les diagrammes constituant une famille ne sont pas forcément tous distincts.

Montrons que les diagrammes 3(a) et 3(b) *où les états r, s, t, q, l, k sont les mêmes* et où les temps se déduisent les uns des autres par rotation sur le cercle β donnent la même contribution. Les éléments de matrice de V associés aux deux diagrammes sont visiblement les mêmes. Les facteurs statistiques f et g relatifs aux lignes autres que celles qui aboutissent en u_1 sont aussi inchangés. Les lignes aboutissant en u_1 voient leurs flèches retournées, ce qui change les f^+ et g^+ en f^- et g^-, et vice-versa. D'après les expressions (22) cette transformation s'écrit

$$f_r^+ f_s^- g_k^- \to f_r^- f_s^+ g_k^+ = f_r^+ f_s^- g_k^- \, e^{\beta \Delta E_1}, \tag{29}$$

où

$$\Delta E_1 = \varepsilon_s + \varepsilon_k - \varepsilon_r$$

est l'énergie d'excitation correspondant à l'interaction u_1 (qui est la même pour les deux diagrammes). Il nous reste à examiner la modification du facteur exponentiel dépendant des temps. Celui-ci s'écrit ici

$$e^{u_1 \Delta E_1 + u_2 \Delta E_2 + u_3 \Delta E_3 + u_4 \Delta E_4}.$$

Comme

$$\Delta E_1 + \Delta E_2 + \Delta E_3 + \Delta E_4 = 0,$$

puisque nous avons affaire à un diagramme sans ligne extérieure, le facteur exponentiel n'est pas modifié par l'addition d'une même constante à tous les temps. Mais lorsqu'au cours de la rotation le point u_1 franchit l'origine, u_1 décroît brusquement de β, ce qui a pour effet de multiplier le facteur exponentiel par $\exp(-\beta \Delta E_1)$. Cette modification compense la modification des facteurs f et g et on voit que le produit complet est invariant.

Lorsqu'un diagramme est connexe, les diagrammes équivalents sont évidemment connexes. Nous pouvons donc appliquer les raisonnements d'invariance à la partie connexe de (28) qui seule intervient dans le développement (27) du potentiel de Gibbs.

Nous allons maintenant utiliser la propriété d'invariance pour simplifier l'intégration par rapport aux temps dans le développement (27). En vertu de cette invariance, chaque intégrale figurant dans (27) est égale à $1/p$ fois la somme des intégrales (toutes égales) prises sur les p domaines

$$\begin{aligned}
&\beta > u_1 > u_2 > u_3 \ldots > u_{p-1} > u_p > 0, \\
&\beta > u_2 > u_3 > u_4 \ldots > u_p > u_1 > 0, \\
&\text{- - - - - - - - - - - - - - - - - - - -} \\
&\beta > u_p > u_1 > u_2 \ldots > u_{p-2} > u_{p-1} > 0.
\end{aligned}$$

En posant

$$u_1 = v_1 + u_p, \; u_2 = v_2 + u_p, \ldots u_{p-1} = v_{p-1} + u_p$$

et en prenant comme nouvelles variables $v_1, \ldots, v_{p-1}, u_p$, on voit que la somme de nos p domaines d'intégration peut être décrite par les inégalités

$$\beta > u_p > 0, \qquad \beta > v_1 > v_2 > \ldots > v_{p-1} > 0.$$

Une variation de u_p à $v_1, v_2, \ldots v_{p-1}$ constants correspond à une rotation d'ensemble sur le cercle β. Elle laisse la fonction à intégrer invariante. On peut dans celle-ci faire $u_p = 0$ et effectuer immédiatement l'intégration sur u_p. Ceci donne un facteur β. Le développement (27) devient alors

$$A = A_0 - \sum_{p=1}^{\infty} \frac{(-)^p}{p} \int_{\beta > v_1 > \ldots > v_{p-1} > 0} dv_1 \ldots dv_{p-1} \langle V(v_1) \ldots V(v_{p-1}) V(0) \rangle_c \quad . \quad (30)$$

L'invariance cyclique recevra encore d'autres applications au paragraphe suivant.

6. La Formulation Indépendante du Temps

Nous allons maintenant effectuer les intégrations par rapport aux temps $v_1, v_2, \ldots v_{p-1}$ dans le développement (30) afin de le mettre sous une forme analogue à celle des développements habituels de la théorie des perturbations indépendantes du temps.

Il sera commode d'utiliser dans ce qui suit la notion *d'énergie du système entre deux interactions*. Nous désignerons par E_i ($i = 1, 2, \ldots p-1$) l'énergie entre les instants v_{i+1} et v_i, et par E_p l'énergie entre les instants v_1 et β (qui sur le cercle des temps équivaut à $v_p = 0$) (fig. 5). Ces énergies sont

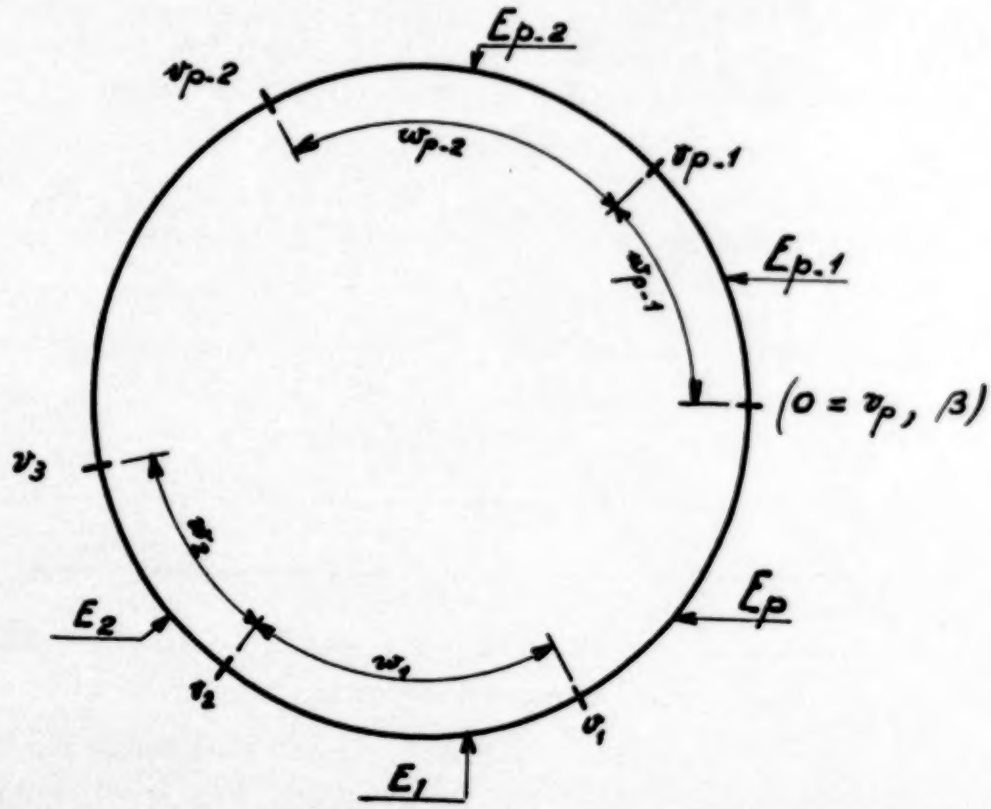

Fig. 5. Notations pour le passage à la formulation indépendante du temps.

définies, à une constante près que nous laisserons arbitraire (toutes les expressions que nous rencontrerons par la suite ne feront intervenir que des différences d'énergie), par les relations

$$\Delta E_{i+1} = E_i - E_{i+1} \qquad (i = 1, 2, \ldots p-1), \qquad \Delta E_1 = E_p - E_1, \quad (31)$$

où les ΔE_i sont les énergies d'excitation aux instants v_i définies par (12).

L'intégrale par rapport aux temps que nous devons calculer s'écrit

$$\int_{\beta > v_1 > \ldots > v_{p-1} > 0} \mathrm{d}v_1 \ldots \mathrm{d}v_{p-1}\, \mathrm{e}^{v_1 \Delta E_1 + \ldots + v_{p-1} \Delta E_{p-1}}. \quad (32)$$

En introduisant les nouvelles variables d'intégration

$$w_1 = v_1 - v_2, \qquad w_2 = v_2 - v_3, \qquad w_{p-2} = v_{p-2} - v_{p-1}, \qquad w_{p-1} = v_{p-1},$$

l'intégrale (32) devient

$$\int \mathrm{d}w_1 \ldots \mathrm{d}w_{p-1}\, \mathrm{e}^{w_1(E_p - E_1) + w_2(E_p - E_2) + \ldots + w_{p-1}(E_p - E_{p-1})}, \quad (33)$$

où les variables $w_1, \ldots w_{p-1}$ sont intégrées de 0 à $+\infty$ avec la restriction

$$w_1 + w_2 + \ldots + w_{p-1} < \beta.$$

On peut s'affranchir de cette inégalité en multipliant l'intégrale par

$$\frac{1}{2\pi i} \int_{+i\infty - a}^{-i\infty - a} \frac{\mathrm{d}\varepsilon}{\varepsilon}\, \mathrm{e}^{\varepsilon(w_1 + w_2 + \ldots w_{p-1} - \beta)}, \quad (34)$$

où l'intégration est effectuée dans le sens descendant le long d'une parallèle à l'axe imaginaire d'abscisse négative $-a$. Si a est choisi assez grand pour que

$$a + E_i - E_p > 0 \quad (i = 1, 2, \ldots, p-1),$$

on peut dans le produit de (33) par (34) intervertir l'ordre des intégrations et calculer d'abord les intégrales en $w_1, w_2, \ldots w_{p-1}$. On obtient l'expression

$$\frac{(-)^{p-1}}{2\pi i} \int_{+i\infty - a}^{-i\infty - a} \frac{\mathrm{d}\varepsilon}{\varepsilon}\, \mathrm{e}^{-\beta\varepsilon} \frac{1}{\varepsilon + E_p - E_1} \ldots \frac{1}{\varepsilon + E_p - E_{p-1}}. \quad (35)$$

Le contour peut être fermé à droite par un grand demi-cercle puisque $\beta > 0$. On obtient alors un contour fermé parcouru dans le sens positif et

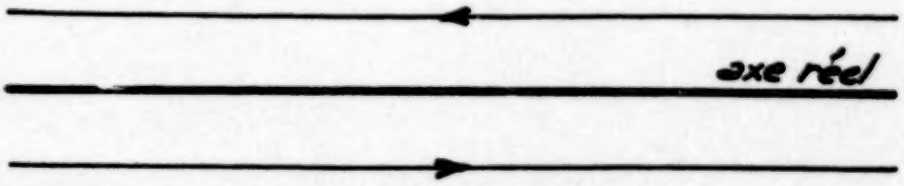

Fig. 6. Le contour d'intégration C dans le plan complexe des ε.

entourant toutes les singularités. Celles-ci se trouvent toutes sur l'axe réel, et le contour peut être déformé suivant le contour C habituel (fig. 6) composé d'une parallèle à l'axe réel en dessous de celui-ci parcourue dans

le sens positif et d'une parallèle située au-dessus parcourue dans le sens négatif. En reportant alors (35) dans (30), on obtient le développement:

$$\boxed{A = A_0 + \sum_{p=1}^{\infty} \frac{1}{2\pi i p} \int_C \frac{d\varepsilon}{\varepsilon} e^{-\beta\varepsilon} \left\langle V \left(\frac{1}{\varepsilon - \mathscr{E}} V \right)^{p-1} \right\rangle_c} . \qquad (36)$$

Dans ce développement, $\mathscr{E}$ désigne l'énergie du système entre deux interactions calculée en prenant pour état d'énergie nulle l'état représenté par l'absence de toute ligne sur le diagramme. En d'autre termes, on a posé:

$$\mathscr{E}_i = E_i - E_p,$$

et on voit que $\mathscr{E}_i$ *est égal à la somme des énergies des lignes montantes diminuée de la somme des énergies des lignes descendantes existant entre les instants* v_{i+1} *et* v_i.

Dans le développement (36), la sommation est étendue à tous les diagrammes connexes distincts équivalents ou non.

Il est commode d'introduire explicitement la constante de couplage en remplaçant dans le développement V par λV. Ceci permet de mettre le développement (36) sous la forme équivalente:

$$\boxed{\begin{aligned} &A = A_0 + \int_0^1 \frac{\partial A}{\partial \lambda} d\lambda, \\ &\text{avec} \\ &\frac{\partial A}{\partial \lambda} = \frac{1}{\lambda} \sum_{p=1}^{\infty} \frac{1}{2\pi i} \int_C \frac{d\varepsilon}{\varepsilon} e^{-\beta\varepsilon} \left\langle \lambda V \left(\frac{1}{\varepsilon - \mathscr{E}} \lambda V \right)^{p-1} \right\rangle_c \end{aligned}} . \qquad (37)$$

Nous allons encore indiquer deux formes du développement de A dont l'intérêt est de montrer clairement la ressemblance de celui-ci avec le développement habituel de l'énergie de liaison du système. Ces deux formes ont toutefois l'inconvénient d'obliger de traiter d'une manière particulière les contributions où certains des $\mathscr{E}_i$ sont nuls, alors qu'aucune distinction de ce genre n'intervient dans les développements (36) ou (37).

Considérons la contribution au potentiel de Gibbs provenant d'un certain diagramme d'ordre p, *pour des choix déterminés des états* $r, s, \ldots k, \ldots$ *associés aux lignes*. Par rotation de ce diagramme nous obtiendrons en tout p diagrammes donnant p contributions égales. Chacune de ces contributions est affectée dans le développement (36) du coefficient $1/p$. Il est évidemment possible de supprimer ce coefficient si on introduit en même temps une restriction éliminant toutes les contributions égales obtenues par rotation du diagramme sauf une. Supposons d'abord les énergies E_i toutes distinctes. Si nous amenons, par une rotation appropriée, l'énergie E_i la plus petite à être l'énergie E_0, *les énergies intermédiaires* $\mathscr{E}_i$ *seront toutes positives*. Le

choix de la rotation étant évidemment unique, nous obtenons bien ainsi une condition permettant de sélectionner une et une seule des p contributions égales.

La situation est un peu différente lorsque $\mathcal{N}+1$ énergies ($\mathcal{N} \geqq 1$) sont égales entre elles et inférieures à toutes les autres. En amenant l'une de ces énergies à être l'énergie E_p, *les énergies intermédiaires* $\mathscr{E}_i$ *seront toutes positives ou nulles*. D'autre part, il est difficile de sélectionner l'une des $\mathcal{N}+1$ contributions égales obtenues en amenant successivement chacune des $\mathcal{N}+1$ énergies E_i minimum à jouer le rôle de E_p. Ceci conduit à prendre la somme de toutes ces contributions pondérée par le coefficient $1/(\mathcal{N}+1)$. Nous obtenons ainsi le développement

$$A = A_0 + \sum_{p=1}^{\infty} \frac{1}{2\pi i(\mathcal{N}+1)} \int_c \frac{d\varepsilon}{\varepsilon} e^{-\beta\varepsilon} \left\langle V \left(\frac{1}{\varepsilon - \mathscr{E}} V \right)^{p-1} \right\rangle_{c, \mathscr{E} \geq 0}, \quad (38)$$

où la sommation sur les états intermédiaires est limitée aux combinaisons donnant des énergies intermédiaires toutes positives ou nulles, et où $\mathcal{N}$ *est pour chaque contribution le nombre des énergies* $\mathscr{E}_i$ *nulles.*

Pour établir une dernière forme du développement de A, nous commencerons par remarquer que l'intégrale (35) prend lorsqu'on remplace la variable d'intégration ε par $\eta = \varepsilon + E_p$ la forme plus symétrique

$$\frac{(-)^{p-1}}{2\pi i} e^{\beta E_p} \int_c d\eta\, e^{-\beta\eta} \frac{1}{\eta - E_1} \frac{1}{\eta - E_2} \cdots \frac{1}{\eta - E_p} \quad (39)$$

qui permet de vérifier facilement à nouveau l'invariance cyclique. En effet, la fonction à intégrer dans (39) ne change pas sous l'effet d'une rotation du diagramme, et il est facile de vérifier que le produit des facteurs statistiques f et g par $\exp(\beta E_p)$ est aussi invariant. Prenons, par exemple, le cas de la rotation représentée par la fig. 3. La relation exprimant l'invariance s'écrit

$$f_r^+ f_s^- g_k^- e^{\beta E_p} = f_r^- f_s^+ g_k^+ e^{\beta E_1}.$$

Cette égalité résulte bien des relations (29) et (31).

Supposons d'abord que les E_i soient tous distincts et considérons à nouveau la contribution au potentiel de Gibbs provenant d'un certain diagramme d'ordre p, pour des choix déterminés des états $r, s, \ldots k, \ldots$ associés aux lignes. D'après le calcul des résidus, les intégrales (35) ou (39) sont égales à la somme des résidus aux p pôles simples. Le pôle $\varepsilon = 0$ dans (35) correspond au pôle $\eta = E_p$ and (38). De même, le pôle $\varepsilon = 0$ de l'intégrale semblable à (35) relative au diagramme de la fig. 3 (b) obtenu en faisant passer l'interaction u_1 du haut vers le bas du diagramme correspond au pole $\eta = E_1$ de (38). En continuant ce processus on voit que les pôles $\varepsilon = 0$ des intégrales (35) relatives aux p diagrammes déduits les uns des autres par rotation, correspondent aux p pôles de l'intégrale (38) relative au

diagramme de départ. Il en résulte qu'on peut dans le développement (36) *supprimer le facteur* $1/p$ *à condition de prendre seulement le résidu au pôle* $\varepsilon = 0$ *de l'intégrale.*

La situation est de nouveau un peu différente lorsque les E_i ne sont pas tous distincts. D'une part, ceci fait apparaître des pôles multiples. D'autre part, un pôle d'ordre O occupera au cours des rotations O fois la position $\varepsilon = 0$. Il en résulte que la contribution correspondante doit être affectée du coefficient $1/O$, et nous aboutissons au développement

$$A = A_0 + \sum_{p=1}^{\infty} \frac{1}{O} \mathrm{Rés}_{\varepsilon=0} \frac{e^{-\beta\varepsilon}}{\varepsilon} \left\langle V \left(\frac{1}{\varepsilon - \mathscr{E}} V \right)^{p-1} \right\rangle_c, \tag{40}$$

où O *est pour chaque contribution l'ordre du pole* $\varepsilon = 0$.

La somme des contributions au développement (40) pour lesquelles $\varepsilon = 0$ est un pôle simple, c'est à dire telles que toutes les énergies intermédiaires $\mathscr{E}_i$ soient différentes de zéro a une forme particulièrement simple:

$$A = A_0 + \sum_{p=1}^{\infty} (-)^{p-1} \left\langle V \left(\frac{1}{\mathscr{E}} V \right)^{p-1} \right\rangle_{c, \mathscr{E} \neq 0} + \ldots . \tag{41}$$

Ecrivons, à titre d'exemple, les formes (36), (38) et (40) de la somme des termes correspondant au diagramme de la fig. 1 et au diagramme qui s'en déduit par rotation:

$$\frac{1}{2} \frac{1}{2\pi i} \int_c \frac{d\varepsilon}{\varepsilon} e^{-\beta\varepsilon} \sum_{r,s,k} \left[\frac{f_r^+ f_s^- g_k^-}{\varepsilon - \varepsilon_r + \varepsilon_s + \omega_k} + \frac{f_r^- f_s^+ g_k^+}{\varepsilon + \varepsilon_r - \varepsilon_s - \omega_k} \right] |\langle sk|v|r\rangle|^2, \tag{36'}$$

$$\frac{1}{2\pi i} \int_c \frac{d\varepsilon}{\varepsilon} e^{-\beta\varepsilon} \left[\sum_{\varepsilon_r > \varepsilon_s + \omega_k} \frac{f_r^+ f_s^- g_k^-}{\varepsilon - \varepsilon_r + \varepsilon_s + \omega_k} + \sum_{\varepsilon_r < \varepsilon_s + \omega_k} \frac{f_r^- f_s^+ g_k^+}{\varepsilon + \varepsilon_r - \varepsilon_s - \omega_k} \right] |\langle sk|v|r\rangle|^2, \tag{38'}$$

$$- \sum_{\varepsilon_r \neq \varepsilon_s + \omega_k} \left[\frac{f_r^+ f_s^- g_k^-}{\varepsilon_r - \varepsilon_s - \omega_k} + \frac{f_r^- f_s^+ g_k^+}{\varepsilon_s + \omega_k - \varepsilon_r} \right] |\langle sk|v|r\rangle|^2. \tag{40'}$$

On vérifie immédiatement l'égalité de ces expressions où nous avons négligé pour simplifier l'écriture les contributions telles que $\varepsilon_r = \varepsilon_s + \omega_k$.

7. Comparaison avec le Développement de Goldstone

Le développement (41) présente une analogie remarquable avec le développement établi par Goldstone [2]) pour l'énergie de l'état fondamental d'un système de particules. Dans les deux cas, les termes du développement sont associés aux différents diagrammes connexes sans lignes extérieures. Les contributions provenant d'un diagramme sont les produits des mêmes éléments de matrice de v et des mêmes dénominateurs en énergie (l'opérateur $\mathscr{E}$ que nous avons introduit peut, en effet, être identifié avec l'opérateur $H_0 - E_0$ de Goldstone).

Si nous omettons, pour l'instant, les contributions à (40) pour lesquelles $O > 1$, *la seule différence entre le développement de A et le développement de Goldstone réside dans les facteurs statistiques* f et g qui n'existent pas dans le développement de Goldstone. Ils y sont remplacés par les conditions que les lignes montantes (particules) doivent être associées aux états d'énergie supérieure à l'énergie de Fermi seulement, et les lignes descendantes (trous) aux états d'énergie inférieure à celle-ci. Ces conditions correspondent à la valeur limite des facteurs statistiques lorsqu'on fait *tendre la température vers zéro.* Si α et β tendent vers l'infini de façon que leur rapport

$$\frac{\alpha}{\beta} = \varepsilon_F$$

reste fixe et égal à l'énergie de Fermi, les facteurs statistiques deviennent en effet:

$$f_r^+ = \begin{cases} 0 \text{ si } \varepsilon_r < \varepsilon_F, \\ 1 \text{ si } \varepsilon_r > \varepsilon_F, \end{cases}$$

$$f_r^- = \begin{cases} 1 \text{ si } \varepsilon_r < \varepsilon_F, \\ 0 \text{ si } \varepsilon_r > \varepsilon_F, \end{cases}$$

$$g_k^+ = 1, \quad g_k^- = 0.$$

Dans ces conditions, le développement (41) devient identique au développement de Goldstone, et A devient égal à l'énergie de liaison du système, comme il fallait s'y attendre d'après la définition (1) (2) de cette quantité.

Il nous reste à examiner les contributions au développement (40) pour lesquelles l'ordre O du pôle $\varepsilon = 0$ est supérieur à 1. Ces termes omis dans (41) disparaissent dans le cas limite d'une température nulle, à condition, cependant, que *l'état fondamental du système non perturbé soit non dégénéré*†. Dans ce cas, les énergies d'excitation intermédiaires $\mathscr{E}_i$ sont, en effet toujours positives. On sait que la condition de non-dégénérescence est indispensable pour l'application des résultats de Goldstone. Le cas où l'état fondamental du système non perturbé est dégénéré qui ne se singularise pas aux températures finies, nécessite une étude spéciale [8]) si on veut déterminer l'énergie de l'état fondamental et des premiers états excités par le passage à la limite $\beta \to +\infty$.

On notera que les lignes descendantes de bosons donnent des contributions nulles. Il faut donc ne considérer que les diagrammes contenant exclusivement des lignes montantes de bosons. On peut alors supprimer les flèches comme dans la théorie des champs habituelle.

† Dans (41) les contributions sont fournies par des résidus de pôles simples. L'intégrale (13) de l'article cité dans la référence [8]) a au contraire un pôle double au point E_0. Ce pole double fait intervenir la quantité $F'(E_0)$ qui est liée à la normalisation $|\langle 0|f\rangle|^2$ de l'état fondamental. Ici, au lieu de nous appuyer sur le calcul de $\langle 0|U(\beta)|0\rangle$, nous avons calculé des traces. De ce fait, les facteurs de normalisation des fonctions d'onde ne peuvent pas apparaître.

L'analogie très grande que nous venons de constater entre le développement du potentiel de Gibbs et le développement de l'énergie de l'état fondamental suggère l'extension à celui-ci des techniques qui ont été développées pour l'étude de l'état fondamental. Nous montrerons dans la seconde partie de ce travail qu'on peut effectuer, dans certains cas, la sommation des diagrammes en échelle comme l'a fait Goldstone et définir une matrice t dépendant de la température semblable à celle de Brueckner et de Bethe et Goldstone [5]).

Bibliographie

1) R. Feynman, Phys. Rev. **91** (1953) 1291;
T. Matsubara, Progr. Theor. Phys. **14** (1955) 351;
K. Watson, Phys. Rev. **103** (1956) 489;
H. Ezawa, Y. Tomozawa and H. Umezawa, Nuovo Cimento **5** (1957) 810;
P. C. Martin, communication privée;
E. Montroll et J. Ward, Physics of Fluids **1** (1958) 55
2) K. Brueckner, Phys. Rev. **100** (1955) 37;
J. Goldstone, Proc. Roy. Soc. A **239** (1957) 267;
N. Hugenholtz, Physica **23** (1957) 481
3) D. ter Haar, Elements of Statistical Mechanics (Rinehart, New York, 1954);
J. Yvon, Nuclear Physics **4** (1957) 1
4) H. Ursell, Proc. Comb. Phil. Soc. **23** (1927) 685;
J. Yvon, Act. Sc. Ind. **203** (1935);
G. Uhlenbeck et E. Beth, Physica **3** (1936) 729;
J. Mayer, J. Chem. Phys. **5** (1937) 67
5) K. Brueckner et C. Levinson, Phys. Rev. **97** (1955) 1344;
H. Bethe et J. Goldstone, Proc. Roy. Soc. A **238** (1957) 551
6) C. Bloch, Nuclear Physics **7** (1958) 451
7) G. Wick, Phys. Rev. **80** (1950) 268
8) C. Bloch et J. Horowitz, Nuclear Physics
9) T. Thouless, Phys. Rev. **107** (1957) 1162

1.E.1:
3.A

Nuclear Physics 7 (1958) 480—487; © *North-Holland Publishing Co., Amsterdam*
Not to be reproduced by photoprint or microfilm without written permission form the publisher

GAMMA RADIATION FOLLOWING THE DECAY OF Mn^{56} AND THE ENERGY LEVELS OF Fe^{56}

C. SHARP COOK

U. S. Naval Radiological Defense Laboratory, San Francisco 24, California

Received 19 March 1958

Abstract: The gamma radiation following the decay of Mn^{56} has been studied using a 4″ diameter by 4″ high NaI(Tl) crystal spectrometer. Two new gamma rays at 2.52 and 3.39 MeV have been found. Relative intensities of the gamma-rays are reported.

1. Introduction

The energy levels in Fe^{56} have been studied by many groups using a rather large variety of experiments. Recent studies [1]) of the α-particle energies from the reaction $Co^{59}(p, \alpha)Fe^{56}$ show that excited levels exist in the Fe^{56} nucleus at 0.844, 2.085, 2.661, 2.964, 3.127 and 3.379 MeV. In addition, levels at 2.940 and 3.388 MeV were found in the inelastic scattering of protons from Fe^{56}, but these levels were only weakly excited by the $Fe^{56}(p, p')Fe^{56*}$ process. Experiments [2–7]) on the decay of Co^{56} have identified levels at 0.845, 2.09, 3.13 and 3.44 MeV, as well as higher levels at 3.84 and 4.10 MeV. Earlier work [8, 9]) on the decay of Mn^{56} identities the Fe^{56} energy levels at 0.845, 2.65 and 2.98 MeV, levels apparently identical with those seen by Mazari *et al.* [1])

The present work studies the relative intensities of the gamma radiation following the decay of Mn^{56} and considers the possibility of fitting into the currently accepted level scheme for Fe^{56} those gamma rays not previously observed in the decay of Mn^{56}.

2. Experimental Procedure, Results and Discussion

Radioactive Mn^{56} was prepared by the $Mn^{55}(n, \gamma)Mn^{56}$ reaction. Collimated gamma radiations were then studied using a 4 inch diameter by 4 inch high NaI(Tl) crystal, DuMont Type 6364 photomultiplier tube and a Penco 100 channel pulse height analyzer. Analysis of data was performed in exactly the same manner as previously described [2]) for the analysis of Co^{56} and Co^{58} gamma radiations.

The pulse height spectra from one of the Mn^{56} sources prepared for this study is shown in fig. 1. The analysis of this distribution by the successive

subtraction of standard shaped pulse height distributions for monoenergetic gamma rays is shown in figs. 2 and 3. The relative intensities of the gamma rays is given in table 1. Errors are assigned on the basis of a combination of statistical errors and consistency between independent analyses of two

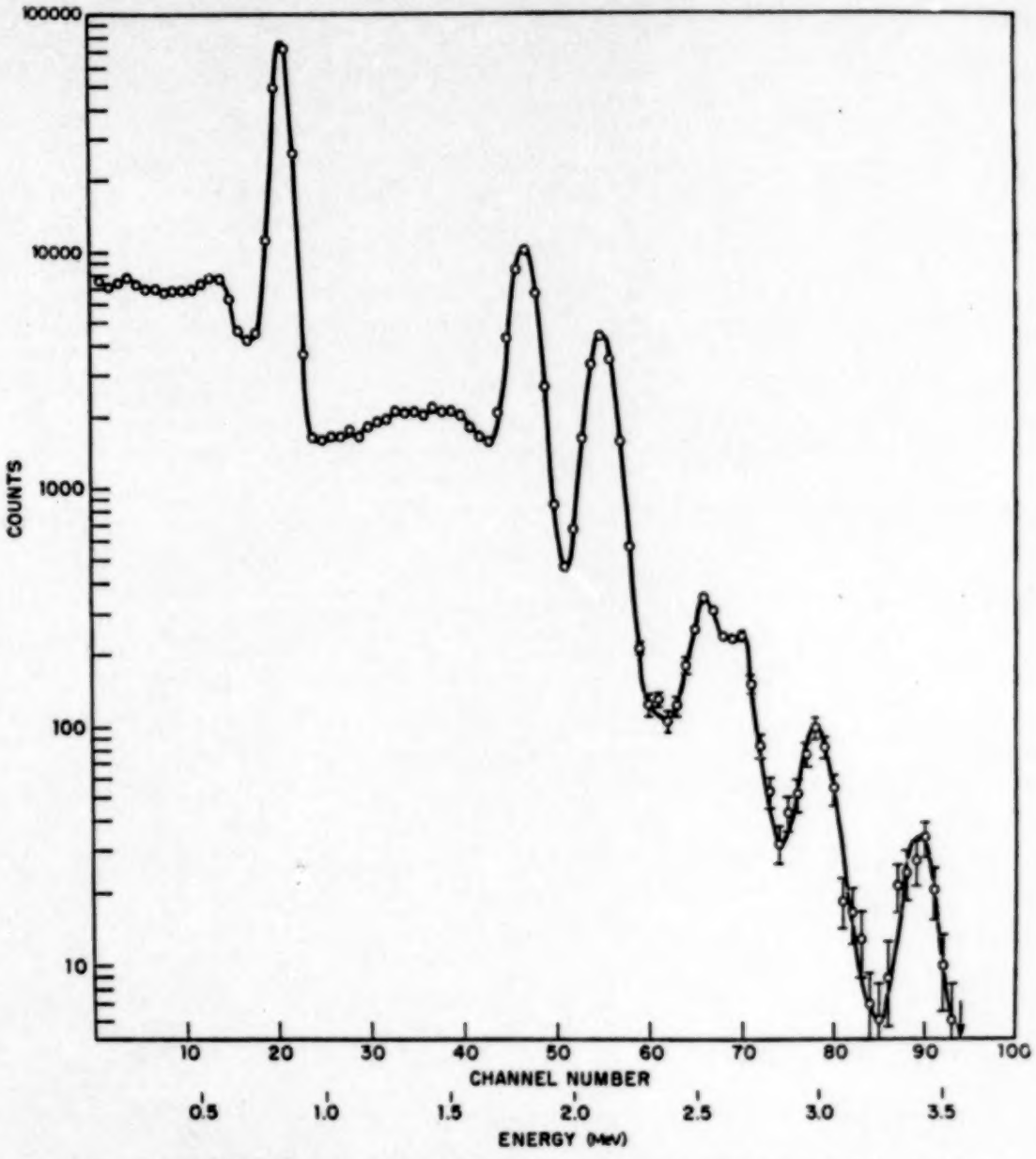

Fig. 1. Pulse height distribution produced in a 4″ diameter by 4″ high NaI(Tl) crystal by a collimated source of gamma rays from Mn^{56}.

Mn^{56} sources. Systematic errors of the same type and same order of magnitude which appear in both studies would not necessarily be apparent in this system of analysis. That the analysis does not appear to possess any significant systematic errors was verified [2]) for Co^{56} by the fact that the calculated sum of the intensities of the gamma-rays feeding the 0.845 MeV level equals,

within experimental error, the intensity of the 0.845 MeV gamma ray.

It can be seen from table 1 that a very weak 3.39 MeV gamma ray and a 2.52 MeV gamma ray, neither previously observed, appear as decay radia-

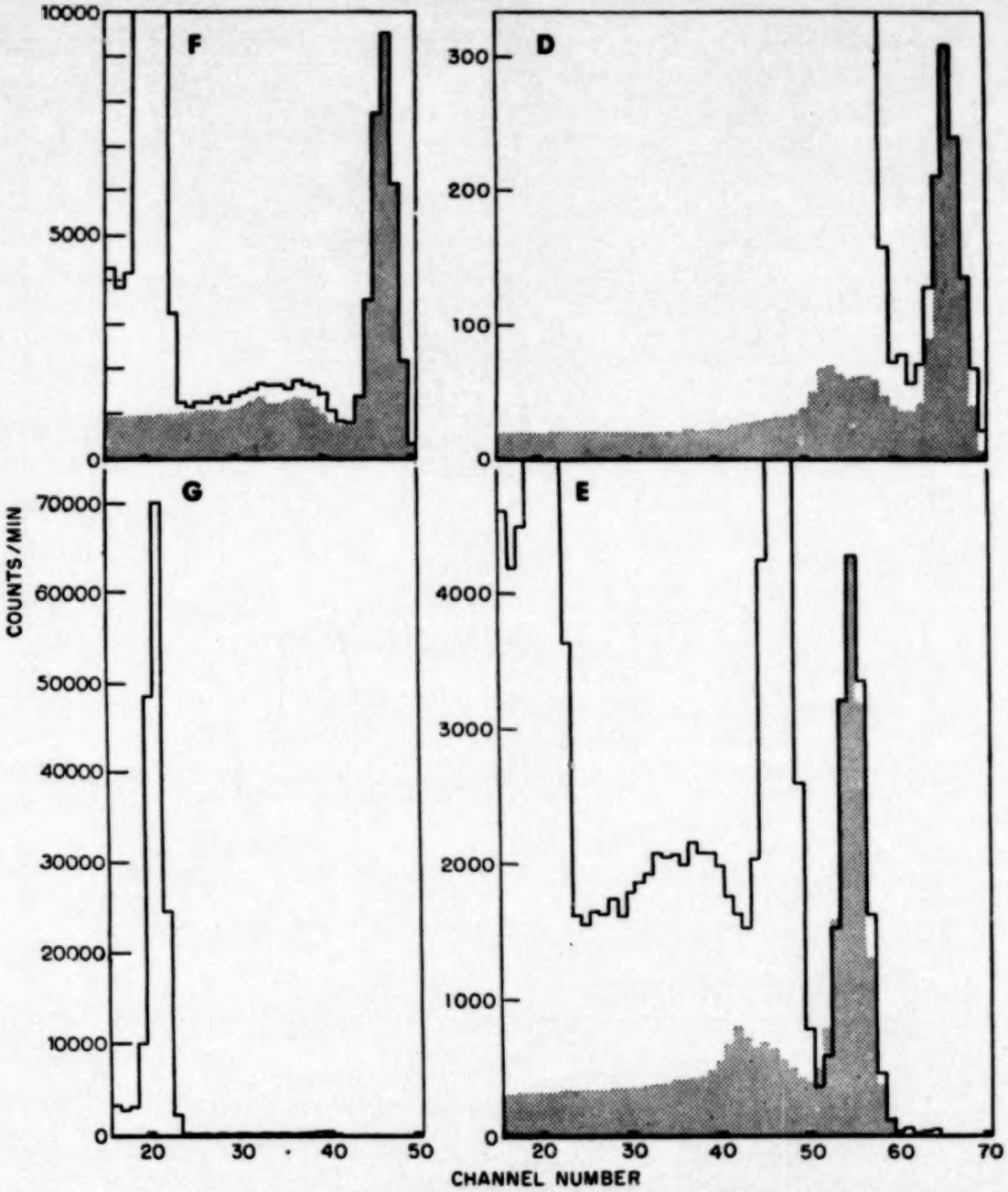

Fig. 2. Analysis of the higher energy portions of the pulse height distribution of fig. 1 by the successive subtraction of pulse height distributions derived from monoenergetic gamma ray sources.

tions following Mn^{56}. These are very probably the same gamma rays quoted previously [2]) as 3.47 MeV and 2.56 MeV gamma rays in the decay of Co^{56} and, if they are, lead to the decay scheme of fig. 4. It would appear that these

two gamma rays originate at either the 3.38 or the 3.39 MeV level found in nuclear reaction studies [1]).

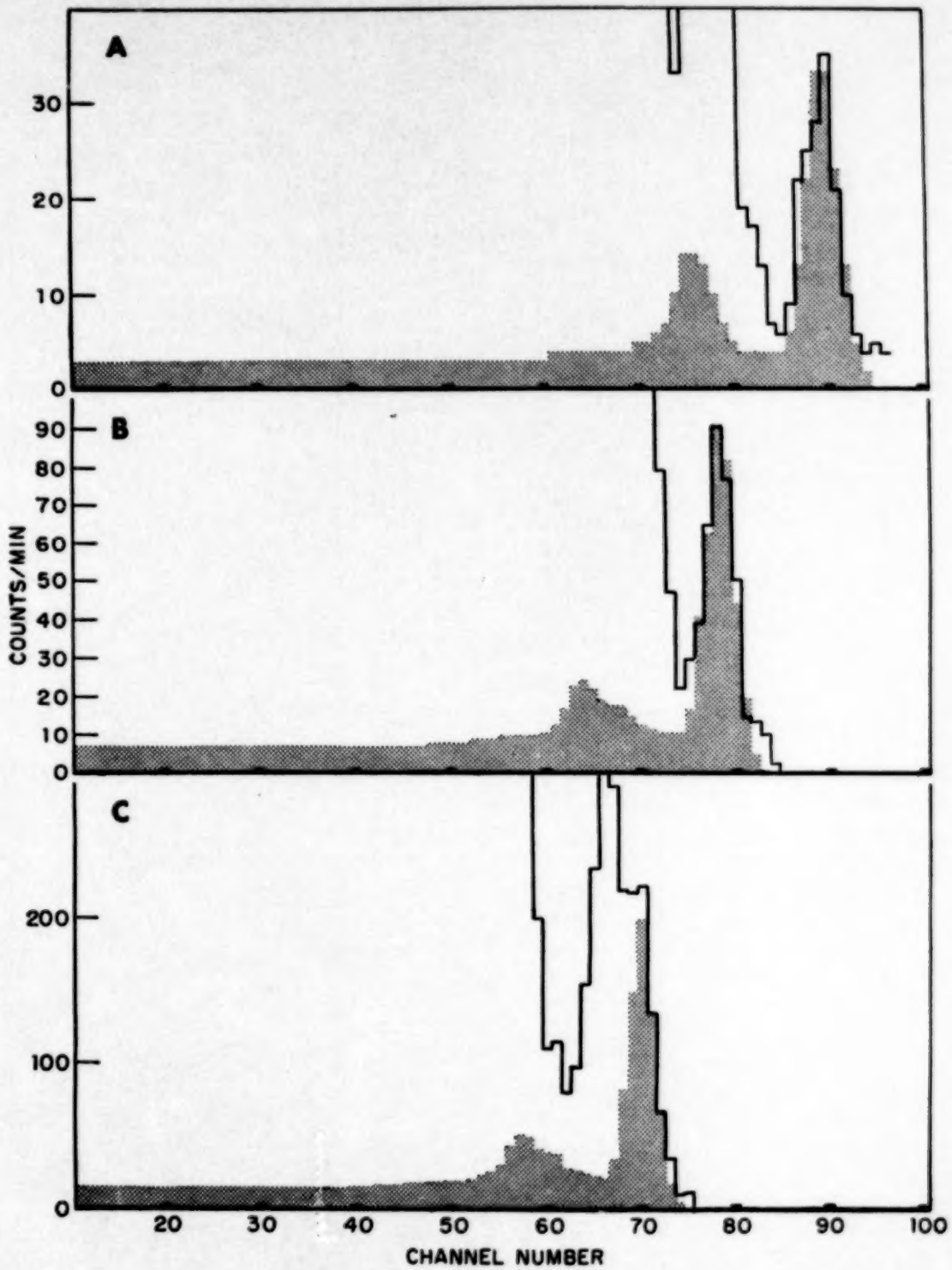

Fig. 3. Continuation of fig. 2 with lower energy region.

A small excess of counts appears in the region between the 0.845 and the

1.81 MeV full energy peaks (see fig. 3). Whether this excess is real is uncertain, for in the analysis of a second source of Mn^{56} the excess was not so

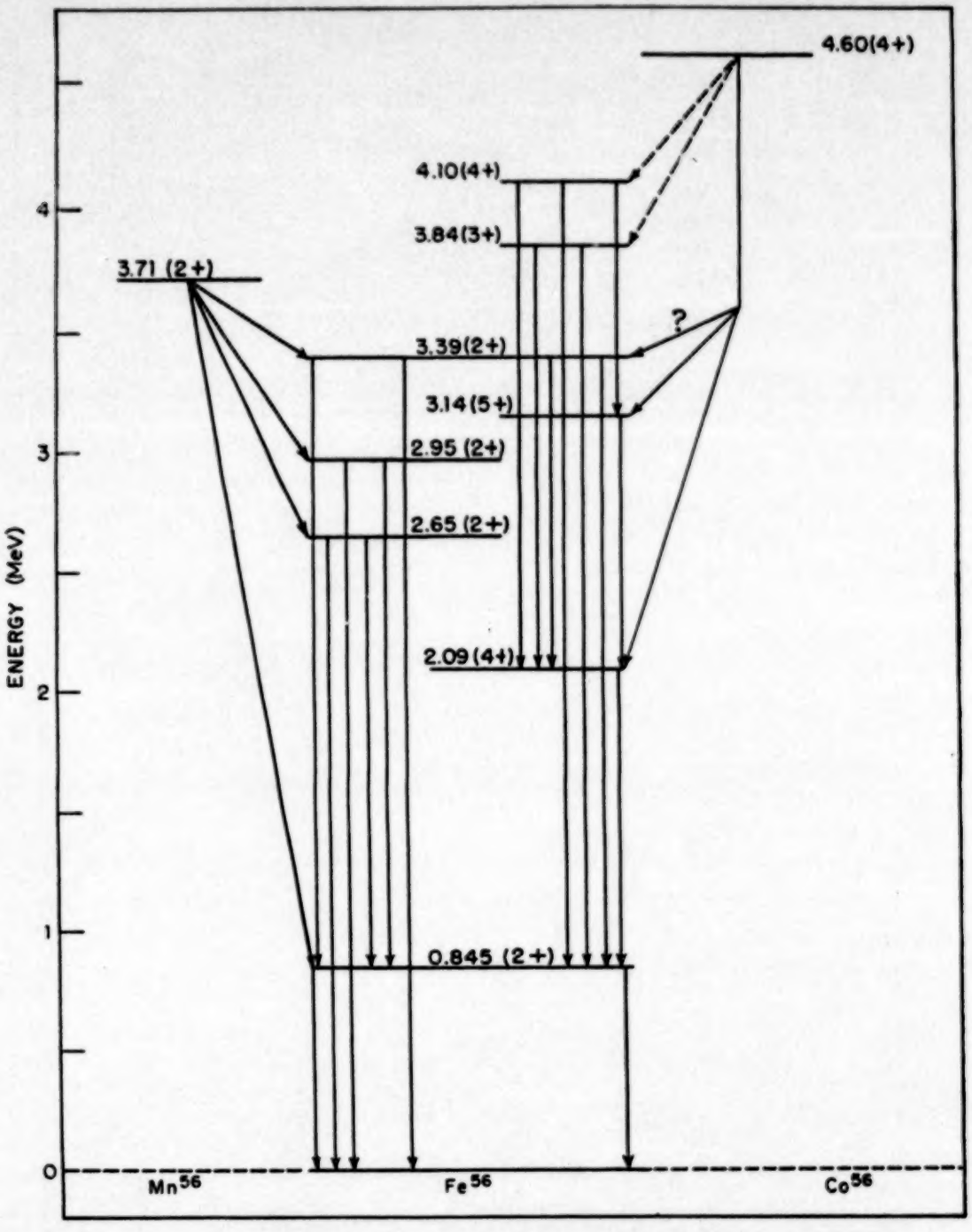

Fig. 4. Nuclear energy levels of Fe^{56}.

readily apparent. A possible gamma ray at 1.35 MeV was listed in the Co^{56} gamma ray analysis. It too appeared as a small excess in the number of counts in the pulse height distribution in this energy region. If the 1.35 MeV

gamma ray really exists in the decay of Mn^{56}, then its intensity relative to the intensity of the 0.845 MeV gamma ray is as measured by the current studies 0.0049 ± 0.0049.

Using the transition probabilities for a single proton [10]), calculations have been made of the expected relative probabilities for the emission of gamma rays from selected single levels. From the 2.65 MeV level the spin change to the ground state and to the 0.845 MeV level are respectively $\Delta I = 2$(no) and $\Delta I = 0$(no). If these are E2 and M1 transitions, as indicated by angular correlation measurements [11]), the expected ratio of intensities would be 0.028. The measured ratio of intensities is 0.024, in excellent agreement.

In like manner the transitions from the 2.95 MeV level to the ground state

TABLE 1

Gamma radiation following Mn^{56}

Gamma ray energy (MeV)	Relative intensity
3.39	0.0021 ± 0.0004
2.95	0.0038 ± 0.0006
2.65	0.0072 ± 0.0007
2.52	0.0115 ± 0.0007
2.12	0.153 ± 0.003
1.81	0.296 ± 0.007
0.845	1.000

[$\Delta I = 2$(no), E2] and to the 0.845 MeV level [$\Delta I = 0$(no), M1] are expected to have a ratio of intensities of 0.030, and have a measured ratio of 0.025, again in very good agreement.

The status of gamma ray transitions from the 3.39 MeV level is not so clear. From this level gamma rays to the ground state and to the 0.845 MeV level are observed experimentally in a ratio of 0.071. If the 3.39 MeV level is a 3+ state the two transitions most logically would be expected to be M3 and M1 respectively. This leads to an expected intensity ratio of 4.4×10^{-7}, very much lower than observed. On the other hand if the 3.39 MeV level is a 2+ level the intensity ratio expected is 0.034 which, while still lower than the observed ratio, is within the proper order of magnitude and is thus reasonable.

If the 3.39 MeV level following the decay of Mn^{56} is 2+, and if this is the same level from which the observed [2]) 3.47 and 2.56 MeV gamma rays originate following the decay of Co^{56}, there is a question how this level is populated in the Co^{56} decay. Assuming that the Co^{56} ground state is 4+, no observable orbital electron capture directly into the 3.39 MeV level would be expected. Orbital electron capture would be expected into either the 3.84 or the 4.10 MeV levels, but if the 3.39 MeV level is populated by transitions

from either of these two levels, gamma radiation at about 450 keV and 610 keV in measurable quantities should have been observed in the Co^{56} gamma ray spectrum, but were not observed.

Using a magnetic spectrometer and uranium radiator three gamma rays have been found [12]) at energies quoted as 2.61, 2.67 and 2.73 MeV. Should there be several levels in the immediate vicinity of 3.39 MeV, indicated also by the proton scattering studies [1]), it is possible that this multiplicity of levels may be used to explain the observed phenomena, but how such an explanation may be made cannot clearly be seen at present.

As seen in fig. 4, four Mn^{56} beta groups should be present with maximum energies of 0.32, 0.76, 1.06 and 2.87 MeV. Using gamma ray intensity measurements as the experimental input, the relative intensities of these beta groups have been determined to be 0.018, 0.154, 0.298 and 0.530. The logft values for these groups are respectively 4.98, 5.36, 5.61 and 7.48. The logft values for the three low energy groups are in the range of allowed transitions, in agreement with the spin-parity assignments of 2+ for both the ground state of Mn^{56} and for the 3.39, 2.95 and 2.65 MeV levels in Fe^{56}. The logft value of 7.48 is somewhat higher than expected for an allowed transition, required if $\Delta I = 0$(no) as indicated in the disintegration scheme. It is not necessarily unreasonably high, however.

No gamma rays have been observed corresponding to transitions between any two of the levels at 3.39, 2.95 and 2.65 MeV. Under any circumstances it would have been difficult to have seen these transitions. Even if the transitions were single particle transitions, M1 radiation, the intensity ratios would have been much less than the intensities of the radiations resulting from transitions to the 0.845 MeV (proportional to the cube of the energy of the radiation). Should these transitions be between vibrational states [13]), E2 radiation, their intensities would be reduced considerably further. Because of the anticipated low intensity, it appears that mere detection of these radiations would be quite difficult.

It is a pleasure to acknowledge the assistance of Mr. R. A. Taylor on electronic matters and of Mr. P. R. Howland and Mr. F. M. Tomnovec for assistance in the preparation of the source used in this study.

References

1) M. Mazari, A. Sperduto and W. W. Buechner, Phys. Rev. **107** (1957) 365
2) C. S. Cook and F. M. Tomnovec, Phys. Rev. **104** (1956) 1407
3) Sakai, Dick, Anderson and Kurbatov, Phys. Rev. **95** (1954) 101
4) M. Sakai, J. Phys. Soc. Japan **10** (1955) 729
5) Poppema, Siekman, Van Wageningen and Tolhoek, Physica **21** (1955) 223
6) Kurbatov, Sathoff, Hisatake and Sakai, Bull. Am. Phys. Soc. **1** (1956) 163; Azuma, Kokoszka, Cartwright and Kurbatov, Bull. Am. Phys. Soc. **3** (1958) 103

7) A. N. Diddens, Ph. D. Thesis, Groningen (1957)
8) H. Slätis and K. Siegbahn, Arkiv Fysik **4** (1952) 485
9) K. Siegbahn, Arkiv Mat. Astron. Fysik **33A** (1946) no. 10
10) S. A. Moszkowski, Theory of Multipole Radiation, in Beta and Gamma Ray Spectroscopy, edited by K. Siegbahn (North Holland Publ. Co., Amsterdam, 1955) pp. 373–395
11) F. R. Metzger and W. B. Todd, Phys. Rev. **92** (1953) 904
12) K. P. Howard, Ph. D. Thesis, Washington University, St. Louis (1956);
Carl Dulgeroff, private communication
13) T. Lindqvist and I. Marklund, Nuclear Physics **4** 189 (1957)

1.E.4:
3.A

Nuclear Physics 7 (1958) 488—502; © *North-Holland Publishing Co., Amsterdam*
Not to be reproduced by photoprint or microfilm without written premission from the publisher

RELATIVE TRANSITION PROBABILITIES IN CERTAIN EVEN NUCLEI

C. F. COLEMAN

Atomic Energy Research Establishment, Harwell, Didcot, Berks

Received 15 February 1958

Abstract: Angular correlation measurements on 2, 2, 0 cascades in Se^{76}, Ge^{72}, Zr^{92} and Te^{122} are reported. An analysis of the available data on such cascades shows that in non-rotational even nuclei the M1 transition probability from the second to the first excited state and the E2 crossover transition probability are inhibited by factors of about 10^4 and 10^2 respectively in relation to the E2 transition probability from the second to the first excited state. For the magic nuclei Zr^{92} and Ce^{140} the corresponding factors are both less than or of the order of unity.

1. Introduction

Goldhaber and Weneser [1]) first pointed out the existence of a number of marked regularities in the level structures of even nuclei outside the rotational regions. Some of these are summarized, in a form due to Wilets and Jean [2]), in fig. 1. Here the ratio E_2/E_1 is plotted for each nucleus against the ratio $E_1/E_{\text{vib.}}$, where E_1 and E_2 are the energies of the first and second excited states of the nucleus, and $E_{\text{vib.}}$ is the energy predicted for the first vibrational state on the hydrodynamical model. The nuclei are seen to fall into three groups. In the first, the rotational nuclei, E_2/E_1 is closely equal to 10/3, and $E_1/E_{\text{vib.}}$ lies between 0.04 and 0.07. In the second group, the existence of which was first pointed out by Goldhaber and Weneser [1]), E_2/E_1 is approximately 2, and $E_1/E_{\text{vib.}}$ lies between 0.18 and 0.38. The mass numbers of these nuclei lie in regions intermediate between those of the rotational nuclei and those associated with the magic numbers. The magic nuclei themselves form a third group, in which E_2/E_1 is less than 2, and $E_1/E_{\text{vib.}}$ exceeds 0.4. The second excited states of the rotational nuclei all have spin 4+, in the nuclei of the intermediate region spins 4+, 2+, and 0+ occur, and in the magic nuclei little systematic evidence is available, though it appears that weakly magic nuclei have level characteristics rather like those of intermediate region nuclei.

Coulomb excitation measurements [3, 4, 5]) have indicated systematic variations in the transition probabilities from the first excited states to the ground states of intermediate region nuclei. These results are usually interpreted in terms of the coefficients C_2 and $B_2/(B_2)_{\text{irrot}}$ of the hydrodynamical

model [6]), but their systematic character is much more clearly revealed by plotting F, the ratio of the observed transition probability to that predicted by the single particle model, for each transition against its energy. Fig. 2 shows a number of results, mainly due to Heydenburg and Temmer [3]), plotted in this way. It is clear that F is given quite well by an expression of the form $F = kE_1^{-2}$, which depends on the magic numbers only through their effects on the value of E_1. The determination of the absolute transition probabilities from the second excited states is difficult, but Stelson and McGowan [7]) have recently detected the Coulomb excitation of 2+ second excited states by measuring coincidences arising from cascade de-excitations through the first excited states. Some information about relative transition

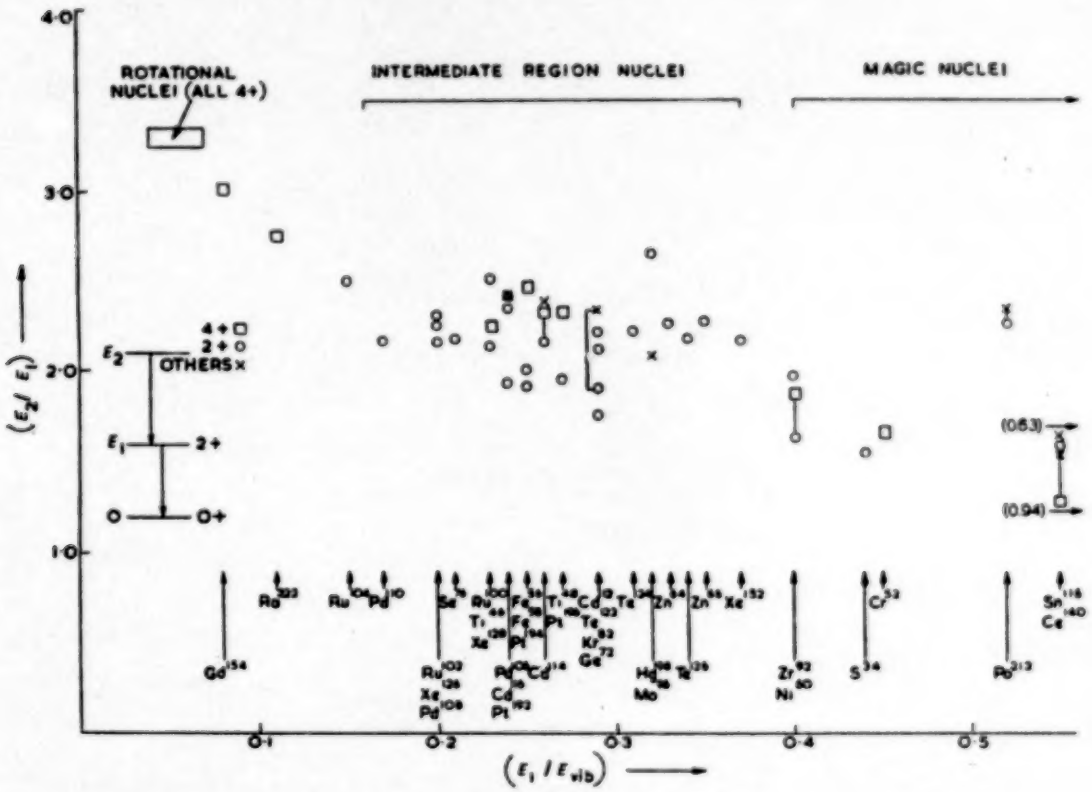

Fig. 1. Wilets-Jean diagram for even nuclei.

References to data not included in the original paper by Wilets and Jean [1]) are as follows:
S^{34}: H. E. Handler and J. R. Richardson, Phys. Rev. **102** (1956) 833
Cr^{52}, Zn^{64}, Ge^{72}, Kr^{82}, Zr^{92}: see ref. [11])
Fe^{56}: H. Frauenfelder, N. Levine, A. Rossi and S. Singer, Phys. Rev. **103** (1956) 352
Ru^{100}, Ru^{102}, Ru^{104}, Pd^{104}, Pd^{106}, Pd^{108}, Cd^{110}, Cd^{112}, Cd^{114}: see ref. [23])
Cd^{116}: see ref. [25]) Ce^{140}: see ref. [19]) Po^{212}: see ref. [26]).

probabilities from the 2+ second excited states can be obtained from angular correlation measurements on the 2, 2, 0, gamma ray cascades, which determine the relative magnitudes of the E2 and M1 transition

probabilities in the $2 \rightarrow 2$ transitions. The ratio of the E2 transition probabilities to the first excited states and to the ground states can then be inferred from a knowledge of the crossover intensities. The results of the present paper, and those of Lindqvist and Marklund [8]), which cover similar ground, qoth confirm the original conclusion of Goldhaber and Weneser [1]), namely, that the E2 transition probabilities for $2 \rightarrow 2$ transitions in the intermediate region nuclei are strongly enhanced in relation to both the corresponding M1 transition probabilities and the E2 crossover transition probabilities.

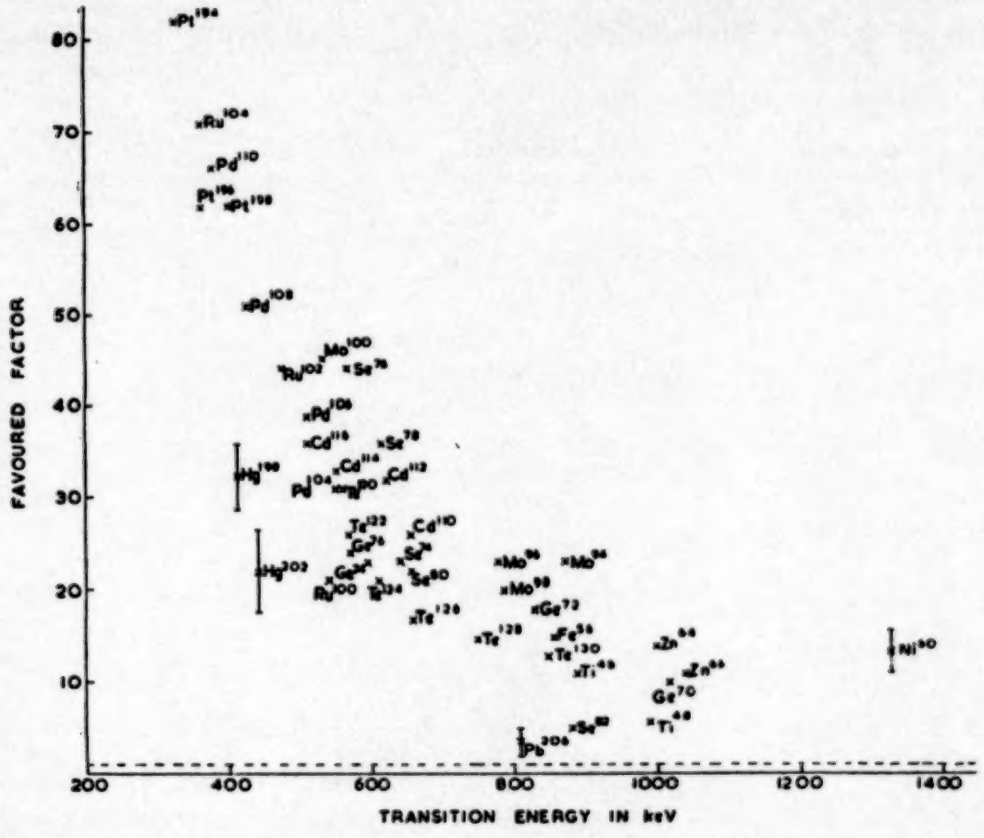

Fig. 2. The favoured factor F as a function of E_1 for intermediate region nuclei.

Ni^{60}: F. R. Metzger, Phys. Rev. **103** (1956) 983
Hg^{198}: W. G. Davey and P. B. Moon, Proc. Phys. Soc. A **66** (1955) 585
Hg^{202}: F. R. Metzger, Phys. Rev. **98** (1955) 200
Pb^{206}: P. H. Stelson and F. K. McGowan [4])
Others: G. M. Temmer and N. P. Heydenburg [3]).

2. Angular Correlation Measurements

The equipment used for these measurements and the method of analysing the results have been described elsewhere [9]). The pulse height selectors in the slow channels were normally set to select the photopeaks from the desired gamma rays. When energetic beta rays were present perspex ab-

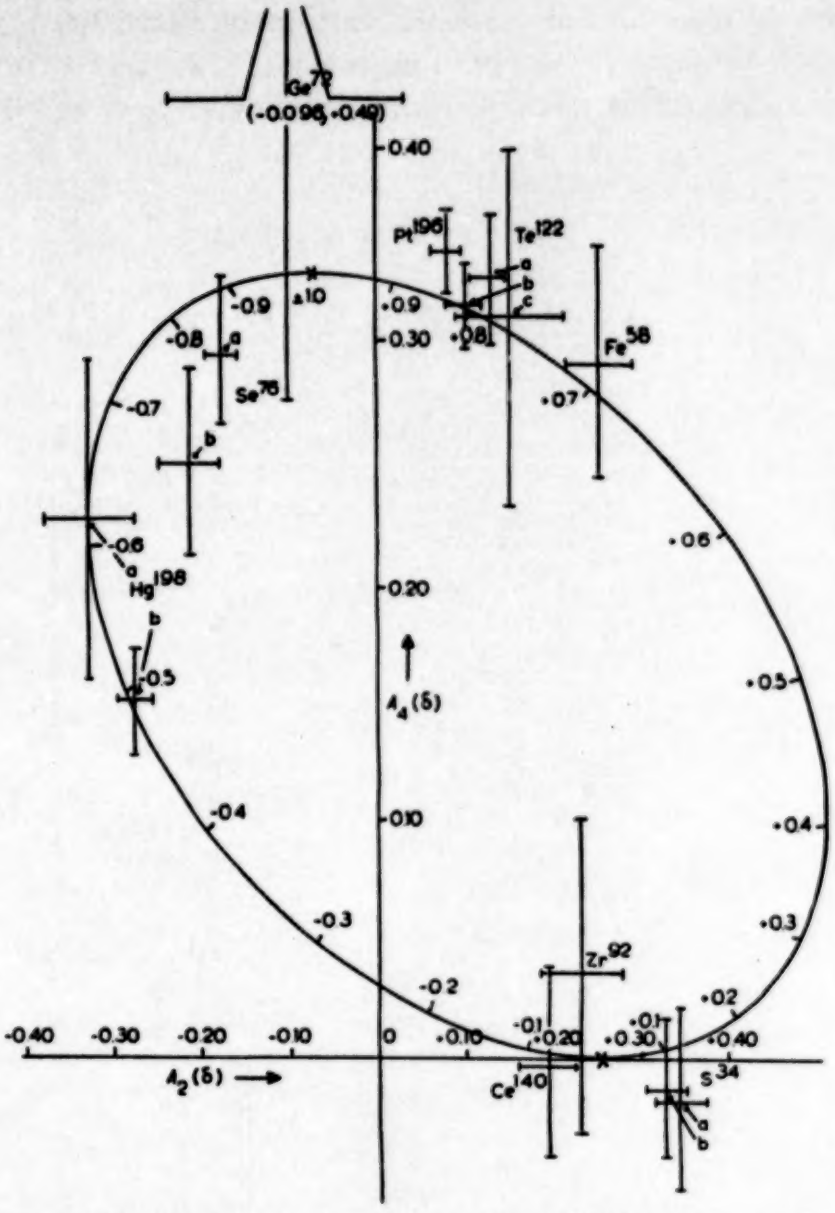

Fig. 3. Parametric plot of 2, 2, 0 angular correlation measurements.

The curve in this diagram is given by the parametric equations $x = A_2(\delta)$ and $y = A_4(\delta)$, where $A_2(\delta)$ and $A_4(\delta)$ are the coefficients of the Legendre polynomials in the angular correlation function for the spin sequence 2(E2+M1)2(E2)0. δ is the mixture ratio for the first transition, and the arc of the curve is labelled with values of the quantity $\delta' = \delta/(1+|\delta|)$. The values of δ^2 used in table 1 have been obtained from this figure. That for Hg^{198} (a) is not consistent with the value quoted in the original paper.

S^{34}: (a) H. E. Handler and J. R. Richardson, Phys. Rev. **102** (1956) 833
(b) P. S. Fisher and G. S. Shute, Phil. Mag. **2** (1957) 1255

Fe^{58}: H. Frauenfelder, N. Levine, A. Rossi and S. Singer, Phys. Rev. **103** (1956) 352
Ge^{72}: present work Se^{76}: (a) see ref. [6]) (b) present work Zr^{92}: present work
Te^{122}: (a) see ref. [6]) (b) present work (c) M. J. Glaubman, Phys. Rev. **98** (1955) 645
Ce^{140}: see ref. [19])
Pt^{196}: R. M. Steffen, Phys. Rev. **89** (1953) 665
Hg^{198}: (a) C. D. Schrader, Phys. Rev. **92** (1953) 928
(b) D. Schiff and F. R. Metzger, Phys. Rev. **90** (1953) 849

sorbers were used in front of the detectors to reduce bremsstrahlung formation. The scintillation spectrum of each source was checked before the correlation measurement, and where impurity peaks were found this is

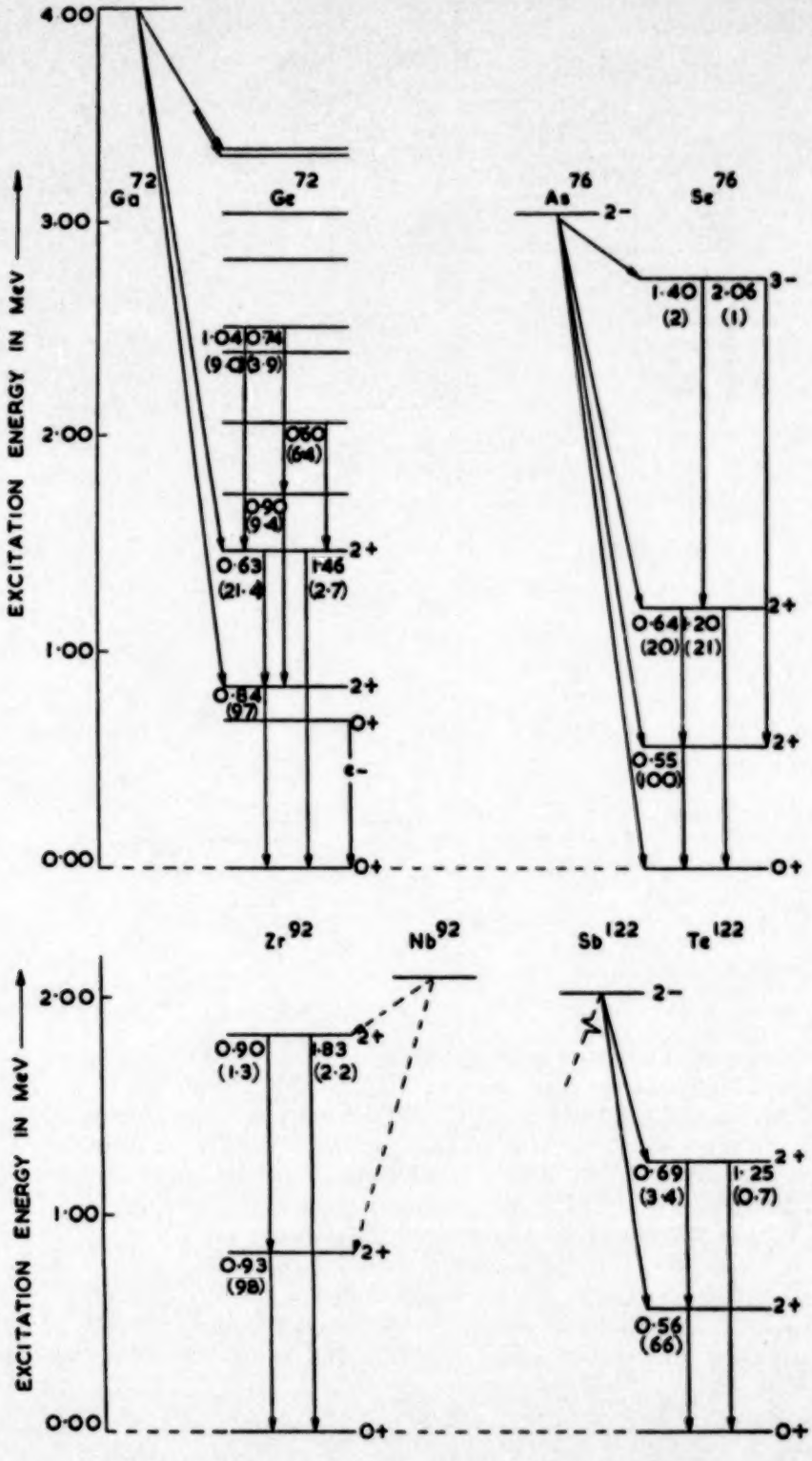

Fig. 4. Decay schemes of Ga^{72}, As^{76}, Nb^{92} and Sb^{122}.

noted in the account of the corresponding experiment. The angular resolution correction was determined from an angular correlation measurement on the 0.69, 0.56 MeV cascade in Te^{122}. The available experimental results on 2, 2, 0 cascades, including those described below, are summarized on a parametric plot [10]) in fig. 3, and the values of δ^2 obtained are collected in table 1.

As^{76}

The decay scheme for this nucleus is given in Nuclear Level Schemes, $A = 40-92$, (edited by K. Way *et al.* [11])) and is shown in fig. 4. Coulomb excitation measurements [3]) indicate a lifetime for the 0.55 MeV level in Se^{76} of about 2×10^{-11} sec, and an upper limit comparable with this was obtained from a delayed coincidence measurement [12]) using the centroid shift technique. Thus reorientation effects in correlations for which this level is the intermediate state will be negligible. Sources of As^{76} were prepared by irradiating 'Specpure' As_2O_3 powder, supplied by Johnson and Matthey, in the reactor BEPO.

Since the beta transition from the 2− ground state of As^{76} to the 2.59 MeV level in Se^{76} is allowed, this level should have odd parity. The angular correlation of the 1.40, 1.20 MeV cascade was measured (see fig. 5), and after correction for the detector angular resolution was found to be

$$W(\theta) = 1-(0.091\pm0.024)\,P_2\,(\cos\theta)+(0.057\pm0.034)\,P_4\,(\cos\theta).$$

This result suggests that the 2.59 MeV state has spin 2, and that the 1.40 MeV transition is a mixture of 85 % E1 and 15 % M2. However, the result is not seriously inconsistent with a spin 3 for the upper level, in which case the upper transition would be almost pure electric dipole, which is much more likely than the E1, M2 mixture required by the first choice. States of spin 3− occurring at excitation energies of a few MeV have also been identified in Ca^{40}, Sr^{88} and Te^{124}, and are the lowest observed odd parity levels in these nuclei.

The angular correlation of the 0.64, 0.55 MeV cascade, after correction for contributions to the observed result from other cascades and for the detector angular resolution, was found to be

$$W(\theta) = 1-(0.209\pm0.031)P_2\,(\cos\theta)+(0.246\pm0.045)P_4\,(\cos\theta).$$

This result is consistent with that of Lindqvist and Marklund [8]), but not with the early result of Kraushaar and Goldhaber [13]), obtained with much less effective energy selection, so that coincidences involving the 1.20 MeV transition were not excluded.

Ga^{72}

The decay scheme of this nucleus, shown in part in fig. 4, is extremely complex [14]). Coulomb excitation measurements give a value of 6×10^{-12} sec

for the lifetime of the 0.81 MeV 2+ excited state in Ge^{72}, and a resonance fluorescence measurement [15]) the value 4.6×10^{-12} sec, so that reorientation effects involving this state will be negligible. Sources were prepared

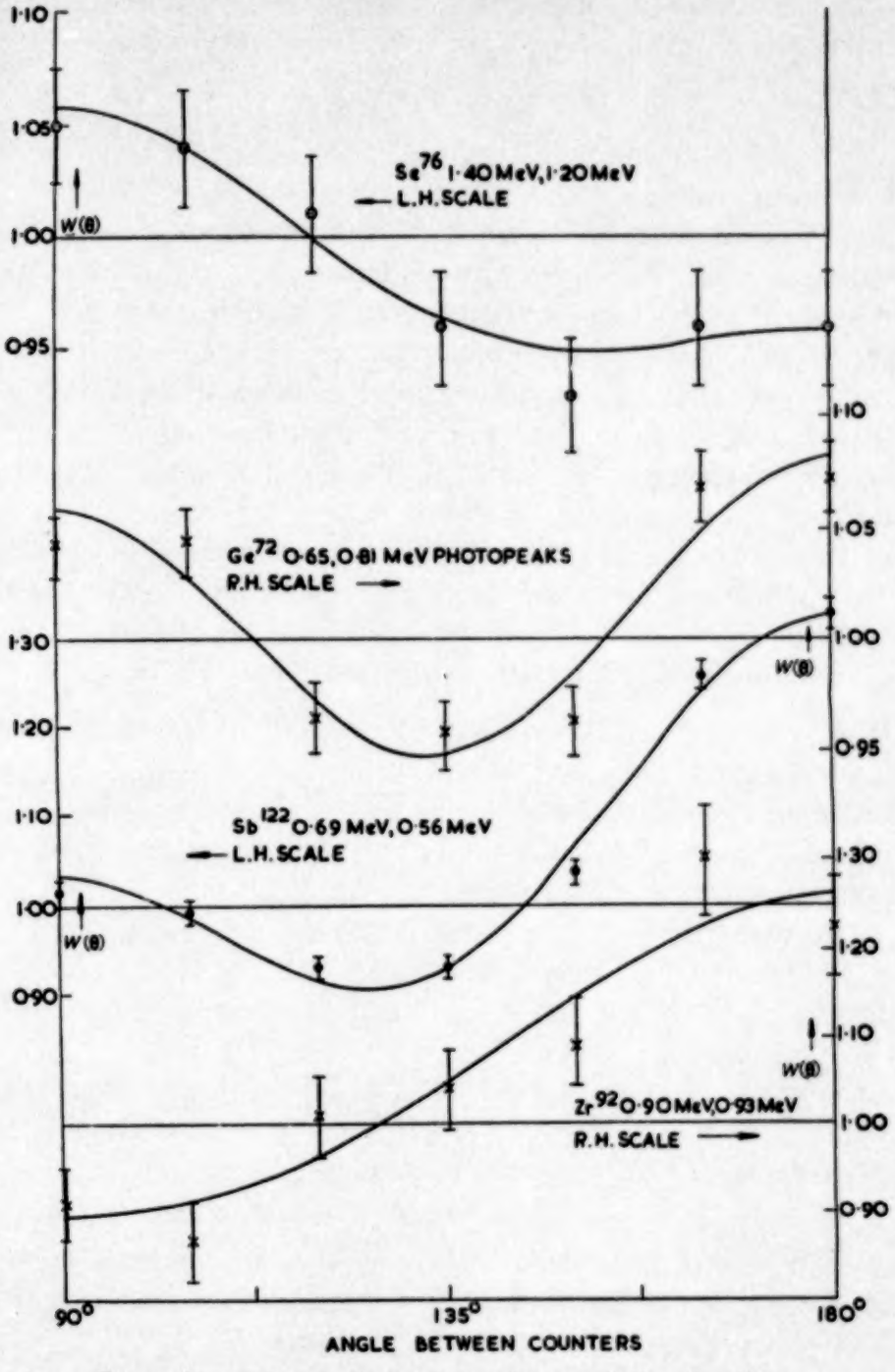

Fig. 5. Examples of observed angular correlation functions.

by irradiating 'specpure' Ga_2O_3 powder, supplied by Johnson and Matthey, in the reactor BEPO. To measure the 0.65, 0.81 MeV angular correlation it was assumed that the Compton background from the higher energy lines

was constant over the 0.65 and 0.81 MeV photopeaks and in the trough between them. Four correlation measurements were made, selecting in turn in the two slow channels the 0.65 and 0.81 MeV photopeaks (see fig. 5), the 0.65 MeV photopeak and the 0.81 MeV trough, the 0.81 MeV photopeak and the 0.81 MeV trough, and finally the 0.81 MeV trough in both. By subtracting suitably normalized amounts of the three latter correlations from the observed 0.65, 0.81 MeV correlation the true correlation was determined, though with large errors because of the repeated subtractions. Corrected for the detector angular resolution it is

$$W(\theta) = 1-(0.096\pm0.13)\, P_2\,(\cos\theta)+(0.49\pm0.21)\, P_4\,(\cos\theta).$$

Thus the 1.4 MeV level has almost certainly spin 2, and the mixing ratio for the 0.63 MeV transition is probably large.

Nb^{92}

The decay scheme given for this nucleus by Hayward *et al.* [16]) and shown in fig. 4 has been confirmed. The trend of the lifetime measurements shown in fig. 2 is such that reorientation effects involving the 0.93 MeV first excited state in Zr^{92} should be negligible. A source of Nb^{92} was produced by a

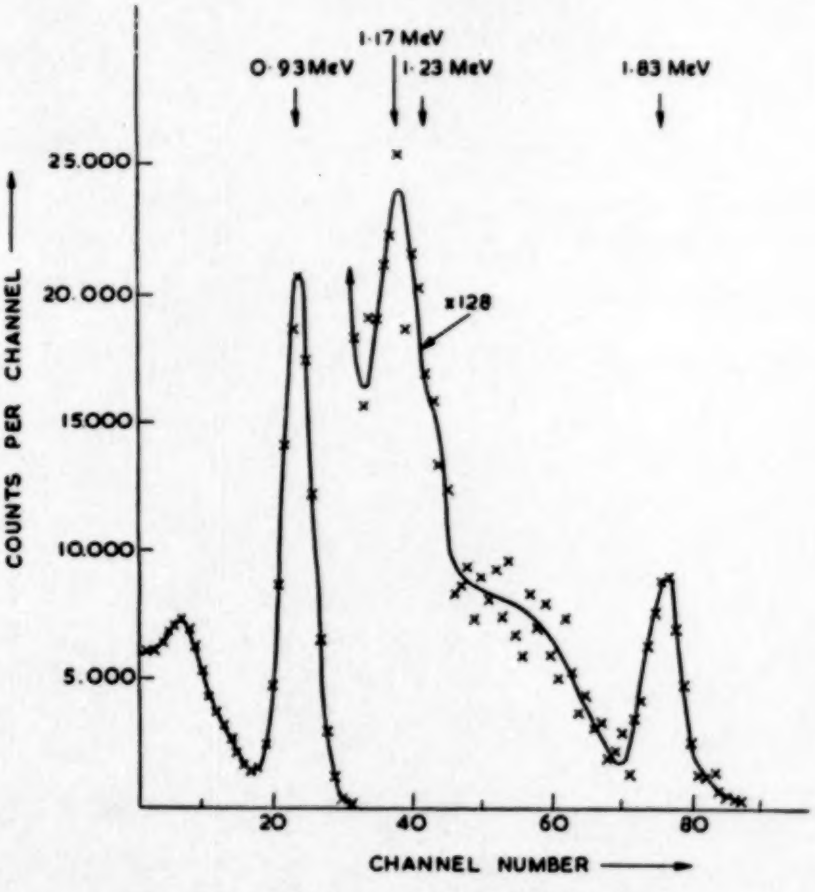

Fig. 6. Scintillation spectrum of Nb^{92} source.

reactor induced (n, p) reaction on molybdenum, followed by chemical purification to remove molybdenum and cobalt activities. Fig. 6 shows the scintillation spectrum of the purified source material, which was prepared by Dr. C. E. Mellish. Impurity peaks amounting to a few per cent of the main Nb^{92} activity are visible at energies of about 1.17 and 1.23 MeV.

The 0.90, 0.93 MeV angular correlation (see fig. 5), after correction for cosmic ray coincidences and for the detector angular resolution, was found to be

$$W(\theta) = 1+(0.236\pm0.049)\ P_2(\cos\theta)+(0.036\pm0.068)\ P_4(\cos\theta).$$

This is not in good agreement with the measured value 1.21 for $W(180°)/W(90°)$ attributed to Hayward *et al.* in ref. [11]).

Sb^{122}

The lifetime of the 0.56 MeV level in Te^{122} has been measured by Temmer and Heydenburg [3]), using Coulomb excitation, and was found to be

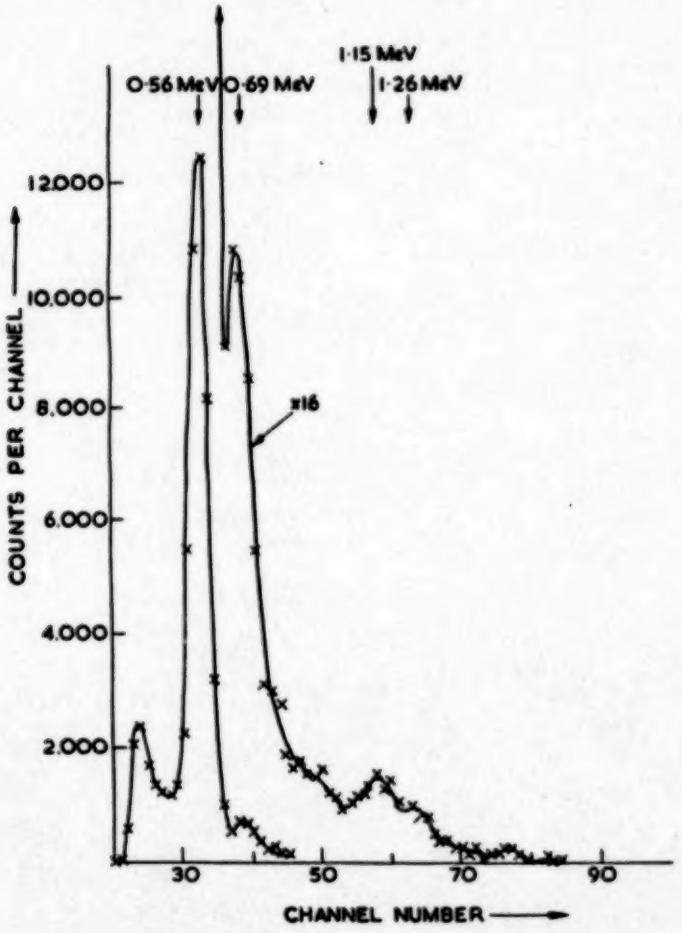

Fig. 7. Scintillation spectrum of Sb^{122} source.

1.4×10^{-11} sec. This is consistent with the limit $\lesssim 10^{-11}$ sec obtained by Sunyar [19]) using a centroid shift technique. These values are such that reorientation effects involving the first excited state will be negligible. A source of Sb^{122} was prepared by irradiating enriched Sb^{121} (95 % Sb^{121}) in the reactor BEPO. The scintillation spectrum was reasonably free from impurity peaks (fig. 7), and in particular the Sb^{124} activity was too weak to disturb the correlation measurements. The observed angular correlation of the 0.69, 0.56 MeV cascade was (see fig. 5)

$$W(\theta) = 1+(0.102\pm0.010)\,P_2(\cos\theta)+(0.233+0.011)\,P_4(\cos\theta).$$

The experimental conditions for this measurement were good, and it was used to determine the angular resolution corrections. If each detector has uniform sensitivity over a cone of semi-angle ϕ radians, the observed values of the coefficients A'_2, A'_4 are related to the values that would be obtained with point detectors by the equations

$$A'_2 = A_2\{1-(3/2)\phi^2\}, \quad A'_4 = A_4\{1-5\phi^2\}.$$

The value of ϕ required to bring the experimental result into agreement with the theoretical predictions for A_2 and A_4 was found to be 12° 20′. Because of inscattering from the lead shields around the detectors this is rather greater than the angle of 10° determined from the physical dimensions of the detectors. The correlation corrected for angular resolution then becomes

$$W(\theta) = 1+(0.110\pm0.11)\,P_2(\cos\theta)+(0.308\pm0.015)\,P_4(\cos\theta),$$

in good agreement with the results of Glaubman [18]) and of Lindqvist and Marklund [8]).

The linear polarization of the 0.69 MeV radiation, when emitted at an angle of 105° to the direction of emission of the following 0.56 MeV radiation, has also been measured [10]). This measurement, taken together with the observed anisotropy of the directional correlation, confirms the value of δ obtained from the parametric plot, shows that it is the 0.69 MeV transition which is mixed, and indicates that this transition involves no parity change.

La^{140}

The angular correlation of the 0.92, 1.60 MeV cascade following the beta decay of this nucleus has been reported previously [19]). A comparison was made, using the centroid shift technique, of coincidences from the (0.82+0.92), 1.60 MeV cascades in Ce^{140} with those from the 1.32, 0.99 MeV cascade in Ti^{48}. Using Heydenburg and Temmer's value [3]) for the lifetime of the 0.99 MeV level in Ti^{48}, a value of $(2.5\pm2)\times10^{-11}$ sec was obtained for the lifetime of the 1.60 MeV first excited state in Ce^{140}. Thus reorientation effects will be negligible in this case also.

3. Interpretation of Results and Conclusions

Three models have been proposed to account for the properties of nuclei in the intermediate region.

(1) The spherical equilibrium model of Goldhaber and Weneser [1]) assumes that the systematic excited levels are vibrational in character, and arise from coupling of the sphercial core to the outer nucleons. As this coupling increases the excitation energy of the first excited state, E_1, diminishes, while the ratio E_2/E_1 rises from an initial value of 2 to values greater than 2.2. The second excited state group is a 3-fold multiplet with spins 0, 2, and 4; the third a 5-fold multiplet with spins 0, 2, 3, 4 and 6. The E2 transition probability from the 2+ second excited state to the first excited state, $T(\mathrm{E2}, 21)$, is much greater than the single particle prediction (see Moskowski's calculations [20])). (In the symbol $T(\mathrm{E2}, 21)$ the last two figures indicate the groups to which the initial and final states belong.) In comparison with $T(\mathrm{E2}, 21)$ the crossover transition probability $T(\mathrm{E2}, 20)$ is appreciably inhibited, and $T(\mathrm{M1}, 21)$ vanishes in the limit of zero coupling.

(2) The model of Wilets and Jean [2]) assumes that the nucleus has a finite equilibrium deformation, but is shape-unstable. That is, the energy associated with any ellipsoidal deformation depends only on the change in the area of the nuclear surface to which it gives rise. The increase in surface area is related to the parameter β, while the shape is described by the parameter γ. On this model E_1 diminishes as γ increases, while E_2/E_1 increases from an initial value of 2 to 2.5. The 0+ state is initially much higher than the other members of the second excited state group, but joins them when E_1/E_{vib} falls to about 0.6. Both $T(\mathrm{E2}, 20)$ and $T(\mathrm{M1}, 21)$ vanish if the nucleus is strictly shape-unstable, but if some γ dependence of the deformation energy is assumed, $T(\mathrm{E2}, 20)$ takes finite values, though $T(\mathrm{M1}, 21)$ remains zero.

(3) The model proposed by Marty [21]) assumes that the equilibrium shape of the nucleus is a non-degenerate ellipsoid, and leads to a second excited state which may have either spin 2 or spin 4, according to the equilibrium value of γ, with a state of the other spin immediately above it.

The experimental data are collected in table 1. The columns list in order the nucleus in which the transitions occur, the ratio E_1/E_{vib}, the ratio E_2/E_1, the intensity ratio δ^2, the relative cross-over intensity, and the ratios

$$\left(\frac{T(\mathrm{E2}, 21)}{T(\mathrm{E2}, 20)}\right)_{\mathrm{exp.}} \Big/ \left(\frac{T(\mathrm{E2}, 21)}{T(\mathrm{E2}, 20)}\right)_{\mathrm{S.P.}}, \quad \left(\frac{T(\mathrm{E2}, 21)}{T(\mathrm{M1}, 21)}\right)_{\mathrm{exp.}} \Big/ \left(\frac{T(\mathrm{E2}, 21)}{T(\mathrm{M1}, 21)}\right)_{\mathrm{S.P.}},$$

where the suffixes denote experimental and single particle theoretical values of the quantities in brackets. For the magic nuclei, in contrast with the assumption used by Alder *et al.* [6]), in analysing similar data, δ may become quite small. The results of Scharenberg *et al.*[22]) on the 0.80, 1.27 MeV

cascade on Sn^{116} appear to contradict this conclusion. However, measurements on In^{116} present considerable experimental difficulties, and the uncertainty in the results for this cascade is such that they are quite compatible with a small value of δ. It is still reasonable to assume that δ is large for nuclei well away from the magic numbers, and figures derived on this assumption are shown for Kr^{82}, Te^{126}, Xe^{126} and Xe^{128}. The table shows that for typical intermediate region nuclei $\left(\frac{T(E2,21)}{T(E2,20)}\right)_{exp.} / \left(\frac{T(E2,21)}{T(E2,20)}\right)_{S.P.}$ is $\approx 10^2$, falling to values ≈ 1 for magic and near magic nuclei. The low value for Se^{76} appears to be due to an unusually large crossover intensity.

TABLE 1

Normalized transition probabilities from 2+ second excited states in even nuclei

Nucleus	$E_1/E_{vib.}$	E_2/E_1	δ^2	$\frac{T(E2,20)}{T(M1+E2,21)}$	$F\frac{(E2,21)}{(E2,20)}$	$F\frac{(E2,21)}{(M1,21)}$	References	
							Col. 4	Col. 5
S^{34}	0.44	1.54	$0.004 \rightarrow 0.03$	0.47 ± 0.1	$1.6 \rightarrow 12$	$5 \rightarrow 40$	a	a
Fe^{58}	0.25	2.00	$3.8 \rightarrow 6.6$	0.3 ± 0.1	$(1.2 \pm 0.4) \times 10^2$	$(5 \rightarrow 8) \times 10^3$	b	b
Ge^{72}	0.29	1.75	$\gtrsim 19$	0.13 ± 0.04	$(5 \pm 1.5) \times 10^3$	$\gtrsim 3 \times 10^4$	fig. 3	c
Se^{76}	0.21	2.15	$16 \rightarrow 100$	1	2.3×10^1	$(2.5 \rightarrow 14) \times 10^4$	fig. 3	d
Kr^{82}	0.29	1.90		0.57	$\approx 7.3 \times 10^1$			d
Zr^{92}	0.40	1.97	< 0.008	1.7	$\lesssim 1.6 \times 10^{-1}$	$\lesssim 5$	fig. 3	d
Te^{122}	0.29	2.24	$10 \rightarrow 21$	0.19 ± 0.04	$(1.0 \pm 0.2) \times 10^2$	$(7 \rightarrow 14) \times 10^3$	fig. 3	e
Te^{126}	0.34	2.18		0.09 ± 0.02	$\approx 2.4 \times 10^2$			f
Xe^{126}	0.20	2.25		0.19 ± 0.04	$\approx 1 \times 10^2$			f
Xe^{128}	0.23	2.12		0.18	$\approx 1.3 \times 10^2$			g
Ce^{140}	0.94	1.60	$\lesssim 0.015$	0.3 ± 0.1	$\lesssim 6$	$\lesssim 5$	h	h
Pt^{192}	0.24	1.93	$\gtrsim 10$	0.23	1.7×10^2	$\gtrsim 1.5 \times 10^4$	i	j
Pt^{194}	0.25	1.91	$\gtrsim 3$	0.31	1.3×10^2	$\gtrsim 5 \times 10^3$	k	l
Pt^{196}	0.27	1.95	$\gtrsim 25 \pm 6$	$\lesssim 0.03$	$\gtrsim 10^3$	$\gtrsim (4 \pm 1) \times 10^4$	fig. 3	m
Hg^{198}	0.32	2.65	$0.73 \rightarrow 1.5$	0.23 ± 0.07	$(4.7 \pm 1.5) \times 10^1$	$(3 \rightarrow 6) \times 10^2$	fig. 3	n

$$F\frac{(E2,21)}{(E2,20)} = \left(\frac{T(E2,21)}{T(E2,20)}\right)_{exp.} / \left(\frac{T(E2,21)}{T(E2,20)}\right)_{S.P.}$$

$$F\frac{(E2,21)}{(M1,21)} = \left(\frac{T(E2,21)}{T(M1,21)}\right)_{exp.} / \left(\frac{T(E2,21)}{T(M1,21)}\right)_{S.P.}$$

a. H. E. Handler and J. R. Richardson, Phys. Rev. **102** (1956) 833
b. H. Frauenfelder, N. Levine, A. Rossi and S. Singer, Phys. Rev. **103** (1956) 352
c. J. J. Kraushaar, E. Brun and W. E. Meyerhof, Phys. Rev. **101** (1956) 139
d. see ref. [11])
e. M. J. Glaubman, Phys. Rev. **98** (1955) 645
f. M. L. Perlman and J. P. Welker, Phys. Rev. **95** (1954) 133
g. N. Benczer, B. Farrelly, L. Koerts and C. S. Wu, Bull. Amer. Phys. Soc. **30** (1955) 9
h. see ref. [19])
i. see ref. [22])
j. see ref. [22])
k. V. R. Potnis, V. S. Dubey and C. E. Mandeville, Phys. Rev. **102** (1956) 459
l. M. T. Thieme and E. Bleuler, Phys. Rev. **102** (1956) 195
m. R. M. Steffen, Phys. Rev. **89** (1953) 665
n. P. E. Cavanagh, J. F. Turner, D. V. Brooker and H. J. Dunster, Proc. Phys. Soc. A **64** (1951) 13

The behaviour of $\left(\frac{T(\mathrm{E2},\ 21)}{T(\mathrm{M1},\ 21)}\right)_{\mathrm{exp.}} / \left(\frac{T(\mathrm{E2},\ 21)}{T(\mathrm{M1},\ 21)}\right)_{\mathrm{S.P.}}$ is even more striking, since for typical intermediate region nuclei, as Lindqvist and Marklund have pointed out, it takes values ranging from 10^3 to greater than 10^5, while for the magic nuclei Zr^{92} and Ce^{140} it is only ≈ 1. The relative behaviour of these ratios reproduces the predictions of both the spherical equilibrium and shape unstable models. However, the rather small values of $\left(\frac{T(\mathrm{E2},\ 21)}{T(\mathrm{E2},\ 20)}\right)_{\mathrm{exp.}} / \left(\frac{T(\mathrm{E2},\ 21)}{T(\mathrm{E2},\ 20)}\right)_{\mathrm{S.P.}}$ are more in keeping with the former, since to be explained on the latter model they would require a considerable departure from the assumption of a γ independent potential.

Evidence for the existence of the 0+ member of the second excited state group predicted by these two models is available for Pd^{106}, Cd^{114}, and Po^{214}. In Pd^{106} the 1.137 MeV 0+ state is well established. Stelson and McGowan[23]) have shown that there is a 2+ state at 1.12 MeV. The 0.624 and 1.131 MeV gamma rays observed by Alburger and Toppel [24]) in the decay of Ag^{106} are probably the transitions from this state to the first excited state and the ground state respectively. The residual departures from the theoretical 0, 2, 0 correlation of the 0.624, 0.513 MeV cascade in Pd^{106}, excited by the decay of Rh^{106}, may arise from a weak branch to this 1.13 MeV 2+ state. Motz [25]) has found states at 1.212, 1.286, 1.308 and 1.368 MeV in Cd^{114}, with spins of 2+ (or 1+), 4+, 0+ and 2+ (or 1+) respectively. The work of Stelson and McGowan [23]) suggests that the 1.212 MeV 2+ state rather than the 1.368 MeV state belongs to the triplet group. In Po^{214} the 1.414 MeV 0+ state has long been known, and recent work by Nielsen [26]) has established the existence of a level at 1.376 MeV with spin 2+ and branching ratios to the ground state and first excited state consistent with those in other nuclei in the intermediate region.

TABLE 2

Normalized transition probabilities from 3+ third excited states in even nuclei

Nucleus	E (keV)	Group Sequence	Spin Sequence	δ^2	$\frac{T(\mathrm{E2},\ 31)}{T(\mathrm{M1+E2},\ 32)}$	$F\frac{(\mathrm{E2},\ 32)}{(\mathrm{E2},\ 31)}$	$F\frac{(\mathrm{E2},\ 32)}{(\mathrm{M1},\ 32)}$	Refs. Col. 5	Refs. Col. 6
Kr^{82}	610	3→2	3→2	3.7→ 6.6	0.72 ± 0.17	$(6.3\pm1.5)\times10^2$	$(5\rightarrow10)\times10^3$	a	a
	1305	3→1	3→2	12 →24				a	
Pt^{192}	136.3	3→2	3→4	4.0 ± 0.4	7.7×10^1	2.2×10^1	$(4\pm0.4)\times10^4$	b	c
	308.5	3→2	3→2	20 →100	0.4	7.3×10^1	$(4\rightarrow20)\times10^4$	b	c
	604.4	3→1	3→2	6 → 10				b	

a. see ref. [27]); b. see ref. [28]); c. see ref. [29]).

The existence of states having the properties to be expected in the 3+ member of the third excited state group appears to have been established in Kr^{82} and Pt^{192}. The 3+ 2.071 MeV state in Kr^{82} was identified by

Waddell and Jensen [27]) from angular correlation measurements. It decays by dominantly E2 transitions to 2+ states at 1.469 and 0.766 MeV. The 3+ 1.357 MeV state in Pt^{192} was identified by Kelman *et al.* [28]) from measurements of the $L_1 : L_2 : L_3$ conversion ratios for the 604.5 keV transition. The relative transition probabilities from the 3+ members of the third excited state groups in these nuclei to the 2+ members of the second excited state groups and the 2+ first excited states are given in table 2, which also makes use of gamma ray intensities determined by Baggerly *et al.* [29]).

Some information on the absolute transition probabilities from 2+ second excited states is now available from the Coulomb excitation measurements of Stelson and McGowan [23]). These workers measured $\frac{T(\mathrm{E2},\ 21)}{T(\mathrm{E2},\ 20)}$ for Pt^{194}, and found a value [7]) too small to be reconciled with either the spherical equilibrium or shape unstable models. A satisfactory model of nuclei in the intermediate region must also account for the systematic variation of the favoured factor F with E_1 shown in fig. 2, where one might have anticipated that $E_1/E_{\mathrm{vib.}}$ would be a more appropriate independent variable. If $T(\mathrm{E2}, 21)$ and $T(\mathrm{E2}, 20)$ are found to show the $(E_1)^3$ energy dependence which characterizes $T(\mathrm{E2}, 10)$ the remaining enhancement of $T(\mathrm{E2}, 21)$ over $T(\mathrm{E2}, 20)$, remembering that the statistical weights of the first excited state and the ground state are 5 and 1 respectively, is reduced to about 5.

It is a pleasure to acknowledge discussions of the various nuclear models with Dr. B. Flowers, Dr. A. M. Lane and Dr. T. H. R. Skyrme, and of the experiments generally with Dr. P. E. Cavanagh. I am grateful to Dr. M. L. Smith of the Electromagnetic Separator Group for supplying the enriched Sb^{121}.

References

1) G. Scharff-Goldhaber and J. Weneser, Phys. Rev. **98** (1955) 212
2) L. Wilets and M. Jean, Phys. Rev. **102** (1956) 788
3) G. M. Temmer and N. P. Heydenburg, Phys. Rev. **104** (1956) 967
4) P. H. Stelson and F. K. McGowan, Phys. Rev. **99** (1955) 112
5) H. Mark, C. McClelland and C. Goodman, Phys. Rev. **98** (1955) 1245
6) K. Alder, A. Bohr, T. Huus, B. Mottelson and A. Winther, Revs. Mod. Phys. **28** (1956) 432
7) F. K. McGowan and P. H. Stelson, Phys. Rev. **106** (1957) 522
8) T. Lindqvist and I. Marklund, Nuclear Physics **4** (1957) 189
9) C. F. Coleman, Phys. Rev. **103** (1956) 647
10) C. F. Coleman, Nuclear Physics **5** (1958) 495
11) Nuclear Level Schemes, $A = 40 \rightarrow 92$, Publication TID 5300 of USAEC (1955)
12) C. F. Coleman, Phil. Mag. **46** (1955) 1135
13) J. J. Kraushaar and M. Goldhaber, Phys. Rev. **89** (1953) 1081
14) J. J. Kraushaar, E. Brun and W. E. Meyerhof, Phys. Rev. **101** (1956) 139
15) F. R. Metzger, Phys. Rev. **101** (1956) 286
16) R. W. Hayward, D. D. Hoppes and H. Ernst, Phys. Rev. **98** (1955) 231A
17) A. W. Sunyar, Bull. Amer. Phys. Soc. **2** (1957) 37

18) M. J. Glaubman, Phys. Rev. **98** (1955) 645
19) C. F. Coleman, Phil. Mag. **46** (1955) 1132
20) S. A. Moskowski, Beta and Gamma Spectroscopy, Ed. K. Siegbahn (N. Holland Publ. Co., Amsterdam, 1955) Ch. XII, p. 373
21) C. Marty, Nuclear Physics **3** (1957) 193
22) R. P. Scharenberg, M. G. Stewart and M. L. Wiedenbeck, Phys. Rev. **101** (1956) 193
23) P. H. Stelson and F. K. McGowan, Bull. Amer. Phys. Soc. **2** (1957) 267
24) D. E. Alburger and B. T. Toppel, Phys. Rev. **100** (1955) 1357
25) H. T. Motz, Phys. Rev. **104** (1956) 1353
26) O. B. Nielsen, reported at Edinburgh Conf. of the Physical Soc. (Dec. 1956)
27) R. C. Waddell and E. N. Jensen, Phys. Rev. **102** (1956) 816
28) V. M. Kelman, R. Y. Metskhvarishvili, V. A. Romanov and V. V. Tuchkevich, Nuclear Physics **4** (1957) 240
29) L. L. Baggerly, P. Marmier, F. Boehm and J. W. M. DuMond, Phys. Rev. **100** (1955) 1364

1.D.2 : 2.L

Nuclear Physics 7 (1958) 503—515; © *North-Holland Publishing Co., Amsterdam*
Not to be reproduced by photoprint or microfilm without written permission from the publisher

INELASTIC SCATTERING OF NUCLEONS AND DEUTERONS FROM SPHEROIDAL NUCLEI†

J. SAWICKI

Palmer Physical Laboratory, Princeton University, Princeton, New Jersey †

Received 21 March 1958

Abstract: A direct interaction theory of the inelastic scattering of nucleons and deuterons from strongly deformed nuclei of $A \approx 25$ is proposed. The nucleus is described by the strong coupling approximation of the unified nuclear model. Two alternative forms of the transition operators are discussed: the projectile-surface interaction and the interparticle forces (projectile-target nucleons). Both the rotational and the individual particle excitations are discussed. As an example of the recent data on the Mg^{24}(d, d′) and Mg^{24}(p, p′) reactions are considered. Angular correlations with γ's are discussed. The case of the 2+ (rotational level) → 0+ E2-radiation is considered in detail.

1. Introduction

The theory of the inelastic scattering of medium energy nucleons and deuterons from nuclei has been extensively developed in the past few years. It has been pointed out that at sufficiently high energies the direct interaction processes play a dominant role, and in the case of deuterons the compound nucleus formation contribution is in general negligible. There are two main types of direct interaction transition operators: interparticle forces for one-particle and collective transitions, and "collective" (mainly projectile-surface) interactions important in cases when vibrational or rotational levels are being excited. The latter type of projectile-nucleus interaction has been investigated in a number of papers (see e.g. refs. [1–6]) using the unified nuclear model with weak or strong coupling. In a recent paper [7]) (further referred to as I) the strong coupling theory was applied also to the inelastic scattering of deuterons from strongly deformed spheroidal nuclei in the region $A \approx 25$. General expressions for the differential cross sections were obtained involving corrections up to the fourth power of the deformation parameter β; these expressions correspond to the excitation of the first few members of the rotational bands based on the ground states. A rather good agreement with the data was obtained in the case of the reaction Mg^{24}(d, d′)Mg^{24*} (1.37 MeV, 2+ level).

The aim of the present paper is to present a more extensive discussion of

† This work was supported by the U.S. Atomic Energy Commission and the Higgins Scientific Trust Fund.

the strong coupling nuclear model characteristics of the angular distributions and cross sections for the inelastic scattering of nucleons and deuterons. General expressions are discussed for the cases of rotational and individual particle excitations induced by collective projectile-deformed core interactions and by interparticle forces between the incident particle and the particles of the target.

2. Rotational Excitations

The method of I was essentially a plane wave Born approximation method with (1) pure strong coupling unified model wave functions for the initial and final nuclei, (2) neglect of all possible exchange amplitudes, (3) the transition operator being V_n+V_p, the effective spheroidally symmetrical interaction potential of the deuteron with the target. The potential function was

$$V = V(\mathscr{r}(r, \omega, \theta_i))$$

where

$$\mathscr{r} = r(1+\zeta), \qquad \zeta = \beta Y_{20}(\omega') = \beta \sum D^2_{\nu 0}(\theta_i) Y_{2\nu}(\omega);$$

here (r, ω) are the (fixed frame) coordinates of the colliding particle in question, θ_i denotes the rotation Eulerian angles, ω' refers to the body frame and D denotes the usual rotation matrix. One can expand V in powers of β or $r\zeta$ and find expressions corresponding to rotational transitions to arbitrarily high lying members of a given band based on the ground state of the target nucleus (the selection rule $K_f = K_i$ ($\Delta K = 0$) being due to the absence of individual particle excitation, i.e. $\Omega_f = \Omega_i$ ($\Delta\Omega = 0$) in Bohr and Mottelson's notation). If one adopts a square well form for V, of depth $\bar{V}_0$ and radius r_0, and keeps terms up to $\propto \beta^2$ in its expansion, one finally gets the form of the differential cross section given in I:

$$\begin{aligned}\sigma(\theta) = \frac{k_f}{k_i}\frac{m^{*2}}{(2\pi\hbar^2)^2}\bar{V}_0{}^2 r_0{}^6 \beta^2 \sum_{l=0,2,4} (I_i l; K_i 0|I_f K_f)^2 \{4\pi |j_2(kr_0)|^2 \delta_{l2} \\ + \tfrac{4}{7}\sqrt{20\pi}\beta[j_2(kr_0)(j_2(kr_0)+\tfrac{1}{2}kr_0 j'_2(kr_0))]\delta_{l2} \\ + 25\beta^2(2l+1)^{-1}(22; 00|l0)^4[j_l(kr_0)+\tfrac{1}{2}kr_0 j'_l(kr_0)]^2\} X + O(\beta^5)\end{aligned} \tag{1}$$

where $\theta = \sphericalangle(\mathbf{k}_i, \mathbf{k}_f)$; m^* is the reduced mass of the particle in question; I_i and I_f are the initial and final nuclear spins; $j(x)$ is the spherical Bessel function; $\mathbf{k}_i, \mathbf{k}_f$ are the initial and final momenta of the free particle, $k = |\mathbf{k}_i - \mathbf{k}_f|$ is the momentum transfer; the factor X is unity for the nucleon case and $X = \eta g(k)^2$ for the deuteron case; $g(k) = \int d(\varrho) e^{-i\mathbf{k}\cdot\rho/2}|\chi(\rho)|^2$ where $\chi(\rho)$ is the internal deuteron S-state wave function; η was assumed to be unity in I (only V_n operating, the proton being assumed to be sufficiently strongly repulsed by the Coulomb field and kept away from the target). Actually $\sigma(\theta)$ is proportional to $|\langle V_n\rangle + \langle V_p\rangle|^2$; if one assumed no Coulomb

repulsion present and an equal contribution from V_p, η would be $2^2 = 4$; the exact expression is much more complicated; however, one could expect an "equivalent" η to lie between 1 and 4. The use of plane waves rather than the true distorted Coulomb waves is obviously rather crude.

In the case of an even target with $I_1 = 0+$ and $I_f = 2+$, eq. (1) reduces to

$$\sigma(\theta)|_{I_f=2+} = \frac{k_f}{k_1}\frac{m^{*2}}{(2\pi\hbar^2)^2}\bar{V}_0^2 r_0^6 \beta^2\{4\pi|j_2(kr_0)|^2 + \tfrac{4}{7}\sqrt{20\pi}\beta[j_2(kr_0)(j_2(kr_0)+\tfrac{1}{2}kr_0 j'_2(kr_0))] + \tfrac{20}{49}\beta^2[j_2(kr_0)+\tfrac{1}{2}kr_0 j'_2(kr_0)]^2\}X + O(\beta^5). \quad (2)$$

If the second rotational member $I_f = 4+$ of the same band $K = 0$ is excited, we have

$$\sigma(\theta)|_{I_f=4+} = \frac{k'_f}{k_1}\frac{m^{*2}}{(2\pi\hbar^2)^2}\bar{V}_0^2 r_0^6 \beta^4 \tfrac{36}{49}[j_4(k'r_0)+\tfrac{1}{2}k'r_0 j'_4(k'r_0)]^2 X' + O(\beta^5); \quad (3)$$

the k''s refer to a different Q-value in this case. Eq. (2) was employed in I to analyze the data on the $Mg^{24}(d, d')Mg^{24*}$ ($Q = -1.37$ MeV) reaction: we took $\beta = 0.42$, $r_0 = 6.2\times10^{-13}$ cm after Haffner [8]), and a Hulthén wave function with the relation $\Gamma = 7\alpha$ between the parameters. The resulting angular distribution for 15.1 MeV incident deuterons is in a nice agreement with Haffner's data except only for one experimental point (at $\theta \approx 20°$), which seems to indicate a forward peaking. However, the recent data by Hinds *et al.* [9]) for 8.9 MeV deuterons have no indication of such a forward peaking in this reaction. The total cross section was found to be 46.5 mb with $\bar{V}_0 = 40$ MeV and $\eta = 1$, as compared to the experimental number 88 mb (with an uncertainty factor of 2). This nice agreement seems to be accidental in view of so many rather arbitrary assumptions involved; however, it is an indication of the right order of magnitude predicted by this type of theory.

The angular distribution computed for $E_d = 8.9$ MeV using the same parameters gives also a nice fit with the data of ref. [9]) (r_0 should be slightly increased to obtain a still better fit). The theoretical curve given by eq. (2) is even better than that of fig. 2 of ref. [9]) corresponding to $|j_2(kr_0)|^2$. Our contributions $\propto \beta$ and β^2 in the curly bracket term of eq. (2) fill in the spurious zeros and increase $\sigma(\theta)$ at backward angles.

The computed total cross section is about 38.2 mb, which is again in agreement with the data of Hinds *et al.* [9]). These authors give also the data for the second excited 4+ state and the third excited (individual particle) 2+ state. However, the resolution of these two states seems to have been poor, since they are very close together (4.12 and 4.23 MeV).

The curve resulting from eq. (3) being essentially a plot of $[k'r_0 \cdot j_3(k'r_0) - 3j_4(k'r_0)]^2$ is in disagreement with the data of fig. 2 of ref. [9]),

in particular at small angles (the curve has a flat peak at about 60°). It is only slightly better than the $|j_4(k'r_0)|^2$ curve plotted in fig. 2 of ref. [9]). The total cross section is only about 1 % of that for the 2+ first rotational state. This is again in disagreement with the data. If it were not possible to blame these discrepancies on poor experimental resolution in this case, the most natural attempt to explain these data would be to employ a distorted wave calculation. It is well known (see, e.g., refs. [3, 10])) that distortions of the free particle wave functions increase the differential cross sections at small angles and can modify the angular distributions and cross sections very notably.

It is also far from obvious that the contributions $\propto \beta$ (leading to the 2+ excitation) and those $\propto \beta^2$ (leading to the 4+ excitation) coming from the second Born approximation are small and negligible.

It is not known either whether the contribution of the intrinsic 2^4-pole deformation to the 4+ excitation is negligible. This is, however, very likely.

The band of $K = 0$ in Mg^{24} seems to be rather clearly pure, i.e., with no admixtures of $K = 1$ or 2 due to the Coriolis forces (rotation-particle coupling) or other couplings, thus violating the strong coupling scheme.

In the distorted wave method, in which the distortion potential is taken to be the spherical part of the complete spheroidal effective potential of interaction between the projectile and the target nucleus (usually assumed to be an optical model well appropriate to the elastic scattering case), the perturbation treatment is much better. If this spherical (main) part is contained in the Green's function of the problem, the remainder of the effective potential is a small contribution due to the spheroidicity (essentially the particle-surface deformation interaction). In this case the contributions to the 2+ excitation coming from the second distorted wave approximation (iteration of the integral equation of the scattering problem) are of higher order in β ($\propto \beta^2$), and those leading to the 4+ excitation are $\propto \beta^3$. A more detailed discussion of the distorted wave case will be given in § 4.

The antisymmetrization of the initial (say) wave function of the system projectile+target in protons and neutrons leads to certain exchange terms in addition to the direct amplitude (discussed above) of the same collective transition operator. These exchange terms, however, involve overlap integrals of the bound-state and continuum-state functions of the same particle, which should be very small in general in a distorted wave approximation, owing to the quasi-orthogonality of the bound-state and properly chosen continuum-state wave functions. Any exchange terms of this type could be of importance for the angular correlation functions discussed in § 4.

3. Excitations by Interparticle Forces

In cases when $K_f \neq K_i$ ($\Delta K \neq 0$) a transition can be caused by an interparticle force between the projectile and one of the nucleons of the spheroidal

target. Generally $\Delta K = K_f - K_i = \Delta\Omega = \Omega_f - \Omega_i$ in the strong coupling model notation. Having to do with a case characterized by a definite ΔK and Ω_i, we know what Ω_f has to be and which Nilsson's orbit was populated from which orbit.

Let us first consider the case of the inelastic scattering of nucleons (protons, say). For the sake of simplicity let us use the plane wave Born approximation. The reaction amplitude antisymmetrized in all space, spin and isospin coordinates of the incident proton and target particle is

$$I^{I_i \to I_f}_{\Delta K}(M_i \mu_p; M_f \mu'_p) \propto \int d\xi\, d\theta_i \int d(t)\, d(p) \Psi^{I_f *}[M_f](\xi, t, \theta_i) e^{-i\mathbf{k}_f \cdot \mathbf{r}_p}$$
$$\times \chi^*_{\mu' p}(\sigma_p) \eta^*_{\tau' p = -\frac{1}{2}}(\tau_p) V_{pt}(|\mathbf{r}_p - \mathbf{r}_t|, \sigma_p, \sigma_t) \frac{1}{\sqrt{2}} \{\Psi^{I_i}[M_i](\xi, t, \theta_i) e^{i\mathbf{k}_i \cdot \mathbf{r}_p} \quad (4)$$
$$\times \chi_{\mu_p}(\sigma_p) \eta_{-\frac{1}{2}}(\tau_p) - \Psi^{I_i}[M_i](\xi, p, \theta_i) e^{i\mathbf{k}_i \cdot \mathbf{r}_t} \chi_{\mu_p}(\sigma_t) \eta_{-\frac{1}{2}}(\tau_t) \delta_{\tau' t, -\frac{1}{2}}\}$$

where ξ denotes the intrinsic coordinates of the subcore, (p) all the coordinates of the incident proton and (t) all those of the target particles, the $\Psi^I[M]$'s are the nuclear bound states, $\chi_\mu(\sigma)$ and $\eta_{\tau'}(\tau)$ the spin and isospin wave functions.

The Nilsson orbital of the particle (t) can be written in the fixed frame in the form

$$\chi_\Omega(t) = \eta_{\tau'}(\tau_t) \sum_{lj} C_{jl}(\Omega) R_{Nl}(\tau) \sum_\mu D^{j*}_{\mu\Omega}(\theta_i) \mathcal{Y}^\mu_{jl\frac{1}{2}}(\omega, \sigma) \quad (5)$$

where the $R_{Nl}(r)$'s are the radial functions, the $\mathcal{Y}$'s the j-eigenfunctions and the $C_{jl}(\Omega)$'s the diagonalisation coefficients. The integration of eq. (4) can be carried out analytically in closed form only under the assumption of a zero-range force

$$V_{pt} \equiv V_{pt}(|\mathbf{r}_p - \mathbf{r}_t|, \sigma_p, \sigma_t) = \delta(\mathbf{r}_p - \mathbf{r}_t) \left(V_1 + V_2 \frac{1 + \boldsymbol{\sigma}_p \cdot \boldsymbol{\sigma}_t}{2}\right). \quad (6)$$

In this approximation the contribution coming from the spin exchange term ($\propto V_2$) and the direct part of the amplitude in eq. (4) is of the same type as that coming from the exchange part of eq. (4) and the direct term of the transition operator ($\propto V_1$).

Performing all the integrations and using the algebraic methods of Racah one can obtain the following final result:

$$I^{I_i \to I_f}_{\Delta K = \Omega_f - \Omega_i}(M_i \mu_p; M_f \mu'_p) \propto \sqrt{\frac{[I_i]}{[I_f]}} \sum_{ls} \sum_{l_i j_i} \sum_{l_f j_f} C_{j_i l_i}(\Omega_i) C_{j_f l_f}(\Omega_f) i^l$$
$$\times \mathcal{R}_{l l_i l_f}(k) \{[j_i][j_f][l_i][l_f]\}^{\frac{1}{2}} (l_i l_f; 00|l0)(I_i s; M_i, \mu_p - \mu'_p | I_f M_f)$$
$$\times (I_i s; K_i, \Omega_f - \Omega_i | I_f K_f)(j_i j_f; -\Omega_i, \Omega_f | s, \Omega_f - \Omega_i) \left[(V_1 - V_2 \delta_{\tau' t, -\frac{1}{2}}) \right. \quad (7)$$
$$\left. \times \delta_{\mu_p \mu' p} \delta_{sl} W(l_i j_i l_f j_f; \tfrac{1}{2} l) - (V_1 \delta_{\tau' t, -\frac{1}{2}} - V_2)(-)^{j_i - l_i - \mu' p} [l]^{\frac{1}{2}}\right.$$

$$\times \sum_{h=0,1} [h]^{\frac{1}{2}}(\tfrac{1}{2}\tfrac{1}{2};\, -\mu'_{\mathrm{p}},\, \mu_{\mathrm{p}}|h,\, \mu_{\mathrm{p}}-\mu'_{\mathrm{p}})(lh;\, 0,\, \mu_{\mathrm{p}}-\mu'_{\mathrm{p}}|s,\, \mu_{\mathrm{p}}-\mu'_{\mathrm{p}}) X \begin{Bmatrix} l_1 & \frac{1}{2} & j_1 \\ l_{\mathrm{t}} & \frac{1}{2} & j_{\mathrm{t}} \\ l & h & s \end{Bmatrix} \Bigg]$$

where $[z] = 2z+1$, $(jj';\, mm'|kM)$ is a Clebsch-Gordan coefficient, $W(\ldots)$ a Racah coefficient, $X\{\vdots\vdots\vdots\}$ a 9-j symbol as defined e.g. in ref. [11]) and

$$\mathscr{R}_{l l_1 l_{\mathrm{t}}}(k) = \int_{r_0}^{\infty} r^2 \mathrm{d}r\, j_l(kr) \mathscr{R}_{N_{\mathrm{t}} l_{\mathrm{t}}}(r) \mathscr{R}_{N_1 l_1}(r). \tag{8}$$

The first term in the square brackets in eq. (7) is the "effective" direct term, the second one the "effective" exchange term †.

In the case of the inelastic scattering of deuterons we get a slightly more complicated result in the same approximation:

$$\begin{aligned} I^{I_1 \to I_{\mathrm{t}}}_{\Delta K = \Omega_{\mathrm{t}} - \Omega_1}(M_1 \mu_{\mathrm{d}};\, M_{\mathrm{t}} \mu'_{\mathrm{d}}) \propto X \sqrt{\frac{[I_1]}{[I_{\mathrm{t}}]}} \sum_{ls} \sum_{l_1 j_1} \sum_{l_{\mathrm{t}} j_{\mathrm{t}}} C_{j_1 l_1}(\Omega_1)\, C_{j_{\mathrm{t}} l_{\mathrm{t}}}(\Omega_{\mathrm{t}})\, i^l \\ \times \mathscr{R}_{l l_1 l_{\mathrm{t}}}(k) \{[j_1][j_{\mathrm{t}}][l_1][l_{\mathrm{t}}]\}^{\frac{1}{2}} (l_1 l_{\mathrm{t}};\, 00|l0)(I_1 s;\, M_1 \mu_{\mathrm{d}},\, -\mu'_{\mathrm{d}}|I_{\mathrm{t}} M_{\mathrm{t}}) \\ \times (I_1 s;\, K_1 \Omega_{\mathrm{t}},\, -\Omega_1|I_{\mathrm{t}} K_{\mathrm{t}})(j_1 j_{\mathrm{t}};\, -\Omega_1,\, \Omega_{\mathrm{t}}|s \Omega_{\mathrm{t}},\, -\Omega_1) \Big[(V_1 - V_2 \delta_{\tau'_{\mathrm{t}}, -\frac{1}{2}}) \\ \times \delta_{\mu_{\mathrm{d}} \mu'_{\mathrm{d}}} \delta_{sl} W(l_1 j_1 l_{\mathrm{t}} j_{\mathrm{t}};\, \tfrac{1}{2} l) - (V_1 \delta_{\tau'_1, -\frac{1}{2}} - V_2) \sum_{\mu_{\mathrm{t}}} \sum_{\mu_{\mathrm{n}}} (-)^{j_1 - l_1 - \mu_{\mathrm{n}}} [l]^{\frac{1}{2}} \\ \times \sum_{h=0,1} [h]^{\frac{1}{2}} (\tfrac{1}{2}\tfrac{1}{2};\, -\mu_{\mathrm{n}},\, \mu_{\mathrm{t}}|h,\, \mu_{\mathrm{t}} - \mu_{\mathrm{n}})(\tfrac{1}{2}\tfrac{1}{2};\, \mu_{\mathrm{n}},\, \mu'_{\mathrm{d}} - \mu_{\mathrm{n}}|1 \mu'_{\mathrm{d}}) \\ \times (\tfrac{1}{2}\tfrac{1}{2};\, \mu_{\mathrm{t}},\, \mu_{\mathrm{d}} - \mu_{\mathrm{t}}|1 \mu_{\mathrm{d}})(lh;\, 0,\, \mu_{\mathrm{t}} - \mu_{\mathrm{n}}|s, \mu_{\mathrm{t}} - \mu_{\mathrm{n}}) X \begin{Bmatrix} l_1 & \frac{1}{2} & j_1 \\ l_{\mathrm{t}} & \frac{1}{2} & j_{\mathrm{t}} \\ l & h & s \end{Bmatrix} \Bigg] \end{aligned} \tag{9}$$

where $\mu_{\mathrm{d}}, \mu'_{\mathrm{d}}$ denote the initial and final projections of the deuteron spin and the factor X has the same meaning as in (1). The approximation of eq. (9) for deuterons is, of course, much worse than the approximation of eq. (7) for protons, since the deuteron induced reactions are generally more complex.

In general, one has then to sum over all the particles contributing to a given transition, i.e., to sum over all $\Omega_1, \Omega_{\mathrm{t}}$'s corresponding to the transition operator $V = \sum_i V_{\mathrm{p}i}$ where $V_{\mathrm{p}i}$ is given by eq. (6) with (t) replaced by (i).

The expressions of eqs. (7)-(8) are not only applicable to the individual particle excitations, but can also describe cases of rotational excitations with $\Omega_{\mathrm{t}} = \Omega_1$ ($\Delta K = 0$). For these cases, eqs. (7)-(9) serve as an alternative to the theory of § 2 (a sum of interparticle forces between the particles of the target described by Nilsson's orbitals and the projectile replaces the "effective" spheroidal well "seen" by the projectile).

† An expression analogous to the direct part of that of eq. (7) was obtained independently by J. S. Blair and E. Henley for the case of α-particle scattering[12]). In the case when Ω_1 is the j-projection of the odd nucleon of an odd-mass nucleus the product $f(K_1, \Omega_1)$ of all factors depending on K_1, Ω_1 should be replaced by $f(K_1, \Omega_1) + (-)^{I_1 - j_1} f(-K_1, -\Omega_1)$ for the usual symmetrization. The same applies to eq. (9).

As an example, consider the reaction $Mg^{24}(p, p')Mg^{24*}$ (2+, 1.37 MeV level). Consider the Mg^{24} nucleus as the spherical O^{16} core plus eight $d_{5/2}$ $[(\frac{1}{2}+)^2, (3/2+)^2]$ particles (4 protons and 4 neutrons). Assume now $V = \sum_{i=1}^{8} V_{pi}$ (summation over these 8 particles). With the help of eq. (7) one arrives at the final result:

$$
\begin{aligned}
I_0^{0\to 2}(0\mu_p, M_f\mu'_p) \propto & \sum_{l_1 j_1}\sum_{l_f j_f}\sum_{\Omega=-3/2}^{+3/2} C_{j_1 l_1}(\Omega)C_{j_f l_f}(\Omega)(j_1 j_f; -\Omega\Omega|20) \\
& \times \mathscr{R}_{2l_1 l_f}(k)\{[j_1][j_f][l_1][l_f]\}^{\frac{1}{2}}(l_1 l_f; 00|20)\Big[(2V_1-V_2) \\
& \times \delta_{\mu_p\mu'_p} W(l_1 j_1 l_f j_f; \tfrac{1}{2}2) - (V_1-2V_2)(-)^{j_1-l_1-\mu'_p}\sqrt{5} \\
& \times \sum_{h=0,1}[h]^{\frac{1}{2}}(\tfrac{1}{2}\tfrac{1}{2}; -\mu'_p, \mu_p|h, \mu_p-\mu'_p)(2h; 0, \mu_p-\mu'_p|2, \mu_p-\mu'_p) \\
& \times X\begin{pmatrix} l_1 & \frac{1}{2} & j_1 \\ l_f & \frac{1}{2} & j_f \\ 2 & h & 2 \end{pmatrix}\Big].
\end{aligned}
\tag{10}
$$

The only allowed value of l is 2; in the direct terms $l = s$ $(= 2)$ according to eq. (7), and in the exchange terms $l = 0$ and 4 are forbidden by the selection rules contained in the 9-j symbol. Therefore, the angular distribution determined by eq. (10) is very closely similar to that given by eq. (1). The possible values of l_1 and l_f are 0 and 2. The angular distribution function is then a combination of the radial integrals of the form

$$\sigma(\theta) = a\mathscr{R}_{222}(k)^2 + 2b\mathscr{R}_{222}(k)\mathscr{R}_{220}(k) + c\mathscr{R}_{220}(k)^2. \tag{11}$$

The general feature of $\sigma(\theta)$ given by eq. (11) is determined by the function $j_2(kr_0)$ present in all the radial integrals: in the Born approixmation with over-all space integration $(r_0 \to 0)$ we would have

$$\mathscr{R}_{222}(k) = \sqrt{\tfrac{2}{5}}e^{-k^2/4\Gamma}(k^2/\Gamma)(14-k^2/\Gamma), \qquad \mathscr{R}_{220}(k) = e^{-k^2/4\Gamma}(k^2/\Gamma)(k^2/\Gamma-8)$$

with arbitrary normalization (the same for both the integrals).

Consider now the individual particle transition in Mg^{24}: 0+ (ground state) $\to$ 2+ (4.23 MeV third excited level). Hinds *et al.* [9]) obtained the angular distribution and the absolute values of the differential cross section for this transition being caused by 8.9 MeV inelastically scattered deuterons. According to the suggestion of Litherland *et al.* [13a]), this state corresponds to $K = 2$ and $\Delta\Omega = \Omega_f - \Omega_i = 2$ formed by a single particle transition: $\Omega_i = -3/2+$ (Nilsson's orbit (7)) to $\Omega_f = \frac{1}{2}+$ (Nilsson's orbit (9)), which seems to be the first particle-excited state for the large deformation of Mg^{24} ($\beta \approx 0.42$ as compared to $\beta \approx 0.34$ for Mg^{25} †. The angular distribution computed from eq. (9) has the form given by eq. (11). Again only $j_2(kr_0)$ determines the shape of the curve; it turns out to be essentially independent of the coefficients a, b and c. The curve computed with the use of the over-all space radial integrations is flatter than that of fig. 2 of ref. [9]) and gives a much better agree-

† Estimated from fig. 3 of ref. [13b]); according to ref. [13a]), $\delta \approx 0.95$, $\beta \approx 0.36$.

ment with the data, in particular for $40° \leqq \theta \leqq 100°$. However, it is in rather striking disagreement with the data at small scattering angles. This could be attributed to (1) a probably rather poor resolution for the 4.12 MeV and 4.23 MeV levels in the experiment of ref. [9]), (2) the finite range effects and the distortion effects of the incoming and outgoing free particle functions which are known to be capable of producing very distinct forward peaks in the angular distributions of the inelastically scattered particles (see refs. [3, 10])).

A systematical experimental study of branching ratios for excitations of rotational and individual particle states for every given spheroidal nucleus would be highly desirable. The cross sections for inelastic scattering exciting rotational levels are known to be large and expected to be larger than those for single particle excitations.

A good test of the unified model would be, for example, the $Mg^{25}(p, p')Mg^{25*}$ reaction at medium energies. In the pure strong-coupling approximation, i.e. if one neglects the possible mixing of bands by the Coriolis force, one has as lowest lying states:

1) ground state: $I_1 = K_1 = \frac{5}{2}+$ (orbit (5)),
2) 0.58 MeV state: $I_f = K_f = \frac{1}{2}$; $\Omega_f = K_f - K_1 + \Omega_1 = \frac{1}{2}+$ (orbit (9), first single particle excitation),
3) 0.98 MeV state: $I_f = \frac{3}{2}$, $K_f = \Omega_f = \frac{1}{2}+$ (orbit (9), first excited member of the rotational band $K_f = \frac{1}{2}$),
4) 1.61 MeV state: $I_f = \frac{7}{2}$, $K_f = K_1 = \frac{5}{2}$, $\Omega_f = \Omega_1 = \frac{5}{2}+$ (orbit (5), first excited member of the ground state rotational band),
5) 1.96 MeV state: $I_f = \frac{5}{2}$ (second excited member of the band $K = \frac{1}{2}$).

An example of a situation when the strong coupling is a poor approximation owing to a strong configuration mixing by rotation-particle coupling is the inelastic scattering from Na^{23} (see ref. [14]) for the structure of this nucleus). Such cases would be of special interest. Proper linear combinations of the strong coupling reaction amplitudes presented above with proper configuration mixing coefficients have to be applied in such cases.

It should be noted finally that in the processes (p, n) or (n, p) the surface coupling mechanism of § 2 is unimportant and only expressions of the type of eq. (7) should be applied.

4. Angular Correlations with γ-Rays

Let us now consider the angular correlations with the successive γ-radiation following an inelastic scattering process.

One can show that in the case of the collective transition operator $\Delta V = -\bar{V}_0 \beta r_0 \sum_\nu D^2_{\nu 0}(\theta_i)^* Y_{2\nu}(\omega)\delta(r - r_0)$ the angular correlation function, in distorted wave approximation, has the general form

$$\Phi[\theta, \Omega_\gamma(\theta_\gamma, \phi_\gamma)] = \sum_{\lambda, \nu, \nu', \mu} (-)^\nu [2\lambda]^{-\frac{1}{2}} Y_{2\lambda\mu}(\Omega_\gamma)^* S_{2\nu}(\theta) S^*_{2\nu'}(\theta)$$
$$\times (22; -\nu\nu'|2\lambda\mu) F_{2\lambda}(LI'_f I_f) W(I_f I_f 22; 2\lambda I_1). \quad (12)$$

Eq. (12) corresponds to a 2^L-pole γ-transition $I_f \to I'_f$; Ω_γ is the solid angle of the direction of propagation of the γ-ray;

$$F_{2\lambda}(LI'_f I_f) = (-)^{I_f - I'_f + 1} [I_f]^{\frac{1}{2}} [L]^{\frac{1}{2}} (LL; 1, -1|2\lambda 0) W(I_f I_f LL; 2\lambda I'_f)$$

is tabulated in ref. [15]); further

$$S_{2\nu}(\theta) = \int d\omega \, Y_{2\nu}(\omega) F_{\mathbf{k}_1}(r_0, \omega) F^*_{\mathbf{k}_f}(r_0, \omega) \quad (13)$$

where $F_{\mathbf{k}_1}$ and $F_{\mathbf{k}_f}$ stand for the initial and final state distorted waves at $r = r_0$. $\Phi[\theta, \Omega_\gamma(\theta_\gamma, \phi_\gamma)]$ is azimuthally symmetric (i.e., independent of ϕ_γ) around the recoil direction only in the plane wave approximation.

Consider now the simplest case: $I_1 = I'_f = 0$, $I_f = 2$, $L = 2$ (E2 transition). An example would be the reaction $Mg^{24}(p, p')Mg^{24*}$ (1.37 MeV) (γ) Mg^{24}. The angular correlation function in this case reduces to

$$\Phi(\theta, \Omega_\gamma) = \sum_{\lambda\nu\nu'\mu} (-)^\nu [2\lambda]^{-\frac{1}{2}} Y_{2\lambda\mu}(\Omega_\gamma)^* S_{2\nu}(\theta) S^*_{2\nu'}(\theta)$$
$$\times (22; -\nu, \nu'|2\lambda\mu)(22; 1, -1|2\lambda 0). \quad (14)$$

This shape of the function $\Phi(\theta, \Omega_\gamma)$ is in general preserved, even if one includes higher order corrections coming from the higher order terms of the β-power series expansion of the spheroidal well † of § 2. The same remains true for the inclusion of the higher iteration terms of the perturbation expansion (2nd and higher order distorted wave Born approximation). This general form is also independent of specific nuclear models applied. Banerjee and Levinson [10b]) obtained the same function $\Phi(\theta, \Omega_\gamma)$ as in eq. (14) using the nuclear shell model, for the reaction $C^{12}(p, p')C^{12*}$ (4.45 MeV)$(\gamma)C^{12}$.

For γ-rays in the reaction plane with $\phi_\gamma = 0$ we have

$$\Phi(\theta, \theta_\gamma) = a(\theta) + b(\theta) \sin^2 2(\theta_\gamma - \theta_0),$$

where the model dependent functions $a(\theta)$ and $b(\theta)$ and θ_0 are given in ref. [10b]), eqs. (38)-(40), in terms of $S_{2\nu}$ (one has to replace the T_ν^2 in these equations by our $S^*_{2\nu}$). This form of $\Phi(\theta, \theta_\gamma)$ is preserved even if one includes spin-orbit couplings (or any forces acting on the spin of the projectile only) both in the transition operator and in the distortion potentials. For spin independent potentials one can write the distorted wave amplitudes $S_{2\nu}$, in the frame with the z-axis along $\mathbf{k}_1$ and the x-axis in the reaction plane, in the form

$$S_{2\nu}(\theta) = \sum_{\lambda L} i^{\lambda - L} Y_{L\nu}(\theta) [\lambda][L]^{\frac{1}{2}} (\lambda 2; 00|L0)(\lambda 2; 0\nu|L\nu)$$
$$\times [j_\lambda(k_1 r_0) - \beta_\lambda h_\lambda^{(1)}(k_1 r_0)][j_L(k_f r_0) - \beta_L{}^* h_L^{(2)}(k_f r_0)]^* \quad (15)$$

† It should be noted that, as shown in ref. [6]), the tapered edge potentials give much better results than the square wells of § 2. Both the "spherical part" of the potential representing the distorting potential in our approximate method and the transition operators should be tapered edge functions.

where $h^{(1)[(2)]}_{\lambda(L)}(x)$ are the usual spherical Hankel functions and $\beta_{\lambda(L)}$ are the usual distortion coefficients $\beta_{\lambda(L)} = \frac{1}{2}(1-\eta_{\lambda(L)})$: cf., e.g. refs. [16, 17]).

In the plane wave case ($\beta_\lambda = \beta_L = 0$) the situation simplifies greatly. If we quantize along the recoil direction $-\mathbf{k} = \mathbf{k}_f - \mathbf{k}_1$, we get

$$S_{2\nu} \to \bar{S}_{20}\delta_{\nu 0} = j_2(kr_0)\delta_{\nu 0}.$$

The correlation function reduces to the well known form first obtained by Satchler [17]):

$$\Phi(\theta, \theta_\gamma) = \sin^2 2\theta_\gamma \tag{16}$$

where θ_γ refers to the recoil direction. Eqs. (12)-(16) apply to the case of deuterons as well so long as we do not introduce exchange terms coming from the antisymmetrization of the wave function of the whole system in identical particles. Such terms are rather inconsistent with the collective transition operator; they will be considered, however, in the case of excitations by interparticle forces, which we now discuss.

For the sake of illustration let us assume the interparticle forces to be of the form given by eq. (6) (i.e., zero range forces with spin exchange). Let us consider the important case $I_1 = I'_f = 0$, $I_f = 2$, $L = 2$ (E2 transition) for an even nucleus, the excited 2+ state being the first excited rotational level. The angular correlation function for such a (p, p', γ) reaction can be shown to be, in the plane wave approximation,

$$\Phi(\theta, \theta_\gamma) = \sum_{\lambda\nu} [2\lambda]^{-\frac{1}{2}} Y_{2\lambda 0}(\theta_\gamma)\mathcal{T}_{\nu\nu}(\theta)(22; -\nu\nu|2\lambda 0)(22; 1, -1|2\lambda 0) \tag{17}$$

where θ_γ again refers to the recoil direction. The matrix $\mathcal{T}_{\nu\nu}(\theta)$ is diagonal in this approximation; the components $\mathcal{T}_{11}$ and $\mathcal{T}_{-1-1}$ are characteristic of the exchange effects (with $\mu_p - \mu'_p = \pm 1$). Explicitly,

$$\begin{aligned}\Phi(\theta, \theta_\gamma) &= -\tfrac{3}{8}\mathcal{T}_{00}\sin^2 2\theta_\gamma + \tfrac{1}{4}(\mathcal{T}_{11}+\mathcal{T}_{-1-1})[2 - \sin^2\theta_\gamma - \sin^2 2\theta_\gamma] \\ &= \mathcal{T}_{11}(1-\tfrac{1}{2}\sin^2\theta_\gamma) - (\tfrac{3}{8}\mathcal{T}_{00}+\tfrac{1}{2}\mathcal{T}_{11})\sin^2 2\theta_\gamma\end{aligned} \tag{18}$$

with

$$\begin{aligned}\mathcal{T}_{00} = \sum\{ll'; l_1 j_1 l_f j_f; l'_1 j'_1 l'_f j'_f\} & T_t(l_1 j_1 l_f j_f) T_{t'}(l'_1 j'_1 l'_f j'_f) \\ \times \left[1 - \{(-)^{j'_1+j_f} + (-)^{j_1+j'_f}\}\frac{1-2\alpha}{2-\alpha} - \tfrac{1}{2}(-)^{j_1+j'_1+j_f+j'_f}\left(\frac{1-2\alpha}{2-\alpha}\right)^2\right] \\ \times W(l_1 j_1 l_f j_f; \tfrac{1}{2} l) W(l'_1 j'_1 l'_f j'_f; \tfrac{1}{2} l'),\end{aligned} \tag{19}$$

$$\begin{aligned}\mathcal{T}_{11} = \mathcal{T}_{-1-1} = \sum\{l \ldots j'_f\} & T_t(\ldots) T_{t'}(\ldots) \\ & \times (-)^{j_1+j'_1} 1.5 \left(\frac{1-2\alpha}{2-\alpha}\right)^2 X \begin{Bmatrix} l_1 & \frac{1}{2} & j_1 \\ l_f & \frac{1}{2} & j_f \\ l & 1 & 2 \end{Bmatrix} X \begin{Bmatrix} l'_1 & \frac{1}{2} & j'_1 \\ l'_f & \frac{1}{2} & j'_f \\ l' & 1 & 2 \end{Bmatrix}.\end{aligned} \tag{20}$$

Here $\alpha = V_2/V_1$ and

$$T_t(l_1 j_1 l_t j_t) = \sum_{\Omega} C_{j_1 l_1}(\Omega) C_{j_t l_t}(\Omega)(j_1 j_t; -\Omega, \Omega|20) \times (l_1 l_t; 00|l0)\{[j_1][j_t][l_1][l_t]\}^{\frac{1}{2}} \mathscr{R}_{tl_1 l_t}(k)\delta_{t2}; \tag{21}$$

all the other quantities involved are defined in § 2, 3.

Using the properties of the T_2's and of the 9-j symbols, and eq. (20), one can show that $\mathscr{T}_{11} \equiv 0$ and one has again the Satchler form $\Phi(\theta, \theta_\gamma) = \sin^2 2\theta_\gamma$. This result ($\mathscr{T}_{11} \equiv 0$) does not hold for finite range forces or when distortion effects are present. Neither does it hold in general for the cases when the 2+ excited level is an individual particle excited level with $\Delta\Omega = K_t \neq 0$. In such cases

$$T_t(l_1 j_1 l_t j_t) = \sum_{\Omega_1 \Omega_t} C_{j_1 l_1}(\Omega_1) C_{j_t l_t}(\Omega_t)(j_1 j_t; -\Omega_1, \Omega_t|2K_t) \times (l_1 l_t; 00|l0)\{[j_1][j_t][l_1][l_t]\}^{\frac{1}{2}} \mathscr{R}_{tl_1 l_t}(k). \tag{22}$$

Eq. (18) determines a particular case of the general shape† of the function

$$\Phi(\theta, \theta_\gamma) = a(\theta) + b(\theta) \sin^2 2(\theta_\gamma - \theta_0) + c(\theta) \sin^2(\theta_\gamma - \theta'_0)$$

characteristic of $I_1 = I'_t = 0, I_t = 2, L = 2$ (E2 transitions). The "isotropic" term $a(\theta)$ and the $\sin^2(\theta_\gamma - \theta'_0)$-term come only from the exchange effects (antisymmetrization and spin exchanges forces). If there is no spin exchange present (pure Wigner forces), then $\alpha \to 0$ but the effect of antisymmetrization still remains. It vanishes ($\mathscr{T}_{11} \equiv 0$) when $\alpha = \frac{1}{2}$. It is seen from eq. (20) that only the spin-flip amplitudes contribute to $\mathscr{T}_{11}$ (viz., $h = h' = 1$ in the 9-j symbol of eq. (10)).

It should be noted again that the general shape of $\Phi(\theta, \theta_\gamma)$ is independent of the nuclear model assumed (for the shell model calculation, cf., e.g., ref.[10b]), eq. (43)). The recent data of Sherr and Yoshiki [18]) on the Mg^{24} reaction seem to indicate the presence of a $\sin^2(\theta_\gamma - \theta'_0)$-term at backward θ-angles. Distortion effects alone, without exchange effects, cannot produce the $\sin^2(\theta_\gamma - \theta'_0)$-term: they produce only the form $a(\theta) + b(\theta) \sin^2 2(\theta_\gamma - \theta_0)$ in the reaction plane. The experiment of Sherr and Yoshiki [18]) seems also to indicate a slight deviation from the forward-backward symmetry shape in the reaction plane predicted by eq. (18) or the general form of $\Phi(\theta, \theta_\gamma)$. This could be due to (1) distortion effects, (2) finite range transition operators together with the spin-flip terms.

† Most generally

$$\Phi(\theta, \theta_\gamma) = \sum_{\lambda\nu\nu'\mu} (-)^{\nu'} [2\lambda]^{-\frac{1}{2}} Y_{2\lambda,\mu}(\theta_\gamma, 0) T_{\nu\nu'}(22; -\nu, \nu'|2\lambda, \mu)(22; 1, -1\,|2\lambda, 0)$$
$$= A + B\cos 4\theta_\gamma + C \sin 4\theta_\gamma + D \cos 2\theta_\gamma + E \sin 2\theta_\gamma$$
$$= a + b \sin^2 2(\theta_\gamma - \theta_0) + c \sin^2(\theta_\gamma - \theta'_0),$$

with

$$A = a + b + \tfrac{1}{2}c, \quad B = -\tfrac{1}{2}b \cos 4\theta_0, \quad C = -\tfrac{1}{2}b \sin 4\theta_0, \quad D = -\tfrac{1}{2}c \cos 2\theta'_0, \quad E = -\tfrac{1}{2}c \sin 2\theta'_0.$$

The same result was independently obtained by J. S. Blair.

The author feels greatly indebted to Dr. J. S. Blair for many invaluable discussions, criticisms and suggestions during the course of this work, and for reading the manuscript. Thanks are due to Professor R. Sherr for his kind interest and several helpful discussions on the angular correlation problem, and to H. Yoshiki for his encouragement on this problem. Several discussions with Dr. C. A. Levinson, Dr. W. Pinkston, H. Yoshiki and C. Bouchiat are greatfully acknowledged.

Note added in proof:

1) Eqs. (7), (9), (10), (19)–(22) can be simplified by the relation

$$\sqrt{[l_1][l_f]}(l_1 l_f;\ 00|l0)W(j_1 l_1 j_f l_f;\ \tfrac{1}{2}l) = (j_1 j_f;\ \tfrac{1}{2}, -\tfrac{1}{2}|l0),\ l_1+l_f-l = \text{even}.$$

The author is indebted to G. R. Satchler for pointing out to him this relation.

2) For a finite range interparticle force

$$V_{pt} \equiv \sum_{k=0}^{\infty} \sum_{\nu} f_k(r_t) \times g_k(r_p) Y^*_{k\nu}(\omega_p) Y_{k\nu}(\omega_t)[1+\tfrac{1}{2}\alpha(1+\boldsymbol{\sigma}_p \cdot \boldsymbol{\sigma}_t)],$$

plane waves representing the free proton states, and the quantization axis along the recoil direction, the (p, p′)-reaction amplitude (4) can be shown to be

$$\begin{aligned}
I^{I_1 \to I_f}_{\Delta K=\Delta\Omega}(M_1\mu_p;\ M_f\mu'_p) \propto{}& \sqrt{\frac{[I_1]}{[I_f]}} \sum_s \sum_{j_1 j_f l_1 l_f} C_{j_1 l_1}(\Omega_1) C_{j_f l_f}(\Omega_f) \\
&\times (I_1 s;\ M_1,\ M_f - M_1 | I_f M_f)(I_1 s;\ K_1 \Delta\Omega | I_f K_f)(j_1 j_f;\ -\Omega_1,\ \Omega_f | s \Delta\Omega) \\
&\times \Big\{ i^l \{[j_1][j_f]\}^{\frac{1}{2}} (j_1 j_f;\ \tfrac{1}{2},\ -\tfrac{1}{2}|l0) \hat{\mathcal{R}}_{l l_1 l_f} \delta_{\mu_p \mu'_p} \delta_{sl} \\
&+ \alpha i^l (-)^{j_1 - l_1 - \mu'_p} \hat{\mathcal{R}}_{l l_1 l_f} \{[j_1][j_f][l_1][l_f]\}^{\frac{1}{2}} (l_1 l_f;\ 00|l0) \\
&\times \sum_{h=0,1} [h]^{\frac{1}{2}} [l]^{\frac{1}{2}} (\tfrac{1}{2}\tfrac{1}{2};\ -\mu'_p,\ \mu_p | h,\ \mu_p - \mu'_p)(lh;\ 0,\ \mu_p - \mu'_p | s,\ \mu_p - \mu'_p) X \begin{Bmatrix} l_1 & \frac{1}{2} & j_1 \\ l_f & \frac{1}{2} & j_f \\ l & h & s \end{Bmatrix} \\
&- 4\pi \sum_{g,h} \sum_{\lambda_f \lambda_1 k} \sum_{\nu_1 \nu_f} (-)^{j_1 - l_1 + \mu'_p - k + \nu_f} Y^*_{\lambda_1 \nu_1}(\theta_{k_1}) Y_{\lambda_f \nu_f}(\theta_{k_f}) i^{\lambda_1 - \lambda_f} \\
&\times \mathcal{R}^{(k)}_{\lambda_f l_1 \lambda_1 l_f}[k] \{[j_1][j_f][\lambda_1][\lambda_f][g][h]\}^{\frac{1}{2}} (\lambda_f k;\ 00|l_1 0)(\lambda_f \lambda_1;\ \nu_f,\ -\nu_1 | g, \nu_f - \nu_1) \\
&\times (\lambda_1 k;\ 00|l_f 0)(\tfrac{1}{2}\tfrac{1}{2};\ -\mu'_p, \mu_p | h, \mu_p - \mu'_p)(gh;\ \nu_1 - \nu_f,\ \mu_p - \mu'_p | s,\ \mu_p - \mu'_p + \nu_1 - \nu_f) \\
&\times W(\lambda_f l_1 \lambda_1 l_f;\ kg) X \begin{Bmatrix} l_1 & \frac{1}{2} & j_1 \\ l_f & \frac{1}{2} & j_f \\ g & h & s \end{Bmatrix} (1+\alpha\delta_{\mu_p, \mu'_p})\delta_{\tau' t, -\frac{1}{2}} \Big\}
\end{aligned}$$

where

$$\hat{\mathcal{R}}_{l l_1 l_f} = \int_{r_0}^{\infty} r_p^2\, dr_p\, j_l(kr_p) g_k(r_p) \int_{r_0}^{\infty} r_t^2\, dr_t\, R_{l_f}(r_t) R_{l_1}(r_t) f_k(r_t),$$

$$\mathcal{R}^{(k)}_{\lambda_f l_1 \lambda_1 l_f} = \int_{r_0}^{\infty} r_p^2\, dr_p\, j_{\lambda_f}(k_f r_p) R_{l_1}(r_p) g_k(r_p) \int_{r_0}^{\infty} r_t^2\, dr_t\, j_{\lambda_1}(k_1 r_t) R_{l_f}(r_t) f_k(r_t).$$

One can show that $\mathcal{T}_{11}$ of eq. (17) is different from zero in this case even if $\Delta\Omega = 0$ i.e. $K_f = K_1$.

References

1) D. M. Brink, Proc. Phys. Soc. A **68** (1955) 994
2) S. Hayakawa and S. Yoshida, Proc. Phys. Soc. A **68** (1955) 656
3) S. Yoshida, Proc. Phys. Soc. A **69** (1955) 688
4) E. V. Inopin, JETP **31** (1956) 901

5) W. N. Gribov, JETP **32** (1957) 842
6) D. M. Chase, L. Wilets and A. R. Edmonds, preprint
7) J. Sawicki, Nuclear Phys. **6** (1958) 613
8) J. W. Haffner, Phys. Rev. **103** (1956) 1398
9) S. Hinds, R. Middleton and G. Parry, Proc. Phys. Soc. A **70** (1957) 900
10) C. A. Levinson and M. K. Banerjee, Annals of Physics (a) **2** (1957) 471; (b) **2** (1957) 499
11) W. T. Sharpe *et al.*, Chalk River report C.R.T.-556
12) J. S. Blair and E. Henley, Bull. Am. Phys. Soc. **1** (1956) 20; Physica **22** (1956) 1126; private communication from Dr. J. S. Blair
13a) A. E. Litherland *et al.*, Chalk River report PD-289 (1957)
13b) R. K. Sheline, Nuclear Phys. **2** (1956) 382
14) E. Paul, private communication from D. A. Bromley
15) L. C. Biedenharn and M. E. Rose, Revs. Mod. Phys. **25** (1953) 729
16) J. Sawicki, Phys. Rev. **106** (1957) 172
17) G. R. Satchler, Proc. Phys. Soc. A **68** (1955) 1037
18) R. Sherr and H. Yoshiki, to be published

4.A:4.E *Nuclear Physics* 7 (1958) 516—525; © *North-Holland Publishing Co., Amsterdam*
Not to be reproduced by photoprint or microfilm without written permission from the publisher

β-ZERFALL DES N^{13} UND FIERZ-INTERFERENZ BEI FERMI-WECHSELWIRKUNG

H. DANIEL und U. SCHMIDT-ROHR
Institut für Physik im Max-Planck-Institut für medizinische Forschung, Heidelberg

Eingegangen am 15. April 1958

Abstract: The β-ray spectrum of the mirror transition $N^{13} \rightarrow C^{13}$ has been investigated with an iron-free lens spectrometer. No deviation from the allowed shape was observed. The Fierz coefficient was measured to be $b = (0.14 \pm 2.37)$ % (standard deviation). Taking into account that only 70 % of the transition rate are due to Fermi interaction an upper limit of 11 % is found for $|b_F|$, b_F being the Fierz coefficient for pure Fermi interaction.

1. Ziel der Untersuchung †

Die Form eines erlaubten β^+-Spektrums wird durch den folgenden Ausdruck wiedergegeben [1]:

$$N(W)\mathrm{d}W = \frac{\xi}{4\pi^3} F(Z,W) pW (W_0 - W)^2 \left(1 - \frac{b}{W}\right) \mathrm{d}W$$

mit

$$\begin{aligned} \xi &= (|C_S|^2 + |C_V|^2 + |C'_S|^2 + |C'_V|^2)|M_F|^2 \\ &\quad + (|C_T|^2 + |C_A|^2 + |C'_T|^2 + |C'_A|^2)|M_{GT}|^2, \qquad (1) \\ b\xi &= \gamma(C_S^* C_V + C_S C_V^* + C_S'^* C'_V + C'_S C_V'^*)|M_F|^2 \\ &\quad + \gamma(C_T^* C_A + C_A^* C_T + C_T'^* C'_A + C_A'^* C_T)|M_{GT}|^2; \end{aligned}$$

$C_S(C'_S)$ = paritätserhaltende (nicht erhaltende) Konstante für skalare Kopplung, usw. Die nicht erklärten Symbole sind in ihrer üblichen [2] Bedeutung gebraucht. In dieser Darstellung sind die Beiträge verbotener Terme vernachlässigt. Solche Beiträge spielen keine Rolle, außer wenn die erlaubten Matrixelemente besonders klein sind; das ist aber bei dem Spiegelübergang $N^{13} \rightarrow C^{13}$ sicher nicht der Fall.

Für die Fierz-Koeffizienten bei Fermi-Wechselwirkung,

$$b_F = \gamma \frac{C_S^* C_V + C_S C_V^* + C_S'^* C'_V + C'_S C_V'^*}{|C_S|^2 + |C_V|^2 + |C'_S|^2 + |C'_V|^2},$$

und bei Gamow-Teller Wechselwirkung,

$$b_{GT} = \gamma \frac{C_T^* C_A + C_T C_A^* + C_T'^* C'_A + C'_T C_A'^*}{|C_T|^2 + |C_A|^2 + |C'_T|^2 + |C'_A|^2},$$

† Eine vorläufige Mitteilung ist bereits früher erschienen [21].

liegen eine Reihe von Abschätzungen vor. Ältere Untersuchungen von Spektralformen ergaben [2]) $|b_{GT}| < 0.2$ und $|b_F| \lesssim 0.2$. Eine gemeinsame Analyse vieler β-Strahler im „$B\varkappa$-Diagramm" führte Kofoed-Hansen und Winther [3]) auf $b_{GT} \approx 0$ und $b_F \approx 0.29$ (die Vorbehalte der Autoren s. ebenda). Aus dem Verhältnis Elektroneneinfang zu Positonenemission erhielten Sherr und Miller [4]) an Na^{22} $b_{GT} = (-2 \pm 4)$ %, Drever, Moljk und Scobie [5]) an F^{18} $b_{GT} = (0.8 \pm 4)$ % und Scobie und Lewis [6]) an C^{11} $b_F = (-4 \pm 18)$ %. Neuerdings untersuchten Yuasa *et al.*[7]) die Form des Y^{90}-Spektrums; sie geben $|b_{GT}| < 6$ % an.

Wenn die Elektronenpolarisation bei erlaubten Übergängen vollständig ist, verschwinden die Fierz-Terme. Es liegt eine große Anzahl von Messungen der Elektronenpolarisation vor [8]), deren neuere alle mit voller Polarisation verträglich sind. Jedoch scheint die Genauigkeit, insbesondere bei Fermi-Übergängen, noch nicht so weit getrieben worden zu sein, daß man kleine obere Grenzen der Fierz-Koeffizienten entnehmen kann.

Zweck der vorliegenden Untersuchung war es, eine kleine obere Grenze für den Fierz-Koeffizienten bei Fermi-Wechselwirkung sicherzustellen. Dazu wurde die Form des β^+-Spektrums von N^{13} untersucht. N^{13} zerfällt größtenteils über Fermi-Wechselwirkung.

Wenn es keine Fierz-Interferenz gibt, ist nach Gleichung (1) der Formfaktor

$$\mathrm{Ff} = \frac{N(W)}{F(Z,W)pW(W_0-W)^2} \tag{2}$$

unabhängig von der Elektronenenergie W, die Kurve Ff gegen W also parallel zur Abszissenachse. Von besonderer Bedeutung ist offensichtlich die genaue Kenntnis der Grenzenergie W_0. Deshalb wurde W_0 mit einer für diesen Zweck besonders geeigneten Methode separat bestimmt.

Zusätzliche Messungen erstreckten sich auf die Halbwertzeit und die Suche nach Kern-γ-Strahlung; Kern-γ-Strahlung könnte eine zweite Komponente im β-Spektrum anzeigen, und Abweichungen von der erlaubten Form im gesamten β-Spektrum wären trotz verschwindender Fierz-Terme möglich.

2. Quellen

Das N^{13} wurde durch Bestrahlen von spektralreinem Graphit mit Deuteronen von 7 MeV im Heidelberger Zyklotron hergestellt. Als Target diente ein massiver Block, der sehr hohe Bestrahlungsintensitäten zuließ. Zur Messung des β-Spektrums wurden einige Milligramm des bestrahlten Materials in einer Reibschale 3 min fein gemahlen und mit einem Tropfen ammoniakalischer Tanninlösung aufgeschlämmt, der etwas Entspannungsmittel („Pril") zugesetzt worden war. Ein Teil der Suspension wurde auf die

Trägerfolie des β-Präparathalters pipettiert und dort eingetrocknet. Dabei bildete sich eine homogene hellgraue Schicht, in der keine Körnerstruktur mit dem Mikroskop auflösbar war. Knapp 10 min nach Bestrahlungsende begannen die Messungen mit dem β-Spektrometer. Die spezifische Aktivität der Quellen betrug bei Meßbeginn etwa 2 mC/mg.

Der Präparathalter war dem früher [9]) beschriebenen ähnlich. Als Trägerfolie diente entweder Aluminium von 240 μg/cm^2 oder Zelluloid von 30 bis 50 μg/cm^2. Beide Folien brachten die gleichen Ergebnisse. Starke Quellen wurden jedoch nur mit Aluminiumfolie hergestellt.

Für die Formbestimmung wurde die Quellendicke zwischen 140 und 300 μg/cm^2 variiert, s. Zif. 4. Zur Messung der Grenzenergie und besonders der Halbwertzeit konnten aber dickere und damit stärkere Quellen benutzt werden.

3. Meßverfahren

Das β-Spektrum wurde mit dem Heidelberger Doppellinsenspektrometer [9]) gemessen, das sich aus verschiedenen Gründen gut zur genauen Aufnahme eines Kontinuums eignet:

(a) Im Gerät wird keinerlei Eisen verwendet. Deshalb sind die Fokussierungseigenschaften unabhängig von der eingestellten Elektronenenergie.

(b) In der Nähe der Quelle befindet sich außer dem Präparathalter keinerlei Materie.

(c) Das Elektronenbündel tangiert die Begrenzungsflächen der Austrittsblende, so daß nur relativ wenige Elektronen an den Blendenrändern gestreut werden.

(d) Der Abstand zwischen Austrittsblende und Detektor ist groß, so daß Elektronen, die an den Blendenrändern gestreut worden sind, den Detektor nicht mehr erreichen.

Aus diesen Gründen ist die Transmission des Gerätes unabhängig von der eingestellten Elektronenenergie, und das Spektrum wird durch Rückstreuung von Elektronen an der Kammerwand u.ä. nicht verfälscht.

Als Detektor diente wie früher [10]) ein Szintillationszähler mit einem Anthracenkristall von 25 mm Durchmesser und 10 mm Stärke. Zur Messung der Grenzenergie des N^{13} wurde der Szintillationszähler mit Einkanal-Diskriminierung benutzt, um so den Untergrund praktisch auszuschalten. Diese Messung beschränkte sich auf den energiereichen Teil des β-Kontinuums. Zur Messung der gesamten Spektralform wurde der Szintillationszähler mit integraler Diskriminierung verwendet. Die Höhe der Diskriminierung wurde variiert. Meistens wurde bei 3V gemessen. Elektronen von 1 MeV riefen bei der angewandten Hochspannung und Verstärkung Impulse von 45 V am Eingang des Diskriminators hervor.

Bei einem solchen Detektor treten Zählverluste insbesondere bei kleinen

Elektronenenergien auf durch Rückstreuung der Elektronen aus dem Kristall. Diese Verluste wurden auf die übliche Weise [11]) durch Aufnahme der Auflösekurve des Szintillationszählers bei festgehaltener Elektronenenergie und Extrapolation dieser Kurve auf die Impulshöhe Null bestimmt. Als Quelle diente ein starkes P^{32}-Präparat. Die Form des P^{32}-Spektrums ging in die Kontrollmessungen nicht ein. Abb. 1 zeigt die Zählkorrektur als Funktion der Elektronenenergie. Die Rückstreuung von Elektronen und Positonen aus Materialien mit kleiner Ordnungszahl ist gleich [12]).

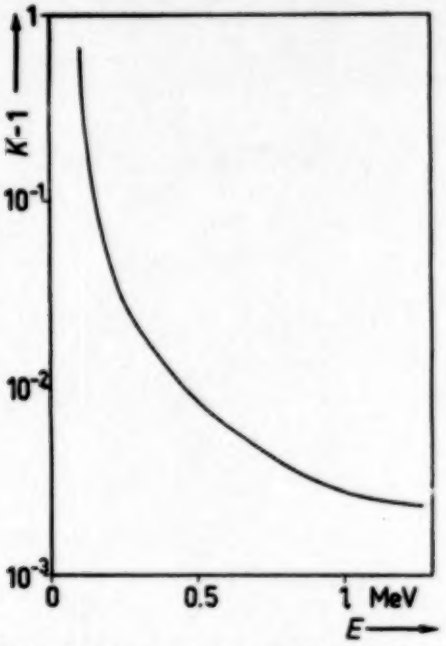

Abb. 1. Korrektion auf Zählverluste durch Rückdiffusion. E = Energie der einfallenden Elektronen, K = Korrektionsfaktor bei integraler Diskriminierung von 3 V.

Die so erhaltene Zählkorrektur wurde geprüft durch Aufnahme des P^{32}-Spektrums mit verschieden hoher integraler Diskriminierung; aus der gemessenen linearen Kurve Zählrate gegen Diskriminator-Vorspannung ließ sich die Korrektur durch Extrapolation auf Null entnehmen. Dieses Verfahren lieferte, obwohl etwas ungenauer als das oben genannte, praktisch die gleichen Resultate.

Eine weitere Kontrolle direkt mit N^{13} ergab sich aus dem Verhältnis Zählrate bei 6V Diskriminierung zu Zählrate bei 3V Diskriminierung, wobei beide Zählraten auf die Zählverluste korrigiert waren (Abb. 2).

Die Totzeit der Zählanordnung wurde mit einem Doppelimpulsgeber bestimmt. Sie betrug bei integraler Diskriminierung von 3V 3.0 μsec. Eine gute Kontrolle der daraus errechneten Totzeitkorrektur lieferte die Messung des zeitlichen Abfalls eines N^{13}-Präparates, s. Zif. 4.

Bei der Auswertung der Messungen ist der natürliche Nulleffekt des Detektors und der durch das Präparat verursachte Untergrund von der

Zählrate abzuziehen. Wie sich herausstellte, war der natürliche Nulleffekt von der Stärke des Magnetfeldes unabhängig. Der durch das Präparat verursachte Untergrund, hervorgerufen durch vagabundierende Positonen und Negatonen und durch Vernichtungsstrahlung, wurde bei Spulenströmen entsprechend Energien oberhalb der β-Grenze des N^{13} und beim Spulenstrom Null gemessen. Für die dazwischen liegenden Werte des Spulenstroms wurde linear interpoliert. Die Zulässigkeit dieser Interpolation wurde durch eine zusätzliche Messung geprüft, bei der die Zählrate als Funktion des

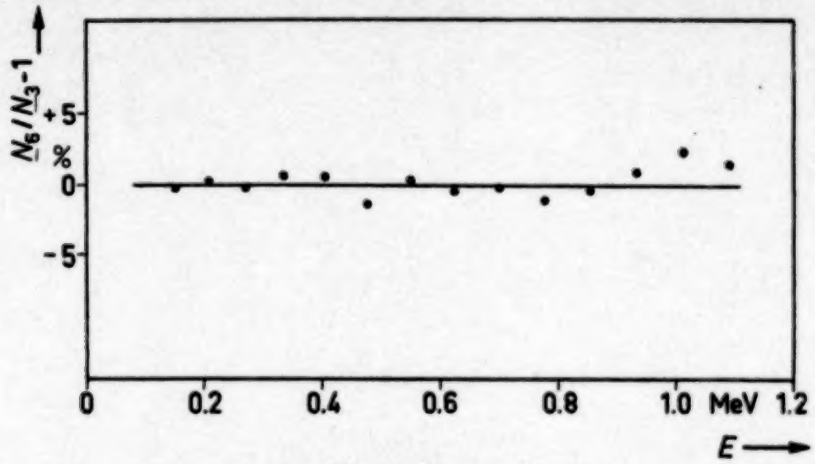

Abb. 2. Hilfsmessung an N^{13} zur Prüfung der Korrektion auf Zählverluste durch Rückdiffusion. N_6 (N_3) = korrigierte Zählrate bei integraler Diskriminierung von 6 (3) V. Bei kleiner Positonenenergie E ist die Statistik gut, bei großer schlecht.

Spulenstroms aufgenommen wurde, während sich ein starkes Gamma-Präparat in der Nähe des Spektrometers, aber außerhalb der Vakuumkammer befand. Wie sich zeigte, ließ sich die Zählrate als Funktion des Spulenstroms durch eine schwach abfallende Gerade darstellen.

Von besonderer Bedeutung ist die Frage, ob das Spektrum durch Rückstreuung vom Präparathalter oder der Unterlage verfälscht werden kann. Beides wurde mit einer starken P^{32}-Quelle geprüft durch Vermehren der für Rückstreuung in Frage kommenden Materie (Ersetzen der drei Streben des Präparathalters durch einen geschlossenen Mantel bzw. Unterlegen von zusätzlicher Al-Folie unter das Präparat). Wie sich herausstellte, kann der von Präparathalter und Trägerfolie zusammen herrührende Fehler im Fierz-Koeffizient b Zif. 4 höchstens die Hälfte des dort angegebenen mittleren Fehlers betragen.

4. Meßergebnisse

Abb. 3 zeigt die mit dem Linsenspektrometer aufgenommene Abfallkurve eines starken N^{13}-Präparates. Hierbei war das Spektrometer auf das Intensitätsmaximum im Spektrum und der Diskriminator auf 3V integral eingestellt. Offenbar verläuft der Abfall rein exponentiell.

Ähnliche Kurven liegen für andere Energien vor, so daß die Reinheit der Quellen gesichert ist. Die Halbwertzeit ergab sich zu 9.96 ± 0.03 min (Fehlergrenze).

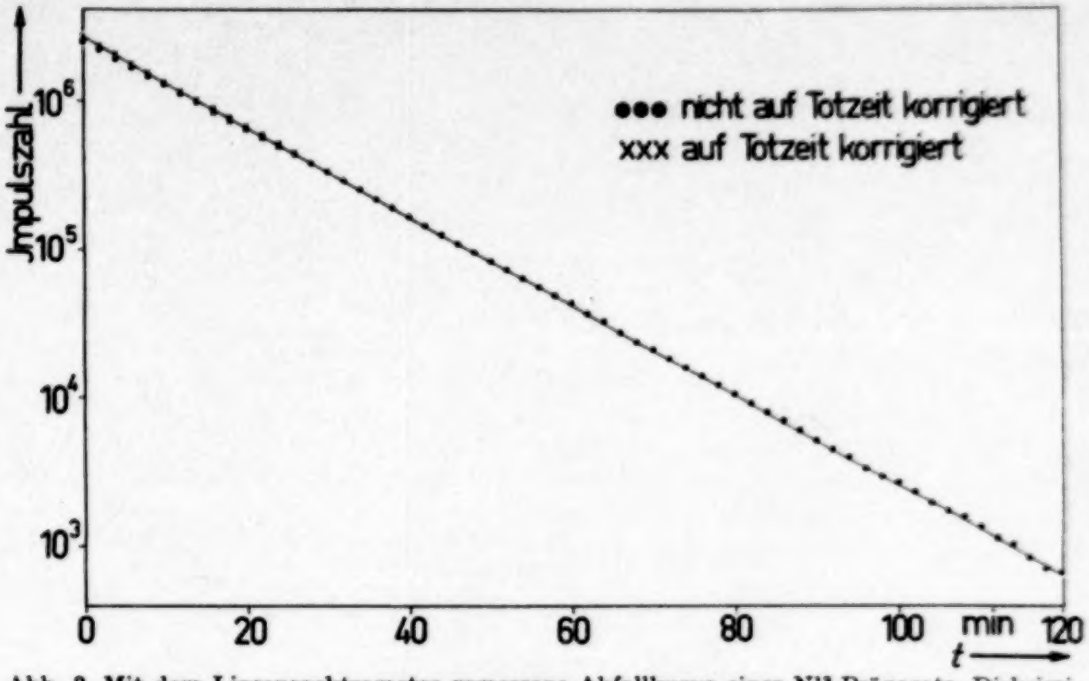

Abb. 3. Mit dem Linsenspektrometer gemessene Abfallkurve eines N^{13}-Präparats. Diskriminierung integral bei 3 V. Der natürliche Nulleffekt des Zählers ist abgezogen.

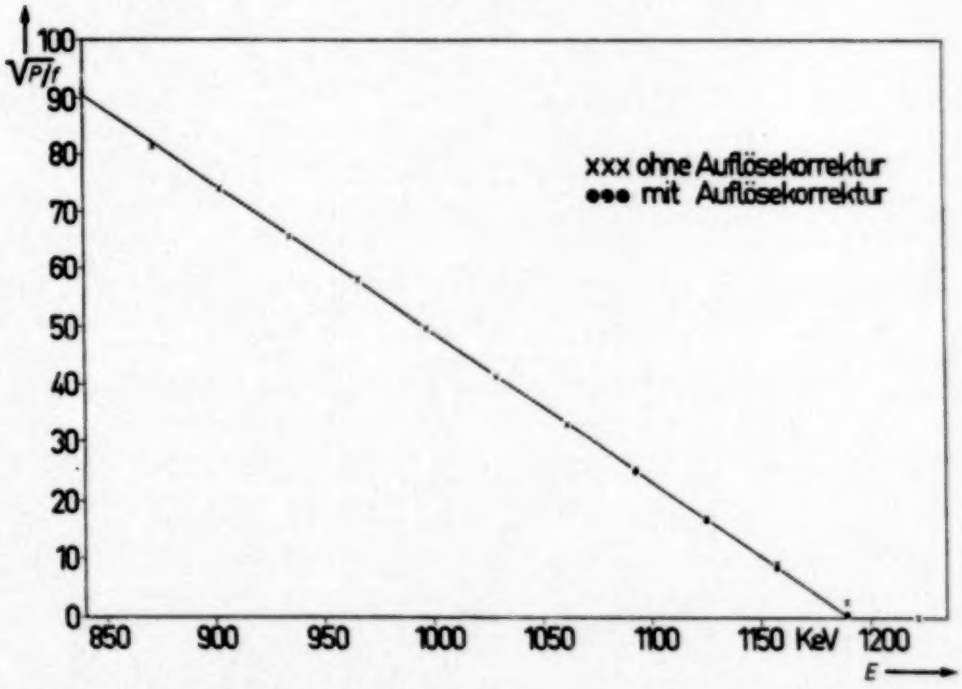

Abb. 4. Energiereicher Teil des β-Spektrums von N^{13} in Fermi-Darstellung.

Abb. 4 zeigt den energiereichen Teil des β-Kontinuums in Fermi-Darstellung. Die Grenzenergie beträgt 1.190 ± 0.003 MeV (Fehlergrenze).

Aus Halbwertzeit und Grenzenergie ermittelt man mit den Tabellen von Djelepov und Siranowa [13]), die bei allen Auswertungen benutzt wurden, einen *ft*-Wert von $ft = 4560 \pm 40$ sec.

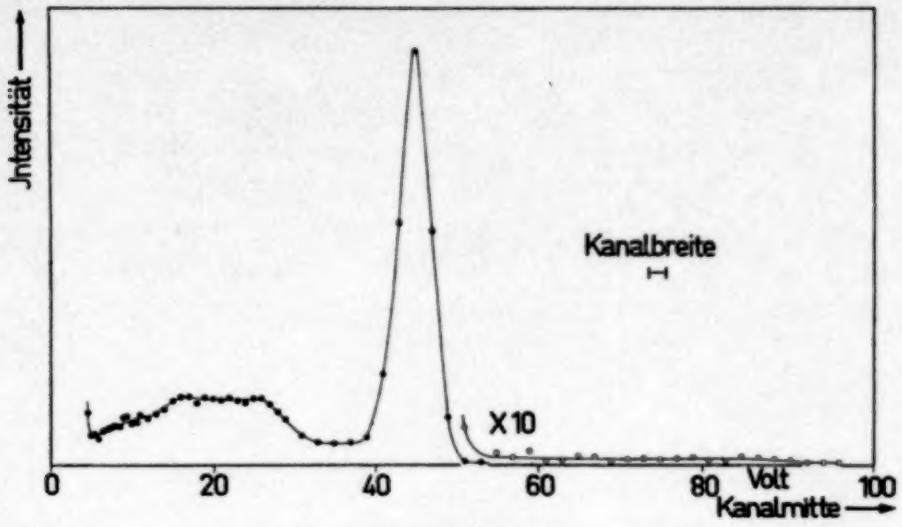

Abb. 5. γ-Spektrum des N^{13}.

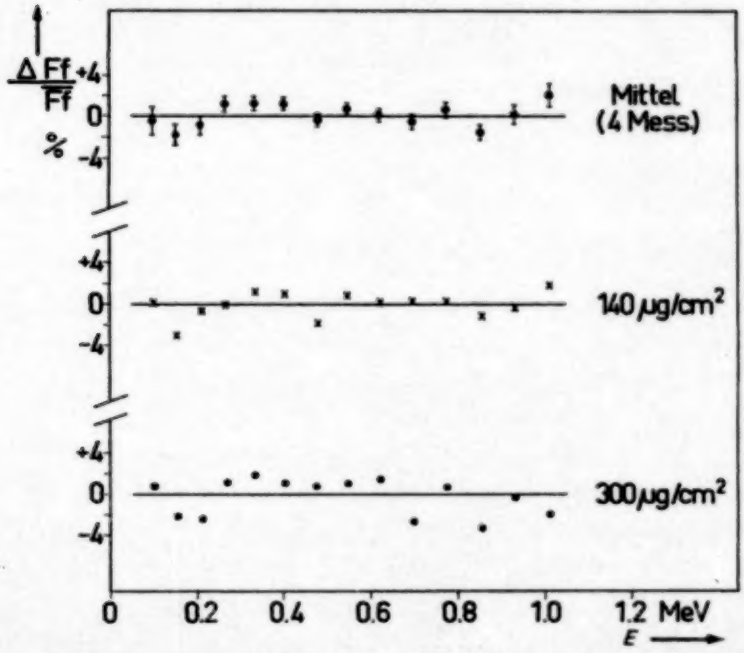

Abb. 6. Formfaktor Ff als Funktion der Positonenenergie *E*. Die obere Kurve stellt das Mittel aller Messungen dar; eingezeichnet sind die statistischen Fehler. Die unteren Kurven sind bei den rechts angeschriebenen Quellendicken aufgenommen worden.

Zur Suche nach Gamma-Strahlung wurde einmal das Spektrum der Compton-Elektronen aus einem dicken Konverter mit dem Linsenspektrometer aufgenommen, zum anderen wurde mit einem NaJ(Tl)-Szintillations-

spektrometer [10]) gemessen. In beiden Fällen zeigte sich keine Kern-Gamma-Strahlung. Abb. 5 gibt das mit dem Szintillationsspektrometer aufgenommene Spektrum wieder. Als obere Intensitätsgrenze einer etwaigen Kern-Gamma-Strahlung wurde im Bereich Gamma-Energie $E_\gamma > 0.58$ MeV 1.0 % pro Zerfall erhalten, im Bereich 0.05 MeV $< E_\gamma <$ 0.42 MeV 2.5 % pro Zerfall.

Für die Aufnahme des β-Kontinuums blieb nach den Vorversuchen Zif. 3 nur noch zu prüfen, ob die verwendeten N^{13}-Quellen dünn genug waren, um das Spektrum im untersuchten Energiebereich nicht zu verfälschen. Dazu wurde die Quellendicke variiert. Abb. 6 zeigt zwei Messungen mit verschieden dicken Quellen und das für die weitere Auswertung genommene Mittel aller Messungen. Offensichtlich spielt die Quellendicke in diesem Bereich noch keine Rolle.

Der Formfaktor wurde stets mit der gesondert gemessenen Grenzenergie von 1.190 MeV errechnet. Ein etwaiger Eichfehler des Spektrometers blieb dabei ohne wesentlichen Einfluß, weil Grenzenergie und Spektralform mit demselben Gerät bestimmt worden waren.

Die Analyse nach der Methode der kleinsten Quadrate ergab für den Fierz-Koeffizient b im N^{13}-Spektrum den Wert $b = (0.14 \pm 2.37)$ % (mittlerer statistischer Fehler).

5. Diskussion

Die hier gemessenen Werte stimmen befriedigend mit den älteren Daten [14]) überein. Das Hauptargument dafür, daß der β-Zerfall des N^{13} nicht komplex ist, liefern nicht die in Zif. 4 angegebenen oberen Intensitätsgrenzen für etwaige begleitende Gamma-Strahlung, sondern die Tatsache, daß bei Kernreaktionen keine Niveaus in C^{13} gefunden worden sind, zu denen eine Positonengruppe vom N^{13} führen könnte [14]). Das Termschema des C^{13} ist eines der am besten bekannten.

Um den Anteil der Fermi-Wechselwirkung am N^{13}-Zerfall zu erhalten, kann man den ft-Wert dieses β^+-Übergangs mit dem ft-Wert des Übergangs $0+ \to 0+$ bei O^{14} vergleichen. Bei O^{14} liegt reine Fermi-Wechselwirkung vor, und die Matrixelemente beider Übergänge lassen sich, unabhängig von Kernmodellen, lediglich aus der Ladungsunabhängigkeit der Kernkräfte errechnen. Bei O^{14} ist [15]) $|M_F|^2 = 2$, bei N^{13} $|M_F|^2 = 1$. Unbedeutende Korrekturen [16]) sind dabei vernachlässigt. Mit der Grenzenergie $E_0 = 1825 \pm 8$ keV, der Halbwertzeit $t = 72.1 \pm 0.4$ sec und dem Positonenverzweigungsverhältnis $R = (99.4 \pm 0.1)$ % [17]) errechnet sich der ft-Wert bei O^{14} zu 3264 ± 70 sec. Der β-Zerfall des N^{13} wird also zu (70 ± 2) % durch Fermi-Wechselwirkung vermittelt.

Setzt man als Beitrag der Statistik zur Fehlergrenze für b Zif. 4 den

dreifachen mittleren Fehler an, so kommt man zu der folgenden oberen Grenze für den Fierz-Koeffizienten bei Fermi-Wechselwirkung: $|b_F| < 11\ \%$.

Aus dem Verschwinden der Fierz-Terme kann man nicht, wie es vor der Entdeckung der Paritätsverletzung geschah, auf die Alternative ST(P)- oder VA-Wechselwirkung schließen. Diese Alternative ergibt sich jedoch nach Hinzunahme der folgenden beiden Annahmen: Invarianz der β-Wechselwirkung gegenüber Zeitumkehr und Gültigkeit der Zweikomponententheorie des Neutrinos.

Bei Invarianz der β-Wechselwirkung gegenüber Zeitumkehr kann man die zehn Kopplungskonstanten C_S, C'_S usw. als reell ansetzen [18]). Bei Gültigkeit der vom theoretischen Standpunkt aus sehr attraktiven Zweikomponententheorie [19]) des Neutrinos bestehen die Gleichungen

$$C_S = \pm C'_S, \qquad C_V = \pm C'_V, \qquad C_T = \pm C'_T, \qquad C_A = \pm C'_A,$$

wobei entweder stets das positive oder stets das negative Vorzeichen zu wählen ist.

Damit erhalten die Fierz-Koeffizienten die frühere [2]) Gestalt

$$b_F = \gamma \frac{2C_S C_V}{|C_S|^2+|C_V|^2} = \gamma \frac{2C'_S C'_V}{|C'_S|^2+|C'_V|^2},$$

$$b_{GT} = \gamma \frac{2C_T C_A}{|C_T|^2+|C_A|^2} = \gamma \frac{2C'_T C'_A}{|C'_T|^2+|C'_A|^2}$$

und können wieder als scharfes Maß für die ST(P)- und VA-Mischung benutzt werden. Die Rückstoßexperimente scheinen jetzt eindeutig für überwiegende VA-Wechselwirkung entschieden zu haben [20]). Aus allen Experimenten über Fierz-Interferenz zusammen gewinnt man dann die Abschätzungen

$$|C_S|/|C_V| < 5\ \%, \qquad |C'_S|/|C'_V| < 5\ \%,$$
$$|C_T|/|C_A| < 2\ \%, \qquad |C'_T|/|C'_A| < 2\ \%.$$

Es muß jedoch betont werden, daß die Gültigkeit der für diese Abschätzungen benötigten beiden Annahmen keineswegs gesichert ist.

Für die Untersuchung wurden Apparate der Deutschen Forschungsgemeinschaft mitverwendet.

Literatur

1) T. D. Lee und C. N. Yang, Phys. Rev. **104** (1956) 254
2) K. Siegbahn (Herausgeber), β- and γ-ray Spectroscopy (North-Holland Publishing Company, Amsterdam, 1955) Kap. IX und XI
3) O. Kofoed-Hansen und A. Winther, Mat. Fys. Medd. Dan. Vid. Selsk. **30** (1956) no. 20
4) R. Sherr und R. H. Miller, Phys. Rev. **93** (1954) 1076

5) R. W. P. Drever, A. Moljk und J. Scobie, Phil. Mag. **1** (1956) 942
6) J. Scobie und G. M. Lewis, Phil. Mag. **2** (1957) 1089
7) T. Yuasa, J. Laberrigue-Frolow und L. Feuvrais, J. phys. rad. **18** (1957) 559
8) Vgl. z. B.: H. Frauenfelder, R. Bobone, E. von Goeler, N. Levine, H. R. Lewis, R. N. Peacock, A. Rossi und G. DePasquali, Phys. Rev. **106** (1957) 386; **107** (1957) 909; H. Frauenfelder, A. O. Hanson, N. Levine, A. Rossi und G. DePasquali, Phys. Rev. **107** (1957) 643; J. Heintze, Z. Physik **148** (1957) 560; **150** (1958) 134; A. de-Shalit, S. Kuperman, H. J. Lipkin und T. Rothem, Phys. Rev. **107** (1957) 1459; M. Deutsch, B. Gittelmann, R. W. Bauer, L. Grodzins und A. W. Sunyar, Phys. Rev. **107** (1957) 1733; F. Boehm, T. B. Novey, C. A. Barnes und B. Stech, Phys. Rev. **108** (1957) 1497; H. Bienlein, R. Fleischmann und H. Wegener, Z. Physik **150** (1958) 80
9) H. Daniel und W. Bothe, Z. Naturforschg. **9a** (1954) 402
10) H. Daniel, Z. Naturforschg. **12a** (1957) 194
11) Vgl. z. B.: F. T. Porter, M. S. Freedman, T. B. Novey und F. Wagner jr., Phys. Rev. **103** (1956) 921
12) G. Marguin, Ann. physique **2** (1957) 318
13) B. S. Djelepov und L. N. Siranowa, Der Einfluß des atomaren elektrischen Feldes auf den β-Zerfall (Akad. Nauk S.S.S.R., Moskau, 1956)
14) Vgl. z. B.: F. Ajzenberg und T. Lauritsen, Revs. Mod. Phys. **27** (1955) 77
15) M. Goeppert Mayer und J. H. D. Jensen, Elementary Theory of Nuclear Shell Structure (John Wiley and Sons, New York, 1955) Kap. X
16) Vgl.: W. M. MacDonald, Bull. Am. Phys. Soc. **3** (1958) 48
17) J. B. Gerhart, Phys. Rev. **95** (1954) 288; R. Sherr, J. B. Gerhart, H. Horie und W. F. Hornyak, Phys. Rev. **100** (1955) 945; D. A. Bromley, E. Almqvist, H. E. Gove, A. E. Litherland, E. B. Paul und A. J. Ferguson, Phys. Rev. **105** (1957) 957; J. R. Penning und F. H. Schmidt, Phys. Rev. **94** (1954) 779
18) J. D. Jackson, S. B. Treiman und H. W. Wyld jr., Phys. Rev. **106** (1957) 517; Nuclear Physics **4** (1957) 206
19) T. D. Lee und C. N. Yang, Phys. Rev. **105** (1957) 1671; L. Landau, Nuclear Physics **3** (1957) 127; A. Salam, Nuovo Cimento **5** (1957) 299
20) W. B. Herrmannsfeldt, D. R. Maxson, P. Stähelin und J. S. Allen, Phys. Rev. **107** (1957) 641; W. B. Herrmannsfeldt, P. Stähelin und J. S. Allen, Bull. Am. Phys. Soc. **3** (1958) 52; B. W. Ridley, Nuclear Physics **6** (1958) 34; M. Goldhaber, L. Grodzins und A. W. Sunyar, Phys. Rev. (im Druck); B. Schimmer u.a., erscheint in Kürze
21) H. Daniel und U. Schmidt-Rohr, Z. Naturforschg. **12a** (1957) 750

1.E.5 *Nuclear Physics* 7 (1958) 526—551; © *North-Holland Publishing Co., Amsterdam*
Not to be reproduced by photoprint or microfilm without written permission from the publisher

DIFFUSION D'ÉLECTRONS DE HAUTE ÉNERGIE ET RÉPARTITION DE LA CHARGE ÉLECTRIQUE DU NOYAU

JEAN REIGNIER
Université Libre de Bruxelles

Reçu le 20 mars 1958

Abstract: The phase-shift η_j of the partial wave j depends on the nuclear charge distribution only through the value at the edge of the nucleus of some function $\gamma_j(r)$, solution of a Riccati equation. We give two methods to calculate this function. These methods are quickly convergent and provide a very precise value of $\gamma_j(r)$ after one or two iterations only. The zero order approximation (the same in both procedures) can be calculated very simply and is already quite close to the exact value. So far as this zero order approximation is concerned the phase-shift η_j depends on the nuclear charge distribution only through the average value of some function $\mathcal{J}_j(\kappa r)$ weighted by the nuclear charge density. We discuss the sensitivity of the differential scattering cross-section to the details of the nuclear charge distribution. At not too high energies (less than about 100 MeV for heavy nuclei), the angular distribution of the scattered electrons depends mainly of the average values $\langle \mathcal{J}_j(\kappa r) \rangle$. Finer details can be reached at higher energies but the static model of the nucleus becomes less founded. In the appendix, we show how the method may be applied to non relativistic nuclear scattering.

1. Introduction

Au cours des dernières années, de nombreux travaux expérimentaux et théoriques ont été publiés sur la diffusion d'électrons de hautes énergies par les noyaux, qui s'est révélée un outil puissant pour l'étude de multiples aspects de la structure nucléaire †. Dans ce travail, nous nous intéressons à son emploi pour déterminer la distribution de la charge électrique du noyau.

Nous considérons la diffusion d'électrons (de Dirac) de haute énergie ($E \gg 1$) †† par une répartition d'électricité statique, à symétrie sphérique (de densité $\rho(r)$) représentant un noyau. Ce modèle convient pour les noyaux moyens et lourds, pas trop déformés et aux énergies inférieures à environ 200 MeV ($\lambda\!\!\!^{-} \gtrsim 10^{-13}$ cm). Il ne tient pas compte des corrections radiatives, ni de l'influence des moments magnétique et quadrupolaire du noyau, ni de la granulation de la charge électrique du noyau: ces effets sont négligeables dans les conditions ci-dessus (voir réf. [1–7]).

La distribution angulaire des électrons diffusés est donnée par [8])

† On trouvera la plupart des références dans les articles revues de Ford et Hill [1]) et de Hofstadter [2]).

†† Dans tout le travail, les unités sont telles que $\hbar = 1$, $c = 1$, $m_e = 1$.

$$\sigma(E,\theta) = \sec^2\tfrac{1}{2}\theta|f(E,\theta)|^2,$$

$$f(E,\theta) = \frac{1}{2iE}\sum_{j=\frac{1}{2}}(j+\tfrac{1}{2})e^{2i\eta_j}(P_{j-\frac{1}{2}}(\cos\theta)+P_{j+\frac{1}{2}}(\cos\theta)). \qquad (1.1)$$

Dans le cas de la diffusion par un noyau étendu, le déphasage η_j de l'onde partielle j (de moment angulaire total j) diffère du déphasage η_j^{R} correspondant à un noyau ponctuel. La contribution du volume fini du noyau

$$\delta_j = \eta_j - \eta_j^{\mathrm{R}} \qquad (1.2)$$

n'est appréciable que si l'énergie est suffisamment élevée, en gros, supérieure à environ $140(j-\frac{1}{2})A^{-\frac{1}{3}}$ MeV, où A est le nombre de masse du noyau diffuseur. Cette contribution se calcule de la façon suivante. Soient $\phi_{1,j}(r)$ et $\phi_{2,j}(r)$ les solutions des équations radiales de Dirac pour l'électron dans le champ du noyau; soient aussi $\varphi_{1,j}^{\mathrm{R}}(r)$ et $\varphi_{2,j}^{\mathrm{R}}(r)$ ($\varphi_{1,j}^{\mathrm{I}}(r)$ et $\varphi_{2,j}^{\mathrm{I}}(r)$) les solutions régulières (irrégulières) à l'origine dans le cas d'un noyau ponctuel et $\eta_j^{\mathrm{R}}(\eta_j^{\mathrm{I}})$ le déphasage correspondant. On a

$$\operatorname{tg}\delta_j = \frac{\sin(\eta_j^{\mathrm{I}}-\eta_j^{\mathrm{R}})}{C_j+\cos(\eta_j^{\mathrm{I}}-\eta_j^{\mathrm{R}})} \qquad (1.3)$$

avec

$$C_j = -\frac{\varphi_{1,j}^{\mathrm{I}}(r_1)-\varphi_{2,j}^{\mathrm{I}}(r_1)\gamma_j(r_1)}{\varphi_{1,j}^{\mathrm{R}}(r_1)-\varphi_{2,j}^{\mathrm{R}}(r_1)\gamma_j(r_1)}, \qquad (1.4)$$

$$\gamma_j(r) = \frac{\phi_{1,j}(r)}{\phi_{2,j}(r)}; \qquad (1.5)$$

r_1 est un point quelconque extérieur au noyau; en pratique, on prend le plus petit point r_1 où la densité $\rho(r)$ peut être considérée comme négligeable (bord du noyau). On voit que le déphasage de l'onde partielle j ne dépend de la distribution d'électricité dans le noyau que par la valeur de la fonction $\gamma_j(r)$ au bord du noyau; les autres grandeurs intervenant dans le calcul correspondent à la diffusion par un noyau ponctuel et ne dépendent donc que de la charge totale.

La plupart des auteurs arrêtent l'analyse à ce stade et calculent $\gamma_j(r_1)$ en intégrant les équations radiales de Dirac et en prenant le quotient des solutions au point r_1. Sauf dans les cas les plus simples (répartition en surface, homogène, etc.) les équations radiales de Dirac sont intégrées numériquement, ce qui représente un travail considérable. On obtient ainsi des résultats très précis mais dont la dépendance en la distribution d'électricité est tout à fait masquée. Dans ce travail, nous calculons $\gamma_j(r)$ directement, sans résoudre les équations radiales de Dirac. Nous donnons deux méthodes de calcul par approximations successives qui convergent très rapidement. L'approximation d'ordre zéro (la même dans les deux procédés) est déjà très proche de la solution exacte et nous permet de déterminer, avec

une bonne approximation, la dépendance de $\gamma_j(r_1)$ et donc de η_j en la densité d'électricité nucléaire. Nous discutons ensuite la sensibilité de la section efficace de diffusion aux détails de la distribution de la charge électrique du noyau.

En utilisant les équations radiales de Dirac, il est aisé de voir que $\gamma_j(r)$ est la solution nulle à l'origine de l'équation de Riccati [9])

$$\frac{d\gamma_j}{dr} + \frac{2j+1}{r}\gamma_j + b(r)(1+\gamma_j^2) = 0 \tag{1.6}$$

où $b(r) = E - V(r)$ est l'énergie cinétique de l'électron † ($V(r)$ étant l'énergie potentielle); cette solution se comporte au voisinage de l'origine comme

$$-\frac{b(0)}{2j+2}r. \tag{1.7}$$

Bodmer [9]) résoud cette équation par approximations successives: l'approximation d'ordre n, $\gamma_{j,n}(r)$, se calcule en remplaçant dans (1.6) $\gamma_j^2(r)$ par son approximation d'ordre $n-1$, $\gamma_{j,n-1}^2(r)$, l'approximation d'ordre zéro étant identiquement nulle. Ce procédé de calcul ne converge que jusqu'au premier pôle de $\gamma_j(r)$; pour notre problème, ceci constitue essentiellement une limitation sur l'énergie des électrons. Par exemple, pour un électron $j = \frac{1}{2}$ et un noyau de plomb, le procédé ne converge qu'aux énergies inférieures à environ 90 MeV; mais la lenteur de la convergence ne le rend pratiquement utilisable qu'aux énergies inférieures à environ 20 MeV, où les erreurs relatives au premier et au second ordre sont déjà respectivement de 10 % et de 1 %. La première approximation qui dépend très simplement de $V(r)$ ne peut pas être utilisée seule pour calculer les déphasages; il est nécessaire d'itérer au moins une fois. Néanmoins, elle est intéressante quand il s'agit de comparer des répartitions entre elles; nous y reviendrons aux paragraphes 4 et 5.

Fowler [10]) a donné le premier une expression approchée de $\gamma_j(r)$ au-delà du premier pôle de la fonction. Il pose $\gamma_j(r) = \operatorname{tg} \phi_j(r)$ et, comme les pôles de $\gamma_j(r)$ sont simples, la fonction $\phi_j(r)$ n'a pas de singularité. Malheureusement, les approximations introduites dans son calcul rendent le résultat trop imprécis pour être utilisé dans le calcul des déphasages.

2. Méthode de Calcul par Approximations Successives

2.1. PRINCIPE

Nous calculons par approximations successives non pas $\gamma_j(r)$ (procédé de Bodmer) mais la différence entre $\gamma_j(r)$ et la solution exacte $\gamma_j^*(r)$ d'un

† $b(r)$ est une fonction continue positive et décroissante; elle peut éventuellement être constante de 0 à r_0 (dans le cas de répartitions ne comportant pas de charge de 0 à r_0); elle vaut $E+\alpha/r$ à l'extérieur du noyau ($\alpha = Z/137$).

problème où $b(r)$ est une constante b^*:

$$\gamma_j^*(r) = \varphi_j(b^* r) \equiv -\frac{J_{j+1}(b^* r)}{J_j(b^* r)} \tag{2.1}$$

($J_\nu(x)$ est la fonction de Bessel d'indice ν en la variable x); nous choisissons ensuite b^* de façon à assurer une convergence rapide [11, 12]).

Posons

$$x = b^* r, \quad \delta b(r) = b(r) - b^*, \quad \theta_j(x) = \gamma_j(r) - \varphi_j(x); \tag{2.2}$$

$\theta_j(x)$ est la solution nulle à l'origine de l'équation

$$\frac{d\theta_j}{dx} + \left(\frac{2j+1}{x} + 2\varphi_j(x)\right)\theta_j = -\frac{\delta b(r)}{b^*}(1+\varphi_j^2(x)) - 2\frac{\delta b(r)}{b^*}\varphi_j(x)\theta_j - \left(1+\frac{\delta b(r)}{b^*}\right)\theta_j^2. \tag{2.3}$$

Le facteur intégrant $xJ_j^2(x)$ permet de transformer (2.3) en une équation intégrale. Pour simplifier l'écriture, posons

$$\begin{aligned}
A_j(x) &= -\frac{1}{xJ_j^2(x)}\int_0^x \frac{\delta b(r')}{b^*}(J_j^2(x') + J_{j+1}^2(x'))x'\,dx', \\
B_j(f(x)) &= \frac{2}{xJ_j^2(x)}\int_0^x \frac{\delta b(r')}{b^*} f(x')J_j(x')J_{j+1}(x')x'\,dx', \\
C_j(f(x)) &= -\frac{1}{xJ_j^2(x)}\int_0^x f(x')J_j^2(x')x'\,dx', \\
D_j(f(x)) &= -\frac{1}{xJ_j^2(x)}\int_0^x \frac{\delta b(r')}{b^*} f(x')J_j^2(x')x'\,dx'.
\end{aligned} \tag{2.4}$$

L'équation intégrale en $\theta_j(x)$ s'écrit alors

$$\theta_j(x) = A_j(x) + B_j(\theta_j(x)) + C_j(\theta_j^2(x)) + D_j(\theta_j^2(x)). \tag{2.5}$$

Nous calculons $\theta_j(x)$ par approximations successives selon la loi

$$\begin{aligned}
\theta_{j,1}(x) &= A_j(x), \\
\theta_{j,n+1}(x) &= A_j(x) + B_j(\theta_{j,n}(x)) + C_j(\theta'^2_{j,n}(x)) + D_j(\theta'^2_{j,n-1}(x)),
\end{aligned} \tag{2.6}$$

où $\theta'^2_{j,n}(x)$ est défini par

$$\theta'^2_{j,n}(x) = \sum_{i=1}^{n} \sum_{\substack{k=1 \\ (k+l=i+1)}}^{i} (\theta_{j,k}(x) - \theta_{j,k-1}(x))(\theta_{j,l}(x) - \theta_{j,l-1}(x)): \tag{2.7}$$

$\theta_{j,n}(x)$ est formé des n premiers termes du développement de $\theta_j(x)$ en série des puissances d'un paramètre lié à la grandeur de $\delta b(r)/b^*$ †; $\theta'^2_{j,n}(x)$

† Si dans la définition (2.6) des approximations successives nous prenions $\theta^2_{j,n}(x)$ au lieu de $\theta'^2_{j,n}(x)$, nous verrions apparaître des termes d'ordre supérieur dès la 3ème approximation, termes qui seraient complétés dans les approximations suivantes. Les deux définitions conduisent finalement au même résultat mais la définition ci-dessus est plus facile à discuter.

contient tous les termes jusqu'à l'ordre $(\delta b(r)/b^*)^{n+1}$ du carré de $\theta_{j,n}(x)$. La fonction $\gamma_j(r)$ est ainsi représentée par le développement

$$\gamma_j(r) = \varphi_j(x)+\theta_{j,1}(x)+(\theta_{j,2}(x)-\theta_{j,1}(x))+\ldots \qquad (2.8)$$

où les termes du membre de droite sont d'ordre 0, 1, 2 . . . en un paramètre lié à la grandeur de $\delta b(r)/b^*$.

2.2. CONVERGENCE DU PROCÉDÉ ET CHOIX DE b^*

Commençons par examiner le cas simple où $b(r)$ est une constante b. Ce cas est trivial puisque nous connaissons la solution exacte

$$\gamma_j(r) = \varphi_j(y), \qquad y = br; \qquad (2.9)$$

mais il nous aide à comprendre le sens du développement (2.8) qui est alors identique au développement en série de Taylor de la fonction $\varphi_j(y)$ autour du point $x = b^* r$. La fonction $\varphi_j(x)$ est analytique entre ses pôles, lesquels sont situés aux zéros $\pm j_j^n$ de $J_j(x)$ (nous désignons par j_ν^n le $n^{\text{ième}}$ zéro positif de $J_\nu(x)$). Le développement en série de Taylor de $\varphi_j(y)$ autour du point x converge si les points $x \pm |y-x|$ appartiennent tous deux à l'un de ces intervalles. Comme le point y se trouve à la distance $|\delta b| r$ du point x, nous obtenons la règle: „le développement (2.8) converge au point r sauf si l'intervalle $(b^* \pm |\delta b|)r$ contient un des zéros j_j^n de $J_j(x)$".

Notre procédé diffère de celui de Bodmer par le fait que nous construisons par approximations successives non pas $\gamma_j(r)$ mais la différence entre $\gamma_j(r)$ et une fonction connue, $\gamma_j^*(r)$, solution (nulle à l'origine) de l'équation pour $b(r) = b^*$; nous disposons ainsi d'un paramètre b^*. Dans le cas particulier considéré ci-dessus, le procédé de Bodmer fournit la solution sous la forme d'un développement en série de Taylor à partir de l'origine alors que notre procédé fournit la solution sous la forme d'un développement en série de Taylor à partir d'un point choisi arbitrairement ($x = b^* r$). Le domaine de convergence du procédé de Bodmer est donc limité par le premier pôle (j_j^1) de $\gamma_j(r)$ alors que notre procédé peut être rendu convergent partout par un choix convenable du paramètre b^*: en un point r donné, il suffit de choisir b^* de telle façon que l'intervalle $(b^* \pm |b-b^*|)r$ ne contienne pas de zéro j_j^n. De plus, nous pouvons encore choisir b^* de façon à assurer une convergence rapide, le meilleur choix étant évidemment $b^* = b$.

Il est beaucoup plus difficile de discuter la convergence du procédé dans le cas général où $b(r)$ n'est plus une constante. Les fonctions $b(r)$ que nous avons à considérer dans ce travail ne sont pas très différentes d'une constante ($E-V(r)$ varie peu du centre au bord du noyau). On peut penser que, tout comme dans le cas $b(r) = \text{c}^{\text{te}}$, le procédé converge sauf si certains intervalles centrés sur $b^* r$ contiennent un des zéros j_j^n de $J_j(x)$. Nous nous contenterons de calculer ces intervalles par perturbation et de discuter à partir de là le choix de b^*; nous vérifierons ensuite ces résultats sur un exemple relatif au

problème qui nous intéresse. Considérons un point R où nous calculons $\gamma_j(r)$ selon le développement (2.8):

$$\gamma_j(R) = \varphi_j(X)+\theta_{j,1}(X)+(\theta_{j,2}(X)-\theta_{j,1}(X))+\ldots, \tag{2.10}$$

avec $X = b^* R$. Associons à $b(r)$ une fonction $u_0(b^*, R)$ constante en la variable r et définie par

$$u_0(b^*, R) = \frac{\int_0^R b(r')r'[J_j^2(x')+J_{j+1}^2(x')]\mathrm{d}r'}{\int_0^R r'[J_j^2(x')+J_{j+1}^2(x')]\mathrm{d}r'}. \tag{2.11}$$

La solution nulle à l'origine de l'équation (1.6) avec $b(r) = u_0(b^*, R)$ est $\varphi_j(u_0(b^*, R)r)$ et son développement (2.8) au point R s'écrit

$$\varphi_j(u_0(b^*, R)R) = \varphi_j(X)+\eta_{j,1}(X)+(\eta_{j,2}(X)-\eta_{j,1}(X))+\ldots; \tag{2.12}$$

ce développement converge sauf si l'intervalle $(b^*\pm|u_0(b^*, R)-b^*|)R$ contient un des zéros j_j^n de $J_j(x)$. La définition (2.11) de $u_0(b^*, R)$ entraîne

$$\theta_{j,1}(X) = \eta_{j,1}(X). \tag{2.13}$$

Les fonctions $\theta_{j,1}(x)$ et $\eta_{j,1}(x)$ sont égales à l'origine et en X. Si $b(r)$ ne diffère pas trop d'une constante, ces fonctions ne sont pas très différentes entre 0 et X; les corrections suivantes $[(\theta_{j,2}(X)-\theta_{j,1}(X)), \ldots$ pour (2.10) et $(\eta_{j,2}(X)-\eta_{j,1}(X)), \ldots$ pour (2.12)], qui se construisent à l'aide des valeurs prises respectivement par $b(r)$ et $\theta_{j,1}(x)$, et par $u_0(b^*, R)$ et $\eta_{j,1}(x)$, pour r variant entre 0 et R, sont du même ordre de grandeur et les séries (2.10) et (2.12) convergent sensiblement en même temps. Nous obtenons ainsi une règle approchée: „le développement converge au point r sauf si l'intervalle $(b^*\pm|u_0(b^*, r)-b^*|)r$ contient un des zéros j_j^n de $J_j(x)$". De plus, ce raisonnement indique que $\varphi_j(u_0(b^*, r)r)$ doit être une approximation de $\gamma_j(r)$; nous vérifierons qu'il en est bien ainsi dans le cas de la diffusion d'électrons par les noyaux.

Considérons maintenant le choix de b^*; d'après la règle de convergence, pour calculer $\gamma_j(r)$ au point R, on prendra

$$b^* = u_0(b^*, R). \tag{2.14}$$

En pratique, comme ce résultat est de toute façon un résultat approché et comme la moyenne $u_0(b^*, R)$ est peu sensible au choix de b^* quand $b(r)$ varie peu de 0 à R, on prendra plus simplement

$$b^* = u_0(\kappa, R) \qquad (b(R) \leqq \kappa \leqq b(0)) \tag{2.15}$$

où κ est une quelconque des valeurs de $b(r)$ de 0 à R.

2.3. EXEMPLE

Vérifions ces conclusions sur un exemple simple où nous pouvons calculer la solution exactement. Prenons une énergie potentielle en escalier

$$V(r) = \begin{cases} V_1 & \text{pour } r < r_0 \\ V_2 & \text{pour } r_0 < r < R \end{cases} \tag{2.16}$$

et calculons $\gamma_{\frac{1}{2}}(r)$ au point R pour différentes valeurs de l'énergie totale E. Prenons des données numériques en accord avec le problème considéré dans ce travail †:

$$\begin{aligned} &R = 1.8\times 10^{-2}, \qquad r_0 = R/2 \\ &V_1 = -48, \qquad\quad V_2 = -32 \\ &0 \leqq E \leqq 400 \qquad \text{(de 40 en 40)}. \end{aligned} \tag{2.17}$$

Dans le tableau 1 ci-dessous, nous donnons, pour chaque valeur de l'énergie, successivement: la valeur de b^* utilisée dans le calcul (c'est-à-dire, $u_0(\kappa, R)$ avec $\kappa = E - V_2$), les approximations d'ordre zéro $[\gamma_{\frac{1}{2},0}(R) = \varphi_{\frac{1}{2}}(u_0(\kappa, R)R)]$, un $(\gamma_{\frac{1}{2},1}(R))$ et deux $(\gamma_{\frac{1}{2},2}(R))$, la solution exacte $(\gamma_{\frac{1}{2}}(R))$, les erreurs relatives de ces différentes approximations (δ_0, δ_1 et δ_2) en pour-mille, et une autre erreur relative

$$\Delta_{\frac{1}{2}} = \frac{|\gamma_{\frac{1}{2}}(R) - \gamma_{\frac{1}{2},0}(R)|}{1+\gamma_{\frac{1}{2}}^2(R)} \tag{2.18}$$

qui s'introduira plus loin et qui est également donnée en pour-mille.

TABLEAU 1

E	$\frac{-V^*}{(b^*=E-V^*)}$	$\gamma_{\frac{1}{2},0}(R)$	$\gamma_{\frac{1}{2},1}(R)$	$\gamma_{\frac{1}{2},2}(R)$	$\gamma_{\frac{1}{2}}(R)$	δ_0 (‰)	δ_1 (‰)	δ_2 (‰)	$\Delta_{\frac{1}{2}}$ (‰)
0	34.0673	−0.2097	−0.2098	−0.2099	−0.2099	0.81	0.53	0.07	0.16
40	34.3612	−0.5105	−0.5108	−0.5111	−0.5111	1.2	0.70	0.04	0.48
80	34.9614	−1.0276	−1.0288	−1.0301	−1.0302	2.5	1.3	0.08	1.2
120	35.9814	−3.2387	−3.2597	−3.2779	−3.2795	12.	6.0	0.49	3.5
160	37.4300	+2.0060	+1.9823	+1.9667	+1.9662	20.	8.2	0.26	8.1
200	38.9062	+0.2046	+0.2004	+0.1975	+0.1975	36.	15.	0.35	6.8
240	39.7676	−0.5338	−0.5353	−0.5372	−0.5371	6.3	3.4	0.06	2.6
280	39.9882	−1.9065	−1.9070	−1.9096	−1.9093	1.5	1.2	0.17	0.61
320	40.0000	+4.8608	+4.8609	+4.8658	+4.8677	1.4	1.4	0.39	0.28
360	39.9869	+0.6280	+0.6283	+0.6292	+0.6293	2.1	1.6	0.08	0.93
400	39.8856	−0.1903	−0.1898	−0.1892	−0.1892	6.2	3.2	0.03	1.1

Dans tous les cas considérés, le procédé de calcul converge très rapidement. L'approximation d'ordre zéro est très proche de la solution exacte, l'erreur relative maximum étant de 3.6 % seulement. Remarquons que l'erreur $\Delta_{\frac{1}{2}}$ est toujours inférieure à 1 %. La correction du premier ordre est faible: b^* est en effet choisi dans ce sens; elle n'améliore pas sensiblement la solution;

† Pour l'or, une répartition homogène de la charge et un rayon de $1.20\times 10^{-13}\, A^{\frac{1}{3}}$ cm, on a

$$R = 1.81\times 10^{-2}, \quad V(0) = -3\alpha/2R \simeq -48, \quad V(R) = -\alpha/R \simeq -32.$$

Le domaine énergétique envisagé va de 0 à environ 200 MeV.

en gros, elle réduit l'erreur de moitié. La correction du second ordre conduit à une excellente approximation, qui diffère de moins de 0.5 $^0/_{00}$ de la solution exacte.

Cette méthode nous permet de calculer $\gamma_j(r)$ avec une grande précision à l'aide de quelques approximations seulement. Les calculs sont beaucoup plus simples qu'une intégration numérique des équations radiales de Dirac. En particulier, la solution approchée

$$\gamma_{j,0}(r) = \varphi_j(u_0(\kappa, r)r) \qquad (b(r) \leqq \kappa \leqq b(0)) \tag{2.19}$$

constitue déjà une bonne approximation de $\gamma_j(r)$ et ne nécessite que le calcul d'une seule intégrale dépendant de l'énergie potentielle de l'électron dans le noyau:

$$\int_0^r V(r')r'\,[J_j^2(\kappa r') + J_{j+1}^2(\kappa r')]\,\mathrm{d}r'. \tag{2.20}$$

Nous allons maintenant étudier cette solution approchée plus en détail et examiner sa validité dans le problème de la diffusion d'électrons de hautes énergies par les noyaux.

3. Solution Approchée Obtenue Directement

3.1. CALCUL

Nous cherchons la solution de l'équation (1.6) qui se comporte au voisinage de l'origine comme (1.7). Si $b(r)$ était une constante, la solution cherchée serait $\varphi_j(br)$. Dans le cas général, nous pouvons essayer de trouver une solution du même type et poser

$$\gamma_j(r) = \varphi_j(z). \tag{3.1}$$

Il est évident que $z(r)$ ne sera en général ni c.^{te} $\cdot\, r$ ni $b(r)r$. Posons encore

$$z(r) = u(r)r; \tag{3.2}$$

$\varphi_j(z)$ satisfait à l'équation (obtenue par dérivation)

$$\begin{aligned} &\frac{\mathrm{d}\varphi_j(z)}{\mathrm{d}r} + \frac{2j+1}{r}\varphi_j(z) + (1+\varphi_j^2(z))\left(u(r) + r\,\frac{\mathrm{d}u(r)}{\mathrm{d}r}\right) \\ &\qquad + \frac{2j+1}{u(r)}\,\frac{\mathrm{d}u(r)}{\mathrm{d}r}\,\varphi_j(z) = 0 \end{aligned} \tag{3.3}$$

et se comporte à l'origine comme

$$-\frac{u(0)}{2j+2}r. \tag{3.4}$$

En comparant (1.6) et (1.7) à (3.3) et (3.4), nous voyons que $\varphi_j(z)$ sera la solution cherchée de (1.6) si $u(r)$ est la solution qui vaut $b(0)$ à l'origine de l'équation

$$\frac{\mathrm{d}u(r)}{\mathrm{d}r} = \frac{b(r)-u(r)}{r f_j(z)} \tag{3.5}$$

avec

$$f_j(x) = 1 - \frac{2j+1}{x} \frac{J_j(x)J_{j+1}(x)}{J_j^2(x)+J_{j+1}^2(x)}; \tag{3.6}$$

$f_j(x)$ est une fonction analytique de x, positive pour toute valeur de x; elle vaut $(2j+2)^{-1}$ à l'origine, 1 aux zéros de $J_j(x)$ et de $J_{j+1}(x)$ et tend vers 1 quand x tend vers l'infini. Nous représentons ci-dessous (fig. 1) les fonctions $f_{\frac{1}{2}}(x)$ et $f_{\frac{3}{2}}(x)$.

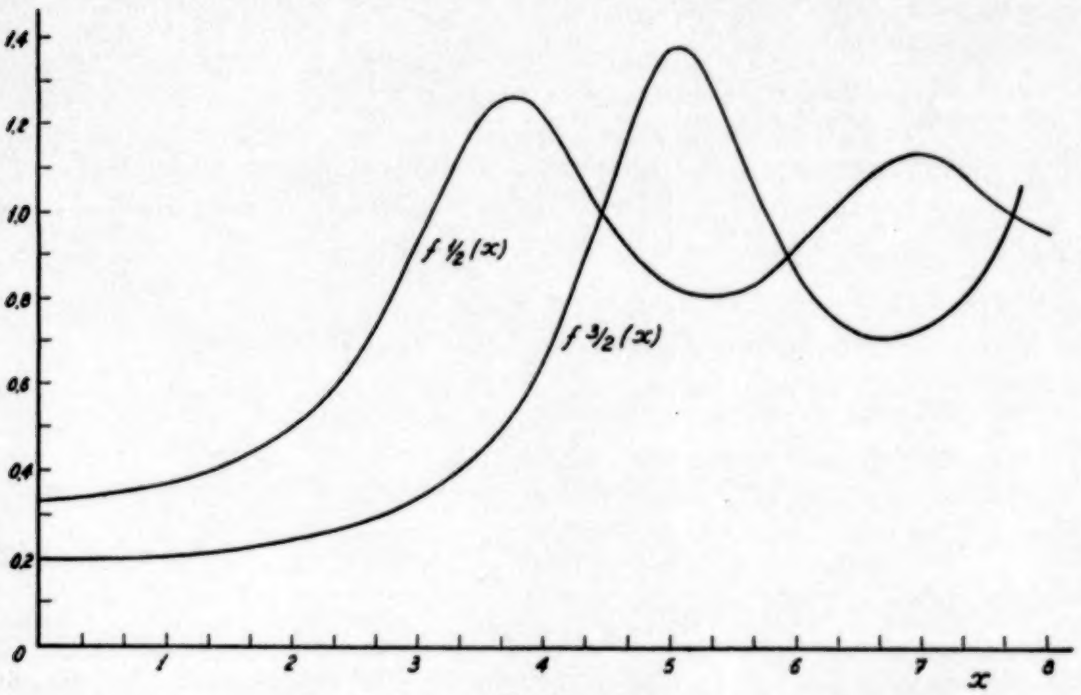

Fig. 1

Introduisons la variable x qui dépend d'un paramètre b^* (positif)

$$x = b^* r \tag{3.7}$$

et ajoutons et soustrayons $(b(r)-u(r))/rf_j(x)$ à l'équation (3.5). A l'aide du facteur intégrant [13])

$$\int_0^r r'[J_j^2(x')+J_{j+1}^2(x')]\mathrm{d}r' = r^2[J_j^2(x)+J_{j+1}^2(x)]f_j(x), \tag{3.8}$$

nous transformons l'équation ainsi modifiée en une équation intégrale:

$$u(r) = u_0(b^*, r)+u_1(b^*, r) \tag{3.9}$$

avec

$$u_0(b^*, r) = \frac{\int_0^r b(r')r'[J_j^2(x')+J_{j+1}^2(x')]\mathrm{d}r'}{\int_0^r r'[J_j^2(x')+J_{j+1}^2(x')]\mathrm{d}r'}, \tag{3.10}$$

$$u_1(b^*, r) = \frac{\int_0^r (b(r')-u(r'))\left(\frac{f_j(x')}{f_j(z')}-1\right)[J_j^2(x')+J_{j+1}^2(x')]\,r'\,dr'}{\int_0^r [J_j^2(x')+J_{j+1}^2(x')]\,r'\,dr'}. \quad (3.11)$$

La solution $u(r)$ de l'équation (3.9) vaut $b(0)$ à l'origine et est donc la solution cherchée. On peut résoudre cette équation par approximations successives; numériquement, les calculs ne présentent aucune difficulté et le procédé converge très rapidement ($u_0(b^*, r)$ étant déjà une bonne approximation); ceci fournit une autre méthode de calcul de $\gamma_j(r)$ par approximations successives. Nous nous limiterons à $u_0(b^*, r)$ et nous allons montrer qu'on peut choisir b^* de façon à obtenir une bonne approximation.

3.2 QUELQUES PROPRIÉTÉS

La fonction $b(r)$ est continue, positive et décroissante †, et nous pouvons la représenter au voisinage de l'origine par

$$b(r) = b(0)+a_0 r^s+O(>s) \qquad (s>0, a_0<0). \quad (3.12)$$

La solution $u(r)$ est alors, au voisinage de l'origine,

$$u(r) = b(0)+\frac{2j+2}{2j+2+s} a_0 r^s+O(>s) \quad (3.13)$$

et on a

$$b(0) \geqq u(r) \geqq b(r), \qquad \frac{du(r)}{dr} \leqq 0; \quad (3.14)$$

les relations (3.14) valent également pour toutes les valeurs de r en vertu de la continuité de $b(r)$ et de $u(r)$. Il en résulte la propriété suivante: en tout point R tel que

$$b(0)R \leqq X_j, \quad (3.15)$$

où X_j est le premier maximum de $f_j(x)(j > -\frac{1}{2})$, on a ††

$$u_0(b(R), R) \leqq u(R) \leqq u_0(b(0), R). \quad (3.16)$$

Pour le voir, écrivons (3.11) au point R sous la forme

$$u_1(b^*, R)\int_0^R r[J_j^2(x)+J_{j+1}^2(x)]\,dr = \int_0^R \frac{du(r)}{dr} r^2[J_j^2(x)+J_{j+1}^2(x)](f_j(x)-f_j(z))\,dr;$$

le premier membre a le signe de $u_1(b^*, R)$ et dans le second membre

† Le cas où $b(r)$ est constante de 0 à r_0 (pas de charge de 0 à r_0) ne pose pas de problème spécial: $u(r) = b(r) =$ c.te de 0 à r_0 et on peut raisonner comme ci-dessous à partir du point r_0; les relations (3.14) sont encore valables.

†† L'égalité n'a lieu pour $R > 0$ que si $b(r) =$ c.te ou si $j = -\frac{1}{2}$.

$$\frac{du(r)}{dr} r^2[J_j^2(x)+J_{j+1}^2(x)]$$

est constamment négatif. Prenons $b^* = b(0)$; quel que soit $r \leqq R$,

$$X_j \geqq b(0)r \geqq u(r)r,$$

et comme $f_j(x)$ est croissante ($j > -\frac{1}{2}$, $0 < x < X_j$), il en résulte que

$$f_j(x) \geqq f_j(z),$$

c'est-à-dire que †

$$u_1(b(0), R) \leqq 0. \tag{3.17a}$$

De même, en prenant $b^* = b(R)$, on a †

$$u_1(b(R), R) \geqq 0. \tag{3.17b}$$

En tenant compte de (3.9), les inégalités (3.17a, b) démontrent (3.16).

De plus, comme $u_0(b^*, r)$ est une fonction continue de b^*, il résulte de (3.16) qu'il correspond au point R une valeur b_1^* de b^* comprise entre $b(0)$ et $b(R)$ et telle que

$$u(R) = u_0(b_1^*, R) \qquad (b(R) \leqq b_1^* \leqq b(0)). \tag{3.18}$$

Notons en passant quelques valeurs de X_j intéressantes pour notre problème:

j	$\frac{1}{2}$	$\frac{3}{2}$	$\frac{5}{2}$	$\frac{7}{2}$	$\frac{9}{2}$
X_j	3.8	5.1	6.4	7.6	8.8

(3.19)

Elles montrent, par exemple, que dans le cas de la diffusion d'électrons par le plomb, avec un modèle nucléaire sphère homogène de rayon 1.2×10^{-13} $A^{\frac{1}{3}}$ cm, la condition (3.15) est satisfaite pour les ondes partielles $j = \frac{1}{2}, \frac{3}{2}, \frac{5}{2}, \frac{7}{2}$ et $\frac{9}{2}$ tant que l'énergie reste inférieure à 80, 115, 155, 185 et 220 MeV, respectivement.

La relation (3.18) est valable indépendamment de la condition (3.15). Appliquons le théorème de la moyenne à (3.11) au point R:

$$u_1(b^*, R) = \left\{\frac{du(r)}{dr} r(f_j(x)-f_j(z))\right\}_{r_0} \qquad 0 \leqq r_0 \leqq R; \tag{3.20}$$

r_0 est un certain point compris entre 0 et R et nous supposons que $r_0 = r_0(b^*, R)$ est une fonction continue de b^* sur le segment $u(R) \leqq b^* \leqq u(0)$. Faisons varier b^* depuis $u(0)$ jusque $u(R)$; $r_0 = r_0(b^*)$ varie de $r_0(u(0))$ à $r_0(u(R))$ et on a

$$\begin{aligned} b^*_{\text{initial}} &= u(0) \geqq u[r_0(u(0))], \\ b^*_{\text{final}} &= u(R) \leqq u[r_0(u(R))]. \end{aligned} \tag{3.21}$$

† L'égalité n'a lieu pour $R > 0$ que si $b(r) = \text{c.}^{\text{te}}$ ou si $j = -\frac{1}{2}$.

Au cours du passage de b^* de $u(0)$ à $u(R)$, il y a renversement de l'inégalité entre b^* et $u(r_0(b^*))$; il existe donc au moins une valeur b_1^* de b^* comprise entre $u(0)$ et $u(R)$ et telle que

$$b_1^* = u[r_0(b_1^*)]. \tag{3.22}$$

Pour cette valeur de b^*, $x(r_0)$ est égal à $z(r_0)$ et $u_1(b_1^*, R)$ s'annule. A un point R donné, il correspond une valeur b_1^* de b^* comprise entre $u(0)$ et $u(R)$ et donc, a fortiori, entre $b(0)$ et $b(R)$ et telle que

$$u(R) = u_0(b_1^*, R) \qquad (b(R) \leqq b_1^* \leqq b(0)), \tag{3.23}$$

c'est-à-dire telle que

$$\gamma_j(R) = \varphi_j(u_0(b_1^*, R)R). \tag{3.24}$$

Remarquons que $\varphi_j(u_0(b_1^*, r)r)$ n'est pas solution de l'équation (1.6) mais à l'origine et au point R elle a même valeur que la solution cherchée.

3.3. VALIDITÉ DE LA SOLUTION APPROCHÉE

Nous ignorons la valeur exacte à donner au paramètre b^* pour satisfaire à (3.24). Nous faisons l'approximation de prendre pour b^* une valeur quelconque comprise entre les bornes de $b(r)$. La solution ainsi obtenue est exacte si $b(r) = \text{c.}^{\text{te}}$ ou si $j = -\frac{1}{2}$ (cas non physique); on retrouve alors les solutions qu'on pouvait calculer directement ($\varphi_j(br)$ et $-\operatorname{tg}\{\int_0^r b(r')\mathrm{d}r'\}$, respectivement). En général, nous commettons une erreur δb^* sur b^* et il en résulte des erreurs $\delta u(r)$ sur $u(r)$, $\delta z(r)$ sur $z(r)$ et $\delta\gamma_j(r)$ sur $\gamma_j(r)$. On a

$$\delta\gamma_j(r) = \delta\varphi_j(z) = \frac{\mathrm{d}\varphi_j(z)}{\mathrm{d}z}\,\delta z(r) = -\delta z(r)\left\{1+\varphi_j^2(z)+\frac{2j+1}{z}\,\varphi_j(z)\right\}, \tag{3.25}$$

$$\frac{\delta\gamma_j(r)}{1+\gamma_j^2(r)} = -r\delta u(r) f_j(z). \tag{3.26}$$

Considérons une fonction $b(r)$ du type

$$b(r) = b(0)+r^s(a_0+a_1 r+\ldots) \qquad (s>0) \tag{3.27}$$

($a_0, a_1, \ldots$ sont des constantes) et définissons les fonctions

$$y_j^{(n)}(x) = \frac{\int_0^x x'^{n+1}[J_j^2(x')+J_{j+1}^2(x')]\,\mathrm{d}x'}{x^n\int_0^x x'\,[J_j^2(x')+J_{j+1}^2(x')]\,\mathrm{d}x'}. \tag{3.28}$$

Ces fonctions $y_j^{(n)}(x)$ sont continues, positives et inférieures à 1; elles prennent la valeur $(2j+2)/(2j+n+2)$ à l'origine et tendent asymptotiquement vers $(n+1)^{-1}$. Nous représentons ci-dessous (fig. 2) les fonctions $y_{\frac{1}{2}}^{(2)}(x)$, $y_{\frac{1}{2}}^{(4)}(x)$ et $y_{\frac{3}{2}}^{(2)}(x)$; les autres $y_j^{(n)}(x)$ ont la même allure générale. On a

$$u_0(b^*, r) = b(0)+r^s(a_0\, y_j^{(s)}(x)+a_1 r y_j^{(s+1)}(x)+\ldots), \tag{3.29}$$

$$\frac{\delta\gamma_j(r)}{1+\gamma_j^2(r)} = -r^{s+1}\{a_0\,\delta y_j^{(s)}(x)+a_1\,r\delta y_j^{(s+1)}(x)+\ldots\}f_j(z). \qquad (3.30)$$

Majorons le second membre de cette dernière expression:

$$\Delta_j \equiv \frac{|\delta\gamma_j(r)|}{1+\gamma_j^2(r)} < r^{s+2} f_j(z)\left\{|a_0|\left|\frac{\mathrm{d}y_j^{(s)}(x)}{\mathrm{d}x}\right|_{\max} + |a_1| r\left|\frac{\mathrm{d}y_j^{(s+1)}(x)}{\mathrm{d}x}\right|_{\max}+\ldots\right\}(b(0)-b(r)). \qquad (3.31)$$

L'erreur commise est d'autant plus grande que la variation de $b(r)$ est plus grande. Dans le cas de la diffusion d'électrons par les noyaux, cette variation

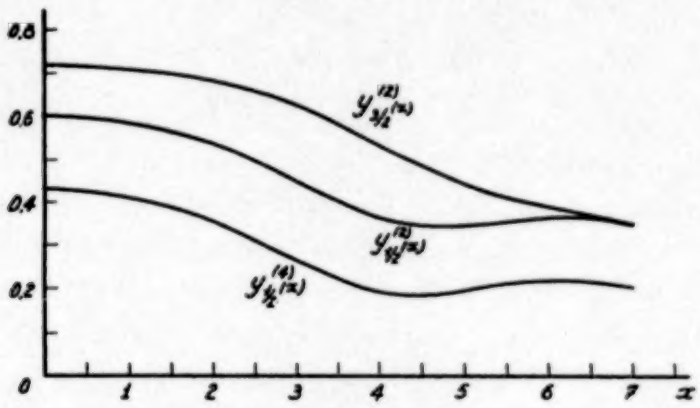

Fig. 2

est suffisamment faible pour obtenir une bonne approximation. Considérons, par exemple, un noyau représenté par une sphère homogène de rayon R et calculons l'erreur maximum Δ_j commise au bord du noyau ($r = R$). On a

$$b(r) = \begin{cases} E+\dfrac{\alpha}{2R}\left(3-\dfrac{r^2}{R^2}\right) & (r \leqq R) \\ E+\dfrac{\alpha}{r} & (r \geqq R) \end{cases} \qquad \left(\alpha = \frac{Z}{137}\right), \qquad (3.32)$$

et, d'après (3.31),

$$\Delta_j < \frac{\alpha^2}{4}\left|f_j(x)\,\frac{\mathrm{d}y_j^{(2)}(x)}{\mathrm{d}x}\right|_{\max}. \qquad (3.33)$$

Les courbes des figures 1 et 2 montrent que le coefficient de $\alpha^2/4$ vaut 0.13 pour $j = \frac{1}{2}$ et 0.15 pour $j = \frac{3}{2}$. Pour le plomb ($\alpha \approx 0.6$) ceci donne

$$\Delta_{\frac{1}{2}} < 1.2\ \%, \qquad \Delta_{\frac{3}{2}} < 1.4\ \%.$$

Nous voyons que l'erreur maximum Δ_j commise au bord du noyau croît proportionnellement à Z^2 et qu'elle est de l'ordre de 1 % pour les noyaux lourds.

3.4. EXEMPLE ET DISCUSSION

Nous avons déjà vérifié sur un cas particulier (§ 2.3) la grande précision de la solution approchée $\varphi_j(u_0(\kappa, r)r)$ $(b(r) \leqq \kappa \leqq b(0))$ quand les données numériques correspondent aux conditions de la diffusion d'électrons par les noyaux. Considérons maintenant le cas d'une répartition homogène de rayon R et calculons $\gamma_j(R)$ et δ_j pour différentes valeurs de l'énergie et différentes ondes partielles, exactement et au moyen de la solution approchée. Nous allons jusqu'au calcul des déphasages afin de mieux juger du domaine de validité de la solution approchée. On peut calculer $\gamma_j(R)$ exactement en intégrant les équations radiales de Dirac (solution sous forme de série) et en prenant le quotient des solutions. Les déphasages δ_j se calculent à l'aide des formules (1.3) et (1.4) et des valeurs calculées des $\gamma_j(R)$. Nous utilisons les tables des fonctions coulombiennes et des déphasages coulombiens publiées par Glassgold et Mack [14]). Nous considérons le cas de l'or ($\alpha = 0.57647$) qui est l'élément de plus grand Z figurant dans ces tables (c'est donc le plus défavorable pour la solution approchée), les valeurs $ER = 1, 2, 3$ (les tables ne vont pas au-delà de $ER = 3$) † et les ondes partielles $j = \frac{1}{2}, \frac{3}{2}, \frac{5}{2}$ et $\frac{7}{2}$, c'est-à-dire celles qui sont appréciablement influencées à la plus haute énergie. Nous calculons la solution approchée pour les valeurs extrêmes de κ:

$$\kappa = b(0) = E + \frac{3\alpha}{2R}, \qquad \kappa = b(R) = E + \frac{\alpha}{R}; \tag{3.34}$$

conformément à ce que nous avons vu précédemment (3.16 et 3.19), les résultats correspondants encadrent le résultat exact (tableau 2). En ce qui concerne les $\gamma_j(R)$, nous vérifions que l'erreur Δ_j est toujours inférieure à 1 %.

Discutons maintenant la validité de la solution approchée pour le calcul des déphasages. La précision requise sur les déphasages dépend des conditions du problème et notamment de l'énergie des électrons et de l'angle de diffusion considéré; elle est d'autant plus grande que l'énergie est plus élevée et l'angle plus grand. Yennie *et al.* [8]) donnent une relation approchée: l'erreur sur les déphasages doit être inférieure à

$$0.2\, E \sqrt{\sigma_{\min}}\, \varepsilon \tag{3.35}$$

où $\sigma_{\min}$ est la section efficace de diffusion au plus grand angle envisagé, et ε l'erreur relative admise sur $\sigma_{\min}$; mais d'après ces auteurs, la relation serait „trop pessimiste". Dans la comparaison avec l'expérience, on admet une erreur relative de 10 % au plus grand angle considéré (110° généralement); l'erreur est alors tout à fait négligeable aux angles plus petits. Une précision de l'ordre de 10^{-4} radian sur les déphasages suffit dans tous les cas. Le tableau 2 montre que nous obtenons cette précision pour les δ_j inférieurs

† Pour un rayon $R = 1.2 \times 10^{-13}\, A^{\frac{1}{3}}$ cm, les énergies considérées sont 28, 57 et 85 MeV.

à environ 10^{-2} radian, c'est-à-dire pour les dernières ondes partielles dont il faut tenir compte dans le calcul de la section efficace de diffusion. Mais une telle précision n'est pas toujours requise; ainsi, pour $ER \lesssim 2$ on peut admettre une erreur de $2-3\times10^{-3}$ radian et les déphasages approchés (tableau

TABLEAU 2

ER	j	$\gamma_j(R)$	Δ_j(%)	δ_j (radian)	$\lvert\Delta\delta_j\rvert$ (10^{-4} rad)	ER	j	$\gamma_j(R)$	Δ_j(%)	δ_j (radian)	$\lvert\Delta\delta_j\rvert$ (10^{-4} rad)
1	$\frac{1}{2}$	−0.7221		−0.2389		2	$\frac{5}{2}$	−0.4304		−0.0041	
		−0.7204	0.12	−0.2407	18			−0.4302	0.02	−0.0042	1
		−0.7235	0.09	−0.2374	15			−0.4307	0.03	−0.0040	1
	$\frac{3}{2}$	−0.3632		−0.0068			$\frac{7}{2}$	−0.3160		−0.0002	
		−0.3630	0.02	−0.0069	1			−0.3159	0.00	−0.0002	0
		−0.3636	0.03	−0.0067	1			−0.3161	0.01	−0.0002	0
	$\frac{5}{2}$	−0.2457		−0.0001		3	$\frac{1}{2}$	+1.1522		−0.7038	
		−0.2456	0.01	−0.0001	0			+1.1660	0.59	−0.7082	44
		−0.2458	0.01	−0.0001	0			+1.1482	0.17	−0.7025	13
	$\frac{7}{2}$	−0.1863		−0.0000			$\frac{3}{2}$	−1.5595		−0.1569	
		−0.1863	0.00	−0.0000	0			−1.5529	0.19	−0.1603	34
		−0.1863	0.01	−0.0000	0			−1.5657	0.18	−0.1538	31
2	$\frac{1}{2}$	−2.6499		−0.4997			$\frac{5}{2}$	−0.6975		−0.0266	
		−2.6212	0.35	−0.5044	47			−0.6970	0.03	−0.0272	6
		−2.6667	0.21	−0.4970	27			−0.6983	0.05	−0.0256	10
	$\frac{3}{2}$	−0.6985		−0.0580			$\frac{7}{2}$	−0.4750		−0.0027	
		−0.6977	0.06	−0.0590	10			−0.4749	0.01	−0.0028	1
		−0.6996	0.07	−0.0568	12			−0.4753	0.02	−0.0026	1

Dans chaque case, on a en descendant: le résultat exact, le résultat approché calculé avec $V^* = -\alpha/R$ et l'erreur correspondante, le résultat approché calculé avec $V^* = -3\alpha/2R$ et l'erreur correspondante.

2) sont tout à fait satisfaisants. Nous voyons donc que nous pouvons utiliser la solution approchée pour le calcul des déphasages des ondes partielles $j \approx ER$. Les autres déphasages sont à calculer au moyen d'une solution plus précise (solution qui peut être fournie par l'un ou l'autre de nos procédés par approximations successives). Notons encore que pour une valeur donnée de ER, les résultats sont meilleurs pour les éléments plus légers que l'or, l'erreur commise sur $\gamma_j(R)$ étant proportionnelle à Z^2.

Un résultat intéressant du tableau 2 est que tous les déphasages δ_j approchés sont exacts à moins de 5×10^{-3} radian près. Nous établissons ainsi que, au moins jusqu'à une précision de cet ordre, le déphasage de l'onde partielle j ne dépend de la répartition de la charge électrique dans le noyau que par

$$\int_0^{r_1} V(r) r [J_j^2(\kappa r) + J_{j+1}^2(\kappa r)] \mathrm{d}r \tag{3.36}$$

où r_1 est un point extérieur au noyau ($V(r_1) = -\alpha/r_1$), $\kappa = E - V^*$, V^* étant une quelconque des valeurs de l'énergie potentielle $V(r)$ de l'électron dans le noyau. Ce point est discuté en détail au paragraphe suivant.

4. Conditions d'Équivalence

Par définition, deux répartitions sont „équivalentes du point de vue de l'onde partielle j et à l'énergie E" si le déphasage de cette onde partielle est le même pour les deux répartitions à l'énergie considérée. D'après le procédé de calcul des déphasages, la condition d'équivalence de deux répartitions du point de vue de l'onde partielle j et à l'énergie E est l'égalité des fonctions $\gamma_j(r)$ correspondantes à l'extérieur des deux répartitions (où le potentiel est coulombien). En calculant ces fonctions par les méthodes développées aux paragraphes précédents, nous obtenons une condition d'équivalence approchée: si les deux répartitions donnent même valeur à (3.36), les déphasages correspondants sont égaux à moins de 5×10^{-3} radian près. En intégrant (3.36) deux fois par parties, en utilisant l'équation au potentiel et le fait que le potentiel est coulombien en r_1 pour les deux répartitions, on obtient [15]) comme condition d'équivalence, l'égalité de †

$$\int_0^{\infty} \rho(r) r^2 \mathscr{J}_j(\kappa r) \mathrm{d}r; \tag{4.1}$$

$\rho(r)$ est la densité d'électricité nucléaire et $\mathscr{J}_j(x)$ est définie par

$$\mathscr{J}_j(x) \equiv \int_0^x \left\{ J_j^2(x') + J_{j+1}^2(x') - \frac{2j+1}{x'} J_j(x') J_{j+1}(x') \right\} \mathrm{d}x'. \tag{4.2}$$

La fonction $\mathscr{J}_j(x)$ est nulle à l'origine, positive et croissante pour $x > 0$. Il est commode de multiplier (4.1) par $4\pi/Ze$, ce qui permet de dire: la condition d'équivalence (approchée) du point de vue de l'onde partielle j et à l'énergie E est l'égalité des moyennes de la fonction $\mathscr{J}_j(\kappa r)$ prise sur le noyau avec les fonctions de poids $\rho(r)$,

$$\langle \mathscr{J}_j(\kappa r) \rangle = \frac{\int_0^{\infty} \rho(r) \mathscr{J}_j(\kappa r) r^2 \, \mathrm{d}r}{\int_0^{\infty} \rho(r) r^2 \, \mathrm{d}r}. \tag{4.3}$$

Le déphasage de l'onde partielle j ne dépend de la densité d'électricité nucléaire que par $\langle \mathscr{J}_j(\kappa r) \rangle$. Il est peu sensible aux valeurs centrales de la densité: du fait que $\mathscr{J}_j(x)$ est nulle à l'origine et ensuite toujours croissante, les valeurs superficielles de $\rho(r)$ sont beaucoup plus importantes que les

† La limite supérieure de l'intégrale est r_1 mais comme $\rho(r > r_1) = 0$, nous pouvons l'étendre jusqu' à l'infini.

valeurs centrales. La sensibilité au centre croît avec l'énergie mais se sature aux très hautes énergies (comparer (4.3), (4.4) et (4.5)).

Pour les petites et les grandes valeurs de ER, où R est de l'ordre des dimensions nucléaires (en unités usuelles, $R \simeq 1.2\times 10^{-13} A^{\frac{1}{3}}$ cm), on trouve aisément des approximations de la condition d'équivalence (4.3), qui devient l'égalité de

$$\langle r^{2j+1}\rangle \quad \text{pour} \quad (ER)^2 \ll 2j+7 \tag{4.4}$$

et de

$$\langle \log r\rangle \quad \text{pour} \quad ER \gg j. \tag{4.5}$$

La condition (4.4) est due à Bodmer [9]). La condition (4.5) montre que toutes les ondes partielles $j \ll ER$ ne dépendent de la densité d'électricité nucléaire que par un même paramètre, $\langle \log r\rangle$. Ravenhall et Yennie [16]) † retrouvent ce résultat sous une forme plus explicite mais moins rigoureuse; pour les répartitions peu différentes d'une répartition homogène, ils obtiennent

$$\eta_j \simeq \frac{Z}{137}\left\{1-\langle \log 2Er\rangle + j(j+1)\left\langle \frac{1}{(2Er)^2}\right\rangle\right\} \quad (ER \gg j); \tag{4.6}$$

le terme dépendant de j est négligeable si $ER \gg j$.

La variation de l'équivalence de deux répartitions avec l'énergie et l'onde partielle considérée est illustrée par la figure 3 ci-dessous. Nous considérons l'équivalence d'une sphère chargée en surface de rayon r_s et d'une sphère homogène de rayon R. Pour chaque valeur de j et de κR, la condition (4.3) détermine le rapport r_s/R. Ce rapport est porté sur le graphique pour quelques valeurs de j en fonction de κR et aussi en fonction de l'énergie pour un

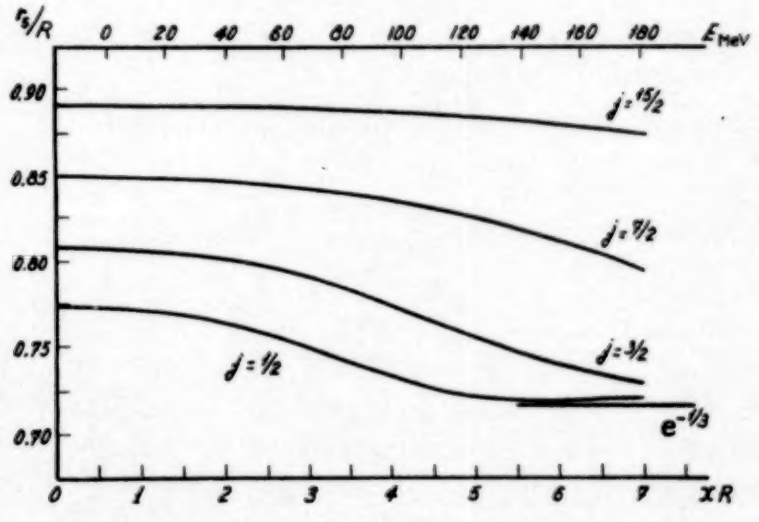

Fig. 3

† Je remercie MM. D. G. Ravenhall et D. R. Yennie pour l'envoi d'un preprint.

noyau d'or de rayon $R = 1.2\times 10^{-13}A^{\frac{1}{3}}$ cm (nous prenons † $\kappa = E+\alpha/R$). Partant à l'origine de la valeur [(4.4)]

$$\left(\frac{r_s}{R}\right)_j = \left(\frac{3}{2j+4}\right)^{\frac{1}{2j+1}} \tag{4.7}$$

les courbes tendent asymptotiquement vers [(4.5)]

$$\frac{r_s}{R} = e^{-\frac{1}{2}} = 0.717. \tag{4.8}$$

On remarque que cette valeur limite est bien près d'être atteinte vers 180 MeV pour les ondes partielles $j = \frac{1}{2}$ et $j = \frac{3}{2}$; d'un autre côté, à la même énergie, l'onde $j = \frac{15}{2}$ (qui entre généralement en ligne de compte dans le calcul de la section efficace) obéit pratiquement encore à la condition de Bodmer.

5. Validité des Conditions d'Équivalence

Les conditions d'équivalence formulées au paragraphe précédent concernent les déphasages des ondes partielles. D'un autre côté, l'équivalence des répartitions est relative à la section efficace de diffusion. Il faut donc examiner dans quelle mesure on peut discuter la section efficace de diffusion à partir de conditions approchées sur les déphasages. La réponse dépend essentiellement du nombre de déphasages δ_j nécessaires dans le calcul de la section efficace de diffusion, nombre qui croît à peu près linéairement avec l'énergie (pour un modèle donné). Pour faciliter la discussion, nous définissons trois domaines énergétiques: les basses, les moyennes et les hautes énergies qui correspondent respectivement à un seul, deux et trois, ou plus de trois δ_j appréciables; les séparations entre ces domaines se situent vers $140A^{-\frac{1}{3}}$ MeV et $280A^{-\frac{1}{3}}$ MeV (pour l'or par exemple, vers 24 et 48 MeV). En ce qui concerne les basses et les moyennes énergies, nous devons nous attendre à ce que nos conditions d'équivalence (4.3) soient valables puisque, comme nous l'avons vu au paragraphe 3, les déphasages approchés peuvent être utilisés dans le calcul de la section efficace de diffusion.

5.1. BASSES ÉNERGIES

Glassgold a examiné la validité des conditions d'équivalence de Bodmer en comparant les sections efficaces de diffusion par des répartitions „équivalentes"[17]). Dans la première partie de son travail, Glassgold considère une répartition homogène de rayon R et la répartition en surface de rayon r_s

† Un autre choix de κ se traduit par un déplacement de l'échelle d'énergie. κ étant compris entre $E+\alpha/R$ et $E+3\alpha/2R$, l'échelle d'énergie peut au maximum se déplacer vers la droite de $\alpha/2R \approx 8.5$ MeV. On peut se rendre compte sur le graphique que l'indétermination sur r_s/R qui en résulte est très faible.

équivalente (au sens de Bodmer) du point de vue de la première onde partielle ($j = \frac{1}{2}$):

$$r_s = \sqrt{\tfrac{3}{5}}\, R = 0.775R. \tag{5.1}$$

Il calcule les sections efficaces de diffusion correspondantes pour divers éléments ($Z = 13$, 29, 50, 74 et 79) et diverses valeurs de ER ($ER = 0.5$, 1.0, 1.5 et 2.0) †.

Pour $ER = 0.5$ et 1.0, la première onde partielle est seule fortement affectée par l'extension finie des répartitions et, d'après Bodmer, les sections efficaces de diffusion par la sphère homogène et par la sphère chargée en surface doivent être égales. Effectivement, Glassgold n'observe que des différences trop faibles pour figurer sur ses graphiques ou pour apparaître expérimentalement (différences de l'ordre de quelques pour-cent). Ceci prouve la validité de la condition d'équivalence de Bodmer dans tout le domaine des basses énergies. La diffusion d'électrons d'énergie inférieure à environ $140\,A^{-\frac{1}{3}}$ MeV ne dépend que du rayon carré moyen de la répartition, $\langle r^2 \rangle$, et ne peut donc fournir que ce paramètre ††. La validité de la condition d'équivalence de Bodmer entraîne a fortiori la validité de notre condition d'équivalence (4.3) intrinsèquement plus précise. D'ailleurs, si une plus grande précision est nécessaire (précision de l'ordre de 1 % sur le rayon de la sphère homogène équivalente, par exemple), c'est au moyen de $\langle \mathcal{J}_{\frac{1}{2}}(\kappa r) \rangle$ qu'il faut comparer les répartitions; c'est aussi cette grandeur que l'on obtiendra à partir de l'expérience.

5.2. ÉNERGIES MOYENNES

Revenons au travail de Glassgold [17]). Pour $ER = 1.5$ et 2.0, deux ondes partielles sont fortement affectées par l'extension finie des répartitions. Pour ces valeurs de ER, Glassgold observe des différences appréciables entre les sections efficaces de diffusion correspondantes aux deux modèles. Ceci est bien naturel et ne nous renseigne pas sur la validité des conditions d'équivalence, puisqu' une répartition homogène et une répartition en surface ne sauraient être simultanément équivalentes (au sens de Bodmer) du point de vue des deux premières ondes partielles, la condition d'équivalence du point de vue de $j = \frac{3}{2}$ étant

$$r_s = (\tfrac{3}{7})^{\frac{1}{2}}\, R = 0.809R \tag{5.2}$$

à comparer à (5.1). Pour tester la validité des conditions d'équivalence aux énergies moyennes, il faut considérer des répartitions à deux paramètres. Glassgold considère notamment un modèle „en double couche"

† Pour $R = 1.2 \times 10^{-13}\, A^{\frac{1}{3}}$ cm, $ER = 1$ correspond à des énergies de 55, 41, 33, 29 et 28 MeV pour $Z = 13$, 29, 50, 74 et 79 respectivement.

†† Ce résultat est dû à Feshbach [18]) mais a été précisé par Bodmer. Pour les éléments légers, on peut le déduire de l'approximation de Born.

$$\rho_{\text{d.c.}}(r) = \frac{Z_1 e}{4\pi r_1^2}\delta(r-r_1) + \frac{Z_2 e}{4\pi r_2^2}\delta(r-r_2), \tag{5.3}$$

les rayons r_1 et r_2 des surfaces électrisées étant les paramètres. Il calcule alors la section efficace de diffusion par une sphère homogène de rayon R pour $Z = 74$ et $ER = 1.903$ et, pour le même élément et à la même énergie, les sections efficaces de diffusion par les répartitions en double couche ($Z_1 = 50$, $Z_2 = 24$) dont les paramètres r_1 et r_2 sont fixés par les conditions

$$\begin{aligned} \langle r^2\rangle_{\text{d.c.}} &= \langle r^2\rangle_{\text{h.}} \\ \langle r^4\rangle_{\text{d.c.}} &= \lambda\langle r^4\rangle_{\text{h.}} \end{aligned} \tag{5.4}$$

avec $\lambda = 0.84,\ 0.88, \ldots 1.16$. Les sections efficaces de diffusion par la répartition homogène et par la répartition en double couche $\lambda = 1.00$ (équivalente au sens de Bodmer à la répartition homogène) diffèrent appréciablement aux grands angles (11 %, assez pour une mise en évidence expérimentale). La répartition en double couche équivalente à la répartition homogène (c'est-à-dire dont la section efficace de diffusion est égale à celle de la répartition homogène) correspond à $\lambda \approx 1.04$. Dans le cas de ces deux modèles et à l'énergie considérée, les conditions d'équivalence sont donc

$$\langle r^2\rangle_{\text{d.c.}} = 1.00\,\langle r^2\rangle_{\text{h.}}, \qquad \langle r^4\rangle_{\text{d.c.}} \approx 1.04\,\langle r^4\rangle_{\text{h.}}. \tag{5.5}$$

Ceci montre que les conditions d'équivalence de Bodmer, valables aux basses énergies ($E \lesssim 140\,A^{-\frac{1}{3}}$ MeV) cessent de l'être aux énergies plus élevées. Une analyse de la diffusion d'électrons en fonction des moments d'ordre pair de la répartition de la charge électrique du noyau ($\langle r^2\rangle, \langle r^4\rangle, \ldots$) n'est donc pas possible.

Nous pouvons utiliser les calculs de Glassgold pour tester nos conditions d'équivalence. D'après (4.3), la répartition en double couche équivalente à la répartition homogène est telle que

$$\langle \mathcal{J}_{\frac{1}{2}}(\kappa r)\rangle_{\text{d.c.}} = \langle \mathcal{J}_{\frac{1}{2}}(\kappa r)\rangle_{\text{h.}}, \qquad \langle \mathcal{J}_{\frac{3}{2}}(\kappa r)\rangle_{\text{d.c.}} = \langle \mathcal{J}_{\frac{3}{2}}(\kappa r)\rangle_{\text{h.}} \tag{5.6}$$

avec

$$E + \frac{\alpha}{R} \lesssim \kappa \lesssim E + \frac{3\alpha}{2R} \qquad (\alpha = Z/137 = 0.540).$$

En résolvant ces équations, on détermine les paramètres r_1 et r_2 de la répartition en double couche équivalente à la répartition homogène; calculant alors les moments, on trouve que, d'après nos conditions d'équivalence, la répartition en double couche équivalente à la répartition homogène est telle que

$$\begin{aligned} \langle r^2\rangle_{\text{d.c.}} &= (1.0035 \pm 0.0005)\langle r^2\rangle_{\text{h.}} \\ \langle r^4\rangle_{\text{d.c.}} &= (1.036 \pm 0.006)\quad \langle r^4\rangle_{\text{h.}} \end{aligned} \tag{5.7}$$

en bon accord avec le résultat de Glassgold (5.5) (l'erreur indiquée correspond à l'incertitude dans le choix de κ).

Les conditions d'équivalence (4.3) nous permettent de déterminer correctement la répartition en double couche équivalente à la répartition homogène. Elles sont donc valables dans le domaine des énergies moyennes. La diffusion d'électrons d'énergie inférieure à environ 280 $A^{-\frac{1}{3}}$ MeV ne dépend de la densité d'électricité nucléaire que par les moyennes $\langle \mathcal{F}_{\frac{1}{2}}(\kappa r) \rangle$ et $\langle \mathcal{F}_{\frac{3}{2}}(\kappa r) \rangle$; une expérience faite dans ce domaine énergétique ne peut nous fournir que la valeur de ces paramètres (à l'énergie considérée).

Les résultats expérimentaux dont on dispose actuellement aux basses et moyennes énergies sont assez imprécis. Il serait intéressant de faire des expériences plus précises dans ces domaines énergétiques où l'on peut fixer des paramètres bien déterminés de la répartition de la charge électrique du noyau.

5.3. HAUTES ÉNERGIES

Le nombre de déphasages δ_j nécessaires et la précision requise sur chacun d'eux augmentent avec l'énergie, ce qui rend l'analyse de plus en plus compliquée. Si les conditions d'équivalence avaient une précision de 10^{-4} radian (ou mieux), deux répartitions équivalentes du point de vue de toutes les ondes partielles appréciablement influencées par l'extension de la charge à une énergie donnée seraient équivalentes à cette énergie (même section efficace de diffusion, à tous les angles considérés); des conditions d'équivalence aussi précises seraient suffisantes mais non nécessaires, car, étant donné la complexité des calculs conduisant à la section efficace de diffusion, il peut s'introduire des compensations telles que de grandes différences dans certains déphasages deviennent tout à fait inobservables (voir l'exemple discuté ci-dessous). En réalité, la situation est encore plus confuse, car nous ne disposons que de conditions précises à 5×10^{-3} radian près (pour les premiers déphasages; l'approximation est meilleure pour les autres). On peut penser que cette précision suffit pour discuter, au moins grossièrement, la dépendance de la section efficace de diffusion en la densité de charge, c'est-à-dire, par exemple, qu'un effet modifiant la quatrième décimale des déphasages est moins significatif qu'un effet modifiant la seconde. Cette interprétation est certainement valable à tous les angles au début du domaine des hautes énergies (3 ou 4 déphasages δ_j importants; en gros, moins de 100 MeV pour les éléments lourds) et aux petits angles aux énergies plus élevées (car la précision requise sur les déphasages est moindre aux petits angles). La section efficace de diffusion, comme les déphasages, est alors surtout sensible aux valeurs superficielles de la densité (dépendance en les moyennes $\langle \mathcal{F}_j(\kappa, r) \rangle$ peu sensibles au centre); autrement dit, on peut

obtenir des détails sur la surface du noyau, la région centrale restant largement indéterminée.

D'un autre côté, il est évident que si l'on considère des énergies de plus en plus élevées et par conséquent un nombre de plus en plus grand d'ondes partielles, l'analyse de la section efficace de diffusion doit finalement révéler la distribution de charge d'une manière de plus en plus détaillée †. Les déphasages sont largement insensibles aux fins détails de la densité (comme par exemple les valeurs centrales), mais aux énergies élevées la superposition d'ondes partielles ayant des déphasages extrêmement voisins peut néanmoins conduire à des sections efficaces sensiblement différentes aux grands angles. Ravenhall et Yennie en donnent un exemple intéressant [16]). Ils considèrent trois modèles de la répartition de la charge électrique d'un noyau d'or [(1): répartition homogène; (2): répartition de Fermi; (3): répartition de Fermi creuse] et ils comparent à 236 MeV (de 10 à 12 déphasages nécessaires) d'une part les déphasages et d'autre part les sections efficaces de diffusion entre 30° et 140°. Pour les valeurs choisies des paramètres, (1) et (2) ont des déphasages très voisins, qui ne diffèrent jamais de plus de 6×10^{-3} radian; quant aux sections efficaces, elles diffèrent aux grands angles par un facteur 30. D'un autre côté, les répartitions (2) et (3) ont des déphasages beaucoup plus différents: les quatre premiers diffèrent de 2 à 3×10^{-2} radian et la différence de chacun des autres déphasages est nettement supérieure à la différence correspondante pour les répartitions (1) et (2); cependant, les sections efficaces sont très voisines, au moins jusque 110° et en tous cas, plus proches l'une de l'autre que celles des répartitions (1) et (2). Les petites différences $(\eta_j^{(1)}-\eta_j^{(2)}) \lesssim 6\times10^{-3}$ radian donnent finalement un effet plus important que les différences $(\eta_j^{(2)}-\eta_j^{(3)})$, individuellement supérieures. Il n'est donc pas possible de discuter de la section efficace de diffusion aux énergies élevées et aux grands angles à partir d'une connaissance approchée des déphasages.

Cet exemple n'est cependant pas décisif quant à l'emploi de nos conditions d'équivalence pour la discussion de la section efficace de diffusion à l'énergie considérée car il s'agit en fait de répartitions qui ne sont pas équivalentes du point de vue de ces conditions. Un test beaucoup plus probant serait par exemple de calculer la section efficace de diffusion à l'aide des déphasages obtenus par notre solution approchée (2.19) et de la comparer à la section efficace de diffusion calculée exactement. Il est certain qu'à partir d'une énergie suffisament élevée nos conditions d'équivalence ne peuvent plus être utilisées pour discuter la section efficace de diffusion (en dépit du fait

† Ceci est particulièrement clair à l'approximation de Born où la densité est la transformée de Fourier du facteur de forme $F(q)$ (voir (2) par exemple); elle se trouve donc univoquement déterminée lorsque l'on connaît $F(q)$ pour toutes les valeurs du transfert d'impulsion $q = 2E \sin \frac{1}{2}\theta$.

que la théorie prévoit correctement le comportement des déphasages, même aux énergies très élevées). A ce moment, l'expérience peut en principe révéler des détails plus fins que les moyennes $\langle \mathcal{J}_j(\kappa r)\rangle$. Mais la question de savoir quels détails de la distribution de la charge sont accessibles aux énergies très élevées est assez académique, étant donné que l'interprétation des expériences à l'aide d'un potentiel statique (correspondant à l'état fondamental du noyau) n'est probablement plus valable au delà d'environ 200 MeV (granulation de la charge). Pour cette raison, il reste intéressant de faire des expériences précises à des énergies plus basses (en-dessous de 100 MeV), où l'interprétation est plus sûre et peut se faire en fonction de paramètres bien déterminés.

5.4. CONCLUSIONS

La diffusion d'électrons d'énergie inférieure à environ 280 $A^{-\frac{1}{3}}$ MeV (basses et moyennes énergies; jusqu'à environ 50 MeV pour les éléments lourds) ne dépend de la densité d'électricité nucléaire $\rho(r)$ que par les moyennes $\langle \mathcal{J}_{\frac{1}{2}}(\kappa r)\rangle$ et $\langle \mathcal{J}_{\frac{3}{2}}(\kappa r)\rangle$. Pour chaque valeur de l'énergie †, l'expérience nous donne ces deux paramètres. A défaut d'une bonne précision, et en particulier, aux basses énergies, on peut plus simplement les remplacer par les moments $\langle r^2\rangle$ et $\langle r^4\rangle$ de la distribution de charge.

Au début du domaine des hautes énergies (de 50 à 100 MeV pour les noyaux lourds (environ)), la diffusion continue à ne dépendre de $\rho(r)$ que par les moyennes $\langle \mathcal{J}_j(\kappa r)\rangle$. Etant donné la complexité croissante du calcul de la section efficace (3, 4 déphasages δ_j importants), il devient plus difficile d'extraire ces paramètres des résultats expérimentaux. Il résulte de cette dépendance (en $\langle \mathcal{J}_j(\kappa r)\rangle$) que l'expérience peut fournir des détails supplémentaires sur la densité aux valeurs pas trop petites de r et, en particulier, à la surface du noyau mais que le centre reste largement indéterminé. Des expériences précises dans ces régions énergétiques (en-dessous de 100 MeV) donneraient déjà une description détaillée de la distribution de la charge électrique du noyau (au moins aux valeurs pas trop petites de r); d'ailleurs, l'interprétation des expériences par un modèle statique du noyau est beaucoup plus fondée en-dessous de 100 MeV qu'aux énergies plus élevées.

Quand l'énergie est si élevée qu'il devient nécessaire de tenir compte de nombreux déphasages δ_j (au-delà d'environ 100 MeV pour les noyaux lourds), il n'est plus possible d'analyser la diffusion à l'aide des moyennes $\langle \mathcal{J}_j(\kappa r)\rangle$. La diffusion d'électrons aux énergies très élevées permet une description de plus en plus détaillée de la densité d'électricité nucléaire; il faut toutefois remarquer que l'on reste limité en énergie car les effets dûs à la granulation de la charge du noyau peuvent devenir importants quand la

† Avec une marge d'environ 10 MeV due à l'arbitraire dans le choix de κ.

longueur d'onde des électrons devient de l'ordre de la distance entre les nucléons ($\lambda_{200\ \mathrm{MeV}} \approx 10^{-13}$ cm).

Ce travail a été effectué sous la direction de Monsieur le Professeur J. Géhéniau. Je le remercie vivement des conseils et des encouragements qu'il n'a cessé de me prodiguer. Mes remerciements vont également à Monsieur le Professeur L. Rosenfeld pour de nombreuses et utiles discussions. Je remercie aussi le Laboratoire de Calcul Numérique de l'Université Libre de Bruxelles qui s'est chargé d'une partie des calculs numériques.

Appendice

Diffusion de Particules non Relativistes

Les méthodes de calcul développées aux paragraphes 2 et 3 sont également utilisables dans l'étude de la diffusion de particules non relativistes par un centre de force. La partie radiale $\psi_l(r)$ de l'onde partielle de moment angulaire orbital $l\hbar$ (unités ordinaires) satisfait à l'équation radiale de Schrödinger

$$\left\{\frac{\mathrm{d}^2}{\mathrm{d}r^2} - \frac{l(l+1)}{r^2} + p^2(r)\right\}\psi_l = 0 \tag{A.1}$$

avec

$$p^2(r) = \frac{2m}{\hbar^2}(E - V(r)); \tag{A.2}$$

nous supposons que l'énergie potentielle $V(r)$ est régulière à l'origine. On peut calculer le déphasage η_l de l'onde partielle de moment angulaire $l\hbar$ si l'on connaît la dérivée logarithmique de $\psi_l(r)$ à l'extérieur du potentiel diffuseur (où il devient négligeable). Plutôt que de résoudre l'équation (A.1) et de calculer ensuite la dérivée logarithmique de $\psi_l(r)$, nous obtenons directement cette dérivée logarithmique en calculant la fonction

$$F_l(r) = \left(\frac{1}{\psi_l(r)}\frac{\mathrm{d}\psi_l(r)}{\mathrm{d}r} + \frac{l}{r}\right)^{-1}: \tag{A.3}$$

$F_l(r)$ est la solution nulle à l'origine de l'équation de Riccati

$$\frac{\mathrm{d}F_l}{\mathrm{d}r} + \frac{2l}{r}F_l - 1 - p^2(r)F_l^2 = 0, \tag{A.4}$$

et on peut résoudre cette équation par les méthodes développées aux paragraphes 2 et 3.

Considérons ici la méthode directe seulement. En posant

$$F_l(r) = \frac{1}{q(r)} \frac{J_{l+\frac{1}{2}}(q(r)\cdot r)}{J_{l-\frac{1}{2}}(q(r)\cdot r)} \tag{A.5}$$

on trouve que $q(r)$ est donné par

$$q^2(r) = q_0{}^2(p^*, r) + q_1{}^2(p^*, r) \tag{A.6}$$

avec

$$q_0{}^2(p^*, r) = \frac{\int_0^r p^2(r') r' J^2_{l+\frac{1}{2}}(p^* r') \mathrm{d}r'}{\int_0^r r' J^2_{l+\frac{1}{2}}(p^* r') \mathrm{d}r'}, \tag{A.7}$$

$$q_1{}^2(p^*, r) = \frac{\int_0^r (p^2(r') - q^2(r')) \left(\frac{g_l(q(r')r')}{g_l(p^* r')} - 1 \right) r' J^2_{l+\frac{1}{2}}(p^* r') \mathrm{d}r'}{\int_0^r r' J^2_{l+\frac{1}{2}}(p^* r') \mathrm{d}r'}; \tag{A.8}$$

dans ces formules, p^* est un paramètre positif et nous avons posé

$$g_l(x) = \frac{2J^2_{l+\frac{1}{2}}(x)}{J^2_{l-\frac{1}{2}}(x) + J^2_{l+\frac{1}{2}}(x) - \frac{2l+1}{x} J_{l-\frac{1}{2}}(x) J_{l+\frac{1}{2}}(x)}. \tag{A.9}$$

La solution approchée

$$F_l(r) \approx \frac{1}{q_0(p^*, r)} \frac{J_{l+\frac{1}{2}}(q_0(p^*, r) r)}{J_{l-\frac{1}{2}}(q_0(p^*, r) r)} \tag{A.10}$$

est une bonne approximation de $F_l(r)$ si $p(r)$ varie peu de 0 à r et si on choisit p^* parmi les valeurs prises par $p(r)$ de 0 à r. On peut améliorer cette solution approchée en calculant (numériquement) une correction $q_1{}^2(p^*, r)$ à $q_0{}^2(p^*, r)$ correction donnée par (A.8) avec $q_0(p^*, r')$ au lieu de $q(r')$; et ce procédé par approximations successives peut se continuer (convergence rapide).

Supposons que le potentiel diffuseur est négligeable pour $r \geqq R$. Nous devons calculer $F_l(R)$; nous voyons que le déphasage η_l ne dépend principalement du potentiel diffuseur que par

$$\int_0^R V(r) r J^2_{l+\frac{1}{2}}(p^* r) \mathrm{d}r, \tag{A.11}$$

p^* étant une quelconque des valeurs de $p(r)$ de 0 à R; nous obtenons donc encore une condition d'équivalence (approchée) pour les potentiels.

Bibliographie

1) K. W. Ford and D. L. Hill, Ann. Rev. Nuc. Sc. **5** (1955) 25
2) R. Hofstadter, Revs. Mod. Phys. **28** (1956) 214
3) D. R. Yennie and H. Suura, Phys. Rev. **105** (1957) 1378
4) B. Hahn, D. G. Ravenhall and R. Hofstadter, Phys. Rev. **101** (1956) 1131
5) B. W. Downs, D. G. Ravenhall and D. R. Yennie, Phys. Rev. **106** (1957) 1285

6) R. R. Lewis Jr., Phys. Rev. **102** (1956) 344
7) L. I. Schiff, Nuovo Cimento **5** (1957) 1223
8) D. R. Yennie, D. G. Ravenhall and R. N. Wilson, Phys. Rev. **95** (1954) 500
9) A. R. Bodmer, Proc. Phys. Soc. A **66** (1953) 1041
10) G. N. Fowler, Proc. Phys. Soc. A **68** (1955) 559
11) J. Reignier, Bull. Ac. R. Belg., Cl. Sc. **41** (1955) 151
12) J. Reignier, Bull. Ac. R. Belg., Cl. Sc. **42** (1956) 173
13) G. N. Watson, Theory of Bessel Functions (Cambridge, 1922)
14) A. E. Glassgold and E. W. Mack, MIT Techn. Rep. no. 65 (1954)
15) J. Reignier, Nuclear Physics **3** (1957) 340
16) D. G. Ravenhall and D. R. Yennie, preprint (1957)
17) A. E. Glassgold, Phys. Rev. **98** (1955) 1360
18) H. Feshbach, Phys. Rev. **84** (1951) 1206

Nuclear Physics 7 (1957) 552; © *North-Holland Publishing Co., Amsterdam*

NEWS ITEM

DOCUMENTATION ATOMIQUE

Le développement prodigieux des sciences et des techniques nucléaires a entraîné un accroissement démesuré de la littérature relative à ces domaines. C'est ainsi par exemple que la bibliothèque de l'Ecole Polytechnique Fédérale à Zurich (désignée comme bibliothèque nationale atomique) s'est vue placée devant le problème de classer 50000 rapports spécialisés. Elle a été obligée d'établir un schéma de classification approprié, assez détaillé pour englober la plupart des cas, assez souple pour s'adapter aux évolutions imprévisibles et rapides. Le système adopté est décimal; il peut s'employer comme système de classification indépendant pour les domaines atomiques, mais peut servir également de subdivision pour une classification décimale quelconque. Les tables de classification seront polycopiées sous peu et pourront être commandées à la Bibliothèque de l'E.P.F., Service de Documentation, Zurich.

Comme les revues constituent actuellement une des sources les plus importantes de la littérature spécialisée, ce Service vient de commencer pour les domaines atomiques la publication de cartes de documentation analogues à celles qu'il édite depuis des années pour l'électrotechnique. Il projette de faire paraître un nombre fixe de cartes par semaine (probablement de 30 à 50), en choisissant les articles les plus intéressants de la presse spécialisée d'une part, des nombreuses revues techniques de la bibliothèque de l'E.P.F. d'autre part. Cette publication sera, à notre connaissance, la première documentation offrant une classification assez spécialisée pour que les groupes engendrés ne soient pas disproportionnés. On envisage d'ailleurs d'étendre et de subdiviser cette classification suivant les nécessités, afin de lui conserver sa valeur aussi longtemps que possible.

Le prix d'abonnement a été fixé, comme pour la documentation électrotechnique, à 0.15 franc suisse la carte. Ci-dessous un spécimen de carte:

SKA
223.14 TH Per.711 384

The Elastic Scattering of 30.5 MeV Alpha-Particles from Ni, Cu and Au. By L. Wayne Swenson, Ulrich Schindewolf and N.S.Wall.
3 figs.
Nucl.Phys., Vol.6(1958)No.2, March, p. 203-209.
Angular distributions of 30 MeV alpha particles elastically scattered from Au, Cu, and Ni measured and compared to pure Coulomb scattering, absence of a significant compound elastic contribution.
11 Literaturnachweis ETH, Zürich. April 58.

2.G

Nuclear Physics 7 (1958) 553—560; © *North-Holland Publishing Co., Amsterdam*

Not to be reproduced by photoprint or microfilm without written permission from the publisher

AN IMPULSE APPROXIMATION FOR THE DEUTERON STRIPPING REACTION

G. RAKAVY

Department of Theoretical Physics, Hebrew University, Jerusalem

Received 10 April 1958

Abstract: The deuteron stripping at low and intermediate energies is treated in a way resembling somewhat the impulse approximation. The neutron-proton interaction is considered twice: first it determines the initial conditions of the problem and then this same interaction is considered as a perturbation inducing transitions between various eigenstates determined by the strong interaction of the target nucleus with the impinging particles.

The nuclear parameters entering the calculation are, besides the reduced widths, the scattering amplitudes of free neutrons and protons. In the present treatment room is made for some resonance phenomena. Also the effect of the Coulomb forces can be treated in a rather straightforward manner.

1. Introduction

The deuteron stripping reaction has been treated in several ways [1]) all yielding essentially the same results. Also the results of the following treatment, which is based on a kind of impulse approximation, are rather similar in their general features; yet this treatment may have some advantage in allowing for resonance-like phenomena in the stripping cross-sections [2]).

The picture underlying the present treatment of the stripping is the following: A bound deuteron approaches the target nucleus. When the neutron or proton (or both) come into the reach of the nuclear forces exerted by the target, the neutron-proton interaction (which formerly held the deuteron together) can be neglected. Now the neutron and proton are scattered independently by the target nucleus as if they were free particles. Until the present stage the influence of the N—P interaction was brought into the picture only by the fact that the incoming neutron and proton waves are not simple plane waves but form some rather complicated wave packets.

If, at the stage that one or both of the particles are inside the target nucleus, the N—P interaction did not exist at all, we would get only scattered free particles. No capture could take place except for the extremely weak capture by the electromagnetic interaction (this is just the usual capture reaction taking place when a free proton or neutron impinges on a nucleus). Thus, the transition of one of the particles to a bound state is induced just

by the formerly neglected N—P interaction. With the hope that the average N—P interaction is small (as indicated by the large ratio of the deuteron radius to the N—P interaction range) we treat this interaction with the usual method of first order perturbation theory.

2. The Procedure in a Simplified Case

In order to bring out the salient points of the calculation, we make the following simplifying assumptions:

(1) We neglect all the spins and consequently also the spin dependence of the nuclear forces.

(2) The Coulomb forces are neglected.

(3) When both the neutron and proton are within the "nuclear matter" of the target nucleus we set the N—P interaction equal to zero. This may be thought of as some saturation effect of nuclear forces.

(4) When the proton and neutron are on or outside of the target surface we use a δ-function for the space dependence of the N—P interaction. This is of course justified by the fact that the interaction range is small compared to the nuclear radius.

We divide the calculation into the following three stages which, in a time dependent picture, can be imagined as occurring successively in time:

Stage 1: A bound deuteron approaches the target nucleus. The deuteron wave function can be expanded into "correlated" neutron and proton plane waves.

Stage 2: Each (neutron or proton) plane wave is scattered by the target nucleus and thereby an outgoing scattered wave is added to it. The scattering amplitudes which appear are characteristic of the target nucleus and should be taken from neutron and proton scattering experiments or should be calculated by some nuclear model †.

Stage 3: After the second stage the particles are left in continuum states (under the influence of the target nucleus) and now the N—P interaction must be taken into account as a perturbation inducing transitions. In general three kinds of transitions are possible:

(a) The proton and neutron which appear in the second stage as "partially" split into free particle waves (by the modification of the plane waves due to the target nucleus) may combine to form a scattered deuteron.

(b) If the energy is high enough transitions to free particle states may occur and we get the splitting of the deuteron into a free neutron and proton.

(c) One of the particles may be caught into a bound state while the other

† As we shall see later we are interested in averages of the scattering amplitudes over rather wide energy intervals and these can be calculated rather reliably by the optical model of the nucleus.

goes out in a continuum state. This is the genuine stripping reaction in which we are interested †.

As we use here the theory of transition probabilities the energy conservation is provided for in a natural way. We must only remember that the energy corresponding to the approximate wave function used in the second stage is really the original energy of the bound deuteron approaching the target.

As a consequence of our assumptions about the N—P interaction and the fact that the wave function of the bound state is appreciably different from zero only within and on the nuclear surface, we need for the calculation of the transition matrix element only the values of the wave functions in the region where both the particles are near the nuclear surface. Therefore, the only property of the bound state that enters into the calculations is the value of the wave function at the nuclear surface. This value is related to the reduced width used in the older treatments [3]).

3. Detailed Calculation of the Simplified Case

3.1. FIRST STAGE

For the internal wave function of the deuteron we shall use the expression

$$\chi_d(r) = \frac{\alpha}{2}\,\frac{e^{-\alpha r}}{r} \quad \left(\alpha = \sqrt{\frac{MB_d}{\hbar^2}} = 0.159\sqrt{B_d} = 0.23\times 10^{13}\,\mathrm{cm}^{-1}\right). \tag{1}$$

This function corresponds to the assumption of a δ-interaction and is infinite at the origin. This infinity does not appear if we assume a finite range for the N—P interaction and therefore we shall take $\chi_d(0)$ to be finite in spite of eq. (1).

The complete wave function describing the approaching deuteron is

$$\varphi_d = \chi_d(r)\cdot e^{i\mathbf{k}_d\cdot\mathbf{r}_0} \tag{2}$$

where

$$\mathbf{r} = \mathbf{r}_1 - \mathbf{r}_2, \qquad \mathbf{r}_0 = (\mathbf{r}_1 + \mathbf{r}_2).$$

This wave function can readily be analysed into plane waves:

$$\begin{aligned}\varphi_d(\mathbf{r}_1;\ \mathbf{r}_2) &= \int_{\mathbf{k}_1}\int_{\mathbf{k}_2} g(\mathbf{k}_1;\mathbf{k}_2)\exp\{i\mathbf{k}_1\cdot\mathbf{r}_1 + i\mathbf{k}_2\cdot\mathbf{r}_2\}\\ &= \int_{\mathbf{k}_1}\int_{\mathbf{k}_2} g(\mathbf{k}_1;\mathbf{k}_2)\exp\{i\mathbf{k}_0\cdot\mathbf{r}_0 + i\mathbf{k}\cdot\mathbf{r}\}\end{aligned} \tag{3}$$

where

$$\mathbf{k}_0 = \mathbf{k}_1 + \mathbf{k}_2, \qquad \mathbf{k} = \tfrac{1}{2}(\mathbf{k}_1 - \mathbf{k}_2).$$

By a straight-forward calculation one gets

$$g(\mathbf{k}_1;\mathbf{k}_2) = \delta(\mathbf{k}_0 - \mathbf{k}_d)G(\mathbf{k}) \tag{4}$$

where

$$G(k) = \int \chi_d(r)e^{-i\mathbf{k}\cdot\mathbf{r}}(\mathrm{d}^3r) = 4\pi\int \frac{\sin kr}{kr}\,\chi_d(r)\cdot r^2\,\mathrm{d}r = \frac{2\sqrt{2\pi\alpha}}{k^2+\alpha^2}\cdot$$

† Transitions of the type (a) are between eigenstates of two different hamiltonians, which are not orthogonal, but in cases (b) and (c) no trouble of this kind is encountered.

3.2. SECOND STAGE

In the region exterior to the target nucleus every plane wave is modified owing to the interaction with the target only by the addition of an out-going part. Therefore in the expansion (3) we have to replace every plane wave by

$$e^{i\mathbf{k}\cdot\mathbf{r}}+f(\theta)\frac{e^{ikr}}{r}=e^{i\mathbf{k}\cdot\mathbf{r}}-2\pi\sum_{lm}i^{l+1}u_l^+(kr)Y_{lm}(\mathbf{k})Y_{lm}^*(\mathbf{r})\{\eta_l(k)-1\}. \quad (5)$$

The total wave function of the proton-neutron system as modified by the target nucleus is

$$\begin{aligned}\Psi_1=&\int_{\mathbf{k}_1}\int_{\mathbf{k}_2}\delta(\mathbf{k}_1+\mathbf{k}_2-\mathbf{k}_d)G(\tfrac{1}{2}|\mathbf{k}_1-\mathbf{k}_2|)\\&\times[e^{i\mathbf{k}_1\cdot\mathbf{r}_1}-2\pi\sum_{l'm'}i^{l'+1}u^+(k_1r_1)Y_{l'm'}(\mathbf{k}_1)Y_{l'm'}^*(\mathbf{r}_1)\{\eta_{l'}'-1\}] \quad (6)\\&\times[e^{i\mathbf{k}_2\cdot\mathbf{r}_2}-2\pi\sum_{l''m''}i^{l''+1}u^+(k_2r_2)Y_{l''m''}(\mathbf{k}_2)Y_{l''m''}^*(\mathbf{r}_2)\{\eta_{l''}''-1\}].\end{aligned}$$

This function is valid only in the exterior region $r_1 \geqq R$, $r_2 \geqq R$.

3.3. THIRD STAGE

At last we have to calculate the cross section for transitions from the initial state (6) to the final state:

$$\Psi_f=\psi_L(r_1)Y_{LM}(\mathbf{r}_1)\{e^{i\mathbf{k}_f\cdot\mathbf{r}_2}-2\pi\sum_{lm}i^{l+1}u^+(k_fr_2)Y_{lm}(\mathbf{k}_f)Y_{lm}^*(\mathbf{r})\{\eta_l(f)-1\}\}. \quad (7)$$

Here we assume for the captured particle a "single particle" state $\psi_L(r_1)Y_{LM}(\mathbf{r}_1)$. The state of the outgoing particle is given by the expression in the curly bracket.

The cross section for transitions from the initial to the final state is calculated by the usual Born approximation:

$$\frac{d\sigma}{d\Omega}=\sqrt{\frac{u_1E_f}{u_fE_1}}\frac{\lambda\!\!\!^{-}_0{}^4}{\lambda^2},\quad \frac{hc}{\lambda}=\frac{1234}{\lambda}=|\langle f|V|i\rangle|. \quad (8)$$

(The interaction energy $|\langle f|V|i\rangle|$ is measured in MeV, length is measured in units of 10^{-13} cm. All wave functions — describing continuum states — are normalized within the volume $\lambda\!\!\!^{-}_0{}^3$, where $\lambda\!\!\!^{-}_0$ is the Compton wave length of the nucleon divided by 2π : $\lambda\!\!\!^{-}_0 = 0.21$.)

Following our assumptions about the nuclear forces we can use for the N—P interaction the following expression:

$$V(\mathbf{r}_1;\mathbf{r}_2)=V_0\delta(\mathbf{r}_1-\mathbf{r}_2)\delta(r_1-R). \quad (9)$$

Using (6) (7) and (9) we get for the transition matrix element

$$\begin{aligned}\langle \mathrm{f}|V|\mathrm{i}\rangle &= \mathrm{Norm}\cdot V_0\cdot \psi_L(R)\int_{\mathbf{k}_1}\int_{\mathbf{k}_2}\delta(\mathbf{k}_1+\mathbf{k}_2-\mathbf{k}_\mathrm{d})G(k)\\ &\times\int_\Omega \mathrm{d}\Omega Y^*_{LM}(\varrho)\{e^{-i\mathbf{k}_f\cdot\rho}-2\pi\sum_{lm}(-i)^{l+1}u^-(k_fR)Y^*_{lm}(\mathbf{k}_f)Y_{lm}(\varrho)[\eta_l^*(\mathrm{f})-1]\}\\ &\times\{e^{i\mathbf{k}_1\cdot\rho}-2\pi\sum_{l'm'}i^{l'+1}u^+(k_1R)Y_{l'm'}(\mathbf{k}_1)Y^*_{l'm'}(\varrho)[\eta_{l'}'(k_1)-1]\}\\ &\times\{e^{i\mathbf{k}_2\cdot\rho}-2\pi\sum_{l''m''}i^{l''+1}u^+(k_2R)Y_{l''m''}(\mathbf{k}_2)Y^*_{l''m''}(\varrho)[\eta_{l''}''(k_2)-1]\}.\end{aligned}\tag{10}$$

Here ϱ indicates a radius vector of length R and direction Ω. The wave functions (6) and (7) are not normalized (in the volume λ_0^3) and therefore we have inserted in (10) a normalizing factor: Norm. If we are interested only in the angular distribution this factor is of no significance.

The Ω integration in (10) can be performed immediately.

The integration over $\mathbf{k}_1$ and $\mathbf{k}_2$ is simplified by the presence of the δ function but still represents a rather complicated problem, especially because of the appearance of k_1 and k_2 in the scattering amplitudes η.

4. Investigation of the Various Terms appearing in Eq. (10)

When we multiply out the expressions in the curly brackets in formula (10) we get one term not containing any η's, other terms containing η (f)'s and not containing the other η's, and also linear and quadratic terms in the η (k_i)'s. In the case that all the η's are small the first term dominates and we get an angular distribution similar to Butler's. Usually this should not be the case and the angular distribution is modified by the presence of the additional terms.

The term not containing any η's can be integrated out explicitly:

$$\begin{aligned}&\text{const.}\times\int_{\mathbf{k}_1}\int_{\mathbf{k}_2}G(k)\delta(\mathbf{k}_1+\mathbf{k}_2-\mathbf{k}_\mathrm{d})\int_\Omega Y^*_{LM}(\varrho)e^{i(\mathbf{k}_1+\mathbf{k}_2-\mathbf{k}_f)\cdot\rho}\\ &=\text{const.}\times 4\pi i^L\chi_\mathrm{d}(0)j_L(|\mathbf{k}_\mathrm{d}-\mathbf{k}_f|R)Y^*_{LM}(\mathbf{k}_\mathrm{d}-\mathbf{k}_f).\end{aligned}\tag{11}$$

The terms arising from the modification of the final state of the scattered particle by the interaction with the residual nucleus (term linear in $\eta_l(\mathrm{f})$ and containing no other η's) are also of a rather simple nature:

$$\begin{aligned}&\text{const.}\times u^-(k_fR)Y^*_{lm}(\mathbf{k}_f)[\eta_l^*(f)-1]\chi_\mathrm{d}(0)\int_\Omega \mathrm{d}\Omega Y^*_{LM}(\varrho)Y_{lm}(\varrho)e^{i\mathbf{k}_\mathrm{d}\cdot\rho}\\ &=\text{const.}\times u^-(k_fR)Y^*_{lM}(\mathbf{k}_f)\,[\eta_l^*(\mathrm{f})-1]\chi_\mathrm{d}(0)\sum_\lambda a_{L l\lambda}(LM;\,l-m|\lambda 0)(-)^M i^\lambda\\ &\quad\times\sqrt{4\pi(2\lambda+1)}j_\lambda(k_\mathrm{d}R);\end{aligned}$$

here we assume $\mathbf{k}_\mathrm{d}$ to define the z axis; and $a_{l_1l_2l_3}$ is given by

$$\left(\frac{(2l_1+1)\,(2l_2+1)}{4\pi(2l_3+1)}\right)^{\frac{1}{2}}(l_1\,0,\,l_2\,0|l_3\,0).$$

The only factor significant for the angular distribution in the above expression is $Y_{lM}(\mathbf{k}_f)$.

The nature of all the other terms containing the scattering amplitudes $\eta'_{l'}(k_1)$ or $\eta''_{l''}(k_2)$ is much more complicated.

A typical term is

$$\int_{\mathbf{k}_1+\mathbf{k}_2=\mathbf{k}_d} G(\tfrac{1}{2}|\mathbf{k}_1-\mathbf{k}_2|)\int_\Omega Y^*_{LM}(\varrho)e^{i(\mathbf{k}_1-\mathbf{k}_f)\rho}u_0^+(k_2R)[\eta_0(k_2)-1]$$
$$= 4\pi i^L\int_{\mathbf{k}_1+\mathbf{k}_2=\mathbf{k}_d} G(\tfrac{1}{2}|\mathbf{k}_1-\mathbf{k}_2|)Y^*_{LM}(\mathbf{k}_1-\mathbf{k}_f)j_L(|\mathbf{k}_1-\mathbf{k}_f|R)u_0^+(k_2R)[\eta_0(k_2)-1].$$

In order to be able to perform the k-integration we must have an explicit expression for the scattering amplitudes. In any case it is almost certain that this k-integration must be performed numerically. An important feature of the above expression is that the $\eta(k)$'s appear in the integral multiplied by a rather slowly varying function of k. We shall return to discuss this point later.

5. The Effect of the Coulomb Forces

In order to take into account the effect of the Coulomb forces we must modify our treatment at several points.

(I) In the first stage we have a deuteron approaching the target. As long as the binding energy of the deuteron is great compared to the variation of the Coulomb energy over distances of the order of magnitude of the deuteron radius we can describe the Coulomb effect as a force acting on the centre of mass of the deuteron. This means that we just need to replace the plane wave describing the motion of the centre of mass by a "Coulomb wave". Therefore we have for the initial wave function

$$\psi_d = e^{i\mathbf{k}_d\cdot\mathbf{r}_0}F(k_d r_0-\mathbf{k}_d\cdot\mathbf{r}_0)\chi_d(r).$$

The analysis of this wave into plane neutron and proton waves can be performed immediately:

$$\psi_d = \int\int g(\mathbf{k}_1,\mathbf{k}_2)e^{i\mathbf{k}_1\cdot\mathbf{r}_1+i\mathbf{k}_2\cdot\mathbf{r}_2},$$
$$g(\mathbf{k}_1,\mathbf{k}_2) = \phi_{\mathbf{k}_d}(k_0)G(k);$$

$G(k)$ is the same as before and

$$\phi_{\mathbf{k}_d}(\mathbf{k}_0) = -\frac{1}{2\pi^2}\lim_{\varepsilon\to 0}\frac{d}{d\varepsilon}\frac{[k_0^2+(\varepsilon-k_d)^2]^{i\alpha}}{[\varepsilon^2+(\mathbf{k}_0-\mathbf{k}_d)^2]^{i\alpha+1}}\quad\left(\alpha=\frac{Ze^2}{\hbar v}\right).$$

The modification introduced by the Coulomb forces in this stage is really only the replacement of the $\delta(\mathbf{k}_0-\mathbf{k}_d)$ function appearing in (4) by the singular function $\phi_{\mathbf{k}_d}(k_0)$. In the present case even in the first term, (11), the k integration is rather complicated.

(II) When the deuteron is near enough to the target the Coulomb forces may polarize it. Yet closer to the target in the region where the nuclear forces begin to be effective one can again neglect the influence of the Coulomb

forces. Therefore in the second stage of the process, where we imagine the neutrons and protons moving (freed from their mutual interaction) in the region of strong nuclear forces of the target, we can neglect the Coulomb interaction. This means that in so far as we neglect the above mentioned polarization effect, we can use the wave function (6) with the δ function replaced by the function $\phi_{\mathbf{k}_d}(\mathbf{k}_0)$.

It should be noticed that the scattering amplitudes used in the description of the initial proton waves, should be calculated as if there existed no Coulomb force acting on the proton. The important influence of the Coulomb force in the usual proton scattering process is related to the fact that the Coulomb force has a much longer range than the nuclear forces, and modifies the wave function in regions far away from the target. In our case, the protons are not free in the far regions, but are bound with the neutron into a deuteron. Therefore, this long range influence has already been included in the modification of the deuteron wave function discussed above. The modification brought about by the Coulomb forces in the region where the nuclear forces are effective is rather hard to estimate, but is supposed to be small.

(III) In the third stage the Coulomb effect is very simple: If the outgoing particle is a proton we must replace the plane wave describing the final state of the proton by a corresponding Coulomb wave. If the outgoing particle is the neutron no modifications are needed in this last stage.

6. Concluding Remarks

The central idea in the present treatment is that one interaction (i.e. the N—P interaction) is used to determine the "initial conditions" and the same interaction is treated afterwards as a perturbation inducing transitions between eigenstates of the system determined by a second strong interaction. The conditions for the validity of such a treatment are not very clear. One condition is of course that within the target nuclear the N—P interaction should be negligible compared with the forces exerted by the target. Another condition which seems to be necessary is that the "collision time" should be small compared with the "internal period" of the impinging deuteron. The first condition is necessary for the validity of the perturbation treatment of the N—P interaction. The second condition is required in order to assure that the "development" of the state caused by the N—P interaction during the collision is insignificant and thereby to justify the use of the "initial conditions" as determined by the N—P intraction.

In practice the above outlined procedure is unambiguous only when the scattering amplitudes of one particle in the field of the target nucleus are equal to the scattering amplitudes in the field of the target nucleus plus the other particle. If the N—P forces were really negligible small compared with the nuclear forces of the target this would be the situation. But as we know,

the scattering amplitudes may show resonances characteristic to a particular nucleus. In this case the treatment is rather ambiguous.

The situation is perhaps really not so bad because in our formulas the scattering amplitudes always appear in integrals over the energy and therefore the exact variations are not so important as their averages over energy regions containing several resonances. These averages are reproduced rather well by the optical model of the nucleus and do not differ much from nucleus to nucleus. These averages are also spin independent (i.e. they depend only on l's but not on j's) which simplifies matters further.

Throughhout the whole treatment it was assumed implicitly that the probability for the formation of a compound nucleus is small and that the interaction of the target with the scattered particles can be replaced by some average potential. This, too, is in accordance with the optical model.

References

1) Thomas, Phys. Rev. **100** (1955) 25. This paper contains a rather complete list of references
2) Bonner *et al.*, Phys. Rev. **101** (1955) 209; Marion and Weber, Phys. Rev. **103** (1956) 1408; McEllistrem *et al.*, Phys. Rev. **104** (1956) 1008
3) Blatt and Weisskopf, Theoretical Nuclear Physics, p. 554

1.E.4:
3.A

Nuclear Physics 7 (1958) 561—568; © *North-Holland Publishing Co., Amsterdam*
Not to be reproduced by photoprint or microfilm without written permission from the publisher

LEVELS AND BRANCHING RATIOS IN Tb^{159}

K. O. NIELSEN, O. B. NIELSEN and O. SKILBREID
Institute for Theoretical Physics, University of Copenhagen

Received 1 May 1958

Abstract: β-ray sources of Gd^{159} were prepared in an electromagnetic isotope separator. The decay scheme $Gd^{159} \rightarrow Tb^{159}$ was reinvestigated in two six-gap β-ray spectrometers. γ-ray spectra coincident with β-rays and conversion lines were recorded on a 100 channel analyzer.

Three γ-transitions of $\approx$ 225, $\approx$ 300, and 364 keV from the 364 keV level to the ground state rotational band were observed, and it was confirmed that the relative intensities disagree with the theoretical branching ratios. It is suggested that the deviation is connected with the fact that the γ-rays are of E1 nature and probably strongly hindered.

1. Introduction

The branching ratios for β- and γ-transition in deformed nuclei in general follow the selection rules calculated within the framework of the unified model [1]). In the decay $Gd^{159} \rightarrow Tb^{159}$, however, some disagreements have been observed [2, 3, 4, 5]). As a closer study of the deviations might lead to a more detailed understanding of the nature of the nuclear states involved, an investigation with improved experimental accuracy was desirable.

18 h Gd^{159} is formed by neutron irradiation in a reactor. The production of β-ray sources of high specific activity by conventional techniques is difficult due to the low neutron cross section of Gd^{158}. Furthermore, strong activities may be induced in small amounts of Sm and Eu, which are often found as impurities in Gd. In the present investigation, isotopically pure sources prepared in an electromagnetic isotope separator [6]) were employed.

In most respects the experimental results confirm earlier measurements, but new information regarding intensities and multipole orders was obtained.

2. Source Preparation

The technique developed for the preparation of radioactive sources of rhenium [7]) could be used with only minor modifications.

As charging material for the ion source waterfree gadolinium chloride ($GdCl_3$)[8, 9]) was used. The compound was prepared before neutron irradiation and was placed in a crucible of graphite or quartz; since $GdCl_3$ is highly hygroscopic, it was kept in an air-tight aluminium container until

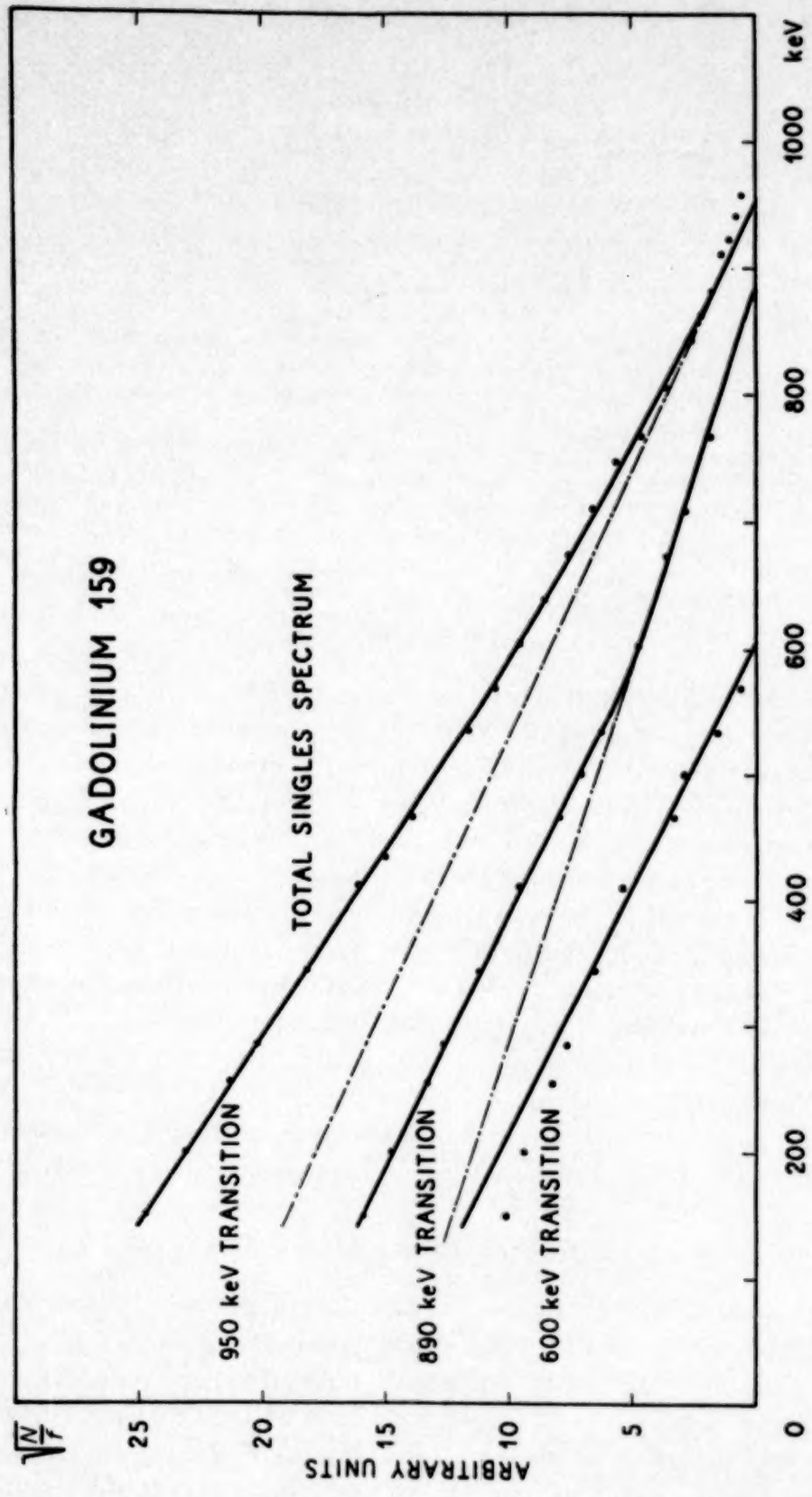

Fig. 1. Fermi analysis of the continuous β-ray spectrum. The separation between the two high energy groups represents a best fit based on the known energy difference rather than a subtraction analysis.

the crucible containing the irradiated material could be introduced into the ion source. The irradiation was performed in the reactor at Saclay in neutron fluxes up to 6×10^{12} neutrons/cm^2.

The optimum duration of a separation is about 25 h[10]) for an 18 h activity, provided that the ion current is kept constant. In such a run, the ion source consumes 300—400 mg $GdCl_3$.

The best source obtained had a strength of about 70 μC on an area of 2×6 mm^2.

An ion beam of stable atoms, corresponding to mass number 159, appeared in several separations and, in one case, it destroyed the 150 μg/cm^2 aluminium foil used as source backing. It had to be assigned to ions of $Yt^{89}Cl_2^{35}$ due to an impurity of ytrium rather than of Tb^{159}. Although the destruction of the foil could be avoided by using gadolinium of high purity, the stable beam probably gave rise to a certain loss of activity due to sputtering.

3. The Spectrometers

The β-ray measurements were performed in two six-gap spectrometers[11,12]). The γ-ray spectra coincident with the conversion lines and the continuous β-ray background were recorded on a 100 channel analyzer.

4. Experimental Results

4.1. γ-RAY AND CONVERSION LINE MEASUREMENTS

The single γ-ray spectrum contains two dominant peaks of about 50 and 365 keV. In addition, weak γ-rays of $\approx$ 80, $\approx$ 225, and $\approx$ 300 keV have been observed [5]). The 57 keV peak is due to γ-rays of 57 keV as well as KX-rays.

The intensities of the conversion lines are given in table 1. Due to the low energy ($\approx$ 5 keV) the K-conversion line of the strong 57 keV transition could not be observed. The conversion lines for the weak 225 and 300 keV transitions were not observed, however, the upper limit which could be placed on K_{225} was sufficient to fix the multipole order.

TABLE 1

E keV	Shell	I line $\times10^4$	Assignment	Conv. Coeff.		K/L ratios		I_γ %	I transition %
				Exp.	Theor.	Exp.	Theor.		
57	L	310	M1		1.35			2.2	26
79	K	18	M1		5	6±1	7	0.04	0.26
225	K	$\lesssim$ 1	E1	$\lesssim$ 0.04	0.028			0.26	0.26
300								0.10	0.10
364	K	8.4	E1	0.008	0.009	$\gtrsim$ 5	7.3	9.3	9.4

The theoretical conversion coefficients and K/L ratios are taken from the tables of Rose *et al.*[19]) and of Sliv and Band [20]).

4.2. β-RAY GROUPS

In addition to the total β-ray spectrum, the partial spectra coincident with β-rays of energies above 20 and 80 keV, respectively, were studied. In these experiments, the γ-ray energies were selected by integral bias discrimination. The most energetic group of 950 ± 10 keV was not γ-coincident. The low energy γ-peak was coincident with a group of about 890 keV, and the 365 keV γ-ray was related to a 600 keV group.

A Fermi analysis of the total β-ray spectrum is given in fig. 1. Due to the small difference in energy between the 950 and 890 keV spectra, a normal subtraction analysis was not feasible, and the separation in the two groups represents a best fit. Therefore, the intensity of 24 % found for the 890 keV transition is not very accurate, but this value as well as the 13 % for the 600 keV group are in close agreement with the intensities which could be calculated on the basis of the known γ-ray efficiencies in the coincidence experiments.

4.3. e$-\gamma$ COINCIDENCE MEASUREMENTS

The spectrum of γ-rays coincident with the lines L_{57} and K_{79} is shown in fig. 2. The two γ-rays of 225 and 300 keV are clearly seen in coincidence with 57 keV, whereas only the 225 keV line appears in coincidence with the K and L lines of the 79 keV transition.

These relations in connection with the β-ray measurements establish the decay scheme fig. 3, apart from the order of the 79 and 225 keV γ-rays. The intermediate level has tentatively been placed at 136 keV, because a level of this energy and similar decay properties are known from Coulomb excitation [13]).

On the basis of the known efficiencies for γ-rays of the crystal in the coincident circuit, it is possible from the intensity of the photo peak in the coincident spectrum to calcultate the relative strength of the two transitions represented by the conversion line and by the γ-ray †. The total intensity of the 57 keV transition being known from the conversion line data (see next section), the 225 keV γ-ray represented 0.26 % of all decays. The same intensity, 0.26 %, was found from the conversion lines for the 79 keV transition, and these results were checked by the coincidence method which indicated that each 79 keV transition was accompanied by 0.95 γ-rays of 225 keV.

The intensity of the 300 keV γ-ray observed in fig. 2 is 0.10 %. This result as well as the intensity of the 225 keV transition are in good agreement with the values of Ballini and Barloutaud [5]), obtained in a single γ-ray spectrum.

† A more detailed discussion on such quantitative γ-ray measurements will be published in a paper on the decay of Tb^{156} [14]).

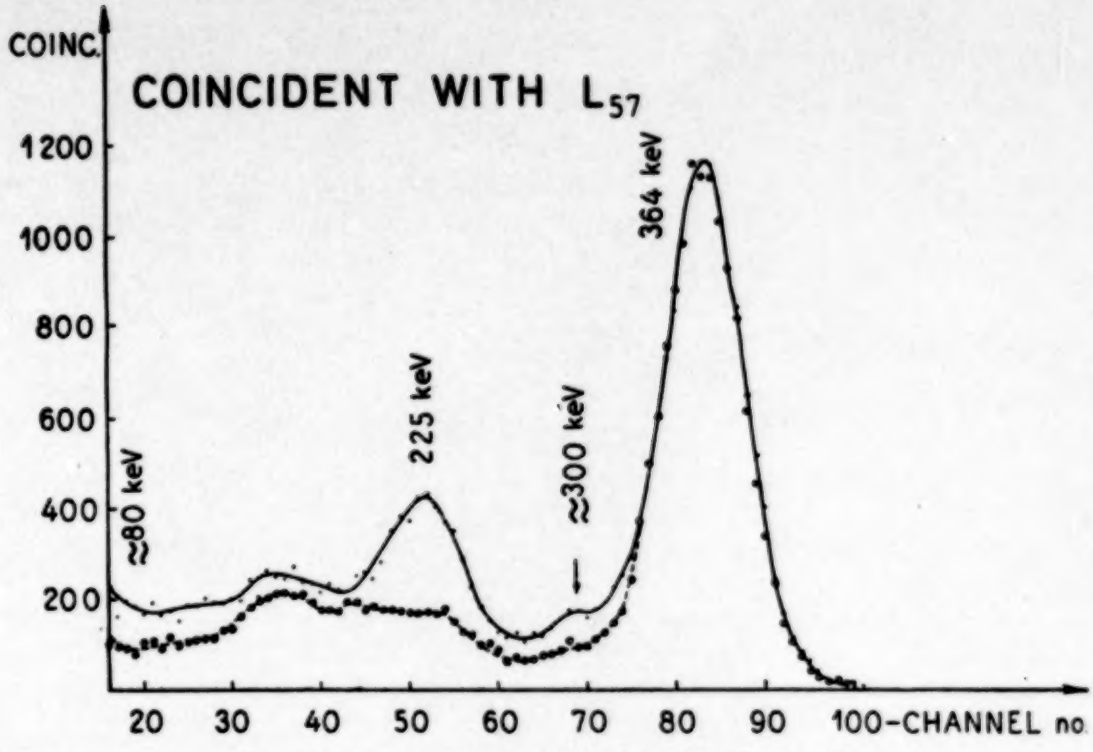

Fig. 2A. γ-ray spectrum coincident with the line L_{57}.

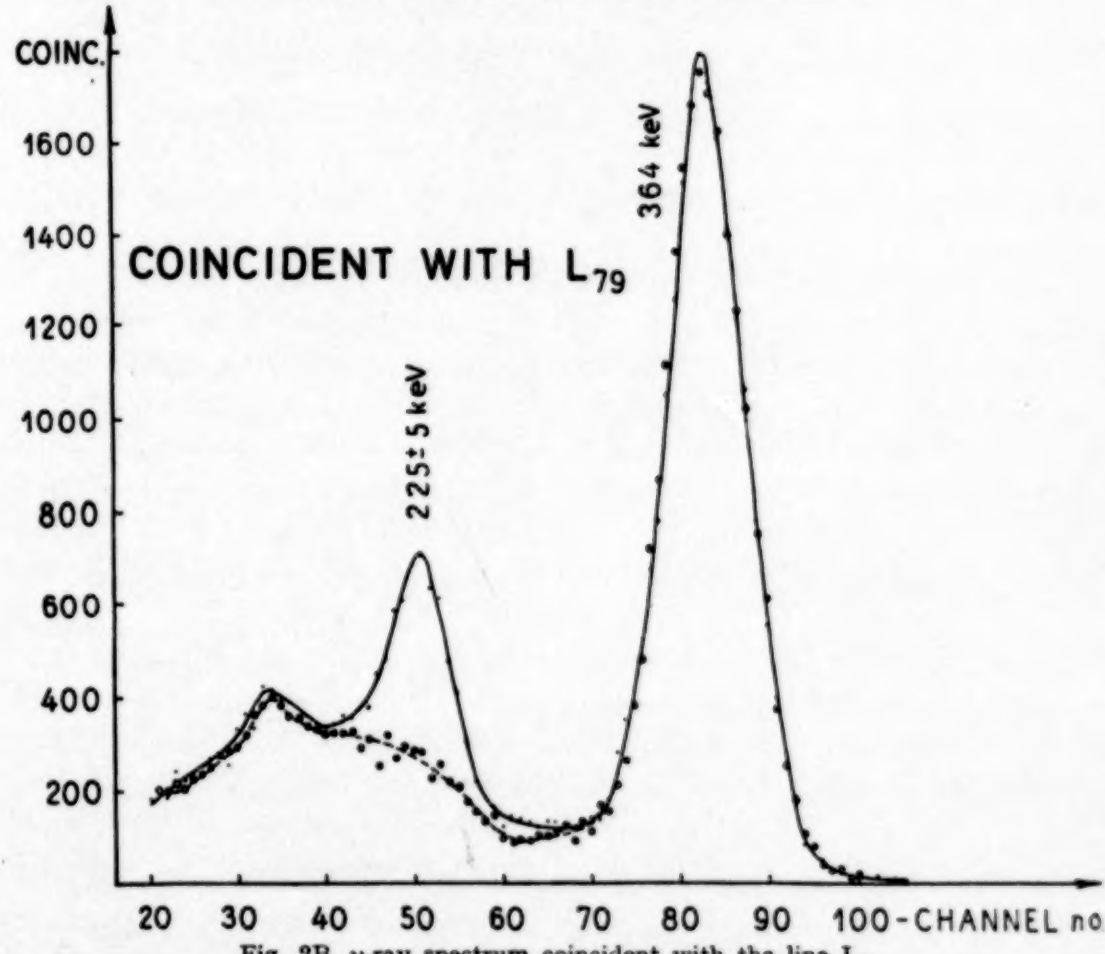

Fig. 2B. γ-ray spectrum coincident with the line L_{79}.
The full-drawn curves include the contributions coincident with the continuous β-ray background, the dotted curves represent the background alone.

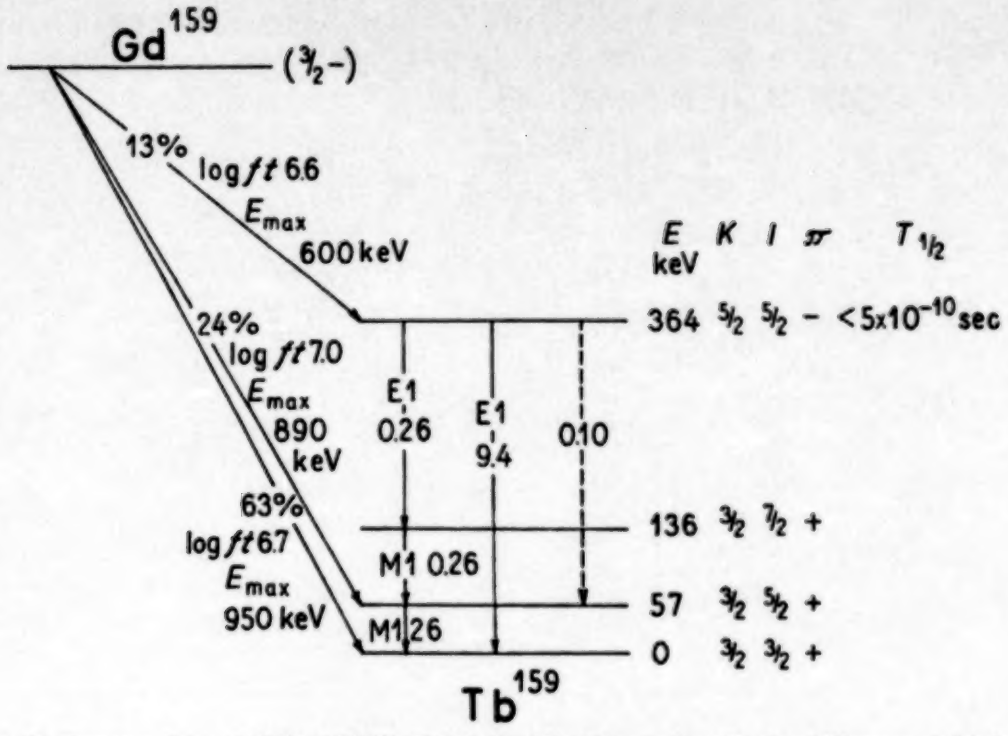

Fig. 3. Decay scheme $Gd^{159} \rightarrow Tb^{159}$. The intensities shown for the transitions are obtained independently from β-ray and conversion line measurements.

5. Multipole Orders and Intensities

The intensities of KX-rays and K Auger lines show the presence of a strong K conversion line which can be attributed only to the 57 keV transition. K conversion is only appreciable for dipole transitions at such a low energy, and the conversion coefficient can be estimated from the ratio of KX-rays to 57 keV γ-rays in the γ-ray spectrum. The two contributions are not resolved, but the shape of the asymmetric peak indicates $\alpha_K \approx 6$, which is consistent with the theoretical M1 value of 8, whereas E1 corresponds to $\alpha_K \approx 1$. A calculation of the total transition intensity on the basis of the L conversion line and the theoretical K/L ratios and L conversion coefficients yields 26 % and 50 % of all decays in the M1 and E1 cases, respectively. Only the M1 assignment is thus in agreement with the intensity of the β-ray group in the coincidence measurements on the β-ray spectrum. The M1 nature is also indicated by the fact that the L_{III} conversion line is weak [2]).

The K/L ratio 6 ± 1 for the 79 keV transition indicates dipole nature, and, since E1 is excluded by the weakness of the γ-ray [5]), the multipole order must be predominantly M1. The total intensity of the transition can then be calculated to 0.26 ± 0.04 % of all decays.

The conversion lines of the 225 keV transition were not observed with certainty, but the upper limit on the intensity just corresponds to an E1 assignment.

The conversion coefficient for the 364 keV transition could, in principle, be determined from the intensities of the K conversion line and the β-ray to the 364 keV level. Due to the relative weakness of this branch, the accuracy was not considered sufficient, and a more reliable determination was made by a comparison with the 662 keV transition in Ba^{137}. The K conversion lines and the γ-rays for the two transitions were measured in identical geometries in the β-ray and in the γ-ray spectrometer. Assuming the conversion coefficient for the 662 keV γ-ray to be 0.095, the conversion coefficient for the 364 keV transition came out as 0.0083, in agreement with the theoretical value of 0.0090 for E1. The total intensity of the transition calculated from the K line and the theoretical E1 conversion coefficient is then 9.4 %, in accord with the result from Fermi analysis.

6. Discussion

The ground state of Tb^{159} has spin $\frac{3}{2}$ [15]) and, according to the classification of Mottelson and Nilsson [16]), even parity. The 57 and 136 keV levels, which have been Coulomb excited, are then the associated rotational states. The 364 keV state decays with E1 transitions to levels which are assumed to be $\frac{3}{2}^+$ and $\frac{7}{2}^+$, and has thus the spin $\frac{5}{2}^-$. A level with this spin and parity is expected among the low lying intrinsic states [16]).

In Dy^{161}, which contains the same (odd) number of neutrons as Gd^{159}, three intrinsic states with spins $\frac{5}{2}^+$, $\frac{5}{2}^-$, and $\frac{3}{2}^-$ have been found with an energy difference less than 75 keV [17,18]). The ground state of Gd^{159} probably corresponds to one of these and, since it decays to states with spin $\frac{3}{2}$ and $\frac{5}{2}$, but not to the assumed $\frac{7}{2}$ state, the $\frac{3}{2}^-$ assignment seems to be the most likely.

The ground states of Tb^{159} and Tb^{161} are presumably the same odd proton states with spin $\frac{3}{2}^+$. Thus, the β-decay of Gd^{159} to the ground state of Tb^{159} connects the same intrinsic states as the decay of Tb^{161} to the $\frac{3}{2}^-$ level in Dy^{161}. It is interesting to note that the two log ft-values in question are almost identical, viz., 6.7 and 6.8.

The theoretical branching ratio for β-transitions from a $\frac{3}{2}$ level to the $\frac{3}{2}$ and $\frac{5}{2}$ states in the ground state rotational band is 1.5 [1]), to be compared with the experimental value 2.0.

The experimental branching ratio for the E1 transitions from the $\frac{5}{2}^-$ state to the $\frac{3}{2}^+$, $\frac{5}{2}^+$, and $\frac{7}{2}^+$ states, 1 : 0.016 : 0.11, deviates considerably from the theoretical value 1 : 0.43 : 0.07. This discrepancy indicates a breakdown in the assumptions underlying the theoretical selection rules, and is probably connected with the fact that the γ-rays are E1's, which are usually strongly hindered. The upper limit of 5×10^{-10} sec. for the lifetime of the 364 keV state [5]) only indicates that the transitions are less than 10^5 slower than the single-particle estimate.

We wish to express our gratitude to Professor Niels Bohr for the ideal working conditions in his Institute. The stimulating contact with Drs. D. R. Bés, B. R. Mottelson, and S. G. Nilsson is gratefully acknowledged.

References

1) G. Alaga, K. Alder, A. Bohr and B. R. Mottelson, Mat. Fys. Medd. Dan. Vid. Selsk. **29** (1955) no. 9
2) W. C. Jordan, J. M. Cork and S. B. Burson, Phys. Rev. **92** (1953) 315
3) N. Marty, Comp. rend. **241** (1956) 389
4) R. Barloutaud and B. Ballini, Comp. rend. **241** (1956) 389
5) B. Ballini and R. Barloutaud, J. phys. radium **17** (1956) 534
6) K. O. Nielsen and O. Skilbreid, Nuclear Instruments **2** (1958) 15
7) K. O. Nielsen and O. B. Nielsen, Nuclear Physics **5** (1958) 319
8) K. O. Nielsen, Nuclear Instruments **1** (1957) 289
9) B. Skytte Jensen, Nuclear Instruments **1** (1957) 323
10) S. Thulin, Ark. Fys. **4** (1951) 363
11) O. B. Nielsen and O. Kofoed Hansen, Mat. Fys. Medd. Dan. Vid. Selsk. **29** (1955) no. 6
12) O. B. Nielsen, to be published
13) N. P. Heydenburg and G. M. Temmer, Phys. Rev. **100** (1955) 150
14) P. Gregers Hansen, N. O. Lassen, O. B. Nielsen and R. K. Sheline, to be published
15) J. M. Baker and B. Bleaney, Proc. Phys. Soc. **68** (1955) 257
16) B. R. Mottelson and S. G. Nilsson, Phys. Rev. **99** (1955) 1615
17) P. Gregers Hansen, O. Nathan, O. B. Nielsen and R. K. Sheline, Nuclear Physics **6** (1958) 630
18) D. R. Bés, Nuclear Physics **6** (1958) 645
19) M. E. Rose, G. H. Goertzel and C. L. Perry, ORNL-1923 (1955);
M. E. Rose, G. H. Goertzel and C. Swift, L-shell internal conversion coefficients, privately distributed;
M. E. Rose, L-shell internal conversion coefficients with finite nuclear size included, privately distributed
20) L. Sliv and J. Band, Tables of Gamma-Ray Internal Conversion Coefficients, Part I (Isdatelstvo Akademia Nauk SSSR, Moscow and Leningrad, 1956)

8.B

Nuclear Physics 7 (1958) 569—572; © *North-Holland Publishing Co., Amsterdam*

Not to be reproduced by photoprint or microfilm without written permission from the publisher

A POSSIBLE EXPERIMENT FOR DETERMINATION OF SPIRALITY OF μ-MESONS

A. Z. DOLGINOV

Physico-Technical Institute, USSR Academy of Sciences, Leningrad

Received 1 March 1958

Abstract: For the determination of the direction of the μ-meson spin with respect to its momentum it is suggested that circular polarization of X-ray quanta emitted by a mesic atom be investigated. This should simultaneously yield information on the degree of depolarization of μ-mesons after a certain level is reached in the mesic atom.

It has been demonstrated in a number of experiments [1, 2]) that μ-mesons created in $\pi \to \mu + \nu$ decay are polarized relative to the direction of their momentum $\mathbf{p}(p, \vartheta, \varphi)$. This result agrees with the predictions of Lee and Yang [3]) which are based on the assumption of parity non-conservation in weak interactions. However, the aforementioned experiments were not sufficient to permit one to determine whether the μ-meson spin was parallel or antiparallel to the direction of motion. On the other hand, elucidation of this problem is important for the verification of the law of conservation of lepton charge. Since slow μ-mesons are produced in $\pi \to \mu + \nu$ decay it is difficult to determine the direction of their spins from circular polarization of the bremsstrahlung.

It will be shown in the present paper that a study of circular polarization of X-ray quanta emitted as a result of transitions, in a mesic atom, of a captured μ-meson should permit one to determine the direction of the spin of the μ-meson relative to its initial momentum. A study of this kind should simultaneously yield information on the degree of depolarization of the μ-meson spin during deceleration, capture and subsequent radioactive or Auger transitions.

The experiments described in ref. [1, 2]) indicate that polarization of μ-mesons does not disappear before the mesons are stopped. Since depolarization is due to relativistic effects and the velocities of μ-mesons in a mesic atom are not large, it may be expected that as the μ-meson successively undergoes transitions to deeper levels in the mesic atom its depolarization will not become complete.

The wave function of the μ-mesic atom can be written in the form

$$\psi = \sum_{\sigma} a^{\xi}{}_{\sigma} \psi_{\sigma} \psi_{lm} \psi_{IM} \tag{1}$$

where ψ_{IM} is the nuclear wave function, ψ_{σ} is the spin part and ψ_{lm} the orbital part of the μ-meson function. $a^{\xi}{}_{\sigma}$ defines the degree of polarization of the meson spin in the shell. The $a^{\xi}{}_{\sigma}$ determine the density matrix

$$\rho(\sigma, \sigma') = \langle a^{\xi *}_{\sigma} a^{\xi}_{\sigma'} \rangle_{\xi} \tag{2}$$

where $\langle\ \rangle_{\xi}$ signifies averaging over the statistical ensemble.

Let the z-axis be chosen along the direction of the initial μ-meson momentum (before stoppage). In such a coordinate system only the diagonal elements of matrix $\rho(\sigma, \sigma) = W(\sigma)$ will not vanish. Here $W(\sigma)$ is the probability of detecting a meson with a spin directed along ($\sigma = \frac{1}{2}$) or opposite ($\sigma = -\frac{1}{2}$) the direction of $\mathbf{p}$.

Consider a radiative transition of a μ-meson from a state with an orbital angular momentum l_0 and total angular momentum j_0 to a state l_1, j_1. Let $\mathbf{k}(k, \theta, \phi)$ denote the momentum of the emitted X-ray quantum. If quanta of definite circular polarization are not selected no appreciable angular correlation of the vectors $\mathbf{p}$ and $\mathbf{k}$ should be expected. Correlation of this type should occur only if initial μ-meson capture takes place from a state with $l \neq 0$ (capture in flight). However the probability of such captures is very small.

If, however, quanta of definite circular polarization are selected, their angular distribution relative to direction $\mathbf{p}$ will be anisotropic. It is not difficult to find this angular distribution by evaluating the radiative transition matrix element.

We then obtain

$$W(\mathbf{p}, \mathbf{k}, \sigma_{\mu}, \sigma_{\gamma}) = 1 - (j_0 - l_0) \lambda_{j_1 j_0} \sqrt{\frac{4j_0 - 2l_0 + 1}{2l_0 + 1}} \sigma_{\mu} \sigma_{\gamma} \cos\theta. \tag{3}$$

Here θ is the angle between the direction of $\mathbf{k}$ and the direction of $\mathbf{p}$; σ_{μ} determines the degree of polarization of the μ-mesons in the shell:

$$\sigma_{\mu} = W(\tfrac{1}{2}) - W(-\tfrac{1}{2}); \tag{4}$$

$\sigma_{\gamma} = 1$ or -1 for right or left hand polarization of the X-ray quanta. For dipole radiation, which is the most probable, one has

$$\lambda_{j_0 - 1, j_0} = \sqrt{\frac{j_0 + 1}{j_0}}, \quad \lambda_{j_0 + 1, j_0} = -\sqrt{\frac{j_0}{j_0 + 1}}, \quad \lambda_{j_0, j_0} = \frac{1}{\sqrt{j_0(j_0 + 1)}}. \tag{5}$$

If radiation of multipolarity 2^L is emitted,

$$\lambda_{j_1 j_0} = \sqrt{2(2j_0 + 1)(2L + 1)}\, W(j_1 L j_0 1; j_0 L),$$

where $W(abcd; ef)$ is a Racah function.

It follows from (3) that the correlation for $l_0 j_0(\gamma) l_1 j_1$ and $l_1 j_1(\gamma) l_0 j_0$ transitions is not the same. In particular, for $P_{\frac{1}{2}} \to S_{\frac{1}{2}}$ and $P_{\frac{3}{2}} \to S_{\frac{1}{2}}$ transitions we correspondingly have

$$W_{\frac{1}{2}} = 1+\tfrac{1}{3}\sigma_\mu \sigma_\gamma \cos\theta; \quad W_{\frac{3}{2}} = 1-\tfrac{5}{6}\sigma_\mu \sigma_\gamma \cos\theta, \tag{6}$$

whereas for $S_{\frac{1}{2}} \to P_{\frac{1}{2}}$ and $S_{\frac{1}{2}} \to P_{\frac{3}{2}}$ transitions

$$W_{\frac{1}{2}} = 1-\sigma_\mu \sigma_\gamma \cos\theta, \quad W_{\frac{3}{2}} = 1+\tfrac{1}{2}\sigma_\mu \sigma_\gamma \cos\theta. \tag{7}$$

If the correlation for the $P_{j_0} \to S_{\frac{1}{2}}$ transition is observed without separating quanta corresponding to $j_0 = \frac{1}{2}$ and $\frac{3}{2}$ in accord with their energy, the resultant correlation will be

$$W_{P\to S} = 1-\tfrac{4}{9}\sigma_\mu \sigma_\gamma \cos\theta. \tag{8}$$

If, however, the $S_{\frac{1}{2}} \to P_{j_1}$ transition is observed without separating quanta for different values of j_1, the resulting correlation will be absent, $W_{S\to P} = \text{const}$, as the weight of state $P_{\frac{3}{2}}$ is twice as great as that of state $P_{\frac{1}{2}}$.

Formulas (3)–(8) show that in order to draw conclusions concerning the direction of the μ-meson spin it should be sufficient to determine the correlation sign for a given circular polarization of the quanta. From the magnitude of σ_μ for various transitions, information can be obtained relating to the degree of depolarization of a μ-meson after it reaches a given level.

Formula (3) is slightly modified if the hyperfine splitting of the level from which the transition under investigation takes place, is comparable to or exceeds its width. Computing, in accord with ref.[4]), the transition probability for this case we obtain an expression which differs from (3) by an additional factor B_ϱ before $\cos\theta$:

$$[\sum_F (2F+1)] B_\varrho = \sum_{F,F'} \frac{(2F+1)|U(Ij_0F1; F'j_0)|^2}{1+(\omega_{FF'}\tau)^2}, \tag{9}$$

where F is the total angular momentum of the mesic atom, I is the nuclear angular momentum, $U(abcd; ef) = \sqrt{(2e+1)(2f+1)}W(abcd; ef)$, $\hbar\omega_{FF'}$ is the energy difference between levels with angular momenta F and F', τ is the lifetime of the level.

Since $B_\varrho \leqq 1$ it should be desirable to use mesic atoms with nuclei for which $I = 0$. Weakening of correlation for $I \neq 0$ can be avoided if a magnetic field strong enough to break the j_0–I coupling is applied parallel to $\mathbf{p}$.

If the mesic atom is located in a magnetic field which is too weak to break the bond between j_0 and I, precession of F in the field will modify the angular correlation. In this case

$$W(\mathbf{p}, \mathbf{k}, \sigma_\mu, \sigma_\gamma, \mathbf{H}) = 1 - \frac{4\pi(j_0-l_0)}{\sum_F (2F+1)} \lambda_{j_1 j_0} \sqrt{\frac{4j_0-2l_0+1}{2l_0+1}} \times \sum_{FF'\varphi\varphi'} \frac{|C^{F'\varphi'}_{F\varphi 1\eta}|^2 U(Ij_0F'1; Fj_0)}{1-i\omega_{F\varphi; F'\varphi'}\tau} \sigma_\mu \sigma_\gamma Y_{1\eta}(\phi\varphi) Y^*_{1\eta}(\vartheta\varphi); \tag{10}$$

$\hbar\omega_{F\varphi;F'\varphi'}$ is the energy difference between states with angular momenta F and F' and their projections φ and φ' in the external magnetic field. In this case the z-axis is chosen along the direction to field **H**. Angles ϑ, φ determine the direction of **p** and angles θ, ϕ the direction of **k** in a system with $Oz||\mathbf{H}$. As above, σ_μ, in accord with (4), specifies the μ-meson polarization relative to **p**.

References

1) R. Garwin, L. Lederman and M. Weinrich, Phys. Rev. **105** (1957) 1415
2) D. Berley, T. Coffin, R. Carwin, L. Lederman and M. Weinrich, Phys. Rev. **106** (1957) 835
3) T. D. Lee and C. N. Yang, Phys. Rev. **104** (1956) 254
4) G. Goertzel, Phys. Rev. **62** (1945) 763; K. Alder, Helv. Phys. Acta **25** (1952) 235

7.A Nuclear Physics 7 (1958) 573—578; © North-Holland Publishing Co., Amsterdam
Not to be reproduced by photoprint or microfilm without written permission from the publisher

ON THE DISPERSION RELATIONS FOR THE COMPTON EFFECT

A. A. LOGUNOV and A. R. FRENKIN
Joint Institute of Nuclear Research, Laboratory of Theoretical Physics, Dubna, U.S.S.R.

Received 12 February 1958

Abstract: A basis underlying the deduction of the dispersion relations for the Compton effect on nucleons in the absence of an unobservable energy region is presented.

1. Introduction

At present the method of dispersion relations is extensively used in quantum field theory. Although this method does not yield complete information on a particular process, it nevertheless does lead to some exact relations between observable quantities. Special interest has been attached to the dispersion relations inasmuch as they may be instrumental in solving experimentally the problem of localizability and causality in interactions between elementary particles. However, in order to show that this is possible it is necessary to prove that these relations always hold in the presence of the two above-mentioned properties. Although the method of dispersion relations was proposed as early as 1954, a number of uncertainties regarding the deduction of these relations still remained up to recent times. It was only at the end of 1956 that N. N. Bogolubov was able to overcome all difficulties and to give a rigorous proof of the dispersion equations for meson-nucleon scattering processes. In order to accomplish this N. N. Bogolubov had to make a profound analysis of the main physical premises underlying the deduction and to prove several refined theorems belonging to a region intermediate between the theory of functions of complex variables and functional analysis. For forward scattering similar proofs were also obtained by Lehmann, Simanzyk and Jost. For the Compton effect on nucleons dispersion relations were derived in ref. [1, 2]).

In the present paper the existence of these relations will be rigorously proved for the case when there are no unobservable energy regions, the method of N. N. Bogolubov being applied for this purpose [3]). As in ref.[2]) no electromagnetic corrections will be taken into account. Our attention will chiefly be directed to a study of the main amplitude term proportional to e^2, that is, only strong interactions will be considered.

2. The Compton Scattering Amplitude

The amplitude for Compton scattering on nucleons can be represented in the form

$$f^{C}(q, q') = \sum_{\mu, \mu'} e_{\nu}{}^{\mu}(\mathbf{q}) e_{\nu'}{}^{\mu'}(\mathbf{q}') T^{C}_{\alpha, \omega}\left(\frac{q+q'}{2}\right) \tag{1}$$

where $\alpha = (\mathbf{p}, s, \mu)$, $\omega = (\mathbf{p}', s', \mu')$; $\mathbf{p}$ is the nucleon momentum. In the reference system in which the sum of the nucleon momenta before and after the reaction is zero, the Fourier transforms of the retarded and advanced matrix elements have the form

$$\begin{aligned} T^{\mathrm{ret}}(E, \mathbf{e}, \mathbf{p}) &= \int dx e^{i(Ex_0 - \mathbf{e}\cdot\mathbf{x}\sqrt{E^2-\mathbf{p}^2})} F^{\mathrm{ret}}(x), \; F^{\mathrm{ret}}(x) = 0 \text{ for } x \lesssim 0, \\ T^{\mathrm{adv}}(E, \mathbf{e}, \mathbf{p}) &= \int dx e^{i(Ex_0 - \mathbf{e}\cdot\mathbf{x}\sqrt{E^2-\mathbf{p}^2})} F^{\mathrm{adv}}(x), \; F^{\mathrm{adv}}(x) = 0 \text{ for } x \gtrsim 0; \end{aligned} \tag{2}$$

E is the quantum energy, $\mathbf{e}$ is a unit vector orthogonal to vector $\mathbf{p}$. The functions T^{ret} and T^{adv} are defined everywhere on the real axis for $|E| > |\mathbf{p}|$. We introduce the function

$$\begin{aligned} T(E, \mathbf{e}, \mathbf{p}) &= T^{\mathrm{ret}}(E, \mathbf{e}, \mathbf{p}) - T^{\mathrm{adv}}(E, \mathbf{e}, \mathbf{p}) \\ &= \frac{(2\pi)^6}{2i} \sum_n \delta(\sqrt{M_n{}^2+E^2-\mathbf{p}^2}+E-\sqrt{M^2+\mathbf{p}^2}) \\ &\qquad \cdot \langle p', s' | J_{\mu}(0) | -\lambda\mathbf{e}, n\rangle\langle -\lambda\mathbf{e}, n | J_{\mu'}(0) | p, s\rangle \\ &- \frac{(2\pi)^6}{2i} \sum_n \delta(\sqrt{M_n{}^2+E^2-\mathbf{p}^2}-E-\sqrt{M^2+\mathbf{p}^2}) \\ &\qquad \cdot \langle p', s' | J_{\mu'}(0) | \lambda\mathbf{e}, n\rangle\langle \lambda\mathbf{e}, n | J_{\mu}(0) | p, s\rangle \\ \lambda^2 &= E^2-\mathbf{p}^2, \quad J_{\mu}(x) = i\frac{\delta S}{\delta A_{\mu}(x)} \cdot S^{+}. \end{aligned} \tag{3}$$

Assuming that the meson-nucleon field system does not possess any bound states with a mass $M < M_n < M + \mu$, it is easy to show that the function $T(E, \mathbf{e}, \mathbf{p})$ has δ singularities at $E = \pm E_2$ and a continuous

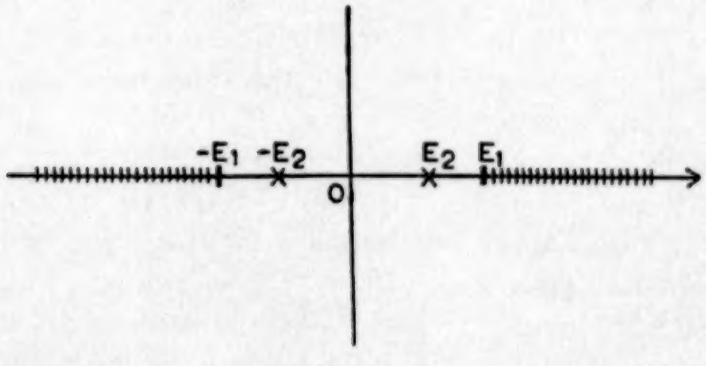

Fig. 1

spectrum which extends from $-\infty$ to $-E_1$, and from E_1 to ∞, with

$$E_1 = \frac{M\mu + \frac{1}{2}\mu^2 - \mathbf{p}^2}{\sqrt{M^2+\mathbf{p}^2}}, \qquad E_2 = \frac{\mathbf{p}^2}{\sqrt{M^2+\mathbf{p}^2}}. \tag{4}$$

Diagramatically this is shown in fig. 1.

In our reference system the threshold of the process is $E_p = |\mathbf{p}|$. For small momenta of the scatterer,

$$\mathbf{p}^2 \leqq \mu^2 \left(\frac{M+\frac{1}{2}\mu}{M+\mu}\right)^2, \tag{5}$$

it is easy to show that

$$E_p \leqq E_1, \tag{6}$$

that is, no unobservable energy region exists.

3. Derivation of Dispersion Relations

We set up a function $\bar{T}(E, \mathbf{e}, \mathbf{p})$ which vanishes if $|E| < E_1$. In order to do this we replace the functions $F^{\mathrm{ret}}(x)$, $F^{\mathrm{adv}}(x)$ in (2) by the functions $\bar{F}^{\mathrm{ret}}(x)$ $\bar{F}^{\mathrm{adv}}(x)$ in the following manner:

$$\bar{F}^{\mathrm{ret}}(x) = \left(\Box^2 - 2\mathbf{p}^2\Box + (4M^2+4\mathbf{p}^2)\frac{\partial^2}{\partial x_0^2} + \mathbf{p}^4\right) F^{\mathrm{ret}}(x) \tag{7}$$

or in momentum space

$$\bar{T}^{\mathrm{ret}}(q, \mathbf{p}) = ([[q'+\tfrac{1}{2}(p'-p)]^2+\mathbf{p}^2]^2 - 4E^2M^2 - 4E^2\mathbf{p}^2)T^{\mathrm{ret}}(q, \mathbf{p}). \tag{8}$$

It is quite obvious that

$$\bar{T}(q, \mathbf{p}) = \bar{T}^{\mathrm{ret}}(q, \mathbf{p}) - \bar{T}^{\mathrm{adv}}(q, \mathbf{p}) = 0 \text{ if } q^0 = E < E_1. \tag{9}$$

We introduce the expressions

$$\begin{aligned} S_{\pm}\int \bar{F}^{\mathrm{ret}}(x) e^{i(Ex_0 - \mathbf{e}\cdot\mathbf{x}\sqrt{E^2-\mathbf{p}^2}) - \varepsilon\mathbf{x}^2}\, dx &= \phi^{\mathrm{r}}(E, \mathbf{e}, \mathbf{p}, \varepsilon), \\ S_{\pm}\int \bar{F}^{\mathrm{adv}}(x) e^{i(Ex_0 - \mathbf{e}\cdot\mathbf{x}\sqrt{E^2-\mathbf{p}^2}) - \varepsilon\mathbf{x}^2}\, dx &= \phi^{\mathrm{a}}(E, \mathbf{e}, \mathbf{p}, \varepsilon), \end{aligned} \tag{10}$$

where $S_{\pm}$ is the symmetrization or antisymmetrization operation with respect to $\mathbf{e}$:

$$S_+ f(\mathbf{e}) = f(\mathbf{e}) + f(-\mathbf{e}), \quad S_- f(\mathbf{e}) = \frac{1}{\lambda}(f(\mathbf{e}) - f(-\mathbf{e})).$$

The functions ϕ^{r}, ϕ^{a} are analytic respectively in the upper or lower half-plane of energy E. On the basis of (9) it follows that

$$\phi^{\mathrm{r}}(E, \mathbf{e}, \mathbf{p}, \varepsilon) = \phi^{\mathrm{a}}(E, \mathbf{e}, \mathbf{p}, \varepsilon) \text{ for } |E| < E_1, \ \mathrm{Im}\, E = 0 \tag{11}$$

and hence a function $\phi(E, \mathbf{e}, \mathbf{p}, \varepsilon)$ exists for which

$$\phi(E, \mathbf{e}, \mathbf{p}, \varepsilon) = \begin{cases} \phi^{\mathrm{r}}(E, \mathbf{e}, \mathbf{p}, \varepsilon) \text{ for } \mathrm{Im}\, E > 0 \\ \phi^{\mathrm{a}}(E, \mathbf{e}, \mathbf{p}, \varepsilon) \text{ for } \mathrm{Im}\, E < 0 \end{cases} \tag{12}$$

and which is analytic throughout the entire energy plane excepting the cuts

$$-\infty < \mathrm{Re}\, E < -E_1; \quad E_1 < \mathrm{Re}\, E < \infty, \quad \mathrm{Im}\, E = 0. \tag{13}$$

On the upper cut lines ϕ equals ϕ^{r} and on the lower ϕ^{a}.

If, for $E \to \infty$, the function $\phi(E, \mathbf{e}, \mathbf{p}, \varepsilon)$ does not increase faster than E^{n+4}, Cauchy's integral theorem with the integration contour depicted in fig. 2 can be applied to the function

$$\frac{\phi(E, \mathbf{e}, \mathbf{p}, \varepsilon)}{(E-E_0)^{n+5}} \tag{14}$$

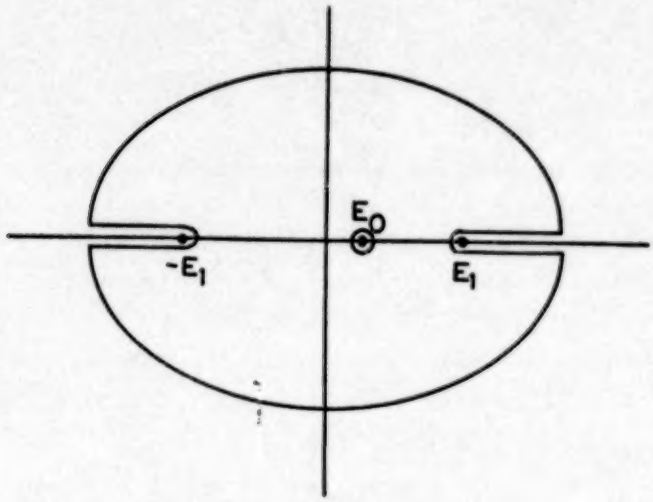

Fig. 2

(where E_0 is a real parameter, $|E_0| < E_1$). If the radius of the large circle approaches infinity and the radii of the small semi-circles approach zero one obtains

$$\phi(E, \mathbf{e}, \mathbf{p}, \varepsilon) = \frac{(E-E_0)^{n+5}}{2\pi i} \int_{-\infty}^{-E_1} \frac{\phi(E'+i0, \mathbf{e}, \mathbf{p}, \varepsilon) - \phi(E'-i0, \mathbf{e}, \mathbf{p}, \varepsilon)}{(E'-E)(E'-E_0)^{n+5}}\, \mathrm{d}E'$$
$$+ \frac{(E-E_0)^{n+5}}{2\pi i} \int_{E_1}^{\infty} \frac{\phi(E'+i0, \mathbf{e}, \mathbf{p}, \varepsilon) - \phi(E'-i0, \mathbf{e}, \mathbf{p}, \varepsilon)}{(E'-E)(E'-E_0)^{n+5}}\, \mathrm{d}E' + P_{n+4}(E). \tag{15}$$

Integration in expression (15) is carried out over the observable region $E_1 > E_p$. However, since the functions ϕ^{r} and ϕ^{a} are defined in the observable region for $\varepsilon = 0$ also, we may put $\varepsilon = 0$ in integrals (15). It is quite evident that the right hand side of expression (15) is an analytic function over the entire plane of the complex variable E, excluding the cuts (13), and for $\varepsilon = 0$ this right hand side defines a function $\phi(E, \mathbf{e}, \mathbf{p}, 0)$ which is analytic over the complete plane E excepting the cuts (13). However, the function $\phi(E, \mathbf{e}, \mathbf{p}, 0)$ differs from the function

$$S_{\pm} G(E, \mathbf{e}, \mathbf{p}) = \begin{cases} S_{\pm} T^{\mathrm{ret}}(E, \mathbf{e}, \mathbf{p}) & \text{for } \mathrm{Im}\, E > 0 \\ S_{\pm} T^{\mathrm{adv}}(E, \mathbf{e}, \mathbf{p}) & \text{for } \mathrm{Im}\, E < 0 \end{cases} \tag{16}$$

only by a factor which vanishes at $E = \pm E_2$. The function $S_\pm G(E, \mathbf{e}, \mathbf{p})$ will therefore be analytic over the whole plane of complex variable E and have first order poles at $E = \pm E_2$ and cuts extending from $-\infty$ to $-E_1$, and from E_1 to $+\infty$. The $S_\pm G(E, \mathbf{e}, \mathbf{p})$ does not increase faster than function E^n as $E \to \infty$.

Thus Cauchy's theorem with the integration contour depicted in fig. 3 can be applied to the function

$$\frac{S_\pm G(E, \mathbf{e}, \mathbf{p})}{(E-E_0)^{n+1}}. \tag{17}$$

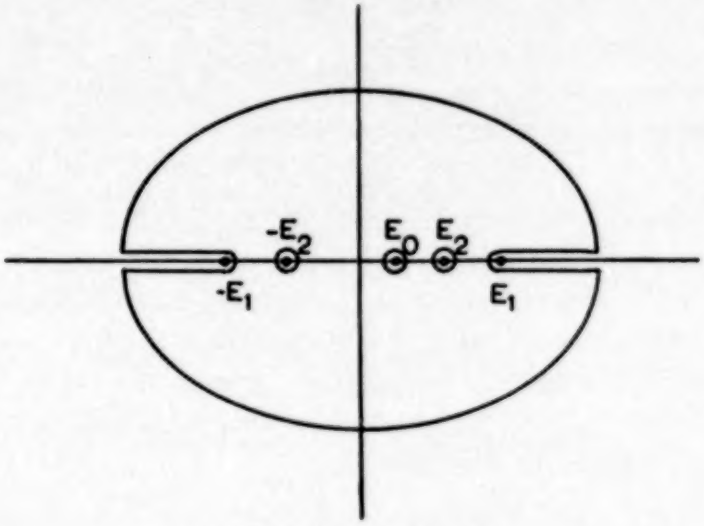

Fig. 3

When the radius of the large circle approaching infinity and the radii of the small semicircles approach zero one obtains

$$\begin{aligned} S_\pm G(E) = {} & \frac{(E-E_0)^{n+1}}{2\pi i}\int_{|E'|\geq E_1} \frac{S_\pm T^{\mathrm{ret}}(E') - S_\pm T^{\mathrm{adv}}(E')}{(E'-E)(E'-E_0)^{n+1}}\,\mathrm{d}E' \\ & + \left(\frac{E-E_0}{-E_0-E_2}\right)^{n+1} \cdot \frac{S_\pm A(\mathbf{p})}{E_2+E} + \left(\frac{E-E_0}{E_2-E_0}\right)^{n+1} \cdot \frac{S_\pm B(\mathbf{p})}{E-E_2} + P_n(E) \end{aligned} \tag{18}$$

where

$$\begin{aligned} S_\pm A(\mathbf{p}) &= \frac{M^2}{\mathbf{p}^2+M^2} \sum_{s''} S_\pm \langle -\mathbf{p}, s'|j_\nu(0)|s'', \lambda\mathbf{e}\rangle\langle s'', \lambda\mathbf{e}|j_\nu(0)|\mathbf{p}, s\rangle \\ S_\pm B(\mathbf{p}) &= \frac{M^2}{\mathbf{p}^2+M^2} \sum_{s''} S_\pm \langle -\mathbf{p}, s'|j_\nu(0)|s'', -\lambda\mathbf{e}\rangle\langle s'', -\lambda\mathbf{e}|j_\nu(0)|\mathbf{p}, s\rangle. \end{aligned} \tag{19}$$

We now perform the transition to real E. Noting that

$$\begin{aligned} \lim_{\varepsilon\to 0} S_\pm G(E+i\varepsilon) &= S_\pm T^{\mathrm{ret}}(E) \\ \lim_{\varepsilon\to 0} S_\pm G(E-i\varepsilon) &= S_\pm T^{\mathrm{adv}}(E) \end{aligned} \qquad (\mathrm{Im}E = 0) \tag{20}$$

and taking into account the definition of the Hermitian and anti-Hermitian parts

$$D_{\alpha,\omega}(E) = \tfrac{1}{2}(T^{\mathrm{ret}}_{\alpha,\omega}(E)+T^{\mathrm{adv}}_{\alpha,\omega}(E)),\ A_{\alpha,\omega}(E) = \frac{1}{2i}(T^{\mathrm{ret}}_{\alpha,\omega}(E)-T^{\mathrm{adv}}_{\alpha,\omega}(E)) \quad (21)$$

the following dispersion relations can readily be obtained:

$$\begin{aligned} S_{\pm}D_{\alpha,\omega}(E) = {} & \frac{(E-E_0)^{n+1}}{\pi}\,\mathrm{P}\int_{|E'|\geq E_1} \mathrm{d}E'\,\frac{S_{\pm}A_{\alpha,\omega}(E')}{(E'-E)\,(E'-E_0)^{n+1}} \\ & + \left(\frac{E-E_0}{-E_2-E_0}\right)^{n+1}\frac{S_{\pm}A(\mathbf{p})}{E+E_2} + \left(\frac{E-E_0}{E_2-E_0}\right)^{n+1}\cdot\frac{S_{\pm}B(\mathbf{p})}{E-E_2} + P_n(E). \end{aligned} \quad (23)$$

In the considerations presented above no assumption was made concerning the degree of increase of the amplitude in E at infinity. If the Compton scattering amplitude at infinity is assumed to possess a pole not higher than the first order, it is not difficult to show, by applying "crossing symmetry," that the dispersion relations (22) are identical with relations (16–17) in ref. [2]).

In conclusion it should be noted that in the deduction of the dispersion relations localizability of only the photon field was assumed. It can be shown that in the absence of an unobservable energy region it is sufficient to assume localizability of the photon or nucleon fields in order to deduce rigorously the dispersion relations[4]).

The authors are deeply grateful to Academician N. N. Bogolubov for a valuable discussion of this paper.

References

1) M. Gell-Mann, M. Goldberger and W. Thirring, Phys. Rev. **95** (1957) 1612
2) N. N. Bogolubov and D. V. Shirkov, Doklady Akad. Nauk SSSR **113** (1957) 527
3) N. N. Bogolubov and D. V. Shirkov, Introduction to the theory of quantized fields (in Russian) (Moscow, 1957)
4) B. M. Stepanov, Doklady Akad. Nauk SSSR **118** (1958) 911

7.C

Nuclear Physics 7 (1958) 579—590; © *North-Holland Publishing Co., Amsterdam*

Not to be reproduced by photoprint or microfilm without written permission from the publisher

SOME POSSIBLE EXPERIMENTS FOR THE INVESTIGATION OF INELASTIC SCATTERING OF NUCLEONS

L. M. SOROKO

Joint Institute of Nuclear Research, Laboratory of Nuclear Problems, Dubna, USSR

Received 9 December 1957

Abstract: Some possible experiments are considered which can be used to study inelastic collisions of nucleons of the type $N+N \to \pi+N+N'$. Processes of this type are most frequent in the $\approx$ 650 MeV energy region. Some non-trivial experiments on the π-meson–nucleon angular correlation are indicated which are based on the existence of azimuthal asymmetry in the emission of these two particles. Similar effects for a polarized nucleon beam are considered. The calculations are performed in terms of ten inelastic transition amplitudes, it being assumed that these transitions yield the main contribution to the total cross section of the $N+N \to \pi+N+N'$ process at 650 MeV.

1. Introduction

Investigations of nucleon scattering processes at energies of $\approx$ 650 MeV, performed with the purpose of carrying out quantitative phase shift analysis, include experiments on elastic as well as inelastic scattering of nucleons. The experiments which should be sufficient for a study of elastic processes include observation of various polarization effects and seem to be well established at present [1,2]). In respect of inelastic processes, for which the total cross section at $\approx$ 650 MeV is approximately equal to the total elastic cross section [3]), no complete set of experiments has as yet been proposed. Only the process $p+p \to \pi^+ + d$ [4–8]) has been treated theoretically, whereas the inelastic processes $p+p \to \pi^+ + n + p$ and $p+p \to \pi^0 + p + p$ which are frequent in the $\approx$ 650 MeV region, have not been examined.

Our purpose is to fill up this gap and to ascertain what can be deduced from experiments on processes of the type $N+N \to \pi+N+N'$. In the present paper the π-meson angular distribution and the π-meson—nucleon angular correlations for unpolarized as well as polarized nucleon beams are analyzed. The calculations are performed for two particular reactions, $p+p \to \pi^+ + n + p$ and $p+p \to \pi^0 + p + p$. In a later paper we intend to consider the polarization of inelastically scattered nucleons and the correlation of their spin states.

2. General Remarks

As is well-known, intense absorption by a scattering centre considerably complicates the character of elastic scattering. In order to determine the

phase shifts of the various partial waves by observing an elastic process one must know the intensity of absorption of these partial waves. The latter can be found by analysing the angular and spin characteristics of emission of secondary particles in all possible types of inelastic processes. The most complicated case is that of π-meson formation, $N+N \to \pi+N+N'$, which is characterized by final emission of three particles.

If the energy of the incident nucleon is known, a given process of this type can be completely characterized by prescribing the energy of one of the particles, the polar angles (θ, φ) defining the direction of emission of the particle in the c.m.s. of the colliding nucleons and also the polar angles of motion of the other two particles in their c.m.s. The differential cross section should therefore depend on five arguments.

In order to prescribe the angular part of the final wave function of three particles, the three-body problem is usually reduced to the two-body problem by introduction of two subsystems. This can be done in two ways. In one case two nucleons enter one of the subsystems. This procedure permits one to add the nucleon spins within a single subsystem and to add the orbital angular momenta in each subsystem separately. This method of introduction of two subsystems is usually termed the (ls)-scheme. The angular part of the set of two subsystems can be written as

$$\psi^{(ls)} = \sum_{m+\mu=M} (l_\pi j m\mu | l_\pi j J M) Y^m_{l_\pi}(\pi) \cdot Y_j{}^\mu(1,2).$$

Taking into account the orbital angular momentum of relative motion of two nucleons and their spins we finally obtain

$$\psi^{(ls)} = \sum_{\substack{m+\mu=M \\ m_l+m_s=\mu \\ m_{s_1}+m_{s_2}=m_s}} \sum \sum (l_\pi j m\mu | l_\pi j J M)(lsm_l m_s | lsj\mu)(s_1 s_2 m_{s_1} m_{s_2} | s_1 s_2 s m_s) \times Y^m_{l_\pi}(\pi) \cdot Y^{m_l}_l(1,2) \cdot \chi^{m_{s_1}}_{s_1}(1) \cdot \chi^{m_{s_2}}_{s_2}(2), \qquad (1)$$

where $Y^m_{l_\pi}(\pi) = Y^m_{l_\pi}(\theta_\pi, \varphi_\pi)$ and $Y^{m_l}_l(1,2) = Y^{m_l}_l(\theta_{12}, \varphi_{12})$ are spherical functions of the corresponding arguments. The angles $(\theta_\pi, \varphi_\pi)$ define the direction of emission of the π-meson in the c.m.s. of the two colliding nucleons and $(\theta_{12}, \varphi_{12})$ the direction of emission of nucleon 1 in the c.m.s. of the inelastically scattered nucleons. In this case nucleon 2 is emitted in the opposite direction, so that $\theta_{21} = \pi - \theta_{12}$ and $\varphi_{21} = \varphi_{12} + \pi$.

Expression (1) for the angular part of the wave function is the most convenient one for experiments in which π-mesons are observed. In contrast, if only nucleons are to be observed the (jj)-scheme of introduction of two subsystems should be more convenient; in this case a π-meson and one of the nucleons enter one of the subsystems. It should be emphasized that representation of the angular part in accord with either the (ls) or (jj) scheme corresponds to two possible ways of expanding the angular part of the wave function of three particles in eigenfunctions of each of the sub-

systems. The expansion which is more convenient, that is, which contains the smallest amount of amplitudes yielding large contributions to the cross section, can only be determined by trial, as the choice of the expansion depends in an intricate manner on the mechanism of π-meson formation and on the nature of the interaction between the emitted particles.

In the (jj)-scheme the angular part of the wave function for three particles can be written in the form

$$\psi^{(jj)} = \sum_{\substack{m+m_j=M \\ m_l+m_{s_1}=m_j \\ m_2+m_{s_2}=m}} \sum \sum (jLm_j m|jLJM)(l_2 s_2 m_2 m_{2s}|l_2 s_2 Lm)(l_\pi s_1 m_l m_{1s}|l_\pi s_1 j m_j) \times Y_{l_2}^{m_2}(2) \cdot Y_{l_\pi}^{m_l}(1) \cdot \chi_{s_1}^{m_{1s}}(1) \cdot \chi_{s_2}^{m_{2s}}(2). \quad (2)$$

The vector diagram of the momenta of secondary particles participating in the process $N+N \to \pi+N+N'$ is represented in fig. 1 for the c.m.s. of the colliding nucleons. If the secondary nucleons can be approximately

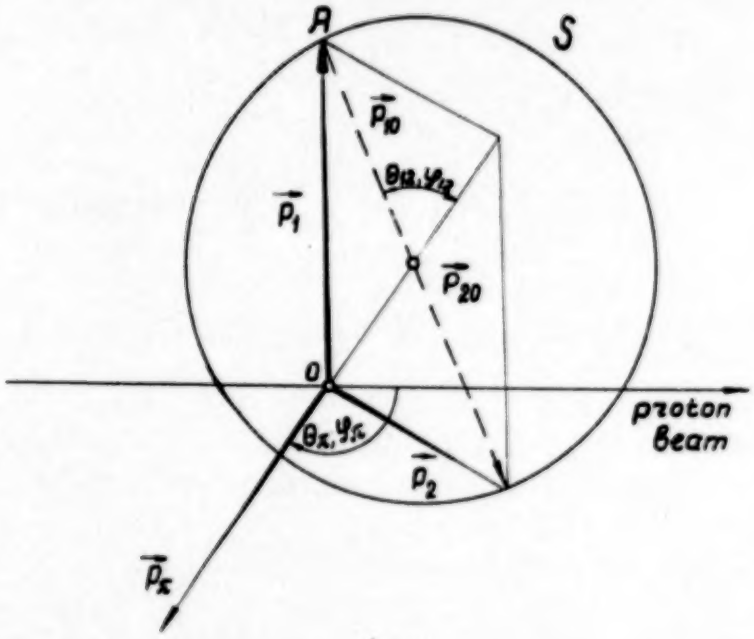

Fig. 1

treated without account of the relativistic increase of their mass, one finds that the locus A of the ends of the nucleon vector will be a sphere of radius $R = \sqrt{M(W-\sqrt{p^2+m^2})-\frac{1}{4}p^2}$, where W is the total kinetic energy in the c.m.s., p is the π-meson momentum and M and m are the nucleon and π-meson masses respectively. It can easily be shown in this case that the differential of the phase volume density for two particles, which in the (ls) scheme is $d^2N/d\Omega(\theta_{12}, \varphi_{12})dW$, is independent of the angles $(\theta_{12}, \varphi_{12})$ and is determined by the magnitude of the radius R. In the (jj) scheme this is not the case and $d^2N/d\Omega(\theta_{\pi 1}, \varphi_{\pi 1})dW$ depends on $\theta_{\pi 1}$ but not on $\varphi_{\pi 1}$.

3. Statement of the Problem

In our calculations we use the formalism developed in ref.[6]) for the analysis of polarization effects in inelastic collisions between nucleons.

The initial function for two protons, of which that contained in the target is unpolarized, can be written in the form

$$\psi_{\text{init}} = \varphi_1 + \varphi_2,$$

where

$$\varphi_1 = \frac{\varepsilon_1}{\sqrt{2}}\sqrt{4\pi}\left\{\sum_{l=0}^{\infty}(-i)^l\sqrt{2l+1}\cdot[1-(-1)^l]\right.$$
$$\cdot\left[q_1\sum_J(l101|l1J1)\cdot Y^1_{J(11)}+\frac{q_2}{\sqrt{2}}\sum_J(l100|l1J0)\cdot Y^0_{J(11)}\right] \qquad (3)$$
$$\left.+\sum_{l=0}^{\infty}(-i)^l\sqrt{2l+1}\cdot[1+(-1)^l]\cdot\frac{q_2}{\sqrt{2}}(l000|l0l0)\cdot Y^0_{l(10)}\right\},$$

$$\varphi_2 = \frac{\varepsilon_2}{\sqrt{2}}\sqrt{4\pi}\cdot\left\{\sum_{l=0}^{\infty}(-i)^l\sqrt{2l+1}\cdot[1-(-1)^l]\right.$$
$$\cdot\left[q_2\sum_J(l10-1|l1J-1)\cdot Y^{-1}_{J(11)}+\frac{q_1}{\sqrt{2}}\sum_J(l100|l1J0)\cdot Y^0_{J(11)}\right] \qquad (4)$$
$$\left.-\sum_{l=0}^{\infty}(-i)^l\sqrt{2l+1}\cdot[1+(-1)^l]\cdot\frac{q_1}{\sqrt{2}}(l000|l0l0)\cdot Y^0_{l(10)}\right\}.$$

The coefficients ε_1 and ε_2 satisfy the condition $|\varepsilon_1|^2 = |\varepsilon_2|^2 = \frac{1}{2}$, $\varepsilon_1^*\,\varepsilon_2 = 0$, and describe an unpolarized target, whereas $q_1 = \cos\frac{1}{2}\vartheta\,e^{-i/2\delta}$, $q_2 = \sin\frac{1}{2}\vartheta\,e^{i/2\delta}$ are coefficients which describe the spin function of a completely polarized proton beam in the direction (ϑ, δ).

In the present work the possibilities which various independent experiments afford are considered for a particular case in which a restricted number of inelastic transition amplitudes are taken into account. Some qualitative generalizations are made on the basis of this particular case. We shall assume that within the framework of the (ls) scheme it is sufficient at primary proton energies of $\approx$ 650 MeV to take into account only those transitions which are given in table 1.

The amplitude of each transition is a function of the π-meson momentum and of the energy of the incident proton. The nucleon momenta will not enter the expression for the cross section as the phase volume of a subsystem of two nucleons is independent of the angles $(\theta_{12}, \varphi_{12})$ at which they move away from each other after collision. This means, in other words, that the angular and momentum parts are completely separated at the termination of the process.

TABLE 1

Type of transition	Transition scheme		Transition amplitude
σ_{10}	$^1S_0 \to (^3S_1p)_0$		$c_1(p_\pi)$
	$^1D_2 \to (^3S_1p)_2$		$c_2(p_\pi)$
	$^3P_0 \to (^1P_1p)_0$		$b_1(p_\pi)$
	$^3P_1 \to (^1P_1p)_1$		$b_2(p_\pi)$
	$^3P_2 \to (^1P_1p)_2$		$b_3(p_\pi)$
	$^3F_2 \to (^1P_1p)_2$		$b_4(p_\pi)$
σ_{11}	$^3P_0 \to (^3P_1p)_0$		$d_1(p_\pi)$
	$^3P_1 \to$	$(^3P_0p)_1$	$d_2(p_\pi)$
		$(^3P_1p)_1$	$d_3(p_\pi)$
		$(^3P_2p)_1$	$d_4(p_\pi)$

4. Results and Discussion

In the present paper we calculate the average values of spin tensors which are directly related to the physical quantities observed experimentally. Thus, for example, the average value of the zero rank spin tensor $\langle T_{00}\rangle$ determines the differential cross section for emission of a π-meson in the direction $(\theta_\pi, \varphi_\pi)$ when the nucleons move in the direction $(\theta_{12}, \varphi_{12})$ with respect to the direction of emission of the π-meson in the c.m.s. of the two nucleons. In this case the relation between the spin tensor $\langle T_{00}\rangle$ and differential cross section is given by the equation

$$\langle T_{00}\rangle(\theta_\pi, \varphi_\pi; \theta_{12}, \varphi_{12}; p_\pi) = \frac{k^2}{\rho_E} \frac{\mathrm{d}^3\sigma(\theta_\pi, \varphi_\pi; \theta_{12}, \varphi_{12}; p_\pi)}{\mathrm{d}\Omega(\theta_\pi, \varphi_\pi)\mathrm{d}\Omega(\theta_{12}, \varphi_{12})\mathrm{d}p_\pi}. \tag{5}$$

Here $k = 1/\lambda$; p_π is the π-meson momentum in the c.m.s. of the colliding nucleons and ρ_E is the phase volume of the three particles and equals $\rho_E = p_\pi^2 \cdot R(p_\pi; W)$.

The final wave function has the form

$$\begin{aligned} F_1 &= \frac{1}{\sqrt{4\pi}}[A_1\chi_0^0 + \alpha_1\chi_1^1 + \beta_1\chi_1^0 + \gamma_1\chi_1^{-1}], \\ F_2 &= \frac{1}{\sqrt{4\pi}}[A_2\chi_0^0 + \alpha_2\chi_1^1 + \beta_2\chi_1^0 + \gamma_2\chi_1^{-1}], \end{aligned} \tag{6}$$

where the coefficients A_1, α_1 etc., are related to the transition amplitudes as follows:

$$A_1 = -iq_1 \frac{3}{\sqrt{2}} \Big[\Big(b_- + \frac{\sqrt{3}}{2} b_2 \Big) \cdot \sin\theta_\pi \cdot \cos\theta_{12} \cdot e^{i\varphi_\pi} + \Big(b_- - \frac{\sqrt{3}}{2} b_2 \Big) \cdot \cos\theta_\pi \cdot \sin\theta_{12} \cdot e^{i\varphi_{12}} \Big] - iq_2 \cdot 3 \Big[\Big(\frac{b_1}{\sqrt{6}} - b_+ \Big) \cdot \sin\theta_\pi \cdot \sin\theta_{12} \cdot \cos(\varphi_\pi - \varphi_{12}) + \Big(\frac{b_1}{\sqrt{6}} + 2b_+ \Big) \cdot \cos\theta_\pi \cdot \cos\theta_{12} \Big],$$

$$\alpha_1 = iq_2 \Big[\frac{c_-}{2i} \sin\theta_\pi \cdot e^{-i\varphi_\pi} + \tfrac{1}{2}\sqrt{\tfrac{3}{2}}\, d_1 (\cos\theta_\pi \cdot \sin\theta_{12} \cdot e^{-i\varphi_{12}} - \sin\theta_\pi \cdot \cos\theta_{12} \cdot e^{-i\varphi_\pi}) \Big] + iq_1 \tfrac{3}{2} \Big[\Big(\sqrt{\tfrac{3}{2}}\, d_3 - \frac{3}{\sqrt{10}} d_4 \Big) \cos\theta_\pi \cdot \cos\theta_{12} - D_- \cdot \sin\theta_\pi \cdot \sin\theta_{12} \cdot e^{i(\varphi_\pi - \varphi_{12})} - \frac{3}{\sqrt{10}} d_4 \cdot \sin\theta_\pi \cdot \sin\theta_{12} \cdot e^{-i(\varphi_\pi - \varphi_{12})} \Big],$$

$$\beta_1 = iq_2 \Big[-\frac{c_+}{2i} \cos\theta_\pi + i \frac{\sqrt{3}}{2} d_1 \cdot \sin\theta_\pi \cdot \sin\theta_{12} \cdot \sin(\varphi_\pi - \varphi_{12}) \Big] + iq_1 \cdot \tfrac{3}{2} \Big[\Big(d_2 - \frac{d_4}{\sqrt{5}} \Big) \sin\theta_\pi \cdot \cos\theta_{12}\, e^{i\varphi_\pi} + \Big(\frac{\sqrt{3}}{2} d_3 + \frac{3}{\sqrt{20}} d_4 \Big) \cos\theta_\pi \cdot \sin\theta_{12} \cdot e^{i\varphi_{12}} \Big],$$

$$\gamma_1 = iq_2 \Big[-\frac{c_-}{2i} \sin\theta_\pi \cdot e^{i\varphi_\pi} + \tfrac{1}{2}\sqrt{\tfrac{3}{2}}\, d_1 (\cos\theta_\pi \cdot \sin\theta_{12} \cdot e^{i\varphi_{12}} - \sin\theta_\pi \cdot \cos\theta_{12} \cdot e^{i\varphi_\pi}) \Big] + iq_1 \cdot \tfrac{3}{2} \cdot D_+ \cdot \sin\theta_\pi \cdot \sin\theta_{12} \cdot e^{i(\varphi_\pi + \varphi_{12})}, \tag{7}$$

$$A_2 = iq_2 \frac{3}{\sqrt{2}} \Big[\Big(b_- + \frac{\sqrt{3}}{2} b_2 \Big) \cdot \sin\theta_\pi \cdot \cos\theta_{12} \cdot e^{-i\varphi_\pi} + \Big(b_- - \frac{\sqrt{3}}{2} b_2 \Big) \cdot \cos\theta_\pi \cdot \sin\theta_{12} \cdot e^{-i\varphi_{12}} \Big] - iq_1\, 3 \Big[\Big(\frac{b_1}{\sqrt{6}} - b_+ \Big) \cdot \sin\theta_\pi \cdot \sin\theta_{12} \cdot \cos(\varphi_\pi - \varphi_{12}) + \Big(\frac{b_1}{\sqrt{6}} + 2b_+ \Big) \cos\theta_\pi \cdot \cos\theta_{12} \Big],$$

$$\alpha_2 = iq_1 \Big[-\frac{c_-}{2i} \sin\theta_\pi\, e^{-i\varphi_\pi} + \tfrac{1}{2}\sqrt{\tfrac{3}{2}}\, d_1 (\cos\theta_\pi \cdot \sin\theta_{12} \cdot e^{-i\varphi_{12}} - \sin\theta_\pi \cdot \cos\theta_{12} \cdot e^{-i\varphi_\pi}) \Big] - iq_2 \cdot \tfrac{3}{2} D_+ \cdot \sin\theta_\pi \cdot \sin\theta_{12} \cdot e^{-i(\varphi_\pi + \varphi_{12})},$$

$$\beta_2 = iq_1 \Big[\frac{c_+}{2i} \cos\theta_\pi + i \frac{\sqrt{3}}{2} d_1 \cdot \sin\theta_\pi \cdot \sin\theta_{12} \cdot \sin(\varphi_\pi - \varphi_{12}) \Big] + iq_2 \cdot \tfrac{3}{2} \Big[\Big(d_2 - \frac{d_4}{\sqrt{5}} \Big) \sin\theta_\pi \cdot \cos\theta_{12} \cdot e^{-i\varphi_\pi} + \Big(\frac{\sqrt{3}}{2} d_3 + \frac{3}{\sqrt{20}} d_4 \Big) \cos\theta_\pi \cdot \sin\theta_{12} \cdot e^{-i\varphi_{12}} \Big],$$

$$\gamma_2 = iq_1\Big[\frac{c_-}{2i}\sin\theta_\pi\cdot e^{+i\varphi_\pi} + \tfrac{1}{2}\sqrt{\tfrac{3}{2}}\,d_1(\cos\theta_\pi\cdot\sin\theta_{12}\cdot e^{i\varphi_{12}} - \sin\theta_\pi\cdot\cos\theta_{12}\cdot e^{i\varphi_\pi})\Big]$$
$$-iq_2\cdot\tfrac{3}{2}\Big[\Big(\sqrt{\tfrac{3}{2}}\,d_3 - \frac{3}{\sqrt{10}}\,d_4\Big)\cdot\cos\theta_\pi\cos\theta_{12} \qquad (7)$$
$$-D_-\cdot\sin\theta_\pi\cdot\sin\theta_{12}\cdot e^{-i(\varphi_\pi-\varphi_{12})} - \frac{3}{\sqrt{10}}\,d_4\cdot\sin\theta_\pi\cdot\sin\theta_{12}\cdot e^{i(\varphi_\pi-\varphi_{12})}\Big],$$

and

$$c_+ = c_1+\sqrt{10}\,c_2,\quad b_+ = \frac{b_3}{\sqrt{6}}+\frac{b_4}{2},$$
$$c_- = c_1-\sqrt{\tfrac{5}{2}}\,c_2,\quad b_- = -\frac{\sqrt{3}}{2}\,b_3+\frac{b_4}{2},\qquad D_\pm = \frac{d_2}{\sqrt{2}}\pm\tfrac{1}{2}\sqrt{\tfrac{3}{2}}\,d_3+\frac{d_4}{2\sqrt{10}}. \qquad (8)$$

We furthermore have

$$\langle T_{00}\rangle = |F_1|^2+|F_2|^2 = \frac{1}{4\pi}\,[|A_1|^2+|\alpha_1|^2+|\beta_1|^2+|\gamma_1|^2+|A_2|^2+|\alpha_2|^2+|\beta_2|^2+|\gamma_2|^2]. \qquad (9)$$

The results of the calculations can easily be represented in the form

$$\langle T_{00}\rangle = \langle T_{00}\rangle_{\text{unpol}}+P\cdot\langle T_{00}\rangle_{\text{pol}}. \qquad (10)$$

Here P is the degree of polarization (along the Oy axis) of the incident proton beam and

$$\langle T_{00}\rangle_{\text{unpol}} = \frac{1}{4\pi}\{f_0+f_1\cdot\cos^2\theta_\pi+f_2\cdot\cos^2\theta_{12}+f_3\cdot\cos^2\theta_\pi\cdot\cos^2\theta_{12} + f_4\cdot\sin\theta_\pi\cdot\cos\theta_\pi\cdot\sin\theta_{12}\cdot\cos\theta_{12}\cdot\cos(\varphi_\pi-\varphi_{12}) \qquad (11)$$
$$+f_5\cdot\sin^2\theta_\pi\cdot\sin^2\theta_{12}\cdot\cos 2(\varphi_\pi-\varphi_{12})\},$$

$$\langle T_{00}\rangle_{\text{pol}} = \frac{1}{4\pi}\{\sin\theta_\pi\cdot\cos\theta_\pi\,[(g_0+g_1\cdot\cos\theta_{12}+g_2\cdot\cos^2\theta_{12})\cdot\cos\varphi_\pi + g_3\cdot\sin^2\theta_{12}\cdot\cos(\varphi_\pi-2\varphi_{12})] \qquad (12)$$
$$+\sin\theta_{12}\cdot\cos\theta_{12}\cdot[(g_4+g_5\cdot\cos^2\theta_\pi)\cdot\cos\varphi_{12}+g_6\cdot\sin^2\theta_\pi\cdot\cos(\varphi_{12}-2\varphi_\pi)]$$
$$+\sin\theta_{12}\cdot[(g_7+g_8\cdot\cos^2\theta_\pi)\cdot\cos\varphi_{12}+g_9\cdot\sin^2\theta_\pi\cdot\cos(\varphi_{12}-2\varphi_\pi)]\}.$$

The values of coefficients $f_0, f_1, \ldots$ and $g_0, g_1, \ldots$ are given in the appendix. The difference between expression (11) and the expression for the differential cross section for inelastic processes involving the emission of two particles is that (11) contains the asymmetry with respect to the azimuthal angle $(\varphi_\pi-\varphi_{12})$ in the form of $\cos(\varphi_\pi-\varphi_{12})$ as well as $\cos 2(\varphi_\pi-\varphi_{12})$. It is natural that both types of asymmetry must be measured, as then two independent coefficients f_4 and f_5 can be determined. The kinematic scheme of the corresponding experiment will be that represented in fig. 2 if the c.m.s. of the colliding nucleons is used. The relation between the radius R and the π-meson momentum shown in the fig. corresponds to a π-meson

energy close to the highest possible energy. For fixed angles θ_π and θ_{12} and also for $\varphi_\pi = 0$, the cross section (11) takes the form

$$\langle T_{00}\rangle_{\text{unpol}} = h_0 + h_1 \cdot \cos\varphi_{12} + h_2 \cdot \cos 2\varphi_{12}.$$

In order to determine the coefficients h_1 and h_2 and hence f_4 and f_5 the measurements should be carried out at the angles $\varphi_{12} = 0°$, 90° and 180°. In

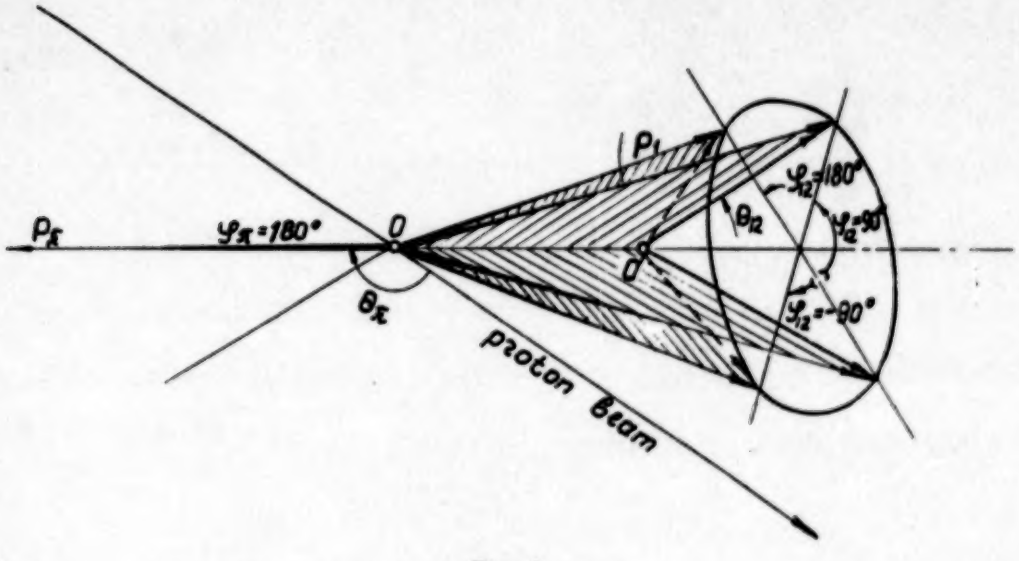

Fig. 2

measuring the asymmetry $\cos 2(\varphi_\pi - \varphi_{12})$ it is profitable to choose angles θ_π and θ_{12} equal to 90° as then the asymmetry $\propto \cos(\varphi_\pi - \varphi_{12})$ vanishes.

Measurement of the coefficient f_5 is important since this coefficient depends only on such transitions which are related to the initial states $^3P_0$, $^3P_2$ and $^3F_2$ of the two protons and is independent of any other of the transitions chosen by us. Apparently, the following general conclusion is true: the contribution to the term with f_5 is made by transitions from those nucleon triplet states in which the orbital and spin momenta are either parallel or antiparallel.

As an example we may consider the reaction $p+p \to \pi^0+p+p$ to which only σ_{11} transitions can contribute. In our particular choice of the initial transitions, measurement of f'_5 directly yields the amplitude of the transition $^3P_0 \to (^3P_1\, p)_0$. Indeed, in this case we have

$$f'_5 = -\tfrac{3}{8}|d_1|^2. \tag{13}$$

The minus sign in (13) means that emission at an angle of $(\varphi_\pi - \varphi_{12}) = 90°$ is more probable than emission at an angle $(\varphi_\pi - \varphi_{12}) = 0^0$.

Less information can be derived from experiments in which only π-mesons are recorded and the nucleons are emitted in arbitrary directions, than from experiments in which one of the nucleons is likewise recorded. Thus if only the π-meson is observed we have

$$\langle T_{00}\rangle_{\text{unpol}}(\theta_\pi, \varphi_\pi; p_\pi) = (f_0+\tfrac{1}{3}f_2)+(f_1+\tfrac{1}{3}f_3)\cdot\cos^2\theta_\pi, \qquad (14)$$

where f_4 and f_5 have completely dropped out and the other coefficients are encountered in pairs.

Examination of the coefficients determining $\langle T_{00}\rangle_{\text{pol}}$ reveals that the coefficients g_1, g_7, g_8, and g_9 contain terms due to interference between σ_{10} and σ_{11} transitions or more precisely, between the $^1S_0 \to (^3S_1\,p)_0$ and $^1D_2 \to (^3S_1 p)_2$ transitions and $^3P_1 \to (^3P_0 p)_1$, $^3P_1 \to (^3P_1 p)_1$, $^3P_1 \to (^3P_2 p)_1$ transitions.

Experiments on a polarized beam, in which only the π-meson is recorded, permit the determination of the quantity

$$\langle T_{00}\rangle_{\text{pol}}(\theta_\pi, \varphi_\pi; p_\pi) = \sin\theta_\pi\cdot\cos\theta_\pi\cdot(g_0+\tfrac{1}{2}g_2)\cdot\cos\varphi_\pi. \qquad (15)$$

Here seven of nine coefficients have dropped out and the remaining two enter as a linear combination. This is a convincing illustration of the statement that experiments, in which besides the π-meson one of the nucleons is recorded, yield much more information than those experiments in which only the π-meson is recorded.

The authors are thankful to S. M. Bilenky, L. I. Lapidus and R. M. Ryndin for valuable discussions and advice.

Appendix

COEFFICIENTS f_i AND g_i FOR THE PROCESS $p+p\to\pi^+ + n + p$

$$\begin{aligned}
f_0 = {} & \tfrac{1}{2}|c_-|^2+\tfrac{9}{4}\{\tfrac{1}{6}|d_1|^2+|d_2|^2+\tfrac{3}{4}|d_3|^2+\tfrac{5}{4}|d_4|^2+\tfrac{4}{\sqrt{5}}|d_2|\cdot|d_4|\cdot\cos(d_2,d_4)\\
& -\tfrac{3}{2}\sqrt{\tfrac{3}{5}}|d_3|\cdot|d_4|\cdot\cos(d_3,d_4)+\tfrac{1}{3}(|b_1|^2+|b_3|^2)+\tfrac{1}{2}|b_4|^2\\
& +\sqrt{\tfrac{2}{3}}|b_3|\cdot|b_4|\cdot\cos(b_3,b_4)-\sqrt{\tfrac{2}{3}}|b_1|\cdot|b_4|\cdot\cos(b_1,b_4)\\
& -\tfrac{2}{3}|b_1|\cdot|b_3|\cdot\cos(b_1,b_3)\},
\end{aligned}$$

$$\begin{aligned}
f_1 = {} & \frac{|c_+|^2-|c_-|^2}{2}+\tfrac{9}{4}\{\tfrac{1}{6}|d_1|^2-|d_2|^2-\tfrac{3}{4}|d_4|^2-\tfrac{4}{\sqrt{5}}|d_2|\cdot|d_4|\cdot\cos(d_2,d_4)-\tfrac{1}{3}|b_1|^2\\
& +\tfrac{7}{6}|b_3|^2+\tfrac{3}{2}|b_2|^2+\tfrac{1}{2}|b_4|^2-4\sqrt{\tfrac{3}{2}}|b_3|\cdot|b_4|\cdot\cos(b_3,b_4)+\sqrt{\tfrac{2}{3}}|b_1|\cdot|b_4|\cdot\cos(b_1,b_4)\\
& +\tfrac{2}{3}|b_1|\cdot|b_3|\cdot\cos(b_1,b_3)-2\sqrt{\tfrac{3}{2}}|b_2|\cdot|b_4|\cdot\cos(b_2,b_4)+3|b_2|\cdot|b_3|\cdot\cos(b_2,b_3)\},
\end{aligned}$$

$$\begin{aligned}
f_2 = {} & \tfrac{9}{4}[\tfrac{1}{6}|d_1|^2-\tfrac{3}{4}|d_3|^2-\tfrac{21}{20}|d_4|^2-\tfrac{6}{\sqrt{5}}|d_2|\cdot|d_4|\cdot\cos(d_2,d_4)\\
& +\tfrac{3}{2}\sqrt{\tfrac{3}{5}}|d_3|\cdot|d_4|\cdot\cos(d_3,d_4)-\tfrac{1}{3}|b_1|^2+\tfrac{3}{2}|b_2|^2+\tfrac{7}{6}|b_3|^2+\tfrac{1}{2}|b_4|^2\\
& +\sqrt{\tfrac{2}{3}}|b_1|\cdot|b_4|\cdot\cos(b_1,b_4)+\tfrac{2}{3}|b_1|\cdot|b_3|\cdot\cos(b_1,b_3)-4\sqrt{\tfrac{2}{3}}|b_3|\cdot|b_4|\cdot\cos(b_3,b_4)\\
& +\sqrt{6}|b_2|\cdot|b_4|\cdot\cos(b_2,b_4)-3|b_2|\cdot|b_3|\cdot\cos(b_2,b_3)],
\end{aligned}$$

$$f_3 = \tfrac{9}{4}[-\tfrac{1}{2}|d_1|^2+\tfrac{3}{2}|d_3|^2+\tfrac{3}{2}|d_4|^2+\tfrac{6}{\sqrt{5}}|d_2|\cdot|d_4|\cdot\cos(d_2,d_4)$$
$$-6\sqrt{\tfrac{3}{5}}|d_3|\cdot|d_4|\cdot\cos(d_3,d_4)+|b_1|^2-3|b_2|^2-\tfrac{1}{2}|b_4|^2$$
$$+5\sqrt{6}|b_3|\cdot|b_4|\cdot\cos(b_3,b_4)+\sqrt{6}|b_1|\cdot|b_4|\cdot\cos(b_1,b_4)$$
$$+2|b_1|\cdot|b_3|\cdot\cos(b_1,b_3)],$$

$$f_4 = 3[-\tfrac{1}{2}|d_1|^2-\tfrac{63}{80}|d_4|^2-\tfrac{9}{8}|d_3|^2+\tfrac{3}{4}\sqrt{3}|d_2|\cdot|d_3|\cdot\cos(d_2,d_3)$$
$$+\tfrac{3}{4}\sqrt{15}|d_3|\cdot|d_4|\cdot\cos(d_3,d_4)-\tfrac{3}{4}\sqrt{\tfrac{1}{5}}|d_2|\cdot|d_4|\cdot\cos(d_2,d_4)+|b_1|^2-\tfrac{9}{4}|b_2|^2$$
$$+\tfrac{1}{3}|b_3|^2-\tfrac{3}{2}|b_4|^2+\sqrt{\tfrac{3}{2}}|b_1|\cdot|b_4|\cdot\cos(b_1,b_4)+|b_1|\cdot|b_3|\cdot\cos(b_1,b_3)$$
$$-\frac{21}{\sqrt{6}}|b_3|\cdot|b_4|\cdot\cos(b_3,b_4)],$$

$$f_5 = \tfrac{3}{2}[-\tfrac{1}{4}|d_1|^2+\tfrac{1}{2}(|b_1|^2+|b_3|^2)+\tfrac{3}{4}|b_4|^2+\sqrt{\tfrac{3}{2}}|b_3|\cdot|b_4|\cdot\cos(b_3,b_4)$$
$$-\sqrt{\tfrac{3}{2}}|b_1|\cdot|b_4|\cdot\cos(b_1,b_4)-|b_1|\cdot|b_3|\cdot\cos(b_1,b_3)],$$

$$g_0 = \tfrac{9}{4}[\tfrac{1}{2}|d_1|\cdot|d_3|\cdot\sin(d_1,d_3)-\frac{1}{\sqrt{20}}|d_1|\cdot|d_4|\cdot\sin(d_1,d_4)$$
$$-|b_1|\cdot|b_2|\cdot\sin(b_1,b_2)-|b_1|\cdot|b_3|\cdot\sin(b_1,b_3)+\frac{1}{\sqrt{3}}|b_1|\cdot|b_4|\cdot\sin(b_1,b_4)$$
$$-|b_2|\cdot|b_3|\cdot\sin(b_2,b_3)-\sqrt{\tfrac{3}{2}}|b_2|\cdot|b_4|\cdot\sin(b_2,b_4)$$
$$-\frac{5}{\sqrt{6}}|b_3|\cdot|b_4|\cdot\sin(b_3,b_4)],$$

$$g_1 = \tfrac{3}{2}[\sqrt{\tfrac{3}{2}}|c_-|\cdot|d_3|\cdot\cos(c_-,d_3)-\frac{3}{\sqrt{10}}|c_-|\cdot|d_4|\cdot\cos(c_-,d_4)$$
$$-|c_+|\cdot|d_2|\cdot\cos(c_+,d_2)+\frac{1}{\sqrt{5}}|c_+|\cdot|d_4|\cdot\cos(c_+,d_4)],$$

$$g_2 = \tfrac{9}{4}[\tfrac{1}{2}|d_1|\cdot|d_3|\cdot\sin(d_1,d_3)-\tfrac{1}{2}\sqrt{\tfrac{3}{5}}|d_1|\cdot|d_4|\cdot\sin(d_1,d_4)$$
$$+3|b_1|\cdot|b_2|\cdot\sin(b_1,b_2)-|b_1|\cdot|b_3|\cdot\sin(b_1,b_3)+|b_1|\cdot|b_4|\cdot\sin(b_1,b_4)$$
$$+5|b_2|\cdot|b_3|\cdot\sin(b_2,b_3)-3\sqrt{\tfrac{3}{2}}|b_2|\cdot|b_4|\cdot\sin(b_2,b_4)$$
$$+\frac{25}{\sqrt{6}}|b_3|\cdot|b_4|\cdot\sin(b_3,b_4)],$$

$$g_3 = \tfrac{9}{4}[\tfrac{1}{2}|d_1|\cdot|d_3|\cdot\sin(d_1,d_3)-\tfrac{1}{2}\sqrt{\tfrac{3}{5}}|d_1|\cdot|d_4|\cdot\sin(d_1,d_4)$$
$$-|b_1|\cdot|b_2|\cdot\sin(b_1,b_2)-|b_1|\cdot|b_3|\cdot\sin(b_1,b_3)+\sqrt{\tfrac{2}{3}}|b_1|\cdot|b_4|\cdot\sin(b_1,b_4)$$
$$-|b_2|\cdot|b_3|\cdot\sin(b_2,b_3)-\sqrt{\tfrac{3}{2}}|b_2|\cdot|b_4|\cdot\sin(b_2,b_4)$$
$$-\frac{5}{\sqrt{6}}|b_3|\cdot|b_4|\cdot\sin(b_3,b_4)],$$

$$g_4 = \tfrac{9}{4}[-\tfrac{1}{2}|d_1|\cdot|d_3|\cdot\sin(d_1,d_3)+\tfrac{1}{2}\sqrt{\tfrac{3}{5}}|d_1|\cdot|d_4|\cdot\sin(d_1,d_4)$$
$$+|b_1|\cdot|b_2|\cdot\sin(b_1,b_2)-|b_1|\cdot|b_3|\cdot\sin(b_1,b_3)+\sqrt{\tfrac{2}{3}}|b_1|\cdot|b_4|\cdot\sin(b_1,b_4)$$
$$+|b_2|\cdot|b_3|\cdot\sin(b_2,b_3)+\sqrt{\tfrac{3}{2}}|b_2|\cdot|b_4|\cdot\sin(b_2,b_4)$$
$$-\frac{5}{\sqrt{6}}|b_3|\cdot|b_4|\cdot\sin(b_3,b_4)],$$

$$g_5 = \tfrac{9}{4}[-\tfrac{1}{2}|d_1| \cdot |d_3| \cdot \sin(d_1, d_3) + \tfrac{1}{2}\sqrt{\tfrac{3}{5}}|d_1| \cdot |d_4| \cdot \sin(d_1, d_4)$$
$$-3|b_1| \cdot |b_2| \cdot \sin(b_1, b_2) - |b_1| \cdot |b_3| \cdot \sin(b_1, b_3)$$
$$+\sqrt{\tfrac{2}{3}}|b_1| \cdot |b_4| \cdot \sin(b_1, b_4) + 3|b_2| \cdot |b_3| \cdot \sin(b_2, b_3)$$
$$+3\sqrt{\tfrac{3}{2}}|b_2| \cdot |b_4| \cdot \sin(b_2, b_4) + \frac{25}{\sqrt{6}}|b_3| \cdot |b_4| \cdot \sin(b_3, b_4)],$$

$$g_6 = \tfrac{9}{4}[-\frac{1}{\sqrt{3}}|d_1| \cdot |d_3| \cdot \sin(d_1, d_3) + \tfrac{1}{2}\sqrt{\tfrac{3}{5}}|d_1| \cdot |d_4| \cdot \sin(d_1, d_4)$$
$$+|b_1| \cdot |b_2| \cdot \sin(b_1, b_2) - |b_1| \cdot |b_3| \cdot \sin(b_1, b_3) + \sqrt{\tfrac{2}{3}}|b_1| \cdot |b_4| \cdot \sin(b_1, b_4)$$
$$+|b_2| \cdot |b_3| \cdot \sin(b_2, b_3) - \frac{5}{\sqrt{6}}|b_3| \cdot |b_4| \cdot \sin(b_3, b_4)$$
$$+\sqrt{\tfrac{3}{2}}|b_2| \cdot |b_4| \cdot \sin(b_2, b_4)],$$

$$g_7 = \tfrac{9}{4}[-\frac{1}{3\sqrt{2}}|c_-| \cdot |d_2| \cdot \cos(c_-, d_2) - \frac{1}{\sqrt{6}}|c_-| \cdot |d_3| \cdot \cos(c_-, d_3)$$
$$-\tfrac{7}{3}\sqrt{\tfrac{1}{10}}|c_-| \cdot |d_4| \cdot \cos(c_-, d_1)],$$

$$g_8 = \tfrac{9}{4}[\tfrac{7}{3}\sqrt{\tfrac{1}{10}}|c_-| \cdot |d_4| \cdot \cos(c_-, d_4) + \frac{\sqrt{2}}{3}|c_-| \cdot |d_2| \cdot \cos(c_-, d_2)$$
$$+\frac{1}{\sqrt{6}}|c_-| \cdot |d_3| \cdot \cos(c_-, d_3) - \frac{1}{\sqrt{3}}|c_+| \cdot |d_3| \cdot \cos(c_+, d_3)$$
$$-\frac{1}{\sqrt{5}}|c_+| \cdot |d_4| \cdot \cos(c_+, d_4)],$$

$$g_9 = \tfrac{3}{2}[\tfrac{1}{2}\sqrt{\tfrac{3}{2}}|c_-| \cdot |d_3| \cdot \cos(c_-, d_3) - \frac{1}{\sqrt{2}}|c_-| \cdot |d_2| \cdot \cos(c_-, d_2)$$
$$-\frac{1}{2\sqrt{10}}|c_-| \cdot |d_4| \cdot \cos(c_-, d_4)].$$

Coefficients f'_i and g'_i for the process $p+p \to \pi^0+p+p$

$$f'_0 = \tfrac{9}{4}[\tfrac{1}{6}|d_1|^2 + |d_2|^2 + \tfrac{3}{4}|d_3|^2 + \tfrac{5}{4}|d_4|^2 + \frac{4}{\sqrt{5}}|d_2| \cdot |d_4| \cdot \cos(d_2, d_4)$$
$$-\tfrac{3}{5}\sqrt{\tfrac{3}{5}}|d_3| \cdot |d_4| \cdot \cos(d_3, d_4)],$$

$$f'_1 = \tfrac{9}{4}[\tfrac{1}{6}|d_1|^2 - |d_2|^2 - \tfrac{3}{4}|d_3|^2 - \frac{4}{\sqrt{5}}|d_2| \cdot |d_4| \cdot \cos(d_2, d_4)],$$

$$f'_2 = \tfrac{9}{4}[\tfrac{1}{6}|d_1|^2 - \tfrac{3}{4}|d_3|^2 - \tfrac{21}{20}|d_4|^2 - \frac{6}{\sqrt{5}}|d_2| \cdot |d_4| \cdot \cos(d_2, d_4)$$
$$+\tfrac{3}{2}\sqrt{\tfrac{3}{5}}|d_3| \cdot |d_4| \cdot \cos(d_3, d_4)],$$

$$f'_3 = \tfrac{9}{4}[-\tfrac{1}{2}|d_1|^2 + \tfrac{3}{2}|d_3|^2 + \tfrac{3}{2}|d_4|^2 + \frac{6}{\sqrt{5}}|d_2| \cdot |d_4| \cdot \cos(d_2, d_4)$$
$$-6\sqrt{\tfrac{3}{5}}|d_3| \cdot |d_4| \cdot \cos(d_3, d_4)],$$

$$f'_4 = 3[-\tfrac{1}{2}|d_1|^2 - \tfrac{63}{80}|d_4|^2 - \tfrac{9}{8}|d_3|^2 + \tfrac{3}{4}\sqrt{3}|d_2| \cdot |d_3| \cdot \cos(d_2, d_3)$$
$$+\tfrac{3}{4}\sqrt{15}|d_3| \cdot |d_4| \cdot \cos(d_3, d_4)],$$

$$f'_5 = -\tfrac{3}{8}|d_1|^2,$$

$$g'_0 = \tfrac{9}{4}[\tfrac{1}{2}|d_1| \cdot |d_3| \cdot \sin(d_1, d_3) - \frac{1}{\sqrt{20}}|d_1| \cdot |d_4| \cdot \sin(d_1, d_4)],$$

$$g'_2 = \tfrac{9}{4}[\tfrac{1}{2}|d_1| \cdot |d_3| \cdot \sin(d_1, d_3) - \tfrac{1}{2}\sqrt{\tfrac{3}{5}}|d_1| \cdot |d_4| \cdot \sin(d_1, d_4)],$$

$$g'_6 = \tfrac{9}{4}[-\frac{1}{\sqrt{3}}|d_1| \cdot |d_3| \cdot \sin(d_1, d_3) + \tfrac{1}{2}\sqrt{\tfrac{3}{5}}|d_1| \cdot |d_4| \cdot \sin(d_1, d_4)],$$

$$g'_3 = g'_2 = -g'_4 = -g'_5,$$

$$g'_1 = g'_7 = g'_8 = g'_9 = 0.$$

References

1) O. Chamberlain, E. Segrè, R. Tripp, K. Wiegand and T. Ypsilantis, Phys. Rev. **105** (1957) 288;
   H. Stapp, T. Ypsilantis, and N. Metropolis, Phys. Rev. **105** (1957) 302
2) V. Vladimirsky and Ya. Smorodinsky, Doklady Akad. Nauk SSSR **104** (1955) 713
3) V. P. Dželepow, V. I. Moskalev and S. V. Medved, Doklady Akad. Nauk SSSR **104** (1955) 380
4) L. Wolfenstein, Phys. Rev. **98** (1955) 766
5) K. Watson and K. Brueckner, Phys. Rev. **83** (1955) 1
6) V. B. Berestetsky, Doklady Akad. Nauk SSSR **94** (1954) 421
7) S. M. Bilenky and L. I. Lapidus, Report of INP, 1955
8) F. Mandl and T. Regge, Phys. Rev. **99** (1955) 1478

8.B

Nuclear Physics 7 (1958) 591—598; © *North-Holland Publishing Co., Amsterdam*

Not to be reproduced by photoprint or microfilm without written permission from the publisher

FIRST ORDER FORBIDDEN β—γ-CORRELATION FOR ORIENTED NUCLEI

A. Z. DOLGINOV and N. P. POPOV

Physico-Technical Institute, U.S.S.R. Academy of Sciences, Leningrad

Received 30 January 1958

Abstract: Explicit formulae for $\beta - \gamma$-correlation of oriented nuclei in first forbidden β-transitions are obtained. All five types of β-interaction are considered and the Coulomb field of an extended nucleus is taken into account. Explicit $\beta - \gamma$-correlation formulae for non-oriented nuclei are obtained as a particular case. Angular as well as polarization correlation is considered.

In a previous paper of one of the authors [1]) a general formula was deduced for the angular and polarization correlation between a β-particle and γ-quantum in transitions of arbitrary order of forbiddenness. In the present paper we consider in detail first forbidden transitions and present explicit formulae which are valid for practical purposes. Since the method of performing the calculations has been outlined in ref.[1]), we shall give directly the final results for the correlation.

Let the z-axis of the coordinate system be directed along the direction of predominant orientation of the nuclear spins. Let $\mathbf{p}(p, \vartheta, \varphi)$ denote the electron momentum, $\mathbf{k}(k, \theta, \phi)$ the γ-quantum momentum and I the γ-quantum multipolarity; j_0, j_1 and j_2 denote the angular momenta of the nuclear levels for the β—γ-transition $j_0(\beta)j_1(\gamma)j_2$; μ_0, μ_1, and μ_2 are projections of the angular momenta of the nuclear levels on the z-axis.

For oriented nuclei the first forbidden β—γ-angular correlation has the form †

$$W(\mathbf{j}_0, \mathbf{p}, \mathbf{k}) = \sum_{S,J,g} \sum_{L \leqq L'} Z^J_{LL'} U^{LL'}_{SgJ} h_g(j_0) B_S F_{SgJ}(\mathbf{p}, \mathbf{k}), \tag{1}$$

$$U^{LL'}_{SgJ} = (-1)^g \sqrt{(2g+1)(2S+1)}\, X(j_1 j_1 S, j_0 j_0 g, L' L J), \tag{2}$$

$$B_S = \sqrt{(2j_1+1)(2I+1)} \left[1 - \frac{S(S+1)}{2I(I+1)}\right] W(j_2 I j_1 S; j_1 I) C^{I0}_{I0S0} \tag{3}$$

$$h_g(j_0) = \sum_{\mu_0} (-1)^{j_0-\mu_0} C^{g0}_{j_0\mu_0 j_0-\mu_0} w(\mu_0). \tag{4}$$

In (1) summation is carried out between the following limits: L and $L' = 0, 1, 2$; $J = 0, 1, 2, 3$; $0 \leqq g \leqq 2j_0$ for $|S-J| \leqq g \leqq S+J$ where S is

† Common factors which do not affect the correlation are disregarded throughout this paper.

even and $0 \leqq S \leqq 2I$. For aligned nuclei (obtained e.g. by Bleaney's [2]) or Pound's [3]) method) only even values of g are possible. For polarized nuclei (obtained e.g. by the Gorter-Rose [4]) method) even as well as odd values of g are possible. Since the coefficient f_g decreases with increasing g it is usually sufficient to take $g \leqq 4$ or even less. The values of $f_g(j) = h_g(j)/j^g$ are presented in ref. [5]). The $X(abc, def, ghi)$ are Fano functions; the properties, explicit form and some particular values of these functions are presented in ref.[6]). The $W(abcd; ef)$ are Racah functions and have been tabulated in ref.[7])

The $C^{\alpha\alpha}_{b\beta c\gamma}$ are Clebsch-Gordan coefficients. $w(\mu_0)$ is the probability of a given value of μ_0 (projection of the angular momentum of the oriented nucleus). The values of $Z^J_{LL'}$ are presented in appendix 1. The quantities $F_{S_g J}(\mathbf{p}, \mathbf{k})$ depend only on the angles of $\mathbf{p}$ and $\mathbf{k}$:

$$F_{S_g J}(\mathbf{p}, \mathbf{k}) = 4\pi i^\gamma \sum_\sigma C^{J\sigma}_{g0S\sigma} Y_{S\sigma}(\theta\phi) Y^*_{J\sigma}(\vartheta\varphi), \tag{5}$$

where $2\gamma = 1+(-1)^{S+g}$. Some particular values of $F_{abc}(\vartheta\varphi\theta\phi)$, which differs from $F_{S_g J}(\mathbf{p}, \mathbf{k})$ only by the factor i^γ, are presented in ref.[1]).

In order to obtain the correlation between the direction of the β-particle and circular polarization of the subsequent γ-quantum, B_{SM} should be substituted for B_S in (1) or (10):

$$B_{SM} = \sqrt{(2j_1+1)(2I+1)}\, C^{IM}_{IMS0} W(j_2 I j_1 S; j_1 I) \tag{6}$$

where $M = 1$ or -1 for right or left circular polarization of the γ-quantum. In the particular case when $S = 1$,

$$B_{1M} = M[j_1(j_1+1) - j_2(j_2+1) + I(I+1)][2I(I+1)\sqrt{j_1(j_1+1)}]^{-1}. \tag{7}$$

The B_{SM} are related to the quantities $F_S(II j_2 j_1)$ tabulated in ref. [8]) by the relation

$$B_{SM} = (-M)^S (2S+1)^{-\frac{1}{2}} F_S(II j_2 j_1). \tag{8}$$

For unpolarized γ-quanta the B_S (formula 3) can be obtained from the B_{SM} by summing over $M = 1$ and -1.

If the observed $\beta-\gamma$-cascade has the form $j_0(\beta)j_1(\gamma)j_2(\gamma_2)\ldots j_{N-1}(\gamma)j_N$ and it is the angular distribution of γ-quanta from the $j_{N-1}(\gamma)j_N$ transition that is being studied, the direction of the remaining quanta being neglected, one should additionally multiply B_S or B_{SM} in formula (1) by the product

$$\prod_{k=2}^{N-1} \sqrt{(2j_k+1)(2j_{k-1}+1)}\, W(j_k I_k S j_{k-1}; j_{k-1} j_k); \tag{9}$$

B_S can be obtained from (3) by replacing j_2 by j_N and j_1 by j_{N-1}. If the γ-transition is of the mixed type (e.g.E2 or M1) B_S should be replaced by expression (13) in ref. [9]).

Putting $g = 0$ in formula (1) we obtain the following expression for

$\beta-\gamma$-correlation of non-oriented nuclei †:

$$W(\mathbf{p},\mathbf{k}) = \sum_{S=0,2} \sum_{L \leq L'} (2S+1) Z^S_{LL'} W(j_0 j_1 LS; L' j_1) B_S P_S(\cos\psi), \quad (10)$$

where ψ is the angle between the directions of $\mathbf{p}$ and $\mathbf{k}$.

If the nuclear charge $Z \ll 2A^{\frac{1}{3}}E$, expression (1) can be considerably simplified:

$$\begin{aligned} W(\mathbf{j}_0,\mathbf{p},\mathbf{k}) = \sum_{S,g} \sqrt{2S+1}\{&[(2j_0+1)^{-1}\delta_{j_1 j_0} Z^0_{00} + \sqrt{\tfrac{1}{3}} \\ &\times W(S j_0 j_1 1; j_0 j_1) Z^0_{11}]\delta_{Sg} P_S(\cos\theta) + (-1)^g \sqrt{2g+1} \\ &\times [Z^1_{01} W(j_0 S j_0 1; j_0 g)\delta_{j_1 j_0} \sqrt{1/3(2j_0+1)} + Z^1_{11} X(j_1 j_1 S, j_0 j_0 g, 111)] \\ &\times F_{Sg1}(\mathbf{p},\mathbf{k})\} h_g(j_0) B_S, \end{aligned} \quad (11)$$

$$Z^0_{00} = \kappa^2 \xi_1^{-} b_{22}, \quad Z^0_{11} = \sqrt{\tfrac{1}{3}}\,\kappa^2 \xi_1^{-}(b_{11}+2b_{66}+2\sqrt{2}\,b_{16}),$$

$$3\sqrt{3}\,Z^1_{11} = \sqrt{2}\,\kappa^3 \xi_3^{0}(c_{11}+2c_{66}+2\sqrt{2}\,c_{16}),$$

$$Z^1_{01} = \tfrac{2}{3}\kappa^3 \xi_3^{0}(c_{12}+\sqrt{2}\,c_{26}).$$

For even values of $S+g+J$

$$\kappa^2 \xi_1^{-} b_{ii'} = (W-1)^2 (E+\gamma)\ \mathrm{Re}\ b^+_{ii'} + (W+1)^2 (E-\gamma)\ \mathrm{Re}\ b^-_{ii'},$$

$$E\xi_3^{0} c_{ii'} = p\ \mathrm{Re}\ (c^+_{ii'}+c^-_{ii'}) - \alpha Z\ \mathrm{Im}\ (c^-_{ii'}-c^+_{ii'}).$$

For odd values of $S+g+J$

$$\kappa^2 \xi_1^{-} b_{ii'} = (W-1)^2 (E+\gamma)\ \mathrm{Im}\ b^+_{ii'} + (W+1)^2 (E-\gamma)\ \mathrm{Im}\ b^-_{ii'},$$

$$E\xi_3^{0} c_{ii'} = p\ \mathrm{Im}\ (c^+_{ii'}+c^-_{ii'}) + \alpha Z\ \mathrm{Re}\ (c^-_{ii'}-c^+_{ii'}).$$

The values of $b_{ii'}$ and $c_{ii'}$ are presented in appendix 1.

Forbiddenness of the β-transition due to smallness of pR is lifted at large values of Z since instead of p the expression $\kappa = \sqrt{(E+V)^2-1}$ enters the integrand and $\kappa \gg p$. As $\kappa \approx V$ where V is the effective depth of the Coulomb well in the vicinity of the nucleus, the energy dependence drops out and the β-transition becomes similar to an allowed transition. Inasmuch as for allowed transitions $\beta-\gamma$-correlation is absent in non-oriented nuclei, it may be expected that the correlation will also be small for first forbidden transitions if $Z \gg 2A^{\frac{1}{3}}E$. This conclusion directly follows from the explicit form of the $Z^J_{LL'}$ in (1). In contrast, a large $\beta-\gamma$-transitions correlation for oriented nuclei should be expected when $Z \gg 2A^{\frac{1}{3}}E$ as such a correlation occurs in allowed transitions. Comparison of (11) with the expression for $\beta-\gamma$-correlation in allowed transitions [1]) shows that in both cases the nature of the correlation is the same (the nuclear matrix elements are of course different).

† $W(\mathbf{p},\mathbf{k})$ is identical with formula (10) in ref.[9]) if it be taken into account that in the notations employed in ref.[9]) $Z^S_{LL'}$ is $(2S+1)^{-1}\sqrt{2L'+1}\,\Sigma_{i \leq k}\,[\mathrm{Re}\ M_{Li}\, M^*_{L'k}] C^{SLL'}_{ik}$. In contrast to ref.[9]) the expressions for $Z^S_{LL'}$ pertain to β-interaction of the general form involving non-conservation of parity.

The correlation between the directions of $\mathbf{j}_0$, $\mathbf{p}$ and $\mathbf{k}$ can be large for aligned nuclei with $Z \gg 2A^{\frac{1}{3}}E$ only if invariance of the theory with respect to time reversal is violated.

Appendix 1

VALUES OF $Z^J_{LL'}$ IN FORMULAE (1) AND (10) FOR EVEN VALUES OF $S+g+J$

$$Z^0_{00} = \kappa^2\varphi_1\xi_1^- b_{22} - 6\kappa^2\varphi_2\xi_1^0 b_{23} + 9\varphi_0\xi_1^+ b_{33} - 2q\kappa^2\varphi_2\xi_1^0 a_{22} + 6q\varphi_0\xi_1^+ a_{23} + q^2\varphi_0\xi_1^+ b_{22},$$

$$\sqrt{3}\,Z^0_{11} = \kappa^2\varphi_1[(\xi_1^- + 2\xi_2^-)b_{11} + (2\xi_1^- + \xi_2^-)b_{66} + 2\sqrt{2}(\xi_1^- - \xi_2^-)b_{16}] + 6\sqrt{3}\,\kappa^2\varphi_2\xi_1^0(\sqrt{2}\,b_{46} + b_{14}) + 27\varphi_0\xi_1^+ b_{44} - 2q\kappa^2\varphi_2\xi_1^0(a_{11} - 2a_{66} + 4\sqrt{2}\,a_{61} - 4\sqrt{2}\,a_{16}) - 6\sqrt{3}\,q\varphi_0\xi_1^+(a_{14} - \sqrt{2}\,a_{46}) + 3q^2\varphi_0\xi_1^+(b_{11} + b_{66}),$$

$$Z^0_{22} = \sqrt{5}\,(\kappa^2\varphi_1\xi_2^- + q^2\varphi_0\xi_1^+)b_{55},$$

$$\sqrt{15}\,Z^2_{11} = -\kappa^2\varphi_1[2\xi_5^-(\sqrt{2}\,b_{11} - \sqrt{2}\,b_{66} + 2b_{16} - b_{61}) + \xi_2^-(\sqrt{2}\,b_{11} + \sqrt{\tfrac{1}{2}}\,b_{66} - 2b_{16})] - 6\sqrt{3}\,\kappa^2\varphi_2\xi_5^0(\sqrt{2}\,b_{14} - b_{64}) + 2q\kappa^2\varphi_2\rho_5^0(\sqrt{2}\,a_{11} + \sqrt{2}\,a_{66} - 2a_{16} - a_{61}),$$

$$2\sqrt{5}\,Z^2_{22} = -\sqrt{14}\,\kappa^2\varphi_1\xi_2^- b_{55},$$

$$\sqrt{5}\,Z^2_{02} = -2\sqrt{2}(\kappa^2\varphi_1\xi_5^- b_{52} - 3\kappa^2\varphi_2\xi_5^0 b_{53} - q\kappa^2\varphi_2\rho_5^0 a_{52}),$$

$$\sqrt{5}\,Z^2_{12} = -\sqrt{2}\{\kappa^2\varphi_1[\xi_5^-(\sqrt{2}\,b_{51} + 2b_{56}) + \xi_2^-(b_{56} - \sqrt{2}\,b_{51})] + 3\sqrt{6}\,\kappa^2\varphi_2\xi_5^0 b_{54} - q\kappa^2\varphi_2\rho_5^0(\sqrt{2}\,a_{51} - 2a_{56})\},$$

$$3\sqrt{3}\,Z^1_{11} = -\sqrt{2}\{\kappa^3\varphi_1[\xi_3^0(c_{11} + 2c_{66} + 2\sqrt{2}\,c_{16}) + 2\xi_4^0(c_{66} - c_{11} - \sqrt{2}\,c_{16} + \sqrt{\tfrac{1}{2}}\,c_{61}) + \xi_6^0(c_{11} + \tfrac{1}{2}c_{66} - \sqrt{2}\,c_{16})] + 6\sqrt{3}\,\kappa\varphi_2[\xi_3^+(c_{14} + \sqrt{2}\,c_{64}) - \xi_4^+(c_{14} - \sqrt{\tfrac{1}{2}}\,c_{64})] + 27\kappa\varphi_0\xi_3^0 c_{44} - 2q\kappa\varphi_2[\rho_3^-(d_{11} - 2d_{66} - \sqrt{2}\,d_{16} + \sqrt{2}\,d_{61}) - \rho_4^-(d_{66} + d_{11} - \sqrt{2}\,d_{16} - \sqrt{\tfrac{1}{2}}\,d_{61})] - 6\sqrt{3}\,q\kappa\varphi_0\xi_3^0(d_{14} - \sqrt{2}\,d_{64}) + 3q^2\kappa\varphi_0\rho_3^0(\tfrac{1}{2}c_{66} - \sqrt{2}\,c_{16})\},$$

$$\sqrt{30}\,Z^1_{22} = (3\kappa^3\varphi_1\xi_6^0 + 5q^2\kappa\varphi_0\rho_3^0)c_{55},$$

$$\sqrt{35}\,Z^3_{22} = -3\sqrt{2}\,\kappa^3\varphi_1\xi_6^0 c_{55},$$

$$3Z^1_{01} = 2\{\kappa^3\varphi_1[\xi_3^0(c_{12} + \sqrt{2}\,c_{26}) + \xi_4^0(2c_{12} - \sqrt{2}\,c_{62})] + 3\kappa\varphi_2[\xi_3^+(\sqrt{3}c_{24} - \sqrt{2}c_{63} - c_{13}) + \xi_4^+(\sqrt{2}c_{63} - 2c_{13})] - 2q\kappa\varphi_2[\rho_3^-(d_{12} + \sqrt{\tfrac{1}{2}}d_{26} - \sqrt{\tfrac{1}{2}}d_{62}) + \rho_4^-(d_{12} - \sqrt{\tfrac{1}{2}}d_{62})] - 3q\kappa\varphi_0\xi_3^0(\sqrt{3}\,d_{42} - d_{31} + \sqrt{2}\,d_{36}) - 9\sqrt{3}\,\kappa\varphi_0\xi_3^0 c_{34} + q^2\kappa\varphi_0\rho_3^0(c_{12} - \sqrt{2}\,c_{26})\},$$

$$3Z^1_{12} = -\sqrt{5}[\kappa^3\varphi_1\xi_4{}^0(2c_{51}+\sqrt{2}\,c_{56})+6\sqrt{3}\,\kappa\varphi_2\xi_4{}^+c_{54} - q\kappa\varphi_2\rho_4{}^-(2d_{51}-\sqrt{2}\,d_{56})-2q^2\kappa\varphi_0\rho_3{}^0(2c_{15}+\sqrt{2}\,c_{56})],$$

$$\sqrt{35}Z^3_{12} = 6\kappa^3\varphi_1\xi_6{}^0(c_{65}-\sqrt{2}\,c_{15}).$$

The following notations have been employed in the expressions for $Z^J_{LL'}$: $\kappa^2 = W^2-1$, $W = E+V$, where E is the electron energy in mc^2 units, including the rest energy ($\hbar = m = c = 1$). For uniform surface distribution of the charge $V = \alpha Z/R$, where R is the nuclear radius. For uniform volume distribution $V = 3\alpha Z/2R$.

The neutrino energy has been denoted by q.

$$\xi_i{}^{\pm}x_{ii'} \equiv (W\pm1)(\beta_i{}^+\,\mathrm{Re}+\alpha_i{}^+\,\mathrm{Im})x^+_{ii'}+(W\mp1)(\beta_i{}^-\,\mathrm{Re}+\alpha_i{}^-\,\mathrm{Im})x^-_{ii'},$$

$$\xi_i{}^0x_{ii'} \equiv (\beta_i{}^+\,\mathrm{Re}+\alpha_i{}^+\,\mathrm{Im})x^+_{ii'}+(\beta_i{}^-\,\mathrm{Re}+\alpha_i{}^-\,\mathrm{Im})x^-_{ii'}.$$

The values of $\beta_i{}^{\pm}$ and $\alpha_i{}^{\pm}$ are deduced from the condition of smooth fitting of the electron wave function onto the nuclear surface. Their explicit form is presented in appendix 3.

$x_{ii'}$ is any one of the quantities $a_{ii'}$, $b_{ii'}$, $c_{ii'}$ or $d_{ii'}$, for which the following relations hold:

$$a^{\pm}_{ii'} = (a^{\mp}_{i'i})^*, \qquad b^{\pm}_{ii'} = (b^{\pm}_{i'i})^*, \qquad c^{\pm}_{ii'} = (c^{\mp}_{i'i})^*, \qquad d^{\pm}_{ii'} = (d^{\pm}_{i'i})^*.$$

The $\rho_i{}^{\pm}x_{ii'}$ and $\rho_i{}^0x_{ii'}$ correspondingly coincide with $\xi_i{}^{\pm}x_{ii'}$ and $\xi_i{}^0x_{ii'}$ if all $\beta_i{}^+$ are replaced by $\beta_i{}^-$ and all $\alpha_i{}^+$ by $\alpha_i{}^-$ and vice versa.

Expressions for $Z^J_{LL'}$ for odd $S+g+J$ can be obtained by replacing in the preceding expressions for $Z^J_{LL'}$ the $\mathrm{Re}\,x^{\pm}_{ii'}$ by $\mathrm{Im}\,x^{\pm}_{ii'}$ and $\mathrm{Im}\,x^{\pm}_{ii'}$ by $\mathrm{Re}\,x^{\pm}_{ii'}$ and changing the sign of $\alpha_i{}^{\pm}$.

For STP-interaction the quantities $x^{\pm}_{ii'}$ have the form

$$a^{\pm}_{ii'} = b^{\pm}_{ii'} = \eta_{ii'}K_iK^*_{i'}, \qquad c^{\pm}_{ii'} = d^{\pm}_{ii'} = \eta'_{ii'}K_iK^*_{i'},$$

$$\eta_{ii'} = C_iC^*_{i'}+C'_iC'^*_{i'}, \qquad \eta'_{ii'} = C_iC'^*_{i'}+C'_iC^*_{i'},$$

$$\eta_{11} = |C_{\mathrm{S}}|^2+|C'_{\mathrm{S}}|^2, \qquad \eta_{33} = |C_{\mathrm{P}}|^2+|C'_{\mathrm{P}}|^2,$$

$$\eta_{13} = C_{\mathrm{S}}C^*_{\mathrm{P}}+C'_{\mathrm{S}}C'^*_{\mathrm{P}}, \qquad \eta_{1k} = C_{\mathrm{S}}C^*_{\mathrm{T}}+C'_{\mathrm{S}}C'^*_{\mathrm{T}},$$

$$\eta_{3k} = C_{\mathrm{P}}C^*_{\mathrm{T}}+C'_{\mathrm{P}}C'^*_{\mathrm{T}} \text{ for } k \neq 1,\ 3,$$

$$\eta_{kk'} = |C_{\mathrm{T}}|^2+|C'^*_{\mathrm{T}}|^2 \text{ for } k, k' = 2,\ 4,\ 5,\ 6,$$

$$\eta_{ii'} = \eta^*_{i'i}.$$

The C_{S}, C_{T}, C_{P}, C_{V} and C_{A} are respectively the scalar, tensor, pseudoscalar, vector and axial vector β coupling constants; C'_{S}, C'_{T} etc., are similar constants before terms which are valid only if parity is not conserved (the terms then contain an extra $\gamma_5 = \gamma_1\gamma_2\gamma_3\gamma_4$, $\gamma_4 = -\beta$). The K_i are nuclear interaction matrix elements. Their explicit form is presented in appendix 2.

For VA-interaction

$$b^{\pm}_{ii'} = -a^{\pm}_{ii'} = \zeta_{ii'} L_i L^*_{i'}, \qquad d^{\pm}_{ii'} = -c^{\pm}_{ii'} = \zeta'_{ii'} L_i L^*_{i'},$$

$$\zeta_{ii'} = C_i C^*_{i'} + C'_i C'^*_{i'}, \qquad \zeta'_{ii'} = C_i C'^*_{i'} + C'_i C^*_{i'},$$

$$\zeta_{11} = \zeta_{44} = \zeta_{14} = |C_V|^2 + |C'_V|^2, \qquad \zeta_{kk'} = |C_A|^2 + |C'_A|^2 \text{ for } k, k' \neq 1,4,$$

$$\zeta_{1k} = \zeta_{4k} = C_V C_A^* + C'_V C'^*_A \text{ for } k \neq 1, 4, \qquad \zeta_{ii'} = \zeta^*_{i'i}.$$

The nuclear matrix elements L_i differ from the respective K_i by the additional matrix β in the integrand.

Expressions for $x_{ii'}$ in the general case of STPVA interaction are given in appendix 4. Since invariance of β-interaction under time inversion has not been assumed, formulae (1) and (10) contain the imaginary part of $x_{ii'}$. If, however, this assumption is made, all terms containing Im $x^{\pm}_{ii'}$ should be discarded and comparison with experiment is significantly simplified. For clarification of the problem of invariance under time inversion it is better to study $\beta-\gamma$-correlation for allowed transitions of oriented nuclei [1]), as in this case the interpretation of the experiments is simpler and less ambiguous.

The values of $Z^J_{LL'}$ cited above refer to the case of surface distribution of the nuclear charge. If a volume distribution of the charge is assumed the following substitution should be made:

$$\varphi_0 \to \varphi_3, \qquad \varphi_1 \xi_1^- \to \varphi_4 \xi_1^- - (3\alpha Z/5R)\xi_1^0 + (3\alpha Z/10\kappa R)^2 \xi_1^+,$$

$$\varphi_2 \xi_1^0 \to \varphi_5 \xi_1^0 - (3\alpha Z/10\kappa^2 R)\xi_1^+, \qquad \varphi_1 \xi_2^- \to \varphi_6 \xi_2^-,$$

$$\varphi_1 \xi_5^- \to \varphi_7 \xi_5^- - (3\alpha Z/10R)\xi_5^0, \qquad \varphi_2 \xi_5^0 \to \varphi_8 \xi_5^0,$$

$$\varphi_1 \xi_3^0 \to [\varphi_4 - 3\alpha ZW/5R\kappa^2 + (3\alpha Z/10\kappa R)^2]\xi_3^0,$$

$$\varphi_1 \xi_4^0 \to \varphi_7 \xi_4^0 - (3\alpha Z/10\kappa^2 R)\xi_4^-, \qquad \varphi_2 \rho_5^0 \to \varphi_8 \rho_5^0,$$

$$\varphi_2 \xi_3^+ \to \varphi_5 \xi_3^+ - (3\alpha Z/10R)\xi_3^0, \qquad \varphi_1 \xi_6^0 \to \varphi_6 \xi_6^0,$$

$$\varphi_2 \rho_3^- \to \varphi_5 \rho_3^- - (3\alpha Z/10R)\rho_3^0, \qquad \varphi_2 \xi_4^+ \to \varphi_8 \xi_4^+,$$

$$\varphi_2 \rho_4^- \to \varphi_8 \rho_4^-,$$

$$V = \frac{\alpha Z}{R} \to \frac{3\alpha Z}{2R}.$$

The values of φ_i are given in appendix 3. With an accuracy to term $\approx (\alpha Z)^2/4$ one may put $\varphi_i = 1$.

To change to a point nucleus one should write $V = 3\alpha Z/2R$ in the formula referring to a surface charge distribution.

Appendix 2

$$K_i = \sqrt{4\pi}\int \psi^*_{j_1\mu_1}\tau O_i \psi_{j_0\mu_0}\,\mathrm{d}\mathbf{r}, \quad L_i = \sqrt{4\pi}\int \psi^*_{j_1\mu_1}\tau\beta O_i \psi_{j_0\mu_0}\,\mathrm{d}\mathbf{r}, \quad C_L \equiv [C^{j_1\mu_1}_{L\Lambda j_0\mu_0}]^{-1},$$

$$O_1 = C_1 r\beta Y_{1\Lambda}, \qquad K_1 = \sqrt{3}\int \beta\mathbf{r}, \qquad K_2 = \int \beta\boldsymbol{\sigma}\cdot\mathbf{r}$$

$$O_2 = C_0 r\beta(\boldsymbol{\sigma}\cdot\mathbf{Y}^1_{00}),$$

$$O_3 = iC_0\beta\gamma_5 Y_{00}, \qquad K_3 = \int i\beta\gamma_5, \qquad K_4 = \int i\beta\boldsymbol{\alpha}$$

$$O_4 = -iC_1\beta(\boldsymbol{\alpha}\cdot\mathbf{Y}^{-1}_{1\Lambda}), \qquad K_5 = \sqrt{\tfrac{3}{4}}\int B^{\beta}_{ij}, \qquad K_6 = -\sqrt{\tfrac{3}{2}}\int \beta\boldsymbol{\sigma}\times\mathbf{r}$$

$$O_5 = C_2 r\beta(\boldsymbol{\sigma}\cdot\mathbf{Y}^{-1}_{2\Lambda}),$$

$$O_6 = -C_1 r\beta(\boldsymbol{\sigma}\cdot\mathbf{Y}^0_{1\Lambda}), \qquad L_1 = \sqrt{3}\int \mathbf{r}, \qquad L_2 = \int \boldsymbol{\sigma}\cdot\mathbf{r} \text{ etc.}$$

$\psi_{j_0\mu_0}$ and $\psi_{j_1\mu_1}$ are the wave functions for the initial and final states of the nucleus: τ is an operator acting on the isobaric spin variables; β, γ_5, $\boldsymbol{\sigma}$ and $\boldsymbol{\alpha}$ are Dirac matrices, $\mathbf{Y}^{\lambda}_{JM}$ is a spherical vector (see ref. [1]).

Appendix 3

$$\beta_1^{\pm} = a^2_{\frac{1}{2}\mp\frac{1}{2}}[(W\pm 1)\kappa]^{-1}, \qquad \beta_2^{\pm} = 9a^2_{\frac{1}{2}\pm\frac{1}{2}}[(W\mp 1)\kappa^3]^{-1},$$

$$\beta_3^{\pm} = a_{\frac{1}{2}\frac{1}{2}}a_{\frac{1}{2}-\frac{1}{2}}\kappa^{-2}\cos(\delta_{\frac{1}{2}\mp\frac{1}{2}}-\delta_{\frac{1}{2}\pm\frac{1}{2}}), \qquad \beta_4^{\pm} = 3a_{\frac{1}{2}\mp\frac{1}{2}}a_{\frac{1}{2}\mp\frac{1}{2}}[(W\pm 1)\kappa^2]^{-1}\cos(\delta_{\frac{1}{2}\mp\frac{1}{2}}-\delta_{\frac{1}{2}\mp\frac{1}{2}}),$$

$$\beta_5^{\pm} = 3a_{\frac{1}{2}\mp\frac{1}{2}}a_{\frac{1}{2}\pm\frac{1}{2}}\kappa^{-3}\cos(\delta_{\frac{1}{2}\mp\frac{1}{2}}-\delta_{\frac{1}{2}\pm\frac{1}{2}}), \qquad \beta_6^{\pm} = 9a_{\frac{1}{2}\frac{1}{2}}a_{\frac{1}{2}-\frac{1}{2}}\kappa^{-4}\cos(\delta_{\frac{1}{2}\pm\frac{1}{2}}-\delta_{\frac{1}{2}\mp\frac{1}{2}}).$$

Here $a_{j\lambda}$ denote the coefficients of fitting the electron wave function onto the nuclear boundary. j is the total angular momentum and $l = j+\lambda$ is the electron orbital angular momentum; $\lambda = \pm\frac{1}{2}$. Tables of numerical values of $a_{j\lambda}$ can be found in ref. [10]). $\delta_{j\lambda}$ is the phase shift of the electron wave function in the nuclear Coulomb field. Tables of $\delta_{j\lambda}$ are also given in ref. [10]).

The difference between $\alpha_i^{\pm}$ and $\beta_i^{\pm}$ is that the former contain sin $(\delta_{j\lambda}-\delta_{j'\lambda'})$ instead of cos $(\delta_{j\lambda}-\delta_{j'\lambda'})$ and $\alpha_1^{\pm} = \alpha_2^{\pm} = 0$.

By neglecting terms smaller than $\approx (\alpha Z)^2$ the following simple expressions for $\beta_i^{\pm}$ and $\alpha_i^{\pm}$ can be obtained:

$$\beta_1^{\pm} = \frac{E\pm\gamma}{W\pm 1}, \qquad \beta_2^{\pm} = [p^2+(\alpha ZE)^2]\kappa^{-2}\beta_1^{\mp},$$

$$\beta_3^{\pm} = \frac{p^2}{\kappa\sqrt{p^2+(\alpha Z)^2}}, \qquad \beta_4^{\pm} = \sqrt{p^2+(\alpha ZE)^2}\,\kappa^{-1}\beta_1^{\pm}\cos\omega_1^{\pm},$$

$$\beta_5^{\pm} = \sqrt{p^2+(\alpha ZE)^2}\,p\kappa^{-2}\cos\omega_2^{\pm}, \qquad \beta_6^{\pm} = 2\frac{p^2[p^2+(\alpha ZE)^2]}{\kappa^3\sqrt{4p^2+(\alpha Z)^2}};$$

$$\alpha_3^{\pm} = \pm\frac{\alpha Z}{p}\beta_3^{\pm}, \qquad \alpha_4^{\pm} = \beta_4^{\pm}\,\mathrm{tg}\,\omega_1^{\pm},$$

$$\alpha_5^{\pm} = \beta_5^{\pm}\,\mathrm{tg}\,\omega_2^{\pm}, \qquad \alpha_6^{\pm} = \mp\frac{\alpha Z}{2p}\beta_6^{\pm};$$

$$\operatorname{tg}\omega_1^{\pm}=\left[\tfrac{3}{4}\frac{\alpha ZE}{p}\pm\tfrac{1}{4}\frac{\alpha Z}{p}\right]\left[1-(\alpha Z)^2+\tfrac{3}{8}\left(\frac{\alpha Z}{p}\right)^2\mp\tfrac{1}{8}\left(\frac{\alpha Z}{p}\right)^2E-\left(\frac{\alpha ZE}{p}\right)^2\right]^{-1}$$

$$\operatorname{tg}\omega_2^{\pm}=\left[\tfrac{3}{4}\frac{\alpha ZE}{p}\pm\tfrac{3}{4}\frac{\alpha Z}{p}\right]\left[1-(\alpha Z)^2-\tfrac{1}{8}\left(\frac{\alpha Z}{p}\right)^2\mp\tfrac{3}{8}\left(\frac{\alpha Z}{p}\right)^2E+\left(\frac{\alpha ZE}{p}\right)^2\right]^{-1},$$

$$\gamma=\sqrt{1-(\alpha Z)^2};$$

$$\varphi_0=1-(\kappa R)^2/5,\qquad \varphi_1=1-3(\kappa R)^2/25,\qquad \varphi_2=1-4(\kappa R)^2/25,$$

$$\varphi_3=1-11(\kappa R)^2/75,\qquad \varphi_4=1-2(\kappa R)^2/35,\qquad \varphi_5=1-7(\kappa R)^2/75,$$

$$\varphi_6=1-3(\kappa R)^2/35,\qquad \varphi_7=1-12(\kappa R)^2/175,\qquad \varphi_8=1-4(\kappa R)^2/35.$$

Appendix 4

The quantities $a_{ii'}$, $b_{ii'}$ etc., have the following form for STPVA interaction:

$$a^{\pm}_{ii'}=(\eta_{ii'}K_iK^*_{i'}-\zeta_{ii'}L_iL^*_{i'})\pm(\chi_{ii'}K_iL^*_{i'}-\chi^*_{i'i}L_iK^*_{i'}),$$

$$b^{\pm}_{ii'}=(\eta_{ii'}K_iK^*_{i'}+\zeta_{ii'}L_iL^*_{i'})\pm(\chi_{ii'}K_iL^*_{i'}+\chi^*_{i'i}L_iK^*_{i'}),$$

$$c^{\pm}_{ii'}=(\eta'_{ii'}K_iK^*_{i'}-\zeta'_{ii'}L_iL^*_{i'})\pm(\chi'_{ii'}K_iL^*_{i'}-\chi'^*_{i'i}L_iK^*_{i'}),$$

$$d^{\pm}_{ii'}=(\eta'_{ii'}K_iK^*_{i'}+\zeta'_{ii'}L_iL^*_{i'})\pm(\chi'_{ii'}K_iL^*_{i'}+\chi'^*_{i'i}L_iK^*_{i'}).$$

The values of $\eta_{ii'}$, $\eta'_{ii'}$, $\zeta_{ii'}$ and $\zeta'_{ii'}$ are the same as those given in appendix 1. For $\chi_{ii'}$ we get

$$\chi_{11}=\chi_{14}=C_{\mathrm{S}}C^*_{\mathrm{V}}+C'_{\mathrm{S}}C'^*_{\mathrm{V}},\qquad \chi_{31}=\chi_{34}=C_{\mathrm{P}}C^*_{\mathrm{V}}+C'_{\mathrm{P}}C'^*_{\mathrm{V}},$$

$$\chi_{k1}=\chi_{k4}=C_{\mathrm{T}}C^*_{\mathrm{V}}+C'_{\mathrm{T}}C'^*_{\mathrm{V}}\quad\text{for}\quad k\neq 1,3,\qquad \chi_{ii'}\neq\chi^*_{i'i},$$

$$\chi_{1k}=C_{\mathrm{S}}C^*_{\mathrm{A}}+C'_{\mathrm{S}}C'^*_{\mathrm{A}},\qquad \chi_{3k}=C_{\mathrm{P}}C^*_{\mathrm{A}}+C'_{\mathrm{P}}C'^*_{\mathrm{A}}\ \text{for}\ k\neq 1,4,$$

$$\chi_{kk'}=C_{\mathrm{T}}C^*_{\mathrm{A}}+C'_{\mathrm{T}}C'^*_{\mathrm{A}}\quad\text{for}\quad k\neq 1,3,\qquad k'\neq 1,4.$$

If $\chi_{ii'}=C_iC^*_{i'}+C'_iC'^*_{i'}$ one has $\chi'_{ii'}=C_iC'^*_{i'}+C'_iC^*_{i'}$.

References

1) A. Z. Dolginov, JETP **33** (1958) 1363; Nuclear Physics **5** (1958) 512
2) B. Bleaney, Proc. Phys. Soc. A **64** (1951) 315
3) R. V. Pound, Phys. Rev. **76** (1949) 1410
4) A. Simon, M. E. Rose and J. M. Jauch, Phys. Rev. **84** (1951) 1155
5) J. A. M. Cox and H. A. Tolhoek, Physica **19** (1953) 673
6) H. Matsunobu and H. Takebe, Progr. of Theor. Phys. **14** (1955) 589; J. W. Stephenson and K. Smith, Proc. Phys. Soc. A **70** (1957) 571
7) L. C. Biedenharn, J. M. Blatt and M. E. Rose, Revs. Mod. Phys. **25** (1953) 729; H. A. Jahn, Proc. Roy. Soc. **205** (1951) 192
8) K. Alder, B. Stech and A. Winter, Phys. Rev. **107** (1957) 728
9) A. Z. Dolginov and I. N. Toptigin, Nuclear Physics **2** (1956) 147
10) L. A. Sliv and B. A. Volchek, Tables of Coulomb phase shifts and amplitudes with account of finite nuclear dimensions. Acad. Sci. USSR (1956)

2.C:6.A *Nuclear Physics* 7 (1958) 599—612; © *North-Holland Publishing Co., Amsterdam*
Not to be reproduced by photoprint or microfilm without written permission from the publisher

A NEW DEVELOPMENT IN THE AREA METHOD OF NEUTRON RESONANCE ANALYSIS

J. E. LYNN

Atomic Energy Research Establishment, Harwell, Berks

Received 28 April 1958

Abstract: The area method of neutron resonance analysis has been extended to include the effect of various interference terms which may enter the formula for the neutron resonance cross section. The principal interference term is that between resonance and potential scattering. A series formula has been found for the area function which takes account of this term when Doppler broadening is negligible. Doppler broadening is treated by numerical computation. The practical application of these formulae is discussed. Interference caused by other resonances may be important. It can be represented by cross terms between resonances and is treated as a correction to the area function.

1. Introduction

In the determination of the parameters of the slow neutron resonances of most nuclei, the so-called "area" method of analysis has been extensively developed by many workers [1,2,3,4]). Reduced to its essentials, the area method depends on the fact that the area above a resonance dip in a curve of neutron transmission plotted against energy is independent of experimental resolution (provided that the energy limits enclosing the area are sufficiently far from the resonance energy [5])). A theoretical expression for the area as a function of the resonance parameters and the sample thickness may be obtained assuming the resonance to have a single-level Breit-Wigner form. This function has a characteristic shape when plotted logarithmically which enables one to deduce the peak cross section and width of the resonance from experimental determinations of the area. Unfortunately, a major assumption upon which the area function has always been calculated is that interference between resonance and potential scattering is an effect which may be neglected. It is the purpose of this paper to describe how the area method may be modified when the interference effect is considered. It is also shown how many-level interference effects may be taken into account.

2. Area Method without Interference

The single-level Breit-Wigner approximation to the (s-wave) neutron cross section of a nucleus with ground state spin I and mass number A at an energy E close to the resonance energy E_R is

$$\sigma(x) = \frac{\sigma_0}{1+x^2} + \frac{2\sigma_0 ax/\lambda\!\!\!^{-}}{1+x^2} + 4\pi a^2 \qquad (1)$$

where $x = (E-E_R)/\frac{1}{2}\Gamma$, Γ is the total width of the resonance, $\sigma_0 \approx 4\pi\lambda\!\!\!^{-2} g_J \Gamma_n/\Gamma$ is the peak cross section, $2\pi\lambda\!\!\!^{-}$ is the de Broglie wavelength of the neutron (in the centre of mass system), Γ_n is the neutron width and g_J is a weighting factor depending on the total angular momentum, J, of the resonant state of the compound nucleus and $4\pi a^2$ is the potential scattering cross section. The second term on the right of eq. (1) represents the interference between the resonance and potential scattering of neutrons.

The transmission at energy E is given by

$$T(x) = e^{-n\sigma(x)} = \exp\left\{-\frac{n\sigma_0}{1+x^2} - \frac{2n\sigma_0 a}{\lambda\!\!\!^{-}} \cdot \frac{x}{1+x^2}\right\} \exp(-4\pi a^2 n) \qquad (2)$$

where n is the number of atoms per cm^2 of the sample. If we write $T_p = \exp(-4\pi n a^2)$ then the area above a resonance dip † is defined as $A_E(\varepsilon) = \int_{-\varepsilon}^{\varepsilon}[1-T(x)/T_p]d(E-E_R)$. The analytical treatment of this paper is concerned with the integral

$$A_x(\xi) = \int_{-\xi}^{\xi}[1-T(x)/T_p]dx = (2/\Gamma)A_E(\varepsilon)$$

where $\xi = 2\varepsilon/\Gamma$.

If the interference term in the exponent of (2) is ignored $A_x(\infty)$ may be evaluated analytically [6]). We call this function $A'_x(\infty)$

$$A'_x(\infty) = \pi n\sigma_0 e^{-n\sigma_0/2}[I_0(n\sigma_0/2)+I_1(n\sigma_0/2)] \qquad (3)$$

where I_m is the Bessel function of imaginary argument of order m [7a]). The asymptotic properties of (3) are such that

$$\lim_{n\sigma_0 \to 0} A'_E(\infty) = \pi n\sigma_0 \Gamma/2, \qquad \text{("thin samples")} \qquad (4)$$

$$\lim_{n\sigma_0 \to \infty} A'_E(\infty) = (\pi n\sigma_0)^{\frac{1}{2}}\Gamma. \qquad \text{("thick samples")} \qquad (5)$$

So far no account has been taken of the Doppler broadening of the resonances due to thermal motion of the atoms in the sample [8, 9]). When this is significant the resonance term $1/(1+x^2)$ is replaced by the function $\Psi(\beta, x)$ where $\beta = 2\Delta/\Gamma$, $\Delta = (4E_R k\theta/A)^{\frac{1}{2}}$, k is Boltzmann's constant and θ is the effective temperature of the sample [9]),

$$\Psi(\beta, x) = \frac{1}{\beta\sqrt{\pi}}\int_{-\infty}^{\infty} \frac{1}{1+y^2} \exp\left\{\frac{-(x-y)^2}{\beta^2}\right\} dy. \qquad (6)$$

Graphs and tables of this function have been presented elsewhere [2, 10]).

† In these calculations, $\lambda\!\!\!^{-}$, Γ_n and Γ are taken to be independent of energy for a given resonance.

$A'_x(\xi)$ as a function of β is now given by

$$A'_x(\xi, \beta) = \int_{-\xi}^{\xi} \{1 - \exp[-n\sigma_0 \Psi(\beta, x)]\} dx.$$

The effect of Doppler broadening on the asymptotic relations (4) and (5) is to increase the range of $n\sigma_0$ over which (4) is a reasonable approximation and to decrease the range of $n\sigma_0$ over which (5) is valid. The aim in using the area method is to determine $A'_E(\infty)$ when $n\sigma_0$ is small thus obtaining a value of $\sigma_0\Gamma$, and also when $n\sigma_0$ is large thus obtaining a value of $\sigma_0\Gamma^2$. From these two determinations the quantities $g_J\Gamma_n$ and Γ are obtained which, in general, is the most information about the widths of a single resonance that a total cross section measurement will give.

3. The Interference Term in the Area Function

3.1. GENERAL BEHAVIOUR OF THE AREA FUNCTION

Fig. 1 illustrates the effect of the interference between resonance and potential scattering. Fig. 1a shows a thick sample transmission curve as a

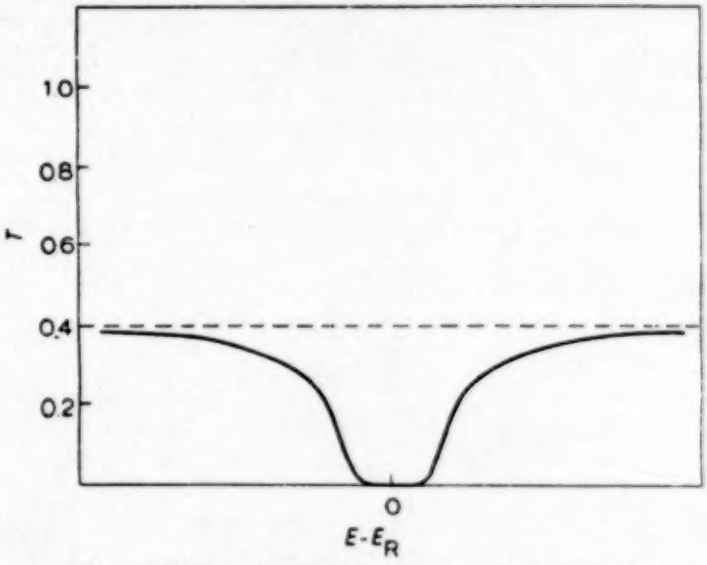

Fig. 1. Effect of interference upon the area A_E;
a) interference ignored — T as function of energy;

function of energy without interference. The dashed line is the value of T_p, the transmission due to potential scattering alone. In order to obtain the area A'_E the transmission curve of fig. 1a must be divided by T_p to give the curve shown in fig. 1b. The hatched area in fig. 1b is A'_E. Figs. 1c and 1d show the same curves as 1a and 1b respectively with the interference term now included. The hatched area is now the area A_E. Notice that the part of the area above the line $T/T_p = 1$, which is hatched in the opposite direction from that below $T/T_p = 1$, is negative. It is apparent that the net effect is a decrease in the area through inclusion of interference.

This net decrease is reflected in the expression which is now to be employed for the area function:

$$A_x(\infty, \beta) = A'_x(\infty, \beta) - C(\beta). \tag{7}$$

Here $C(\beta)$ is a positive quantity which takes the interference into account. It is shown in appendices 1 and 2 that $C(\beta)$ may be evaluated as an infinite series

$$C(\beta) = \sum_{m=1}^{\infty} C_m(\beta). \tag{8}$$

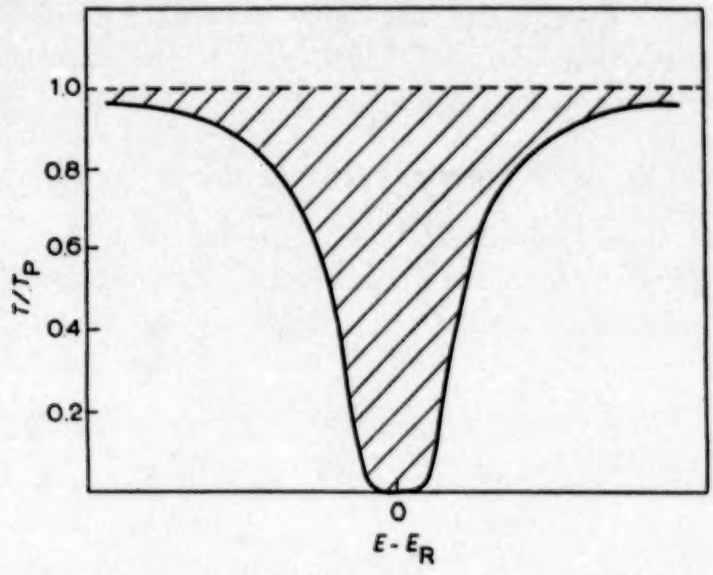

Fig. 1. b) interference ignored — T/T_p as function of energy; the hatched area is A'_E;

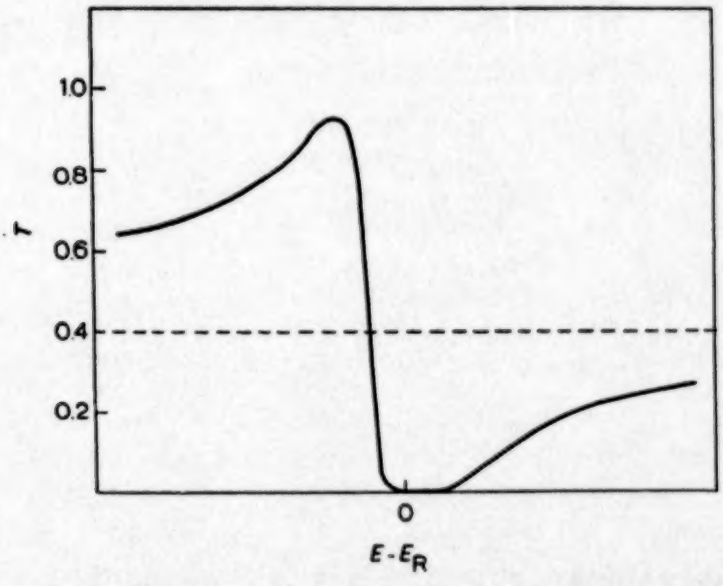

Fig. 1 c) interference included — T as function of energy;

When $\beta = 0$,

$$C_m = \pi n \sigma_0 e^{-n\sigma_0/2} \frac{(2m-3)!!}{(2m)!} \left(\frac{2n\sigma_0 a^2}{\lambda^2}\right)^m [I_{m-1}(n\sigma_0/2) + I_m(n\sigma_0/2)]. \tag{9}$$

Some approximate numerical calculations have been made of the quantities $C_m(\beta)$ when $\beta \neq 0$ for $m = 1$, 2 and 3 (figs. 2, 3 and 4). $C_m(\beta)$ decreases

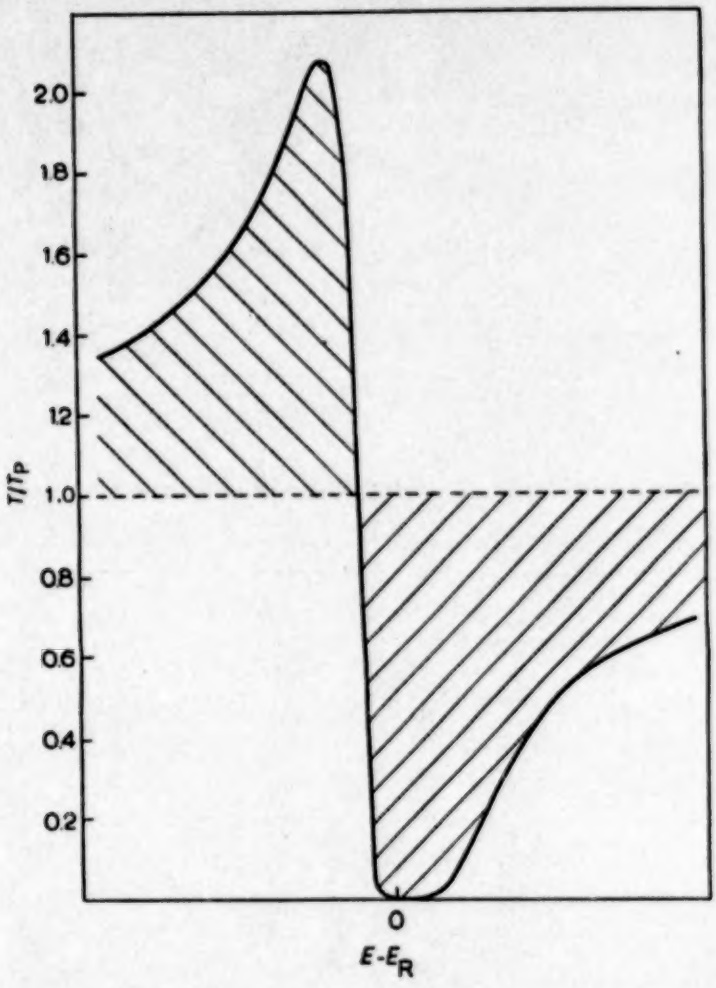

Fig. 1 d) interference included — T/T_p as function of energy; hatched area below the dashed line is positive, above the dashed line is negative.
Total gives A_E.

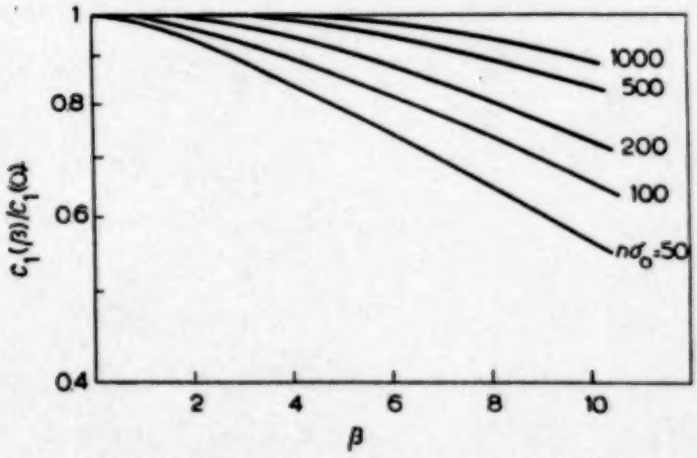

Fig. 2. $C_m(\beta)/C_m(0)$ for $m = 1$ as function of β for different $n\sigma_0$.

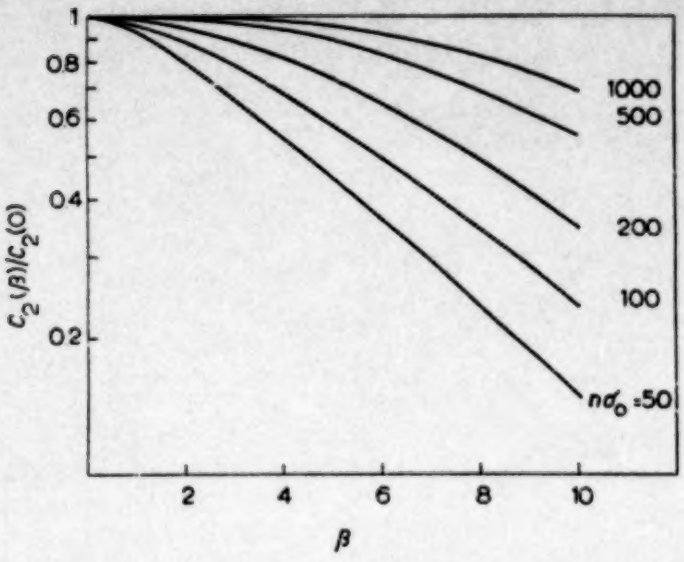

Fig. 3. $C_m(\beta)/C_m(0)$ for $m = 2$ as function of β for different $n\sigma_0$.

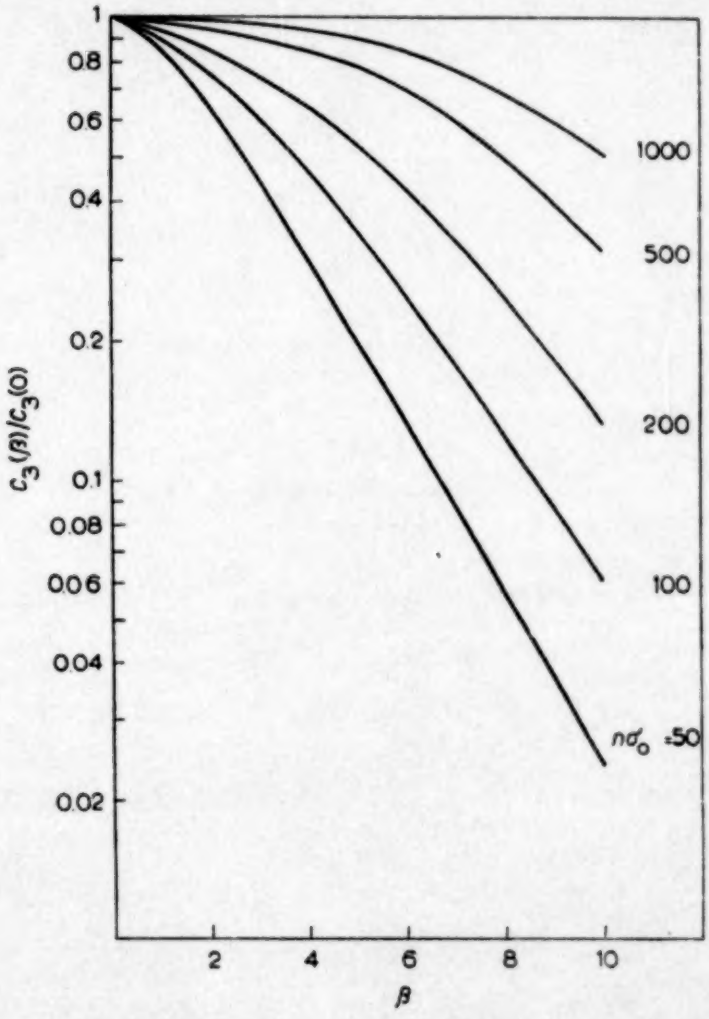

Fig. 4. $C_m(\beta)/C_m(0)$ for $m = 3$ as function of β for different $n\sigma_0$.

with increasing β, the decrease being more rapid the greater the value of m and the smaller the value of $n\sigma_0$. For all values of $2n\sigma_0 a^2/\lambda^2$ likely to be met in practice $\sum_m C_m$ is a rapidly converging series. No more than five terms of the series are ever likely to be needed to compute C with reasonable accuracy.

The quantity C is important for low energy resonances only when $n\sigma_0$ is large compared with unity. When $n\sigma_0$ is large one may take advantage of the asymptotic expansions of the Bessel functions to obtain (see appendix 1)

$$\lim_{n\sigma_0 \to \infty} A_x(\infty) = 2\sqrt{\pi n\sigma_0}\left\{1 - \sum_{m=1}^{\infty} \frac{(2m-3)!!}{(2m)!}\left(\frac{2n\sigma_0 a^2}{\lambda^2}\right)^m\right\}. \qquad (10)$$

The behaviour of this quantity as a function of $2n\sigma_0 a^2/\lambda^2$ is shown by the full curve in fig. 5. The broken curve in the same figure is $\lim A'_x(\infty) = 2\sqrt{\pi n\sigma_0}$

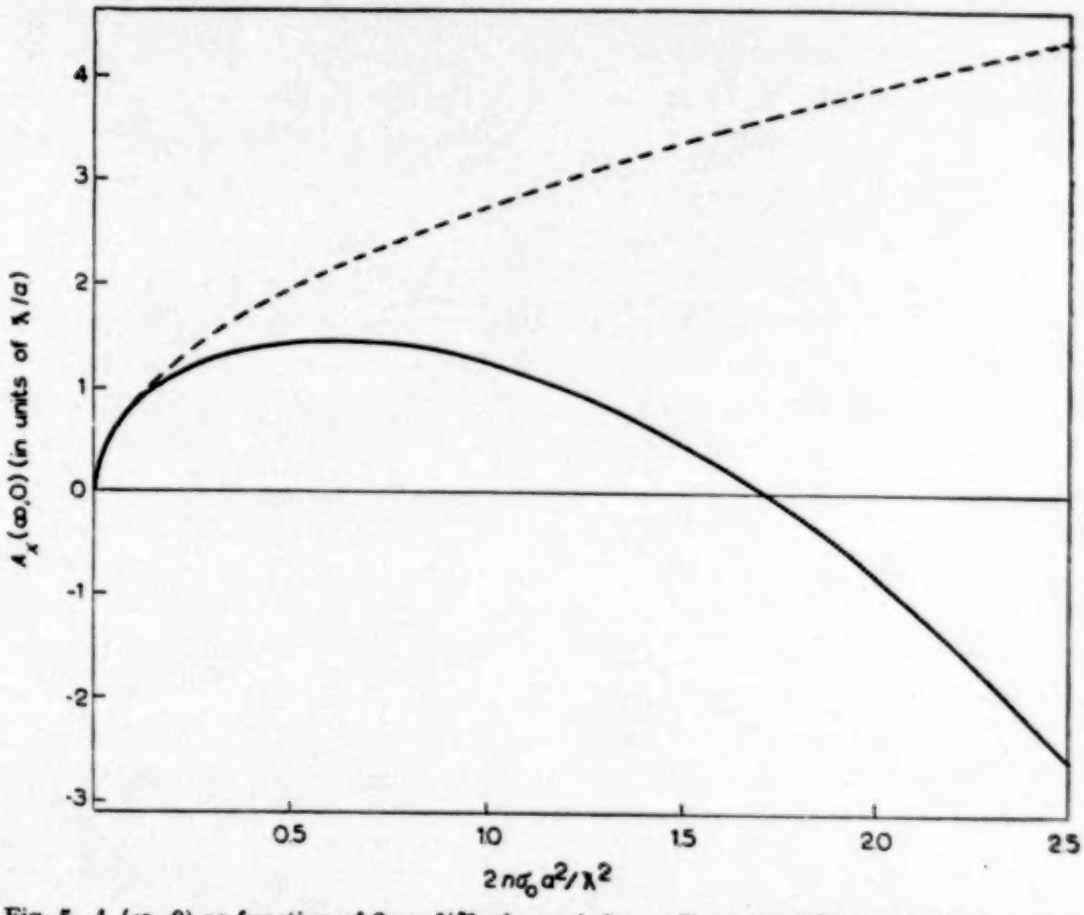

Fig. 5. $A_x(\infty, 0)$ as function of $2n\sigma_0 a^2/\lambda^2$ when n is large. Since $2\sigma_0 a^2/\lambda^2$ is a fixed parameter for a given resonance this curve describes the effect of increasing sample thickness on the area. The broken curve is the corresponding curve calculated neglecting interference (i.e. $A'_x(\infty, 0)$).

which is the usual formula for the area for thick samples neglecting interference. It is apparent that the effect of interference on the area is to limit drastically the range of validity of the asymptotic relation (5). The use of this latter gives too low a value of $\sigma_0 \Gamma^2$; in fact, it is so much reduced that

nowhere can (5) be considered valid for an elastic scattering resonance of a heavy nucleus above about 1 keV neutron energy.

3.2. CORRECTION TERM IN CONVENTIONAL AREA ANALYSIS

For resonances well below 1 keV (5) may still be a useful relationship but for accurate analysis C should be taken into consideration as a small correction term. In this case only the first term, $C_1(\beta)$, of the expansion (8) is required. This is accurately given by $A'_x(\infty, 0)n\sigma_0 a^2/\lambda\!\!\!^{-2}$ when $\beta = 0$. When $\beta \neq 0$, the ratio $C_1(\beta)/C_1(0)$ can be obtained from fig. 2. The quantity measured is proportional to $A_x(\infty, \beta)$. From this $A'_x(\infty, \beta)$ is obtained by the relation

$$A'_x(\infty, \beta) = A_x(\infty, \beta) + C_1(\beta). \tag{11}$$

From this $n\sigma_0\Gamma^2$ is obtained by the conventional method of area analysis. An approximate value of $n\sigma_0$ for the correction term is obtained in the first instance by disregarding the correction; $n\sigma_0$ is then improved by successive approximation. The value of a must be obtained from the potential scattering cross section, $4\pi a^2$.

3.3. NEW AREA METHOD TO DETERMINE σ_0 AND Γ

When C is no longer small compared with A_x, the shape of the area function (fig. 5) may be used to determine resonance parameters. Two features of the area function are particularly striking. First, there is a maximum in the function. Second, A_x changes sign fairly sharply as the sample thickness increases.

As an example consider the information that may be obtained from these two features, (for $\beta = 0$ and large $n\sigma_0$, eq. (10), fig. 5). Under these conditions $A_x(\infty, 0)$ has a maximum when $n\sigma_0 = 0.305\lambda\!\!\!^{-2}/a^2$. The maximum value of $A_E(\infty, 0)$ is $0.664\Gamma\lambda\!\!\!^{-}/a$. Since the maximum is broad and flat it should be possible to determine this quantity experimentally. For a sample thickness, n, which is a little different from that for which the area is a maximum ($n_{\max}$) the area is given by

$$A_E(\infty, 0) \approx \frac{\Gamma\lambda\!\!\!^{-}}{a}\left[0.664 - 0.266\left(\frac{n}{n_{\max}} - 1\right)^2\right].$$

The zero value of $A_x(\infty, 0)$ occurs when $n\sigma_0 = 0.85\lambda\!\!\!^{-2}/a^2$. The fall of $A_x(\infty, 0)$ through zero is steep and a fairly accurate experimental determination of $\sigma_0 a^2$ is possible.

Since it is not $A_E(\infty)$ but rather $A_E(\varepsilon)$ which is determined from the experiment, where ε is large compared with Γ, it is necessary to apply a wing correction term, (see appendix 3). The quantities which occur in the wing correction term, $\Delta A_E(\varepsilon)$ are $\sigma_0\Gamma^2$ and $\sigma_0 a^2$. These are determined approximately from the maximum value of $A_E(\varepsilon)$ and the position of its zero and improved by successive approximations.

3.4. CORRECTIONS DUE TO MANY-LEVEL EFFECTS

Although the single-level Breit-Wigner formula (1) is generally a very useful approximation for low energy neutron resonances, we find that for precise analysis of neutron cross sections some rather small but nevertheless significant many-level effects must be taken into consideration. The effect of these on the area is treated approximately in appendix 4 and the results are summarized here.

We assume the cross section contains an energy dependent potential scattering term such that $T_p(x) = T_p(0)(1+rx)$. This gives rise to an additional energy dependent factor in the interference term which is now written

$$\frac{sx}{1+x^2}(1+tx)$$

r, s and t are energy independent coefficients. The area which should be evaluated from the experimental data in this case is $\hat{A}_E(\varepsilon) = (\Gamma/2)\hat{A}_x(\xi)$ where

$$\hat{A}_x(\xi) = \int_{-\xi}^{\xi} [1-T(x)/T_p(0)]\mathrm{d}x. \tag{12}$$

The corresponding quantity $A_x(\infty)$ reduced to the single level case (i.e. all energy dependent many level effects eliminated) is given by

$$A_x(\infty) = A'_x(\infty)-C \approx \hat{A}_x(\xi)+\Delta A_x(\xi)-(nst+nsr)[2\xi-A'_x(\xi)]. \tag{13}$$

Here C and $\Delta A_x(\infty)$ are obtained from eqs. (9) and (18) respectively on replacing $a/\lambda\!\!\!^{-}$ by $s/2\sigma_0$.

In the case of slow neutron resonances which decay only by elastic scattering or radiative capture

$$s = \sigma_0[2a_J/\lambda\!\!\!^{-} - \sum_{S\neq R} \Gamma_{Sn}/(E_S-E_R)] \tag{13a}$$

where S denotes all other resonances which interfere with R, the resonance in question, viz. those which have the same spin J. The coefficients t and r are given by

$$t = \frac{\Gamma_R}{2}\left(\frac{2a_J}{\lambda\!\!\!^{-}} - \sum_{S\neq R}\frac{\Gamma_{Sn}}{E_S-E_R}\right)^{-1} \sum_{S\neq R}\frac{\Gamma_{Sn}}{(E_S-E_R)^2} \tag{13b}$$

$$r = \frac{\Gamma_R}{2}\cdot 4\pi\lambda\!\!\!^{-} n \sum_J g_J a_J \sum_{S'\neq R}\frac{\Gamma_{S'n}}{(E_{S'}-E_R)^2}. \tag{13c}$$

In (13c) the sum over S′ includes all resonances, not only those interfering with R. A spin dependent potential scattering length a_J appears in eqs. (13). This spin-dependence arises from the fact that strong distant resonances of different spins may be contributing to the cross section in the neighbourhood of E_R, although the energy dependence of this contribution is negligible.

Appendix 1

Calculation of the Area Function: Doppler Broadening Absent

From the definition of the area function $A_x(\infty)$ and the single-level Breit-Wigner formula (1) one may expand the part of T/T_p which contains the interference term as exponent to obtain

$$A_x(\infty) = \int_{-\infty}^{\infty} \left[1-\exp\left(-\frac{n\sigma_0}{1+x^2}\right) \mathrm{d}x\right] - \sum_{m=1}^{\infty} \frac{(2n\sigma_0 a/\lambda)^{2m}}{(1+x^2)^{2m}} \int_{-\infty}^{\infty} \frac{x^{2m}}{(1+x^2)^{2m}} \exp\left(-\frac{n\sigma_0}{1+x^2}\right) \mathrm{d}x. \quad (14)$$

The integrals in (14) may be evaluated by making the substitution $x = \tan\theta$. The first integral on the right hand side of (15) is $A'_x(\infty)$ (eq. (3)). The other integrals in (14) are a general family and are evaluated by the following steps:

$$\int_{-\infty}^{\infty} \frac{x^{2m}}{(1+x^2)^{2m}} \exp\left(-\frac{n\sigma_0}{1+x^2}\right) \mathrm{d}x = \frac{\mathrm{e}^{-n\sigma_0/2}}{2^{2m-2}} \int_{-\pi/2}^{\pi/2} \sin^2\theta \sin^{2m-2} 2\theta \mathrm{e}^{-\frac{n\sigma_0}{2}\cos 2\theta} \mathrm{d}\theta.$$

After integrating the right hand side by parts and rearrangement (including the substitution $2\theta = \varphi$)

$$\int_{-\infty}^{\infty} \frac{x^{2m}}{(1+x^2)^{2m}} \exp\left(-\frac{n\sigma_0}{1+x^2}\right) \mathrm{d}x = \frac{\mathrm{e}^{-n\sigma_0/2}}{2^{2m-1}} \int_0^{\pi} \sin^{2m-2}\varphi \mathrm{e}^{-(n\sigma_0/2)\cos\varphi} \mathrm{d}\varphi + \frac{n\sigma_0 \mathrm{e}^{-n\sigma_0/2}}{2^{2m}(2m-1)} \int_0^{\pi} \sin^{2m}\varphi \mathrm{e}^{-(n\sigma_0/2)\cos\varphi} \mathrm{d}\varphi.$$

By the use of Poisson's integrals for the Bessel Functions [7b])

$$\int_{-\infty}^{\infty} \frac{x^{2m}}{(1+x^2)^{2m}} \exp\left(-\frac{n\sigma_0}{1+x^2}\right) \mathrm{d}x = \frac{\pi n\sigma_0 \mathrm{e}^{-n\sigma_0/2}}{(2n\sigma_0)^m} (2m-3)!![I_{m-1}(n\sigma_0/2)+I_m(n\sigma_0/2)].$$

Hence the eqs. (7), (8) and (9) are obtained for $\beta = 0$.

Tables of the Bessel functions of imaginary argument have been given by Watson [7]) and by Wrinch and Wrinch [11]). Where these tables are incomplete (for large values of the argument) C_m may be calculated from the asymptotic expansions for the Bessel functions [7c]) with the result

$$C_m = \frac{(2m-3)!!}{(2m)!} (\pi n\sigma_0)^{\frac{1}{2}} \left(\frac{2n\sigma_0 a^2}{\lambda^2}\right)^m \sum_{\nu=0}^{\infty} \frac{(-)^\nu \Gamma(m+\nu-\frac{1}{2})}{\Gamma(\nu+1)\Gamma(m-\nu-\frac{1}{2})} \frac{1}{(n\sigma_0)^\nu} \left(\frac{2m-1}{m-\nu-\frac{1}{2}}\right). \quad (15)$$

From (15) the limiting result (10) is obtained. Eqs. (7), (8) and (9) have been used to compute $A_x(\infty, \beta = 0)$ for a number of values of $n\sigma_0$ and $2n\sigma_0 a^2/\lambda^2$ (table 1).

TABLE 1

Table of the area function $A_s(\infty, 0)$

$n\sigma_0$ \ $2n\sigma_0 a^2/\lambda^2$	0	10^{-3}	10^{-2}	0.0316	0.100	0.316	1.00	1.50	2.00	2.50	3.00
0.2	0.598	0.598	0.595	0.589	0.569	0.504	0.298	0.147	− 0.0049	− 0.157	− 0.310
0.6	1.64	1.64	1.63	1.61	1.56	1.38	0.810	0.389	− 0.039	− 0.350	− 0.907
1.0	2.52	2.52	2.51	2.48	2.39	2.12	1.24	0.577	− 0.094	− 0.778	− 1.47
2	4.23	4.23	4.21	4.17	4.02	3.56	2.05	0.901	− 0.028	− 1.51	− 2.77
4	6.58	6.58	6.55	6.48	6.25	5.53	3.12	1.26	− 0.070	− 2.76	− 4.93
10	10.9	10.9	10.9	10.8	10.4	9.16	5.07	1.81	− 1.69	− 5.47	− 9.56
16	13.7	13.7	13.6	13.5	13.0	11.5	6.31	2.15	− 2.36	− 7.27	− 12.6
20	15.7	15.7	15.6	15.4	14.9	13.1	7.19	2.41	− 2.80	− 8.49	− 14.7
30	19.3	19.3	19.2	19.0	18.3	16.1	8.81	2.88	− 3.61	−10.7	− 18.6
60	27.3	27.3	27.2	26.9	26.0	22.9	12.5	3.93	− 5.44	−15.8	− 27.6
74	30.4	30.4	30.3	29.9	28.9	25.5	13.9	4.44	− 5.93	−17.4	− 30.1
100	35.4	35.3	35.2	34.8	35.6	29.6	16.1	5.07	− 7.09	−20.6	− 35.6
200	50.1	50.1	49.8	49.3	47.6	42.0	22.8	7.10	−10.2	−29.3	− 50.9
400	70.9	70.8	70.5	69.7	67.3	59.4	32.2	9.99	−14.5	−41.8	− 72.3
1000	112	112	111	110	106	93.9	50.9	15.7	−23.1	−66.4	−115

Appendix 2

Calculation of the Area Function: Doppler Broadening Present

When Doppler broadening is appreciable, eq. (14) becomes

$$A_x(\infty,\beta)=\int_{-\infty}^{\infty}\{1-\exp[-n\sigma_0\Psi(\beta,x)]\}\mathrm{d}x - \sum_{m=1}^{\infty}\frac{(2n\sigma_0 a/\lambda)^{2m}}{(2m)!}\int_{-\infty}^{\infty}\Phi^{2m}(\beta,x)\exp[-n\sigma_0\Psi(\beta,x)]\mathrm{d}x \quad (16)$$

where Ψ is given by (6) and Φ, the Doppler broadened interference term, is $\Phi(\beta,x)=(1/\beta\sqrt{\pi})\int_{-\infty}^{\infty}(y/1+y^2)\exp\{-(x-y)^2/\beta^2\}\mathrm{d}y$. The integrals on the right hand side have to be computed numerically. The first integral $A'_x(\infty,\beta)$ has been quite extensively computed [2,3,4]). Approximate numerical computations of the remaining integrals up to $m=3$ have been made in the present work. Eq. (17) then is in the form of (7) and (8) and the ratios $C_m(\beta)/C_m(0)$ are shown in figs. 2, 3 and 4 as functions of β.

Appendix 3

Wing Corrections and Basic Level

In the evaluation of areas from experimental data one must know the value of T_p (the basic transmission) which enters the area definition. Also, the area evaluated is $A_E(\varepsilon)$ where ε is such that the transmission term due to the resonance term in (1) is approximately equal to 0.9. To convert $A_E(\varepsilon)$ to $A_E(\infty)$, the computed function, a wing correction term $\Delta A_E(\varepsilon)$ must be added to $A_E(\varepsilon)$.

If ε is large compared with Γ (and small compared with the level spacing) then a simple calculation gives, to second order of approximation

$$\Delta A_E(\varepsilon)=\frac{n\sigma_0\Gamma^2}{2\varepsilon}\left\{\left[1-\frac{2n\sigma_0 a^2}{\lambda^2}\right]-\frac{n\sigma_0\Gamma^2}{12\varepsilon^2}\left[\tfrac{1}{2}-\frac{2n\sigma_0 a^2}{\lambda^2}\right]\right\}. \quad (17)$$

The basic transmission may be found by taking the transmission at an equal energy difference on each side of the resonance, this energy difference being large compared with the width of the resonance but rather less than half the level spacing. If a small correction is made to these values to remove the transmission due to the resonance term, their product is T_p^2, the interference transmission thus being eliminated.

Appendix 4

Many-level Effects and their Inclusion in the Area Function

If the energy independent coefficient of the interference term in (1) and the transmission due to potential scattering are replaced by polynomials in x

then it is clear that the area $\hat{A}_x(\xi)$ defined by

$$\hat{A}_x(\xi) = \int_{-\xi}^{\xi} [1-T(x)/T_p(0)]\mathrm{d}x$$

may be expanded in the manner of eq. (14) and the integrals which appear may be evaluated. For simplicity only the case of linear functions of x are considered in this paper. Thus if $T_p(x) = T_p(0)(1+rx)$ and the interference term is written $sx(1+tx)/(1+x^2)$ then it is easily shown that

$$\begin{aligned}\hat{A}_x(\xi) = &\int_{-\xi}^{\xi} \left\{1-\exp\left(-\frac{n\sigma_0}{1+x^2}\right)\right\} \mathrm{d}x \\ &- \sum_{m=1}^{\infty} \frac{(-)^m}{m!}(ns)^m \sum_{q=0}^{m} \binom{m}{q} t^q \int_{-\xi}^{\xi} \frac{x^{m+q}}{(1+x^2)^m} \exp\left(-\frac{n\sigma_0}{1+x^2}\right) \mathrm{d}x \qquad (18) \\ &-r \sum_{m=1}^{\infty} \frac{(-)^m}{m!}(ns)^m \sum_{q=0}^{m} \binom{m}{q} t^q \int_{-\xi}^{\xi} \frac{x^{m+q+1}}{(1+x^2)^m} \exp\left(-\frac{n\sigma_0}{1+x^2}\right) \mathrm{d}x.\end{aligned}$$

Under the condition that ξ and $1/t$ are much greater than ns eq. (13) is obtained as an approximation to (18). It remains to show how this result is of value in dealing with many-level effects. Note that if the method of Appendix 3 is used to find $T_p(0)$ the terms in t disappear from (18) and (13).

By means of a procedure similar to that described by Feshbach, Porter and Weisskopf [12]) one may expand the total cross section expression of Wigner and Eisenbud [13]) in the case when the elements of the part of the derivative matrix due to all levels S, other than the main level R under consideration, are small compared with unity. The resulting expression for the cross section contains the usual single-level terms for the level R, and the analogous terms for the wings of the other levels S, together with cross terms between factors due to the level R and factors due to the other levels S which interfere with R. Most of these cross terms may be shown to be very small for the s-wave neutron cross section at energies below a few keV. By means of arguments concerning the very many channel nature of radiative capture, all cross terms involving radiative capture matrix elements may be omitted from consideration. Thus, in the case when radiative capture is the only reaction, the only many-level term which is expected to be significant, in general, is of the form:

$$\sigma_{ML} = -\frac{\sigma_0 x}{1+x^2} \sum_{S \neq R} \frac{\Gamma_{Sn}}{E_S - E}.$$

This may be expanded in terms of x giving

$$\sigma_{ML}(x) = -\frac{\sigma_0 x}{1+x^2} \sum_{S \neq R} \frac{\Gamma_{Sn}}{E_S - E_R} \left(1 + \frac{x}{x_{SR}} + \ldots\right) \qquad (19)$$

where $x_{SR} = (E_S - E_R)/\frac{1}{2}\Gamma_R$. This expression for σ_{ML} may now be included in

(1) to give the first-order many-level form of the cross section near the resonance R:

$$\sigma(x)=\frac{\sigma_0}{1+x^2}+\frac{\sigma_0 x}{1+x^2}\left[\frac{2a_J}{\lambda}-\sum_{S\neq R}\frac{\Gamma_{Sn}}{E_S-E_R}\right]$$
$$\cdot\left[1-\left(\frac{2a_J}{\lambda}-\sum_{S\neq R}\frac{\Gamma_{Sn}}{E_S-E_R}\right)^{-1}\sum_{S\neq R}\frac{\frac{1}{2}\Gamma_R\Gamma_{Sn}}{(E_S-E_R)^2}x\right]+4\pi\sum_J g_J a_J^2+\sum_{S,S'\neq R}\sigma_{SW}. \tag{20}$$

$\sum_{S,S'}\sigma_{SW}$ is the sum of the single-level wings of the levels S including levels S′ which do not interfere with R (i.e. have different spin J). This term is to be considered, for purposes of area analysis, as contributing to T_p. Thus, both T_p and the coefficient of the interference term may be treated as linear functions of x provided $|E-E_R|\ll|E_S-E_R|$ for all S. For†

$$\sum_{S,S'}\sigma_{SW}=-\sum_J 4\pi\lambda a_J g_J\sum_{S,\,S'\neq R}\frac{\Gamma_{Sn}}{E_S-E_R}\left(1+\frac{x}{x_{SR}}+\ldots\right) \tag{21a}$$

and

$$T_p(x)\approx T_p(0)\left[1+n4\pi\lambda\sum_J g_J a_J\sum_{S,\,S'\neq R}\frac{\frac{1}{2}\Gamma_R\Gamma_{Sn}}{(E_S-E_R)^2}x\right] \tag{21b}$$

where

$$T_p(0)=\exp\left[-n4\pi\sum_J g_J a_J^2\{1-(\lambda/a_J)\sum_{S,\,S'\neq R}\Gamma_{Sn}/(E_S-E_R)\}\right]. \tag{21c}$$

From eqs. (20) and (21) eqs. (13a, b and c) may be derived.

† Only the interference contributions to the wings are included in (21a). In general, the resonance contributions are negligible.

References

1) W. W. Havens Jr. and L. J. Rainwater, Phys. Rev. **83** (1951) 1123
2) E. Melkonian, W. W. Havens Jr. and L. J. Rainwater, Phys. Rev. **92** (1953) 702
3) F. G. P. Seidl, D. J. Hughes, H. Palevsky, J. S. Levin, W. Y. Kato and N. G. Sjöstrand, Phys. Rev. **95** (1954) 476
4) D. J. Hughes, J. Nuclear Energy **1** (1955) 237
5) J. E. Lynn and E. R. Rae, J. Nuclear Energy **4** (1957) 418
6) R. Ladenburg and F. Reiche, Ann. der Phys. **42** (1913) 181
7) G. N. Watson, Theory of Bessel Functions, 2nd Edition, (Cambridge University Press, Cambridge, 1944) (a) p. 77; (b) p. 25; (c) p. 203
8) H. A. Bethe, Revs. Mod. Phys. **9** (1937) 140
9) W. E. Lamb, Phys. Rev. **55** (1939) 190
10) M. E. Rose, W. Miranker, P. Leak and G. Rabinowitz, Brookhaven National Laboratory Report BNL. 257 (1953)
11) H. E. H. Wrinch and D. Wrinch, Phil. Mag. **45** (1923) 846
12) H. Feshbach, C. E. Porter and V. F. Weisskopf, Phys. Rev. **96** (1954) 448
13) E. P. Wigner and L. Eisenbud, Phys. Rev. **72** (1947) 29

2.C

Nuclear Physics 7 (1958) 613—621; © *North-Holland Publishing Co., Amsterdam*

Not to be reproduced by photoprint or microfilm without written permission from the publisher

THE LOW ENERGY NEUTRON RESONANCES OF BISMUTH

J. E. LYNN, M. C. MOXON and F. W. K. FIRK

Atomic Energy Research Establishment, Harwell, Berks

Received 28 April 1958

Abstract: The neutron transmission of bismuth has been measured as a function of neutron energy between 300 eV and 4000 eV for samples of different thickness. The analysis of the measurements gives the following parameters. The resonance at 784 ± 9 eV may be described by the combinations of parameters $\sigma_0 a_R^2/\lambda\!\!\!^{-2}_R = 5.68 \pm 0.22$ barn, $\Gamma \lambda\!\!\!^{-}_R/a_R = 77.4 \pm 3.3$ eV and the resonance at 2230±40 eV by $\sigma_0 a_R^2/\lambda\!\!\!^{-2}_R = 3.78 \pm 0.20$ barn and $\Gamma \lambda\!\!\!^{-}_R/a_R = 196 \pm 11$ eV. The interpretation of these results is that the two resonances correspond to states of the compound nucleus of different total angular momentum J. Hence the effective potential scattering cross section in the region 0—3 keV averages 9.46±0.3 barn. The probable spins of the two resonances are $J = 5$ for the 784 eV resonance and $J = 4$ for the 2230 eV resonance and the widths, Γ, are 4.34±0.15 eV and 16.6±0.7 eV respectively. This interpretation implies that the spin of the large resonance observed at about 12 keV by other workers is $J = 4$ and its width is ≈ 400 eV. The true potential scattering cross section then turns out to be approximately 10.4±0.3 barn.

1. Introduction

The low energy neutron cross section of bismuth is known to contain resonances having widths and spacings which are large for a heavy nucleus [1]). The present study was made to measure the widths of the lowest energy resonances with precision and to determine the angular momentum, J, of the states of the compound nucleus associated with the resonances. The method used to analyse the transmission measurements is described in the preceding paper [2]) (hereafter referred to as I).

2. Experimental

The neutron transmission of bismuth was measured as a function of neutron energy between 300 eV and 4000 eV for samples of metallic bismuth, the thickness ranging from $n = 0.022 \times 10^{24}$ atoms cm^{-2} to $n = 0.192 \times 10^{24}$ atoms cm^{-2}. The energy measurements were made by time-of-flight methods, the pulsed neutron source being the Harwell 15 MeV linear electron accelerator [3]). The flight path length was 31.8 m and the timing channels were of 1 μsec duration, the nominal resolution thus being 0.032 μsec m^{-1}. The method of determining background has been described previously [4]).

3. Analysis of Data

Some of the measured transmission curves are shown in fig. 1. Visual inspection indicates that the resonance energies are about 800 eV and 2300 eV. The areas $\hat{A}_E(\varepsilon)$ (eq. (12) of I) of the resonance dips were calculated from the transmission curves with cut-off points ε approximately 200 eV and 380 eV respectively. $T_p(E_R)$ was evaluated by the procedure of appendix 3 of I.

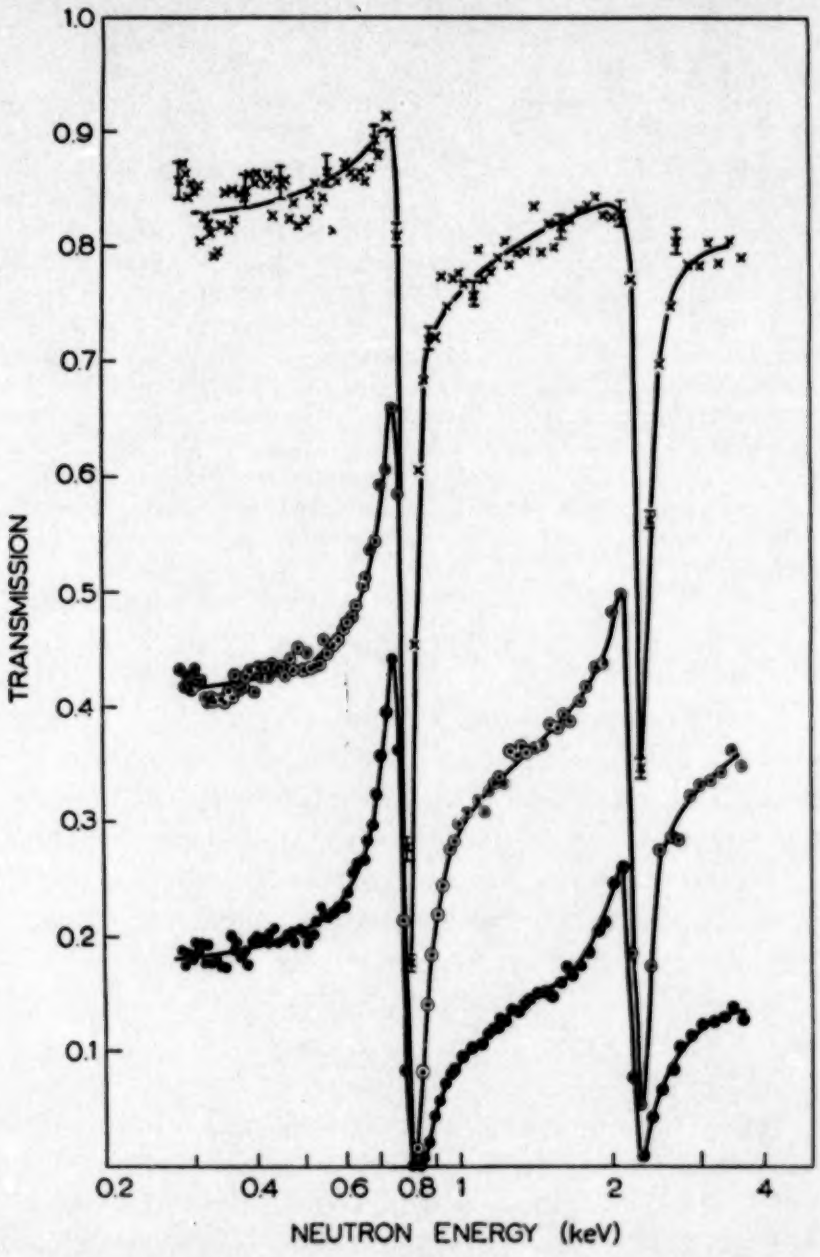

Fig. 1. Measured curves of the transmission of neutrons through metallic bismuth. The samples contain $n = 0.0218, 0.100, 0.192 \times 10^{24}$ atom cm^{-2}, in the order from the top of the figure.

An important source of error in the evaluation of $A_E(\varepsilon)$ arises from inaccurate determination of the resonance energy. In general this is not

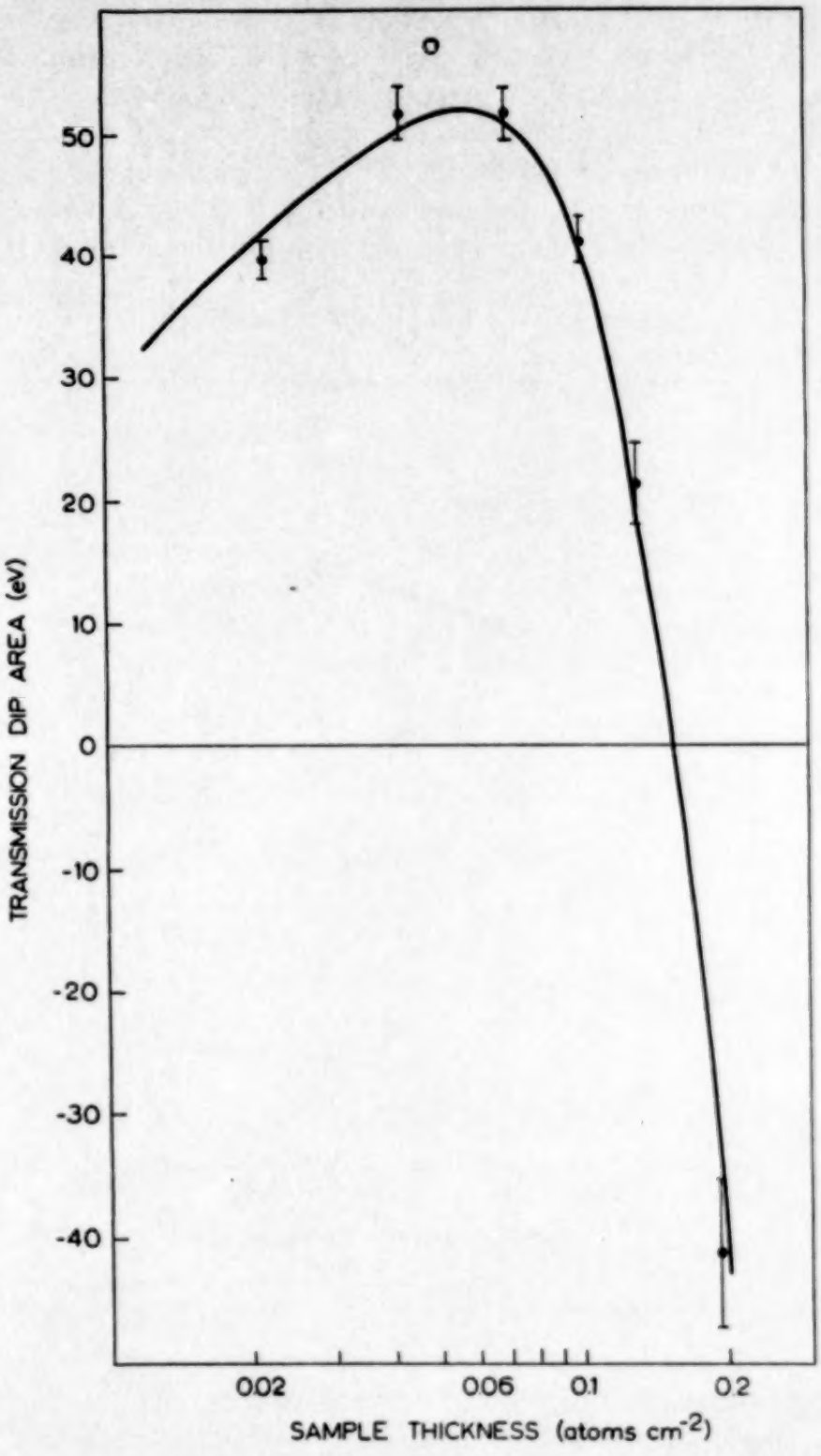

Fig. 2. Areas $A_E(\infty)$ of the transmission dips due to the 784 eV resonance of bismuth plotted against sample thickness. The full curve is the best fit of the theoretical area function to the experimental points.

sufficiently well determined by simple inspection of the highly asymmetric shapes illustrated in fig. 1. In appendix 1 of this paper a method is developed which enables the resonance energy to be fixed fairly reliably for thick samples. By this method the resonance energies are found to be 784 ± 3 eV and 2230 ± 10 eV. The stated errors take no account of systematic errors in the zero of the time scale but are relative to the energies of the other points in the transmission curves. The error caused in $\hat{A}_E(\varepsilon)$ by an error $\delta\varepsilon$ in the estimate of the resonance energy is calculated in appendix 2. It is

$$\delta\hat{A}_E(\varepsilon) = 2n\sigma_0 \frac{a^2}{\lambda\!\!\!^{-2}} \cdot \frac{\Gamma\lambda\!\!\!^{-}}{a} \left\{ 1 - \frac{1}{2\varepsilon} \frac{n\sigma_0\Gamma^2}{2\varepsilon} \left(1 - \tfrac{2}{3} n\sigma_0 a^2/\lambda\!\!\!^{-2}\right) \right\} \frac{\delta\varepsilon}{\varepsilon}.$$

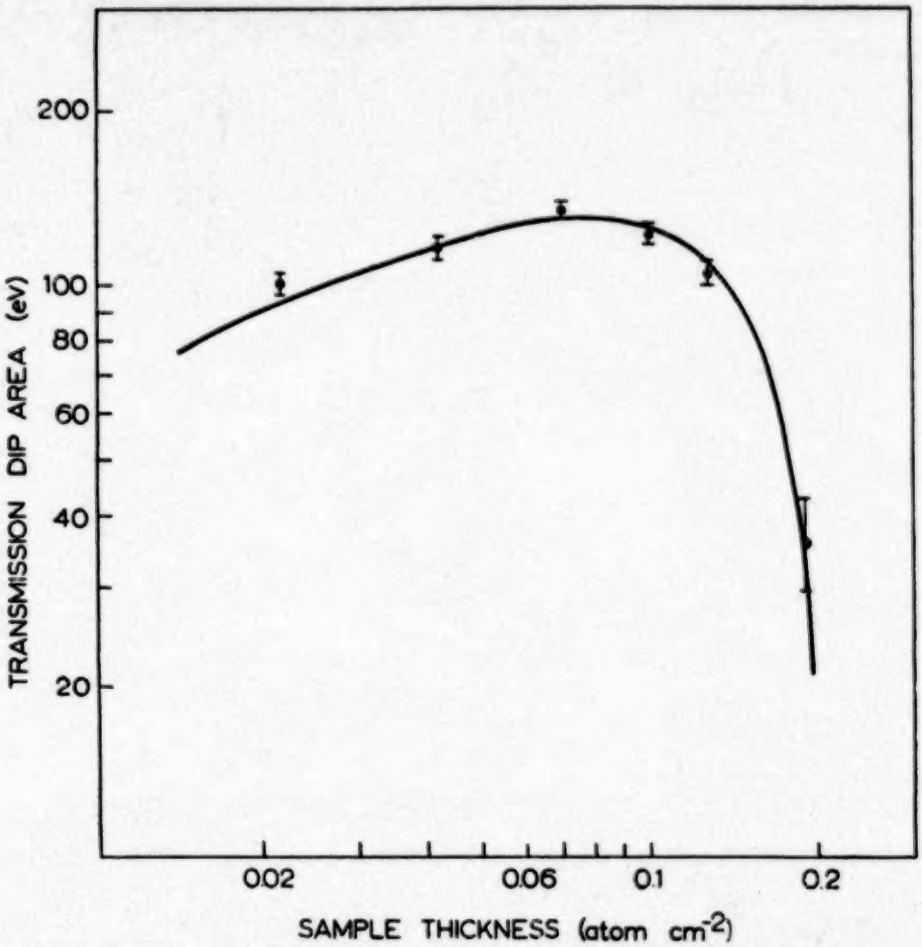

Fig. 3. Areas $A_E(\infty)$ of the transmission dips due to the 2230 eV resonance of bismuth plotted against sample thickness. The full curve is the best fit of the theoretical area function to the experimental points.

Wing correction terms to take account of the area beyond the cut-off point ε are described in appendix 3 of I. Preliminary analysis of the areas indicates that the resonances do not interfere so that the many-level corrections that must be made to the areas (eq. (13) of I) are confined to the term in s (eq. (13a) of I). After making all these corrections (using successive

approximations) values of $A_E(\infty)$ for different sample thicknesses are obtained. These are shown in fig. 2 for the 784 eV resonance and in fig. 3 for the 2230 eV resonance.

The smooth curves in fig. 2 and 3 are the best fits of the theoretical forms for $A_E(\infty, 0)$ (obtained from eqs. (7), (8) and (9) of I; Doppler broadening is negligible for these resonances). These fits determine the values of $\sigma_0 a_R^2/\lambda\!\!\!^{-}_R^2$ and $\Gamma\lambda\!\!\!^{-}_R/a_R$ for the two resonances. Here a_R is the effective potential scattering length and $2\pi\lambda\!\!\!^{-}_R$ the de Broglie wavelength at the resonance energy E_R. The results are given in table 1.

TABLE 1

Results of analysis of data and its interpretation

(The dashed panels are considered the more improbable interpretation)

E_R (eV)	$\frac{\sigma_0 a_R^2}{\lambda\!\!\!^{-}_R^2}$ (b)	$\frac{\Gamma\lambda\!\!\!^{-}_R}{a_R}$ (eV)	J	Γ (eV)	Γ_γ (meV)	Γ_n (eV)	σ_p
784±9	5.68±0.22	77.4±3.3	5	4.34±0.15	44±3	4.30±0.15	10.4±0.4
			4	4.80±0.2	40±3	4.76±0.20	12.8±0.4
2230±40	3.78±0.2	196 ±11	4	16.7 ±0.7		16.7 ±0.7	
			5	15.3 ±0.7		15.3 ±0.7	
12×10^3	–	–	4	≈ 400		≈ 400	
			5	≈1100		≈1100	

4. Resonance Parameters

The quantity $\sigma_0 a_R^2/\lambda\!\!\!^{-}_R^2$ is related to the widths and spin, J, of the resonance through

$$\frac{\sigma_0 a_R^2}{\lambda\!\!\!^{-}_R^2} = 4\pi a_R^2 g_J \frac{\Gamma_n}{\Gamma} \tag{1}$$

where $g_J = (2J+1)/2(2I+1)$ ($I = \frac{9}{2}$ for Bi^{209}). The thermal capture cross section is so low that Γ_n/Γ differs from unity only by about one per cent for both of the resonances under consideration, and may be replaced by unity in order to consider the spins of the resonances.

4.1. ANGULAR MOMENTUM OF COMPOUND NUCLEUS STATES

It is observed (see table 1) that $g_J a_R^2$ for the 784 eV resonance is considerably greater than for the 2230 eV resonance. This implies that the two resonances have different J. If they were the same, there would be inter-

ference so that a_{2230} would be greater than a_{784} owing to the positive contribution to a at 2230 eV from the 784 eV resonance and the negative contribution to a at 784 eV from the 2230 eV resonance (this argument is valid when, as here, there is no greatly varying contribution from other levels). Thus, the sum of $\sigma_0 a_R^2/\lambda\!\!\!^{-}_R{}^2$ for the two resonances gives approximately the effective potential scattering cross section in the region of 0 to 3 keV. The effective potential scattering cross section is the true potential scattering cross section modified by the contribution of distant levels. If the latter were negligible the ratio of $\sigma_0 a_R^2/\lambda\!\!\!^{-}_R{}^2$ of the two resonances would be the ratio of their spin weighting factors, 11 : 9. The fact that this ratio is larger than 11/9 shows that other levels do contribute. If it is assumed that only the large level which has been observed at 12 keV [1]) contributes appreciably to the cross section below 3 keV then it is clear that the spins of the 12 keV and 2.23 keV levels are the same, and that the value of $\sigma_0 a_R^2/\lambda\!\!\!^{-}_R{}^2$ for the 784 eV level gives the true potential scattering cross section. If $J = 4$ for the 784 eV level the true potential scattering cross section is greater than 12.65 barns. If $J = 5$, it is greater than 10.3 barn. The potential scattering cross sections of most other heavy nuclei appear to lie in the range of about 10 to 11 barn [5]). It appears most likely therefore that the spins associated with the resonances are as follows: 748 eV, $J = 5$; 2230 eV, $J = 4$; 12 keV, $J = 4$.

4.2. TOTAL WIDTHS

The assignment of spins to the resonances allows the determination of $a_R/\lambda\!\!\!^{-}_R$ and hence Γ. The values are given in table 1.

4.3. RADIATIVE CAPTURE WIDTHS

The thermal capture cross section, σ_γ, at very low energy E is related to the partial widths of the resonances by

$$\sigma_\gamma = \sum_R \frac{\pi \lambda\!\!\!^{-}_R{}^2 g_{JR} \Gamma_{nR} \Gamma_{\gamma R}}{E_R^{\frac{1}{2}} E^{\frac{1}{2}}}.$$

If $\Gamma_{\gamma R}$ is assumed to be the same for each resonance then substitution of the parameters and the thermal absorption cross section of 32 ± 2mb [5]) in this formula gives $\Gamma_\gamma = 44 \pm 3$ meV.

4.4. POTENTIAL SCATTERING CROSS SECTION

The above value for Γ_γ justifies its neglect in equating Γ_n/Γ to unity in (1). The effective potential scattering (i.e. the sum of the two entries in column 2 of table 1) is 9.5 ± 0.3 barn. This agrees with the observed value of 9.8 ± 0.1 barn (from resonance parameters and observed cross section curve, fig. 4). The true potential scattering cross section as found in § 4.1 and corrected for Γ_γ is probably 10.4 ± 0.4 barn.

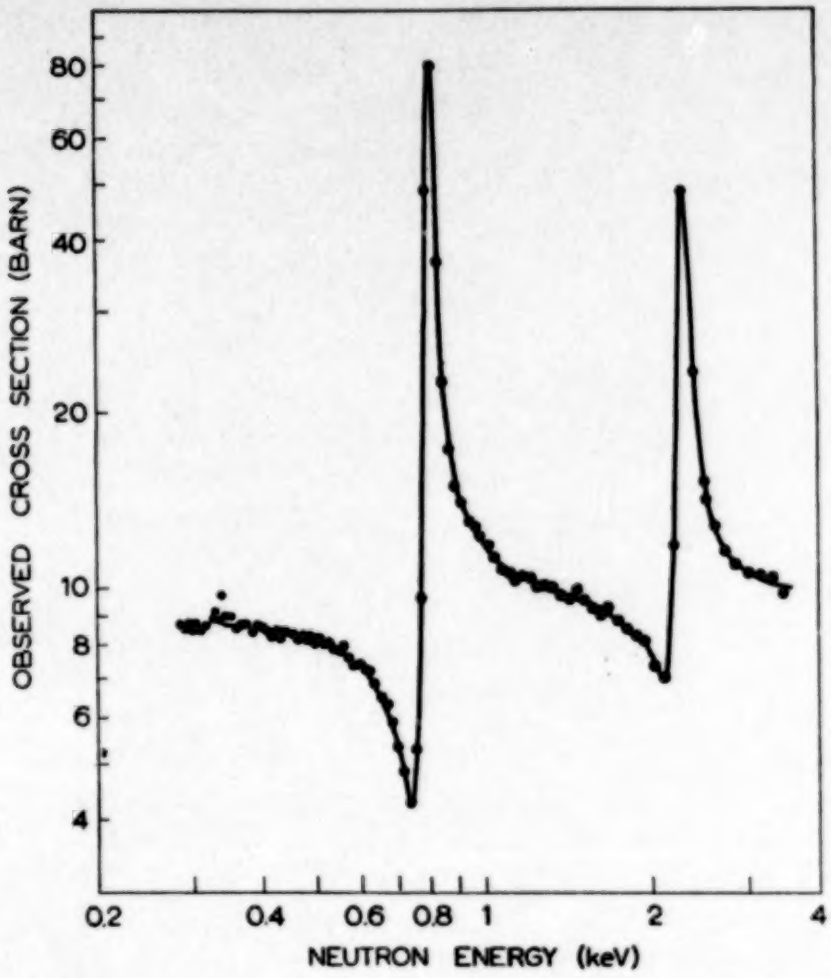

Fig. 4. Observed cross section of bismuth as function of energy. Errors are less than the circles.

Appendix 1

Determination of Resonance Energy

The solid line in fig. 5 shows a calculated transmission curve in the neighbourhood of a resonance where interference asymmetry is strong and the sample is thick. The most distinctive feature is a rather sharp almost linear step. The effect of rather poor resolution is shown by the dashed curve which was obtained by folding into the solid curve the resolution function shown by the triangle. Resolution decreases the slope of the step but the true curve and the resolution-broadened curve intersect at about half-way up the step. Thus, the actual observation of the transmission curve even with poor resolution enables one to determine the energy of a unique point on the curve. The position of this point with respect to the resonance energy is given by

$$E_{\frac{1}{2}}-E_{\mathrm{R}}=\frac{-2n\sigma_0 a_{\mathrm{R}}^2/\lambda\!\!\!^{-}_{\mathrm{R}}^2+\sqrt{(2n\sigma_0 a_{\mathrm{R}}^2/\lambda\!\!\!^{-}_{\mathrm{R}}^2)^2-2y\cdot 2n\sigma_0 a_{\mathrm{R}}^2/\lambda\!\!\!^{-}_{\mathrm{R}}^2-(ya_{\mathrm{R}}/\lambda\!\!\!^{-}_{\mathrm{R}})^2}}{y}\cdot\frac{\Gamma\lambda\!\!\!^{-}_{\mathrm{R}}}{4a_{\mathrm{R}}}$$

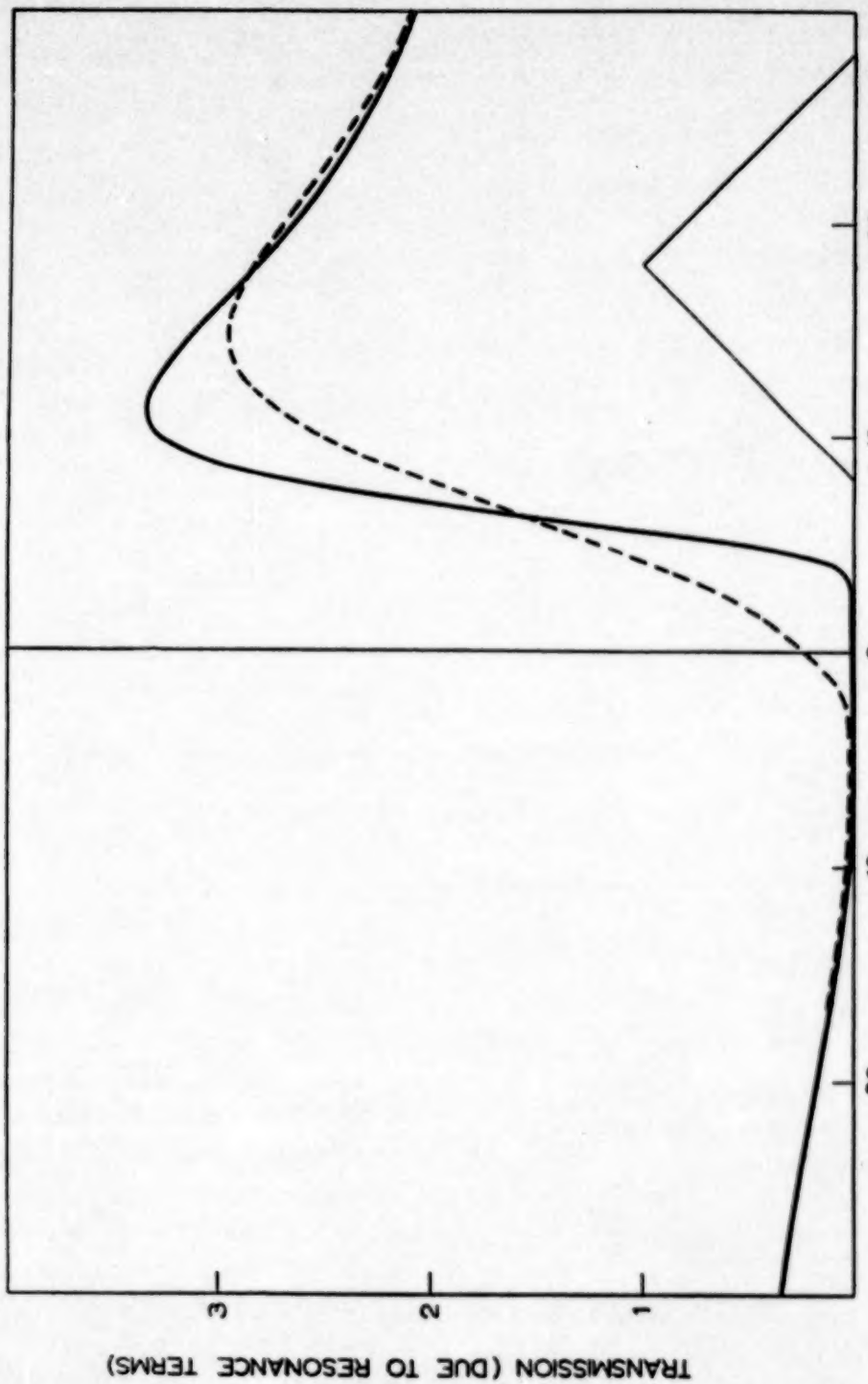

Fig. 5. This shows the effect of resolution (dashed curve) upon the true transmission (full curve) when the sample is very black at resonance and there is considerable interference. The triangle is the resolution function employed.

where $y = \ln(T_{\frac{1}{2}}/T_p)$, $T_{\frac{1}{2}}$ is the transmission at $E_{\frac{1}{2}}$, the point half-way up the interference step. In order to determine $E_{\frac{1}{2}}$ there must be at least two observations of the transmission on the step. The parameters, sample thickness and resolution used in calculating the curves of fig. 5 are roughly those corresponding to the case of the 2230 eV resonance using the thickest sample.

Appendix 2

Area Correction for Resonance Energy Error

If the resonance energy has been wrongly estimated by an amount $\delta\varepsilon$ the area calculated from the observations is

$$A_E(\varepsilon)+\delta A_E(\varepsilon) = \int_{-(\varepsilon-\delta\varepsilon)}^{\varepsilon+\delta\varepsilon} [1-T/T_p]\mathrm{d}(E-E_R)$$

$$\therefore \delta A_E(\varepsilon) = \int_{\varepsilon}^{\varepsilon+\delta\varepsilon} [1-T/T_p]\mathrm{d}(E-E_R)+\int_{-(\varepsilon-\delta\varepsilon)}^{-\varepsilon} [1-T/T_p]\mathrm{d}(E-E_R). \quad (2)$$

If $\varepsilon \gg \Gamma$, eq. (2) of I may be replaced by the first few terms of its expansion and $1+x^2$ may be replaced by x^2. After substitution of this approximation for T in (2) and integration

$$\delta A_E(\varepsilon) \approx \frac{2n\sigma_0 a^2}{\lambda\!\!\!^{-}_R{}^2} \cdot \frac{\Gamma\lambda\!\!\!^{-}}{a} \left\{ 1 - \frac{1}{2\varepsilon} \cdot \frac{n\sigma_0\Gamma^2}{2\varepsilon} \left(1-\tfrac{2}{3}n\sigma_0 a^2/\lambda\!\!\!^{-2}\right) \right\} \frac{\delta\varepsilon}{\varepsilon}$$

to second order. $\delta\varepsilon/\varepsilon$ is assumed small compared with unity.

References

1) L. M. Bollinger, D. A. Dahlberg, R. R. Palmer and G. E. Thomas, Phys. Rev. **100** (1955) 126
2) J. E. Lynn, Nuclear Physics **7** (1958) 599
3) E. R. Wiblin, Proceedings of the International Conference on the Peaceful Uses of Atomic Energy **4** (United Nations, New York, 1956) 35
4) J. E. Lynn, F. W. K. Firk and M. C. Moxon, Nuclear Physics **5** (1958) 603
5) K. K. Seth, Ph. D. thesis, University of Pittsburgh (1957)
6) D. J. Hughes and J. A. Harvey, Neutron Cross Sections, BNL report 325 (1955)

2.B *Nuclear Physics* **7** (1958) 622—642; © *North-Holland Publishing Co., Amsterdam*
Not to be reproduced by photoprint or microfilm without written permission from the publisher

THE POLARIZATION OF DEUTERONS AND PARTICLES OF ARBITRARY SPIN

L. J. B. GOLDFARB
Department of Theoretical Physics, University of Manchester

Received 22 March 1958

Abstract: General formulae are given for the polarization of particles of arbitrary spin which are emitted in a nuclear scattering or reaction process, and also for the angular distribution associated with processes involving incident particles of arbitrary spin that are polarized. These formulae are applied to the particular process of elastic scattering of deuterons by He^4 where a narrow resonance is found to exist at the deuteron laboratory energy of 1.069 MeV. This resonance is attributed to a well-defined intermediate state with a unique set of quantum numbers for the initial and final states. In general, the polarization of deuterons is described by tensors of first and second rank; however in this case, the former tensors vanish while the tensors of second rank are independent of the nuclear matrix element and they attain large values for various scattering angles. Thus, the scattering process serves as an efficient polarizer of deuterons. Alternatively, it serves as an efficient analyser of deuteron polarization of rank two.

A calculation is made of the polarization of deuterons which are elastically scattered by spinless nuclei where the interaction is described by a potential. This potential is assumed to involve only the vector $\mathbf{r}$, joining the centre of mass of the deuteron to that of the nucleus, and the spins of the nucleons in the deuteron, $\boldsymbol{\sigma}_P$ and $\boldsymbol{\sigma}_N$. The most general potential involves central terms, $V(r)$, spin-orbit terms of the type $W(r)\frac{1}{2}\hbar\mathbf{l}\cdot(\boldsymbol{\sigma}_P+\boldsymbol{\sigma}_N)$, where $\mathbf{l}$ is the deuteron angular-momentum operator and tensor terms of the type $U(r)T_{12}$, where

$$T_{12}=3\frac{\boldsymbol{\sigma}_P\cdot\mathbf{r}\boldsymbol{\sigma}_N\cdot\mathbf{r}}{r^2}-\boldsymbol{\sigma}_P\cdot\boldsymbol{\sigma}_N.$$

The polarization can be detected in a second scattering by the same nuclei or by using the He^4 scattering process as an analyser. The calculation in Born approximation shows that in the latter case, the angular distribution when expressed as a function of the angle between the two scattering planes, shows a left-right asymmetry for tensor forces and no such asymmetry for spin-orbit forces.

1. Introduction

The large polarization exhibited by nucleons that are emitted in nuclear reactions leads one to consider the possibility of obtaining beams of polarized deuterons from nuclear processes. That deuterons can be polarized has been shown directly by Chamberlain *et al.*[1]), who subjected a beam of 167 MeV deuterons to a double scattering by C^{12}. They measured the angular distribution of the doubly scattered beam at a pair of fixed scattering angles and found it to be of the form

$$W(\varphi) = p+q\cos\varphi+r\cos 2\varphi \qquad (1.1)$$

where φ is the angle between the two planes of scattering. The deuterons are polarized by the first scattering process and exhibit their polarization in a second scattering.

In contrast to the case of spin-$\frac{1}{2}$ particles, the state of polarization of a beam of deuterons is described both by a tensor of the first rank (vector) and of the second rank (Dalitz[2]); Lakin [3])). Lakin investigated the properties of the tensors and arrived at several selection rules for simple reactions, including the relations of the parameters p, q and r in (1.1) to the components of the polarization tensors. Some detailed geometrical considerations of the state of polarization of the deuterons have also been given by MacDowell [4]).

A more general approach by Simon [5]) leads to general selection rules for the polarization of particles of arbitrary spin and to explicit formulae for the tensors. By an alternative derivation (cf. the review article by Devons and Goldfarb [6])) some of the tedious algebra associated with the summation over magnetic quantum numbers is avoided by the use of density matrices, efficiency matrices and tensors derived therefrom. A general expression for the angular distribution in nuclear processes involving polarized particles of arbitrary spin can be directly found using the above formalism. The expressions for the angular distribution and the polarization tensors which are equivalent to those to be found in ref.[5,6]) are included in section 2. They simplify greatly for the case of spin 1 and it is one of the purposes of this paper to give specific formulae for the polarization of deuterons which are scattered by or react with nuclei of arbitrary spin †.

The usual description of nuclear reactions requires that we introduce a scattering matrix, S, with a related reaction matrix, $R(R = S-1)$, to characterize the probability amplitude for a particular process to occur. The R-matrix has elements specifying the transition from an initial state to a final state where each state is associated with a definite set of quantum numbers. They arise for each state in the vector addition of the spin and relative orbital angular momentum of the incident or outgoing particle together with the spin of the target or residual nucleus to yield the total angular momentum of the system. If the spins are first coupled together, they yield the channel-spin quantum number which, together with the orbital angular-momentum and total angular-momentum quantum numbers, provides a description of the R-matrix in the channel-spin representation [9]). On the other hand, the R-matrix may be described in the $\mathscr{L}$-representation [6,10]), where the spin of the particle is coupled to its orbital

† J. W. MacDowell and J. Tiomno [7]) have developed formulae for the scattering of deuterons by spinless nuclei, using a method of Lepore [8]) which is appropriate for $\mathbf{l}\cdot\mathbf{s}$ potentials. Our formulae in section 2 apply to any spin and are not restricted to scattering processes.

angular momentum to form L which is then coupled to the nuclear spin to give the total angular momentum. In either case, the matrices each correspond to a definite value of the total angular momentum, and are independent of the components of angular momenta.

One of the features of spin-$\frac{1}{2}$ polarization is that it depends on the imaginary part of RR'^*, where R and R' are two reaction matrix elements in either the channel-spin or $\mathscr{L}$-representation. It therefore vanishes if there is only one matrix element †. The second-rank polarization of the deuteron, on the other hand, depends on the real part of RR'^* and, as a consequence, polarization can arise from a single reaction matrix element. An example is the resonant scattering of deuterons by He^4 at 1.069 MeV which is adequately explained by a single assignment of quantum numbers for R. The polarization is calculated in section 3. Of great interest is the fact that the magnitude of the polarization is independent of the dynamics of the process, i.e. of the particular nature of R, but it is merely a function of the angles characterizing the measurements, i.e. of the geometry of the process.

In the last section the polarization of deuterons, elastically scattered by spinless nuclei, is calculated in Born approximation. The interaction between the deuteron and nucleus is represented phenomenologically by an arbitrary central potential and by spin-orbit terms of the form $W(r)\mathbf{l}\cdot\mathbf{s}$ and

$$U(r)T_{12} = \left(3\frac{\boldsymbol{\sigma}_P\cdot\mathbf{r}\boldsymbol{\sigma}_N\cdot\mathbf{r}}{r^2} - \boldsymbol{\sigma}_P\cdot\boldsymbol{\sigma}_N\right)$$

where

$$\mathbf{s} = \tfrac{1}{2}\hbar(\boldsymbol{\sigma}_P+\boldsymbol{\sigma}_N),$$

$\mathbf{l}$ is the orbital angular-momentum operator which operates on the deuteron coordinate and $\mathbf{r}$ is the vector joining the deuteron to the centre of mass of the nucleus. The tensor force is postulated in analogy with the S_{12} operator which accounts for the binding of neutron and proton in the deuteron; however, the vector $\mathbf{r}$ has a different significance in this case. Although a realistic representation of the deuteron interaction with the nucleus should be a function of the variables of the proton, neutron and the nucleons in the nucleus, the potentials considered here are presented in order to provide a first orientation to the study of polarization. A significant qualitative difference in polarization arises in the two cases since, if the He^4 scattering process is used as an analyser of the polarization, the doubly-scattered deuteron beam exhibits a left-right asymmetry for the tensor interaction and no such asymmetry for the $\mathbf{l}\cdot\mathbf{s}$ interaction.

† In the case of elastic scattering, polarization, in principle, can arise on account of the interference between potential and resonance scattering; but we will ignore this possibility.

2. General Formulae for Arbitrary Spin

2.1. ANGULAR DISTRIBUTIONS FOR POLARIZED PARTICLES

We will mainly follow the notation used by Devons and Goldfarb [6]) for the representation of angular-momentum states. The angular-momentum quantum numbers are represented by Latin letters and their components (magnetic quantum numbers) by the Greek equivalent. Thus, $a\alpha$, $b\beta$, and $c\gamma$ are the quantum numbers for target, compound nucleus and residual nucleus, respectively. If no compound-nucleus formation takes place, $b\beta$ designates the total angular momentum of the system of nucleus plus particle. The incident particle is described by quantum numbers $L_1 \Lambda_1$ which arise from the vector addition of l_1 and s_1, i.e. of the states $|l_1 \lambda_1\rangle$ and $|s_1 \sigma_1\rangle$. The representation used in this treatment is the total angular-momentum representation, or $\mathscr{L}$-representation, where $\mathscr{L}$ is a collective symbol for l, s and L. The alternative scheme, the channel-spin representation, which is frequently used for nuclear reactions has the virtue that if polarization effects are not present the angular distribution involves an incoherent summation over channel-spin quantum numbers. This advantage is lost, however, if polarization is present and it is then more convenient to deal with the $\mathscr{L}$-representation.

We use the formalism introduced by Coester and Jauch[11]) and by Fano [12]) with density and efficiency matrices and the derived quantities, the statistical and efficiency tensors. The method proves to be very appropriate for the study of polarization phenomena. It consists in describing the reaction or scattering process by means of a change in the density matrix, ρ, through the reaction matrix, R. The density matrix is multiplied by ε, the efficiency matrix, which depends on the detection of the outgoing particle and residual nucleus. In a certain representation, q, the matrix ε is diagonal and the probability of detection is given by

$$W = \sum_q \langle q|\rho|q\rangle\langle q|\varepsilon|q\rangle = \text{trace } \rho\varepsilon. \tag{2.1}$$

This can likewise be represented in terms of the representation of interest, as follows:

$$W = \sum_{bb'\beta\beta' BB'} \langle b\beta B|\rho|b'\beta' B'\rangle\langle b'\beta' B'|\varepsilon|b\beta B\rangle. \tag{2.2}$$

Here, the quantum numbers B, B' designate quantum numbers aside from $b\beta$, $b'\beta'$ which are necessary to describe the state of the complete system. It is more convenient to use statistical tensors $\rho_{k_b \kappa_b}(bB, b'B')$ and efficiency tensors $\varepsilon_{k_b \kappa_b}(bB, b'B')$ defined as

$$\rho_{k_b \kappa_b}(bB, b'B') = \sum_{\beta\beta'} (-)^{b'-\beta'}(b\beta, b'-\beta'|k_b \kappa_b)\langle b\beta B|\rho|b'\beta' B'\rangle \tag{2.3a}$$

and

$$\varepsilon_{k_b \kappa_b}(bB, b'B') = \sum_{\beta\beta'} (-)^{b'-\beta'} (b\beta, b'-\beta'|k_b \kappa_b)\langle b\beta B|\varepsilon|b'\beta' B'\rangle \quad (2.3b)$$

where $(b\beta, b'-\beta'|k_b \kappa_b)$ is a Clebsch-Gordan coefficient. The probability is then given by

$$W = \sum_{bb' BB' k_b \kappa_b} \rho_{k_b \kappa_b}(bB, b'B')\varepsilon^*_{k_b \kappa_b}(bB, b'B'). \quad (2.4)$$

These tensors are particularly convenient since they can be transformed in terms of tensors which describe separately the state of preparation of the incident particle and target nucleus or the process of detection of the outgoing particle and the recoil nucleus. For example, to account for the detection of the decay products, we use, the relation $\mathbf{b} = \mathbf{L}_2 + \mathbf{c}$ and transform $\varepsilon_{k_b \kappa_b}$ as follows:

$$\varepsilon_{k_b \kappa_b}(bB, b'B') = \sum_{k_2 \kappa_2 k_c \kappa_c} \varepsilon_{k_2 \kappa_2}(\mathscr{L}_2 \mathscr{L}'_2)\varepsilon_{k_c \kappa_c}(cc')(k_2 \kappa_2, k_c \kappa_c|k_b \kappa_b) \cdot \hat{b}\hat{b}' \hat{k}_2 \hat{k}_c \begin{Bmatrix} L_2 & c & b \\ L'_2 & c' & b' \\ k_2 & k_c & k_b \end{Bmatrix} \quad (2.5)$$

where the last term in parentheses is the 9-j symbol and the superscript ("stat") provides a short-hand notation for the statistical factor, e.g. $\hat{b} \equiv \sqrt{2b+1}$, etc. The dynamics of the process are described by the change in the density matrix from the initial value $\rho^{(i)}$ to the final value $\rho^{(f)}$, given by

$$\rho^{(f)} \propto R^\dagger \rho^{(i)} R. \quad (2.6)$$

This leads to an expression for the statistical tensor describing the final state in terms of the initial statistical tensor. The latter tensor accounts for the state of preparation of the incident particle and target nucleus, and is transformed in terms of $\rho_{k_1 \kappa_1}(\mathscr{L}_1 \mathscr{L}'_1)$ and $\rho_{k_a \kappa_a}(aa')$ according to (2.5), using the relation $\mathbf{b} = \mathbf{L}_1 + \mathbf{a}$. The tensors $\rho_{k_1 \kappa_1}(\mathscr{L}_1 \mathscr{L}'_1)$ and $\varepsilon_{k_2 \kappa_2}(\mathscr{L}_2 \mathscr{L}'_2)$ are further transformed into tensors which describe the preparation or measurement of the direction of propagation of the particles and of their states of polarization.

The general expression for the angular distribution can be shown to be [6])

$$W(\Omega_1, \Omega_2) = \frac{\lambda^2}{4\hat{a}^2 \hat{s}_1^2} \sum_{\substack{k \kappa_1 \kappa_2 bb' \\ \mathscr{L}_1 \mathscr{L}'_1 \mathscr{L}_2 \mathscr{L}'_2}} A_{k\kappa_1}(\mathscr{L}_1 \mathscr{L}'_1; abb') A^*_{k\kappa_2}(\mathscr{L}_2 \mathscr{L}'_2; cbb') \cdot RR'^* \mathscr{D}^k_{\kappa_2 \kappa_1}(\mathscr{R}_2^{-1} \mathscr{R}_1), \quad (2.7)$$

where $R \equiv \langle c\mathscr{L}_2 b|R|a\mathscr{L}_1 b\rangle$, $R' \equiv \langle c\mathscr{L}'_2 b'|R|a\mathscr{L}'_1 b'\rangle$ and Ω_1, Ω_2 are the angles in the centre-of-mass system characterizing the directions of motion and polarization of the incident and outgoing particles, respectively. The angular dependence is contained in $\mathscr{D}$ which is the matrix corresponding to

the rotation from the coordinate axes of the second radiation, to those of the first radiation. $\mathscr{R}_i$ represents the rotation from an arbitrary set of axes to those characterizing the ith radiation. $\lambda\!\!\!^{-}$ is the reduced wave length in the centre-of-mass system. The expression $A_{k\kappa}$ is given by

$$A_{k\kappa}(\mathscr{L}_1\mathscr{L}'_1; abb') = 4\pi\hat{s}_1^{\,2}\hat{b}\hat{b}'(-)^{a+k-L_1-b'}W(bb'L_1L'_1; ka)c_{k\kappa}(\mathscr{L}_1\mathscr{L}'_1) \tag{2.8}$$

where $c_{k\kappa}(\mathscr{L}_1\mathscr{L}'_1)$, the radiation parameter, is

$$c_{k\kappa}(\mathscr{L}_1\mathscr{L}'_1) = \frac{\hat{L}_1\hat{L}'_1\hat{l}_1\hat{l}'_1(-)^{l'_1}}{4\pi}\sum_{k_i k_s}(l_1 0, l'_1 0|k_i 0)(k_i 0, k_s\kappa|k\kappa) \cdot \hat{k}_i\hat{k}_s \begin{Bmatrix} l_1 & l'_1 & k_i \\ s_1 & s_1 & k_s \\ L_1 & L'_1 & k \end{Bmatrix} \rho_{k_s\kappa}(s). \tag{2.9}$$

The expression for $A_{k\kappa}(\mathscr{L}_2\mathscr{L}'_2; cbb')$ is the same as above except for the replacement of ρ by ε and the suffix 1 by 2. If the beam is unpolarized, or if detection is insensitive to polarization, the spin tensors $\rho_{k_s\kappa}(s)$, $\varepsilon_{k_s\kappa}(s)$ are proportional to $\delta_{k_s 0}\delta_{\kappa 0}$. In these cases $c_{k\kappa}$ reduces to

$$c_{k0}(\mathscr{L}_1\mathscr{L}'_1) = \frac{\hat{L}_1\hat{L}'_1\hat{l}_1\hat{l}'_1(-)^{k+s_1-L_1}}{4\pi\hat{s}_1^{\,2}}(l_1 0, l'_1 0|k0)W(l_1l'_1L_1L'_1; ks_1) \tag{2.10}$$

and $A_{k\kappa}$ becomes A_k where

$$A_k(\mathscr{L}_1\mathscr{L}'_1; abb') = \hat{L}_1\hat{L}'_1\hat{l}_1\hat{l}'_1\hat{b}\hat{b}'(-)^{a-s_1-b'}(l_1 0, l'_1 0|k0) \cdot W(l_1l'_1L_1L'_1; ks_1)\, W(bb'L_1L'_1; ka). \tag{2.11}$$

The angular distribution, $W_0(\theta)$, is for unpolarized particles and involves only the angle, θ, between incident and outgoing particles. It is given by

$$W_0(\theta) = \frac{\lambda\!\!\!^{-2}}{4\hat{a}^2\hat{s}_1^{\,2}}\sum_{kbb'\mathscr{L}_1\mathscr{L}'_1\mathscr{L}_2\mathscr{L}'_2} A_k(\mathscr{L}_1\mathscr{L}'_1; abb')A_k(\mathscr{L}_2\mathscr{L}'_2; cbb') \cdot q(bb'; L_1L'_1, L_2L'_2, l_1l'_1, l_2l'_2)\,\mathrm{Re}\,(RR'^*)P_k(\cos\theta), \tag{2.12}$$

where q is a contraction factor which avoids some duplication in the summation and satisfies

$$q(bb'; L_1L'_1, L_2L'_2, l_1l'_1, l_2l'_2) = \begin{cases} 0 \\ 2 \end{cases}$$

when $b \lesseqgtr b'$, or when $b = b'$ and any of the following conditions hold:

$$L_1 \lesseqgtr L'_1$$
$$L_1 = L'_1 \quad \text{and} \quad L_2 \lesseqgtr L'_2$$
$$L_1 = L'_1, L_2 = L'_2 \quad \text{and} \quad l_1 \lesseqgtr l'_1$$
$$L_1 = L'_1, L_2 = L'_2, l_1 = l'_1 \quad \text{and} \quad l_2 \lesseqgtr l'_2.$$

Also, $q(bb; L_1L_1, L_2L_2, l_1l_1, l_2l_2) = 1$.

We will be concerned with the use of the reaction or scattering process, either as a polarizer or an analyser. In either case, one of the $A_{k\kappa}$ factors reduces to A_k and the rotation matrix reduces to a Legendre function. If $\mathscr{R}_1^{-1}\mathscr{R}_2$ is denoted by the Euler angles χ, θ, ψ, the displacement from one coordinate system to the other is described by a rotation χ about the z-axis of the first radiation, followed successively by rotations θ about the new y-axis and ψ about the new z-axis. We use the relations

$$\mathscr{D}^k_{\kappa_2\kappa_1}(\mathscr{R}_2^{-1}\mathscr{R}_1) = \mathscr{D}^{k*}_{\kappa_1\kappa_2}(\mathscr{R}_1^{-1}\mathscr{R}_2) = \mathscr{D}^{k*}_{\kappa_1\kappa_2}(\chi, \theta, \psi) \tag{2.13}$$

and

$$\mathscr{D}^k_{\kappa_1 0}(\chi, \theta, \psi) = \frac{\sqrt{4\pi}}{\hat{k}} Y_k^{\kappa_1}(\theta, \chi) = \sqrt{\frac{(k-\kappa_1)!}{(k+\kappa_1)!}}\,(-)^{\kappa_1\delta\kappa_1,|\kappa_1|}\,P_k^{|\kappa_1|}(\cos\theta)\mathrm{e}^{-i\kappa_1\chi}$$
$$= P_k(\cos\theta), \quad \text{if} \quad \kappa_1 = 0$$

where $P_k(\cos\theta)$ and $P_k^{\kappa}(\cos\theta)$ are the Legendre coefficient and associated Legendre functions of the first kind (see Jahnke and Emde [13]).

The angular distribution for a process in which the polarization of the incident beam is characterized by the statistical tensor $\rho_{k_s\kappa}(s)$ is found to be

$$W(\Omega_1, \Omega_2)$$
$$= W_0(\theta)\Bigg[1 + \frac{\hat{\lambda}^2}{4\hat{a}^2 W_0(\theta)} \sum_{bb'\mathscr{L}_1\mathscr{L}'_1\mathscr{L}_2\mathscr{L}'_2 k} \frac{A_k(\mathscr{L}_1\mathscr{L}'_1; abb')A_k(\mathscr{L}_2\mathscr{L}'_2; cbb')}{(l_1 0, l'_1 0|k0)W(l_1 l'_1 L_1 L'_1; ks_1)}$$
$$\cdot q(bb'; \mathscr{L}_1\mathscr{L}'_1, \mathscr{L}_2\mathscr{L}'_2)(-)^{k+s_1-L_1+l'_1} \sum_{k_l, k_s(\neq 0)} (l_1 0, l'_1 0|k_l 0)\hat{k}_l\hat{k}_s \begin{Bmatrix} l_1 & l'_1 & k_l \\ s_1 & s_1 & k_s \\ L_1 & L'_1 & k \end{Bmatrix} \tag{2.14}$$
$$\cdot B_1(k_l k_s k; RR'^*)\Bigg]$$

where

$$B_1(k_l k_s k; RR'^*) = \rho_{k_s 0}(s)(k_l 0, k_s 0|k0)P_k(\cos\theta)\ \mathrm{Re}\ (RR'^*)$$
$$+2\sum_{\kappa>0}(-)^{\kappa}\sqrt{\frac{(k-\kappa)!}{(k+\kappa)!}}\,(k_l 0, k_s \kappa|k\kappa) \tag{2.14a}$$
$$\cdot P_k^{\kappa}(\cos\theta)\begin{cases}\mathrm{Re}\,(\rho_{k_s\kappa}(s)\mathrm{e}^{i\kappa\chi})\ \mathrm{Re}\ (RR'^*) \ldots \text{even } k_s \\ -\mathrm{Im}\,(\rho_{k_s\kappa}(s)\mathrm{e}^{i\kappa\chi})\ \mathrm{Im}\ RR'^* \ldots \text{odd } k_s\end{cases}.$$

The real or imaginary expressions are used depending on whether k_s is even or odd respectively.

Similarly, if the process serves as a polarizer, the angular distribution is characterized by the efficiency tensors describing the sensitivity of the detector to the polarization of the outgoing particles. The distribution is given by (2.14) where the suffix 1 is replaced by 2 and

$$B_2(k_i k_s k; RR'^*) = \varepsilon_{k_s 0}(s)(k_i 0, k_s 0|k0)P_k(\cos\theta)\,\mathrm{Re}\,(RR'^*)$$
$$+2\sum_{\kappa>0}(-)^\kappa\sqrt{\frac{(k-\kappa)!}{(k+\kappa)!}}\,(k_i 0, k_s \kappa|k\kappa)$$
$$\cdot P_k^\kappa(\cos\theta)\begin{cases}\mathrm{Re}\,(\varepsilon_{k_s\kappa}(s)e^{i\kappa\chi})\,\mathrm{Re}\,(RR'^*)\ldots\text{even } k_s\\ \mathrm{Im}\,(\varepsilon_{k_s\kappa}(s)e^{i\kappa\chi})\,\mathrm{Im}\,(RR'^*)\ldots\text{odd } k_s\end{cases}. \tag{2.14b}$$

The significance of χ differs in the two cases. We denote the unit vector normal to the plane of the process by $\mathbf{n}$, i.e. $\mathbf{n} = \mathbf{k}_1 \times \mathbf{k}_2$, where $\mathbf{k}_1, \mathbf{k}_2$ are unit propagation vectors of the particle before and after the reaction. The quantity χ in the first case is the angle between $+\mathbf{n}$ and the y-axis used to describe the polarization of the incident beam, while in the second case χ is the angle between $-\mathbf{n}$ and the y-axis describing the polarization-efficiency of the detectors. The z-axis is along the direction of the particle whose polarization is of interest.

The quantity $W(\Omega_1, \Omega_2)$ refers to particles of arbitrary spin, s. The expression in the channel-spin representation can be obtained in a similar fashion and the results are given in ref. [6]). The case of γ-rays requires separate treatment [5, 6]), using the $\mathscr{L}$-representation.

2.2. DISTRIBUTION OF SPIN TENSORS

An alternative approach is to find the probability for the process in the spin-representation, using the approach of Wolfenstein [14]), Tolhoek [15]) and others. We are interested in finding the relative probability, $W(s)$ for response of a detector whose efficiency is characterized by ε to the state of polarization of the particles of spin s, which is represented by the density matrix ρ. This is given by

$$W(s) = \sum_{\sigma\sigma'\Sigma\Sigma'}\langle s\sigma\Sigma|\rho|s\sigma'\Sigma'\rangle\langle s\sigma'\Sigma'|\varepsilon|s\sigma\Sigma\rangle$$
$$= \sum_{k_s\kappa\Sigma\Sigma'}\rho_{k_s\kappa}(s\Sigma, s\Sigma')\varepsilon^*_{k_s\kappa}(s\Sigma, s\Sigma'). \tag{2.15}$$

The measurement or production of the polarization states is likewise characterized by the efficiency tensor $\varepsilon_{k_s\kappa}(s)$ and the statistical tensor $\rho_{k_s\kappa}(s)$, which we will refer to collectively as spin tensors.

There are two cases of interest:

(1) The reaction serves as a polarizer, i.e. the outgoing beam is of spin s, and its polarization is measured by means of a polarization-sensitive detector. In this case, the quantities Σ and Σ' represent quantum numbers such as a, b, $\mathscr{L}_1$, $\mathscr{L}_2$ etc., characterizing $\rho_{k_s\kappa}$ in addition to other quantities corresponding to the properties of the detector which determine $\varepsilon_{k_s\kappa}$. The detection usually involves measurement of the angular distribution of particles in a second process in terms of the coordinate system defining the first process. The incoming beam of particles is unpolarized, although we need not assume this in the discussion that follows.

(2) The reaction serves as an analyser, i.e. the incoming beam of spin s is polarized and the polarization is measured by the angular distribution of the outgoing beam in terms of the coordinate system used to specify the polarization. Here, $\rho_{k_s\kappa}$ is a function of parameters representing the mode of preparation of the polarization, while $\varepsilon_{k_s\kappa}$ includes the quantum numbers $a, b, \mathscr{L}_1, \mathscr{L}_2$, etc.

The spin-tensor distribution corresponding to no polarization of the incoming beam and no measurement of polarization of the outgoing particles is denoted by W_0 and obtains when $k_s = \kappa = 0$. We can write $W(s)$ in the form

$$W(s) = W_0[1+\eta(s) \sum_{\Sigma, \Sigma', \kappa, k_s(\neq 0)} \rho_{k_s\kappa}(s\Sigma, s\Sigma')\varepsilon^*_{k_s\kappa}(s\Sigma, s\Sigma')] \quad (2.15a)$$

where $\eta(s)$ depends on the choice of normalization of the zero-rank tensors.

The tensor, $\rho_{k_s\kappa}(s)$, has been defined by Simon and Welton [16]) as the mean value of an irreducible tensor operator satisfying certain commutation properties with the angular-momentum operators. We use a different definition:

$$\rho_{k_s\kappa}(s) \equiv \overline{T_{k_s\kappa}} = \text{trace } \rho T_{k_s\kappa} = \sum_{\sigma\sigma'} \langle s\sigma|\rho|s\sigma'\rangle\langle s\sigma'|T_{k_s\kappa}|s\sigma\rangle, \quad (2.16)$$

where the horizontal bar represents the mean value of the operator.

The tensor $T_{k\kappa}$ is only dependent on s, σ, σ', k and κ, and from (2.3a) has matrix elements

$$\langle s\sigma'|T_{k\kappa}|s\sigma\rangle = (-)^{s-\sigma'}(s\sigma, s-\sigma'|k\kappa). \quad (2.16a)$$

If we represent the angular-momentum operator $\mathbf{s}$ by the Cartesian components † s_1, s_2, s_3, then $T_{k\kappa}$ satisfies the following commutation rules:

$$\begin{aligned} [(s_1 \mp i s_2), T_{k\kappa}] &= -\sqrt{(k\mp\kappa)(k\pm\kappa+1)}\,T_{k\kappa\pm1} \\ [s_3, T_{k\kappa}] &= -\kappa T_{k\kappa}. \end{aligned} \quad (2.17)$$

The inverse relation to (2.16), viz. the expression of the density matrix, ρ, in terms of $T_{k_s\kappa}$,

$$\langle s\sigma|\rho|s\sigma'\rangle = \sum_{k_s\kappa} \rho^*_{k_s\kappa}(s)\langle s\sigma|T_{k_s\kappa}|s\sigma'\rangle \quad (2.18)$$

follows as a consequence of the relation

$$\text{trace } (T_{k\kappa}\, T_{k'\kappa'}(-)^\kappa) = \delta_{kk'}\delta_{\kappa-\kappa'}.$$

The explicit values of $T_{k_s\kappa}$ up to and including the second rank are

† The subscripts 1, 2 and 3 correspond to the x, y and z coordinate axes. Assuming the z-axis to be the axis of quantization, the operator s_3 yields the eigenvalue $\hbar\sigma_3$. To conform with our previous notation, σ_3 is equivalent to σ.

$$T_{00} = \frac{1}{\hat{s}} \qquad T_{20} = \frac{\sqrt{5}[3s_3^2/\hbar^2 - s(s+1)]}{\hat{s}\sqrt{(2s-1)s(s+1)(2s+3)}}$$

$$T_{10} = \frac{\sqrt{3}\, s_3}{\hbar\hat{s}\sqrt{s(s+1)}} \qquad T_{2\pm1} = \frac{\mp\sqrt{15}[(s_1 \mp is_2)s_3 + s_3(s_1 \mp is_2)]}{\hbar^2\hat{s}\sqrt{(2s-1)s(2s+2)(2s+3)}} \tag{2.19}$$

$$T_{1\pm1} = \frac{\mp\sqrt{3}(s_1 \mp is_2)}{\hbar\hat{s}\sqrt{2s(s+1)}} \qquad T_{2\pm2} = \frac{\sqrt{15}(s_1 \mp is_2)(s_1 \mp is_2)}{\hbar^2\hat{s}\sqrt{(2s-1)s(2s+2)(2s+3)}}.$$

Thus, the tensors for spin $s = \frac{1}{2}$ are

$$\rho_{00}(\tfrac{1}{2}) = \frac{1}{\sqrt{2}}, \quad \rho_{10}(\tfrac{1}{2}) = \frac{P_3}{\sqrt{2}}, \quad \rho_{1\pm1}(\tfrac{1}{2}) = \mp\tfrac{1}{2}(P_1 \mp iP_2) \tag{2.20}$$

where

$$\bar{\mathbf{s}} \equiv \tfrac{1}{2}\hbar\,\mathbf{P}$$

and the density matrix in the spin-$\frac{1}{2}$ representation, by virtue of (2.18) and (2.19), becomes

$$\rho = \tfrac{1}{2}(1 + \mathbf{P}\cdot\boldsymbol{\sigma}) \tag{2.21}$$

where $\boldsymbol{\sigma}$ is the Pauli spin-matrix operator (use is made of the Hermitian property of the tensors: $\rho_{k,\kappa}(s) = (-)^{\kappa}\rho^{*}_{k,-\kappa}(s)$).

We now consider the case $s = 1$. Introduce the vector $\mathbf{P}$ and tensor P_{ij}:

$$\bar{\mathbf{s}} \equiv \hbar s\mathbf{P} = \hbar\mathbf{P}$$

$$P_{ij} \equiv \frac{3}{2\hbar^2}[\overline{s_i s_j} + \overline{s_j s_i}] - 2\delta_{ij}. \tag{2.22}$$

The spin tensors are

$$\rho_{00}(1) = \frac{1}{\sqrt{3}} \qquad \rho_{20}(1) = \frac{1}{\sqrt{6}}P_{33}$$

$$\rho_{10}(1) = \frac{1}{\sqrt{2}}P_3 \qquad \rho_{2\pm1}(1) = \mp\tfrac{1}{3}(P_{13} \mp iP_{23}) \tag{2.23}$$

$$\rho_{1\pm1}(1) = \mp\tfrac{1}{2}(P_1 \mp iP_2) \quad \rho_{2\pm2}(1) = \tfrac{1}{6}(P_{11} - P_{22}) \mp \frac{i}{3}P_{12}.$$

By definition, P_{ij} represents the components of a traceless, symmetric tensor, having real values. The density matrix in the spin-1 representation is a 3×3 matrix, obtained from (2.18), (2.19) and (2.23) where we use for s_1, s_2 and s_3 the matrices, explicitly given in (3.4).

Similarly, from (2.3b) we can relate the efficiency tensor $\varepsilon_{k,\kappa}(s)$ to $T_{k,\kappa}$ as follows:

$$\varepsilon_{k,\kappa}(s) = T^{\mathrm{d}}_{k,\kappa} = \text{trace}\,(\varepsilon T_{k,\kappa}) \tag{2.24}$$

so that the efficiency tensors are the spin operators weighted by the efficiency of the detector.

Their explicit values for $k_s = 0, 1, \ldots$ are:

$$\varepsilon_{00}(s) = \frac{1}{\hat{s}}, \quad \varepsilon_{10}(s) = \frac{\sqrt{3}\, s_3{}^{\mathrm{d}}}{\hbar\hat{s}\sqrt{s(s+1)}}, \quad \varepsilon_{1\pm1}(s) = \mp \frac{\sqrt{3}(s_1{}^{\mathrm{d}} \mp i s_2{}^{\mathrm{d}})}{\hbar\hat{s}\sqrt{2s(s+1)}}, \ldots \tag{2.25}$$

The quantities $s_1{}^{\mathrm{d}}$, $s_2{}^{\mathrm{d}}$ and $s_3{}^{\mathrm{d}}$ represent the mean values of the spin operators as measured by a detector whose properties are fully described by the efficiency matrix ε. For the case $s = \frac{1}{2}$, we introduce the vector $\mathbf{P}^{\mathrm{d}}$:

$$\mathbf{P}^{\mathrm{d}} \equiv \frac{2}{\hbar}\mathbf{s}^{\mathrm{d}}. \tag{2.26}$$

For $s = 1$, we construct the vector $\mathbf{P}^{\mathrm{d}}$ and tensor P_{ij}^{d} such that

$$\begin{aligned} \mathbf{P}^{\mathrm{d}} &\equiv \frac{1}{\hbar}\mathbf{s}^{\mathrm{d}} \\ P_{ij}^{\mathrm{d}} &\equiv \frac{3}{2\hbar^2}[(s_i s_j)^{\mathrm{d}} + (s_j s_i)^{\mathrm{d}}] - 2\delta_{ij}. \end{aligned} \tag{2.27}$$

The normalization of trace ρ = trace $\varepsilon = 1$ is a matter of convention. As a result the spin-tensor distribution has a leading term corresponding to $k_s = 0$ of $1/\hat{s}^2$. In order to convert the relative distribution into a cross-section, we must therefore multiply the result by $\hat{s}^2 W_0$. With this normalization, the spin-tensor distribution $W(s)$ for $s = \frac{1}{2}$ is

$$W(\tfrac{1}{2}) = \text{trace } \rho\varepsilon = \sum_{k_s \kappa} \rho_{k_s \kappa}(\tfrac{1}{2}) \varepsilon^*_{k_s \kappa}(\tfrac{1}{2}) = W_0[1 + \mathbf{P} \cdot \mathbf{P}^{\mathrm{d}}] \tag{2.28a}$$

and for $s = 1$,

$$\begin{aligned} W(1) = W_0\{1 &+ \tfrac{3}{2}\mathbf{P} \cdot \mathbf{P}^{\mathrm{d}} + \tfrac{1}{2} P_{33} P_{33}^{\mathrm{d}} + \tfrac{2}{3}(P_{13} P_{13}^{\mathrm{d}} + P_{32} P_{32}^{\mathrm{d}} + P_{21} P_{21}^{\mathrm{d}}) \\ &+ \tfrac{1}{6}(P_{11} - P_{22})(P_{11}^{\mathrm{d}} - P_{22}^{\mathrm{d}})\}. \end{aligned} \tag{2.28b}$$

It is clear from the above that an expression for $W(\Omega_1, \Omega_2)$ as in (2.14) provides direct information concerning the polarization of a particle of arbitrary spin s, which is produced in a nuclear process. The expression for B_2 in (2.14b) contains the terms $\varepsilon_{k_s \kappa}(s)$ and one has merely to take the coefficient $\varepsilon_{k_s \kappa}(s)$ in $W(\Omega_1, \Omega_2)$ to find $\rho^*_{k_s \kappa}(s)$, taking care that the tensors are appropriately normalized. For spin-$\frac{1}{2}$ and spin-1 particles, the expression for B_2 can be written in terms of $\mathbf{P}^{\mathrm{d}}$ and P_{ij}^{d} and the expression for $W(\Omega_1, \Omega_2)$ can be compared to (2.28) to find the quantities $\mathbf{P}$ and P_{jl}.

The selection rules for polarization as found by Simon [5]) easily follow from (2.14). As a consequence of parity conservation, k and k_l are either even or odd. This also follows from the fact that $(l0, l'0|k_l 0)$ vanishes unless $l + l' + k$ is even. If the intermediate state is of well-defined parity, $l_2 + l'_2$ is even so that k is even and from (2.14) k_l is also even. Similarly if $l_2 + l'_2$ is odd, both k and k_l are odd. It then follows from the expression

for B_2 that $\rho_{k_s 0}(s)$ vanishes unless k_s is even. Furthermore, if Im (RR'^*) is zero, only even-rank polarization is present. Thus, for $s = \frac{1}{2}$, where $k_s = 0$ or 1, no polarization is possible. It is also possible to show that first-rank polarization is perpendicular to the plane of the process, i.e. $\mathbf{P}$ is in the direction $\mathbf{n}_1 = \mathbf{k}_1 \times \mathbf{k}_2$. Higher-rank polarization requires for its specification the angle that the y-axis makes with $\mathbf{n}_1$. The z-axis is assumed to be along the direction of propagation of the particle whose polarization is being studied.

An interesting conclusion from (2.14) concerns the existence of non-isotropic angular distributions, even though only S-waves are involved. For example, if a reaction is characterized by incoming particles with $l = 0$, but which have even-rank polarization, then, if the outgoing particles are emitted in states with $l > 0$ and $b > \frac{1}{2}$, the angular distribution is non-isotropic. In this case, $k = k_s > 2$. If the incoming particles are non-polarized, $k_s = 0$ and the distribution is isotropic. Similarly, it is possible to produce particles with polarization of even rank, even though $l = 0$, provided the spin is greater than $\frac{1}{2}$.

Consider $s = 1$ and the quantity $B_2(k_i\, 2k;\, RR')$. This is found to be

$$B_2(k_i 2k; RR'^*) = \Bigg\{ \frac{(k_i 0,\, 20|k0)}{\sqrt{6}} P^{\mathrm{d}}_{33} P_k(\cos\theta) - \frac{2(k_i 0,\, 21|k1)}{3\sqrt{k(k+1)}} (P^{\mathrm{d}}_{13} \cos\chi + P^{\mathrm{d}}_{23} \sin\chi) P_k^1(\cos\theta) + \frac{(k_i 0,\, 22|k2)}{3\sqrt{(k+1)k(k-1)(k-2)}} [(P^{\mathrm{d}}_{11} - P^{\mathrm{d}}_{22}) \cos 2\chi + 2P^{\mathrm{d}}_{12} \sin 2\chi] P_k^2(\cos\theta) \Bigg\} \mathrm{Re}\ (RR' \tag{2.29}$$

It then follows that the angular dependence of $P_{ij}(\theta_1, \chi)$ where $\cos\theta_1 = \mathbf{k}_1 \cdot \mathbf{k}_2$, can be separated as follows:

$$\begin{aligned} P_{13} &\equiv p_{13}(\theta_1) \cos\chi \\ P_{23} &\equiv p_{23}(\theta_1) \sin\chi \\ P_{11} - P_{22} &\equiv [p_{11}(\theta_1) - p_{22}(\theta_1)] \cos 2\chi \\ P_{12} &\equiv p_{12}(\theta_1) \sin 2\chi \end{aligned} \tag{2.30}$$

where $p_{ij}(\theta_1) \equiv P_{ij}(\theta_1, 0)$. Similarly we can define P^{d}_{ij} in terms of p^{d}_{ij}. If we arrange the z- and y-axes to be along $\mathbf{k}_2$ and $-\mathbf{n}_1$, respectively, it follows that $\chi = 0$. Furthermore, if detection is made by subjecting the outgoing beam to another scattering or reaction and if $\mathbf{n}_2$ is the normal to the second plane with $\cos\phi = \mathbf{n}_1 \cdot \mathbf{n}_2$, then the angular distribution $W(\Omega_1, \Omega_2)$ is given by

$$\begin{aligned} W(\Omega_1, \Omega_2) = W_0(\theta_1, \theta_2) \{ 1 &+ \tfrac{3}{2} P_2(\theta_1, 0) P_2^{\mathrm{d}}(\theta_1, 0) \cos\phi + \tfrac{1}{2} p_{33}(\theta_1) p^{\mathrm{d}}_{33}(\theta_2) \\ &- \tfrac{2}{3} p_{13}(\theta_1) p^{\mathrm{d}}_{13}(\theta_2) \cos\phi + \tfrac{1}{6} [p_{11}(\theta_1) - p_{22}(\theta_1)][p^{\mathrm{d}}_{11}(\theta_2) - p^{\mathrm{d}}_{22}(\theta_2)] \cos 2\phi \}. \end{aligned} \tag{2.31}$$

The explicit expression for $\mathbf{P}$ is found by inserting the expression $B_2(k_i\, 1k;$

RR'^*) into (2.14) and comparing the result with (2.28b). This simplifies to (cf. ref. [6]))

$$P_2(\theta_1, 0) = \frac{\lambda^2}{24\hat{a}^2 W_0} \sum_{bb'\mathscr{L}_1\mathscr{L}'_1\mathscr{L}_2\mathscr{L}'_2 k} A_k(\mathscr{L}_1\mathscr{L}'_1; abb')A_k(\mathscr{L}_2\mathscr{L}'_2; cbb')q(bb'; \mathscr{L}_1\mathscr{L}'_1, \mathscr{L}_2\mathscr{L}'_2) \cdot \frac{L_2(L_2+1)-l_2(l_2+1)-L_2'(L'_2+1)+l'_2(l'_2+1)}{k(k+1)} P_k^1(\cos\theta_1)\ \mathrm{Im}\ (RR'^*). \tag{2.32}$$

There is no component of **P** perpendicular to the y-axis. The expressions for P_{ij} are more complicated but they can easily be found by substituting (2.29) into (2.14) and identifying the coefficients of P_{ij}^{d} as in (2.31).

The expression $B_1(k_i 2k; RR'^*)$ is found by (2.14) to be identical with (2.29) except that P_{ij}^{d} is replaced by P_{ij} and χ denotes the angle between **n** and the y-axis. From (2.28b), it then follows that P_{ij}^{d} can be written as in (2.30). If the process is elastic scattering followed by a second elastic scattering, and if the energy degradation is ignored, then for equal scattering angles, θ, we have

$$\begin{aligned} P_2(\theta, 0) &= P_2^{\mathrm{d}}(\theta, 0) \\ P_{ij}(\theta, 0) &= P_{ij}^{\mathrm{d}}(\theta, 0). \end{aligned} \tag{2.33}$$

3. Polarization of Deuterons in Resonance Scattering by He^4

Examination of (2.14) shows that although the presence of polarization of spin-$\frac{1}{2}$ particles requires the non-vanishing of Im (RR'^*), the polarization tensors of even rank that are associated with higher spins, involve Re (RR'^*). Consequently it is possible for polarization to arise by virtue of a single matrix element. Furthermore, the quantity $|R|^2$ in this case is common to the 'polarized' and 'unpolarized' distribution, so that the extent of polarization is *independent* of $|R|^2$.

An example of this situation is provided by the scattering of deuterons by He^4. A sharp resonance was found by Lauritsen *et al.*[17]) at $E_{\mathrm{d}} = 1.069$ MeV (laboratory energy) with an observed width of 23 keV. This resonance is attributed to scattering from the 2.189 MeV level of Li^6, and Lauritsen and co-workers were able to demonstrate that a consistent interpretation of the angular distribution is provided by assuming only $l = 2$ waves are effective †. The excited level of Li^6 is uniquely identified by $b=3$ and positive

† Lauritsen *et al.* also consider the possibility of formation of the ground state of Li^6 by S-wave deuterons. Although a reasonable selection of parameters for this competing process leads to a somewhat better fit with the experimental data, they point out that the effect of the ground state is not established with certainty. For reasons of simplicity we assume that only one intermediate state is involved.

parity since $a = c = 0$. The channel-spin representation is identical with the $\mathscr{L}$-representation and the results of the previous section can be easily applied to this process. We ignore the Coulomb contribution by considering scattering at only energies close to E_d, where the resonance amplitude is expected to be large compared to the Coulomb amplitude.

The unpolarized distribution $W_0(\theta)$, from (2.12) is found to be:

$$\begin{aligned} W_0(\theta) &= \tfrac{7}{12}\lambda^2|R|^2[1+\tfrac{48}{49}P_2(\cos\theta)+\tfrac{22}{49}P_4(\cos\theta)] \\ &\equiv \frac{\lambda^2|R|^2}{84}q(\theta) \end{aligned} \tag{3.1}$$

where

$$q(\theta) = 49+48\,P_2(\cos\theta)+22\,P_4(\cos\theta). \tag{3.2}$$

Polarization of only rank 2 is present and the components P_{ij}, P^d_{ij} are calculated from (2.14). The resultant polarization is found to be given by the following:

$$\begin{aligned} q(\theta)P_{33} &= -2[7+12\,P_2(\cos\theta)+16P_4(\cos\theta)] \\ q(\theta)P_{13} &= 3[4P^1{}_2(\cos\theta)+3P_4{}^1(\cos\theta)]\cos\chi \\ q(\theta)P_{23} &= 3[4P_2{}^1(\cos\theta)+3P_4{}^1(\cos\theta)]\sin\chi \\ q(\theta)P_{12} &= -2[6P_2{}^2(\cos\theta)+P_4{}^2(\cos\theta)]\sin 2\chi \\ q(\theta)(P_{11}-P_{22}) &= -4[6P_2{}^2(\cos\theta)+P_4{}^2(\cos\theta)]\cos 2\chi \end{aligned} \tag{3.3}$$

where χ is the angle between the y-axis, specifying the polarization and $-\mathbf{n}(=\mathbf{k}_2\times\mathbf{k}_1)$. The polarization tensors P^d_{ij} are equal to P_{ij}, provided that in this case, χ is interpreted as the angle between the y-axis of the detector and $+\mathbf{n}$.

It is interesting to compare the results with the maximum and minimum polarizations possessed by a spin-1 particle. These are easily found by representing the spin eigenfunction, $\chi(1)$, in terms of the basic spin-1 eigenfunctions, as $\chi(1) = \sum_m a_m\chi_m$, where $m = -1$, 0 and $+1$. The spin operators are the usual matrices

$$s_1 = \frac{\hbar}{\sqrt{2}}\begin{pmatrix}0&1&0\\1&0&1\\0&1&0\end{pmatrix}, \qquad s_2 = \frac{\hbar}{\sqrt{2}}\begin{pmatrix}0&-i&0\\i&0&-i\\0&i&0\end{pmatrix}, \qquad s_3 = \hbar\begin{pmatrix}1&0&0\\0&0&0\\0&0&-1\end{pmatrix}. \tag{3.4}$$

Inserting (3.4) into (2.22) we find maximum and minimum values for P_{ij} as shown in table 1.

TABLE 1

Maximum and minimum values of P_{ij}

P_{ij}	Maximum	Minimum
P_{33}	1	-2
P_{13}, P_{23}	$\frac{3}{2}$	$-\frac{3}{2}$
$P_{11}-P_{22}$	3	-3
P_{12}	$\frac{3}{2}$	$-\frac{3}{2}$

The values of P_{jj} or P^{d}_{ij}, divided by the maximum numerical values that are theoretically possible, are plotted in fig. 1 with the assumption that $\chi = 0$. The absolute values of P_{13}, P_{33} and $P_{11}-P_{22}$ have their maxima at widely differing angles. These occur for P_{33} at $\theta = 0$ and 90°, for P_{13} at

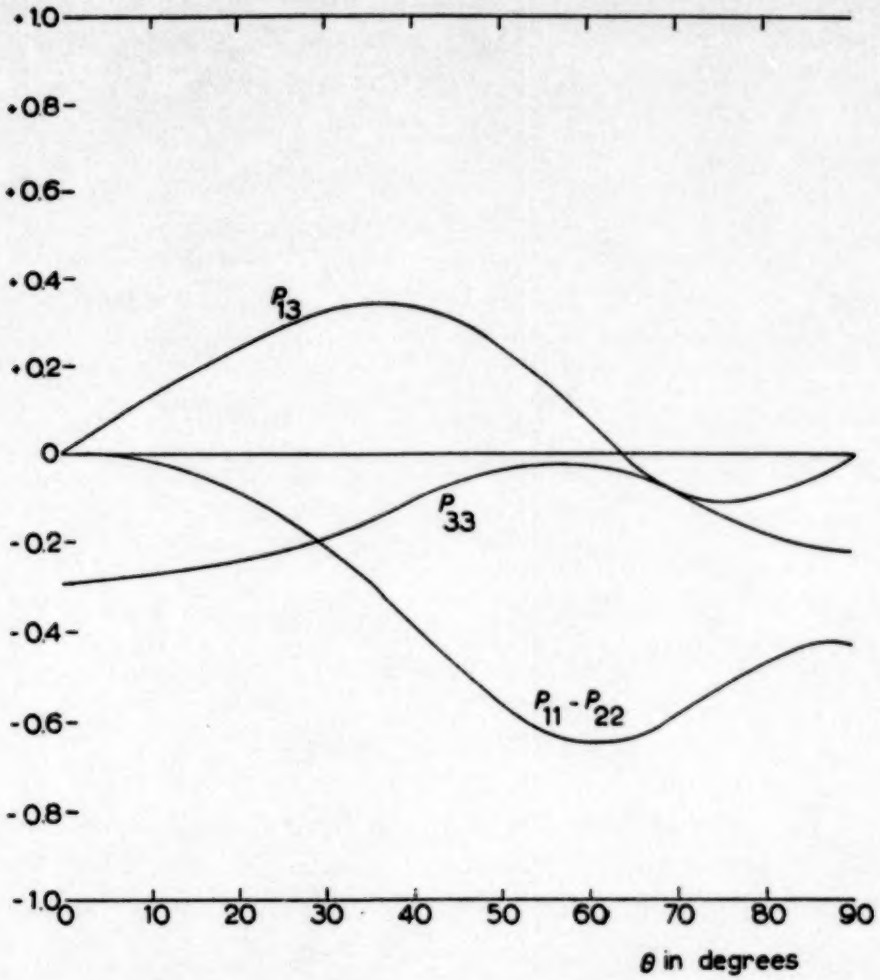

Fig. 1. Components of second-rank polarization of the deuteron in the resonance reaction $d+He^4 \rightarrow d+He^4$ divided by their maximum magnitudes in any state of polarization.

$\theta \approx 35°$ and for $P_{11}-P_{12}$ at $\theta \approx 60°$. It is to be noted that in the latter case, $P_{11}-P_{22} \approx 65\ \%$ of the maximum theoretical values. The scattering serves as a selective polarizer or detector in the sense that scattering through a certain value brings to prominence one of the components, P_{ij}, over the other components. The large values of P^{d}_{ij} for certain angles indicate that the process serves as a highly efficient detector of rank-2 polarization of the deuteron. The narrow width of the resonance makes unfeasible any double-scattering process, since the target nucleus is only twice as heavy as the deuteron and absorbs a significant fraction of its kinetic energy. Furthermore, the low energy of the scattered deuterons restricts the usefulness of

the polarizer to a few reactions involving only light nuclei. On the other hand, the process serves as an efficient analyser of the polarization of deuterons from pick-up processes and also of higher-energy deuterons scattered by nuclei. We examine this latter possibility in the next section.

4. Polarization of Deuterons Scattered by Spinless Nuclei

Detailed study [18]) has been given to the observation of large polarization effects of slow neutrons which are scattered by heavy nuclei. The presence of polarization is interpreted as a consequence of the strong $\mathbf{l}\cdot\mathbf{s}$ forces which are used when describing the nuclear scattering in terms of the optical model. Born-approximation estimates indicate identically zero polarization if the interaction is described by a real potential. Thus, the observed polarization is, to a good approximation, a manifestation of the imaginary potential which accounts for the absorption of nucleons to form a compound nucleus. This approximation has a limited validity for nucleon-nuclei scattering with energies up to ≈ 100 MeV.

4.1. SPIN-ORBIT INTERACTIONS OF THE TYPE $\mathbf{l}\cdot\mathbf{s}$

A similar approach is now given to elastic deuteron scattering. For simplicity, we consider only target nuclei that are spinless and we describe the interaction of the deuteron with nucleus, as if the deuteron were a point-particle whose spin arises from the symmetrical combination of spins of two nucleons. The interaction potential is assumed to be of the form

$$H'_1 = V(r)+W(r)\mathbf{l}\cdot\mathbf{s}+W'(r)\mathbf{l}\cdot(\mathbf{s}_P-\mathbf{s}_N) \tag{4.1}$$

where $\mathbf{l}=\mathbf{r}\times(\hbar/i)\nabla$, $\mathbf{s}=\frac{1}{2}\hbar(\boldsymbol{\sigma}_P+\boldsymbol{\sigma}_N)$, and $\mathbf{r}$ refers to the vector joining the centre-of-mass of the deuteron to the centre of the nucleus. The functions $V(r)$, $W(r)$ and $W'(r)$ are arbitrary functions of r and may be complex.

The deuteron wave which is scattered through angles θ, φ in the centre-of-mass system is asymptotically described by a spherical wave of the form

$$\psi_{sc}\sim\frac{e^{ikr}}{r}\sum_{mm'}M_{m'm}(\theta,\varphi)a_m\chi_{m'} \tag{4.2}$$

where a_m are the relative amplitudes of the initial spin states of a spin-1 particle corresponding to the state χ_m. If the beam of deuterons is initially unpolarized, $\overline{a_m a^*_{m'}}=\frac{1}{3}\delta_{mm'}$.

The matrix M is evaluated in Born approximation as

$$M_{m'm}=\frac{-\mu}{2\pi\hbar}\int e^{-i\mathbf{k}_2\cdot\mathbf{r}}H'_{m'm}e^{i\mathbf{k}_1\cdot\mathbf{r}}d\mathbf{r} \tag{4.3}$$

where μ is the reduced mass of the deuteron and $H'_{m'm}$ is

$$H'_{m'm}\equiv\langle\chi_{m'}|H'|\chi_m\rangle. \tag{4.4}$$

The angular integration is straightforward, leading to

$$M(\theta) = A(\theta) + \frac{i}{\hbar} B(\theta)\mathbf{s}\cdot\mathbf{n} \tag{4.5}$$

where

$$A(\theta) = -\frac{2\mu}{\hbar^4} k^2 \sin\theta \int_0^\infty \frac{\sin Kr}{Kr} V(r) r^2 \, dr \tag{4.6a}$$

$$B(\theta) = -\frac{2\mu}{\hbar^4} k^2 \sin\theta \int_0^\infty \frac{\sin Kr - Kr\cos Kr}{K^3 r} W(r) r^2 \, dr. \tag{4.6b}$$

and where

$$K = |\mathbf{k}_1 - \mathbf{k}_2|,\ k = |\mathbf{k}_1| = |\mathbf{k}_2| \text{ and } \mathbf{n} = \mathbf{k}_1 \times \mathbf{k}_2.$$

The quantity $A(\theta)$ is to be multiplied by the unit 3×3 matrix.

The antisymmetrical term in the interaction, $W'(r)\mathbf{l}\cdot(\mathbf{s}_P - \mathbf{s}_N)$ gives no contribution since the triplet eigenfunctions are symmetrical in spin.

The polarization of the outgoing beam is calculated along the lines indicated by Wolfenstein [19]). Thus, the initial and final density matrices are connected by the relation

$$\rho^{(f)} \propto M^\dagger \rho^{(i)} M \tag{4.7}$$

and ρ is given by (2.18) and (2.16). We find

$$\rho^{(f)}_{k\kappa}(1) = \text{trace}\,(\rho^{(f)} T_{k\kappa}) \propto \text{trace}\,[M^\dagger \sum_{k'\kappa'} \rho^{(i)}_{k'\kappa'}(1) T_{k'\kappa'} M T_{k\kappa}]. \tag{4.8}$$

For an unpolarized initial beam, $\rho^{(i)}_{k'\kappa'}(1) = 1/\sqrt{3}\,\delta_{k'0}\delta_{\kappa'0}$. Also $\rho^{(f)}$ is normalized so that $\rho^{(f)}_{00}(1) = 1/\sqrt{3}$. As a result, the final spin-tensors $\rho^{(f)}_{k\kappa}(1)$ are given as

$$\rho^{(f)}_{k\kappa}(1) = \frac{\text{trace}\,(M^\dagger M T_{k\kappa})}{\text{trace}\,(M^\dagger M)}. \tag{4.9}$$

Alternatively, suppose the initial beam is polarized and the polarization is described by the spin-tensors $\rho^{(i)}_{k\kappa}(1)$. If the polarization is measured by the angular distribution, i.e. by polarization-insensitive detectors, $\varepsilon_{k\kappa}(1) = (1/\sqrt{3})\delta_{k0}\delta_{\kappa 0}$. The angular distribution as a consequence of (4.8) is of the form

$$W = \sum_{k\kappa} \rho^{(f)}_{k\kappa}(1)\varepsilon^*_{k\kappa}(1) = \frac{\sqrt{3}\sum_{k'\kappa'} \rho^{(i)}_{k'\kappa'}\,\text{trace}\,(M^\dagger T_{k'\kappa'} M T_{k\kappa}\,\delta_{k0}\,\delta_{\kappa 0})}{\text{trace}\,(M^\dagger M)}. \tag{4.10}$$

Thus, the efficiency of measurement of $\rho_{k'\kappa'}(1)$ is given as

$$\varepsilon_{k'\kappa'}(1) = \frac{\text{trace}\,(M^\dagger T_{k'\kappa'} M)}{\text{trace}\,(M^\dagger M)}. \tag{4.11}$$

The equivalence of the two expressions in (4.9) and (4.11) has been proved for the case of nucleon-nucleon scattering by Wolfenstein and

Ashkin [19]) and by Dalitz [2]). Their procedure consists in finding the most general interaction, M, for the system and evaluating the expressions in (4.9) and (4.11). In particular, it is necessary that M be invariant under time-reversal. On the other hand, the equality of $\rho_{k\varkappa}(s)$ and $\varepsilon_{k\varkappa}(s)$ for scattering processes follows naturally from (2.14) for two spin-$\frac{1}{2}$ particles, and has already been noticed for spin-1 particles (2.33), although care must be given to the proper choice of coordinate axes used to define $\rho_{k\varkappa}(s)$ and $\varepsilon_{k\varkappa}(s)$.

The polarization vector $\mathbf{P}$ and the tensor P_{ij} are easily found by inserting the matrices $T_{k\varkappa}$ evaluated by use of (2.19) and (3.4), into (4.9) and using (2.23). The result is†

$$\begin{aligned} &P_1 = P_3 = 0, \quad P_2(\theta) = \frac{-2\,\mathrm{Im}\,[A(\theta)B^*(\theta)]}{W_0(\theta)} \\ &P_{13} = P_{32} = P_{21} = 0 \\ &P_{33}(\theta) = \frac{-|B(\theta)|^2}{W_0(\theta)}, \quad P_{11}(\theta) - P_{22}(\theta) = \frac{-3|B(\theta)|^2}{W_0(\theta)} \end{aligned} \tag{4.12}$$

and the unpolarized distribution is given by

$$W_0(\theta) = 3|A(\theta)|^2 + |B(\theta)|^2. \tag{4.13}$$

The y-axis is assumed to be along $-\mathbf{n}$. The scattering also serves as a detector of polarization where $\mathbf{P}^{\mathrm{d}}$ and P^{d}_{ij} are identical with $\mathbf{P}$ and P_{ij}.

It is to be noted that, in contrast to the case of scattering of nucleons, polarization effects obtain even in the absence of an imaginary central potential. The angular distribution for a double-scattering process is of the form

$$\begin{aligned} &W(\theta_1, \theta_2, \phi) \\ &= W_0^{(1)}(\theta_1) W_0^{(2)}(\theta_2)[1 + l_1(\theta_1, \theta_2) + m_1(\theta_1, \theta_2)\cos\phi + n_1(\theta_1, \theta_2)\cos 2\phi] \end{aligned} \tag{4.14}$$

where the scattering is through angles θ_1 and θ_2, while ϕ is the angle between the scattering planes. The coefficients $l_1(\theta_1, \theta_2)$, $m_1(\theta_1, \theta_2)$, $n_1(\theta_1, \theta_2)$ are

$$\begin{aligned} &l_1(\theta_1, \theta_2) = \tfrac{1}{2} P_{33}(\theta_1) P_{33}(\theta_2), \quad m_1(\theta_1, \theta_2) = P_2(\theta_1) P_2(\theta_2) \\ &n_1(\theta_1, \theta_2) = \tfrac{1}{6}[P_{11}(\theta_1) - P_{22}(\theta_1)][P_{11}(\theta_2) - P_{22}(\theta_2)]. \end{aligned} \tag{4.14a}$$

The presence of a term varying as $\cos\phi$, i.e. a 'left-right' asymmetry, depends on the presence of an imaginary central potential, assuming that the quantity $W(r)$ in (4.1) is real. On the other hand, the other terms contributing to the polarized intensity are independent of the central potential and depend on the absolute value of $W(r)$.

If the analyser is resonance scattering by He^4,

$$W(\theta_1, \theta_2, \phi) = W_0^{(1)}(\theta_1) W_0^{(2)}(\theta_2)[1 + l_2(\theta_1, \theta_2) + n_2(\theta_1, \theta_2)\cos 2\phi] \tag{4.15}$$

where

† In the following, quantities such as $\mathbf{P}(\theta, 0)$ and $P_{ij}(\theta, 0)$ are written, for simplicity, as $\mathbf{P}(\theta)$ and $P_{ij}(\theta)$.

$$l_2(\theta_1, \theta_2) = \tfrac{1}{2} P_{33}(\theta_1) P^{\mathrm{d}}_{33}(\theta_2),$$
$$n_2(\theta_1, \theta_2) = \tfrac{1}{6}[P_{11}(\theta_1) - P_{22}(\theta_1)][P^{\mathrm{d}}_{11}(\theta_2) - P^{\mathrm{d}}_{22}(\theta_2)] \tag{4.15a}$$

and the quantities P^{d}_{33}, $P^{\mathrm{d}}_{11} - P^{\mathrm{d}}_{22}$, $W^{(2)}_0(\theta_2)$ are found from (2.30), (3.3) and (3.1). In this case, there is no 'left-right' asymmetry, even if the central part of the interaction is complex. The quantities $l_2(\theta_1, \theta_2)$ and $n_2(\theta_1, \theta_2)$ are evaluated by measurements of the 'unpolarized intensity', $W^{(1)}_0(\theta_1) W^{(2)}_0(\theta_2)$ together with the quantities $W(\phi = 0°) \pm W(\phi = 90°)$.

4.2. TENSOR INTERACTIONS

The interaction potential (4.1) is not the most general expression which is a function of $\mathbf{r}$, $\boldsymbol{\sigma}_{\mathrm{P}}$ and $\boldsymbol{\sigma}_{\mathrm{N}}$. One should also include a tensor

$$T_{12} = 3 \frac{\boldsymbol{\sigma}_{\mathrm{P}} \cdot \mathbf{r} \boldsymbol{\sigma}_{\mathrm{N}} \cdot \mathbf{r}}{r^2} - \boldsymbol{\sigma}_{\mathrm{P}} \cdot \boldsymbol{\sigma}_{\mathrm{N}}.$$

The tensor differs from the usual tensor potential, S_{12}, since $\mathbf{r}$ does not represent the relative vector of protons and neutron in the deuteron. We now consider an alternative interaction, H'_2 given by

$$H'_2 = V(r) + U(r) T_{12}. \tag{4.16}$$

The evaluation of $M(\theta)$ (see Ashkin and Wu[20]) leads to

$$M(\theta) = A(\theta) + C(\theta) N(\theta), \tag{4.17}$$

where $A(\theta)$ is as in (4.6a), and

$$C(\theta) = \frac{2\mu}{\hbar^2} \int_0^\infty \left[\sin Kr + - \frac{3 \sin Kr - Kr \cos Kr}{(Kr)^3} \right] U(r) r^2 \, \mathrm{d}r. \tag{4.18}$$

The matrix $N(\theta)$ has elements given by

$$N(\theta) = \begin{pmatrix} -\frac{1}{2}(1 - 3\cos\theta) & \frac{3}{\sqrt{2}} \sin\theta & -3\cos^2\theta/2 \\ \frac{3}{\sqrt{2}} \sin\theta & 1 - 3\cos\theta & -\frac{3}{\sqrt{2}} \sin\theta \\ -3\cos^2\theta/2 & -\frac{3}{\sqrt{2}} \sin\theta & -\frac{1}{2}(1 - 3\cos\theta) \end{pmatrix} \tag{4.19}$$

where the y-axis is taken to be along $-\mathbf{n}$. The resultant of $\mathbf{P}$ and P_{ij} are calculated to be

$$\begin{aligned} \mathbf{P} &= 0 \\ P_{23} = P_{12} &= 0 \\ P_{33}(\theta) &= \frac{-2(1 - 3\cos\theta) \ \mathrm{Re}\{C^*(\theta)[A(\theta) + C(\theta)]\}}{W_0(\theta)} \end{aligned} \tag{4.20}$$

$$P_{13}(\theta) = \frac{6 \sin\theta \,\mathrm{Re}\{C^*(\theta)[A(\theta)+C(\theta)]\}}{W_0(\theta)} \tag{4.20}$$

$$P_{11}(\theta)-P_{22}(\theta) = \frac{-3(1+\cos\theta)\,\mathrm{Re}\left\{C^*(\theta)\left[A(\theta)+C(\theta)\left(\frac{5-3\cos\theta}{2}\right)\right]\right\}}{W_0(\theta)}$$

and

$$W_0(\theta) = |A(\theta)|^2+8|C(\theta)|^2. \tag{4.21}$$

The angular distribution for a double scattering is again given by (4.14) where $l_1(\theta_1, \theta_2)$ and $n_1(\theta_1, \theta_2)$ are given in (4.14a). However, $m_1(\theta_1, \theta_2)$ is replaced by $m'_1(\theta_1, \theta_2)$ where

$$m'_1(\theta_1, \theta_2) = \tfrac{2}{3} P_{13}(\theta_1) P_{13}(\theta_2). \tag{4.22}$$

The 'left-right' asymmetry, arises now from second-rank polarization and not vector-polarization, since the latter vanishes identically.

Of particular interest is the fact that if the analyser is the resonance scattering by He^4, there is now a term varying as $\cos\phi$, i.e.

$$W(\theta_1, \theta_2, \phi)$$
$$= W_0^{(1)}(\theta_1) W_0^{(2)}(\theta_2)[1+l_2(\theta_1, \theta_2)+m_2(\theta_1, \theta_2)\cos\phi+n_2(\theta_1, \theta_2)\cos 2\phi] \tag{4.23}$$

where $l_2(\theta_1, \theta_2)$ and $n_2(\theta_1, \theta_2)$ are defined as in (4.15a) and

$$m_2(\theta_1, \theta_2) = \tfrac{2}{3} P_{13}(\theta_1) P^{\mathrm{d}}_{13}(\theta_2). \tag{4.24}$$

This is in contrast to the distribution arising from $\mathbf{l}\cdot\mathbf{s}$ forces (4.15).

It therefore follows that if the interaction involves only the vector joining the nucleus to the centre-of-mass of the deuteron and the individual spins of the deuteron components, the Born approximation estimates lead to a 'left-right' asymmetry only if tensor terms of the form T_{12} are included in the interaction.

Since the polarization effects probably increase markedly with energy, the scattering should be performed at high energies. This also decreases the importance of the Coulomb scattering which has been neglected. The usual procedure of analysing the polarization of the deuterons scattered by the spinless nuclei is to perform a second scattering. But, if the polarization effect is small as is apparent by the results of Chamberlain *et al.*[1]) for 167 MeV deuterons, then the efficiency of the second-scattering process is likewise small. It then might be feasible to decelerate the high-energy ($\approx$ 25 MeV, say) polarized deuterons to 1.069 MeV and to use the highly efficient He^4 analyser whose efficiency as a function of scattering angle is indicated in fig. 1. One might also examine the possibility of producing polarized deuterons in some other resonance scattering process, e.g. from C^{12}. Such a process could then serve as an analyser of the polarization arising from the first scattering.

It is a pleasure to acknowledge the helpful discussions the author had with Professor S. Devons and, in particular, his suggestion concerning the use of the He^4-scattering process as a polarizer of deuterons.

References

1) O. Chamberlain, E. Segrè, R. Tripp, C. Wiegand and T. Ypsilantis, Phys. Rev. **95** (1954) 1104
2) R. H. Dalitz, Proc. Phys. Soc. A **65** (1952) 175
3) W. Lakin, Phys. Rev. **98** (1955) 139
4) S. W. MacDowell, An. Acad. Brasilieira de Ciencias **27** (1956) no. 4
5) A. Simon, Phys. Rev. **92** (1953) 1050
6) S. Devons and L. J. B. Goldfarb, Angular Correlations, Handbuch der Physik, Volume 42 (Springer, 1957)
7) S. W. MacDowell and J. Tiomno, An Acad. Brasilieira de Ciencias (1956)
8) J. V. Lepore, Phys. Rev. **79** (1950) 137
9) J. M. Blatt and L. C. Biedenharn, Revs. Mod. Phys. **24** (1952) 258
10) G. R. Satchler, Proc. Phys. Soc. A **68** (1955) 1041
11) F. Coester and J. M. Jauch, Helv. Phys. Acta **26** (1953) 3
12) U. Fano, Nat. Bureau Standards Report NBS 1214 (1952) unpublished
13) E. Jahnke and F. Emde, Tables of Functions with Formulae and Curves (Dover Publications (1945)
14) see for example: L. Wolfenstein, Annual Rev. Nuclear Science **6** (1956) 43
15) H. A. Tolhoek, Revs. Mod. Phys. **28** (1956) 277
16) A. Simon and T. A. Welton, Phys. Rev. **90** (1953) 1036
17) T. Lauritsen, T. Huus and S. G. Nilsson, Phys. Rev. **92** (1953) 1501
18) E. Fermi, Nuovo Cimento **11** (1954) 407; W. Heckrotte, Phys. Rev. **94** (1954) 1797; B. T. Malenka, Phys. Rev. **95** (1954) 522
19) L. Wolfenstein and J. Ashkin, Phys. Rev. **85** (1952) 947
20) J. Ashkin and T. Y. Wu, Phys. Rev. **73** (1948) 973

8.A *Nuclear Physics* 7 (1958) 643—645; © *North-Holland Publishing Co., Amsterdam*
Not to be reproduced by photoprint or microfilm without written permission from the publisher

TWO EVENTS OF MESONIC DECAY OF HYPERFRAGMENTS IN FLIGHT

A. FILIPKOWSKI, E. SKRZYPCZAK, A. SOMOGYI †
Institute of Nuclear Research, Warsaw
and
A. WRÓBLEWSKI
Institute of Physics, Warsaw University

Received 31 March 1958

In a systematic scanning in a part of a stack of Ilford G5 emulsions, exposed to a 300 MeV/c K^- beam from the Berkeley Bevatron, we found 553 stars produced in interactions at rest of K^--mesons with emulsion nuclei. From this sample we established 6 certain mesonic decays of hyperfragments and 17 events which were considered as possible non-mesonic decays. In the latter case, however, the possibility of π^- or Σ^- stars cannot be excluded. Two of the mesonic decays of hyperfragments appeared to be decays in flight.

Having no information about the thickness of the emulsion and its humidity during the exposure, we were obliged to do some calibration work in order to calculate the shrinkage factor s and the ratio z defined as

$$z = \frac{\text{stopping power of our emulsion}}{\text{stopping power of Barkas' emulsion [1])}}.$$

For this purpose we made range measurements of (1) 30 tracks of μ^+-mesons from π^+ decays at rest, (2) 8 tracks of protons from decays at rest $\Sigma^+ \rightarrow p + \pi$ and (3) 2 tracks of Σ^- hyperons from interactions at rest $K^- + (\text{free})p \rightarrow \Sigma^- + \pi^+$. On the basis of these measurements, using the correlation method of Fry and White [2]) we obtain the data collected in table 1.

TABLE 1

	Mean range (μ)	s	z
(1)	607 ± 7	2.48 ± 0.13	1.007 ± 0.023
(2)	1682 ± 14	2.36 ± 0.08	1.001 ± 0.009
(3)	705 ± 7	—	1.007 ± 0.029
Mean values		2.39 ± 0.07	1.002 ± 0.008

As the mean value of z appeared to be equal to unity we were justified in using the range-energy relation given by Barkas [1]), without introducing any corrections.

† On leave from the Central Research Institute for Physics of the Hungarian Academy of Sciences, Department of Cosmic Rays, Budapest.

From the mean values of the ranges R_p and R_{Σ^-} we have calculated the masses of Σ^+ and Σ^- hyperons. The results are

$$M_{\Sigma^-} = 1196.3 \pm 1.0 \text{ MeV}$$
$$M_{\Sigma^+} = 1189.5 \pm 1.1 \text{ MeV}$$

The errors quoted above include the measurement errors, straggling, the 1 % error of the energy-range relation and the uncertainties in the masses of particles entering into the calculations [3]).

The results of measurements of the two hyperfragments decays in flight are listed in table 2.

TABLE 2

	R_{htr}	R_π	R_1	R_2	φ_π	φ_1	φ_2	θ_{htr}	θ_π	θ_1	θ_2
Event 1	603 ± 10	31940 ± 1100	194 ± 5	–	89°.7 ± 1°	306°.1 ± 1°	–	−80°.4 ± 0°.4	−77°.9 ± 0°.6	55°.6 ± 1°.7	–
Event 2	203 ± 2	3270 ± 110	1767 ± 41	41 ± 1	136°.3 ± 0°.4	352.°2 ± 0.°3	5°.0 ±1°	32°.6 ± 0°.4	−19°.3 ± 1°	48°.2 ± 0°.8	−45°.8 ± 0°.8

R = ranges in microns, φ = angles in the plane of emulsion measured from the projected direction of flight of hyperfragment, θ = dip angles.

Event 1 is the uniquely defined decay of a $^4H_\Lambda$ hyperfragment corresponding to the scheme

$$^4H_\Lambda \rightarrow \pi^- + {}^4He:$$

within the limits of error the three tracks are coplanar and the transverse momenta of the secondaries are balanced. The binding energy of Λ^0 in the $^4H_\Lambda$ is equal to $B_{\Lambda^0} = 0.1 \pm 1.2$ MeV, taking the value of the mass from ref. [3]). The velocity of $^4H_\Lambda$ at the point of decay was $\beta = 0.0740 \pm 0.0017$ and, using the tables of H. Fay *et al.* [4]), the time of flight was found to be $\tau = 2.2 \times 10^{-11}$ sec. From the primary star, which is of the 4+0K$^-$ type, a π_0 meson is emitted, giving rise to an electron pair at the distance of $\approx 25\mu$ from the point of K$^-$ capture.

Event 2 corresponds to a hyperfragment emitted from the 4+0K$^-$ star and decaying into three charged particles, the resulting momentum of which is too large to be carried away by one or more neutrons. It is clearly a decay in flight. The detailed analysis showed that with a great probability it was one of the following two cases:

$$^3H_\Lambda \rightarrow \pi^- + p + p + n,$$
$$^4H_\Lambda \rightarrow \pi^- + d + p + n.$$

Nevertheless it was not possible to exclude some other explanations, having, however, much smaller probabilities. The calculations of the time of flight of the hyperfragment yields for all reasonable schemes 0.6×10^{-11} sec $< \tau < 1.1 \times 10^{-11}$ sec.

We are greatly indebted to Prof. E. Segrè and his collaborators for the exposure of the stack in the Bevatron beam, and to Dr. S. Goldhaber and her collaborators for the processing of the emulsions. Thanks are due to Prof. M. Danysz and Dr. J. Gierula for many helpful discussions. One of us (A. S.) wishes to express his sincere thanks to the Institute of Nuclear Research of the Polish Academy of Sciences for the invitation and facilities to participate in this work.

References

1) W. H. Barkas, UCRL – 3769 (1957)
2) W. F. Fry and G. R. White, Phys. Rev. **90** (1953) 207
3) L. W. Alvarez, Reports of the VII Rochester Conference **4** (1957) 2
4) H. Fay, K. Gottstein and K. Hain, Suppl. Nuovo Cimento **11** (1954) 234

2.A.2 *Nuclear Physics* 7 (1958) 646—654; © *North-Holland Publishing Co., Amsterdam*
Not to be reproduced by photoprint or microfilm without written permission from the publisher

PHENOMENOLOGICAL ANALYSIS OF REACTIONS OF THE $a + a' \rightarrow b + b'$ TYPE

S. M. BILENKY, L. I. LAPIDUS, L. D. PUZIKOV and R. M. RYNDIN
Joint Institute of Nuclear Research. Laboratory of Theoretical Physics, Dubna, USSR

Received 12 February 1958

Abstract: Conditions for the construction from experimental data of the matrix for reactions of the $a+a' \rightarrow b+b'$ type are considered on basis of general principles of quantum mechanics. The reaction matrix M is expanded in a complete set of irreducible tensor operators $T^{JM}(j_b, j_a)$ and the number of complex scalar functions which determine it is computed for the case when invariance under space rotations and reflections is taken into account. Time reversal invariance of the interaction leads to relations between polarization effects in the direct and inverse reactions. The number of experiments required for complete construction of the reaction matrix in the presence of several channels can be determined on basis of unitarity of the S matrix.

The general form of the azimuthal dependence of the angular distribution of the reaction products (for arbitrary spins) is derived in the appendix.

1. Introduction

It has been shown in ref.[1,2]) that in a phenomenological analysis of the experimental data on elastic scattering the conditions of space rotation and reflection invariance, symmetry under time reversal and also the unitarity conditions permit one to determine the number of experiments required for complete construction of the scattering matrix. A similar analysis is carried out below for an arbitrary reaction of the type

$$a+a' \rightarrow b+b'. \tag{1}$$

The spins of the particles are denoted here as i_1 and i_2 for a and a′ and I_1 and I_2 for b and b′. The analysis is carried out by application of the method of construction of the reaction amplitudes as functions of the initial and final wave vectors and spin operators; this method is a direct extension of the procedure proposed by Wolfenstein and Ashkin [3]), Dalitz [4]) and Lakin [5]).

2. Construction of Reaction Matrix

By definition, the reaction matrix after acting on the initial spin function χ_a yields the amplitude of the outgoing wave in the final state

$$f_b = \sqrt{\frac{v_a}{v_b}}\, M_{ba}(\mathbf{n}_b, \mathbf{n}_a)\chi_a. \tag{2}$$

Here $\mathbf{n}_a$ and $\mathbf{n}_b$ are unit vectors directed along the relative momenta of the initial and final states and v_a and v_b are the corresponding velocities. M is a scalar for reactions in which the relative intrinsic parities of the particles do not change and is a pseudoscalar if the intrinsic parity changes. For convenience of investigation of the symmetry properties of matrix M we make use of the complete set of operators $T^{JM}(j_b, j_a)$ which transform according to the irreducible representation of weight $(2J+1)$ of the three dimensional rotation group

$$T^{JM}(j_b, j_a) = A(j_b, j_a, J) \sum_{m_a, m_b} (j_a J m_a M | j_a J j_b m_b) \chi_{j_b m_b} \chi^{+}_{j_a m_a} \tag{3}$$

where j_a and j_b are the total spins of the system in the initial and final states, $\chi_{j_a m_a}$ and $\chi_{j_b m_b}$ denote the respective spin functions. Coefficients $A(j_a, j_b, J)$ satisfy the condition

$$A^*(j_b, j_a, J)\sqrt{2j_b+1} = (-1)^{j_a - j_b}\sqrt{2j_a+1}\, A(j_a, j_b, J), \tag{4}$$

which for $j_a = j_b$ reduces to the requirement that $A(j_a, j_a, j)$ be real. Otherwise the value of $A(j_a, j_a, J)$ depends on how the tensors $T^{JM}(j_b, j_a)$ are normalized.

Condition (4) follows from the requirement

$$\overset{+}{T}{}^{JM}(j_b, j_a) = (-1)^M T^{J-M}(j_a, j_b). \tag{5}$$

During space reflections the $T^{JM}(j_b, j_a)$ transforms as J rank tensors for even J and as J rank pseudotensors for odd J.

Expanding M in terms of the operators in (3) we get

$$M_{ba}(\mathbf{n}_b, \mathbf{n}_a) = \sum_{JMj_a j_b} \phi^{JM}_{j_b j_a}(\mathbf{n}_b, \mathbf{n}_a) T^{JM}(j_b, j_a). \tag{6}$$

From invariance of M under rotations it follows that the functions $\phi^{JM}_{j_b j_a}$ can be represented in the form

$$\phi^{JM}_{j_b j_a}(\mathbf{n}_b, \mathbf{n}_a) = \sum_{\lambda} a^{\lambda}_{j_b j_a J} \psi^{\lambda *}_{JM}(\mathbf{n}_b, \mathbf{n}_a), \tag{7}$$

where the $a^{\lambda}_{j_b j_a J}$ are arbitrary complex scalar functions which depend on the energy and $\mathbf{n}_a \cdot \mathbf{n}_b$ and

$$\psi^{\lambda}_{JM}(\mathbf{n}_b, \mathbf{n}_a) = \sum_{\mu, \mu'} (r-\lambda, r+\lambda, \mu\mu' | r-\lambda, r+\lambda, JM) y_{r-\lambda, \mu}(\mathbf{n}_a) y_{r+\lambda, \mu'}(\mathbf{n}_b) \tag{8}$$

are independent functions of two unit vectors $\mathbf{n}_a$ and $\mathbf{n}_b$ which transform according to the irreducible representation of the rotation group of weight $(2J+1)$.

If the relative intrinsic parity does not change, one gets

$$2r = J \qquad \text{for even } J$$
$$2r = J+1 \qquad \text{for odd } J.$$

If the relative parity changes,

$$2r = J+1 \qquad \text{for even } J$$
$$2r = J \qquad \text{for odd } J.$$

The number of values of λ depends on the properties of the Clebsch-Gordan coefficients in (8) and equals

$$N(J) = J+1 \qquad \text{for even } J$$
$$N(J) = J \qquad \text{for odd } J,$$

if the intrinsic parity does not change and

$$N(J) = J \qquad \text{for even } J$$
$$N(J) = J+1 \qquad \text{for odd } J$$

if the intrinsic parity in (1) changes.

In order to determine the total number of experiments required for construction of the reaction amplitude, we present the number $N_0(i_1, i_2, I_1, I_2)$ of $a^{\lambda}_{j_a j_b J}$ functions. This number is

$$N_0(i_1, i_2, I_1, I_2) = \sum_{|I_1-I_2|}^{I_1+I_2} \sum_{|i_1-i_2|}^{i_1+i_2} \sum_{|j_a-j_b|}^{j_a+j_b} N(J).$$

If the spins of all the particles participating in the reactions are integers then

$$N_0(i_1, i_2, I_1, I_2) = \tfrac{1}{2}(2i_1+1)(2i_2+1)(2I_1+1)(2I_2+1) \pm (-1)^{i_1+i_2+I_1+I_2}. \quad (9)$$

In all other cases

$$N_0(i_1, i_2, I_1, I_2) = \tfrac{1}{2}(2i_1+1)(2i_2+1)(2I_1+1)(2I_2+1). \quad (10)$$

The upper sign in (9) refers to the case when the intrinsic parity is constant and the lower to the case when it changes.

3. Time Reversal Invariance

It can be seen that the condition of invariance under rotation reduces the number of terms in matrix M from

$$(2i_1+1)(2i_2+1)(2I_1+1)(2I_2+1) \text{ to } N_0(i_1, i_2, I_1, I_2).$$

If in (1) b equals a and b′ equals a′ (elastic scattering of particles with arbitrary spins) further reduction of the number of terms in the expansion of M, and hence of the number of required experiments, can be attained [2]) by taking into account invariance under time reversal.

In the general case of reaction (1) time reversal symmetry yields a relation between the matrices M of the direct and inverse reactions. If $M_{ab}(\mathbf{n}_a, \mathbf{n}_b)$ denotes the matrix of the reaction which is the reciprocal of (1) then

$$k_a M^{+}_{ba}(\mathbf{n}_b, \mathbf{n}_a) = k_b T M_{ab}(-\mathbf{n}_a, -\mathbf{n}_b) T^{-1}, \quad (11)$$

where $\mathbf{k}_a$ and $\mathbf{k}_b$ are the momenta of relative motion in the initial and final states and T is a time reversal operator. The action of the latter on a function

with definite values of the square of the angular momentum and of its projection is defined by the equation [7])

$$T\psi_{JM} = (-1)^{J-M}\psi_{J-M}. \tag{12}$$

The law of transformation of $T^{JM}(j_a, j_b)$ under time reversal follows from (12):

$$TT^{JM}(j_a, j_b)T^{-1} = (-1)^{J-M}T^{J-M}(j_a, j_b). \tag{13}$$

Employing the expansion

$$M_{ab}(\mathbf{n}_a, \mathbf{n}_b) = \sum_{JMj_aj_b}\sum_{\lambda} b^{\lambda}_{j_aj_bJ}\psi^{\lambda *}_{JM}(\mathbf{n}_a, \mathbf{n}_b)T^{JM}(j_a, j_b) \tag{14}$$

and using relations (13), (5) and also the relations

$$\psi^{\lambda}_{JM}(\mathbf{n}_b, \mathbf{n}_a) = (-1)^{2r-J}\psi^{-\lambda}_{JM}(\mathbf{n}_a, \mathbf{n}_b) \tag{15}$$

and

$$\psi^{\lambda}_{JM}(-\mathbf{n}_a, -\mathbf{n}_b) = (-1)^{2r}\psi^{\lambda}_{JM}(\mathbf{n}_a, \mathbf{n}_b), \tag{16}$$

one obtains from (11) the relation between the scalar expansion coefficients of matrices M for the direct and inverse reactions

$$k_a a^{\lambda}_{j_bj_aJ} = k_b b^{-\lambda}_{j_aj_bJ}. \tag{17}$$

Formulae (11) or (17) permit one to construct the matrix of the inverse reaction knowing M of the direct reaction and vice versa.

Experimentally measurable mean values of the spin operators in the direct and inverse reactions can be directly related on basis of condition (11). Under real conditions either the mean values of the spin operators of separate particles (unpolarized cross section, vector and tensor polarizations in beam) or else the mean values of their direct products (polarization correlation) are measured. It is therefore convenient to expand the density matrix, referring to the polarization state of the particles, into direct products of irreducible tensor operators of separate particles.

One gets

$$\rho_a = \frac{1}{(2i_1+1)(2i_2+1)}\sum_{J=0}^{2i_1}\sum_{J'=0}^{2i_2}\sum_{M=-J}^{J}\sum_{M'=-J'}^{J'}\langle T^{JM}T^{J'M'}\rangle \overset{+}{T}{}^{JM}\overset{+}{T}{}^{J'M'} \tag{18}$$

for the density matrix of particles a and a′ and

$$\rho_b = \frac{1}{(2I_1+1)(2I_2+1)}\sum_{K=0}^{2I_1}\sum_{K'=0}^{2I_2}\sum_{N=-K}^{K}\sum_{N'=-K'}^{K'}\langle \theta^{KN}\theta^{K'N'}\rangle \overset{+}{\theta}{}^{KN}\overset{+}{\theta}{}^{K'N'} \tag{19}$$

for b and b′.

Operators T^{JM} and $T^{J'M'}$ act on the spin variables of particles a and a′; and θ^{KN}, $\theta^{K'N'}$ on spin variables of b and b′ respectively.

The expressions for T^{JM} can be obtained from (3) by putting $j_a = j_b = i_1$; the value of $A(i_1, i_1, J)$ is defined by the condition

$$\mathrm{tr}\ \overset{+}{T}{}^{JM}T^{JM} = 2i_1+1. \tag{20}$$

Under similar conditions for $T^{J'M'}$, θ^{KN} and $\theta^{K'N'}$, i_1 must be replaced by i_2, I_1 and I_2 respectively. The quantities $\langle T^{JM}T^{J'M'}\rangle$ for the direct reaction are prescribed by the conditions of the experiment. The quantities $\langle\theta^{KN}\theta^{K'N'}\rangle$ can then be expressed through $\langle T^{JM}T^{J'M'}\rangle$ and the matrix of the direct reaction, $M_{ba}(\mathbf{n}_b, \mathbf{n}_a)$:

$$\sigma_{ba}\langle\theta^{KN}\theta^{K'N'}\rangle = \frac{1}{(2i_1+1)(2i_2+1)}\sum_{JJ'MM'}\langle T^{JM}T^{J'M'}\rangle \mathrm{tr}\,\theta^{KN}\theta^{K'N'} \times M_{ba}(\mathbf{n}_b, \mathbf{n}_a)\overset{+}{T}{}^{JM}\overset{+}{T}{}^{J'M'}M_{ba}(\mathbf{n}_b, \mathbf{n}_a) \quad (21)$$

and

$$\sigma_{ba} = \mathrm{tr}\, M_{ba}\rho_a M_{ba}^{+}. \quad (22)$$

For the inverse reaction

$$\sigma_{ab}\langle T^{JM}T^{J'M'}\rangle = \frac{1}{(2I_1+1)(2I_2+1)}\sum_{KK'NN'}\langle\theta^{KN}\theta^{K'N'}\rangle \times \mathrm{tr}\, T^{JM}T^{J'M'}M_{ab}(\mathbf{n}_a, \mathbf{n}_b)\overset{+}{\theta}{}^{KN}\overset{+}{\theta}{}^{K'N'}M_{ab}(\mathbf{n}_a, \mathbf{n}_b) \quad (23)$$

and

$$\sigma_{ab} = \mathrm{tr}\, M_{ab}\rho_b M_{ab}^{+}. \quad (24)$$

From (11) and (13) we obtain†

$$\begin{aligned} &k_a^2\,\mathrm{tr}\,\theta^{KN}\theta^{K'N'}M_{ba}(\mathbf{n}_b, \mathbf{n}_a)\overset{+}{T}{}^{JM}\overset{+}{T}{}^{J'M'}M_{ba}^{+}(\mathbf{n}_b, \mathbf{n}_a) \\ &\quad = (-1)^{J+J'+K+K'+M+M'+N+N'} \\ &\quad \times k_b^2\,\mathrm{tr}\, T^{J-M}T^{J'-M'}M_{ab}(-\mathbf{n}_a, -\mathbf{n}_b)\overset{+}{\theta}{}^{K-N}\overset{+}{\theta}{}^{K'-N'}M_{ab}^{+}(-\mathbf{n}_a, -\mathbf{n}_b). \end{aligned} \quad (25)$$

For $J = J' = K = K' = 0$, that is, when all θ and T reduce to unit matrices, the well known relation between the unpolarized cross sections σ_{ab}^0 and σ_{ba}^0 follows from (25) if account is made of the fact that σ_{ab}^0 and σ_{ba}^0 can be expressed through M as follows:

$$\sigma_{ba}^0 = \frac{1}{(2i_1+1)(2i_2+1)}\,\mathrm{tr}\, M_{ba}M_{ba}^{+}$$

and

$$\sigma_{ab}^0 = \frac{1}{(2I_1+1)(2I_2+1)}\,\mathrm{tr}\, M_{ab}M_{ab}^{+}.$$

In the general case, (25) yields the relation between the contribution to the mean value of operator $\theta^{KN}\theta^{K'N'}$ in the direct reaction (the contribution arising from the fact that the mean value of $T^{JM}T^{J'M'}$ is not zero in the initial state) and the contribution to the mean value of $T^{J-M}T^{J'-M'}$ (which is due to the fact that in the initial state of the inverse reaction the mean value of $\theta^{K-N}\theta^{K'-N'}$ does not vanish).

† A similar expression has been obtained by M. I. Shirokov [8]), to whom the authors express their appreciation for making available the results of his work prior to publication. Validity of (25) for elastic scattering in some reactions has been established by a number of authors [1-5, 9, 10, 11]).

4. Determination of Reaction Matrix

We shall now proceed to analyze the conditions underlying the determination of the reaction matrix from the experimental data. If not all simultaneously operative reactions are taken into account, M_{ba} can be reconstructed only with an accuracy to a common phase factor. Since the functions $a^{\lambda}_{j_a j_b J}$ are complex, the number of necessary experiments is

$$2N_0(i_1, i_2, I_1, I_2)-1$$

where N_0 is defined in (9) and (10).

If reactions proceeding along parallel channels are investigated simultaneously with reaction (1), then for determination of the total number of required experiments, not only the symmetry properties considered above but the unitarity condition for the S matrix should also be used [1,12]; also see [13]).

If only two reaction channels are involved, the unitarity condition can be represented as follows:

$$\begin{aligned}
&2\pi i[M^{+}_{aa}(\mathbf{n}_a, \mathbf{n}'_a)-M_{aa}(\mathbf{n}'_a, \mathbf{n}_a)]\\
&\quad = k_a\int d\omega(\mathbf{n})\{M^{+}_{aa}(\mathbf{n}, \mathbf{n}'_a)M_{aa}(\mathbf{n}, \mathbf{n}_a)+M^{+}_{ba}(\mathbf{n}, \mathbf{n}'_a)M_{ba}(\mathbf{n}, \mathbf{n}'_a)\},\\
&2\pi i[M^{+}_{ab}(\mathbf{n}_a, \mathbf{n}_b)-M_{ba}(\mathbf{n}_b, \mathbf{n}_a)]\\
&\quad = \int d\omega(\mathbf{n})\{k_a M^{+}_{ab}(\mathbf{n}, \mathbf{n}_b)M_{aa}(\mathbf{n}, \mathbf{n}_a) + k_b M^{+}_{bb}(\mathbf{n}, \mathbf{n}_b)M_{ba}(\mathbf{n}, \mathbf{n}_a)\},\\
&2\pi i[M^{+}_{bb}(\mathbf{n}_b, \mathbf{n}'_b)-M_{bb}(\mathbf{n}'_b, \mathbf{n}_b)]\\
&\quad = k_b\int d\omega(\mathbf{n})\{M^{+}_{bb}(\mathbf{n}, \mathbf{n}_b')M_{bb}(\mathbf{n}, \mathbf{n}_b)+M^{+}_{ab}(\mathbf{n}, \mathbf{n}'_b)M_{ab}(\mathbf{n}, \mathbf{n}_b)\}.
\end{aligned} \tag{26}$$

In accord with (9) and (10) the number of scalar functions in matrix M_{ba} is $N_0(i_1, i_2, I_1, I_2)$. The number of independent scalar functions reduces to

$$N(i_1, i_2) = \tfrac{1}{2}N_0(i_1, i_2, i_1, i_2)+\tfrac{1}{2}(2i_1+1)(2i_2+1) \tag{27}$$

for matrix M_{aa} and to

$$N(I_1, I_2) = \tfrac{1}{2}N_0(I_1, I_2, I_1, I_2)+\tfrac{1}{2}(2I_1+1)(2I_2+1) \tag{28}$$

for matrix M_{bb}, if time reversal invariance is taken into account. Thus the total number of scalar functions entering the reaction matrices of the processes under consideration is

$$N(i_1, i_2)+N(I_1, I_2)+N_0(i_1, i_2, I_1, I_2).$$

These functions are complex and hence all values cited above should be doubled. However, equations (26) lead to integral relations between the scalar functions in the expansion of M. The number of these relations coincides with the total number of coefficients in matrices M_{aa}, M_{bb} and M_{ab} and this precisely equals the necessary number of experiments (it being assumed that all experiments are performed at a prescribed energy).

The considerations presented here for the case of two channels can be directly extended to the case of an arbitrary number of channels.

In conclusion the authors consider it a pleasant duty to express their appreciation to Professor Ya. A. Smorodinsky for interesting discussions of the problems considered here.

Appendix

It is of interest to investigate the azimuthal dependence of the angular distribution of the products of reaction (1) when the incident beam (particle a) is polarized and the target is not polarized. In this case the cross section for the reaction has the following form

$$\sigma_{ba}(\mathbf{n}_b, \mathbf{n}_a)=\mathrm{tr}\,\rho_a M_{ba}^{+} M_{ba}=\frac{1}{(2i_1+1)(2i_2+1)}\sum_{JM}\langle T^{JM}\rangle \mathrm{tr} T^{JM} M_{ba}^{+} M_{ba}. \quad (A.1)$$

Since $M_{ba}^{+} M_{ba}$ is a quadratic matrix of the order $(2i_1+1)(2i_2+1)$ it can be expanded in orthogonal products $T^{JM} T^{J'M'}$. Making use of the condition of invariance of $M_{ba}^{+} M_{ba}$ under space rotations and reflections we get

$$M_{ba}^{+} M_{ba}=\sum_{J\lambda} A_J{}^{\lambda} \sum_{M} \psi_{JM}^{\lambda *} T^{JM}+Q, \quad (A.2)$$

where, analogously to (7), $A_J{}^{\lambda}$ are arbitrary scalar functions and Q contain as multipliers the operators $T^{J'M'}$ for $J' \neq 0$. From (A.1) and (A.2) it follows that

$$\sigma_{ba}(\mathbf{n}_b, \mathbf{n}_a) = \sum_{J\lambda} A_J{}^{\lambda} \sum_{M=-J}^{J} \langle T^{JM}\rangle \psi_{JM}^{\lambda *}(\mathbf{n}_b, \mathbf{n}_a). \quad (A.3)$$

The azimuthal dependence of the cross section is due to terms with $M \neq 0$. Therefore the sum over M in (A.3) can be represented as follows:

$$\langle T^{J0}\rangle \psi_{J0}^{\lambda *}+\sum_{M=1}^{J}\{[\langle T^{JM}\rangle \psi_{JM}^{\lambda *}+\langle T^{J-M}\rangle \psi_{J-M}^{\lambda *}\}$$
$$=\langle T^{J0}\rangle \psi_{J0}^{\lambda *}+\sum_{M=1}^{J}\{\langle T^{JM}\rangle \psi_{JM}^{\lambda *}+(-1)^{J-M}\langle T^{J-M}\rangle \psi_{JM}^{\lambda}\}. \quad (A.4)$$

To obtain the latter expression use was made of the relation

$$\psi_{J-M}^{\lambda *} = (-1)^{J-M}\psi_{JM}^{\lambda}, \quad (A.5)$$

which follows from the definition of the functions ψ_{JM}^{λ} if it be taken into account that, in accord with (12), the phases of the spherical functions are chosen so that

$$y_{lm}^{*} = (-1)^{l-m} y_{l-m}.$$

In the following it will be considered that polarization of particle a is the result of a reaction with unpolarized particles. In this case, as will be shown below,

$$\langle T^{JM}\rangle = (-1)^{J+M}\langle T^{J-M}\rangle \quad (A.6)$$

(in the coordinate system in which the z-axis is directed along $\mathbf{n}_a$ and the x-axis is perpendicular to the first reaction plane). The expression (A.4) then reduces to

$$\langle T^{J0}\rangle \psi^{\lambda *}_{J0} + \sum_{M=1}^{J} \langle T^{JM}\rangle \{\psi^{\lambda *}_{JM} + \psi^{\lambda}_{JM}\}$$

or

$$\langle T^{J0}\rangle \psi^{\lambda *}_{J0} + \sum_{M=1}^{J} \langle T^{JM}\rangle B^{\lambda}_{JM}\, 2\cos M\varphi, \tag{A.7}$$

since in the chosen system

$$\psi^{\lambda}_{JM} = e^{iM\varphi} B^{\lambda}_{JM}, \qquad B^{\lambda *}_{JM}(\theta) = B^{\lambda}_{JM}(\theta).$$

From (A.7), (A.3) and (A.4) it follows that

$$\sigma_{ba}(\mathbf{n}_b, \mathbf{n}_a) = \sum_{J=0}^{2i_1} \sum_{\lambda} A_J{}^{\lambda} \{\langle T^{J0}\rangle \psi^{\lambda *}_{J0} + 2 \sum_{M=1}^{J} \langle T^{JM}\rangle B^{\lambda}_{JM} \cos M\varphi\} \tag{A.8}$$

and this can be transformed to

$$\sigma_{ba}(\mathbf{n}_b, \mathbf{n}_a) = \sigma^0_{ba}(\mathbf{n}_b, \mathbf{n}_a) + \sum_{q=1}^{i_1} \langle T^{2q0}\rangle A_{2q}(\theta) + \sum_{K=1}^{2i_1} \cos K\varphi \sin^K\theta \sum_{J=K}^{2i_2} B_J(\theta)\langle T^{JK}\rangle. \tag{A.9}$$

In virtue of property (A.6) only terms with even J remain in the first sum in (A.9).

We now return to the proof of relations (A.6). For $\langle T^{JM}\rangle$ we have

$$\sigma_0 \langle T^{JM}\rangle = \frac{1}{n} \operatorname{tr} MM^+ T^{JM},$$

where the quantities σ_0 and MM^+ refer to a reaction in which particle a is produced; n is the number of initial spin states of this reaction. Employing for MM^+ an expansion of the same type as (A.2)

$$MM^+ = \sum_{J\lambda} C_J{}^{\lambda} \sum_{M} \psi^{\lambda}_{JM} \overset{+}{T}{}^{JM} + R, \tag{A.10}$$

we get

$$\sigma_0 \langle T^{JM}\rangle = \frac{1}{n} \sum_{\lambda} C_J{}^{\lambda} \psi^{\lambda}_{JM}. \tag{A.11}$$

In the chosen coordinate system the ψ^{λ}_{JM} are real ($2r$ is an even number as MM^+ is always a scalar). Making use of this circumstance we immediately obtain (A.6) from (A.11) and (A.3).

References

1) L. D. Puzikov, R. M. Ryndin and Ya. A. Smorodinsky, JETP **32** (1957) 592; Nuclear Physics **3** (1957) 436
2) L. D. Puzikov, JETP (in print)
3) L. Wolfenstein and J. Ashkin, Phys. Rev. **85** (1952) 947

4) R. H. Dalitz, Proc. Roy. Soc. A **65** (1952) 175
5) W. Lakin, Phys. Rev. **98** (1955) 139
6) G. Racah, Phys. Rev. **62** (1942) 438
7) R. Huby, Proc. Phys. Soc. A **67** (1952) 1103
8) M. I. Shirokov, JETP **33** (1957) 975
9) A. I. Baz, JETP **32** (1957) 628
10) L. I. Lapidus, JETP, **33** (1957) 204; Nuclear Physics **4** (1957) 145
11) L. I. Lapidus, JETP (in print)
12) R. M. Ryndin and Ya. A. Smorodinsky, JETP **32** (1957) 1584
13) Yu. A. Golfand, JETP **31** (1956) 224

8.A

Nuclear Physics 7 (1958) 655—671; © *North-Holland Publishing Co., Amsterdam*

Not to be reproduced by photoprint or microfilm without written permission from the publisher

MEASUREMENT OF LONGITUDINAL POLARIZATION OF ELECTRONS EMITTED IN β-DECAY

A. I. ALIKHANOV, G. P. ELISEIEV and V. A. LIUBIMOV †

USSR Academy of Sciences, Moscow

Received 13 December 1957

Abstract: The longitudinal polarization of Coulomb β-transition electrons has been measured for several electron energies. The polarization value was found to be equal to $-v/c$ for all the substances measured. It is proved that the most probable relationships among the coupling constants in β-decay are

$$C_T = -C'_T, \quad C_S = -C'_S, \quad C_V = C'_V, \quad C_A = C'_A.$$

1. Introduction

With the discovery of non-conservation of parity in weak interaction [1]), the pattern of β-decay has beccome more involved. Whereas previously β-decay could be characterized essentially by four (to be precise, five) coupling constants, the number of constants has now doubled, as half of them reflect non-conservation of parity. And since, generally speaking, the coupling constants can be complex, the number of parameters increases to 16. On the other hand, new effects have become known, in which the relationship between the constants can be discovered by physical measurements. One such effect, as is well-known, is the longitudinal polarization of electrons in the β-decay of non-polarized nuclei [2]).

Depending on the type of the transition in the β-active nuclei, different combinations of coupling constants can be derived from measurements on electron longitudinal polarization. If the polarization is measured with a high degree of accuracy, with due consideration of electron energy, a study of heavy nuclei involving first forbidden transitions (so-called Coulomb transitions) should yield the greatest possible amount of information about the coupling constants which can in principle be derived from measurements of longitudinal polarization of electrons emitted from non-polarized nuclei.

In the present investigation we endeavour to measure with the highest possible accuracy the longitudinal polarization of electrons of different energy from elements with Coulomb transitions, such as Tm^{170} ($\Delta J = 1$; yes), Re^{186} ($\Delta J = 1$; yes), Sm^{153} ($\Delta J = 1,0$; yes), Au^{198} ($\Delta J = 0$; yes),

† Paper submitted to the Padua-Venice Conference on September 27, 1957 and to the Moscow Conference on November 23, 1957.

and Lu^{177} ($\Delta J = 1$; yes) or ($\Delta J = 0$; yes), containing a mixture of Gamov-Teller and Fermi interactions. For comparison, measurements were also carried out with Sr^{90} and Y^{90}, which have unique transitions and a pure Gamov-Teller interaction and for which one might with greater reason expect an electron polarization equal to $-v/c$.

2. Experimental Set-Up

To measure longitudinal polarization we made use of the Mott scattering method. This consists in measuring the azimuthal asymmetry of transversely polarized electrons singly scattered through a large angle by a scatterer with a large Z-value.

To obtain greater stability and reproducibility of the results, we strived to make our apparatus as simple as possible. We did not use external fields, electric or electric + magnetic, for transforming longitudinal polarization into transvesre, since these methods introduce errors which are difficult to control. Transformation of longitudinal polarization to transverse was achieved by deflection of the electron trajectory in nuclear Coulomb fields during multiple scattering at an angle close to 90° of the electrons in a relatively thick scatterer. When polarization is transformed by application of external fields, such as in a curved condenser, the upper limit of the electron energy at which polarization can be measured is not high; the reason of this is that sufficiently high electric field intensities cannot be obtained because of vacuum breakdown. Our method is obviously free from this handicap.

Fig. 1 shows the set-up used. The electron passages were made sufficiently wide to increase the aperture ratio of the device. However, despite considerable straggling of the values of the electron trajectory angles, the geometrical correction reducing the azimuthal asymmetry due to angular scattering was found to be only ≈ 6 % (since the average angle of scattering of the electrons from scatterer I (transformer) was close to 90°). The thin gold scatterer II (analyzer) was placed perpendicularly to the axis of the instrument. This position of scatterer II ensured maximum symmetry of the whole assembly. The electrons experiencing scattering in scatterers I and II were recorded by a telescope consisting of two Geiger counters in coincidence. An aluminium filter stopping low-energy electrons was inserted between the counters. The counters were arranged at an angle of 112.5° to the instrument axis in such a way that the rather small solid angle of the counter telescope viewed the entire scatterer area illuminated by the electrons. This mutual position of the counters and scatterer II ensured maximal intensity. The counters, together with scatterer II, could be rotated about the instrument axis without affecting the vacuum. To reduce the

admixture of electrons scattered from the walls of the instrument, baffles were made in the electron beam channel. The baffles were thin (0.5 mm) duralumin diaphragms.

The Tm, Lu, Sm, and Sr+Y sources consisted of an even layer of finely dispersed active powder, deposited on a 10 μ thick aluminium foil. Re was deposited electrolytically on an aluminium foil covered with a very thin layer of platinum. Au was deposited on an aluminium foil by evaporation

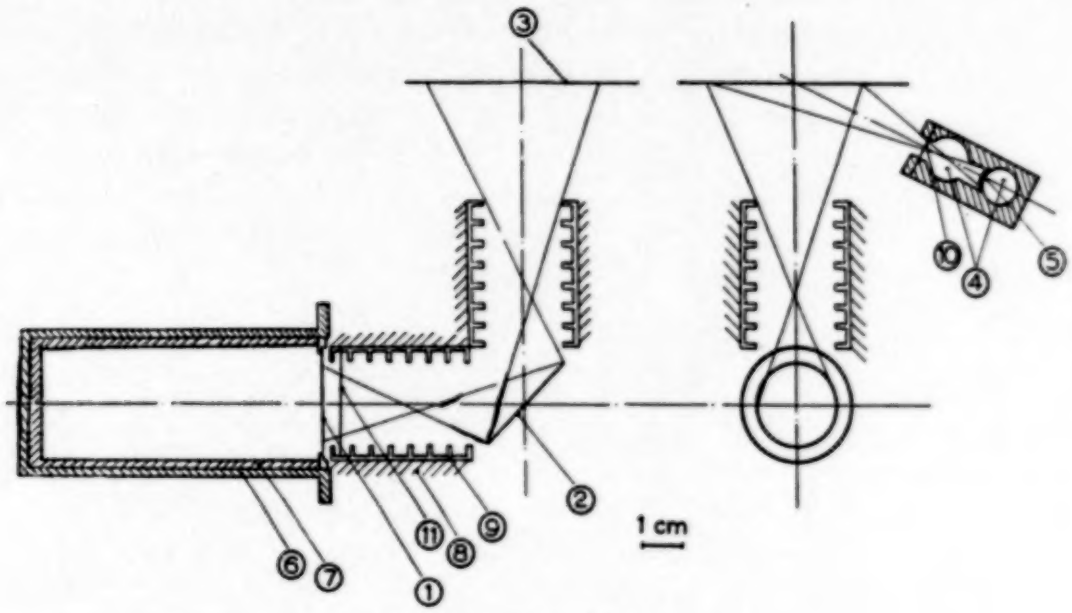

Fig. 1. Experimental set-up.
1. source; 2. scatterer I (transformer); 3. scatterer II (analyzer); 4. Geiger counters; 5. aluminium filter between the counters; 6. brass vessel; 7. plexiglass vessel; 8. instrument body; 9. duralumin diaphragms; 10. polyethylene film; 11. thin collodion film.

in vacuum with subsequent activation. The aluminium foil and sources were attached to a duralumin ring, which was placed in a brass vessel coated on the inside with plexiglass. In some cases a thin film of collodion was placed before the source to protect the instrument from contamination by the active substance.

Two identical instruments were made. The body of the one was of brass and lead, 1, while the body of the other was made of lead and tungsten, 2.

3. Measurements

The azimuthal asymmetry of scattering

$$\Delta = 200\frac{I_1-I_2}{I_1+I_2}$$

was measured in a plane perpendicular to the plane of electron deflection caused by the first scattering. This was performed at several values of the

mean electron energy $\bar{\varepsilon}$ (I_1 is the intensity of scattering in the azimuthal direction $[\boldsymbol{v}_2 \times \boldsymbol{v}_1]$, where $\boldsymbol{v}_1$ is the electron velocity prior to and $\boldsymbol{v}_2$ is the velocity after scattering in scatterer I; I_2 refers to the opposite direction). Electrons were selected according to their energy by interposing an aluminium filter of definite thickness ρ between the counters and by employing scatterer I with a thickness τ. In each experiment with a definite mean electron energy $\bar{\varepsilon}$ measurements of the azimuthal asymmetry A_k were performed at various thicknesses t_k of scatterer II.

Three series of measurements were performed: the first with instrument 1, the second with instrument 2, and the third with instrument 2, in which two counter telescopes were employed. The azimuthal asymmetry of scattering was determined as the average of the azimuthal asymmetry values in each of the telescopes. This ruled out errors due to a possible change in the electron flux during the measurements, as well as to possible non-uniformity of the thickness of scatterer II.

3.1. REPRODUCIBILITY OF RESULTS

A necessary condition for reliability of the statistical accuracy of the measurements is the absence of non-statistical scattering. This can be ascertained by the degree of coincidence and from the actual scattering of the results of repeated measurements around a mean value.

Altogether eighty measurements of azimuthal asymmetry were carried out. For a number of points two or more measurements were performed (in total 53 such repeated measurements). Although the measurements were performed with different instruments, the overwhelming majority of them were in good agreement. Out of the 53 repeated measurements, 40 coincide with the mean values within the limits of the experimental errors, 10 do not coincide by more than 1 error, 2 by 2 errors, and 1 by 3 errors; the last three measurements were not taken into account in calculating the mean values for the reproducible measurements. The mean values of the measured azimuthal asymmetry may be seen in table 1.

2.2. CONTROL EXPERIMENTS

a) Asymmetry of instrumental origin was determined by measuring scattering of electrons in an aluminium foil used as scatterer II. In calculating the instrumental asymmetry, it was taken into account, moreover, that azimuthal asymmetry in the case of scattering in aluminium should be $\approx 1/12$ the values of electron scattering in gold of equivalent thickness [3]. The measurements revealed that the instrumental asymmetry value (A_p) did not depend on the substance of the source, but only on the electron energy and varied from 0 to -2.

b) The flux of electrons reflected back from the aluminium backing of the source and from the plexiglass vessel was measured experimentally with the aid of a point source covered above by a small shield impenetrable

TABLE I

ρ, τ (mg/cm²)	$\bar{\varepsilon}$ (keV)	t(mg/cm²)Au / element thickness (mg/cm²)	1.97	0.92	0.39	0.24	0.12	$\bar{A}_0$	$\bar{A}_{0\ corr.}$	$\bar{A}_{th}$	$\langle\sigma\rangle/(-v)$
			$\bar{A} = 200\ (I_1-I_2)/(I_1+I_2)$								
$\rho_1 = 1.0$ Al; $\tau_1 = 3.0$ Au	145	Tm 0.8			22.0±0.9	25.3±1.2	28.0±2.0	33.0±1.3	36.6±1.8	36.2	1.01±0.05
	140	Sm 1.1				23.1±1.4	29.0±1.6	32.0±1.5	35.7±1.9	35.7	1.00±0.05
	130	Lu 0.3			15.1±1.9	19.0±2.6	22.8±2.8	26.3±1.9	29.6±2.3	30.5	0.97±0.07
	130	Sr+Y 1.5				31.6±3.7	24.8±2.8	33.8±3.6	37.3±4.1	35.0	1.06±0.12
$\rho_2 = 2.6$ Al; $\tau_2 = 6.0$ Au	260	Tm		22.1±0.9	29.8±1.2	31.5±1.5	33.8±2.8	37.5±1.1	39.2±1.5	42.3	0.93±0.04
	250	Sm				31.9±2.5		37.6±3.8	39.3±3.8	42.1	0.93±0.09
	200	Lu	14.0±1.3	23.7±2.0	30.0±4.0			42.5±4.4	44.4±4.6	42.7	1.04±0.11
	260	Re 0.1		23.3±2.6	38.0±4.8			43.2±4.4	45.2±4.6	42.7	1.06±0.11
	220	Sr+Y		21.4±1.7	35.7±1.8	33.6±4.8		41.5±2.5	43.4±2.7	42.1	1.03±0.06
$\rho_3 = 5.2$ Al; $\tau_3 = 13$ Au	390	Tm	18.1±1.3	25.7±0.9	30.4±1.3	33.5±2.8		37.5±1.6	41.2±1.9	40.6	1.01±0.05
	360	Sm			30.6±2.3			36.7±3.0	40.4±3.3	40.6	1.00±0.08
	390	Au 0.2			23.8±2.6	36.8±4.0		33.6±2.5	36.8±2.9	36.6	1.00±0.08
	450	Sr+Y	15.5±1.2	23.1±1.5	28.0±2.0			33.0±3.1	36.2±3.4	38.3	0.94±0.09
$\rho_4 = 10.4$ Al; $\tau_4 = 20.0$ Au	520	Tm	16.2±2.8	27.4±2.1	32.0±2.9			35.2±2.1	36.6±2.2	37.0	0.99±0.06
	520	Au	18.2±2.1	24.2±2.6	30.0±5.8			33.3±2.8	34.5±2.9	35.9	0.96±0.08
	650	Sr+Y	18.9±2.2	23.6±2.7				30.7±3.1	31.8±3.2	32.5	0.98±0.10

ρ = thickness of the filter between the Geiger counters; τ = thickness of scatterer I (transformer); $\bar{\varepsilon}$ = mean electron energy; t = thickness of scatterer II (analyzer); $\bar{A}$ = mean measured value of azimuthal asymmetry; $\bar{A}_0$ = azimuthal asymmetry extrapolated to zero thickness of scatterer II; $\bar{A}_{0\ corr.}$ is the azimuthal asymmetry with the following corrections introduced: (1) instrumental asymmetry A_p, (2) electron backscattering δ_μ, (3) electrons scattered from the instrument walls δ_η; $\bar{A}_{th}$ = expected azimuthal asymmetry for electrons with a polarization equal to $-v$; $\langle\sigma\rangle/(-v)$ is the longitudinal electron polarization in $(-v)$ units.

to electrons, so that no direct radiation could reach the counter. The relative number of back-scattered electrons depended on the electron energy and varied from 0.5 to 1.5 %. Since the back-scattered electrons mainly have a polarization opposite to that of the "forward" electrons, the corrections δ_β to the measured values of azimuthal asymmetry must be somewhat higher, viz. (0.8—2.0)%.

c) Similarly, measurements were made on the fraction of electrons scattered by the diaphragms near the source and by the instrument walls. The corrections δ_γ to the azimuthal asymmetry in this case were (3.5—1.9)%.

d) Measurements of azimuthal asymmetry at different azimuthal angles showed that at all energies the effect was most pronounced in a plane perpendicular to the plane of deflection of the electron trajectory after scattering in scatterer I.

e) K. A. Ter-Martirosyan has shown that in multiple scattering of electrons through an angle ψ in a light substance, the electron spin turns by an angle† $\varphi = \psi(1-\sqrt{1-v^2})$, where $v = v/c$. Measurements in which equivalent thicknesses of Al and Au were employed as scatterer I (transformer) revealed that the azimuthal asymmetry effect does not depend on the substance of scatterer I.

f) In measurements with a Au^{198} source, the Geiger counters were subjected to strong γ-radiation. Measurements of electron polarization were performed in the 300—700 keV interval, with sufficiently thick aluminium filters between the coincidence counters to ensure that electrons produced by the γ-rays ($\varepsilon_\gamma \approx 400$ keV) did not cause any significant number of coincidences in the counters. The resolution of the counting device was sufficiently high and the background of chance coincidences did not exceed (0.5—1.0)%.

The fraction of photo- and Compton-electrons produced by the γ-rays was measured by shielding the source with a plexiglass screen impenetrable to electrons, but not to the γ-rays. The azimuthal asymmetry correction due to this effect was ≈ 2 %.

† The following expression for the angle of rotation of the spin in the scattering plane can easily be derived in the Born approximation for an elementary scattering act:

$$\sin\varphi_i = \frac{1-(1-\sqrt{1-v^2})\sin^2\frac{1}{2}\psi_i}{1-v^2\sin^2\frac{1}{2}\psi_i}(1-\sqrt{1-v^2})\sin\psi_i.$$

For $\psi_i \ll 1$ this expression goes over into to the formula $\varphi_i = (1-\sqrt{1-v^2})\,\psi_i$ for deflection of the spin in an electric condenser.

The correction $(Z/137)\,\frac{1}{2}\psi_i$, which arises from application of the Born approximation is small even for heavy nuclei if $\psi_i \ll 1$. Thus this formula may be expected to be valid for small angles (multiple scattering) as in the case of scattering on heavy nuclei. If multiple scattering occurs in a single plane the following relation should evidently hold between the resultant angles $\varphi = \Sigma_i \varphi_i$ and $\psi = \Sigma_i \psi_i$:

$$\varphi = (1-\sqrt{1-v^2})\,\psi.$$

3.3. DETERMINATION OF THE EXTRAPOLATED VALUE OF THE AZIMUTHAL ASYMMETRY OF SCATTERING CORRESPONDING TO SINGLE SCATTERING

To determine electron polarization we must know the azimuthal asymmetry corresponding to single electron scattering. In actual measurements the electrons scattered from scatterers of finite thickness always contain a fraction of multiply scattered electrons. This distorts the magnitude of the azimuthal asymmetry effect. However, the correction can be obtained experimentally.

It has been shown by Artsimovich [4]) that the intensity of electrons of a given energy, scattered in a layer of thickness t is

$$I(t) = I_0[t+\gamma(\varepsilon)\cdot t^2] = I'(t)+I''(t)$$

where $I'(t) = I_0 t$ is the intensity of single scattering, and $I''(t) = I_0\gamma(\varepsilon)t^2$ is the intensity of multiple scattering. Scattering of polarized electrons is characterized by the azimuthal asymmetry:

$$\Delta(t) = 200\frac{I'_1(t)-I'_2(t)+I''_1(t)-I''_2(t)}{I'_1(t)+I'_2(t)+I''_1(t)+I''_2(t)} = 200\,\frac{I'_1(t)-I'_2(t)+I''_1(t)-I''_2(t)}{I'(t)+I''(t)}$$

$$= 200\frac{I'_1(t)-I'_2(t)}{I'(t)\left[1+\dfrac{I''(t)}{I'(t)}\right]}+200\frac{I''_1(t)-I''_2(t)}{I''(t)\left[1+\dfrac{I'(t)}{I''(t)}\right]} = \frac{\Delta_0}{1+\gamma(\varepsilon)t}+\frac{\xi(\varepsilon)\Delta_0\gamma(\varepsilon)t}{1+\gamma(\varepsilon)t}$$

$$\approx \Delta_0\frac{1}{1+\gamma(\varepsilon)[1-\xi(\varepsilon)]t} = \Delta_0\frac{1}{1+\alpha(\varepsilon)t},$$

where $\Delta_0 = 200(I'_1-I'_2)/I'$ is the azimuthal asymmetry for single scattering, and $\xi(\varepsilon)\Delta_0$ is the azimuthal asymmetry for multiple scattering, with $\xi(\varepsilon) < 1$.

We thus obtain that the inverse values Δ_k of azimuthal asymmetry of electrons possessing a given energy ε scattered in scatterers II of different thicknesses t_k are linearly related to t_k:

$$\frac{1}{\Delta_k} = \frac{1}{\Delta_0}+\frac{\alpha(\varepsilon)t_k}{\Delta_0}.$$

The quantity $\overline{\alpha(\varepsilon)}$ as a function of the energy (fig. 2) was derived from the data obtained for different substances at different energies. The extrapolated values $\bar{\Delta}_0$ for each substance and each energy were found according to the formula

$$\bar{\Delta}_0 = (1/k)\sum_k \Delta_k[1+\overline{\alpha(\varepsilon)}t_k]$$

under the condition that $\overline{\alpha(\varepsilon)}t_k < 1$. The extrapolated values $\bar{\Delta}_0$ with due consideration for the above mentioned corrections Δ_p, δ_μ and δ_η are given in table 1; $\Delta_{0\,\mathrm{corr}} = \delta_\mu\delta_\eta\,(1/k)\sum_k(\Delta_k-\Delta_p)[1+\overline{\alpha(\varepsilon)}t_k]$. From these data it is evident that the measured values of azimuthal asymmetry weakly vary over

a wide range of energy. This means that an exact knowledge of the electron energy spectrum is not essential in determining the degree of electron polarization with the help of our instrument.

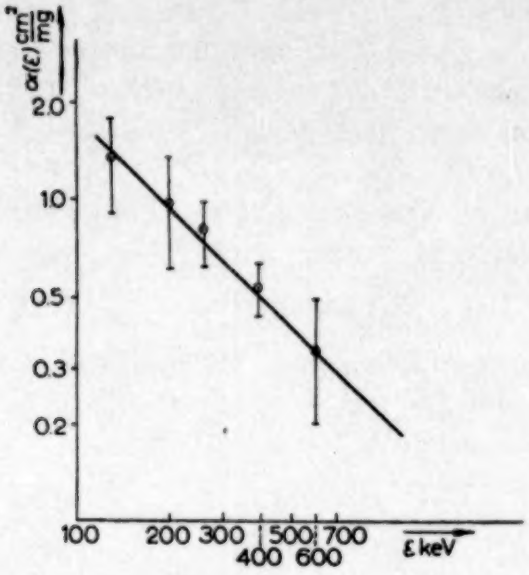

Fig. 2

3.4. ELECTRON ENERGY SPECTRA

The energy spectrum of electrons experiencing double scattering and recorded by the counter can be represented as

$$\frac{\partial n}{\partial \varepsilon} = f_0 \sigma(\tau)\sigma_0 \varphi(\rho)$$

where f_0 is the electron spectrum of the source, $\sigma(\tau)$ is the cross-section for multiple scattering of electrons in scatterer I of thickness τ through an angle of 90°; σ_0 is the cross-section for single scattering through an angle of 112.5° and $\varphi(\rho)$ is the fraction of the electrons passing through the aluminium filter of thickness ρ. The values of σ_0 and $\varphi(\rho)$ are known[3,6]. The energy spectra of Au^{198} (950 keV boundary energy) and Lu^{177} (500 keV boundary energy) electrons which experienced multiple scattering through $\approx 90°$ were carefully measured with a spectrometer. For Lu^{177} the measurements were performed with 3 mg/cm² Au and 6 mg/cm² Au scatterers I; for Au^{198}, with 3 mg/cm² Au, 6 mg/cm² Au, 13 mg/cm² Au, and 20 mg/cm² Au scatterers I. As an illustration, figs. 3a, 3b give the electron spectra of Lu^{177} ($\bar{\varepsilon} = 130$ keV) and Au^{198} ($\bar{\varepsilon} = 360$ keV); the spectra refer to multiple scattering through an angle of 90° and single scattering through an angle of 112.5°. The Lu and Au electron spectra contain conversion lines with conversion electron energies of 98 keV, 137 keV for Lu and 325 keV and $\approx$ 400 keV for Au. Since the conversion electrons are not polarized, their contribution to the spectrum must be taken into account in determining the expected scattering

asymmetry. This contribution could be determined directly from the β-spectrum shape of the multiply scattered electrons.

The electron spectra of Re^{186}, Tm^{170} and Sm^{153} practically coincide with

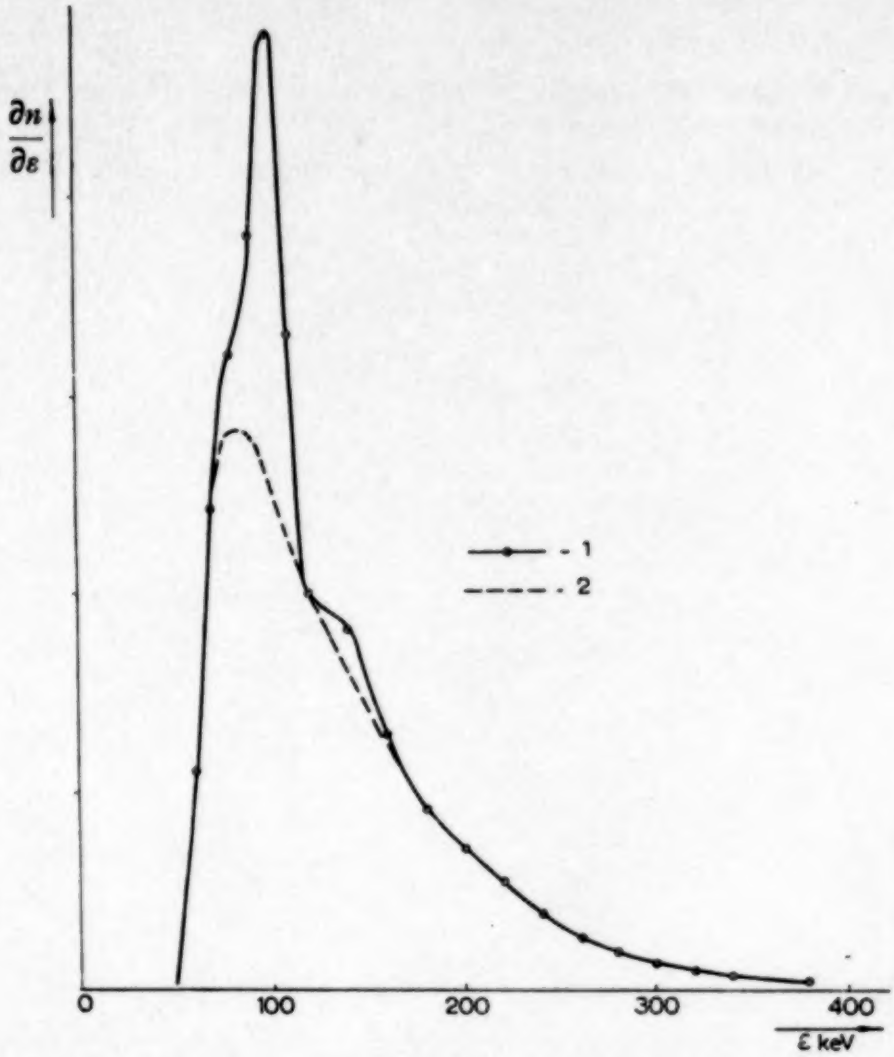

Fig. 3a. Spectrum of Lu^{177} electrons experiencing double scattering and causing coincidence in Geiger counters ($\bar{\varepsilon}_1 = 130$ keV, $\rho_1 = 1.0$ mg/cm² Al, $\tau_1 = 3.0$ mg/cm² Au).
1. spectrum including conversion electrons; 2. spectrum without conversion electrons.

those of Au^{198} which do not contain conversion electrons. The electron spectra of $Sr^{90}+Y^{90}$ were calculated.

3.5. CALCULATION OF THE EXPECTED VALUE OF THE SCATTERING AZIMUTHAL ASYMMETRY

In order to determine the degree of longitudinal polarization of electrons in units of $-v$ the measured values should be compared with the expected values $\bar{A}_{th}$ of azimuthal asymmetry in the scattering of electrons possessing a longitudinal polarization $-v$ and a known energy spectrum $\partial n/\partial \varepsilon$

$$\Delta_{\text{th}i} = \frac{\int \Delta_{\text{th}i} \frac{\partial n'_i}{\partial \varepsilon} d\varepsilon}{\int \frac{\partial n'_i}{\partial \varepsilon} d\varepsilon} = 200\, v \frac{\int S \langle \sigma_\perp \rangle_i \delta_g \delta_Z \delta_{\text{sh}} (1 - \frac{1}{2}\theta^2) \int \frac{\partial n'_i}{\partial \varepsilon} d\varepsilon}{\int \frac{\partial n_i}{\partial \varepsilon} d\varepsilon}$$

where

1) $\partial n'_i/\partial \varepsilon$ is the electron energy spectrum without conversion electrons in the i-th experiment; the latter is characterized by a filter of thickness ρ_i between the counters and a scatterer I (transformer) of thickness τ_i;

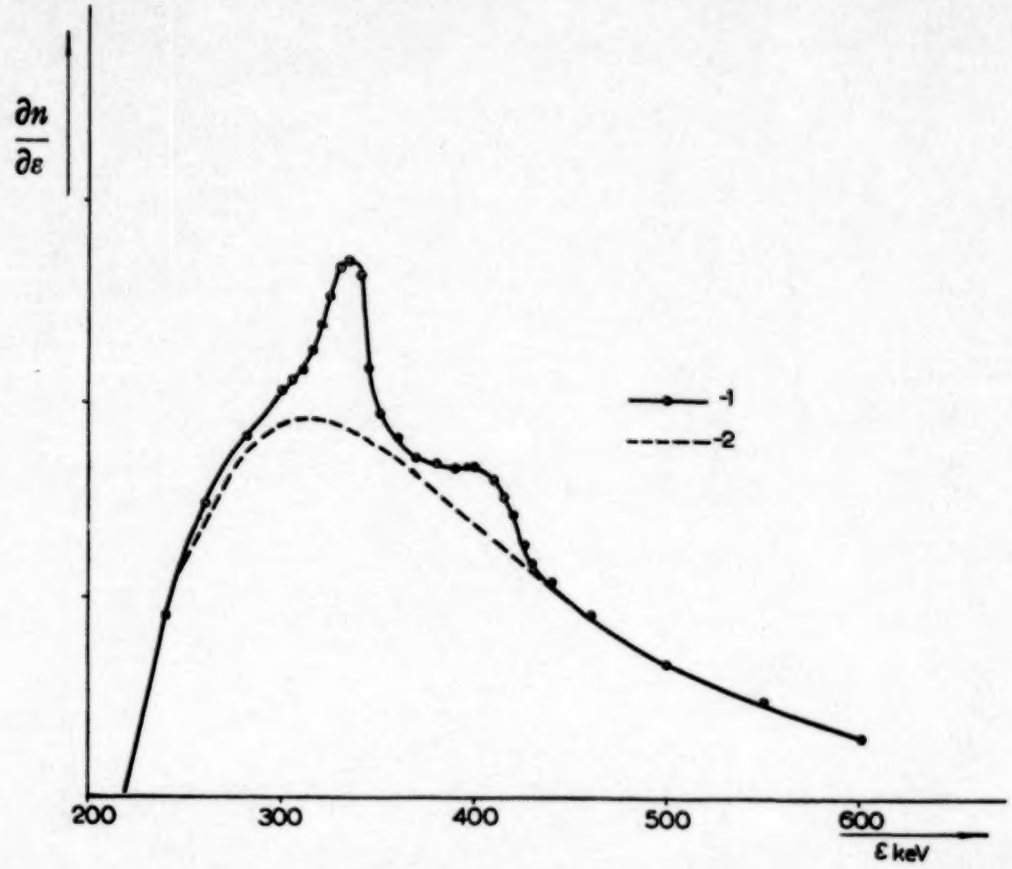

Fig. 3b. Spectrum of Au^{198} electrons experiencing double scattering and causing coincidence in Geiger counters ($\bar{\varepsilon}_3 = 390$ keV, $\rho_3 = 5.2$ mg/cm² Al, $\tau_3 = 13$ mg/cm² Au). 1. spectrum with conversion electrons; 2. spectrum without conversion electrons.

2) $\partial n_i/\partial \varepsilon$ is the same as above, but includes conversion electrons;

3) S is the azimuthal asymmetry in the scattering on mercury ($Z = 80$) of completely transversely polarized electrons with an energy ε; the relevant quantity has been taken from the Sherman tables [3]);

4) δ_g is the correction to account for the solid angles of the instrument;

5) δ_Z is the correction for the tabulated values of S due to scattering taking place on gold ($Z = 79$);

6) δ_{sh} is the correction due to the shielding effect. This correction was found on the basis of the data presented in ref.[5]) by extrapolating the results

to the energies with which we operated. The correction was calculated by K. A. Ter-Martirosyan;

7) $(1-\frac{1}{2}\theta)$ is the depolarization in the source; θ^2 is the mean square of the multiple-scattering angle [6]). These values, as a function of energy, are listed in table 2.

8) $\langle\sigma_\perp\rangle_i$ is the perpendicular spin component relative to the trajectory of an electron of energy ε deflected through an angle of 90° as a result of multiple scattering in scatterer I possessing a thickness τ_i. The magnitude of this projection was computed by the Monte Carlo method by G. Adelson-Velsky, A. Birzgal and A. Kronrod on an electronic computer †. A correction for depolarization of the electrons in scatterer I is included.

Depolarization is due to deflection of the electron spin in the electric field of the nucleus. Depolarization does not occur if multiple scattering of the electron occurs in a plane formed by the trajectories of the electron before it entered the scatterer and after exit from the scatterer (providing the electron trajectory is not a closed loop). Polarization occurs if the electron leaves this plane during scattering.

Calculations show that the deflection of the electron spin due to multiple deflection in a Coulomb field is approximately 5 % smaller than that predicted by the "condenser", formula

$$\varphi = \psi(1-\sqrt{1-v^2})$$

A family of curves $\langle\sigma_\perp\rangle_i$ for various energies of electrons scattered from scatterer I of different thicknesses τ_i is presented in fig. 4.

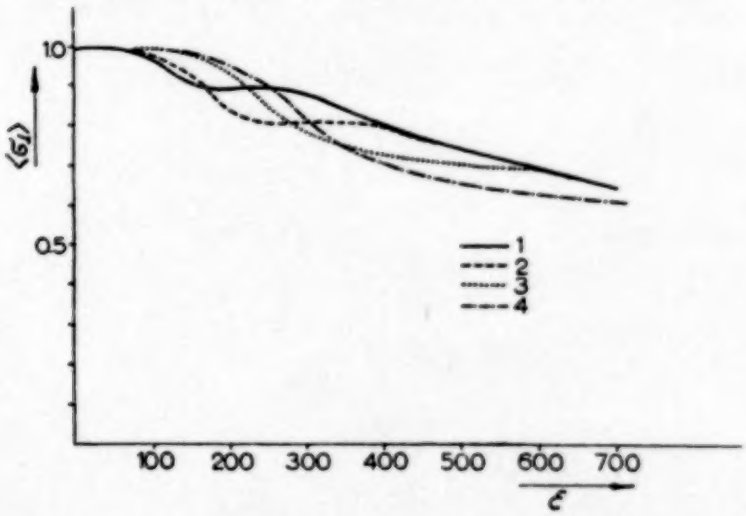

Fig. 4. Dependence of perpendicular spin component on energy of electron deflected through an angle of 90° with respect to the initial direction; the deflection is a result of multiple scattering in scatterer I whose thickness is
1. $\tau_1 = 3.0$ mg/cm² Au; 2. $\tau_2 = 6.0$ mg/cm² Au; 3. $\tau_3 = 13.0$ mg/cm² Au; 4. $\tau_4 = 20.0$ mg/cm² Au.

† The authors are indebted to I. S. Bruk, Head of the Guidance Machine Laboratory of the USSR Academy of Sciences, for providing the opportunity to perform these calculations.

TABLE 2

ε(keV)	70	100	150	200	250	300	400	500	600	700	800	900	1000	1200	1400
v	0.48	0.55	0.63	0.69	0.74	0.77	0.83	0.86	0.89	0.91	0.92	0.93	0.94	0.95	0.96
S	0.38	0.39	0.40	0.41	0.40	0.39	0.37	0.35	0.33	0.31	0.29	0.28	0.25	0.22	0.17
$100(\delta_e-1)$	−5.2	−5.5	−6.2	−6.8	−7.3	−7.7	−8.1	−7.8	−7.1	−6.2	−5.1	−4.1	−3.0	−2.0	−1.5
$100(\delta_Z-1)$	−2.3	−2.3	−2.2	−2.1	−2.0	−1.9	−1.8	−1.7	−1.7	−1.6	−1.5	−1.5	−1.4	−1.4	−1.4
$100(\delta_{sh}-1)$	−11.0	−6.5	−1.3	0	0	0	0	0	0	0	0	0	0	0	0
$(1-\frac{1}{2}\theta^2)_{Sr+Y}$	0.89	0.94	0.97	0.98	0.99	0.99	1.00	1.00	1.00	1.00	1.00	1.00	1.00	1.00	1.00
$(1-\frac{1}{2}\theta^2)_{Tm}$	0.93	0.97	0.98	0.99	0.99	1.00	1.00	1.00	1.00	1.00	1.00	1.00	1.00	1.00	1.00
$(\Delta_{th})_{Sr+Y}$	25	33	41	44	44	44	40	37	34	30	28	25	23	17	12
$(\Delta_{th})_{Tm,Sm}$	26	34	41	45	44	44	40	37	34	30	28	25	23	17	12
$(\Delta_{th})_{Lu,Re}$	28	35	42	45	44	44	40	37	34	30	28	25	23	17	12

TABLE 3

Element	$Sr^{90}+Y^{90}$	Tm^{170}	Sm^{153}	Lu^{177}	Re^{186}	Au^{198}	average
$\langle\bar{\sigma}\rangle/(-v)$	0.99 ± 0.037 (±0.05)	0.98 ± 0.015 (±0.03)	0.98 ± 0.037 (±0.05)	1.00 ± 0.058 (±0.06)	1.06 ± 0.106 (±0.11)	0.97 ± 0.055 (±0.06)	0.98 ± 0.01 (±0.03)

Values of electron longitudinal polarization $\langle\bar{\sigma}\rangle/(-v)$ averaged over the energy. Statistical errors are indicated in the table. Errors taking into account systematic corrections are between brackets.

Details of the calculations will be published separately by their authors.

The expected azimuthal asymmetry values Δ_{th} for Tm, Lu, Re, Au, Sm and Sr + Y for different energies, calculated with the aid of these spectra, are listed in table 1.

4. Discussion of the Results

The longitudinal polarization values in $-v$ units $\langle\sigma\rangle_i/(-v) = \Delta_{0\,corr}/\Delta_{th}$ are presented in fig. 5 for various values of energy. It is evident from these data that the electron polarization $\langle\sigma\rangle_i/(-v)$ of all the measured

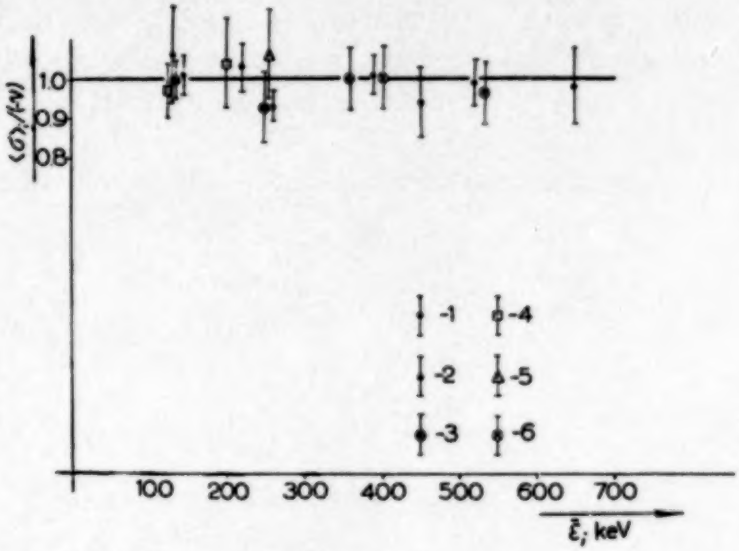

Fig. 5. Electron longitudinal polarization $\langle\sigma\rangle_i/-v$ at different energies.
1. $Sr^{90}+Y^{90}$; 2. Tm^{170}; 3. Sm^{153}; 4. Lu^{177}; 5. Re^{186}; 6. Au^{198}.

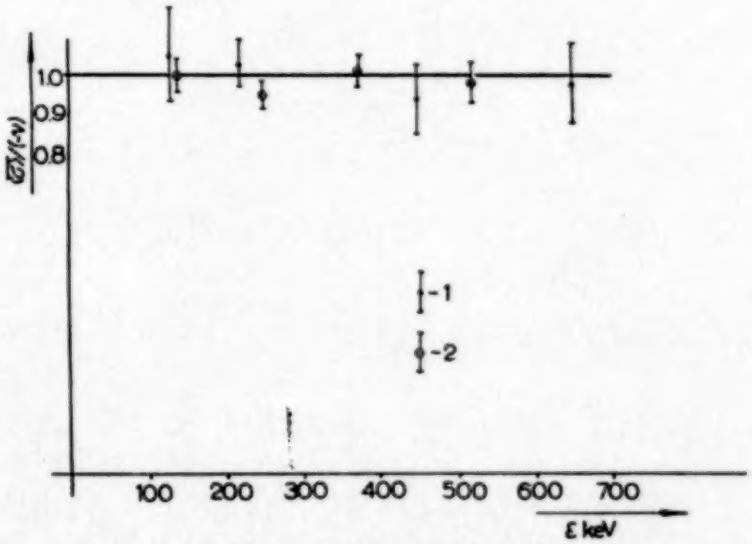

Fig. 6. The energy dependence of longitudinal electron polarization $\langle\bar{\sigma}\rangle/-v$ for Coulomb transitions.
1. $Sr^{90}+Y^{90}$; 2. Coulomb transitions.

elements does not, within experimental error, depend on energy. Table 3 lists the $\langle\bar{\sigma}\rangle/(-v)$ values for the investigated elements, averaged over energy. The mean values of $\langle\bar{\sigma}\rangle/(-v)$ as a function of energy for Coulomb transitions as compared with the polarization of $Sr^{90}+Y^{90}$ electrons are given in fig. 6.

The following conclusions may be drawn from these data:

1. The longitudinal polarizations of the electrons of all measured elements are identical to within (2—11) %. (The overall errors given do not include errors due to the systematic corrections which are identical for all elements).

2. The electron longitudinal polarization is equal to $-v$ to within ≈ 3 % on the average for all elements.

3. With an accuracy of (4—7) % the longitudinal polarization of Coulomb transition electrons does not depend on the energy in the 100—600 keV interval.

For first forbidden Coulomb transitions the longitudinal polarization may be represented as [7])

$$W\cdot\langle\sigma_E\rangle/v=2\mathrm{Re}\left\{(C_S C_S'^*-C_V C_V'^*)|M_F|^2+(C_T C_T'^*-C_A C_A'^*)\,(|M_{GT}|^2+|M_{GT}'|^2)\right.$$
$$\left.+\frac{Z}{137Ev}\,[(C_T C_V'^*+C_T' C_V^*)M_F^* M_{GT}-(C_S C_A'^*+C_S' C_A^*)M_F\cdot M_{GT}^*]\right\}$$
$$-2\,\mathrm{Im}\left\{-(C_T C_S'^*-C_A C_V'^*)M_F^* M_{GT}+(C_T'^* C_S-C_A'^* C_V)M_F\cdot M_{GT}^*\right.$$
$$\left.+\frac{Z}{137Ev}\,[(C_S C_V'^*+C_S' C_V^*)|M_F|^2+(C_T C_A'^*+C_T' C_A^*)\,(|M_{GT}|^2+|M_{GT}'|^2)]\right\},$$

$$W=(|C_T|^2+|C_T'|^2+|C_A|^2+|C_A'|^2)(|M_{GT}|^2+|M_{GT}'|^2)$$
$$+(|C_S|^2+|C_S'|^2+|C_V|^2+|C_V'|^2)|M_F|^2$$
$$-2\mathrm{Im}\,[(C_T^* C_S+C_T'^* C_S'+C_A^* C_V+C_A'^* C_V')M_F\cdot M_{GT}^*]$$
$$-\frac{2\gamma_1}{E}\cdot\mathrm{Re}\,[(C_S C_V'^*+C_S' C_V'^*)|M_F|^2+(C_T C_A'^*+C_T' C_A'^*)\,(|M_{GT}|^2+|M_{GT}'|^2)]$$
$$+\frac{2\gamma_1}{E}\,\mathrm{Im}[(C_S C_A'^*+C_S' C_A'^*)M_F\cdot M_{GT}^*-(C_T C_V'^*+C_T' C_V'^*)M_F^* M_{GT}]$$

where E is the total electron energy in mc^2 units, and $\gamma_1=\sqrt{1-(Z/137)^2}$.

On the basis of our data the expression $\langle\sigma_E\rangle$ may be assumed to equal $-v$, irrespective of the energy or of the values of the matrix elements (since the electron polarization for the measured substances is identical, and different substances must have different matrix elements). We then obtain 9 equations for the coupling constants:

$$|C_S+C'_S|^2+|C_V-C'_V|^2 = 0 \quad (1)$$

$$|C_T+C'_T|^2+|C_A-C'_A|^2 = 0 \quad (2)$$

$$\mathrm{Re}(C_S C_V^*+C'_S C'^*_V) = 0 \quad (3)$$

$$\mathrm{Re}(C_T C_A^*+C'_T C'^*_A) = 0 \quad (4)$$

$$\mathrm{Im}(C_S C'^*_V+C'_S C_V^*) = 0 \quad (5)$$

$$\mathrm{Im}(C_T C'^*_A+C'_T C_A^*) = 0 \quad (6)$$

$$\mathrm{Re}(C_T C'^*_S+C_S C'^*_T-C_V C'^*_A-C_A C'^*_V+C_T C_S^*+C'^*_T C'_S+C_A C_V^*+C'^*_A C'_V)=0 \quad (7)$$

$$\mathrm{Re}(+C_S C_A^*+C'_S C'^*_A+C_T C_V^*+C'_T C'^*_V) = 0 \quad (8)$$

$$\mathrm{Im}(+C_S C'^*_A+C'_S C_A^*+C_T C'^*_V+C'_T C_V^*) = 0. \quad (9)$$

It is easy to see that the maximum number of relationships has been obtained, which can be determined from experiments involving measurement of the longitudinal polarization of the electrons from non-polarized nuclei. Eqs. (3)—(4) were obtained earlier (absence of Fierz terms). Eqs. (1)—(2) were obtained from measurements of the longitudinal polarization (with an accuracy of 10—20 %) in allowed and other transitions without measurement of the energy dependence of polarization [8]).

The relationships

$$C_S = -C'_S, \quad C_T = -C'_T, \quad C_V = C'_V, \quad C_A = C'_A$$

follow from eqs. (1)—(2).

If these relationships are valid, this is the maximum information that can be obtained from the value of the longitudinal polarization of electrons emitted from non-polarized nuclei. Indeed, in this case all the equations are identically satisfied. However, the accuracy with which these relationships can be obtained from equations (1)—(2) is not high. For the sake of simplicity let there be only one type of interaction, T. Then

$$|C_T+C'_T|^2 = \delta(|C_T|^2+|C'_T|^2)$$

where δ indicates how much the electron polarization differs from $-v$. In our case this is the precision of the measurements, and is 0.03.

In a first approximation

$$C_T = -C'_T(1+\alpha), \quad \alpha^2 = 2\delta = 0.06,$$
$$\therefore \alpha \approx 0.25.$$

The relation between the constants can thus be determined from eqs. (1)—(2) with a precision no better than 20—30 %.

Let us consider another possibility. Suppose that the constants $|C|$ and $|C'|$ are equal in absolute value and $C = -C'$, which is precisely the case in a 2-component neutrino model. Moreover, it must be assumed that $|C_V|$

and $|C_A|$ are small as required by the available experimental data [8]). For the sake of simplicity we shall consider only tensor and vector interactions. Then for the allowed transitions, which lead only to eqs. (1)–(2), we obtain

$$\frac{-|C_T|^2|M_{GT}|^2+|C_V|^2|M_F|^2}{|C_T|^2|M_{GT}|^2+|C_V|^2|M_F|^2} = -\frac{1-|\rho|^2}{1+|\rho|^2} \approx -(1-2|\rho|^2)$$

$$\therefore |\rho| = \frac{|C_V||M_F|}{|C_T||M_{GT}|} \approx 0.2,$$

since $2|\rho|^2 = 0.1$ is the highest accuracy with which electron polarization for allowed transitions has yet been measured.

For electron polarization in Coulomb transitions and its energy dependence, eqs. (3)–(9) are also valid, as stated above. Eqs. (3)–(6), (8), (9) are the most sensitive to the relations between the constants. It follows from these equations that the following relations must obtain between the coupling constants:

$$\frac{C_T}{C'_T} = \frac{C'_S}{C_S} = -\frac{C_V}{C'_V} = -\frac{C'_A}{C_A}.$$

From the negative polarization of the negatons, say, of Sr^{90} (pure Gamov-Teller transition) and from the positive polarization of Cl^{34} positons (pure Fermi transition) [9]), it follows, assuming $|C| = |C'|$, that

$$C_T = -C'_T, \quad C_S = -C'_S, \quad C_V = C'_V, \quad C_A = C'_A,$$

the accuracy of these equalities being higher.

Indeed, for electron polarization in the event of a Coulomb transition we have in the case under consideration

$$\frac{-|C_T|^2|M_{GT}|^2+|C_V|^2|M_F|^2 \pm \frac{2Z}{137Ev} C_T C_V^* |M_{GT}||M_F|}{|C_T|^2|M_{GT}|^2+|C_V|^2|M_F|^2} = -\frac{1-|\rho|^2 \pm \frac{2Z}{137Ev}\rho}{1+|\rho|^2} \approx -1 \pm 1.5\rho$$

with $Z/137 \approx 0.5$, $E \approx 1.2$, $v \approx 0.6$; whence, since $1.5\rho \approx 0.05$,

$$\rho = \frac{C_V^*|M_F|}{C_T^*|M_{GT}|} \approx 0.03.$$

Insofar as the electron polarization of all the measured Coulomb transitions is identical and it is improbable that the ratios $|M_F|/|M_{GT}|$ for all of them should be small to the same extent, it follows that the contribution of vector interaction in which $C_V = -C'_V$ should be very small. This is likewise true for axial-vector interaction.

On the basis of the above considerations we conclude that the results presented in this paper on the electron longitudinal polarization for Coulomb transitions and its energy dependence, most probably point to the following relationships between the coupling constants in β-decay:

$$C_T = -C'_T, \quad C_S = -C'_S, \quad C_V = C'_V, \quad C_A = C'_A.$$

These relations correspond to a 2-component electron model. Thus the results of the present experiment are consistent with the 2-component neutrino model only if the pair of coupling constants for vector and axial-vector interaction or the pair for scalar and tensor interaction vanish.

The authors consider it their pleasant duty to express their thanks to K. A. Ter-Martirosyan, who calculated some of the corrections in the present experiment and who took an active part in discussing the results obtained, to G. Adelson-Belsky, A. P. Birzgal, A. S. Kronrod and V. B. Berestetsky, who calculated the correction for electron depolarization in multiple scattering, to E. F. Tretyakov and G. Grishuk, who measured the spectra of Au^{198} and Lu^{177} electrons which experienced multiple scattering at $\approx 90°$, and to M. P. Anikina, who prepared the β-active sources, as well as to B. L. Ioffe and A. P. Rudik for their participation in the discussion.

References

1) C. S. Wu, E. Ambler, R. W. Hayward, D. D. Hoppes and R. P. Hudson, Phys. Rev. **105** (1957) 1413;
R. L. Garwin, L. M. Lederman and M. Weinrich, Phys. Rev. **105** (1957) 1415
2) T. D. Lee and C. N. Yang, Phys. Rev. **104** (1956) 254;
L. Landau, Nuclear Physics **3** (1957) 127;
T. D. Lee and C. N. Yang, Phys. Rev. **105** (1957) 1671
3) N. Sherman, Phys. Rev. **103** (1956) 1601
4) L. Artsimovich, JETP **9** (1939) 927
5) C. B. O. Mohr and L. F. Tassic, Proc. Phys. Soc. **67** (1954) 711
6) Experimental Nuclear Physics, edited by Segrè, pp. 239–241 and 247–257
7) V. B. Berestetsky, B. L. Ioffe, A. P. Rudik and K. A. Ter-Martirosyan, Phys, Rev. (in print)
8) H. Frauenfelder, R. Bobone, E. von Goeler, N. Levine, H. R. Levis, R. N. Peacock, A. Rossi and G. de Pasquali, Phys. Rev. **106** (1957) 386;
A. I. Alikhanov, G. P. Eliseiev, V. A. Liubimov and B. V. Ershler, JETP **32** (1957) 1344;
M. E. Vishnevsky, V. K. Grigoriev, V. A. Yergakov, S. Ya. Nikitin, Ye. V. Pushkin and Yu. V. Trebukhovsky, Nuclear Physics **4** (1957) 271;
P. E. Cavanagh, I. E. Turner, C. E. Coleman, C. A. Card and B. W. Ridley (in print);
N. Benezer Koller, A. Schwarzschild, I. B. Vise and C. S. Wu, Phys. Rev. (in print);
F. Boehm, T. Novey, C. Barnes and B. Stech (in print)
9) M. Deutsch, B. Gittelman, R. W. Bauer, L. Grodzyns and A. W. Sunyar, Phys. Rev. **107** (1957) 1733

3.A *Nuclear Physics* 7 (1958) 672—676; © *North-Holland Publishing Co., Amsterdam*
Not to be reproduced by photoprint or microfilm without written permission from the publisher

CORRÉLATION ANGULAIRE DES PAIRES MONOPOLAIRES DU CALCIUM 40

S. GORODETZKY, P. CHEVALLIER, R. ARMBRUSTER, A. GALLMANN et G. SUTTER
Institut de Recherches Nucléaires, Strasbourg

Received 1 May 1958

Abstract: The angular correlation of the internal pairs from the first excited level (3.35 MeV) of ^{40}Ca obtained in a(p, p′) reaction confirms that the transition from this level to the fundamental level 0^+ has the character of an electric monopole (E0).

1. Introduction

Le calcium 40 est un noyau doublement magique. On peut s'attendre ainsi [1]) à ce que son premier niveau excité (3.35 MeV) soit $J = 0^+$ et non $J = 2^+$. R. D. Bent, W. Bonner et J. H. McCrary [2]), utilisant la réaction ^{40}Ca (p, p′) ^{40}Ca, ont montré au moyen d'un spectromètre magnétique que ce niveau 3.35 MeV se désexcitait par émission de paires, aucun rayonnement gamma de la même énergie n'étant trouvé. R. B. Day [3]) utilisant la réaction ^{40}Ca (n, n′) ^{40}Ca a mis en évidence une ligne gamma de 508 keV dont le seuil correspond à une énergie de neutrons de 3.36 ± 0.05 MeV. Il interprète cette ligne comme étant due à la dématérialisation de positons provenant du premier niveau excité du ^{40}Ca.

Nous avons repris cette étude au moyen de la réaction ^{40}Ca (p, p′) ^{40}Ca en utilisant la méthode de corrélation angulaire des paires de conversion interne.

2. Dispositif Expérimental

La mesure de la corrélation angulaire des paires d'électrons a été faite au moyen du spectromètre beta que montre la fig. 1. Les cristaux sont des scintillateurs plastiques dont les dimensions sont telles que les électrons y perdent toute leur énergie. Le temps de résolution du circuit rapide est de $2\tau = 5 \times 10^{-9}$ sec, une coïncidence lente à 10^{-7} sec est faite entre la coïncidence rapide et les canaux de discrimination. De plus les canaux proportionnels sont ouverts par la coïncidence lente au moyen d'une porte fonctionnant à 10^{-6} sec. Les impulsions proportionnelles à l'énergie du négaton et du positon d'une même paire sont additionnées et envoyées sur un analyseur à 100 canaux RIDL. On obtient ainsi une raie de sommation corres-

spondant à l'énergie cinétique totale de la paire, c'est à dire à l'énergie de la transition étudiée moins 1.02 MeV. La résolution de la raie de somme est de 18 % pour la transition de 3.35 MeV du ^{40}Ca et de 14 % pour celle de 6.05 MeV de ^{16}O. Le calibrage en énergie des deux canaux proportionnels s'effectue au moyen de la raie de conversion interne (624 keV) du ^{137}Cs et des „Compton edges" des rayonnements gamma de 1.28 MeV du ^{22}Na et de 2.61 MeV du ThC" (fig. 2).

La boîte de corrélation est à fenêtres minces d'aluminium (1/10 mm) espacées chacune de l'autre de façon à avoir un angle multiple de 30° à partir de la cible.

La cible bombardée par des protons de 4.43 MeV était une pièce de calcium métallique naturel qui contient 96.97 % de ^{40}Ca. La discrimination utilisée était de 511 ± 25 keV afin d'éliminer toutes les coïncidences pouvant

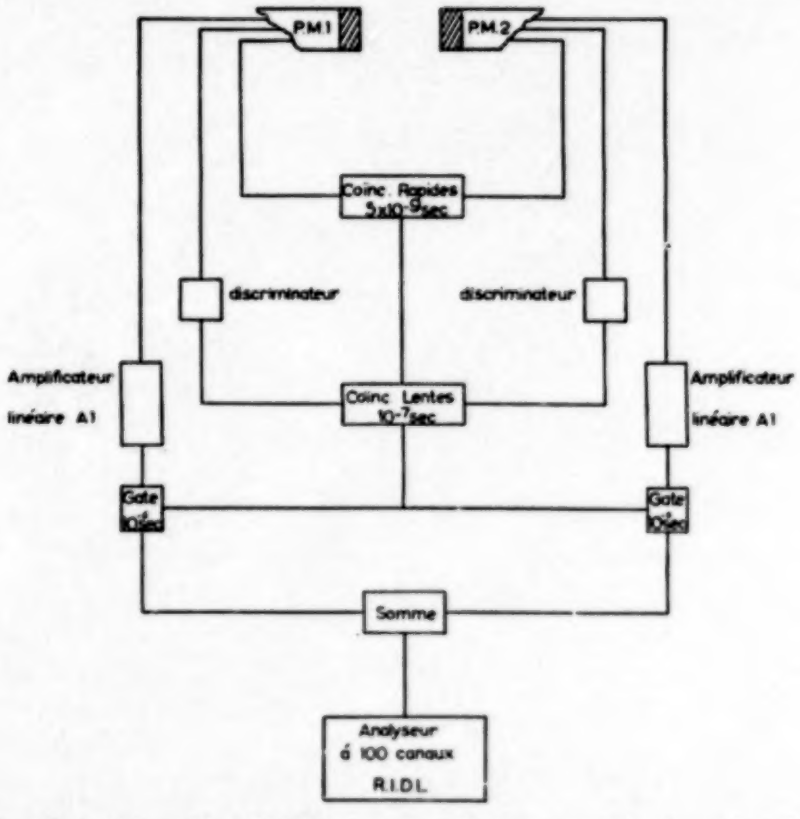

Fig. 1. Schéma du spectromètre utilisé pour la corrélation angulaire des paires de conversion interne. Les cristaux sont des scintillateurs plastiques dont le rendement lumineux est 60 % de celui d'un cristal d'anthracène.

être dues à des rayonnements gamma diffusés d'un cristal dans l'autre par choc Compton.

3. Résultats

La fig. 3 montre le résultat expérimental normalisé à l'angle 30° avec les courbes théoriques monopolaire électrique E0 et dipolaire électrique E1. Les

courbes théoriques correspondant à des modes de transition différents n'ont pas été calculées car se trouvant en dessous de la courbe E1.

La courbe théorique E0 est, compte tenu des corrections géométriques, de la forme

$$y = 1+(0.961\pm0.005)\cos\theta.$$

La courbe expérimentale tracée est

$$y = 1+0.955\cos\theta.$$

Nous avions, au préalable, fait une grossière courbe d'excitation de la radiation d'annihilation des positons avec un cristal NaI 1.5″ × 1.5″ utilisant les énergies de protons $E_p = 3$ MeV, 3.5 MeV, 4 MeV et 4.43 MeV. La raie de

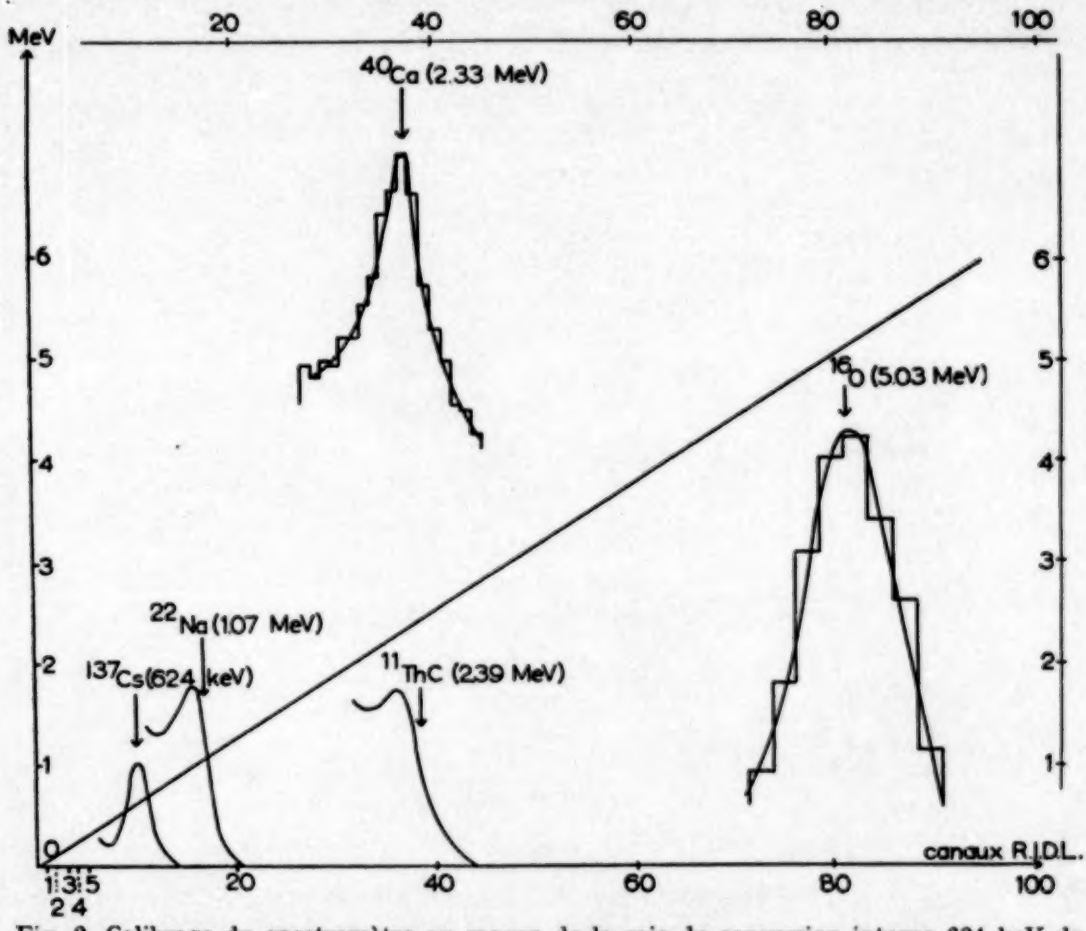

Fig. 2. Calibrage du spectromètre au moyen de la raie de conversion interne 624 keV du ^{137}Cs des „Compton edges" des rayonnements gamma 1.28 MeV de ^{22}Na et 2.62 MeV de ThC", la position de ceux-ci étant pris au $\frac{3}{4}$ de la hauteur maxima.
La figure montre également une raie de somme pour ^{16}O et ^{40}Ca à 30°. La raie de ^{40}Ca laisse apparaître un renflement sur le côté gauche ceci correspondant à des électrons sortant par les bords du cristal en fin de parcours. Ce phénomène n'est pas visible sur la raie de ^{16}O la discrimination utilisée dans ce cas étant de 2 MeV.

511 keV, invisible à 3 MeV et 3.5 MeV, apparaît très nettement à partir de 4 MeV.

Nous avons de plus, pour l'énergie utilisée $E_p = 4.43$ MeV, déterminé la proportion des rayonnements gamma 3.73 MeV et 3.90 MeV provenant des deuxième et troisième états excités du ^{40}Ca et de la radiation de 511 keV, car la résolution du spectromètre beta utilisé ne permet pas de distinguer parfaitement entre les paires provenant des niveaux 3.35 MeV, 3.73 MeV et 3.90 MeV. Cette analyse nous a permis de conclure que les paires provenant des niveaux 3.73 MeV et 3.90 MeV sont au moins 5000 fois moins importantes que celles provenant du niveau 3.35 MeV. Le nombre absolu de paires par protons a pu d'autre part être mesuré pour cette cible épaisse de ^{40}Ca : 2.5×10^{-9} paire/proton.

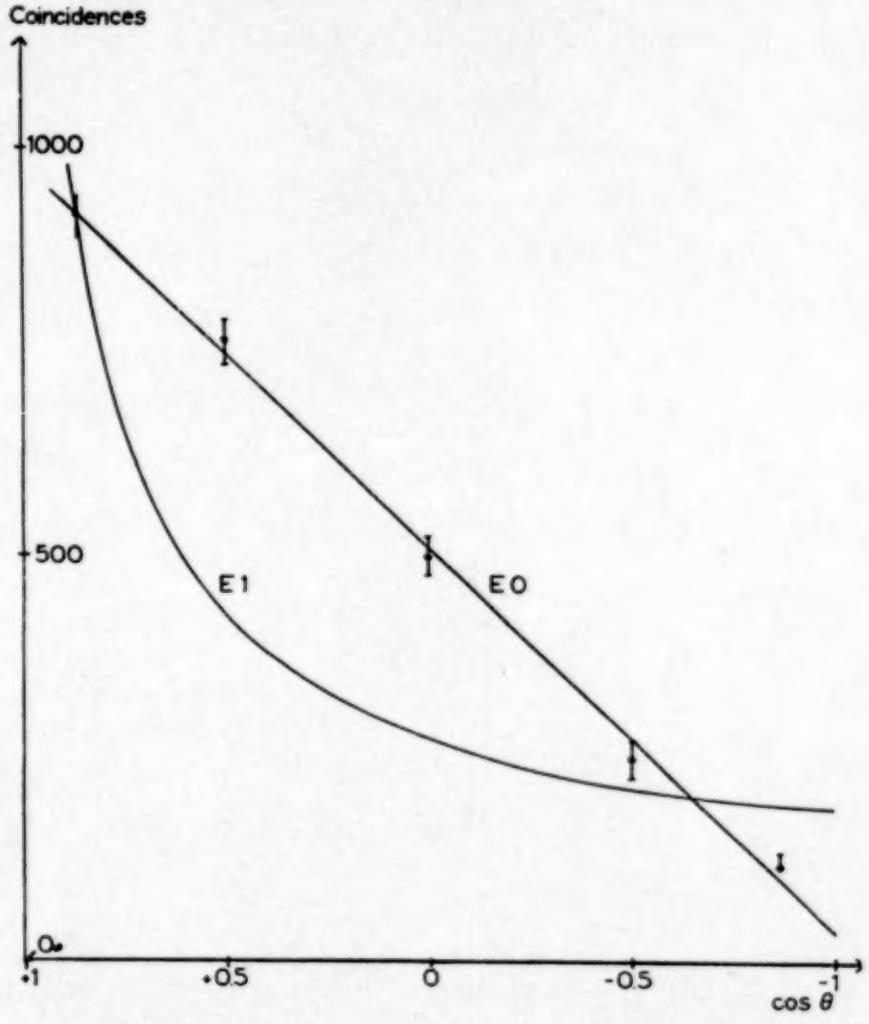

Fig. 3. Corrélation angulaire des paires monopolaires du ^{40}Ca.

Nous tenons à remercier le Centre d'Études Nucléaires de Saclay qui a mis obligeament à notre disposition l'accélérateur Van de Graaff de 5 MeV et nous sommes en particulier très reconnaissants à Monsieur Cotton pour l'aide qu'il nous a apportée dans la réalisation de ce travail.

Bibliographie

1) G. Sharff-Goldhaber, Phys. Rev. **90** (1953) 587
2) R. D. Bent, T. W. Bonner and J. H. McCrary, Phys. Rev. **98** (1955) 1325
3) R. B. Day, Phys. Rev. **102** (1956) 767

9.A *Nuclear Physics* 7 (1958) 677—686; © *North-Holland Publishing Co., Amsterdam*
Not to be reproduced by photoprint or microfilm without written permission from the publisher

INVESTIGATION OF EXTENSIVE AIR SHOWERS CONTAINING NUCLEAR ACTIVE PARTICLES

G. BOZÓKI, E. FENYVES, T. SÁNDOR and A. SOMOGYI
Central Research Institute of Physics, Department for Cosmic Rays, Budapest

Received 9 May 1958

Abstract: The exponent of the density spectrum of the electronic component of extensive air showers containing nuclear active particles was determined to be $\gamma = 1.34 \pm 0.08$ assuming that the density of nuclear active particles is proportional to the density of electrons in air showers. The agreement of the exponent found in the present experiment with that determined earlier for extensive air showers ($\gamma = 1.43 \pm 0.02$) with the same arrangement, which however, consisted only of the electron detectors supports the above assumption. From this it follows that the density spectrum of nuclear active particles has the form of a power law with an exponent approximately equal to γ. Furthermore, the decoherence curve between the electron and nuclear active particle detectors was measured. The experimental results are briefly discussed.

1. Introduction

In a course of measurements concerning the nuclear active component of extensive air showers we have investigated the density spectrum of air showers containing nuclear active particles.

Jánossy has pointed out earlier [1]) that in an extensive air shower arrangement consisting of n large counters of surface S an additional small counter of surface s has the effect of reducing by one the exponent of the "effective" density spectrum of those showers causing the $(n+1)$-fold coincidences between the $n+1$ counters of the arrangement. This means that if

$$s \ll S$$

the rate of the $(n+1)$-fold coincidences as a function of the surface of the large counters S will be given by †

$$c(S_1, S_2, \ldots S_n, s) = \text{const.}\, S^{\gamma-1} \tag{1}$$

where γ is the exponent of the unbiased integral density spectrum

$$N(x) = Hx^{-\gamma}. \tag{2}$$

The above considerations can be extended — as suggested by Jánossy — to the case of an extensive air shower arrangement consisting of n unshielded

† For a detailed discussion see ref. [1]).

counters (S) and a nuclear active particle detector the effective surface of which is not much larger than S †.

If we assume that the density of nuclear active particles is nearly proportional to the density of electrons — the constant factor being of the order of 10^{-2} for showers of energies and distances from the core as selected by the commonly used experimental arrangements, — then we can expect the nuclear active particle detector to have the same effect as a small unshielded counter.

On the other hand measuring the effective γ – value with an arrangement of the type described above the assumption as to the density of the nuclear active particles in an extensive shower can be checked [1]).

These considerations led us to measure the dependence of the frequency of extensive air showers containing energetic nuclear active particles (extensive penetrating showers) detected with an air shower arrangement [3]) and a penetrating shower detector [4]) connected in coincidence, on the surface S of the unshielded counters.

2. Experimental Arrangement

The arrangement consisted of four unshielded counter sets 1, 2, 3 and 4 serving as electron detectors and a detector N for nuclear active particles (fig. 1). Each unshielded set consisted of 10 counters, each counter having a sensitive surface of 320 cm². By using from 1 to 10 counters of each set the surface S of the unshielded sets could be varied from 320 to 3200 cm².

The detector N was a conventional penetrating shower arrangement (fig. 2) consisting of four trays A, B, C and D containing 10 counters each embedded in a lead block. The total amount of lead between the counter trays A and D was 170 g/cm² and the thickness of the absorber above the top counters A was varied in the course of the measurements between 110 and 230 g/cm² ††.

We have selected by means of discriminators the events by which at least two and three counters, respectively, of each of the sets A, B, C and D, each consisting of 10 counters, were discharged. Denoting these coincidences ($A_{\geq 2}, B_{\geq 2}, C_{\geq 2}, D_{\geq 2}$) and ($A_{\geq 3}, B_{\geq 3}, C_{\geq 3}, D_{\geq 3}$) by N_2 and N_3, respectively, we have measured the following coincidences between the detector of nuclear active particles N (selecting the events N_2 and N_3) and the unshielded counter sets 1—4: (N_2, 1), (N_3, 1), (N_2, 1, 2), (N_3, 1, 2), (N_2, 1, 2, 3, 4) and (N_3, 1, 2, 3, 4).

† About the bias introduced by a nuclear active particle detector on the density spectrum see also ref. [2]).

†† This change in the thickness of the top absorber had a negligible effect on the number of extensive penetrating showers and — what is more — the intensity of all penetrating showers (local and extensive) was not affected to any appreciable degree, the small changes of intensity being in both cases within the limits of the statistical errors.

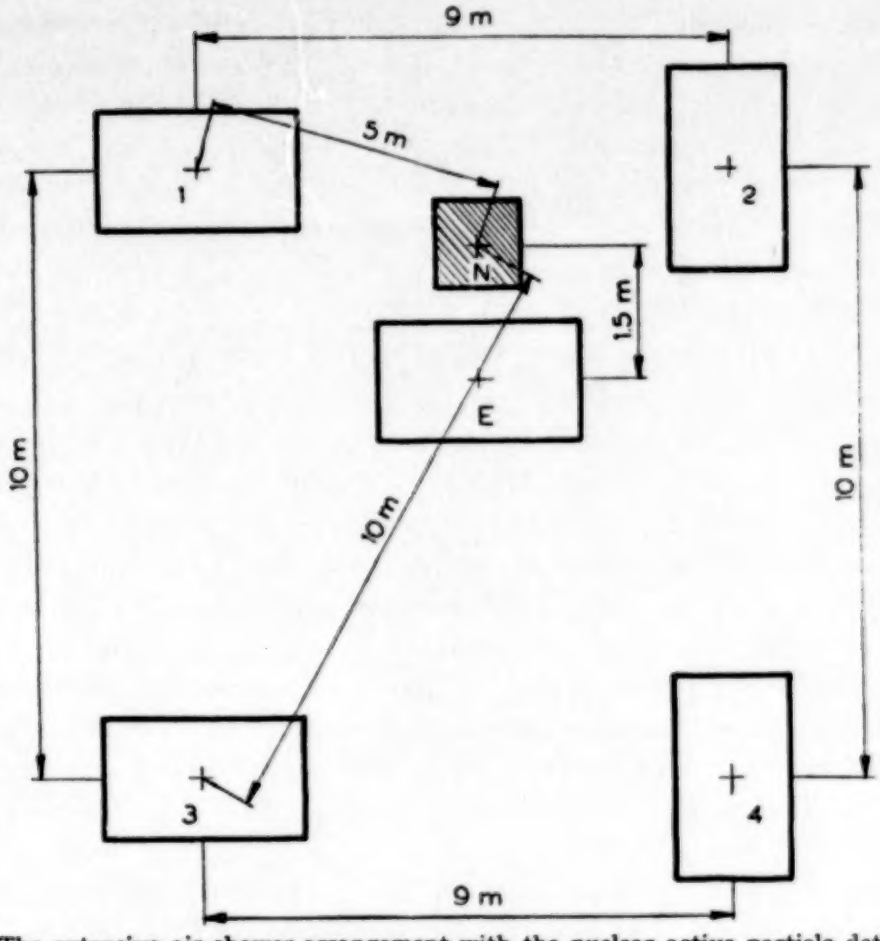

Fig. 1. The extensive air shower arrangement with the nuclear active particle detector N.

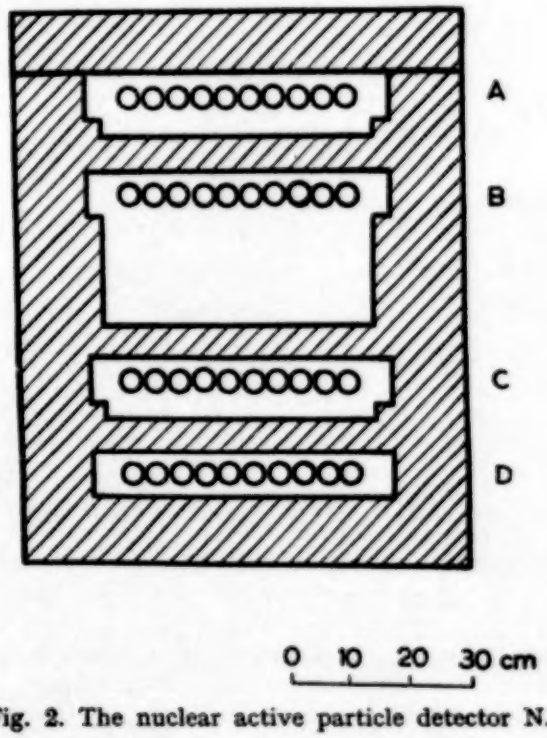

Fig. 2. The nuclear active particle detector N.

counters (S) and a nuclear active particle detector the effective surface of which is not much larger than S †.

If we assume that the density of nuclear active particles is nearly proportional to the density of electrons — the constant factor being of the order of 10^{-2} for showers of energies and distances from the core as selected by the commonly used experimental arrangements, — then we can expect the nuclear active particle detector to have the same effect as a small unshielded counter.

On the other hand measuring the effective γ – value with an arrangement of the type described above the assumption as to the density of the nuclear active particles in an extensive shower can be checked [1]).

These considerations led us to measure the dependence of the frequency of extensive air showers containing energetic nuclear active particles (extensive penetrating showers) detected with an air shower arrangement [3]) and a penetrating shower detector [4]) connected in coincidence, on the surface S of the unshielded counters.

2. Experimental Arrangement

The arrangement consisted of four unshielded counter sets 1, 2, 3 and 4 serving as electron detectors and a detector N for nuclear active particles (fig. 1). Each unshielded set consisted of 10 counters, each counter having a sensitive surface of 320 cm². By using from 1 to 10 counters of each set the surface S of the unshielded sets could be varied from 320 to 3200 cm².

The detector N was a conventional penetrating shower arrangement (fig. 2) consisting of four trays A, B, C and D containing 10 counters each embedded in a lead block. The total amount of lead between the counter trays A and D was 170 g/cm² and the thickness of the absorber above the top counters A was varied in the course of the measurements between 110 and 230 g/cm² ††.

We have selected by means of discriminators the events by which at least two and three counters, respectively, of each of the sets A, B, C and D, each consisting of 10 counters, were discharged. Denoting these coincidences ($A_{\geq 2}, B_{\geq 2}, C_{\geq 2}, D_{\geq 2}$) and ($A_{\geq 3}, B_{\geq 3}, C_{\geq 3}, D_{\geq 3}$) by N_2 and N_3, respectively, we have measured the following coincidences between the detector of nuclear active particles N (selecting the events N_2 and N_3) and the unshielded counter sets 1—4: (N_2, 1), (N_3, 1), (N_2, 1, 2), (N_3, 1, 2), (N_2, 1, 2, 3, 4) and (N_3, 1, 2, 3, 4).

† About the bias introduced by a nuclear active particle detector on the density spectrum see also ref. [2]).

†† This change in the thickness of the top absorber had a negligible effect on the number of extensive penetrating showers and — what is more — the intensity of all penetrating showers (local and extensive) was not affected to any appreciable degree, the small changes of intensity being in both cases within the limits of the statistical errors.

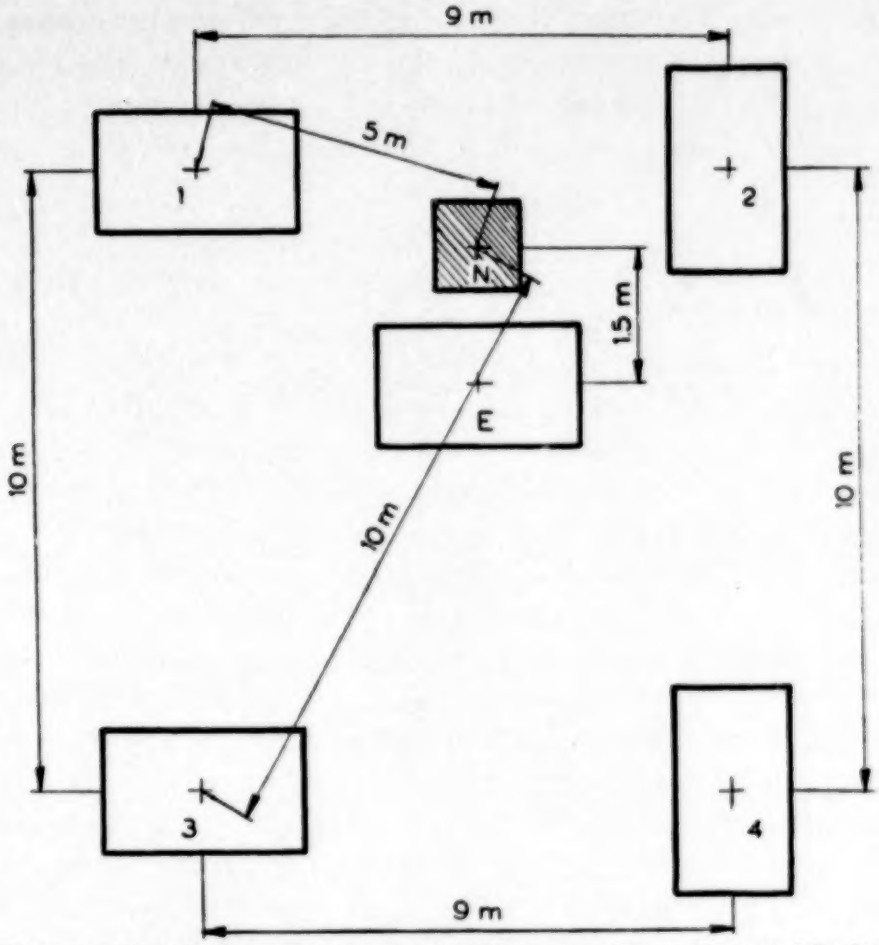

Fig. 1. The extensive air shower arrangement with the nuclear active particle detector N.

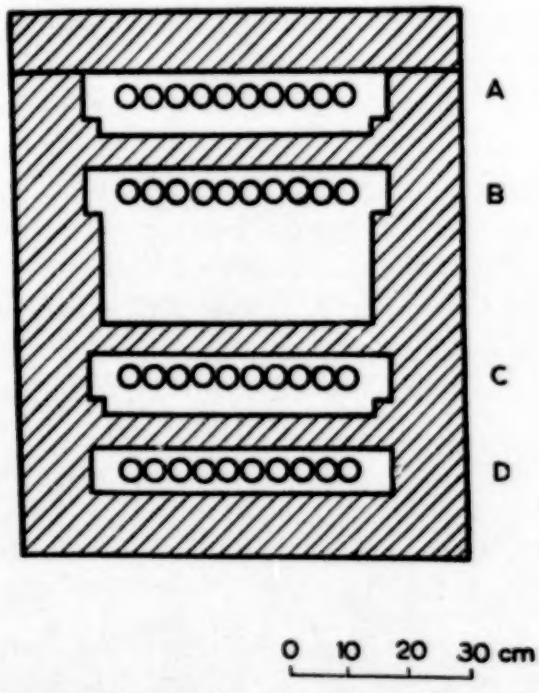

Fig. 2. The nuclear active particle detector N.

At a distance of 1.5 m from the detector N was placed a further unshielded set of counters (E) † identical with the sets 1—4 and the coincidences (N_2, E) and (N_3, E) were also measured. The measurements were carried out at Csillebérc, Budapest, 410 m above sea level.

3. Results

3.1. THE DENSITY SPECTRUM OF EXTENSIVE AIR SHOWERS CONTAINING NUCLEAR ACTIVE PARTICLES.

Practically all coincidences N_2 and N_3 were caused by nuclear disintegrations produced in the lead block by incoming nuclear active particles and thus the coincidences between N_2 (or N_3) and the unshielded counter trays were caused by extensive air showers containing nuclear active particles.

This statement is based on the estimation of the number of events N_2 and N_3 caused by the μ-meson component. The maximum value of the probability of discharging two or more counters of a counter set like the trays A, B, C or D by the μ-meson component, e.g. by μ-mesons and the knock-on showers produced by them in the lead block was experimentally determined for each counter set, the average value being approximately 3 % ††. From this value the maximum rate of coincidences N_2 expected to be caused by the μ-meson component was evaluated to be $\approx$ 0.01 c/h (and much less for N_3). This value is roughly 0.2 % of the rates for N_2 actually observed which varied between 4.84 ± 0.09 and 4.62 ± 0.12 c/h (and much less for the case of N_3) according to the thickness of absorber above the top counters.

Thus we can say that practically all detected cases were indeed caused by extensive air showers containing nuclear active particles.

As was pointed out in the introduction of this paper the detector N having a not too large effective surface may cause the same saturation effect as an additional small counter. The effective surface of the detector N cannot be determined exactly, but its order of magnitude can be easily estimated.

The surface of each counter tray A—D amounted to 1500 cm², the surface of the absorber in which nuclear disintegrations can be produced has the same order of magnitude and the efficiency of the detector for nuclear active particles passing through the top absorber is of the order of magnitude of 10^{-1}. Taking into account that the density of energetic nuclear active particles is about 1/100 of the density of electrons or less [5]) and further that the surface of electron detectors has the same order of magnitude as the surface of the detector N, the effect caused by the detector must be nearly equivalent to the effect of an additional counter of an effective surface three orders of magnitude smaller than that of the large ones.

† This tray served in another set of measurements for discriminating between local and extensive penetrating showers.

†† A detailed description of these measurements will be published elsewhere.

Thus we can expect, if our original assumptions are valid, that relation (1) holds, i.e. that the rate of extensive-penetrating showers varies with $S^{\gamma-1}$.

The measured rates of the various coincidences as functions of the surface S of the unshielded counter trays are given in table 1 and plotted in fig. 3.

TABLE 1

Rate of coincidences vs. surface

Type of coincidences	S(cm²)				
	320	640	960	1600	3200
(N_2, 1)	0.176±0.016		0.276±0.021		0.379±0.016
(N_3, 1)	0.095±0.015		0.155±0.019		0.240±0.018
(N_2, 1, 2)	0.112±0.012	0.155±0.013		0.189±0.035	0.241±0.013
(N_3, 1, 2)	0.058±0.012	0.104±0.015		0.130±0.025	0.150±0.015
(N_2, 1, 2, 3, 4)	0.093±0.011				0.200±0.017
(N_3, 1, 2, 3, 4)	0.046±0.010				0.091±0.014

Approximating the coincidence rate vs. surface curves by a power-law expression the respective exponents can be evaluated by the method of least squares; the values obtained are given in table 2.

TABLE 2

Type of coincidences	Exponent corresponding to the c/h vs S curve
(N_2, 1)	0.32±0.09
(N_3, 1)	0.39±0.16
(N_2, 1, 2)	0.31±0.10
(N_3, 1, 2)	0.33±0.19
(N_2, 1, 2, 3, 4)	0.34±0.15
(N_3, 1, 2, 3, 4)	0.30±0.27

The exponents thus obtained from the experimental curves are the same inside the limits of statistical errors. The different curves correspond to the same physical phenomenon and therefore the best value of the exponent γ can be evaluated by calculating the weighted mean value of the exponents obtained from the different experimental data.

The different combinations of coincidences between unshielded counter trays and N_2 or N_3 were measured simultaneously and did not give statistically independent information; during the first part of the measurements all

coincidences involving N_2 and during the second all those involving N_3 were counted.

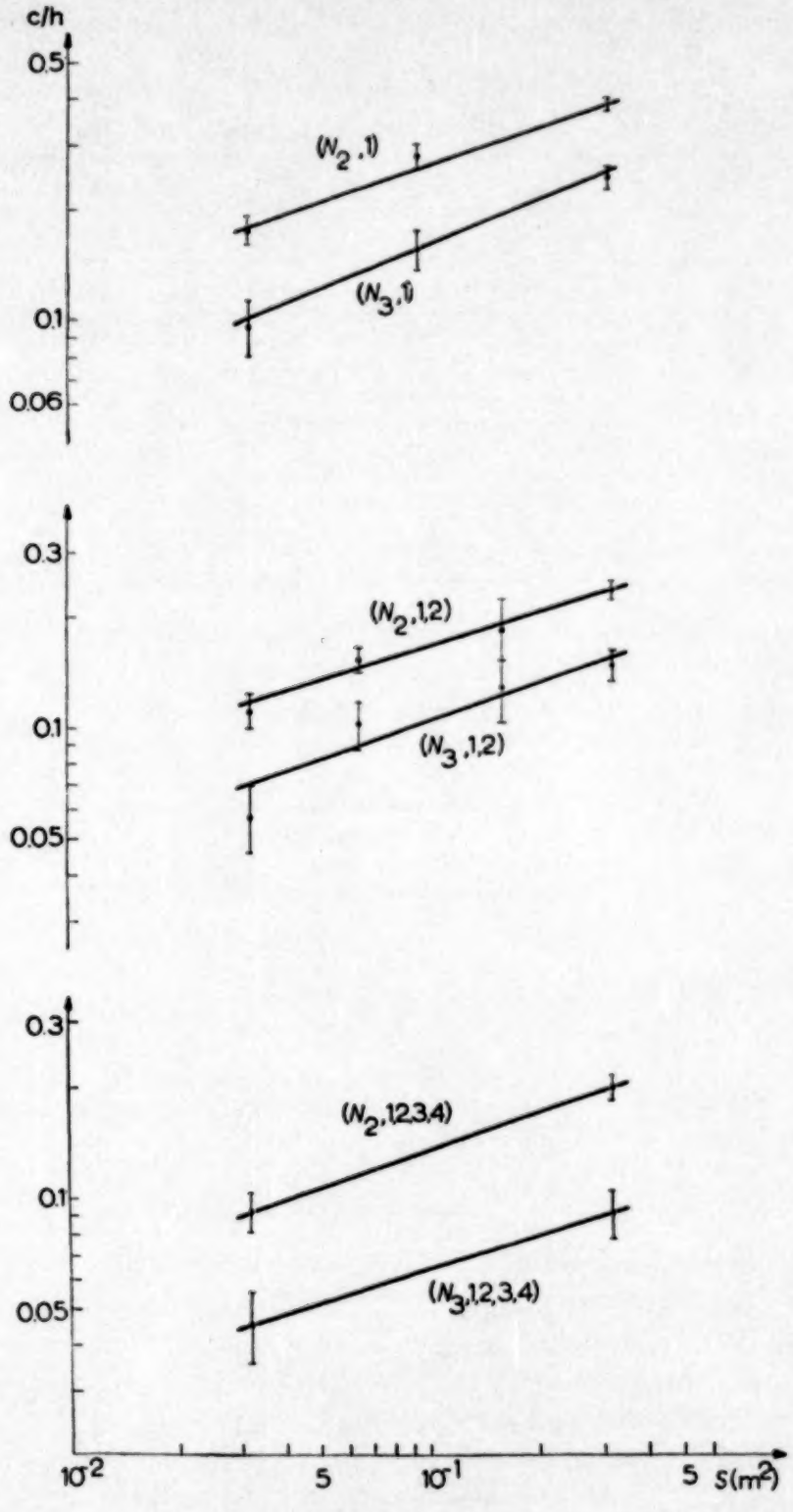

Fig. 3. The rate in c/h of coincidences vs. the surface S of the unshielded counter trays.

Thus, the rates of coincidence, giving the maximum independent information are (N_2, 1) and (N_3, 1). The mean value of the exponents corresponding to these curves is

$$\gamma - 1 = 0.34 \pm 0.08$$

and thus the exponent of the density spectrum of the electronic component of extensive air showers containing nuclear active particles is obtained as

$$\gamma = 1.34 \pm 0.08.$$

Some of the authors of the present investigations [3,6]) have determined earlier — using the same arrangement of unshielded counter trays and varying the surface S — the value of γ as

$$\gamma = 1.43 \pm 0.02.$$

This is in good agreement with the value found in the present experiment for extensive air showers containing nuclear active particles.

3.2. CHANGE OF THE RATE OF COINCIDENCES WITH THE DISTANCE BETWEEN THE ELECTRON DETECTOR AND THE DETECTOR OF NUCLEAR ACTIVE PARTICLES

Besides the above-mentioned coincidences we have measured the rate of coincidences between the detector and single electron detectors which were placed at various distances from the detector N : (N_2, E), (N_2, 1) (N_2, 3) and the same combinations with N_3, the corresponding distances being 1.5, 5 and 10 m.

The measured data are collected in table 3 and the decoherence curves plotted in fig. 4. In consequence of the poor statistics of the experimental data it is not possible to draw detailed conclusions from them and thus only an approximate treatment of the data can be given.

TABLE 3

Rate of coincidences vs. distance

Type of coincidences of the detector N	d(m)		
	1.5	5	10
N_2	0.459 ± 0.022	0.379 ± 0.016	0.401 ± 0.023
N_3	0.269 ± 0.018	0.240 ± 0.018	0.204 ± 0.025

The decoherence curves can be roughly approximated in the usual way by a power-law expression

$$c(d) = \text{const.}\ d^{-\beta} \qquad (3)$$

where $c(d)$ is the rate of coincidences, d the distance between the detector N and the electron detector and β the exponent of the decoherence curve.

It can be seen from the figure that the slopes of both curves are equal inside the statistical errors and the weighted mean value of β can be estimated as

$$\beta = 0.10 \pm 0.08.$$

If we assume, as we did in the determination of the value of γ that the density of the nuclear active component is proportional to the density of

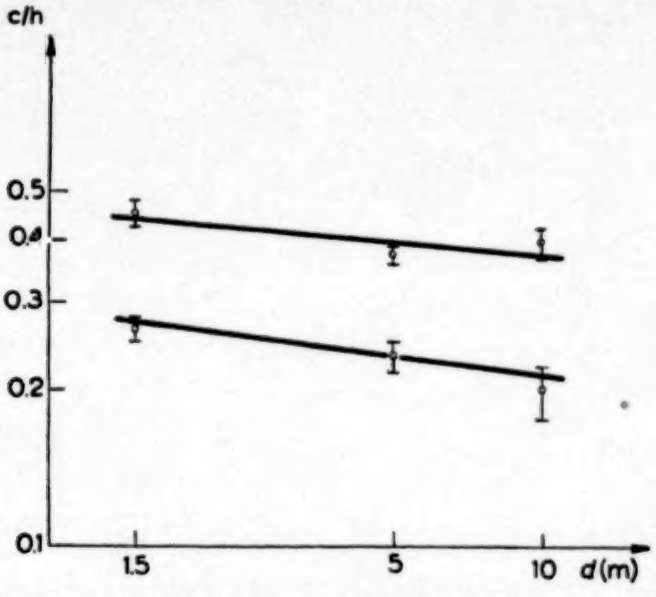

Fig. 4. The rate in c/h of coincidences vs. the distance d between the electron and nuclear active particle detectors.

electrons, we expect that the value of the above exponent is nearly equal to that of the decoherence curve measured with the unshielded counters only. Some of the authors have determined this value earlier with four unshielded counter trays, varying the length of the sides of the square in the corners of which the trays were placed [6,7]) as

$$\beta' = 0.20 \pm 0.01.$$

Taking into account the very great statistical error of the value of β determined in the present investigations the two values do not differ significantly, the result being thus not inconsistent with the original assumption concerning the proportionality between the densities of electrons and nuclear active particles.

4. Discussion

4.1. VALIDITY OF THE BASIC ASSUMPTION

The determination of the exponent of the density spectrum of extensive air showers containing nuclear active particles is based on the assumption that the density of nuclear active particles is — at least on the average — proportional to the density of electrons for showers of the energy range and

for distances from the core as selected by our experimental arrangement. This assumption is strongly supported by the good agreement between the values of γ found with the present arrangement for extensive penetrating air showers and for extensive air showers, respectively. Earlier investigations of extensive penetrating showers carried out by several authors [8,9,10,11]) gave also similar results (cf. § 4.2). Thus the proportionality — at least on the average — between the density of electrons and nuclear active particles in extensive air showers seems to be very probable.

From this it follows that the density spectrum of the nuclear active particles has the form of a power law with an exponent approximately equal to γ, the value found for the electronic component, i.e.

$$N(x_{\text{n.a.}}) = k \cdot x_{\text{n.a.}}^{-\gamma'}; \quad \gamma' \approx \gamma, \tag{4}$$

where $N(x_{\text{n.a.}})$ is the integral density spectrum of nuclear active particles and k is a constant.

4.2. COMPARISON WITH OTHER EXPERIMENTS

Similar experiments concerning the density spectrum of the electronic component of extensive penetrating showers were carried out near sea level by Broadbent and Jánossy[8]) and at mountain altitudes by Cool and Piccioni[9]) Anishtchenko *et al.*[10]) and Farrow [11]). The exponents of the density spectrum determined by these authors are collected in table 4.

TABLE 4

Author	Exponent corresponding to the c/h vs. S curve $(\gamma-1)$
Broadbent and Jánossy [8])	0.56 ± 0.10
Cool and Piccioni [9])	0.5
Anishtchenko *et al.* [10])	0.4
Farrow [11])	0.64
present exp.	0.34 ± 0.08

Taking into account the statistical errors (or the large inaccuracy of measurements, where the errors are not indicated) and the differing experimental conditions, there seems to be no significant disagreement between the result arrived at here and those published formerly.

Anishtchenko *et al.* point out that the exponent found by them for extensive penetrating air showers agrees well with the exponent ($\gamma = 1.4$) found earlier by Zatsepin *et al.*[12]) for extensive air showers, from which the proportionality between the densities of electrons and nuclear active particles follows.

Broadbent and Jánossy[8]) have measured also the decoherence curve and have found also a very slow decrease in the coincidence rate with increasing distance between the penetrating shower detector and the electron detectors. The value of β determined from their data by means of eq. (3) is (0.11 ± 0.08) and is in good agreement with the value found in the present experiment.

The authors are indebted to Prof. L. Jánossy for suggesting this experiment and his continuous interest in the work and many helpful discussions.

References

1) L. Jánossy, Colston Papers **1** (1949) 103
2) D. Broadbent and L. Jánossy, Proc. Roy. Soc. A **192** (1948) 364
3) J. Koch, T. Sándor, A. Somogyi and J. Szivek, Reports of the Central Research Institute of Physics **1** (1953) 61 (in Hungarian)
4) G. Bozóki, E. Fenyves and L. Jánossy, Reports of the Central Research Institute of Physics (in the press)
5) K. Greisen, The Extensive Air Showers, Progress in Cosmic Ray Physics III (North Holland Publ. Co., Amsterdam, 1956)
6) L. Jánossy, Nuovo Cimento Suppl. **1** (1955) 247
7) T. Sándor and A. Somogyi, Reports of the Central Research Institute of Physics **2** (1954) 466 (in Hungarian)
8) D. Broadbent and L. Jánossy, Proc. Roy. Soc. A **191** (1947) 517
9) R. L. Cool and O. Piccioni, Phys. Rev. **82** (1951) 306
10) J. W. Anishtchenko, G. I. Zatsepin, I. L. Rosenthal and L. I. Saritcheva, JETF **22** (1952) 143
11) L. A. Farrow, Phys. Rev. **107** (1957) 1687
12) G. T. Zatsepin, V. V. Miller, I. L. Rosenthal and L. H. Eidus, JETF **17** (1947) 1125

Nuclear Physics **7** (1958) 687—690; © *North-Holland Publishing Co., Amsterdam*

BOOK REVIEWS

I. EMIN (Editor), *Russian-English glossary of solid state physics* (Consultants Bureau, New York 1958. 90 pages. $ 10).

This is one instalment of a comprehensive glossary in course of publication. The method seems to have been to collect the technical terms and phrases occurring in the recent volumes of the specialized Russian journals.

L.R.

L. LANDAU and Y. SMORODINSKY, *Lectures on nuclear theory* (1955) (Consultants Bureau, New York 1958. 83 pages. $ 15).

We have here a real jewel of an elementary introduction into the main concepts of nuclear theory: with extremely simple means, the authors succeed in leading the reader straight into the heart of the matter: they present him (in spite of their modest disclaimer) with a comprehensive survey of the subject, always bringing out the essential points with admirable lucidity, and leave him well-armed for a more detailed study. This book should be in the hands of every student; to this end, however, it ought to be reprinted in book form at a reasonable price.

L.R.

O.E.E.C. (Editor), *The industrial challenge of nuclear energy: II. Research, uses, social problems* (European Productivity Agency of the OEEC, Paris 1958. 301 pages. 20 s.)

The Organisation for European Economic Co-operation publishes in book form the complete proceedings of its second 'information conference on nuclear energy for management' held at Amsterdam on 24—28 June 1957. It forms an authoritative and comprehensive review of the main technical and economic aspects of the question, with some account of the scientific background, which cannot fail to be extremely useful to wide sections of the public. The various topics are ably treated by experts, addressing an audience of industrialists and administrators. The only 'social problems' deemed of interest for this audience are those concerned with protection from the effects of radioactivity.

The interest of this excellent survey of the present situation would have been enhanced still further if it had relied less exclusively on American experience, and included more information about comparable developments in the Soviet Union. This lack of balance appears to be connected with the set-up of the Organisation sponsoring the conference: from the extremely interesting and spirited contribution of Prof. L. Nicolaidis on 'Nuclear energy in Europe' (p. 31—42), one gathers that although the OEEC Agency 'has no political aims' (p. 39) it may be hampered by political interference; the purchases of fissile material from American producers, e.g., 'are not always free from conditions other than commercial, and are subject to conditions associated with control which encroach upon national sovereignty' (p. 35). When Prof. Nicolaidis speaks of 'Free Europe' (p. 32), he no doubt uses the word 'free' in the propitiatory sense in which his ancestors called the stormy Black Sea 'hospitable'.

L.R.

M. BAYET, *Physique électronique des gaz et des solides* (Masson, Paris 1958. 246 pages. 4900 fr. fr.)

L'auteur a rassemblé dans ce livre, sous forme très résumée, les idées théoriques principales qui gouvernent l'analyse des phénomènes variés et compliqués de la conduction électronique dans les gaz et les solides. Pour le développement de ces idées et la description détaillée des phénomènes, il renvoie à un petit nombre de traités spéciaux, bien choisis. Le traitement du sujet est surtout classique (il comprend un bon résumé de la théorie des plasmas); les aspects quantiques ne sont mentionnés que très sommairement. L'ensemble, caractérisé par la traditionnelle clarté d'exposition des ouvrages pédagogiques français, constitue un utile vade-mecum pour l'étudiant et le spécialiste.

L.R.

A. Sokolow, *Quantenelektrodynamik* (Akademie-Verlag, Berlin, 1957, X-324 pages. DM 29.)

This book is a somewhat enlarged and revised German translation of the first part of the work entitled 'The Quantum Theory of Fields' which appeared in Russian in 1952. (The second part, an introduction to the general theory of elementary particles, was written by Prof. D. Ivanenko and has also been translated into German.) The present work aims at giving a rather thorough treatment of what one may now call 'classical quantum electrodynamics', i.e. a survey of the basic properties of free and interacting photons and electrons, presenting in a very elaborate way the actual calculation methods and working out the results in great detail. Hereby the author prefers to dwell very much on the calculational side of the individual selected topics rather than to give an exhaustive treatment of the more recent basic questions and problems connected with quantum field theory. From this follow all the virtues and drawbacks of the book.

The first, introductory, chapter deals with the properties and canonical quantisation of scalar fields, then investigates the general structure and types of solution of Maxwell's equations. This is followed by the quantisation of the vector potential. (It is interesting to note that the author starts with finding out the commutation rules for the creation-annihilation operators and constructs therefrom the covariant commutation rules for the field operators.) Then a detailed survey of the Dirac equation and related problems follows (noteworthy is here a rather unusual but very effective method developed to calculate the squares of various matrix elements and their averages). This chapter terminates naturally with the quantisation of the Dirac field.

Chapters II and III form the bulk and the best part of the work. After the general treatment of the interaction between charged particles and the electromagnetic field we get a brief but interesting treatment of the longitudinal field and Coulomb's law and, as a kind of surprise at this place, Breit's and Møller's formulae. Only then follows the theory of dipole radiation and photo effect. The continuity of the presentation is a bit endangered here by the insertion of a chapter on radiation damping, after which we again return to the previous line by investigating the properties of multipole-radiation. (In this section we also find an interesting summary of the author's studies on synchrotron-radiation.) Again a short interlude, on mathematical properties of emission probability, follows; then comes the theory of Čerenkov radiation; dispersion of light (including Compton and Raman effects); elastic scattering of charged particles in a Coulomb field; bremsstrahlung. A short introduction on the question of negative energy states precedes the treatment of pair creation and pair annihilation (including a brief theory of positonium) and this is followed by a naturally short and somewhat qualitative, nevertheless very fascinating, section on the theory of cascade-showers.

The last chapter deals with the theory of the vacuum. The methods employed here are direct but rather unusual and though the author manages to make very clear the physical meaning of the various terms which he obtains in the course of calculating the 'additional energy' of an electron with the electromagnetic vacuum and the polarisation of the electron-pair vacuum, the manipulations may seem to the initiated reader cumbersome and *ad hoc*. The problem of renormalisation is just touched upon. On the other hand we get some insight of the handling of regularisation methods. The last three sections treat in great detail the classical, Bohr-Sommerfeld, Schrödinger and Dirac theories of the hydrogen atom, its fine and hyperfine structure and the Zeeman-effect, making use of the formulae deduced on the previous pages to calculate also the vacuum corrections to the above mentioned phenomena.

The author does not make use of manifestly covariant presentation and of the now already quite familiar covariant perturbation theory and graph-methods. This seems to be regrettable as, firstly, these methods are usually even simpler and easier to follow than the older presentation, and, secondly, the student thereby does not become acquainted with the so powerful armament which would enable him to follow the current literature.

P. Roman

Physics of Fission (Consultants Bureau Inc., New York, 1957. 140 pages $ 30).

This is one of several translations of Russian articles to be published in a venture by an American concern, Consultants Bureau, Inc. Although one may approve of the principle

of making such translations available, it is hard to maintain much enthusiasm for this particular book after noting its price. For a fairly small paper-back, it is very expensive.

The same set of papers have also been translated and published by Pergamon Press as Volume 2 of Division II of their *International Series of Monographs on Nuclear Energy*. The price is much less, £ 3, and the book is free of the proofreading errors and mistranslations mentioned below.

The book is a handy and readable summary of fission phycics. It is not exhaustive but mentions most important aspects of the subject. It is also quite up-to-date, containing results published until 1957, including those presented at the Geneva Conference in 1955. It is especially useful, in that no other up-to-date review article on fission is available before Wheeler's article appears in the Encyclopaedia of Physics. The only comparable survey is the Report on the Conference at Chalk River in 1956. (This is actually more informative in many detailed respects than the present book.)

There are twelve articles, all of them authoritative. They cover both experiment and theory. The first article by B. T. Geilikman is devoted to the theoretical situation. It assumes some previous knowledge of the subject and omits elementary explanations. It avoids unnecessary details, and exposes the successes and failures of various theories in a most skilful manner. Indeed, it is a classic example of how a short survey should be composed. The only criticism is that it is a little too bare in places. It makes a bad impression to find that a quantity x appearing on the second page is not defined. (Unfortunately this is not the only instance of slipshod proof-reading in the book. A short perusal unearthed several others, such as the transposition of figures 6 and 7 on page 29.)

The following five contributions deal with aspects of low-energy fission. After a short article by Yu. S. Zamyatnin on the steps observed in plots of (n, f) cross-sections against neutron energy, there is a thorough survey by A. N. Murin of experimental data on the mass and charge distribution of fission products. The next contribution is a theoretical paper by V. G. Nosov on fission close to threshold. This contains some interesting speculations on the energy dependence of fission widths, which make plausible the constancy of observed (n, f) cross-sections. The fifth article by I. M. Frank is on anisotropy in fission processes, and overlaps other papers in several places. (This overlapping occurs frequently and one has the impression that if all the papers were synthesized, the size of the book would be halved.)

The sixth article by B. G. Erozolimsky is distinguished by a mis-translation of the title. Instead of being about "Neutron Fission", it is concerned with "Fission Neutrons", quite a different matter. This error occurs in spite of the translator being a "bilingual physicist", and one wonders about the presence of less evident errors. The article itself is well up to the high standard of others in the book. It reviews the data on the numbers of fission neutrons and their spectra, and mentions the semi-empirical analyses that have been made in the absence of a proper theory.

The next three articles deal with high-energy fission. The first by N. A. Perfilov, discusses data on fission into more than two fragments, and various characteristic features of high energy fission. Then follows an account by N. S. Ivanova of particular experiments with high energy protons with emphasis on the light charged particles emitted. This article mentions work done with the 660 MeV protons from the Russian synchrocyclotron, and contains an especially interesting discussion on the question of whether fission occurs directly from excited nuclei left by the emission of knock-out particles, or only after the evaporation of some neutrons. This question is taken up again in the next paper by V. P. Shamov in which data on photographic plates in presented and analysed.

Spontaneous Fission is described in the next two contributions. The first, by K. A. Petrzhak, is a general survey of the subject. From the references, one gathers that it is almost a monopoly of Western laboratories. The second paper is a short one that draws attention to some interesting correlations between alpha decay and fission lifetimes. This is an aspect of the subject which has hitherto been mainly studied in Russia.

The last paper by L. E. Lazareva and N. V. Nikitina is devoted to photo-fission. Like the other articles, it is admirably written, containing an outline of all relevant facts without unnecessary details.

A. M. Lane

Physics of nuclear fission (Supplement no. 1 of the Soviet journal Atomnaya Energiya), translated by J. E. S. Bradley (Pergamon Press, London &c. 1958. vi—182 pages. 60s.)

This is the book alluded to in Dr. Lane's review of the same translation published by the Consultants Bureau. The blemishes explicitly mentioned in the latter review are absent from the present volume; in particular, the quantity x occurring on p. 2 *is* duly defined in the text on the same page. A competent "corrector" has added a number of valuable footnotes, mainly referring to later developments.

The production is excellent in every respect: clear print of text and diagrams, photographs reproduced on special paper, and neat binding. The price is rather high, and yet it sounds cheap in comparison with that charged for the shabby American version.

L. R.

HERBERT GOLDSTEIN, *The attenuation of gamma rays and neutrons in reactor shields* (U. S. Government Printing Office, Washington 1957. xi—295 pages. $ 2)

This book, which has been prepared by the Nuclear Development Corporation of America for the U.S.A.E.C., gives in an excellent way a treatment of the fundamental problems involved in nuclear reactor shielding.

After a review of background information, such as definition of radiation intensities and the biological effects of radiation, a discussion is given of the different types of radiation sources of interest for reactor shield design. This discussion is followed by a description of shielding measurement equipment, mainly the LTSF and the BSR of the ORNL. The last two chapters, which cover the main subject of the book, contain a treatment of the attenuation of gamma rays and fast neutrons, respectively. Here different methods for attenuation calculations, particularly the method of moments for the solution of the Boltzmann equation and the Monte Carlo methods, are outlined. Further the results of numerical calculations and experiments are compared.

It ought to be emphasized that the book is unusually well-written, and its value is further increased by the large number of graphs and tables. At the end of each chapter a thorough list of references is given, of which some however are still classified.

Even though this book mainly deals with the fundamental aspects of nuclear radiation shielding, it is also of great value to the practical shield designer. This is not only due to the fact that it contains much information on nuclear data to be used in shield calculations, but also, and this is most important, because it gives the nuclear engineer a vivid impression of the background for and the limitations of the present status of reactor shield design.

P. L. Ølgaard

Nuclear Physics **7** (1958) 691; © *North-Holland Publishing Co., Amsterdam*

ERRATA

V. G. SOLOVIEV, The hypothesis of conservation of combined parity &c. (Nuclear Physics **6** (1958) 618).

In the *Note added in proof* on p. 624, the number of the reference quoted in the first line should be 9 and not 2.

N. Zeldes, Nuclear energies and the shell model, Nuclear Physics **7** (1958) 27

pp. 27, 28, 29	pagination	*add 26 to the page numbers in the table of contents*
p. 40	fig. 3a 1st part	*connect by a bold broken line segment the* S_p *values of* Sr^{86} *and* Mo^{90}
p. 41	lines 6, 7	*delete* and also in the transmercury elements
	line 8	*delete refs.* 18) *and* 33)
p. 44	line 9	*add* of the first kind *after* discontinuity
p. 73	fig. 12	*delete the thin line segment from* Em^{222} *to* Ra^{223}
p. 74	line 11	*write* different from *instead of* smaller than
p. 75	line 2	*add* and also the Q value *after* identification
p. 76	line 2	*add* (see also § 4.1) *after* terms
p. 77	line 14	*write* (46) *instead of* (45)
p. 94	line 11	*add* of Zr *after* protons

R. E. White, A. Chisholm and D. Brown, Polarization in the elastic scattering of 2—3 MeV neutrons by deuterons, Nuclear Physics **7** (1958) 233.

The abstract line 3 should read

0.58 ± 0.05 at 2.26 MeV and
0.40 ± 0.20 at 3.1 MeV.

AUTHOR INDEX

ALIKHANOV, A. I., G. P. ELISEIEV and V. A. LIUBIMOV, Measurement of longitudinal polarization of electrons emitted in β-decay . . . 655

ANDERSEN, S. L., K. GJÖTTERUD, T. HOLTEBEKK and O. LÖNSJÖ, Beams of different masses in electrostatic accelerators 384

ARMBRUSTER, R., *see* Gorodetzky

AUSTERN, N., Note on effective range theory 195

BÄCKSTRÖM, G., O. BERGMAN and J. BURDE, Transitions in Hg^{199} following the decay of Au^{199} 263

BARASHENKOV, V. S., On the interaction between K-mesons, pions, nucleons and hyperons 146

BERGMAN, O., *see* Bäckström

BILENKY, S. M., L. I. LAPIDUS, L. D. PUZIKOV and R. M. RYNDIN, Phenomenological analysis of reactions of the $a+a' \to b+b'$ type 646

BLOCH, C., Sur la détermination de l'état fondamental d'un système de particules 451

BLOCH, C. et C. DE DOMINICIS, Un développement du potentiel de Gibbs d'un système quantique composé d'un grand nombre de particules 459

BOOTH, N. E., F. L. HEREFORD, M. HUQ, G. W. HUTCHINSON, MARGARET E. LAW, A. M. SEGAR and D. H. WHITE, Azimuthal symmetry in proton scattering at 980 MeV 284

BOZÓKI, G., E. FENYVES, T. SÁNDOR and A. SOMOGYI, Investigation of extensive air showers containing nuclear active particles 677

BROWN, D., *see* White

BURDE, J., *see* Bäckström

CHEVALLIER, P., *see* Gorodetzky

CHISHOLM, A., *see* White

COESTER, F., Bound states of a many-particle system 421

COLEMAN, C. F., Relative transition probabilities in certain even nuclei 488

CORINALDESI, E., Particles and symmetries 305

DANIEL, H. und U. SCHMIDT-ROHR, β-Zerfall des N^{13} und Fierz-Interferenz bei Fermi-Wechselwirkung 516

DE DOMINICIS, C., *see* Bloch

DE-SHALIT, A., Energy levels in odd-mass and even nuclei. . . . 225

DOLGINOV, A. Z., A possible experiment for determination of spirality of μ-mesons 569

DOLGINOV, A. Z. and N. P. POPOV, First order forbidden $\beta-\gamma$-correlation for oriented nuclei 591

ELISEIEV, G. P., *see* Alikhanov
FENYVES, E., *see* Bozóki
FILIPKOWSKI, A., E. SKRZYPCZAK, A. SOMOGYI and A. WRÓBLEWSKI, Two events of mesonic decay of hyperfragments in flight 643
FIRK, F. W. K., *see* Lynn
FRENKIN, A. R., *see* Logunov
FRÖHLICH, H., Speculations on the masses of particles 148
GALLMANN, A., *see* Gorodetzky
GJÖTTERUD, K., *see* Andersen
GOLDEMBERG, J. and L. MARQUEZ, Measurements of (γ, d) and (γ, np) reactions in the threshold region 202
GOLDFARB, L. J. B., The polarization of deuterons and particles of arbitrary spin 622
GOLDSTEIN, S., *see* Lipkin
GORODETZKY, S., P. CHEVALLIER, R. ARMBRUSTER, A. GALLMANN et G. SUTTER, Corrélation angulaire des paires monopolaires du calcium 40 672
GREEN, H. S., Dirac matrices, teleparallelism and parity conservation 373
HAIG, FRANK R., Studies in lithium-7 and nitrogen-13 429
HARADA, K., *see* Oda
HEREFORD, F. L., *see* Booth
HILLMAN, P., *see* Maris
HILLMAN, P., *see* Tyrén
HOLTEBEKK, T., *see* Andersen
HUQ, M., *see* Booth
HUTCHINSON, G. W., *see* Booth
ISOYA, A., H. OHMURA and T. MOMOTA, The angular distributions of the long-range alpha-particles from the reaction $F^{19}(p, \alpha_0)O^{16}$ . . . 116
ISOYA, A., Analysis of the yield curves and the angular distributions of the reactions $F^{19}(p, \alpha_0)O^{16}$ and $F^{19}(p, \alpha_\pi)O^{16}$ 126
KAMEFUCHI, S., Reformulation of the theory of the neutrino 411
KANELLOPOULOS, Th., *see* Wildermuth
KONUMA, M., *see* Umezawa
LAPIDUS, L. I., *see* Bilenky
LAW, MARGARET E., *see* Booth
LIPKIN, H. J. and S. GOLDSTEIN, Rotational properties of the two-dimensional anisotropic harmonic oscillator II. The collective-intrinsic description 184
LIUBIMOV, V. A., *see* Alikhanov
LOGUNOV, A. A. and A. R. FRENKIN, On the dispersion relations for the Compton effect 573
LÖNSJÖ, O., *see* Andersen
LYNN, J. E., A new development in the area method of neutron

resonance analysis 599
LYNN, J. E., M. C. MOXON and F. W. K. FIRK, The low energy neutron resonances of bismuth 613
MA, S. T., The causal function and the causality condition 163
MARIS, TH. A. J., P. HILLMAN and H. TYRÉN, Quasi-elastic scattering and nuclear structure 1
MARIS, TH. A. J., *see* Tyrén
MARQUEZ, L., *see* Goldemberg
MIHAILOVIĆ, M. V. and B. POVH, The half-lives of some short-lived isotopes 296
MOMOTA, T., *see* Isoya
MORAVCSIK, M. J., Analytic forms of the deuteron wave function . . 113
MOXON, M. C., *see* Lynn
NAKAGAWA, K., *see* UMEZAWA
NIELSEN, K. O., O. B. NIELSEN and O. SKILBREID, Levels and branching ratios in Tb^{159} 561
NIELSEN, O. B., *see* K. O. Nielsen
NISHIMURA, K., Inelastic scattering of 96 MeV protons 425
ODA, N. and K. HARADA, Inelastic scattering of protons at intermediate energies 251
OHMURA, H., *see* Isoya
PIENAAR, H. J., *see* Van der Spuy
POPOV, N. P., *see* DOLGINOV
POVH, B., *see* Mihailović
PUZIKOV, L. D., *see* Bilenky
RAKAVY, G., An impulse approximation for the deuteron stripping reaction 553
REIGNIER, J., Diffusion d'électrons de haute énergie et répartition de la charge électrique du noyau 526
RIAZUDDIN, Charge dependent effects on scattering lengths of np and pp systems 217
RIAZUDDIN, On the difference of π^0-nucleon and $\pi^{\pm}$-nucleon coupling constants 223
RUELLE, D., Représentation du spin isobarique des particules à interactions fortes 443
RYNDIN, R. M., *see* Bilenky
SÁNDOR, T., *see* Bozóki
SATCHLER, G. R., *see* Sawicki
SAWICKI, J. and G. R. SATCHLER, Shape effects in deuteron stripping on spheroidal nuclei 289
SAWICKI, J., Inelastic scattering of nucleons and deuterons from spheroidal nuclei 503
SCHMIDT-ROHR, U., *see* Daniel

SEGAR, A. M., *see* Booth
SHARP COOK, C., Gamma radiation following the decay of Mn^{56} and the energy levels of Fe^{56} 480
SIMONS, L., Some properties of the irregular rotational spectra in odd-mass nuclei 209
SKILBREID, O., *see* K. O. Nielsen
SKRZYPCZAK, E., *see* Filipkowski
SOMOGYI, A., *see* Filipkowski
SOMOGYI, A., *see* Bozóki
SOROKO, L. M., Some possible experiments for the investigation of inelastic scattering of nucleons. 579
STREATER, R. F. and J. C. TAYLOR, Notes on meson decays 276
SUTTER, G., *see* Gorodetzky
TAKABAYASI, T., Right-left asymmetry and two-component neutrino 237
TAYLOR, J. C., *see* Streater
TIBELL, G., *see* Tyrén
TYRÉN, H., P. HILLMAN and TH. A. J. MARIS, High energy (p, 2p) reactions and proton binding energies 10
TYRÉN, H. and TH. A. J. MARIS, Inelastic scattering of 185 MeV protons on elements between Ca and Zn 24
TYRÉN, H., G. TIBELL and TH. A. J. MARIS, The scattering of 185 MeV protons from deuterium and neon 281
TYRÉN, H., *see* Maris
UMEZAWA, H., M. KONUMA and K. NAKAGAWA, The hyperon decays and the structure of interactions. 169
VAN DER SPUY, E. and H. J. PIENAAR, Relation of scattering phases to interaction parameters 389
VAN DER SPUY, E. and H. J. PIENAAR, The interaction of two alpha-particles 397
WHITE, D. H., *see* Booth
WHITE, R. E., A. CHISHOLM and D. BROWN, Polarization in the elastic scattering of 2—3 MeV neutrons by deuterons (see also erratum p. 691) 233
WILDERMUTH, K. and TH. KANELLOPOULOS, The "cluster model" of the atomic nuclei. 150
WRÓBLEWSKI, A., *see* Filipkowski
ZELDES, N., Nuclear energies and the shell model (see also errata p. 691) 27

SUBJECT INDEX

1. Nuclear Structure

1.B *Two-and three-body problems*

Analytic forms of the deuteron wave function, M. J. Moravcsik 113
Note on effective range theory, N. Austern 195
Polarization in the elastic scattering of 2−3 MeV neutrons by deuterons, R. E. White, A. Chisholm and D. Brown (see also erratum p. 691) . 233

1.C *Many-particle systems*

Bound states of a many-particle system, F. Coester 421
Sur la détermination de l'état fondamental système de particules, Claude Bloch 451
Un développement du potentiel de Gibbs d'un système quantique composé d'un grand nombre de particules, Claude Bloch et Cyrano de Dominicis 459

1.D *Nuclear models*

1.D.1 *Shell model*

Nuclear energies and the shell model, Nissan Zeldes (see also errata p. 691) 27
Energy levels in odd-mass and even nuclei, A. De-Shalit 225
Studies in lithium-7 and nitrogen-13, Frank R. Haig 429

1.D.2 *Collective model*

Rotational properties of the two-dimensional anisotropic harmonic oscillator II. The collective-intrinsic description, H. J. Lipkin and S. Goldstein 184
Some properties of the irregular rotational spectra in odd-mass nuclei, L. Simons 209
Shape effects in deuteron stripping on spheroidal nuclei, J. Sawicki and G. R. Satchler 289
Inelastic scattering of nucleons and deuterons from spheroidal nuclei, J. Sawicki 503

1.D.3 *Other models*

The "cluster model" of the atomic nuclei, K. Wildermuth and Th. Kanellopoulos. 150

1.D.4 *Relationship between different models*

Inelastic scattering of 96 MeV protons, Keiichi Nishimura 425

1.E *Properties of nuclei*

1.E.1 *Energy levels*

Quasi-elastic scattering and nuclear structure, Th. A. J. Maris, P. Hillman and H. Tyrén 1
High energy (p, 2p) reactions and proton binding energies, H. Tyrén, P. Hillman and Th. A. J. Maris 10
Energy levels in odd-mass and even nuclei, A. De-Shalit 225
Studies in lithium-7 and nitrogen-13, Frank R. Haig. 429
Gamma radiation following the decay of Mn^{56} and the energy levels of Fe^{56}, C. Sharp Cook 480

1.E.2 *Binding energies; Masses*

Nuclear energies and the shell model, Nissan Zeldes (see also errata p. 691) 27

1.E.4 *Transition probabilities; Cross sections*

Transitions in Hg^{199} following the decay of Au^{199}, G. Bäckström, O. Bergman and J. Burde 263

Relative transition probabilities in certain even nuclei, C. F. Coleman 488

Levels and branching ratios in Tb^{159}, K. O. Nielsen, O. B. Nielsen and O. Skilbreid 561

1.E.5 *Nuclear radii; Matter distributions*

Diffusion d'électrons de haute énergie et répartition de la charge électrique du noyau, Jean Reignier 526

2. Nuclear Reactions

2.A *General properties*

2.A.2 *General theory*

Phenomenological analysis of reactions of the $a+a' \rightarrow b+b'$ type, S. M. Bilenky, L. I. Lapidus, L. D. Puzikov and R. M. Ryndin . . 646

2.B *Angular distributions; Correlations; Polarization*

The angular distributions of the long-range alpha-particles from the reaction F^{19} (p, α_0)O^{16}, A. Isoya, H. Ohmura and T. Momota 116

Analysis of the yield curves and the angular distributions of the reactions F^{19}(p, α_0)O^{16} and F^{19}(p, α_π)O^{16}, A. Isoya 126

Polarization in the elastic scattering of 2–3 MeV neutrons by deuterons R. E. White, A. Chisholm and D. Brown (see also erratum p. 691) . 233

The polarization of deuterons and particles of arbitrary spin, L. J. B. Goldfarb 622

2.C *Resonance reactions; R-matrix theory*

Beams of different masses in electrostatic accelerators, S. L. Andersen, K. Gjötterud, T. Holtebekk and O. Lönsjö 384

A new development in the area method of neutron resonance analysis, J. E. Lynn. 599

The low energy neutron resonances of bismuth, J. E. Lynn, M. C. Moxon and F. W. K. Firk 613

2.G *Stripping and pick-up*

Shape effects in deuteron stripping on spheroidal nuclei, J. Sawicki and G. R. Satchler 289

An impulse approximation for the deuteron stripping reaction, G. Rakavy 553

2.I *Photonuclear processes*

Measurements of (γ, d) and (γ, np) reactions in the threshold region, J. Goldemberg and L. Marquez 202

The half-lives of some short-lived isotopes, M. V. Mihailović and B. Povh 296

2.L *Scattering processes (except two-nucleon system and meson scattering)*

Quasi-elastic scattering and nuclear structure, Th. A. J. Maris, P. Hillman and H. Tyrén 1

High energy (p, 2p) reactions and proton binding energies, H. Tyrén, P. Hillman and Th. A. J. Maris 10

Inelastic scattering of 185 MeV protons on elements between Ca and Zn, H. Tyrén and Th. A. J. Maris 24

Polarization in the elastic scattering of 2—3 MeV neutrons by deuterons, R. E. White, A. Chisholm and D. Brown (see also erratum p. 691) . 233
Inelastic scattering of protons at intermediate energies, N. Oda and K. Harada 251
The scattering of 185 MeV protons from deuterium and neon, H. Tyrén, G. Tibell and Th. A. J. Maris 281
Azimuthal symmetry in proton scattering at 980 MeV, N. E. Booth, F. L. Hereford, M. Huq, G. W. Hutchinson, Margaret E. Law, A. M. Segar and D. H. White 284
Relation of scattering phases to interaction parameters, E. van der Spuy and H. J. Pienaar 389
The interaction of two alpha-particles, E. van der Spuy and H. J. Pienaar . 397
Inelastic scattering of 96 MeV protons, Keiichi Nishimura 425
Inelastic scattering of nucleons and deuterons from spheroidal nuclei, J. Sawicki 503

3. Electromagnetic Radiation

3.A *Gamma radiation*

Transitions in Hg^{199} following the decay of Au^{199}, G. Bäckström, O. Bergman and J. Burde 263
Gamma radiation following the decay of Mn^{56} and the energy levels of Fe^{56}, C. Sharp Cook 480
Relative transition probabilities in certain even nuclei, C. F. Coleman . . 488
Levels and branching ratios in Tb^{159}, K. O. Nielsen, O. B. Nielsen and O. Skilbreid 561
Corrélation angulaire des paires monopolaires du calcium 40, S. Gorodetzky. P. Chevallier, R. Armbruster, A. Gallmann et G. Sutter 672

4. Beta Decay; Parity

4.A *General theory*

β-Zerfall des N^{13} und Fierz-Interferenz bei Fermi-Wechselwirkung, H. Daniel und U. Schmidt-Rohr 516

4.E *Analysis of data*

β-Zerfall des N^{13} und Fierz-Interferenz bei Fermi-Wechselwirkung, H. Daniel und U. Schmidt-Rohr 516

6. Methods and Instruments

6.A *Experimental*

Beams of different masses in electrostatic accelerators, S. L. Andersen, K. Gjötterud, T. Holtebekk and O. Lönsjö 384
A new development in the area method of neutron resonance analysis, J. E. Lynn 599

6.B *Theoretical*

Analytic forms of the deuteron wave function, M. J. Moravcsik 113

6.C *Constants, standards and units*

Document S.U.N. 57—9 299

7. Quantum Field Theory

7.A *General*

The causal function and the causality condition, S. T. Ma 163
On the dispersion relations for the Compton effect, A. A. Logunov and A. R. Frenkin 573

7.C *π-meson field (scattering and nuclear forces)*

Charge dependent effects on scattering lengths of np and pp systems, Riazuddin 217
On the difference of π^0-nucleon and $\pi\pm$-nucleon coupling constants, Riazuddin 223
Some possible experiments for the investigation of inelastic scattering of nucleons, L. M. Soroko 579

8. Elementary Particles

8.A *Experimental*

Two events of mesonic decay of hyperfragments in flight, A. Filipkowski, E. Skrzypczak, A. Somogyi and A. Wróblewski 643
Measurement of longitudinal polarization of electrons emitted in β-decay, A. I. Alikhanov, G. P. Eliseiev and V. A. Liubimov 655

8.B *Theory; transformation properties*

On the interaction between K-mesons, pions, nucleons and hyperons, V. S. Barashenkov 146
Speculations on the masses of particles, H. Fröhlich 148
The hyperon decays and the structure of interactions, H. Umezawa, M. Konuma and K. Nakagawa 169
Right-left asymmetry and two-component neutrino, T. Takabayasi . . . 237
Notes on meson decays, R. F. Streater and J. C. Taylor 276
Particles and symmetries, E. Corinaldesi 305
Dirac matrices, teleparallelism and parity conservation, H. S. Green . . . 373
Reformulation of the theory of the neutrino, S. Kamefuchi 411
Représentation du spin isobarique des particules à interactions fortes, D. Ruelle 443
A possible experiment for determination of spirality of μ-mesons, A. Z. Dolginov 569
First order forbidden $\beta-\gamma$-correlation for oriented nuclei, A. Z. Dolginov and N. P. Popov 591

9. Cosmic Radiation

9.A *General*

Investigation of extensive air showers containing nuclear active particles, G. Bozóki, E. Fenyves, T. Sándor and A. Somogyi 677

10. News Items

10.A *News item*

Documentation Atomique 552

10.D *Book reviews*

Flügge, S. V., editor, Handbuch der Physik — Encyclopedia of Physics, Vol. 39 (L.R.) 111

BOGOLIUBOV, N. N. i D. V. SHIRKOV, Vvedenie v teoriiu kvantovannych polei [Introduction into the theory of quantized fields] (L. R.) 297
FLÜGGE, S.V., editor, Handbuch der Physik-Encyclopedia of Physics Vol. 5/1 (L. R.) 298
EMIN, I., editor, Russian-English glossary of solid state physics (L. R.) . . 687
LANDAU, L. and Y. SMORODINSKY, Lectures on nuclear theory (L. R.) . . 687
O.E.E.C., editor, The industrial challenge of nuclear energy: II. Research, uses, social problems (L. R.). 687
BAYET, M., Physique électronique des gaz et des solides (L. R.) 687
SOKOLOW, A., Quantenelektrodynamik (P. Roman) 688
Physics of Fission (A. M. Lane) 689
Physics of nuclear fission (L. R.). 690
GOLDSTEIN, H., The attenuation of gamma rays and neutrons in reactor shields (P. L. Ølgaard) 690

10.E *Errata*

V. G. SOLOVIEV, Nuclear Physics **6** (1958) 618 691
N. ZELDES, Nuclear Physics **7** (1958) 27 691
R. E. WHITE, A. CHISHOLM and D. BROWN, Nuclear Physics **7** (1958) 233 . 691